INSECTS AT THE CENTER OF INTERACTIONS WITH OTHER ORGANISMS

EDITED BY: Patrizia Falabella, Michel Cusson and Anne-Nathalie Volkoff
PUBLISHED IN: Frontiers in Physiology

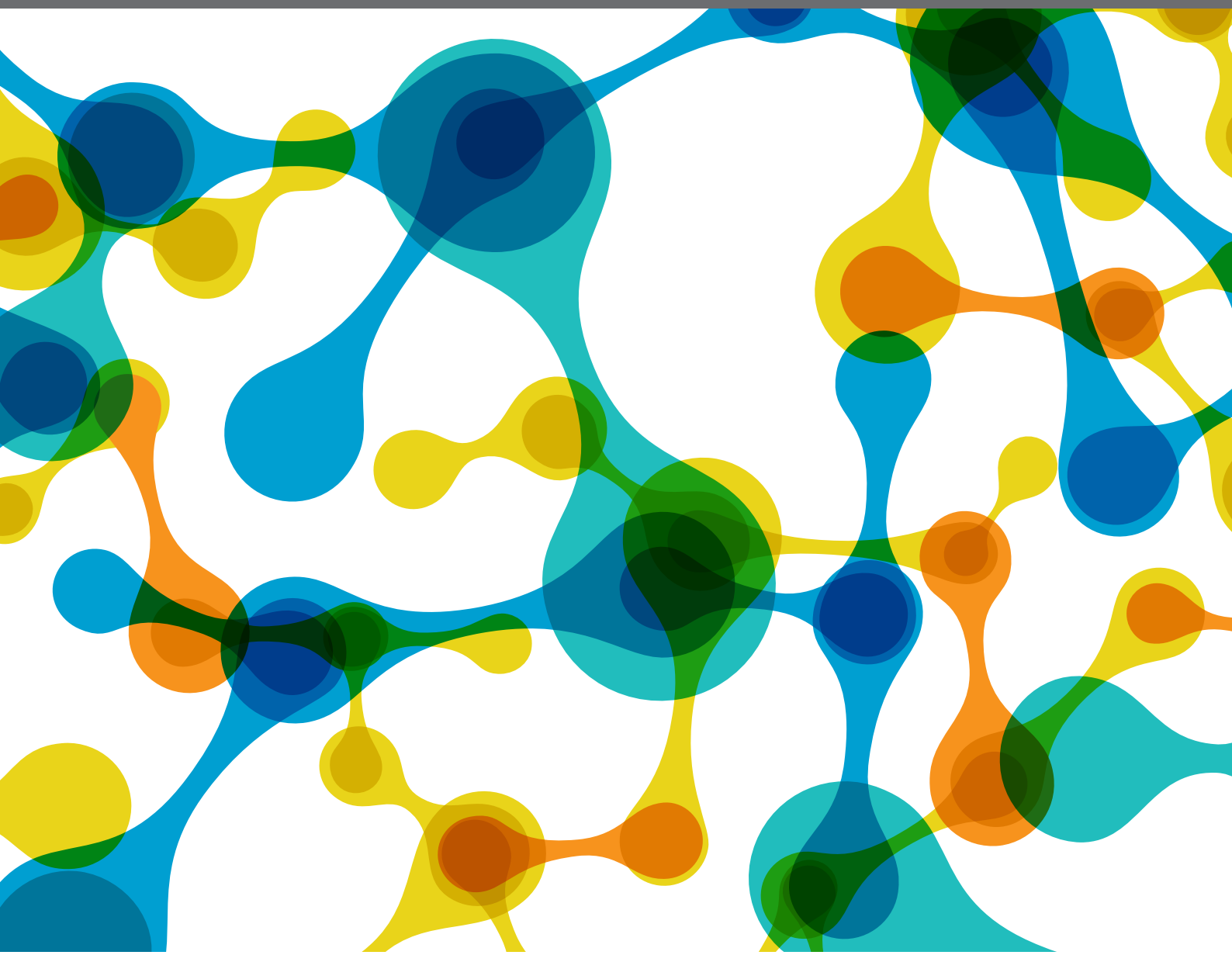

frontiers Research Topics

frontiers

ISSN 1664-8714
ISBN 978-2-88963-940-3
DOI 10.3389/978-2-88963-940-3

About Frontiers

Frontiers is more than just an open-access publisher of scholarly articles: it is a pioneering approach to the world of academia, radically improving the way scholarly research is managed. The grand vision of Frontiers is a world where all people have an equal opportunity to seek, share and generate knowledge. Frontiers provides immediate and permanent online open access to all its publications, but this alone is not enough to realize our grand goals.

Frontiers Journal Series

The Frontiers Journal Series is a multi-tier and interdisciplinary set of open-access, online journals, promising a paradigm shift from the current review, selection and dissemination processes in academic publishing. All Frontiers journals are driven by researchers for researchers; therefore, they constitute a service to the scholarly community. At the same time, the Frontiers Journal Series operates on a revolutionary invention, the tiered publishing system, initially addressing specific communities of scholars, and gradually climbing up to broader public understanding, thus serving the interests of the lay society, too.

Dedication to Quality

Each Frontiers article is a landmark of the highest quality, thanks to genuinely collaborative interactions between authors and review editors, who include some of the world's best academicians. Research must be certified by peers before entering a stream of knowledge that may eventually reach the public - and shape society; therefore, Frontiers only applies the most rigorous and unbiased reviews.
Frontiers revolutionizes research publishing by freely delivering the most outstanding research, evaluated with no bias from both the academic and social point of view. By applying the most advanced information technologies, Frontiers is catapulting scholarly publishing into a new generation.

What are Frontiers Research Topics?

Frontiers Research Topics are very popular trademarks of the Frontiers Journals Series: they are collections of at least ten articles, all centered on a particular subject. With their unique mix of varied contributions from Original Research to Review Articles, Frontiers Research Topics unify the most influential researchers, the latest key findings and historical advances in a hot research area! Find out more on how to host your own Frontiers Research Topic or contribute to one as an author by contacting the Frontiers Editorial Office: researchtopics@frontiersin.org

INSECTS AT THE CENTER OF INTERACTIONS WITH OTHER ORGANISMS

Topic Editors:
Patrizia Falabella, University of Basilicata, Italy
Michel Cusson, Department of Natural Resources (Canada), Canada
Anne-Nathalie Volkoff, Institut National de la Recherche Agronomique Centre Montpellier, France

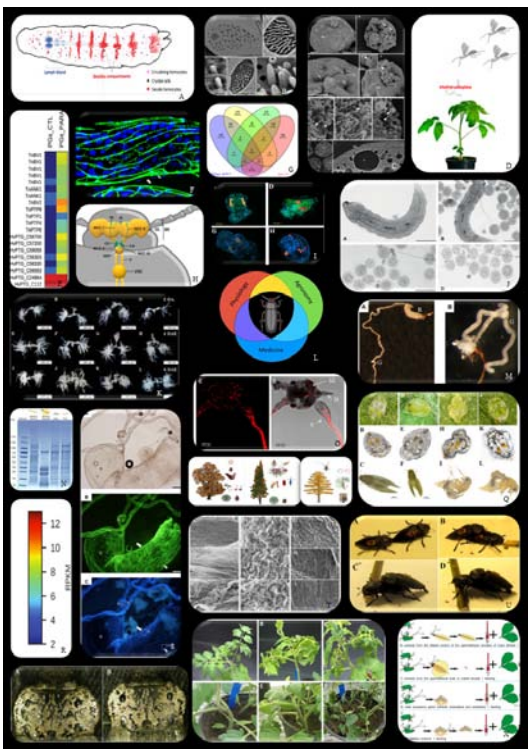

(A) Figure from "Chami Kim-Jo, Jean-Luc Gatti and Marylène Poirié (2019). Drosophila Cellular Immunity Against Parasitoid Wasps: A Complex and Time-Dependent Process. Front. Physiol. 10:603. doi: 10.3389/fphys.2019.00603"

(B) Figure from "Giuseppe Bari, Andrea Scala, Vita Garzone, Rosanna Salvia, Cem Yalcin, Pasqua Vernile, Antonella Maria Aresta, Osvaldo Facini, Rita Baraldi, Sabino A. Bufo, Heiko Vogel, Enrico de Lillo, Francesca Rapparini and Patrizia Falabella (2019). Chemical Ecology of *Capnodis tenebrionis* (L.) (Coleoptera: Buprestidae): Behavioral and Biochemical Strategies for Intraspecific and Host Interactions. Front. Physiol. 10:604. doi: 10.3389/fphys.2019.00604"

(C) Figure from "Rosanna Salvia, Annalisa Grimaldi, Rossana Girardello, Carmen Scieuzo, Andrea Scala, Sabino A. Bufo, Heiko Vogel and Patrizia Falabella (2019). *Aphidius ervi Teratocytes* Release Enolase and Fatty Acid Binding Protein Through Exosomal Vesicles. Front. Physiol. 10:715. doi: 10.3389/fphys.2019.00715"

(D) Figure from "Mariangela Coppola, Gianfranco Diretto, Maria Cristina Digilio, Sheridan Lois Woo, Giovanni Giuliano, Donata Molisso, Francesco Pennacchio, Matteo Lorito and Rosa Rao (2019). Transcriptome and Metabolome Reprogramming in Tomato Plants by *Trichoderma harzianum* strain T22 Primes and Enhances Defense Responses Against Aphids. Front. Physiol. 10:745. doi: 10.3389/fphys.2019.00745"

(E) Figure from "Rosanna Salvia, Marisa Nardiello, Carmen Scieuzo, Andrea Scala, Sabino A. Bufo, Asha Rao, Heiko Vogel and Patrizia Falabella (2018). Novel Factors of Viral Origin Inhibit TOR Pathway Gene Expression X. Front. Physiol. 9:1678. doi: 10.3389/fphys.2018.01678"

(F) Figure from "Sébastien Cambier, Olivia Ginis, Sébastien J. M. Moreau, Philippe Gayral, Jack Hearn, Graham N. Stone, David Giron, Elisabeth Huguet and Jean-Michel Drezen (2019). Gall Wasp Transcriptomes Unravel Potential Effectors Involved in Molecular Dialogues With Oak and Rose. Front. Physiol. 10:926. doi: 10.3389/fphys.2019.00926"

(G) Figure from "Mariangela Coppola, Gianfranco Diretto, Maria Cristina Digilio, Sheridan Lois Woo, Giovanni Giuliano, Donata Molisso, Francesco Pennacchio, Matteo Lorito and Rosa Rao (2019). Transcriptome and Metabolome Reprogramming in Tomato Plants by *Trichoderma harzianum* strain T22 Primes and Enhances Defense Responses Against Aphids. Front. Physiol. 10:745. doi: 10.3389/fphys.2019.00745"

(H) Figure from "Zbigniew Adamski, Sabino A. Bufo, Szymon Chowański, Patrizia Falabella, Jan Lubawy, Paweł Marciniak, Joanna Pacholska-Bogalska, Rosanna Salvia, Laura Scrano, Małgorzata Słocińska, Marta Spochacz, Monika Szymczak, Arkadiusz Urbański, Karolina Walkowiak-Nowicka and Grzegorz Rosiński (2019). Beetles as Model Organisms in Physiological, Biomedical and Environmental Studies – A Review.
Front. Physiol. 10:319. doi: 10.3389/fphys.2019.00319"

(I) Figure from "Surapathrudu Kanakala, Svetlana Kontsedalov, Galina Lebedev and Murad Ghanim (2019). Plant-Mediated Silencing of the Whitefly *Bemisia tabaci Cyclophilin* B and Heat Shock Protein 70 Impairs Insect Development and Virus Transmission. Front. Physiol. 10:557. doi: 10.3389/fphys.2019.00557"

(J) Figure from "Rosanna Salvia, Annalisa Grimaldi, Rossana Girardello, Carmen Scieuzo, Andrea Scala, Sabino A. Bufo, Heiko Vogel and Patrizia Falabella (2019). *Aphidius ervi Teratocytes* Release Enolase and Fatty Acid Binding Protein Through Exosomal Vesicles. Front. Physiol. 10:715. doi: 10.3389/fphys.2019.00715"

(K) Figure from "Lin Quan Ge, Sui Zheng, Hao Tian Gu, Yong Kai Zhou, Ze Zhou, Qi Sheng Song and David Stanley (2019). Jinggangmycin-Induced UDP-Glycosyltransferase 1-2-Like is a Positive Modulator of Fecundity and Population Growth in *Nilaparvata lugens* (Stål) (Hemiptera: Delphacidae).
Front. Physiol. 10:747. doi: 10.3389/fphys.2019.00747 "

(L) Figure from "Zbigniew Adamski, Sabino A. Bufo, Szymon Chowański, Patrizia Falabella, Jan Lubawy, Paweł Marciniak, Joanna Pacholska-Bogalska, Rosanna Salvia, Laura Scrano, Małgorzata Słocińska, Marta Spochacz, Monika Szymczak, Arkadiusz Urbański, Karolina Walkowiak-Nowicka and Grzegorz Rosiński (2019). Beetles as Model Organisms in Physiological, Biomedical and Environmental Studies – A Review.
Front. Physiol. 10:319. doi: 10.3389/fphys.2019.00319"

(M) Figure from "Sébastien Cambier, Olivia Ginis, Sébastien J. M. Moreau, Philippe Gayral, Jack Hearn, Graham N. Stone, David Giron, Elisabeth Huguet and Jean-Michel Drezen (2019). Gall Wasp Transcriptomes Unravel Potential Effectors Involved in Molecular Dialogues With Oak and Rose. Front. Physiol. 10:926. doi: 10.3389/fphys.2019.00926"

(N) Figure from "Gianandrea Salerno, Francesca Frati, Eric Conti, Ezio Peri, Stefano Colazza and Antonino Cusumano (2019). Mating Status of an Herbivorous Stink Bug Female Affects the Emission of Oviposition-Induced Plant Volatiles Exploited by an Egg Parasitoid. Front. Physiol. 10:398. doi: 10.3389/fphys.2019.00398"

(O) Figure from "Marisa Skaljac, Heiko Vogel, Natalie Wielsch, Sanja Mihajlovic and Andreas Vilcinskas (2019). Transmission of a Protease-Secreting Bacterial Symbiont Among Pea Aphids via Host Plants. Front. Physiol. 10:438. doi: 10.3389/fphys.2019.00438"

(P) Figure from "Alberto Santini and Andrea Battisti (2019). Complex Insect–Pathogen Interactions in Tree Pandemics. Front. Physiol. 10:550. doi: 10.3389/fphys.2019.00550"

(Q) Figure from "Surapathrudu Kanakala, Svetlana Kontsedalov, Galina Lebedev and Murad Ghanim (2019). Plant-Mediated Silencing of the Whitefly *Bemisia tabaci* Cyclophilin B and Heat Shock Protein 70 Impairs Insect Development and Virus Transmission. Front. Physiol. 10:557. doi: 10.3389/fphys.2019.00557"

(R) Figure from "Rosanna Salvia, Marisa Nardiello, Carmen Scieuzo, Andrea Scala, Sabino A. Bufo, Asha Rao, Heiko Vogel and Patrizia Falabella (2018). Novel Factors of Viral Origin Inhibit TOR Pathway Gene Expression X. Front. Physiol. 9:1678. doi: 10.3389/fphys.2018.01678"

(S) Figure from "Sébastien Cambier, Olivia Ginis, Sébastien J. M. Moreau, Philippe Gayral, Jack Hearn, Graham N. Stone, David Giron, Elisabeth Huguet and Jean-Michel Drezen (2019). Gall Wasp Transcriptomes Unravel Potential Effectors Involved in Molecular Dialogues With Oak and Rose. Front. Physiol. 10:926. doi: 10.3389/fphys.2019.00926"

(T) Figure from "Gong Chen, Qi Su, Xiaobin Shi, Huipeng Pan, Xiaoguo Jiao and Youjun Zhang (2018). Persistently Transmitted Viruses Restrict the Transmission of Other Viruses by Affecting Their Vectors. Front. Physiol. 9:1348. doi: 10.3389/fphys.2018.01348"

(U) Figure from "Giuseppe Bari, Andrea Scala, Vita Garzone, Rosanna Salvia, Cem Yalcin, Pasqua Vernile, Antonella Maria Aresta, Osvaldo Facini, Rita Baraldi, Sabino A. Bufo, Heiko Vogel, Enrico de Lillo, Francesca Rapparini and Patrizia Falabella (2019). Chemical Ecology of *Capnodis tenebrionis* (L.) (Coleoptera: Buprestidae): Behavioral and Biochemical Strategies for Intraspecific and Host Interactions. Front. Physiol. 10:604. doi: 10.3389/fphys.2019.00604"

(V) Figure from "Giuseppe Bari, Andrea Scala, Vita Garzone, Rosanna Salvia, Cem Yalcin, Pasqua Vernile, Antonella Maria Aresta, Osvaldo Facini, Rita Baraldi, Sabino A. Bufo, Heiko Vogel, Enrico de Lillo, Francesca Rapparini and Patrizia Falabella (2019). Chemical Ecology of *Capnodis tenebrionis* (L.) (Coleoptera: Buprestidae): Behavioral and Biochemical Strategies for Intraspecific and Host Interactions. Front. Physiol. 10:604. doi: 10.3389/fphys.2019.00604"

(W) Figure from "Surapathrudu Kanakala, Svetlana Kontsedalov, Galina Lebedev and Murad Ghanim (2019). Plant-Mediated Silencing of the Whitefly *Bemisia tabaci* Cyclophilin B and Heat Shock Protein 70 Impairs Insect Development and Virus Transmission. Front. Physiol. 10:557. doi: 10.3389/fphys.2019.00557"

(X) Figure from "Gianandrea Salerno, Francesca Frati, Eric Conti, Ezio Peri, Stefano Colazza and Antonino Cusumano (2019). Mating Status of an Herbivorous Stink Bug Female Affects the Emission of Oviposition-Induced Plant Volatiles Exploited by an Egg Parasitoid. Front. Physiol. 10:398. doi: 10.3389/fphys.2019.00398"

Citation: Falabella, P., Cusson, M., Volkoff, A.-N., eds. (2020). Insects at the Center of Interactions with Other Organisms. Lausanne: Frontiers Media SA. doi: 10.3389/978-2-88963-940-3

Table of Contents

frontiers in Physiology

EDITORIAL
published: 23 June 2020
doi: 10.3389/fphys.2020.00616

Editorial: Insects at the Center of Interactions With Other Organisms

Anne-Nathalie Volkoff[1]*, *Michel Cusson*[2]* and *Patrizia Falabella*[3]*

[1] INRAE Institut National de Recherche pour l'Agriculture, l'alimentation et l'Environnement, Montpellier, France, [2] Laurentian Forestry Centre, Natural Resources Canada, Quebec City, QC, Canada, [3] Department of Sciences, University of Basilicata, Potenza, Italy

Keywords: biomimicry, insects, behavior, ecology, biotechnology, environment

Editorial on the Research Topic

Insects at the Center of Interactions With Other Organisms

Insects represent the largest and most diverse group of living organisms and are involved in a wide spectrum of interactions with other organisms. Many such interactions have been the focus of scientific investigations, including some reported here in a collection of *Frontiers in Physiology* papers published under the Research Topic "Insects at the center of interactions with other organisms." Below is an overview of the subject matters and key findings of each article included in this collection. As you will come to appreciate, these studies are very diverse, both in terms of the subject organisms and research tools used to shed light on the interactions under investigation, but all of them report on cases in which insects are at the center of interactions with other organisms.

OPEN ACCESS

Edited and reviewed by:
Ioannis Eleftherianos, George Washington University, United States

***Correspondence:**
Anne-Nathalie Volkoff
anne-nathalie.volkoff@inrae.fr
Michel Cusson
michel.cusson@canada.ca
Patrizia Falabella
patrizia.falabella@unibas.it

Specialty section:
This article was submitted to Invertebrate Physiology, a section of the journal Frontiers in Physiology

Received: *24 April 2020*
Accepted: *15 May 2020*
Published: *23 June 2020*

Citation:
Volkoff A-N, Cusson M and Falabella P (2020) Editorial: Insects at the Center of Interactions With Other Organisms. Front. Physiol. 11:616. doi: 10.3389/fphys.2020.00616

INSECTS AS MODEL ORGANISMS FOR BIOLOGICAL AND BIOMEDICAL STUDIES

Insects, with over 1 million described species, have a worldwide distribution and display an amazing ability to adapt to all types of environmental conditions so long as in presence of organic substances as a food source. In addition, their breeding is easy and inexpensive and several of their biochemical pathways at the cellular level are very similar to those of vertebrates, allowing us to extrapolate some findings about their biology and physiology to vertebrates (a famous case being research on drosophila development and immunity (Anderson and Nusslein-Volhard, 1984; Lemaitre et al., 1996), which led to the discovery of Toll-like receptors in humans). For these reasons, many insects have been used as model organisms in biological, medical and environmental research. In recent years, species in the order Coleoptera have increasingly been used as model organisms in biomedical and environmental studies. In this Research Topic, Adamsky et al. review current knowledge regarding the use of beetles as model organisms and the practical applications resulting from it to various fields of the life sciences.

HOST-PARASITOID INTERACTIONS

Parasitoid wasps represent one of the most abundant and diversified groups of insects on Earth, and interactions between parasitoids and their invertebrate hosts have been extensively studied. Parasitoids have long fascinated researchers as biological models to explore host-parasite co-evolution, insect development and immunity, insect behavior, or have been studied because they are natural enemies of insect pests and thus widely used as biological control agents.

Parasitoids exhibit different life habits and widely diverse interactions with their hosts. Complex physiological interactions are found between parasitoids that develop within a living insect

(so called koinobiont endoparasitoids). Because of this particular life cycle, this group of parasitoids have developed fine-tuned strategies allowing them to deal with their host's immunity, development or metabolism in order to allow proper development of their progeny. Strategies include injection into the host, by the female wasp, of venom proteins or viral particles produced in the genital track. Acquisition of knowledge on the molecular mechanisms underlying these complex interactions has largely benefitted, in the recent years, from the emergence of high-throughput technologies combined with more classical biochemical and cellular biology techniques. For instance, the whole arsenal of proteins produced in the venom gland of drosophila parasitoids in the genus *Leptopilina* has been elucidated thanks to a combined transcriptomic and proteomic approach. A review of the advances achieved in this field is presented in a paper by Kim-Jo et al. The review also highlights how the field of parasitoid "venomics" contributed to advance knowledge of insect cellular immunity. Similarly, knowledge on the mutualistic viruses produced in the ovaries of braconid and ichneumonid wasps has considerably advanced in recent years. The viral particles are injected into a caterpillar host upon oviposition by the female wasp. The packaged viral genome includes hundreds of genes that are expressed in the parasitized insect where their expression leads to alterations of the physiology of the parasitoid's host. Two papers present novel data on how the parasitized insect is affected in these biological systems and thus contribute to an understanding of how koinobiont parasitoids regulate the physiology of their host to ensure the development of their progeny. A first study by Merlin and Consoli analyses the transcriptome of caterpillars parasitized by the virus-carrying braconid wasp *Cotesia flavipes*, allowing them to establish an extensive list of lepidopteran genes potentially involved in host immune response, metabolism and development, and showing that transcription is strongly affected by parasitism. Another study by Salvia, Nardiello et al. investigates the manipulation of host development by the braconid wasp *Toxoneuron nigriceps* using different approaches; the authors, here, nicely demonstrate the involvement of viral proteins in blocking ecdysteroidogenesis in host prothoracic glands, through alterations of the PI3K/Akt/TOR pathway at the transcriptional level. Finally, beyond maternal factors, host suitability may be promoted by factors released by the developing, immature wasp. Some parasitoid species, upon egg hatch, release unusual giant serosal cells called teratocytes, responsible, among other functions, for extra-oral digestion of host tissues. In this issue, using biochemical and cellular biology approaches, Salvia, Grimaldi et al. report on the unconventional mechanism by which teratocytes from the braconid wasp *Aphidius ervi* release enolase and fatty acid binding proteins, and reveal that these proteins are probably released via an exosome secretion pathway.

INSECT-NEMATODE INTERACTIONS

With a parasitic life history similar to that of parasitoid wasps, parasitic nematodes also develop within living insects. To complete their life cycle, nematodes rely on symbiotic bacteria responsible for the death of the insect, the nematode then feeding on the insect cadaver. Intricate interactions also exist between the insect and the complex formed by the nematode and its mutualistic bacteria. In this issue, Ozakman and Eleftherianos provide insights into the signaling pathways that are activated in insects when they are infected with entomopathogenic nematodes; they show, using mutant flies, that lipid metabolism is affected in nematode-infected insects via the regulation of the activin and BMP branches of TGF-ß signaling.

INSECTS AND THEIR INTERACTIONS WITH ENDOSYMBIONTS

Bacterial symbionts of insects are very common and, in many instances, can have profound effects on the physiology of their insect hosts. The reality of their prevalence is highlighted by the recent characterization of specific microbial communities in many insects, thanks to new genomic sequencing technologies. Plant sap-sucking insects form a well-studied group in terms of their association with primary symbionts, which supply them with essential nutrients; these insects are also known to harbor diverse secondary symbionts. In addition to their role in insect nutritional ecology, bacterial symbionts can mediate several other ecologically relevant traits, including defense toward pathogens and parasites, adaptation to environment, influences on insect-plant interactions, and impact on population dynamics (for an overview see Su et al., 2013). In the Research Topic, several contributing papers explore the role of endosymbionts in a variety of plant sap-sucking insect life traits, using different approaches. A study by Li et al. examines the effects of the secondary bacterial symbiont *Cardinium* on the ecological adaptation of whiteflies. To this end, they analyze differentially expressed miRNAs between infected and uninfected insects; their results lead to the conclusion that symbionts can improve the fitness of their host by increasing its tolerance to environmental stresses via miRNA regulation of gene expression. In another paper, Skaljac et al. show the importance of symbionts in insect-plant interactions. Through an analysis of tissue localization of the secondary bacterial symbiont *Serratia symbiotica* in pea aphid, the authors reveal the presence of the symbiont in several tissues from the aphid's digestive tract, including the salivary glands and the stylet. Consequently, the bacteria were also detected in plant tissues, where they could, by secreting proteases, facilitate digestion of plant proteins and alter plant defense. A third paper addresses the role of symbiotic bacteria in host defense against pathogens. Gonella et al. analyzed the expression of immune genes in the sugar-feeding leafhopper *Euscelidius variegatus*, following exposure to the secondary bacterial symbiont *Asaia*. They conclude that a component of the Ras/Raf pathway is activated by *Asaia* and could potentially mediate the role the symbiont plays in limiting phytoplasma acquisition by the insect.

INSECTS AS VECTORS OF PLANT PATHOGENS

Because vector-borne plant diseases can have severe economic and environmental impacts, the factors responsible for, or limiting, their transmission have received much research attention. Insects can vector many plant diseases, including viruses, bacteria and fungi. Consequently, the molecular mechanisms underlying insect-phytopathogen interactions have been intensively studied. Two papers in this Research Topic address the factors that may affect transmission of the tomato yellow leaf curl virus (TYLCV) by whiteflies. These factors include insect vector proteins, as shown by Kanakala et al.. Using bioassays and RNAi technology to knock-down two whitefly gene products previously shown to interact with the TYLCV in the insect midgut, the authors confirmed the role of cyclophilin B and heat shock protein 70 in the whitefly's ability to transmit the virus. Chen G. et al. examined another factor that can affect virus transmission by insects. The authors compared transmission by whiteflies and western flower thrips of two persistently transmitted viruses that can co-infect the two insect species. Their results indicate that presence of TSWV reduces the ability of whiteflies to transmit the TYLCV, and inversely, that the presence of TYLCV in thrips reduces the transmission of TSWV, thus showing a negative effect of co-infections on virus transmission in both biological systems.

Vector-borne plant viruses may also have direct or indirect effects on the insect vectors. Ding et al. explored the molecular mechanisms underlying the response of whiteflies to the plant pathogens they vector (TYLCV, ToCV, TYLCV&ToCV co-infection), using a transcriptomic approach. They identified a list of insect genes that are differentially regulated in infected and non-infected insects. Studying this type of system from the angle of insect nutrition, Guo et al. assessed the effects of TYLCV infection on nutrient availability for different whitefly biotypes. The authors show that TYLCV infection of tomato plants significantly affected the amount of free amino acids in the phloem sap of the tomato plants and of free amino acids in whitefly honeydew. The authors also show that the better performance of the Q biotype is related to its superior ability to obtain free amino acids from the virus-infected plants.

Insects can also be indirect vectors of plant diseases and can thus contribute to emergence of new pandemics. A paper by Santini and Battisti, based on an analysis of three major pandemics affecting forest and urban trees in temperate ecosystems, illustrates how such pandemics can be initiated by the introduction of a non-native pathogen that exploits well-developed interactions between native non-aggressive organisms and insects associated with trees.

INSECT AND PLANT TROPHIC INTERACTIONS

Herbivorous insects often have intricate relationships with their host plants. Insects rely on a series of chemical cues to locate their host plant, especially plant volatiles such as terpenoids and other compounds emitted from leaves; their response to host plant odors varies with the physiological status of both the plant and the insect. Indeed, plants perceive damage-associated and insect-associated molecular patterns via receptors that activate diverse signaling networks resulting in local and systemic responses. Several papers in the present collection provide insights into the complex interactions between insects and plants and how they affect tritrophic interactions in agro-ecological systems. Cambier et al. explored the molecular mechanisms underlying cynipid gall induction in woody plants. By analyzing the transcriptome of ovaries and venom glands of two cynipid wasps, the authors identified candidate proteins involved in gall induction, including cellulases and potential plant defense suppressors. Bari et al. analyzed the communication strategies adopted by adults of the Mediterranean flat-headed root-borer. By combining morphological studies, bioassays, chemical and transcriptomic analyses, the authors discovered that females regulate mate recognition and acceptance via pronotal secretions related to volatiles emitted from their host plant. Finally, two papers examined interactions between parasitoids (third trophic level) and volatiles emitted by the plant in response to insect damage, and the factors affecting these interactions. Bertoldi et al. examined the role of host-parasitoid coevolution in the "efficiency" of this interaction. Their results indicate that the egg parasitoid *Trissolcus japonicus* efficiently exploits volatiles produced by tomato plants following egg deposition and infliction of feeding punctures by its coevolved host *Halyomorpha halys*; however, it does not respond to cues associated with a novel host, *Podisus maculiventris*. The study by Salerno et al. contributes to elucidating the source and the nature of the elicitor responsible for the recruitment of the egg parasitoid *Trissolcus basalis* by emitting plants following oviposition by stink bugs. By combining olfactometer observations and protein analysis, they identified a candidate protein specifically produced in response to mating in the dilated portion of the stink bug's spermathecal complex.

EFFECTS OF BIOTIC AND ABIOTIC FACTORS ON INSECT LIFE TRAITS

Insects live in a wide variety of environments and are therefore exposed to multiple biotic and abiotic factors that may seriously impact on their life traits. Understanding how these factors affect, positively or negatively, insect life traits can shed light on their population ecology and dynamics and, *in fine*, may lead to the development of novel sustainable pest control strategies. The effects different factors have on insect life traits are addressed in this Research Topic; these factors include the nutritional characteristics of their food sources and the presence of pesticides in the environment. Abedi et al. evaluated different commercial cultivars of pomegranate on life traits of a major pomegranate pest, the carob moth. Through biochemical analyses and bioassays, they show that biochemical characteristics of cultivars significantly affect life history traits and demographical parameters in the pest. Results led to a classification of the pomegranate cultivars as susceptible or resistant, a knowledge that is critical to the development of integrated pest management practices.

The effect of diet was also investigated by Chen E. et al. who evaluated its impact on susceptibility of the cabbage looper to the AcMNPV baculovirus. Microscopic observations and transcriptomic analyses clearly showed an effect of diet composition on the thickness of the peritrophic membrane of the caterpillars' midgut, an effect that results from differences in chitin deacetylase and chitinase expression, which in turn has consequences for looper susceptibility to the baculovirus. Pesticides can negatively affect beneficial insects, and in particular pollinators. To assess the global impact of pesticides on pollinators, methods for residue detection are needed. Favaro et al. present a practical and reliable approach to identify the source of pesticide residues from pollen collected by honeybees based on pollen and multi-residual chemical analyses. Thanks to an experimental setup at the landscape scale, the authors were able to identify various sources of contamination during the apple blossom season. In addition to their detrimental effects on beneficial insects, pesticides directed against one organism can have unexpected effects on another organism. For instance, Ge et al. provide evidence that applications of the antibiotic jinggangmycin, normally used to control a rice fungal pathogen, stimulates planthopper reproduction via an upregulation of an UDP-glucuronosyltransferase in the insect, which is shown to be a positive modulator of the insect's reproductive biology. This paper underscores the importance of assessing the side effects of a given control product on the entire community of the targeted pest, under natural conditions.

MICROORGANISMS FOR THE DEFENSE OF PLANTS FROM PHYTOPHAGOUS INSECTS

Plant defenses can also be triggered by microorganisms. Fungi in the genus *Trichoderma* are efficient inducers of systemic resistance in plants (Bisen et al., 2016) and largely used as biocontrol agents against plant pathogens. In addition to their role in promoting plant growth, nutrient uptake, and induction of plant defense responses against different biotic and abiotic stresses (Zehra et al., 2017), *Trichoderma* fungi also protect the plant from herbivorous insects, as shown in two papers of this Research Topic by Coppola, Cascone et al. and Coppola, Diretto et al. In these two studies, each conducted using a different *Trichoderma* species, the authors used transcriptomics, proteomics and bioassay approaches to show that treatment with the biological control agent induces transcriptional changes for a wide array of defense-related genes in tomato plants, but also alters plant metabolic pathways. These alterations result in better protection of the tomato plant against two major tomato insect pests (an aphid and a noctuid moth). Interestingly, the treatments also lead to the release of volatile organic compounds that attract aphid parasitoids.

We hope you enjoy reading the articles in this collection!

AUTHOR CONTRIBUTIONS

MC, PF, and A-NV wrote, edited, and finalized this manuscript. All authors contributed to the article and approved the submitted version.

FUNDING

This report was supported by the University of Basilicata.

ACKNOWLEDGMENTS

We would like to thank all authors' contributions to this Research Topic. We also thank all reviewers who assisted us and helped to improve manuscripts with their comments and precious suggestions, as well as the Frontiers editorial team for its support on the Research Topic management.

REFERENCES

Anderson, K. V., and Nusslein-Volhard, C. (1984). Information for the dorsal-ventral pattern of the *Drosophila* embryo is stored as maternal mRNA. *Nature* 311, 223–27.

Bisen, K., Keswani, C., Patel, J. S., Sarma, B. K., and Singh, H. B. (2016). "*Trichoderma* spp.: efficient inducers of systemic resistance in plants," in *Microbial-Mediated Induced Systemic Resistance in Plants,* eds. D. Choudhary and A. Varma (Singapore: Springer), 185–195.

Lemaitre, B., Nicolas, E., Michaut, L., Reichhart, J. M., and Hoffmann, J. A. (1996). The dorsoventral regulatory gene cassette spätzle/toll/cactus controls the potent antifungal response in drosophila adults. *Cell* 86, 973–983.

Su, Q., Zhou, X., and Zhang, Y. (2013). Symbiont-mediated functions in insect hosts. *Commun. Integr. Biol*. 6:e23804. doi: 10.4161/cib.23804

Zehra, A., Meena, M., Dubey, M. K., Aamir, M., and Upadhyay, R. S. (2017). Synergistic effects of plant defense elicitors and *Trichoderma harzianum* on enhanced induction of antioxidant defense system in tomato against Fusarium wilt disease. *Bot. Stud.* 58:44. doi: 10.1186/s40529-017-0198-2

Conflict of Interest: The authors declare that the research was conducted in the absence of any commercial or financial relationships that could be construed as a potential conflict of interest.

frontiers in Physiology

ORIGINAL RESEARCH
published: 01 October 2018
doi: 10.3389/fphys.2018.01261

Persistently Transmitted Viruses Restrict the Transmission of Other Viruses by Affecting Their Vectors

*Gong Chen[1,2,3], Qi Su[2,4], Xiaobin Shi[2], Huipeng Pan[2], Xiaoguo Jiao[2,5] and Youjun Zhang[2]**

[1] College of Plant Protection, Hunan Agricultural University, Changsha, China, [2] Department of Plant Protection, Institute of Vegetables and Flowers, Chinese Academy of Agricultural Sciences, Beijing, China, [3] Hunan Provincial Key Laboratory for Biology and Control of Plant Diseases and Insect Pests, Hunan Agricultural University, Changsha, China, [4] College of Agriculture, Yangtze University, Jingzhou, China, [5] Hubei Collaborative Innovation Center for Green Transformation of Bio-Resources, College of Life Sciences, Hubei University, Wuhan, China

Diverse pathogens, plant hosts, insect vectors, and non-vector herbivores coexist and interact in natural systems. An example is the cooccurrence of insects *Bemisia tabaci* Q and *Frankliniella occidentalis* and the pathogens tomato yellow leaf curl virus (TYLCV) and tomato spotted wilt virus (TSWV) on the same plant. In addition, both TYLCV and TSWV are persistently transmitted in these insect species. However, TSWV reduces the fitness of *B. tabaci* Q; therefore, we investigated whether TSWV affects the transmission of TYLCV to tomato. Both TYLCV and TSWV are persistently transmitted. Although *B. tabaci* Q cannot transmit TSWV, we found that this insect species is able to acquire and retain this virus serotype, indicating that the effects of TSWV on TYLCV transmission in the current study result from effects on the vector. The acquisition, retention, and transmission of TYLCV by *B. tabaci* Q were reduced when the insect vector contained TSWV. Additionally, the TYLCV acquisition and transmission by *B. tabaci* Q were reduced when the host plant was inoculated with TSWV before TYLCV or simultaneously with TYLCV. We also found that *F. occidentalis* fecundity and transmission of TSWV were reduced when *F. occidentalis* contained TYLCV. Our findings are consistent with the hypothesis that persistently transmitted viruses can restrict the transmission of other viruses by affecting their insect vectors.

Keywords: persistently transmitted virus, vector transmission, ecological interaction, adaptive manipulation, pathogen competition

OPEN ACCESS

Edited by:
Anne-Nathalie Volkoff, Institut National de la Recherche Agronomique, France

Reviewed by:
Daniele Pereira Castro, Fundação Oswaldo Cruz (Fiocruz), Brazil
Jing Zhao, Weifang University of Science and Technology, China

****Correspondence:***
Youjun Zhang
zhangyoujun@caas.cn

Specialty section:
This article was submitted to Invertebrate Physiology, a section of the journal Frontiers in Physiology

Received: *26 May 2018*
Accepted: *21 August 2018*
Published: *01 October 2018*

Citation:
Chen G, Su Q, Shi X, Pan H, Jiao X and Zhang Y (2018) Persistently Transmitted Viruses Restrict the Transmission of Other Viruses by Affecting Their Vectors. Front. Physiol. 9:1261. doi: 10.3389/fphys.2018.01261

INTRODUCTION

Research has increasingly indicated that vector-borne parasites can manipulate some phenotypes of their vectors or hosts in ways that enhance parasite transmission (Lefèvre and Thomas, 2008; Mauck et al., 2012; Blanc and Michalakis, 2016). Pathogen-induced changes in host-plant phenotypic traits often result in increased attraction of vectors to infected host plants or in other changes in vector performance on infected host plants; the effects of these changes in the host on the interactions between the vector and pathogen can be mutualistic, neutral, or antagonistic (Hammond and Hardy, 1988; Fereres and Moreno, 2009). Pathogen-induced changes in vectors can strongly affect transmission efficiency and vector fitness and can thus have significant effects on agricultural and other ecosystems and on human health (Ajayi and Dewar, 1983; Hammond and Hardy, 1988; Mauck et al., 2010, 2012). The interactions between persistently transmitted viruses

and vectors have often been studied, but research is lacking on the interactions between persistently transmitted viruses and non-insect-vectors (Su et al., 2016). The persistently transmitted viruses require vectors to feed on an infected host for a sustained period to acquire and circulate (and sometimes replicate) virions, and then disperse to a new, healthy host (Mauck et al., 2012).

In natural systems, the evolution of pathogen effects on host characteristics, including those that influence the interactions with insect vectors, is likely to be influenced by complex ecological interactions involving host plants, insect vectors, non-vector herbivores, and multiple pathogens (Salvaudon et al., 2013). For example, pathogen-induced changes in a host-plant phenotypic trait that enhance insect-vector recruitment may also increase pathogen transmission via increased herbivory. In addition, parasite-induced changes in herbivores that directly or indirectly affect herbivore fitness may influence parasite transmission (Pan et al., 2012). The existing literature shows that insect vectors prefer to settle on, or at least do not avoid settling on, host plants infected with persistently transmitted viruses and that insect vectors show no preference or reduced preference for host plants infected with non-persistently transmitted viruses relative to healthy plants (Ingwell et al., 2012; Mauck et al., 2016, 2012). Moreover, persistently transmitted viruses typically enhance host plant quality for insect vectors, resulting in increased insect vector longevity, fecundity, or survival. In contrast, non-persistently transmitted viruses usually reduce or have no influence on host plant quality (Mauck et al., 2012).

Although increases in insect vector fitness caused by persistently transmitted viruses have been extensively studied (Mauck et al., 2012), the influence of persistently transmitted viruses on non-vector insects have seldom been investigated. Just as host plants may be simultaneously fed upon by non-vector and vector herbivorous insects, they may be simultaneously infected by multiple viruses, and such multiple infections of a single host plant are likely to occur in the field. As a consequence, herbivorous insects may simultaneously ingest several pathogens, and we have observed simultaneous outbreaks of tomato yellow leaf curl virus (TYLCV), tomato spotted wilt virus (TSWV), *Frankliniella occidentalis*, and *Bemisia tabaci* in the same greenhouse. Previous studies have documented a mutualistic relationship between TYLCV and *B. tabaci* Q (Pan et al., 2012; Chen et al., 2013). In addition, our previous results showed that TSWV can reduce the fitness of *B. tabaci* on pepper (*Capsicum annuum* L) (Pan et al., 2013). Many other studies have indicated that parasites can influence the transmission of pathogens by changing the host quality for vectors (Ebbert and Nault, 2001; Taylor and Hurd, 2001; Pan et al., 2012; Liu et al., 2013) or by changing the cues (attractants) used by the foraging insect vectors to locate host plants (Jennersten, 1988; Eigenbrode et al., 2002; Jiménez-Martínez et al., 2004a,b).

Tomato yellow leaf curl virus is a destructive begomovirus of tomato plants and is transmitted by *B. tabaci* in a circulative and persistent manner (Cohen and Nitzany, 1966; Mehta et al., 1994; Caciagli et al., 1995). TSWV is another persistently transmitted virus. Like most tospoviruses, TSWV replicates in its insect vectors (*F. occidentalis* and other thrips) and is transmitted in the vector's saliva during persistent feeding (Elliott, 1996; Ullman et al., 2002). TSWV also can enhance the fitness of *F. occidentalis* (Maris et al., 2004). Unlike TYLCV, TSWV is not transmitted by *B. tabaci* (Zhao et al., 2015). Similarly, TYLCV is not transmitted by *F. occidentalis*. When these insects feed on host plants that are infected by both TSWV and TYLCV, they are likely to ingest both viruses.

The sweet potato whitefly, *B. tabaci* (Gennadius) (Hemiptera: Aleyrodidae), is a vector of begomoviruses. It causes serious damage in many crops by direct feeding and by vectoring plant viruses. The most current molecular evidence reveals that *B. tabaci* actually includes at least 24 genetically distinct but morphologically indistinguishable cryptic species (De Barro et al., 2011). The most damaging and widespread cryptic species are the Mediterranean genetic group (biotype Q) and the Middle East–Asia Minor 1 genetic group (biotype B). *F. occidentalis* is also an important agronomic pest and has a worldwide distribution (Ullman et al., 1997). It reduces plant growth, deforms plant organs, and causes cosmetic damage in the form of silver scars on leaves and flowers (Kirk and Terry, 2003). The small size and slender shape, short reproductive cycle, high fecundity, and polyphagous feeding behavior of *B. tabaci* and *F. occidentalis* help make them successful invasive species (Brown et al., 1995; Morse and Hoddle, 2006).

As noted earlier, the performance of *B. tabaci* is reduced when it feeds on TSWV-infected pepper plants (Pan et al., 2013). Based on these results, we hypothesized that persistently transmitted viruses can restrict the transmission of other viruses by affecting their vectors. The current study describes how the acquisition of TSWV by *B. tabaci* Q affects the whitefly's ability to acquire, retain, and transmit TYLCV; how the order in which a host plant is infected with the two viruses affects the whitefly's ability to acquire TYLCV from that plant; and how the infection of tomato by TSWV affects the whitefly's ability to transmit TYLCV. We also describe how the acquisition of TYLCV by *F. occidentalis* affects its fecundity and its ability to transmit TSWV.

RESULTS

Detection of TSWV RNA in *B. tabaci* Q as Affected by Acquisition Access Period (AAP)

Tomato spotted wilt virus RNA was detected in 40% of the *B. tabaci* Q adults after a 3-h AAP on TSWV-infected pepper leaves (**Table 1**). The percentage of Q adults with detectable TSWV RNA increased as the AAP increased and was 100% with a 24-h AAP.

Retention of TSWV RNA by *B. tabaci* Q

All *B. tabaci* Q adult females that probably were infected by TSWV (these adult females had a 72-h AAP) contained detectable TSWV RNA in the 5 d following their transfer onto healthy non-host cotton plants (**Table 1**). Thereafter, the percentage of adults with detectable TSWV RNA ranged from 50 to 100%.

TABLE 1 | Efficiency of TSWV acquisition and retention by *Bemisia tabaci* Q. *B. tabaci* Q adult females were assayed for TSWV RNA after they had a 0- to 48-h acquisition access period (AAP) on TSWV-infected pepper plants.

TSWV acquisition from pepper		TSWV retention on cotton	
AAP (h)[a]	Adults with TSWV RNA (%)	Duration of feeding (d)[a]	Adults with TSWV RNA (%)
0	0	0	100
3	40	5	100
6	50	10	90
12	90	15	100
24	100	20	50
48	100		

[a] *Ten whiteflies were assayed at each time point. After a 72-h AAP, females were transferred to cotton plants, a nonhost for TSWV, and subsequently assayed for TSWV RNA after 0- to 20-d feeding periods.*

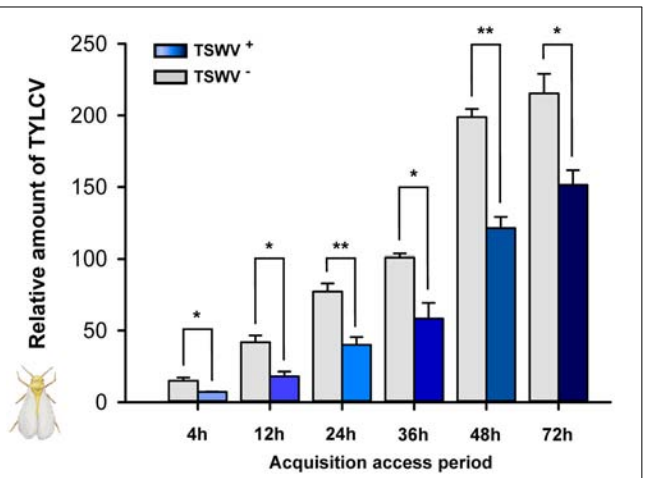

FIGURE 1 | Acquisition of TYLCV DNA by *Bemisia tabaci* Q females as affected by previous exposure of the whiteflies to TSWV. TSWV$^+$ or TSWV$^-$: *B. tabaci* Q females that had a 72-h acquisition access period (AAP) on TSWV-infected pepper plants or on noninfected pepper plants, respectively, before they fed on TYLCV-infected tomato plants. The *B. tabaci* Q used for TSWV$^+$ were assumed to contain TSWV based on **Table 1**. Values are means ± SE. Asterisks indicate significant differences between TSWV$^+$ vs. TSWV$^-$ treatments (one-way analysis of variance, $^*P < 0.05$, $^{**}P < 0.01$).

Acquisition of TYLCV DNA by *B. tabaci* Q Females Carrying TSWV

Tomato yellow leaf curl virus acquisition was significantly lower for *B. tabaci* Q females that had previously fed on TSWV-infected pepper plants rather than on healthy pepper plants (**Figure 1**). For all treatments, TYLCV DNA reached maximal viral loads in *B. tabaci* Q females after a 48-h AAP.

Acquisition of TYLCV DNA by *B. tabaci* Q Females From Tomato Plants Inoculated in Different Order With Both TSWV and TYLCV

Relative to TYLCV acquisition by *B. tabaci* Q females on tomato plants inoculated only with TYLCV (Control, **Figure 2A**), TYLCV acquisition was significantly lower on plants that had been first inoculated with TSWV and then with TYLCV (TSWV-TYLCV, **Figure 2B**) or that had been concurrently (Concurrent, **Figure 2C**) inoculated with both viruses (**Figure 2**). TYLCV acquisition, however, did not significantly differ on control tomato plants and tomato plants that had first been inoculated with TYLCV and then with TSWV.

Retention of TYLCV DNA by *B. tabaci* Q Females Carrying TSWV

As indicated by q-PCR, the relative amount of TYLCV on day 0, when the *B. tabaci* Q females were transferred to cotton plants, was lower in females previously exposed to TSWV (they had fed on TSWV-infected pepper plants before they fed on TYLCV-infected tomato plants) than in females not exposed to TSWV (**Figure 3A**). The TYLCV titer decreased gradually in all treatments but was always lower in females that presumably contained TSWV than in females that did not (**Figure 3A**). The rate at which the TYLCV titer declined did not significantly differ between females that were or were not exposed to TSWV ($F_{1,4} = 1.101$, $P = 0.353$) (**Figure 3B**).

Transmission of TYLCV to Tomato by *B. tabaci* Q Females Carrying TSWV

Tomato yellow leaf curl virus transmission, as indicated by the relative amount of TYLCV in tomato leaves exposed to one viruliferous adult *B. tabaci* Q female, was lower by females that contained both viruses (they were exposed to TSWV first) than by females that contained only TYLCV ($F_{1,14} = 15.836$, $P = 0.00137$) (**Figure 4**).

Transmission of TYLCV by *B. tabaci* Q to TSWV-Infected Tomato Plants vs. Healthy Tomato Plants

As indicated by the relative quantities of TYLCV in the plants, the transmission of TYLCV by *B. tabaci* Q adult females (one female per plant) was lower to TSWV-infected tomato plants than to healthy tomato plants ($F_{1,14} = 9.305$, $P = 0.00864$) (**Figure 5**).

Detection of TYLCV DNA in *F. occidentalis* Second-Instar Nymphs and Newly Emerged Adults

Tomato yellow leaf curl virus was detected by PCR in all *F. occidentalis* second-instar nymphs that had fed on TYLCV-infected tomato plants and in all adults that emerged from those nymphs (**Figure 6A**).

Fecundity of *F. occidentalis* Females on TYLCV-Infected and Healthy Tomato Plants

Fecundity was significantly lower for *F. occidentalis* females on TYLCV-infected tomato plants than on healthy tomato plants ($F_{1,18} = 68.747$, $P < 0.001$) (**Figure 6B**).

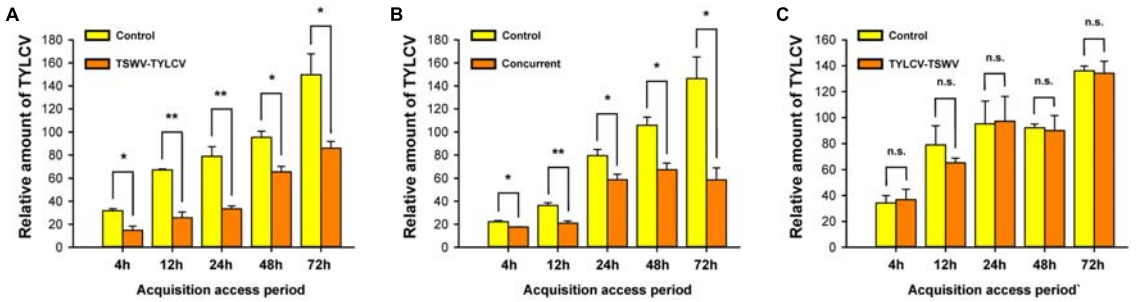

FIGURE 2 | Acquisition of TYLCV DNA by *B. tabaci* Q females from tomato plants inoculated in different order with both TSWV and TYLCV. TSWV-TYLCV: plants were inoculated with TSWV and 2 weeks later with TYLCV. TYLCV-TSWV: plants were inoculated with TYLCV and 2 weeks later with TSWV. Concurrent: plants were simultaneously inoculated with both viruses. Control: plants were inoculated with TYLCV and were mock-inoculated 2 weeks later. **(A)** Acquisition ability of TYLCV DNA by *B. tabaci* Q females from TSWV-TYLCV plants. **(B)** Acquisition ability of TYLCV DNA by *B. tabaci* Q females from concurrent plants. **(C)** Acquisition ability of TYLCV DNA by *B. tabaci* Q females from TYLCV-TSWV plants. Values are means ± SE. Asterisks indicate significant differences between treatments vs. control (one-way analysis of variance; $*P < 0.05$, $**P < 0.01$, and n.s. indicates not significant, $P > 0.05$).

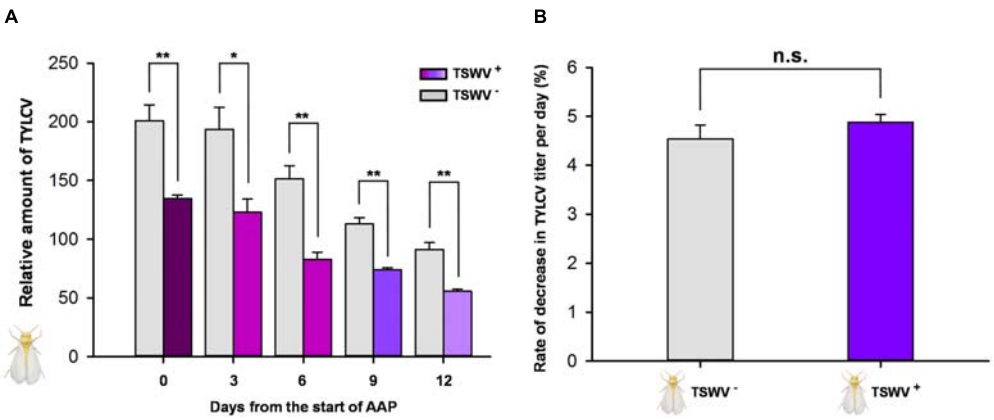

FIGURE 3 | Retention of TYLCV DNA by *B. tabaci* Q females after transfer to nonhost (cotton) plants as affected by previous exposure of the whiteflies to TSWV. $TSWV^+$ or $TSWV^-$: *B. tabaci* Q females that had a 72-h AAP on TSWV-infected pepper plants or on noninfected pepper plants, respectively, before they fed on TYLCV-infected tomato plants. The *B. tabaci* Q used for $TSWV^+$ were assumed to contain TSWV based on **Table 1**. **(A)** Relative quantity of TYLCV retained. **(B)** Rate at which TYLCV titer decreased in *B. tabaci* Q females. Values are means ± SE. Asterisks indicate significant differences between $TSWV^+$ vs. $TSWV^-$ treatments (one-way analysis of variance; $*P < 0.05$, $**P < 0.01$, and n.s. indicates not significant, $P > 0.05$).

Transmission of TSWV by *F. occidentalis* Females to Healthy Tomato Plants as Affected by Previous Exposure of Thrips to TYLCV-Infected Tomato Plants

The transmission of TSWV, as indicated by the amount of virus in tomato leaves exposed to one adult *F. occidentalis* female, was reduced if the thrips had been previously exposed to a TYLCV-infected tomato plant ($F_{1,22} = 447.544$, $P < 0.001$) (**Figure 6C**).

MATERIALS AND METHODS

Plant Cultures, TSWV Inoculation, TYLCV Inoculation, and *B. tabaci* and *F. occidentalis* Populations

Pepper (*Capsicum annuum* L., cv Zhongjiao 6), cotton (*Gossypium herbaceum* L., cv DP99B), and tomato (*Solanum lycopersicum* L., cv Zhongza 9) were grown as described previously (Chen et al., 2013). Pepper can be infected by TSWV and TYLCV, but cotton cannot be infected by TSWV and TYLCV. Hence, we chose pepper to be the virus host plant and chose cotton to be the control plant.

Tomato spotted wilt virus was maintained on *Datura stramonium*. The virus inoculum was prepared by grinding infected plant material in chilled 0.01 M phosphate buffer, pH 7, containing 1% (wt:vol) sodium sulfite and 2% (wt:vol) PVP. The inoculum was mechanically transmitted by rubbing the ground material onto the upper leaves of the pepper plants, which had been dusted with carborundum. Pepper plants were inoculated at the three-true-leaf stage. Pepper plants were assumed to be infected with TSWV when they developed characteristic symptoms that include plant stunting, bronzing, or chlorosis of leaves. Infection was then determined for inoculated and non-inoculated control plants by the molecular methods described in the next section. When these healthy and TSWV-infected plants

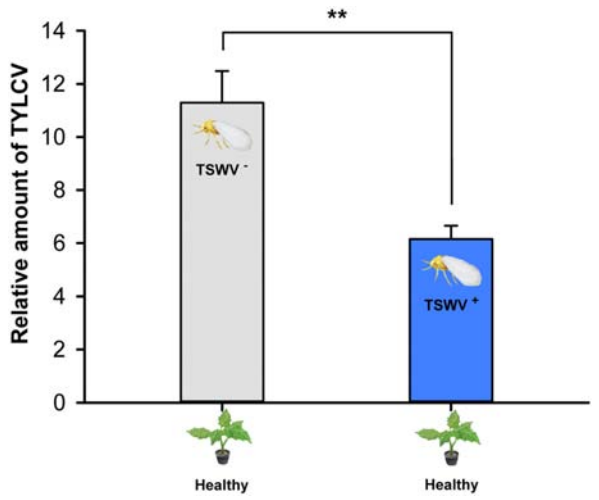

FIGURE 4 | Transmission of TYLCV DNA to tomato plants by *Bemisia tabaci* Q females as affected by previous exposure of the whiteflies to TSWV. TSWV$^+$ or TSWV$^-$: *B. tabaci* Q females that had a 72-h AAP on TSWV-infected pepper plants or on noninfected pepper plants, respectively, before they fed on tomato plants. The *B. tabaci* Q used for TSWV$^+$ were assumed to contain TSWV based on **Table 1**. Values are means ± SE. Asterisks indicate significant differences between TSWV$^+$ vs. TSWV$^-$ treatments (one-way analysis of variance, $^{**}P < 0.01$).

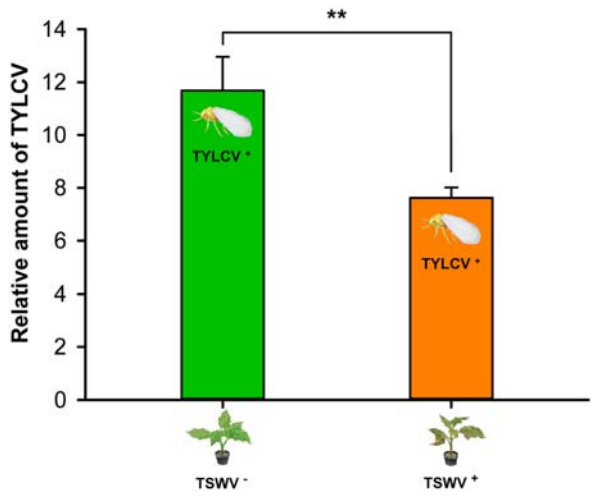

FIGURE 5 | Transmission of TYLCV DNA to tomato plants by *Bemisia tabaci* Q females as affected by previous infection of the tomato plants by TSWV. TSWV$^+$ or TSWV$^-$: Tomato plants inoculated with TSWV or mock-inoculated, respectively, before they were exposed to *Bemisia tabaci* Q females that contained TYLCV. TYLCV$^+$: Females that acquired TYLCV from another TYLCV-infected plant. Values are means ± SE. Asterisks indicate significant differences between TSWV$^+$ vs. TSWV$^-$ treatments (one-way analysis of variance, $^{**}P < 0.01$).

had developed to the six–seven-true-leaf stage, they were used in the experiments. (Pan et al., 2013).

Tomato yellow leaf curl virus-infected tomato plants were obtained by carrier (*Agrobacterium tumefaciens*) -mediated inoculation using a TYLCV clone (GenBank accession ID: AM282874) that was initially isolated from tomato in China (Wu et al., 2006). TYLCV inoculum was prepared and plants were inoculated with TSWV as described by Chen et al. (2013). To account for the effects of the inoculation process, control treatments were mock-inoculated with a noncarrier buffer.

Since its collection in Beijing, China, in 2009, the *B. tabaci* Q population used in this research has been maintained on poinsettia plants (*Euphorbia pulcherrima* Wild. ex. Klotz.) in insect-proof screen cages under natural light and controlled temperature (26 ± 2°C) in a greenhouse. The purity of the *B. tabaci* Q population has been monitored as described by Chu et al. (2010).

Since its collection from melon (*Cucumis melo* L.) in a glasshouse at the Institute of Vegetables and Flowers, Chinese Academy of Agricultural Sciences (CAAS), Beijing, China, in 2003, the *F. occidentalis* population has been reared with fresh green bean pods Phaseolus vulgaris in a climate-controlled chamber (27 ± 1°C, 16 L: 8 days) (Zhang et al., 2013).

RT-PCR Detection of TSWV in Pepper Plants and in *B. tabaci* Q

Total RNAs were extracted from pepper plants and *B. tabaci* Q using TRIzol reagent following the manufacturer's protocol (Invitrogen). The resulting total RNA was resuspended in nuclease-free water and was quantified with a spectrophotometer (Thermo Scientific). Reverse transcription was then performed on 1.0 μg of each RNA sample, and the first-strand cDNA was synthesized using the PrimeScript RT reagent kit according to the manufacturer's protocol (TaKaRa Biotechnology, Dalian Co., Ltd). Specific primers (forward primer NF302: 5′-5′GGGTCAGGCTTGTTGAGGAAAC-3′ and reverse primer NR575: 5′-TTCCCTAAGGCTTCCCTGGTG-3′) were used to detect TSWV (Mason et al., 2003). Polymerase chain reaction amplifications were performed in 20-μl reactions containing 1 μl of cDNA, 1 μl of each primer (10 μM each), 7 μl of ddH2O, and 10 μl of 2 × Tap10 Master Mix (Biosubstrate Technologies, Beijing, China). At the same time, PCR amplifications with negative control (template was ddH2O) and positive control (template was the tomato plant cDNA that contains TSWV) were performed. The cycling conditions were: 2 min of activation at 94°C followed by 30 cycles of 30 s at 94°C, 30 s at 60°C, and 30 s at 72°C; and a final extension of 5 min at 72°C. The PCR products were electrophoresed on a 1.5% agarose gel in a 0.5 × TBE buffer and were visualized by Gelview staining (Boonham et al., 2002; Pan et al., 2013).

Acquisition of TSWV by *B. tabaci* Q

A pepper plant at the seven-true-leaf stage that had been inoculated with TSWV and that showed clear symptoms of TSWV infection was used as the virus source. The plant, which was enclosed in an insect-proof cage, was infested with approximately 200 newly emerged (0 to 24 h) *B. tabaci* Q females. Care was taken to transfer the whiteflies evenly onto all leaves of the TSWV-infected pepper plant. After AAPs of 3, 6, 12, 24, and 48 h, 10 adults were randomly collected from the top second

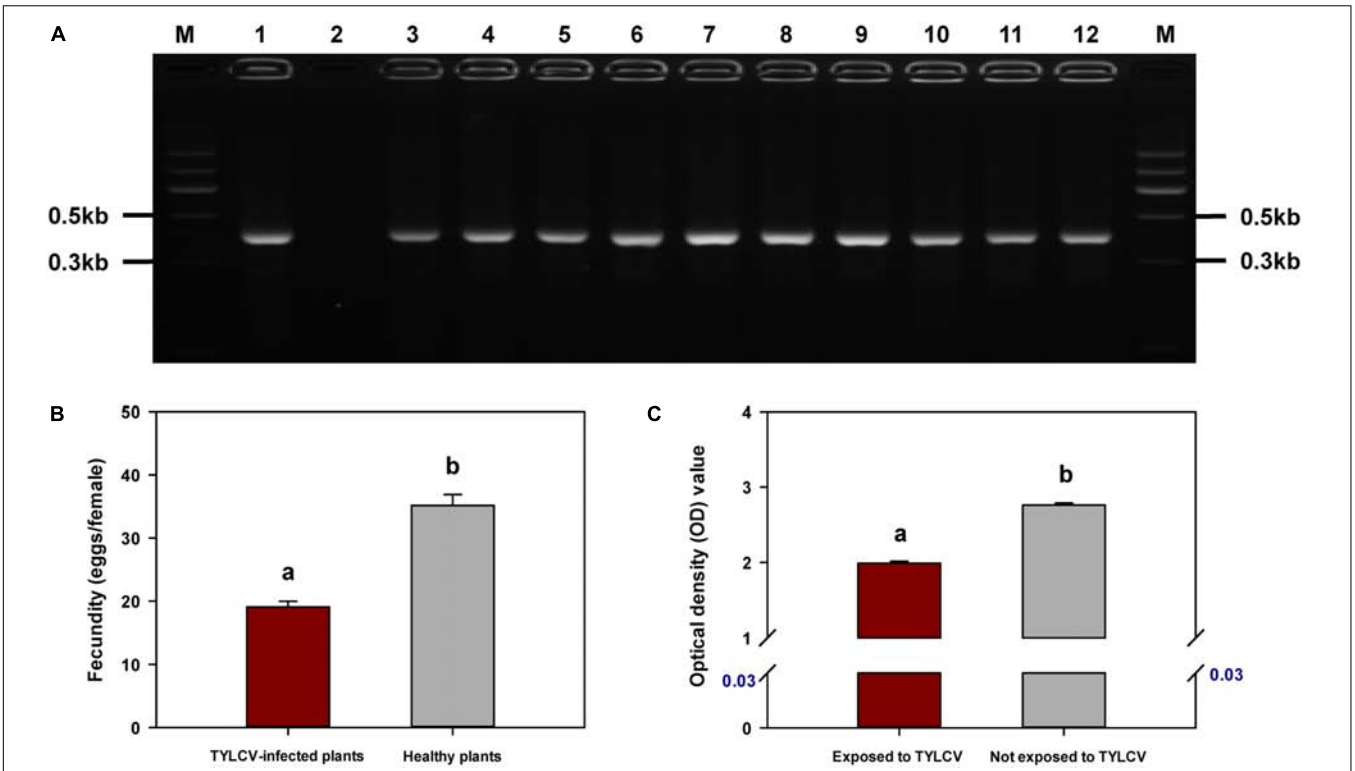

FIGURE 6 | Acquisition of TYLCV by *Frankliniella occidentalis* **(A)**, fecundity of *F. occidentalis* as affected by TYLCV **(B)**, and transmission of TSWV by *F. occidentalis* as affected by previous exposure of the thrips to TYLCV **(C)**. **(A)** PCR amplification of TYLCV was performed with the DNA extracted from *F. occidentalis* second-instar nymphs (lanes 3–7; one nymph per lane) and newly emerged adults (lanes 8–12; one adult per lane) obtained from a TYLCV-infected tomato plant. Amplification products were visualized by agarose gel electrophoresis with Gelview staining. Lane 1: positive control; lane 2: negative control; lane M: Marker II (Tiangen). **(B)** Number of eggs laid by each female placed in a clip-cage attached to a leaf of a healthy or a TYLCV-infected tomato plant. Values are means ± SE of 10 replicate plants (three adults per plant). **(C)** The OD value of TSWV analysis obtained by DAS-ELISA indicated the difference between *F. occidentalis* that were exposed and not exposed to TYLCV. The number in blue indicates the mean OD value of healthy tomato plants. Values are means ± SE. For **(B,C)**, different letters indicate significant differences between treatments ($P < 0.05$).

and third leaves of the TSWV-infected pepper plant. During the collection of adults, care was taken not to disturb other whiteflies on the TSWV-infected pepper plant. Ten adults that had not been placed on the plant (0-h AAP) were also collected. The collected adults were stored at −80°C and were later individually assayed for TSWV RNA by RT-PCR as described in the previous section.

Retention of TSWV RNA by *B. tabaci* Q

Approximately 200 *B. tabaci* Q adult females that had access to a TSWV-infected pepper plant for 72 h and that were known to contain TSWV (see **Table 1**) were placed on a healthy cotton plant, which is not a host plant of TSWV. One group of 10 live adults was collected at 5, 10, 15, and 20 days after placement. At day 14, the adults remaining on the cotton plant were transferred onto a new cotton plant so that the new adults that emerged from the progeny were not collected at day 15 and 20. The collected insects were stored at −80°C and were later individually assayed for TSWV RNA by RT-PCR.

Quantification of TVLCV DNA by q-PCR

To quantify TYLCV acquisition and retention, the MiniBEST universal genomic DNA extraction kit ver.5.0, Cod: 9765 (TaKaRa Biotechnology, Dalian Co., Ltd.) was used to extract the DNA from female whiteflies. To quantify TYLCV in tomato plants, a plant genomic DNA kit (Tiangen Biotech, Beijing, Co., Ltd.) was used to extract the DNA from tomato leaves. **Table 2** lists the primers used for the quantification of TYLCV. The q-PCR reaction conditions for samples from plants were described by Pan et al. (2012), and those for samples from insects were described by Pakkianathan et al. (2015). TYLCV DNA was quantified with SuperReal PreMix Plus (SYBR Green) (Tiangen Biotech). Four technical replicates were amplified for each sample. The comparative cycle threshold $2^{-\Delta C_T}$ method was used to calculate the relative quantities of TYLCV.

Acquisition of TYLCV by *B. tabaci* Q Carrying TSWV

About 450 newly emerged *B. tabaci* Q adult females were placed in leaf clip-cages (50 adults per clip-cage) on the top second and third leaves (one clip-cage per leaf) of TSWV-infected pepper plants (at the six-true-leaf stage, about 2 weeks after virus inoculation) and healthy (mock-inoculated) pepper plants for a 72-h AAP. These adults were subsequently moved into replicate

TABLE 2 | Primer sequences used for q-PCR analysis.

Gene or source of DNA	Primer	Primer sequence (5′ to 3′)	Reference
TYLCV	TY-F	GTCTACACGCTTACGCC	Pan et al., 2012
	TY-R	GCAATCTTCGTCACCC	
Bemisia tabaci	β-actin-F	TCTTCCAGCCATCCTTCTTG	Pakkianathan et al., 2015
	β-actin-R	CGGTGATTTCCTTCTGCATT	
Tomato	UBI-F	TCGTAAGGAGTGCCCTAATGCTGA	Pan et al., 2012
	UBI-R	CAATCGCCTCCAGCCTTGTTGTAA	

screen cages containing one TYLCV-infected tomato plant. There were 150 adults per replicate screen cage, with three replicate screen cages for adults from TSWV-infected pepper plants and three for adults from healthy pepper plants. After AAPs of 4, 12, 24, 36, 48, and 72 h, adults were randomly collected from symptomatic tomato leaves in each cage. Then, 20 females per replicate cage were stored at −80°C. The content of TVLCV DNA in these females was subsequently assessed by q-PCR as described later.

Acquisition of TYLCV DNA by *B. tabaci* Q Females From Tomato Plants Inoculated in Different Order With Both TSWV and TYLCV

The acquisition of TYLCV by *B. tabaci* Q was tested as described earlier in this report, but the plants were inoculated with TYLCV and TSWV in different order. In the first case, we measured TYLCV acquisition from tomato plants that were first inoculated with TSWV and then inoculated with TYLCV 2 weeks later, or that were first mock-inoculated and then inoculated with TYLCV 2 weeks later. In the second case, we measured TYLCV acquisition from tomato plants that were simultaneously inoculated with TYLCV and TSWV, or that were simultaneously mock-inoculated and inoculated with TYLCV. In the third case, we measured TYLCV acquisition from tomato plants that were first inoculated with TYLCV and then inoculated with TSWV 2 weeks later, or that were first inoculated with TYLCV and were then mock-inoculated 2 weeks later. The content of TVLCV DNA in these females was subsequently assessed by q-PCR as described later.

Retention of TYLCV DNA by *B. tabaci* Q Carrying TSWV

Newly emerged *B. tabaci* Q adult females were subjected to a 72-h AAP on TSWV-infected and healthy (mock-inoculated) pepper plants as described earlier. These adults were subsequently released into replicate screen cages containing one TYLCV-infected tomato plant as described earlier. After a 72-h AAP, the adult females in each replicate screen cage were transferred to a new replicate screen cage containing one healthy cotton plant, which is not a host of TYLCV. Twenty adult females were collected randomly from each screen cage after 0, 3, 6, 9, and 12 d and were stored at −80°C. The content of TVLCV DNA in these females was tested by q-PCR as described later.

Transmission of TYLCV by *B. tabaci* Q Carrying TSWV

About 200 newly emerged *B. tabaci* Q adult females were placed in clip-cages (50 females per cage) on the top second and third leaves (one clip-cage per leaf) of TSWV-infected pepper plants (at the six-true-leaf stage, about 2 weeks after virus inoculation) and healthy (mock-inoculated) pepper plants. After a 72-h AAP, the adults were moved into insect-proof screen cages containing TYLCV-infected tomato plants (one plant and 100 adult females per cage). After a 72-h AAP, the adult females were collected and placed in clip-cages attached to healthy tomato plants with three true leaves; each plant had one clip-cage that contained one adult female. Each of two treatments (one female carrying TSWV or one control female) was represented by eight replicate clip-cages. After the clip-cages had been in greenhouse for 48 h, all of the whiteflies were removed, and the plants were kept in whitefly-proof screen cages. After 10 d, the first two youngest leaves of each tomato plant were collected (Mason et al., 2008; Péréfarres et al., 2011), and the DNA in the leaves was extracted and tested for TYLCV by q-PCR as described later.

Transmission of TYLCV by *B. tabaci* Q to TSWV-Infected Tomato Plants vs. Healthy Tomato Plants

About 200 newly emerged *B. tabaci* Q adult females were moved into insect-proof cages containing TYLCV-infected tomato plants (one plant and 100 adult females per cage). After a 72-h AAP, the adult females were collected and placed in clip-cages attached to TSWV-infected tomato plants and healthy tomato plants with three true leaves; each plant had one clip-cage that contained one adult female. Each of the two treatments (TYLCV-viruliferous adults on TSWV-infected tomato plants or on healthy tomato plants) was represented by eight replicate clip-cages. After the clip-cages had been in place for 48 h, all of the whiteflies were removed, and the tomato plants were kept in whitefly-proof screen cages. After 10 d, the first two youngest leaves of each tomato plant were collected (Mason et al., 2008; Péréfarres et al., 2011), and the DNA was extracted from the tomato leaves and tested for TYLCV by q-PCR as described later.

Acquisition of TYLCV by *F. occidentalis*

A tomato plant at the seven-true-leaf stage that had been inoculated with TYLCV and that showed clear symptoms of TYLCV infection was used as the virus source. The plant, which was enclosed in a thrips-proof screen cage, was infested with

approximately 200 *F. occidentalis* adults. Adult females were allowed to oviposit on the tomato plant for 2 days. The second-instar nymphs and the newly emerged adults (0 to 24 h) were then collected and later assayed for TYLCV DNA by PCR as described by Ghanim et al. (2007). This was performed with five replicate TYLCV-infected plants.

F. occidentalis Fecundity as Affected by TYLCV

One newly emerged adult female *F. occidentalis* was collected from a colony feeding on healthy bean pods. The adult was placed in a clip-cage attached to a leaf of a healthy (mock-inoculated) or TYLCV-infected tomato plant; each plant had three clip-cages, and each treatment was represented by 10 replicate plants. Seven days later, these infested leaves were detached, and the number of live nymphs and eggs were counted using a stereomicroscope. The data from the three infested leaves from each plant were pooled and treated as one biological replicate (n = 10). *F. occidentalis* fecundity was reported as the mean number of offspring per thrips.

Transmission of TSWV by *F. occidentalis* Carrying TYLCV

Newly hatched *F. occidentalis* nymphs (0–6 h since hatching) were placed in a thrips-proof cage (50 nymphs per cage) containing a TYLCV-infected tomato plant or a healthy (mock-inoculated) tomato plant for a 24-h AAP. These nymphs were then transferred to another cage containing a TSWV-infected tomato plant for a 48-h AAP. The transmission of TSWV by the adults was then assessed by a leaf disk assay (with leaf disks from a healthy tomato plant) as previously described (Wijkamp and Peters, 1993; Tedeschi et al., 2001). Each of the two treatments was represented by 12 replicates. In addition, the concentration of TSWV in leaf disk extracts was assessed by using a DAS-ELISA kit supplied by Adgen Phytodiagnostics (Neogen Europe (Ayr), Ltd.) and by following the manufacturer's recommendations. Absorbance and optical density (OD) were determined with a fluorescence microplate reader (SpectraMax M2e, Molecular Devices) at a wavelength of 405 nm.

Data Analysis

One-way analyses of variance (ANOVAs) were used to determine whether treatment effects were significant. SPSS 17.0 (SPSS Inc., Chicago, IL, United States) was used for all statistical analyses.

DISCUSSION

Although *B. tabaci* Q cannot transmit TSWV (Zhao et al., 2015), we showed in this study that it can acquire and retain TSWV. In the interaction between TSWV, *B. tabaci* Q, and host plants, it follows that any effects of TSWV on *B. tabaci* Q are direct, i.e., do not result from the changes in the host plant that could occur following TSWV transmission. Previous exposure of *B. tabaci* Q to TSWV reduced the whitefly's ability to acquire, retain, and transmit TYLCV (**Figures 1**, **3**, **4**), and the whitefly's ability to acquire TYLCV from tomato plants was reduced if the plants were inoculated with TSWV before TYLCV or concurrently with TYLCV (**Figures 2A,B**). Previous exposure of tomato plants to TSWV reduced the transmission of TYLCV to those plants by *B. tabaci* Q (**Figure 5**). We also found that *F. occidentalis* can acquire TYLCV (**Figure 6A**) and that its fecundity was lower on TYLCV-infected tomato plants than on healthy tomato plants (**Figure 6B**). Moreover, the transmission of TSWV by *F. occidentalis* was reduced when the thrips had previously fed on TYLCV-infected plants (**Figure 6C**). These results are consistent with our hypothesis that a persistently transmitted virus can suppress the transmission of a second virus by decreasing some fitness characteristics of its vector and by competing with the second virus in the host plant.

The current study provides additional evidence that transmission efficiency can be significantly affected by changes in vector fitness. Previous research has indicated that virus transmission can be affected by insect vector characteristics; TYLCV-carried whiteflies fed more readily than noncarried whiteflies, and spent more time salivating into sieve tube elements (Liu et al., 2013). Similarly, the potato leafroll virus infection of potato alters the feeding behavior of its aphid vector (Alvarez et al., 2007). The transmission of TYLCV, for example, differs among *B. tabaci* biotypes (Chu et al., 2006; Pan et al., 2012; Ning et al., 2015). Virus transmission is also often greater for female than for male piercing-sucking insect vectors (Ghanim and Czosnek, 2000). For example, female adults of the planthopper *Peregrinus maidis* are more efficient vectors of the rice stripe virus than male adults (Narayana and Muniyappa, 1996), and female adults of *B. tabaci* Q are more efficient vectors of TYLCV than male adults (Ning et al., 2015). In some cases, however, male insects are more efficient vectors. Male thrips, for example, are more efficient vectors than female thrips (van de Wetering et al., 1999; Stafford et al., 2011). Transmission can also be affected by endosymbiotic bacteria that produce a GroEL homolog, which seems to protect begomoviruses in the *B. tabaci* hemolymph (Morin et al., 1999, 2000; Gottlieb et al., 2010; Himler et al., 2011). The transmission of TYLCV by *B. tabaci* is enhanced by the endosymbiotic bacterium *Hamiltonella* sp. (Gottlieb et al., 2010; Su et al., 2013). Transmission is also affected by immune responses such as autophagy; the activation of autophagy significantly reduces TYLCV (Medeiros et al., 2004; Wang et al., 2016).

Persistently transmitted viruses can substantially increase the fitness of their vectors and thereby increase virus transmission (Mauck et al., 2012). For example, TYLCV can improve the performance of *B. tabaci* Q, including their body size, longevity, fecundity, and so on (Pan et al., 2012; Chen et al., 2013); TSWV infection increases *F. occidentalis* oviposition and makes them develop faster (Maris et al., 2004); and persistently transmitted viruses enhance aphid performance (including in terms of growth, reproduction, and survival) on infected plants (Montllor and Gildow, 1986; Castle and Berger, 1993; Jiménez-Martínez et al., 2004a). Our previous results indicated that TSWV can

reduce the longevity and fecundity of *B. tabaci* on pepper plants (Pan et al., 2013). The current results revealed that prior feeding on TSWV-infected plants reduces the ability of *B. tabaci* Q to acquire, retain, and transmit TYLCV and that prior feeding on TYLCV-infected plants reduces *F. occidentalis* fecundity and its ability to transmit TSWV. In other words, the current study provides additional evidence that transmission efficiency can be significantly affected by changes in vector fitness.

The results of the current study have several possible explanations. We have two hypotheses. First, the ingestion of a persistently transmitted virus (virus 1) may activate autophagy in the vector (vector 2) of a second virus (virus 2), which would decrease the titer and gene expression of virus 2 in vector 2. This is possible because autophagy, which is an intrinsic antiviral process, can decrease the infection of a persistently transmitted plant virus by reducing the amount of viral coat protein and DNA (Wang et al., 2016). This hypothesis is related to the insect's immune response "memory" or prolonged immune response to a virus that can interfere in another virus. Second, the presence of virus 1 in vector 2 could induce changes in the feeding behavior of vector 2, thereby affecting the acquisition of virus 2. Determining whether either of these explanations is correct will require additional research.

The objective of this study was to assess the effects of one persistently transmitted virus on the transmission of another persistently transmitted virus. The results are consistent with the view that, while persistently transmitted viruses can substantially increase the fitness (including longevity, body size, fecundity) of their vectors, they can also decrease the fitness of vectors of other viruses. These characteristics may help the vector population of persistently transmitted viruses to spread in the field, where there is significant competition among persistently transmitted viruses and other pathogens for host resources.

AUTHOR CONTRIBUTIONS

GC contributed to the chemical ecological laboratory work, performed the major part of entomological manipulations, participated in data analysis, conception and design of the study, and drafting of the manuscript. QS carried out the ecological manipulations. XS contributed to viral and microbiological manipulations. HP contributed to insect and plant husbandry and data collection. XJ carried out the statistical analyses. YZ contributed to the conception and design of the study, coordinated the study, and helped in drafting the manuscript. All authors gave final approval for publication.

FUNDING

This work was supported by the State Key Program of National Natural Science Foundation of China (31420103919, 31801799), the 973 Program (2013CB127602), the National Natural Science Foundation of China (31572014, 31801799), the Beijing Natural Science Foundation (6131002), the Beijing Training Project For The Leading Talents in S and T (LJRC201412), the Graduate Research and Innovation Project in Hunan Province (CX2015B248), and the Beijing Key Laboratory for Pest Control and Sustainable Cultivation of Vegetables. The granting agencies had no role in study design, data collection and analysis, decision to publish, or preparation of the manuscript.

ACKNOWLEDGMENTS

The authors are grateful to Dr. Mark C. Mescher (ETH Zürich) for his invaluable advice on the previous version of the manuscript, and Dr. Xueping Zhou (Institute of Biotechnology, Zhejiang University, Hangzhou, China) for providing the infectious TYLCV clone.

REFERENCES

Ajayi, O., and Dewar, A. M. (1983). The effect of barley yellow dwarf virus on field populations of the cereal aphids, *Sitobion avenae* and *Metopolophium dirhodum*. *Ann. Appl. Biol.* 103, 1–11. doi: 10.1111/j.1744-7348.1983.tb02734.x

Alvarez, A., Garzo, E., Verbeek, M., Vosman, B., Dicke, M., and Tjallingii, W. (2007). Infection of potato plants with potato leafroll virus changes attraction and feeding behaviour of *Myzus persicae*. *Entomol. Exp. Appl.* 125, 135–144. doi: 10.1111/j.1570-7458.2007.00607.x

Blanc, S., and Michalakis, Y. (2016). Manipulation of hosts and vectors by plant viruses and impact of the environment. *Curr. Opin. Insect Sci.* 16, 1–8. doi: 10.1016/j.cois.2016.05.007

Boonham, N., Smith, P., Walsh, K., Tame, J., Morris, J., Spence, N., et al. (2002). The detection of Tomato spotted wilt virus (TSWV) in individual thrips using real time fluorescent RT-PCR (TaqMan). *J. Virol. Methods* 101, 37–48. doi: 10.1016/S0166-0934(01)00418-9

Brown, J. K., Frohlich, D. R., and Rosell, R. C. (1995). The sweetpotato or silverleaf whiteflies: biotypes of *Bemisia tabaci* or a species complex? *Annu. Rev. Entomol.* 40, 511–534. doi: 10.1146/annurev.en.40.010195.002455

Caciagli, P., Bosco, D., and Al-Bitar, L. (1995). Relationships of the Sardinian isolate of tomato yellow leaf curl geminivirus with its whitefly vector *Bemisia tabaci*. *Gen. Eur. J. Plant Pathol.* 101, 163–170. doi: 10.1007/BF01874762

Castle, S. J., and Berger, P. H. (1993). Rates of growth and increase of *Myzus persicae* on virus-infected potatoes according to type of virus-vector relationship. *Entomol. Exp. Appl.* 69, 51–60. doi: 10.1111/j.1570-7458.1993.tb01727.x

Chen, G., Pan, H. P., Xie, W., Wang, S. L., Wu, Q. J., Fang, Y., et al. (2013). Virus infection of a weed increases vector attraction to and vector fitness on the weed. *Sci. Rep.* 3:2253. doi: 10.1038/srep02253

Chu, D., Wan, F. H., Zhang, Y. J., and Brown, J. K. (2010). Change in the biotype composition of *Bemisia tabaci* in Shandong Province of China from 2005 to 2008. *Environ. Entomol.* 39, 1028–1036. doi: 10.1603/EN09161

Chu, D., Zhang, Y. J., Brown, J. K., Cong, B., Xu, B. Y., Wu, Q. J., et al. (2006). The introduction of the exotic Q biotype of *Bemisia tabaci* from the Mediterranean region into China on ornamental crops. *Florida Entomol.* 89, 168–174. doi: 10.1653/0015-4040(2006)89[168:TIOTEQ]2.0.CO;2

Cohen, S., and Nitzany, F. E. (1966). Transmission and host range of the tomato yellow leaf curl virus. *Phytopathology* 56, 1127–1131.

De Barro, P. J., Liu, S. S., Boykin, L. M., and Dinsdale, A. (2011). *Bemisia tabaci*: a statement of species status. *Annu. Rev. Entomol.* 56, 1–19. doi: 10.1146/annurev-ento-112408-085504

Ebbert, M. A., and Nault, L. R. (2001). Survival in Dalbulus leafhopper vectors improves after exposure to maize stunting pathogens. *Entomol. Exp. Appl.* 100, 311–324. doi: 10.1046/j.1570-7458.2001.00878.x

Eigenbrode, S. D., Ding, H., Shiel, P., and Berger, P. H. (2002). Volatiles from potato plants infected with potato leafroll virus attract and arrest the virus

vector, *Myzus persicae* (Homoptera; Aphididae). *Proc. R. Soc. B* 269, 455–460. doi: 10.1098/rspb.2001.1909

Elliott, R. M. (1996). *The Bunyaviridae*. New York, NY: Plenum Press, 337. doi: 10.1007/978-1-4899-1364-7

Fereres, A., and Moreno, A. (2009). Behavioural aspects influencing plant virus transmission by homopteran insects. *Virus Res.* 141, 158–168. doi: 10.1016/j.virusres.2008.10.020

Ghanim, M., and Czosnek, H. (2000). Tomato yellow leaf curl geminivirus (TYLCV-Is) is transmitted among whiteflies (*Bemisia tabaci*) in a sex-related manner. *J. Virol.* 74, 4738–4745. doi: 10.1128/JVI.74.10.4738-4745.2000

Ghanim, M., Sobol, I., Ghanim, M., and Czosnek, H. (2007). Horizontal transmission of begomoviruses between *Bemisia tabaci* biotypes. *Arthropod Plant Inte* 1, 195–204. doi: 10.1007/s11829-007-9018-z

Gottlieb, Y., Zchori-Fein, E., Mozes-Daube, N., Kontsedalov, S., Skaljac, M., Brumin, M., et al. (2010). The transmission efficiency of tomato yellow leaf curl virus by the whitefly *Bemisia tabaci* is correlated with the presence of a specific symbiotic bacterium species. *J. Virol.* 84, 9310–9317. doi: 10.1128/JVI.00423-10

Hammond, A. M., and Hardy, T. N. (1988). "Quality of diseased plants as hosts for insects," in *Plant Stress-Insect Interactions*, ed. E. E. A. Heinrichs (Verdun: INIA-ICARDA), 381–431.

Himler, A. G., Adachi-Hagimori, T., Bergen, J. E., Kozuch, A., Kelly, S. E., Tabashnik, B. E., et al. (2011). Rapid spread of a bacterial symbiont in an invasive whitefly is driven by fitness benefits and female bias. *Science* 332, 254–256. doi: 10.1126/science.1199410

Ingwell, L. L., Eigenbrode, S. D., and Bosque–Pérez, N. A. (2012). Plant viruses alter insect behavior to enhance their spread. *Sci. Rep.* 2:578. doi: 10.1038/srep00578

Jennersten, O. (1988). Insect dispersal of fungal disease: effects of Ustilago infection on pollinator attraction in *Viscaria vulgaris*. *Oikos* 51, 163–170. doi: 10.2307/3565638

Jiménez-Martínez, E. S., Bosque-Pérez, N. A., Berger, P. H., and Zemetra, R. S. (2004a). Life history of the bird cherry-oat aphid, *Rhopalosipum padi* (Homoptera: Aphididae), on transgenic and untransformed wheat challenged with Barley yellow dwarf virus. *J. Econ. Entomol.* 97, 203–212. doi: 10.1104/pp.109.142661

Jiménez-Martínez, E. S., Bosque-Pérez, N. A., Berger, P. H., Zemetra, R. S., Ding, H., and Eigenbrode, S. D. (2004b). Volatile cues influence the response of *Rhopalosiphum padi* (Homoptera: Aphididae). to Barley yellow dwarf virus-infected transgenic and untransformed wheat. *Environ. Entomol.* 33, 1207–1216. doi: 10.1603/0046-225X-33.5.1207

Kirk, W. D. J., and Terry, L. I. (2003). The spread of the western flower thrips *Frankliniella occidentalis* (Pergande). *Agric. For. Entomol.* 5, 301–310. doi: 10.1046/j.1461-9563.2003.00192.x

Lefèvre, T., and Thomas, F. (2008). Behind the scene, something else is pulling the strings: emphasizing parasitic manipulation in vector-borne diseases. *Infect. Genet. Evol.* 8, 504–519. doi: 10.1016/j.meegid.2007.05.008

Liu, B. M., Preisser, E. L., Chu, D., Pan, H. P., Xie, W., Wang, S. L., et al. (2013). Multiple forms of vector manipulation by a plant-infecting virus: *Bemisia tabaci* and tomato yellow leaf curl virus. *J. Virol.* 87, 4929–4937. doi: 10.1128/JVI.03571-12

Maris, P. C., Joosten, N. N., Goldbach, R. W., and Peters, D. (2004). Tomato spotted wilt virus infection improves host suitability for its vector *Frankliniella occidentalis*. *Phytopathology* 94, 706–711. doi: 10.1094/PHYTO.2004.94.7.706

Mason, G., Caciagli, P., Accotto, G. P., and Noris, E. (2008). Real-time PCR for the quantitation of tomato yellow leaf curl *Sardinia virus* in tomato plants and in *Bemisia tabaci*. *J. Virol. Methods* 147, 282–289. doi: 10.1016/j.jviromet.2007.09.015

Mason, G., Roggero, P., and Tavella, L. (2003). Detection of Tomato spotted wilt virus in its vector *Frankliniella occidentalis* by reverse transcription-polymerase chain reaction. *J. Virol. Methods* 109, 69–73. doi: 10.1016/S0166-0934(03)00048-X

Mauck, K., Bosque-Pérez, N. A., Eigenbrode, S. D., De Moraes, C. M., and Mescher, M. C. (2012). Transmission mechanisms shape pathogen effects on host-vector interactions: evidence from plant viruses. *Funct. Ecol.* 26, 1162–1175. doi: 10.1111/j.1365-2435.2012.02026.x

Mauck, K. E., De Moraes, C. M., and Mescher, M. C. (2010). Deceptive chemical signals induced by a plant virus attract insect vectors to inferior hosts. *Proc. Natl. Acad. Sci. U.S.A.* 107, 3600–3605. doi: 10.1073/pnas.0907191107

Mauck, K. E., De Moraes, C. M., and Mescher, M. C. (2016). Effects of pathogens on sensory-mediated interactions between plants and insect vectors. *Curr. Opin. Plant Biol.* 32, 53–61. doi: 10.1016/j.pbi.2016.06.012

Medeiros, R. B., Resende, R. O., and de Avila, A. C. (2004). The plant virus Tomato Spotted Wilt *Tospovirus* activates the immune system of its main insect vector. *Frankliniella occidentalis*. *J. Virol.* 78, 4976–4982. doi: 10.1128/JVI.78.10.4976-4982.2004

Mehta, P., Wyman, J. A., Nakhla, M. K., and Maxwell, D. P. (1994). Transmission of tomato yellow leaf curl geminivirus by *Bemisia tabaci* (Homoptera: Aleyrodidae). *J. Econ. Entomol.* 87, 1291–1297. doi: 10.1093/jee/87.5.1291

Montllor, C. B., and Gildow, F. E. (1986). Feeding responses of two grain aphids to barley yellow dwarf virus-infected oats. *Entomol. Exp. Appl.* 42, 63–69. doi: 10.1111/j.1570-7458.1986.tb02188.x

Morin, S., Ghanim, M., Sobol, I., and Czosnek, H. (2000). The GroEL protein of the whitefly *Bemisia tabaci* interacts with the coat protein of transmissible and nontransmissible begomoviruses in the yeast two-hybrid system. *Virology* 276, 404–416. doi: 10.1006/viro.2000.0549

Morin, S., Ghanim, M., Zeidan, M., Czosnek, H., Verbeek, M., and van den Heuvel, J. F. (1999). A GroEL homologue from endosymbiotic bacteria of the whitefly *Bemisia tabaci* is implicated in the circulative transmission of tomato yellow leaf curl virus. *Virology* 256, 75–84. doi: 10.1006/viro.1999.9631

Morse, J. G., and Hoddle, M. S. (2006). Invasion biology of thrips. *Annu. Rev. Entomol.* 51, 67–89. doi: 10.1146/annurev.ento.51.110104.151044

Narayana, Y. D., and Muniyappa, V. (1996). Virus-vector relationships of a planthopper (*Peregrinus maidis*)-borne sorghum stripe tenuivirus. *Int. J. Pest Manage.* 42, 165–170. doi: 10.1080/09670879609371990

Ning, W., Shi, X., Liu, B., Pan, H., Wei, W., Zeng, Y., et al. (2015). Transmission of *Tomato Yellow* Leaf *Curl Virus by Bemisia tabaci* as affected by whitefly sex and biotype. *Sci. Rep.* 5, 10744. doi: 10.1038/srep10744

Pakkianathan, B. C., Kontsedalov, S., Lebedev, G., Mahadav, A., Zeidan, M., Czosnek, H., et al. (2015). Replication of tomato yellow leaf curl virus in its whitefly vector. *Bemisia tabaci*. *J. Virol.* 89, 9791–9803. doi: 10.1128/JVI.00779-15

Pan, H. P., Chen, G., Li, F., Wu, Q. J., Wang, S. L., Xie, W., et al. (2013). Tomato spotted wilt virus infection reduces the fitness of a non-vector herbivore on pepper. *J. Econ. Entomol.* 106, 924–928. doi: 10.1603/EC12365

Pan, H. P., Chu, D., Yan, W. Q., Su, Q., Liu, B. M., Xie, W., et al. (2012). Rapid spread of Tomato yellow leaf curl virus in China is aided differentially by two invasive whiteflies. *PLoS One* 7:e34817. doi: 10.1371/journal.pone.0034817

Péréfarres, F., Hoareau, M., Chiroleu, F., Reynaud, B., Dintinger, J., and Lett, J. M. (2011). A novel synthetic quantification standard including virus and internal report targets: application for the detection and quantification of emerging begomoviruses on tomato. *Virol. J.* 8, 1–9. doi: 10.1186/1743-422X-8-389

Salvaudon, L., De Moraes, C. M., and Mescher, M. C. (2013). Outcomes of co-infection by two potyviruses: implications for the evolution of manipulative strategies. *Proc. R. Soc. B* 280:20122959. doi: 10.1098/rspb.2012.2959

Stafford, C. A., Walker, G. P., and Ullman, D. E. (2011). Infection with a plant virus modifies vector feeding behavior. *Proc. Natl. Acad. Sci. U.S.A.* 108, 9350–9355. doi: 10.1073/pnas.1100773108

Su, Q., Mescher, M. C., Wang, S. L., Chen, G., Xie, W., Wu, Q. J., et al. (2016). Tomato yellow leaf curl virus differentially influences plant defence responses to a vector and a non-vector herbivore. *Plant Cell. Environ.* 39, 597–607. doi: 10.1111/pce.12650

Su, Q., Pan, H., Liu, B., Chu, D., Xie, W., Wu, Q., et al. (2013). Insect symbiont facilitates vector acquisition, retention, and transmission of plant virus. *Sci. Rep.* 3, 1367. doi: 10.1038/srep01367

Taylor, P. J., and Hurd, H. (2001). The influence of host haematocrit on the blood feeding success of *Anopheles stephensi*: implications for enhanced malaria transmission. *Parasitology* 122, 491–496. doi: 10.1017/S0031182001007776

Tedeschi, R., Ciuffo, M., Mason, G., Roggero, P., and Tavella, L. (2001). Transmissibility of four tospoviruses by a thelytokous population of *Thrips tabaci* from Liguria, northwestern Italy. *Phytoparasitica* 29, 37–45. doi: 10.1007/BF02981812

Ullman, D. E., Medeiros, R. B., Campbell, L. R., Whitfield, A. E., Sherwood, J. L., and German, T. L. (2002). Thrips as vectors of tospoviruses. *Adv. Bot. Res.* 36, 113–140. doi: 10.1016/S0065-2296(02)36061-0

Ullman, D. E., Sherwood, J. L., and German, T. L. (1997). "Thrips as vectors of plant pathogens," in *Thrips as Crop Pests. Institute of Arable Crops Research*, ed. T. Lewis (Harpenden: Rothamsted), 539–565.

van de Wetering, F., van der Hoek, M., Goldbach, R., and Peters, D. (1999). Differences in tomato spotted wilt virus vector competency between males and females of *Frankliniella occidentalis*. *Entomol. Exp. Appl.* 93, 105–112. doi: 10.1046/j.1570-7458.1999.00567.x

Wang, L. L., Wang, X. R., Wei, X. M., Huang, H., Wu, J. X., Chen, X. X., et al. (2016). The autophagy pathway participates in resistance to tomato yellow leaf curl virus infection in whiteflies. *Autophagy* 12, 1560–1574. doi: 10.1080/15548627.2016.1192749

Wijkamp, I., and Peters, D. (1993). Determination of the median latent period of two tospoviruses in *Frankliniella occidentalis*, using a novel leaf disk assay. *Phytopathology* 83, 986–991. doi: 10.1094/Phyto-83-986

Wu, J. B., Dai, F. M., and Zhou, X. P. (2006). First report of Tomato yellow leaf curl virus in China. *Plant Dis.* 155, 439–448. doi: 10.1094/PD-90-1359C

Zhang, Z. J., Zhang, P. J., Li, W. D., Zhang, J. M., Huang, F., Yang, J., et al. (2013). De novo transcriptome sequencing in *Frankliniella occidentalis* to identify genes involved in plant virus transmission and insecticide resistance. *Genomics* 101, 296–305. doi: 10.1016/j.ygeno.2013.02.005

Zhao, W. W., Wan, Y. R., Wen, X., Xu, B. Y., Zhang, Y. J., and Wang, S. L. (2015). Effect of Spinosad resistance on transmission of tomato spotted wilt virus by the western flower thrips (Thysanoptera: Thripidae). *J. Econ. Entomol.* 109, 62–69. doi: 10.1093/jee/tov278

Conflict of Interest Statement: The authors declare that the research was conducted in the absence of any commercial or financial relationships that could be construed as a potential conflict of interest.

frontiers in Physiology

ORIGINAL RESEARCH
published: 04 October 2018
doi: 10.3389/fphys.2018.01348

The Effect of Diet on Midgut and Resulting Changes in Infectiousness of AcMNPV Baculovirus in the Cabbage Looper, *Trichoplusia ni*

Elizabeth Chen[1,2], *Dennis Kolosov*[3], *Michael J. O'Donnell*[3], *Martin A. Erlandson*[4], *Jeremy N. McNeil*[2] *and Cam Donly*[1,2]*

[1] London Research and Development Centre, Agriculture and Agri-Food Canada, London, ON, Canada, [2] Department of Biology, University of Western Ontario, London, ON, Canada, [3] Department of Biology, McMaster University, Hamilton, ON, Canada, [4] Saskatoon Research and Development Centre, Agriculture and Agri-Food Canada, Saskatoon, SK, Canada

Insecticide resistance has been reported in many important agricultural pests, and alternative management methods are required. Baculoviruses qualify as an effective, yet environmentally benign, biocontrol agent but their efficacy against generalist herbivores may be influenced by diet. However, few studies have investigated the tritrophic interactions of plant, pest, and pathogen from both a gene expression and physiological perspective. Here we use microscopy and transcriptomics to examine how diet affects the structure of peritrophic matrix (PM) in *Trichoplusia ni* larvae and consequently their susceptibility to the baculovirus, AcMNPV. Larvae raised on potato leaves had lower transcript levels for chitinase and chitin deacetylase genes, and possessed a thicker and more multi-layered PM than those raised on cabbage or artificial diet, which could contribute to their significantly lower susceptibility to the baculovirus. The consequences of these changes underline the importance of considering dietary influences on pathogen susceptibility in pest management strategies.

Keywords: cabbage looper, AcMNPV baculovirus, chitinase, chitin deacetylase, midgut transcriptome, pathogen resistance, peritrophic matrix, midgut pH

OPEN ACCESS

Edited by:
Patrizia Falabella,
University of Basilicata, Italy

Reviewed by:
Yuan-Xi Li,
Nanjing Agricultural University, China
Dandan Wei,
Southwest University, China

***Correspondence:**
Cam Donly
cam.donly@agr.gc.ca

Specialty section:
This article was submitted to Invertebrate Physiology, a section of the journal Frontiers in Physiology

Received: *26 June 2018*
Accepted: *06 September 2018*
Published: *04 October 2018*

Citation:
Chen E, Kolosov D, O'Donnell MJ, Erlandson MA, McNeil JN and Donly C (2018) The Effect of Diet on Midgut and Resulting Changes in Infectiousness of AcMNPV Baculovirus in the Cabbage Looper, Trichoplusia ni. Front. Physiol. 9:1348. doi: 10.3389/fphys.2018.01348

INTRODUCTION

Baculoviruses are entomopathogens with high host specificity but some, such as the Autographa californica multicapsid nucleopolyhedrovirus (AcMNPV), can infect a wide range of lepidopterans (Clem and Passarelli, 2013). Once ingested, the alkaline pH of the larval midgut dissolves the viral occlusion body (OB), releasing the occlusion-derived virions (ODVs) that rapidly pass through the midgut peritrophic matrix (PM) and infect the microvilli of columnar midgut epithelium cells (Granados and Lawler, 1981). However, the infection process can be affected by the larval food source (Duffey et al., 1995; Cory and Hoover, 2006) as this shapes the environment of the gut (Keating et al., 1990; Brodersen et al., 2012). Secondary metabolites (phenolics, flavonoids, and tannins) affect the palatability of plant tissue and influence caterpillar growth, which in turn affects larval behavior and plant-pest interactions (Sarfraz et al., 2011).

Brassica spp. synthesize glucosinolates, a significant class of natural defense compounds, which when ingested by insects are hydrolysed by myrosinase to produce isothiocyanates, oxazolidine thiones, epithionitroles, and nitrils (sometimes known as the "mustard oil bomb,"

Grubb and Abel, 2006). These compounds are toxic repellents to some insects (Mithen et al., 2000; Lambrix et al., 2001; Talalay and Fahey, 2001; Agrawal and Kurashige, 2003) but others have evolved counter-adaptations including reduced plant cell disruption, rapid absorption of intact glucosinolates and rapid metabolic conversion of glucosinolates to harmless compounds (Winde and Wittstock, 2011). Although the functional basis of glucosinolate detoxification remains to be determined, there is transcriptomic evidence that glutathione S-transferases and cytochrome P450s are involved (Wadleigh and Yu, 1988; Whiteman et al., 2012; Kumar et al., 2013). *Solanum* spp. produce glycoalkaloids as natural defense compounds which inhibit acetylcholinesterase and butyrylcholinesterase, both of which catalyze the hydrolysis of the neurotransmitter acetylcholine, as well as interfering with calcium and sodium ion transport across cell membranes (Schwarz et al., 1995). In insect herbivores, the mechanisms of counter-adaptation are predominantly present in the fat body, which contains detoxification enzymes and ABC transporters (Yang et al., 2007).

Lepidopterans have both biochemical and physical gut attributes to counteract the challenges of a wide diet range. As one of the most alkaline environments in a natural system, a high midgut pH retains the nutritional quality of ingested plant proteins and offsets the toxicity of their host plant's defensive compounds (Woodham, 1983). Maintaining a pH $>$ 8 prevents the antidigestive effects of tannin-protein-aggregates (Felton and Duffey, 1991). The physical peritrophic matrix (PM), which separates the gut content from the midgut wall, is another protective feature of the lepidopteran midgut. The PM consists of a proteinaceous matrix embedded in a chitin substructure that serves in the combined roles of digestion and absorption of nutrients, mechanical protection, toxin nullification, and pathogen restriction (Spence, 1991). However, while more toxic diets can induce thicker PM formation which affords greater protection from toxins and pathogens, there is a possible trade-off relating to digestive efficiency. For example, the growth rate of *Heliothis virescens* was reported to be lower when larvae were fed a more toxic diet that resulted in a thicker PM, although there was an additional effect as the larvae had a lower susceptibility to viral pathogens (Plymale et al., 2008).

Trichoplusia ni is a generalist herbivore capable of feeding on plants from many families, including Solanaceae and Brassicaceae. Its larval PM is typical of most lepidopterans, forming as a thin layer at the anterior end of the midgut and becoming progressively thicker as additional components are added to its structure by the midgut epithelium (Adang and Spence, 1981; Harper and Granados, 1999; Toprak et al., 2014). As it is thinnest and most porous at the anterior region this could help explain why the vast majority of AcMNPV infections in *T. ni* are initiated in the anterior midgut (Javed et al., 2016). The components contributing to PM architecture, synthesis, and function include structural (peritrophins, mucins, glycoproteins, lipases), microvesicle delivery (gelsolin, annexin), framework (chitin synthase, chitinase, chitin deacetylase), and hormonal effectors (ecdysone, juvenile hormone related) (Hegedus et al., 2016).

In the present study, we undertook experiments to confirm that variable diets could alter the susceptibility of *T. ni* larvae to viral infections (Cory and Hoover, 2006; Shikano et al., 2010) and to determine if larval diet affected the structure of the PM. In addition, using RNA-seq analysis, we investigated larval midgut gene expression to determine if the expression of various categories of genes whose products could influence PM structure differed with diet.

MATERIALS AND METHODS

Insect Rearing, Diet, and Virus

All insects used were obtained from a *T. ni* culture reared on cabbage under a 16L:8D photoperiod at 25°C at Agriculture and Agri-Food Canada's (AAFC) London Research and Development Centre (LRDC). Golden Acre Cabbage (*Brassica oleraceae*) and Kennebec Potato (*Solanum tuberosum*) were grown in a greenhouse at 16L:8D photoperiod at 25°C while the McMorran wheat germ-based artificial diet (Adkisson et al., 1960) was purchased from Insect Production Services (Great Lakes Forestry Centre, Sault Ste. Marie, ON, Canada). Virus used for infections was derived from the AcMNPV bacmid bMON14272 backbone repaired with *gfp* under the control of the OpMNPV *ie1* promoter (Javed et al., 2016).

Bioassays

Fourth instar larvae were placed in 5.5 cm diameter petri dishes lined with moist filter paper and provided with either a 6 mm diameter potato or cabbage leaf disc (cut from the leaves of plants that were ∼1 month old) or a 5 mm^3 cube of artificial diet. The food samples were treated with viral doses calculated from preliminary bioassays: 15, 25, 50, 100, or 200 OBs on cabbage, 50, 100, 150, 250, or 400 OBs on potato, or 25, 50, 100, 200, or 350 OBs on artificial diet. The concentrations obtained using serial dilution were confirmed with hemocytometer counts. Controls for the three diet treatments were treated with 0.05% Triton X-100 in water, the solution used to suspend the OBs. In all cases, the virus was applied in a 2 μl droplet and on leaf disks the droplet was allowed to dry before being fed to insects. In the case of artificial diet, a square of parafilm was placed underneath the cube to ensure the solution was not absorbed by the filter paper. Once the treated food was completely consumed, untreated food was provided for 7 days post treatment or until the larvae pupated. There were three replicates of ten larvae per concentration per diet treatment and mortality was recorded daily. LD_{50} values were estimated and Fieller's method used to calculate subsequent 95% confidence intervals in the R add-on package *drc* (Cox, 1990; Ritz et al., 2015). Each continuous dose response curve was modeled based on the parameters of identical lower and upper limits with only binomial responses (alive or dead) and the results were compared pairwise within *drc* for identity based on slope and LD_{50} using a one-way ANOVA. GraphPad Prism software was used to generate **Figure 1** showing the curves.

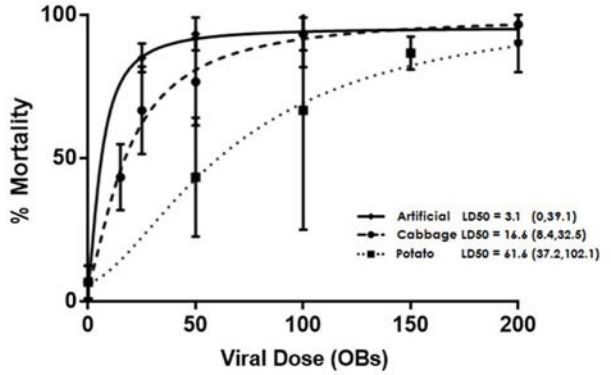

FIGURE 1 | Dose dependent mortality of AcMNPV-treated 4th instar *T. ni* larvae that were raised on artificial diet, cabbage, or potato. Error bars depict 95% confidence intervals.

Double-Barrelled Ion-Selective Microelectrode Midgut pH Measurements

Construction of double-barrelled ion-selective microelectrodes has been described in detail in Ianowski et al. (2002) and Ianowski and O'Donnell (2004) so the modified protocol used is described briefly. Double-barrelled "theta" glass microcapillaries were pulled to a fine point using a vertical micropipette puller PE-2 (Narashige, Japan). The pH-barrel was silanized to aid retention of the hydrophobic H^+ ionophore cocktail, as described by Ianowski et al. (2002). The ion-selective barrel was then filled with a solution containing 100 mM sodium citrate and 100 mM NaCl (pH = 6.0). The reference barrel was filled with 150 mM KCl. Finally, the ion-selective barrel was tip-filled with Hydrogen ionophore I cocktail B. Each barrel was connected through chlorided silver wires to the inputs of a high-input impedance differential electrometer (HiZ-223, Warner Instruments, Hamden, CT) which was referenced to a bath electrode filled with 3M KCl in 4% agar. The pH microelectrodes were calibrated in TAPS-buffered solutions of pH 8, 9, and 10 with ionic strength approximating that of *T. ni* diet.

Ten 4th instar larvae from each of the three diets were pinned straight while submerged in saline solution. A longitudinal incision was made along the length of the caterpillar to expose the midgut so that a pH microelectrode could be inserted into the anterior lumen of the midgut and the pH recorded. All measurements were performed *in situ*, i.e., without removing the gut from the animal and completed within 5 min from the end of dissection. Microelectrode voltages were low-pass filtered at 2 Hz, digitized and recorded using a PowerLab data acquisition system (AD Instruments, Colorado Springs, CO) and analyzed using Chart software (Ad Instruments). pH values were calculated from microelectrode voltages which were stable to within 0.1 mV over 10 s. The pH data for the three diets were analyzed using a one-way ANOVA and assessed for significance using the Holm–Sidak method (Sidak, 1967; Holm, 1979).

Scanning Electron Microscopy (SEM)

Larvae were reared on each of the three diets until the 4th instar (head capsule size 1.0–1.3 mm), at which time their midguts were dissected out, the food bolus removed, so that the PM could be cut lengthwise and immersed in Sorenson's phosphate buffer (pH 7.4) containing 2.5% glutaraldehyde as a primary fixative. After triple buffer rinsing, samples were fixed in 1% osmium tetroxide for 1 h, triple rinsed again, and then dehydrated in a graded ethanol series before being dried in a graded hexamethyldisilazane series (Shivley and Miller, 2009). Samples were mounted, gold sputtered, and observed with a Hitachi 3400-N VP-SEM. Three midgut samples per diet category were processed and the anterior, middle, and posterior regions of the resulting PMs from the larvae reared on differing diets were compared.

Transmission Electron Microscopy (TEM)

The initial steps of TEM preparation were identical to those used for SEM, up to and including the fixation in 1% osmium tetroxide and secondary wash. Following that, TEM preparation included dehydration in a graded acetone series before infiltration and embedding in epon-araldite resin and finally baking at 60°C for 48 h. Coarse trimming was done using a razor blade and finer sectioning done on a Sorval Ultracut with a diamond knife. All sections were from the anterior region of the PM and netted on copper grids. Samples were post stained in the dark for 20 min with uranyl acetate, rinsed in five water droplets, stained for 2 min with lead citrate, and rinsed in three water droplets. Grid samples were examined and images taken using a Philips CM10 TEM 60 KV. The midguts from three larvae from each diet category were examined.

RNA Extraction, RNA-seq, and Transcriptomic Analysis

Midguts of 4th instar larvae from each diet category were dissected in Calpode's insect saline (pH = 7.2, 10.7 mM NaCl, 25.8 mM KCl, 90 mM glucose, 29 mM $CaCl_2$, 20 mM $MgCl_2$, and 5 mM HEPES), immediately suspended in RNAlater buffer (Ambion, Fisher Scientific) and stored at −20°C until RNA

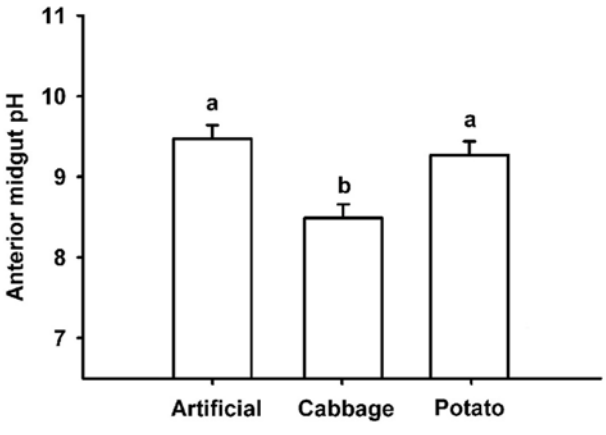

FIGURE 2 | pH values in anterior midguts of 4th instar *T. ni* raised on artificial diet, cabbage, and potato. Different letters represent significant differences $p < 0.001$ using a one-way ANOVA coupled with a *post-hoc* multiple comparison Holm–Sidak test.

extraction. Total RNA was extracted from five pooled midguts using an RNeasy mini kit (Qiagen), and replicated three times for each diet treatment. The quality and quantity of RNA were assessed using a 2100 Bioanalyzer (Agilent). RNA samples were diluted to 300 ng/μL in DEPC-treated water. Strand-specific libraries were constructed and sequencing performed on the Illumina HiSeq 2000 platform using 100 bp single-end reads protocol at McGill University and Génome Québec Innovation Centre (Montreal, QC, Canada).

Messenger RNA-seq reads were mapped to a reference *T. ni* transcriptome containing 58,200 contigs that was previously assembled from 3 tissue-specific transcriptomes (Javed et al., 2017). Subsequent analysis and data handling were done using CLC Genomics Workbench version 10.0.1 (Qiagen Bioinformatics). Before mapping, library reads with <50 nucleotides were discarded. Gene expression tracks were then generated from RNA-seq analysis. Finally, all potential pairings of different diets were tested for differential expression. The output from DESeq analysis included normalized mean number of reads assigned to a contig, $\log_2$ fold change, and its statistical significance. A contig was considered differentially expressed if the absolute value of the $\log_2$ fold change was ≥3 and the adjusted *p*-value was ≤0.001 following Benjamini-Hochberg false discovery rate (FDR) correction (Benjamini and Yekutieli, 2001). Contigs corresponding to genes of interest were screened from all those found to be differentially expressed. Contig IDs without annotation were analyzed by BLASTN comparison with the NCBI database. The NCBI accessions and descriptions of matching entries using an E-value cut-off of 0.001 are reported in **Supplementary Table 1**.

RESULTS

Diet Based *T. ni* Bioassay Lethality Curves

Larval diets had a significant effect on the susceptibility of *T. ni* larvae to AcMNPV baculovirus (**Figure 1**), with LD_{50s} of 3.1 OBs (95% CI: 0, 39.1); 16.6 OBs (95% CI: 8.4, 32.5); and 61.6 OBs (95% CI: 37.2, 102.1) for larvae reared on artificial diet, cabbage, and potato respectively. The LD_{50s} for larvae reared on artificial diet and cabbage did not differ significantly ($p > 0.05$, F-ratio = 2.76, $df = 2$) but both differed significantly from the LD_{50} value for larvae reared on potato (cabbage: $p = 0.0019$, F-ratio = 7.81, $df = 2$; artificial diet: $p < 0.001$, F-ratio = 14.16, $df = 2$).

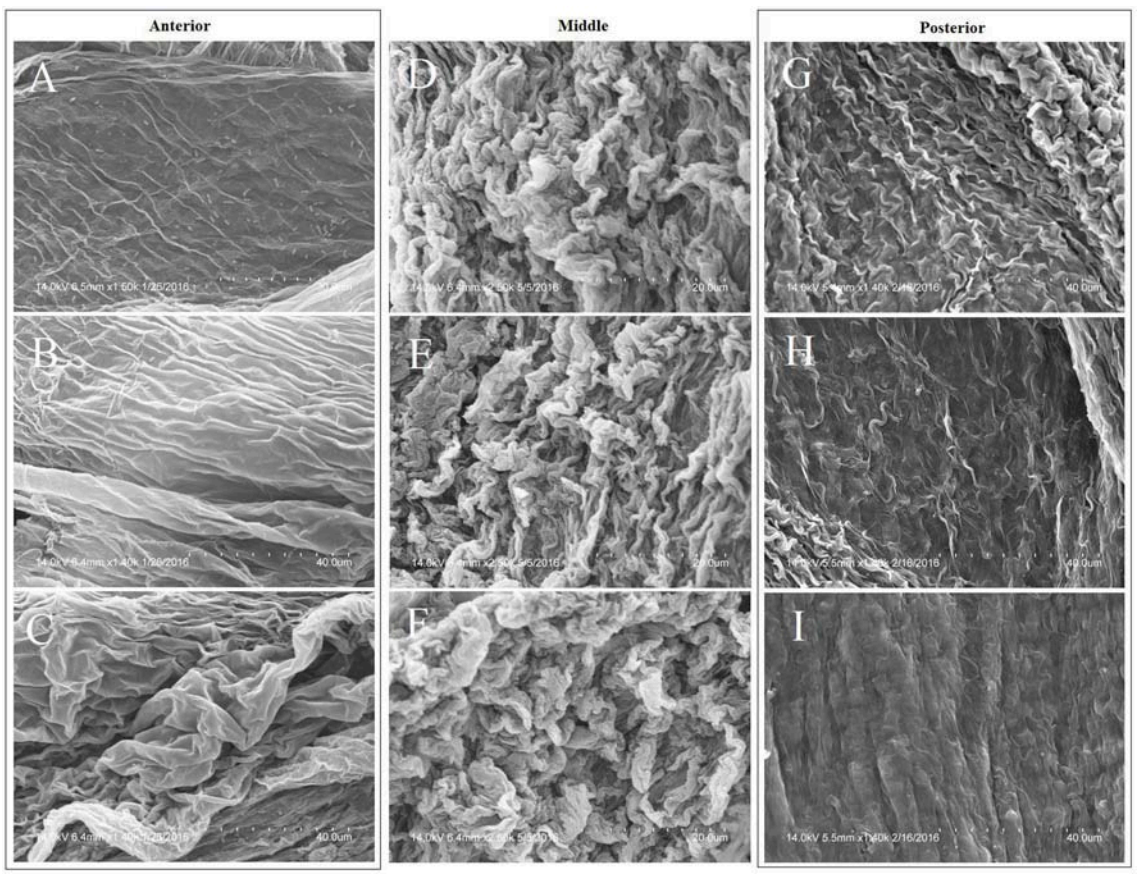

FIGURE 3 | Morphological variation in the anterior, middle, and posterior sections of the PM of a cabbage-raised *T. ni* midgut per regional characteristics: left column = anterior; middle column = middle; right column = posterior. Magnification of images are: **(A)** = 1,500×; **(B)** = 1,400×; **(C)** = 1,400×; **(D–F)** = 2,500×; **(G–I)** = 1,400×. Images **(A–I)** are in spatial, sequential order along the length of the midgut.

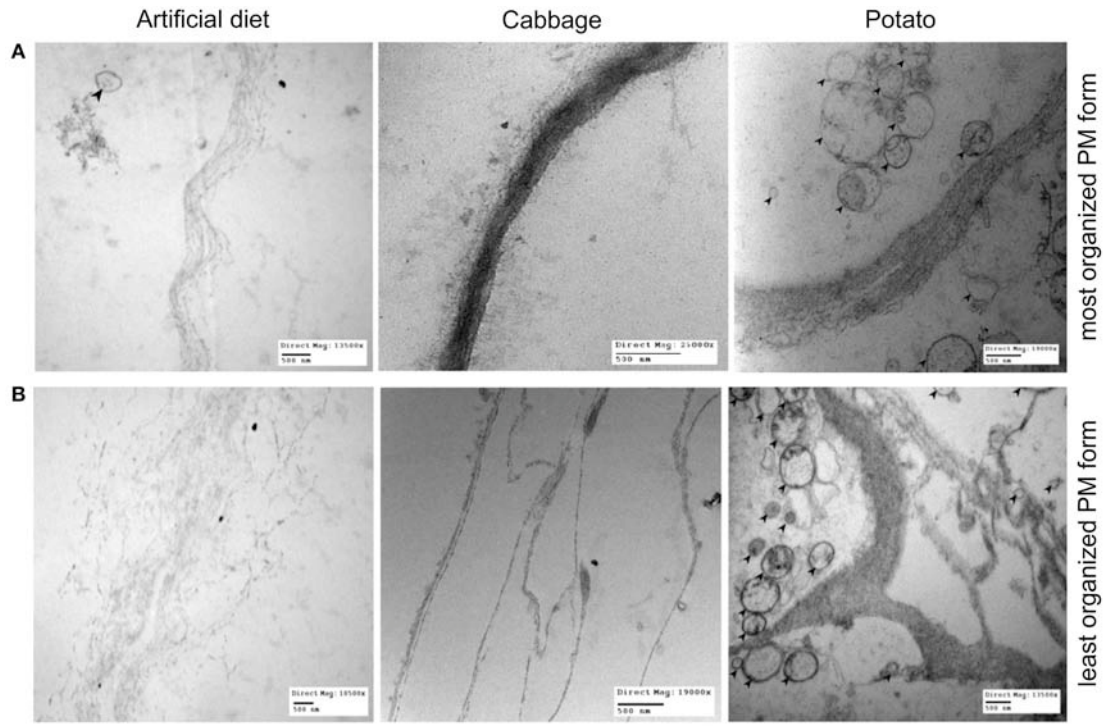

FIGURE 4 | The range of PM morphology observed in 4th instar *T. ni* larvae raised on 3 different diets: artificial diet, cabbage, and potato. **(A)** Depicts an example of the most organized appearance of the PM for each diet and **(B)** depicts an example of the least organized. Note the bends/kinks present in the example of PM of potato-fed larvae at its least organized (bottom right image). Left column: larvae raised on artificial diet (top image magnification = 13,500×; bottom image magnification = 10,500×). Middle column: larvae raised on cabbage (top image magnification = 25,000×; bottom image magnification = 19,000×). Right column: larvae raised on potato (top image magnification = 10,500×; bottom image magnification = 13,500×). Bars = 500 nm. Black arrows point to microvesicles, which are present significantly more in potato-fed larval PMs regardless of the level of organization.

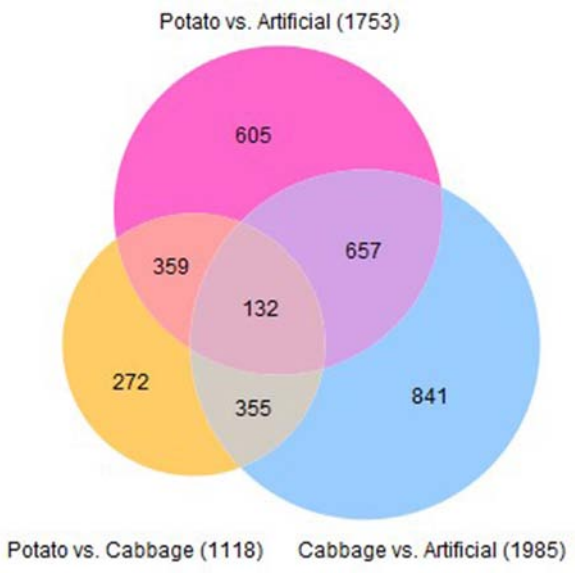

FIGURE 5 | Venn diagram describing the number of contigs significantly differentially expressed in midguts of 4th instar *T. ni* raised on three diets.

Measurements of Anterior Midgut pH

Diet had a significant effect on the pH in the anterior midgut of 4th instar *T. ni*, with larvae raised on cabbage having a significantly less alkaline pH (X = 8.44; SD ± 0.26) than those raised on artificial diet (X = 9.48; SD ± 0.53) or potato (X = 9.28; SD ± 0.52) (**Figure 2**). Statistically significant differences were determined using a one-way ANOVA coupled with a Holm-Sidak multiple comparison test ($p < 0.001$, F-ratio = 14.726). The degrees of freedom between groups = 2; the residual degrees of freedom = 27.

SEM Characterization of the PM

The structural differences between the anterior, middle, and posterior sections of the midgut are presented in **Figure 3**. The anterior region has relatively shallow but extensive folds, transitioning into tight coils in the middle region and becoming degraded and sloughed at the posterior end.

While the anterior region of the PM can be morphologically differentiated from the middle and posterior sections, significant morphological differences between the anterior regions of larvae raised on the three diets were not observed.

TABLE 1 | Summary of differentially expressed contigs in midguts between all diet group pairs for 4th instar *T. ni*.

Gene category	Contig ID	Contig length (bp)	Sequence description	Cabbage relative to artificial	Potato relative to cabbage	Potato relative to artificial
Chitin Synthase	gi|687040850	227	Chitin synthase A	–	–	↓ 13x
Chitinases	11990	1,399	Chitinase domain	↓ 3x	–	–
	17052/16243/ gi|687056067	1,186	Viral-like chitinase	↓ 10x	–	↓ 13x
	17700	676	Chitinase	–	–	↓ 8x
	gi|687027891	9,581	Chitinase 10	–	↓ 4x	↓ 10x
	gi|687027960	3,179	Chitinase 3	↓ 9x	–	↓ 13x
	gi|687094659/8386	1,202	Chitinase 2	↓ 17x	↓ 4x	↓ 68x
	gi|687131816	2,030	Endochitinase A1-like	–	–	↓ 3x
Chitin Deacetylase	16131/11096	1,843	Chitin deacetylase 1	–	↓ 2x	↓ 6x
Glycoprotein	838	4,146	Glycoprotein 1-like	↓ 3x	–	–
	9115	789	Glycoprotein 2B-like	↑ 3x	–	–
	12335	654	Glycoprotein 2B-like	↑ 3x	–	–
	12706	1,400	Glycoprotein 1-like	↓ 4x	–	↓ 4x
	13031	1,431	Glycoprotein 1-like	↑ 3x	–	–
	13710	2,774	Glycoprotein 2C-like	↑ 25x	–	↑ 34x
	13711	2,440	Glycoprotein 2C-like	↑ 32x	–	↑ 42x
	13714	559	Glycoprotein 2C-like	↑ 28x	–	–
	17683	603	Glycoprotein 2C-like	–	–	↑ 6x
	18285	471	Endocuticle structural glycoprotein ABD-5-like	↑ 7x	–	↑ 7x
	18333	590	Glycoprotein ABD-5-like	↑ 8x	–	–
Ecdysone Inducibles	3024	1,783	Ecdysone-induced protein 74EF isoform A	↑ 4x	–	↑ 4x
	5946	453	Ecdysone receptor transcript variant X2	↓ 5x	–	↓ 4x
	6995	571	Ecdysteroid-induced (E75)	–	–	↓ 4x
	8772	1,940	Zinc finger protein on ecdysone puffs	↓ 3x	–	–
	16286	1,185	3-dehydrecdysone 3b-reductase	↓ 4x	–	↓ 6x
	18136	2,470	20-hydroxy-ecdysone receptor	↓ 3x	↑ 15x	↑ 4x
	gi|687100743	380	Ecdysone oxidase gene	↓ 4x	–	↓ 4x
Juvenile hormone inducibles	2789	3,733	Juvenile hormone-inducible protein	↓ 5x	–	–
	4247	1,993	Juvenile hormone epoxide hydrolase precursor	–	↑ 3x	–
	6007	1,020	Juvenile hormone epoxide hydrolase-like	–	↓ 7x	↓ 11x
	9577	2,010	Juvenile hormone esterase-like isoform	↓ 4x	–	–
	11982	494	Juvenile hormone esterase precursor (JHE)	↓ 19x	–	↓ 27x
	13294	2,389	Juvenile hormone epoxide hydrolase-like protein	–	↓ 5x	–
	14365	2,322	Juvenile hormone esterase-like	–	–	↓ 5,811x
	16406	2,351	Juvenile hormone sensitive hemolymph protein	–	–	↓ 8x
	16491	850	Juvenile hormone-inducible protein	–	↓ 3x	↓ 4x
	17075	1,195	Juvenile hormone esterase-like	–	–	↓ 5x
	17228	1,428	Juvenile hormone epoxide hydrolase-like	–	–	↓ 25x

(Continued)

TABLE 1 | Continued

Gene category	Contig ID	Contig length (bp)	Sequence description	Cabbage relative to artificial	Potato relative to cabbage	Potato relative to artificial
	18269	714	Juvenile hormone binding-like protein	↓ 24x	–	↓ 78x
	gi|687052097	205	Juvenile hormone esterase precursor (JHE)	↓ 25x	–	↓ 35x
Gelsolin	14408	1,099	Gelsolin-like	↑ 3x	–	–
Mucins	2899	4,725	Mucin-12-like	–	–	↓ 8x
	8946	4,324	Mucin-2-like	↓ 3x	–	↓ 6x
	16236	442	Intestinal mucin	–	↑ 10x	↑ 11x
	17180	417	Mucin-5AC	–	–	↓ 7x
	gi|687050021	288	Mucin-5AC	↓ 13x	–	–
	gi|687060229	294	Mucin-5AC-like	↓ 16x	–	↓ 19x
	gi|687064266	219	Mucin-5AC-like	↓ 19x	–	↓ 13x
	gi|687073777	537	Mucin-5AC-like	↓ 17x	–	↓ 10x
	gi|687079129	295	Mucin-5AC-like	↓ 8x	–	↓ 10x
	gi|687080496	259	Mucin-5AC-like	↓ 12x	–	↓ 5x
	gi|687085871	401	Mucin-2-like	↑ 5x	–	–
	gi|687093538	984	Mucin-5AC	–	–	↓ 12x
Lipases	3030	1,018	Lipase 3-like	↑ 8x	↓ 7x	–
	10385	437	Lipase (Lipn004)	–	–	↓ 3x
	10606	1,230	Lipase 3-like	↓ 4x	↓ 6x	↓ 26x
	11520	893	Lipase-like	–	–	↓ 3x
	15809	1,398	Lipase 1-like	–	↓ 4x	↓ 4x
	16200	153	Insect intestinal lipase 7	–	↑ 4x	–
	16325	797	Insect intestinal lipase 6	–	↑ 4x	–
	16375	977	Insect intestinal lipase 6	↓ 3x	↓ 4x	↓ 15x
	16377	660	Lipase 3-like	↑ 3x	–	↑ 6x
	16389	885	Lipase-like	–	↓ 159x	↓ 96x
	16607	559	Lipase ABHD12	↓ 5x	–	↓ 5x
	16887	568	Lipase member H-like	↑ 23x	–	↑ 48x
	17002	670	Bile salt-activated lipase-like	↑ 5x	–	↑ 3x
	17081	483	Lipase-like	–	–	↓ 4x
	17396	880	Lipase 3-like	↑ 69x	–	↑ 35x
	gi|687078584	265	Lipase-like	↓ 26x	↑ 608x	↑ 23x
	gi|687085460	404	Lipase-like	↓ 20x	↑ 468x	↑ 23x
	gi|687101661	671	Lipase-related Protein 1-like	↓ 6x	–	↑ 4x
	gi|687116092	1,317	Lipase-like	↓ 4x	–	↑ 4x
	gi|687125502	266	Lipase	↓ 5x	–	–

Dash, no significant change; ↑, increased; ↓, decreased.

TEM Characterization of the PM

TEM imaging revealed significant morphological variability of the *T. ni* PM, both within and between diets, and the simplest morphologies are shown in **Figure 4A**. The PM of larvae reared on both artificial diet and cabbage is thin (≤500 nm in thickness) but with a more dense and uniform appearance in the cabbage treatment. In potato-raised larvae, the PM is usually thin (≤500 nm in thickness) but with its layers separated, thus spanning several microns.

By comparison, the most complex forms of PM (**Figure 4B**) have very different levels of organization, having thicker, less organized and more numerous layers than those shown in **Figure 4A**. Larvae reared on artificial diet vary from having a PM that exhibits separated laminae, spanning several microns, to one that is almost completely unraveled, with little structural integrity. In cabbage-raised larvae, the PM has divided laminae and further divided internal fibrils spanning several microns, but each layer is well defined. The structure of the PM in the potato treatment has bends and kinks of multiple fibrils and

divided laminae, showing a much greater level of disorganization than in larvae from the other two diet treatments. This highly disorganized form of the PM in larvae reared on potato is the main form present and its prevalence over the simple form was greatest in this treatment group. Furthermore, regardless of form, the PM of larvae raised on potato also featured more numerous microvesicles (**Figures 4A,B**).

mRNA Sequenced Read Processing and Quality Control

The sequencing of 9 libraries constructed from larval midgut RNA extracted from insects fed 3 different diets yielded 652,598,015 reads, with raw reads per library ranging from 57.8 to 80.3 million reads, with a mean of 72.5 million. The percentage of reads remaining after trimming ranged between 95.8 and 97.7%, with the average read length being 99.8 bp. The proportion of reads per sample mapping to the reference transcriptome ranged from 94.6 to 96.5%. The number of uniquely mapped reads per sample ranged from 48.4 to 64.2 million, with a mean of 58.8 million. The percentage of uniquely mapped reads ranged from 81.6 to 87.3%. All statistics stated are reported in **Supplementary Table 2**.

Diet Induced Transcriptomic Responses in *T. ni* Midgut

Using a cut-off of $\geq$3 absolute fold change and a FDR-corrected *p*-value of $\leq$0.001, the total number of contigs significantly differentially expressed for cabbage vs. artificial diet was 1,985; potato vs. cabbage was 1,118 and potato vs. artificial diet was 1,753. There were 132 shared contigs between all diets (**Figure 5**).

From the contigs that were differentially expressed, we selected those within gene categories encoding products likely to be involved in the PM's architecture, synthesis, and function, for further analysis. The following gene categories were included: structural (peritrophins, mucins, glycoproteins, lipases), microvesicle delivery (gelsolin, annexin), framework (chitin synthase, chitinase, chitin deacetylase) and hormonal effectors (ecdysone and juvenile hormone related). The overall midgut comparisons between 4th instar *T. ni* raised on different diets are presented in **Table 1** while the comparison with expanded statistics are given in **Supplementary Tables 3–5**. Of all the gene categories of interest, the downregulation of contigs corresponding to chitinase and chitin deacetylase were most correlated with diet toxicity.

DISCUSSION

Physiological Differences in Gut pH With Different Diets

It has been suggested that larval gut pH may play a role in resistance to pathogens and that gut pH can be significantly altered by diet (Keating et al., 1990). However, while our data supported the idea that diet can influence gut pH levels, as observed between diet treatments (**Figure 2**), there was no evident relationship between these differences and the significant differences in the susceptibility to the virus in *T. ni* larvae reared on different diets. Larvae reared on potato and artificial diet had an alkaline pH in the midgut well within the 9–11 range reported for most lepidopteran larvae (Dow, 1992), while those raised on cabbage had a less alkaline pH, possibly due to the high ascorbic acid content of cabbage. However, despite having a significantly lower gut pH, larvae fed cabbage were not the most susceptible to the virus, having an LD_{50} in between those reared on artificial diet and potato (**Figure 1**). The lack of effect may be related to the fact that the pH remained above 8, which is sufficiently alkaline to dissolve OBs effectively (Martin and Martin, 1983; Felton and Duffey, 1991).

Morphological and Transcriptional Differences in *T. ni* Midgut and PM

Our results suggest that the different susceptibility of larvae reared on different treatments are the result of changes in the

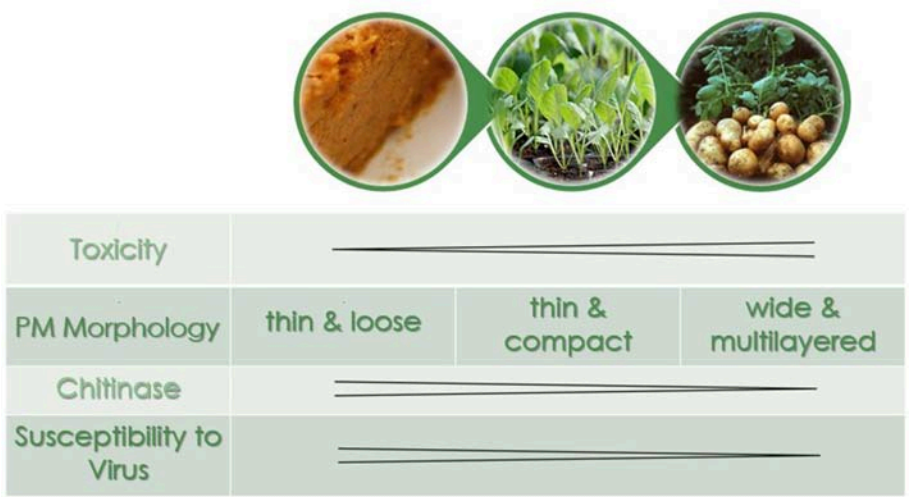

FIGURE 6 | The peritrophic matrix morphology, chitinase expression levels, and susceptibility to virus as a function of diet in 4th instar *T. ni*. In order of increasing toxicity are artificial diet, cabbage, and potato.

PM structure induced by diet, especially in the anterior end of the midgut where most AcMNPV baculovirus infections in *T. ni* occur (Javed et al., 2016). Larvae reared on artificial diet, the most susceptible to the baculovirus, not only had thin ($\leq$1 μm) and fragile PMs, they had high levels of chitinase transcripts (**Table 1**), the products of which would actively degrade chitin structures like the PM. Thus, such a thin PM would not provide a very effective barrier against viral infection. In comparison, while the PM of larvae reared on cabbage, a preferred host plant, was also thin ($\leq$1 μm), it was more uniform and dense than that seen in larvae fed artificial diet. Furthermore, the lower transcript levels of chitinases observed in the midgut of these insects would result in less degradation of the PM, which could lower the susceptibility to the baculovirus. The LD_{50} for larvae raised on potato, a non-preferred host plant laden with defensive biologically active secondary metabolites (Friedman, 2006), was higher than that for the other two treatments. This could be explained, at least in part by the fact that these larvae had thicker and less organized layers in the PM and the lowest chitinase and chitin deacetylase transcript levels. In addition the PM of larvae reared on potato also had more microvesicles (**Figure 4**), consistent with repair/reinforcement, as microvesicle membranes become partially soluble in alkaline pH and, when close to the intestinal lumen, release their contents which become incorporated into the PM (Eisemann and Binnington, 1994; Terra, 2001). The proposed relationships between diet chemistry and the corresponding effects on 4th instar *T. ni* PM morphology, chitinase gene expression regulation, and susceptibility to baculovirus are summarized in **Figure 6**.

Other potential modulators of the PM are the levels of ecdysone- and JH-induced gene expression in the midgut environment, through resulting changes to synthesis of their corresponding protein products. This is because ecdysone and JH work antagonistically to coordinate molting, a process during which the insect's chitin content is drastically altered (Truman and Riddiford, 2002). For example ecdysone induces molting, which is correlated with a thickening of the PM (Toprak et al., 2014), and larvae reared on potato had increased transcript levels of 20-hydroxyecdysone receptor and reduced levels of those for ecdysone oxidase. The latter catalyzes the conversion of ecdysone into 3-dehydroecdysone, diverting it from being processed into the active form, 20-hydroxyecdysone, which acts on ecdysone receptors to stimulate molting (Takeuchi et al., 2005). Thus differential expression of both gene groups could result in a PM with morphological characteristics of a molting, rather than a feeding, larva.

Detoxification Gene Responses to Plant Allelochemicals

The midgut's ability to detoxify plant toxins is an essential characteristic that allows insects, especially generalist species, to cope with a diversity of secondary plant compounds. Many cytochrome P450s are important enzymes in the functionalization step of detoxification (Stevens et al., 2000; Cianfrogna et al., 2002; Li et al., 2002). Glutathione S-transferases (GSTs) convert lipophilic xenobiotics into hydrophilic compounds for excretion or sequestration (Francis et al., 2005; Després et al., 2007) while UDP-glucosyl transferases (UGTs) detoxify benzoxazinoids by conjugation with a sugar (Wouters et al., 2014). All three major detoxifying enzyme families were represented in the top 50 contigs with the biggest changes in midgut transcript levels between larvae reared on potatoes and cabbage (**Supplementary Table 6**), a pattern that was much more pronounced than when comparing the midgut results of larvae reared on artificial diet with either of the host plants (**Supplementary Tables 7**, **8**). These detoxifying enzyme genes were predominantly downregulated in midguts of potato-raised larvae. A similar response was found in a comparison of midgut transcriptomes of *T. ni* larvae fed on tomato (*Solanaceae*) or *Arabidopsis thaliana* (*Brassicaceae*) (Herde and Howe, 2014), two different plant species from the same families we used in this study. Herde and Howe (2014) hypothesized that anti-nutritive proteins found in *Solanaceae* elicit large-scale remodeling of digestive enzymes and that the metabolic costs associated with digestive flexibility constrain an insect's ability to detoxify secondary metabolites when feeding on plants using this defensive strategy. However, it is difficult to isolate the relative importance of such effects on insect health from those resulting from the thickened PM, as a thicker PM could also reduce digestion and result in decreased nutrition (Plymale et al., 2008), but in nature both probably play a role.

CONCLUSIONS

We found that diet affects the susceptibility of *T. ni* larvae to AcMNPV virus infection and this would appear to be mediated through alterations to the structure of the PM and not through changes to midgut pH. Examination of gene expression in the midgut using RNA-seq showed many changes in gene expression in larvae raised on potato compared with those raised on cabbage or artificial diet, most noticeably with respect to lowered transcript levels of chitinase and chitin deacetylase genes. This could explain the thickened and multi-layered PM seen in these larvae, which could provide a more effective barrier to baculovirus infection. These changes in gene expression provide leads for further experiments, using directed approaches such as RNA interference to selectively silence individual candidate genes, to identify the specific mechanisms involved.

AUTHOR CONTRIBUTIONS

EC and CD: conceived and designed the experiments; EC, DK, and MO: performed the experiments; MO and ME: contributed reagents, materials, and analysis tools; EC, CD, and JM: wrote the manuscript; DK and ME: edited the manuscript. All authors read and approved the final document.

ACKNOWLEDGMENTS

This study was funded by Agriculture and Agri-Food Canada. The authors would like to thank: Dr. Richard Gardiner and Ms. Karen Nygard (the Biotron facility at the University of Western

Ontario)—for use and training of microscopy processing and imaging machinery, Dr. Brent J. Sinclair (University of Western Ontario) and Dr. Aiming Wang (Agriculture and Agri-Food Canada) for advice and comments throughout the duration of this study, and Ms. Emine Kaplanoglu and Mr. Patrick Chapman (Agriculture and Agri-Food Canada) for their bioinformatics assistance.

SUPPLEMENTARY MATERIAL

The Supplementary Material for this article can be found online at: https://www.frontiersin.org/articles/10.3389/fphys.2018.01348/full#supplementary-material

NCBI Sequence Read Archive submissions can be found under accession SRP124718.

REFERENCES

Adang, M. J., and Spence, K. D. (1981). Surface morphology of peritrophic membrane formation in the cabbage looper, *Trichoplusia ni*. *Cell Tissue Res.* 218, 141–147. doi: 10.1007/BF00210100

Adkisson, P. L., Vanderzant, E. S., Bull, D. L., and Allison, W. E. (1960). A wheat germ medium for rearing the pink bollworm. *J. Econ. Entomol.* 53, 759–762. doi: 10.1093/jee/53.5.759

Agrawal, A. A., and Kurashige, N. S. (2003). A role for isothiocyanates in plant resistance against the specialist herbivore *Pieris rapae*. *J. Chem. Ecol.* 29, 1403–1415. doi: 10.1023/A:1024265420375

Benjamini, Y., and Yekutieli, D. (2001). The control of the false discovery rate in multiple testing under dependency. *Ann. Stat.* 29, 1165–1188. doi: 10.1214/aos/1013699998

Brodersen, G., Johns, R., Lapointe, R., Thumbi, D., Thurston, G., Lucarotti, C. J., et al. (2012). Larval diet prior to and following virus ingestion influences the efficacy of two nucleopolyhedroviruses in whitemarked tussock moth (*Orgyia leucostigma*) caterpillars. *Can. Entomol.* 144, 447–457. doi: 10.4039/tce.2012.2

Cianfrogna, J., Zangerl, A., and Berenbaum, M. (2002). Dietary and developmental influences on induced detoxification in an oligophage. *J. Chem. Ecol.* 28, 1349–1364. doi: 10.1023/A:1016292317948

Clem, R. J., and Passarelli, A. L. (2013). Baculoviruses: sophisticated pathogens of insects. *PLOS Pathog.* 9:e1003729. doi: 10.1371/journal.ppat.1003729

Cory, J. S., and Hoover, K. (2006). Plant-mediated effects in insect-pathogen interactions. *Trends Ecol. Evol.* 21, 278–286. doi: 10.1016/j.tree.2006.02.005

Cox, C. (1990). Fieller's theorem, the likelihood and the Delta method. *Biometrics* 46, 709–718. doi: 10.2307/2532090

Després, L., David, J. P., and Gallet, C. (2007). The evolutionary ecology of insect resistance to plant chemicals. *Trends Ecol. Evol.* 22, 298–307. doi: 10.1016/j.tree.2007.02.010

Dow, J. A. (1992). pH gradients in lepidopteran midgut. *J. Exp. Biol.* 172:355–375.

Duffey, S. S., Hoover, K., Bonning, B., and Hammock, B. D. (1995). "The impact of host plant on the efficacy of baculoviruses," in *Reviews in Pesticide Toxicology*, eds M. Roe and R. Kuhr (Raleigh, NC: CTI Toxicology Communications), 137–275.

Eisemann, C. H., and Binnington, K. C. (1994). The peritrophic membrane: its formation, structure, chemical composition and permeability in relation to vaccination against ectoparasitic arthropods. *Int. J. Parasitol.* 24, 15–26. doi: 10.1016/0020-7519(94)90055-8

Felton, G., and Duffey, S. S. (1991). Reassessment of the role of gut alkalinity and detergency in insect herbivory. *J. Chem. Ecol.* 17, 1821–1836. doi: 10.1007/BF00993731

Francis, F., Vanhaelen, N., and Haubruge, E. (2005). Glutathione S-transferases in the adaptation to plant secondary metabolites in the *Myzus persicae* aphid. *Arch. Insect Biochem.* 58, 166–174. doi: 10.1002/arch.20049

Friedman, M. (2006). Potato glycoalkaloids and metabolites: roles in the plant and in the diet. *J. Agric. Food Chem.* 54, 8655–8681. doi: 10.1021/jf061471t

Granados, R. R., and Lawler, K. A. (1981). *In vivo* pathway of *Autographa californica* baculovirus invasion and infection. *Virology* 108, 297–308. doi: 10.1016/0042-6822(81)90438-4

Grubb, C. D., and Abel, S. (2006). Glucosinolate metabolism and its control. *Trends Plant Sci.* 11, 78–100. doi: 10.1016/j.tplants.2005.12.006

Harper, M. S., and Granados, R. R. (1999). Peritrophic membrane structure and formation of larval *Trichoplusia ni* with an investigation on the secretion patterns of a PM mucin. *Tissue Cell* 31, 202–211. doi: 10.1054/tice.1999.0023

Hegedus, D. D., Toprak, U., and Erlandson, M. (2016). "Chapter 3: Lepidopteran peritrophic matrix, composition, function, and formation," in *Short Views on Insect Genomics and Proteomics, Entomology in Focus 4*, ed C. Raman (New York, NY: Springer International Publishing).

Herde, M., and Howe, G. A. (2014). Host plant-specific remodeling of midgut physiology in the generalist insect herbivore *Trichoplusia ni*. *Insect Biochem. Mol.* 50, 58–67. doi: 10.1016/j.ibmb.2014.03.013

Holm, S. (1979). A simple sequentially rejective multiple test procedure. *Scand. J. Stat.* 6, 65–70.

Ianowski, J. P., Christensen, R. J., and O'Donnell, M. J. (2002). Intracellular ion activities in Malpighian tubule cells of *Rhodnius prolixus*: Evaluation of Na^+-K^+-$2Cl^-$ cotransport across the basolateral membrane. *J. Exp. Biol.* 205, 1645–1655.

Ianowski, J. P., and O'Donnell, M. J. (2004). Basolateral ion transport mechanisms during fluid secretion by Drosophila Malpighian tubules: Na^+ recycling, Na^+:K^+:$2Cl^-$ cotransport and Cl^- conductance. *J. Exp. Biol.* 207, 2599–2609. doi: 10.1242/jeb.01058

Javed, M. A., Coutu, C., Theilmann, D. A., Erlandson, M. A., and Hegedus, D. D. (2017). Proteomics analysis of *Trichoplusia ni* midgut epithelial cell brush border membrane vesicles. *Insect Sci.* doi: 10.1111/1744-7917.12547. [Epub ahead of print].

Javed, M. A., Harris, S., Willis, L. G., Theilmann, D. A., Donly, B. C., Erlandson, M. A., et al. (2016). Microscopic investigation of AcMNPV infection in the *Trichoplusia ni* midgut. *J. Invertebr. Pathol.* 141, 24–33. doi: 10.1016/j.jip.2016.10.006

Keating, S. T., Schultz, J. C., and Yendol, W. G. (1990). The effect of diet on Gypsy Moth (*Lymantria dispar*) larval midgut pH, and its relationship with larval susceptibility to a baculovirus. *J. Invertebr. Pathol.* 56, 317–326. doi: 10.1016/0022-2011(90)90118-P

Kumar, P., Pandit, S. S., Steppuhn, A., and Baldwin, I. T. (2013). Natural history-driven, plant mediated RNAi-based study reveals CYP6B46's role in a nicotine-mediated antipredator herbivore defense. *Proc. Natl. Acad. Sci. U.S.A.* 111, 1245–1252. doi: 10.1073/pnas.1314848111

Lambrix, V., Reichelt, M., Mitchell-Olds, T., Kleibenstein, D. J., and Gershenzon, J. (2001). The Arabidopsis epithiospecifier protein promotes the hydrolysis of glucosinolates to nitriles and influences *Trichoplusia ni* herbivory. *Plant Cell* 13, 2793–2807. doi: 10.1105/tpc.13.12.2793

Li, X., Berenbaum, M. R., and Schuler, M. A. (2002). Plant allelochemicals differentially regulate *Helicoverpa zea* cytochrome P450 genes. *Insect Mol. Biol.* 11, 343–351. doi: 10.1046/j.1365-2583.2002.00341.x

Martin, J. S., and Martin, M. M. (1983). Precipitation of ribulose-1,5-bis-phosphate carboxylase/oxygenase by tannic acid, quebracho, and oak foliage extracts. *J. Chem. Ecol.* 9, 285–294. doi: 10.1007/BF00988046

Mithen, R. F., Dekker, M., Verkerk, R., Rabot, S., and Johnson, I. T. (2000). The nutritional significance, biosynthesis, and bioavailability of glucosinolates in human foods. *J. Sci. Food Agric.* 80, 967–984. doi: 10.1002/(SICI)1097-0010(20000515)80:7<967::AID-JSFA597>3.0.CO;2-V

Plymale, R., Grove, M. J., Cox-Foster, D., Ostiguy, N., and Hoover, K. (2008). Plant mediated alteration of the peritrophic matrix and baculovirus infection in lepidopteran larvae. *J. Insect Physiol.* 54, 737–749. doi: 10.1016/j.jinsphys.2008.02.005

Ritz, C., Baty, F., Streibig, J. C., and Gerhard, D. (2015). Dose-response analysis using R. *PLoS ONE* 10:e014621. doi: 10.1371/journal.pone.0146021

Sarfraz, R. M., Cervantes, V., and Myers, J. H. (2011). The effect of host plant species on performance and movement behaviour of the cabbage looper *Trichoplusia ni* and their potential influences on infection by *Autographa*

californica multiple nucleopolyhedrovirus. *Agric. Forest Entomol.* 13, 157–164. doi: 10.1111/j.1461-9563.2010.00504.x

Schwarz, M., Glick, D., Lowenenstein, Y., and Soreq, H. (1995). Engineering of human cholinesterases explains and predicts diverse consequences of administration of various drugs and poisons. *Pharmacol. Ther.* 67, 283–322. doi: 10.1016/0163-7258(95)00019-D

Shikano, I., Ericsson, J. D., Cory, J. S., and Myers, J. H. (2010). Indirect plant-mediated effects on insect immunity and disease resistance in a tritrophic system. *Basic Appl. Ecol.* 11, 15–22. doi: 10.1016/j.baae.2009.06.008

Shivley, S., and Miller, W. R. (2009). The use of HDMS (hexamethyldisilazane) to replace Critical Point Drying (CPD) in the preparation of tardigrades for SEM (Scanning Electron Microscope) imaging. *Trans Kansas Acad. Sci.* 112, 198–200. doi: 10.1660/062.112.0407

Sidak, Z. (1967). Rectangular confidence regions for the means of multivariate normal distributions. *J. Am. Stat. Assoc.* 62, 626–633. doi: 10.1080/01621459.1967.10482935

Spence, K. D. (1991). "Structure and physiology of the peritrophic membrane," in *Physiology of the Insect Epidermis,* eds K. Binnington and A. Petnakaran (Melbourne, VIC: CSIRO), 77–93.

Stevens, J. L., Snyder, M. J., Koener, J. F., and Feyereisen, R. (2000). Inducible P450s of the CYP9 family from larval *Manduca sexta* midgut. *Insect Biochem. Mol.* 30, 559–568. doi: 10.1016/S0965-1748(00)00024-2

Takeuchi, H., Rigden, D. J., Ebrahimi, B., Turner, P. C., and Rees, H. H. (2005). Regulation of ecdysteroid signalling during Drosophila development: identification characterization and modelling of ecdysone oxidase, an enzyme involved in control of ligand concentration. *Biochem. J.* 389, 637–645. doi: 10.1042/BJ20050498

Talalay, P., and Fahey, J. W. (2001). Phytochemicals from cruciferous plants protect against cancer by modulating carcinogen metabolism. *J. Nutr.* 131, 3027S−3033S. doi: 10.1093/jn/131.11.3027S

Terra, W. R. (2001). The origin and functions of the insect peritrophic membrane and peritrophic gel. *Arch. Insect Biochem.* 47, 47–61. doi: 10.1002/arch.1036

Toprak, U., Hegedus, D. D., Baldwin, D., Coutu, C., and Erlandson, M. (2014). Spatial and temporal synthesis of *Mamestra configurata* peritrophic matrix through a larval stadium. *Insect Biochem. Mol. Biol.* 54, 89–97. doi: 10.1016/j.ibmb.2014.09.002

Truman, J. W., and Riddiford, L. M. (2002). Endocrine insights into the evolution of metamorphosis in insects. *Annu. Rev. Entomol.* 47, 467–500. doi: 10.1146/annurev.ento.47.091201.145230

Wadleigh, R. W., and Yu, S. J. (1988). Detoxification of isothiocyanate allelochemicals by glutathione transferase in three lepidopteran species. *J. Chem. Ecol.* 14, 1279–1288. doi: 10.1007/BF01019352

Whiteman, N. K., Gloss, A. D., Sackton, T. B., Groen, S. C., Humphrey, P. T., Lapoint, R. T. (2012). Genes involved in the evolution of herbivory by a leaf-mining, drosophilid fly. *Genome Biol. Evol.* 4, 900–916. doi: 10.1093/gbe/evs063

Winde, I., and Wittstock, U. (2011). Insect herbivore counter-adaptations to the plant glucosinolate-myrosinase system. *Phytochemistry* 72, 1566–1575. doi: 10.1016/j.phytochem.2011.01.016

Woodham, A. A. (1983). "The nutritional evaluation of leaf protein concentrates," in *Leaf Protein Concentrates*, eds L. Telek and H. D. Graham (Westport, CT: AVI Publishing Company), 415–433.

Wouters, F. C., Reichelt, M., Glauser, G., Bauer, E., Erb, M., Gershenzon, J., et al. (2014). Reglucosylation of the benzoxazinoid DIMBOA with inversion of stereochemical configuration is a detoxification strategy in lepidopteran herbivores. *Angew. Chem.* 126, 11502–11506. doi: 10.1002/ange.201406643

Yang, J., McCart, C., Woods, D. J., Terhzaz, S., Greenwood, K. G., and Dow, J. A. (2007). A Drosophila systems approach to xenobiotic metabolism. *Physiol. Genomics* 30, 223–231. doi: 10.1152/physiolgenomics.00018.2007

Conflict of Interest Statement: The authors declare that the research was conducted in the absence of any commercial or financial relationships that could be construed as a potential conflict of interest.

frontiers in Physiology

ORIGINAL RESEARCH
published: 12 November 2018
doi: 10.3389/fphys.2018.01580

Genome-Wide Profiling of *Cardinium*-Responsive MicroRNAs in the Exotic Whitefly, *Bemisia tabaci* (Gennadius) Biotype Q

*Hongran Li, Xiaoying Wei, Tianbo Ding and Dong Chu**

Key Lab of Integrated Crop Pest Management of Shandong Province, College of Plant Health and Medicine, Qingdao Agricultural University, Qingdao, China

Although the bacterial symbiont *Cardinium* has profound effects on the ecological adaptation of its host, the whitefly *Bemisia tabaci* (Gennadius) biotype Q (hereafter referred to as *B. tabaci* Q), the molecular mechanism underlying interactions between these two organisms is not yet fully understood. In this study, sRNA libraries were constructed, amplified, and sequenced for *Cardinium*-infected (C^{+}) and uninfected (C^{*-}) *B. tabaci* Q with identical genetic backgrounds. Subsequently, the genes targeted by the differentially expressed miRNAs were predicted by integrating the *B. tabaci* Q genome data. A total of 125 known and 100 novel miRNAs were identified, among which 23 significant differentially expressed miRNAs were identified in both libraries. It is noteworthy that an analysis of target genes showed that *Cardinium*-responsive miRNA-regulated genes were functional in apoptosis, reproduction, development, immune response, thermotolerance and insecticide resistance. GO and KEGG pathway analysis revealed that some miRNA-target genes are closely associated with energy metabolism. A major finding of this study was the identification of several miRNAs that may be involved in physiological processes in response to environmental stress, i.e., insecticides and high temperatures. This information will provide a foundation to help further elucidate the functions of *Cardinium* in *B. tabaci* Q.

Keywords: *Bemisia tabaci* biotype Q, *Cardinium*, insect-symbiont interaction, microRNA, expression analysis

OPEN ACCESS

Edited by:
Michel Cusson,
Natural Resources Canada, Canada

Reviewed by:
Mauro Mandrioli,
Università degli Studi di Modena e Reggio Emilia, Italy
Xiaoling Tan,
Chinese Academy of Agricultural Sciences, China

***Correspondence:**
Dong Chu
chinachudong@qau.edu.cn

Specialty section:
This article was submitted to Invertebrate Physiology, a section of the journal Frontiers in Physiology

Received: *05 July 2018*
Accepted: *23 October 2018*
Published: *12 November 2018*

Citation:
Li H, Wei X, Ding T and Chu D (2018) Genome-Wide Profiling of Cardinium-Responsive MicroRNAs in the Exotic Whitefly, Bemisia tabaci (Gennadius) Biotype Q. Front. Physiol. 9:1580. doi: 10.3389/fphys.2018.01580

INTRODUCTION

Most phloem-feeding insects are infected with maternally inherited intracellular bacteria that have been categorized as either obligate symbionts or facultative symbionts (Gaelen et al., 2009). One of these facultative symbionts, *Candidatus Cardinium hertigii* (hereafter referred as *Cardinium*), was initially characterized in *Encarsia* wasps (Zchori-Fein et al., 2004). The symbiont has been shown to be a reproductive manipulator in several arthropod taxa through various means including cytoplasmic incompatibility (CI), feminization, and induction of parthenogenesis (White et al., 2011; Penz et al., 2012). Further, more recent research has demonstrated that *Cardinium* can also affect the fitness of its host (Harris et al., 2010; Fang et al., 2014).

Our long-term field surveys showed that the infection rate by *Cardinium* remains at a low level (12.2%) in the exotic sweet potato whitefly, *Bemisia tabaci* (Gennadius) Q (hereafter referred to

as *B. tabaci* Q) in the Shandong Province, China (Chu et al., 2011). Further research revealed that competitive ability and fitness are diminished in *Cardinium*-infected *B. tabaci* populations compared to the *Cardinium*-uninfected population (Fang et al., 2014). Fitness (survival and reproductive success) of a field collected strain of *Cardinium*-infected *B. tabaci* Q, however, was shown to have unexpectedly improved after being reared under constant laboratory conditions for > 3 years (Li Hong-Ran, unpublished data). We speculated that the potential negative effect of *Cardinium* on its host whitefly may be the result of environmental stress under field conditions, i.e., in response to insecticides and high temperatures. To date, little information is available regarding the molecular mechanism underlying the *Cardinium*-mediated phenotypes of their whitefly hosts (Li et al., 2018). A more thorough understanding of this mechanism will help understand the ecological adaptation and population dynamics of this introduced pest.

MicroRNAs (abbreviated as miRNAs) are numerous non-coding small RNAs (sRNAs) (20–24 nt) involved in the regulation of gene expression post-transcriptionally, through repression of mRNA translation or degradation of mRNA in the cytoplasm (Bühler et al., 2006; Bartel, 2009; Iliopoulos et al., 2009). As a result of ongoing research, the significant roles of miRNAs in the manipulation of metabolism, development, and epigenetic inheritance are becoming better understood (Esau et al., 2006; Carlsbecker et al., 2010; Wang et al., 2018). Accumulating evidence has indicated that miRNAs are involved in regulating diverse biological processes such as apoptosis, hematopoiesis, and patterning of the nervous and immune systems in various groups of insects (Bushati and Cohen, 2007; Asgari, 2013; Xu et al., 2017). More recently, dramatic changes in the expression levels of miRNAs have also been documented in response to symbiont and host interactions. For instance, the microRNA, aae-miR-2940-5p, which is highly enriched in *Wolbachia*-infected mosquitoes, may be involved in mediating the regulation of pelo in *Aedes aegypti* (Asad et al., 2018). Also, *Wolbachia* is able to use host miRNAs to regulate host gene expression, and manipulation of the mosquito metalloprotease gene via aae-miR-2940 is crucial for efficient maintenance of the endosymbiont (Hussain et al., 2011). An analysis of target genes in the two-spotted spider mite, *Tetranychus urticae*, showed that *Wolbachia*-responsive miRNAs regulate genes associated with lysosome function, apoptosis, sphingolipid metabolism, and lipid transport in both sexes, as well as reproduction in females (Rong et al., 2014). Because miRNAs are involved in infections by bacterial symbionts, such as *Wolbachia*, we postulated that the host miRNAs might also be involved in *Cardinium*-host interactions. A test of this hypothesis would provide insights into *Cardinium*-mediated phenotypes in host whiteflies.

Based on our current knowledge, sufficient data are available to characterize the profiles of miRNAs in whiteflies. Our previous results showed different expression levels of miRNAs in *B. tabaci* B vs. Q (Guo et al., 2013). Furthermore, Wang et al. (2016) investigated the expression profiles of miRNAs in *B. tabaci* B in response to viral infection. Still, insufficient research has been directed at exploring the potential role of miRNAs in *B. tabaci*

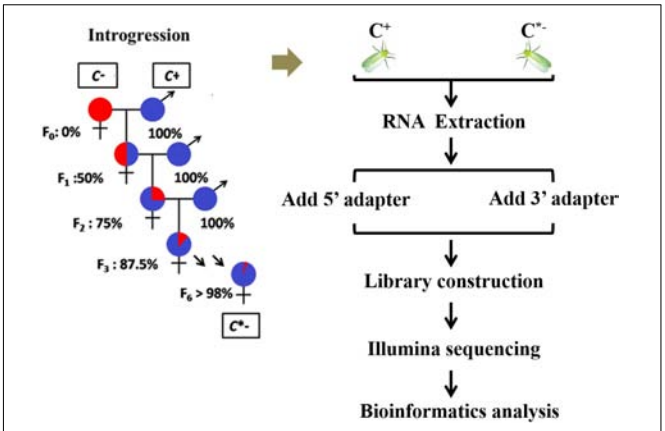

FIGURE 1 | Experimental design and schematic diagram of the workflow used in this study.

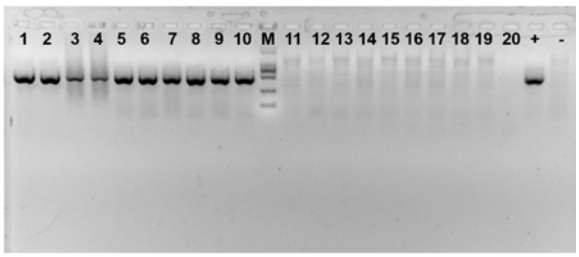

FIGURE 2 | Amplification product of *Cardinium*-infected and uninfected *Bemisia tabaci* Q using specific primers. 1–10: *Cardinium*-infected *B. tabaci* Q; 11–20: *Cardinium*-uninfected *B. tabaci* Q; + : positive control; -: negative control; M: DL2000 DNA marker.

following symbiont infection. In this study, we first established a *Cardinium*-infected *B. tabaci* Q strain (abbreviated as C^+) and an uninfected strain (abbreviated as C^{*-}) with identical genetic backgrounds. Deep sequencing of four sRNA libraries was then conducted for both C^+ and C^{*-}. Subsequently, bioinformatics analyses were carried out to categorize the sRNAs, assess differential expression of known and novel miRNAs, predict their targets and perform their functional annotation. These data will provide novel insight into the mechanism of insect-symbiont interactions, especially for *Cardinium* in *B. tabaci* Q.

MATERIALS AND METHODS

Whitefly Colony

The *B. tabaci* Q colony used in this study was established from individuals originally collected in the Shandong Province, China, in July 2012, and maintained in separate cultures for 3 years on potted cotton plants (Lu-Mian-Yan 21 cultivar). Whiteflies were kept in isolated screen cages under constant conditions of 27 ± 1°C, with a 16/8 h light/dark photoperiod, and 70 ± 5% RH. An introgressive backcrossing scheme was used to homogenize nuclear genetic backgrounds of infected and uninfected whiteflies for 6 generations, using the method

described by Turelli and Hoffmann (1991). After completion of the introgression series, > 98% of nuclear alleles were expected to be shared between the C^+ and C^{*-} whiteflies; the two strains were then regarded as having a nearly identical genetic background (**Figure 1**). The one day-old adult females that were prepared for RNA isolation were selected from these *Cardinium*-infected and uninfected *B. tabaci* Q strains. To obtain newly emerged adult females, all adult whiteflies were removed from cotton leaves containing whitefly pupae each evening (at 6:00 pm). The following morning (at 8:00 am), newly emerged adults were individually collected and transferred into plastic tubes and sexed using a stereomicroscope (Luan et al., 2008; López and Andorno, 2009). All samples were stored at −80°C until needed for RNA isolation.

Cardinium Detection in Populations

Presence of the symbiont *Cardinium* in each population was verified every 30 days from a sample of 20 adults using PCR primers to amplify a portion of the 16S rRNA gene (**Figure 2**). The primers used were CLO-F (5′- GCGGTGTAAAATGAGCGTG -3′) and CLO-R1 (5′- ACCTMTTCTTAACTCAAGCCT -3′) (Weeks et al., 2003). All PCRs were performed using 13 μL samples of a solution containing 1 × buffer, 0.16 mM of each dNTP, 0.5 mM of each primer, 0.5 unit Taq DNA polymerase (Takara, Dalian, China), and 2 μL template DNA. Cycling conditions consisted of initial denaturation at 95°C for five min, followed by 35 cycles of 1 min at 94°C for denaturation, 1 min at 58°C for annealing and 1 min at 72°C for elongation, plus a final extension step at 72°C for 7 min. All amplicons were electrophoresed, along with a negative (sterile water instead of DNA) and positive controls (DNA from previous sequencing) of the symbiont on a 1.0% agarose gel, and visualized using *Gelview* staining.

Small RNA Library Construction for Illumina Sequencing

Total RNA was isolated from the C^+ and C^{*-} strains using the Trizol reagent (Invitrogen Catalog No. 15596-026) with a slight modification of the procedure recommended by the manufacturer. In this procedure, RNA was purified several times with isopropanol and 75% ethyl alcohol. Total RNA (>3 μg) of good quality was used to construct an sRNA library for each sample by using a TruSeq small RNA Sample Pre Kit (Illumina). Briefly, total RNA was ligated with 5′ and 3′ adapters followed by reverse transcription using RT primers. After PCR amplification of the cDNAs, amplified PCR products within the 130–160 bp size range were purified on an 8% polyacrylamide gel (100 V, 80 min). The libraries were constructed with purified RNAs and were sequenced on an Illumina HiSeq 2500/2000 platform at the Novogene Company, Beijing, China.

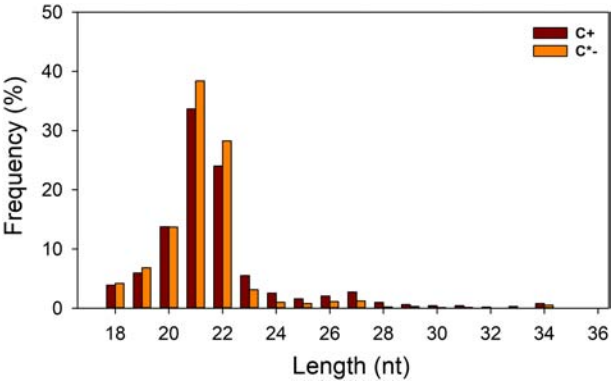

FIGURE 3 | Length distribution of small RNAs in the two libraries. C^+, *Cardinium*-infected *B. tabaci* Q; C^{*-}, *Cardinium*-uninfected *B. tabaci* Q.

Bioinformatics Analysis of Sequencing Data

After Illumina sequencing, raw data were processed using Novogene' s Perl and Python scripts. Clean data were screened to remove reads containing more than three N (undetermined bases), reads with 5′ adapter contaminants, reads without 3′ adapter or the insert tags, those containing

TABLE 1 | Statistics of small RNA sequences in C^+ and C^{*-} libraries.

Group of reads	Number of sequences				Total
	C^+1	C^+2	$C^{*-}1$	$C^{*-}2$	
Raw data	11008300	11159082	10968649	11029471	44165502
Clean reads	10752028	10895385	10675963	10738383	43061759
Mapped total reads	9922549	10113477	10137941	10270736	40444703
Mapped unique reads	2610855	2500937	2786945	2825947	10724684
Mapped total sRNA	1234106	895124	1515005	1748357	5392592
Mapped unique sRNA	592	523	644	671	2430
Mapped hairpin	152	154	152	162	170
Mapped mature[§]	111	110	109	120	125
Novel miRNA	89	81	91	96	100
Novel miRNA*	57	52	65	64	72

[§] *indicates known miRNAs; *indicates passenger strand.*

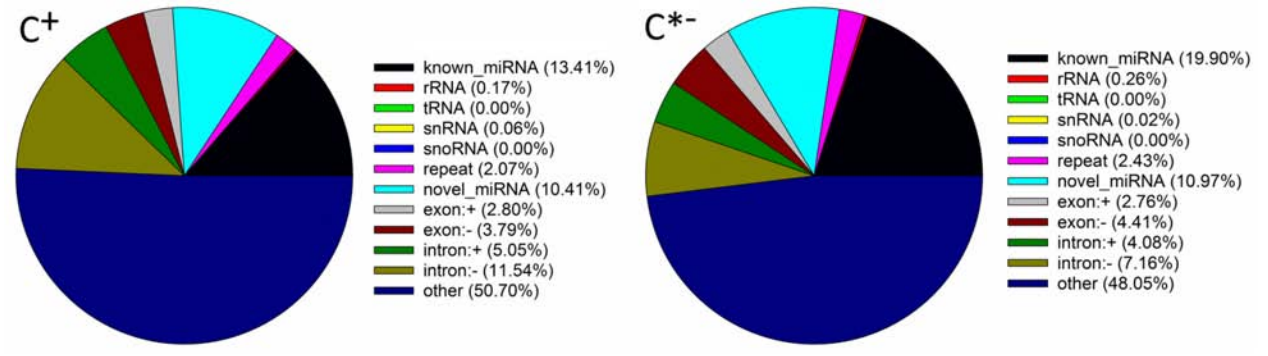

FIGURE 4 | Classification of sRNAs in the C $^{+}$ and C*$^{-}$ libraries. snRNA, small nuclear RNA; snoRNA, small nucleolar RNA; exon: + , same orientation with mRNA exon; exon: -, reverse orientation with mRNA exon; intron: + , same orientation with mRNA intron; intron: -, reverse orientation with mRNA intron; other, unannotated sRNA.

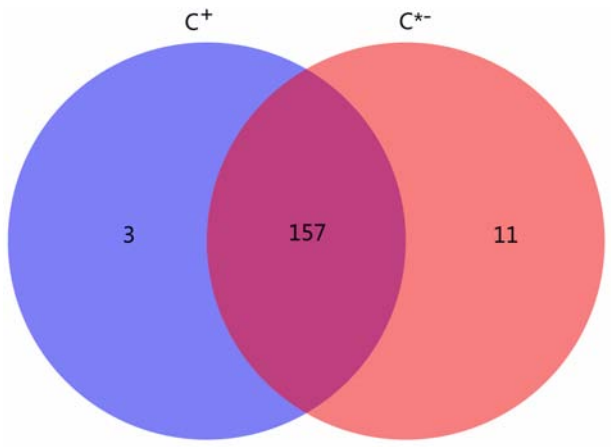

FIGURE 5 | Venn chart of miRNA expression in the C $^{+}$ vs. C*$^{-}$ strains. The blue circle represents C $^{+}$, *Cardinium*-infected *B. tabaci* Q; the red circle represents C*$^{-}$, *Cardinium*-uninfected *B. tabaci* Q.

poly A, T, G, or C and low quality reads obtained from the raw data. Then, sRNA sequences of 18–35 nt were selected to conduct all downstream analyses. To prevent every unique sRNA mapping to multiple non-coding RNA (ncRNAs), we used the following priority rule: known miRNA > rRNA > tRNA > snRNA > snoRNA > repeat > gene > novel miRNA so that every unique sRNA mapped to only one annotation. The Bowtie software was used to map the sRNA tags to the *B. tabaci* Q genome[1]) with less than 2 bp mismatch to analyze their distribution and expression (Langmead et al., 2009).

Next, the mappable sRNA tags were used to search the release of version 20.0 of miRBase to identify known miRNAs in *B. tabaci*. Known miRNAs were defined as sequences that were identical to sequences from *Drosophila melanogaster* or other insects (*Aedes aegypti*, *Apis mellifera*, *Tribolium castaneum* and *Bombyx mori*) as outlined previously (Guo et al., 2013). Then, rRNAs, tRNAs, snRNAs, and snoRNAs were removed by mapping the remained sRNA tags to Rfam[2]. Repeat sequences were discarded by using a repeat sequence database[3], and protein coding genes were filtered by mapping to the exon and intron of mRNAs of *B. tabaci*. Finally, novel miRNAs were predicted by exploring the secondary structure, the Dicer cleavage site and the minimum free energy of the former unannotated sRNA tags that could be mapped to the reference sequence by integrating two available software, miREvo and mirdeep2 (Wen et al., 2010; Friedlander et al., 2011).

Differential Expression Analysis of miRNAs Between C $^{+}$ and C*$^{-}$ Strains

miRNA levels (transcripts per million; TPM) were estimated using the following normalization formula: Normalized expression = (mapped read count/total reads)*1,000,000 (Zhou et al., 2010). Since there were two biological replicates for each sample, differential expression analysis of miRNAs between libraries was performed using the DESeq R package (1.8.3) (Anders and Huber, 2010). *P*-values were adjusted using the method of Benjamini and Hochberg (1995). The threshold level of collected *P*-values was set as 0.05 for significant differential expression.

Target Prediction and Enrichment Analysis

We used the miRanda software to identify genes targeted by miRNAs in the genome of *B. tabaci*[4] (Enright et al., 2003). To further reveal functions related to the putative target genes, GO and KEGG enrichment analysis of the predicted target genes was performed using the GOSeq/topGO2.12 and KOBAS 2.0 software (Mao et al., 2005; Kanehisa et al., 2008; Young et al., 2010).

[1]http://gigadb.org/dataset/100286

[2]http://rfam.xfam.org/

[3]http://www.repeatmasker.org/cgi-bin/WEBRepeatMasker/

[4]http://gigadb.org/dataset/100286

TABLE 2 | List of all significantly differentially expressed miRNAs in C^+ vs. C^{*-} strains.

sRNA	Potential miRNA	Log2-fold change	Target gene id	Gene description
novel_140	*	2.8072	BTA021458.1	Apoptosis-stimulating of p53 protein 2
			BTA017976.1	Glutathione S-transferase
			BTA011400.1	Heat shock protein 70 B2
novel_256	ppc-miR-2235a-9-3p	1.1904	BTA026695.3	Multidrug resistance-associated protein 4
			BTA029742.1	Cytochrome P450 9e2
			BTA019100.1	Activator of 90 kDa heat shock protein ATPase homolog 1
novel_27	cte-miR-87b	1.0441	BTA002500.1	Cytochrome P450 6k1
ame-bantam		0.70975		
novel_24	bmo-miR-13b-3p	0.69232	BTA004618.1	Multidrug resistance-associated protein 7
novel_1	ame-bantam	0.66426		
ame-miR-87		0.64842		
novel_152	pxy-miR-2b	0.63995		
novel_5	tca-miR-13a-3p	0.57691		
tca-miR-13a-3p		0.49866	BTA019714.1	Homeotic protein female sterile
ame-miR-281		0.38728		
aae-miR-277-3p		0.38109	BTA028304.1	Multidrug resistance protein MexA
dme-miR-277-3p		0.38109		
novel_19	*	−1.1005	BTA013163.1	Non-lysosomal glucosylceramidase
			BTA027909.1	30S ribosomal protein S11
bmo-miR-993b-5p		−0.99651	BTA004944.1	Larval cuticle protein A1A
bmo-miR-993a-5p		−0.96172	BTA029040.1	Polyribonucleotide nucleotidyltransferase
tca-miR-993-5p		−0.96172	BTA017354.1	Pupal cuticle protein Edg-84A
novel_193	pma-miR-133a	−0.93463	BTA017001.1	Histone H3.3
novel_36	dps-miR-927-3p	−0.73363	BTA022535.1	Meiosis arrest female protein 1 homolog
novel_42	bmo-miR-2765	−0.70818	BTA027376.1	Apoptosis-resistant E3 ubiquitin protein ligase 1
dme-miR-305-5p		−0.67412	BTA013707.1	Adult-specific rigid cuticular protein 12.4
tca-miR-305-5p		−0.66718	BTA023288.2	Cuticle protein 8
novel_3	lva-miR-278-3p	−0.44769		

*Potential miRNA, miRNA sequences of B. tabaci that were similar to those in other species but differed in some nucleotide positions. *indicates miRNA sequences were not found in other species in miRBase Version 20.0.*

The dataset that was studied in this article is available in the NCBI (SRA) public repository under accession number SRP076077.

Validation of Differentially Expressed miRNAs via qRT-PCR

Total RNA was extracted from the C^+ and C^{*-} whiteflies (taken from the same treatment samples as used for library construction). Reverse transcription was performed by Mir-X^{TM} miRNA First-Strand Synthesis Kit (Takara catalog no. 638313) under the following conditions: 37°C for 1 h, 85°C for 5 min, and then held at 4°C. Levels of miRNA were assessed in four biological and two technical replicates of each sample, using SYBR Premix EX TaqTM II (Takara catalog no. RR820A). The cDNA was quantified in 20μL reactions, containing 7.2 μL ddH_2O, 10 μL SYBR Advantage Premix (2X), 0.8 μL miRNA-specific Primer (10 uM), mRQ 3′ Primer (supplied with the Kit No. RR820A) and 2 μL template cDNA. The primers used in this study are provided in **Supplementary Table S1**. The reactions were incubated at 95°C for 10 s, followed by 40 cycles of 95°C for 5 s, 60°C for 20 s. A dissociation curve was obtained to ensure that only one product was amplified after the amplification phase. The $2^{-\Delta\Delta Ct}$ method for relative quantification of gene expression was used to determine the level of miRNA expression.

RESULTS AND DISCUSSION

Overview of the Analysis of sRNA Libraries

In this study, we generated two replicate sRNA libraries for each of the C^+ and C^{*-} strains (**Table 1**), totaling 44 million raw reads. About 43 million clean reads remained after the filtering step (see section "Materials and Methods" for details). Analysis of the length distribution among the 18–35 nt sRNAs examined here indicated that the highest proportion of small RNAs, in both strain-specific libraries, was in the 21–22 nt range (57.71 and 66.64% in the C^+ and C^{*-} libraries, respectively) (**Figure 3**). The proportion of small RNAs in the 21–22 nt range is consistent with that observed for miRNAs in animals (Li et al., 2011). But in previous studies examining miRNAs in *B. tabaci* B/Q and non-viruliferous whiteflies, length distribution showed maximum enrichment for 21–23 nt or

28–30 nt sRNAs (Guo et al., 2013; Wang et al., 2016). This difference may be due to sample treatment prior to library construction. Here, only one day-old adult females were utilized for total RNA isolation, whereas the whiteflies used in previous reports were neither isolated by sex nor segregated by time of emergence.

The mapped sRNAs fell in one of 12 categories, including known miRNAs, rRNAs, tRNA, snRNA, snoRNA, repeat, novel miRNAs, exon, intron and unannotated sRNAs (**Figure 4**). The percentages of known miRNAs in the C^{*-} libraries (19.90%) were higher than those in the C^{+} libraries (13.41%), whereas the corresponding values for novel miRNAs were similar (10.97 and 10.41%, respectively). Thus, differences of both length distribution and composition of two sRNA libraries suggest that infection by *Cardinium* may inhibit the synthesis of miRNAs in *B. tabaci*. The same results were found in *T. urticae* infected with the symbiont *Wolbachia* (Rong et al., 2014).

Identification of Known and Novel miRNA

Sequences in our libraries identical to miRNA sequences of *D. melanogaster*, *Aedes aegypti*, *Apis mellifera*, *T. castaneum* and *B. mori* were considered to be potentially known miRNAs. Following a BLASTn search against the miRBase 20.0 and subsequent sequence analysis, a total of 125 known miRNAs were identified in the four libraries (**Table 1** and **Supplementary Table S2**). Next, we used the miRNA prediction software miRDeep2 to identify putative novel miRNAs by searching against the *B. tabaci* Q genome sequence[5]. In total, 100 novel miRNAs were identified from both libraries (**Table 1**). To determine whether these novel miRNAs are known in other species, we used these miRNA sequences to search against all nucleotide sequences in miRBase Version 20.0. The results showed that 79 novel miRNA sequences of *B. tabaci* were similar to those in other species, but differed in some nucleotide positions, while 21 novel miRNA sequences were not found in other species (**Supplementary Table S3**). Thus, 21 novel miRNAs are putatively specific to whiteflies and could thus have a species-specific functions.

Among all identified known and novel miRNAs, three miRNAs [novel-122 (efu-miR-9216), novel-156 (hsa-miR-4762-3p) and tca-miR-263b-5p] were detected only in C^{+} and 11 miRNAs were found only in C^{*-}, while 157 miRNAs were found in both libraries (**Figure 5**). miR-263a/b affects expression of genes contributing to cellular and humoral immunity in *Manduca sexta* and regulates immunity-related signal transduction by affecting the expression of genes related to the *Galleria mellonella* tumor necrosis factor receptor superfamily, suggesting that the specific tca-miR-263b-5p in *Cardinium*-infected *B. tabaci* Q may be a regulator of immune processes (Mukherjee and Vilcinskas, 2014; Zhang et al., 2014). An earlier study also reported that miR-263a/b negatively regulates apoptosis, chaeta development and compound eye morphogenesis in *D. melanogaster*, suggesting that tca-miR-263b-5p may play a role in cell apoptosis in C^{+} strain (Hilgers et al., 2010).

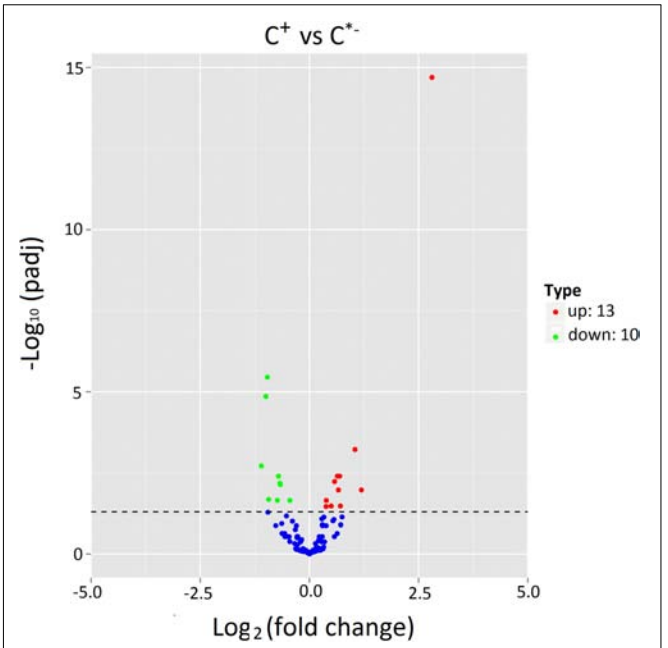

FIGURE 6 | Expression of miRNAs in C^{+} vs. C^{*-}. The x-axis represents the fold change of miRNA expression in different samples; the y-axis represents the significance of the variances on transcription levels of miRNAs. Each point represents one miRNA. Red points represent the up-regulated miRNAs. Blue points indicate equally expressed miRNAs. Green points represent down-regulated miRNAs. $P < 0.05$.

Differentially Expressed miRNAs Between C^{+} and C^{*-} Strains

The expression levels of known and novel miRNAs in C^{+} and C^{*-} libraries were compared after normalization (normalized expression = actual miRNA count/total count of clean reads × 100000). We identified 23 differentially expressed miRNAs, including 13 up-regulated miRNAs and 10 down-regulated miRNAs in the C^{+} strain relative to the C^{*-} strain (**Table 2** and **Figure 6**). The strongest up-regulation was observed for novel-140, novel-27 (cte-miR-87b), novel-256 (ppc-miR-2235a-9-3p) and ame-bantam, while the strongest down-regulation was observed for novel-19, tca-miR-993-5p, bmo-miR-993b-5p and novel-193 (pma-miR-133a).

For up-regulated miRNAs, previous studies showed that bantam miRNA simultaneously stimulates cell proliferation and prevents apoptosis in *Drosophila*, indicating that an up-regulated level of ame-bantam in the C^{+} strain may help resist apoptotic cell death (Brennecke et al., 2003). miR-87 has been reported to be associated with anti-pathogen and immune responses (Liu et al., 2015). Thus up-regulation of novel-27 (cte-miR-87b) in the present study suggests it may play a role in immune responses in *Cardinium*-infected *B. tabaci* Q. With respect to down-regulated miRNAs, lmi-miR-133 was shown to mediate phenotypic plasticity and behavioral changes between social and

[5]http://gigadb.org/dataset/100286

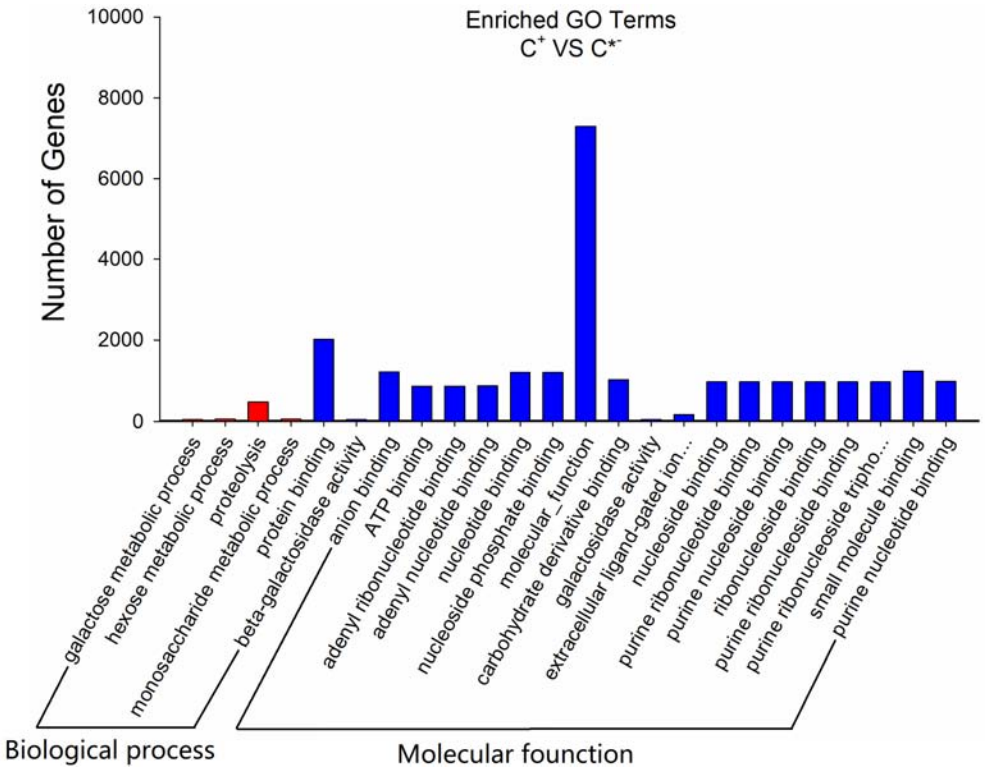

FIGURE 7 | GO analysis results of the target genes of C^+ vs. C^{*-} strains. The *x*-axis is the GO category; the *y*-axis is the number of genes.

solitary phases of henna and pale locusts by targeting key players in the dopamine synthesis pathway, indicating that novel-193 (pma-miR-133a) may modulate phenotypic plasticity in *B. tabaci* Q (Yang et al., 2014).

Prediction of Target Genes for Differentially Expressed miRNAs

To further clarify the biological functions of the differentially expressed miRNAs, we analyzed the targets of 23 of them. A total of 12760 target genes for these 23 sRNAs listed in **Table 2** were predicted. Among them, the number of target genes for each differentially expressed miRNAs ranged from 339 to more than one thousand. These results are consistent with previous findings indicating multiple miRNAs can be used to regulate a single gene and, conversely, that a single miRNA can target multiple genes, confirming the complexity of the miRNA-gene regulation network (Thomson et al., 2011).

To further assess the presumptive functions of the genes predicted to be targeted by differentially expressed miRNAs, GO (Gene Ontology) annotation enrichment was performed. GO ontologies containing four different biological processes and 20 molecular functions were predicted (**Figure 7** and **Supplementary Table S4**). The enrichment of each GO term within biological processes was compared, and most were involved in metabolic processes. As for molecular functions, the molecular function terms and most related binding terms comprised most of the targets, which is consistent with a regulatory role in transcription and translation for these miRNAs (Hobert, 2008). In addition, a KEGG (Kyoto Encyclopedia of Genes and Genomes) pathway analysis was preformed to elucidate the biological interpretation of the genes targeted by differentially expressed miRNAs (**Figure 8**). A total of 90 highly diversified biochemical pathways were identified that involved the miRNA-targeted genes, after considering a corrected *p*-value and the number of genes involved (**Supplementary Table S5**). Furthermore, a total of 1739 genes were enriched in the top 20 pathways. The "Metabolic pathways" category was the most significantly enriched term with 812 genes, followed by "Carbon metabolism" (98 genes) and "Starch and sucrose metabolism" (82 genes). The "rich factor" (x axis of **Figure 8**) represents the ratio of the number of differentially expressed genes to the total number of unigenes in the pathway. The most significant degree of enrichment was observed for the glycolysis "Glycolysis/Gluconeogenesis," "Inositol phosphate metabolism" and "Nitrogen metabolism" pathways, all related to energy metabolism.

Cardinium-Responsive miRNAs May Be Associated With Apoptosis Process in *B. tabaci* Q

The target genes of several significantly differentially expressed miRNAs in *B. tabaci* Q have been identified to be associated with apoptosis (**Table 2**). The gene BTA013163.1, targeted by

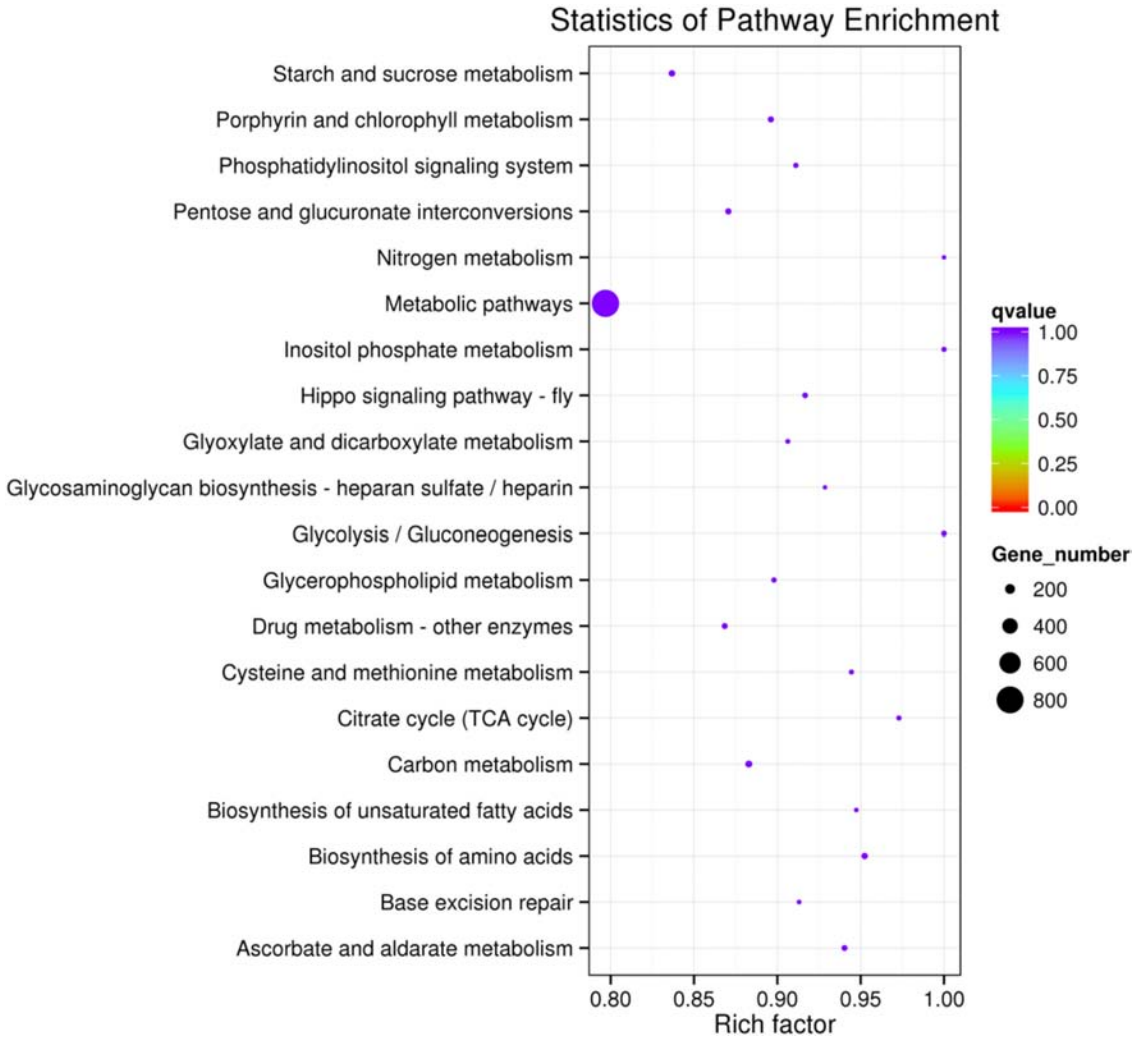

FIGURE 8 | The 20 most enriched KEGG pathways based on target genes of differentially expressed miRNAs in C^+ vs. C^{*-} strains. The *x*-axis shows the rich factor. The *y*-axis shows the pathway names. The size of each point represents the number of genes enriched in a particular pathway. The larger the value of the rich factor and the smaller the value of *q*-value indicate a more significant degree of enrichment.

down-regulated novel_19, encodes glucosylceramidase, whose deficiency can cause neurodegeneration and apoptosis in the brain of mice (Enquist et al., 2007). The observed down-regulation of novel_19 in C^+ strain may indicate its role in inhibiting apoptosis. Moreover, the gene BTA021458.1 targeted by novel_140 codes for Apoptosis-stimulating of p53 protein 2. Therefore, the observed up-regulation of novel_140 in C^+ strain may also indicate its role in decreasing apoptosis. It is well known that *Wolbachia* and *Cardinium* infection can lead to decreases in apoptosis in their respective hosts, *Drosophila mauritiana* and *Encarsia suzannae* (Fast et al., 2011; Mann et al., 2017). Female-biased genes encoding ribosomal proteins indicate an increase in general translational activity of *Cardinium* in female wasps (Mann et al., 2017). In this study, the gene BTA027909.1 targeted by down-regulated novel_19, encodes 30S ribosomal protein S11, indicating a potential increase in general translational activity of *Cardinium*. We, therefore, speculated that *Cardinium* in *B. tabaci* Q probably could inhibit apoptosis in its host, which in turn, would be beneficial to the maintenance of *Cardinium* itself.

Cardinium-Responsive miRNAs May Regulate Reproduction and Development in *B. tabaci* Q

Cardinium can induce a number of reproductive disruptions in arthropods to optimize its transmission in a manner similar to that described for *Wolbachia,* including CI and feminization (Gotoh et al., 2007; White et al., 2011). CI was expected to an increase in the production of symbiont-infected females in the population (Poinsot et al., 2003; Werren et al., 2008). In the present study, some target genes of differentially expressed miRNAs were found to be related to female reproduction. For example, the target gene BTA017001.1

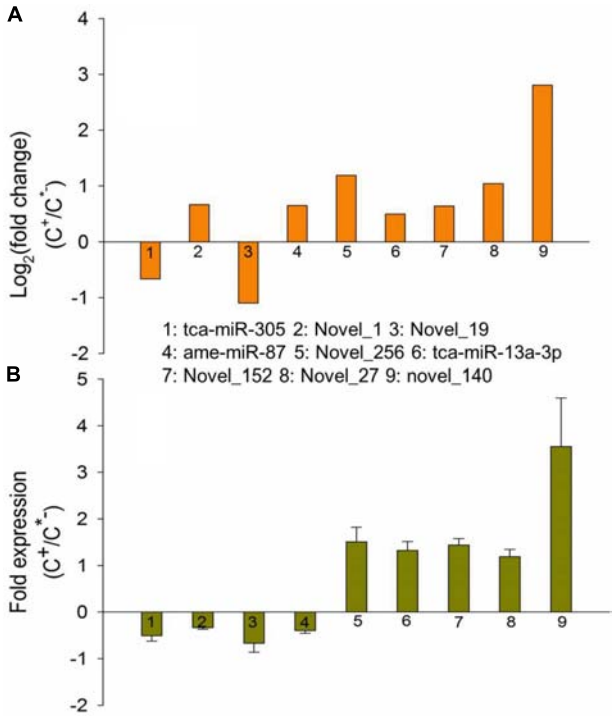

FIGURE 9 | Expression patterns of differentially expressed miRNAs identified based on Illumina sequencing **(A)** and qRT-PCR **(B)**. *X*-axis, name of the miRNAs that were selected for qRT-PCR assessment; column above the *X*-axis: miRNAs that were up-regulated in the C^+ strain; column below the *X*-axis: miRNAs that were upregulated in the C^{*-} strain.

(targeted by novel_193) codes for Histone H3.3, which is believed to play an essential role in early developmental manifestations of CI (Serbus et al., 2008). In addition, the gene BTA022535.1, which is targeted by down-regulation of novel_36, codes for "meiosis arrest female protein 1 homolog" and is involved in oogenesis (**Table 2**).The miRNA tca-miR-13a-3p was up-regulated, which is expected to result in the down-regulation of BTA019714.1, a gene involved in female sterility. Moreover, target genes BTA013707.1 (targeted by dme-miR-305-5p), BTA017354.1 (targeted by tca-miR-993-5p), BTA023288.2 (targeted by tca-miR-305-5p) and BTA004944.1 (targeted by bmo-miR-993b-5p) code for cuticle protein in specific developmental stages. The down-regulated miRNAs should result in enhanced cuticular protein production, which may be related to growth and development. Thus, our results appear to support previous observations to the effect that *Cardinium* may manipulate host female reproduction and development, although this hypothesis will need to be further tested (Rong et al., 2014).

Cardinium-Responsive miRNAs May Be Essential in *B. tabaci* Q Under Stress Conditions

Accumulating evidence indicates that miRNAs play an important role in drug resistance, as revealed by miRNA expression profiling (Xin et al., 2008; Ma et al., 2010; Zheng et al., 2010). In the present study, target gene BTA004618.1 (targeted by novel_24) codes for multidrug resistance-associated protein 7, and target genes such as BTA017976.1 (targeted by novel_140), BTA002500.1 (targeted by novel_27) and BTA029742.1 (targeted by novel_256) are related to glutathione S-transferase and cytochrome P450. In addition, target gene BTA026695.3 (targeted by novel_256) and BTA028304.1 (targeted by aae-miR-277-3p) are related to drug resistance as well. Those up-regulated miRNAs may reduce their targeted gene expression. Additionally, the target gene BTA011400.1 (targeted by novel_140) and BTA019100.1 (targeted by novel_256), encoding "Heat shock protein (HSP) 70 B2" and "Activator of 90 kDa HSP ATPase homolog 1." The up-regulated miRNAs may result in reduced HSP protein production, which may depress tolerance. Taken together, our observations support our earlier speculation that the C^+ strain may have lower thermotolerance, insecticide resistance and detoxification than the C^{*-} strain.

qPCR Validation of Differentially Expressed miRNAs

To further validate the expression patterns of miRNAs identified in this work, we randomly selected nine differentially expressed miRNAs to measure the expression levels via quantitative real time polymerase chain reaction (qRT-PCR). The results showed that seven miRNAs had qPCR expression patterns similar to those revealed by our RNA-seq analysis in the C^+ and C^{*-} strains. For example, novel-140 had been found to be highly expressed in the C^+ strain, displaying a 2.8 log2-fold change compared with the C^{*-} strain (**Table 2** and **Figure 9A**), while similar results were obtained through a qPCR assessment, where approximately 4 times greater expression was found in the C^+ strain (**Figure 9B**). However, two miRNAs, novel_1 and ame-miR-87, exhibited a decrease in expression in C^+ as compared to C^{*-} strain, which is the opposite of what the Illumina sequencing revealed. The reason for these differences is currently unknown. Overall, the qPCR results tend to indicate that the Illumina sequencing data accurately reflected the expression level of miRNAs.

CONCLUSION

Using high-throughput sRNA sequencing, we screened out 23 miRNAs exhibiting differential expression in response to *Cardinium* infection in *B. tabaci* Q. These miRNAs are involved in several biological processes, including cell apoptosis, reproduction and development. The major finding of this study is the identification of several miRNAs overexpressed in infected whiteflies that target genes involved in thermotolerance and insecticide resistance, pointing to a compromised resistance to heat and xenobiotic stresses in C^+ individuals. These findings may help explain fitness variation among *Cardinium*-infected *B. tabaci* Q whiteflies in response to environmental stress. In general, our

findings lay a solid foundation for further functional study of the interactions between *Cardinium* and its host whitefly, *B. tabaci* Q.

ETHICS STATEMENT

The present research complies with all laws of the country (China) in which it was performed and was approved by the Department of Science and Technology of the Qingdao Agricultural University, China (Permit Number: 20110712).

AUTHOR CONTRIBUTIONS

DC contributed to experimental design and management. HL carried out the data analysis and drafted the manuscript. XW and TD participated in data analysis. All authors read and approved the final manuscript.

FUNDING

This research was supported by the National Natural Science Foundation of China (31572064) and the Taishan Mountain Scholar Constructive Engineering Foundation of Shandong.

ACKNOWLEDGMENTS

We thank Novogene Company (Beijing) for helping with small RNA sequencing.

SUPPLEMENTARY MATERIAL

The Supplementary Material for this article can be found online at: https://www.frontiersin.org/articles/10.3389/fphys.2018.01580/full#supplementary-material

REFERENCES

Anders, S., and Huber, W. (2010). Differential expression analysis for sequence count data. *Genome Biol.* 11:R106. doi: 10.1186/gb-2010-11-10-r106

Asad, S., Hussain, M., Hugo, L., Osei-Amo, S., Zhang, G., Watterson, D., et al. (2018). Suppression of the pelo protein by *Wolbachia* and its effect on dengue virus in *Aedes aegypti*. *PLoS Negl. Trop. Dis.* 12:e0006405. doi: 10.1371/journal.pntd.0006405

Asgari, S. (2013). MicroRNA functions in insects. *Insect Biochem. Mol. Biol.* 43, 388–397. doi: 10.1016/j.ibmb.2012.10.005

Bartel, D. P. (2009). MicroRNAs: target recognition and regulatory functions. *Cell* 136, 215–233. doi: 10.1016/j.cell.2009.01.002

Benjamini, Y., and Hochberg, Y. (1995). Controlling the false discovery rate: a practical and powerful approach to multiple testing. *J. R. Stat. Soc.* 57, 289–300.

Brennecke, J., Hipfner, D. R., Stark, A., Russell, R. B., and Cohen, S. M. (2003). bantam encodes a developmentally regulated microRNA that controls cell proliferation and regulates the proapoptotic gene hid in *Drosophila*. *Cell* 113, 25–36. doi: 10.1016/S0092-8674(03)00231-9

Bühler, M., Verdel, A., and Moazed, D. (2006). Tethering RITS to a nascent transcript initiates RNAi- and heterochromatin-dependent gene silencing. *Cell* 125, 873–886. doi: 10.1016/j.cell.2006.04.025

Bushati, N., and Cohen, S. M. (2007). microRNA functions. *Annu. Rev. Cell Dev. Biol.* 23, 175–205. doi: 10.1146/annurev.cellbio.23.090506.123406

Carlsbecker, A., Lee, J. Y., Roberts, C. J., Dettmer, J., Lehesranta, S., Zhou, J., et al. (2010). Cell signalling bymicroRNA165/6 directs gene dose-dependent root cell fate. *Nature* 465, 316–321. doi: 10.1038/nature08977

Chu, D., Gao, C. S., De Barro, P., Zhang, Y. J., Wan, F. H., and Khan, I. A. (2011). Further insights into the strange role of bacterial endosymbionts in whitefly, *Bemisia tabaci*: comparison of secondary symbionts from biotypes B and Q in China. *Bull. Entomol. Res.* 101, 477–486. doi: 10.1017/S0007485311000083

Enquist, I. B., Bianco, C. L., Ooka, A., Nilsson, E., Månsson, J. E., Ehinger, M., et al. (2007). Murine models of acute neuronopathic Gaucher disease. *Proc. Natl. Acad. Sci. U.S.A.* 104, 17483–17488. doi: 10.1073/pnas.0708086104

Enright, A. J., John, B., Gaul, U., Tuschl, T., Sander, C., and Marks, D. (2003). MicroRNA targets in *Drosophila*. *Genome Biol.* 5:R1. doi: 10.1186/gb-2003-5-1-r1

Esau, C., Davis, S., Murray, S. F., Yu, X. X., Pandey, S. K., Pear, M., et al. (2006). miR-122 regulation of lipid metabolism revealed by in vivo antisense targeting. *Cell Metab.* 3, 87–98. doi: 10.1016/j.cmet.2006.01.005

Fang, Y. W., Liu, L. Y., Zhang, H. L., Jiang, D. F., and Chu, D. (2014). Competitive ability and fitness differences between two introduced populations of the invasive whitefly *Bemisia tabaci* Q in China. *PLoS One* 6:e100423. doi: 10.1371/journal.pone.0100423

Fast, E. M., Toomey, M. E., Panaram, K., Desjardins, D., Kolaczyk, E. D., and Frydman, H. M. (2011). *Wolbachia* enhance *Drosophila* stem cell proliferation and target the germline stem cell niche. *Science* 334, 990–992. doi: 10.1126/science.1209609

Friedlander, M. R., Mackowiak, S. D., Li, N., Chen, W., and Rajewsky, N. (2011). miRDeep2 accurately identifies known and hundreds of novel microRNA genes in seven animal clades. *Nucleic Acids Res.* 40, 37–52. doi: 10.1093/nar/gkr688

Gaelen, R. B., Benjamin, B. N., Colin, F., and Nancy, A. M. (2009). Evolution and diversity of facultative symbionts from the aphid subfamily Lachninae. *Appl. Environ. Microb.* 75, 5328–5335. doi: 10.1128/AEM.00717-09

Gotoh, T., Noda, H., and Ito, S. (2007). Cardinium symbionts cause cytoplasmic incompatibility in spider mites. *Heredity* 98, 13–20. doi: 10.1038/sj.hdy.6800881

Guo, Q., Tao, Y. L., and Chu, D. (2013). Characterization and comparative profiling of miRNAs in invasive *Bemisia tabaci* (Gennadius) B and Q. *PLoS One* 9:e59884. doi: 10.1371/journal.pone.0059884

Harris, L., Kelly, S., Hunter, M., and Perlman, S. (2010). Population dynamics and rapid spread of Cardinium, a bacterial endosymbiont causing cytoplasmic incompatibility in *Encarsia pergandiella* (Hymenoptera: Aphelinidae). *Heredity* 104, 239–246. doi: 10.1038/hdy.2009.130

Hilgers, V., Bushati, N., and Cohen, S. M. (2010). *Drosophila* microRNAs 263a/b confer robustness during development by protecting nascent sense organs from apoptosis. *PLoS Biol.* 2010:e1000396. doi: 10.1371/journal.pbio.1000396

Hobert, O. (2008). Gene regulation by transcription factors and microRNAs. *Science* 319, 1785–1786. doi: 10.1126/science.1151651

Hussain, M., Frentiu, F. D., Moreira, L. A., O'Neill, S. L., and Asgaria, S. (2011). *Wolbachia* uses host microRNAs to manipulate host gene expression and facilitate colonization of the dengue vector *Aedes aegypti*. *Proc. Natl. Acad. Sci. U.S.A.* 108, 9250–9255. doi: 10.1073/pnas.1105469108

Iliopoulos, D., Hirsch, H. A., and Struhl, K. (2009). An epigenetic switch involving NF-kappaB, Lin28, Let-7 MicroRNA, and IL6 links inflammation to cell transformation. *Cell* 139, 693–706. doi: 10.1016/j.cell.2009.10.014

Kanehisa, M., Araki, M., Goto, S., Hattori, M., Hirakawa, M., Itoh, M., et al. (2008). KEGG for linking genomes to life and the environment. *Nucleic Acids Res.* 36, 480–484. doi: 10.1093/nar/gkm882

Langmead, B., Trapnell, C., Pop, M., and Salzberg, S. L. (2009). Ultrafast and memory-efficient alignment of short DNA sequences to the human genome. *Genome Biol.* 10:R25. doi: 10.1186/gb-2009-10-3-r25

Li, H. R., Harwood, J. D., Liu, T. X., and Chu, D. (2018). Novel proteome and acetylome of *Bemisia tabaci* Q in response to Cardinium infection. *BMC Genomics* 19:523. doi: 10.1186/s12864-018-4907-3

Li, T. T., Wu, R. M., Zhang, Y., and Zhu, D. H. (2011). A systematic analysis of the skeletal muscle miRNA transcriptome of chicken varieties with divergent skeletal muscle growth identifies novel miRNAs and differentially expressed miRNAs. *BMC Genomics* 12:186. doi: 10.1186/1471-2164-12-186

Liu, Y. X., Zhou, Y. H., Wu, J. Y., Zheng, P. M., Li, Y. J., Zheng, X. Y., et al. (2015). The expression profile of Aedes albopictus miRNAs is altered by dengue virus serotype-2 infection. *Cell Biosci.* 5:16. doi: 10.1186/s13578-015-0009-y

López, S. N., and Andorno, A. V. (2009). Evaluation of the local population of *Eretmocerus mundus* (Hymenoptera: Aphelinidae) for biological control of *Bemisia tabaci* biotype B (Hemiptera: Aleyrodidae) in greenhouse peppers in Argentina. *Biol. Control* 50, 317–323. doi: 10.1016/j.biocontrol.2009.05.002

Luan, J. B., Ruan, Y. M., Zhang, L., and Liu, S. S. (2008). Pre-copulation intervals, copulation frequencies, and initial progeny sex ratios in two biotypes of whitefly, *Bemisia tabaci*. *Entomol. Exp. Appl.* 129, 316–324. doi: 10.1111/j.1570-7458.2008.00777.x

Ma, J., Dong, C., and Ji, C. (2010). MicroRNA and drug resistance. *Cancer Gene Ther.* 17, 523–531. doi: 10.1038/cgt.2010.18

Mann, E., Stouthamer, C. M., Kelly, S. E., Dzieciol, M., Hunter, M. S., and Schmitz-Esser, S. (2017). Transcriptome sequencing reveals novel candidate genes for Cardinium hertigii-caused cytoplasmic incompatibility and host-cell interaction. *mSystems* 21:e00141-17. doi: 10.1128/mSystems.00141-17

Mao, X., Cai, T., Olyarchuk, J. G., and Wei, L. (2005). Automated genome annotation and pathway identification using the KEGG orthology (KO) as a controlled vocabulary. *Bioinformatics* 21, 3787–3793. doi: 10.1093/bioinformatics/bti430

Mukherjee, K., and Vilcinskas, A. (2014). Development and immunity-related microRNAs of the lepidopteran model host *Galleria mellonella*. *BMC Genomics* 15:705. doi: 10.1186/1471-2164-15-705

Penz, T., Schmitz-Esser, S., Kelly, S. E., Cass, B. N., Müller, A., Woyke, T., et al. (2012). Comparative genomics suggests an independent origin of cytoplasmic incompatibility in Cardinium hertigii. *PLoS Genet.* 8:e1003012. doi: 10.1371/journal.pgen.1003012

Poinsot, D., Charlat, S., and Merçot, H. (2003). On the mechanism of *Wolbachia* induced cytoplasmic incompatibility: confronting the models with the facts. *Bioessays* 25, 259–265. doi: 10.1002/bies.10234

Rong, X., Zhang, Y. K., Zhang, K. J., and Hong, X. Y. (2014). Identification of *Wolbachia*-responsive microRNAs in the two-spotted spider mite, *Tetranychus urticae*. *BMC Genomics* 15:1122. doi: 10.1186/1471-2164-15-1122

Serbus, L. R., Casper-Lindley, C., Landmann, F., and Sullivan, W. (2008). The genetics and cell biology of *Wolbachia*-host interactions. *Annu. Rev. Genet.* 42, 683–707. doi: 10.1146/annurev.genet.41.110306.130354

Thomson, D. W., Bracken, C. P., and Goodall, G. J. (2011). Experimental strategies for microRNA target identification. *Nucleic Acids Res.* 39, 6845–6853. doi: 10.1093/nar/gkr330

Turelli, M., and Hoffmann, A. A. (1991). Rapid spread of an inherited incompatibility factor in California *Drosophila*. *Nature* 353, 440–442. doi: 10.1038/353440a0

Wang, B., Wang, L. L., Chen, F. Y., Yang, X. L., Ding, M., Zhang, Z. K., et al. (2016). MicroRNA profiling of the whitefly *Bemisia tabaci* middle East-Aisa Minor I following the acquisition of Tomato yellow leaf curl China virus. *Virol. J.* 13, 183–197. doi: 10.1186/s12985-016-0469-7

Wang, Z. Z., Ye, X. Q., Shi, M., Li, F., Wan, Z. H., Zhou, Y. N., et al. (2018). Parasitic insect-derived mi RNAs modulate host development. *Nat. Commun.* 9:2205. doi: 10.1038/s41467-018-04504-1

Weeks, A. R., Velten, R., and Stouthamer, R. (2003). Incidence of a new sex-ratio-distorting endosymbiotic bacterium among arthropods. *Proc. R. Soc. Lond. B* 270, 1857–1865. doi: 10.1098/rspb.2003.2425

Wen, M., Shen, Y., Shi, S., and Tang, T. (2010). miREvo: an integrative microRNA evolutionary analysis platform for next-generation sequencing experiments. *BMC Bioinformatics* 13:140. doi: 10.1186/1471-2105-13-140

Werren, J. H., Baldo, L., and Clark, M. E. (2008). *Wolbachia*: master manipulators of invertebrate biology. *Nat. Rev. Microbiol.* 6, 741–751. doi: 10.1038/nrmicro1969

White, J. A., Kelly, S. E., Cockburn, S. N., Perlman, S. J., and Hunter, M. S. (2011). Endosymbiont costs and benefits in a parasitoid infected with both *Wolbachia* and Cardinium. *Heredity* 106, 585–591. doi: 10.1038/hdy.2010.89

Xin, F., Li, M., Balch, C., Thomson, M., Fan, M., Liu, Y., et al. (2008). Computational analysis of microRNA profiles and their target genes suggests significant involvement in breast cancer antiestrogen resistance. *Bioinformatics* 25, 430–434. doi: 10.1093/bioinformatics/btn646

Xu, J., Xu, X. X., Li, S. Z., Wang, S., Xu, X. J., Zhou, X. Q., et al. (2017). Genome-Wide Profiling of *Plutella xylostella* immunity-related miRNAs after *Isaria fumosorosea* infection. *Front. Physiol.* 8:1054. doi: 10.3389/fphys.2017.01054

Yang, M., Wei, Y., Jiang, F., Wang, Y., Guo, X., He, J., et al. (2014). MicroRNA-133 inhibits behavioral aggregation by controlling dopamine synthesis in locusts. *PLoS Genet.* 10:e1004206. doi: 10.1371/journal.pgen.1004206

Young, M. D., Wakefield, M. J., Smyth, G. K., and Oshlack, A. (2010). goseq: gene ontology testing for RNA-seq datasets. *Genome Biol.* 11:R14. doi: 10.1186/gb-2010-11-2-r14

Zchori-Fein, E., Perlman, S. J., Kelly, S. E., Katzir, N., and Hunter, M. S. (2004). Characterization of a 'Bacteroidetes' symbiont in *Encarsia* wasps (Hymenoptera: Aphelinidae): proposal of 'Candidatus Cardinium hertigii'. *Int. J. Syst. Evol. Microbiol.* 54, 961–968. doi: 10.1099/ijs.0.02957-0

Zhang, X., Zheng, Y., Jagadeeswaran, G., Ren, R., Sunkar, R., and Jiang, H. (2014). Identification of conserved and novel microRNAs in Manduca sexta and their possible roles in the expression regulation of immunity-related genes. *Insect Biochem. Mol. Biol.* 47, 12–22. doi: 10.1016/j.ibmb.2014.01.008

Zheng, T., Wang, J., Chen, X., and Liu, L. (2010). Role of microRNA in anticancer drug resistance. *Int. J. Cancer* 126, 2–10. doi: 10.1002/ijc.24782

Zhou, L., Chen, J., Li, Z., Li, X., Hu, X. D., Huang, Y., et al. (2010). Integrated profiling of microRNAs and mRNAs: microRNAs located on Xq27.3 associate with clear cell renal cell carcinoma. *PLoS One* 5:e15224. doi: 10.1371/journal.pone.0015224

Conflict of Interest Statement: The authors declare that the research was conducted in the absence of any commercial or financial relationships that could be construed as a potential conflict of interest.

frontiers in Physiology

ORIGINAL RESEARCH
published: 26 November 2018
doi: 10.3389/fphys.2018.01678

Novel Factors of Viral Origin Inhibit TOR Pathway Gene Expression

Rosanna Salvia[1†], Marisa Nardiello[1†], Carmen Scieuzo[1†], Andrea Scala[1†], Sabino A. Bufo[1], Asha Rao[2], Heiko Vogel[3] and Patrizia Falabella[2]*

[1] Department of Sciences, University of Basilicata, Potenza, Italy, [2] Department of Biology, Texas A&M University, College Station, TX, United States, [3] Department of Entomology, Max Planck Institute for Chemical Ecology, Jena, Germany

Polydnaviruses (PDVs) are obligate symbionts of endoparasitoid wasps, which exclusively attack the larval stages of their lepidopteran hosts. The Polydnavirus is injected by the parasitoid female during oviposition to selectively infect host tissues by the expression of viral genes without undergoing replication. *Toxoneuron nigriceps* bracovirus (*Tn*BV) is associated with *Toxoneuron nigriceps* (Hymenoptera: Braconidae) wasp, an endoparasitoid of the tobacco budworm larval stages, *Heliothis virescens* (Lepidoptera: Noctuidae). Previous studies showed that *Tn*BV is responsible for alterations in host physiology. The arrest of ecdysteroidogenesis is the main alteration which occurs in last (fifth) instar larvae and, as a consequence, prevents pupation. *Tn*BV induces the functional inactivation of *H. virescens* prothoracic glands (PGs), resulting in decreased protein synthesis and phosphorylation. Previous work showed the involvement of the PI3K/Akt/TOR pathway in *H. virescens* PG ecdysteroidogenesis. Here, we demonstrate that this cellular signaling is one of the targets of *Tn*BV infection. Western blot analysis and enzyme immunoassay (EIA) showed that parasitism inhibits ecdysteroidogenesis and the phosphorylation of the two targets of TOR (4E-BP and S6K), despite the stimulation of PTTH contained in the brain extract. Using a transcriptomic approach, we identified viral genes selectively expressed in last instar *H. virescens* PGs, 48 h after parasitization, and evaluated expression levels of PI3K/Akt/TOR pathway genes in these tissues. The relative expression of selected genes belonging to the TOR pathway (*tor*, *4e-bp,* and *s6k*) in PGs of parasitized larvae was further confirmed by qRT-PCR. The down-regulation of these genes in PGs of parasitized larvae supports the hypothesis of *Tn*BV involvement in blocking ecdysteroidogenesis, through alterations of the PI3K/Akt/TOR pathway at the transcriptional level.

Keywords: Polydnavirus, *Tn*BV, PI3K/Akt/TOR, ecdysteroidogenesis, prothoracic glands

OPEN ACCESS

Edited by:
Guy Smagghe,
Ghent University, Belgium

Reviewed by:
Takashi Koyama,
University of Copenhagen, Denmark
Shelley Adamo,
Dalhousie University, Canada

***Correspondence:**
Patrizia Falabella
patrizia.falabella@unibas.it

† These authors have contributed equally to this work

Specialty section:
This article was submitted to Invertebrate Physiology, a section of the journal Frontiers in Physiology

Received: *02 June 2018*
Accepted: *08 November 2018*
Published: *26 November 2018*

Citation:
Salvia R, Nardiello M, Scieuzo C, Scala A, Bufo SA, Rao A, Vogel H and Falabella P (2018) Novel Factors of Viral Origin Inhibit TOR Pathway Gene Expression. Front. Physiol. 9:1678. doi: 10.3389/fphys.2018.01678

Abbreviations: 4E-BP, translational repressor 4E-binding protein; Akt, protein kinase B; ANOVA, analysis of variance; BE, brain equivalent; BLAST, basic local alignment search tool; BSA, bovine serum albumin; ECL, enhanced chemo luminescence; EIA, enzyme immunoassay; GO, Gene Ontology; NCBI, National Center for Biotechnology Information; PBS, phosphate-buffered saline; PDV, polydnavirus; PG, prothoracic gland; PI3K, phosphoinositide 3-kinase; PTP, protein tyrosine phosphatase; PTTH, prothoracicotropic hormone; S6K, p70 ribosomal protein S6 kinase; SEM, standard error of mean; TBS-T, tris-buffered saline-Tween 20; *Tn*BV, *Toxoneuron nigriceps* bracovirus; TOR, target of rapamycin.

INTRODUCTION

Toxoneuron nigriceps (Viereck) (Hymenoptera: Braconidae) is a solitary braconid endoparasitoid wasp of the tobacco budworm *Heliothis virescens* (Fabricius) (Lepidoptera: Noctuidae) larval stages. During oviposition, *T. nigriceps* female injects several maternal factors into the host (Lewis and Vinson, 1968; Pennacchio et al., 1993), which are able to modulate the host immune system and endocrine balance, in order to create a suitable environment for parasitoid progeny development (Beckage and Gelman, 2004; Pennacchio and Strand, 2006; Falabella et al., 2007; Moreau and Asgari, 2015). Maternal factors include protein rich venom (Laurino et al., 2016) and the ovarian calyx fluid, composed of ovarian proteins and an obligate symbiotic virus belonging to the Polydnaviridae family, the *Toxoneuron nigriceps* bracovirus (*Tn*BV) (Lewis and Vinson, 1968). The genome of Polydnaviruses (PDVs) consists of multiple double-stranded segmented circular DNA, integrated as provirus into the wasp genome, specifically associated in a mutualistic symbiosis (Webb et al., 2000; Webb and Strand, 2005). PDVs integrated into the parasitoid genome replicate exclusively in wasp ovaries, where their circular genome is generated from linear DNA copies of insect chromosomes (Varricchio et al., 1999; Volkoff et al., 2010; Dupuy et al., 2011). PDVs express their genes, without any replication event, in several host tissues, causing alterations in their physiology and enabling parasitoid larvae to survive, grow and finally pupate in silken cocoons (Strand and Burke, 2014). Thus, successful development of parasitoid wasp ensures vertical transmission of the integrated viral genome to the next generation (Strand, 2010).

In *H. virescens* larvae parasitized by *T. nigriceps*, the main infection target tissues are haemocytes and prothoracic glands (PGs) (Stoltz and Vinson, 1979; Wyder et al., 2003), where *Tn*BV expresses several genes belonging to different families encoding protein tyrosine phosphatases (PTPs), the largest gene family in bracovirus (Provost et al., 2004; Falabella et al., 2006, 2007; Webb et al., 2006), ankyrin motif protein (ANK) (Falabella et al., 2007; Salvia et al., 2017), UDP dehydrogenase, proteins containing Ben domains (Park and Kim, 2010; Falabella et al., unpublished data). Other viral genes expressed in the host are *Tn*BV1, implicated in immune suppression (Varricchio et al., 1999; Malva et al., 2004) and activating caspase proteins (Lapointe et al., 2005) and *Tn*BV2 encoding a retroviral aspartyl protease (Falabella et al., 2003). Previous studies reported that *H. virescens* PGs explanted from parasitized last (fifth) instar larvae do not respond to the stimulus of the prothoracicotropic hormone (PTTH), the neuropeptide that triggers ecdysone production (Pennacchio et al., 1997, 1998a). Besides the inhibition of ecdysteroidogenesis, a decrease of protein synthesis and a complete inhibition of PTTH-induced phosphorylation of some unidentified proteins in PGs of parasitized larvae were observed (Pennacchio et al., 1997, 1998a). Moreover, it was demonstrated that *Tn*BV is responsible for the functional inactivation of PGs and thus for blocking host pupation (Pennacchio et al., 1998a) due to the reduction of ecdysone biosynthesis in parasitized last instar larvae. Recent work reported that the TOR pathway is involved in ecdysteroidogenesis in some lepidopteran species (Gu et al., 2012; Kemirembe et al., 2012), including *H. virescens* (Scieuzo et al., 2018).

In this work, we show that specific *Tn*BV genes are expressed in PGs of *H. virescens* last instar larvae and we argue that they could be involved in blocking ecdysteroidogenesis, at least in part, through negative regulation of the PI3K/Akt/TOR pathway at the transcriptional level.

MATERIALS AND METHODS

Insect Rearing and Staging

Toxoneuron nigriceps wasps were reared on larval stages of its host, *Heliothis virescens*, according to Vinson et al. (1973). *Heliothis virescens* larvae were maintained on a standard artificial diet developed by Vanderzant et al. (1962). Rearing temperature was maintained at 29 ± 1°C for the host, parasitized host larvae and cocoons. *Toxoneuron nigriceps* adults were kept at 25 ± 1°C and fed with water and honey. In both cases, a 16:8 light/dark photoperiod and a relative humidity of 70 ± 5% were adopted. Late 2 or early 3 days old last (fifth) instar larvae of *H. virescens* were individually parasitized by *T. nigriceps* and maintained as described by Pennacchio et al. (1994). *H. virescens* last instar larvae were staged according to Webb and Dahlman (1985) and synchronized as reported by Pennacchio et al. (1992).

Dissection of Prothoracic Glands

The prothoracic glands (PGs) from parasitized and non-parasitized *H. virescens* 3 days old last instar larvae were dissected in 1X phosphate-buffered saline (PBS) as previously reported (Pennacchio et al., 1998a).

Glands were incubated at 25°C in 100 μl of Grace's insect medium (Sigma-Aldrich, St. Louis, MO, United States) for 30 min (time of rest) in order to reduce the possibility of their activation by experimental manipulation, as reported for *Manduca sexta* PGs (Bollenbacher et al., 1983; Smith et al., 1986).

Extraction of Prothoracicotropic Hormone

The brain extract containing PTTH (hereafter referred to as PTTH) was prepared by homogenizing brains dissected from an equal number of *H. virescens* 3 and early 4 days old last instar larvae and stored in ice-cold Grace's insect medium (Sigma-Aldrich, St. Louis, MO, United States). The homogenate was placed in boiling water for 2 min, cooled to 4°C on ice and centrifuged at 15,000 g at 4°C for 5 min (Pennacchio et al., 1997). Before being used, PTTH extract was filtered with a 0.20 μm Sterile Syringe Filter (Corning Incorporated, Corning, NY, United States) and then diluted in Grace's insect medium to 0.1 brain equivalent/μl (BE/μl) and either used immediately for the experiments described below or stored at −80°C.

Analysis of Protein Phosphorylation

The effect of parasitism on the phosphorylation of the TOR targets 4E-BP and S6K was studied in PGs explanted from parasitized and non-parasitized last instar larvae, under six different experimental conditions: basal PGs incubated in Grace's

insect medium (Sigma-Aldrich, St. Louis, MO, United States) from non-parasitized larvae; basal PGs incubated in Grace's insect medium from parasitized larvae; stimulated PGs with 0.1 BE/μl PTTH from non-parasitized larvae; stimulated PGs with 0.1 BE/μl PTTH from parasitized larvae; PGs from non-parasitized larvae incubated with 1 μM rapamycin (Calbiochem, catalog number 553210, San Diego, CA, United States), a specific inhibitor of TOR; PGs from non-parasitized larvae incubated with 1 μM rapamycin and stimulated with 0.1 BE/μl PTTH.

After dissection and initial incubation (as described above), PGs were incubated for 3 h at 25°C, for all the experimental conditions, except for incubation with rapamycin, in which PGs were pre-incubated with rapamycin alone for 30 min, then transferred to fresh medium containing the same dose of the inhibitor with or without PTTH 0.1 BE/μl.

After the incubation, a pool of 20 PGs for each of these conditions was lysed directly in 2X Laemmli buffer (Laemmli, 1970), to block protease and phosphatase activity. The extracted proteins were separated by 12% polyacrylamide gel electrophoresis and then transferred on a Whatman nitrocellulose membrane (Protran, Dassel, Germany).

Specific antibodies were used to evaluate phosphorylation of the two TOR targets: anti-phospho-4E-BP (Cell Signaling catalog number 2855S, Danvers, MA, United States) and anti-phospho-S6K (Millipore catalog number 04-393, Temecula, CA, United States) (Gu et al., 2012; Scieuzo et al., 2018). Signals obtained with the anti-actin antibody (Abcam, catalog number 75186, Cambridge, United Kingdom) were used as loading controls as reported for other Lepidoptera (Smith et al., 2014). All antibodies were diluted 1:1000 in tris-buffered saline and 0.1% Tween 20 (TBS-T) with 5% bovine serum albumin (BSA), and the incubation was carried out for 16 h. Membranes were sequentially incubated with each of the three antibodies. Goat anti-rabbit conjugated to horseradish peroxidase (Invitrogen, Carlsbad, CA, United States), diluted 1:15,000 in TBS-T, was used as secondary antibody. Detection was carried out using enhanced chemiluminescence (ECL) (LiteAB Blot Kit – Euroclone, Pavia, Italy) and signals were measured by a Chemidoc^{TM} MP System (Bio-Rad, Milan, Italy).

In vitro Biosynthesis of Ecdysone

Following the dissection of PGs, Grace's insect medium was replaced with a fresh medium containing stimulators or inhibitors, as described in section Analysis of Protein Phosphorylation. Ecdysone released in the medium was determined by a competitive enzyme immunoassay (EIA), using anti-ecdysone as primary antibody and 20-hydroxyecdysone-peroxidase conjugated as tracer, as previously described (Kingan, 1989; Scieuzo et al., 2018). All experiments were performed on a single PG, in three technical replicates for each of the six biological replicates.

RNA Extraction and Prothoracic Glands *de novo* Transcriptome Assembly

In order to identify genes differentially expressed in *H. virescens* PGs from parasitized and non-parasitized last instar larvae, a transcriptome analysis was conducted. Total RNA from 300 PGs explanted from 3 days old last instar parasitized (48 h post-parasitism) and synchronized non-parasitized larvae, was extracted using TRI-Reagent (Sigma-Aldrich, St. Louis, MO, United States), according to the manufacturer's protocol. An additional DNase (Turbo DNase, Ambion Inc., Austin, TX, United States) treatment was carried out before the second purification step to remove any remaining DNA. The DNase enzyme was removed, and the RNA was further purified by using the RNeasy MinElute Clean up Kit (Qiagen, Venio, Netherlands), following the manufacturer's protocol, and eluted in 20 μl of RNA Storage Solution (Ambion Inc., Austin, TX, United States). RNA integrity was verified on an Agilent 2100 Bioanalyzer using the RNA Nano chips (Agilent Technologies, Palo Alto, CA, United States) and RNA quantity was determined by Nanodrop ND-1000 spectrophotometer (Thermo Scientific, Waltham, MA, United States). Poly(A)+ RNA was isolated from 5 μg total RNA for PGs from parasitized and non-parasitized larvae using the Ambion MicroPoly(A) Purist Kit according to the manufacturer's instructions (Life Technologies, Carlsbad, CA, United States).

Sequencing was carried out by the Max Planck Genome Center[1] using standard TruSeq procedures on an Illumina HiSeq2500 sequencer, generating approximately 40 mio paired-end (2 × 100 bp) reads for each of the tissue samples. Quality control measures, including the filtering of high-quality reads based on the score given in FASTQ files, removal of reads containing primer/adaptor sequences and trimming of read lengths, were carried out using CLC Genomics Workbench v9.1[2]. The *de novo* transcriptome assembly was carried out with the same software, selecting the presumed optimal consensus transcriptome as previously described (Vogel et al., 2014). All obtained sequences (contigs) were used as query for a BLASTX searches (Altschul et al., 1997) against the non-redundant database of the National Center for Biotechnology Information (NCBI), considering all hits with an *e*-value < 1E-3. The transcriptome was annotated using BLAST, Gene Ontology (GO) and InterPro terms (InterProScan, EBI), enzyme classification (EC) codes, and metabolic pathways (Kyoto Encyclopedia of Genes and Genomes, KEGG) as implemented in BLAST2GO v4.1[3]. Based on the BLAST hits, the contigs were assigned to either insect or virus (i.e., *Tn*BV) origin. To optimize the annotation of data, we used GO slim, which uses a subset of the complete GO terms that provides a broader overview of the transcriptome ontology content.

Digital Gene Expression Analysis

Digital gene expression analysis was carried out by using CLC Genomics workbench v9.1 to generate BAM (mapping) files and QSeq Software (DNAStar Inc.) to remap the Illumina reads onto the reference transcriptome and then counting the sequences to estimate expression levels, using previously described parameters for read mapping and normalization (Vogel et al., 2014;

[1]http://mpgc.mpipz.mpg.de/home/

[2]http://www.clcbio.com

[3]http://www.blast2go.de

Jacobs et al., 2016). In particular, the expression abundance of each conting was calculated based on the reads per kilobase per million mapped reads (RPKM) method (Mortazavi et al., 2008), using the formula:

RPKM (A) = (10,00,000 × C × 1,000)/(N × L), where RPKM (A) is the abundance of gene A, C is the number of reads that uniquely aligned to gene A, N is the total number of reads that uniquely aligned to all genes, and L is the number of bases in gene A. The RPKM method is able to eliminate the influence of different gene lengths and sequencing discrepancy in the calculation of expression abundance.

Quantitative RT-PCR (qRT-PCR)

To evaluate the relative expression of *tor, 4ebp,* and *s6k* genes in parasitized and non-parasitized *H. virescens* PGs, quantitative RT-PCR (qRT-PCR) experiments were carried out on an ABI PRISM® 7500 Fast Real-Time PCR System Thermal Cycler (Applied Biosystems, Foster City, CA, United States), with cDNA samples prepared from 3 days old last instar parasitized and non-parasitized PGs, following the guidelines reported in Minimum Information Required for Publication of Quantitative Real-Time PCR experiments (MIQE) (Bustin et al., 2009) and minimum information necessary for quantitative real-time PCR experiments (Johnson et al., 2014). Based on their relative expression levels obtained from our RNAseq data showing that five candidate control genes were not affected by parasitization (**Supplementary Figure S1**), Glyceraldehyde-3-phosphate dehydrogenase (*Gapdh*), elongation factor 1-alpha (*ef1a*) and ribosomal protein L13 (*rp13*) were chosen as reference genes for normalization of qRT-PCR data. Specific primers for each *H. virescens* gene (*tor, s6k, 4ebp*) and reference genes were designed using Primer 3.0[4] (**Supplementary Table S1**).

Genes of interest and reference gene sequences were obtained from the PG *de novo* transcriptome assembly (Scieuzo et al., 2018).

PCR amplifications were performed using GoTaq qPCR Master Mix (Promega, Madison, WI, United States). The reactions were carried out in a 20 µl volume containing 20 ng cDNA and 0.3 µmol/L final primer concentration. Cycling conditions for all genes were: 2 min at 95°C, followed by 40 cycles of 15 s at 95°C and 1 min at 58°C. At the end of each run, a melting curve analysis was performed to confirm the specificity of PCR products. All amplification reactions were run in triplicate (technical replicates) and included negative controls (non-template reactions, replacing cDNA with ultrafiltered sterile water). All qRT-PCR analyses were performed for a set of three biological replicates. In order to evaluate gene expression levels, relative quantification was performed using equations described by Liu and Saint (2002), based on PCR amplification efficiencies of reference and target genes. Amplification efficiency of each target gene and endogenous genes was determined according to the equation $E = 10^{-1/S} - 1$ (Lee et al., 2006), where S is the slope of the standard curve generated from three serial 10-fold dilutions of cDNA. Quantification analysis of amplification was performed using the comparative CT (ΔCT) method. The efficiencies of the amplicons were approximately equal (*gapdh* parasitized = 0.98; *gapdh* non-parasitized = 0.96; *ef* parasitized = 0.82; *ef* non-parasitized = 0.86; *rpl13* parasitized = 0.91; *rpl13* non-parasitized = 0.93; *tor* parasitized = 0.89; *tor* non-parasitized = 0.88; *4ebp* parasitized = 0.97; *4ebp* non-parasitized = 0.94; *s6k* parasitized = 0.88; *s6k* non-parasitized = 0.87).

[4]http://bioinfo.ut.ee/primer3-0.4.0

Statistical Analysis

qRT-PCR data were expressed as mean ± SEM (standard error of mean) of independent biological replicates and were compared by a one-way analysis of variance (ANOVA) and Bonferroni *post hoc* test using GraphPad Prism 6.00 software for Windows (GraphPad Software, La Jolla, CA, United States[5]). Enzyme immunoassay data were expressed as mean ± SEM (standard error of mean) of independent biological replicates and were compared by a two-way analysis of variance (ANOVA) with Treatment (3 levels: Parasitized, non-parasitized Control and non-parasitized Rapamycin-treated) as the first factor and PTTH-stimulated (2 levels: yes, no) as the second factor. *Post hoc* Means Comparison test was done with both Tukey and SNK tests. In order to correct heteroscedasticity and non-normality, checked with Levene and Shapiro–Wilk tests, data were square root transformed before the analysis. All the statistical analysis was done using Systat 13 (Systat Software, Inc., San Jose, CA, United States[6]).

[5]www.graphpad.com

[6]www.systatsoftware.com

RESULTS

Phosphorylation of 4E-BP and S6K Proteins in Parasitized and Non-parasitized Prothoracic Glands

In order to verify the effect of parasitism on the TOR pathway and a potential impact on *Heliothis virescens* ecdysteroidogenesis, western blot analyses were performed on protein extracts from PGs, previously incubated under different conditions (basal, PTTH, rapamycin, PTTH added with rapamycin) explanted from non-parasitized and parasitized last instar (fifth) larvae. The phosphorylation of the main targets of TOR kinase was detected using antibodies against phospho-4E-BP and phospho-S6K, respectively.

The *in vitro* exposure of PGs explanted from 3 days old last instar non-parasitized larvae to PTTH contained in brain extract enhanced the phosphorylation level of both 4E-BP and S6K proteins. No phosphorylation signals were detected in PGs explanted from non-parasitized larvae, treated with rapamycin (with or without PTTH stimulation) and from parasitized larvae (with or without PTTH stimulation) (**Figure 1**).

In vitro Effect of Parasitism on Ecdysteroidogenesis

The *in vitro* biosynthetic activity of PGs explanted from *H. virescens* 3 days old last instar parasitized and non-parasitized

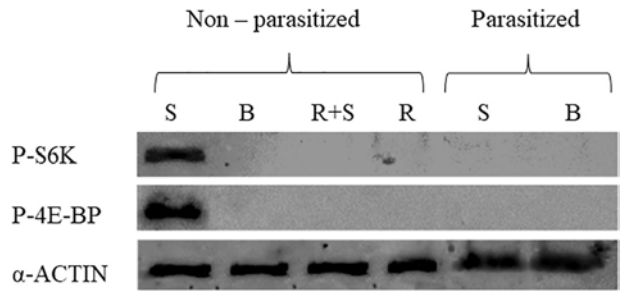

FIGURE 1 | Phosphorylation of TOR target proteins, 4E-BP and S6K, in prothoracic glands, explanted from parasitized and non-parasitized larvae, under different experimental conditions. Basal prothoracic glands (B) or stimulated prothoracic glands with PTTH extract (S), rapamycin (R), explanted from parasitized or non-parasitized larvae. Prothoracic glands (PGs) from 3 days old last instar parasitized and non-parasitized larvae were incubated with 0.1 BE/μl PTTH (stimulated, S). Non-parasitized PGs were also pre-incubated with 1 μM rapamycin for 30 min, then transferred to fresh medium containing the same dose of the inhibitor with (stimulated, R+S) or without (R) 0.1 BE/μl PTTH. Parasitized and non-parasitized (basal, B) glands were incubated in Grace's insect medium. Incubation was maintained for 3 h in each condition at 25°C. Glands lysed in Laemmli buffer 2X, were analyzed by western blot using antibodies against phospho-4E-BP (20 kDa), phospho-S6K (70 kDa). Each lane represents the equivalent of 20 prothoracic glands. The quantity of loaded proteins was verified by the endogenous control, α-Actin (42 kDa).

larvae, in response to activators or inhibitors, is reported in **Figure 2** and **Supplementary Table S2**.

Ecdysone production was strongly enhanced by PTTH stimulation of non-parasitized PGs in comparison to all other experimental conditions. In the presence of rapamycin, the ecdysone production following PTTH-stimulation, although significantly lower compared to stimulation conditions, was significantly higher than basal or rapamycin-treated non-parasitized PGs, and basal or PTTH-stimulated parasitized PGs. In both PTTH-stimulated and non-stimulated parasitized PGs the titre of ecdysone was lower to that released by basal non-parasitized PGs (**Supplementary Table S3**).

Transcriptome Analyses of Parasitized and Non-parasitized (Combined) *H. virescens* Prothoracic Glands

For functional annotations, all sequences were subjected to Gene Ontology (GO) analyses in Blast2GO revealing that of the total number of contigs, 61% (40,290) shared significant similarity to proteins with assigned molecular functions in the GO database (Altschul et al., 1997). The analyses of the combined transcriptome allowed the identification of 18 contigs of viral origin selectively transcribed and putatively expressed in parasitized PGs. Among these, 6 contigs could be assigned to general bracovirus genes, while 12 could be assigned specifically to *Tn*BV, as visualized in the heat map with the normalized mapped read (RPKM) counts (**Figure 3**).

Using the transcriptome and RNAseq mapping data, it was also possible to evaluate the transcript levels of all genes encoding for proteins involved in the cell signaling pathway PI3K/Akt/TOR. As shown in the respective heat map (**Figure 4**), in PGs extracted from parasitized larvae all of the identified genes are downregulated compared to control (non-parasitized) PGs.

Moreover, the transcript levels of genes codifying for proteins involved both in MAPK pathway and in the biosynthesis of ecdysone (*Halloween* genes) were evaluated. In PGs extracted from parasitized larvae, 57 of the 58 identified transcripts encoding for proteins belonging to the MAPK pathway are downregulated compared to control (non-parasitized larvae PGs) (**Figure 5**). The downregulation of 5 among the 6 identified contigs corresponding to *Halloween* genes is also observed in PGs extracted from parasitized larvae compared to non-parasitized larvae PGs (control) (**Figure 6**).

Gene Expression Levels in Parasitized and Non-parasitized Prothoracic Glands

In order to confirm the transcriptomic analysis, showing a downregulation of TOR pathway genes, we analyzed the relative expression of *tor*, *4ebp,* and *s6k* genes by quantitative Real time PCR (qRT-PCR) in parasitized and non-parasitized PGs. Our results showed that all tested genes displayed lower expression levels in parasitized PGs. The expression levels were statistically significantly different compared to those in non-parasitized samples (**Figure 7**).

DISCUSSION

The serine/threonine protein kinase Target of Rapamycin (TOR) is one of the key proteins involved in the control of several cell processes. TOR belongs to the phosphoinositide 3-kinase/protein kinase B (PI3K/Akt) pathway and its activation is modulated by the combination of signaling pathways following intracellular stimuli, such as nutrients and growth factors. The TOR protein and other proteins belonging to its cellular cascade are highly conserved among eukaryotes from yeast to mammals, including insects (Zhang et al., 2000; Rexin et al., 2015; Gonzalez and Hall, 2017). The alteration of the PI3K/Akt pathway, which leads to the overexpression or the inactivation of TOR kinase, seems to be critical in a number of diseases, such as cancer and diabetes (Ali et al., 2017), or neurological diseases such as Parkinson (Xu et al., 2014; Tiwari and Pal, 2017) and Alzheimer (Tang et al., 2015; Tramutola et al., 2015). TOR therefore represents one of the major therapeutic targets in these pathological alterations. The macrolide rapamycin and its analogs are highly specific inhibitors of TOR and they are considered therapeutic molecules with antitumor (Calimeri and Ferreri, 2017; Faes et al., 2017; Liu et al., 2017) and immunosuppressive activity (McMahon et al., 2011; Hamdani et al., 2017; Yee and Tan, 2017), and with promising activity against neurological disease (Wang et al., 2014; Maiese, 2016). These molecules have a unique mechanism of action: they first bind FK506-binding protein (FKBP12), a 12 kDa immunophilin, and then this complex inhibits the serine/threonine kinase TOR (Russell et al., 2011).

The use of rapamycin or its analogs has also side effects: dose-dependent cytopenia, hyperlipidemia, thrombosis and pulmonary, cardiovascular, skin or bone damages (Bhat et al., 2013). The identification of new genes and molecules able to

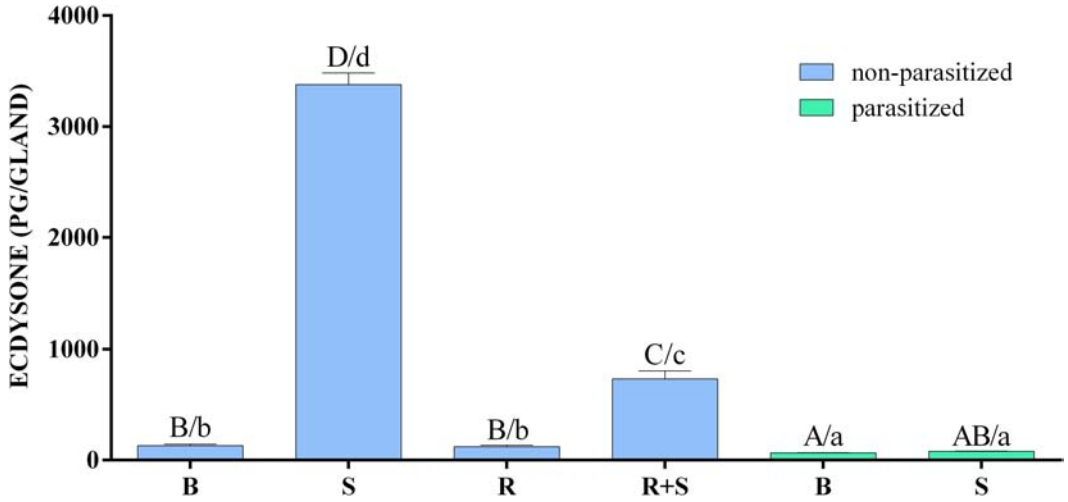

FIGURE 2 | Inhibitory effect of parasitism and rapamycin on the synthesis of ecdysone by prothoracic glands of *H. virescens*. Prothoracic glands (PGs) explanted from parasitized and non-parasitized 3 days old last instar larvae were incubated in Grace's insect medium with (stimulated, S) or without (basal, B) 0.1 BE/μl PTTH. Non-parasitized PGs were also pre-incubated with 1 μM rapamycin for 30 min, then transferred to fresh medium containing the same dose of the inhibitor with (rapamycin stimulated, R+S) or without (rapamycin basal, B) 0.1 BE/μl PTTH. Parasitized and non-parasitized (basal) glands were incubated in Grace's insect medium. Incubation was maintained for 3 h in each condition at 25°C, after which the ecdysone produced was determined by enzyme immunoassay (EIA). Data are expressed as mean ± SEM of $n = 6$ experiments. Statistical analysis was performed by a two-way analysis of variance (ANOVA). *Post hoc* Means Comparison test was done with both Tukey and SNK tests. Different letters indicate significant differences ($p < 0.05$). Uppercase letters refer to the Tukey *post hoc* test and lowercase letters to the SNK test.

modulate/inhibit the TOR pathway with a similar or different mechanism as rapamycin can be considered an important goal to enrich the strategy and tools employable in cancer therapy or in pathology related to TOR pathway deregulation.

Beside the important roles regarding the regulation of cell growth and proliferation in response to environmental and nutritional conditions, in insects the TOR pathway is involved in ecdysone biosynthesis by PGs or analogous organs, stimulated by the PTTH. In previous work we demonstrated the involvement of the PI3K/Akt/TOR pathway in ecdysteroidogenesis stimulated by PTTH, contained in the brain extract, in *Heliothis virescens* PGs (Scieuzo et al., 2018). Here we show that this cellular signaling pathway is one of the targets of infection by *Tn*BV, the Polydnavirus associated with the endoparasitoid wasp *Toxoneuron nigriceps*.

T. nigriceps oviposits into all larval instars of *H. virescens*, which can reach the stage of mature larva (last instar) but become developmentally arrested failing pupation. The PGs functional inactivation is responsible for blocking pupation of the parasitized host last instar larvae (Tanaka and Vinson, 1991; Pennacchio et al., 1997, 1998a,b, 2001). The reduced biosynthetic activity of host PGs was due to their infection by transcriptionally active *Tn*BV, suggesting that viral gene expression in PGs might play a role in the disruption of the PTTH signal transduction pathway (Pennacchio et al., 1998a).

Our recent studies showing a PI3K/Akt/TOR signaling involvement in PTTH-stimulated ecdysteroidogenesis by *H. virescens* PGs, confirmed that PTTH rapidly enhanced the phosphorylation of translational repressor 4E-binding protein (4E-BP) and p70 ribosomal protein S6 kinase (S6K), two well-known downstream targets of TOR. Moreover, we also demonstrated that rapamycin blocked phosphorylation of 4E-BP and S6K in PTTH-stimulated PGs and strongly inhibited PTTH-stimulated ecdysteroidogenesis (Scieuzo et al., 2018).

In the present study the possible role of *Tn*BV on the PI3K/Akt/TOR pathway in PTTH-stimulated ecdysone biosynthesis in *H. virescens* PGs was investigated. Interestingly, our results confirm that a parasitism event completely inhibits PTTH-mediated stimulation of ecdysone biosynthesis in PGs of parasitized larvae, as suggested in previous work (Pennacchio et al., 1997, 1998a; Falabella et al., 2006), and demonstrate that one of the *Tn*BV effects is linked to PI3K/Akt/TOR pathway alteration. The impact of *Tn*BV on ecdysteroidogenesis is more dramatic than the effect of rapamycin: parasitism totally inhibited ecdysone production of PTTH-stimulated PGs, whereas the effect of rapamycin was partial. This difference can be explained on the basis of our previous study (Scieuzo et al., 2018) and other studies on lepidopteran species (Lin and Gu, 2007; Gu et al., 2011) which demonstrated that both MAPK and PI3K/Akt/TOR pathways are independently involved in PTTH-stimulated ecdysteroidogenesis, but rapamycin only affects the TOR pathway. Evidently the expression of *Tn*BV genes in *H. virescens* PGs affects PTTH-stimulated ecdysteroidogenesis pathways at different levels and also with different mechanisms. Moreover, the PTTH-stimulated phosphorylation of 4E-BP and S6K, detected only in non-parasitized PGs, indicates that the PI3K/Akt/TOR pathway is directly stimulated by the neuropeptide hormone, as previously demonstrated (Scieuzo et al., 2018); no phosphorylation signal was detected in parasitized PGs, both basal and stimulated, apparently similar to

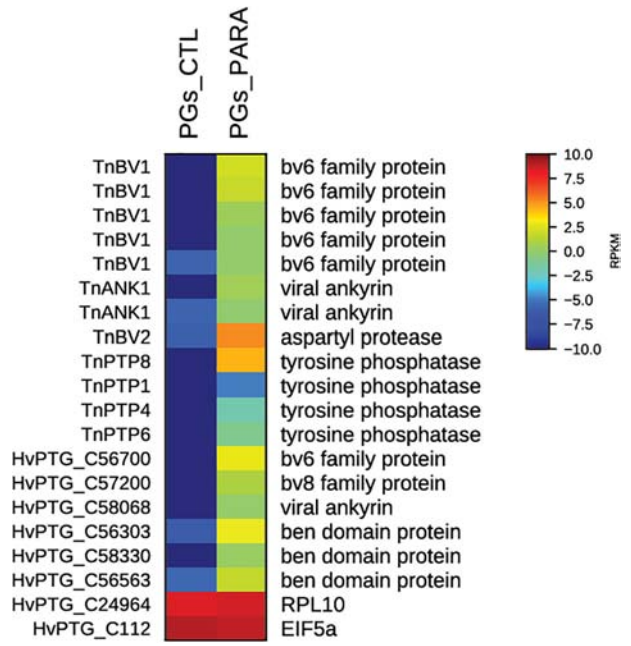

FIGURE 3 | Heat map showing relative expression levels of *Tn*BV genes in PGs from parasitized (PGs_PARA) and non-parasitized (PGs_CTL) *H. virescens* larvae. Viral genes are exclusively expressed in PGs from parasitized larvae. The housekeeping genes *RPl10* and *EIF5a* are used for normalization and are shown to confirm the uniform expression of these control genes across samples. The map is based on log2-transformed RPKM values shown in the gradient heat map (blue represents weakly-expressed genes, and red represents strongly-expressed genes).

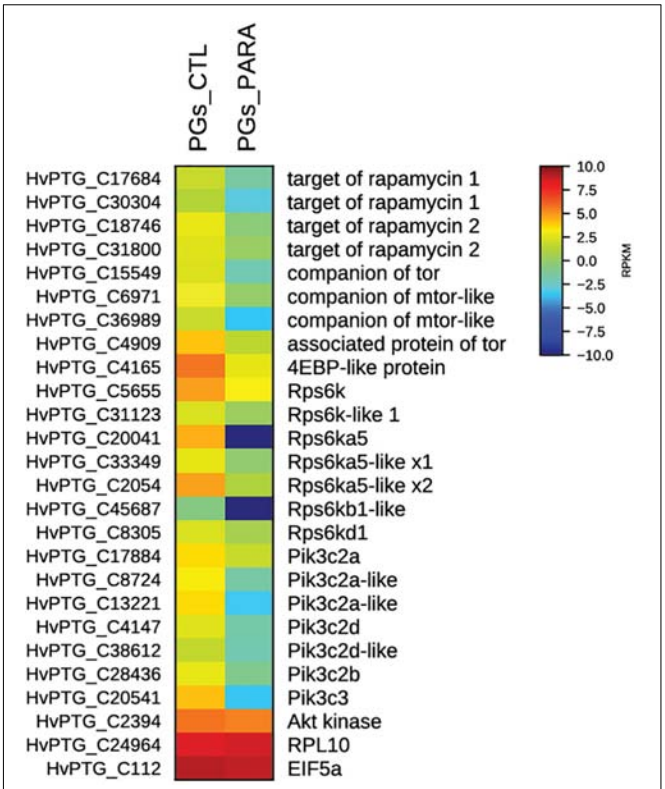

FIGURE 4 | Heat map showing relative expression levels of all TOR pathway genes in PGs from parasitized (PGs_PARA) and non-parasitized (PGs_CTL) larvae. Genes belonging to the TOR pathway are downregulated in parasitized larvae compared to the control (non-parasitized). The housekeeping genes *RPl10* and *EIF5a* are used for normalization and are shown to confirm the uniform expression of these control genes across samples. The map is based on log2⁻ transformed RPKM values shown in the gradient heat map (blue represents weakly-expressed genes, and red represents strongly-expressed genes).

the effect of PG incubation with rapamycin (Gu et al., 2011, 2012; Scieuzo et al., 2018). *In vitro* ecdysone biosynthesis evaluation showed that non-parasitized PGs, treated with rapamycin (R) and stimulated with PTTH extract (R+S), produced a significantly lower amount of ecdysone in comparison to non-parasitized PGs stimulated with PTTH extract (S), but a significantly higher amount of ecdysone in comparison to both untreated parasitized PGs (B) and those stimulated with PTTH extract (S), confirming that a parasitism event completely blocks ecdysteroidogenesis. This confirms, above all, that PI3K/Akt/TOR is not the only pathway involved in *H. virescens* ecdysteroidogenesis, suggesting that parasitization affects all the signaling pathways involved in ecdysteroidogenesis (Scieuzo et al., 2018).

Taken together, our results indicate that the infection of host PGs by *Tn*BV alters ecdysone production, at least in part, by modulating the TOR pathway through the expression of one or more viral genes. In support of this hypothesis, we identified all viral genes expressed in PGs, comparing the expression levels of transcripts in parasitized and non-parasitized PGs. Among these were previously identified and, in some cases, functionally characterized *Tn*BV genes (Varricchio et al., 1999; Falabella et al., 2003; Provost et al., 2004) such as *TnBV1*, *TnBV2*, *TnBVank1*, *ptp1*, *ptp4*, *ptp6,* and *ptp8*. *Tn*BVank1 displays significant sequence similarity with members of the IkB family (Silverman and Maniatis, 2001; Thoetkiattikul et al., 2005; Falabella et al., 2007; Bitra et al., 2012; Salvia et al., 2017). These proteins are generally involved in the control of NF-kB signaling pathways both in insects and vertebrates (Silverman and Maniatis, 2001).

Using *Drosophila melanogaster* as a model to functionally characterize *Tn*BV genes, it was shown that *Tn*BVank1 expression in host germ cells altered the microtubule network in oocytes (Duchi et al., 2010; Valzania et al., 2014). Subsequently, Valzania et al. (2014) confirmed that the expression of *Tn*BVank1 in PG cells strongly reduced ecdysone biosynthesis and, as a consequence, inhibited the transition of *D. melanogaster* larval to pupal stage, mimicking the developmental arrest observed in *H. virescens* larvae parasitized by *T. nigriceps*.

These results support the hypothesis that *Tn*BVank1, expressed in *H. virescens* PGs, could actively participate in inducing ecdysone titer reduction. *Tn*BVank1 influences different physiological pathways involved in both the disruption of cytoskeletal structure of PG cells and in affecting the sterol delivery from endosomal compartments trough the interaction with Alix, as reported for *D. melanogaster* (Valzania

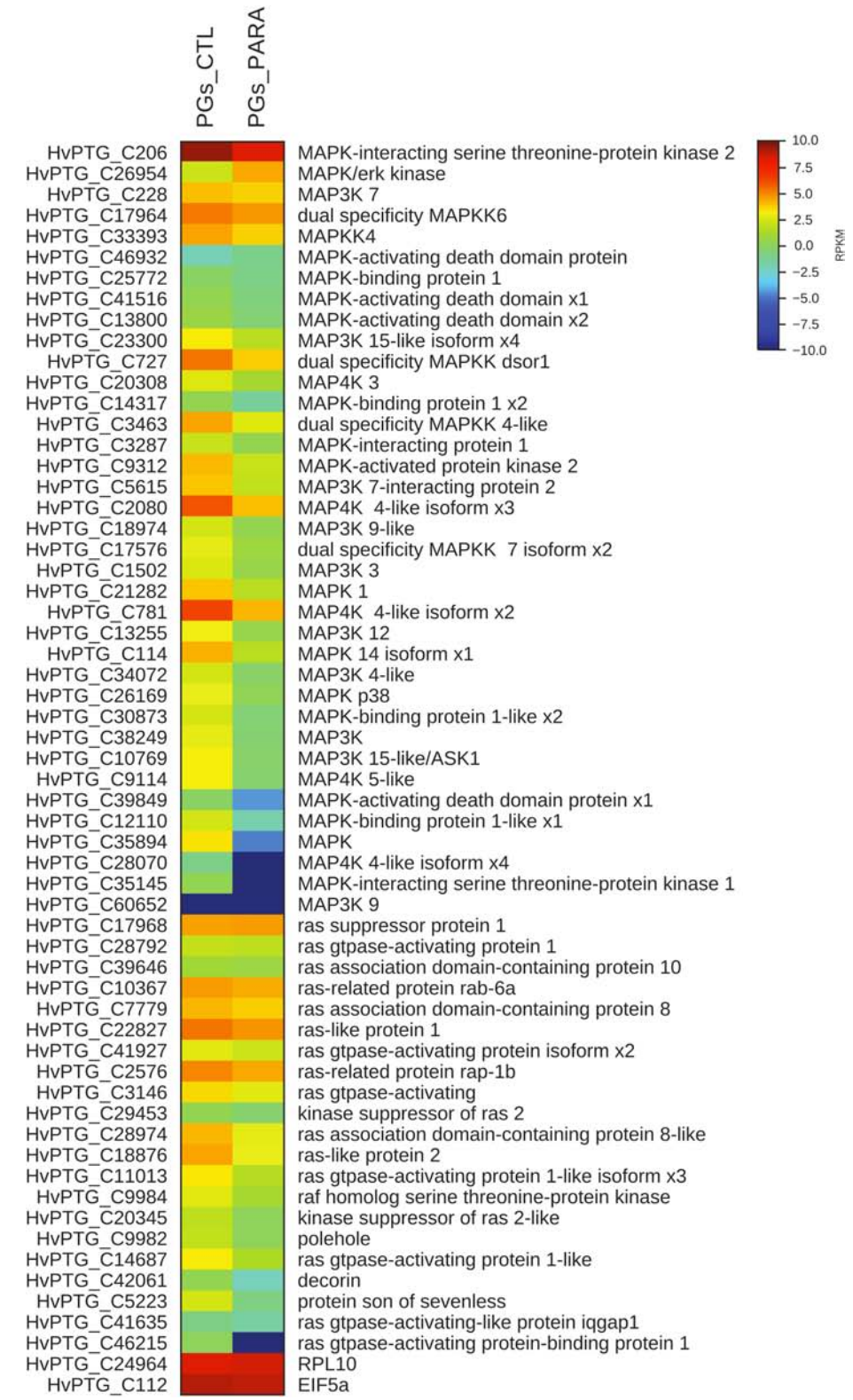

FIGURE 5 | Heat map showing relative expression levels of MAPK pathway genes in PGs from parasitized (PGs_PARA) and non-parasitized (PGs_CTL) larvae. Genes belonging to the MAPK pathway are downregulated in parasitized larvae compared to the control (non-parasitized). The housekeeping genes *RPl10* and *EIF5a* are used for normalization and are shown to confirm the uniform expression of these control genes across samples. The map is based on $\log2^{-}$ transformed RPKM values shown in the gradient heat map (blue represents weakly-expressed genes, and red represents strongly-expressed genes).

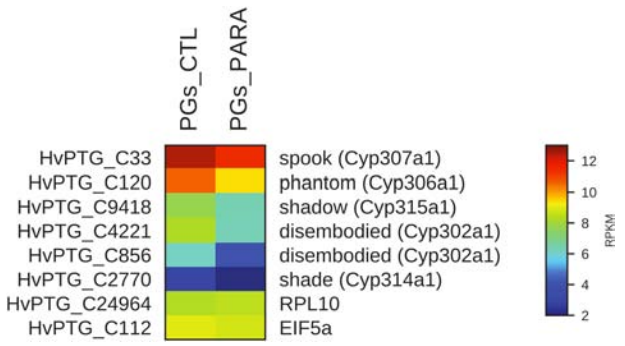

FIGURE 6 | Heat map showing relative expression levels of *Halloween* genes in PGs from parasitized (PGs_PARA) and non-parasitized (PGs_CTL) larvae. *Halloween* genes are downregulated in parasitized larvae compared to the control (non-parasitized). The housekeeping genes *RPl10* and *EIF5a* are used for normalization and are shown to confirm the uniform expression of these control genes across samples. The map is based on log2$^-$ transformed RPKM values shown in the gradient heat map (blue represents weakly-expressed genes, and red represents strongly-expressed genes).

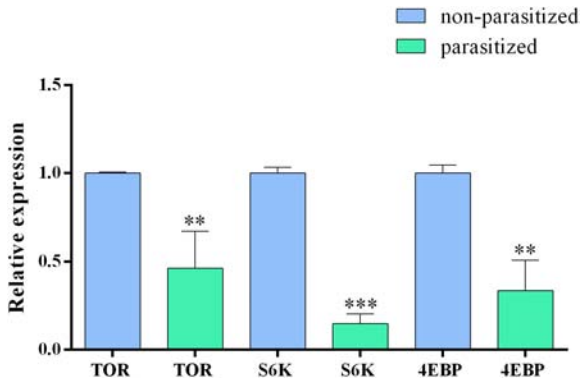

FIGURE 7 | Relative expression level of *tor, s6k,* and *4ebp* genes in basal parasitized and basal non-parasitized PGs. Gene expression levels were quantified by qRT-PCR. Data represent the mean of three independent replicates ± SEM. Statistically significant differences between samples are indicated with asterisk (**$p \leq 0.01$ and ***$p \leq 0.001$, one way ANOVA and Bonferroni *post hoc* <0.05). Reference genes: *gapdh, rp13, and ef*. Calibrator sample: non-parasitized PGs.

et al., 2014). This multifunctional activity of *Tn*BVank1 is not surprising. The expression of this gene in *H. virescens* immune cells was demonstrated to induce apoptosis through the interaction with Alix, besides its irreversible inhibition of NF-kB translocation in cell nuclei, thus blocking the expression of key genes and inducing apoptotic phenomena (Falabella et al., 2007; Salvia et al., 2017). The reduced gland size observed in *D. melanogaster* larvae (Valzania et al., 2014) and the low basal production of ecdysteroids in PGs of *H. virescens* parasitized larvae were also reported (Pennacchio et al., 1997, 1998b). Here we demonstrate that in naturally parasitized larvae these symptoms were associated with a disruption of PTTH signaling by active *Tn*BV infection of PGs (Pennacchio et al., 1998a). It is highly plausible that at least part of these effects could be attributable to the expression of *Tn*BVank1 in the parasitized host.

Although the effects of other viral genes should be analyzed *in vivo* or *in vitro*, we can speculate on possible roles of different *Tn*BV genes in the suppression of ecdysteroidogenesis.

Among the 13 putative PTPs identified in the *Tn*BV genome, 8 PTP genes have a full protein tyrosine phosphatase domain (Provost et al., 2004; Falabella et al., 2006).

Our results demonstrate that PTP1, 4, 6, and 8 are specifically expressed in parasitized PGs. These PTPs together with PTP7 (Provost et al., 2004; Falabella et al., 2006), could dephosphorylate PG proteins phosphorylated by tyrosine kinases following PTTH stimulation. The expression of *Tn*BV PTP7 (24 h after parasitism) (Falabella et al., 2006) and of *Tn*BV PTP1, PTP4, PTP6, and PTP8 (reported here) specifically in PGs, confirms that PTP expression is host tissue-specific.

Members of the *Tn*BV PTP gene family, expressed at different times during parasitism, could be good candidates for a functional involvement in host PG inactivation through dephosphorylation of regulatory proteins. These proteins are possibly involved in the extremely intricate PTTH-stimulated ecdysone secretion pathway. However, at least in case of *H. virescens* and other Lepidoptera, this pathway is not yet fully identified. Since *Tn*BV PTPs belong to the classical PTPs (Provost et al., 2004), they dephosphorylate only tyrosine residues, and it is reasonable to hypothesize that *Tn*BV PTPs do not directly affect the TOR pathway (Brunn et al., 1997; Aoki et al., 2001). The target/s of viral PTPs still remain/s unknown.

The effect of parasitism on PGs could act on different levels to ensure the total inhibition of PG biosynthetic activity. Indeed, we demonstrate an alternative way to control the TOR pathway at the transcriptional level through expression of one or more *Tn*BV genes in PGs of parasitized larvae. The down-regulation of TOR genes, especially *tor, s6k,* and *4ebp,* was confirmed by qRT-PCR experiments. Although it remains unclear which of the *Tn*BV genes are involved, *TnBVank1* could play a role, also because of its ability to block NF-kB-mediated gene expression regulation (Falabella et al., 2007; Dan et al., 2008; Oeckinghaus et al., 2011).

The expression of *Tn*BV genes in PGs seems to alter TOR metabolic pathway, influencing essential steps for the synthesis of ecdysone. However in *H. virescens* at least two independent pathways contribute to ecdysteroidogenesis: MAPK and PI3K/Akt/TOR cellular signaling (Scieuzo et al., 2018). RNA-seq data showed a down-regulation of genes involved in both PI3K/Akt/TOR, MAPK pathways, and in the biosynthesis of ecdysone (*Halloween* genes). These findings suggest that the massively reduced amounts of ecdysone following *T. nigriceps* parasitism could be ascribed to the expression of *Tn*BV genes in PGs. Further studies are needed to obtain more information regarding the possible mechanism of action of *Tn*BV proteins on these pathways. Further characterization of other viral proteins would allow a better understanding of the mechanisms involved in the inhibition of ecdysone synthesis, and could provide a range of candidates potentially capable of inhibiting more steps of the PI3K/Akt/TOR pathway. The possible use of viral proteins in synergy with rapamycin or its analogs can be a turning point in

medical treatment with the PI3K/Akt/TOR pathway as possible therapeutic target.

DATA AVAILABILITY

The short read data have been deposited in the EBI short read archive (SRA) with the following sample accession numbers: ERS2859514-ERS2859515 (PGs of non-parasitized *H. virescens* larvae) and ERS2859516 (PGs of *T. nigriceps* parasitized *H. virescens* larvae). The complete study can also be accessed directly using the following URL: http://www.ebi.ac.uk/ena/data/view/PRJEB29401.

ETHICS STATEMENT

Insects used in this work were treated as well as possible given the constraints of the experimental design.

AUTHOR CONTRIBUTIONS

PF designed the experiments, wrote and critically revised the paper. HV, RS, MN, CS, AS, AR, and SB contributed to the data interpretation and critically revised the paper. RS and CS performed the western blot experiments. AS, MN, and RS performed the samples collection and RT-qPCR. MN and CS performed the enzyme immunoassay. HV performed the *de novo* transcriptome assembly and analysis. All authors read and approved the manuscript.

FUNDING

This work was supported by the Max Planck Society and the University of Basilicata (RIL funds).

ACKNOWLEDGMENTS

We would like to thank Prof. Paolo Fanti, University of Basilicata, for the assistance in statistical analysis.

SUPPLEMENTARY MATERIAL

The Supplementary Material for this article can be found online at: https://www.frontiersin.org/articles/10.3389/fphys.2018.01678/full#supplementary-material

FIGURE S1 | Heat map showing relative expression levels of five candidate reference genes in PGs from parasitized (PGs_PARA) and non-parasitized (PGs_CTL) larvae. Eukaryotic translation initiation factor 5A-1 (*eif5a*), ribosomal protein L10 (*rpl10*), Glyceraldehyde-3-phosphate dehydrogenase (*Gapdh)*, elongation factor 1-alpha (*ef1a)* and ribosomal protein L13 (*rp13)* were pre-selected as candidate reference genes for normalization of qRT-PCR data since they were not affected by parasitization. *Gapdh, ef1a* and *rp13* were subsequently chosen as reference genes.

TABLE S1 | Primers used for qRT-PCR. F: forward, R: reverse.

TABLE S2 | Ecdysone released by prothoracic glands in different experimental conditions. Data are expressed as mean of ecdysone concentrations (pg/gland) ± SEM of n = 6 experiments. Different letters indicate significant differences ($p < 0.05$). Uppercase letters refer to the Tukey *post hoc* test and lowercase letters to the SNK test.

TABLE S3 | Raw data of enzyme immunoassay (EIA) **(a)** and Two-Way ANOVA statistical output **(b)**.

REFERENCES

Ali, M., Bukhari, S. A., and Lee, H. W. (2017). Upstream signalling of mTORC1 and its hyperactivation in type 2 diabetes (T2D). *BMB Rep.* 50, 601–609. doi: 10.5483/BMBRep.2017.50.12.206

Altschul, S. F., Madden, T. L., Schaffer, A. A., Zhang, J., Zhang, Z., Miller, W., et al. (1997). Gapped BLAST and PSI-BLAST: a new generation of protein database search programs. *Nucleic Acids Res.* 25, 3389–3402. doi: 10.1093/nar/25.17.3389

Aoki, M., Blazek, E., and Vogt, P. K. (2001). A role of the kinase mTOR in cellular transformation induced by the oncoproteins P3k and Akt. *Proc. Natl. Acad. Sci. U.S.A.* 98, 136–141. doi: 10.1073/pnas.98.1.136

Beckage, N. E., and Gelman, D. B. (2004). Wasp parasitoid disruption of host development: implications for new biologically based strategies for insect control. *Annu. Rev. Entomol.* 49, 299–330. doi: 10.1146/annurev.ento.49.061802.123324

Bhat, M., Sonenberg, N., and Gores, G. J. (2013). The mTOR pathway in hepatic malignancies. *Hepatology* 58, 810–818. doi: 10.1002/hep.26323

Bitra, K., Suderman, R. J., and Strand, M. R. (2012). Polydnavirus Ank proteins bind NF-κB homodimers and inhibit processing of relish. *PLoS Pathog.* 8:e1002722. doi: 10.1371/journal.ppat.1002722

Bollenbacher, W. E., O'Brien, M. A., Katahira, E. J., and Gilbert, L. I. (1983). A kinetic analysis of the action of insect prothoracicotropic hormone. *Mol. Cell. Endocrinol.* 32, 27–46. doi: 10.1016/0303-7207(83)90096-5

Brunn, G. J., Fadden, P., Haystead, T. A., and Lawrence, J. C. (1997). The mammalian target of rapamycin phosphorylates sites having a (Ser/Thr)-Pro motif and is activated by antibodies to a region near its COOH terminus. *J. Biol. Chem.* 272, 32547–32550. doi: 10.1074/jbc.272.51.32547

Bustin, S. A., Benes, V., Garson, J. A., Hellemans, J., Huggett, J., Kubista, M., et al. (2009). The MIQE guidelines: minimum information for publication of quantitative real-time PCR experiments. *Clin. Chem.* 55, 611–622. doi: 10.1373/clinchem.2008.112797

Calimeri, T., and Ferreri, A. J. M. (2017). m-TOR inhibitors and their potential role in haematological malignancies. *Br. J. Haematol.* 177, 684–702. doi: 10.1111/bjh.14529

Dan, H. C., Cooper, M. J., Cogswell, P. C., Duncan, J. A., Ting, J. P. Y., and Baldwin, A. S. (2008). Akt-Dependent Regulation of NF-κB Is Controlled by mTOR and Raptor in Association with IKK. *Genes Dev.* 22, 1490–1500. doi: 10.1101/gad.1662308

Duchi, S., Cavaliere, V., Fagnocchi, L., Grimaldi, M. R., Falabella, P., Graziani, F., et al. (2010). The impact on microtubule network of a bracovirus IkappaB-like protein. *Cell. Mol. Life Sci.* 67, 1699–1712. doi: 10.1007/s00018-010-0273-2

Dupuy, C., Periquet, G., Serbielle, C., Bézier, A., Louis, F., and Drezen, J. M. (2011). Transfer of a chromosomal Maverick to endogenous bracovirus in a parasitoid wasp. *Genetica* 139, 489–496. doi: 10.1007/s10709-011-9569-x

Faes, S., Santoro, T., Demartines, N., and Dormond, O. (2017). Evolving significance and future relevance of anti-angiogenic activity of mTOR inhibitors in cancer therapy. *Cancers* 9:E152. doi: 10.3390/cancers9110152

Falabella, P., Caccialupi, P., Varricchio, P., Malva, C., and Pennacchio, F. (2006). Protein tyrosine phosphatases of Toxoneuron nigriceps bracovirus as potential disrupters of host prothoracic gland function. *Arch. Insect Biochem. Physiol.* 61, 157–169. doi: 10.1002/arch.20120

Falabella, P., Varricchio, P., Gigliotti, S., Tranfaglia, A., Pennacchio, F., and Malva, C. (2003). Toxoneuron nigriceps polydnavirus encodes a putative aspartyl protease highly expressed in parasitized host larvae. *Insect Mol. Biol.* 12, 9–17. doi: 10.1046/j.1365-2583.2003.00382.x

Falabella, P., Varricchio, P., Provost, B., Espagne, E., Ferrarese, R., Grimaldi, A., et al. (2007). Characterization of the IκB-like gene family in polydnaviruses associated with wasps belonging to different Braconid subfamilies. *J. Gen. Virol.* 88, 92–104. doi: 10.1099/vir.0.82306-0

Gonzalez, A., and Hall, M. N. (2017). Nutrient sensing and TOR signalling in yeast and mammals. *EMBO J.* 36, 397–408. doi: 10.15252/embj.201696010

Gu, S. H., Yeh, W. L., Young, S. C., Lin, P. L., and Li, S. (2012). TOR signaling is involved in PTTH stimulated ecdysteroidogenesis by prothoracic glands in the silkworm. *Bombyx mori. Insect Biochem. Mol. Biol.* 42, 296–303. doi: 10.1016/j.ibmb.2011.12.010

Gu, S. H., Young, S. C., Lin, J. L., and Lin, P. L. (2011). Involvement of PI3K/Akt signaling in PTTH-stimulated ecdysteroidogenesis by prothoracic glands of the silkworm. *Bombyx mori. Insect Biochem. Mol. Biol.* 41, 197–202. doi: 10.1016/j.ibmb.2010.12.004

Hamdani, S., Thiolat, A., Naserian, S., Grondin, C., Moutereau, S., Hulin, A., et al. (2017). Delayed and short course of rapamycin prevents organ rejection after allogeneic liver transplantation in rats. *World J. Gastroenterol.* 14, 6962–6972. doi: 10.3748/wjg.v23.i38.6962

Jacobs, C., Steiger, S., Heckel, D. G., Wielsch, N., Vilcinskas, A., and Vogel, H. (2016). Sex, offspring and carcass determine antimicrobial peptide expression in the burying beetle. *Sci. Rep.* 6:25409. doi: 10.1038/srep25409

Johnson, G., Nour, A. A., Nolan, T., Huggett, J., and Bustin, S. (2014). Minimum information necessary for quantitative real-time PCR experiments. *Methods Mol. Biol.* 1160, 5–17. doi: 10.1007/978-1-4939-0733-5_2

Kemirembe, K., Liebmann, K., Bootes, A., Smith, W. A., and Suzuki, Y. (2012). Amino acids and TOR signaling promote prothoracic gland growth and the initiation of larval molts in the tobacco hornworm *Manduca sexta*. *PLoS One* 7:e44429. doi: 10.1371/journal.pone.0044429

Kingan, T. G. (1989). A competitive enzyme-linked immunosorbent assay: applications in the assay of peptides, steroids, and cyclic nucleotides. *Anal. Biochem.* 183, 283–289. doi: 10.1016/0003-2697(89)90481-8

Laemmli, U. K. (1970). Cleavage of structural proteins during the assembly of the head of bacteriophage T4. *Nature* 227, 680–685. doi: 10.1038/227680a0

Lapointe, R., Wilson, R., Vilaplana, L., O'Reilly, D. R., Falabella, P., Douris, V., et al. (2005). Expression of a Toxoneuron nigriceps polydnavirus-encoded protein causes apoptosis-like programmed cell death in lepidopteran insect cells. *J. Gen. Virol.* 86(Pt 4), 963–971. doi: 10.1099/vir.0.80834-0

Laurino, S., Grossi, G., Pucci, P., Flagiello, A., Bufo, S. A., and Bianco, G. (2016). Identification of major Toxoneuron nigriceps venom proteins using an integrated transcriptomic/proteomic approach. *Insect Biochem. Mol. Biol.* 76, 49–61. doi: 10.1016/j.ibmb.2016.07.001

Lee, C., Kim, J., Shin, S. G., and Hwang, S. (2006). Absolute and relative QPCR quantification of plasmid copy number in *Escherichia coli*. *J. Biotechnol.* 123, 273–280. doi: 10.1016/j.jbiotec.2005.11.014

Lewis, W. J., and Vinson, S. B. (1968). Egg and larval development of *Cardiochiles nigriceps*. *Ann. Entomol. Soc. Am.* 61, 561–656. doi: 10.1093/aesa/61.3.561

Lin, J. L., and Gu, S. H. (2007). In vitro and in vivo stimulation of extracellular signal-regulated kinase (ERK) by the prothoracicotropic hormone in prothoracic gland cells and its developmental regulation in the silkworm. *Bombyx mori. J. Insect Physiol.* 53, 622–631. doi: 10.1016/j.jinsphys.2007.03.004

Liu, W., and Saint, D. A. (2002). A new quantitative method of real time reverse transcription polymerase chain reaction assay based on simulation of polymerase chain reaction kinetics. *Anal. Biochem.* 302, 52–59. doi: 10.1006/abio.2001.5530

Liu, Y., Pandeswara, S., Dao, V., Padrón, A., Drerup, J. M., Lao, S., et al. (2017). Biphasic rapamycin effects in lymphoma and carcinoma treatment. *Cancer Res.* 77, 520–531. doi: 10.1158/0008-5472.CAN-16-1140

Maiese, K. (2016). Targeting molecules to medicine with mTOR, autophagy and neurodegenerative disorders. *Br. J. Clin. Pharmacol.* 82, 1245–1266. doi: 10.1111/bcp.12804

Malva, C., Varricchio, P., Falabella, P., La Scaleia, R., Graziani, F., and Pennacchio, F. (2004). Physiological and molecular interaction in the host-parasitoid system *Heliothis virescens*-Toxoneuron Nigriceps: current status and future perspectives. *Insect Biochem. Mol. Biol.* 34, 177–183. doi: 10.1016/j.ibmb.2003.09.008

McMahon, G., Weir, M. R., Li, X. C., and Mandelbrot, D. A. (2011). The evolving role of mTOR inhibition in transplantation tolerance. *J. Am. Soc. Nephrol.* 22, 408–415. doi: 10.1681/ASN.2010040351

Moreau, S., and Asgari, S. (2015). Venom proteins from parasitoid wasps and their biological functions. *Toxins* 7, 2385–2412. doi: 10.3390/toxins7072385

Mortazavi, A., Williams, B. A., McCue, K., Schaeffer, L., and Wold, B. (2008). Mapping and quantifying mammalian transcriptomes by RNA-Seq. *Nat. Methods* 5, 621–628. doi: 10.1038/nmeth.1226

Oeckinghaus, A., Hayden, M. S., and Ghosh, S. (2011). Crosstalk in NF-kappaB signaling pathways. *Nat. Immunol.* 12, 695–708. doi: 10.1038/ni.2065

Park, B., and Kim, Y. (2010). Transient transcription of a putative RNase containing BEN domain encoded in *Cotesia plutellae* bracovirus induces an immunosuppression of the diamondback month. *Plutella xylostella*. *J. Invertebr. Pathol.* 105, 156–163. doi: 10.1016/j.jip.2010.06.003

Pennacchio, F., Falabella, P., and Vinson, S. B. (1998a). Regulation of *Heliothis virescens* prothoracic glands by *Cardiochiles nigriceps* polydnavirus. *Arch. Insect Biochem. Physiol.* 38, 1–10.

Pennacchio, F., Falabella, P., Sordetti, R., Varricchio, P., Malva, C., and Vinson, S. B. (1998b). Prothoracic gland inactivation in *Heliothis virescens* (F.) (*Lepidoptera:Noctuidae*) larvae parasitized by *Cardiochiles nigriceps* (V.) (*Hymenoptera:Braconidae*). *J. Insect Physiol.* 44, 845–857. doi: 10.1016/S0022-1910(98)00016-X

Pennacchio, F., Malva, C., and Vinson, S. B. (2001). "Regulation of host endocrine system by the endophagous braconid *Cardiochiles nigriceps* and its polydnavirus," in *Endocrine Interactions of Insect Parasites and Pathogens*, eds J. P. Edward and R. J. Weaver (Oxford: BIOS), 123–132.

Pennacchio, F., Sordetti, R., Falabella, P., and Vinson, S. B. (1997). Biochemical and ultrastructural alterations in prothoracic glands of *Heliothis virescens* (F.) (Lepidoptera: Noctuidae) last instar larvae parasitized by *Cardiochiles nigriceps* (V.) (Hymenoptera: Braconidae). *Insect Biochem. Mol. Biol.* 27, 439–450. doi: 10.1016/S0965-1748(97)00016-7

Pennacchio, F., and Strand, M. R. (2006). Evolution of developmental strategies in parasitic hymenoptera. *Ann. Rev. Entomol.* 51, 233–258. doi: 10.1146/annurev.ento.51.110104.151029

Pennacchio, F., Vinson, S. B., and Tremblay, E. (1992). Host regulation effects of *Heliothis virescens* (F.) larvae induced by teratocytes of *Cardiochiles nigriceps* (V.) (Lepidoptera, Noctuidae – Hymenoptera, Braconidae). *Arch. Insect Biochem. Physiol.* 19, 177–192. doi: 10.1002/arch.940190304

Pennacchio, F., Vinson, S. B., and Tremblay, E. (1993). Growth and development of *Cardiochiles nigriceps* (V.) (*Hymenoptera, Braconidae*) larvae and their synchronization with some changes of the hemolymph composition of their host, *Heliothis virescens* (F.) (Lepidoptera, Noctuidae). *Arch. Insect Biochem. Physiol.* 24, 65–77. doi: 10.1002/arch.940240202

Pennacchio, F., Vinson, S. B., Tremblay, E., and Ostuni, A. (1994). Alteration of ecdysone metabolism in *Heliothis virescens* (F.) (Lepidoptera, Noctuidae) larvae induced by *Cardiochiles nigriceps* (V.) (Hymenoptera, Braconidae). *Insect Biochem. Mol. Biol.* 24, 383–394.

Provost, B., Varricchio, P., Arana, E., Espagne, E., Falabella, P., Huguet, E., et al. (2004). Bracovirus contain a large multigene family coding for protein tyrosine phosphatases. *J. Virol.* 78, 13090–13103. doi: 10.1128/JVI.78.23.13090-13103.2004

Rexin, D., Meyer, C., Robaglia, C., and Veit, B. (2015). TOR signalling in plants. *Biochem. J.* 15, 1–14. doi: 10.1042/BJ20150505

Russell, R. C., Fang, C., and Guan, K. L. (2011). An emerging role for TOR signalling in mammalian tissue and stem cell physiology. *Development* 138, 3343–3356. doi: 10.1242/dev.058230

Salvia, R., Grossi, G., Amoresano, A., Scieuzo, C., Nardiello, M., and Giangrande, C. (2017). The multifunctional polydnavirus TnBVANK1 protein: impact on host apoptotic pathway. *Sci. Rep.* 7:11775. doi: 10.1038/s41598-017-11939-x

Scieuzo, C., Nardiello, M., Salvia, R., Pezzi, M., Chicca, M., and Leis, M. (2018). Ecdysteroidogenesis and development in *Heliothis virescens* (Lepidoptera: Noctuidae): focus on PTTH-stimulated pathways. *J. Insect Physiol.* 15, 57–67. doi: 10.1016/j.jinsphys.2018.02.008

Silverman, N., and Maniatis, T. (2001). NF-kB signaling pathways in mammalian and insect innate immunity. *Genes Dev.* 15, 2321–2342. doi: 10.1101/gad.909001

Smith, W. A., Combest, W. L., and Gilbert, L. I. (1986). Involvement of cyclic AMP-dependent protein kinase in prothoracicotropic hormone-stimulated ecdysone synthesis. *Mol. Cell. Endocrinol.* 47, 25–33. doi: 10.1016/0303-7207(86)90012-2

Smith, W. A., Lamattina, A., and Collins, M. (2014). Insulin signaling pathways in lepidopteran ecdysone secretion. *Front. Physiol.* 5:19. doi: 10.3389/fphys.2014.00019

Stoltz, D. B., and Vinson, S. B. (1979). Viruses and parasitism in insects. *Adv. Virus Res.* 24, 125–171. doi: 10.1016/S0065-3527(08)60393-0

Strand, M. R. (2010). "Polydnaviruses," in *Insect Virol*, eds S. Asgari and K. N. Johnson (Norwich: Caister Academic Press), 216–241.

Strand, M. R., and Burke, G. R. (2014). Polydnaviruses: nature's genetic engineers. *Ann. Rev. Virol.* 1, 333–354. doi: 10.1146/annurev-virology-031413-085451

Tanaka, T., and Vinson, S. B. (1991). Depression of prothoracic gland activity of *Heliothis virescens* by venom and calyx fluids from the parasitoid. *Cardiochiles nigriceps. J. Insect Physiol.* 37, 139–144. doi: 10.1016/0022-1910(91)90099-L

Tang, Z., Ioja, E., Bereczki, E., Hultenby, K., Li, C., Guan, Z., et al. (2015). mTOR mediates tau localization and secretion: implication for Alzheimer's disease. *Biochim. Biophys. Acta* 1853, 1646–1657. doi: 10.1016/j.bbamcr.2015.03.003

Thoetkiattikul, H., Beck, M. H., and Strand, M. R. (2005). Inhibitor κB-like proteins from a polydnavirus inhibit NF-κB activation and suppress the insect immune response. *Proc. Nat. Acad. Sci. U.S.A.* 102, 11426–11431. doi: 10.1073/pnas.0505240102

Tiwari, P. C., and Pal, R. (2017). The potential role of neuroinflammation and transcription factors in Parkinson disease. *Dialogues Clin. Neurosci.* 19, 71–80.

Tramutola, A., Triplett, J. C., Di Domenico, F., Niedowicz, D. M., Murphy, M. P., Coccia, R., et al. (2015). Alteration of mTOR signaling occurs early in the progression of Alzheimer disease (AD): analysis of brain from subjects with pre-clinical AD, amnestic mild cognitive impairment and late-stage AD. *J. Neurochem.* 133, 739–749. doi: 10.1111/jnc.13037

Valzania, L., Romani, P., Tian, L., Li, S., Cavaliere, V., Pennacchio, F., et al. (2014). A polydnavirus ANK protein acts as virulence factor by disrupting the function of prothoracic gland steroidogenic cells. *PLoS One* 9:e95104. doi: 10.1371/journal.pone.0095104

Vanderzant, E. S., Richardson, C. D., and Fort, S. W. Jr. (1962). Rearing of the bollworm on artificial diet. *J. Econ. Entomol.* 55:140. doi: 10.1673/031.007.3501

Varricchio, P., Falabella, P., Sordetti, R., Graziani, F., Malva, C., and Pennacchio, F. (1999). *Cardiochiles nigriceps* polydnavirus: molecular characterization and gene expression in parasitized *Heliothis virescens* larvae. *Insect Biochem. Mol. Biol.* 29, 1087–1096. doi: 10.1016/S0965-1748(99)00087-9

Vinson, S. B., Guillot, F. S., and Hays, D. B. (1973). Rearing of *Cardiochiles nigriceps* in the laboratory, with *Heliothis virescens* as hosts. *Ann. Entomol. Soc. Am.* 66:1172. doi: 10.1093/aesa/66.5.1170

Vogel, H., Badapanda, C., Knorr, E., and Vilcinskas, A. (2014). RNA-sequencing analysis reveals abundant developmental stage-specific and immunity-related genes in the pollen beetle *Meligethes aeneus*. *Insect Mol. Biol.* 23, 98–112. doi: 10.1111/imb.12067

Volkoff, A. N., Jouan, V., Urbach, S., Samain, S., Bergoin, M., and Wincker, P. (2010). Analysis of virion structural components reveals vestiges of the ancestral ichnovirus genome. *PLoS Pathog.* 6:e1000923. doi: 10.1371/journal.ppat.1000923

Wang, C., Yu, J. T., Miao, D., Wu, Z. C., Tan, M. S., and Tan, L. (2014). Targeting the mTOR signaling network for Alzheimer's disease therapy. *Mol. Neurobiol.* 49, 120–135. doi: 10.1007/s12035-013-8505-8

Webb, B. A., Beckage, N. E., Hayakawa, Y., Krell, P. J., and Lanzrein, B. (2000). "Family polydnaviridae," in *Virus Taxonomy: Seventh Report of the International Committee on Taxonomy of Viruses*, eds M. H. V. Van Regenmortel (Cambridge, MA: Academic Press), 253–260.

Webb, B. A., and Dahlman, D. L. (1985). Developmental pathology of *Heliothis virescens* larvae parasitized by *Microplitis croceipes*: parasite-mediated host developmental arrest. *Arch. Insect Biochem. Physiol.* 2, 1–139. doi: 10.1002/arch.940020203

Webb, B. A., and Strand, M. R. (2005). "The biology and genomics of polydnaviruses," in *Comprehensive Molecular Insect Science*, Vol. 6, eds L. I. Gilbert, K. Iatrou, and S. S. Gill (San Diego: Elsevier), 260–323.

Webb, B. A., Strand, M. R., Dickey, S. E., Beck, M. H., Hilgarth, R. S., Barney, W. E., et al. (2006). Polydnavirus genomes reflect their dual roles as mutualists and pathogens. *Virology* 347, 160–174. doi: 10.1016/j.virol.2005.11.010

Wyder, S., Blank, F., and Lanzrein, B. (2003). Fate of polydnavirus DNA of the egg–larval parasitoid *Chelonus inanitus* in the host *Spodoptera littoralis*. *J. Insect Physiol.* 49, 491–500. doi: 10.1016/S0022-1910(03)00056-8

Xu, Y., Liu, C., Chen, S., Ye, Y., Guo, M., Ren, Q., et al. (2014). Activation of AMPK and inactivation of Akt result in suppression of mTOR-mediated S6K1 and 4E-BP1 pathways leading to neuronal cell death in in vitro models of Parkinson's disease. *Cell. Signal.* 26, 1680–1689. doi: 10.1016/j.cellsig.2014.04.009

Yee, M. L., and Tan, H. H. (2017). Use of everolimus in liver transplantation. *World J. Hepatol.* 18, 990–1000. doi: 10.4254/wjh.v9.i23.990

Zhang, H., Stallock, J. P., Ng, J. C., Reinhard, C., and Neufeld, T. P. (2000). Regulation of cellular growth by the Drosophila target of rapamycin dTOR. *Genes Dev.* 14, 2712–2724. doi: 10.1101/gad.835000

Conflict of Interest Statement: The authors declare that the research was conducted in the absence of any commercial or financial relationships that could be construed as a potential conflict of interest.

frontiers in Physiology

REVIEW
published: 28 March 2019
doi: 10.3389/fphys.2019.00319

Beetles as Model Organisms in Physiological, Biomedical and Environmental Studies – A Review

Zbigniew Adamski[1,2], Sabino A. Bufo[3,4], Szymon Chowański[1], Patrizia Falabella[3], Jan Lubawy[1], Paweł Marciniak[1], Joanna Pacholska-Bogalska[1], Rosanna Salvia[3], Laura Scrano[5], Małgorzata Słocińska[1], Marta Spochacz[1], Monika Szymczak[1], Arkadiusz Urbański[1], Karolina Walkowiak-Nowicka[1] and Grzegorz Rosiński[1]*

[1] Department of Animal Physiology and Development, Institute of Experimental Biology, Faculty of Biology, Adam Mickiewicz University in Poznań, Poznań, Poland, [2] Laboratory of Electron and Confocal Microscopy, Faculty of Biology, Adam Mickiewicz University in Poznań, Poznań, Poland, [3] Department of Sciences, University of Basilicata, Potenza, Italy, [4] Department of Geography, Environmental Management & Energy Studies, University of Johannesburg, Johannesburg, South Africa, [5] Department of European and Mediterranean Cultures, University of Basilicata, Matera, Italy

OPEN ACCESS

Edited by:
Fernando Ariel Genta, Fundação Oswaldo Cruz (Fiocruz), Brazil

Reviewed by:
Jake Socha, Virginia Tech, United States
Carlos Peres Silva, Federal University of Santa Catarina, Brazil
Rodrigo Nunes Da Fonseca, Federal University of Rio de Janeiro, Brazil

***Correspondence:**
Zbigniew Adamski
zbigniew.adamski@amu.edu.pl; ed@amu.edu.pl

Specialty section:
This article was submitted to Invertebrate Physiology, a section of the journal Frontiers in Physiology

Received: *19 October 2018*
Accepted: *11 March 2019*
Published: *28 March 2019*

Citation:
Adamski Z, Bufo SA, Chowański S, Falabella P, Lubawy J, Marciniak P, Pacholska-Bogalska J, Salvia R, Scrano L, Słocińska M, Spochacz M, Szymczak M, Urbański A, Walkowiak-Nowicka K and Rosiński G (2019) Beetles as Model Organisms in Physiological, Biomedical and Environmental Studies – A Review. Front. Physiol. 10:319. doi: 10.3389/fphys.2019.00319

Model organisms are often used in biological, medical and environmental research. Among insects, *Drosophila melanogaster*, *Galleria mellonella*, *Apis mellifera*, *Bombyx mori*, *Periplaneta americana,* and *Locusta migratoria* are often used. However, new model organisms still appear. In recent years, an increasing number of insect species has been suggested as model organisms in life sciences research due to their worldwide distribution and environmental significance, the possibility of extrapolating research studies to vertebrates and the relatively low cost of rearing. Beetles are the largest insect order, with their representative – *Tribolium castaneum* – being the first species with a completely sequenced genome, and seem to be emerging as new potential candidates for model organisms in various studies. Apart from *T. castaneum*, additional species representing various Coleoptera families, such as *Nicrophorus vespilloides*, *Leptinotarsa decemlineata*, *Coccinella septempunctata*, *Poecilus cupreus*, *Tenebrio molitor* and many others, have been used. They are increasingly often included in two major research aspects: biomedical and environmental studies. Biomedical studies focus mainly on unraveling mechanisms of basic life processes, such as feeding, neurotransmission or activity of the immune system, as well as on elucidating the mechanism of different diseases (neurodegenerative, cardiovascular, metabolic, or immunological) using beetles as models. Furthermore, pharmacological bioassays for testing novel biologically active substances in beetles have also been developed. It should be emphasized that beetles are a source of compounds with potential antimicrobial and anticancer activity. Environmental-based studies focus mainly on the development and testing of new potential pesticides of both chemical and natural origin. Additionally, beetles are used as food or for their valuable supplements. Different beetle families are also used as bioindicators. Another important research area using beetles as models is behavioral ecology studies, for instance, parental care. In this paper, we review the current knowledge regarding beetles as model organisms and their practical application in various fields of life science.

Keywords: beetles, model organisms, bioactive compounds, agronomy, immunology, neuroendocrinology, biomonitoring

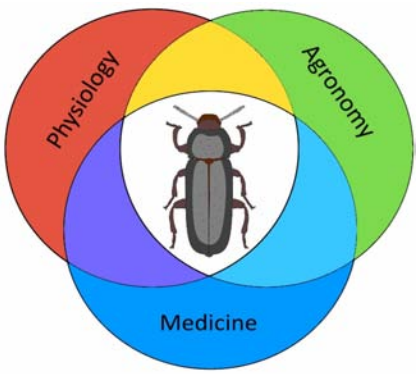

GRAPHICAL ABSTRACT | Beetles at the center of life sciences, more and more often used as model organisms.

INTRODUCTION

Insects are novel model organisms to examine human diseases and to establish drug toxicity due to the conservation of their signaling pathways, energy metabolism and structural components with mammals. Furthermore, insects are cost-effective, easy to rear and time-efficient in the early steps of drug discovery and physiological processes investigation. For over 100 years, the fruit fly, *Drosophila melanogaster*, has been a powerful tool in genetic, behavioral and molecular biology studies. Beyond *Drosophila*, some other insects such as *Galleria mellonella*, *Bombyx mori*, *Periplaneta americana*, and *Locusta migratoria* have been used in biological, medical and environmental research (Stankiewicz et al., 2012; Wang et al., 2014; Soumya et al., 2017; Mikulak et al., 2018). In addition to these insect species, scientists have been recently searching for new model insects for studies in physiological and environmental studies.

During the last decade, the interest of scientists on the Coleoptera order increased, the richest order in the animal kingdom with approximately 400,000 species constituting almost 25% of all known animal life-forms and occupying most terrestrial environments (Stork et al., 2015). Beetles interact with plants and other organisms as well as dead and decaying biotic materials, thus playing a key role in natural and human-dominated ecosystems (McKenna et al., 2009). They have survived major floral and faunal disasters and several mass extinctions over their 300 million years of history (McKenna et al., 2016). Furthermore, many beetle species are serious pests in many areas of the world, leading to significant losses in the nutritional value of plants and agricultural products (Tribolium Genome Sequencing Consortium, 2008). Therefore, the sequencing of some beetle genomes has provided a powerful tool for revealing genomic innovations contributing to the evolutionary success of beetles and understanding of insecticide resistance mechanisms, the specificity and effectiveness of insecticides and biological agents, the interactions of host plants with microorganisms, and, finally, the development of new protection methods.

So far, 11 genomic sequences are available for 11 beetle species; among them, 7 have been published (McKenna, 2018). The first sequenced beetle genome was the red flour beetle, *T. castaneum,* an important pest of agricultural products (Tribolium Genome Sequencing Consortium, 2008). The *T. castaneum* genome contains large expansions of odorant receptors, gustatory receptors, and genes putatively involved in detoxification, which reflects the ability of the pest to interact with a diverse chemical environment. Some developmental processes of *T. castaneum* are more representative and comparable to those of mammals than those of *Drosophila* (Schroder et al., 2008). The ancestral genes involved in cell-to-cell communication expressed in the growth zone crucial for axial extension in short-term development make *T. castaneum* ideal for studying the evolution of development, such as segment specifications (Von Dassow et al., 2000) or multilevel selection (Goodnight, 2005). Genetic knowledge, and, in particular, easy genetic manipulations of gene expression RNA interference (RNAi) (Bucher et al., 2002; Knorr et al., 2018) at different stages of *T. castaneum* development make this beetle an even more valuable model in a number of research fields, for example, identification of targets for selective insect control. Currently, *T. castaneum* is a one of the most convenient genetic models for post-genomic studies such as RNA expression profiling, proteomics and functional genomics, mechanisms of insect immunity (Altincicek and Vilcinskas, 2007), gene–food interactions (Grunwald et al., 2013) or host–pathogen relationships (Milutinović et al., 2013).

A short time after the *T. castaneum* genome was sequenced, other beetle genomes were also sequenced; in 2013, the mountain pine beetle, *Dendroctonus ponderosae*, an important forest pest (Keeling et al., 2013), and in 2015, the coffee berry borer, *Hypothenemus hampei,* and the burying beetle, *N. vespilloides,* (Cunningham et al., 2015b; Vega et al., 2015) genomes were published. In their genomes, genes putatively involved in detoxification and plant cell wall degradation, as well as gene of bacterial sucrose-6-phosphate hydrolase, with proposed relevance to digestive physiology have been found. Furthermore, it was found that the *N. vespilloides* genome has an active DNA methylation system and genes responsible for social behavior. The genomes of *Oryctes borbonicus* (Meyer et al., 2016) and *Anoplophora glabripennis* (McKenna et al., 2016) were published in 2016.

Of particular interest is the sequencing of the genome of the Colorado potato beetle, *Leptinotarsa decemlineata*, one of the main pests that is difficult to manage, which has a special ability to adapt to solanaceous plants and changing environmental conditions (Schoville et al., 2018). The *L. decemlineata* genome analysis supports a rapid evolutionary change and confirms the genomic basis of phytophagy and insecticide resistance. It was found that *L. decemlineata* has evolved resistance to over 50 pesticides. Adaptations to plant nutrition have been observed in gene expansions that are putatively involved in digestion and detoxification, as well in gustatory receptors for bitter taste. The spectacular ability to exploit novel host plants and unusual resistance together with the newly released genome make *L. decemlineata* a good model system for agricultural pest

genomics and developing sustainable methods to control this pest (Schoville et al., 2018).

Sequencing of genomes combined with the development of proteomic techniques such as mass spectrometry enables the understanding of the evolutionary and genomic basis of the biodiversity of beetles' genomes and importantly, applying new technologies to the exploitation of beetle genomes for human purposes. However, the majority of beetles intensively developed in many research areas, e.g., *Tenebrio molitor*, *Coccinella septempunctata*, *Poecilus cupreus* and many others, still have unknown genomes. We suppose that it is only a matter of time because beetles are convenient and inexpensive animal models, invaluable for studying physiological processes during insect development and biomedical and pharmacological research between invertebrates and vertebrates.

Many physiological mechanisms of insects exhibit a high level of similarity or identity with higher animals (Altincicek et al., 2008; Ntwasa et al., 2012). The neuroendocrine system exhibits similarities at the structural, functional and developmental levels between beetles and vertebrates (Hartenstein, 2006). Signaling molecules such as hormones and neuropeptides of insects have physiological counterparts in mammals, indicating that they are highly conserved in the animal kingdom. This fact provides an opportunity to perform comparative studies between invertebrates and vertebrates concerning neurobiology and the role of signaling molecules in animal physiology. This approach may be promising for the treatment of many human diseases, such as obesity, metabolic syndrome or cardiovascular diseases (Chowański et al., 2017a).

Furthermore, beetle models have been developed at the early steps of pharmacological studies for testing the activity of new substances of both synthetic and natural plant or animal origin. Moreover, Coleopterans themselves are a source of compounds with a potential antimicrobial and antitumor activity, which could likely be used in cancer therapy and immunology (Słocińska et al., 2008; Chowański et al., 2017a; Walkowiak-Nowicka et al., 2018). For these reasons, the use of beetle model systems for screening of drugs and active agents seems to be reasonable.

Vertebrate models have many limitations: long generation time, low fecundity, high housing costs and ethical permissions. Recently, *T. castaneum* has been used as an early warning system for environmental effectors, such as nutrients or pharmaceutics, effects on the health and lifespan of living organisms (Denell, 2008; Grunwald et al., 2013; Bingsohn et al., 2016). Additionally, beetles are used as food or sources of valuable food supplements.

In this paper, we review the current state of knowledge regarding beetles as model organisms in biomedical and environmental studies. We show the applications of beetle models in different fields of research, such as neuroendocrinology, immunology, pharmacology and toxicology. Moreover, we indicate the importance of beetles in environmental studies including agriculture, food production or ecosystem monitoring, which are closely interrelated with physiological studies as well.

NEUROENDOCRINOLOGY

Through the process called neuroendocrine integration, the nervous system and the endocrine system interplay together in regulation of function and homeostasis maintenance. Different studies have emphasized the similarities between the neuroendocrine system of vertebrates and arthropods (especially insects, including beetles) at the structural, functional, and developmental levels (Hartenstein, 2006; De Loof et al., 2012). The hormone-producing neurons are called neurosecretory cells (NSCs). In vertebrates, they are located mainly in the hypothalamus. NSCs, besides innervating brain centers and thereby influencing neural circuits as "neuromodulators," send their axons to the peripheral neurohaemal glands (posterior pituitary gland) in which hormones produced by the NSCs are stored and released. The stimulatory neurohormones are also transported by the portal blood vessel system to the anterior pituitary, where they cause the release of a specific hypophyseal hormone (McKinley et al., 2016). Insects do not have any region of a brain that can be considered as a morphological and physiological counterpart of the hypothalamus, nor any portal blood vessel system in their brain (De Loof et al., 2012). However, the corresponding structures would be groups of NSCs located in the brain protocerebrum, such as the *pars intercerebralis* (PI), *pars lateralis* (PL), or tritocerebrum. NSCs are also located in the suboesophageal and/or ventral nerve cord ganglia. PI/PL project their axons toward peripheral targets, which are the paired neurohaemal organs *corpora cardiaca* (CC) and *corpora allata* (CA) situated in the beetle's head capsule on both sides of the proximal end of the aorta, and form a retrocerebral complex (Sliwowska et al., 2001; Urbański et al., 2018). Like the mammalian pituitary gland, the CC of insects/beetles consists of two distinct lobes: an unpaired ventral storage lobe, containing the NSCs' terminals located in the PI and PL, and a more lateral glandular neurohaemal lobe, which also has its own NSCs (**Figure 1**).

Despite anatomical and functional similarities in the neuroendocrine system, there is a great resemblance of the signaling molecules of invertebrates and vertebrates, which is summarized in: (Chowański et al., 2017a). Most of the hormones or neurohormones found in the animal kingdom are short polypeptides produced by proteolytic cleavage from larger precursor proteins, called prohormones. Major examples of neuropeptides found in insects/beetles and their analogs in vertebrates are adipokinetic hormones (AKHs) that resemble mammalian glucagon, insulin-like peptides (ILPs) that resemble mammalian insulin, tachykinin-related peptides (TRPs) that resemble mammalian tachykinins, and many others (Chowański et al., 2017a). Considering all the above described structural and functional similarities, an increasing number of studies has been conducted under the neuroendocrine regulation of various physiological processes. There are two main areas of interest in biomedical aspects: (a) the use of simple insect models of the neuroendocrine system for detailed study of the complex mechanisms of neurohaemal regulation in mammals and other higher vertebrates to reveal the principles of various disorders; (b) a source of biologically active substances as a basis for new

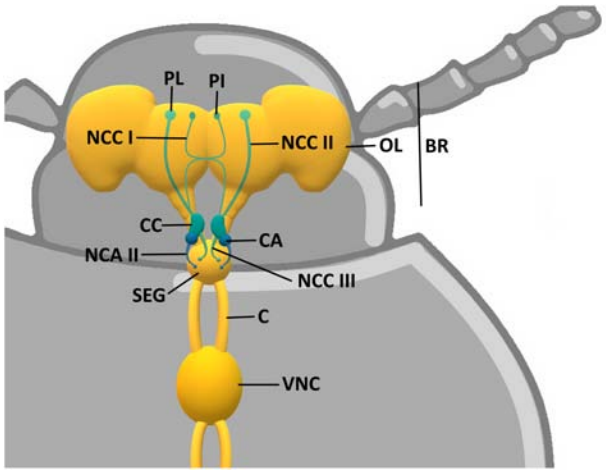

FIGURE 1 | Scheme of *Tenebrio molitor* neuroendocrine system. BR, brain; OP, optical lobe; PI, *pars intercerebralis*; PL, *pars lateralis*; NCC I, NCC II, and NCC III, *nervi corporis cardiaci* I, II, and III; CC, *corpora cardiaca*; CA, *corpora allata*; NCA II, *nervi corporis allati* II; SEG, suboesophageal ganglion; C, connectives; VNC, ventral nerve cord.

agents used in therapy of disorders. Below, we describe some examples of research conducted on insect neuropeptides in the context of biomedical studies.

Food Intake

Feeding behavior and energy homeostasis is under strict neuroendocrine and endocrine control (Monteleone et al., 2018). Key players in this process in vertebrates are the so-called metabolic hormones, such as leptin, ghrelin or cholecystokinin (CCK), as well as neuropeptides, e.g., neuropeptide Y or orexins (Monteleone et al., 2018). In invertebrates, there are several analogs and homologs of these molecules that are similar on both the structural and functional level and sometimes common in origin. Sulfakinins (SKs) are insect homologs of mammalian gastrin/cholecystokinin (Rehfeld, 2017). They have been identified in various insects in two forms: containing sulfated or non-sulfated tyrosine (Nässel and Williams, 2014). This structural similarity together with the well-conserved *C*-terminal amino acid sequence HMRFa puts SKs in the family of CCK-like peptides. In mammals, CCK is a pleiotropic peptide responsible for various physiological processes, mainly as a regulator of satiety signaling (Rehfeld, 2017). Similarities between CCK and SKs were also found at the functional level. Studies on the beetles *T. castaneum* and *Zophobas atratus* showed that SKs inhibit food consumption and regulate energy metabolism in these species and hence may be a part of the insect brain-gut axis (Yu et al., 2013; Słocińska et al., 2015b). CCK signaling disorders in humans are associated with various illnesses, such as obesity or depression (Coulter et al., 2017; Klockars et al., 2018). Thus, SKs may be a good source of potent agents used for the treatment of these diseases in the future. This approach is even more possible since a similarity between CCK receptors and SK receptors has been shown (Słocińska et al., 2015a; Yu et al., 2015).

Cardiovascular Diseases – A New Approach Using the Insect Heart

Cardiovascular disorders (CVDs) are among the most common diseases in the world. Therefore, it is important to gain extensive knowledge about the mechanisms that cause certain diseases or, on the other hand, find various substances that modify the activity of the heart to create a solid basis for further progress in the treatment of CVDs. Research on various insect models, including beetles, are very promising in this field (Szymczak et al., 2014; Zhu et al., 2017; Pacholska-Bogalska et al., 2018). The heart/myocardium of insects has been shown to be a convenient biomedical model. The spectrum of neurotransmitters, neuropeptides and peptide hormones that affect contractility and regulate normal heart rhythm is quite large (Chowański et al., 2016). Among them, many exhibit structural similarities to mammalian peptides/hormones (Chowański et al., 2017a). For example, myosuppressins, due to the highly conserved *C*-terminal amino acid sequence FLRFa, belong to the superfamily of RFamide peptides (Fukusumi et al., 2006). It has been demonstrated that mammalian RFamides inhibit the contractility of the vertebrate/insect myocardium (Nichols et al., 2012). The cardioinhibitory effects of myosuppressin were also observed in studies on the *Z. atratus* myocardium (Marciniak et al., 2010b). Small, highly specific molecules are the preferred candidates for drug discovery, partly due to delivery, synthesis and cost. In addition, the components of transduction mechanisms are targets for the development of therapeutic strategies for the treatment of diseases, such as heart failure. Furthermore, the insect G protein-coupled receptor for myosuppressin resembles mammalian GPCRs (Leander et al., 2015).

Growth, Development and Reproduction Regulators

In insects, two groups of neuropeptides are proven to be involved in the regulation of growth, metamorphosis and reproduction by regulation of production and secretion of the juvenile hormone (JH) by CA (Feyereisen, 1985), stimulatory allatotropins or inhibitory allatostatins. Among allatostatins, three separate families can be distinguished, which vary structurally (Lubawy et al., 2018). The most interesting of these families for biomedical research seems to be the so-called PISCF/ASTC allatostatins. Structural similarities between mature somatostatin and mature PISCF/ASTCs are not very relevant. However, the resemblance between the vertebrate somatostatin/cortistatin precursors and the arthropod ASTC/ASTCC precursors consists of a disulfide bridge at the *C*-terminal end of these two precursors. Moreover, insect ASTC receptors are closely related to somatostatin receptors (Veenstra, 2009). In *T. castaneum*, ASTC receptor was shown to be shorter than other insect receptors but similar in size to human SSTR3 receptor (Audsley et al., 2013). ASTCs are thus considered arthropod somatostatin homologs (Veenstra, 2009). Next, the physiological resemblance is also evident. Human somatostatin acts on different tissues in the human body and in general, is known as an inhibitory peptide (Gahete et al., 2010). The same situation occurs in insects, as was shown in

beetle models. PISCF/ASTCs were shown to be inhibitory in *T. castaneum* and *T. molitor* (Abdel-latief and Hoffmann, 2010, 2014; Lubawy et al., 2013). These similarities provide a starting point for fundamental studies about the pharmacology of human somatostatin receptors (SSTRs). Insect allatostatin C sequences may yield useful peptides to produce new ligands. Ligands for SSTRs are still needed to treat different endocrinopathies such as Cushing's disease or acromegaly (Langlois et al., 2018; Paragliola and Salvatori, 2018).

Diuresis Regulators

Other neuropeptides that are of interest in biomedical research are nonapeptides, oxytocin, and arginine vasopressin. In mammals, they are produced and released by the posterior lobe of the pituitary gland and influence many tissues and organs. To date, it is known that oxytocin and vasopressin mediate a range of physiological functions that are important for osmoregulation, reproduction, complex social behaviors, memory and learning. Comparing amino acid sequences of mature peptides across invertebrates and mammals, it is clear that some positions are highly conserved. For example, they have the same length and position of Cys residues crucial for forming disulfide bonds (Gruber, 2014). Moreover, invertebrate receptors for vasopressin show a high degree of similarity to mammalian ones (Liutkeviciute et al., 2016). Recently, 260 species of arthropods were searched for the presence of the inotocin peptide GPCR signaling system, and it was shown that not all of the insect orders possess this signaling system. Trichoptera, Lepidoptera, Siphonaptera, Mecoptera, and Diptera lack the presence of inotocin genes, which suggests that this peptide-receptor system was probably lost in their common ancestors (Liutkeviciute et al., 2016). For this reason, beetles seem to be better models to study inotocin signaling than the insect commonly used in biomedical research, *D. melanogaster*. Among Coleoptera, all 20 analyzed species exhibited evidence for the presence of the inotocin signaling system (Liutkeviciute et al., 2016). Vasopressin-like peptides and their receptors were already characterized from the *T. castaneum* beetle and were shown to be crucial for diuresis regulation in this species (Aikins et al., 2008).

Owing to this structural and physiological importance, ligands of oxytocin and vasopressin receptors have potential therapeutic applications for novel treatment approaches to different osmoregulatory disorders such as diabetes insipidus, as well as cardiovascular or even mental disorders (Gruber, 2014; Di Giglio et al., 2017).

IMMUNOLOGY

The immune system of insects is based primarily on innate immune mechanisms that might be divided into cellular and humoral responses. The cellular response includes all processes in which morphotic components of insect haemolymph, haemocytes, participate. We indicate three main cellular mechanisms: phagocytosis, nodulation and encapsulation (Strand, 2008; Urbański et al., 2014). The humoral response includes processes in which molecules such as antimicrobial peptides (AMPs), lysozyme or phenoloxidase (PO) participate, for which the concentration increases dramatically after a pathogen infection (Bulet et al., 1999; Wojda et al., 2009). However, distinction between these two types of immune response is artificial, because pathogen recognition by haemocytes is crucial for the activation of humoral responses, and humoral mechanisms stimulate the activity of haemocytes (Strand, 2008; Urbański et al., 2017).

The use of beetles as model organisms in biomedical studies is associated with the similarity of basic immune mechanisms, such as pathogen recognition, immunodeficiency, and molecular pathways such as Toll and JAK/STAT signaling (Altincicek et al., 2008; Vogel et al., 2014; **Figure 2**). In each of these mechanisms, their individual components have vertebrate counterparts, starting from the receptors (e.g., beetle Toll receptor and mammalian Toll-like receptor) and ending with transcription factors (e.g., transcription factor Dif characteristic for immunodeficiency pathways belongs to the NF-κB transcription factor family) (Maxton-Küchenmeister et al., 1999; Chen et al., 2000; Yokoi et al., 2012; Johnston et al., 2014). Moreover, recent studies generally concerning molecular similarities between insects and vertebrates indicated that beetles have retained many ancestral genes compared to those of other insect orders (Savard et al., 2006; Van der Zee et al., 2008). Many of these genes were found in vertebrates and beetles but not in fruit flies. Also, beetle immune-related genes often have a higher level of similarity and identity with vertebrate analogs than those observed in *Drosophila* species, for example, insect Toll protein and vertebrate Toll-like receptor. Furthermore, the similarities of the insect and vertebrate immune systems are present also in the regulation of their function, for example, by serpins (serine protease inhibitors) (Gooptu and Lomas, 2009; Jiang et al., 2011). All of these studies clearly indicate that beetles are useful models for studies concerning the molecular basis of the innate immune response and its evolution (Savard et al., 2006; Ntwasa et al., 2012). Moreover, the availability of the full genome sequence of several beetle species allows for genetic manipulation, including gene knockdowns using RNAi, and leads to unquestionable progress in the use of beetles in these kinds of studies (Rajamuthiah et al., 2015).

Similarities between beetles and vertebrates are also evident in the regulation of haemocyte activity during the cellular response. The similarity can be exemplified by the regulation of phagocytosis in both animal groups by focal adhesion kinase (FAK) and mitogen-activated protein kinase pathways (MAPK) (McLeish et al., 1998; Tang et al., 2014).

AGRONOMY AND ECOLOGY

Crop Growth, Food Production and New Sources of Nutrition

Beetles play an important role in agriculture and food production. However, their influence on these fields of studies can be positive and negative. In our review, we focus on the use of beetles as alternative sources of food and their role in maintaining a good

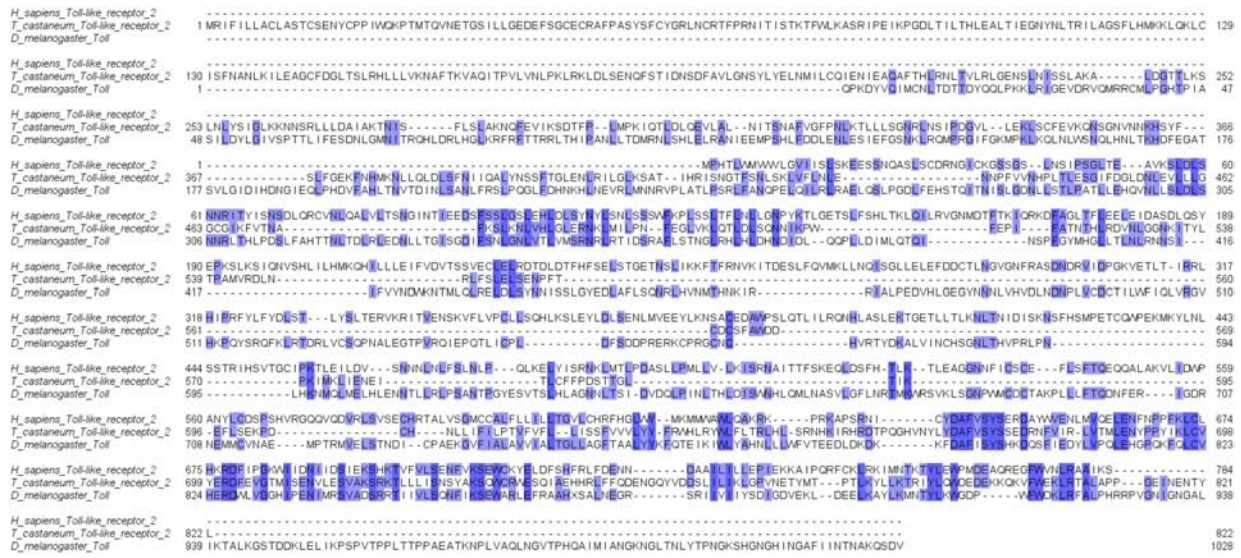

FIGURE 2 | An exemplary comparison of similarity between important parts of insect and mammalian immune systems. Alignment of human Toll-like receptor 2 sequence and its structural homologs identified in *Tribolium castaneum* and *Drosophila melanogaster.* Color indicates identity in the amino acid sequence. The sequences of receptors were obtained from a BLAST search in a public database (NCBI) using the blastp algorithm to analyze the transcriptomic data of *Homo sapiens, T. castaneum* (AN: PRJNA15718) and *D. melanogaster* (AN: PRJNA164). The alignment was made using JalView software (ver. 2.10.).

condition of cultivated fields as well as their importance for ecosystem stability.

It is obvious that the present-day world needs to develop alternative sources of proteins for livestock feed as well as for the human diet, considering the production of high-protein foods is extremely expensive, due to the costs concerning money spent directly on animal farming and costs resulting from space-, water- and environment-consumption. The production of 1 kg of beef consumes 15,000 L of water and 330 m^2 of soil and introduces 16.4 kg of CO_2 into the environment (FAO, 2013). Moreover, livestock production is the world's largest user of land (Foley et al., 2011). Thus, searching for new, less expensive sources of nutrient-rich and high-caloric food is a large challenge for contemporary society. Insects are of a great interest as a possible solution due to their capability to satisfy two different requirements: (1) they are an important source of protein and other nutrients and (2) their use as food has ecological advantages over conventional meat and, in the long run, leads to economic benefits (Belluco et al., 2013). Globally, the most commonly consumed insects are beetles (Coleoptera); they account 31% percent of insects used as a food. Overall, insect breeding should not compete for space or other resources with plant culture; instead that, it should complement it, e.g., insects may feed on plants or plant parts that are unsuitable for human consumption or on organic wastes (FAO, 2013). It is also suggested that insects can be a huge source of plant cell wall degrading enzymes (Pauchet et al., 2010; Busch et al., 2017). Therefore, insects are able to contribute significantly to cycles of matter (Katayama et al., 2008). In this way, organic wastes can be used for feed production *via* insects. Ramos-Elorduy et al. (2002) used *T. molitor* larvae reared on organic wastes as a supplementation to the diet of broiler chickens. Dried and milled larvae were added to fodder at a concentration of 5 or 10% of total weight. The addition of larvae to the basic diet did not significantly affect food intake, weight gain, or feed efficiency (Ramos-Elorduy et al., 2002). Moreover, addition of fermented *T. molitor* and *Z. atratus* to broiler meal lead to reduction of caecal *Escherichia coli* and *Salmonella spp*. and increased IgG and IgA levels. Most likely, these effects are combined results of chitin and probiotics contained in this forage (Islam and Yang, 2016; Gasco et al., 2018). Similar results were also obtained in studies on European sea bass fingerlings, in which *T. molitor* enhances lysozyme activity (Gasco et al., 2018; Henry et al., 2018). Beetle forage may also be used as meal for aquatic invertebrates. Panini et al. (2017a,b) showed that replacing fishmeal with mealworm meal does not alter protein content in the muscles of *Litopenaeus vannamei* shrimp, but it increased the lipid content. However, for a human nutritional perspective, the lipid content of the shrimps is considered low and within the optimal concentration (Panini et al., 2017a,b). An advantage of insects as a food/fodder is that they have higher feed conversion efficiency in comparison to conventional livestock, i.e., they need less feed to produce 1 kg of biomass (Rumpold and Schluter, 2013). For example, the average daily gain of *T. molitor* larvae is 2 and 25 times higher than that for pigs and beef cattle, respectively, and they produce much less CO_2 (g/kg mass gain) than the mentioned livestock. Moreover, the production of other greenhouse gasses (N_2O, CH_4, and NH_3) is also significantly lower (Oonincx et al., 2010). Life cycle assessment studies covering all energy costs of biomass production by organisms have been performed (e.g., food consumption, feed production, transport, electricity, etc.). Studies conducted by Oonincx and de Boer (2012) showed that production of 1 kg of dry biomass and production of 1 kg of edible proteins by larvae of two beetle species, *T. molitor* and *Z. atratus*,

requires definitely fewer natural resources than cattle, pigs and chicken. Thus, for every 1 ha of land required for producing mealworm protein, 2.5 ha would be required for producing a similar amount of milk protein, 2–3.5 ha for pork or chicken protein, and 10 ha for beef protein (FAO, 2013). The efficiency of food conversion into biomass may significantly differ in insects depending on the diet composition. However, insects can be bred on organic byproducts, wastes which cannot be used in the case of pigs, sheep, or beef cattle. Larvae of three tenebrionid beetles, *T. molitor*, *Z. atratus*, and *Alphitobius diaperinus*, fed with organic byproducts from beer brewing, bread/cookie baking, potato processing and bioethanol production still retained high efficiency of food conversion into biomass comparable to that of conventional livestock (van Broekhoven et al., 2015).

Beetles exert an important impact on the condition of cultivated fields. They take part in pest management and soil fertilization and reduce weeds. Two groups are especially important: dung beetles (Scarabaeoidea) and ground beetles (Carabidae). Scarabaeoidea, the coprophagous beetles that feed on animal excreta as both adults and larvae, provide several key functions to agroecosystems. By manipulating feces, dung beetles play an important role in the nutrient cycle, trophic regulation, soil fertilization and biological pest control (Nichols et al., 2008). Studies on the dung beetle, *Onthophagus lenzii*, showed that the beetles' activity significantly affects cow dung decomposition. In the first 5 days, rapid organic nitrogen decomposition is noted, regardless of dung beetle activity. After 15 days, dung beetles accelerate or initiate another ammonification process in residual cow dung and dung balls. They do so by producing aerobic conditions through a rapid decrease in moisture content (Kazuhira et al., 1991). Thus, a soil is fertilized with nitrogen, sulfur and phosphorus forms available for plants. Bang et al. (2005) found that adding one of three tested dung beetle species (*Copris ochus*, *C. tripartitus*, and *O. lenzii*) to cultivated fields increased the annual yield of perennial ryegrass by approximately 20%, and adding all of the species together gave 11% greater yield than that of the control.

The second mentioned group, the ground beetles, has an effective role in weed reduction (granivorous and omnivorous) and pest control (predators). Among all agricultural practices, the management of weeds has historically been the most resource-demanding practice performed by growers (Kulkarni et al., 2015). Seed consumption by Carabidae beetles (e.g., *Pseudoophonus rufipes*, *Harpalus affinis*, and *Amara aenea*) can help to reduce seed stock of a weed species in the range of 65 to 90% (Honek et al., 2005). Weed seed consumption rates of up to 74% have been documented for *Viola arvensis*, *Stellaria media*, and *Capsella bursa-pastoris* in agricultural habitats (Jonason et al., 2013). Within plant-feeding carabids, two "functions" can be distinguished: (1) utilization of green plant parts and fruits for supplementing beetles and (2) feeding on seeds by so-called "spermophagus" species (Kulkarni et al., 2015). The second group of Carabidae beetles forms a large group of formidable predators in the insect world. The following species might be given as examples: *P. cupreus*, *Bembidion lampros*, *Trechus quadristriatus*, *Carabus auratus*, and *Pterostichus melanarius*. Carabidae beetles living on the surface of the soil capture and consume a wide assortment of soil dwelling insects. The potential of carabids for pest control has been recognized a long time ago by observant farmers (Holland, 2002). Exemplary data show their importance. Field data indicate that Carabidae beetles' predation caused an 81% decrease in emerging adults of *Sitodiplosis mosellana* and their parasites (Kromp, 1999). The field population of eggs and first-instar larvae of the cabbage root fly (*Delia radicum*) might even be reduced by 90% by such carabids as *B. lampros* and *T. quadristriatus* (Finch and Elliott, 1992). Another result shows that the population of *L. decemlineata*, in presence of such Carabidae species as *C. auratus* or *P. melanarius,* undergoes reduction of up to 30% (Kromp, 1999).

Pest Management

Among pests, beetles are the one of the most important and largest groups, often with global importance (Spochacz et al., 2018). Therefore, many studies are carried out to check the effect of pesticides against them. Development of resistance to pesticides focuses interest of scientists, from the fields of life sciences to economy and law. *L. decemlineata* has developed resistance against 56 insecticides, *T. castaneum* against 32, and an important pest of rape, *Meligethes aeneus,* against 27 ones (Arthropod-Pesticide-Resistance-Database, 2018). Due to their resistance to numerous xenobiotics, the beetles are models for testing various aspects of this phenomenon, including genetic, enzymatic, physiological and behavioral (Zhang et al., 2012; Crossley et al., 2017; Schoville et al., 2018), as well as models of the evolutionary processes to explain the basis of development of resistance (Pelissie et al., 2018). The level of resistance may increase as much as 2,000 times (Alyokhin et al., 2008). The phenomenon has been studied on economically important beetles: *L. decemlineata*, *Eriopis connexa*, *Cryptolaemus montrouzieri*, *M. aeneus*, and *Sitophilus zeamais* (Guedes et al., 2006; Alyokhin et al., 2008; Zhang et al., 2012; Rodrigues et al., 2013; Stratonovitch et al., 2014). The mechanisms of resistance include alterations at various levels of biological organization and lead to altered behavior and reorganization of physiological processes or structure of cuticle. Therefore, detoxification requires an investment of large amounts of energy. The trade-off of energy between detoxification and insect development is an important topic in the research on resistance. Guedes et al. (2006) suggested that insecticide-resistant beetles are characterized by significantly higher mobilization of energy reserves. The different energy management of the resistant and susceptible strains manifests also, for example, in a different structure of trophocytes. This finding suggests that the metabolism of resistant strain is biased toward detoxification rather than development. Therefore, insecticides and other xenobiotics slow down insects' development, inhibit molting, and decrease emergence (Weissenberg et al., 1998; Adamski et al., 2005; Chaieb, 2010; Barbosa et al., 2018). Some tests indicated that resistance to insecticides may lead to decreased fitness in the insecticide-free environment and results in decreased generation-time and differentially biased sex ratio (Gordon et al., 2015).

Ultrastructural and enzymatic malfunctions and malformations are correlated with the toxicity of insecticidal

compounds, including natural ones. Beetles are used also as model organisms to help explain their mode of action. The involvement of esterases (Cutler et al., 2005) and factors which regulate cytochromes (Kalsi and Palli, 2017) in detoxification of pesticides was proved using beetles. The activity of several enzymes important in pesticide resistance, such as glutathione *S*-transferase, superoxide dismutase, and catalase, was described in model beetle organisms (Papadopoulos et al., 1999; Kostaropoulos et al., 2001; Adamski et al., 2003; Kolawole and Kolawole, 2014; Lambkin and Furlong, 2014; Abdelsalam et al., 2016). Several ultrastructural effects in non-target tissues were described in coleopterans: condensation of chromatin, disruption of biological membranes or malformations of mitochondria (Adamski et al., 2005; Abdelsalam et al., 2016). Hence, cyto-physiological alterations are key reactions explaining the mechanisms of toxicity but also the development of resistance in pests.

Cutler et al. (2005) indicate that pests may be resistant to pesticides that have not been widely used yet. For example, cross-resistance was observed for *L. decemlineata* in Canada (Scott et al., 2015). This phenomenon is of a huge importance to crop protection. Therefore, beetles have also been taken into consideration during construction of mathematical and computer models that simulate the development of resistance and to plan strategies of pesticide management (Argentine et al., 1994; Clift et al., 1997; Stratonovitch et al., 2014; Sudo et al., 2018). *L. decemlineata* has been proposed as an important species for the development of predictive strategies to minimize the resistance to pesticides (Kitaev et al., 2017). This species is also a reference model in research, where resistance of two or more species is confronted (Arain et al., 2017; Spit et al., 2017).

Beetles are amongst the most important species, both as pests and as predators, that limit herbivory. Therefore, regulation of their reproduction, fertility, fecundity, and development is a focus of interest in plant protection and agronomy and is crucial for integrated pest management programs. Mating behavior includes items such as partner recognition, courtship, and copulation. One of the most studied groups is Coccinellidae because of its important role in the reduction of aphids. Lately, the invasiveness of *Harmonia axyridis* has been observed. The sexual behavior of this species has been described as a 5-step process: "approach," "watch," "examine," "mount," and "attempt to copulate" (Obata, 1987). In another ladybird species, *Adelia bipunctata,* no "watching" step occurs (Hemptinne et al., 1998). A peculiar sexual behavior was observed in *Tenuisvalvae notata,* where a male spins two times on the back of a female after the copulation, which was not connected with body adjustment (dos Santos et al., 2017). Pheromones, vision and acoustic signals for communication between two individuals play a very important role in sexual behavior. The sexual behavior of lady beetles relies on pheromones; during the female reproductive cycle particular compounds can be identified. These compounds can be used to manipulate the behavior of insects, and due to this effect, they can be applied as new insect pest management strategies (Fassotte et al., 2016). Some insects, for example, bark beetles, use courtship songs during mating. According to Lindeman and Yack (2015), male *Dendroctonus valens* (Curculionidae) produce acoustic signals while approaching the female gallery. In this way, a female can choose a male grounding on the quality of the male song. The abovementioned studies may inform the use of non-chemical attractants in the future.

An interesting application of beetles in pest management was described for ambrosia beetles, a group of the subfamilies of Scolytidae and Platypodinae (Curculionidae) that are known for cultivating fungi in the galleries they dig inside tree barks. Most of the species of ambrosia beetles attack damaged or dead trees without any negative economic effect. However, there are species (*Platypus koryoensis*, *Xylosandrus compactus*, and *Austroplatypus incompertus*) that are invasive to new habitats and may cause significant losses (Vannini et al., 2017). *A. incompertus* is able to infest healthy, undamaged trees, decreasing the quality of wood. After infestation, the cultivation process is maintained with symbiotic fungi whose spores are released by insects from special morphological structures, the mycangia. In this way, ambrosia beetles are also vectors of fungal infections among trees (Moon et al., 2012). Recent studies have shown that ethanol present in trees promotes the growth of fungi and inhibits the appearance of other non-symbiotic fungi such as *Aspergillus*. Hence, ambrosia beetles choose trees with stem tissues containing ethanol to increase the effectiveness of food production (Ranger et al., 2018). This compound also attracts another ambrosia beetle, *Trypodendron lineatum*, and therefore, it can be used for pest management (Moeck, 1970).

Harmonia axyridis is known to be an invasive species in many countries that contains the native species *A. bipunctata* and *C. septempunctata*. The latest research showed the existence of factors that can promote the invasiveness of harlequin lady beetles (Verheggen et al., 2017). One of them is aggregation behavior, which appears among adults and pupae *H. axyridis*. It has been proved that gregarious pupation decreases mortality in pupae (Roberge et al., 2016) and that adult beetles can aggregate both in wintering and non-wintering conditions (Durieux et al., 2015). Additionally, it was documented that individuals of this species follow objects with highly contrasting colors (Nalepa et al., 2005).

Altogether, the complex, multilevel investigations on insect physiology and behavior may lead to the discovery of novel substances and manners for pest management. In addition, in the field of pesticides and their effects on beetles, in-depth studies focusing on both main and side effects, from the biochemical level through cellular, physiological and organismal effects and up to the ecosystems, are necessary for the proper estimation of their toxicity. The wide range of these studies may show the most realistic effects of pesticides on beneficial organisms.

Biomonitoring

Heavy metals, pesticides, and even radiation alter most of the earth's ecosystems. Therefore, many living organisms are used as models and bioindicators in the monitoring and assessing of the state of the environment and changes in ecosystems and provide warning signals for imminent ecological changes (Nouchi, 2012; Testi et al., 2012; Kalkan and Altuğ, 2015; Parmar et al., 2016; Siddig et al., 2016). Among species that raise great interest in the field of ecosystem monitoring, beetles have started

to attract attention as biological indicators of environmental contaminants (Zödl and Wittmann, 2003). The coleopterans may be found in almost every type of habitat in which any insect is found, and the niches that are inhabited by many species of Coleoptera are often inaccessible for other insects. Some beetle species are also immensely sensitive to changes occurring in their environments (Osman and Shonouda, 2017; Shonouda and Osman, 2018). Taking this fact into consideration along with well-established and standardized collecting methods (Spence and Niemelä, 1994) and readily available keys for identification, coleopterans are perfect organisms for bioindication. Ground beetles (Carabidae) are the most commonly used bioindicators, notably when trying to assess environmental pollution (Abildsnes and Tømmerås, 2000; Ghannem et al., 2018). Other families, such as Curculionidae, Tenebrionidae, and Staphylinidae, are also used (Shonouda and Osman, 2018). Agricultural activities strongly influence the assemblage of ground beetles found in woody habitats and grasslands. In general, more disturbed habitats support ground beetle fauna of smaller average body size (Petit and Usher, 1998). It has been shown that increased agricultural management leads to a decreased number of Carabidae forest species as well as number of individuals in hedgerows (Burel et al., 2004). Changes were correlated to the type of crops cultured between hedgerows. The relative abundance of large carabid species decreased, while small, mobile and more ubiquitous species were favored where cereal crops were cultured. However, some scientists report that even though total richness and composition of the species pools are the same, the rate of beetle species accumulation depends on the type of agricultural practice (Fahrig et al., 2011). Other researchers also showed that human influence, for example, cultivation of orchards, causes qualitative changes in beetle species composition in comparison to that of natural forest habitats (Allegro and Sciaky, 2003). Agricultural and veterinary practice can cause a change in beetle population, as was evaluated in Canada in a study considering endectocides (e.g., doramectin and eprinomectin; macrocyclic lactones that are veterinary parasiticides used to control nematodes and arthropods affecting livestock) (Floate, 2006). Cattle that were exposed to those products excreted metabolites, that were subsequently tested on dung beetles such as *Onthophagus nuchicornis* or *Aphodius prodromus*. The abovementioned endectocides, globally used in treating ectoparasites, reduced useful insect diversity and might cause the accumulation of dung on pastures (Floate, 2006).

Carabidae beetles can also be used as biodiversity indicators. The richness in beetle species can reflect the diversity of other taxa inhabiting a given environment. For example, Pearson and Cassola (1992) have shown the correlation between the richness of tiger beetles (Carabidae: Cicindelinae) and birds and butterflies. Carabid species richness has also been shown to have a positive correlation with that of other beetle families (Scarabaeidae and Pselaphidae) (Oliver and Beattie, 1996). Moreover, observations and quality-checking of beetle species richness and populations' homogeneity/heterogeneity are also used to control the stability of unique habitats, for example, rainforests. Davis (2000) showed that usage of reduced-impact logging in the Malaysian rainforest leaves more equitable and species-rich communities of dung beetles. The dung beetle species richness is also notably higher in primary rainforests, where the majority of species are more abundant than in secondary ones, and plantation sites harbored an impoverished subset of primary forest species (Gardner et al., 2008). Knowledge about these correlations can be a useful tool in monitoring human influence on the natural environment.

Beetles can also be used for determination of heavy metal pollution. Elevated concentrations of lead and mercury were observed in zoophagous species and in some mycetophagous species of Staphylinidae, respectively (Bohac, 1989). Lagisz and Laskowski (2008) showed that an increase in zinc and lead levels in *P. oblongopunctatus* can cause a reduction in elytra length. This evidence shows that pollutants may affect body size, causing its decrease. This effect is probably the result of a negative effect on species development. Similar results were obtained for *P. cupreus* whose body size decreases notably with an increase of heavy metals in food (Maryanski et al., 2002). In addition to direct toxic effects, heavy metal pollutants may alter locomotory behavior, as was shown in larvae of *P. cupreus* exposed to copper (Bayley et al., 1995), and it affects reproducibility by causing degeneration of the flagella of spermatids (Shonouda and Osman, 2018).

Although coleopteran insects include the most important pests, many beetles are beneficial for ecosystems, and they are not regarded as destructive animals. Therefore, environmental studies often focus on the effects on whole beetle communities, observing alterations in the presence of beetle species and their behavior (Lee et al., 2001; Sivčev et al., 2017). Carabid beetles belong to the group of important soil-inhabiting species that are beneficial for soil quality. They prey on other insects; therefore they limit populations of herbivores. The species are noted, among others, in potato fields. Therefore, these beetles are the objects of numerous toxicity tests. They include not only lethality but also a broad range of effects, including altered activity of enzymes, ultrastructural malformations (Giglio et al., 2017), developmental parameters, mortality (Heimbach, 1998), and population and field effects (Huusela-Veistola, 1996; Markó and Kádár, 2005). Because of their importance in the environment as mentioned above, beetles are also used in standardized tests required for regulatory approval of veterinary and agrotechnical products, and the low toxicity of insecticides to non-target species is one of the crucial points taken under consideration. The Organization for Economic Co-operation and Development (OECD) as well as International Organization for Biological and Integrated Control (IOBC), Beneficial Arthropod Regulatory Testing Group (BART) and European and Mediterranean Plant Protection Organization (EPPO) Joint Initiative and EU developed series of tests that are used to determine the risk factors and potential adverse effects of newly introduced chemicals to non-target, beneficial arthropods. Four beetle species that are widely distributed around the globe and easy to breed in culture are used as indicators in those tests. *Aleochara bilineata* (Staphylinidae) is commonly used as a model organism for ground dwelling arthropods, *C. septempunctata* (Coccinellidae) for leaf-dwelling insects, *P. cupreus* (Carabidae) as a member of carabid beetles that are encountered frequently in agriculture sites and *Aphodius constans* (Scarabaeidae) as a model for ecologically

important insects associated with fresh dung insects (Candolfi and Blümel, 2000; Römbke et al., 2007).

SOURCE OF BIOACTIVE AGENTS

Antimicrobial Peptides

Recently, studies on compounds that protect beetles against pathogen infection have shown that this group of insects might be a useful source of antimicrobial and antitumor agents. This supposition is related to the fact that the beetles are characterized by a broad spectrum of AMPs, small bioactive compounds (usually $\leq$ 20 kDa) that act against bacteria, viruses, fungi, protozoa or other parasites (Vilcinskas et al., 2013; Chowański et al., 2017a). An astonishing example is the invasive harlequin ladybeetle *H. axyridis*. Vilcinskas et al. (2013) identified in this species 50 genes encoding various AMPs. However, the specificity of action very often is characteristic for the class (Chowański et al., 2017a). Regarding medical applications, the most important are defensins and their synthetic analogs (Ntwasa et al., 2012; Ishibashi, 2016). Defensins belong to the AMPs class of cysteine-rich peptides and mainly have antimicrobial activity against Gram-positive bacteria (Chowański et al., 2017a). However, some members of this AMPs class also possess activity against Gram-negative bacteria, fungi, and protozoa (Tonk et al., 2015). Their importance is associated with the fact that beetle defensins and defensin-derived AMPs exhibited promising activity against MRSA (methicillin-resistant *Staphylococcus aureus*) and *Pseudomonas aeruginosa*, bacteria that cause the largest number of nosocomial infections (Rajamuthiah et al., 2015; Ishibashi, 2016). An additional advantage of defensins compared to antibiotics is the fact that the bacteria did not develop AMPs resistance during a 30-day experiment (Iwasaki et al., 2007). Due to the above AMPs activities, clinical applications of defensin-derived AMPs have been examined, for example, as AMPs-containing bandages that suppresses MRSA proliferation (Saido-Sakanaka et al., 2005; Nakamura et al., 2011).

The potential for therapeutic application of beetle AMPs is related not only to their antimicrobial properties but also to the minimal cytotoxic effect toward normal mammalian cells. This property is associated with the fact that these compounds do not act on electrically neutral cell membranes. It should be highlighted that this specific action of defensins could be useful in anticancer treatment because several types of cancer, similar to bacteria, are characterized by negatively charged phospholipid membranes. To date, antitumor activity of defensin-derived AMPs (based on the *A. dichotoma* defensin) and harmoniasin isolated from the ladybeetle *H. axyridis* and its synthetic analog HaA4 have been confirmed, for example, in human leukemia cells (Kim et al., 2013). Their cytotoxicity is correlated with the induction of apoptosis and necrosis in the tested cell lines. CopA3, a peptide isolated from the dung beetle *Copris tripartitus*, also has similar activities. This anticancer peptide acts on human gastric cancer cells and leukemia cells (Kang et al., 2012; Lee et al., 2015).

Non-peptide Compounds

Not only the peptides have therapeutic potential but also several non-peptide compounds. One of the best-known examples of these substances is cantharidin. Cantharidin is a terpenoid synthesized only by beetles belonging to the Meloidae (blister beetles) and Oedemeridae (pollen-feeding beetles) families (Ghoneim, 2013). Interestingly, dried body of the *Mylabris phalerata* beetle was used in traditional Chinese medicine for the treatment of many diseases (Moed et al., 2001; Yin et al., 2013). This potential medical use has been confirmed in recent studies that especially showed a broad spectrum of antitumor activity of this compound (Efferth et al., 2005; Lu et al., 2014). These results are associated with the fact that cantharidin treatment not only leads to apoptosis and necrosis of tumor cells but also causes inhibition of protein, RNA and DNA synthesis and tumor cell migration and proliferation (Sagawa et al., 2008; Hsia et al., 2016). Despite antitumor activities, cantharidin may have other biological activities, such as stimulation of bone marrow or sexual arousal (Ghoneim, 2013; Torbeck et al., 2014). However, the biggest problem with the medical usage of cantharidin is the toxicity of this compound to the mucosa, mainly the ureter, kidney and gastrointestinal tract (Yu and Zhao, 2016). However, the studies conducted by Yu and Zhao (2016) showed a very interesting perspective. In this study, the authors tested the action of cantharidin after its bioconversion by the photosynthetic bacteria *Rhodobacter sphaeroides* cultured on medium containing this compound. Bioconversion not only led to a decrease in toxicity but also increased anti activity of cantharidin against HepG-2 (human liver cancer), BEL-7406 (human liver cancer), and A549 (human lung cancer) cell lines (Yu and Zhao, 2016).

The beetle *Blaps japanensis* is also suitable as a donor of compounds that have been used for a long time for the treatment of many diseases such as fever, cough, rheumatism, cancer and inflammatory disorders. Recently, it has been revealed that the compounds responsible for those activities are called blapsols, which are active against cyclooxygenase (COX) enzymes (Yan et al., 2015). The opposite effect is provided by molossusamides extracted from *Catharsius molossus*. Research conducted by Lu et al. (2015) showed that these compounds have inhibitory properties against COX-1 and COX-2, which may be useful in anti-inflammatory therapy of chronic diseases.

The next compound that can also be considered in clinical application is pederin. Pederin is an amide with two tetrahydropyran rings detected in haemolymph and eggs of rove beetles of the genus *Paederus*, *Paederidus*, and *Megalopaederus* (Ghoneim, 2013). However, the beetle organism does not participate in the production of pederin. This amide is synthesized by the symbiotic bacteria *P. aeruginosa*. Like cantharidin, pederin is characterized by high toxicity, and contact of this substance with the skin leads very often to a characteristic irritation called Paederus dermatitis. Despite its toxic effects, pederin is characterized by antitumor activity. This amide, for example, induced apoptosis in human myeloid leukemia cells or HeLa cells (Samani et al., 2014; El-Hafeez and Rakha, 2017).

Other compounds that can be used in anticancer treatment are methyl-1,4-benzoquinones, ethyl-1,4-benzoquinones and

1-pentadecene isolated from the beetle *Ulomoides dermestoides*. Crespo et al. (2011) evaluated the cytotoxicity of these compounds on the A549 human lung carcinoma epithelial cell line and showed that they reduce cell viability and induce DNA damage.

Beetles are not only a source of antimicrobial and antitumor agents. Some compounds may also be useful as anticoagulants. Lee et al. (2017) described the antiplatelet and antithrombotic activity of two metabolites isolated from *T. molitor*. These compounds inhibit intrinsic blood coagulation pathways by inhibiting factor Xa (FXa), which can prevent the continuous production of thrombin and, at the same time, retain activity for primary homeostasis (Bauer, 2006).

Other Bioactive Agents

Insect-based bioactive products can also be developed as a therapeutic agent for obesity. Seo et al. (2017) used ethanol extract of *T. molitor* larvae and revealed its anti-adipogenic and anti-obesity effect without cytotoxicity *in vitro* and *in vivo*. This extract caused up to a 90% reduction of lipid accumulation and triglyceride content in mature adipocytes of mice. Body weight gain was attenuated after oral administration of *T. molitor* larvae powder, and hepatic steatosis was reduced (Seo et al., 2017).

Xu et al. (2016) reported anticoagulant activity of crude extract of *Holotricha diomphalia* larvae (CEHDL) *in vitro* and *in vivo*. The anticoagulation activity of CEHDL was confirmed by hydrolysing fibrinogen and fibrin, for which inactivation by proteinase inhibitors, metal ions, heat and solutions with acidic or basic pH does not readily occur. CEHDL could be a promising antithrombotic agent used in medicine (Xu et al., 2016).

BEETLES AS MODEL ORGANISMS IN BIOMEDICINE

Insects have been used as model organisms in biomedical research for a long time. The first and most widely studied insect is undoubtedly *D. melanogaster*. Apart from Dipteran models, representatives of other orders of insects such as Lepidoptera or Orthoptera have also been used in recent years (Wilson-Sanders, 2011; Entwistle and Coote, 2018). An increasing amount of attention is devoted to the order Coleoptera, with one of the main representatives being *T. castaneum*. It has recently been used as a model in various types of biomedical research (Mukherjee et al., 2015; Schmidt-Ott and Lynch, 2016). Here, we describe the main examples.

Neurodegenerative Diseases

Missense mutations in the human protein kinase PINK1 gene (PTEN-induced kinase 1, hPINK1) are thought to cause hereditary Parkinson's disease with an early onset (Valente et al., 2004; Deas et al., 2009; Woodroof et al., 2011). hPINK1 differs from other protein kinases due to the presence of three unique insertions within the kinase domain and a *C*-terminal extension of an unknown function that bears no homology to any known protein domain (Kumar et al., 2017). hPINK1, which has been proposed to act as the main regulator of mitochondrial quality control and promotes the elimination of damaged mitochondria *via* autophagy (McWilliams and Muqit, 2017), is difficult to study due to its low *in vitro* kinase activity. Woodroof et al. (2011) showed that insect orthologs of PINK1 remained active *in vitro*. The PINK1 protein from the *T. castaneum* beetle (TcPINK1), despite some structural differences in comparison to hPINK1 (Woodroof et al., 2011), exhibits catalytic activity toward ubiquitin, Parkin and generic substrates (Woodroof et al., 2011; Kazlauskaite et al., 2015). It has been shown that motor defects of *Drosophila* PINK1 null flies, similar to those that occur in Parkinson's disease, can be rescued *in vivo* by crossing lines that overexpress *Tc*PINK1 (Woodroof et al., 2011). *Tc*PINK1 is also easier to produce *in vitro* than hPINK1, which facilitates studying its structure. Study of the three-dimensional structure of the *Tc*PINK1 protein revealed details of its domain structure and function, including kinase domain loop insertions involved in controlling PINK1 activity and affecting its interactions with other proteins and the *C*-terminal domain, which is involved in the enzyme activity of PINK1. It has been shown that some of these futures are also part of the human PINK1 protein (Kumar et al., 2017). The use of *Tc*PINK1 provides molecular insights into the mechanisms of hPINK1 kinase activity and ubiquitin substrate recognition. *Tc*PINK1 was also used to investigate the impact of Parkinson's disease-associated PINK1 missense mutations, of which nearly all are located within the kinase domain (Woodroof et al., 2011; Kumar et al., 2017). Some of these properties have been shown to be features of the human PINK1 protein (Kumar et al., 2017).

The *T. castaneum* beetle has also been used to study the function of a weakly characterized orphan cytokine receptor-like factor 3 (CRLF3). CRLF3 belongs to the family of type I cytokine receptors, which also includes the classical erythropoietin receptor (EpoR), thrombopoietin receptor, prolactin receptor or growth hormone receptor. The *Crlf3* gene is well conserved, and orthologs have been identified in vertebrates including humans and various insect species, such as *T. castaneum* and the cricket *Gryllus bimaculatus* but not *D. melanogaster* (Wyder et al., 2007; Hahn et al., 2017). Erythropoietin (Epo)-mediated neuroprotection and neuroregeneration have been described in insects: the grasshopper *Chorthippus biguttulus*, the locust *L. migratoria* (Ostrowski et al., 2011; Miljus et al., 2014), the beetle *T. castaneum* and the cricket *G. bimaculatus* but not *D. melanogaster* (Hahn et al., 2017). So far, no orthologs of Epo or the classical EpoR have been identified in invertebrate species.

Using the *T. castaneum* beetle as a simpler genetic model, it has been shown that Epo-like signaling molecules are ligands of CRLF3 and that CRLF3 plays a role in EPO-mediated neuroprotection, as knockdown of *Tc*-CRLF3 expression abolished the protective effect of Epo on *T. castaneum* brain neurons exposed to hypoxia (Hahn et al., 2017). This result suggests that the insect cytokine receptor CRLF3 serves as a neuroprotective receptor for an Epo-like cytokine and that vertebrate CRLF3, similar to its insect ortholog, may represent a tissue protection-mediating receptor. It has also been indicated that insects such as *T. castaneum* (but not *D. melanogaster*) can be used to search for additional tissue-protective Epo-receptors with conserved orthologs, as well as alternative ligands that

activate neuroprotective receptors such as CRLF3 and can have mammalian orthologs with a similar function. An advantage of using insects in Epo-receptor studies is that insects do not possess erythrocytes and the classic EpoR, so studies do not have to consider interference by the abovementioned mechanisms (Hahn et al., 2017).

Aging

Aging is a natural biological process associated with adverse changes at the molecular, cellular and tissue levels that determine the lifespans of organisms. Due to the genetic and phenotypic similarities of organisms, it is thought that the basic mechanisms of aging may be evolutionarily conserved from yeast to mammals, including humans (Barbieri et al., 2003; Bonafe et al., 2003; Bartke et al., 2013).

Insects became models of various aspects of aging and models for aging research at the tissue and genetic levels. The heart of insects, for example, has been the subject of studies related to cardiovascular diseases and aging (Ocorr et al., 2007b; Piazza and Wessells, 2011). The genetic basis of changes in heart function during aging in humans is not well-determined, partly due to the complex relationship between genes, age, disease and lifestyle (Lakatta, 2002). This complexity is the reason why simpler animal genetic models can be more useful for discovering basic mechanisms. Insects are excellent objects to study cardiac aging due to their short lifespan, many conserved genes and simple heart structure that facilitates the detection of changes. Moreover, the activity of their heart can be examined without causing premature death (Ocorr et al., 2007a) in part because oxygen is supplied through the tracheal system, which is separated from the circulatory system. Physiological changes in the endogenous activity of the insect myocardium during development and aging have been described mainly in *D. melanogaster* (Nishimura et al., 2011). It has been shown that in *D. melanogaster*, the resting heart rate declines progressively with age (Paternostro et al., 2001), the cardiac response to various stimuli is impaired in older flies (Paternostro et al., 2001; Wessells and Bodmer, 2007) and resistance to sudden stress decreases dramatically with age (Wessells et al., 2004). It has also been demonstrated that the majority of older wild-type flies exhibit non-rhythmic heart contraction patterns, including frequent asystole/bradycardia and ectopic beats (Ocorr et al., 2007b; Santalla et al., 2014). Similar changes in the heart rhythm have been detected in *T. molitor* beetles (Pacholska-Bogalska et al., 2018). In older beetles, more abnormalities in heart rhythm, arrhythmias, were detected. In this group of beetles, the incidence of arrhythmia and the arrhythmicity index were higher than in a group of younger beetles (Pacholska-Bogalska et al., 2018). This finding suggests that the beetle heart preparations can also be used as a model in the studies on aging and for testing cardioactive drugs as well.

Host–Pathogen Interactions

The aforementioned structural and functional homologies of the immune system in insects and vertebrates, the large body size, fast development and availability of genome sequences of beetles result in the fact that beetles are very often used as models in studies concerning various aspects of host–pathogen interactions. For example, *T. castaneum* and that Gram-positive bacteria *Bacillus thuringiensis* or protozoan *Nosemia sp.* are used as a model for studying antagonistic interactions and co-evolution between hosts and their pathogens, including Red Queen-related questions (Kerstes et al., 2012; Milutinović et al., 2013). Moreover, the pair of *T. molitor* and *S. aureus* is very useful in research on immune mechanisms related to persistent infection (Dobson et al., 2012). This is a fundamental question, especially through the prism of the current problem with bacterial resistance to antibiotics.

Pharmacology and Toxicology

Insects can be used in preclinical pharmacology research on drugs and as an early warning system to indicate epigenetic risk factors connected with the consequences caused by drugs in subsequent generations. The standard procedure to preclinical studies usually requires that at least two non-human species be tested. Searching for alternatives according to the 3 Rs – reduction, refinement and replacement of vertebrates – an increasing number of groups of researchers is looking for alternative models for research (Wilson-Sanders, 2011). Bingsohn et al. (2016) used *T. castaneum* and tested diets, which were supplemented with a psychoactive drug – valproic acid (VPA), a histone deacetylase inhibitor – on the development, longevity and reproduction of this beetle. VPA is widely used in the treatment of many human diseases such as epilepsy, migraine and bipolar disorder. It was found that in *T. castaneum*, VPA delayed development, increased female body weight and decreased fertility and fecundity in comparison to the control diet, and these results correspond to studies in vertebrate models. Even in the untreated generation of F1 beetles, the expression of epigenetic regulatory genes was induced, which confirms the potential usefulness of insects for screening for epigenetic effects of drugs (Bingsohn et al., 2016).

The pharmacological properties of cardioactive compounds can be easily tested using semi-isolated beetle hearts and the microdensitometric technique described by Gäde and Rosiński (1990). Confirmation of the usefulness of this study model and technique comes from the results obtained, for example, by Marciniak et al. (2009, 2010a), Chowański and Rosiński (2017), Chowański et al. (2017b), Lubawy et al. (2018) and others. Our group used the heart of *Z. atratus* as a non-mammalian model to detect changes caused by drugs. We used selected benzodiazepines as test compounds. Benzodiazepines are a class of drugs widely prescribed because of their pharmacological importance in relieving anxiety and insomnia and their sedative and anticonvulsant actions, which are based on allosteric modulation of the GABA receptor (Krueger, 1995; Gavish et al., 1999; Słocińska et al., 2004). The action of benzodiazepines and GABA (endogenous receptor ligand) were assayed in the semi-isolated heart of the *Z. atratus* beetle using a video microscopy technique and computer-based method of image acquisition and analysis (Marciniak and Rosiński, 2010). We observed that increasing concentrations (10^{-12} to 10^{-5} M) of benzodiazepines (Ro5-4864 and diazepam) and GABA induce chrono- and inotropic effects in the heart of *Z. atratus*. An inotropic-negative and dose-dependent action of the examined substances was observed (Słocińska et al., 2011).

The calculated effective concentration (EC_{50}) is 3.9×10^{-10} M and 2.1×10^{-10} M for diazepam and GABA, respectively. However, we did not observe any significant effect of benzodiazepines on the contraction frequencies of the heart. In this case, the EC_{50} value is 2.3×10^{-9} M for 4′-chlorodiazepam and 1.8×10^{-7} M for diazepam (Słocińska et al., 2011). These data are supported by and consistent with data obtained in other animals (Surinkaew et al., 2011). Negative inotropic effects were observed with the use of benzodiazepines in various mammalian models, including papillary muscle from the right and left ventricles of guinea pigs, isolated rat and rabbit hearts, and isolated canine atrium (Holck and Osterrieder, 1985; Mestre et al., 1985; Saegusa et al., 1987; Edoute et al., 1993; Brown et al., 2008). Nevertheless, the results observed across the diverse animals confirm the insect model as a useful non-mammalian system for the evaluation changes in heart activity related to drug action or aging.

Beetles are also good models for pharmacological studies of anti-arrhythmic drugs such as digoxin. Cardiac glycosides are the featured group of plant glycosides that have strong anti-arrhythmic properties. For this reason, they are widely used as first-line treatment of various types of arrhythmias in humans and for the treatment of heart failure resulting in construction defects or abnormal heart function (Evans et al., 2009). In the case of anti-arrhythmic drugs, *Z. atratus* was found as a useful organism in research concerning cardioactivity of this group of drugs. For example, digoxin causes an anti-arrhythmic effect on *Z. atratus* myocardium. The positive chronotropic effect of digoxin increased with increasing drug concentration (10^{-11}–10^{-9} M) (Kowalski, 2011). The anti-arrhythmic action of digoxin was also confirmed by the use of a pharmacological agent – terfenadine, which provokes artificial arrhythmia (Chan et al., 2009). Application of digoxin after treatment of the insect heart with terfenadine restored the basic heart rhythm.

All cardiac glycosides affect the heart, and similar effects are observed in 99% of animals and humans. To date, a similar effect of glycosides on the heart has been demonstrated in mice, rats, guinea pigs, dogs, pigs, chimpanzees and humans (Kolińska et al., 2016). The exact place of action of this class of compounds is the sodium-potassium pump (Na/K-ATPase) located in the cell membrane of cardiomyocytes. Cardiac glycosides cause an increase in energy demand of the myocardium but do not require an increase of ATP synthesis by cardiomyocytes (O'Neil, 2001). A similar manner of drug action was observed in the heart of beetles as was obtained in humans, which confirms the possibility of leading screening research on a non-mammalian model.

Several substances of plant origin are often used to modulate muscle and heart contractions (Loizzo et al., 2008). Based on the functional similarity of the insect and mammalian hearts, these substances can be first tested in insects. Several experiments were carried out on beetles to assess the cardioactive properties of glycoalkaloids extracted from plants of the *Solanaceae* family. We have shown that extract prepared from potato leaves inhibited cardiac activity in *Z. atratus* adults (Marciniak et al., 2010a). Similar activity of the extract was observed *in vivo* on pupae of the same species. The extract reduced the amplitude of heart contractions in both the retrograde and anterograde phase of myocardium activity. Moreover, changes in the duration of both phases of the heartbeat were observed (Marciniak et al., 2010a; Ventrella et al., 2015).

Behavioral Studies

Parental care of *Nicrophorus* (Silphidae) remains a remarkable phenomenon among insects. Both parents, male and female, bury a carcass and prepare it by removing feathers and fur. Ball formed out of the carcass is next preserved with excreted anal and oral substances. After careful preparation, the female lays eggs. Hatched larvae are fed by both parents until their pupation. Despite the fact that in further larval development larvae are able to feed themselves, parents support this process to accelerate larval growth. At the same time, larvae begging is observed (Urbański, 2013). The complexity of burying beetle behavior and possibility to obtain large number of individuals provides that these beetles are one of the model organisms in the field behavioral ecology, including the physiological and molecular basis of parental care. Recently, research conducted on burying beetles clearly indicated that neurohormones and biogenic amines are crucial for the regulation of this process (Scott and Panaitof, 2004; Cunningham et al., 2015a; Panaitof et al., 2016). Moreover, a comparison between burying beetles and non-social beetles showed that the evolutionary basis of parental care is not related to the presence of specific genes but rather to methylation processes (Cunningham et al., 2015a). Burying beetles are also good model organisms in research about chemical signaling. Research conducted by Engel et al. (2016) and Steiger and Stokl (2017) proved that pheromonal signals regulated parent and offspring behavior, including inhibition of copulation and parental care synchronization.

Some coleopterans are exceptional in their social behavior. Therefore, they are objects of intensive basic studies that, in the future, may yield important information on the functioning of social animals and extrapolation of animal social behavior to human society or even in the design of robots (Miklósi and Gácsi, 2012). The first reported beetle with eusociality features was *A. incompertus* (Curculionidae) (Kent and Simpson, 1992). The biology and feeding behavior were described in a subchapter on pest management. Recent studies showed not only that one gallery is inhabited by a single core family but also that insects are divided into groups consisting of an inseminated mother, infertile female workers, larvae and their caretakers (Smith et al., 2018). Research on *Xyleborinus saxenii* confirmed that ambrosia beetles are very social. Division of labor between larvae and adults was observed. Larvae are responsible for enlarging and maintaining the hygiene the gallery; moreover, they participate in brood care (Biedermann and Taborsky, 2011).

Other Biomedical Studies

As mentioned before, due to the homology of basic immune mechanisms, beetles are good candidates to play roles as models in a broad range of trials. This applicability also arises from the fact that in contrast to vertebrates, insects breed rapidly, produce many offspring and are more ethically acceptable, which allows them to be used for high-throughput screening, including

tests concerning the effects of pharmaceuticals and other active compounds (Bingsohn et al., 2016).

The first example of such studies was a test conducted on the dung beetles *Onthophagus taurus* and *Euoniticellus fulvus*, which were fed on feces collected from sheep that were treated with ivermectin and albendazole (Wardhaugh et al., 2001). Those two substances are used as broad-spectrum antiparasitic drugs. Usage of those substances results in a decreased number of developing larvae. In insects that survived exposure to the tested drugs, delayed sexual maturation was observed. Bioassays conducted on dung beetles are especially important because they play a role in nutrient cycling and are essential to the long-term maintenance of pasture hygiene and productivity (Wardhaugh et al., 2001).

There are also many natural compounds that were in truth isolated from insects but not from beetles and possess verified activity in model beetles that can be used in further studies. One such substance is yamamarin – a pentapeptide (DILRG) isolated from the silk moth *Antheraea yamamai*. It was shown that this peptide is probably physiologically involved in the regulation of a process called diapause (Sato et al., 2010). Additionally, Walkowiak-Nowicka et al. (2018) showed the immunotropic activity of yamamarin by testing its impact on selected functions of the immune system of *T. molitor*. This compound also possesses strong cardioinhibitory effects on semi-isolated hearts of this beetle species (Szymanowska-Dziubasik et al., 2008). Thanks to formerly described activities of the pentapeptide in beetles, it was possible to show that this compound causes growth arrest in a murine leukemia cell line expressing the human gene Bcr/Abl (Sato et al., 2010) or reversible growth arrest of rat hepatoma cells due to its cytotoxic activity (Yang et al., 2007).

Another compound isolated from insect species is alloferon (HGVSGHGQHGVHG), which was found in the *Calliphora vicina* fly. According to Lee et al. (2011) and Chernysh and Kozuharova (2013), alloferon could stimulate NK cell cytotoxicity toward cancer cells, especially leukemia cells, and inhibit replication of Kaposi's sarcoma-associated herpesvirus. When Kuczer et al. (2013, 2016) and Matusiak et al. (2014) conducted *in vivo* studies on the beetle *T. molitor*, it was found that this tridecapeptide and its structural analogs could increase PO activity and induce haemocyte apoptosis. These results indicated that beetles might be very useful model organisms for testing the cytotoxicity of various compounds.

Next, an example is the research conducted by Bourel et al. (2001) on two necrophagous beetles, *Dermestes frischi* and *Thanatophilus sinuatus*. Insects were reared on substrates containing different dosages of morphine that were calculated to create tissue concentrations similar to those encountered in human deaths due to opiate overdose. That conducted study demonstrates the potential for use of those two beetles as alternative species to use in toxicological analyses (Bourel et al., 2001).

SUMMARY AND PERSPECTIVES

With an increasing number of fully sequenced and annotated insect genomes, omics technologies and bioinformatics can be used to exploit this huge amount of sequence information for the study of different biological aspects of insect model organisms. In the postgenomic era, the international i5K project (http://i5k.github.io/,2018) played an important role in understanding the genomes of various insect species. This project was aimed at sequencing the genome of each species known to be important in agriculture and also all known disease vectors, insects with important ecosystem functions and insects that are models in biological and biomedical research (representatives of all families).

In this review, we have provided a broad discussion of the research carried out on various beetle species and indicated the

TABLE 1 | Chosen examples of beetle usage in different fields of life science.

Field of life science	Application		
Medicine	Models	Neurodegenerative disorders	Parkinson's disease
		Aging	Heart aging
		Host–pathogen interactions	Persistent infections
		Pharmacology and toxicology	Benzodiazepines
		Behavior	Parental care
	Bioactive agents	Antimicrobial peptides	Defensins and their analogs
		Non-peptide agents	Cantharidin
Physiology	Neuroendocrinology	Study similarities between the neuroendocrine system of vertebrates and arthropods	Food intake
			Cardiovascular diseases
			Growth, development, and reproduction
			Diuresis
	Immunology	Study similarity of basic immune mechanisms	Phagocytosis and pathogen recognition
			Toll and Jak/STAT pathways
Agronomy	New source of nutrition	Animal feed	Aquatic feed
	Crop growth	Pest management, soil fertilization and reduce weeds	Toxicity of alkaloids
	Biomonitoring	Assessment of environmental pollution	Diversity of indicator species

possibilities of using these insects as model organisms in the fields of molecular biology, physiology, ecophysiology, pharmacology and toxicology and indicated the importance of beetles in agriculture, food production or ecosystem monitoring (**Table 1**). Due to the increasing need for food for humans and harvested animals, research on that field may be an important in near future. Next, research on new generations of insecticides seem to be an intensively developing area of natural sciences.

The huge amount of data obtained from research conducted on beetles not only has contributed to a better understanding of the molecular and physiological mechanisms of the functioning of insect organisms but also has a significant meaning for our knowledge of the comparative aspects with regard to vertebrates. In beetles, an increasing number of new biologically active substances regulating various physiological processes have been identified, as demonstrated both in homologous and heterologous bioassays, including, to a lesser extent, in relation to vertebrate cells or tissues. We suppose that searching for counterparts of mammalian metabolic pathways and diseases in insects will rise into an intensive trend in science in the near future. For a number of new substances produced by insects, only one type of biological activity has been identified, and their wider physiological role is unknown. Because many substances often exhibit pleiotropic biological activity, there is a need to understand a wider spectrum of biological activity for newly discovered compounds. It is also necessary to develop new, specific and sensitive physiological, pharmacological or ecophysiological bioassays. In the future, broader research on beetles and their various substances will not only increase our knowledge of the functioning of insect organisms but may also have significant practical implications for biomedical applications, environmental monitoring or food production.

In the last decade, we have been observing new trends in the development of modern biotechnology, where besides medical, industrial, food and plant protection biotechnology, the term "Yellow Biotechnology" was introduced as an alternative term for insect biotechnology, opening new horizons for multidisciplinary research in the field of experimental entomology (Vilcinskas, 2013). Insect biotechnology has been defined as the use of biotechnology to develop insects, their molecules, cells or organs into products and services for specific applications in medicine, plant protection and industry. Beetles (e.g., *Tribolium confusum*, *T. castaneum*, *T. molitor*, and other beetles) that feed on crops or stored products are still the most important competitors for human nutrition on a global scale. Therefore, for practical reasons, there is a need for further development of new bioassays using model beetle species for not only those feeding on plants and stored products but also those species with potentially high biomedical or industrial significance.

AUTHOR CONTRIBUTIONS

All the authors are responsible for the general idea of the manuscript and text editing. ZA and SC are responsible for the formal edition of the manuscript. MSł coordinated the introduction. MSz, JP-B, PM, KW-N, AU, and MSł coordinated a description of neuroendocrinological, immunological, pharmacological aspects, aging, model organisms, and bioactive agents. MSp, SC, JL, and ZA coordinated the description of beetles in agronomy and ecology. GR coordinated the summary and perspectives.

FUNDING

This work was partially supported by the National Science Centre, Poland by Grant Nos. 2015/19/N/NZ4/00729 (KW-N), 2015/17/N/NZ4/02330 (JL), 2016/21/N/NZ4/00123 (AU), and 2013/09/D/NZ3/00002 (PM) and the Ministry of Science and Higher Education by Grant No. IP2014028173 (PM).

REFERENCES

Abdel-latief, M., and Hoffmann, K. H. (2010). Neuropeptide regulators of the juvenile hormone biosynthesis (*in vitro*) in the beetle, *Tenebrio molitor* (Coleoptera, Tenebrionidae). *Arch. Insect Biochem. Physiol.* 74, 135–146. doi: 10.1002/arch.20359

Abdel-latief, M., and Hoffmann, K. H. (2014). Functional activity of allatotropin and allatostatin in the pupal stage of a holometablous insect, *Tribolium castaneum* (Coleoptera, Tenebrionidae). *Peptides* 53, 172–184. doi: 10.1016/j.peptides.2013.10.007

Abdelsalam, S. A., Alzahrani, A. M., Elmenshawy, O. M., and Abdel-Moneim, A. M. (2016). Spinosad induces antioxidative response and ultrastructure changes in males of red palm weevil *Rhynchophorus ferrugineus* (Coleoptera: Dryophthoridae). *J. Insect Sci.* 16, 106. doi: 10.1093/jisesa/iew089

Abildsnes, J., and Tømmerås, B. Å (2000). Impacts of experimental habitat fragmentation on ground beetles (Coleoptera, Carabidae) in a boreal spruce forest. *Ann. Zool. Fenn.* 37, 201–212.

Adamski, Z., Banaszkiewicz, M., and Ziemnicki, K. (2005). Ultrastuctural alterations induced by fenitrothion on fat body cells and midgut cells of *Tenebrio molitor* L. (Insecta, Coleoptera) larvae. *J. Biol. Res.* 3, 15–22.

Adamski, Z., Ziemnicki, K., Fila, K., Zikic, R., and Stajn, A. (2003). Effects of long-term exposure to fenitrothion on *Spodoptera exigua* and *Tenebrio molitor* larval development and antioxidant enzyme activity. *Biol. Lett.* 40, 43–52.

Aikins, M. J., Schooley, D. A., Begum, K., Detheux, M., Beeman, R. W., and Park, Y. (2008). Vasopressin-like peptide and its receptor function in an indirect diuretic signaling pathway in the red flour beetle. *Insect Biochem. Mol. Biol.* 38, 740–748. doi: 10.1016/j.ibmb.2008.04.006

Allegro, G., and Sciaky, R. (2003). Assessing the potential role of ground beetles (Coleoptera, Carabidae) as bioindicators in poplar stands, with a newly proposed ecological index (FAI). *For. Ecol. Manage.* 175, 275–284. doi: 10.1016/S0378-1127(02)00135-4

Altincicek, B., Knorr, E., and Vilcinskas, A. (2008). Beetle immunity: identification of immune-inducible genes from the model insect *Tribolium castaneum*. *Dev. Comp. Immunol.* 32, 585–595. doi: 10.1016/j.dci.2007.09.005

Altincicek, B., and Vilcinskas, A. (2007). Identification of immune-related genes from an apterygote insect, the firebrat *Thermobia domestica*. *Insect Biochem. Mol. Biol.* 37, 726–731. doi: 10.1016/j.ibmb.2007.03.012

Alyokhin, A., Baker, M., Mota-Sanchez, D., Dively, G., and Grafius, E. (2008). Colorado potato beetle resistance to insecticides. *Am. J. Potato Res.* 85, 395–413. doi: 10.1007/s12230-008-9052-0

Arain, M. S., Wan, P.-J., Shakeel, M., Farooq, M., Hu, X.-X., Shah, S. A. H., et al. (2017). Toxicity of butene-fipronil, in comparison with seven other insecticides,

in *Leptinotarsa decemlineata* and *Drosophila melanogaster*. *Phytoparasitica* 45, 103–111. doi: 10.1007/s12600-016-0560-z

Argentine, J., Clark, J. M., and Ferro, D. (1994). Computer simulation of insecticide resistance management strategies for control of Colorado potato beetle (Coleoptera: Chrysomelidae). *J. Agric. Entomol.* 11, 137–155.

Arthropod-Pesticide-Resistance-Database (2018). *Arthropod Pesticide Resistance Database*. East Lansing, MI: Michigan State University.

Audsley, N., Vandersmissen, H. P., Weaver, R., Dani, P., Matthews, J., Down, R., et al. (2013). Characterisation and tissue distribution of the PISCF allatostatin receptor in the red flour beetle, *Tribolium castaneum*. *Insect Biochem. Mol. Biol.* 43, 65–74. doi: 10.1016/j.ibmb.2012.09.007

Bang, H. S., Lee, J.-H., Kwon, O. S., Na, Y. E., Jang, Y. S., and Kim, W. H. (2005). Effects of paracoprid dung beetles (Coleoptera: Scarabaeidae) on the growth of pasture herbage and on the underlying soil. *Appl. Soil. Ecol.* 29, 165–171. doi: 10.1016/j.apsoil.2004.11.001

Barbieri, M., Bonafe, M., Franceschi, C., and Paolisso, G. (2003). Insulin/IGF-I-signaling pathway: an evolutionarily conserved mechanism of longevity from yeast to humans. *Am. J. Physiol. Endocrinol. Metab.* 285, E1064–E1071. doi: 10.1152/ajpendo.00296.2003

Barbosa, P. R., Oliveira, M. D., Barros, E. M., Michaud, J., and Torres, J. B. (2018). Differential impacts of six insecticides on a mealybug and its coccinellid predator. *Ecotoxicol. Environ. Saf.* 147, 963–971. doi: 10.1016/j.ecoenv.2017.09.021

Bartke, A., Sun, L. Y., and Longo, V. (2013). Somatotropic signaling: trade-offs between growth, reproductive development, and longevity. *Physiol. Rev.* 93, 571–598. doi: 10.1152/physrev.00006.2012

Bauer, K. A. (2006). New anticoagulants: anti IIa vs anti Xa—is one better? *J. Thromb. Thrombolysis* 21, 67–72. doi: 10.1007/s11239-006-5579-4

Bayley, M., Baatrup, E., Heimbach, U., and Bjerregaard, P. (1995). Elevated copper levels during larval development cause altered locomotor behavior in the adult carabid beetle *Pterostichus cupreus* L. (Coleoptera: Carabidae). *Ecotoxicol. Environ. Saf.* 32, 166–170. doi: 10.1006/eesa.1995.1098

Belluco, S., Losasso, C., Maggioletti, M., Alonzi, C. C., Paoletti, M. G., and Ricci, A. (2013). Edible insects in a food safety and nutritional perspective: a critical review. *Compr. Rev. Food. Sci. Food Saf.* 12, 296–313. doi: 10.1111/1541-4337.12014

Biedermann, P., and Taborsky, M. (2011). Larval helpers and age polyethism in ambrosia beetles. *Proc. Natl. Acad. Sci. U.S.A.* 108, 17064–17069. doi: 10.1073/pnas.1107758108

Bingsohn, L., Knorr, E., and Vilcinskas, A. (2016). The model beetle *Tribolium castaneum* can be used as an early warning system for transgenerational epigenetic side effects caused by pharmaceuticals. *Comp. Biochem. Physiol. C Toxicol. Pharmacol.* 18, 57–64. doi: 10.1016/j.cbpc.2016.03.002

Bohac, J. (1989). "Accumulation of heavy metals in the bodies of staphylinid beetles (Coleoptera, Staphylinidae)," in *Proceedings of the 5th International Conference on Bioindicatores Deteriorisationis Regionis*, eds J. Bohac and V. Ruzicka (Ceske Budejovice: Institute of Landscape Ecology CAS), 319–321.

Bonafe, M., Barbieri, M., Marchegiani, F., Olivieri, F., Ragno, E., Giampieri, C., et al. (2003). Polymorphic variants of insulin-like growth factor I (IGF-I) receptor and phosphoinositide 3-kinase genes affect IGF-I plasma levels and human longevity: cues for an evolutionarily conserved mechanism of life span control. *J. Clin. Endocrinol. Metab.* 88, 3299–3304. doi: 10.1210/jc.2002-021810

Bourel, B., Tournel, G., Hédouin, V., Goff, M. L., and Gosset, D. (2001). Determination of drug levels in two species of necrophagous Coleoptera reared on substrates containing morphine. *J. Forensic Sci.* 46, 600–603. doi: 10.1520/JFS15010J

Brown, D. A., Aon, M. A., Akar, F. G., Liu, T., Sorarrain, N., and O'rourke, B. (2008). Effects of 4'-chlorodiazepam on cellular excitation–contraction coupling and ischaemia–reperfusion injury in rabbit heart. *Cardiovasc. Res.* 79, 141–149. doi: 10.1093/cvr/cvn053

Bucher, G., Scholten, J., and Klingler, M. (2002). Parental RNAi in Tribolium (Coleoptera). *Curr. Biol.* 12, R85–R86. doi: 10.1016/S0960-9822(02)00666-8

Bulet, P., Hetru, C., Dimarcq, J.-L., and Hoffmann, D. (1999). Antimicrobial peptides in insects; structure and function. *Dev. Comp. Immunol.* 23, 329–344. doi: 10.1016/S0145-305X(99)00015-4

Burel, F., Butet, A., Delettre, Y., and de La Peña, N. M. (2004). Differential response of selected taxa to landscape context and agricultural intensification. *Landsc. Urban Plan.* 67, 195–204. doi: 10.1016/S0169-2046(03)00039-2

Busch, A., Kunert, G., Heckel, D. G., and Pauchet, Y. (2017). Evolution and functional characterization of CAZymes belonging to subfamily 10 of glycoside hydrolase family 5 (GH5_10) in two species of phytophagous beetles. *PLoS One* 12:e0184305. doi: 10.1371/journal.pone.0184305

Candolfi, M., and Blümel, S. (2000). *Guidelines to Evaluate Side-Effects of Plant Protection Products to Non-Target Arthropods: IOBC, BART and EPPO Joint Initiative*. Ghent: IOBC/WPRS.

Chaieb, I. (2010). Saponins as insecticides: a review. *Tunis. J. Plant Prot.* 5, 39–50.

Chan, P. K., Lin, C. C., and Cheng, S. H. (2009). Noninvasive technique for measurement of heartbeat regularity in zebrafish (*Danio rerio*) embryos. *BMC Biotechnol.* 9:11. doi: 10.1186/1472-6750-9-11

Chen, G., Handel, K., and Roth, S. (2000). The maternal NF-kappaB/dorsal gradient of *Tribolium castaneum*: dynamics of early dorsoventral patterning in a short-germ beetle. *Development* 127, 5145–5156.

Chernysh, S., and Kozuharova, I. (2013). Anti-tumor activity of a peptide combining patterns of insect alloferons and mammalian immunoglobulins in naive and tumor antigen vaccinated mice. *Int. Immunopharmacol.* 17, 1090–1093. doi: 10.1016/j.intimp.2013.10.014

Chowański, S., Adamski, Z., Lubawy, J., Marciniak, P., Pacholska-Bogalska, J., Słocińska, M., et al. (2017a). Insect peptides - perspectives in human diseases treatment. *Curr. Med. Chem.* 24, 3116–3152. doi: 10.2174/0929867324666170526120218

Chowański, S., Lubawy, J., Urbański, A., and Rosiński, G. (2016). Cardioregulatory functions of neuropeptides and peptide hormones in insects. *Protein Pept. Lett.* 23, 913–931. doi: 10.2174/0929866523666160728102842

Chowański, S., and Rosiński, G. (2017). Myotropic effects of cholinergic muscarinic agonists and antagonists in the beetle *Tenebrio molitor* L. *Curr. Pharm. Biotechnol.* 18, 1088–1097. doi: 10.2174/1389201019666180124233440

Chowański, S., Spochacz, M., Szymczak, M., and Rosiński, G. (2017b). Effect of biogenic amines on the contractile activity of visceral muscles in the beetle *Tenebrio molitor*. *Bull. Insectology* 70, 209–220.

Clift, A., Herron, G., and Terras, M. (1997). DEMANIR, a simulation model of insecticide resistance development and management. *Math. Comput. Simul.* 43, 243–250. doi: 10.1016/S0378-4754(97)00006-2

Coulter, L., Ibrahimi, M., Patel, R., and Agius, M. (2017). Linking the psychosocial aetiology and neurobiology of unipolar depression. *Psychiatr. Danub.* 29, 441–446.

Crespo, R., Villaverde, M. L., Girotti, J. R., Güerci, A., Juárez, M. P., and de Bravo, M. G. (2011). Cytotoxic and genotoxic effects of defence secretion of *Ulomoides dermestoides* on A549 cells. *J. Ethnopharmacol.* 136, 204–209. doi: 10.1016/j.jep.2011.04.056

Crossley, M. S., Chen, Y. H., Groves, R. L., and Schoville, S. D. (2017). Landscape genomics of Colorado potato beetle provides evidence of polygenic adaptation to insecticides. *Mol. Ecol.* 26, 6284–6300. doi: 10.1111/mec.14339

Cunningham, C. B., Douthit, M. K., and Moore, A. J. (2015a). Expression of octopaminergic receptor genes in 4 nonneural tissues in female *Nicrophorus vespilloides* beetles. *Insect Sci.* 22, 495–502. doi: 10.1111/1744-7917.12133

Cunningham, C. B., Ji, L., Wiberg, R. A., Shelton, J., McKinney, E. C., Parker, D. J., et al. (2015b). The genome and methylome of a beetle with complex social behavior, *Nicrophorus vespilloides* (Coleoptera: Silphidae). *Genome Biol. Evol.* 7, 3383–3396. doi: 10.1093/gbe/evv194

Cutler, G. C., Tolman, J. H., Scott-Dupree, C. D., and Harris, C. R. (2005). Resistance potential of colorado potato beetle (Coleoptera: Chrysomelidae) to novaluron. *J. Econ. Entomol.* 98, 1685–1693. doi: 10.1093/jee/98.5.1685

Davis, A. J. (2000). Does reduced-impact logging help preserve biodiversity in tropical rainforests? A case study from Borneo using dung beetles (Coleoptera: Scarabaeoidea) as indicators. *Environ. Entomol.* 29, 467–475. doi: 10.1603/0046-225X-29.3.467

De Loof, A., Lindemans, M., Liu, F., De Groef, B., and Schoofs, L. (2012). Endocrine archeology: do insects retain ancestrally inherited counterparts of the vertebrate releasing hormones GnRH, GHRH, TRH, and CRF? *Gen. Comp. Endocrinol.* 177, 18–27. doi: 10.1016/j.ygcen.2012.02.002

Deas, E., Plun-Favreau, H., and Wood, N. W. (2009). PINK1 function in health and disease. *EMBO Mol. Med.* 1, 152–165. doi: 10.1002/emmm.200900024

Denell, R. (2008). Establishment of tribolium as a genetic model system and its early contributions to evo-devo. *Genetics* 180, 1779–1786. doi: 10.1534/genetics.104.98673

Di Giglio, M. G., Muttenthaler, M., Harpsoe, K., Liutkeviciute, Z., Keov, P., Eder, T., et al. (2017). Development of a human vasopressin V1a-receptor antagonist from an evolutionary-related insect neuropeptide. *Sci. Rep.* 7:41002. doi: 10.1038/srep41002

Dobson, A. J., Johnston, P. R., Vilcinskas, A., and Rolff, J. (2012). Identification of immunological expressed sequence tags in the mealworm beetle *Tenebrio molitor*. *J. Insect Physiol.* 58, 1556–1561. doi: 10.1016/j.jinsphys.2012.09.009

dos Santos, E. A., Silva-Torres, C. S., Barbosa, P. R., Torres, J. B., and Blassioli-Moraes, M. C. (2017). Sexual behavior in ladybird beetles: sex with lights on and a twist for *Tenuisvalvae notata* (Coleoptera: Coccinellidae). *Behav. Process.* 144, 93–99. doi: 10.1016/j.beproc.2017.09.006

Durieux, D., Fassotte, B., Deneubourg, J., Brostaux, Y., Vandereycken, A., Joie, E., et al. (2015). Aggregation behavior of *Harmonia axyridis* under non-wintering conditions. *Insect Sci.* 22, 670–678. doi: 10.1111/1744-7917.12144

Edoute, Y., Giris, J., Ben-Haim, S. A., Lochner, A., Weizman, A., Hayam, G., et al. (1993). Ro 5-4864 and PK 11195, but not diazepam, depress cardiac function in an isolated working rat heart model. *Pharmacology* 46, 224–230. doi: 10.1159/000139049

Efferth, T., Rauh, R., Kahl, S., Tomicic, M., Böchzelt, H., Tome, M. E., et al. (2005). Molecular modes of action of cantharidin in tumor cells. *Biochem. Pharmacol.* 69, 811–818. doi: 10.1016/j.bcp.2004.12.003

El-Hafeez, A. A. A., and Rakha, O. M. (2017). *Paederus alfieri* extract induces apoptosis in human myeloid leukemia K562 cells. *Asian J. Pharm. Clin. Res.* 10, 72–75.

Engel, K., Stokl, J., Schweizer, R., Vogel, H., Ayasse, M., Ruther, J., et al. (2016). A hormone-related female anti-aphrodisiac signals temporary infertility and causes sexual abstinence to synchronize parental care. *Nat. Commun.* 7:11035. doi: 10.1038/ncomms11035

Entwistle, F. M., and Coote, P. J. (2018). Evaluation of greater wax moth larvae, *Galleria mellonella*, as a novel in vivo model for non-tuberculosis *Mycobacteria* infections and antibiotic treatments. *J. Med. Microbiol.* 67, 585–597. doi: 10.1099/jmm.0.000696

Evans, W. C., Evans, D., and Trease, G. E. (2009). *Trease and Evan's Pharmacognosy*. Edinburgh: Saunders.

Fahrig, L., Baudry, J., Brotons, L., Burel, F. G., Crist, T. O., Fuller, R. J., et al. (2011). Functional landscape heterogeneity and animal biodiversity in agricultural landscapes. *Ecol. Lett.* 14, 101–112. doi: 10.1111/j.1461-0248.2010.01559.x

FAO (2013). *Edible Insects: Future Prospects for Food and Feed Security*. Rome: Food and Agriculture Organization of the United Nations.

Fassotte, B., Francis, F., and Verheggen, F. (2016). The scent of love: how important are semiochemicals in the sexual behavior of lady beetles? *J. Pest Sci.* 89, 347–358. doi: 10.1007/s10340-016-0735-x

Feyereisen, R. (1985). "Regulation of juvenile hormone titer: synthesis," in *Comprehensive Insect Physiology, Biochemistry and Pharmacology*, eds G. A. Kerkut and L. I. Gilbert (Oxford: Pergamon Press), 391–403.

Finch, S., and Elliott, M. S. (1992). Predation of cabbage root fly eggs by carabidae. *IOBC/WPRS Bull.* 15, 176–183.

Floate, K. D. (2006). Endectocide use in cattle and fecal residues: environmental effects in Canada. *Can. J. Vet. Res.* 70, 1–10.

Foley, J. A., Ramankutty, N., Brauman, K. A., Cassidy, E. S., Gerber, J. S., Johnston, M., et al. (2011). Solutions for a cultivated planet. *Nature* 478, 337–342. doi: 10.1038/nature10452

Fukusumi, S., Fujii, R., and Hinuma, S. (2006). Recent advances in mammalian RFamide peptides: the discovery and functional analyses of PrRP, RFRPs and QRFP. *Peptides* 27, 1073–1086. doi: 10.1016/j.peptides.2005.06.031

Gäde, G., and Rosiński, G. (1990). The primary structure of the hypertrehalosemic neuropeptide from tenebrionid beetles: a novel member of the AKH/RPCH family. *Peptides* 11, 455–459. doi: 10.1016/0196-9781(90)90042-4

Gahete, M. D., Cordoba-Chacon, J., Duran-Prado, M., Malagon, M. M., Martinez-Fuentes, A. J., Gracia-Navarro, F., et al. (2010). Somatostatin and its receptors from fish to mammals. *Ann. N. Y. Acad. Sci.* 1200, 43–52. doi: 10.1111/j.1749-6632.2010.05511.x

Gardner, T. A., Hernández, M. I., Barlow, J., and Peres, C. A. (2008). Understanding the biodiversity consequences of habitat change: the value of secondary and plantation forests for neotropical dung beetles. *J. Appl. Ecol.* 45, 883–893. doi: 10.1111/j.1365-2664.2008.01454.x

Gasco, L., Finke, M., and Van Huis, A. (2018). Can diets containing insects promote animal health? *J. Insects Food Feed* 4, 1–4. doi: 10.3920/JIFF2018.x001

Gavish, M., Bachman, I., Shoukrun, R., Katz, Y., Veenman, L., Weisinger, G., et al. (1999). Enigma of the peripheral benzodiazepine receptor. *Pharmacol. Rev.* 51, 629–650.

Ghannem, S., Touaylia, S., and Boumaiza, M. (2018). Beetles (Insecta: Coleoptera) as bioindicators of the assessment of environmental pollution. *Hum. Ecol. Risk Assess.* 24, 456–464. doi: 10.1673/031.011.17201

Ghoneim, K. S. (2013). Human dermatosis caused by vesicating beetle products (Insecta), cantharidin and paederin: an overview. *World J. Med. Sci.* 1, 1–26.

Giglio, A., Cavaliere, F., Giulianini, P. G., Mazzei, A., Talarico, F., Vommaro, M. L., et al. (2017). Impact of agrochemicals on non-target species: *Calathus fuscipes* Goeze 1777 (Coleoptera: Carabidae) as model. *Ecotoxicol. Environ. Saf.* 142, 522–529. doi: 10.1016/j.ecoenv.2017.04.056

Goodnight, C. J. (2005). Multilevel selection: the evolution of cooperation in non-kin groups. *Popul. Ecol.* 47, 3–12. doi: 10.1007/s10144-005-0207-2

Gooptu, B., and Lomas, D. A. (2009). Conformational pathology of the serpins: themes, variations, and therapeutic strategies. *Annu. Rev. Biochem.* 78, 147–176. doi: 10.1146/annurev.biochem.78.082107.133320

Gordon, J., Potter, M., and Haynes, K. (2015). Insecticide resistance in the bed bug comes with a cost. *Sci. Rep.* 5:10807. doi: 10.1038/srep10807

Gruber, C. W. (2014). Physiology of invertebrate oxytocin and vasopressin neuropeptides. *Exp. Physiol.* 99, 55–61. doi: 10.1113/expphysiol.2013.072561

Grunwald, S., Adam, I. V., Gurmai, A. M., Bauer, L., Boll, M., and Wenzel, U. (2013). The red four beetle *Tribolium castaneum* as a model to monitor food safety and functionality. *Adv. Biochem. Eng. Biotechnol.* 135, 111–122. doi: 10.1007/10_2013_212

Guedes, R., Oliveira, E., Guedes, N., Ribeiro, B., and Serrao, J. (2006). Cost and mitigation of insecticide resistance in the maize weevil, *Sitophilus zeamais*. *Physiol. Entomol.* 31, 30–38. doi: 10.1017/S0007485308005737

Hahn, N., Knorr, D. Y., Liebig, J., Wustefeld, L., Peters, K., Buscher, M., et al. (2017). The insect ortholog of the human orphan cytokine receptor CRLF3 is a neuroprotective erythropoietin receptor. *Front. Mol. Neurosci.* 10:223. doi: 10.3389/fnmol.2017.00223

Hartenstein, V. (2006). The neuroendocrine system of invertebrates: a developmental and evolutionary perspective. *J. Endocrinol.* 190, 555–570. doi: 10.1677/joe.1.06964

Heimbach, U. (1998). Testing the effects of plant protection products on larvae of the carabid beetle *Poecilus cupreus* (Coleoptera, Carabidae) in the laboratory, method and results. *IOBC WPRS Bull.* 21, 21–28.

Hemptinne, J., Lognay, G., and Dixon, A. (1998). Mate recognition in the two-spot ladybird beetle, Adalia bipunctata: role of chemical and behavioural cues. *J. Insect Physiol.* 44, 1163–1171. doi: 10.1016/S0022-1910(98)00081-X

Henry, M., Gasco, L., Chatzifotis, S., and Piccolo, G. (2018). Does dietary insect meal affect the fish immune system? The case of mealworm, *Tenebrio molitor* on European sea bass, *Dicentrarchus labrax*. *Dev. Comp. Immunol.* 81, 204–209. doi: 10.1016/j.dci.2017.12.002

Holck, M., and Osterrieder, W. (1985). The peripheral, high affinity benzodiazepine binding site is not coupled to the cardiac Ca2+ channel. *Eur. J. Pharmacol.* 118, 293–301. doi: 10.1016/0014-2999(85)90140-2

Holland, J. M. (2002). *The Agroecology of Carabid Beetles*. Andover, MA: Intercept.

Honek, A., Martinkova, Z., and Saska, P. (2005). Post-dispersal seed predation of *Taraxacum officinale* (dandelion) seed. *J. Ecol.* 93, 310–318. doi: 10.1111/j.1365-2745.2005.00987.x

Hsia, T.-C., Yu, C.-C., Hsiao, Y.-T., Wu, S.-H., Bau, D.-T., Lu, H.-F., et al. (2016). Cantharidin impairs cell migration and invasion of human lung cancer NCI-H460 cells via UPA and MAPK signaling pathways. *Anticancer Res.* 36, 5989–5997. doi: 10.21873/anticanres.11187

http://i5k.github.io/ (2018). *i5k: Sequencing Five Thousand Arthropod Genomes*. Available at: http://i5k.github.io/

Huusela-Veistola, E. (1996). Effects of pesticide use and cultivation techniques on ground beetles (Col., Carabidae) in cereal fields. *Ann. Zool. Fenn.* 33, 197–205.

Ishibashi, J. (2016). Applications of antimicrobial peptides derived from the defensin of the rhinoceros beetle *Allomyrina dichotoma*. *Juntendo Med. J.* 62, 112–119. doi: 10.14789/jmj.62.112

Islam, M., and Yang, C. (2016). Efficacy of mealworm and super mealworm larvae probiotics as an alternative to antibiotics challenged orally with *Salmonella* and *E. coli* infection in broiler chicks. *Poult. Sci.* 96, 27–34. doi: 10.3382/ps/pew220

Iwasaki, T., Saido-Sakanaka, H., Asaoka, A., Taylor, D., Ishibashi, J., and Yamakawa, M. (2007). In vitro activity of diastereomeric antimicrobial peptides alone and in combination with antibiotics against methicillin-resistant *Staphylococcus aureus* and *Pseudomonas aeruginosa*. *J. Insect Biotechnol. Sericology* 76, 25–29.

Jiang, R., Zhang, B., Kurokawa, K., So, Y.-I., Kim, E.-H., Hwang, H. O., et al. (2011). 93-kDa twin-domain serine protease inhibitor (Serpin) has a regulatory function on the beetle Toll proteolytic signaling cascade. *J. Biol. Chem.* 286, 35087–35095. doi: 10.1074/jbc.M111.277343

Johnston, P. R., Makarova, O., and Rolff, J. (2014). Inducible defenses stay up late: temporal patterns of immune gene expression in *Tenebrio molitor*. *G3* 4, 947–955. doi: 10.1534/g3.113.008516

Jonason, D., Smith, H. G., Bengtsson, J., and Birkhofer, K. (2013). Landscape simplification promotes weed seed predation by carabid beetles (Coleoptera: Carabidae). *Landsc. Ecol.* 28, 487–494. doi: 10.1007/s10980-013-9848-2

Kalkan, S., and Altuğ, G. (2015). Bio-indicator bacteria & environmental variables of the coastal zones: The example of the Güllük Bay, Aegean Sea, Turkey. *Mar. Pollut. Bull.* 95, 380–384. doi: 10.1016/j.marpolbul.2015.04.017

Kalsi, M., and Palli, S. R. (2017). Transcription factor cap n collar C regulates multiple cytochrome P450 genes conferring adaptation to potato plant allelochemicals and resistance to imidacloprid in *Leptinotarsa decemlineata* (Say). *Insect Biochem. Mol. Biol.* 83, 1–12. doi: 10.1016/j.ibmb.2017.02.002

Kang, B.-R., Kim, H., Nam, S.-H., Yun, E.-Y., Kim, S.-R., Ahn, M.-Y., et al. (2012). CopA3 peptide from *Copris tripartitus* induces apoptosis in human leukemia cells via a caspase-independent pathway. *BMB Rep.* 45, 85–90. doi: 10.5483/BMBRep.2012.45.2.85

Katayama, N., Ishikawa, Y., Takaoki, M., Yamashita, M., Nakayama, S., Kiguchi, K., et al. (2008). Entomophagy: a key to space agriculture. *Adv. Space Res.* 41, 701–705. doi: 10.1016/j.asr.2007.01.027

Kazlauskaite, A., Martinez-Torres, R. J., Wilkie, S., Kumar, A., Peltier, J., Gonzalez, A., et al. (2015). Binding to serine 65-phosphorylated ubiquitin primes Parkin for optimal PINK1-dependent phosphorylation and activation. *EMBO Rep.* 16, 939–954. doi: 10.15252/embr.201540352

Kazuhira, Y., Hdeaki, K., Takuro, K., and Toshiharu, A. (1991). Nitrogen mineralization and microbial populations in cow dung, dung balls and underlying soil affected by paracoprid dung beetles. *Soil Biol. Biochem.* 23, 649–653. doi: 10.1016/0038-0717(91)90078-X

Keeling, C. I., Yuen, M. M., Liao, N. Y., Docking, T. R., Chan, S. K., Taylor, G. A., et al. (2013). Draft genome of the mountain pine beetle, *Dendroctonus ponderosae* Hopkins, a major forest pest. *Genome Biol.* 14:R27. doi: 10.1186/gb-2013-14-3-r27

Kent, D., and Simpson, J. (1992). Eusociality in the beetle *Austroplatypus incompertus* (Coleoptera: Curculionidae). *Naturwissenschaften* 79, 86–87. doi: 10.1007/BF01131810

Kerstes, N. A., Bérénos, C., Schmid-Hempel, P., and Wegner, K. M. (2012). Antagonistic experimental coevolution with a parasite increases host recombination frequency. *BMC Evol. Biol.* 12:18. doi: 10.1186/1471-2148-12-18

Kim, I.-W., Lee, J. H., Kwon, Y.-N., Yun, E.-Y., Nam, S.-H., Ahn, M.-Y., et al. (2013). Anticancer activity of a synthetic peptide derived from harmoniasin, an antibacterial peptide from the ladybug *Harmonia axyridis*. *Int. J. Oncol.* 43, 622–628. doi: 10.3892/ijo.2013.1973

Kitaev, K., Mardanshin, I., Surina, E., Leontieva, T., Udalov, M., and Benkovskaya, G. (2017). Modeling genetic processes underlying the development of resistance to fipronil in the populations of Colorado potato beetle (*Leptinotarsa decemlineata* Say). *Russ. J. Genet.* 7, 36–45. doi: 10.1134/S2079059717010063

Klockars, A., Levine, A. S., and Olszewski, P. K. (2018). Hypothalamic integration of the endocrine signaling related to food intake. *Curr. Top. Behav. Neurosci.* doi: 10.1007/7854_2018_54 [Epub ahead of print].

Knorr, E., Fishilevich, E., Tenbusch, L., Frey, M. L. F., Rangasamy, M., Billion, A., et al. (2018). Gene silencing in *Tribolium castaneum* as a tool for the targeted identification of candidate RNAi targets in crop pests. *Sci. Rep.* 8:2061. doi: 10.1038/s41598-018-20416-y

Kolawole, A. O., and Kolawole, A. N. (2014). Insecticides and bio-insecticides modulate the glutathione-related Antioxidant defense system of Cowpea storage Bruchid (*Callosobruchus maculatus*). *Int. J. Insect Sci.* 6, 79–88. doi: 10.4137/IJIS.S18029

Kolińska, A., Marciniak, P., Adamski, Z., and Rosiński, G. (2016). [Alkaloids - natural cardioactive substances]. *Kosmos* 65, 247–256.

Kostaropoulos, I., Papadopoulos, A. I., Metaxakis, A., Boukouvala, E., and Papadopoulou-Mourkidou, E. (2001). Glutathione *S*-transferase in the defence against pyrethroids in insects. *Insect Biochem. Mol. Biol.* 31, 313–319. doi: 10.1016/S0965-1748(00)00123-5

Kowalski, M. (2011). [*Activity of Antiarrhythmic Drugs on the Heart of the Beetle Zophobas atratus*]. Master's thesis, Poznań Adam Mickiewicz University, Poznań.

Kromp, B. (1999). Carabid beetles in sustainable agriculture: a review on pest control efficacy, cultivation impacts and enhancement. *Agric. Ecosyst. Environ.* 74, 187–228. doi: 10.1016/S0167-8809(99)00037-7

Krueger, K. E. (1995). Molecular and functional properties of mitochondrial benzodiazepine receptors. *Biochim. Biophys. Acta* 1241, 453–470. doi: 10.1016/0304-4157(95)00016-X

Kuczer, M., Czarniewska, E., Majewska, A., Rozanowska, M., Rosinski, G., and Lisowski, M. (2016). Novel analogs of alloferon: synthesis, conformational studies, pro-apoptotic and antiviral activity. *Bioorg. Chem.* 66, 12–20. doi: 10.1016/j.bioorg.2016.03.002

Kuczer, M., Czarniewska, E., and Rosinski, G. (2013). Novel biological effects of alloferon and its selected analogues: structure-activity study. *Regul. Pept.* 183, 17–22. doi: 10.1016/j.regpep.2013.03.010

Kulkarni, S. S., Dosdall, L. M., and Willenborg, C. J. (2015). The role of ground beetles (Coleoptera: Carabidae) in weed seed consumption: a review. *Weed Sci.* 63, 355–376. doi: 10.1614/WS-D-14-00067.1

Kumar, A., Tamjar, J., Waddell, A. D., Woodroof, H. I., Raimi, O. G., Shaw, A. M., et al. (2017). Structure of PINK1 and mechanisms of Parkinson's disease-associated mutations. *eLife* 6:e29985. doi: 10.7554/eLife.29985

Lagisz, M., and Laskowski, R. (2008). Evidence for between-generation effects in carabids exposed to heavy metals pollution. *Ecotoxicology* 17, 59–66. doi: 10.1007/s10646-007-0176-7

Lakatta, E. G. (2002). Age-associated cardiovascular changes in health: impact on cardiovascular disease in older persons. *Heart Fail. Rev.* 7, 29–49. doi: 10.1023/A:1013797722156

Lambkin, T. A., and Furlong, M. J. (2014). Application of spinosad increases the susceptibility of insecticide-resistant *Alphitobius diaperinus* (Coleoptera: Tenebrionidae) to pyrethroids. *J. Econ. Entomol.* 107, 1590–1598. doi: 10.1603/EC13473

Langlois, F., Chu, J., and Fleseriu, M. (2018). Pituitary-directed therapies for Cushing's disease. *Front. Endocrinol.* 9:164. doi: 10.3389/fendo.2018.00164

Leander, M., Bass, C., Marchetti, K., Maynard, B. F., Wulff, J. P., Ons, S., et al. (2015). Cardiac contractility structure-activity relationship and ligand-receptor interactions; the discovery of unique and novel molecular switches in myosuppressin signaling. *PLoS One* 10:e0120492. doi: 10.1371/journal.pone.0120492

Lee, J., Menalled, F., and Landis, D. (2001). Refuge habitats modify impact of insecticide disturbance on carabid beetle communities. *J. Appl. Ecol.* 38, 472–483. doi: 10.1046/j.1365-2664.2001.00602.x

Lee, J. H., Kim, I.-W., Kim, S.-H., Yun, E.-Y., Nam, S.-H., Ahn, M.-Y., et al. (2015). Anticancer activity of CopA3 dimer peptide in human gastric cancer cells. *BMB Rep.* 48, 324–329. doi: 10.5483/BMBRep.2015.48.6.073

Lee, N., Bae, S., Kim, H., Kong, J. M., Kim, H.-R., Cho, B. J., et al. (2011). Inhibition of lytic reactivation of Kaposi's sarcoma-associated herpesvirus by alloferon. *Antivir. Ther.* 16, 17–26. doi: 10.3851/IMP1709

Lee, W., Kim, M. A., Park, I., Hwang, J. S., Na, M., and Bae, J. S. (2017). Novel direct factor Xa inhibitory compounds from *Tenebrio molitor* with anti-platelet aggregation activity. *Food Chem. Toxicol.* 109, 19–27. doi: 10.1016/j.fct.2017.08.026

Lindeman, A., and Yack, J. (2015). What is the password? Female bark beetles (Scolytinae) grant males access to their galleries based on courtship song. *Behav. Process.* 115, 123–131. doi: 10.1016/j.beproc.2015.03.009

Liutkeviciute, Z., Koehbach, J., Eder, T., Gil-Mansilla, E., and Gruber, C. W. (2016). Global map of oxytocin/vasopressin-like neuropeptide signalling in insects. *Sci. Rep.* 6:39177. doi: 10.1038/srep39177

Loizzo, M. R., Saab, A. M., Tundis, R., Menichini, F., Bonesi, M., Piccolo, V., et al. (2008). In vitro inhibitory activities of plants used in Lebanon traditional medicine against angiotensin converting enzyme (ACE) and digestive enzymes related to diabetes. *J. Ethnopharmacol.* 119, 109–116. doi: 10.1016/j.jep.2008.06.003

Lu, J., Sun, Q., Tu, Z.-C., Lv, Q., Shui, P.-X., and Cheng, Y.-X. (2015). Identification of *N*-acetyldopamine dimers from the dung beetle *Catharsius molossus* and Their COX-1 and COX-2 inhibitory activities. *Molecules* 20, 15589–15596. doi: 10.3390/molecules200915589

Lu, S., Gao, Y., Huang, X., and Wang, X. (2014). Cantharidin exerts anti-hepatocellular carcinoma by miR-214 modulating macrophage polarization. *Int. J. Biol. Sci.* 10, 415–425. doi: 10.7150/ijbs.8002

Lubawy, J., Czarniewska, E., Kuczer, M., and Rosiński, G. (2013). [Allatostatins - pleiotropic insect neurohormones]. *Post. Biol. Kom.* 40, 385–400. doi: 10.1016/j.npep.2018.05.003

Lubawy, J., Marciniak, P., Kuczer, M., and Rosiński, G. (2018). Myotropic activity of allatostatins in tenebrionid beetles. *Neuropeptides* 70, 26–36. doi: 10.1016/j.npep.2018.05.003

Marciniak, P., Adamski, Z., Bednarz, P., Słocińska, M., Ziemnicki, K., Lelario, F., et al. (2010a). Cardioinhibitory properties of potato glycoalkaloids in beetles. *Bull. Environ. Contam. Toxicol.* 84, 153–156. doi: 10.1007/s00128-009-9921-3

Marciniak, P., Audsley, N., Kuczer, M., and Rosiński, G. (2010b). Identification of myotropic neuropeptides from the brain and *corpus cardiacum-corpus allatum* complex of the beetle, *Zophobas atratus*. *J. Insect Sci.* 10, 156. doi: 10.1673/031.010.14116

Marciniak, P., and Rosiński, G. (2010). Comparison of proctolin and FMRFamide actions on the motility of male and female beetle reproductive tracts. *Invertebr. Rep. Dev.* 54, 1–6. doi: 10.1080/07924259.2010.9652310

Marciniak, P., Słocińska, M., Bednarz, P., Grodecki, S., Konopińska, D., and Rosiński, G. (2009). Effects of arginine substitutions on the cardioinhibitory activity of the Led-NPF-I neuropeptide. *Pesticides* 1-4, 57–62.

Markó, V., and Kádár, F. (2005). Effects of different insecticide disturbance levels and weed patterns on carabid beetle assemblages. *Acta Phytopathol. Entomol. Hung.* 40, 111–143. doi: 10.1556/APhyt.40.2005.1-2.11

Maryanski, M., Kramarz, P., Laskowski, R., and Niklinska, M. (2002). Decreased energetic reserves, morphological changes and accumulation of metals in carabid beetles (*Poecilus cupreus* L.) exposed to zinc- or cadmium-contaminated food. *Ecotoxicology* 11, 127–139. doi: 10.1023/A:1014425113481

Matusiak, A., Kuczer, M., Czarniewska, E., Rosiński, G., and Kowalik-Jankowska, T. (2014). Copper (II) complexes of alloferon 1 with point mutations (H1A) and (H9A) stability structure and biological activity. *J. Inorg. Biochem.* 138, 99–113. doi: 10.1016/j.jinorgbio.2014.05.012

Maxton-Küchenmeister, J., Handel, K., Schmidt-Ott, U., Roth, S., and Jäckle, H. (1999). Toll homolog expression in the beetle *Tribolium* suggests a different mode of dorsoventral patterning than in *Drosophila* embryos. *Mech. Dev.* 83, 107–114. doi: 10.1016/S0925-4773(99)00041-6

McKenna, D. D. (2018). Beetle genomes in the 21st century: prospects, progress and priorities. *Curr. Opin. Insect Sci.* 25, 76–82. doi: 10.1016/j.cois.2017.12.002

McKenna, D. D., Scully, E. D., Pauchet, Y., Hoover, K., Kirsch, R., Geib, S. M., et al. (2016). Genome of the Asian longhorned beetle (*Anoplophora glabripennis*), a globally significant invasive species, reveals key functional and evolutionary innovations at the beetle-plant interface. *Genome Biol.* 17:227. doi: 10.1186/s13059-016-1088-8

McKenna, D. D., Sequeira, A. S., Marvaldi, A. E., and Farrell, B. D. (2009). Temporal lags and overlap in the diversification of weevils and flowering plants. *Proc. Natl. Acad. Sci. U.S.A.* 106, 7083–7088. doi: 10.1073/pnas.0810618106

McKinley, M., O'Loughlin, V., and Bidle, T. (2016). *Anatomy & Physiology: An Integrative Approach*. New York, NY: McGraw-Hill Education.

McLeish, K. R., Klein, J. B., Coxon, P. Y., Head, K. Z., and Ward, R. A. (1998). Bacterial phagocytosis activates extracellular signal regulated kinase and p38 mitogen-activated protein kinase cascades in human neutrophils. *J. Leukoc. Biol.* 64, 835–844. doi: 10.1002/jlb.64.6.835

McWilliams, T. G., and Muqit, M. M. (2017). PINK1 and Parkin: emerging themes in mitochondrial homeostasis. *Curr. Opin. Cell Biol.* 45, 83–91. doi: 10.1016/j.ceb.2017.03.013

Mestre, M., Carriot, T., Belin, C., Uzan, A., Renault, C., Dubroeucq, M. C., et al. (1985). Electrophysiological and pharmacological evidence that peripheral type benzodiazepine receptors are coupled to calcium channels in the heart. *Life Sci.* 36, 391–400. doi: 10.1016/0024-3205(85)90126-2

Meyer, J. M., Markov, G. V., Baskaran, P., Herrmann, M., Sommer, R. J., and Rodelsperger, C. (2016). Draft genome of the scarab beetle *Oryctes borbonicus* on La Reunion Island. *Genome Biol. Evol.* 8, 2093–2105. doi: 10.1093/gbe/evw133

Miklósi, Á, and Gácsi, M. (2012). On the utilization of social animals as a model for social robotics. *Front. Psychol.* 3:75. doi: 10.3389/fpsyg.2012.00075

Mikulak, E., Gliniewicz, A., Przygodzka, M., and Solecka, J. (2018). *Galleria mellonella* L. as model organism used in biomedical and other studies. *Przegl. Epidemiol.* 72, 57–73.

Miljus, N., Heibeck, S., Jarrar, M., Micke, M., Ostrowski, D., Ehrenreich, H., et al. (2014). Erythropoietin-mediated protection of insect brain neurons involves JAK and STAT but not PI3K transduction pathways. *Neuroscience* 258, 218–227. doi: 10.1016/j.neuroscience.2013.11.020

Milutinović, B., Stolpe, C., Peuβ, R., Armitage, S. A., and Kurtz, J. (2013). The red flour beetle as a model for bacterial oral infections. *PLoS One* 8:e64638. doi: 10.1371/journal.pone.0064638

Moeck, H. A. (1970). Ethanol as the primary attractant for the ambrosia beetle *Trypodendron lineatum* (Coleoptera: Scolytidae). *Can. Entomol.* 102, 985–995. doi: 10.4039/Ent102985-8

Moed, L., Shwayder, T. A., and Chang, M. W. (2001). Cantharidin revisited: a blistering defense of an ancient medicine. *Arch. Dermatol.* 137, 1357–1360. doi: 10.1001/archderm.137.10.1357

Monteleone, A. M., Castellini, G., Volpe, U., Ricca, V., Lelli, L., Monteleone, P., et al. (2018). Neuroendocrinology and brain imaging of reward in eating disorders: a possible key to the treatment of anorexia nervosa and bulimia nervosa. *Prog. Neuropsychopharmacol. Biol. Psychiatry* 80, 132–142. doi: 10.1016/j.pnpbp.2017.02.020

Moon, M.-J., Park, J.-G., Seo, S.-T., and Kim, K.-H. (2012). Microstructure of the prothoracic mycangia in the ambrosia beetle *Platypus koryoensis* (Coleoptera: Curculionidae: Platypodinae). *J. Asia Pac. Entomol.* 15, 51–57. doi: 10.1016/j.aspen.2011.08.010

Mukherjee, K., Twyman, R. M., and Vilcinskas, A. (2015). Insects as models to study the epigenetic basis of disease. *Prog. Biophys. Mol. Biol.* 118, 69–78. doi: 10.1016/j.pbiomolbio.2015.02.009

Nakamura, M., Iwasaki, T., Tokino, S., Asaoka, A., Yamakawa, M., and Ishibashi, J. (2011). Development of a bioactive fiber with immobilized synthetic peptides designed from the active site of a beetle defensin. *Biomacromolecules* 12, 1540–1545. doi: 10.1021/bm1014969

Nalepa, C., Kennedy, G., and Brownie, C. (2005). Role of visual contrast in the alighting behavior of *Harmonia axyridis* (Coleoptera: Coccinellidae) at overwintering sites. *Environ. Entomol.* 34, 425–431. doi: 10.1603/0046-225X-34.2.425

Nässel, D. R., and Williams, M. J. (2014). Cholecystokinin-like peptide (DSK) in *Drosophila*, not only for satiety signaling. *Front. Endocrinol.* 5:219. doi: 10.3389/fendo.2014.00219

Nichols, E., Spector, S., Louzada, J., Larsen, T., Amezquita, S., and Favila, M. E. (2008). Ecological functions and ecosystem services provided by Scarabaeinae dung beetles. *Biol. Conserv.* 141, 1461–1474. doi: 10.1016/j.biocon.2008.04.011

Nichols, R., Bass, C., Demers, L., Larsen, B., Li, E., Blewett, N., et al. (2012). Structure-activity studies of RFamide-related peptide-1 identify a functional receptor antagonist and novel cardiac myocyte signaling pathway involved in contractile performance. *J. Med. Chem.* 55, 7736–7745. doi: 10.1021/jm300760m

Nishimura, M., Ocorr, K., Bodmer, R., and Cartry, J. (2011). *Drosophila* as a model to study cardiac aging. *Exp. Gerontol.* 46, 326–330. doi: 10.1016/j.exger.2010.11.035

Nouchi, I. (2012). "Plants as bioindicators of air pollutants," in *Air Pollution and Plant Biotechnology: Prospects for Phytomonitoring and Phytoremediation*, eds K. Omasa, H. Saji, S. Youssefian, and N. Kondo (Tokyo: Springer Science & Business Media).

Ntwasa, M., Goto, A., and Kurata, S. (2012). Coleopteran antimicrobial peptides: prospects for clinical applications. *Int. J. Microbiol.* 2012:101989. doi: 10.1155/2012/101989

Obata, S. (1987). Mating behavior and sperm transfer in the ladybird beetle, *Harmonia axyridis* Pallas: Coleoptera: Coccinellidae. *Appl. Entomol. Zool.* 22, 434–442. doi: 10.1303/aez.22.434

Ocorr, K., Perrin, L., Lim, H.-Y., Qian, L., Wu, X., and Bodmer, R. (2007a). Genetic control of heart function and aging in *Drosophila*. *Trends Cardiovasc. Med.* 17, 177–182. doi: 10.1016/j.tcm.2007.04.001

Ocorr, K., Reeves, N. L., Wessells, R. J., Fink, M., Chen, H. S., Akasaka, T., et al. (2007b). KCNQ potassium channel mutations cause cardiac arrhythmias in *Drosophila* that mimic the effects of aging. *Proc. Natl. Acad. Sci. U.S.A.* 104, 3943–3948.

Oliver, I., and Beattie, A. J. (1996). Designing a cost-effective invertebrate survey: A test of methods for rapid assessment of biodiversity. *Ecol. Appl.* 6, 594–607. doi: 10.2307/2269394

O'Neil, M. J. (2001). *The Merck Index: An Encyclopedia of Chemicals, Drugs, and Biologicals*. Whitehouse Station, NJ: Merck.

Oonincx, D. G., and de Boer, I. J. (2012). Environmental impact of the production of mealworms as a protein source for humans - a life cycle assessment. *PLoS One* 7:e51145. doi: 10.1371/journal.pone.0051145

Oonincx, D. G., van Itterbeeck, J., Heetkamp, M. J., van den Brand, H., van Loon, J. J., and van Huis, A. (2010). An exploration on greenhouse gas and ammonia production by insect species suitable for animal or human consumption. *PLoS One* 5:e14445. doi: 10.1371/journal.pone.0014445

Osman, W., and Shonouda, M. (2017). X-ray metal assessment and ovarian ultrastructure alterations of the beetle, *Blaps polycresta* (Coleoptera, Tenebrionidae), inhabiting polluted soil. *Environ. Sci. Pollut. Res.* 24, 14867–14876. doi: 10.1007/s11356-017-9095-1

Ostrowski, D., Ehrenreich, H., and Heinrich, R. (2011). Erythropoietin promotes survival and regeneration of insect neurons in vivo and in vitro. *Neuroscience* 188, 95–108. doi: 10.1016/j.neuroscience.2011.05.018

Pacholska-Bogalska, J., Szymczak, M., Marciniak, P., Walkowiak-Nowicka, K., and Rosinski, G. (2018). Heart mechanical and hemodynamic parameters of a beetle, *Tenebrio molitor*, at selected ages. *Arch. Insect Biochem. Physiol.* 99:e21474. doi: 10.1002/arch.21474

Panaitof, S. C., Yaeger, J. D. W., Speer, J. P., and Renner, K. J. (2016). Biparental behavior in the burying beetle *Nicrophorus orbicollis*: a role for dopamine? *Curr. Zool.* 62, 285–291. doi: 10.1093/cz/zow032

Panini, R. L., Freitas, L. E. L., Guimarães, A. M., Rios, C., da Silva, M. F. O., Vieira, F. N., et al. (2017a). Potential use of mealworms as an alternative protein source for Pacific white shrimp: digestibility and performance. *Aquaculture* 473, 115–120. doi: 10.1016/j.aquaculture.2017.02.008

Panini, R. L., Pinto, S. S., Nóbrega, R. O., Vieira, F. N., Fracalossi, D. M., Samuels, R. I., et al. (2017b). Effects of dietary replacement of fishmeal by mealworm meal on muscle quality of farmed shrimp *Litopenaeus vannamei*. *Food Res. Int.* 102, 445–450. doi: 10.1016/j.foodres.2017.09.017

Papadopoulos, A., Stamkou, E., Kostaropoulos, I., and Papadopoulou-Mourkidou, E. (1999). Effect of organophosphate and pyrethroid insecticides on the expression of GSTs from*Tenebrio molitor* larvae. *Pestic. Biochem. Physiol.* 63, 26–33. doi: 10.1006/pest.1998.2391

Paragliola, R. M., and Salvatori, R. (2018). Novel somatostatin receptor ligands therapies for acromegaly. *Front. Endocrinol.* 9:78. doi: 10.3389/fendo.2018.00078

Parmar, T. K., Rawtani, D., and Agrawal, Y. (2016). Bioindicators: the natural indicator of environmental pollution. *Front. Life Sci.* 9, 110–118. doi: 10.1080/21553769.2016.1162753

Paternostro, G., Vignola, C., Bartsch, D. U., Omens, J. H., McCulloch, A. D., and Reed, J. C. (2001). Age-associated cardiac dysfunction in *Drosophila melanogaster*. *Circ. Res.* 88, 1053–1058. doi: 10.1161/hh1001.090857

Pauchet, Y., Wilkinson, P., Chauhan, R., and Ffrench-Constant, R. H. (2010). Diversity of beetle genes encoding novel plant cell wall degrading enzymes. *PLoS One* 5:e15635. doi: 10.1371/journal.pone.0015635

Pearson, D. L., and Cassola, F. (1992). World-wide species richness patterns of tiger beetles (Coleoptera: Cicindelidae): indicator taxon for biodiversity and conservation studies. *Conserv. Biol.* 6, 376–391. doi: 10.1046/j.1523-1739.1992.06030376.x

Pelissie, B., Crossley, M. S., Cohen, Z. P., and Schoville, S. D. (2018). Rapid evolution in insect pests: the importance of space and time in population genomics studies. *Curr. Opin. Insect Sci.* 26, 8–16. doi: 10.1016/j.cois.2017.12.008

Petit, S., and Usher, M. B. (1998). Biodiversity in agricultural landscapes: the ground beetle communities of woody uncultivated habitats. *Biodivers. Conserv.* 7, 1549–1561. doi: 10.1023/A:1008875403868

Piazza, N., and Wessells, R. J. (2011). Drosophila models of cardiac disease. *Prog. Mol. Biol. Transl. Sci.* 100, 155–210. doi: 10.1016/B978-0-12-384878-9.00005-4

Rajamuthiah, R., Jayamani, E., Conery, A. L., Fuchs, B. B., Kim, W., Johnston, T., et al. (2015). A defensin from the model beetle *Tribolium castaneum* acts synergistically with Telavancin and Daptomycin against multidrug resistant *Staphylococcus aureus*. *PLoS One* 10:e0128576. doi: 10.1371/journal.pone.0128576

Ramos-Elorduy, J., Gonzalez, E. A., Hernandez, A. R., and Pino, J. M. (2002). Use of *Tenebrio molitor* (Coleoptera: Tenebrionidae) to recycle organic wastes and as feed for broiler chickens. *J. Econ. Entomol.* 95, 214–220. doi: 10.1603/0022-0493-95.1.214

Ranger, C., Biedermann, P., Phuntumart, V., Beligala, G., Ghosh, S., Palmquist, D., et al. (2018). Symbiont selection via alcohol benefits fungus farming by ambrosia beetles. *Proc. Natl. Acad. Sci. U.S.A.* 115, 4447–4452. doi: 10.1073/pnas.1716852115

Rehfeld, J. F. (2017). Cholecystokinin—from local gut hormone to ubiquitous messenger. *Front. Endocrinol.* 8:47. doi: 10.3389/fendo.2017.00047

Roberge, C., Frechette, B., Labrie, G., Dumont, F., and Lucas, E. (2016). Gregarious pupation act as a defensive mechanism against cannibalism and intraguild predation. *Insect Sci.* 23, 612–620. doi: 10.1111/1744-7917.12209

Rodrigues, A. R., Torres, J. B., Siqueira, H. A., and Lacerda, D. P. (2013). Inheritance of lambda-cyhalothrin resistance in the predator lady beetle *Eriopis connexa* (Germar) (Coleoptera: Coccinellidae). *Biol. Control* 64, 217–224. doi: 10.1016/j.biocontrol.2012.11.018

Römbke, J., Hempel, H., Scheffczyk, A., Schallnass, H.-J., Alvinerie, M., and Lumaret, J.-P. (2007). Environmental risk assessment of veterinary pharmaceuticals: development of a standard laboratory test with the dung beetle *Aphodius constans*. *Chemosphere* 70, 57–64. doi: 10.1016/j.chemosphere.2007.07.027

Rumpold, B. A., and Schluter, O. K. (2013). Potential and challenges of insects as an innovative source for food and feed production. *Innov. Food Sci. Emerg.* 17, 1–11. doi: 10.1016/j.ifset.2012.11.005

Saegusa, K., Furukawa, Y., Ogiwara, Y., Takeda, M., and Chiba, S. (1987). Pharmacologic basis of responses to midazolam in the isolated, cross-perfused, canine right atrium. *Anesth. Analg.* 66, 711–718. doi: 10.1213/00000539-198708000-00003

Sagawa, M., Nakazato, T., Uchida, H., Ikeda, Y., and Kizaki, M. (2008). Cantharidin induces apoptosis of human multiple myeloma cells via inhibition of the JAK/STAT pathway. *Cancer Sci.* 99, 1820–1826. doi: 10.1111/j.1349-7006.2008.00872.x

Saido-Sakanaka, H., Ishibashi, J., Momotani, E., and Yamakawa, M. (2005). Protective effects of synthetic antibacterial oligopeptides based on the insect defensins on Methicillin-resistant *Staphylococcus aureus* in mice. *Dev. Comp. Immunol.* 29, 469–477. doi: 10.1016/j.dci.2004.09.005

Samani, F., Monfared, A. S., Zabihi, E., Khafri, S., Karimi, M., and Niaki, H. A. (2014). Evaluation of the effects of paederus beetle extract and gamma irradiation on HeLa cells. *Iran. J. Basic Med. Sci.* 17, 303–306.

Santalla, M., Valverde, C. A., Harnichar, E., Lacunza, E., Aguilar-Fuentes, J., Mattiazzi, A., et al. (2014). Aging and CaMKII alter intracellular Ca2+ transients and heart rhythm in *Drosophila melanogaster*. *PLoS One* 9:e101871. doi: 10.1371/journal.pone.0101871

Sato, Y., Yang, P., An, Y., Matsukawa, K., Ito, K., Imanishi, S., et al. (2010). A palmitoyl conjugate of insect pentapeptide yamamarin arrests cell proliferation and respiration. *Peptides* 31, 827–833. doi: 10.1016/j.peptides.2010.02.017

Savard, J., Tautz, D., and Lercher, M. J. (2006). Genome-wide acceleration of protein evolution in flies (Diptera). *BMC Evol. Biol.* 6:7. doi: 10.1186/1471-2148-6-7

Schmidt-Ott, U., and Lynch, J. A. (2016). Emerging developmental genetic model systems in holometabolous insects. *Curr. Opin. Genet. Dev.* 39, 116–128. doi: 10.1016/j.gde.2016.06.004

Schoville, S. D., Chen, Y. H., Andersson, M. N., Benoit, J. B., Bhandari, A., Bowsher, J. H., et al. (2018). A model species for agricultural pest genomics: the genome of the Colorado potato beetle, *Leptinotarsa decemlineata* (Coleoptera: Chrysomelidae). *Sci. Rep.* 8:1931. doi: 10.1038/s41598-018-20154-1

Schroder, R., Beermann, A., Wittkopp, N., and Lutz, R. (2008). From development to biodiversity - *Tribolium castaneum*, an insect model organism for short germband development. *Dev. Genes Evol.* 218, 119–126. doi: 10.1007/s00427-008-0214-3

Scott, I. M., Tolman, J. H., and MacArthur, D. C. (2015). Insecticide resistance and cross-resistance development in Colorado potato beetle *Leptinotarsa decemlineata* Say (Coleoptera: Chrysomelidae) populations in Canada 2008-2011. *Pest. Manag. Sci.* 71, 712–721. doi: 10.1002/ps.3833

Scott, M., and Panaitof, S. (2004). Social stimuli affect juvenile hormone during breeding in biparental burying beetles (Silphidae: *Nicrophorus*). *Horm. Behav.* 45, 159–167. doi: 10.1016/j.yhbeh.2003.09.012

Seo, M., Goo, T. W., Chung, M. Y., Baek, M., Hwang, J. S., Kim, M. A., et al. (2017). *Tenebrio molitor* larvae inhibit adipogenesis through AMPK and MAPKs signaling in 3T3-L1 adipocytes and obesity in high-fat diet-induced obese mice. *Int. J. Mol. Sci.* 18:E518. doi: 10.3390/ijms18030518

Shonouda, M., and Osman, W. (2018). Ultrastructural alterations in sperm formation of the beetle, *Blaps polycresta* (Coleoptera: Tenebrionidae) as a biomonitor of heavy metal soil pollution. *Environ. Sci. Pollut. Res.* 25, 7896–7906. doi: 10.1007/s11356-017-1172-y

Siddig, A. A., Ellison, A. M., Ochs, A., Villar-Leeman, C., and Lau, M. K. (2016). How do ecologists select and use indicator species to monitor ecological change? Insights from 14 years of publication in Ecological Indicators. *Ecol. Indic.* 60, 223–230. doi: 10.1016/j.ecolind.2015.06.036

Sivčev, L., Sivčev, I., Graora, D., Tomić, V., Dudić, B., Büchs, W., et al. (2017). Effects of insecticides intended for *Ceutorhynchus napi* Gyll. control in oilseed rape on ground beetles. *Pestic. Fitomed.* 32, 223–230. doi: 10.2298/PIF1704223S

Sliwowska, J., Rosinski, G., and Nassel, D. R. (2001). Cardioacceleratory action of tachykinin-related neuropeptides and proctolin in two coleopteran insect species. *Peptides* 22, 209–217. doi: 10.1016/S0196-9781(00)00384-3

Słocińska, M., Czubak, T., Marciniak, P., Jarmuszkiewicz, W., and Rosiński, G. (2015a). The activity of the nonsulfated sulfakinin Zopat-SK-1 in the neck-ligated larvae of the beetle *Zophobas atratus*. *Peptides* 69, 127–132. doi: 10.1016/j.peptides.2015.04.023

Słocińska, M., Gartych, M., and Rosiński, G. (2011). "The action of benzodiazepines on the heart activity of *Zophobas atratus* beetle," in *Proceedings of the Sixth International Symposium on Molecular Insect Science*, Vol. 2, (Amsterdam: Elsevier).

Słocińska, M., Marciniak, P., Jarmuszkiewicz, W., and Rosiński, G. (2015b). New metabolic activity of the nonsulfated sulfakinin Zopat-SK-1 in the insect fat body. *Peptides* 68, 157–163. doi: 10.1016/j.peptides.2014.05.010

Słocińska, M., Marciniak, P., and Rosiń, G. (2008). Insects antiviral and anticancer peptides: new leads for the future? *Protein Pept. Lett.* 15, 578–585.

Słocińska, M., Szewczyk, A., Hryniewiecka, L., and Kmita, H. (2004). Benzodiazepine binding to mitochondrial membranes of the amoeba *Acanthamoeba castellanii* and the yeast *Saccharomyces cerevisiae*. *Acta Biochim. Pol.* 51, 953–962.

Smith, S. M., Kent, D. S., Boomsma, J. J., and Stow, A. J. (2018). Monogamous sperm storage and permanent worker sterility in a long-lived ambrosia beetle. *Nat. Ecol. Evol.* 2:1009. doi: 10.1038/s41559-018-0533-3

Soumya, M., Reddy, H., Nageswari, G., and Venkatappa, B. (2017). Silkworm (*Bombyx mori*) and its constituents: a fascinating insect in science and research. *J. Entomol. Zool. Stud.* 5, 1701–1705.

Spence, J. R., and Niemelä, J. K. (1994). Sampling carabid assemblages with pitfall traps: the madness and the method. *Can. Entomol.* 126, 881–894. doi: 10.4039/Ent126881-3

Spit, J., Philips, A., Wynant, N., Santos, D., Plaetinck, G., and Broeck, J. V. (2017). Knockdown of nuclease activity in the gut enhances RNAi efficiency in the Colorado potato beetle, *Leptinotarsa decemlineata*, but not in the desert locust, *Schistocerca gregaria*. *Insect Biochem. Mol. Biol.* 81, 103–116. doi: 10.1016/j.ibmb.2017.01.004

Spochacz, M., Chowański, S., Walkowiak-Nowicka, K., Szymczak, M., and Adamski, Z. (2018). Plant-derived substances used against beetles – pests of stored crops and food – and their mode of action: a review. *Compr. Rev. Food Sci.* 17, 1339–1366. doi: 10.1111/1541-4337.12377

Stankiewicz, M., Dabrowski, M., and de Lima, M. E. (2012). Nervous system of *Periplaneta americana* cockroach as a model in toxinological studies: a short historical and actual view. *J. Toxicol.* 2012:143740. doi: 10.1155/2012/143740

Steiger, S., and Stokl, J. (2017). Pheromones involved in insect parental care and family life. *Curr. Opin. Insect Sci.* 24, 89–95. doi: 10.1016/j.cois.2017.09.006

Stork, N. E., McBroom, J., Gely, C., and Hamilton, A. J. (2015). New approaches narrow global species estimates for beetles, insects, and terrestrial arthropods. *Proc. Natl. Acad. Sci. U.S.A.* 112, 7519–7523. doi: 10.1073/pnas.1502408112

Strand, M. R. (2008). The insect cellular immune response. *Insect Sci.* 15, 1–14. doi: 10.1111/j.1744-7917.2008.00183.x

Stratonovitch, P., Elias, J., Denholm, I., Slater, R., and Semenov, M. A. (2014). An individual-based model of the evolution of pesticide resistance in heterogeneous environments: control of *Meligethes aeneus* population in oilseed rape crops. *PLoS One* 9:e115631. doi: 10.1371/journal.pone.0115631

Sudo, M., Takahashi, D., Andow, D., Suzuki, Y., and Yamanaka, T. (2018). Optimal management strategy of insecticide resistance under various insect life histories: Heterogeneous timing of selection and interpatch dispersal. *Evol. Appl.* 11, 271–283. doi: 10.1111/eva.12550

Surinkaew, S., Chattipakorn, S., and Chattipakorn, N. (2011). Roles of mitochondrial benzodiazepine receptor in the heart. *Can. J. Cardiol.* 27, 262.e3–262.e 13. doi: 10.1016/j.cjca.2010.12.023

Szymanowska-Dziubasik, K., Marciniak, P., Rosiński, G., and Konopińska, D. (2008). Synthesis, cardiostimulatory, and cardioinhibitory effects of selected insect peptides on *Tenebrio molitor*. *J. Pept. Sci.* 14, 708–713. doi: 10.1002/psc.977

Szymczak, M., Marciniak, P., and Rosiński, G. (2014). [Insect myocardium - model in biomedical studies]. *Post. Biol. Kom.* 41, 59–78.

Tang, B., Chen, J., Hou, Y., and Meng, E. (2014). Transcriptome immune analysis of the invasive beetle *Octodonta nipae* (Maulik)(Coleoptera: Chrysomelidae) parasitized by *Tetrastichus brontispae* Ferrière (Hymenoptera: Eulophidae). *PLoS One* 9:e91482. doi: 10.1371/journal.pone.0091482

Testi, A., Fanelli, G., Crosti, R., Castigliani, V., and D'Angeli, D. (2012). Characterizing river habitat quality using plant and animal bioindicators: a case study of Tirino River (Abruzzo Region, Central Italy). *Ecol. Indic.* 20, 24–33. doi: 10.1016/j.ecolind.2012.01.027

Tonk, M., Knorr, E., Cabezas-Cruz, A., Valdés, J. J., Kollewe, C., and Vilcinskas, A. (2015). *Tribolium castaneum* defensins are primarily active against Gram-positive bacteria. *J. Invertebr. Pathol.* 132, 208–215. doi: 10.1016/j.jip.2015.10.009

Torbeck, R., Pan, M., de Moll, E., and Levitt, J. (2014). Cantharidin: a comprehensive review of the clinical literature. *Dermatol. Online J.* 20:13030/qt45r512w0.

Tribolium Genome Sequencing Consortium (2008). The genome of the model beetle and pest *Tribolium castaneum*. *Nature* 452, 949–955. doi: 10.1038/nature06784

Urbański, A. (2013). [Behavior of necrophagus beetles, *Nicrophorus* species (Coleoptera: Silphidae)]. *Kosmos* 4, 525–534.

Urbański, A., Czarniewska, E., Baraniak, E., and Rosinski, G. (2014). Developmental changes in cellular and humoral responses of the burying beetle *Nicrophorus vespilloides* (Coleoptera, Silphidae). *J. Insect Physiol.* 60C, 98–103. doi: 10.1016/j.jinsphys.2013.11.009

Urbański, A., Czarniewska, E., Baraniak, E., and Rosiński, G. (2017). Impact of cold on the immune system of burying beetle, *Nicrophorus vespilloides* (Coleoptera: Silphidae). *Insect Sci.* 24, 443–454. doi: 10.1111/1744-7917.12321

Urbański, A., Lubawy, J., Marciniak, P., and Rosiński, G. (2018). Myotropic activity and immunolocalization of selected neuropeptides of the burying beetle *Nicrophorus vespilloides* (Coleoptera: Silphidae). *Insect Sci.* doi: 10.1111/1744-7917.12569 [Epub ahead of print].

Valente, E. M., Abou-Sleiman, P. M., Caputo, V., Muqit, M. M., Harvey, K., Gispert, S., et al. (2004). Hereditary early-onset Parkinson's disease caused by mutations in PINK1. *Science* 304, 1158–1160. doi: 10.1126/science.1096284

van Broekhoven, S., Oonincx, D. G., van Huis, A., and van Loon, J. J. (2015). Growth performance and feed conversion efficiency of three edible mealworm species (Coleoptera: Tenebrionidae) on diets composed of organic by-products. *J. Insect Physiol.* 73, 1–10. doi: 10.1016/j.jinsphys.2014.12.005

Van der Zee, M., Da Fonseca, R. N., and Roth, S. (2008). TGFβ signaling in *Tribolium*: vertebrate-like components in a beetle. *Dev. Genes Evol.* 218, 203–213. doi: 10.1007/s00427-007-0179-7

Vannini, A., Contarini, M., Faccoli, M., Valle, M. D., Rodriguez, C., Mazzetto, T., et al. (2017). First report of the ambrosia beetle *Xylosandrus compactus* and associated fungi in the Mediterranean maquis in Italy, and new host–pest associations. *EPPO Bull.* 47, 100–103. doi: 10.1111/epp.12358

Veenstra, J. A. (2009). Allatostatin C and its paralog allatostatin double C: the arthropod somatostatins. *Insect Biochem. Mol. Biol.* 39, 161–170. doi: 10.1016/j.ibmb.2008.10.014

Vega, F. E., Brown, S. M., Chen, H., Shen, E., Nair, M. B., Ceja-Navarro, J. A., et al. (2015). Draft genome of the most devastating insect pest of coffee worldwide: the coffee berry borer, *Hypothenemus hampei*. *Sci. Rep.* 5:12525. doi: 10.1038/srep12525

Ventrella, E., Marciniak, P., Adamski, Z., Rosiński, G., Chowański, S., Falabella, P., et al. (2015). Cardioactive properties of *Solanaceae* plant extracts and pure glycoalkaloids on *Zophobas atratus* Fab. *Insect Sci.* 22, 251–262. doi: 10.1111/1744-7917.12110

Verheggen, F. J., Vogel, H., and Vilcinskas, A. (2017). Behavioral and immunological features promoting the invasive performance of the harlequin ladybird *Harmonia axyridis*. *Front. Ecol. Evol.* 5:156. doi: 10.3389/fevo.2017.00156

Vilcinskas, A. (2013). *Yellow Biotechnology I: Insect Biotechnologie in Drug Discovery and Preclinical Research*. New York, NY: Springer. doi: 10.1007/978-3-642-39863-6

Vilcinskas, A., Mukherjee, K., and Vogel, H. (2013). Expansion of the antimicrobial peptide repertoire in the invasive ladybird *Harmonia axyridis*. *Proc. R. Soc. B. Biol. Sci.* 280:20122113. doi: 10.1098/rspb.2012.2113

Vogel, H., Badapanda, C., Knorr, E., and Vilcinskas, A. (2014). RNA-sequencing analysis reveals abundant developmental stage-specific and immunity-related genes in the pollen beetle *Meligethes aeneus*. *Insect Mol. Biol.* 23, 98–112. doi: 10.1111/imb.12067

Von Dassow, G., Meir, E., Munro, E. M., and Odell, G. M. (2000). The segment polarity network is a robust developmental module. *Nature* 406, 188–192. doi: 10.1038/35018085

Walkowiak-Nowicka, K., Nowicki, G., Kuczer, M., and Rosiński, G. (2018). New activity of yamamarin, an insect pentapeptide, on immune system of mealworm, *Tenebrio molitor*. *Bull. Entomol. Res.* 108, 351–359. doi: 10.1017/S0007485317000839

Wang, X., Fang, X., Yang, P., Jiang, X., Jiang, F., Zhao, D., et al. (2014). The locust genome provides insight into swarm formation and long-distance flight. *Nat. Commun.* 5:2957. doi: 10.1038/ncomms3957

Wardhaugh, K., Holter, P., and Longstaff, B. (2001). The development and survival of three species of coprophagous insect after feeding on the faeces of sheep treated with controlled-release formulations of ivermectin or albendazole. *Aust. Vet. J.* 79, 125–132. doi: 10.1111/j.1751-0813.2001.tb10721.x

Weissenberg, M., Levy, A., Svoboda, J. A., and Ishaaya, I. (1998). The effect of some *Solanum* steroidal alkaloids and glycoalkaloids on larvae of the red flour beetle, *Tribolium castaneum*, and the tobacco hornworm, *Manduca sexta*. *Phytochemistry.* 47, 203–209. doi: 10.1016/S0031-9422(97)00565-7

Wessells, R. J., and Bodmer, R. (2007). Cardiac aging. *Semin. Cell Dev. Biol.* 18, 111–116. doi: 10.1016/j.semcdb.2006.12.011

Wessells, R. J., Fitzgerald, E., Cypser, J. R., Tatar, M., and Bodmer, R. (2004). Insulin regulation of heart function in aging fruit flies. *Nat. Genet.* 36, 1275–1282. doi: 10.1038/ng1476

Wilson-Sanders, S. E. (2011). Invertebrate models for biomedical research, testing, and education. *ILAR J.* 52, 126–152. doi: 10.1093/ilar.52.2.126

Wojda, I., Kowalski, P., and Jakubowicz, T. (2009). Humoral immune response of *Galleria mellonella* larvae after infection by *Beauveria bassiana* under optimal and heat-shock conditions. *J. Insect Physiol.* 55, 525–531. doi: 10.1016/j.jinsphys.2009.01.014

Woodroof, H. I., Pogson, J. H., Begley, M., Cantley, L. C., Deak, M., Campbell, D. G., et al. (2011). Discovery of catalytically active orthologues of the Parkinson's disease kinase PINK1: analysis of substrate specificity and impact of mutations. *Open Biol.* 1:110012. doi: 10.1098/rsob.110012

Wyder, S., Kriventseva, E. V., Schroder, R., Kadowaki, T., and Zdobnov, E. M. (2007). Quantification of ortholog losses in insects and vertebrates. *Genome Biol.* 8:R242. doi: 10.1186/gb-2007-8-11-r242

Xu, X., Liu, W., Li, W., and Liu, S. (2016). Anticoagulant activity of crude extract of *Holotrichia diomphalia* larvae. *J. Ethnopharmacol.* 177, 28–34. doi: 10.1016/j.jep.2015.11.015

Yan, Y.-M., Li, L.-J., Qin, X.-C., Lu, Q., Tu, Z.-C., and Cheng, Y.-X. (2015). Compounds from the insect *Blaps japanensis* with COX-1 and COX-2 inhibitory activities. *Bioorg. Med. Chem. Lett.* 25, 2469–2472. doi: 10.1016/j.bmcl.2015.04.085

Yang, P., Abe, S., Sato, Y., Yamashita, T., Matsuda, F., Hamayasu, T., et al. (2007). A palmitonyl conjugate of an insect pentapeptide causes growth arrest in mammalian cells and mimics the action of diapause hormone. *J. Insect Biotechnol. Sericology* 76, 63–69.

Yin, F., Zhu, J., Hao, J., Cui, J., and Yang, J. (2013). Synthesis, characterization, crystal structure and antitumor activities of a novel demethylcantharidato bridged copper (II) phenanthroline complex. *Sci. China Chem.* 56, 481–489. doi: 10.1007/s11426-013-4865-1

Yokoi, K., Koyama, H., Minakuchi, C., Tanaka, T., and Miura, K. (2012). Antimicrobial peptide gene induction, involvement of Toll and IMD pathways and defense against bacteria in the red flour beetle, *Tribolium castaneum*. *Results Immunol.* 2, 72–82. doi: 10.1016/j.rinim.2012.03.002

Yu, M., and Zhao, Y. (2016). Cantharis by photosynthetic bacteria biotransformation: reduced toxicity and improved antitumor efficacy. *J. Ethnopharmacol.* 186, 151–158. doi: 10.1016/j.jep.2016.03.058

Yu, N., Nachman, R. J., and Smagghe, G. (2013). Characterization of sulfakinin and sulfakinin receptor and their roles in food intake in the red flour beetle *Tribolium castaneum*. *Gen. Comp. Endocrinol.* 188, 196–203. doi: 10.1016/j.ygcen.2013.03.006

Yu, N., Zotti, M. J., Scheys, F., Braz, A. S., Penna, P. H., Nachman, R. J., et al. (2015). Flexibility and extracellular opening determine the interaction between ligands and insect sulfakinin receptors. *Sci. Rep.* 5:12627. doi: 10.1038/srep12627

Zhang, Y., Jiang, R., Wu, H., Liu, P., Xie, J., He, Y., et al. (2012). Next-generation sequencing-based transcriptome analysis of *Cryptolaemus montrouzieri* under insecticide stress reveals resistance-relevant genes in ladybirds. *Genomics* 100, 35–41. doi: 10.1016/j.ygeno.2012.05.002

Zhu, S., Han, Z., Luo, Y., Chen, Y., Zeng, Q., Wu, X., et al. (2017). Molecular mechanisms of heart failure: insights from *Drosophila*. *Heart Fail. Rev.* 22, 91–98. doi: 10.1007/s10741-016-9590-3

Zödl, B., and Wittmann, K. J. (2003). Effects of sampling, preparation and defecation on metal concentrations in selected invertebrates at urban sites. *Chemosphere* 52, 1095–1103. doi: 10.1016/S0045-6535(03)00442-9

Conflict of Interest Statement: The authors declare that the research was conducted in the absence of any commercial or financial relationships that could be construed as a potential conflict of interest.

frontiers in Physiology

ORIGINAL RESEARCH
published: 03 April 2019
doi: 10.3389/fphys.2019.00302

Transcriptome Profiling of the Whitefly *Bemisia tabaci* MED in Response to Single Infection of *Tomato yellow leaf curl virus*, *Tomato chlorosis virus*, and Their Co-infection

Tian-Bo Ding[1], *Jie Li*[1], *Er-Hu Chen*[2], *Jin-Zhi Niu*[2] *and Dong Chu*[1]*

[1] *Key Laboratory of Integrated Crop Pest Management of Shandong Province, College of Plant Health and Medicine, Qingdao Agricultural University, Qingdao, China,* [2] *Key Laboratory of Entomology and Pest Control Engineering, College of Plant Protection, Southwest University, Chongqing, China*

OPEN ACCESS

Edited by:
Patrizia Falabella, University of Basilicata, Italy

Reviewed by:
Jing Zhao, Weifang University of Science and Technology, China
Murad Ghanim, Agricultural Research Organization (ARO), Israel

***Correspondence:**
Dong Chu
chinachudong@sina.com

Specialty section:
This article was submitted to Invertebrate Physiology, a section of the journal Frontiers in Physiology

Received: *19 October 2018*
Accepted: *07 March 2019*
Published: *03 April 2019*

Citation:
Ding T-B, Li J, Chen E-H, Niu J-Z and Chu D (2019) Transcriptome Profiling of the Whitefly Bemisia tabaci MED in Response to Single Infection of Tomato yellow leaf curl virus, Tomato chlorosis virus, and Their Co-infection. Front. Physiol. 10:302. doi: 10.3389/fphys.2019.00302

Tomato yellow leaf curl virus (TYLCV) and *Tomato chlorosis virus* (ToCV) are two of the most devastating cultivated tomato viruses, causing significant crop losses worldwide. As the vector of both TYLCV and ToCV, the whitefly *Bemisia tabaci* Mediterranean (MED) is mainly responsible for the rapid spread and mixed infection of TYLCV and ToCV in China. However, little is known concerning *B. tabaci* MED's molecular response to TYLCV and ToCV infection or their co-infection. We determined the transcriptional responses of the whitefly MED to TYLCV infection, ToCV infection, and TYLCV&ToCV co-infection using Illumina sequencing. In all, 78, 221, and 60 differentially expressed genes (DEGs) were identified in TYLCV-infected, ToCV-infected, and TYLCV&ToCV co-infected whiteflies, respectively, compared with non-viruliferous whiteflies. Differentially regulated genes were sorted according to their roles in detoxification, stress response, immune response, transport, primary metabolism, cell function, and total fitness in whiteflies after feeding on virus-infected tomato plants. Alterations in the transcription profiles of genes involved in transport and energy metabolism occurred between TYLCV&ToCV co-infection and single infection with TYLCV or ToCV; this may be associated with the adaptation of the insect vector upon co-infection of the two viruses. Gene Ontology (GO) and Kyoto Encyclopedia of Genes and Genomes (KEGG) pathway enrichment analyses demonstrated that the single infection with TYLCV or ToCV and the TYLCV&ToCV co-infection could perturb metabolic processes and metabolic pathways. Taken together, our results provide basis for further exploration of the molecular mechanisms of the response to TYLCV, ToCV single infection, and TYLCV&ToCV co-infection in *B. tabaci* MED, which will add to our knowledge of the interactions between plant viruses and insect vectors.

Keywords: ***Bemisia tabaci*, *Tomato yellow leaf curl virus*, *Tomato chlorosis virus*, co-infection, transcriptome**

INTRODUCTION

More than 75% of plant viruses are transmitted by insect vectors, most of which belong to hemipteran (suborder Homoptera) families, such as whiteflies, aphids, and planthoppers (Hogenhout et al., 2008). *Bemisia tabaci* (Gennadius) (Hemiptera: Aleyrodidae), commonly known as the sweetpotato whitefly, has caused tremendous damage to the tomato crops in greenhouses and fields worldwide (Valverde et al., 2004). *B. tabaci* is a cryptic species complex consisting of at least 39 cryptic species (Alemandri et al., 2015), among which the Middle East-Asia Minor (MEAM1) (formerly referred to as biotype B) and the Mediterranean (MED) (formerly referred to as biotype Q) species have become the most destructive alien species in many regions of the world (De Barro et al., 2011). The whitefly MED was first detected in China in 2003 (Chu et al., 2006), and has gradually displaced MEAM1 and become the dominant cryptic species of *B. tabaci* in China (Pan et al., 2011; Rao et al., 2011). The whitefly is an effective vector of numerous plant viruses, the majority of which are Begomoviruses. Several viruses belonging to other genera, including *Crinivirus*, *Ipomovirus*, *Torradovirus*, and *Carlavirus*, can also be transmitted by whiteflies (Navas-Castillo et al., 2011; Polston et al., 2014).

Tomato yellow leaf curl virus (TYLCV) (Geminiviridae), the type member of the genus *Begomovirus*, is one of the most devastating viruses of cultivated tomato worldwide; the virus is transmitted by *B. tabaci* in a persistent circulative manner (Czosnek, 2007; Hogenhout et al., 2008). In China, TYLCV was first detected in 2006 in Shanghai (Wu et al., 2006), and has rapidly spread to many provinces, including Zhejiang, Jiangsu, Shandong, Hebei, and Beijing (Ji et al., 2008; Mugiira et al., 2008; Sun et al., 2009; Zhang et al., 2010; Zhou et al., 2010; Pan et al., 2012). A previous study has confirmed that *B. tabaci* MEAM1 and MED contributed to the TYLCV epidemic across China, and that the introduction of MED accelerated the prevalence of TYLCV (Pan et al., 2012). Recently, another devastating tomato virus, *Tomato chlorosis virus* (Closteroviridae: *Crinivirus*), has reached an outbreak level in several areas of the Chinese mainland, including Beijing, Tianjin, Shandong, Henan, Jiangsu, Neimenggu, and Guangdong (Zhao et al., 2013; Liu et al., 2014; Gao et al., 2015; Hu et al., 2015; Wu et al., 2016; Zheng et al., 2016; Tang et al., 2017; Wei et al., 2018), resulting in significant crop losses. ToCV is uniquely transmitted in a semi-persistent mode by two distinct whitefly genera, *Bemisia* and *Trialeurodes*, viz. *B. tabaci*, *T. abutilonea*, and *T. vaporariorum* (Wisler et al., 1998; Wintermantel and Wisler, 2006). Furthermore, previous research suggests that the rapid spread of ToCV in China was associated with the transmission by MED (Dai et al., 2016; Shi et al., 2018). Notably, the co-infection of TYLCV and ToCV have been detected in several regions of China, including Shandong and Jiangsu Provinces (Zhao et al., 2014; Wu et al., 2016). Following the confirmation of the transmission of TYLCV and ToCV by *B. tabaci* MED in China, we speculated that the TYLCV&ToCV co-infection in the field was probably due to the spread of *B. tabaci* MED.

Interactions between plant viruses and insect vectors are important for both the dispersal of the plant viruses and the population dynamics of the insect (Stout et al., 2006). Plant viruses can have direct or indirect impacts on insect vectors. For example, two Begomoviruses [*Tabacco curly shoot virus* (TbCSV) and *Tomato yellow leaf curl China virus* (TYLCCNV)] infecting tobacco plants significantly increased the fecundity and longevity of their insect vector *B. tabaci* MEAM1 (Jiu et al., 2007). In addition, TYLCV infection also benefitted its vector *B. tabaci* MED by improving the growth, survival, and reproduction (Su et al., 2015). However, ToCV infection decreased the performance of *B. tabaci* MED on tomato plants as measured by declines in longevity and fecundity (Li et al., 2018).

Next-generation sequencing has been shown to be an efficient means of examining the interaction mechanisms between plant viruses and insects. Many transcriptome studies have been performed to analyze the responses to diverse viral infections in whiteflies. When *B. tabaci* MEAM1 was infected with TYLCCNV, the immune responses were activated, and detoxification activity and energy costs were simultaneously attenuated (Luan et al., 2011, 2013). Early studies also revealed that a number of genes involved in transport, binding, metabolism, signal transduction, receptors and lysosomes were differentially regulated when *B. tabaci* MEAM1 fed on TYLCV- and ToCV-infected tomato plants (Kaur et al., 2017; Hasegawa et al., 2018). However, previous viral transcriptome studies were mainly performed on *B. tabaci* MEAM1, and the focus was limited to the response to a single virus infection. Little is known concerning how *B. tabaci* MED responds to single TYLCV and ToCV infection. Moreover, the molecular response of *B. tabaci* to the co-infection with TYCLV and ToCV remains unknown.

In this study, we compared the transcriptional responses in *B. tabaci* MED after feeding on TYLCV- and ToCV-infected, TYLCV&ToCV co-infected and uninfected tomato plants during a 24-h acquisition access period (AAP), respectively. A number of genes involved in defense response, transport, primary metabolism, cell function, and fitness responded to viral infection. We also used the Gene Ontology (GO) and Kyoto Encyclopedia of Genes and Genomes (KEGG) databases to further annotate the functions of the differentially expressed genes (DEGs). Additionally, we compared the similarities and differences between MED whiteflies infected by a single virus (TYLCV or ToCV) and whiteflies co-infected by TYLCV&ToCV. The results provide a comprehensive view of the molecular response to diverse forms of viral infection in the MED whitefly and yield new insights into the interactions between insect vectors and multiple viruses. To our knowledge, this is the first study to analyze the transcriptional changes in response to viral co-infection in whitefly vectors.

MATERIALS AND METHODS

Insect Culture and Virus Source

A colony of *B. tabaci* MED originating in 2012 from Ji'nan, Shandong, China has been maintained on cotton plants (*Gossypium hirsutum* L. cv. Lu-Mian 21), a non-host for TYLCV and ToCV for 6 years. The TYLCV-infected,

ToCV-infected, and TYLCV&ToCV co-infected tomato plants (*Solanum lycopersicum* M) were collected from Qingdao, Shandong, China in 2014, and the viruses were maintained using tomato plants (*S. lycopersicum* M. cv. Zhongza 9) via whitefly transmission as described previously (Li et al., 2018). Both the whiteflies and the plants were cultured in separate climate chambers at 27°C, 60% RH, and a 16:8 (L: D) of photoperiod. The *B. tabaci* MED population was confirmed using the *Vsp* I-based mtCOI-RFLP method (Chu et al., 2012).

Virus Acquisition and Sample Collection

To obtain the viruliferous and non-viruliferous whiteflies, 2,400 female adults were collected and transferred onto TYLCV-infected, ToCV-infected, TYLCV&ToCV co-infected, and uninfected tomato plants for 24 h. Approximately 200 live whiteflies were collected from virus-infected or uninfected tomato plants following a 24-h AAP for each of the two biological replications. The whiteflies were frozen in liquid nitrogen and stored at −80°C. To confirm virus acquisition and determine the efficiency of acquisition for each virus, DNA was extracted from 15 individuals fed on TYLCV-infected and TYLCV&ToCV co-infected tomato plants using a TIANamp Micro DNA Kit (TIANGEN, China). Total RNA was extracted from 15 individuals fed on ToCV-infected and TYLCV&ToCV co-infected tomato plants using TRIzol Reagent (Thermo Fisher, USA). The first-strand cDNA was synthesized following the procedures for the PrimerScript RT Reagent Kit (Perfect real-time) (TaKaRa, Japan). PCR analyses for the detection of TYLCV and ToCV were conducted using Golden Star T6 Super PCR Mix (TsingKe, China) with the primers TYLCV-F/R (Li et al., 2012) and ToCV-F/R (Dovas et al., 2002), respectively (**Supplementary Table S1**). The individuals fed on the uninfected tomato plants served as the negative control.

cDNA Library Preparation and Sequencing

Total RNA was extracted separately from viruliferous and non-viruliferous whiteflies using TRIzol Reagent (Thermo Fisher, USA) according to the manufacturer's protocol. RNA quality and concentration were verified using 1% agarose gels, a NanoPhotometer® spectrophotometer (IMPLEN, USA), and the Qubit RNA Assay Kit in a Qubit® 2.0 Fluorometer (Life Technologies, USA). The integrity of total RNA was determined using the RNA Nano 6000 Assay Kit of the Bioanalyzer 2100 system (Agilent Technologies, USA).

The cDNA libraries were generated from 1.5 μg RNA of each sample using NEBNext® Ultra™ RNA Library Prep Kit for Illumina (NEB, USA) following the manufacturer's instructions, and the index codes were added to attribute sequences to each sample. The quality of the libraries was evaluated using the Agilent Bioanalyzer 2100 system. The cDNA libraries were sequenced for 125/150 bp paired-end reads on an Illumina HiSeq Xten platform (Novogene Bioinformatics Technology Co. Ltd, China).

Transcriptome Assembly and Differential Expression Analysis

In order to obtain clean data, the raw reads were cleaned by removing any reads containing adapter, reads containing poly-N, and low quality reads. The genomes of *B. tabaci* MED (Xie et al., 2017) and MEAM1 (Chen et al., 2016) were used for alignment of the clean reads. Indices of the reference genomes were built using Bowtie v2.2.3 (Langmead and Salzberg, 2012), and the high-quality paired-ended clean reads were aligned to the reference genome using HISAT 2.0.4 (Kim et al., 2015). The reads numbers mapped to each gene were counted using HTSeq v0.6.1. The FPKM (expected number of Fragments Per Kilobase of transcript sequence per Million base pairs sequenced) of each gene was calculated based on the length of the gene and the reads count mapped to that gene. Differential expression analysis of viruliferous and non-viruliferous whiteflies was performed using the DESeq2 R package (1.0) (Love et al., 2014). The resulting *P*-values were adjusted using Benjamini and Hochberg's approach for controlling the false discovery rate (FDR) (Benjamini and Hochberg, 1995). Genes with an adjusted *P*-value (*q*-value) < 0.05 found by DESeq were assigned as differentially expressed. The identification of genes related to viruses infection was conducted based on the gene annotation and differential expression analysis.

GO and KEGG Pathway Analysis

GO enrichment analysis of the differential expression of genes across the samples was carried out using the GOseq R package (Young et al., 2010). Additionally, the statistical enrichment of the differential expression genes in KEGG pathways was implemented by the KOBAS software.

RT-qPCR Validation

To validate the DEG analysis results, the expression profiles of 11 genes were measured by RT-qPCR with SDHA as the internal control gene (Li et al., 2013). Primers for RT-qPCR were designed using the Primer 3.0 software (http://bioinfo.ut.ee/primer3-0.4.0/) and are listed in **Supplementary Table S1**. All of the whitefly samples for the RT-qPCR validation were prepared according to the method described above. Each treatment contained three biological replications. The same total RNA extraction and cDNA synthase methods were used as described above for the detection of ToCV in whiteflies. RT-qPCR assays were performed in 20 μL using the SYBR Premix Ex Taq™ II (Perfect Real Time) (TaKaRa, Dalian, China) according to the manufacturer's instructions. The reactions were conducted using a qTower 2.2 real-time PCR Thermal Cycler (Analytikjena, Germany) under the following conditions: 95°C for 2 min; 40 cycles of 95°C for 15 s and 60°C for 30 s; melting curve generation (60°C to 95°C). The relative expression ratios were calculated using the $2^{-\Delta\Delta CT}$ method (Livak and Schmittgen, 2001).

RESULTS

Virus Infection Status of Whiteflies Selected for RNA-Seq

In order to make sure the basis of comparison between virus-infected and non-viruliferous colonies of *B. tabaci* MED, the

TABLE 1 | Summary statistics of RNA-Seq libraries from *Bemisia tabaci* MED fed for 24 h on virus-infected or uninfected tomato plants.

Sample[a]	Raw reads number	Clean reads number	Clean reads rate (%)	Mapped to genome	
				Mapped number	Mapping rate (%)
TYLCV-1	32,076,630	31,266,388	97.47	25,731,071	82.30
TYLCV-2	34,205,824	33,444,404	97.77	27,497,666	82.22
ToCV-1	32,752,142	31,958,512	97.58	26,320,948	82.36
ToCV-2	31,876,568	31,182,608	97.82	25,499,858	81.78
TYLCV&ToCV-1	43,101,948	41,978,676	97.39	34,195,336	81.46
TYLCV&ToCV-2	32,569,312	31,723,612	97.4	25,648,753	80.85
NV-1	30,475,776	29,813,838	97.83	24,387,996	81.80
NV-2	34,931,068	34,065,894	97.52	27,934,857	82.00

[a] *TYLCV: TYLCV-infected whiteflies; ToCV: ToCV-infected whiteflies; TYLCV&ToCV: TYLCV&ToCV co-infected whiteflies; NV: uninfected (non-viruliferous) whiteflies*

infection rates were estimated for the whiteflies feeding on virus-infected tomato plants for 24 h. Both the infection rates of TYLCV and ToCV reached 100% in the whiteflies after a 24-h AAP feeding on TYLCV and ToCV singly infected tomato plants (**Supplementary Figure S1**). However, the lower infection rates of TYLCV (93.33%) and ToCV (80%) were observed in the whiteflies feeding on TYLCV&ToCV co-infection plants (**Supplementary Figure S1**).

Overview of Illumina Sequencing and Transcriptome Assembly

To determine the transcriptome profiles of *B. tabaci* MED in response to TYLCV infection, ToCV infection, and TYLCV&ToCV co-infection, we performed RNA-seq analysis of female adults that had fed on the respective tomato plants for 24 h Eight cDNA libraries of viruliferous and non-viruliferous whiteflies were sequenced, generating 30,475,776 and 43,101,948 raw reads, respectively (**Table 1**). After cleaning and quality checks, 29,813,838 to 41,978,676 clean reads were obtained and mapped to the whitefly (*B. tabaci* MED) reference genome, for the mapping rates of 80.85 to 82.36% (**Table 1**). Additionally, Pearson's correlation analysis indicated that the two replicated libraries of each treatment were highly correlated (Pearson's $r = 0.958–0.968$) (**Supplementary Figure S2**).

Global Patterns of Gene Expression in Response to Different Patterns of Viral Infection

A total of 359 genes were differentially expressed in whiteflies feeding on TYLCV-infected, ToCV-infected, and TYLCV&ToCV co-infected tomato plants compared to whiteflies that fed on uninfected tomato plants (**Figure 1A**). In TYLCV and ToCV infected whiteflies, 78 (43 upregulated, 35 downregulated) and 221 (88 upregulated, 133 downregulated) DEGs were detected, while only 60 (38 upregulated, 22 downregulated) genes were differentially expressed due to TYLCV&ToCV co-infection (**Figure 1A**).

Although most of the DEGs in response to different patterns of viral infection were diverse, there were seven common genes differentially expressed in whiteflies feeding on TYLCV-infected, ToCV-infected, and TYLCV&ToCV co-infected tomato plants (**Figure 1B**). Totals of 42.31% and 14.93% of the virus-responsive genes were shared between TYLCV- and ToCV-infected whiteflies. Compared to non-viruliferous whiteflies, only ten DEGs were in common between TYLCV-infected and TYLCV&ToCV co-infected whiteflies. However, greater proportions of common genes altered by ToCV (7.69%) and TYLCV&ToCV (28.33%) were identified (**Figure 1B**).

Differentially Regulated Genes Associated With Detoxification

Compared to non-viruliferous whiteflies, three differentially regulated cytochrome P450 (P450) genes involved in detoxification were identified in TYLCV-infected whiteflies. One P450 gene was significantly upregulated, while the other two P450 genes were significantly downregulated (**Table 2**). We found a total of 12 DEGs encoding detoxification enzymes in ToCV-infected whiteflies, including five P450s (one upregulated, four downregulated), a downregulated carboxylesterase (CarE), four downregulated UDP-glucuronosyltransferases (UGTs), and two upregulated ATP-binding cassette transporters (ABCs) (**Table 2**). Only one P450 gene, *BTA015105.1*, was identified and downregulated in response to TYLCV&ToCV co-infection (**Table 2**); the same gene was also detected in TYLCV and ToCV singly infected whiteflies with the same expression pattern.

Differentially Regulated Genes Associated With Stress and Immune Response

A majority of stress response related genes were upregulated in TYLCV-infected whiteflies; these included two alpha-crystallin B chain-like genes, a heat shock protein 70 (HSP70), and a heat shock protein 90 (HSP90) (**Table 3**). While the gene *BTA014707.1*, which encodes superoxide dismutase (SOD), was significantly downregulated (**Table 3**). In accordance with TYLCV-infected whiteflies, four of five stress responsive genes were upregulated in whiteflies feeding on ToCV-infected tomato plants, including an HSP70, a Gulia lazarillo, a peroxidase, and a glutathione peroxidase (**Table 3**). The co-infection with TYLCV and ToCV could also significantly depress the transcription level of the SOD gene *BTA014707.1* (**Table 3**).

Five DEGs related to the immune response were identified in TYLCV-infected whiteflies, including one upregulated

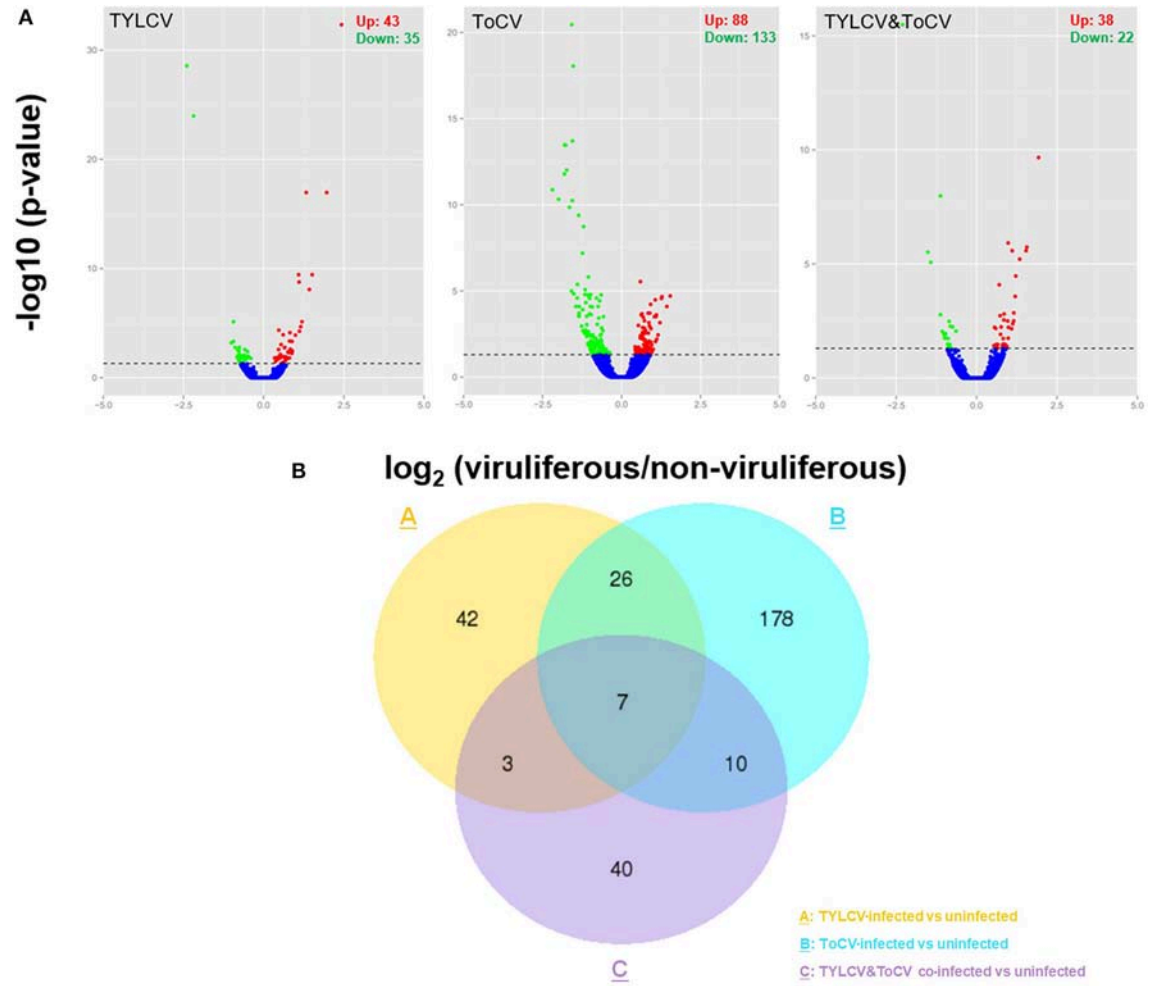

FIGURE 1 | Differentially expressed genes (DEGs) in *Bemisia tabaci* MED in response to TYLCV infection, ToCV infection, and TYLCV&ToCV co-infection. **(A)** Volcano plots of differentially expressed genes in whiteflies infected with TYLCV, ToCV, and TYLCV&ToCV compared to non-viruliferous whiteflies. Dots above the horizontal dotted line indicate the DEGs with an adjusted *P*-value < 0.05. Red dots denote significantly upregulated genes, while green dots denote significantly downregulated genes. **(B)** Venn diagram depicting unique and common DEGs in whiteflies in response to TYLCV infection, ToCV infection, and TYLCV&ToCV co-infection.

sequestosome-1, one downregulated scavenger receptor, and three differentially expressed genes encoding the cathepsins (one upregulated and two downregulated) (**Table 3**). Additionally, nine immune related genes were differentially expressed in whiteflies when infected with ToCV (**Table 3**). The genes encoding prophenoloxidase subunit 2, serpin, and ferritin were upregulated, while one hemocyanin subunit gene was downregulated (**Table 3**). Five genes associated with the lysosome, including two cathepsin B genes and three cathepsin F genes, were all downregulated (**Table 3**). Only two cathepsin B genes associated with the lysosome were classified as being associated with the immune response in TYLCV&ToCV co-infected whiteflies, and both were upregulated (**Table 3**).

Differentially Regulated Genes Associated With Transport

Four genes associated with transport were all downregulated in TYLCV-infected whiteflies compared with non-viruliferous whiteflies (**Table 4**). A total of 18 DEGs implicated in transport were identified in ToCV-infected whiteflies, and the expression levels of 14 genes were decreased (**Table 4**). Among these downregulated genes, five genes (*BTA02849.1*, *BTA029270.2*, *BTA019411.1*, *BTA024233.1*, and *BTA016669.3*) were identified as glucose transporters (**Table 4**). However, among the DEGs in TYLCV&ToCV co-infected whiteflies, four genes related to transport were all upregulated (**Table 4**).

Differentially Regulated Genes Associated With Energy Metabolism, Lipid Metabolism, and Protein Synthesis and Amino Acid Metabolism

After feeding on TYLCV-infected tomato plants, only one gene that was considered to be involved in energy metabolism, annotated as ATP synthase gamma chain,

TABLE 2 | Differentially regulated genes associated with detoxification.

Virus infection	Gene ID	Annotation	V[a]	NV[b]	FC[c]	q-value	Direction	Gene ID-B[d]
TYLCV	BTA009037.1	Cytochrome P450	770.83	458.24	0.65	0.0018	Up	Bta07286
	BTA025848.1	Cytochrome P450	1563.21	2287.27	−0.50	0.0042	Down	Bta07221
	BTA015105.1	Cytochrome P450	1861.63	2688.60	−0.48	0.0104	Down	Bta08018
ToCV	BTA009039.1	Cytochrome P450	337.76	163.53	0.82	0.0254	Up	Bta07284
	BTA015105.1	Cytochrome P450	805.62	2640.14	−1.58	3.44E−21	Down	Bta08018
	BTA025209.1	Cytochrome P450	115.10	290.08	−0.95	0.0147	Down	Bta02801
	BTA025872.1	Cytochrome P450	2350.89	3801.35	−0.63	0.0085	Down	Bta05554
	BTA025848.1	Cytochrome P450	1450.12	2246.02	−0.60	0.0020	Down	Bta07221
	BTA010352.1	Carboxylesterase	641.86	1020.42	−0.61	0.0147	Down	Bta08899
	BTA016010.1	UDP-glucuronosyltransferase	38.88	125.80	−1.03	0.0146	Down	Bta06665
	BTA011174.1	UDP-glucuronosyltransferase	13.30	123.24	−0.94	0.0263	Down	Bta02603
	BTA018877.1	UDP-glucuronosyltransferase	226.41	407.25	−0.73	0.0106	Down	Bta02228
	BTA013275.1	UDP-glucuronosyltransferase	594.47	919.64	−0.58	0.0201	Down	Bta01304
	BTA029281.1	ATP-binding cassette sub-family G member 1	129.47	36.42	0.97	0.0327	Up	Bta07822
	BTA007131.3	ATP-binding cassette sub-family G member 4	1381.80	836.57	0.67	0.0014	Up	Bta09316
TYLCV&ToCV	BTA015105.1	Cytochrome P450	1744.82	2849.69	−0.64	0.0087	Down	Bta08018

[a] *Read count values from virus-infected whiteflies.*
[b] *Read count values from non-viruliferous whiteflies.*
[c] *Fold change (log2 ratio) of gene expression.*
[d] *Mapped genes in Bemisia tabaci MEAM1 genome.*

was significantly downregulated in whiteflies (**Table 5**). Six genes involved in carbohydrate metabolism and three genes involved in ATP metabolism were differentially expressed in ToCV-infected whiteflies (**Table 5**). Moreover, four genes (*BTA020543.1*, *BTA021845.1*, *BTA020828.1*, and *BTA001223.1*) associated with carbohydrate metabolism and two genes (*BTA029804.1* and *BTA020850.1*) associated with ATP metabolism appeared among the DEGs in TYLCV&ToCV co-infected whiteflies (**Table 5**).

We also identified and analyzed four genes associated with lipid metabolism in TYLCV-infected whiteflies, all of which were downregulated except lipase (**Table 5**). A majority of the lipid metabolism genes were downregulated in ToCV-infected whiteflies; the transcription levels of only two genes encoding glycerol-3-phosphate acyltransferase and acetyl-CoA carboxylase increased (**Table 5**). Similar with TYLCV-infection and ToCV-infection, two lipid metabolism related genes (fatty acid oxidation complex subunit alpha and lipid phosphate phosphohydrolase 1) were significantly downregulated in TYLCV&ToCV co-infected whiteflies (**Table 5**).

For protein synthesis and amino acid metabolism, five genes were upregulated and three genes were downregulated in TYLCV-infected whiteflies, while 14 genes (four upregulated and ten downregulated) were responsive to ToCV infection in *B. tabaci* MED (**Table 5**). A total of seven genes associated with protein synthesis and amino acid metabolism were identified in TYLCV&ToCV co-infected whiteflies (**Table 5**). The two genes encoding tryptophan-tRNA ligase and alanine aminotransferase, which were found in the two single virus-infected whiteflies, were also detected in TYLCV&ToCV co-infected whiteflies (**Table 5**), suggesting common functions in response to viral infection.

Differentially Regulated Genes Associated With Cell Function and Other Functions

Only one gene involved in cell function, which is encoding Alpha-tubulin N-acetyltransferase, was upregulated in response to TYLCV infection (**Table 6**). Compared to TYLCV infection, more differentially regulated genes (three upregulated, six downregulated) associated with cell function were identified in ToCV-infected whiteflies (**Table 6**). In addition, two genes involved in cell functions (one upregulated, one downregulated) were altered in TYLCV&ToCV co-infected whiteflies (**Table 4**), while the gene *BTA030040.1* encoding condensing-2 complex subunit D3 was also differentially expressed in ToCV-infected whiteflies.

In response to TYLCV infection, ToCV infection and TYLCV&ToCV co-infection, the vitellogenin genes were all upregulated in whiteflies (**Table 6**). We also detected that two genes encoding juvenile hormone-inducible proteins (**Table 6**), exhibited the downregulated transcription profiles with ToCV infection. The follicle cell protein, which is also associated with reproduction, was identified in TYLCV&ToCV co-infected whiteflies (**Table 6**). Moreover, our analysis showed both single infection with TYLCV or ToCV and TYLCV & ToCV co-infection could reduce the transcription level of methyltransferase (**Table 6**).

Differentially Regulated Genes Associated With Unknown Protein

Among the TYLCV- and ToCV-responsive DEGs, seven and ten genes' functions were still unknown, while the comment gene *BTA023229.1* showed opposite regulation between these two viruses infection (**Supplementary Table S2**).

TABLE 3 | Differentially regulated genes associated with stress and immune response.

Virus infection	Gene ID	Annotation	V[a]	NV[b]	FC[c]	*q*-value	Direction	Gene ID-B[d]
STRESS RESPONSE								
TYLCV	BTA029550.1	Alpha-crystallin B chain-like	141.75	44.63	0.88	0.0060	Up	Bta03915
	BTA005970.1	Alpha-crystallin B chain-like	1749.54	883.32	0.82	7.61E−05	Up	Bta14756
	BTA025691.1	Heat shock 70 kDa protein	1494.46	877.45	0.66	0.0017	Up	Bta15531
	BTA010369.1	Heat shock protein 90	50110.85	35537.34	0.47	4.61E−05	Up	Bta01899
	BTA014707.1	Superoxide dismutase [Cu-Zn]	30.26	466.43	−2.40	2.70E−29	Down	Bta10955
ToCV	BTA025691.1	Heat shock 70 kDa protein	1549.02	861.63	0.73	0.0137	Up	Bta15531
	BTA019619.1	Glial Lazarillo	411.82	221.36	0.74	0.0257	Up	Bta06480
	BTA015175.2	Peroxidase	4338.36	2626.00	0.66	0.0026	Up	Bta02200
	BTA020045.1	Glutathione peroxidase	1817.27	1259.68	0.49	0.0441	Up	Bta00070
	BTA018068.2	Gamma-interferon-inducible lysosomal thiol reductase putative	1270.66	2035.76	−0.63	0.0014	Down	Bta01175
TYLCV&ToCV	BTA014707.1	Superoxide dismutase [Cu-Zn]	32.82	494.34	−2.30	3.19E−16	Down	Bta10955
IMMUNE RESPONSE								
TYLCV	BTA027235.2	Sequestosome-1	5622.29	3545.15	0.61	0.0001	Up	Bta11513
	BTA007837.2	Scavenger receptor class B member, putative	98.53	242.91	−0.89	0.0017	Down	Bta10257
	BTA015120.1	Cathepsin B	166.31	60.50	0.81	0.0160	Up	Bta08035
	BTA028172.1	Cathepsin F	71.19	165.91	−0.76	0.0251	Down	Bta20004
	BTA016813.2	Cathepsin B	2848.14	4454.23	−0.56	0.0135	Down	Bta03880
ToCV	BTA026427.4	Prophenoloxidase subunit 2	874.27	504.16	0.73	0.0005	Up	Bta15615
	BTA008155.2	Serpin	1544.38	1039.13	0.52	0.0476	Up	Bta12484
	BTA021911.1	Ferritin	1557.21	1063.45	0.51	0.0262	Up	Bta07622
	BTA028748.2	Hemocyanin subunit, putative	45284.19	72407.11	−0.65	1.68E−05	Down	Bta12158
	BTA000144.1	Cathepsin B	991.74	3347.14	−1.55	2.03E−14	Down	Bta08697
	BTA016813.2	Cathepsin B	1487.95	4374.04	−1.36	4.10E−10	Down	Bta03880
	BTA028172.1	Cathepsin F	36.32	162.92	−1.34	0.0002	Down	Bta20004
	BTA001253.1	Cathepsin F-like protease	513.12	975.17	−0.78	0.0125	Down	Bta02143
	BTA024606.1	Cathepsin F	8789.26	13205.92	−0.54	0.0429	Down	Bta11871
TYLCV&ToCV	BTA015120.1	Cathepsin B	289.98	64.13	1.09	0.0070	Up	Bta08035
	BTA022401.1	Cathepsin B	5378.46	3428.27	0.60	0.0066	Up	Bta14750

[a] *Read count values from virus-infected whiteflies.*
[b] *Read count values from non-viruliferous whiteflies.*
[c] *Fold change (log2 ratio) of gene expression.*
[d] *Mapped genes in Bemisia tabaci MEAM1 genome.*

Seven unknown proteins were differentially expressed in TYLCV&ToCV co-infected whiteflies, with three upregulated and four downregulated, while the gene *BTA027611.2* was similarly downregulated in ToCV-infected whiteflies (**Supplementary Table S2**).

GO and KEGG Enrichment Analysis of DEGs

GO assignment was performed to classify the functions of the DEGs in response to viral infection. There were 60, 175, and 46 genes among DEGs in response to TYLCV infection, ToCV infection and TYLCV&ToCV co-infection, respectively. These were categorized under biological process, cellular component, and molecular function categories, respectively (**Figure 2**; **Supplementary Table S3**). Under the biological process category, metabolic process, and single-organism metabolic process represented the most abundant subcategories in TYLCV-infected, ToCV-infected, and TYLCV&ToCV co-infected whiteflies. The third most represented GO terms in TYLCV-infected and TYLCV&ToCV co-infected whiteflies were both protein metabolic process, while organonitrogen compound metabolic process was present as the third largest group in ToCV-infected whiteflies. Fewer DEGs were enriched in the cellular component category, and cytoplasm was the largest subcategory among the three types of viruliferous whiteflies. In TYLCV- and ToCV-infected whiteflies, catalytic activity, hydrolase activity, and anion binding were the most abundant molecular function categories. For whiteflies exposed to TYLCV&ToCV, the DEGs were significantly enriched in catalytic activity, hydrolase activity, and peptidase activity under the molecular function category.

Moreover, we found that 57, 184, and 44 genes among TYLCV, ToCV, and TYLCV&ToCV responsive genes, respectively, were mapped to the KEGG database and classified into 11 categories (**Figure 3**; **Supplementary Table S4**). The terms of the four

TABLE 4 | Differentially regulated genes associated with transport.

Virus infection	Gene ID	Annotation	V[a]	NV[b]	FC[c]	*q*-value	Direction	Gene ID-B[d]
TYLCV	BTA001187.1	Transmembrane protein	43.22	180.38	−1.01	0.0006	Down	Bta09390
	BTA019353.1	Choline transporter-like protein 2	96.99	223.71	−0.80	0.0110	Down	Bta08036
	BTA011410.1	Transporter, putative	361.41	591.09	−0.59	0.0248	Down	Bta13176
	BTA007080.3	Vesicular glutamate transporter 3	995.02	1545.42	−0.56	0.0104	Down	Bta07710
ToCV	BTA029391.1	Annexin	753.13	287.07	1.11	0.0003	Up	Bta06534
	BTA001779.2	Sulfate anion transporter 1	463.49	231.99	0.85	0.0029	Up	Bta12218
	BTA005197.1	Solute carrier family 22 member 4	821.61	485.67	0.68	0.0066	Up	Bta09537
	BTA006299.2	Sodium/nucleoside cotransporter 1	665.38	439.55	0.54	0.0483	Up	Bta01801
	BTA007148.1	Solute carrier family 12 member 2	81.78	186.88	−0.91	0.0135	Down	Bta02878
	BTA028491.1	Facilitated glucose transporter protein 1	64.97	266.52	−1.40	2.63E−05	Down	Bta00944
	BTA029270.2	Facilitated glucose transporter protein 1	206.08	444.35	−0.91	0.0035	Down	Bta11822
	BTA019411.1	Solute carrier family 2, facilitated glucose transporter member 8	17.88	94.84	−1.34	0.0003	Down	Bta09677
	BTA024223.1	Solute carrier family 2, facilitated glucose transporter member 8	203.47	470.58	−1.01	0.0002	Down	Bta02936
	BTA016669.3	Solute carrier family 2, facilitated glucose transporter member 8	42.95	128.37	−1.00	0.0164	Down	Bta08290
	BTA019353.1	Choline transporter-like protein 2	60.80	219.68	−1.40	4.24E−06	Down	Bta08036
	BTA007080.3	Vesicular glutamate transporter 3	565.54	1517.51	−1.24	6.54E−08	Down	Bta07710
	BTA007961.1	Sugar transporter 12	88.99	278.56	−1.23	0.0001	Down	Bta08137
	BTA011410.1	Transporter, putative	221.52	580.43	−1.05	0.0023	Down	Bta13176
	BTA026936.3	Transporter, putative	200.83	450.19	−1.01	2.76E−05	Down	Bta01592
	BTA019415.2	Transporter, putative	115.00	263.92	−0.95	0.0036	Down	Bta09672
	BTA027285.1	Transporter, putative	59.75	145.36	−0.87	0.0474	Down	Bta15790
	BTA008826.1	Protein transport protein Sec61 subunit alpha isoform 2	756.83	1246.58	−0.64	0.0149	Down	Bta10727
TYLCV&ToCV	BTA017507.1	Protein transport protein Sec23A, putative	89.38	24.54	0.94	0.0411	Up	Bta07971
	BTA024080.1	Facilitated trehalose transporter Tret1	3260.64	1562.61	0.83	0.0186	Up	Bta07748
	BTA006299.2	Sodium/nucleoside cotransporter 1	878.09	474.44	0.76	0.0058	Up	Bta01801
	BTA009195.1	Proton-coupled amino acid transporter 1	7601.78	4484.92	0.71	8.28E−05	Up	Bta01722

[a] *Read count values from virus-infected whiteflies.*
[b] *Read count values from non-viruliferous whiteflies.*
[c] *Fold change (log2 ratio) of gene expression.*
[d] *Mapped genes in Bemisia tabaci MEAM1 genome.*

most represented pathways in whiteflies fed on TYLCV were: metabolic pathways (10), protein processing in the endoplasmic reticulum (4), lysosome (3), and biosynthesis of amino acids (3). In ToCV-infected whiteflies, the highest number of genes also belonged to metabolic pathways (37), followed by ribosome (8), lysosome (7), and fatty acid metabolism (7). Compared to non-viruliferous whiteflies, the four terms of pathways most represented in TYLCV&ToCV co-infected whiteflies were metabolic pathways (7), lysosome (4), protein processing in the endoplasmic reticulum (4), and spliceosome (3).

Validation of DEGs by RT-qPCR

To validate the data from the DGE analyses, RT-qPCR was conducted on 11 randomly selected differentially expressed genes (**Figure 4**). We analyzed the transcription profiles of nine annotated genes (*BTA017585.2*, vitellogenin; *BTA021906.3*, fatty acid oxidation complex subunit alpha; *BTA001187.1*, transmembrane protein; *BTA009039.1*, P450; *BTA000144.1*, cathepsin B; *BTA028491.1*, facilitated glucose transporter protein 1; *BTA005969.2*, methyltransferase; *BTA009053.1*, pre-mRNA-processing factor 19; *BTA011510.1*, lipid phosphate phosphohydrolase 1), and two genes encoding unknown proteins (*BTA000384.1* and *BTA004369.1*). The results showed that 10 of the selected genes exhibited concordant expression patterns for both RT-qPCR and DGE (**Figure 4**). However, the expression trend of one gene (*BTA000144.1*) was inconsistent between RT-qPCR and DGE (**Figure 4**), which might have been due to the sensitivity of biases existing between the two methods. Nevertheless, the high consistency between the transcription profiles obtained by RT-qPCR and DGE confirmed the reliability of our DGE results.

DISCUSSION

Several transcriptome studies on whiteflies responding to TYLCV or ToCV infection have been conducted, and these

TABLE 5 | Differentially regulated genes associated with energy metabolism, lipid metabolism, and protein synthesis and amino acid metabolism.

Virus infection	Gene ID	Annotation	V[a]	NV[b]	FC[c]	*q*-value	Direction	Gene ID-B[d]
ENERGY METABOLISM								
TYLCV	BTA007709.1	ATP synthase gamma chain	612.89	921.90	−0.52	0.0160	Down	Bta04620
ToCV	BTA028949.1	Beta-galactosidase	359.73	169.87	0.87	0.0083	Up	Bta05309
	BTA011369.1	Alpha-glucosidase	1623.32	970.45	0.69	0.0003	Up	Bta11975
	BTA006577.1	Alpha-glucosidase	295.44	668.78	−1.03	2.17E−05	Down	Bta08426
	BTA018902.1	Alpha-glucosidase	149.28	349.03	−0.93	0.0105	Down	Bta07764
	BTA029066.1	L-lactate dehydrogenase	47.56	126.75	−0.90	0.0441	Down	Bta04403
	BTA029698.1	Alpha-amylase	294.51	524.22	−0.71	0.0261	Down	Bta04553
	BTA007709.1	ATP synthase gamma chain	1355.42	905.28	0.54	0.0188	Up	Bta04620
	BTA006898.1	Pyruvate carboxylase	6609.41	4815.26	0.43	0.0262	Up	Bta05449
	BTA007224.1	Aconitate hydratase	2261.39	3193.00	−0.47	0.0414	Down	Bta04424
TYLCV&ToCV	BTA020543.1	Alpha-glucosidase family 31	2000.60	647.23	1.22	3.33E−05	Up	Bta06849
	BTA021845.1	Alpha-glucosidase	2023.34	1005.97	0.85	0.0029	Up	Bta03818
	BTA020828.1	Alpha-glucosidase	3566.17	1716.10	0.81	0.0378	Up	Bta07453
	BTA001223.1	Glucan endo-1,3-beta-glucosidase	282.61	84.63	1.20	0.0003	Up	Bta06115
	BTA029804.1	AAA-ATPase-like domain-containing protein	73.75	11.98	0.91	0.0426	Up	Bta10446
	BTA020850.1	Malate dehydrogenase	94.48	278.14	−1.00	0.0124	Down	Bta20007
LIPID METABOLISM								
TYLCV	BTA023227.1	Lipase	3647.63	1500.63	1.09	3.61*E*−10	Up	Bta06883
	BTA021906.3	Fatty acid oxidation complex subunit alpha	56.09	609.10	−2.18	1.10*E*−24	Down	Bta00757
	BTA011510.1	Lipid phosphate phosphohydrolase 1	2.53	93.52	−0.77	0.0035	Down	Bta05886
	BTA005102.1	Lipid storage droplets surface-binding protein 1	432.25	735.17	−0.63	0.0129	Down	Bta04143
ToCV	BTA020719.1	Glycerol-3-phosphate acyltransferase, putative	910.38	523.43	0.72	0.0014	Up	Bta09237
	BTA006414.1	Acetyl-CoA carboxylase, putative	3531.39	2235.29	0.62	0.0003	Up	Bta14032
	BTA021906.3	Fatty acid oxidation complex subunit alpha	75.22	598.08	−2.00	4.82E−11	Down	Bta00757
	BTA007925.1	Acyl-CoA synthetase family member 2, mitochondrial	4.08	72.52	−1.58	1.04E−05	Down	Bta14516
	BTA000223.1	Delta(24)-sterol reductase	69.00	183.77	−1.04	0.0035	Down	Bta11167
	BTA024237.1	Fatty acid synthase	41.42	113.10	−0.91	0.0427	Down	Bta07569
	BTA024999.2	Lipase member H-A	247.42	443.44	−0.73	0.0147	Down	Bta03971
	BTA005102.1	Lipid storage droplets surface-binding protein 1	328.21	721.93	−0.98	8.17E−05	Down	Bta04143
	BTA027702.1	Serine palmitoyltransferase	157.37	340.51	−0.86	0.0205	Down	Bta12350
TYLCV&ToCV	BTA021906.3	Fatty acid oxidation complex subunit alpha	136.80	645.54	−1.42	8.42E−06	Down	Bta00757
	BTA011510.1	Lipid phosphate phosphohydrolase 1	3.11	99.10	−1.12	0.0017	Down	Bta05886
PROTEIN SYNTHESIS AND AMINO ACID METABOLISM								
TYLCV	BTA001324.1	Methionine-tRNA ligase	107.08	15.48	1.16	2.06E−05	Up	Bta08529
	BTA029395.1	Msx2-interacting protein	934.45	508.46	0.66	0.0296	Up	Bta14735
	BTA008003.1	Branched-chain-amino-acid aminotransferase	1981.69	1330.59	0.52	0.0074	Up	Bta10673
	BTA018918.1	Methionyl-tRNA formyltransferase	951.32	634.42	0.52	0.0160	Up	Bta01802
	BTA013101.2	Glutamate synthase [NADH], amyloplastic	3773.52	2854.37	0.38	0.0319	Up	Bta06960
	BTA026974.1	Alanine aminotransferase 1	3.01	64.65	−0.81	0.0031	Down	Bta15725
	BTA019051.2	Tryptophan-tRNA ligase	2085.22	2872.14	−0.43	0.0160	Down	Bta06820
	BTA009050.1	Aminopeptidase N	3128.54	4197.32	−0.40	0.0171	Down	Bta07276
ToCV	BTA026807.1	Polycomb complex protein BMI-1	42.85	1.51	0.90	0.0213	Up	Bta09503
	BTA013962.1	Eukaryotic translation initiation factor 1A	1585.75	872.38	0.76	0.0027	Up	Bta13313
	BTA012766.1	Ribosomal protein S18	3925.47	2437.28	0.65	0.0002	Up	Bta04518
	BTA025030.1	ATP-dependent RNA helicase	14477.58	10584.86	0.43	0.0179	Up	Bta02498
	BTA027577.1	ATP-dependent RNA helicase A, putative	74.57	246.20	−1.14	0.0027	Down	Bta05044
	BTA026974.1	Alanine aminotransferase 1	8.18	63.49	−1.06	0.0111	Down	Bta15725

(Continued)

TABLE 5 | Continued

Virus infection	Gene ID	Annotation	V[a]	NV[b]	FC[c]	*q*-value	Direction	Gene ID-B[d]
	BTA009050.1	Aminopeptidase N	1821.95	4121.58	−1.05	1.57*E*−06	Down	Bta07276
	BTA027461.1	Thymus-specific serine protease	463.00	1101.57	−0.97	0.0043	Down	Bta01281
	BTA012512.1	Aspartate aminotransferase	89.49	231.65	−0.95	0.0176	Down	Bta04470
	BTA004061.1	60S ribosomal protein L27a	139.97	289.81	−0.85	0.0122	Down	Bta07190
	BTA011516.1	Ribosomal protein L11	1015.61	1927.32	−0.79	0.0078	Down	Bta03518
	BTA014806.1	40S ribosomal protein S17	428.91	737.17	−0.70	0.0077	Down	Bta00569
	BTA019051.2	Tryptophan-tRNA ligase	1690.76	2820.37	−0.70	3.73E−05	Down	Bta06820
	BTA014721.1	Xaa-Pro aminopeptidase 1	1081.78	1733.67	−0.62	0.0146	Down	Bta03997
TYLCV&ToCV	BTA004604.1	Eukaryotic translation initiation factor 2 subunit 1	326.24	38.97	1.54	2.60*E*−06	Up	Bta01070
	BTA007461.1	SNW domain-containing protein 1	139.01	33.76	1.13	0.0042	Up	Bta09073
	BTA004061.1	60S ribosomal protein L27a	748.72	312.81	0.97	0.0031	Up	Bta07190
	BTA015861.2	U4/U6.U5 tri-snRNP-associated protein 1	139.37	50.54	0.91	0.0419	Up	Bta03973
	BTA019051.2	Tryptophan-tRNA ligase	4918.92	3044.21	0.61	0.0346	Up	Bta06820
	BTA009053.1	Pre-mRNA-processing factor 19	183.82	573.58	−0.99	0.0180	Down	Bta07273
	BTA026974.1	Alanine aminotransferase 1	10.53	68.53	−0.89	0.0491	Down	Bta15725

[a] *Read count values from virus-infected whiteflies.*
[b] *Read count values from non-viruliferous whiteflies.*
[c] *Fold change (log2 ratio) of gene expression.*
[d] *Mapped genes in Bemisia tabaci MEAM1 genome.*

have provided a large amount of valuable information on the interaction among tomato viruses, whiteflies, and plants (Kaur et al., 2017; Geng et al., 2018; Hasegawa et al., 2018). However, these studies mainly focused on infection by a single virus and were conducted on *B. tabaci* MEAM1. Thus, in the present study, we performed transcriptome analyses of *B. tabaci* MED after the whiteflies had fed on TYLCV-infected, ToCV-infected, TYLCV&ToCV co-infected, and uninfected tomatoes for 24 h to compare the gene expression pattern differences between whiteflies infected by a single virus and by both viruses. A total of 265,433,932 clean reads were obtained from eight cDNA libraries, with an average mapping rate of 81.85% to the whitefly (*B. tabaci* MED) reference genome (Xie et al., 2017). Comparative transcriptome analyses identified 359 DEGs between viruliferous and non-viruliferous whiteflies. The number of DEGs in response to ToCV infection (221 genes) was greater than that in response to TYLCV infection (78 genes). This was in accordance with previous studies with MEAM1, wherein more genes were differentially expressed on acquisition for 24 h with ToCV than TYLCV (Kaur et al., 2017; Hasegawa et al., 2018). Only 60 DEGs were detected in whiteflies feeding on TYLCV&ToCV co-infected tomato plants compared to whiteflies feeding on uninfected tomatoes. The number of TYLCV&ToCV-responsive DEGs was clearly less than those of TYLCV or ToCV, and this may be related to the complex interactions between the two viruses in the insect vectors or in the plants.

Detoxification enzymes of insects, including P450s, CarEs, UGTs, and ABCs, are important in the metabolism of xenobiotics, such as plant allelochemicals and insecticides (Scott et al., 1998; Ferry et al., 2004; Despres et al., 2007; Dermauw and Van Leeuwen, 2014). More genes associated with detoxification were regulated in ToCV-infected whiteflies than in TYLCV-infected and TYLCV&ToCV co-infected whiteflies. P450s were the main detoxification enzymes among the DEGs in virus-infected whiteflies, especially in TYLCV-infected and TYLCV&ToCV co-infected whiteflies. Furthermore, most of P450 genes were downregulated in response to the virus infection (2 of 3 genes for TYLCV infection, 4 of 5 genes for ToCV infection, 1 of 1 gene for TYLCV&ToCV co-infection). Four downregulated UGT genes were detected in ToCV-infected whiteflies, indicating that the glucuronidation of plant toxins might be inhibited by ToCV infection. Moreover, we found that the majority of detoxification enzyme genes were downregulated in the virus-infected whiteflies, which was consistent with a DGE analysis of *B. tabaci* MEAM1 in response to TYLCCNV infection (Luan et al., 2013). Whitefly susceptibility to insecticides might therefore be altered by virus infection. ABC transporters are mainly involved in the transport of xenobiotics/plant allelochemicals in arthropods (Dermauw and Van Leeuwen, 2014). The ABC gene ABCB FT/P-gp of *Drosophila melanogaster* is involved in colchicine transport (Wu et al., 1991; Tapadia and Lakhotia, 2005). Additionally, an ABC transporter with similar functions in nicotine excretion was identified in the tobacco hornworm *Manduca sexta* (Murray et al., 1994; Gaertner et al., 1998; Govind et al., 2010). It is noteworthy that two ABC genes identified in ToCV-infected whiteflies were significantly upregulated. These results suggest that improving the transport efficiency might be a whitefly strategy for coping with the plant toxins induced by viral infection.

The alpha-crystallin B chain-like proteins belonging to the small heat shock proteins (sHSP) as well as the heat shock

TABLE 6 | Differentially regulated genes associated with cell function and other functions.

Virus infection	Gene ID	Annotation	V[a]	NV[b]	FC[c]	*q*-value	Direction	Gene ID-B[d]
CELL FUNCTION								
TYLCV	BTA020985.1	Alpha-tubulin N-acetyltransferase	379.57	192.15	0.76	0.0045	Up	Bta09955
ToCV	BTA001245.1	Histone H2B	42.91	0.44	1.22	0.0007	Up	Bta02155
	BTA007206.1	THAP domain-containing protein 4	249.31	115.92	0.86	0.0193	Up	Bta02969
	BTA008661.1	Inositol-3-phosphate synthase 1-B	280.56	137.12	0.84	0.0117	Up	Bta05168
	BTA030040.1	Condensin-2 complex subunit D3	274.86	572.85	−0.93	8.48E−05	Down	Bta02114
	BTA027341.1	E3 ubiquitin-protein ligase RNF139	56.76	147.20	−0.91	0.0379	Down	Bta02577
	BTA030041.1	SAP30-binding protein	30.13	92.20	−0.93	0.0427	Down	Bta02111
	BTA001462.1	G2/mitotic-specific cyclin-B3, putative	604.60	909.87	−0.54	0.0294	Down	Bta03554
	BTA027371.1	Cyclin-A1	1211.97	1703.48	−0.46	0.0346	Down	Bta07538
	BTA002011.1	5′ nucleotidase	1765.92	2426.65	−0.43	0.0480	Down	Bta07799
TYLCV&ToCV	BTA015504.1	Gelsolin	308.71	103.03	0.98	0.0180	Up	Bta11052
	BTA030040.1	Condensin-2 complex subunit D3	305.82	618.31	−0.85	0.0033	Down	Bta02114
OTHERS								
TYLCV	BTA019847.1	Vitellogenin	343607.6	242741.13	0.46	0.0159	Up	Bta07852
	BTA017585.2	Vitellogenin	113734.64	88528.55	0.34	0.0159	Up	Bta11903
	BTA005969.2	Methyltransferase	240.90	538.14	−0.94	7.79E−06	Down	Bta20014
ToCV	BTA017585.2	Vitellogenin	133350.16	86931.65	0.60	2.90E−06	Up	Bta11903
	BTA005969.2	Methyltransferase	122.19	528.44	−1.77	3.53E−14	Down	Bta20014
	BTA008678.3	Juvenile hormone-inducible protein 26-like protein	18.42	74.00	−0.94	0.0414	Down	Bta10000
	BTA023744.1	Juvenile hormone-inducible protein	73.59	173.61	−0.93	0.0123	Down	Bta00804
	BTA004540.1	Aldo/keto reductase	50.08	127.77	−0.92	0.0270	Down	Bta10339
TYLCV&ToCV	BTA017585.2	Vitellogenin	142603.78	93831.08	0.56	0.0060	Up	Bta11903
	BTA004564.1	Follicle cell protein 3C-1	440.15	798.59	−0.75	0.0058	Down	Bta14365
	BTA005969.2	Methyltransferase	292.28	570.38	−0.81	0.0054	Down	Bta20014

[a] *Read count values from virus-infected whiteflies.*
[b] *Read count values from non-viruliferous whiteflies.*
[c] *Fold change (log2 ratio) of gene expression.*
[d] *Mapped genes in Bemisia tabaci MEAM1 genome.*

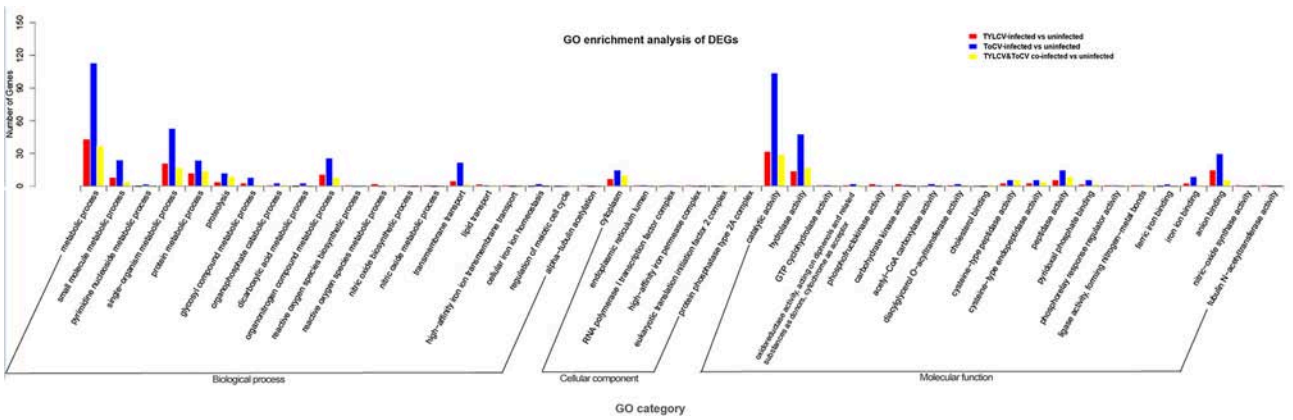

FIGURE 2 | GO enrichment analysis of DEGs in *Bemisia tabaci* MED in response to TYLCV infection, ToCV infection, and TYLCV&ToCV co-infection. Bars represent the number of DEGs classified into 46 GO terms under three main categories (biological process, cellular component, and molecular function).

proteins (HSP70 and HSP90) were significantly upregulated in TYLCV-infected whiteflies. The sHSPs are involved in the destabilizing effects of stressful conditions on cellular integrity (Jong et al., 1993), while HSPs are involved in preventing aggregation of denatured proteins in response to several stress factors, including oxidative, osmotic, and temperature

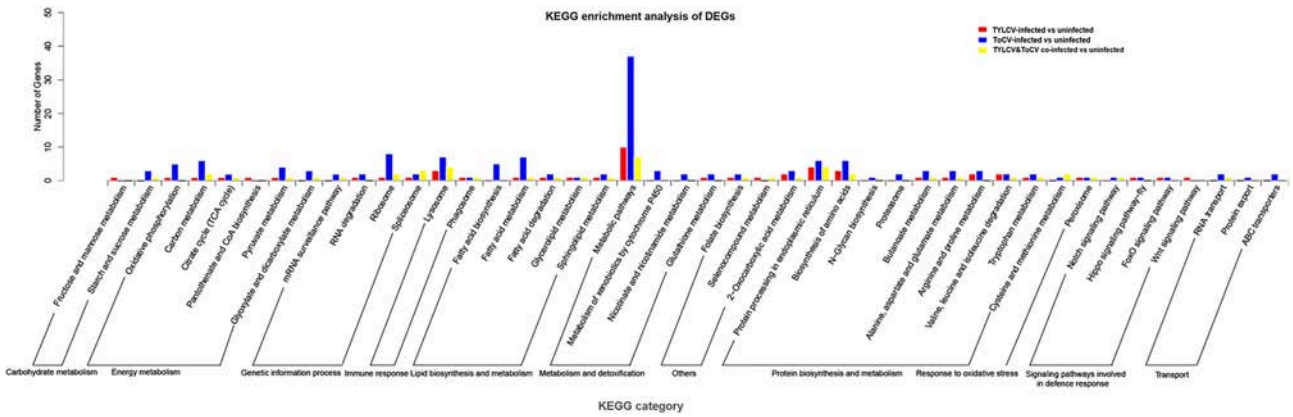

FIGURE 3 | KEGG pathways enrichment analysis of DEGs in *Bemisia tabaci* MED in response to TYLCV infection, ToCV infection, and TYLCV&ToCV co-infection. Bars represent the number of DEGs classified into 44 KEGG terms under 11 main categories (metabolism and detoxification, response to oxidative stress, transport, signaling pathways involved in defense response, immune response, genetic information process, carbohydrate metabolism, protein biosynthesis and metabolism, lipid biosynthesis and metabolism, energy metabolism, and others).

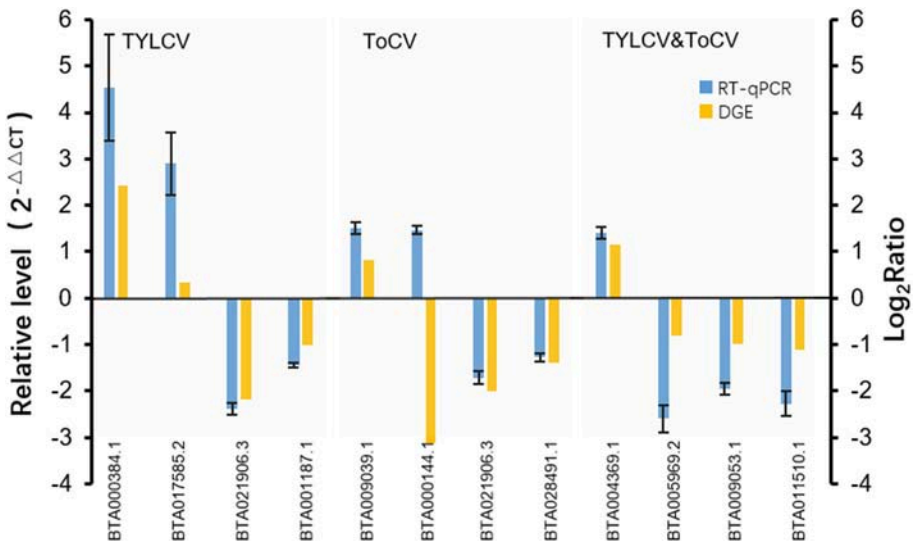

FIGURE 4 | Verification of DEGs by RT-qPCR. Expression levels of 11 selected genes were measured by RT-qPCR using the $2^{-\Delta\Delta CT}$ method. The 11 selected genes contained nine annotated genes (*BTA017585.2*, vitellogenin; *BTA021906.3*, fatty acid oxidation complex subunit alpha; *BTA001187.1*, transmembrane protein; *BTA009039.1*, P450; *BTA000144.1*, cathepsin B; *BTA028491.1*, facilitated glucose transporter protein 1; *BTA005969.2*, methyltransferase; *BTA009053.1*, pre-mRNA-processing factor 19; *BTA011510.1*, lipid phosphate phosphohydrolase 1), and two genes encoding unknown proteins (*BTA000384.1*, *BTA004369.1*). The *X* axis represents the gene ID numbers of the 11 selected genes; the left *Y* axis represents the relative gene expression levels measured by RT-qPCR, while the right *Y* axis represents the $\log_2$Ratio of the genes resulting from DGE.

stresses (Lindquist, 1986; Johnston et al., 1998; Sorensen et al., 2003). In addition to the HSP70 gene, we also identified the Glilial Lazarillo (GLaz) gene, a homolog of apolipoprotein D, exhibiting a positive response to the ToCV infection. This protein has been shown to play a protective role in stress situations in *D. melanogaster* (Sanchez et al., 2006). In contrast with the regulation of detoxification enzyme genes, most of the genes associated with stress response showed increased transcription profiles in response to either TYLCV or ToCV infection.

The innate immune system is the major weapon used by insects to fight against foreign invaders such as pathogens (Hoffmann, 1995; Irving et al., 2001). When infected by plant viruses, the cellular and humoral immune response systems are activated in insects (Luan et al., 2011; Xu et al., 2012; Shrestha et al., 2017). In the present study, higher numbers of immune response-related genes were activated in ToCV-infected whiteflies than in TYLCV-infected or TYLCV&ToCV co-infected whiteflies. Furthermore, a number of cathepsin genes were differentially expressed in whiteflies after feeding

on virus-infected tomato plants. The cathepsins have been implicated in virus transmission, apoptosis, and signaling (Kubo et al., 2012; Sim et al., 2012; Saikhedkar et al., 2015). Similar to our findings, Hasegawa et al. (2018) and Kaur et al. (2017) have identified many differentially regulated genes belonging to the cathepsin B and F families in *B. tabaci* MEAM1 after feeding on TYLCV- and ToCV-infected tomatoes. Only two upregulated cathepsin B genes were found in TYLCV&ToCV co-infected whiteflies, suggesting the possible involvement of immune responses and transmission of these two viruses. Previous studies have shown that the high expression of immune genes in whiteflies with symbionts could lead to a fitness cost (Ghosh et al., 2018). Then, it can be speculated that the inducement of immune response genes may attenuate the performance of TYLCV&ToCV co-infected whiteflies on host plants. Additionally, the altered gene encoding a class B scavenger receptor, a type of surface receptor that is considered to be a regulator of phagocytosis (Franc et al., 1999; Geng et al., 2018), was found in TYLCV-infected whiteflies. Autophagy-related genes have previously been shown to be important in resistance to Begomovirus infection in whiteflies (Luan et al., 2011; Wang et al., 2016). We also identified an upregulated gene encoding sequestosome-1, which is classified as an autophagosome cargo protein, in response to TYLCV infection in whiteflies. After feeding on ToCV-infected tomato plants, the transcription level of the gene encoding the hemocyanin subunit was significantly decreased, in contrast to the transcription profile of the same gene in TYLCV-infected *B. tabaci* MEAM1 (Hasegawa et al., 2018). Hemocyanins are involved in antiviral functions in arthropods (Dolashka and Voelter, 2013), and these results suggest that the immune response modes of hemocyanins may differ according to diverse viral infections.

Our analysis identified a downregulated choline transporter-like protein gene associated with TYLCV infection. In humans, the choline transporter is a cell membrane transporter that carries choline to cholinergic neurons for acetylcholine synthesis (Okuda and Haga, 2000). The transcription level of the choline transporter-like protein was significantly decreased in ToCV-infected whiteflies, suggesting that both TYLCV and ToCV inhibit the normal transmission of neuron signals in whiteflies. Several members of the annexin group have essential roles in vesicular trafficking, adhesion, apoptosis, and viral infection (Iseki et al., 2009; Patel et al., 2011; Ma et al., 2012). For example, annexin A1 (ANXA1) was confirmed to play a detrimental role in influenza infection and positively regulated virus titers in viral infection experiments using mice (Arora, 2014). A similar role was found for salmon annexin 1 during the infection of infectious pancreatic necrosis virus (IPNV) (Hwang et al., 2007). Thus, the overexpression of the annexin gene in ToCV-infected whiteflies may contribute to the survival and transmission of the virus in vectors. The glucose transporter proteins are related to the interaction with viruses (Huang et al., 2015), and a number of facilitated glucose transporter genes were differentially regulated in ToCV-infected whiteflies *B. tabaci* MEAM1 (Kaur et al., 2017). In our study, a total of five facilitated glucose transporter genes were detected in ToCV-infected whiteflies, which suggests that these genes may participate in the interaction with ToCV *in vivo* and may be associated with virus transmission. We noticed that all four transport related genes were upregulated in TYLCV&ToCV co-infected whiteflies, while most of those genes in TYLCV- and ToCV-infected whiteflies were downregulated. The transporter proteins may exhibit positive actions, such as improving the transferring efficiency of trehalose by the upregulated facilitated trehalose transporter Tret 1 gene, in order to defend against the viral co-infection.

Most of the differentially regulated genes associated with energy metabolism encode glucosidases containing alpha-glucosidases and beta-glucosidases. Glucosidases are mainly involved in the hydrolysis of carbohydrates; they also play important roles in normal cellular function and pathogen defense (Bourne and Henrissat, 2001). Two of three alpha-glucosidase genes were downregulated in ToCV-infected whiteflies. Expression of beta-glucosidase genes in *Frankliniella occidentalis* was also depressed by TSWV infection (Zhang et al., 2013). Here, all four glucosidase genes were all upregulated in response to TYLCV&ToCV co-infection, indicating that the activation of glucosidase genes may be involved in the immune defense to co-infection with the two viruses and the complex interactions between whiteflies and viruses.

Lipid metabolism of insect vectors can be disturbed by plant viruses; this has been demonstrated in several studies and is considered to be a hallmark of cellular changes associated with viral infection (Luan et al., 2011; Xu et al., 2012; Zhang et al., 2013). Most genes in this study associated with lipid metabolism were downregulated in TYLCV-infected (3 of 4 genes) and ToCV-infected (7 of 9 genes) whiteflies, while both of the two lipid metabolism-related genes identified in TYLCV&ToCV co-infected whiteflies were downregulated. This result indicates that both single infection with TYLCV or ToCV and co-infection with TYLCV&ToCV can significantly inhibit the lipid metabolism of *B. tabaci* MED. Luan et al. (2011) also found that most genes involved in lipid metabolism were downregulated in *B. tabaci* MEAM1 when feeding on TYLCCNV-infected plants. However, other studies have shown contrasting results in TSWV-infected thrips and demonstrated that lipid metabolism in *F. occidentalis* and *F. fusca* was active in response to TSWV infection (Zhang et al., 2013; Shrestha et al., 2017).

Higher numbers of DEGs involved in protein synthesis and amino acid metabolism were identified in ToCV-infected whiteflies than in TYLCV-infected and TYLCV&ToCV co-infected whiteflies, and the majority of those genes (10 of 14 genes) were downregulated in response to ToCV infection. This suggests that protein synthesis and amino acid metabolism in whiteflies can be inhibited by ToCV infection, which is consistent with the results of previous studies on *Sogatella furcifera* and *Campoletis sonorensis* (Shelby and Webb, 1997; Xu et al., 2012). Two genes encoding eukaryotic translation initiation factors (eIF), which are involved in the initiation phase of eukaryotic translation, were upregulated in ToCV-infected and TYLCV&ToCV co-infected whiteflies. Wang et al. (2014) revealed that eIF4B of the host could inhibit influenza A virus (IAV) replication by upregulating the expression level of a key protein (interferon-induced transmembrane protein 3, IFITM3) that protects the host from virus infection. Thus, it

can be inferred that the upregulation of eIF genes in viruliferous whiteflies may be a strategy in response to ToCV infection and TYLCV&ToCV co-infection. Interestingly, the two genes encoding 60S ribosomal protein L27a and tryptophan-tRNA ligase were downregulated in ToCV-infected whiteflies, but they exhibited opposite regulation profiles in TYLCV&ToCV co-infected whiteflies. The shift in gene expression may result from the alteration of insect and host plant physiologies caused by the co-infection with the two viruses.

Virus infection can lead to cellular DNA damage and the host cells will activate repair mechanisms (Huang et al., 2011). In ToCV-infected whiteflies, the histone H2B gene, which is involved in repair of DNA and regulation of transcription (Ronnigen et al., 2015), was significantly upregulated. This suggests that the histone H2B gene may help attenuate the cell damage wrought by ToCV infection. Additionally, viruses are able to alter the host cell cycle to achieve the replication and expression of their genomes, a phenomenon that has been demonstrated in geminivirus infection (Emmett et al., 2005; Ascencio-lbanez et al., 2008; Geng et al., 2018). Although ToCV cannot replicate in insect vectors, two cyclin genes (G2/motic-specific cyclin-B3 and cyclin-A1), which function in controlling the progression of cells through the cell cycle (Galderisi et al., 2003), were downregulated in ToCV-infected whiteflies. This result demonstrates that ToCV infection also disturbs the normal cell cycle in whiteflies. TYLCV&ToCV co-infection induced the expression of the gelsolin gene, an important actin regulator that is associated with the inhibition of apoptosis (Koya et al., 2000). These alterations of the cell functions caused by viruses may be an adaption or a defense strategy of insect vectors in response to viral infection.

Plant viruses can have direct and indirect effects that influence the fecundity, longevity, and survival rate of the vectors (Belliure et al., 2005; Jiu et al., 2007; Li et al., 2018). Consistent with this, our DGE analysis found several reproduction-related genes and development-related genes differentially regulated in the virus-infected whiteflies. Two vitellogenin genes were upregulated in TYLCV-infected whiteflies, supporting the result that feeding on TYLCV-infected tomato plants can increase the fecundity of *B. tabaci* MED (Su et al., 2015). Previous study showed that whiteflies MED had a shorter development time on ToCV-infected tomato plants than on healthy tomato plants (Shi et al., 2018). We also found that two juvenile hormone-inducible protein genes were both downregulated in ToCV-infected whiteflies.

GO enrichment analysis showed that the DEGs in TYLCV-infected, ToCV-infected, and TYLCV&ToCV co-infected whiteflies were all highly enriched in three functional subcategories: the metabolic process, catalytic activity, and single-organism metabolic process. Previous reports demonstrate that plant viruses can change the defense response and nutrition status of the host plants (Shi et al., 2013; Mauck et al., 2014), which might alter the expression patterns of genes involved in metabolic processes and catalytic activity. We also found several differentially regulated genes enriched in the cytoplasm, indicating that those virus-responsive genes were mainly distributed in the cytoplasm among the cellular component. Additionally, there were several DEGs classified as iron ion binding in whiteflies infected with TYLCV (three genes), ToCV (nine genes), and TYLCV&ToCV (one gene) compared with non-viruliferous whiteflies. Iron-binding proteins are vital in iron transport and sequestering iron, but an overabundance can lead to oxidative stress (Strickler-Dinglasan et al., 2006). It is also known that the major iron-binding proteins in insects play important roles in iron transport (Bartfield and Law, 1990) and immunity (Yoshiga et al., 1997, 1999). Therefore, the DEGs belonging to the iron ion binding group may participate in the defense responses to viral infection and oxidative stress.

In accordance with the results of the GO assignment, the KEGG pathway analysis showed that most DEGs in TYLCV-infected, ToCV-infected, and TYLCV&ToCV co-infected whiteflies were enriched in metabolic pathways. A majority of the genes involved in metabolic pathways were downregulated both in the TYLCV-infected (8 of 10 genes) and TYLCV&ToCV (5 of 7 genes) co-infected whiteflies. A previous study showed that 72.18% of genes enriched in primary metabolism were downregulated in TSWV-infected *F. occidentalis* (Zhang et al., 2013), which is similar to our results. However, there were 14 upregulated genes enriched in metabolic pathways in ToCV-infected whiteflies. Kaur et al. (2017) also confirmed the upregulation of metabolic pathways in ToCV-infected *B. tabaci* MEAM1. The lysosome pathway was among the most represented categories in TYLCV-infected, ToCV-infected, and TYLCV&ToCV co-infected whiteflies compared with non-viruliferous whiteflies, indicating an immune response in whiteflies during the early stages of viral infection. As expected, a number of DEGs were also enriched in the lysosome pathway in ToCV-infected *B. tabaci* MEAM1 compared with non-viruliferous whiteflies (Kaur et al., 2017), and several lysosome genes were also found to be differentially regulated in TYLCV-infected *B. tabaci* MEAM1 (Hasegawa et al., 2018). Notably, all four genes from the lysosome pathway in TYLCV&ToCV co-infected whiteflies were upregulated, while only one gene was upregulated in both TYLCV- and ToCV-infected whiteflies. We can speculate that co-infection with two viruses may induce a stronger antiviral response than single infection with either TYLCV or ToCV. Additionally, four and three genes upregulated in TYLCV infected and TYLCV&ToCV co-infected whiteflies, respectively, were significantly enriched in the pathway of protein processing in the endoplasmic reticulum, indicating that protein synthesis might be enhanced by TYLCV infection and TYLCV&ToCV co-infection.

CONCLUSION

We conducted a transcriptome analysis on the whitefly *B. tabaci* MED in response to TYLCV infection, ToCV infection, and TYLCV&ToCV co-infection. *B. tabaci* MED genes responsive to viral infection were identified, including genes associated with defense response, transport, primary metabolism, cell function, and total fitness. Shifts in the expression of genes involved in transport and energy metabolism occurred between

TYLCV&ToCV co-infection and single infection with TYLCV or ToCV, indicating different responses to diverse patterns of viral infection. GO and KEGG pathway enrichment analyses revealed that the metabolic process and metabolic pathways were significantly disturbed by single infection with TYLCV or ToCV as well as TYLCV&ToCV co-infection. These data increase our understanding of the whitefly-virus interaction and provide new insights into the molecular mechanisms involved in response to co-infection with different viruses. The findings may be useful for discovery of novel molecular targets that could block the spread of whitefly-transmitted viruses and help control insect vector whiteflies.

DATA AVAILABILITY

The RNA-seq reads have been submitted to the SRA at NCBI under the accession PRJNA490883.

AUTHOR CONTRIBUTIONS

T-BD and DC conceived the study. T-BD conducted the experiments. T-BD, JL, E-HC, and J-ZN analyzed the data. T-BD drafted the manuscript. E-HC and J-ZN revised and enhanced the manuscript. All authors read and approved the final manuscript.

ACKNOWLEDGMENTS

This work was supported by the National Natural Science Foundation of P. R. China (31501707), High-level Talents Funds of Qingdao Agricultural University (6631115033), the Taishan Mountain Scholar Constructive Engineering Foundation of Shandong, and the Agricultural Science and Technology Innovation Project of Shandong Academy of Agricultural Sciences (CXGC2016B11). We also would like to thank LetPub (www.letpub.com) for providing linguistic assistance during the preparation of this manuscript.

SUPPLEMENTARY MATERIAL

The Supplementary Material for this article can be found online at: https://www.frontiersin.org/articles/10.3389/fphys.2019.00302/full#supplementary-material

REFERENCES

Alemandri, V., Vaghi Medina, C. G., Dumon, A. D., Arguello Caro, E. B., Mattio, M. F., Garcia Medina, S., et al. (2015). Three members of the *Bemisia tabaci* (Hemiptera: Aleyrodidae) cryptic species complex occur sympatrically in Argentine horticultural crops. *J. Econ. Entomol.* 108, 405–413. doi: 10.1093/jee/tov017

Arora, S. (2014). Functional characterization of annexin A1 in toll like receptor 7 signaling and influenza virus infection. Doctor's thesis, National University of Singapore, Singapore.

Ascencio-lbanez, J. T., Sozzani, R., Lee, T. J., Chu, T. M., Wolfinger, R. D., Cella, R., et al. (2008). Global analysis of Arabidopsis gene expression uncovers a complex array of changes impacting pathogen response and cell cycle during geminivirus infection. *Plant Physiol.* 148, 436–454. doi: 10.1104/pp.108.121038

Bartfield, N. S., and Law, J. H. (1990). Isolation and molecular cloning of transferrin from the tobacco hornworm, *Manduca sexta*. *J. Biol. Chem.* 265, 21684–21691.

Belliure, B., Janssen, A., Maris, P. D., and Sabelis, M. (2005). Herbivore arthropods benefit from vectoring plant virus. *Ecol. Lett.* 8, 70–79. doi: 10.1111/j.1461-0248.2004.00699.x

Benjamini, Y., and Hochberg, Y. (1995). Controlling the false discovery rate: a practical and powerful approach to multiple testing. *J. R. Stat. Soc.* 57, 289–300. doi: 10.1111/j.2517-6161.1995.tb02031.x

Bourne, Y., and Henrissat, B. (2001). Glycoside hydrolases and glycosyltransferases: families and functional modules. *Curr. Opin. Struc. Biol.* 11, 593–600. doi: 10.1016/S0959-440X(00)00253-0

Chen, W. B., Hasegawa, D. K., Kaur, N., Kliot, A., Valle Pinheiro, P., Luan, J. B., et al. (2016). The draft genome of whitefly *Bemisia tabaci* MEAM1, a global crop pest, provides novel insights into virus transmission, host adaptation, and insecticide resistance. *BMC Biol.* 14:110. doi: 10.1186/s12915-016-0321-y

Chu, D., Hu, X., Gao, X., Zhao, H., Nichols, R. L., and Li, X. (2012). Use of mitochondrial cytochrome oxidase I polymerase chain reaction-restriction fragment length polymorphism for identifying subclades of *Bemisia tabaci* Mediterranean group. *J. Econ. Entomol.* 105, 242–251. doi: 10.1603/EC11039

Chu, D., Zhang, Y. J., Brown, J. K., Cong, B., Xu, B. Y., Wu, Q. J., et al. (2006). The introduction of the exotic Q biotype of *Bemisia tabaci* Mediterranean group. *J. Econ. Entomol.* 105, 242–251.

Czosnek, H. (2007). *Tomato Yellow Leaf curl virus Disease: Management, Molecular Biology, Breeding for Resistance*. Dordrecht: Springer.

Dai, H. J., Liu, Y. G., Zhu, X. P., Liu, Y. J., and Zhao, J. (2016). Tomato chlorosis virus (ToCV) transmitted by Bemisia tabaci biotype Q of Shouguang in Shandong Province. *J. Plant Protect.* 43, 162–167. doi: 10.13802/j.cnki.zwbhxb.2016.01.024

De Barro, P., Liu, S. S., Boykin, L. M., and Dinsdale, A. B. (2011). *Bemisia tabaci*: a statement of species status. *Annu. Rev. Entomol.* 56, 1–19. doi: 10.1146/annurev-ento-112408-085504

Dermauw, W., and Van Leeuwen, T. (2014). The ABC gene family in arthropods: comparative genomics and role in insecticide transport and resistance. *Insect. Biochem. Molec.* 45, 89–110. doi: 10.1016/j.ibmb.2013.11.001

Despres, L., David, J. P., and Gallet, C. (2007). The evolutionary ecology of insect resistance to plant chemicals. *Trends Ecol. Evol.* 22, 298–307. doi: 10.1016/j.tree.2007.02.010

Dolashka, P., and Voelter, W. (2013). Antiviral activity of hemocyanins. *Invert. Surviv. J.* 10, 120–127.

Dovas, C. I., Katis, N. I., and Avgelis, A. D. (2002). Multiplex detection of criniviruses associated with epidemics of a yellowing disease of tomato in Greece. *Plant Dis.* 86, 1345–1349. doi: 10.1094/PDIS.2002.86.12.1345

Emmett, S. R., Dove, B., Mahoney, L., Wurm, T., and Hiscox, J. A. (2005). The cell cycle and virus infection. *Methods Mol. Biol.* 296, 197–218. doi: 10.1385/1-59259-857-9:197

Ferry, N., Edwards, M. G., Gatehouse, J. A., and Gatehouse, A. M. R. (2004). Plant-insect interactions: molecular approaches to insect resistance. *Curr. Opin. Biotech.* 15, 155–161. doi: 10.1016/j.copbio.2004.01.008

Franc, N. C., Heitzier, P., and White, K. (1999). Requirement for croquemort in phagocytosis of apoptotic cells in *Drosophila*. *Science* 284, 1991–1994. doi: 10.1126/science.284.5422.1991

Gaertner, L. S., Murray, C. L., and Morris, C. E. (1998). Transepithelial transport of nicotine and vinblastine in isolated Malpighian tubules of the tobacco hornworm (*Manduca sexta*) suggests a P-glycoprotein-like mechanism. *J. Exp. Biol.* 201, 2637–2645.

Galderisi, U., Jori, F. P., and Giordano, A. (2003). Cell cycle regulation and neural differentiation. *Oncogene* 22, 5208–5219. doi: 10.1038/sj.onc.1206558

Gao, L. L., Sun, G. Z., Wang, Y., Gao, W., Zhang, C. X., Zhang, A. S., et al. (2015). Molecular detection and identification of *Tomato chlorosis virus* in Tianjin. *Acta Agriculturae Boreali-Sinica* 30, 211–215. doi: 10.7668/hbnxb.2015.03.036

Geng, L., Qian, L. X., Shao, R. X., Liu, Y. Q., Liu, S. S., and Wang, X. W. (2018). Transcriptome profiling of whitefly guts in response to *Tomato yellow leaf curl virus* infection. *Virol. J.* 15:14. doi: 10.1186/s12985-018-0926-6

Ghosh, S., Bouvaine, S., Richardson, S. C. W., Ghanim, M., and Maruthi, M. N. (2018). Fitness costs associated with infections of secondary endosymbionts in the cassava whitefly species *Bemisia tabaci*. *J. Pest Sci.* 91, 17–28. doi: 10.1007/s10340-017-0910-8

Govind, G., Mittapalli, O., Griebel, T., Allmann, S., Bocker, S., and Baldwin, I. T. (2010). Unbiased transcriptional comparisons of generalist and specialist herbivores feeding on progressively defenseless *Nicotiana attenuata* plants. *PLoS ONE* 5:e8735. doi: 10.1371/journal.pone.0008735

Hasegawa, D. K., Chen, W. B., Zheng, Y., Kaur, N., Wintermantel, W. M., and Simmons, A. M. (2018). Comparative transcriptome analysis reveals networks of genes activated in the whitefly, *Bemisia tabaci* when fed on tomato plants infected with *Tomato yellow leaf curl virus*. *Virology* 513, 52–64. doi: 10.1016/j.virol.2017.10.008

Hoffmann, J. A. (1995). Innate immunity of insects. *Curr. Opin. Immunol.* 7, 4–10.

Hogenhout, S. A., Ammar el-D., Desouky, A., Whitfield, A. E., and Redinbaugh, M. G. (2008). Insect vector interactions with persistently transmitted viruses. *Annu. Rev. Phytopathol.* 46, 327–359. doi: 10.1146/annurev.phyto.022508.092135

Hu, J. A., Wan, X. J., Li, Z. J., Huang, W., Li, W. G., and Ying, F. Q. (2015). Molecular identification on *Tomato chlorosis virus* in Henan Province. *China Vegetables* 12, 25–28. doi: 10.3969/j.issn.1000-6346.2015.12.007

Huang, H. T., Chan, H. L., Shih, T. Y., and Chen, L. L. (2015). A study of the role of glucose transporter 1 (Glut1) in white spot syndrome virus (WSSV) infection. *Fish Shellfish Immun.* 46, 305–314. doi: 10.1016/j.fsi.2015.06.034

Huang, N., Wu, W., Yang, K., Passarelli, A. L., Rohrmann, G. F., and Glem, R. J. (2011). Baculovirus infection induce a DNA damage response that is required for efficient viral replication. *J. Virol.* 85, 12547–12556. doi: 10.1128/JVI.05766-11

Hwang, H. J., Chang, H. M., Han, G. K., Kim, J. Y., Lee, J. M., Park, J. W., et al. (2007). Identification and functional analysis of salmon annexin 1 induced by a virus infection in a fish cell line. *J. Virol.* 81:13816. doi: 10.1128/JVI.02822-06

Irving, P., Troxler, L., Heuer, T. S., Belvin, M., Kopczynski, C., Reichhart, J. M., et al. (2001). A genome-wide analysis of immune responses in *Drosophila*. *Proc. Natl. Acad. Sci. U.S.A.* 98, 15119–15124. doi: 10.1073/pnas.261573998

Iseki, Y., Imoto, A., Okazaki, T., Harigae, H., and Takahashi, S. (2009). Identification of annexin 1 as a PU. 1 target gene in leukemia cells. *Leukemia Res.* 33, 1658–1663. doi: 10.1016/j.leukres.2009.04.010

Ji, Y. H., Xiong, R. Y., Cheng, Z. B., Zhou, T., Zhao, T. M., Yu, W. G., et al. (2008). Molecular diagnosis of *Tomato yellow leaf curl* disease in Jiangsu Province. *Acta Horticulturae Sinica* 35, 1815–1818. doi: 10.3724/SP.J.1005.2008.01083

Jiu, M., Zhou, X. P., Tong, L., Xu, J., Yang, X., Wan, F. H., et al. (2007). Vector-virus mutualism accelerates population increase of an invasive whitefly. *PLoS ONE* 2:e182. doi: 10.1371/journal.pone.0000182

Johnston, J. A., Ward, C. L., and Kopito, R. R. (1998). Aggresomes: a cellular response to misfolded proteins. *J. Cell Biol.* 143, 1883–1898. doi: 10.1083/jcb.143.7.1883

Jong, W. W. D., Leunissen, J. A., and Voorter, C. E. (1993). Evolution of the alpha-crystallin/small heat-shock protein family. *Mol. Biol. Evol.* 10:103.

Kaur, N., Chen, W., Zheng, Y., Hasegawa, D. K., Ling, K. S., Fei, Z., et al. (2017). Transcriptome analysis of the whitefly, *Bemisia tabaci* MEAM1 during feeding on tomato infected with the crinivirus, *Tomato chlorosis virus*, identifies a temporal shift in gene expression and differential regulation of novel orphan genes. *BMC Genom.* 18:370. doi: 10.1186/s12864-017-3751-1

Kim, D., Langmead, B., and Salzberg, S. L. (2015). HISAT: a fast spliced aligner with low memory requirements. *Nat. Methods* 12, 357–360. doi: 10.1038/nmeth.3317

Koya, R. C., Fujita, H., Shimizu, S., Ohtsu, M., Takimoto, M., Tsujimoto, Y., et al. (2000). Gelsolin inhibits apoptosis by blocking mitochondrial membrane potential loss and cytochrome c release. *J. Biol. Chem.* 275, 15343–15349. doi: 10.1074/jbc.275.20.15343

Kubo, Y., Hayashi, H., Matsuyama, T., Sato, H., and Yamamoto, N. (2012). Retrovirus entry by endocytosis and cathepsin proteases. *Adv. Virol.* 2012:640894. doi: 10.1155/2012/640894

Langmead, B., and Salzberg, S. L. (2012). Fast gapped-read alignment with Bowtie 2. *Nat. Methods* 9, 357–359. doi: 10.1038/nmeth.1923

Li, C. B., Cui, Y. L., Zhang, L. Y., and Li, C. Y. (2012). Molecular detection of *Tomato yellow leaf curl virus* (TYLCV). *Hereditas* 34, 366–370. doi: 10.3724/SP.J.1005.2012.00366

Li, J., Ding, T. B., Chi, H., and Chu, D. (2018). Effects of *Tomao chlorosis virus* on the performance of its key vector, *Bemisia tabaci*, in China. *J. Appl. Entomol.* 142, 296–304. doi: 10.1111/jen.12477

Li, R. M., Xie, W., Wang, S. L., Wu, Q. J., Yang, N. N., Yang, X., et al. (2013). Reference gene selection for qRT-PCR analysis in the sweetpotato whitefly, *Bemisia tabaci* (Hemiptera: Aleyrodidae). *PLoS ONE* 8:e53006. doi: 10.1371/journal.pone.0053006

Lindquist, S. L. (1986). The heat-shock response. *Annu. Rev. Biochem.* 55, 1151–1191. doi: 10.1146/annurev.bi.55.070186.005443

Liu, Y. G., Wei, J. P., Qiao, N., Li, M. Q., Liu, X. M., and Zhu, X. P. (2014). The occurrence and management of *Tomato chlorosis virus* in Shandong Province. *China Vegetables* 5, 67–69. doi: 10.3969/j.issn.1000-6346.2014.05.018

Livak, K. J., and Schmittgen, T. D. (2001). Analysis of relative gene expression data using real time quantitative PCR and the $2(-\Delta\Delta CT)$ method. *Methods* 25, 402–408. doi: 10.1006/meth.2001.1262

Love, M. I., Huber, W., and Anders, S. (2014). Moderated estimation of fold change and dispersion for RNA-seq data with DESeq 2. *Genome Biol.* 15:550. doi: 10.1186/s13059-014-0550-8

Luan, J. B., Li, J. M., Varela, N., Wang, Y. L., Li, F. F., Bao, Y. Y., et al. (2011). Global analysis of the transcriptional response of whitefly to *Tomato yellow leaf curl china virus* reveals the relationship of coevolved adaptations. *J. Virol.* 85, 3330–3340. doi: 10.1128/JVI.02507-10

Luan, J. B., Wang, Y. L., Wang, J., Wang, X. W., and Liu, S. S. (2013). Detoxification activity and energy cost is attenuated in whiteflies feeding on *Tomato yellow leaf curl China virus*-infected tobacco plants. *Insect Mol. Biol.* 22, 597–607. doi: 10.1111/imb.12048

Ma, H., Kien, F., Maniere, M., Zhang, Y., and Lararde, N. (2012). Human annexin A6 interacts with influenza A virus protein M2 and negatively modulates infection. *J. Virol.* 86, 1789–1801. doi: 10.1128/JVI.06003-11

Mauck, K. E., De Moraes, C. M., and Mescher, M. C. (2014). Biochemical and physiological mechanisms underlying effects of *Cucumber mosaic virus* on host-plant traits that mediate transmission by aphid vectors. *Plant Cell Environ.* 37, 1427–1439. doi: 10.1111/pce.12249

Mugiira, R. B., Liu, S. S., and Zhou, X. P. (2008). *Tomato yellow leaf curl virus* and *Tomato leaf curl Taiwan virus* invade south-ease coast of China. *J. Phytopathol.* 156, 217–221. doi: 10.1111/j.1439-0434.2007.01345.x

Murray, C. L., Quaglia, M., Arnason, J. T., and Morris, C. E. (1994). A putative nicotine pump at the metabolic blood-brain-barrier of the tobacco hornworm. *J. Neurobiol.* 25, 23–34. doi: 10.1002/neu.480250103

Navas-Castillo, J., Fiallo-Olive, E., and Sanchez-Campos, S. (2011). Emerging virus diseases transmitted by whiteflies. *Annu. Rev. Phytopathol.* 49, 219–248. doi: 10.1146/annurev-phyto-072910-095235

Okuda, T., and Haga, T. (2000). Functional characterization of the human high-affinity choline transporter. *FEBS Lett.* 484, 92–97. doi: 10.1016/S0014-5793(00)02134-7

Pan, H. P., Chu, D., Ge, D. Q., Wang, S. L., Wu, Q. J., Xie, W., et al. (2011). Further spread of and domination by *Bemisia tabaci* (Hemiptera: Aleyrodidae) biotype Q on field crops in China. *J. Econ. Entomol.* 104, 978–985. doi: 10.1603/EC11009

Pan, H. P., Chu, D., Yan, W. Q., Su, Q., Liu, B. M., Wang, S. L., et al. (2012). Rapid spread of *Tomato yellow leaf curl virus* in China is aided differentially by two invasive whiteflies. *PLoS ONE* 7:e34817. doi: 10.1371/journal.pone.0034817

Patel, D. M., Ahmad, S. F., Weiss, D. G., Gerke, V., and Kuznetsov, S. A. (2011). Annexin Al is a new functional linker between actin filaments and phagosomes during phagocytosis. *J. Cell Sci.* 124(Pt 4), 578–588. doi: 10.1242/jcs.076208

Polston, J. E., De Barro, P., and Boykin, L. M. (2014). Transmission specificities of plant viruses with the newly identified species of the *Bemisia tabaci* species comples. *Pest Manag. Sci.* 70, 1547–1552. doi: 10.1002/ps.3738

Rao, Q., Luo, C., Zhang, H., Guo, X., and Devine, G. J. (2011). Distribution and dynamics of *Bemisia tabaci* invasive biotypes in central China. *B. Entomol. Res.* 101, 81–88. doi: 10.1017/S0007485310000428

Ronnigen, T., Shah, A., Oldenburg, A. R., Vekterud, K., Delbarre, E., Moskaug, J. O., et al. (2015). Prepatterning of differentiation-driven nuclear lamin A/C-associated chromatin domains by GlcNAcylated histone H2B. *Genome Res.* 25, 1825–1835. doi: 10.1101/gr.193748.115

Saikhedkar, N., Summanwar, A., Joshi, R., and Giri, A. (2015). Cathepsins of lepidopteran insects: aspects and prospects. *Insect Biochem. Molec.* 64, 51–59. doi: 10.1016/j.ibmb.2015.07.005

Sanchez, D., Lopez-Arias, B., Torroja, L., Canal, I., Wang, X. H., Bastiani, M. J., et al. (2006). Loss of Glial Lazarillo, a homolog of apolipoprotein D, reduces lifespan and stress resistance in *Drosophila*. *Curr. Biol.* 16, 680–686. doi: 10.1016/j.cub.2006.03.024

Scott, J. G., Liu, N., and Wen, Z. (1998). Insect cytochromes P450: diversity, insecticide resistance and tolerance to plant toxins. *Comp. Biochem. and Phys. C* 121, 147–155. doi: 10.1016/S0742-8413(98)10035-X

Shelby, K. S., and Webb, B. A. (1997). Polydnavirus infection inhibits translation of specific growth-associated host proteins. *Insect Biochem. Molec.* 27, 263–270. doi: 10.1016/S0965-1748(96)00095-1

Shi, X. B., Pan, H. P., Xie, W., Wu, Q. J., Wang, S. L., Liu, Y., et al. (2013). Plant virus differentially alters the plant's defense response to its closely related vectors. *PLoS ONE* 8:e83520. doi: 10.1371/journal.pone.0083520

Shi, X. B., Tang, X., Zhang, X., Zhang, D. Y., Li, F., Yan, F., et al. (2018). Transmission efficiency, preference and behavior of *Bemisia tabaci* MEAM1 and MED under the influence of *Tomato chlorosis virus*. *Front. Plant Sci.* 8:2271. doi: 10.3389/fpls.2017.02271

Shrestha, A., Champagne, D. E., Culbreath, A. K., Rotenberg, D., Whitfield, A. E., and Srinivasan, R. (2017). Transcriptome changes associated with *Tomato spotted wilt virus* infection in various life stages of its thrips vector, *Fankliniella fusca* (Hinds). *J. Gen. Virol.* 98, 2156–2170. doi: 10.1099/jgv.0.000874

Sim, S., Ramirez, J. L., and Dimopoulos, G. (2012). Dengue virus infection of the *Aedes aegypti* salivary gland and chemosensory apparatus induces genes that modulated infection and blood-feeding behavior. *PLoS Pathog.* 8:e1002631. doi: 10.1371/journal.ppat.1002631

Sorensen, J. G., Kristensen, T. N., and Loeschcke, V. (2003). The evolutionary and ecological role of heat shock proteins. *Ecol. Lett.* 6, 1025–1037. doi: 10.1046/j.1461-0248.2003.00528.x

Stout, M. J., Thaler, J. S., and Thomma, B. P. H. J. (2006). Plant-mediated interactions between pathogenic microorganisms and herbivorous arthropods. *Annu. Rev. Entomol.* 51, 663–689. doi: 10.1146/annurev.ento.51.110104.151117

Strickler-Dinglasan, P. M., Guz, N., Attardo, G., and Aksoy, S. (2006). Molecular Characterization of iron binding proteins from *Glossina morsitans morsitans* (Diptera: Glossinidae). *Insect Biochem. Molec.* 36, 921–933. doi: 10.1016/j.ibmb.2006.09.003

Su, Q., Preisser, E. L., Zhou, X. M., Xie, W., Liu, B. M., Wang, S. L., et al. (2015). Manipulation of host quality and defense by a plant virus improves performance of whitefly vectors. *J. Econ. Entomol.* 108, 11–19. doi: 10.1093/jee/tou012

Sun, Z. W., Yang, J. X., Zhang, M. Z., and Li, X. D. (2009). Occurrence and control of *Tomato yellow leaf curl virus* disease in Shandong Province. *China Vegetables* 21, 5–6.

Tang, Y. F., He, Z. F., She, X. M., and Lan, G. B. (2017). Molecular identification of *Tomato chlorosis virus* infecting tomato in Guangdong Province. *Plant Prot.* 43, 133–137. doi: 10.3969/j.issn.0529-1542.2017.02.022

Tapadia, M. G., and Lakhotia, S. C. (2005). Expression of mdr49 and mdr65 multidrug resistance genes in larval tissues of *Drosophila melanogaster* under normal and stress conditions. *Cell Stress Chaperone.* 10, 7–11. doi: 10.1379/CSC-67R.1

Valverde, R. A., Sim, J., and Lotrakul, P. (2004). Whitefly transmission of sweet potato viruses. *Virus Res.* 100, 123–128. doi: 10.1016/j.virusres.2003.12.020

Wang, L. L., Wang, X. R., Wei, X. M., Huang, H., Wu, J. X., Chen, X. X., et al. (2016). The autophagy pathway participates in resistance to *tomato yellow leaf curl virus* infection in whiteflies. *Autophagy* 12, 1560–1574. doi: 10.1080/15548627.2016.1192749

Wang, S., Chi, X. J., Wei, H. T., Chen, Y. H., Chen, Z. L., Huang, S. L., et al. (2014). Influenza A virus-induced degradation of eukaryotic translation initiation factor 4B contributes to viral replication by suppressing IFITM3 protein expression. *J. Virol.* 88, 8375–8385. doi: 10.1128/JVI.00126-14

Wei, K. K., Li, J., Ding, T. B., and Chu, D. (2018). Research progress on distribution, identification method of *Tomato chlorosis virus* (ToCV) and whitefly transmission characteristics. *China Vegetables* 1, 19–24.

Wintermantel, W. M., and Wisler, G. C. (2006). Vector specificity, host range, and genetic diversity of *Tomato chlorosis virus*. *Plant Dis.* 90, 814–819. doi: 10.1094/PD-90-0814

Wisler, G. C., Li, R. H., Liu, H. Y., Lowry, D., and Duffus, J. E. (1998). *Tomato chlorosis virus*: a new whitefly-transmitted, phloem-limited, bipartite closterovirus of tomato. *Phytopathology* 88, 402–409. doi: 10.1094/PHYTO.1998.88.5.402

Wu, C. T., Budding, M., Griffin, M. S., and Croop, J. M. (1991). Isolation and characterization of *Drosophila* multidrug resistance gene homologs. *Mol. Cell. Biol.* 11, 3940–3948. doi: 10.1128/MCB.11.8.3940

Wu, J. B., Dai, F. M., and Zhou, X. P. (2006). First report of *Tomato yellow leaf curl virus* in China. *Plant Dis.* 90:1359. doi: 10.1094/PD-90-1359C

Wu, S. H., Li, T. F., Zhao, W. H., Cheng, Z. B., Guo, Q. Y., Zhao, T. M., et al. (2016). Molecular identification on mixed infection of *Tomato yellow leaf curl virus* and *Tomato chlorosis virus* on tomato in Jiangsu Province. *Acta Horticulturae Sinica* 43, 89–99.

Xie, W., Chen, C. H., Yang, Z. Z., Guo, L. T., Yang, X., Wang, D., et al. (2017). Genome sequencing of the sweetpotato whitefly *Bemisia tabaci* MED/Q. *GigaScience* 6, 1–7. doi: 10.1093/gigascience/gix018

Xu, Y., Zhou, W. W., Zhou, Y. J., Wu, J. X., and Zhou, X. P. (2012). Transcriptome and comparative gene expression analysis of *Sogatella furcifera* (Horvath) in response to *Southern rice black-streaked dwarf* virus. *PLoS ONE* 7:e36238. doi: 10.1371/journal.pone.0036238

Yoshiga, T., Georgieva, T., Dunkov, B. C., Harizanova, N., Ralchev, K. L., and Law, J. H. (1999). *Drosophila melanogaster* transferrin. *Eur. J. Biochem.* 260, 414–420. doi: 10.1046/j.1432-1327.1999.00173.x

Yoshiga, T., Hernandez, V. P., Fallon, A. M., and Law, J. H. (1997). Mosquito transferrin, an acute-phase protein that is up-regulated upon infection. *Proc. Natl. Acad. Sci. U.S.A.* 94, 12337–12342. doi: 10.1073/pnas.94.23.12337

Young, M. D., Wakefield, M. J., Smyth, G. K., and Oshlack, A. (2010). Gene ontology analysis for RNA-seq: accounting for selection bias. *Genome Biol.* 11:R14. doi: 10.1186/gb-2010-11-2-r14

Zhang, A. H., Zhang, S. M., Liu, S., Di, D. P., and Miao, H. Q. (2010). Occurrence and distribution of *Tomato yellow leaf curl* disease in Hebei Province. *Plant Prot.* 36, 127–129. doi: 10.3969/j.issn.0529-1542.2010.04.027

Zhang, Z. J., Zhang, P. J., Li, W. D., Zhang, J. M., Huang, F., Yang, J., et al. (2013). *De novo* transcriptome sequencing in *Frankliniella occidentalis* to identify genes involved in plant virus transmission and insecticide resistance. *Genomics* 101, 296–305. doi: 10.1016/j.ygeno.2013.02.005

Zhao, L. M., Li, G., Liu, Y. G., Guo, J. J., Wei, J. P., and Zhu, X. P. (2014). Molecular identification on mixed infections of *Tomato chlorosis virus* and *Tomato yellow leaf curl virus*. *China Vegetables* 12, 15–20. doi: 10.3969/j.issn.1000-6346.2014.12.006

Zhao, R., Wang, R., Wang, N., Fan, Z. F., Zhou, T., Shi, Y. C., et al. (2013). First report of *Tomato chlorosis virus* in China. *Plant Dis.* 97:1123. doi: 10.1094/PDIS-12-12-1163-PDN

Zheng, H. X., Xia, J. X., Zhou, X. M., and Zhang, Y. J. (2016). Be on alert of rapid diffusion of *Tomato chlorosis virus* transmitted by whitefly in China. *China Vegetables* 4, 22–26. doi: 10.3969/j.issn.1000-6346.2016.04.009

Zhou, T., Shi, Y. C., Chen, X. Y., and Fan, Z. F. (2010). Identification and control of *Tomato yellow leaf curl virus* disease in Beijing. *Plant Prot.* 36, 116–118. doi: 10.3969/j.issn.0529-1542.2010.02.026

Conflict of Interest Statement: The authors declare that the research was conducted in the absence of any commercial or financial relationships that could be construed as a potential conflict of interest.

frontiers in Physiology

ORIGINAL RESEARCH
published: 12 April 2019
doi: 10.3389/fphys.2019.00398

Mating Status of an Herbivorous Stink Bug Female Affects the Emission of Oviposition-Induced Plant Volatiles Exploited by an Egg Parasitoid

*Gianandrea Salerno[1], Francesca Frati[1], Eric Conti[1], Ezio Peri[2], Stefano Colazza[2] and Antonino Cusumano[3]**

[1] Dipartimento di Scienze Agrarie, Alimentari ed Ambientali, Università degli Studi di Perugia, Perugia, Italy, [2] Dipartimento di Scienze Agrarie, Alimentari e Forestali, Universitá degli Studi di Palermo, Palermo, Italy, [3] UMR 1333 DGIMI, INRA, Université de Montpellier, Montpellier, France

OPEN ACCESS

Edited by:
Patrizia Falabella, University of Basilicata, Italy

Reviewed by:
David Rivers, Loyola University Maryland, United States
Patricia C. Fernandez, National Scientific and Technical Research Council (CONICET), Argentina

***Correspondence:**
Antonino Cusumano
cusumanoantonino@tiscali.it

Specialty section:
This article was submitted to Invertebrate Physiology, a section of the journal Frontiers in Physiology

Received: *14 November 2018*
Accepted: *22 March 2019*
Published: *12 April 2019*

Citation:
Salerno G, Frati F, Conti E, Peri E, Colazza S and Cusumano A (2019) Mating Status of an Herbivorous Stink Bug Female Affects the Emission of Oviposition-Induced Plant Volatiles Exploited by an Egg Parasitoid. Front. Physiol. 10:398. doi: 10.3389/fphys.2019.00398

Insect parasitoids are under selection pressure to optimize their host location strategy in order to maximize fitness. In parasitoid species that develop on host eggs, one of these strategies consists in the exploitation of oviposition-induced plant volatiles (OIPVs), specific blends of volatile organic compounds released by plants in response to egg deposition by herbivorous insects. Plants can recognize insect oviposition via elicitors that trigger OIPVs, but very few elicitors have been characterized so far. In particular, the source and the nature of the elicitor responsible of egg parasitoid recruitment in the case of plants induced with oviposition by stink bugs are still unknown. In this paper, we conducted behavioral and molecular investigations to localize the source of the elicitor that attracts egg parasitoids and elucidate the role of host mating in elicitation of plant responses. We used as organism study model a tritrophic system consisting of the egg parasitoid *Trissolcus basalis*, the stink bug host *Nezara viridula* and the plant *Vicia faba*. We found that egg parasitoid attraction to plant volatiles is triggered by extracts coming from the dilated portion of the stink bug spermathecal complex. However, attraction only occurs if extracts are obtained from mated females but not from virgin ones. Egg parasitoid attraction was not observed when extracts coming from the accessory glands (mesadene and ectadene) of male hosts were applied, either alone or in combination to plants. SDS-PAGE electrophoresis correlated with olfactometer observations as the protein profile of the dilated portion of the spermathecal complex was affected by the stink bug mating status suggesting post-copulatory physiological changes in this reproductive structure. This study contributed to better understanding the host location process by egg parasitoids and laid the basis for the chemical characterization of the elicitor responsible for OIPV emission.

Keywords: *Trissolcus basalis*, *Nezara viridula*, *Vicia faba*, indirect plant defenses, OIPVs, elicitor

INTRODUCTION

Hymenopteran parasitoids play a key ecological role in many ecosystems and these insects have been recently suggested to be the most species-rich group within the animal kingdom (Forbes et al., 2018). Many parasitoid species are natural enemies of insect pests, which can be used in integrated pest management with the aim of reducing pesticide applications (van Lenteren, 2012; Heimpel and Mills, 2017). One of the key aspects for the success of a parasitoid species as biological control agent is its host finding efficiency: parasitoids can exploit a wide array of cues when foraging for hosts, among which chemical cues convey essential information (Fatouros et al., 2008; Colazza et al., 2014). When parasitoids are far from their hosts, they can use volatile chemicals to narrow-down the area in which hosts are present, whereas contact chemicals become progressively more important once in the close proximity or in contact with the host (Vinson, 1998).

Egg parasitoids have evolved the capacity to develop exclusively on host eggs (Godfray, 1994). The ability to kill the pest before the crop feeding stage makes them very attractive in biological pest control as crop damage is kept to a minimum (Tamiru et al., 2015; Fatouros et al., 2016). Due to this adaptation, egg parasitoids face specific challenges as host eggs are generally inconspicuous and their quality decreases rapidly with egg age because of embryo development (Vinson, 1998; Fatouros et al., 2008). To cope with these challenges, egg parasitoids have evolved specific strategies in order to discover patches where host eggs have just been laid or where gravid host females are present. One of these strategies consists in the exploitation of oviposition-induced plant volatiles (OIPVs), specific blends of volatile organic compounds released by plants in response to egg deposition by herbivorous insects (Hilker and Fatouros, 2015).

Oviposition-induced plant volatiles are known to be widespread within the plant kingdom, as they have been reported to occur in several plant species, regardless of being gymnosperms or angiosperms, annuals or perennials (Fatouros et al., 2016). Depending on the egg deposition modality of the herbivores, OIPV emission can be associated with mechanical damage, as in the elm leaf beetle *Xanthogaleruca luteola* (Meiners and Hilker, 2000) and in the pine sawflies *Diprion pini* and *Neodiprion sertifer* (Hilker et al., 2002; Mumm et al., 2003), or OIPV emission can occur without obvious mechanical damage, as in the case of oviposition by butterflies and moths (Tamiru et al., 2011; Fatouros et al., 2012, Salerno et al., 2013). In the case of the stink bug *Nezara viridula*, a combination of feeding and oviposition activity is required for the emission of OIPVs that recruit egg parasitoids (Colazza et al., 2004; Moujahed et al., 2014, Frati et al., 2017).

Plants can recognize insect oviposition via elicitors that trigger OIPV release or changes in plant cuticular waxes leading to parasitoid recruitment (Hilker and Fatouros, 2015). Very few elicitors have been characterized so far but their chemical nature and origin can vary broadly. In the pine sawfly *D. pini*, the active principle attracting the egg parasitoid *Chrysonotomyia ruforum* to Scots pines is localized in the oviduct secretions and it has been shown to be of proteinaceous nature (Hilker et al., 2005). In *Pieris* butterflies, antiaphrodisiacs (benzyl cyanide and indole) transferred by the male butterfly to the female during mating induce changes in the epicuticular waxes of brassicaceous plants leading to arrestment of *Trichogramma* wasps (Fatouros et al., 2009; Blenn et al., 2012). Thus, in the latter case, it is remarkable to note that egg parasitoids gain reliable information for host location using a sophisticated strategy that involves exploitation of host sexual communication mediated by the plant.

The source and the nature of the elicitor responsible of egg parasitoid recruitment by leguminous plants induced with stink bug oviposition and feeding is still unknown. Previous studies have shown that scelionid egg parasitoids can eavesdrop the sexual communication of their stink bug hosts (Laumann et al., 2007, 2011) and distinguish between mated and virgin host adults: for example the egg parasitoid *Trissolcus basalis* searches intensively in patches contaminated with contact chemicals left by *N. viridula* host adults with a preference for those cues released by females in a pre-ovipositional state (Colazza et al., 1999). The egg parasitoid *Trissolcus brochymenae* exhibits an even more finely-tuned strategy to locate the host *Murgantia histrionica* as the wasp can discriminate between mated females that have not yet laid eggs and those that already had (Salerno et al., 2009). In particular, morphological and physiological alterations in the dilated portion of the spermathecal complex (=bursa copulatrix) after mating have been shown to be important for egg parasitoid attraction (Salerno et al., 2009). After copulation, the physiological status of females changes, with possible consequences for the chemical profile of cuticular hydrocarbons (Zahn et al., 2008), which are used by egg parasitoids to discriminate between male and female hosts (Colazza et al., 2007; Salerno et al., 2009).

In this paper, we investigated if the mating status of an herbivorous stink bug female affects the elicitation of OIPVs exploited by an egg parasitoid. In addition to sperm, stink bug males also transfer other seminal substances during mating which have been detected in female organs such as the dilated portion of the spermathecal complex and the ovary (including the common oviduct) (Koshiyama et al., 1993, Salerno and Cusumano, personal observations). These proteinaceous substances are produced in male accessory glands (ectadene and mesadene) and have been suggested to have nutritional functions for the females (McLain, 1980; Kon et al., 1993). Using as model study organisms the tritrophic system consisting of the egg parasitoid *T. basalis*, the host *N. viridula* and the plant *Vicia faba*, we conducted behavioral and molecular investigations to localize the source of the elicitor that attracts egg parasitoids and elucidate the role of host mating in elicitation of plant responses. We tested two alternative hypothesis: (1) substances transferred from host males to females during mating could be directly implicated in the attraction of the egg parasitoid toward OIPVs; (2) mating induces physiological changes in host females that indirectly trigger OIPV emission and egg parasitoid attraction.

MATERIALS AND METHODS

Insects and Plants

The *N. viridula* colony, established from material collected in cultivated and uncultivated fields around Perugia, was reared under controlled conditions (24 ± 2°C; 70 ± 5% RH;16 h:8 h L:D) inside clear plastic food containers (30 cm × 19.5 cm × 12.5 cm) with 5 cm diameter mesh-covered holes for ventilation. Bugs were fed with a diet of sunflower seeds and seasonal fresh vegetables. Food was changed every 2–3 days, and separate cages were used for nymphs and adults. Egg masses were collected daily and used to maintain colonies of both *N. viridula* and *T. basalis*. The *N. viridula* colony was supplemented regularly with field-collected bugs.

The colony of *T. basalis* was originally established from wasps emerging from *N. viridula* egg masses, located in wild and cultivated fields around Perugia. The parasitoid was reared on *N. viridula* egg masses that were glued on paper strips. Wasps were maintained in 85 ml glass tubes, fed with a honey-water solution and kept in controlled climatic chamber under the same rearing conditions of *N. viridula*. After emergence, male and female wasps were kept together to allow mating. For all bioassays, 2–4 days old females. All tested wasps were naïve (i.e., they had no previous contact with plants).

Seeds of broad bean plants (*V. faba* cv. Superaguadulce) were individually planted in plastic pots (9 cm × 9 cm × 13 cm) filled with a mixture of agriperlite (Superlite, Gyproc Saint-Gobain, PPC Italia, Italy), vermiculite (Silver, Gyproc Saint-Gobain, PPC Italia, Italy), and sand (1:1:1) and grown in a climate controlled chamber (24 ± 2°C, 45 ± 10%RH, 12 h:12 h L:D). Plants were watered daily and, from 1 week post-germination, fertilized with an aqueous solution (1.4 g/l) of fertilizer (5-15-45, N-P-K, Plantfol, Valagro, Italy). Plants with approximately 4 expanded leaves were used for experiments.

Treatments

The test plants used in the bioassays were always exposed to *N. viridula* females and subjected to the following treatments (**Figure 1**): (1) feeding; (2) feeding + oviposition; (3) ovarian eggs + feeding; (4) ovarian eggs + extracts from the dilated portion of the spermathecal complex of mated females + feeding; (5) extracts from the dilated portion of the spermathecal complex of mated females + feeding; (6) extracts from the dilated portion of the spermathecal complex of virgin females + feeding; (7) extracts from the spermathecal bulb + feeding; (8) male accessory gland extracts (mesadene and ectadene) + feeding; (9) mesadene extracts + feeding; (10) ectadene extract + feeding. Previous studies have shown that parasitoid attraction is not observed when plants are induced with eggs only leading to the exclusion of egg deposition treatment from the current study (Colazza et al., 2004). Similarly, previous works have shown that OIPV recruiting egg parasitoids are emitted only when egg deposition occurs in combination with feeding activity of stink bugs (Colazza et al., 2004); thus we decided to include stink bug feeding activity in all the treatments.

For all treatments (1–10), a mated *N. viridula* female was placed for 24 h on the lower surface of a leaf in the central plant portion, inside a "clip cage" made of two modified plastic Petri dishes (Ø = 10 cm; *h* = 1 cm), with a mesh- covered hole in the bottom and the rim covered by a small sponge ring. This plant–bug complex was kept in a controlled environment cabinet (24 ± 2°C, 55 ± 10% RH; 12 h:12 h L:D) allowing the insect to feed and oviposit (treatment 2) or to feed (treatments 1,3-10) and after 24 h the insect was removed. For treatments 1,3-10, plants where the females oviposited were discarded. For treatments 3–10 ovarian eggs and/or extracts were applied together with the insect exposure. Treated plants were used for all the bioassays 24h after the end of the insect exposure. Healthy plants with an empty clip cage applied on a leaf for 24h, were used as controls (24 h after the clip removal).

To exclude an effect of the glue that stink bug females use to attach eggs on the leaves, plants with ovarian eggs were used in treatments 3 and 4. Plants with ovarian eggs (treatment 3) were obtained by applying carefully with a tiny brush 30 ovarian eggs near the clip cage confining the *N. viridula* female onto the lower leaf surface. Ovarian eggs were collected by dissecting *N. viridula* mated females. Females were previously anesthetized at −4°C for 3 min and dissected with the aid of micro-scissors in phosphate buffered saline solution (PBS).

To obtain plants treated with extracts from the spermathecal complex of females and from male accessory glands (treatments 4–10), stink bugs were anesthetized and dissected with the aid of micro-scissors as described above. From stink bug females, the spermathecal apparatus was removed from the abdomen and separated in: (a) the dilated portion of the spermathecal complex and (b) the spermathecal bulb, which were placed in different 1.5 ml Eppendorf tubes containing 10 μl of PBS each (one organ/tube). Tissues were disrupted with the aid of a pestle, then centrifuged at 10000 × *g* for 5 min at 4°C and finally 10 μl of supernatant (=1 bug equivalent) was collected from each sample to be used for plant induction. Stink bug males were anesthetized and dissected similarly to females, and male accessory glands (mesadene and ectadene) were isolated using micro-scissors and placed separately in Eppendorf tubes containing 10 μl of PBS (one organ/tube). Tissues were disrupted, centrifuged at the same conditions as described for females, and 10 μl of supernatant was collected.

In the treatments 4–7, plants were induced with extracts obtained from female stink bugs. In particular, for treatment 4, 30 ovarian eggs were placed into contact with the extract from the spermathecal complex for 3 min and then eggs were carefully applied to a plant leaf with a brush as described above. 10 μl of extract obtained from the dilated duct of the spermathecal complex of mated or virgin females was applied directly onto the leaf in treatments 5 and 6, respectively. For treatment 7, 10 μl of extract obtained from the spermathecal bulb of mated females was applied onto the leaf of one plant.

In the treatments 8–10, plants were treated with extract obtained from accessory glands of virgin males (mesadene and ectadene). One bug equivalent (10 μl) of each gland was used for treatment 8 whereas mesadene and ectadene extracts were

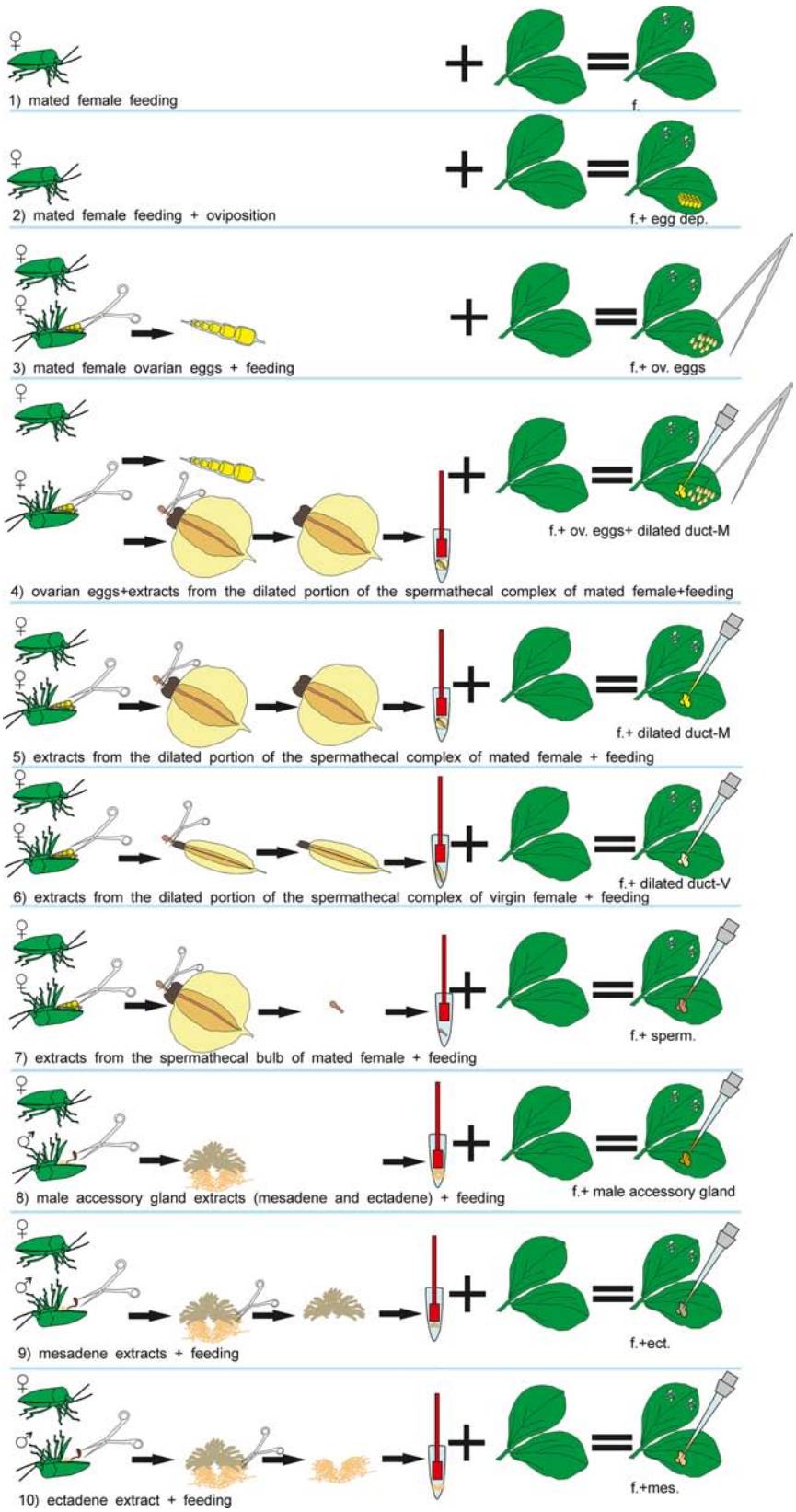

FIGURE 1 | Visual summary of *Nezara viridula* dissections and subsequent treatments of *Vicia faba* plants.

used separately to induce plants for treatment 9 and treatment 10 respectively.

Y-Tube Bioassays

Wasps' responses to volatile chemicals from differently treated *V. faba* plants were investigated with a dual choice Y-tube olfactometer made from a polycarbonate body (stem 9 cm; arms 8 cm at 130° angle; ID 1.5 cm) sandwiched between two glass plates. A stream of clean air (medical-grade compressed air, N_2:O_2 80:20), humidified by bubbling through a water jar, was regulated in each arm by a flowmeter at about 0.40 l min^{-1}. The device was illuminated from above by two 22-W cool white fluorescent tubes, and from below by an infrared source (homogeneous emission of wavelengths at 950 nm provided by 108 LEDs). Before entering the olfactometer arms, each airstream passed through a cylindrical glass chamber (Ø = 12 cm; h = 52 cm) with an O-ring sealed middle joint, containing a treated plant as odor source. The stimuli were randomly assigned at the beginning of the bioassays and were switched regularly to avoid possible bias in the system. At every switch, the whole system was changed with clean parts. At the end of the bioassays, the polycarbonate olfactometer and all glass parts were cleaned with water. The glass parts were then cleaned with acetone and baked overnight at 180°C. Wasp females were singly introduced into the Y-tube olfactometer at the entrance of the stem and allowed to move freely for 10 min. Their behavior was recorded using a monochrome CCD video camera (Sony SSC M370 CE) fitted with a 12.5–75 mm/F 1.8 zoom lens. The camera lens was covered with an infrared pass filter (Kodak Wratten filter 87 Å) to remove visible wavelengths. Analog video signals from the camera were digitized by a video frame grabber (Canopus® ADVC 110, Grass Valley CA, United States).

Digitized data were processed by XBug, a video tracking and motion analysis software (Colazza et al., 1999). Wasp response was measured in terms of residence time, i.e., the time spent by the wasps in each arm during the entire bioassay. The Y-tube olfactometer bioassays were carried out as paired choices, in which plants treated as described in the previous section were always tested *versus* healthy plants used as control. For each paired combination at least 20 replicates have been carried out (see **Figure 2**).

Protein Concentration and SDS-PAGE

To investigate changes in morphology and protein content occurring in the dilated portion of the spermathecal complex after mating, virgin and mated females were dissected as described above and for each female we quantified: (1) the area of the dilated portion of the spermathecal complex measured under an Olympus MVX10 stereoscope fitted with a XC50 camera using the Olympus cellSens digital imaging software; (2) the protein concentration in the dilated portion using the Bradford bioassays (Bradford, 1976). For each group, 6–7 replicates were carried out.

SDS-PAGE gel electrophoresis was carried out to compare the protein profiles of male accessory glands (ectadene and mesadene) with the profile of the dilated portion of the spermathecal complex in females (both virgin and mated ones). For each of the four groups, gland extracts were obtained as described in the previous section and samples containing 20 μg of proteins, derived by pooling together 5 insects, were loaded in each lane. The proteins in the samples were separated using Precast 4–15% Ready Gel (Bio-Rad), under denaturating conditions. Electrophoresis was performed in 25 mM Tris-HCl pH 8.8, 195 mM glycine, and 0.1% (w/v) SDS at a constant current of 30 mA. Gels were stained with Coomassie Brilliant blue R-250 (Bio-Rad). Preliminary SDS-PAGE electrophoresis loading lanes with extracts from single spermathecal organs were replicated 3–4 times for virgin and mated females, respectively, to evaluate the consistency of protein profile patterns (see **Supplementary Figure 1**).

Statistical Analyses

For the olfactometer bioassays, data was tested for normality (Shapiro-Wilk test). Because there was no significant deviation from normal distribution, the time spent by wasp females in each arm was statistically compared by parametric paired t-tests for dependent samples. Linear models were used to test the effect of mating status on the protein concentration of the dilated portion of the spermathecal complex, using the area of the dilated portion as covariate in the model. Significance of the variables in the model was determined using Likelihood Ratio Tests (LRTs) comparing the full model with and without the variable in question starting with interaction effects (Crawley, 2007). Model fit was assessed with residual plots. SDS-PAGE gel obtained by loading lanes with extracts from single spermathecal organs of virgin and mated females were analyzed with the software program Scion Image (Scion Corp., Frederick, MY, United States) in order to assess protein amounts. The detailed steps for relative quantification of band proteins can be found in the software manual[1]. Relative areas of the most characteristic bands associated with virgin and mated females were compared with t-tests after checking that assumptions of normality were met (Shapiro-Wilk test). Olfactometer data were analyzed using the STATISTICA7 software (StatSoft Inc., 2001) whereas all other analyses were carried out using the R software version 3.4.4 (R Core Team, 2013).

RESULTS

Olfactometer Bioassays

Trissolcus basalis females were significantly attracted to volatiles emitted by plants induced with a combination of feeding and oviposition activity of *N. viridula* (t = −2.10, df = 45, P = 0.0411) (**Figure 2**). On the contrary, wasps did not prefer plants induced only with stink bug feeding activity when tested against control plants (t = −0.10, df = 35, P = 0.9203). Similarly, the addition of ovarian eggs to plants damaged by stink bug feeding did not trigger parasitoid attraction (t = 0.99, df = 38, P = 0.3265). Regardless of the application of ovarian eggs, *T. basalis* attraction was restored when extracts coming from the dilated portion of the spermathecal complex of mated females were applied to plants (ovarian eggs + feeding + spermathecal extracts: t = 2.73,

[1]http://mesonpi.cat.cbpf.br/e2002/cursos/NotasAula/ScnImage.pdf

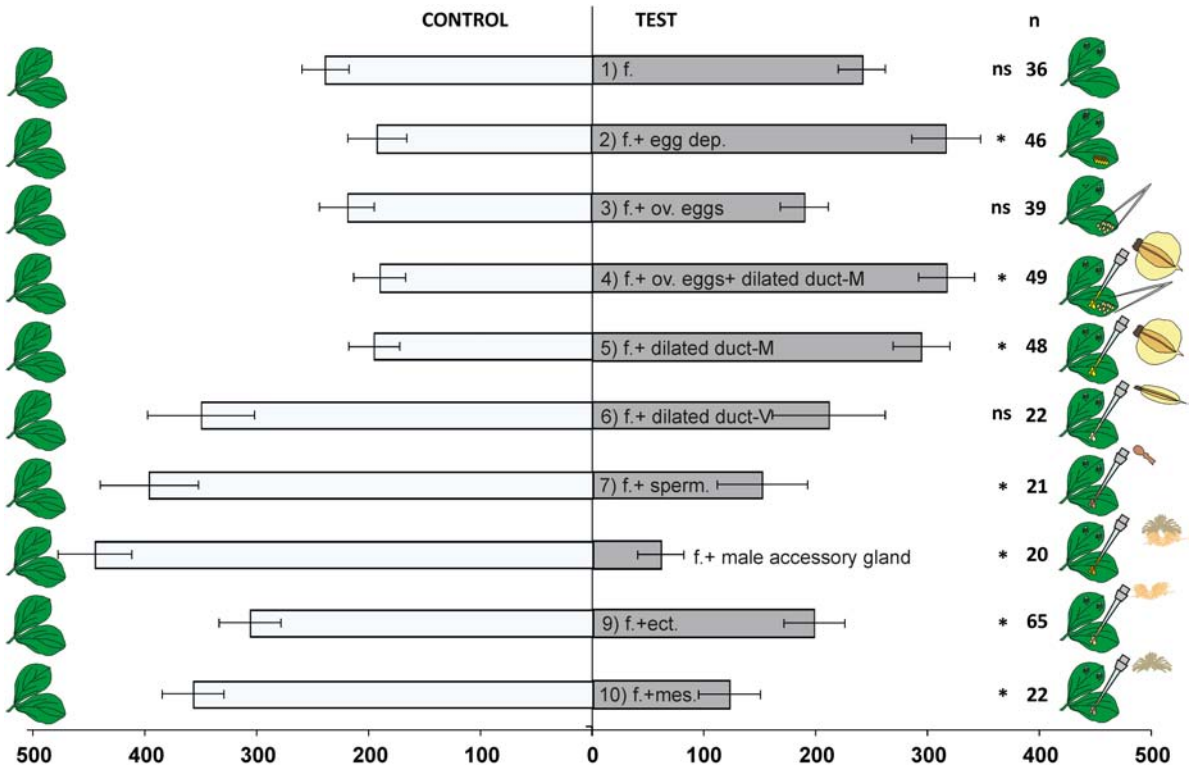

FIGURE 2 | Response of *Trissolcus basalis* females in a Y-tube olfactometer to volatiles from *V. faba* plants subjected to different treatments *versus* healthy plants (used as controls). f. = feeding; egg dep. = oviposition; ov. eggs = ovarian eggs; dilated duct-M = dilated portion of the spermathecal complex in mated females; dilated duct-V = dilated portion of the spermatechal complex in virgin females; sperm. = spermathecal bulb, mes. = mesadene, ect. = ectadene. N = number of replicates. Bars represent mean (±SE) of the time spent by wasp females in each arm over an observation period of 600 s (*t*-test for dependent samples, ns = not significant; $*P < 0.05$).

df = 48, $P = 0.0088$; feeding + spermathecal extracts: $t = 2.22$, df = 47, $P = 0.0315$). On the contrary, extracts coming from the dilated portion of the spermathecal complex of virgin females did not trigger parasitoid attraction when tested over control plants ($t = -1.43$, df = 21, $P = 0.1670$). Parasitoids preferred the control plants when tested against *N. viridula* feeding-induced plants which were treated with extracts coming from the spermathecal bulb ($t = -2.76$, df = 20, $P = 0.0121$). A similar preference for control plants was observed when extracts coming from the male accessory glands (mesadene and ectadene) were applied, either alone (ectadene: $t = -2.09$, df = 64, $P = 0.0409$; mesadene: $t = -4.59$, df = 21, $P = 0.0002$) or in combination ($t = -7.30$, df = 19, $P < 0.0001$) to plants damaged by *N. viridula* feeding activity.

Protein Concentration and SDS-PAGE

Protein concentration in the dilated portion of the spermathecal complex was significantly affected by mating status (GLM: $\chi^2 = 4.96$, df = 1, $P = 0.0259$) as well as by the area of the organ ($\chi^2 = 14.25$, df = 1, $P = 0.0002$) whereas there was no significant mating status × area interaction ($\chi^2 = 0.71$, df = 1, $P = 0.3979$) (**Figure 3**).

The SDS-PAGE profile of the dilated portion of the spermathecal complex consists of several proteins ranging in size from ∼10 to ∼170 kDa (**Figure 4**). The protein profile appears to be different between virgin and mated females although we cannot exclude the possibility that protein profiles simply differ in expression levels. Consistency of the whole protein profiles was observed among replicates of individual mated females ($N = 4$) as well as among virgin females ($N = 3$) (**Supplementary Figure 1**). Relative quantification of protein amount is different in characteristic bands associated with mated females (band n. 3 at ∼70 kDa, bands n. 8–9 at ∼35 kDa) or virgin females (bands 4–7 between 40 and 55 kDa). Some bands appear to be present only in mated (band n. 10 at ∼10 kDa) or virgin females (band n. 1–2 at ∼100 kDa) (**Supplementary Table 1**). The protein profile of male accessory glands (mesadene and ectadene) is very similar between them but no analogous similarity is found in terms of protein content between male accessory glands and the dilated portion of the spermathecal complex of mated females, except for a band of ∼70 kDa which deserves to be better investigated.

DISCUSSION

In this paper we show that mating status of the stink bug host affects the emission of OIPVs in leguminous plants leading to

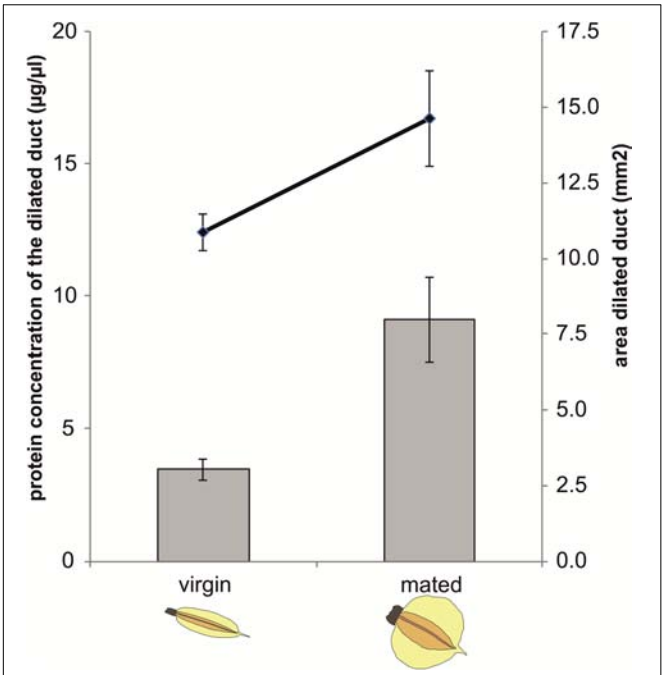

FIGURE 3 | Protein concentration and size of the dilated portion of the spermathecal complex in virgin and mated *Nezara viridula* females. Bars represent means ± SE of protein concentrations (µg/µl) in virgin and mated bugs. Lines represent means ± SE of the size of the organs (mm^2) in virgin and mated bugs (GLM, $^*P < 0.05$). For each group, 6–7 replicates were carried out.

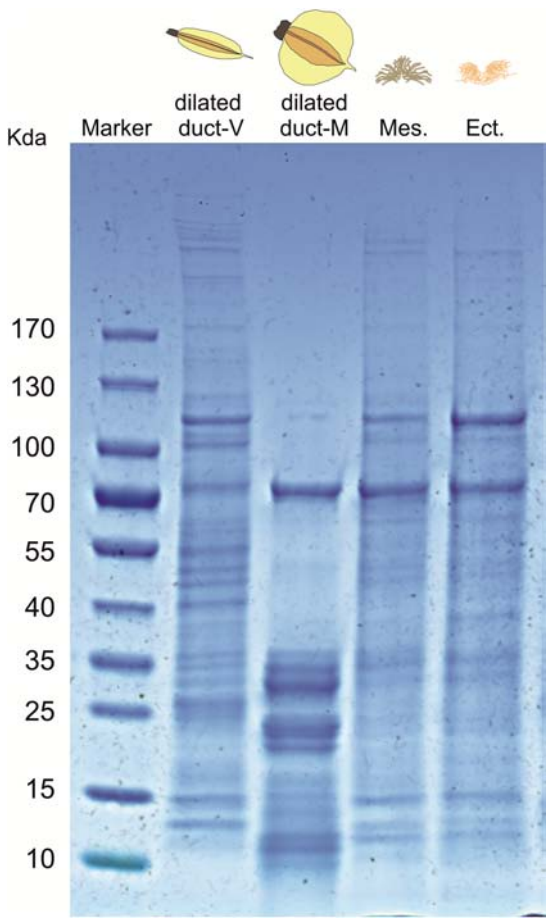

FIGURE 4 | SDS-PAGE profile of: the dilated portion of the spermathecal complex in virgin (V) and mated (M) *Nezara viridula* females; male accessory gland mesadene (Mes) and ectadene (Ect). Each lane was loaded with biological material derived by pooling five stink bug insects. An equivalent lane from the same gel (4–15% SDS-PAGE) showing the molecular mass of the protein marker is presented on the left stained with Coomassie Brilliant blue R-250.

egg parasitoid response. Previous investigations have shown that *N. viridula* feeding and oviposition activities are required to induce *V. faba* plant volatiles that are attractive for *T. basalis* (Colazza et al., 2004; Moujahed et al., 2014, Frati et al., 2017). Application of ovarian eggs does not mimic the effect of oviposition in terms of parasitoid recruitment unless secretions belonging to the dilated portion of the spermathecal complex are also applied onto plant leaves. Interestingly, these secretions trigger wasp attraction even without the concurrent application of host eggs on the plant: however, the parasitoid response occurs only when stink bugs are mated, which suggests that the role of the dilated portion of the spermathecal complex as a source of the elicitor of OIPVs is strictly dependent on the host mating status.

In another tritrophic system it was shown that, during mating, male butterfly transfers antiaphrodisiacs (benzyl cyanide and indole) to the female butterfly along with sperm, to reduce attractiveness toward conspecific males (Andersson et al., 2003). Traces of antiaphrodisiacs were detected into female accessory glands and, when in contact with brassicaceous plants, these compounds induce wax epicuticular changes that arrest *Trichogramma* egg parasitoids (Fatouros et al., 2009). However, application of antiaphrodisiacs do not fully mimic egg deposition in terms of plant defences, as these compounds do not trigger OIPVs attracting *Trichogramma* parasitoids (Fatouros et al., 2015). This is similar to our findings, as *T. basalis* attraction could not be restored when secretions from *N. viridula* male accessory glands were applied to *V. faba* plants highlighting the intricacy of plant responses to insect egg deposition. In our model-study system we found that parasitoids were repelled when extracts from mesadene and ectadene were applied alone or in combination to the plants. As a similar effect was also found when plants were treated with spermathecal bulb extracts containing sperm, it is possible to argue that the elicitor is not a male-derived substance(s) capable *alone* to trigger in the plant the emission of volatiles that attract egg parasitoids. Whereas it is difficult to interpret these repellence effects in the light of the foraging strategy of egg parasitoids, these results confirmed the importance of mating for the elicitation of OIPVs, suggesting that female-derived substances are also needed for restoring parasitoid attraction.

In several heteropteran species, mating is a complex process that can last several days during which sperm and associated seminal fluids are transferred from males to females (Schrader, 1960; Mitchell and Mau, 1969; Mau and Mitchell, 1978; Kasule, 1986; Koshiyama et al., 1993; Wang and Millar, 1997; Ho and Millar, 2001a,b). Because seminal fluid proteins are known to be transferred during mating in *N. viridula* (Kon et al., 1993; Koshiyama et al., 1993), we investigated the protein profiles of male accessory glands and of the dilated portion of the spermathecal complex (in both virgin and mated females) to look for pattern similarities. SDS-PAGE results suggest that the protein profile of the dilated portion of the spermathecal complex is affected by the insect mating status although expression studies are needed to confirm increased abundance (a band at ∼70 kDa, and multiple bands at ∼35 kDa) or presence of specific proteins (a band at ∼10 kDa) only in mated females. This finding correlated with the behavioral assays, since only secretions from *N. viridula* mated bugs elicit *T. basalis* attraction to *V. faba* plant volatiles. Nonetheless, additional investigations are clearly required to provide evidence for the proteinaceous nature of the elicitor but it should be noted that the only identified elicitors of OIPV release and parasitoid recruitment are small proteinaceous compounds (Hilker et al., 2005). In addition, SDS-PAGE indicated no clear similarity of the protein patterns among male accessory glands and the dilated portion of the spermathecal complex of mated females, except for a band of ∼70 kDa which should be investigated with expression studies.

Here we propose two possible scenarios to explain our results. (1) Mating event triggers changes in the physiological status of the females, which, in turn, are *indirectly* responsible of egg parasitoid recruitment. In fact, it is known that seminal fluid proteins produced in reproductive tract tissues of male insects and transferred to females during mating induce numerous physiological and behavioral post-mating changes in females (Gillott, 2003; Avila et al., 2011). The fact that, according to our SDS-PAGE results, some proteins seem to be only present in the dilated portion of the spermathecal complex of virgin females (and disappear in mated ones) could be a further indication of the complexity of these post-mating changes. Thus, in our study, physiological changes stimulated by seminal fluids in *N. viridula* could trigger OIPV emission in *V. faba* and *T. basalis* attraction. (2) Alternatively, compounds transferred by males to females during mating (i.e., a putative protein of ∼70 kDa) are *directly* responsible of egg parasitoid recruitment only in the presence of a "suitable chemical background" provided by the females. In fact, extracts of male accessory glands do not elicit an attraction response in the wasp, and activity is triggered only by the dilated portion of the spermathecal complex of mated females. Because SDS-PAGE suggests presence of a protein of ∼70 kDa that seems to be shared both in male accessory glands and in the bursa copulatrix of mated females, further investigations should be carried out in order to confirm that this protein is transferred during copulation and whether it is involved in elicitation of plant responses. Although we are not aware of any study showing activity of a putative elicitor only when in combination with the "right chemical mixture," the importance of the background composition has been demonstrated in the chemical ecology of plant volatiles recruiting egg parasitoids. In fact, for the egg parasitoid *C. ruforum*, the key compound (*E*)-β-farnesene is only attractive when present in a contrasting background odor from undamaged pine twigs (Mumm and Hilker, 2005).

To conclude here we report that mating of *N. viridula* is essential to trigger, in *V. faba* plants, emission of volatiles that attract the parasitoid *T. basalis*. Our behavioral assays provide evidence that the source of the elicitor is localized in the dilated portion of spermathecal complex of mated *N. viridula* females and our SDS-PAGE investigations indicate that mating affects the whole protein profile of this organ. While the behavioral results correlate with changes in the dilated portion of the spermathecal complex of virgin and mated stink bug females, further behavioral assays are needed to clarify the chemical nature of the elicitor responsible of plant-mediated parasitoid attraction. In particular, treatments with proteinases are required to test if the activity of secretions coming from the dilated spermathecal duct of mated females is lost after enzymatic digestion. If the proteinaceous nature of the elicitor is confirmed, then a combined transcriptomic and proteomic approach targeting male accessory glands and the dilated portion of the spermathecal complex of virgin and mated females is needed for the chemical characterization of the proteins. A transcriptomic analysis would also allow to identify candidate genes whose function could be further studied, for example using the RNA interference technology which is known to be efficient in true bugs.

ETHICS STATEMENT

The study used insects, but none of the manipulations involved in experiments raise ethical issues. All animal care and experimentation complied with the guidelines provided by the Association for the Study of Animal Behavior (ASAB) and the Animal Behavior Society (ABS).

AUTHOR CONTRIBUTIONS

All authors conceived and designed the experiments, interpreted the results, and drafted and revised the article. GS, FF, and AC performed the experiments and analyzed the data.

FUNDING

This research was partially supported by the Marie Skłodowska-Curie Research and Innovation Staff Exchange (RISE) H2020-MSCA-RISE-2015 of the European Union with the project Impact of invasive alien true bug species in native trophic webs—INVASIoN (GA 690952).

ACKNOWLEDGMENTS

We thank Andrea Lucchetti for rearing the insects, Ange Lorenzi for assistance with Bradford assays and Anne-Sophie Gosselin for assistance with SDS-PAGE electrophoresis.

SUPPLEMENTARY MATERIAL

The Supplementary Material for this article can be found online at: https://www.frontiersin.org/articles/10.3389/fphys.2019.00398/full#supplementary-material

REFERENCES

Andersson, J., Borg-Karlson, A. K., and Wiklund, C. (2003). Antiaphrodisiacs in pierid butterflies: a theme with variation! *J. Chem. Ecol.* 29, 1489–1499. doi: 10.1023/A:1024277823101

Avila, F. W., Sirot, L. K., LaFlamme, B. A., Rubinstein, C. D., and Wolfner, M. F. (2011). Insect seminal fluid proteins: identification and function. *Annu. Rev. Entomol.* 56, 21–40. doi: 10.1146/annurev-ento-120709-144823

Blenn, B., Bandoly, M., Küffner, A., Otte, T., Geiselhardt, S., Fatouros, N. E., et al. (2012). Insect egg deposition induces indirect defense and epicuticular wax changes in *Arabidopsis thaliana*. *J. Chem. Ecol.* 38, 882–892. doi: 10.1007/s10886-012-0132-8

Bradford, M. M. (1976). A rapid and sensitive method for the quantitation of microgram quantities of protein utilizing the principle of protein-dye binding. *Anal. Biochem.* 72, 248–254. doi: 10.1016/0003-2697(76)90527-3

Colazza, S., Aquila, G., De Pasquale, C., Peri, E., and Millar, J. G. (2007). The egg parasitoid *Trissolcus basalis* uses n-nonadecane, a cuticular hydrocarbon from its stink bug host *Nezara viridula*, to discriminate between female and male hosts. *J. Chemi. Ecol.* 33, 1405–1420. doi: 10.1007/s10886-007-9300-7

Colazza, S., Cusumano, A., Giudice, D. L., and Peri, E. (2014). Chemo-orientation responses in hymenopteran parasitoids induced by substrate-borne semiochemicals. *BioControl* 59, 1–7. doi: 10.1007/s10526-013-9546-7

Colazza, S., Fucarino, A., Peri, E., Salerno, G., Conti, E., and Bin, F. (2004). Insect oviposition induces volatile emission in herbaceous plants that attracts egg parasitoids. *J. Exp. Biol.* 207, 47–53. doi: 10.1242/jeb.00732

Colazza, S., Salerno, G., and Wajnberg, E. (1999). Volatile and contact chemicals released by *Nezara viridula* (Heteroptera: Pentatomidae) have a kairomonal effect on the egg parasitoid *Trissolcus basalis* (Hymenoptera: Scelionidae). *Biol. Control* 16, 310–317. doi: 10.1006/bcon.1999.0763

Crawley, M. J. (2007). *The R Book*. Hoboken, NJ: John Wiley & Sons. doi: 10.1002/9780470515075

Fatouros, N. E., Cusumano, A., Danchin, E. G., and Colazza, S. (2016). Prospects of herbivore egg-killing plant defenses for sustainable crop protection. *Ecol. Evol.* 6, 6906–6918. doi: 10.1002/ece3.2365

Fatouros, N. E., Dicke, M., Mumm, R., Meiners, T., and Hilker, M. (2008). Foraging behavior of egg parasitoids exploiting chemical information. *Behav. Ecol.* 19, 677–689. doi: 10.7717/peerj.3326

Fatouros, N. E., Lucas-Barbosa, D., Weldegergis, B. T., Pashalidou, F. G., van Loon, J. J., Dicke, M., et al. (2012). Plant volatiles induced by herbivore egg deposition affect insects of different trophic levels. *PLoS One* 7:e43607. doi: 10.1371/journal.pone.0043607

Fatouros, N. E., Paniagua Voirol, L. R., Drizou, F., Doan, Q. T., Pineda, A., Frago, E., et al. (2015). Role of large cabbage white butterfly male-derived compounds in elicitation of direct and indirect egg-killing defenses in the black mustard. *Front. Plant Sci.* 6:794. doi: 10.3389/fpls.2015.00794

Fatouros, N. E., Pashalidou, F. G., Cordero, W. V., van Loon, J. J., Mumm, R., Dicke, M., et al. (2009). Anti-aphrodisiac compounds of male butterflies increase the risk of egg parasitoid attack by inducing plant synomone production. *J. Chem. Ecol.* 35, 1373–1381. doi: 10.1007/s10886-009-9714-5

Forbes, A. A., Bagley, R. K., Beer, M. A., Hippee, A. C., and Widmayer, H. A. (2018). Quantifying the unquantifiable: why Hymenoptera — not Coleoptera — is the most speciose animal order. *BMC Ecol.* 18:21. doi: 10.1186/s12898-018-0176-x

Frati, F., Cusumano, A., Conti, E., Colazza, S., Peri, E., Guarino, S., et al. (2017). Foraging behaviour of an egg parasitoid exploiting plant volatiles induced by pentatomids: the role of adaxial and abaxial leaf surfaces. *PeerJ.* 5:e3326. doi: 10.7717/peerj.3326

Gillott, C. (2003). Male accessory gland secretions: modulators of female reproductive physiology and behavior. *Annu. Rev. Entomol.* 48, 163–184. doi: 10.1146/annurev.ento.48.091801.112657

Godfray, H. C. J. (1994). *Parasitoids: Behavioral and Evolutionary Ecology*. Princeton, NJ: Princeton University Press.

Heimpel, G. E., and Mills, N. J. (2017). *Biological Control: Ecology and Applications*. Cambridge: Cambridge University Press. doi: 10.1017/9781139029117

Hilker, M., and Fatouros, N. E. (2015). Plant responses to insect egg deposition. *Annu. Rev. Entomol.* 60, 493–515. doi: 10.1146/annurev-ento-010814-020620

Hilker, M., Kobs, C., Varama, M., and Schrank, K. (2002). Insect egg deposition induces *Pinus sylvestris* to attractegg parasitoids. *J. Exp. Biol.* 205, 455–461.

Hilker, M., Stein, C., Schroeder, R., Varama, M., and Mumm, R. (2005). Insect egg deposition induces defenceresponses in *Pinus sylvestris*: characterisation of the elicitor. *J. Exp. Biol.* 208, 1849–1854. doi: 10.1242/jeb.01578

Ho, H. Y., and Millar, J. G. (2001a). Identification and synthesis of male-produced sex pheromone components of the stink bugs *Chlorochroa ligata* and *Chlorochroa uhleri*. *J. Chem. Ecol.* 27, 2067–2095.

Ho, H. Y., and Millar, J. G. (2001b). Identification and synthesis of a male-produced sex pheromone from the stink bug *Chlorochroa sayi*. *J. Chem. Ecol.* 27, 1177–1201.

Kasule, F. K. (1986). Repetitive mating and female fitness in *Dysdercus cardinalis* (Hemiptera: Phyrrhocoridae). *Zool. J. Linn. Soc.* 88, 191–199. doi: 10.1111/j.1096-3642.1986.tb01187.x

Kon, M., Oe, A., and Numata, H. (1993). Intra-and interspecific copulations in the two congeneric green stink bugs, *Nezara antennata* and *N. viridula* (Heteroptera, Pentatomidae), with reference to postcopulatory changes in the spermatheca. *J. Ethol.* 1, 83–89. doi: 10.1007/BF02350041

Koshiyama, Y., Tsumuki, H., Muraji, M., Fujisaki, K., and Nakasuji, F. (1993). Transfer of male secretions to females through copulation in *Menida scotti* (Heteroptera: Pentatomidae). *Appl. Entomol. Zool.* 28, 325–332. doi: 10.1303/aez.28.325

Laumann, R. A., Čokl, A., Lopes, A. P., Fereira, J. B., Moraes, M. C., and Borges, M. (2011). Silent singers are not safe: selective response of a parasitoid to substrate-borne vibratory signals of stink bugs. *Anim. Behaviour.* 82, 1175–1183. doi: 10.1016/j.anbehav.2011.08.017

Laumann, R. A., Moraes, M. C., Čokl, A., and Borges, M. (2007). Eavesdropping on sexual vibratory signals of stink bugs (Hemiptera: Pentatomidae) by the egg parasitoid *Telenomus podisi*. *Anim. Behav.* 73, 637–649. doi: 10.1016/j.anbehav.2006.09.011

Mau, R. F. L., and Mitchell, W. C. (1978). Development and reproduction of the oriental stink bug *Plutia stali* (Emiptera: Pentatomidae). *Ann. Entomol. Soc. Am.* 71, 756–757. doi: 10.1093/aesa/71.5.756

McLain, D. K. (1980). Female choice and the adaptive significance of prolonged copulation in *Nezara viridula* (Hemiptera: Pentatomidae). *Psyche* 87, 325–336. doi: 10.1155/1980/70498

Meiners, T., and Hilker, M. (2000). Induction of plant synomones by oviposition of a phytophagous insect. *J. Chem. Ecol.* 26, 221–232. doi: 10.1023/A:1005453830961

Mitchell, W. C., and Mau, R. F. L. (1969). Sexual activity and longevity of the southern green stink bug. *Nezara viridula*. *Ann. Entomol. Soc. Am.* 62, 1246–1247. doi: 10.1093/aesa/62.6.1246

Moujahed, R., Frati, F., Cusumano, A., Salerno, G., Conti, E., Peri, E., et al. (2014). Egg parasitoid attraction toward induced plant volatiles is disrupted by a non-host herbivore attacking above or belowground plant organs. *Front. Plant Sci.* 5:601. doi: 10.3389/fpls.2014.00601

Mumm, R., and Hilker, M. (2005). The significance of background odour for an egg parasitoid to detect plants with host eggs. *Chem. Sens.* 30, 337–343. doi: 10.1093/chemse/bji028

Mumm, R., Schrank, K., Wegener, R., Schulz, S., and Hilker, M. (2003). Chemical analysis of volatiles emitted by *Pinus sylvestris* after induction by insect oviposition. *J. Chem. Ecol.* 29, 1235–1252. doi: 10.1023/A:1023841909199

R Core Team (2013). *R: A Language and Environment for Statistical Computing*. Vienna: R Foundation for Statistical Computing.

Salerno, G., De Santis, F., Iacovone, A., Bin, F., and Conti, E. (2013). Short-range cuesmediate parasitoid searchingbehavior on maize: the role of oviposition-induced plant synomones. *Biol. Control* 64, 247–254. doi: 10.1016/j.biocontrol.2012.12.004

Salerno, G., Frati, F., Conti, E., De Pasquale, C., Peri, E., and Colazza, S. (2009). A finely tuned strategy adopted by an egg parasitoid to exploit chemical traces from host adults. *J. Exp. Biol.* 212, 1825–1831. doi: 10.1242/jeb.028308

Schrader, F. (1960). Evolutionary aspects of aberrant meiosis in some pentatomidae (Heteroptera). *Evolution* 14, 498–508. doi: 10.1111/j.1558-5646.1960.tb03116.x

StatSoft Inc. (2001). *Statistica (Data Analysis Software System), Version 6*. Vigonza, PD: StatSoft Italia S.R.L.

Tamiru, A., Bruce, T. J. A., Woodcock, C. M., Caulfield, J. C., Midega, C. A. O., Ogol, C. K. P. O., et al. (2011). Maize landraces recruit egg and larval parasitoids in response to egg deposition by a herbivore. *Ecol. Lett.* 14, 1075–1083. doi: 10.1111/j.1461-0248.2011.01674.x

Tamiru, A., Khan, Z. R., and Bruce, T. J. A. (2015). New directionsfor improving crop resistance to insects by breeding for egg induced defence. *Curr. Opin. Insect. Sci.* 9, 51–55. doi: 10.1016/j.cois.2015.02.011

van Lenteren, J. C. (2012). The state of commercial augmentative biological control: plenty of natural enemies, but a frustrating lack of uptake. *BioControl* 57, 1–20. doi: 10.1007/s10526-011-9395-1

Vinson, S. B. (1998). The general host selection behavior of parasitoid Hymenoptera and a comparison of initial strategies utilized by larvaphagous and oophagous species. *Biol. Control* 11, 79–96. doi: 10.1006/bcon.1997.0601

Wang, Q., and Millar, J. G. (1997). Reproductive behavior of *Thyanta pallidovirens* (Heteroptera: Pentatomidae). *Ann. Entomol. Soc. Am.* 90, 380–388. doi: 10.1093/aesa/90.3.380

Zahn, D. K., Girling, R. D., McElfresh, J. S., Cardé, T. R., and Millar, J. G. (2008). Biology and reproductive behavior of *Murgantia histrionica* (Heteroptera:Pentatomidae). *Ann. Entomol. Soc. Am.* 101, 215–228. doi: 10.1603/0013-8746(2008)101[215:BARBOM]2.0.CO;2

Conflict of Interest Statement: The authors declare that the research was conducted in the absence of any commercial or financial relationships that could be construed as a potential conflict of interest.

frontiers in Physiology

ORIGINAL RESEARCH
published: 17 April 2019
doi: 10.3389/fphys.2019.00438

Transmission of a Protease-Secreting Bacterial Symbiont Among Pea Aphids via Host Plants

*Marisa Skaljac[1], Heiko Vogel[2], Natalie Wielsch[2], Sanja Mihajlovic[1] and Andreas Vilcinskas[1,3]**

[1] Branch for Bioresources, Fraunhofer Institute for Molecular Biology and Applied Ecology, Giessen, Germany, [2] Entomology Department, Max Planck Institute for Chemical Ecology, Jena, Germany, [3] Institute for Insect Biotechnology, Justus-Liebig University of Giessen, Giessen, Germany

Aphids are economically important pest insects that damage plants by phloem feeding and the transmission of plant viruses. Their ability to feed exclusively on nutritionally poor phloem sap is dependent on the obligatory symbiotic bacterium *Buchnera aphidicola*, but additional facultative symbionts may also be present, a common example of which is *Serratia symbiotica*. Many *Serratia* species secrete extracellular enzymes, so we hypothesised that *S. symbiotica* may produce proteases that help aphids to feed on plants. Molecular analysis, including fluorescence *in situ* hybridization (FISH), revealed that *S. symbiotica* colonises the gut, salivary glands and mouthparts (including the stylet) of the pea aphid *Acyrthosiphon pisum*, providing a mechanism to transfer the symbiont into host plants. *S. symbiotica* was also detected in plant tissues wounded by the penetrating stylet and was transferred to naïve aphids feeding on plants containing this symbiont. The maintenance of *S. symbiotica* by repeated transmission via plants may explain the high frequency of this symbiont in aphid populations. Proteomic analysis of the supernatant from a related but cultivable *S. symbiotica* strain cultured in liquid medium revealed the presence of known and novel proteases including metalloproteases. The corresponding transcripts encoding these *S. symbiotica* enzymes were detected in *A. pisum* and in plants carrying the symbiont, although the mRNA was much more abundant in the aphids. Our data suggest that enzymes from *S. symbiotica* may facilitate the digestion of plant proteins, thereby helping to suppress plant defense, and that the symbionts are important mediators of aphid–plant interactions.

Keywords: symbiosis, extracellular proteases, phloem sap, *Serratia symbiotica*, *Vicia faba*

OPEN ACCESS

Edited by:
Patrizia Falabella, University of Basilicata, Italy

Reviewed by:
Clare L. Casteel, University of California, Davis, United States
Marylène Poirié, Université Côte d'Azur, France

***Correspondence:**
Andreas Vilcinskas
Andreas.Vilcinskas@agrar.uni-giessen.de

Specialty section:
This article was submitted to Invertebrate Physiology, a section of the journal Frontiers in Physiology

Received: *12 November 2018*
Accepted: *01 April 2019*
Published: *17 April 2019*

Citation:
Skaljac M, Vogel H, Wielsch N, Mihajlovic S and Vilcinskas A (2019) Transmission of a Protease- Secreting Bacterial Symbiont Among Pea Aphids via Host Plants. Front. Physiol. 10:438. doi: 10.3389/fphys.2019.00438

INTRODUCTION

Aphids are major crop pests, causing both direct feeding damage and the transmission of important plant viruses (Van Emden and Harrington, 2017). The pea aphid (*Acyrthosiphon pisum* Harris) is a model for the analysis of symbiosis, and its genome sequence was the first to be published among hemipteran insects (Consortium, 2010; Oliver et al., 2014). These species have specialised

mouthparts, including a stylet that penetrates plant tissues such as sieve tubes in order to withdraw the phloem sap (Powell et al., 2006). The adaptation of aphids to this exclusive diet is facilitated by the obligatory bacterial symbiont *Buchnera aphidicola*, which compensates for the lack of nutrients by providing essential amino acids (Hansen and Moran, 2011). Aphids may also carry a variety of facultative bacterial symbionts (e.g., *Serratia symbiotica*, *Hamiltonella defensa*, and *Regiella insecticola*) that act as mutualists or parasites depending on the context of the environmental interactions (Oliver et al., 2010, 2014).

Facultative symbionts are found in multiple aphid tissues (including the haemolymph, gut, and reproductive system), and are sometimes co-localised with *B. aphidicola* within specialised structures known as bacteriomes (Moran et al., 2005; Skaljac et al., 2018). Most symbiotic bacteria (obligatory and facultative) are maternally inherited, whereas the extracellular and scattered localization of facultative symbionts facilitates their horizontal transfer, promoting rapid spreading to new hosts (Russell et al., 2003; Chiel et al., 2009; Oliver et al., 2010). Many studies have revealed phylogenetically closely related symbionts in evolutionarily distant hosts, suggesting that bacteria are horizontally transmitted between diverse insect species (Moran et al., 2005, 2008; Ahmed et al., 2013; Skaljac et al., 2017). The complex horizontal transmission routes include shared plants and parasitoids, resulting in the acquisition of novel ecological traits by the host (Russell et al., 2003; Chiel et al., 2009; Caspi-Fluger et al., 2012; Gehrer and Vorburger, 2012; Gonella et al., 2015; Chrostek et al., 2017).

The genus *Serratia* has spread to diverse habitats and the species in this genus have evolved multiple ecological functions (Petersen and Tisa, 2013). Whereas *S. symbiotica* is one of the most common facultative symbionts of aphids (Manzano-Marín et al., 2012), other *Serratia* species are pathogens associated with humans, insects, nematodes, and plants (Petersen and Tisa, 2013). The ubiquity of the genus is correlated with its ability to produce a large number of extracellular proteins (e.g., proteases, lipases, DNAses, and chitinases) that enable the species to thrive within or in close contact with many hosts (Petersen and Tisa, 2014). There are several classes of bacterial proteases, the most common of which is the metalloproteases (Miyoshi, 2013), and their major physiological role is to degrade environmental proteins for bacterial heterotrophic nutrition (Wu and Chen, 2011).

Although *S. symbiotica* is predominantly a mutualist, it acts as a facultative and protective symbiont in *A. pisum* and the black bean aphid (*Aphis fabae* Scopoli), but it has established co-obligate (nutritional) associations with aphids of the Lachninae subfamily and *B. aphidicola* (Manzano-Marin and Latorre, 2016). *S. symbiotica* provides many benefits but it also imposes costs on *A. pisum* by inhibiting reproduction, development and survival (Laughton et al., 2014; Skaljac et al., 2018). Insects must control their symbiont population in order to ensure the success of both partners, and this is frequently associated with trade-offs between investment in life-history traits and the regulation of symbionts (Login et al., 2011; Laughton et al., 2014).

The vast majority of bacterial symbionts have proven difficult to cultivate in the laboratory due to their lifestyle, gene loss, and dependence on host metabolites (Dale and Moran, 2006; Stewart, 2012). However, several cultivable strains of *S. symbiotica* have recently been isolated from *A. fabae* and the sage aphid (*A. passeriniana* Del Guercio; Sabri et al., 2011; Foray et al., 2014; Grigorescu et al., 2018). These strains are transitional forms between free-living and host-dependent symbiotic bacteria and they provide unique opportunities to study different multi-trophic interactions, such as the tritrophic relationship between symbionts, insects and plants (Foray et al., 2014; Renoz et al., 2017).

Bacterial symbionts frequently play a key role in plant–insect interactions, with important implications for plant defence and plant utilisation by insects (Frago et al., 2012; Sugio et al., 2015; Chrostek et al., 2017). Although the diversity of insect symbionts associated with plants has been investigated in detail, the role of symbiotic bacteria in such interactions is unclear. For example, *Rickettsia* spp. and *Wolbachia* spp. infect the sweet potato whitefly (*Bemisia tabaci* Gennadius) and are horizontally transmitted via the host plant to uninfected peers or even different species (Caspi-Fluger et al., 2012; Li S.J. et al., 2017; Li Y.H. et al., 2017). Furthermore, *Cardinium* spp. are transferred between different phloem-feeding insects via plants carrying the symbiont (Gonella et al., 2015). A common factor in many of these studies is that bacterial symbionts are found in different insect organs, including the salivary glands and stylet, enabling insect hosts to inoculate plant tissues with symbionts. Furthermore, *Wolbachia* spp. and *Rickettsia* spp. associated with *B. tabaci* are viable and persist in reservoir plants for an extended duration, suggesting potential interactions with the plant, such as nutrient uptake (Caspi-Fluger et al., 2012; Chrostek et al., 2017; Li S.J. et al., 2017; Li Y.H. et al., 2017).

Bacterial symbionts are known to help their insect hosts overcome plant defense and adapt to host plants. As a defence mechanism, plants frequently produce inhibitors to destroy proteases secreted by herbivorous insects, thus stopping them from digesting plant proteins (Hansen and Moran, 2014; Sugio et al., 2015; Wielkopolan and Obrepalska-Steplowska, 2016). In turn, insects may produce new protease isoforms that are resistant to plant inhibitors, or they may produce proteases at a higher rate (Wielkopolan and Obrepalska-Steplowska, 2016). Remarkably, gut bacteria in the Western corn rootworm (*Diabrotica virgifera virgifera* LeConte) and the velvet bean caterpillar (*Anticarsia gemmatalis* Hübner) produce additional proteases that help the insects to overcome the protease inhibitors produced by plants (Sugio et al., 2015).

Aphids inject infested plants with saliva containing proteases that digest phloem sap proteins, and these enzymes can be inhibited by the broad-spectrum metalloprotease inhibitor EDTA (Furch et al., 2015). Given that *Serratia* spp. are known to secrete a variety of extracellular enzymes (Hase and Finkelstein, 1993; Renoz et al., 2017), we hypothesise that *S. symbiotica* proteases may help aphids to exploit plants more efficiently by digesting plant proteins. We therefore investigated the localization of *S. symbiotica* in aphid mouthparts and wounded plants, analysed the proteome of *S. symbiotica* cultured in liquid

medium to identify secreted proteases, and determined whether the transcripts encoding these enzymes are present in the aphids and also their host plants.

MATERIALS AND METHODS

Aphids and Bacterial Symbionts

Maintenance of Aphids and Detection of Symbionts

Parthenogenetic *A. pisum* clone LL01 was reared under controlled conditions on the host plant *Vicia faba* var. *minor* as previously described (Luna-Ramirez et al., 2017; Will et al., 2017). The LL01 clone was obtained from Dr. Torsten Will (Justus-Liebig University, Giessen, Germany) and has been used in our research since 2009. We have previously shown that every individual carries *B. aphidicola* and *S. symbiotica* (Luna-Ramirez et al., 2017; Skaljac et al., 2018). A previously established, *Serratia*-free *A. pisum* line was used as a control, whereas the original (infected) aphid line is described hereafter as *Serratia*-positive (Skaljac et al., 2018). The infection status of these aphid lines was regularly checked to detect any potential contamination, especially the presence of *S. symbiotica* in the *Serratia*-free line.

We detected *S. symbiotica* in aphids and plants by extracting total DNA from *Serratia*-positive or *Serratia*-free aphids and *V. faba* tissues using the CTAB method (Luna-Ramirez et al., 2017). We then used *Serratia*-specific primers to detect *S. symbiotica* 16S rDNA in the aphids and *V. faba* plants by PCR (**Supplementary Table S1**). Amplicons were eluted using the NucleoSpin Gel and PCR Clean-up kit (Macherey-Nagel, Düren, Germany), and sequenced for verification on a 3730xl DNA analyzer (Macrogen Europe, Amsterdam, Netherlands). The resulting sequences were screened against the NCBI nr database using BLAST. The nucleotide sequences of the *S. symbiotica* 16S rDNA identified in this study were deposited in GenBank under accession numbers MH447605–MH447629 (whole aphid body), MH447630 (aphid gut), and MH447631–MH447632 (*V. faba* carrying *S. symbiotica*).

Proteomic analysis was carried out using the cultivable *S. symbiotica* strain CWBI-2.3 (DSM no. 23270), originally isolated from *A. fabae*. This strain was obtained from the Leibniz Institute DSMZ (Braunschweig, Germany) and was cultivated as recommended by the supplier. Briefly, the strain was grown in 535 liquid medium at 28°C overnight in a shaking incubator at 200 rpm. Cells were harvested by centrifugation at 453 × *g* for 30 min at 10°C, and the supernatant was stored at −80°C.

Quantification and Visualisation of *S. symbiotica* in *A. pisum* and Its Host Plants

At least three biological replicates of 30 adult *A. pisum* (10 days old) from *Serratia*-positive and *Serratia*-free aphid lines were released into Petri dishes containing *V. faba* discs (2 cm diameter) on 1% agar. After 2 days, aphids were collected in groups of 10 and stored in absolute ethanol at −20°C. Small strips of *V. faba* disc (2 cm × 3 mm) were cut from each replicate immediately after feeding and also 5 and 10 days post-feeding. All insect and plant samples were surface sterilised as previously described (Grigorescu et al., 2018) before DNA or further RNA extraction to ensure that *S. symbiotica* cells and gene expression represented bacteria present inside the tissues.

The abundance of *S. symbiotica* in the *A. pisum* and *V. faba* samples was determined by quantitative PCR (qPCR) as previously described with modifications (Luna-Ramirez et al., 2017). Briefly, genomic DNA was extracted using the CTAB method and a 133-bp fragment of the *S. symbiotica* dnaK gene (**Supplementary Table S1**) was amplified using the StepOnePlus Real-Time PCR System (Applied Biosystems, Waltham, MA, United States). The 10-μL reaction mixture comprised 2 μL of DNA template (50 ng/μL), 10 μM of each specific primer and 5 μL of Power SYBR Green PCR Master Mix (Applied Biosystems). For each sample, three independent reactions were carried out for each primer pair. The relative abundance of the *dnaK* gene in the *Serratia*-positive and *Serratia*-free aphid lines was determined after normalisation to the *ribosomal protein L32* (*rpl32*) reference gene in aphids (Pfaffl, 2001). Furthermore, the relative abundance of *S. symbiotica* in *V. faba* plants exposed to the two aphid lines was determined after normalisation to the *V. faba* actin reference gene (**Supplementary Table S1**). Significant differences in abundance were confirmed using Student's *t*-test in IBM SPSS v23 (Armonk, New York, NY, United States), with statistical significance defined as $p < 0.05$.

We visualised *S. symbiotica* by fluorescence *in situ* hybridization (FISH) in dissected mouthparts, salivary glands and guts of adult aphids as we previously described (Luna-Ramirez et al., 2017). In addition, hand-cut longitudinal stem sections of *V. faba* seedlings that were highly infested with aphids for at least 10 days were analysed by FISH as previously reported (Ghanim et al., 2009). Negative controls consisted of uninfected samples and no-probe staining (**Supplementary Figures S1**, **S2** and **Supplementary Table S2**). The primers and probe used for the quantification and visualisation of *S. symbiotica* are listed in **Supplementary Table S1**.

Horizontal Transmission of *S. symbiotica* Between *A. pisum* Individuals via Host Plants

To determine whether *S. symbiotica* detected in *V. faba* plants can be acquired by *Serratia*-free aphids, 30 aphids (10 days old) from the *Serratia*-positive line were fed on *V. faba* discs in five replicates for 2 days and then removed (**Supplementary Figure S4**). Meanwhile, 30 age-synchronised aphids (2 days old) from the *Serratia*-free line were released onto each *V. faba* disc previously occupied by the *Serratia*-positive aphids (**Supplementary Figure S3**). The *Serratia*-free aphids were allowed to feed for 3 days before transfer to a cage containing non-infested *V. faba* plants. These aphids are described hereafter as *Serratia*-reinfected and were kept in the rearing cage for the next 2 months to ensure the bacterial symbiont could spread among the aphid population.

The *V. faba* discs, mothers from both aphid lines and their randomly selected offspring were tested by PCR for the presence of *S. symbiotica* (**Figure 1**). Two months after infection, at least 30 *Serratia*-reinfected aphids were individually tested by PCR to confirm the transmission of *S. symbiotica* (**Figure 1** and **Supplementary Table S3**). The nucleotide sequences of

S. symbiotica 16*S* rDNA identified in this study were deposited in GenBank under accession numbers MK424314–MK424325 for the *Serratia*-reinfected aphids. The three aphid lines were strictly separated to prevent contamination. However, to avoid false positive transmission results due to potential contamination with the symbiont, we also included a negative control comprising *Serratia*-free aphids as both donors and recipients (**Supplementary Table S3**).

Phylogenetic Analysis of *S. symbiotica*

A phylogenetic tree was constructed using MEGA v7.0 (Kumar et al., 2016). DNA sequence similarities among *Serratia* species were investigated using the BLAST search tool[1]. ClustalW was used for multiple sequence alignments with default parameters. The phylogenetic tree was constructed using the maximum-likelihood method with a Tamura-Nei distance matrix. Bootstrap analysis of 1000 replicates was used to deduce confidence levels. The phylogenetic tree was displayed, manipulated and annotated using iTOL v4.2 (Letunic and Bork, 2016).

Proteomic Analysis of *S. symbiotica* CWBI-2.3 Culture Medium and Identification of Genes Encoding Proteolytic Enzymes in Aphids and Plants

Liquid Chromatography–Mass Spectrometry (LC-MS)

The concentrated supernatant of *S. symbiotica* CWBI-2.3 cells in 535 medium was fractionated by sodium dodecyl sulfate polyacrylamide gel electrophoresis (SDS-PAGE) in 16.5% tricine gradient gels (BioRad, Munich, Germany). The protein bands were stained with Coomassie Brilliant Blue and excised from the gel matrix for tryptic digestion as previously described (Shevchenko et al., 2006). For LC-MS analysis, samples were reconstituted in 50 μL aqueous 1% formic acid and 1 μL of the peptide mixture was injected into a UPLC M-class system (Waters, Eschborn, Germany) coupled online to a Synapt G2-si mass spectrometer equipped with a T-WAVE-IMS device (Waters). Data were acquired in data-dependent acquisition (DDA) and data-independent acquisition (DIA) modes, the latter described as enhanced MS^E. DIA analysis was supported by ion mobility separation, i.e., high-definition enhanced MS^E ($HDMS^E$) analysis (Distler et al., 2016).

Data Processing and Protein Identification

DDA raw data were first searched against a small database containing common contaminants to remove them (ProteinLynx Global Server v2.5.2, Waters). Remaining spectra were interpreted *de novo* to yield peptide sequences and used as queries for homology-based searching with MS-BLAST (Shevchenko et al., 2001) installed on a local server. MS-BLAST searches were performed against the NCBI nr database and a refined *S. symbiotica* database generated by the *in silico* translation of predicted *S. symbiotica* genes. In parallel, MS/MS spectra were searched against the NCBI nr database combined with the refined *S. symbiotica* database using MASCOT v2.5.1. $HDMS^E$ data were searched against the refined *S. symbiotica* protein database and a database containing common contaminants (human keratins and trypsin).

Identification and Expression Analysis of *S. symbiotica* Protease Genes in Aphids and Plants

Proteolytic enzymes detected in the supernatant of the *S. symbiotica* CWBI-2.3 strain (**Supplementary Table S4**) allowed the analysis of the corresponding genes in *S. symbiotica* infecting *A. pisum* and its infested host plants. Complementary DNA (cDNA) sequences for most of the *S. symbiotica* proteases were identified using the Ensembl Bacteria browser[2] or NCBI databases[3]. Gene-specific PCR primers were designed using Primer3 v4.1.0[4] to amplify specific regions of the transcribed cDNAs (Koressaar and Remm, 2007; **Supplementary Table S1**).

Total RNA was extracted from the previously described samples, i.e., aphids from *Serratia*-positive and *Serratia*-free lines, *V. faba* containing or lacking the symbiont, and *S. symbiotica* CWBI-2.3, using the Direct-zol RNA MiniPrep Plus Kit (Zymo Research, Freiburg, Germany). RNA (100 ng) was transcribed using the RevertAid First Strand cDNA synthesis kit (Thermo Fisher Scientific, Dreieich, Germany) to obtain first-strand cDNA. Amplicons from *V. faba* samples infested with *Serratia*-positive aphids were re-amplified because the quantity was low, and were cloned (**Supplementary Figures S5**, **S6**) before sequencing together with amplicons from the *Serratia*-positive aphids and the supernatant of *S. symbiotica* CWBI-2.3. Cloning and sequencing were carried out as previously described (Skaljac et al., 2018). Accession numbers for the *S. symbiotica* protease genes are listed in **Table 1**. The sequences were used to design qRT-PCR primers (**Supplementary Table S1**) in PrimerQuest (Integrated DNA Technologies, Coralville, IA, United States[5]). Control samples (*Serratia*-free aphids and their host plants, as well as non-infested *V. faba* plants), were negative for the expression of *S. symbiotica* protease genes. *S. symbiotica* CWBI-2.3 cDNA was used as a positive control (**Supplementary Figure S5**).

The *S. symbiotica* genes previously shown to be expressed in *V. faba* carrying *S. symbiotica* (*DegQ*, *HtpX*, *YfgC*, *SohB,* and *PepA*) were chosen for further expression analysis by qRT-PCR because they may be important for tritrophic interactions between symbionts, insects and plants (**Table 1**). The expression of the five selected genes in *Serratia*-free and *Serratia*-positive aphids was evaluated by qRT-PCR after normalisation to the expression level of the *rpl32* reference gene (Pfaffl, 2001). For each sample, three independent reactions were carried out for each primer pair. The qPCR protocol described above was modified so that the cDNA template was diluted 1:2 with RNase-free water before qRT-PCR (2 μL in a total volume of 10 μL). The relevant target genes and primers are listed in **Table 1** and **Supplementary Table S1**. Data were analysed as described above.

[1]http://blast.ncbi.nlm.nih.gov/Blast.cgi

[2]http://bacteria.ensembl.org/index.html

[3]https://www.ncbi.nlm.nih.gov/

[4]http://primer3.ut.ee/

[5]http://eu.idtdna.com/PrimerQuest

TABLE 1 | Overview of the genes encoding proteolytic enzymes with associated GenBank accession numbers from *S. symbiotica* expressed in *A. pisum* and its host plant *V. faba* (for additional explanations, see Results section "Proteolytic enzymes associated with *S. symbiotica*").

Protein identification from supernatant of *S. symbiotica* CWBI-2.3, with GenBank accession number for top-scoring protein of *S. symbiotica*	Samples with identified mRNA from *S. symbiotica* including GenBank accession numbers obtained in this study			Potential molecular function and biological process of a protein[§]
	Serratia-positive aphid line	*V. faba* carrying *S. symbiotica*	Culture of *S. symbiotica* CWBI-2.3	
Serine endopeptidase (*DegP*) CDS55594.1	MH458199	nd	MH458200	Hydrolase and protease activity; involved in stress response
Serine endopeptidase (*DegQ*) CDS55928.1	MH458201-MH458202		nd	
Putative IgA-specific serine endopeptidase CDS57070.1	nd	nd	nd	nd
Zn-dependent endopeptidase (*HtpX*) CDS58211.1	MH458203-MH458214			Metalloendopeptidase activity; involved in stress response
Putative M48 family peptidase (*YfgC*) CDS57423.1	MH458227-MH458232			
Putative peptidase (*SohB*) CDS58397.1	MH458196-MH458198; MH458233			Serine-type endopeptidase activity; proteolysis
Peptidase D (*PepD*) CDS55732.1	MH458218	nd	MH458219	Metallopeptidase (Zn peptidase like) activity
Aminopeptidase A (*PepA*) CDS56273.1	MH458215-MH458217			Aminopeptidase (metallopeptidase) activity; proteolysis
Aminopeptidase N (*PepN*) CDS57483.1	MH458220-MH458222	nd	MH458223-MH458226	Aminopeptidase (metallopeptidase) activity

nd – not determined; [§]Molecular function and biological process suggested by https://www.uniprot.org; https://www.ebi.ac.uk/interpro/; https://www.ncbi.nlm.nih.gov.

RESULTS

S. symbiotica in *A. pisum* and Its Host Plants

Detection and Visualisation of *S. symbiotica*

Polymerase chain reaction analysis showed that *S. symbiotica* was present in every individual of the *Serratia*-positive line, in multiple tissues including the salivary glands and gut (**Supplementary Table S2**) confirming findings from our previous study (Skaljac et al., 2018). We found no evidence of the symbiont in the *Serratia*-free line over many generations of rearing under laboratory conditions (**Figure 1**). Furthermore, the same PCR also showed that *S. symbiotica* was present in *V. faba* plants infested with *Serratia*-positive aphids, whereas no symbionts were detected in the plants exposed to the *Serratia*-free aphid line (**Figure 1**).

Fluorescence *in situ* hybridization analysis with a probe specific for *S. symbiotica* was used to confirm the PCR data (**Supplementary Table S2**) and to reveal the distribution of *S. symbiotica* within aphid and *V. faba* tissues. The *S. symbiotica* signal was abundant in the aphid gut (**Figures 2C,D**), but also in salivary glands and associated mouthparts (stylet, mandibles, labrum, food, and salivary canal) (**Figures 2A–D**). At this resolution, we were unable to determine whether *S. symbiotica* was present in one or both canals, but in either case our results indicated its route into aphids with the phloem sap or outward with the saliva. We also observed *S. symbiotica* cells in *V. faba* tissues wounded by the penetrating stylet (**Figures 2E,F**). The symbiont was not detected in non-infested host plants or those infested with the *Serratia*-free line.

Quantification by qPCR revealed that *S. symbiotica* was remarkably abundant in *Serratia*-positive aphids (**Supplementary Table S5** and **Figure 3A**). Furthermore, we detected large numbers of *S. symbiotica* in *V. faba* plants after exposure to aphids from the *Serratia*-positive line for 2 days. When the aphids were removed from the host plants, the numbers of *S. symbiotica* fell progressively at the subsequent testing points, 5 and 10 days post-feeding (**Figure 3B** and **Supplementary Table S5**). However, *S. symbiotica* was still significantly more abundant in these plants, even 10 days post-feeding, compared to plants exposed to aphids from the *Serratia*-free line (**Figure 3B** and **Supplementary Table S5**).

Phylogenetic Placement of *S. symbiotica*

Our phylogenetic analysis of *S. symbiotica* incorporated 28 partial 16*S* rDNA sequences derived from the analysis of *A. pisum* and *V. faba* specimens. These sequences were compared with reference sequences from GenBank. *S. symbiotica* from the aphids and *V. faba* plants in this study clustered together with *S. symbiotica* CWBI-2.3 isolated from *A. fabae*, but also with most of the *S. symbiotica* sequences identified in other clones of *A. pisum* (**Supplementary Figure S4**).

Horizontal Transmission of *S. symbiotica* in Aphids via Host Plants

The detection of *S. symbiotica* in the mouthparts of *Serratia*-positive aphids and wounded plant tissues exposed to these aphids led us to investigate whether this symbiont was transmitted to naïve aphids after feeding on *V. faba* plants containing the bacteria. When *V. faba* discs were exposed to *Serratia*-positive aphids for 2 days, the bacterial symbiont was

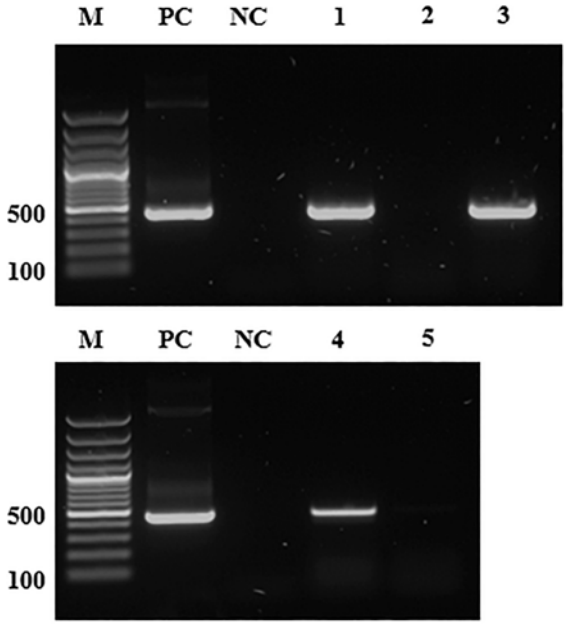

FIGURE 1 | The detection of *S. symbiotica* genomic DNA by PCR. M, DNA marker (size in base pairs); PC, positive control (pGEM T-Easy vector with *S. symbiotica* 16*S* rDNA); NC, negative control (distilled water); lane 1, *Serratia*-positive aphids; lane 2, *Serratia*-free aphids; lane 3, *Serratia*-reinfected aphids (2 months after infection event); lane 4, *V. faba* plant infested with *Serratia*-positive aphids; lane 5, *V. faba* plant infested with *Serratia*-free aphids. The *Serratia* specific primers used for PCR are listed in **Supplementary Table S1**. Amplicon size ∼480 bp.

detected by PCR in all plant samples (**Figure 1**). Sequences from *S. symbiotica* detected in the plant were identical to those in the *Serratia*-positive aphids (**Supplementary Figure S4**). Releasing *Serratia*-free aphids to feed on plant discs carrying the symbiont for 3 days enabled the transmission of the symbiont to naïve aphids. This was confirmed by PCR analysis and sequencing 2 months after the infection event (**Figure 1** and **Supplementary Table S3**). The incubation period of 2 months enabled *S. symbiotica* to spread among all formerly *Serratia*-free aphids, thus increasing the likelihood of inducing the previously observed biological effects and fitness costs (Skaljac et al., 2018). We did not detect *S. symbiotica* following the exposure of *V. faba* to *Serratia*-free aphids (**Figure 1**). During our experiments, no symptoms of bacterial disease were observed in *V. faba* infested with *Serratia*-positive aphids, indicating that the symbiont is not phytopathogenic in nature.

Proteolytic Enzymes Associated With *S. symbiotica*

Identification of Proteolytic Enzymes Released by *S. symbiotica* CWBI-2.3

Sodium dodecyl sulfate polyacrylamide gel electrophoresis analysis of the *S. symbiotica* CWBI-2.3 culture supernatant revealed a remarkable number of potentially secreted proteins (**Supplementary Figure S7**). In total, 246 different extracellular proteins were identified by LC-MS/MS and characterised, representing numerous categories of biological processes (**Supplementary Table S6**). Among these proteins, we identified 15 enzymes with predicted proteolytic activity, including metalloproteases (**Supplementary Table S4**). These enzymes potentially facilitate the degradation of host plant proteins as their annotations suggest[6,7,8]. In total, nine *S. symbiotica* proteases with complete genomic information were included for further analysis (**Table 1**): the serine endopeptidases DegP and DegQ, the putative IgA-specific Zn-dependent serine endopeptidase HtpX, the putative M48 family peptidase YfgC, the putative peptidase SohB, peptidase D (PepD), aminopeptidase A (PepA) and aminopeptidase N (PepN).

S. symbiotica Genes Encoding Proteolytic Enzymes in *A. pisum* and Its Host Plants

Having identified nine *S. symbiotica* CWBI-2.3 extracellular proteases for further analysis, we tested different aphid and plant samples for the presence of the corresponding transcripts. The *DegP*, *DeqQ*, *HtpX*, *YfgC*, *SohB*, *PepD*, *PepA,* and *PepN* transcripts were detected in *Serratia*-positive aphids (**Table 1**). Furthermore, the *DegQ*, *HtpX*, *YfgC*, *SohB,* and *PepA* transcripts were also present (albeit at much lower levels) in plants previously exposed to the *Serratia*-positive aphids (**Table 1** and **Supplementary Figure S5**). The *DegQ*, *HtpX*, *YfgC*, *SohB,* and *PepA* transcripts representing serine endopeptidases and metallopeptidases were selected for further qRT-PCR analysis because they may be relevant in the context of aphid–plant interactions. Quantitative RT-PCR analysis revealed that these five genes were more strongly expressed in *Serratia*-positive aphids than *Serratia*-free aphids (**Supplementary Table S5** and **Figure 4**). The same transcripts were below the level of detection in *V. faba* tissues previously infested with *Serratia*-positive aphids (**Supplementary Figure S5**).

DISCUSSION

Previous studies have shown that *S. symbiotica* colonises several *A. pisum* tissues, specifically the bacteriocytes, gut and haemolymph (Moran et al., 2005; Sabri et al., 2013; Luna-Ramirez et al., 2017; Skaljac et al., 2018). The experiments described here allow us to expand that distribution to include the aphid salivary glands and associated mouthparts (**Figures 2A–D**). Furthermore, *S. symbiotica* was detected in the stylet and in wounded plant tissues, providing strong evidence that aphids inoculate host plants with their bacterial symbionts (**Figures 2E,F**). In agreement with our data, recent studies of bacterial symbionts (e.g., *Rickettsia* spp., *Wolbachia* spp., and *Cardinium* spp.) associated with herbivorous insects (e.g., *B. tabaci* or *Scaphoideus titanus* Ball) reported that bacteria found in the feeding apparatus and gut were also observed in the host plants (Skaljac et al., 2010; Brumin et al., 2012; Caspi-Fluger et al., 2012; Chrostek et al.,

[6]https://www.uniprot.org
[7]https://www.ebi.ac.uk/interpro/
[8]https://www.ncbi.nlm.nih.gov

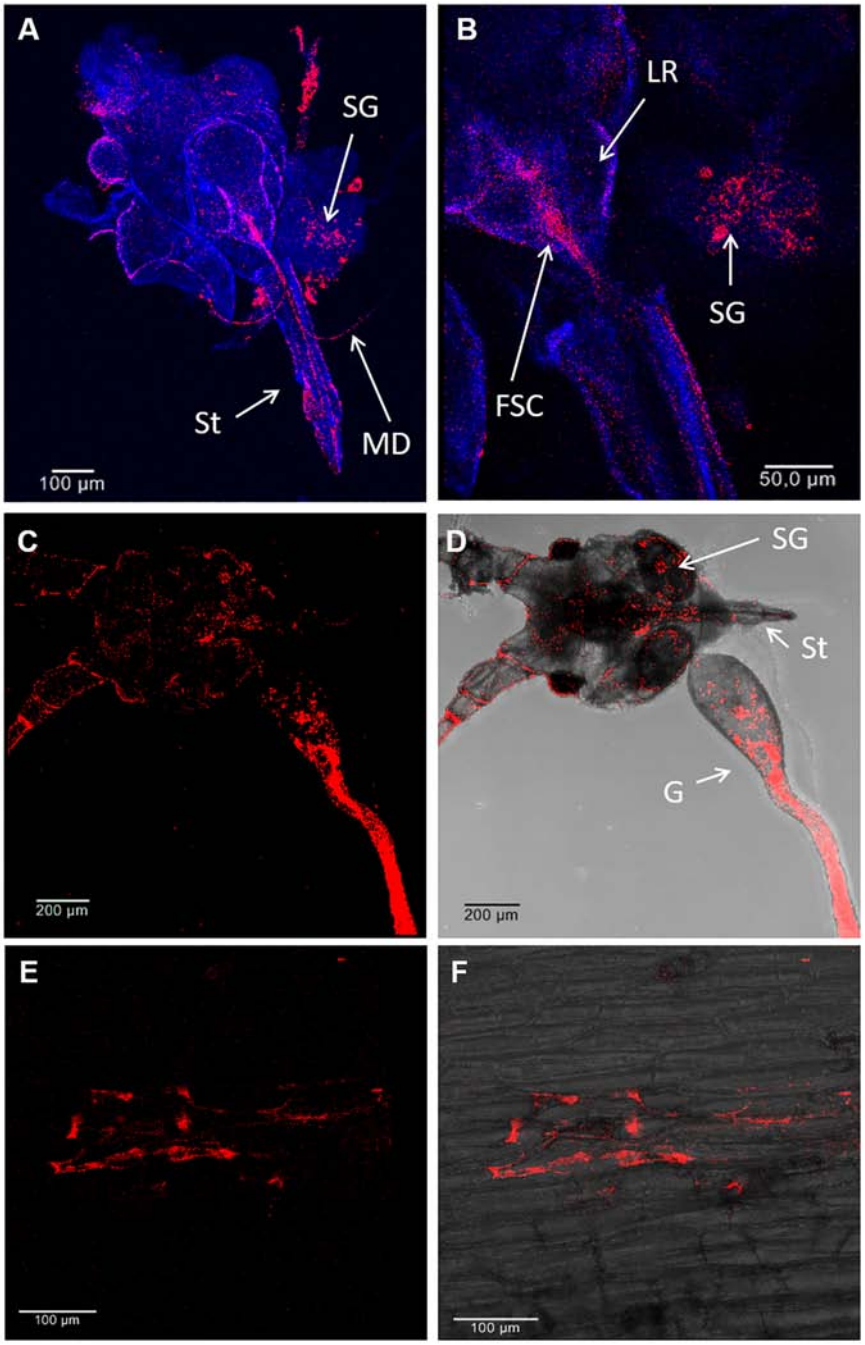

FIGURE 2 | Localization of *S. symbiotica* by fluorescence *in situ* hybridization (FISH) in *A. pisum* mouthparts and *V. faba* tissues. Detection of *S. symbiotica* (red) in the head (mouthparts, salivary glands and gut) of a 10-day-old adult aphids **(A–D)** and *V. faba* longitudinal stem sections under dark field **(E)** and bright field **(F)** imaging. Nuclei were counterstained with DAPI (dark blue). Abbreviations: MD, mandible; SG, salivary gland; St, stylet; LR, labrum; FSC, food and salivary canal; G, gut.

2017; Li S.J. et al., 2017; Li Y.H. et al., 2017). The localization of cultivable strains of *S. symbiotica* (e.g., CWBI-2.3) associated mainly with *Aphis* species is currently thought to be limited to the gut, with no cells detected in the haemolymph (Pons et al., 2019). *S. symbiotica* CWBI-2.3 is able to colonise the entire *A. pisum* gut within just a few days after artificial infection via a specialised diet, without triggering an immune response or affecting survival (Renoz et al., 2015). It would be interesting to determine whether non-cultivable *S. symbiotica* strains are localised differently in the *A. pisum* as previously shown for

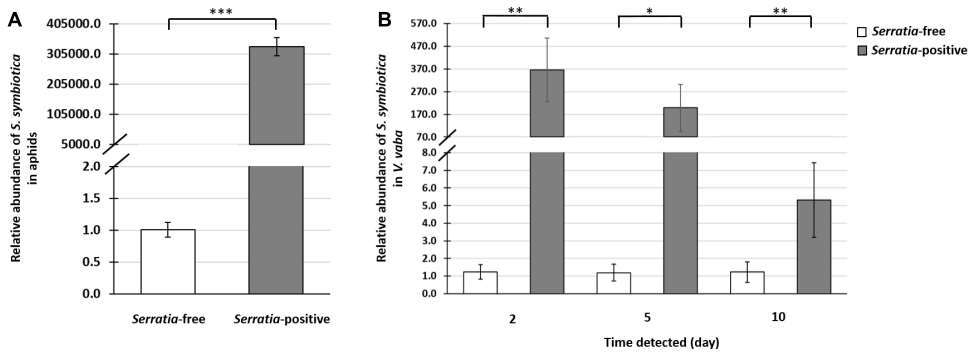

FIGURE 3 | Quantitative PCR analysis of *S. symbiotica* in *A. pisum* and *V. faba*. Data show the relative abundance of the *S. symbiotica dnaK* gene compared to the *rpl32* reference gene in aphids and the *actin* reference gene in plants. This was used to determine the abundance of *S. symbiotica* in the *Serratia*-positive and *Serratia*-free aphid lines **(A)**, and in *V. faba* leaves after exposure to each aphid line, after retention times of 2, 5, and 10 days **(B)**. Statistical significance is indicated as follows: $*p < 0.05$, $**p < 0.01$, $***p < 0.001$.

Rickettsia spp. in *B. tabaci* (Gottlieb et al., 2008; Caspi-Fluger et al., 2011). We detected *S. symbiotica* in many *A. pisum* tissues (**Figure 2D**), including the bacteriome and ovarioles, whereas a more restricted distribution was reported in earlier studies (Moran et al., 2005; Luna-Ramirez et al., 2017).

In Israeli populations of *B. tabaci*, *Rickettsia* spp. displayed a "scattered" distribution, in which the symbiont was present in the haemocoel, excluding the bacteriocytes, or a "confined" distribution, in which it was restricted to bacteriocytes (Caspi-Fluger et al., 2011). In contrast, we previously reported that *Rickettsia* spp. are distributed in all *B. tabaci* tissues, including both the haemocoel and bacteriocytes (Skaljac et al., 2010). The *Rickettsia* strains with different localization patterns often featured identical sequences, suggesting they are closely related (Caspi-Fluger et al., 2011). However, even the same symbionts can show different localization patterns and fulfil diverse functions in their insect hosts, depending on the environmental conditions (Gottlieb et al., 2008; Caspi-Fluger et al., 2011).

Our results revealed the remarkable abundance of *S. symbiotica* in *V. faba* plants after only 2 days of exposure to *Serratia*-positive aphids (**Figure 3B**). When the aphids were removed from the feeding site, the *S. symbiotica* load decreased over the subsequent 10 days (**Supplementary Table S5**). A similar decline in the number of whitefly-associated *Rickettsia* spp. was reported in cotton leaves (Li Y.H. et al., 2017), suggesting that the production of chemical defence compounds in plants may correlate with the decline of symbionts in plant tissues. In addition to the retention time of *S. symbiotica* in *V. faba*, the viability of symbionts in plant tissues is another key requirement for successful interactions with either the plant or naïve insects (Chrostek et al., 2017). The detection of *S. symbiotica* mRNAs in *V. faba* tissues revealed that the symbiont remains alive and transcriptionally active in the plant (**Table 1**). This was previously shown in the *Rickettsia* and *Wolbachia* symbionts of *B. tabaci* (Caspi-Fluger et al., 2012; Li S.J. et al., 2017; Li Y.H. et al., 2017). Future studies should include experiments to determine whether *S. symbiotica* is able to multiply in the host plants as previously described for phytopathogenic *S. marcescens* (Petersen and Tisa, 2013).

The transmission of symbionts via host plants can have a significant impact on the ecology and evolution on both the symbiont and its insect host (Chrostek et al., 2017). For instance, *Rickettsia* spp. has rapidly spread among populations of *B. tabaci* across the southwestern United States, significantly affecting life-history traits by accelerating development, promoting survival into adulthood, and encouraging the production of more offspring (Himler et al., 2011). At the same time, the transmission of *Rickettsia* spp. via plants may have favoured the rapid spreading of this symbiont among populations of *B. tabaci* (Caspi-Fluger et al., 2012). Symbionts help herbivorous insects to utilise plants (e.g., the gut bacteria in *D. virgifera virgifera*), whereas other bacteria have evolved from arthropod symbionts into insect-vectored plant pathogens (e.g., *Arsenophonus* spp.; Sugio et al., 2015; Chrostek et al., 2017). This shows the complexity of the interactions between insects, their symbionts and plants in response to different selection pressures (Shah and Walling, 2017).

We investigated the possibility that *S. symbiotica* was transmitted to uninfected aphids via the host plant, as previously shown for other insect–symbiont systems (Chrostek et al., 2017). Accordingly, we found that when *V. faba* plants containing *S. symbiotica* were fed to uninfected aphids, the plants acted as reservoirs for the efficient transmission of symbionts, resulting in the reinfection of all exposed individuals (**Figure 1** and **Supplementary Table S3**). Several studies have indicated that symbionts of herbivorous insects can be transmitted via honeydew (Darby and Douglas, 2003; Chrostek et al., 2017; Pons et al., 2019). We previously detected *S. symbiotica* in the honeydew of *Serratia*-positive *A. pisum*, so this transmission route cannot be ruled out in natural environments (Skaljac et al., 2018). The transmission route of cultivable *S. symbiotica* strains (e.g., CWBI-2.3) is unknown in *Aphis* species, but this study provides important clues to support the plant reservoir hypothesis. Bacterial symbionts are transmitted maternally with high fidelity. We previously detected *S. symbiotica* in the bacteriomes and ovarioles of *A. pisum* suggesting that this symbiont probably spreads via both horizontal and vertical transmission (Luna-Ramirez et al., 2017).

Given that *S. symbiotica* is one of the most common symbionts of aphids and that *Serratia* species can secrete extracellular enzymes to fulfil their roles in diverse ecological niches, we propose that some of the proteins secreted by *S. symbiotica* (especially proteolytic enzymes) might help the aphids to exploit their host plants more efficiently (Manzano-Marín et al., 2012; Petersen and Tisa, 2013; Sugio et al., 2015; Renoz et al., 2017). In order to test this hypothesis, we used the cultivable *S. symbiotica* strain CWBI-2.3 to identify extracellular proteases and investigate the abundance of the corresponding transcripts in aphids and *V. faba* plants. Our proteomic analysis of the *S. symbiotica* CWBI-2.3 culture supernatant revealed a diverse spectrum of secreted proteins, in agreement with the recently published membrane and cytosolic proteome of this species (Renoz et al., 2017; **Supplementary Tables S4**, **S6**). Our study has expanded the spectrum of *S. symbiotica* proteolytic enzymes (Renoz et al., 2017) to include serine endopeptidases (DegP and DegQ), M48 family metallopeptidases (HtpX and YfgC), aminopeptidases (PepA and PepN) and the other peptidases listed in **Supplementary Table S4**. Proteases are well-known virulence factors in pathogenic *Serratia* species (Petersen and Tisa, 2014) and they play important roles in the degradation of tissues that allow *Serratia* spp. to survive and proliferate within the host (Matsumoto, 2004).

The proteomic analysis of candidate *S. symbiotica* proteases in host plant tissues is not feasible due to the competition from endogenous plant proteins, so we focused on the highly sensitive detection of the corresponding transcripts. Most of the *S. symbiotica* CWBI-2.3 genes encoding proteases in the culture medium were also detected in both *Serratia*-positive aphids and in plants containing symbiont cells (**Table 1**). The *S. symbiotica* protease genes identified in *V. faba* were strongly expressed in *Serratia*-positive aphids (**Figure 4** and **Supplementary Table S5**), suggesting that *S. symbiotica* may indeed help aphids to digest phloem sap proteins and potentially to resist protease inhibitors (Zhu-Salzman and Zeng, 2015). Several studies have highlighted the importance of symbiotic bacteria in the ability of insects to exploit host plants more efficiently by suppressing plant defence mechanisms and/or by expanding the host plant range. For example, this has been shown for *B. tabaci* and its symbiont *H. defensa,* and in the Colorado potato beetle (*Leptinotarsa decemlineata* Say) and its symbionts representing the bacterial genera *Stenotrophomonas*, *Pseudomonas,* and *Enterobacter* (Frago et al., 2012; Su et al., 2015; Sugio et al., 2015; Chung et al., 2017).

In this study, transcripts encoding candidate proteases were present at very low levels in plants previously infested with *Serratia*-positive aphids (**Supplementary Figure S5**). This suggests that the detection of transcripts in *V. faba* is most likely associated with the presence of the symbiont (**Table 1**). On the other hand, the abundance of *S. symbiotica* in aphid tissues (**Figures 2A–D**, **3A**) together with the strong expression of protease genes associated with *Serratia*-positive aphids (**Figure 4**) suggest that the proteases may be active in the aphid gut and salivary glands but not necessarily in the host plant. These assumptions are supported by previous studies showing that plant-derived protease inhibitors inactivate digestive enzymes in the insect gut, preventing the digestion and absorption of nutrients (Ryan, 1990; Hansen and Moran, 2014). Therefore, *S. symbiotica* proteases are more likely to fulfil their role in the aphid gut (or salivary glands) rather than the host plants.

In summary, we investigated the localization of *S. symbiotica* in aphid mouthparts and host plant tissues and confirmed the transmission of this symbiont via plants, potentially explaining its high frequency among aphid populations. We expanded the repertoire of proteolytic enzymes produced by *S. symbiotica* in liquid medium and confirmed the strong expression of the corresponding genes in aphids and their weaker expression in infested host plants. We conclude that plants serve as reservoirs for the transmission of protease-secreting bacterial symbionts among aphids, suggesting that such symbionts could be

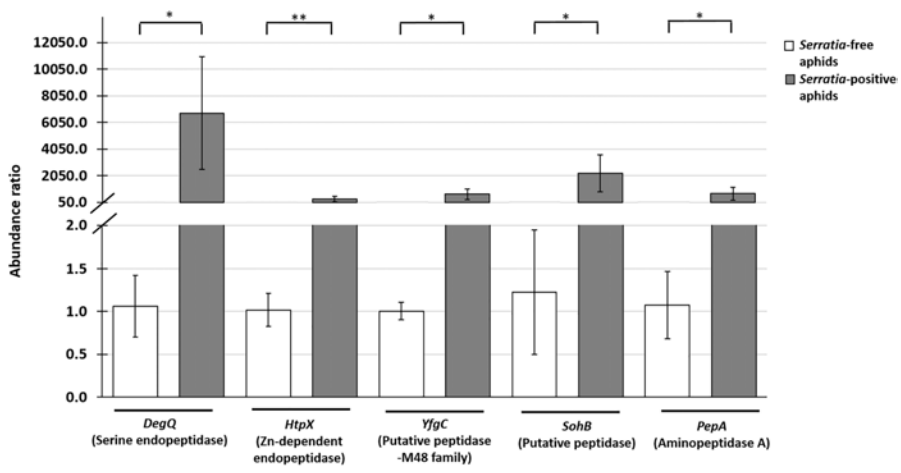

FIGURE 4 | Quantitative RT-PCR analysis showing the relative expression of five *S. symbiotica* genes (*DegQ*, *HtpX*, *YfgC*, *SohB,* and *PepA*) encoding proteolytic enzymes associated with the host plant (**Table 1**) in *Serratia*-positive and *Serratia*-free aphids. The expression data were normalised to the aphid reference gene *rpl32*. Statistical significance is indicated as follows: $*p < 0.05$, $**p < 0.01$.

important mediators of aphid–plant interactions. Investigating the precise nature of the symbiotic relationship described in this study will help to determine whether *S. symbiotica* uses proteases to spread among insect hosts, while in return enabling the insect to exploit plants more efficiently by the suppression of protease inhibitors.

There may be ecological and genomic differences between the two *S. symbiotica* strains used in this study, and accordingly some of the symbiotic proteases originating from the uncultivable strain may have been overlooked. Therefore, future studies should investigate extracellular proteases originating from different *S. symbiotica* strains released under diverse ecological conditions (e.g., exposure to a range of host plants). Furthermore, it would be interesting to determine the precise functions of the proteases listed in **Table 1** to see whether any of them are specifically involved in the suppression of plant defences, the digestion of plant proteins or the proliferation of the symbiont. It would also be valuable to compare defence mechanisms in plants attacked by *Serratia*-positive and *Serratia*-free aphids because this symbiont may have the potential to evolve into a plant pathogen that uses aphids as vectors.

AUTHOR CONTRIBUTIONS

MS, HV, NW, and SM contributed to the study design, carried out the molecular laboratory work, analysed the data, and drafted the manuscript. AV conceived, designed, and coordinated the study, and helped draft the manuscript. All authors agreed to be accountable for the content of the article and give approval for its publication.

FUNDING

This study was financially supported by the Hessen State Ministry of Higher Education, Research and the Arts (HMWK) via the LOEWE Research Center "Insect Biotechnology and Bioresources."

ACKNOWLEDGMENTS

We would like to acknowledge Jens Grotmann, Phillipp Kirfel, Tobias Kessel, Maximilian Seip and Katja Michaelis from Fraunhofer IME (Giessen, Germany), and Sebastian Beer from University of Applied Sciences Mittelhessen, Institute of Bioprocess Engineering and Pharmaceutical Technology (Giessen, Germany) for their valuable help in this study. We thank Dr. Richard M. Twyman for editing the manuscript.

SUPPLEMENTARY MATERIAL

The Supplementary Material for this article can be found online at: https://www.frontiersin.org/articles/10.3389/fphys.2019.00438/full#supplementary-material

REFERENCES

Ahmed, M. Z., De Barro, P. J., Ren, S. X., Greeff, J. M., and Qiu, B. L. (2013). Evidence for horizontal transmission of secondary endosymbionts in the *Bemisia tabaci* cryptic species complex. *PLoS One* 8:e53084. doi: 10.1371/journal.pone.0053084

Brumin, M., Levy, M., and Ghanim, M. (2012). Transovarial transmission of Rickettsia spp. and organ-specific infection of the whitefly *Bemisia tabaci*. *Appl. Environ. Microbiol.* 78, 5565–5574. doi: 10.1128/AEM.01184-12

Caspi-Fluger, A., Inbar, M., Mozes-Daube, N., Katzir, N., Portnoy, V., Belausov, E., et al. (2012). Horizontal transmission of the insect symbiont Rickettsia is plant-mediated. *Proc. Biol. Sci.* 279, 1791–1796. doi: 10.1098/rspb.2011.2095

Caspi-Fluger, A., Inbar, M., Mozes-Daube, N., Mouton, L., Hunter, M. S., and Zchori-Fein, E. (2011). Rickettsia 'in' and 'out': two different localization patterns of a bacterial symbiont in the same insect species. *PLoS One* 6:e21096. doi: 10.1371/journal.pone.0021096

Chiel, E., Inbar, M., Gottlieb, Y., Kelly, S. E., Asplen, M. K., Hunter, M. S., et al. (2009). Almost there: transmission routes of bacterial symbionts between trophic levels. *PLoS One* 4:e4767. doi: 10.1371/journal.pone.0004767

Chrostek, E., Pelz-Stelinski, K., Hurst, G. D. D., and Hughes, G. L. (2017). Horizontal transmission of intracellular insect symbionts via plants. *Front. Microbiol.* 8:2237. doi: 10.3389/fmicb.2017.02237

Chung, S. H., Scully, E. D., Peiffer, M., Geib, S. M., Rosa, C., Hoover, K., et al. (2017). Host plant species determines symbiotic bacterial community mediating suppression of plant defenses. *Sci. Rep.* 7:39690. doi: 10.1038/srep39690

Consortium, I. A. G. (2010). Genome sequence of the pea aphid *Acyrthosiphon pisum*. *PLoS Biol.* 8:e1000313. doi: 10.1371/journal.pbio.1000313

Dale, C., and Moran, N. A. (2006). Molecular interactions between bacterial symbionts and their hosts. *Cell* 126, 453–465. doi: 10.1016/j.cell.2006.07.014

Darby, A. C., and Douglas, A. E. (2003). Elucidation of the transmission patterns of an insect-borne bacterium. *Appl. Environ. Microbiol.* 69, 4403–4407. doi: 10.1128/AEM.69.8.4403-4407.2003

Distler, U., Kuharev, J., Navarro, P., and Tenzer, S. (2016). Label-free quantification in ion mobility-enhanced data-independent acquisition proteomics. *Nat. Protoc.* 11, 795–812. doi: 10.1038/nprot.2016.042

Foray, V., Grigorescu, A. S., Sabri, A., Haubruge, E., Lognay, G., Francis, F., et al. (2014). Whole-genome sequence of serratia symbiotica strain CWBI-2.3T, a free-living symbiont of the black bean aphid *Aphis fabae*. *Genome Announc.* 2:e00767-14. doi: 10.1128/genomeA.00767-14

Frago, E., Dicke, M., and Godfray, H. C. (2012). Insect symbionts as hidden players in insect-plant interactions. *Trends Ecol. Evol.* 27, 705–711. doi: 10.1016/j.tree.2012.08.013

Furch, A. C., van Bel, A. J., and Will, T. (2015). Aphid salivary proteases are capable of degrading sieve-tube proteins. *J. Exp. Bot.* 66, 533–539. doi: 10.1093/jxb/eru487

Gehrer, L., and Vorburger, C. (2012). Parasitoids as vectors of facultative bacterial endosymbionts in aphids. *Biol. Lett.* 8:613. doi: 10.1098/rsbl.2012.0144

Ghanim, M., Brumin, M., and Popovski, S. (2009). A simple, rapid and inexpensive method for localization of tomato yellow leaf curl virus and *Potato leafroll* virus in plant and insect vectors. *J. Virol. Methods* 159, 311–314. doi: 10.1016/j.jviromet.2009.04.017

Gonella, E., Pajoro, M., Marzorati, M., Crotti, E., Mandrioli, M., Pontini, M., et al. (2015). Plant-mediated interspecific horizontal transmission of an intracellular symbiont in insects. *Sci. Rep.* 5:15811. doi: 10.1038/srep15811

Gottlieb, Y., Ghanim, M., Gueguen, G., Kontsedalov, S., Vavre, F., Fleury, F., et al. (2008). Inherited intracellular ecosystem: symbiotic bacteria share bacteriocytes in whiteflies. *FASEB J.* 22, 2591–2599. doi: 10.1096/fj.07-101162

Grigorescu, A. S., Renoz, F., Sabri, A., Foray, V., Hance, T., and Thonart, P. (2018). Accessing the hidden microbial diversity of aphids: an illustration of

how culture-dependent methods can be used to decipher the insect microbiota. *Microb. Ecol.* 75, 1035–1048. doi: 10.1007/s00248-017-1092-x

Hansen, A. K., and Moran, N. A. (2011). Aphid genome expression reveals host–symbiont cooperation in the production of amino acids. *Proc. Natl. Acad. Sci. U.S.A.* 108, 2849–2854. doi: 10.1073/pnas.1013465108

Hansen, A. K., and Moran, N. A. (2014). The impact of microbial symbionts on host plant utilization by herbivorous insects. *Mol. Ecol.* 23, 1473–1496. doi: 10.1111/mec.12421

Hase, C. C., and Finkelstein, R. A. (1993). Bacterial extracellular zinc-containing metalloproteases. *Microbiol. Rev.* 57, 823–837.

Himler, A. G., Bergen, J. E., Kozuch, A., Kelly, S. E., Tabashnik, B. E., Chiel, E., et al. (2011). Rapid spread of a bacterial symbiont in an invasive whitefly is driven by fitness benefits and female bias. *Science* 332:254. doi: 10.1126/science.1199410

Koressaar, T., and Remm, M. (2007). Enhancements and modifications of primer design program Primer3. *Bioinformatics* 23, 1289–1291. doi: 10.1093/bioinformatics/btm091

Kumar, S., Stecher, G., and Tamura, K. (2016). MEGA7: molecular evolutionary genetics analysis version 7.0 for Bigger Datasets. *Mol. Biol. Evol.* 33, 1870–1874. doi: 10.1093/molbev/msw054

Laughton, A. M., Fan, M. H., and Gerardo, N. M. (2014). The combined effects of bacterial symbionts and aging on life history traits in the pea aphid, *Acyrthosiphon pisum*. *Appl. Environ. Microbiol.* 80, 470–477. doi: 10.1128/AEM.02657-13

Letunic, I., and Bork, P. (2016). Interactive tree of life (iTOL) v3: an online tool for the display and annotation of phylogenetic and other trees. *Nucleic Acids Res.* 44, W242–W245. doi: 10.1093/nar/gkw290

Li, S. J., Ahmed, M. Z., Lv, N., Shi, P. Q., Wang, X. M., Huang, J. L., et al. (2017). Plant-mediated horizontal transmission of *Wolbachia* between whiteflies. *ISME J.* 11, 1019–1028. doi: 10.1038/ismej.2016.164

Li, Y. H., Ahmed, M. Z., Li, S. J., Lv, N., Shi, P. Q., Chen, X. S., et al. (2017). Plant-mediated horizontal transmission of Rickettsia endosymbiont between different whitefly species. *FEMS Microbiol. Ecol.* 93:fix138. doi: 10.1093/femsec/fix138

Login, F. H., Balmand, S., Vallier, A., Vigneron, A., Rochat, D., Heddi, A., et al. (2011). Antimicrobial peptides keep insect endosymbionts under control. *Science* 334, 362–365. doi: 10.1126/science.1209728

Luna-Ramirez, K., Skaljac, M., Grotmann, J., Kirfel, P., and Vilcinskas, A. (2017). Orally delivered scorpion antimicrobial peptides exhibit activity against pea aphid (*Acyrthosiphon pisum*) and its bacterial symbionts. *Toxins* 9:E261. doi: 10.3390/toxins9090261

Manzano-Marín, A., Lamelas, A., Moya, A., and Latorre, A. (2012). Comparative genomics of *Serratia* spp.: two paths towards endosymbiotic life. *PLoS One* 7:e47274. doi: 10.1371/journal.pone.0047274

Manzano-Marin, A., and Latorre, A. (2016). Snapshots of a shrinking partner: genome reduction in *Serratia symbiotica*. *Sci. Rep.* 6:32590. doi: 10.1038/srep32590

Matsumoto, K. (2004). Role of bacterial proteases in pseudomonal and serratial keratitis. *Biol. Chem.* 385, 1007–1016. doi: 10.1515/BC.2004.131

Miyoshi, S. I. (2013). Extracellular proteolytic enzymes produced by human pathogenic vibrio species. *Front. Microbiol.* 4:339. doi: 10.3389/fmicb.2013.00339

Moran, N. A., McCutcheon, J. P., and Nakabachi, A. (2008). Genomics and evolution of heritable bacterial symbionts. *Annu. Rev. Genet.* 42, 165–190. doi: 10.1146/annurev.genet.41.110306.130119

Moran, N. A., Russell, J. A., Koga, R., and Fukatsu, T. (2005). Evolutionary relationships of three new species of *Enterobacteriaceae* living as symbionts of aphids and other insects. *Appl. Environ. Microbiol.* 71, 3302–3310. doi: 10.1128/AEM.71.6.3302-3310.2005

Oliver, K. M., Degnan, P. H., Burke, G. R., and Moran, N. A. (2010). Facultative symbionts in aphids and the horizontal transfer of ecologically important traits. *Annu. Rev. Entomol.* 55, 247–266. doi: 10.1146/annurev-ento-112408-085305

Oliver, K. M., Smith, A. H., and Russell, J. A. (2014). Defensive symbiosis in the real world – advancing ecological studies of heritable, protective bacteria in aphids and beyond. *Funct. Ecol.* 28, 341–355. doi: 10.1111/1365-2435.12133

Petersen, L. M., and Tisa, L. S. (2013). Friend or foe? A review of the mechanisms that drive *Serratia* towards diverse lifestyles. *Can. J. Microbiol.* 59, 627–640. doi: 10.1139/cjm-2013-0343

Petersen, L. M., and Tisa, L. S. (2014). Molecular characterization of protease activity in *Serratia* sp. strain SCBI and its importance in cytotoxicity and virulence. *J. Bacteriol.* 196, 3923–3936. doi: 10.1128/JB.01908-14

Pfaffl, M. W. (2001). A new mathematical model for relative quantification in real-time RT-PCR. *Nucleic Acids Res.* 29:e45. doi: 10.1093/nar/29.9.e45

Pons, I., Renoz, F., Noël, C., and Hance, T. (2019). New insights into the nature of symbiotic associations in aphids: infection process, biological effects and transmission mode of cultivable *Serratia symbiotica* bacteria. *Appl. Environ. Microbiol.* doi: 10.1128/AEM.02445-18

Powell, G., Tosh, C. R., and Hardie, J. (2006). Host plant selection by aphids: behavioral, evolutionary, and applied perspectives. *Annu. Rev. Entomol.* 51, 309–330. doi: 10.1146/annurev.ento.51.110104.151107

Renoz, F., Champagne, A., Degand, H., Morsomme, P., Foray, V., Hance, T., et al. (2017). Toward a better understanding of the mechanisms of symbiosis: a comprehensive proteome map a nascent insect symbiont. *PeerJ Preprints* 5:e3291. doi: 10.7717/peerj.3291

Renoz, F., Noël, C., Errachid, A., Foray, V., and Hance, T. (2015). Infection dynamic of symbiotic bacteria in the pea aphid *Acyrthosiphon pisum* gut and host immune response at the early steps in the infection process. *PLoS One* 10:e0122099. doi: 10.1371/journal.pone.0122099

Russell, J. A., Latorre, A., Sabater-Munoz, B., Moya, A., and Moran, N. A. (2003). Side-stepping secondary symbionts: widespread horizontal transfer across and beyond the Aphidoidea. *Mol. Ecol.* 12, 1061–1075. doi: 10.1046/j.1365-294X.2003.01780.x

Ryan, C. A. (1990). Protease inhibitors in plants: genes for improving defenses against insects and pathogens. *Ann. Rev. Pathol.* 28, 425–449. doi: 10.1146/annurev.py.28.090190.002233

Sabri, A., Leroy, P., Haubruge, E., Hance, T., Frere, I., Destain, J., et al. (2011). Isolation, pure culture and characterization of *Serratia symbiotica* sp. nov., the R-type of secondary endosymbiont of the black bean aphid *Aphis fabae*. *Int. J. Syst. Evol. Microbiol.* 61(Pt 9), 2081–2088. doi: 10.1099/ijs.0.024133-0

Sabri, A., Vandermoten, S., Leroy, P. D., Haubruge, E., Hance, T., Thonart, P., et al. (2013). Proteomic investigation of aphid honeydew reveals an unexpected diversity of proteins. *PLoS One* 8:e74656. doi: 10.1371/journal.pone.0074656

Shah, J., and Walling, L. (2017). Editorial: advances in plant-hemipteran interactions. *Front. Plant Sci.* 8:1652. doi: 10.3389/fpls.2017.01652

Shevchenko, A., Sunyaev, S., Loboda, A., Shevchenko, A., Bork, P., Ens, W., et al. (2001). Charting the proteomes of organisms with unsequenced genomes by MALDI-quadrupole time-of-flight mass spectrometry and BLAST homology searching. *Anal. Chem.* 73, 1917–1926. doi: 10.1021/ac0013709

Shevchenko, A., Tomas, H., Havlis, J., Olsen, J. V., and Mann, M. (2006). In-gel digestion for mass spectrometric characterization of proteins and proteomes. *Nat. Protoc.* 1, 2856–2860. doi: 10.1038/nprot.2006.468

Skaljac, M., Kanakala, S., Zanic, K., Puizina, J., Pleic, I. L., and Ghanim, M. (2017). Diversity and phylogenetic analyses of bacterial symbionts in three whitefly species from Southeast Europe. *Insects* 8:E113. doi: 10.3390/insects8040113

Skaljac, M., Kirfel, P., Grotmann, J., and Vilcinskas, A. (2018). Fitness costs of infection with *Serratia symbiotica* are associated with greater susceptibility to insecticides in the pea aphid *Acyrthosiphon pisum*. *Pest. Manag. Sci.* 74, 1829–1836. doi: 10.1002/ps.4881

Skaljac, M., Zanic, K., Ban, S. G., Kontsedalov, S., and Ghanim, M. (2010). Co-infection and localization of secondary symbionts in two whitefly species. *BMC Microbiol.* 10:142. doi: 10.1186/1471-2180-10-142

Stewart, E. J. (2012). Growing unculturable bacteria. *J. Bacteriol.* 194, 4151–4160. doi: 10.1128/JB.00345-12

Su, Q., Oliver, K. M., Xie, W., Wu, Q., Wang, S., and Zhang, Y. (2015). The whitefly-associated facultative symbiont *Hamiltonella defensa* suppresses induced plant defences in tomato. *Funct. Ecol.* 29, 1007–1018. doi: 10.1111/1365-2435.12405

Sugio, A., Dubreuil, G., Giron, D., and Simon, J. C. (2015). Plant-insect interactions under bacterial influence: ecological implications and underlying mechanisms. *J. Exp. Bot.* 66, 467–478. doi: 10.1093/jxb/eru435

Van Emden, H. F., and Harrington, R. (2017). *Aphids as Crop Pests*. Wallingford: CABI. doi: 10.1079/9781780647098.0000

Wielkopolan, B., and Obrepalska-Steplowska, A. (2016). Three-way interaction among plants, bacteria, and coleopteran insects. *Planta* 244, 313–332. doi: 10.1007/s00425-016-2543-1

Will, T., Schmidtberg, H., Skaljac, M., and Vilcinskas, A. (2017). Heat shock protein 83 plays pleiotropic roles in embryogenesis, longevity, and fecundity of the pea aphid *Acyrthosiphon pisum*. *Dev. Genes Evol.* 227, 1–9. doi: 10.1007/s00427-016-0564-1

Wu, J.-W., and Chen, X. L. (2011). Extracellular metalloproteases from bacteria. *Appl. Microbiol. Biotechnol.* 92:253. doi: 10.1007/s00253-011-3532-8

Zhu-Salzman, K., and Zeng, R. (2015). Insect response to plant defensive protease inhibitors. *Annu. Rev. Entomol.* 60, 233–252. doi: 10.1146/annurev-ento-010814-020816

Conflict of Interest Statement: The authors declare that the research was conducted in the absence of any commercial or financial relationships that could be construed as a potential conflict of interest.

frontiers in Physiology

ORIGINAL RESEARCH
published: 01 May 2019
doi: 10.3389/fphys.2019.00489

Amino Acid Utilization May Explain Why *Bemisia tabaci* Q and B Differ in Their Performance on Plants Infected by the *Tomato yellow leaf curl virus*

*Litao Guo[1,2†], Qi Su[3†], Jin Yin[2], Zezhong Yang[2], Wen Xie[2], Shaoli Wang[2], Qingjun Wu[2], Hongying Cui[4] and Youjun Zhang[2]**

[1] Institute of Bast Fiber Crops, Chinese Academy of Agricultural Sciences, Changsha, China, [2] Department of Plant Protection, Institute of Vegetables and Flowers, Chinese Academy of Agricultural Sciences, Beijing, China, [3] Institute of Insect Sciences, College of Agriculture, Yangtze University, Jingzhou, China, [4] Department of Entomology, College of Plant Protection, China Agricultural University, Beijing, China

To make plants more attractive to vectors of viruses, plant-infecting viruses can alter host plant physiology. The recent outbreaks of *Tomato yellow leaf curl virus* (TYLCV) relate to the spread of its primary vector, the whitefly *Bemisia tabaci*. Here, we investigated the question of whether the better performance of *B. tabaci* Q, relative to that of the B biotype, on TYLCV-infected tomato plants could be explained by differences in the ability of the *B. tabaci* Q and B to obtain free amino acids from the virus-infected plants. We found that the TYLCV infection of tomato plants significantly affected the mole percentage (mol%) of free amino acids in the phloem sap of the tomato plants and the mol% of free amino acids in *B. tabaci* adults and *B. tabaci* honeydew. The TYLCV infection caused the mol% of a larger number of free amino acids to rise in *B. tabaci* Q than in B, and the analysis of honeydew indicated that, when feeding on TYLCV-infected plants, *B. tabaci* Q was better able to use the free amino acids than *B. tabaci* B. The results suggest that *B. tabaci* Q is better adapted than B to feed on TYLCV-infected plants, and that TYLCV alters the *B. tabaci* B–Q competitive interaction in favor of Q.

Keywords: *Bemisia tabaci*, adaptation, *Tomato yellow leaf curl virus*, free amino acid, virus-herbivore interactions

OPEN ACCESS

Edited by:
Michel Cusson,
Natural Resources Canada, Canada

Reviewed by:
Yuan-Xi Li,
Nanjing Agricultural University, China
Tomas Erban,
Crop Research Institute (CRI), Czechia

****Correspondence:***
Youjun Zhang
zhangyoujun@caas.cn

† These authors have contributed equally to this work

Specialty section:
This article was submitted to Invertebrate Physiology, a section of the journal Frontiers in Physiology

Received: *11 October 2018*
Accepted: *08 April 2019*
Published: *01 May 2019*

Citation:
Guo L, Su Q, Yin J, Yang Z, Xie W, Wang S, Wu Q, Cui H and Zhang Y (2019) Amino Acid Utilization May Explain Why Bemisia tabaci Q and B Differ in Their Performance on Plants Infected by the Tomato yellow leaf curl virus. Front. Physiol. 10:489. doi: 10.3389/fphys.2019.00489

INTRODUCTION

Bemisia tabaci (Gennadius) (Hemiptera: Aleyrodidae) is a devastating agricultural pest worldwide (De Barro et al., 2011). It is a cryptic species complex consisting of at least 36 morphologically indistinguishable species (Boykin and De Barro, 2014) that differ in host range (Iida et al., 2009; Chu et al., 2012), feeding behavior (Liu et al., 2012), virus transmission (Pan et al., 2013a), insecticide resistance (Horowitz et al., 2005; Luo et al., 2010; Pan et al., 2015), or endosymbiont composition (Gottlieb et al., 2006; Chiel et al., 2007). Two of the most invasive and devastating genotypes of the species are B (Middle East-Asia Minor 1) and Q (Mediterranean) (Dinsdale et al., 2010; De Barro et al., 2011). In most parts of China, *B. tabaci* Q has gradually displaced *B. tabaci* B and has become the predominant *B. tabaci* genotype (Pan et al., 2011, 2015; Zheng et al., 2017).

Because of their polyphagous nature and adaptability, *B. tabaci* B and Q are highly invasive (Inbar and Gerling, 2008). *B. tabaci* B and Q have spread in as many as 60 countries during the last two decades (De Barro et al., 2011; Pan et al., 2015). *B. tabaci* harm plants by transmitting 311 plant

viruses, sucking phloem sap, and excreting honeydew (Gilbertson et al., 2015). The rapid spread of *B. tabaci* B and Q has come together with outbreaks of begomoviruses in the cropping systems of China and many other countries (Shi et al., 2014).

As a single-stranded-DNA plant virus, *Tomato yellow leaf curl virus* (TYLCV) is phloem-limited, exhibits tissue tropism in the plant phloem, and produces characteristic symptoms on plants (Czosnek and Ghanim, 2002). In many tropical and subtropical areas, it is a destructive pathogen of the Solanaceae and causes significant yield losses. Within *B. tabaci* populations, TYLCV is transmitted transovarially, i.e., from female whiteflies to offspring, contributing significantly to its global spread (Ghanim et al., 1998; Wei et al., 2017). When feeding on a TYLCV-infected host plant, *B. tabaci* ingests TYLCV virions through the stylet. The ingested virions are then delivered to midgut epithelial cells, from where they moved to the hemolymph, and circulate until they access the salivary glands, which enables transmission to the plant phloem (Cicero et al., 1995; Hunter et al., 1998; Ghanim et al., 2001; Czosnek and Ghanim, 2002).

Plants are frequently damaged by insects and insect-vectored pathogens. In plant–pathogen–vector systems, the pathogen can directly affect the insect vector or indirectly affect the insect vector through an alteration of plant physiology (Belliure et al., 2005; Colvin et al., 2006; Stout et al., 2006). For example, Stout et al. (2006) studied nutrition-related interactions between aphids and virus-infected plants and concluded that the performance of aphids is often related to the nutritional quality of phloem sap as phloem-feeders, aphids, and other phloem feeding insects, such as whiteflies, absorb a diet that contains fairly high levels of free amino acids (Buchanan et al., 2000). Host selection and insect development are correlated with the diet's relative quality and feeding efficiency (Montllor, 1989). Many studies have examined how such tripartite interactions affect the population dynamics of insect vectors and plant pathogens, and the invasiveness of alien species (Colvin et al., 2006; Stout et al., 2006; Jiu et al., 2007; Pan et al., 2013a; Su et al., 2015, 2016).

Recent research has indicated that TYLCV-infected host plants have different effects on *B. tabaci* B and Q host preference and feeding behavior (Fang et al., 2013; Liu et al., 2013). In general, TYLCV and *B. tabaci* B seem to be neutral or antagonistic (Liu et al., 2009; Pan et al., 2013a; Shi et al., 2013), whereas TYLCV and *B. tabaci* Q seem to be mutualistic or neutral (Matsuura and Hoshino, 2009; Li et al., 2011; Pan et al., 2013a; Shi et al., 2013). However, the mechanisms underlying the nutrition-related interactions (especially with respect to free amino acids) are not completely understood.

For the present research, we hypothesized that *B. tabaci* Q was better adapted than B for feeding on TYLCV-infected tomato plants and that this difference was associated with variations in the levels of free amino acids in the plants, the whiteflies, and the honeydew produced by these whiteflies. We first examined how the free amino acid composition of the phloem sap of tomato plants was modified by TYLCV infection. After allowing B and Q adults to feed on healthy and virus-infected tomato plants, we assessed how virus-induced changes in phloem amino acids affect the nutritional status of *B. tabaci* B and Q, as indicated by the composition of free amino acids in the adults and in their honeydew.

MATERIALS AND METHODS

Plant Cultures and *B. tabaci* Populations

Tomato (*Solanum lycopersicum* Miller, cv. Zhongza 9) was used in our experiments and were held in a glasshouse with natural light and a controlled temperature (26 ± 2°C).

Bemisia tabaci Q specimens were collected from poinsettia, *Euphorbia pulcherrima* Wild. EX Klotz., in Beijing, China in 2009, whereas *B. tabaci* B whiteflies were originally collected in 2004 from a cabbage field, *Brassica oleracea* L. cv. Jingfeng 1, in Beijing, China (Pan et al., 2012).

From the time of their collection, the *B. tabaci* B and Q insects used in this study were reared on tomato (*S. lycopersicum* Mill. cv. Zhongza 9), in a glasshouse with natural light and a controlled temperature (26 ± 2°C). The method used for monitoring the purity of the populations was the same as that described previously (Chu et al., 2010).

TYLCV Inoculation

In our experiments, the method of TYLCV inoculation was the same as that described previously (Pan et al., 2013a). The GenBank accession ID of the TYLCV genome is AM282874.

Amino Acid Analyses

Sampling and Assaying of Amino Acids in the Phloem Sap

To assess the impact of the TYLCV infection on plant nutritional quality, we collected and analyzed the phloem sap of healthy and TYLCV-infected tomato plants as described by Su et al. (2015). In brief, phloem sap from the fifth expanded leaf was sampled. The leaf was immersed in 600 μl of 5 mM Na_2EDTA (pH 7.5). The leaf in the EDTA solution was incubated in a light-proof box at 25°C; a saturated solution of KH_2PO_4 was put in the box to maintain high relative humidity. After 90 min, the leaf was discarded and the phloem exudate in the EDTA solution was frozen at −20°C until it was used for amino acid analysis. Free amino acid content of phloem exudates were analyzed with an automatic amino acid analyzer S433 (Sykam, Munich, Germany). All analyses were performed on three biological replicates.

Sampling and Assaying of Amino Acids in *B. tabaci* Adults

Newly emerged B and Q adults were collected from healthy and TYLCV-infected tomato plants. We analyzed the amino acid content of B. tabaci adults using the approach described in Pan et al. (2013b). A 20 mg whitefly adult (representing one replicate) was fully homogenized with a 2 mL-glass homogenizer, shaken for 2 min on the vortex shaker (QL-866, Qilinbeier), and then centrifuged at 14,000 rpm for 10 min in centrifuge (5417R, Eppendorf, Germany). One mL of the supernatant was mixed with an equal volume of n-hexane. The mixture was then centrifuged at 10,000 rpm for 10 min, after which the supernatant was discarded and 0.5 mL of the underlayer was drawn and mixed

with an equal volume of 8% sulfosalicylic acid. The latter was centrifuged at 10,000 rpm for 10 min (to remove protein). Then, 0.5 mL of the supernatant was concentrated to dryness and re-dissolved in 0.75 mL of double-distilled water. The extracts were passed through a 0.45 μm filter, and an analysis of free amino acid content was performed as described for phloem sap. All analyses were performed on three biological replicates.

Sampling and Assaying of Amino Acids in the Honeydew of *B. tabaci* Adults

Newly emerged B and Q adults feeding on healthy tomato plants were moved to the TYLCV-infected or healthy tomato plants. These whiteflies were placed on the back side of leaves (50 adults per leaf), and their honeydew was collected on aluminum foil in a clip collection cage (2.5 cm diameter) for 48 h (Wilkinson and Douglas, 1995). The honeydew should be kept dry because the amino acids of honeydew would be broken during collection (Sandström and Moran, 2001), and was dried in a Speed-vac. The dry honeydew samples were dissolved in 50 μL of 80% methanol, and an analysis of free amino acid content was performed as described for phloem sap. All analyses were performed on three biological replicates.

Statistical Analyses

The concentration of every amino acid was transformed to the mole percentage (mol%) of total amino acids. A one-way analysis of the variance (ANOVA) and the least significant difference (LSD) test (SPSS 17.0 for Windows; SPSS, Chicago, IL, United States) were used to compare the mol% of individual amino acids in the phloem sap of healthy and TYLCV-infected tomato plants. A two-way analysis of the variance and the LSD test (SPSS 17.0 for Windows; SPSS, Chicago, IL, United States) was used to compare the mol% of individual amino acids of whiteflies whole body and honeydew.

RESULTS

Free Amino Acids in the Phloem Sap of Healthy and TYLCV-Infected Tomato Plants

Twenty free amino acids were detected in healthy tomato plants, and the same 20 plus proline (Pro) were detected in TYLCV-infected tomato plants. The TYLCV infection increased the mol% of histidine (His) (+212%, $F_{1,8}$ = 92.159, $P < 0.001$), isoleucine (Ile) (+42%, $F_{1,8}$ = 6.937, P = 0.030), leucine (Leu) (+79%, $F_{1,8}$ = 13.769, P = 0.006), valine (Val) (+70%, $F_{1,8}$ = 7.468, P = 0.026), asparagine (Asn) (+470%, $F_{1,8}$ = 181.163, $P < 0.001$), and tyrosine (Tyr) (+153%, $F_{1,8}$ = 11.007, P = 0.011) in the phloem sap of tomato plants. However, the virus infection decreased the relative concentration of lysine (Lys) (−77%, $F_{1,8}$ = 92.159, $P < 0.001$), phenylalanine (Phe) (−16%, $F_{1,8}$ = 8.384, P = 0.020), tryptophan (Trp) (−43%, $F_{1,8}$ = 19.116, P = 0.002), aspartate (Asp) (−29%, $F_{1,8}$ = 10.538, P = 0.012), glutamate (Glu) (−30%, $F_{1,8}$ = 6.011, P = 0.040), glycine (Gly) (−37%, $F_{1,8}$ = 17.374, P = 0.003), phosphoserine (PSer) (−41%, $F_{1,8}$ = 20.778, P = 0.002), taurine (Tau) (−41%, $F_{1,8}$ = 18.516, P = 0.003), and urease (Urea) (−42%, $F_{1,8}$ = 29.528, P = 0.001) in the phloem sap of tomato plants. (**Figure 1**).

Free Amino Acids in *B. tabaci* B and Q Adults

A total of 24 free amino acids were detected in both *B. tabaci* B and Q adults that fed on infected and healthy plants (**Table 1**). Genotypes significantly affected the mol% of the essential amino acids arginine (Arg), Ile, and Phe in the adults (**Table 1**). Genotypes also significantly affected the mol% of the non-essential amino acids ornithine (Orn) and β-aminoisobutyric acid (β-AiBA) in the adults. Virus infection significantly influenced the mol% of the essential amino acids Arg and Trp, and of the non-essential amino acids Asn, cysteine (Cys), Glu, Gly, Orn, Pro, Tyr, and β-AiBA in adults. The interaction of genotypes and

TABLE 1 | ANOVA results for the effects of *B. tabaci* genotypes and virus (TYLCV) on the mol% of free amino acids in *B. tabaci* adults.

Amino acid[a]		Genotype[c]	Virus[d]	Genotype*virus
	Arginine (Arg)	*	**	n.s.
	Histidine (His)	n.s.	n.s.	n.s.
	Isoleucine (Ile)	*	n.s.	n.s.
	Leucine (Leu)	n.s.	n.s.	n.s.
Essential	Lysine (Lys)	n.s.	n.s.	n.s.
amino acids[b]	Methionine (Met)	n.s.	n.s.	n.s.
	Phenylalanine (Phe)	*	n.s.	*
	Threonine (Thr)	n.s.	n.s.	n.s.
	Tryptophan (Trp)	n.s.	**	n.s.
	Valine (Val)	n.s.	n.s.	n.s.
	Alanine (Ala)	n.s.	n.s.	n.s.
	Asparagine (Asn)	n.s.	**	n.s.
	Aspartate (Asp)	n.s.	n.s.	n.s.
	Cysteine (Cys)	n.s.	*	n.s.
	Glutamate (Glu)	n.s.	**	n.s.
	Glycine (Gly)	n.s.	*	n.s.
	Ornithine (Orn)	***	**	n.s.
Non-essential	Proline (Pro)	n.s.	***	n.s.
amino acids	Serine (Ser)	n.s.	n.s.	n.s.
	Tyrosine (Tyr)	n.s.	**	n.s.
	α-Aminoadipic acid (α-Aaa)	n.s.	n.s.	n.s.
	β-Alanine (β-Ala)	n.s.	n.s.	n.s.
	β-Aminoisobutyric acid (β-AiBA)	*	*	n.s.
	γ-Aminobutyric acid (γ-Aba)	n.s.	n.s.	n.s.

*[a]Abbreviated amino acid names are in parentheses. [b]Essential amino acids as defined by Morris (1991). [c]B. tabaci B and B. tabaci Q. [d]Tomato plants with and without TYLCV. *, **, and *** indicate P < 0.05, P < 0.01, and P < 0.001 (LSD test, n = 3), respectively; n.s. indicates non-significant.*

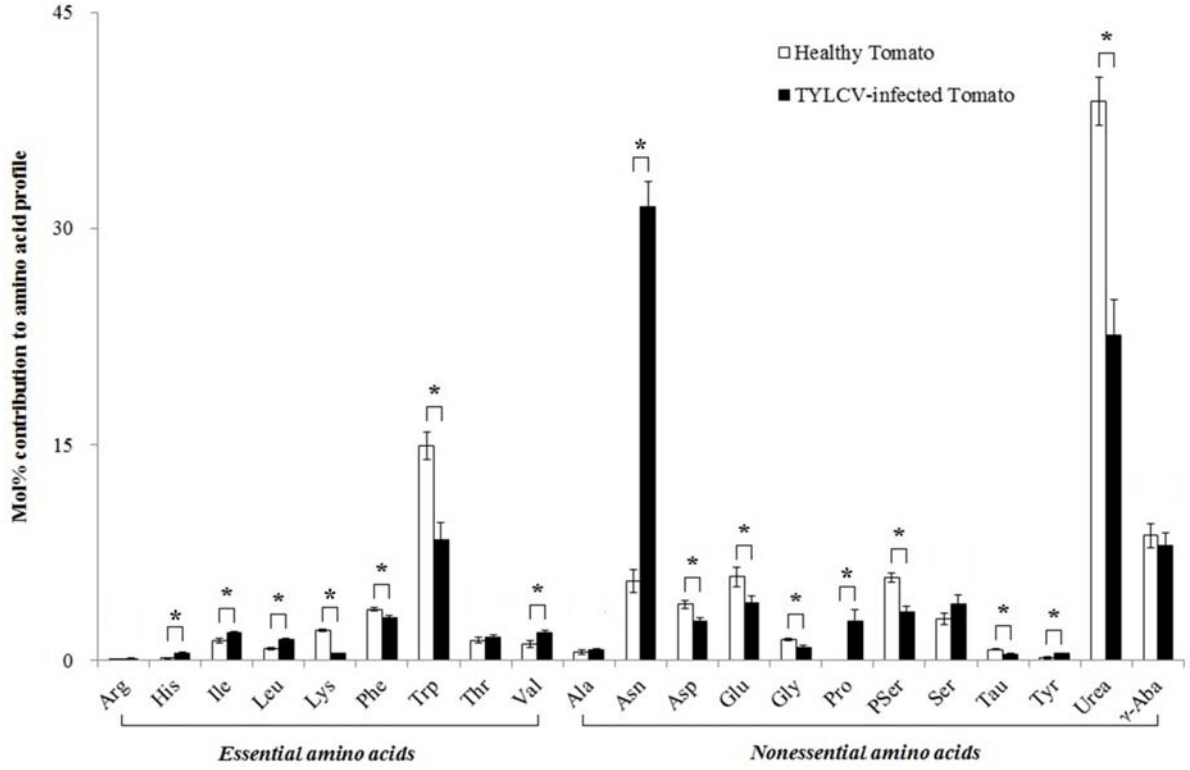

FIGURE 1 | The mol% of free amino acids in the phloem sap of healthy and TYLCV-infected tomato plants. Values are means (± SE) of three replicates. *Indicates significant differences between healthy and TYLCV-infected tomato plants at $P < 0.05$; LSD test. For abbreviations, see **Table 1**.

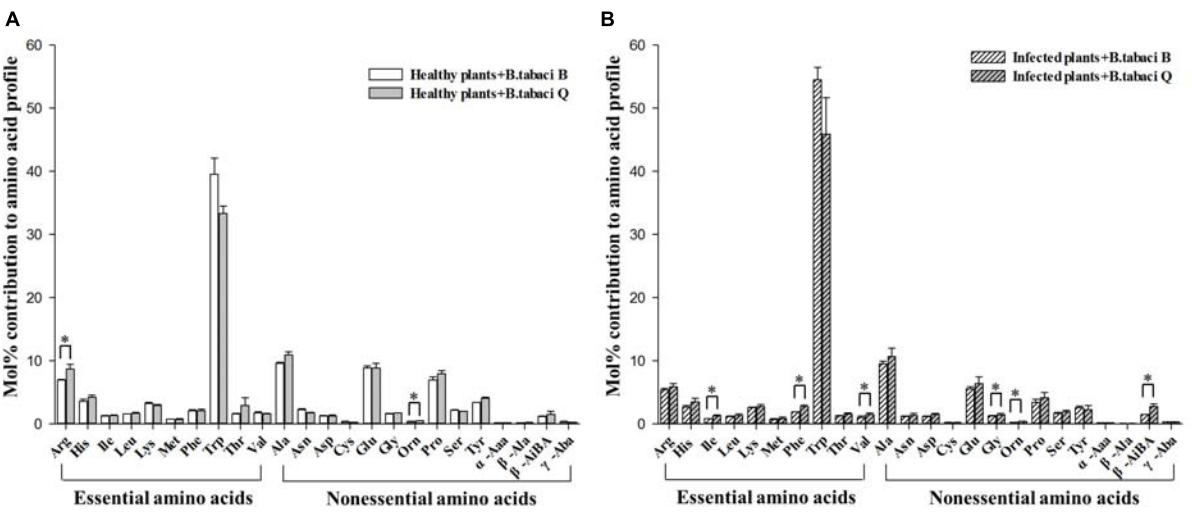

FIGURE 2 | The mol% of free amino acids in *B. tabaci* B and Q adults that fed on **(A)** healthy tomato plants or on **(B)** TYLCV-infected tomato plants. Values are means (± SE) of three replicates. *Indicates a significant difference between B and Q at $P < 0.05$; LSD test. For abbreviations, see **Table 1**.

the virus infection significantly affected the mol% of the essential amino acid Phe in adults (**Table 1**).

When adults fed on healthy plants, the mol% of Arg and Orn were higher in Q than in B (**Figure 2A** and **Supplementary Table S1**); Arg is essential, but Orn is not. When adults fed on virus-infected plants, the mol% of Ile, Phe, Val, Gly, Orn, and β-AiBA were higher in Q than in B (**Figure 2B** and **Supplementary Table S1**); Ile, Phe, and Val are essential amino acids, but the others are not. When adults fed on either TYLCV-infected or healthy tomato plants, the mol% was

not significantly higher in B than in Q for any free amino acid (**Figure 2**).

Free Amino Acids in the Honeydew of *B. tabaci* Adults

A total of 22 free amino acids were found in the honeydew of *B. tabaci* adults that fed on TYLCV-infected and healthy tomato plants. Genotypes significantly influenced the mol% of the essential amino acids Ile, threonine (Thr), and Val, and the mol% of the non-essential amino acids Glu, Pro, Tyr, and β-Alanine (β-Ala) in the honeydew. The virus infection significantly affected the mol% of all the essential amino acids except Arg, and significantly affected the mol% of the non-essential amino acids Asn, Asp, Glu, Orn, Pro, and Tyr in the honeydew. The interaction of genotypes and the virus significantly affected the mol% of the essential amino acid Ile and of the non-essential amino acid β-Ala in the honeydew (**Table 2**).

The mol% of five essential amino acids (Ile, Leu, Lys, Thr, and Val) and four non-essential amino acids (Asp, Glu, Pro, and Tyr) were lower in the honeydew produced by B adults that fed on TYLCV-infected tomato plants rather than on healthy plants, and the mol% of two essential amino acid (Met and Trp) and two non-essential amino acids (Asn and Orn) were higher in the honeydew produced by B adults that fed on TYLCV-infected tomato plants rather than on healthy plants (**Figure 3A**, **Table 3** and **Supplementary Table S2**). The mol% of five essential amino acids (Ile, Lys, Phe, Thr, and Val) and four non-essential amino acids (Asp, Glu, Pro, and Tyr) were lower in the honeydew produced by Q adults that fed on TYLCV-infected tomato plants than on healthy plants, and the mol% of only two non-essential amino acids (Asn and Orn) were higher in the honeydew produced by Q adults that fed on TYLCV-infected tomato plants rather than on healthy plants (**Figure 3B**, **Table 3** and **Supplementary Table S2**).

TABLE 2 | ANOVA results for the effects of *B. tabaci* genotypes and virus (TYLCV) on the mol% of free amino acids in the honeydew of *B. tabaci* adults.

Amino acid[a]		Genotypes[c]	Virus[d]	Genotype*virus
	Arg	n.s.	n.s.	n.s.
	Ile	*	***	*
	Leu	n.s.	*	n.s.
Essential	Lys	n.s.	**	n.s.
amino acids[b]	Met	n.s.	**	n.s.
	Phe	n.s.	*	n.s.
	Thr	**	**	n.s.
	Trp	n.s.	**	n.s.
	Val	*	**	n.s.
	Ala	n.s.	n.s.	n.s.
	Asn	n.s.	**	n.s.
	Asp	n.s.	**	n.s.
	Glu	**	**	n.s.
	Gly	n.s.	n.s.	n.s.
	Orn	n.s.	***	n.s.
Non-essential	Pro	*	**	n.s.
amino acids	Ser	n.s.	n.s.	n.s.
	Tyr	*	**	n.s.
	α-Aaa	n.s.	n.s.	n.s.
	β-Ala	**	n.s.	**
	β-AiBA	n.s.	n.s.	n.s.
	γ-Aba	n.s.	n.s.	n.s.

*[a]Abbreviated names of amino acid. [b]Essential amino acids as defined by Morris (1991). [c]B. tabaciB and B. tabaci Q. [d]Tomato plants with and without TYLCV. *, **, and *** indicate P < 0.05, P < 0.01, and P < 0.001 (LSD test, n = 3), respectively; n.s. indicates non-significant.*

DISCUSSION

Research has shown that vectored viruses can alter host plant phenotypes so as to change interactions with other organisms, including interactions between plants, viruses, and insect vectors of viruses (Mauck et al., 2012, 2018; Casteel and Falk, 2016; Eigenbrode and Bosque-Perez, 2016; Mauck, 2016). Insect-vectored viruses can alter many host plant factors, including odors, induced defenses, visual and tactile characteristics, sugars, free amino acids, and secondary metabolites (Bosque-Perez and Eigenbrode, 2011; Casteel et al., 2014; Mauck et al., 2014a,b). In our study, TYLCV significantly altered the free amino acid concentration in the phloem sap of tomato plants (**Figure 1**), an observation that is consistent with earlier studies on other interactions between plants and pathogens (Casteel et al., 2014; Su et al., 2015). Amino acids are important nutrients because they are required for cell growth regulation, hormone metabolism, nerve transmission, protein synthesis, the production of metabolic energy, and nitrogen metabolism (Castagna et al., 1997; Curis et al., 2007; Manna et al., 2009; Wu, 2009; Wu et al., 2014). Lys and Asn are directly related to antiviral activity and the regulation of the immune function, respectively, and Trp is the only amino acid with enhanced immune function (Wu, 2009). Posttranslational modifications of Lys are related to *Leishmania* survival (Nayak et al., 2018). In an earlier study, a positive correlation was observed between the number of *B. tabaci* individuals (feeding and eggs) and the amino acid content of a plant (Crafts-Brandner, 2002). The concentrations of Ser, Ala, Pro, Phe, Asn, Glu, Asp, Arg, and Trp play a role in

TABLE 3 | The number of free amino acids whose mol% were higher or lower in the honeydew of *B. tabaci* adults (genotypes B and Q) that fed on TYLCV-infected tomato plants vs. healthy tomato plants.

Mol%[a]	Genotypes	Free amino acids in the honeydew	
		Essential amino acids	Non-essential amino acids
Lower	B	5 (Ile, Leu, Lys, Thr, Val)	4 (Asp, Glu, Pro, Tyr)
	Q	5 (Ile, Lys, Phe, Thr, Val)	4 (Asp, Glu, Pro, Tyr)
Higher	B	2 (Met, Trp)	2 (Asn,Orn)
	Q	0	2 (Asn, Orn)

[a]Lower and Higher indicate that the mol% were lower or higher, respectively, in the honeydew derived from virus-infected plants than in the honeydew derived from healthy plants.

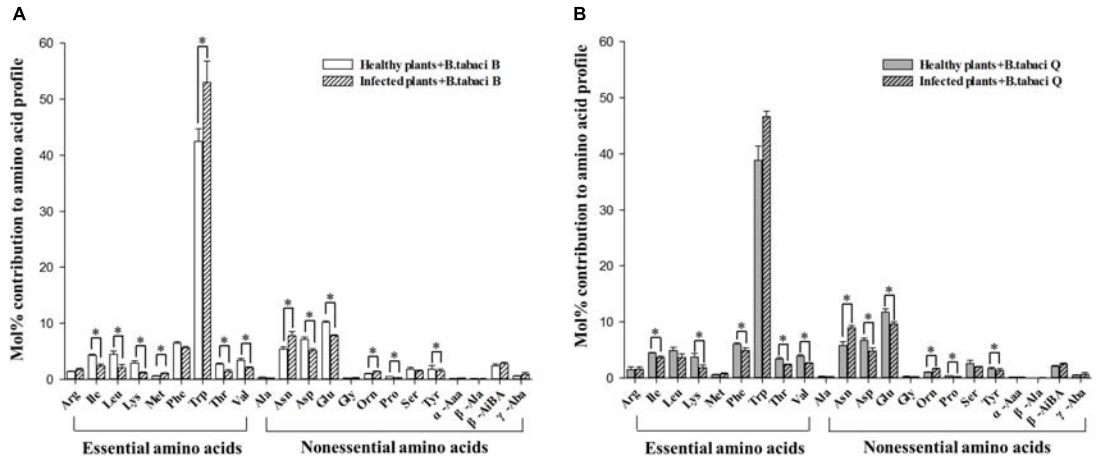

FIGURE 3 | The mol% of free amino acids in the honeydew of **(A)** *B. tabaci* B adults and **(B)** *B. tabaci* Q adults that fed on healthy and TYLCV-infected tomato plants. Value are means (± SE) of three replicates. *Indicates a significant difference between healthy and infected plants at $P < 0.05$; LSD test. For abbreviations, see **Table 1**.

the survival rate of *B. tabaci*, while the concentrations of Asp, Glu, Arg, His, and Asn are related to oviposition by *B. tabaci* (Thompson, 2006). In our study, the mol% of Lys, Trp, and Urea were much lower, and the mol% of Asn was much higher in TYLCV-infected tomato plants than in healthy tomato plants. Our results are consistent with a previous study that found that TYLCV increases free amino acids (His, Ile, Leu, Val, Asn, and Tyr) in the infected tomato phloem sap (Su et al., 2015); the latter study also found that TYLCV attenuates the induction of defenses against *B. tabaci* Q. In contrast to the latter study, the current research assessed the effects of TYLCV on both *B. tabaci* Q and B to advance our understanding of how the virus might affect competition between the two genotypes.

Because virus-infected plants often display better nutritional quality, more efficient absorption of nutrients, or repressed anti-herbivore defenses, many insect herbivores select virus-infected plants (Mauck et al., 2012; Wang et al., 2012; Angeles-López et al., 2016). Our study revealed that *B. tabaci* Q is better able to use TYLCV-infected plants as a source of amino acids, as compared with *B. tabaci* B. In our study, when feeding on TYLCV-infected tomato plants, *B. tabaci* Q had a higher mol% of amino acids (Ile, Phe, Val, Gly, Orn, and β-AiBA) than *B. tabaci* B (**Figure 2B** and **Supplementary Table S1**). TYLCV also had different effects on the mol% of some free amino acids in *B. tabaci* Q and B adults. The amino acid mol% of *B. tabaci* Q was relatively high as a consequence of feeding on TYLCV-infected plants, indicating that *B. tabaci* Q is better adapted to feeding on TYLCV-infected tomato plants than *B. tabaci* B. As is well known, many amino acids, especially essential amino acids obtained through the diet, cannot be synthesized in insects, but are necessary for normal development (Hansen and Moran, 2011; Boudko, 2012). Research on aphid-virus-host interactions has shown that aphid performance is associated with the nutritional quality of phloem sap (Stout et al., 2006). For example, *Aphis gossypii* Glover feeding on *Zucchini yellow mosaic virus*-infected *Cucurbita pepo* had longer longevity and higher fecundity than when feeding on healthy plants. In addition, the differences were associated with higher amino acid concentrations in the virus-infected plant's phloem sap (Blua et al., 1994). In contrast, lowered concentrations of amino acids in the phloem sap of wheat plants infected by two *Barley yellow dwarf virus* strains reduced the suitability of wheat for the aphid *Sitobion avenae* (Fabricius) (Fiebig et al., 2004). In the latter study, the assimilation of amino acids was also lower for aphids feeding on virus-infected plants than on non-infected plants (Fiebig et al., 2004).

We analyzed amino acids in honeydew excreted by *B. tabaci* adults to assess the assimilation of amino acids by adults. The number of free amino acids whose mol% in honeydew was reduced by the TYLCV infection of tomato plants was the same for *B. tabaci* Q and B, but the number of free amino acids whose mol% in honeydew was increased by TYLCV infection was less for *B. tabaci* Q than B (**Table 3**). This result suggests that the efficiency of amino acid utilization was higher in *B. tabaci* Q than for B. The changes in the mol% of free amino acids in honeydew may help explain why *B. tabaci* Q performs better than *B. tabaci* B on TYLCV-infected plants (Pan et al., 2013a).

Taken together, our study shows that *B. tabaci* Q is better adapted than *B. tabaci* B for feeding on TYLCV-infected tomato plants. These results are in agreement with earlier observations indicating that *B. tabaci* Q may more effectively spread TYLCV than *B. tabaci* B, and that *B. tabaci* Q performs better on TYLCV-infected plants than on healthy plants (Pan et al., 2013a). This mutualistic relationship between TYLCV and *B. tabaci* Q may help explain why *B. tabaci* Q has gradually displaced *B. tabaci* B during TYLCV outbreaks in China and elsewhere.

AUTHOR CONTRIBUTIONS

LG, JY, and YZ conceived and designed the experiments. LG and JY performed the experiments. LG and QS analyzed the data.

LG, SW, QW, ZY, WX, HC, and YZ contributed to the reagents, materials, and analysis tools. LG, QS, JY, WX, SW QW, and YZ wrote the manuscript.

FUNDING

This research was supported by the National Natural Science Foundation of China (31420103919, 31701818, 31601638, and 31601637), National Key R&D Program of China (2017YFD0200400), China Agriculture Research System (CARS-24-C-02), Technology Innovation Program of the Chinese Academy of Agricultural Sciences (CAAS-ASTIP-IVFCAAS and CAAS-ASTIP-IBFCCAAS), the Natural Science Foundation of Hunan (2018JJ3582), and the Beijing Key Laboratory for Pest Control and Sustainable Cultivation of Vegetables. The funding agencies had no role in study design, data collection and analysis, decision to publish, or preparation of the manuscript.

SUPPLEMENTARY MATERIAL

The Supplementary Material for this article can be found online at: https://www.frontiersin.org/articles/10.3389/fphys.2019.00489/full#supplementary-material

REFERENCES

Angeles-López, Y. I., Rivera-Bustamante, R. F., and Heil, M. (2016). Colonization by phloemfeeding herbivore overrides effects of plant virus on amino acid composition in phloem of chili plants. *J. Chem. Ecol.* 42, 985–988. doi: 10.1007/s10886-016-0747-2

Belliure, B., Janssen, A., Maris, P. C., Peters, D., and Sabelis, M. W. (2005). Herbivore arthropods benefit from vectoring plant viruses. *Ecol. Lett.* 8, 70–79. doi: 10.1111/j.1461-0248.2004.00699.x

Blua, M. J., Perring, T. M., and Madore, M. A. (1994). Plant virus-induced changes in aphid population development and temporal fluctuations in plant nutrients. *J. Chem. Ecol.* 20, 691–707. doi: 10.1007/BF02059607

Bosque-Perez, N. A., and Eigenbrode, S. D. (2011). The influence of virus-induced changes in plants on aphid vectors, insights from luteovirus pathosystems. *Virus Res.* 159, 201–205. doi: 10.1016/j.virusres.2011.04.020

Boudko, D. Y. (2012). Molecular basis of essential amino acid transport from studies of insect nutrient amino acid transporters of the SLC6 family (NAT-SLC6). *J. Insect. Physiol.* 58, 433–449. doi: 10.1016/j.jinsphys.2011.12.018

Boykin, L. M., and De Barro, P. J. (2014). A practical guide to identifying members of the *Bemisia tabaci* species complex, and other morphologically identical species. *Front. Ecol. Evol.* 2:45. doi: 10.3389/fevo.2014.00045

Buchanan, B. B., Gruissem, W., and Jones, R. L. (2000). *Biochemistry and Molecular Biology of Plants*. Rockville, MD: American Society of Plant Physiologists.

Castagna, M., Shayakul, C., Trotti, D., Sacchi, V. F., Harvey, W. R., Hediger, M. A., et al. (1997). Molecular characteristics of mammalian and insect amino acid transporters, implications for amino acid homeostasis. *J. Exp. Biol.* 200, 269–286.

Casteel, C. L., and Falk, B. W. (2016). "Plant virus-vector interactions, more than just for virus transmission," in *Current Research Topics in Plant Virology*, eds A. Wang and X. Zhou (Cham: Springer International Publishing), 217–240. doi: 10.1007/978-3-319-32919-2_9

Casteel, C. L., Yang, C., Nanduri, A. C., De Jong, H. N., Whitham, S. A., and Jander, G. (2014). The NIa-Pro protein of Turnip mosaic virus improves growth and reproduction of the aphid vector, *Myzus persicae* (green peach aphid). *Plant J.* 77, 653–663. doi: 10.1111/tpj.12417

Chiel, E., Gottlieb, Y., Inbar, M., Zchori, E., and Ghanim, M. (2007). Biotype-dependent secondary symbiont communities in sympatric populations of *Bemisia tabaci*. *Bull. Entomol. Res.* 97, 407–413.

Chu, D., Tao, Y. L., Zhang, Y. J., Wan, F. H., and Brown, J. K. (2012). Effects of host, temperature and relative humidity on competitive displacement of two invasive *Bemisia tabaci* biotypes (Q and B). *Insect. Sci.* 19, 595–603. doi: 10.1111/j.1744-7917.2011.01500.x

Chu, D., Zhang, Y. J., and Wan, F. H. (2010). Cryptic invasion of the exotic *Bemisia tabaci* biotype Q occurred widespread in Shandong Province of China. *Fla. Entomol.* 93, 203–207. doi: 10.1653/024.093.0209

Cicero, J. M., Hiebert, E., and Webb, S. E. (1995). The alimentary canal of *Bemisia tabaci* and *Trialeurodes abutilonea* (Homoptera, Sternorrhyncha), histology, ultrastructure and correlations to function. *Zoomorphology* 115, 31–39. doi: 10.1007/bf00397932

Colvin, J., Omongo, C. A., Govindappa, M. R., Stevenson, P. C., Gowda, M. M. N., Gibson, G., et al. (2006). Host-plant viral infection effects on arthropod-vector population growth, development and behaviour, management and epidemiological implications. *Adv. Virus Res.* 67, 419–452. doi: 10.1016/s0065-3527(06)67011-5

Crafts-Brandner, S. J. (2002). Plant nitrogen status rapidly alters amino acid metabolism and excretion in *Bemisia tabaci*. *J. Insect Physiol.* 48, 33–41. doi: 10.1016/s0022-1910(01)00140-8

Curis, E., Crenn, P., and Cynober, L. (2007). Citrulline and the gut. *Curr. Opin. Clin. Nutr. Metab. Care* 10, 620–626. doi: 10.1097/mco.0b013e32829fb38d

Czosnek, H., and Ghanim, M. (2002). The circulative pathway of begomoviruses in the whitefly vector *Bemisia tabaci*—insights from studies with tomato yellow leaf curl virus. *Ann. Appl. Biol.* 140, 215–231. doi: 10.1111/j.1744-7348.2002.tb00175.x

De Barro, P. J., Liu, S. S., Boykin, L. M., and Dinsdale, A. (2011). *Bemisia tabaci*, a statement of species status. *Annu. Rev. Entomol.* 56, 1–19. doi: 10.1146/annurev-ento-112408-085504

Dinsdale, A., Cook, L., Riginos, C., Buckley, Y. M., and De Barro, P. (2010). Refined global analysis of *Bemisia tabaci* (Hemiptera, Sternorrhyncha, Aleyrodoidea, Aleyrodidae) mitochondrial cytochrome oxidase 1 to identify species level genetic boundaries. *Ann. Entomol. Soc. Am.* 103, 196–208. doi: 10.1603/an09061

Eigenbrode, S. D., and Bosque-Perez, N. A. (2016). "Chemical ecology of aphid-transmitted plant viruses," in *Vector-Mediated Transmission of Plant Pathogens*, ed. J. K. Brown (St. Paul, MN: APS), 3–19. doi: 10.1094/9780890545355.001

Fang, Y., Jiao, X. G., Xie, W., Wang, S. L., Wu, Q. J., Shi, X. J., et al. (2013). Tomato yellow leaf curl virus alters the host preferences of its vector *Bemisia tabaci*. *Sci. Rep.* 3:2876. doi: 10.1038/srep02876

Fiebig, M., Poehling, H. M., and Borgemeister, C. (2004). Barley yellow dwarf virus, wheat, and Sitobion avenae, a case of trilateral interactions. *Entomol. Exp. Appl.* 110, 11–21. doi: 10.1111/j.0013-8703.2004.00115.x

Ghanim, M., Morin, S., and Czosnek, H. (2001). Rate of tomato yellow leaf curl virus (TYLCV) translocation in the circulative transmission pathway of its vector, the whitefly *Bemisia tabaci*. *Phytopathology* 91, 188–196. doi: 10.1094/phyto.2001.91.2.188

Ghanim, M., Morin, S., Zeidan, M., and Czosnek, H. (1998). Evidence for transovarial transmission of tomato yellow leaf curl virus by its vector, the whitefly *Bemisia tabaci*. *Virology* 240, 295–303. doi: 10.1006/viro.1997.8937

Gilbertson, R. L., Batuman, O., Webster, C. G., and Adkins, S. (2015). Role of the insect supervectors *Bemisia tabaci* and Frankliniella occidentalis in the emergence and global spread of plant viruses. *Annu. Rev. Virol.* 2, 67–93. doi: 10.1146/annurev-virology-031413-085410

Gottlieb, Y., Ghanim, M., Chiel, E., Gerling, D., Portnoy, V., Steinberg, S., et al. (2006). Identification and localization of a Rickettsia sp. in *Bemisia tabaci* (Homoptera, Aleyrodidae). *Appl. Environ. Microbiol.* 72, 3646–3652. doi: 10.1128/aem.72.5.3646-3652.2006

Hansen, A., and Moran, N. A. (2011). Aphid genome expression reveals host–symbiont cooperation in the production of amino acids. *Proc. Natl. Acad. Sci. U.S.A.* 108, 2849–2854. doi: 10.1073/pnas.1013465108

Horowitz, A. R., Kontsedalov, S., Khasdan, V., and Ishaaya, I. (2005). Biotypes B and Q of *Bemisia tabaci* and their relevance to neonicotinoid and pyriproxyfen resistance. *Arch. Insect. Biochem.* 58, 216–225. doi: 10.1002/arch.20044

Hunter, W. B., Hiebert, E., Webb, S. E., Tsai, J. K., and Polston, J. E. (1998). Location of geminiviruses in the whitefly *Bemisia tabaci* (Homoptera, Aleyrodidae). *Plant Dis.* 82, 1147–1151. doi: 10.1094/PDIS.1998.82.10.1147

Iida, H., Kitamura, T., and Honda, H. I. (2009). Comparison of egg-hatching rate, survival rate and development time of the immature stage between B-and Q-biotypes of *Bemisia tabaci* (Gennadius) (Homoptera, Aleyrodidae) on various agricultural crops. *Appl. Entomol. Zool.* 44, 267–273. doi: 10.1303/aez.2009.267

Inbar, M., and Gerling, D. (2008). Plant-mediated interactions between whiteflies, herbivores and natural enemies. *Ann. Rev. Entomol.* 53, 431–448. doi: 10.1146/annurev.ento.53.032107.122456

Jiu, M., Zhou, X. P., Tong, L., Xu, J., Yang, X., Wan, F. H., et al. (2007). Vector-virus mutualism accelerates population increase of an invasive whitefly. *PLoS One* 2:e182. doi: 10.1371/journal.pone.0000182

Li, M., Liu, J., and Liu, S. S. (2011). Tomato yellow leaf curl virus infection of tomato does not affect the performance of the Q and ZHJ2 biotypes of the viral vector *Bemisia tabaci*. *Insect. Sci.* 18, 40–49. doi: 10.1111/j.1744-7917.2010.01354.x

Liu, B. M., Preisser, E. L., Chu, D., Pan, H. P., Xie, W., Wang, S. L., et al. (2013). Multiple forms of vector manipulation by a plant-infecting virus, *Bemisia tabaci* and tomato yellow curl leaf virus. *J. Virol.* 87, 4929–4937. doi: 10.1128/JVI.03571-12

Liu, B. M., Yan, F. M., Chu, D., Pan, H. P., Jiao, X. G., Xie, W., et al. (2012). Difference in feeding behaviors of two invasive whiteflies on host plants with different suitability, implication for competitive displacement. *Int. J. Biol. Sci.* 8, 697–706. doi: 10.7150/ijbs.4108

Liu, J., Zhao, H., Jiang, K., Zhou, X. P., and Liu, S. S. (2009). Differential indirect effects of two plant viruses on an invasive and an indigenous whitefly vector, implications for competitive displacement. *Ann. Appl. Biol.* 155, 439–448. doi: 10.1111/j.1744-7348.2009.00366.x

Luo, C., Jones, C. M., Zhang, F., Denholm, I., and Gorman, K. (2010). Insecticide resistance in *Bemisia tabaci* biotype Q (Hemiptera, Aleyrodidae) from China. *Crop Protect.* 29, 429–434. doi: 10.1016/j.cropro.2009.10.001

Manna, P., Sinha, M., and Sil, P. C. (2009). Taurine plays a beneficial role against cadmium-induced oxidative renal dysfunction. *Amino Acids* 36, 417–428. doi: 10.1007/s00726-008-0094-x

Matsuura, S. M., and Hoshino, S. H. (2009). Effect of tomato yellow leaf curl disease on reproduction of *Bemisia tabaci* Q biotype (Hemiptera, Aleyrodidae) on tomato plants. *Appl. Entomol. Zool.* 44, 143–148. doi: 10.1007/s13744-014-0223-z

Mauck, K., Bosque-Pérez, N. A., Eigenbrode, S. D., De Moraes, C. M., and Mescher, M. C. (2012). Transmission mechanisms shape pathogen effects on host–vector interactions, evidence from plant viruses. *Funct. Ecol.* 26, 1162–1175. doi: 10.1111/j.1365-2435.2012.02026.x

Mauck, K. E. (2016). Variation in virus effects on host plant phenotypes and insect vector behavior, what can it teach us about virus evolution? *Curr. Opin. Virol.* 21, 114–123. doi: 10.1016/j.coviro.2016.09.002

Mauck, K. E., Chesnais, Q., and Shapiro, L. R. (2018). Chapter seven - evolutionary determinants of host and vector manipulation by plant viruses. *Adv. Virus Res.* 101, 189–250. doi: 10.1016/bs.aivir.2018.02.007

Mauck, K. E., De Moraes, C. M., and Mescher, M. C. (2014a). Biochemical and physiological mechanisms underlying effects of Cucumber mosaic virus on host-plant traits that mediate transmission by aphid vectors. *Plant Cell Environ.* 37, 1427–1439. doi: 10.1111/pce.12249

Mauck, K. E., De Moraes, C. M., and Mescher, M. C. (2014b). Evidence of local adaptation in plant virus effects on host–vector interactions. *Integr. Comp. Biol.* 54, 193–209. doi: 10.1093/icb/icu012

Montllor, C. B. (1989). "The influence of plant chemistry on aphid feeding behavior," in *Insect Plant Interactions*, Vol. 3, ed. E. Bernays (Boca Raton, FL: CRC Press), 125–173.

Morris, J. G. (1991). "Nutrition," in *Environmental and Metabolic Animal Physiology*, ed. C. L. Prosser (New York, NY: John Wiley & Sons), 231–276.

Nayak, A., Akpunarlieva, S., Barrett, M., and Burchmore, R. (2018). A defined medium for *Leishmania* culture allows definition of essential amino acids. *Exp. Parasitol.* 185, 39–52. doi: 10.1016/j.exppara.2018.01.009

Pan, H., Preisser, E. L., Chu, D., Wang, S., Wu, Q., Carrière, Y., et al. (2015). Insecticides promote viral outbreaks by altering herbivore competition. *Ecol. Appl.* 25, 1585–1595. doi: 10.1890/14-0752.1

Pan, H. P., Chu, D., Ge, D. Q., Wang, S. L., Wu, Q. J., Xie, W., et al. (2011). Further spread of and domination by *Bemisia tabaci* (Hemiptera, Aleyrodidae) biotype Q on field crops in China. *J. Econ. Entomol.* 104, 978–985. doi: 10.1603/ec11009

Pan, H. P., Chu, D., Liu, B. M., Shi, X. B., Guo, L. T., Xie, W., et al. (2013a). Differential effects of an exotic plant virus on its two closely related vectors. *Sci. Rep.* 3:2230. doi: 10.1038/srep02230

Pan, H. P., Su, Q., Jiao, X. G., Zhou, L., Liu, B. M., Xie, W., et al. (2013b). Relative amount of symbionts in *Bemisia tabaci* (Gennadius) Q changes with host plant and establishing the method of analyzing free amino acid in *B. tabaci*. *Commun. Integr. Biol.* 6:e23397. doi: 10.4161/cib.23397

Pan, H. P., Li, X. C., Ge, D. Q., Wang, S. L., Wu, Q. J., Xie, W., et al. (2012). Factors affecting population dynamics of maternally transmitted endosymbionts in *Bemisia tabaci*. *PLoS One* 7:e30760. doi: 10.1371/journal.pone.0030760

Sandström, J. P., and Moran, N. A. (2001). Amino acid budgets in three aphid species using the same host plant. *Physiol. Entomol.* 26, 202–211. doi: 10.1046/j.0307-6962.2001.00235.x

Shi, X., Pan, H., Xie, W., Wu, Q., Wang, S., Liu, Y., et al. (2013). Plant virus differentially alters the plant's defense response to its closely related vectors. *PLoS One* 8:e83520. doi: 10.1371/journal.pone.0083520

Shi, X., Pan, H., Zhang, H., Jiao, X., Xie, W., Wu, Q., et al. (2014). *Bemisia tabaci* Q carrying tomato yellow leaf curl virus strongly suppresses host plant defenses. *Sci. Rep.* 4:5230. doi: 10.1038/srep05230

Stout, M. J., Thaler, J. S., and Thomma, B. P. H. J. (2006). Plant-mediated interactions between pathogenic microorganisms and herbivorous arthropods. *Annu. Rev. Entomol.* 51, 663–689. doi: 10.1146/annurev.ento.51.110104.151117

Su, Q., Mescher, M. C., Wang, S. L., Chen, G., Xie, W., Wu, Q. J., et al. (2016). Tomato yellow leaf curl virus differentially influences plant defence responses to a vector and a non-vector herbivore. *Plant Cell Environ.* 39, 597–607. doi: 10.1111/pce.12650

Su, Q., Preisser, E. L., Zhou, X. M., Xie, W., Liu, B. M., Wang, S. L., et al. (2015). Manipulation of host quality and defense by a plant virus improves performance of whitefly vectors. *J. Econ. Entomol.* 108, 11–19. doi: 10.1093/jee/tou012

Thompson, W. M. O. (2006). Influence of amino acids on cassava biotype *Bemisia tabaci* (Gennadius) (Homoptera: Aleyrodidae) when feeding on an artificial system. *J. Entomol.* 3, 198–203. doi: 10.3923/je.2006.198.203

Wang, J., Bing, X. L., Li, M., Ye, G. Y., and Liu, S. S. (2012). Infection of tobacco plants by a begomovirus improves nutritional assimilation by a whitefly. *Entomol. Exp. Appl.* 144, 191–201. doi: 10.1111/j.1570-7458.2012.01278.x

Wei, J., He, Y. Z., Guo, Q., Guo, T., Liu, Y. Q., Zhou, X. P., et al. (2017). Vector development and vitellogenin determine the transovarial transmission of begomoviruses. *Proc. Natl. Acad. Sci. U.S.A.* 114, 6746–6751. doi: 10.1073/pnas.1701720114

Wilkinson, T. L., and Douglas, A. E. (1995). Why pea aphids (*Acyrthosiphon pisum*) lacking symbiotic bacteria have elevated levels of the amino acid glutamine. *J. Insect. Physiol.* 41, 921–927. doi: 10.1016/0022-1910(95)00063-z

Wu, G. (2009). Amino acids, metabolism, functions, and nutrition. *Amino Acids* 37, 1–17. doi: 10.1007/s00726-009-0269-0

Wu, G., Bazer, F. W., Dai, Z., Li, D., Wang, J., Wu, Z., et al. (2014). Amino acid nutrition in animals, protein synthesis and beyond. *Annu. Rev. Anim. Biosci.* 2, 387–417. doi: 10.1146/annurev-animal-022513-114113

Zheng, H. X., Xie, W., Wang, S. L., Wu, Q. J., Zhou, X. M., and Zhang, Y. J. (2017). Dynamic monitoring (B versus Q) and further resistance status of Q-type *Bemisia tabaci* in China. *Crop Protect.* 94, 115–122. doi: 10.1016/j.cropro.2016.11.035

Conflict of Interest Statement: The authors declare that the research was conducted in the absence of any commercial or financial relationships that could be construed as a potential conflict of interest.

frontiers in Physiology

ORIGINAL RESEARCH
published: 08 May 2019
doi: 10.3389/fphys.2019.00557

Plant-Mediated Silencing of the Whitefly *Bemisia tabaci* Cyclophilin B and Heat Shock Protein 70 Impairs Insect Development and Virus Transmission

Surapathrudu Kanakala, Svetlana Kontsedalov, Galina Lebedev and Murad Ghanim*

Department of Entomology, Agricultural Research Organization, The Volcani Center, Rishon LeZion, Israel

OPEN ACCESS

Edited by:
Michel Cusson,
Natural Resources Canada, Canada

Reviewed by:
Aram Megighian,
University of Padova, Italy
Haonan Zhang,
University of California, Riverside, United States

****Correspondence:***
Murad Ghanim
ghanim@agri.gov.il

Specialty section:
This article was submitted to Invertebrate Physiology, a section of the journal Frontiers in Physiology

Received: *25 December 2018*
Accepted: *24 April 2019*
Published: *08 May 2019*

Citation:
Kanakala S, Kontsedalov S, Lebedev G and Ghanim M (2019) Plant-Mediated Silencing of the Whitefly Bemisia tabaci Cyclophilin B and Heat Shock Protein 70 Impairs Insect Development and Virus Transmission. Front. Physiol. 10:557. doi: 10.3389/fphys.2019.00557

The whitefly *B. tabaci* is a global pest and transmits extremely important plant viruses especially begomoviruses, that cause substantial crop losses. *B. tabaci* is one of the top invasive species worldwide and have developed resistance to all major pesticide classes. One of the promising alternative ways for controlling this pest is studying its genetic makeup for identifying specific target proteins which are critical for its development and ability to transmit viruses. *Tomato yellow leaf curl virus* (TYLCV) is the most economically important and well-studied begomovirus transmitted by *B. tabaci,* in a persistent-circulative manner. Recently, we reported that *B. tabaci* Cyclophilin B (*CypB*) and heat shock protein 70 proteins (*hsp70*) interact and co-localize with TYLCV in the whitefly midgut, on the virus transmission pathway, and that both proteins have a significant role in virus transmission. Here, we extended the previous work and used the *Tobacco rattle virus* (TRV) plant-mediated RNA silencing system for knocking down both genes and testing the effect of their silencing on whitefly viability and virus transmission. Portions of these two genes were cloned into TRV constructs and tomato plants were infected and used for whitefly feeding and transmission experiments. Following whitefly feeding on TRV-plants, the expression levels of *cypB* and *hsp70* in adult *B. tabaci* significantly decreased over 72 h feeding period. The knockdown in the expression of both genes was further shown in the first generation of silenced whiteflies, where phenotypic abnormalities in the adult, wing, nymph and bacteriosomes development and structure were observed. Additionally, high mortality rates that reached more than 80% among nymphs and adults were obtained. Finally, silenced whitefly adults with both genes showed decreased ability to transmit TYLCV under lab conditions. Our results suggest that plant-mediated silencing of both *cypB* and *hsp70* have profound effects on whitefly development and its ability to transmit TYLCV.

Keywords: *Bemisia tabaci*, silencing, Cyclophilin B, Hsp70, *Tobacco rattle virus*

INTRODUCTION

Insect vectors of plant pathogens are distributed worldwide and are the driving force for disseminating more than 70% of the plant viruses worldwide (Hogenhout et al., 2008). The whitefly *Bemisia tabaci* is a supervector and transmits more than 100 plant viruses, most importantly Begomoviruses (family *Geminiviridae*), the largest genus of plant infecting viruses that causes enormous economic losses worldwide (Czosnek et al., 2017; Kanakala and Ghanim, 2018). The transmission of many plant viruses by *B. tabaci* and its ability to develop resistance against many pesticides makes it one of the most devastating insect pests known in agriculture (Skaljac et al., 2017).

The interaction between viruses and plant proteins that have roles in the infection process were previously studied to some extend (Hanley-Bowdoin et al., 2013). However, very little is known about insect proteins that participate in the transmission of plant viruses by insect vectors, especially those that have roles in circulative transmission, most importantly *B. tabaci*-transmitted begomviruses (Kanakala and Ghanim, 2016a), and the identification of such proteins and verifying their roles in the transmission remain a major challenge. The most studied system in this regards is the circulative transmission of *Tomato yellow leaf curl virus* from Israel (TYLCV-IL) by *B. tabaci* (Ghanim, 2014). Several *B. tabaci* proteins have been identified and verified by various methods and the results have confirmed the role of these proteins in the circulative transmission of TYLCV. Those proteins include two heat shock proteins, a GroEL chaperone encoded by endosymbiotic bacteria of *B. tabaci,* and recently a cyclophilin B (CypB) protein (Ghanim, 2014; Rosen et al., 2015; Kanakala and Ghanim, 2016a, 2018). Those proteins were shown to interact with TYLCV and their inhibition influenced the persistence, circulation, and transmission of the virus. The interaction between the candidate proteins and their specific antibodies could interfere with the virus–protein interaction and thus influence the virus transmission and persistence in the insect. For example, it was demonstrated that feeding *B. tabaci* with specific anti-CypB, anti-Hsp70 and anti-GroEL specific antibodies caused significant effects on TYLCV persistence and transmission, and its localization in the midgut (Kanakala and Ghanim, 2016a).

RNA silencing by introducing gene-specific dsRNA molecules is another approach that have been widely used to study insect development and virus–vector interactions in many organisms including insects (Kanakala and Ghanim, 2016a). For example, several delivery methods were used for introducing dsRNAs into *B. tabaci,* including injection for silencing genes expressed in the midgut and salivary glands and those that have a role in egg development (Ghanim et al., 2007). Artificial feeding through membranes was used for the silencing of several candidate genes such as an actin ortholog, ADP/ATP translocase, alpha-tubulin, ribosomal protein L9 (*RPL9*), and Vacuolar-type ATP*ase* A subunit, which caused varying levels of mortality (Upadhyay et al., 2011). Similar feeding methods were used for knocking down the cytochrome P450 monooxygenase *CYP6M1* gene, which showed increased mortality and influenced the detoxification ability of imidacloprid and nicotine in both MEAM1 and MED *B. tabaci* species (Li et al., 2015). Recently, the expression of dsRNA of whitefly genes inside the entomopathogenic fungi, *Isaria fumosorosea* (Chen et al., 2015) and endosymbiotic bacteria (Whitten et al., 2016) were successfully used to induce silencing of target genes in the insect host. Further recent studies demonstrated that whiteflies feeding on transgenic tobacco plants expressing dsRNA against the *v-ATPase A* gene (Thakur et al., 2014) and the osmoregulators *aquaporin* (*AQP*) and *alpha glucosidase,* (*AGLU*) (Raza et al., 2016), significantly reduced the expression level of targeted genes in *B. tabaci* and caused high mortality rates after feeding. So far, none of the gene silencing cases reported from *B. tabaci* were related to virus transmission.

Cyclophilins (Cyps) are a large family of cellular proteins with prolyl isomerase activity that have many molecular roles as chaperons and as signaling molecules (Wang and Heitman, 2005). Recently, CypB from the cereal aphid *Schizaphis graminum* was shown to interact with *Cereal yellow dwarf virus* (CYDV-RPV), and its expression was correlated with higher ability of some aphid biotypes to transmit CYDV-RPV (Tamborindeguy et al., 2013). We have recently shown that CypB interacts with TYLCV in *B. tabaci,* while inhibiting this protein with a specific inhibitor influenced the virus stability in the gut, and its transmission by the insect (Kanakala and Ghanim, 2016a). In a similar study, we demonstrated that *B. tabaci* Hsp70 interacted with TYLCV in the gut. But unlike CypB, feeding whiteflies with anti-Hsp70 specific antibodies resulted in higher transmission rates of TYLCV. This result suggested that Hsp70 had a protective role against the virus, which has been shown to induce various negative effects to the insect (Götz et al., 2012; Ghanim, 2014). Heat shock proteins (Hsps) belong to a multifunctional chaperon families that are upregulated by cells under stress, such as viral and bacterial infections, and play a crucial role in various cellular processes (Li and Srivastava, 2004). Since both CypB and Hsp70 were implicated in the transmission of TYLCV by *B. tabaci*, both proteins were selected as candidates for plant-mediated whitefly gene silencing using the *Tobacco rattle virus* (TRV) system and testing the effect of their knock-down on TYLCV transmission and whitefly development. Here we show that silencing both *CypB* and *Hsp70* genes in *B. tabaci* resulted in impaired nymphal, adult and endosymbiont development, as well as reduced fecundity and high mortality in the progeny of *B. tabaci* adults, which were exposed to TRV-silencing plants. Silencing both genes further resulted in reduced TYLCV transmission ability and confirmed the role of both genes in TYLCV–whitefly interactions.

MATERIALS AND METHODS

Insects, Virus Source, and Plants

B. tabaci B biotype (MEAM1) populations used in this study were reared on cotton seedlings (*Gossypium hirsutum* L. cv. pima) maintained inside insect-proof cages within growth chambers at 26°C, 60% relative humidity and a 14 h light/10 h dark photoperiod. One-week-old adult whiteflies were used for the

feeding experiments. Tomato seedlings (*Solanum lycopersicum* cv. Avigail) plants were agroinoculated with partial tandem repeats (PTR) construct of TYLCV DNA A (Navot et al., 1991), and new infected plants were generated by whitefly-mediated inoculation which were used as the virus source for the experiments in this study. The purity of *B. tabaci* B biotype was confirmed using microsatellite Bem 23 primers and cytochrome C oxidase (COI) gene sequencing (De Barro et al., 2003). Presence of TYLCV in insects and plants was confirmed using the V1 and C473 primers (Ghanim et al., 1998) (**Supplementary Table S1**). Tomato plants at their three to five true leaf stages were used for virus transmission experiments.

Generation of Recombinant *Tobacco Rattle Virus* (TRV) Vectors

Total RNA of *B. tabaci* and tomato plants were extracted using TriZol reagent (Invitrogen, United States) and the first strand cDNA was synthesized using Verso cDNA kit (Thermo scientific, Fermentas) following the manufacturer's instructions. Fragments of *B. tabaci cypB* and *hsp70* genes were amplified from the cDNA with Bt *CypB* F/R and Bt *Hsp70* F/R primers pairs, respectively (**Supplementary Table S1**). For silencing tomato *CypB* gene as a control, a fragment of 302 base pairs was amplified using tomato cDNA as a template with the primers Tom *CypB* F/R primers pairs. All the fragments were T/A cloned into the pGMET vector (Promega), excised using *Eco*R1 and *Bam*H1 and ligated to *Tobacco rattle virus* 2 (TRV 2) using the same restriction enzymes. The silencing TRV vectors including TRV1 and TRV2 were kindly provided by Prof. Henryk Czosnek from the Hebrew University of Jerusalem. The tomato gene *Hsp90* was chosen as positive control to evaluate the silencing effect mediated by TRV, while TRV1 and TRV2 alone were used a negative control.

Agroinoculations and Virus Detection

The TRV1 and four TRV2 constructs: TRV2-Bt*CypB*, TRV2-Bt*Hsp70*, TRV2-Tom*CypB* and TRV2-Tom*Hsp90* were separately transformed into *Agrobacterium tumefaciens* C58 strain. The transformed *A. tumefaciens* cells were grown at 28°C in Luria–Bertani (LB) medium containing kanamycin and rifampicin (50 μg/mL each) for 24 h. pellets were resuspended in 10 mM $MgCl_2$, 10mM MES (2-(*N*-Morpholino) ethanesulfonic acid) and 120 mM acetosyringone) and kept at 25°C for 3 h. The suspensions of *A. tumefaciens* cells were diluted to OD_{600} of 0.8. Each recombinant TRV2 virus construct was mixed with TRV1 virus in equal concentrations and inoculations of 2-week-old 30 tomato seedlings was performed by agro-infiltration (Senthil-Kumar and Mysore, 2014). Agroinoculated plants were maintained under 25 ± 2°C in growth rooms and phenotypic changes were recorded periodically. After 7 days post inoculation (dpi), the movement of TRV1 and four TRV2 constructs in tomato plants was detected by reverse transcription PCR (RT-PCR) analysis with vector and target gene specific primers (**Supplementary Table S1**). PCR positive plants were later transferred to insect-proof cages for insect bioassays.

B. tabaci Bioassays With TRV-Inoculated Plants

B. tabaci RNAi bioassays were performed with 2-week-old plants after agroinoculation with the respective construct. Two plants from each combination, TRV1+TRV2-Bt*CypB*, TRV1+TRV2-Bt*Hsp70*, and TRV1+TRV2 as control were transferred to individual insect-proof cages. For feeding experiments, newly hatched whiteflies from cotton plants were used as non-viruliferous insects. Other newly hatched whiteflies were transferred to TYLCV-infected tomato plants for 48 h acquisition access period and those were used as viruliferous insects. For each replicate around 300 viruliferous or non-viruliferous whiteflies were transferred to each group of plants in insect-proof cages. Quantification of target gene mRNAs was carried out from adults that were fed on the plants for 24 h, 72 h, and 168 h. After 1 week, additional insects were removed from the plants for analyzing the progeny. Plants were monitored every day for counting egg hatch and nymphal development. First generation progeny (nymphs) on all groups of TRV plants were collected and used for quantitative Real Time PCR (qRT-PCR), fluorescent *in situ* hybridization (FISH) assays and for light microscopy.

B. tabaci mortality assay was performed using 15 adult female whiteflies which were fed on all plant groups using clip-on-leaf cages. After 48 h, adults were removed from the leaf cage, and the exposed leaf area was marked with marker and eggs were counted. Plants were shifted to insect free cages and were monitored every 2 days for mortality and fecundity tests. Egg mortality was assessed after 8–10 days by counting number of viable nymphs. Eggs that had failed to hatch or dried out, or nymphs that had died on hatching, were scored as dead. Plants were maintained to collect first generated whiteflies. About 15 first generation female whiteflies were collected from the above assay and were fed on new tomato plants leaves to test fecundity. The experiments were repeated three times and five biological replicates were included in each experiment.

DNA and RNA Extractions, RT-PCR, and qRT-PCR

For total RNA extractions, adult whiteflies (30 whiteflies/replicate) and nymphs (50 nymphs/replicate) were collected at each time point from tomato plants and RNA was isolated using TRIzol reagent (Sigma-Aldrich) then was treated with DN*ase*I according to the manufactures recommendations (Thermo Scientific). RNA (100 ng) was used as a template for cDNA synthesis in 25 μl reaction mixtures by using Verso cDNA kit (Thermo Scientific, Fermentas). For DNA isolation, a pool of 50 nymphs per replicate was isolated using CTAB (cetyltrimethylammonium bromide) method (Shahjahan et al., 1995). The same DNA was used for the screening all three symbionts *Portiera*, *Hamiltonella,* and *Rickettsia* using 16S rDNA specific primers (**Supplementary Table S1**). PCRs were carried out as previously described (Chiel et al., 2007). For qPCR, 3 ng of DNA was used in triplicates for each DNA sample. Five to six biological replicates and three technical ones for each biological replicates were used in all experiments.

The plant DNA was extracted from 100 mg of tomato leaf tissue, as described previously (Kanakala and Ghanim, 2016a). For qPCR, 50 ng of DNA was used in triplicates for each DNA sample. RNA was extracted from 100 mg of leaf tissue using TRIzol (Sigma-Aldrich), and the cDNA synthesis was performed as instructed by the manufacturer using Verso cDNA kit (Thermo Scientific, Fermentas). To ensure the validity of the data, cDNA was used for qRT-PCR in triplicate for each cDNA sample.

Target mRNAs and TYLCV in adult whiteflies and bacterial density in nymphs were quantified by qRT-PCR using Fast SYBR Green Rox mix (Thermo Scientific) using Rotor-Gene 6000 machine (Corbett Robotics Pty Ltd., Brisbane, QLD, Australia) and the accompanying software for qPCR data processing and analysis. The cycling conditions were: 15 min activation at 95°C, 45 cycles of 10 s at 95°C, 20 s at 60°C and 25 s at 72°C. Tomato β-*actin* and *B. tabaci* β-*actin* (Sinisterra et al., 2005), α-*tubulin/BT-C02/BT-E06* (Mahadav et al., 2009) genes were used as internal controls for normalization after validation. The primers used for tomato and *B. tabaci* and symbionts are given in **Supplementary Table S1**. All assays were carried out in triplicates in each of three biologically independent experiments.

Fluorescence *in situ* Hybridization (FISH)

FISH was performed as previously described (Gottlieb et al., 2006). Briefly, nymphs were fixed overnight in Carnoy's fixative (chloroform:ethanol:glacial acetic acid, 6:3:1, vol/vol). After fixation, the samples were decolorized in 6% H_2O_2 in ethanol for 2 h and then hybridized overnight in hybridization buffer (20 mM Tris–HCl pH 8.0, 0.9 M NaCl, 0.01% wt/vol sodium dodecyl sulfate, 30% vol/vol formamide) containing 10 pmol fluorescent probe/mL. For specific targeting of *Portiera Rickettsia* and *Hamiltonella*, the probes BTP1-Cy3 (5′-Cy3-TGTCAGTGTCAGCCCAGAAG-3′) (Gottlieb et al., 2006), Rb1-Cy5 (5′-Cy5-TCCACGTCGCCGTCTTGC-3′) (Gottlieb et al., 2006) and BTH-Cy5 (5′-CCAGATTCCCAGACTTTACTCA-3′) (Gottlieb et al., 2008), respectively, were used. Nymphs were stained with DAPI (4′,6′-diamidino-2-phenylindole) at 0.1 mg mL^{-1}. The stained samples were mounted whole in hybridization buffer and viewed under an IX81 Olympus FluoView500 confocal laser-scanning microscope. For each treatment, 20–30 nymphs were viewed. Optical confocal sections (100-μm thick) were sometimes prepared from each specimen for better visualization of the signal.

Transmission of TYLCV Following Feeding on Tomato Plants Expressing *CypB* and *hsp70* dsRNA

To assess the implication of CypB and Hsp70 in the transmission of TYLCV, 1-week-old *B. tabaci* adults were given acquisition on TRV-Bt*CypB* and TRV-Bt*hsp70* inoculated plants for a week. The insects were then transferred to TYLCV-infected tomato plants for additional 48 h acquisition access period and subsequently single whiteflies were transferred to tomato plants in their three-leaf stage for 7 days. Whiteflies fed on TRV alone and TYLCV-infected plants for 48 h served as a controls. Tomato plants were grown in a potting mix in 1.5L pots under artificial light and maintained inside insect-free greenhouse under controlled temperature as detailed above. The whiteflies that were incubated with the plants were tested for TYLCV acquisition. The plants were monitored for the development of disease symptoms after 28 days post inoculation. DNA was extracted from symptomatic and non-symptomatic tomato plants and subjected to PCR for detecting TYLCV with specific coat protein (CP) primers V61 and V473 (Ghanim et al., 1998). The experiments were triplicated with 20 plants for each replicate.

Statistical Analysis

A one-way analysis of variance using Tukey's HSD adjustment test for multiple comparisons at a family-wise error rate of 5% was used for comparing all possible pairs of treatments. The connected letters in **Figures 1–3**, **5–7** provide a graphical summary: treatments not connected by the same letter are significantly different (i.e., Tukey adjusted p-value < 0.05). Error bars on the barplots are standard error of mean.

RESULTS

Testing the System With TRV-Mediated Silencing of Tomato Genes

Tomato plants transiently expressing dsRNA of *B. tabaci* and tomato target genes were generated by agroinfiltration. After a week, total RNA from agroinfiltrated plants was subjected to reverse transcription-PCR to amplify the target genes and TRV using specific primers. Amplification of the desired bands and virus confirmed the systemic movement of the TRV and target gene mRNA required for inducing siRNA production. First, the working system was tested for the ability to silence tomato genes. Plants agroinfiltrated with pTV::Tom-*CypB* construct, made for silencing the tomato *CypB* gene caused significant leaf petiole rolling and leaf crinkling, while the plants remained retarded until 8 weeks after infiltration, and those symptoms extended until death (**Figures 1A–C**). The expression of the tomato *CypB* gene in those agroinfiltrated plants was monitored using qRT-PCR analysis, and the results showed significant decrease in the transcript levels at 7 dpi which were further reduced to significantly lower levels by 14 and 21 dpi (**Figure 1G**). The expression of the tomato *CypB* gene, however, remained stable in the control plants which were not infiltrated or which were infiltrated with control TRV1 and TRV2 constructs (**Figure 1G**). Tomato plants were also co-infiltrated with pTV::Tom-*Hsp90* construct targeted to the endogenous heat shock protein 90 gene of tomato (Moshe et al., 2016) as an additional positive control. The virus propagation was visualized in stems 1 week after agroinfiltration and the stem became necrotic and plants died 24 days post infiltration as previously described (**Figures 1D–F**) (Moshe et al., 2016). The levels of the tomato *Hsp90* transcripts over time showed gradual decrease over 21 dpi (**Figure 1H**), compared to the controls in which the levels of the transcript remained stable over the course of the experiment. Altogether, the above results confirmed the ability of the TRV system to knock down the expression of tomato target genes to very low levels and cause significant phenotypes in the plant that resulted in death.

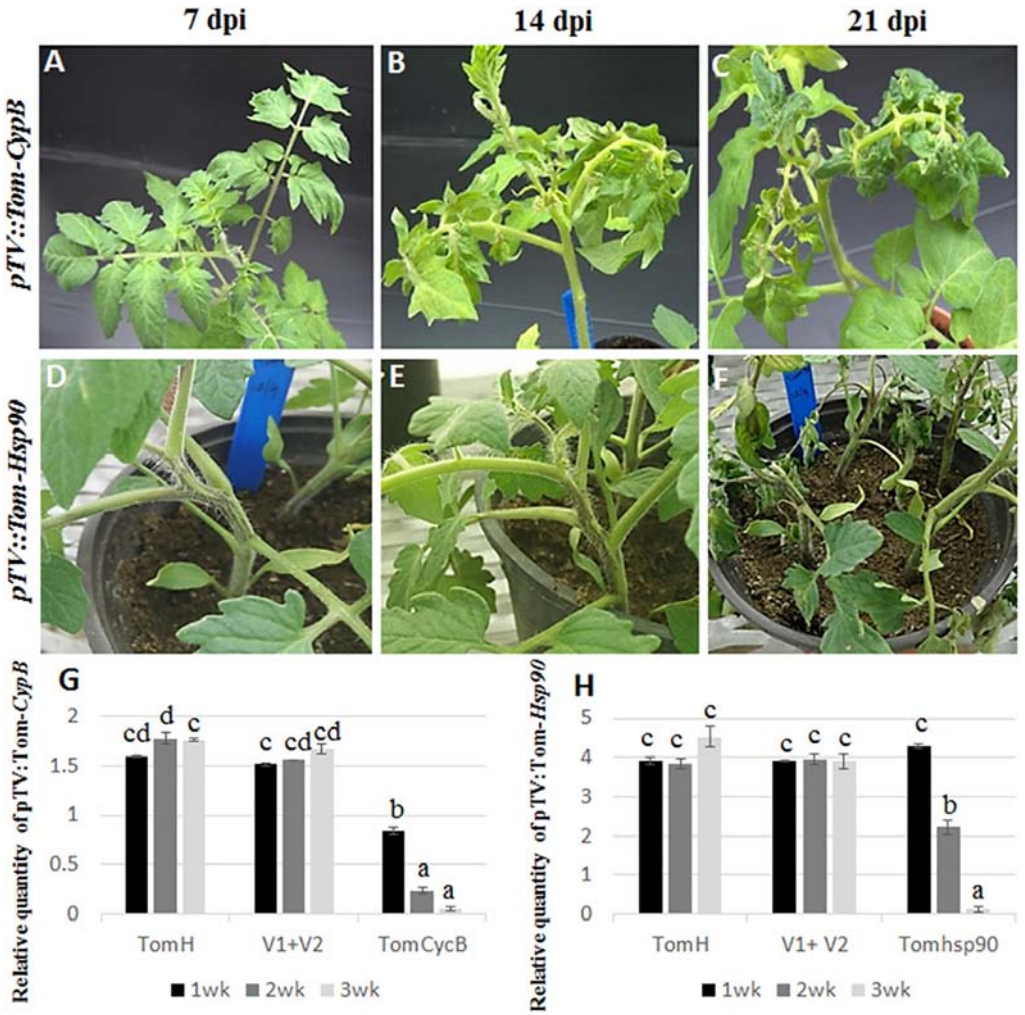

FIGURE 1 | Silencing of tomato *Cyp B* and *Hsp 90* genes. Silencing of *CypB* **(A–C)** induces leaf petiole rolling and leaf crinkling after 14 and 21 days post infection. Silencing of tomato *Hsp90* gene **(D–F)** induces cell death after 21 days post infection. **(G)** qRT-PCR of tomato *CypB* **(G)** and *Hsp90* **(H)** genes in three TRV lines at 7, 14, and 21 days post infection showing effective silencing of both genes compared to the controls. TomH is a non-agroinfiltrated tomato control. V1+V1 is a control agroinfiltrated with both control plasmids. TomCycB and TomHsp90 are plant agroinfiltrated with the respective gene for silencing (CycB or Hsp90).

TRV-Mediated Silencing of *B. tabaci* Genes and the Effect on Virus Levels

Selected regions of the cDNA of *CypB* and *Hsp70* genes were used for dsRNA expression in tomato plants (**Supplementary Figure S1**). The *CypB* gene codes for a Cyclophilin B gene (accession number KX268377) and the RNAi construct was designed to target the conversed two β sheets and α-helices from amino acids 1–77 which are conserved in *B. tabaci* compared to other arthropods (Kanakala and Ghanim, 2016a). This gene family exhibits a peptidylpropyl *cis–trans* isomerases activity (PPIases) and highly conserved Cyclosporin (CsA)-binding residues. On the other hand, the *Hsp70* gene codes for heat shock protein 70, which are important for protein folding and responding to a variety of stresses in the cell (Morano, 2007). *Hsp70*-RNAi construct was designed to be specific to nucleotides unique to the conserved protein domain family NLPC_P60. *B. tabaci CypB* and *Hsp70* are sufficiently different from the tomato *CypB* and *Hsp70* genes, thus they were expected to be suitable for knockdown and obtaining specific results for *B. tabaci* genes. The CypB and Hsp70 amino acid phylogenetic analysis of *B. tabaci* and tomato genes are shown in **Supplementary Figure S2**.

To evaluate the ability of TRV-infected plants to express *B. tabaci CypB* and *Hsp70* dsRNA and induce silencing in whiteflies, tomato plants were agroinfiltrated with the TRV::Bt *CypB* and TRV::Bt *Hsp70* constructs separately. Agroinfiltration with TRV::Bt *CypB* (**Figure 2B**) and TRV::Bt *Hsp70* (**Figure 2C**) did not affect tomato plant development, and no major visible morphological differences were observed between those plants and control plants (**Figure 2A**). Next, the effect of the expressed dsRNA of *B. tabaci CypB* and *Hsp70* genes in tomato using TRV was tested on the whitefly development, gene expression and TYLCV transmission by feeding assays. Following feeding on

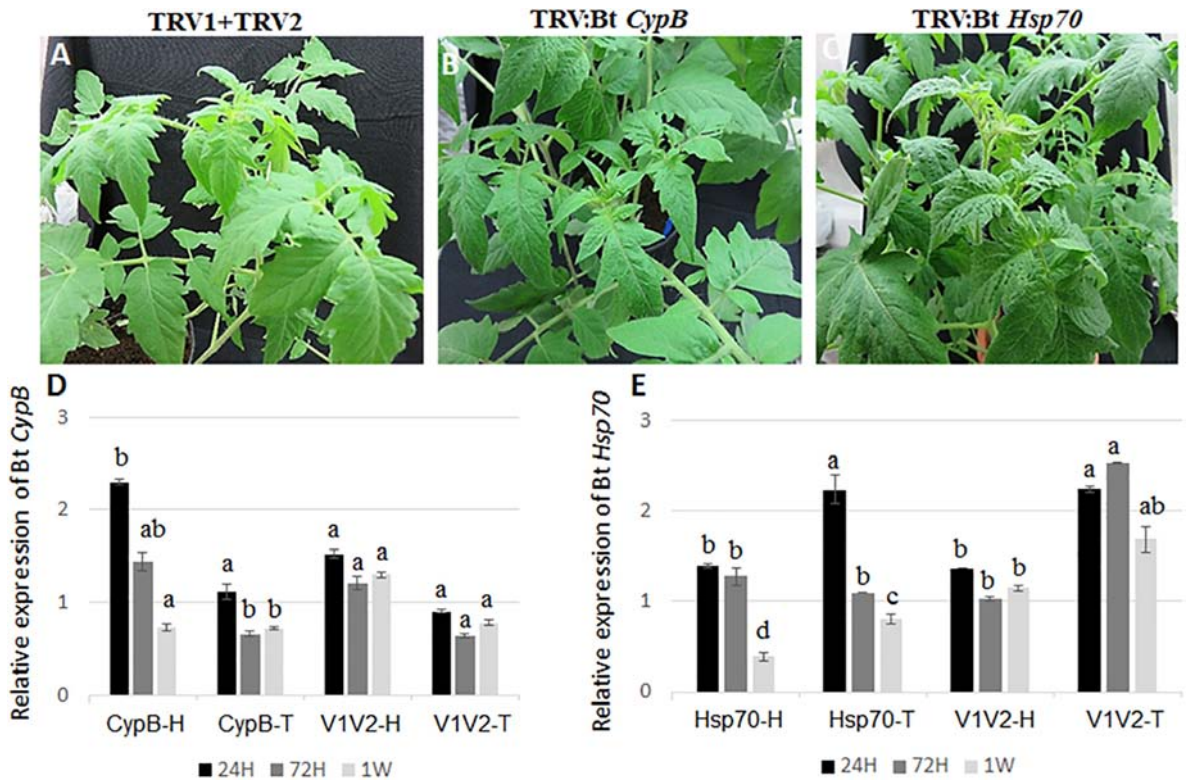

FIGURE 2 | Development of tomato plants after agroinfiltration with **(A)** TRV1+TRV2 (control), **(B)** TRV::Bt *CypB*, **(C)** TRV::Bt *Hsp70*. The pictures shown were takes 4 weeks post agroinfiltration. **(D)** Relative expression of Bt *CypB* in healthy tomato (CypB-H), TYLCV-infected tomato (CypB-T) and in control plants infected (V1V2-T) and uninfected (V1V2-H) with TYLCV after agroinfiltration with both TRV constructs. **(E)** Relative expression of Bt *Hsp70* in healthy tomato (Hsp70-H), TYLCV-infected tomato (Hsp70-T) and in control plants infected (V1V2-T) and uninfected (V1V2-H) with TYLCV after agroinfiltration with both TRV constructs. Bt, *Bemisia tabaci*.

pTV::Bt *CypB*, pTV::Bt *Hsp70*, TRV alone and mock inoculated plant leaves at three time intervals (24 h, 72 h, and 1 week), total RNA was extracted from both viruliferous and non-viruliferous whiteflies feeding on those plants and used in qRT-PCR. For Bt *CypB*, a gradual and significant down-regulation was observed from 24 h up to 1 week in non-viruliferous whiteflies (**Figure 2D**), while in viruliferous whiteflies a significant decrease in the expression was observed only at 72 h and 1 week compared to the levels at 24 h (**Figure 2D**). After *Hsp70* silencing, significant decrease in the expression was observed after 1 week in non-viruliferous whiteflies, while a gradual significant decrease was observed at 72 h and 1 week after the start of the feeding in viruliferous whiteflies (**Figure 2E**). The levels of the transcripts of both *CypB* and *Hsp70* genes remained stable in viruliferous and non-viruliferous whiteflies fed on the TRV1+TRV2 control plants (**Figures 2D,E**). Next, the virus levels in these experiments were also measured at the same time points where gene expression was measured. The results showed that the most significant effect on virus levels was observed in viruliferous whiteflies feeding on TRV::Bt *Hsp70* dsRNA expressing plants after 72 h post whitefly release, while in the rest of the treatments the virus levels did not significantly decrease at the same magnitude, possibly due to virus degradation over time (**Figure 3**).

TRV-Mediated Silencing of *CypB* and *Hsp70* Induce Morphological Abnormalities in First Generation

In the next experiments, we monitored whether the effects of gene silencing induced in the adults that fed on the dsRNA-expressing TRV plants, can be passed to the next generation and induce silencing and possibly phenotypic changes. Tomato plants agroinfiltrated with the pTV::Bt *CypB*, pTV::Bt *Hsp70*, TRV alone and mock inoculated plants were used for feeding adult whiteflies for 48 h after which they were transferred to cotton plants for egg lay. This transfer to cotton was performed to avoid any dsRNA acquisition by the next generation individuals from plants, and any observed effects would be attributed to dsRNA acquired from the previous generation. After a week, microscopic observations on the cotton leaves surfaces showed no difference in hatching between treatments and control insects. In all the agroinfiltrated groups, crawlers were observed over the leaf surface in search for a suitable settling site. Progeny collected from the pTV::Bt *CypB*, pTV::Bt *Hsp70* showed phenotypic changes in second and third instar stages compared to TRV alone and mock infiltrated (**Figure 4**). Over all, different phenotypes were observed between nymphs fed on Bt *CypB* and Bt *Hsp70* dsRNA-expressing plants. In the control insects, all instars looked

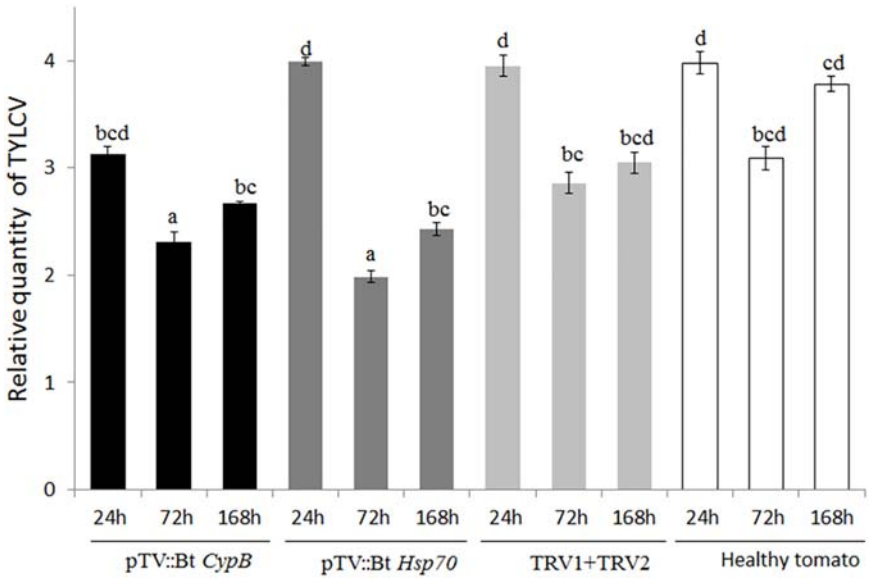

FIGURE 3 | Quantification of TYLCV levels in *B. tabaci* adults feeding on plants expressing dsRNA against *Cyp* B and *Hsp70* after 24 h, 72 h, and 1 week (168 h), compared to mock inoculated plants and plants inoculated with both TRV1 and TRV2 alone as a control.

oval in shape and flattened dorso-ventrally (**Figures 4A,B,D,E**). In case of nymphs feeding on *CypB* dsRNA-expressing plants, they appeared irregular in shape and eventually dried and fall off the leaves (**Figures 4G,H**). Interestingly, great effect on development at red-eyed nymph stage was noted and the red eyes were not observed as in normal development. Nymphs fed on pTV::Bt *Hsp70* plants showed different phenotypic changes and the nymphs became flat and thin in size, edges of the nymph became more transparent and gradually dissolved on the leaf surface and dried (**Figures 4J,K**). We further examined the morphology of adults in the first generation of insects that have fed on dsRNA-expressing plants. In both TRV *CypB*- and TRV *Hsp70* dsRNA-expressing plants on which the first generation was feeding, the adults exhibited curled winged morphology and lighter color of the body (**Figures 4I,L**), compared to control whiteflies that fed on control plants (**Figures 4C,F**). These whiteflies could not fly because of the wing morphology, hardly moved on the leaf, and died within 2–3 days without laying any eggs.

In these experiments, we quantified mRNAs levels in *B. tabaci* nymphs of the first generation that developed on the TRV-*CypB*, TRV-*Hsp70*, TRV alone and mock inoculated tomato plants using qRT-PCR in pools of second and third nymphal stages. The results showed dramatic suppression of the endogenous *CypB* and *Hsp70* mRNAs (**Figure 5**). Quantification of the amount of *CypB* and *Hsp70* genes were normalized against constitutively expressed *B. tabaci* α-tubulin levels. We observed ∼3 times depletion of C*ypB* in nymphs when fed on TRV-*CypB* plants. Simultaneously, the expression of *Cyp* D and G genes, which were previously studied by us, was tested and found to be reduced by ∼2.5 and 1.5 times, respectively (**Figure 5**). These results imply that knockdown of *CypB* could affect other *Cyp* genes in the whitefly. In the case of *Hsp70,* mRNA levels were reduced by ∼4 times when fed on TRV-*Hsp70*, compared to the controls.

Effect of TRV-Mediated Silencing of *CypB* and *Hsp70* on Mortality, Fecundity, and Virus Transmission

The effect of silencing *CypB* and *Hsp70* on adult whitefly mortality and fecundity were examined. Experiments were performed over a period of 2 weeks in which adults were given access to TRV-silencing plants for both genes and the cumulative mortality and fecundity (number of laid eggs) were recorded.

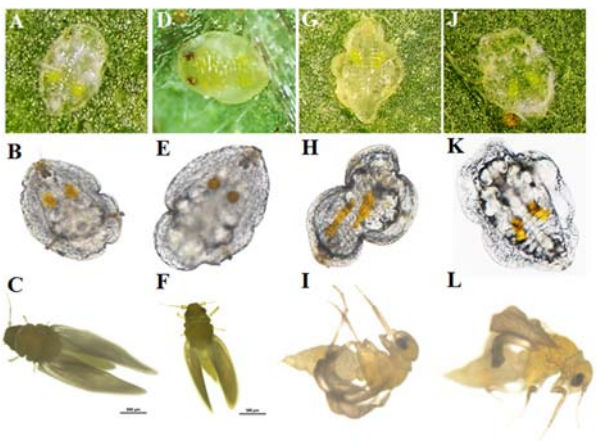

FIGURE 4 | Phenotypes of nymphs and adults of *B. tabaci* first generation after feeding on plants expressing dsRNA against *CypB* and *Hsp70*. **(A–C)** Nymphs and adult offspring of whiteflies that fed on healthy tomato leaves. **(D–F)** Nymphs and adult offspring of whiteflies that fed on TRV-agroinfiltrated tomato. **(G–I)** Nymphs and adult offspring of whiteflies that fed on pTV::Bt *CypB* dsRNA expressing tomato leaves. **(J–L)** Nymphs and adult offspring of whiteflies that fed on pTV::Bt *Hsp70* dsRNA expressing tomato leaves.

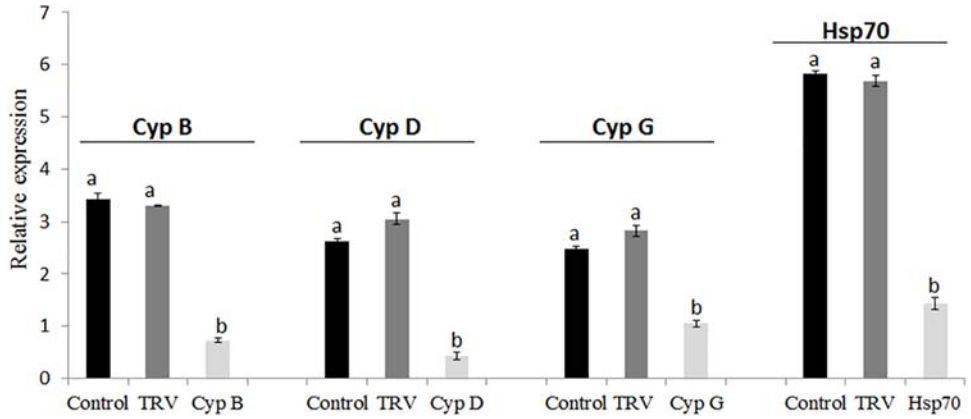

FIGURE 5 | Quantification of *B. tabaci Cyp* genes (*CypB*, *CypD*, and *CypG*) and *Hsp70* transcripts in next generation nymphs feeding on healthy and TRV control plants, and on pTV::Bt *CypB* and pTV::Bt *Hsp70* dsRNA-expressing tomato plants.

Surprisingly, we obtained very high mortality levels that reached 81.8% after feeding on TRV-*CypB* plants, and 85.6% when the adults were fed on TRV-*Hsp70* plants, compared to the TRV and mock control plants where the mortality reached 20% and 16%, respectively.

Females that did not die following feeding on the TRV-silencing plants were recovered from all treatments. Ten females for each replicate were used for egg lay over a course of 2 weeks. The results showed that females feeding on TRV-*CypB* or TRV-*Hsp70* plants laid 38.6% and 19.4% less eggs, respectively, compared to the control TRV and mock plants (**Figure 6**).

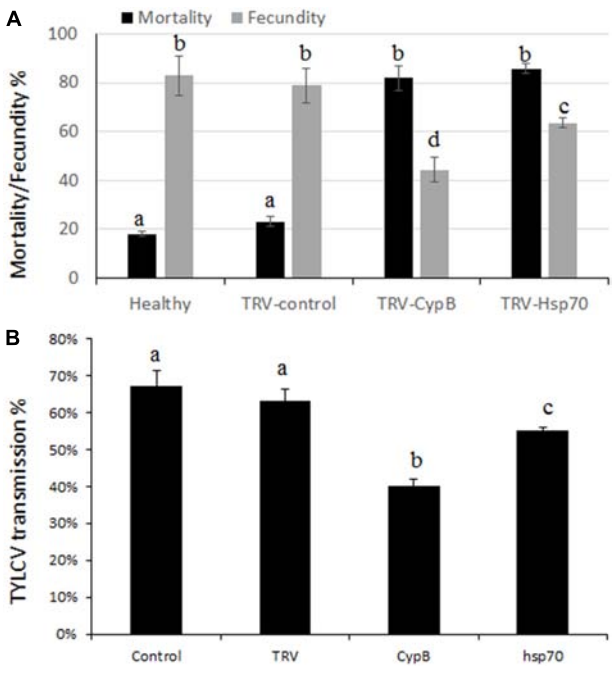

FIGURE 6 | Effect of TRV-silencing *CypB* and *Hsp70* on mortality and fecundity **(A)** and on TYLCV transmission **(B)**.

Some of the recovered females after feeding on silencing plants for both genes were used for virus transmission experiments. Adult MEAM1 females fed on TRV-*CypB* and TRV-*Hsp70* expressing plants for a week or on TRV alone and mock agroinfiltrated plants as control, were caged with TYLCV-infected plants for a 48 h acquisition access period. Subsequently, single whiteflies were transferred to tomato plants in their three-leaf stage for 7 days inoculation access period. In the TRV-*CypB* and TRV-*Hsp70* infected plants, 40% and 55% transmission rates were obtained on average, compared to ∼67% transmission rate when the whiteflies were fed on control plants (**Figure 6**).

Silencing *CypB* and *Hsp70* Induce Endosymbiont Displacement and Reduce *Rickettsia* Amounts

B. tabaci is associated with bacterial endosymbionts that contribute to its successful biology and interactions with the environment (Gottlieb et al., 2008; Gueguen et al., 2010; Skaljac et al., 2017). *Portiera* is the primary endosymbiont while there were seven additional secondary symbionts reported from *B. tabaci* cryptic species around the world. The amounts and density of these different symbionts can be influenced from internal genetic factors in the whiteflies, as well as external environmental factors, which in turn can influence the whitefly biology (Brumin et al., 2011). In the current study, we tested whether the location and densities of the three endosymbionts *Portiera, Rickettsia,* and *Hamiltonella* that infect the MEAM1 species that we used in this study are influenced following the silencing of *CypB* and *Hsp70.* As seen in **Figure 7**, the location of all tested symbionts did not change between the control (**Figures 7A,B,E,F**), and insects that where fed on silencing plants (**Figures 7C,D,G,H**). *Portiera* and *Hamiltonella* colocalized inside the bacteriome cells, while *Rickettsia* localized outside the those cells, and occupied outside organs in the body cavity as previously reported (Gottlieb et al., 2008; Brumin et al., 2012). However, the most notable difference between the control and silenced insects was the shape and structure of the bacteriome

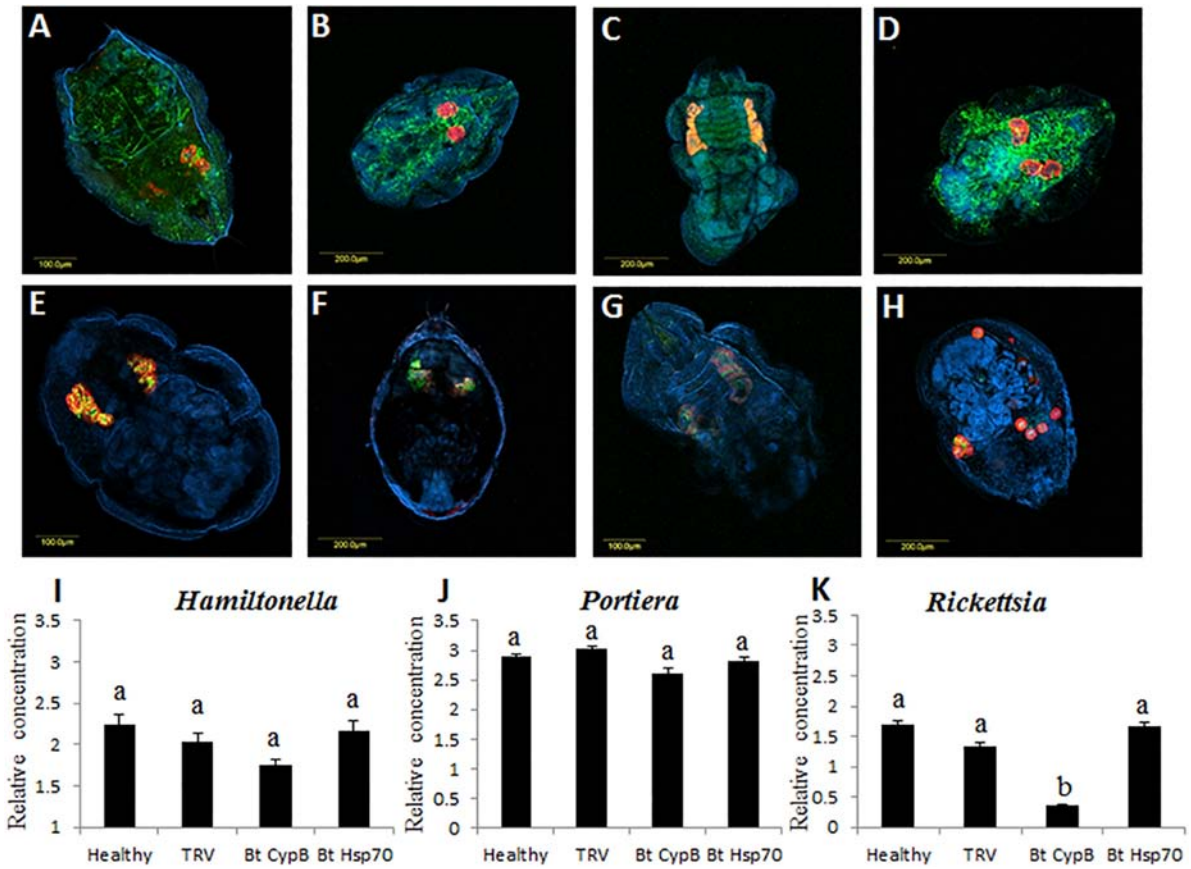

FIGURE 7 | Effect of *CypB* and *Hsp70* silencing on localization and densities of bacterial symbionts in *B. tabaci.* Localization of *Portiera* (red) and *Rickettsia* (green) is shown in **(A)** and localization of *Portiera* (red) and *Hamiltonella* (green) is shown in **(E)**, in both cases the insects were fed on healthy control plants. **(B,F)** are the same treatments and the insects were fed on TRV control plants. **(C,G)** the insects were fed on TRV-*CypB* plants in which *CypB* was silenced and in **(D,H)** the insects were fed on TRV-*Hsp70* plants in which *Hsp70* was silenced. In **(I–K)** quantification of the symbionts *Hamiltonella, Portiera,* and *Rickettsia,* respectively, using qPCR in healthy and TRV control plants and in TRV-*CypB* and TRV-*Hsp70* plants in which both the investigated genes *CypB* and *Hsp70* were silenced.

cells. In the control insects, the cells looked intact and appeared as one structure, while in the insects in which *CypB* was silenced, the bacteriome looked elongated and the cells partially disintegrated (**Figures 7C,G**). In the insects in which *Hsp70* was silenced, the phenotypes were even more severe where the bacteriome cells looked completely disintegrated, and the cells appeared all over the body when *Portiera* and *Hamiltonella* were localized (**Figure 7H**). When the densities of the three symbionts were measured after silencing using qPCR, the amounts of *Portiera* and *Hamiltonella* did not significantly differ compared with the controls, however, the amounts of *Rickettsia* were significantly reduced when *CypB* was silenced, a result that could be observed in the FISH results (**Figure 7C**).

DISCUSSION

In this study, we attempted to develop an RNAi-based approach for controlling one of the most important insect pests known in agriculture, by targetting two proteins that have been previously implicated in TYLCV transmission by *B. tabaci.* Over the past decade and since RNA interference (RNAi) was discovered, this technology has been described as a promise to develop effective, friendly and inexpensive technologies for making crops resistant to insect pests (Baum et al., 2007; Mao et al., 2007). Indeed, hundreds of research results described the effective use of RNAi in causing mortality or reducing insect pest populations, including insect vectors by delivering dsRNA into the insects in various ways (Gordon and Waterhouse, 2007; Price and Gatehouse, 2008; Kumar et al., 2012, 2014; Wuriyanghan and Falk, 2013; Kanakala and Ghanim, 2016b). Here, we took advantage of the ability of *B. tabaci* to feed on tomato, to test the effectiveness of RNAi in causing mortality and reducing virus transmission. This was done by silencing cyclophilin B and Hsp70, two genes with verified role in TYLCV transmission. We also used the TRV silencing system since it was shown to be very effective and robust in tomato, and has been shown to produce stable dsRNA/siRNA against target gene in plants (Kanakala and Ghanim, 2016b).

For testing the functionality of this system, we silenced the tomato cyclophilin and Hsp90 genes. These experiments demonstrated the robustness of the silencing system, especially when *Hsp90* was silenced and the results obtained were as

previously reported (Moshe et al., 2016). Next, *CypB* and *Hsp70* were targeted. Many recent studies demonstrated the ability to induce silencing in whiteflies, but none targeted genes involved in the insect–virus interactions or used the TRV plant-mediated silencing system (Ghanim et al., 2007; Thakur et al., 2014; Chen et al., 2015; Li et al., 2015; Raza et al., 2016; Whitten et al., 2016). TRV-mediated silencing of both *B. tabaci CypB* and *Hsp70* genes resulted in significant reduction in their expression (**Figure 2**). The silencing was consistent and reproducible 7 days post TRV inoculation and was observed in adults and nymphal stages feeding on the phloem of TRV plants expressing dsRNA for both genes (**Figure 2**, 1 week after silencing). After this successful silencing, subsequent experiments were designed to test the effectiveness of silencing *CypB* and *Hsp70* in viruliferous and non-viruliferous whitefly adults, and the results showed that the presence of the virus influenced the silencing potency, as well as the virus levels in the whitefly, confirming the role of these two genes in the whitefly–virus interactions.

Previous research studies in insects pests showed the effectiveness of RNAi in inducing phenotypic changes, as well as lethality, for example in planthoppers (Wu et al., 2012; Zhou et al., 2013; Xi et al., 2015), as we observed here. Although the experiments did not result in complete mortality and developmental arrest of all the nymphs on the leaves, highly significant number of nymphs did show phenotypic abnormalities, suggesting that the plant-mediated TRV silencing is an effective approach for dsRNA delivery by feeding in the plant phloem. The fact that silencing both *CypB* and *Hsp70* resulted in very high mortality rates suggests important roles that they play in the insect development, although the phenotypes obtained with both genes were not similar confirming their different roles in development. In the case of *Hsp70* the phenotypes appeared as drying of the nymphs and adults, suggesting internal factors that result in these drastic changes, while in the in the case of *CypB* more morphological changes in the nymphs were obtained. This may be attributed to the downregulation of the other *Cyp* genes (*CypD* and *CypG),* which when silenced together with *CypB* may contribute to more drastic effects on interactions with other genes, misregulation in their cumulative roles in correct folding of proteins and more drastic phenotypes as we observed. *Hsp70* is expressed almost in every cell and organ and have unusual sequence conservation and functional roles (Boorstein et al., 1994; Karlin and Brocchieri, 1998). It belongs to a large multifunction chaperone family with expanded cellular processes including disaggregation or proteins, prevention of aggregation, correct folding pf proteins, direction of proteins to their targets including translocation across membranes and targeting proteins to specific cellular domains (Pratt et al., 1999; Pishvaee et al., 2000). Many proteins of this family have overlapping roles because of the many functions they have to fulfill, thus they are present ubiquitously in the cell. It also known that some plant viruses encode their own Hsp70 proteins which facilitate virus transport cell to cell in the plant (Alzhanova et al., 2001; Aoki et al., 2002), and have roles in the virus life cycle and replication (Wang et al., 2009). Similar to HSp70s, *Cyp* genes which belong to the peptidyl-prolyl isomerases proteins (PPIases or Cyps), have important roles in the proper folding, chaperone functions and as modulators for human virus replication (Frausto et al., 2013). They were shown to interact with the capsid protein of the human immunodeficiency virus type 1 (HIV-1) (Schaller et al., 2011) and influenza A virus M1 protein (Liu et al., 2009) and were shown to play a key role in the viral replication cycle. They were also shown to contribute to the transmission of B/CYDV circulation and transmission by aphids (Tamborindeguy et al., 2013), and were hypothesized to play a role in chaperoning these viruses to various membrane bound vesicles (Yang et al., 2008).

One of the major effects that we observed following the silencing of both *Hsp70* and *CypB* is the disruption of the endosymbiont location in the insect, however the amounts of the endosymbionts were not disrupted except in the case of *Rickettsia* that was reduced following the silencing of *CypB*. Silencing *Hsp70* showed a dramatic effect on the location of the bacteriosome cells and they appeared disintegrated from the main bacteriome and dispersed in the cytoplasm. These results are supported by previous research in which it was shown that *Rickettsia,* which is the only symbiont that localizes outside of bacteriosome cells is influenced by stress and environmental factors such as heat and virus infection (Brumin et al., 2012; Kliot et al., 2014; Su et al., 2014). However, the effect of silencing *Hsp70* on the integrity of the bacteriome is novel and have not been associated with silencing insect genes in the whitefly or other insects that harbor endosymbiotic bacteria.

Silencing of insect genes is known to influence insect fertility and fecundity as was shown in several reports (Thakur et al., 2014; Mysore et al., 2015; Upadhyay et al., 2016). In our study, we also observed decreased fertility and fecundity when both *B. tabaci CypB* and *Hsp70* were silenced. These effects correlated with decrease in number of eggs laid and the number of hatched eggs. Targeting *CypB* by silencing caused decrease in fecundity more than that of *Hsp70*. The decrease in fecundity and fertility correlated well with the levels of gene expression measured from whole body and nymphs preparations, suggesting that silencing those genes not only results in the mortality of the first generation adults, but also in the reduction of their next generation. Silencing *B. tabaci* vitellogenin (*vg*) gene has been previously shown to be a potent target for decreasing fecundity and inducing mortality (Upadhyay et al., 2016).

The results we obtained here, showed that the siRNA signal could be passed from the feeding females on the plants to its offspring, where it induced silencing in the next generation. Similar results demonstrated the passage of silencing signal between generations (Grentzinger et al., 2012; Abdellatef et al., 2015). Reduced *CypB* expression in next generation nymphs and the wing morphology we observed in the next generation adults as well as the phenotypic changes in the development of nymphs suggest an efficient mechanism by which the silencing signal is transferred. Whiteflies fed on *CypB* dsRNA-expressing plants died earlier than those fed on pTV::Bt *Hsp70*, TRV alone and mock inoculated plants, thus we were not able to test the effect on following generations.

The effect on virus transmission following silencing was an important goal of this study. The results showed that TYLCV transmission was reduced by 27% after *CypB*

plant-mediated silencing, and less than that when *Hsp70* was silenced. These results are consistent with previous results in which inhibition of *CypB* resulted in decreased TYLCV transmission by *B. tabaci* by 43% (Kanakala and Ghanim, 2016a). As mentioned above, TYLCV transmission was reduced only by 12% after *Hsp70* silencing confirming previous results in which this protein was shown to pose an inhibitory role against TYLCV (Götz et al., 2012).

Taking these data together, our work demonstrated that targeting two previously identified genes in whitefly–virus interactions, *CypB* and *Hsp70*, could result in inhibiting the virus transmission and the quantity and location of endosymbionts in the insect. However, because these genes have many other functional roles in the cell, their silencing resulted in drastic phenotypic changes in nymphs and adults and in high mortality, and this silencing signal was heritable. Thus, those genes could serve as important targets for developing resistant plants against *B. tabaci*.

AUTHOR CONTRIBUTIONS

SuK and MG conceived and designed the study, analyzed the data, and wrote the manuscript. SuK, SvK, and GL conducted the experiments.

FUNDING

This research was performed at The Volcani Center, Rishon LeZion, Israel and did not receive external funding. SK received a postdoctoral fellowship from the Israel-India program for supporting Indian postdocs in Israel.

SUPPLEMENTARY MATERIAL

The Supplementary Material for this article can be found online at: https://www.frontiersin.org/articles/10.3389/fphys.2019.00557/full#supplementary-material

FIGURE S1 | Partial sequences of the Bt *CypB*, Bt *Hsp70*, and Tomato *CypB*. **(A)** Bt *CypB* and **(B)** Bt *Hsp70* were amplified by PCR using gene-specific primers linked to *Eco*R1/*Bam*H1 restriction sites. **(C)** Tomato *CypB* was amplified by PCR using gene-specific primers linked to *EcoR1/BamH1* restriction sites. **(D)** The constructs of tobacco rattle virus vectors: the cDNA fragments were inserted into the multiple cloning site of pTRV2 vector to produce tobacco rattle virus constructs.

FIGURE S2 | Phylogenetic tree of *B. tabaci* CypB **(A)** and hsp70 **(B)** and other arthropods, fungal species, *Solanum lycopersicum* and *H. sapiens*. Phylogenetic tree was generated using MEGA 6 (Tamura et al., 2013) with maximum likelihood method. Numbers next to the branches indicated bootstrap value of each internal branch in the phylogenetic tree nodes from 1,000 replicates.

TABLE S1 | Primers used in this study for PCR and qRT-PCR analysis.

REFERENCES

Abdellatef, E., Will, T., Koch, A., Imani, J., Vilcinskas, A., and Kogel, K. H. (2015). Silencing the expression of the salivary sheath protein causes transgenerational feeding suppression in the aphid *Sitobion avenae*. *Plant Biotechnol. J.* 13, 849–857. doi: 10.1111/pbi.12322

Alzhanova, D. V., Napuli, A. J., Creamer, R., and Dolja, V. V. (2001). Cell-to-cell movement and assembly of a plant closterovirus: roles for the capsid proteins and Hsp70 homolog. *EMBO J.* 20, 6997–7007. doi: 10.1093/emboj/20.24.6997

Aoki, K., Kragler, F., Xoconostle-Cazares, B., and Lucas, W. J. (2002). A subclass of plant heat shock cognate 70 chaperones carries a motif that facilitates trafficking through plasmodesmata. *Proc. Natl. Acad. Sci. U.S.A.* 99, 16342–16347. doi: 10.1073/pnas.252427999

Baum, J. A., Bogaert, T., Clinton, W., Heck, G. R., Feldmann, P., Ilagan, O., et al. (2007). Control of coleopteran insect pests through RNA interference. *Nat. Biotechnol.* 25, 1322–1326. doi: 10.1038/nbt1359

Boorstein, W. R., Ziegelhoffer, T., and Craig, E. A. (1994). Molecular evolution of the HSP70 multigene family. *J. Mol. Evol.* 38, 1–17. doi: 10.1007/BF00175490

Brumin, M., Kontsedalov, S., and Ghanim, M. (2011). *Rickettsia* influences thermotolerance in the whitefly *Bemisia tabaci* B biotype. *Insect Sci.* 18, 57–66. doi: 10.1111/j.1744-7917.2010.01396.x

Brumin, M., Levy, M., and Ghanim, M. (2012). Transovarial transmission of *Rickettsia* spp. and organ-specific infection of the whitefly Bemisia tabaci. *Appl. Environ. Microbiol.* 78, 5565–5574. doi: 10.1128/AEM.01184-12

Chen, X., Li, L., Hu, Q., Zhang, B., Wu, W., Jin, F., et al. (2015). Expression of dsRNA in recombinant *Isaria fumosorosea* strain targets the TLR7 gene in *Bemisia tabaci*. *BMC Biotechnol.* 15:64. doi: 10.1186/s12896-015-0170-8

Chiel, E., Gottlieb, Y., Zchori-Fein, E., Mozes-Daube, N., Katzir, N., Inbar, M., et al. (2007). Biotype-dependent secondary symbiont communities in sympatric populations of *Bemisia tabaci*. *Bull. Entomol. Res.* 97, 407–413. doi: 10.1017/S0007485307005159

Czosnek, H., Hariton-Shalev, A., Sobol, I., Gorovits, R., and Ghanim, M. (2017). The incredible journey of begomoviruses in their whitefly vector. *Viruses* 9:273. doi: 10.3390/v9100273

De Barro, P. J., Scott, K. D., Graham, G. C., Lange, C. L., and Schutze, M. K. (2003). Isolation and characterization of microsatellite loci in *Bemisia tabaci*. *Mol. Ecol. Notes* 3, 40–43. doi: 10.1046/j.1471-8286.2003.00344.x

Frausto, S. D., Lee, E., and Tang, H. (2013). Cyclophilins as modulators of viral replication. *Viruses* 5, 1684–1701. doi: 10.3390/v5071684

Ghanim, M. (2014). A review of the mechanisms and components that determine the transmission efficiency of Tomato yellow leaf curl virus (Geminiviridae; Begomovirus) by its whitefly vector. *Virus Res.* 186, 47–54. doi: 10.1016/j.virusres.2014.01.022

Ghanim, M., Kontsedalov, S., and Czosnek, H. (2007). Tissue-specific gene silencing by RNA interference in the whitefly *Bemisia tabaci* (Gennadius). *Insect Biochem. Mol. Biol.* 37, 732–738. doi: 10.1016/j.ibmb.2007.04.006

Ghanim, M., Morin, S., Zeidan, M., and Czosnek, H. (1998). Evidence for transovarial transmission of tomato yellow leaf curl virus by its vector the whitefly *Bemisia tabaci*. *Virology* 240, 295–303. doi: 10.1006/viro.1997.8937

Gordon, K. H., and Waterhouse, P. M. (2007). RNAi for insect-proof plants. *Nat. Biotechnol.* 25:1231. doi: 10.1038/nbt1107-1231

Gottlieb, Y., Ghanim, M., Chiel, E., Gerling, D., Portnoy, V., Steinberg, S., et al. (2006). Identification and localization of a *Rickettsia* sp in *Bemisia tabaci* (Homoptera: Aleyrodidae). *Appl. Environ. Microbiol.* 72, 3646–3652. doi: 10.1128/AEM.72.5.3646-3652.2006

Gottlieb, Y., Ghanim, M., Gueguen, G., Kontsedalov, S., Vavre, F., Fleury, F., et al. (2008). Inherited intracellular ecosystem: symbiotic bacteria share bacteriocytes in whiteflies. *FASEB J.* 22, 2591–2599. doi: 10.1096/fj.07-101162

Götz, M., Popovski, S., Kollenberg, M., Gorovits, R., Brown, J. K., Cicero, J. M., et al. (2012). Implication of *Bemisia tabaci* heat shock protein 70 in begomovirus-whitefly interactions. *J. Virol.* 86, 13241–13252. doi: 10.1128/JVI.00880-12

Grentzinger, T., Armenise, C., Brun, C., Mugat, B., Serrano, V., Pelisson, A., et al. (2012). piRNA-mediated transgenerational inheritance of an acquired trait. *Genome Res.* 22, 1877–1888. doi: 10.1101/gr.136614.111

Gueguen, G., Vavre, F., Gnankine, O., Peterschmitt, M., Charif, D., Chiel, E., et al. (2010). Endosymbiont metacommunities, mtDNA diversity and the evolution of the *Bemisia tabaci* (Hemiptera: Aleyrodidae) species complex. *Mol. Ecol.* 19, 4365–4376. doi: 10.1111/j.1365-294X.2010.04775.x

Hanley-Bowdoin, L., Bejarano, E. R., Robertson, D., and Mansoor, S. (2013). Geminiviruses: masters at redirecting and reprogramming plant processes. *Nat. Rev. Microbiol.* 11, 777–788. doi: 10.1038/nrmicro3117

Hogenhout, S. A., Ammar, E. D., Whitfield, A. E., and Redinbaugh, M. G. (2008). Insect vector interactions with persistently transmitted viruses. *Annu. Rev. Phytopathol.* 46, 327–359. doi: 10.1146/annurev.phyto.022508.092135

Kanakala, S., and Ghanim, M. (2016a). Implication of the whitefly *Bemisia tabaci* Cyclophilin B protein in the transmission of tomato yellow leaf curl virus. *Front. Plant Sci.* 7:1702. doi: 10.3389/fpls.2016.01702

Kanakala, S., and Ghanim, M. (2016b). RNA interference in insect vectors for plant viruses. *Viruses* 8:329. doi: 10.3390/v8120329

Kanakala, S., and Ghanim, M. (2018). "Whitefly-transmitted begomoviruses and advances in the control of their vectors," in *Genes, Genetics and Transgenics for virus resistance in plants*, ed. B. Patil (Poole: Ciaster Academic Press), 201–220.

Karlin, S., and Brocchieri, L. (1998). Heat shock protein 70 family: multiple sequence comparisons function and evolution. *J. Mol. Evol.* 47, 565–577. doi: 10.1007/PL00006413

Kliot, A., Cilia, M., Czosnek, H., and Ghanim, M. (2014). Implication of the bacterial endosymbiont *Rickettsia* spp. in the whitefly *Bemisia tabaci* interactions with tomato yellow leaf curl virus. *J. Virol.* 88, 5652–5660. doi: 10.1128/JVI.00071-14

Kumar, P., Pandit, S. S., and Baldwin, I. T. (2012). *Tobacco rattle virus* vector: a rapid and transient means of silencing *Manduca sexta* genes by plant mediated RNA interference. *PLoS One* 7:e31347. doi: 10.1371/journal.pone.0031347

Kumar, P., Pandit, S. S., Steppuhn, A., and Baldwin, I. I. (2014). Natural history-driven, plant-mediated RNAi-based study reveals CYP6B46's role in a nicotine-mediated antipredator herbivore defense. *Proc. Natl. Acad. Sci. U.S.A.* 111, 1245–1252. doi: 10.1073/pnas.1314848111

Li, J., Li, X., Bai, R., Shi, Y., Tang, Q., An, S., et al. (2015). RNA interference of the P450 CYP6CM1 gene has different efficacy in B and Q biotypes of *Bemisia tabaci*. *Pest. Manag. Sci.* 71, 1175–1181. doi: 10.1002/ps.3903

Li, Z., and Srivastava, P. (2004). Heat-shock proteins. *Curr. Protoc. Immunol.* 58, A.1T.1–A.1T.6. doi: 10.1002/0471142735.ima01ts58

Liu, X., Sun, L., Yu, M., Wang, Z., Xu, C., Xue, Q., et al. (2009). Cyclophilin A interacts with influenza A virus M1 protein and impairs the early stage of the viral replication. *Cell Microbiol.* 11, 730–741. doi: 10.1111/j.1462-5822.2009.01286.x

Mahadav, A., Kontsedalov, S., Czosnek, H., and Ghanim, M. (2009). Thermotolerance and gene expression following heat stress in the whitefly *Bemisia tabaci* B and Q biotypes. *Insect Biochem. Mol. Biol.* 39, 668–676. doi: 10.1016/j.ibmb.2009.08.002

Mao, Y. B., Cai, W. J., Wang, J. W., Hong, G. J., Tao, X. Y., Wang, L. J., et al. (2007). Silencing a cotton bollworm P450 monooxygenase gene by plant-mediated RNAi impairs larval tolerance of gossypol. *Nat. Biotechnol.* 25, 1307–1313. doi: 10.1038/nbt1352

Morano, K. A. (2007). New tricks for an old dog: the evolving world of Hsp70. *Ann. NY Acad. Sci.* 1113, 1–14. doi: 10.1196/annals.1391.018

Moshe, A., Gorovits, R., Liu, Y., and Czosnek, H. (2016). Tomato plant cell death induced by inhibition of HSP90 is alleviated by Tomato yellow leaf curl virus infection. *Mol. Plant. Pathol.* 17, 247–260. doi: 10.1111/mpp.12275

Mysore, K., Sun, L., Tomchaney, M., Sullivan, G., Adams, H., Piscoya, A. S., et al. (2015). siRNA-Mediated Silencing of *doublesex* during female development of the dengue vector mosquito *Aedes aegypti*. *PLoS Negl. Trop. Dis.* 9:e0004213. doi: 10.1371/journal.pntd.0004213

Navot, N., Pichersky, E., Zeidan, M., Zamir, D., and Czosnek, H. (1991). Tomato yellow leaf curl virus: a whitefly-transmitted geminivirus with a single genomic component. *Virology* 185, 151–161. doi: 10.1016/0042-6822(91)90763-2

Pishvaee, B., Costaguta, G., Yeung, B. G., Ryazantsev, S., Greener, T., Greene, L. E., et al. (2000). A yeast DNA J protein required for uncoating of clathrin-coated vesicles in vivo. *Nat. Cell Biol.* 2, 958–963. doi: 10.1038/35046619

Pratt, W. B., Silverstein, A. M., and Galigniana, M. D. (1999). A model for the cytoplasmic trafficking of signalling proteins involving the hsp90-binding immunophilins and p50cdc37. *Cell Signal.* 11, 839–851. doi: 10.1016/S0898-6568(99)00064-9

Price, D. R., and Gatehouse, J. A. (2008). RNAi-mediated crop protection against insects. *Trends Biotechnol.* 26, 393–400. doi: 10.1016/j.tibtech.2008.04.004

Raza, A., Malik, H. J., Shafiq, M., Amin, I., Scheffler, J. A., Scheffler, B. E., et al. (2016). RNA Interference based approach to down regulate osmoregulators of whitefly (*Bemisia tabaci*): potential technology for the control of whitefly. *PLoS One* 11:e0153883. doi: 10.1371/journal.pone.0153883

Rosen, R., Kanakala, S., Kliot, A., Pakkianathan, B. C., Farich, B. A., Santana-Magal, N., et al. (2015). Persistent, circulative transmission of begomoviruses by whitefly vectors. *Curr. Opin. Virol.* 15, 1–8. doi: 10.1016/j.coviro.2015.06.008

Schaller, T., Ocwieja, K. E., Rasaiyaah, J., Price, A. J., Brady, T. L., Roth, S. L., et al. (2011). HIV-1 capsid-cyclophilin interactions determine nuclear import pathway, integration targeting and replication efficiency. *PLoS Pathog.* 7:e1002439. doi: 10.1371/journal.ppat.1002439

Senthil-Kumar, M., and Mysore, K. S. (2014). *Tobacco rattle virus*–based virus-induced gene silencing in *Nicotiana benthamiana*. *Nat. Protoc.* 9, 1549–1562. doi: 10.1038/nprot.2014.092

Shahjahan, R. M., Hughes, K. J., Leopold, R. A., and DeVault, J. D. (1995). Lower incubation temperature increases yield of insect genomic DNA isolated by the CTAB method. *Biotechniques* 19, 332–334.

Sinisterra, X. H., McKenzie, C. L., Hunter, W. B., Powell, C. A., and Shatters, R. G. Jr. (2005). Differential transcriptional activity of plant-pathogenic begomoviruses in their whitefly vector (*Bemisia tabaci*, Gennadius: Hemiptera *Aleyrodidae*). *J. Gen. Virol.* 86, 1525–1532. doi: 10.1099/vir.0.80664-0

Skaljac, M., Kanakala, S., Zanic, K., Puizina, J., Pleic, I. L., and Ghanim, M. (2017). Diversity and phylogenetic analyses of bacterial symbionts in three whitefly species from Southeast Europe. *Insects* 8:113. doi: 10.3390/insects8040113

Su, Q., Xie, W., Wang, S., Wu, Q., Ghanim, M., and Zhang, Y. (2014). Location of symbionts in the whitefly *Bemisia tabaci* affects their densities during host development and environmental stress. *PLoS One* 9:e91802. doi: 10.1371/journal.pone.0091802

Tamborindeguy, C., Bereman, M. S., Deblasio, S., Igwe, D., Smith, D. M., White, F., et al. (2013). Genomic and proteomic analysis of *Schizaphis graminum* reveals cyclophilin proteins are involved in the transmission of Cereal yellow dwarf virus. *PLoS One* 8:e71620. doi: 10.1371/journal.pone.0071620

Tamura, K., Stecher, G., Peterson, D., Filipski, A., and Kumar, S. (2013). MEGA6: molecular evolutionary genetics analysis version 6.0. *Mol. Biol. Evol.* 30, 2725–2729. doi: 10.1093/molbev/mst197

Thakur, N., Upadhyay, S. K., Verma, P. C., Chandrashekar, K., Tuli, R., and Singh, P. (2014). Enhanced whitefly resistance in transgenic tobacco plants expressing double stranded RNA of v-ATPase A gene. *PLoS One* 9:e87235. doi: 10.1371/journal.pone.0087235

Upadhyay, S. K., Chandrashekar, K., Thakur, N., Verma, P. C., Borgio, J. F., Singh, P. K., et al. (2011). RNA interference for the control of whiteflies (*Bemisia tabaci*) by oral route. *J. Biosci.* 36, 153–161. doi: 10.1007/s12038-011-9009-1

Upadhyay, S. K., Singh, H., Dixit, S., Mendu, V., and Verma, P. C. (2016). Molecular characterization of vitellogenin and vitellogenin receptor of Bemisia tabaci. *PLoS One* 11:e0155306. doi: 10.1371/journal.pone.0155306

Wang, P., and Heitman, J. (2005). The cyclophilins. *Genome. Biol.* 6:226. doi: 10.1186/gb-2005-6-7-226

Wang, R. Y., Stork, J., Pogany, J., and Nagy, P. D. (2009). A temperature sensitive mutant of heat shock protein 70 reveals an essential role during the early steps of tombusvirus replication. *Virology* 394, 28–38. doi: 10.1016/j.virol.2009.08.003

Whitten, M. M., Facey, P. D., Del Sol, R., Fernández-Martínez, L. T., Evans, M. C., Mitchell, J. J., et al. (2016). Symbiont-mediated RNA interference in insects. *Proc. R. Soc. B* 283:20160042. doi: 10.1098/rspb.2016.0042

Wu, W. J., Wang, Y., Huang, H. J., Bao, Y. Y., and Zhang, C. X. (2012). Ecdysone receptor controls wing morphogenesis and melanization during rice planthopper metamorphosis. *J. Insect Physiol.* 58, 420–426. doi: 10.1016/j.jinsphys.2012.01.012

Wuriyanghan, H., and Falk, B. W. (2013). RNA Interference towards the potato psyllid, *Bactericera cockerelli*, is induced in plants infected with recombinant *Tobacco mosaic virus* (TMV). *PLoS One* 8:e66050. doi: 10.1371/journal.pone.0066050

Xi, Y., Pan, P. L., and Zhang, C. X. (2015). The β-N-acetylhexosaminidase gene family in the brown planthopper,

Nilaparvata lugens. *Insect Mol. Biol.* 24, 601–610. doi: 10.1111/imb.12187

Yang, X., Thannhauser, T. W., Burrows, M., Cox-Foster, D., Gildow, F. E., and Gray, S. M. (2008). Coupling genetics and proteomics to identify aphid proteins associated with vector-specific transmission of polerovirus (*Luteoviridae*). *J. Virol.* 82, 291–299. doi: 10.1128/JVI.01736-07

Zhou, W. W., Liang, Q. M., Xu, Y., Gurr, G. M., Bao, Y. Y., Zhou, X. P., et al. (2013). Genomic insights into the glutathione S-transferase gene family of two rice planthoppers, *Nilaparvata lugens* (Stål) and *Sogatella furcifera* (Horváth) (Hemiptera: Delphacidae). *PLoS One* 8:e56604. doi: 10.1371/journal.pone.0056604

Conflict of Interest Statement: The authors declare that the research was conducted in the absence of any commercial or financial relationships that could be construed as a potential conflict of interest.

frontiers in Physiology

MINI REVIEW
published: 08 May 2019
doi: 10.3389/fphys.2019.00550

Complex Insect–Pathogen Interactions in Tree Pandemics

Alberto Santini[1] *and Andrea Battisti*[2]*

[1] *Institute for Sustainable Plant Protection, National Research Centre, Sesto Fiorentino, Italy,* [2] *Department of Agronomy, Food, Natural Resources, Animals and the Environment, University of Padua, Padua, Italy*

Tree pandemics are a major cause of economic and ecological loss in forest and urban ecosystems. They often depend on the introduction of a non-native pathogen, which is occupying the niche of a native, non-aggressive organism. Complex interactions with native insects carrying fungi and nematodes can be established based on the proximity of the aggressive pathogenic agents. Here we review three major pandemics of forest and urban trees in temperate ecosystems at world scale, i.e., the Dutch elm disease, the cypress canker, and the pine wilt disease. For each system, the relationships between aggressive and non-aggressive fungi and nematodes with the native insect vectors are presented. Hidden players such as insects, microorganisms or plants, which may have the role of facilitating or contrasting the performance of the agents, are also considered. Results suggest that pandemics rely on the introduction of a non-native pathogen that exploits well-developed interactions between native non-aggressive organisms and insects associated with trees. The success of the invaders depends on the morpho-physiological proximity of the players and on the mutual benefits resulting from the associations. Deciphering such interactions in native systems may help to predict the outcome of the introduction of new pathogens and the development of new tree pandemics.

Keywords: Dutch elm disease, cypress canker disease, pine wilt disease, vector, facilitator, antagonist

OPEN ACCESS

Edited by:
Michel Cusson,
Natural Resources Canada, Canada

Reviewed by:
Louis Bernier,
Laval University, Canada
Mauro Mandrioli,
University of Modena and Reggio Emilia, Italy

***Correspondence:**
Andrea Battisti
andrea.battisti@unipd.it

Specialty section:
This article was submitted to Invertebrate Physiology, a section of the journal Frontiers in Physiology

Received: *03 January 2019*
Accepted: *18 April 2019*
Published: *08 May 2019*

Citation:
Santini A and Battisti A (2019) Complex Insect–Pathogen Interactions in Tree Pandemics. Front. Physiol. 10:550. doi: 10.3389/fphys.2019.00550

INTRODUCTION

When the Iron curtain collapsed at the end of the 1980s, probably none would have imagined that we were contributing to the last constitutive act of a new epoch, the Anthropocene (Crutzen and Stoermer, 2000; Crutzen, 2002; Lewis and Maslin, 2015). According to other authors (Rosenzweig, 2001), this was the start of the Homogocene, a term more related to invasion biology, which highlights the increasing rate of anthropogenic homogenization defined as the "gradual replacement of native biotas by locally expanding non-natives" (Olden et al., 2004). Plants and associated organisms have generally evolved in isolated assemblages, but when humans carry non-native pathogenic organisms into new environments, the latter may find suitable hosts lacking resistance genes and environments favoring their pathogenic behavior (Santini et al., 2018). This process may result in epidemics of newly emerging diseases, and, eventually, in a pandemic, i.e., a global epidemic. This process is greatly facilitated by the presence in the new environment of similar climatic conditions and of hosts phylogenetically related to those present in the native environment.

Pandemics may benefit from strict associations between plants and their herbivores and pathogens, which have developed through long periods of co-evolutionary change in species

(Schluter, 2009). Such associations can occur even among very different taxa of microorganisms, arthropods, and plants (Biere and Tack, 2013). In some cases it is not just a dual interaction, but a very complex interaction among many organisms that shaped the genetic outcome of different species and the entire ecosystem. In some cases, the introduction of new pathogens is not followed by a disease epidemic until a new association with an insect vector is established. New associations between native insect vectors and non-native pathogens of trees resulted into a more efficient pathogen transmission, which are increasingly reported (Battisti et al., 1999; Brasier, 2001; Sousa et al., 2001; Lu et al., 2010; Luchi et al., 2012).

Aim of this review is to analyze factors that determined the success of three pandemics that affected trees, namely Dutch elm disease, cypress canker disease, and pine wilt disease (**Table 1**). All of them are well-known for their heavy economic, ecological, and landscape impacts. The common trait to the three pandemics is that a non-native pathogen has occupied the niche of a non-aggressive, native agent, replacing it almost completely in the invasion area. In addition, the relationships established by the native non-aggressive organism with a number of facilitating or antagonistic factors have been somewhat transferred to the non-native pathogens, with consequences that are difficult to predict.

CASE STUDY 1: DUTCH ELM DISEASE

Dutch elm disease is caused by some Ascomycete fungi of the genus *Ophiostoma* (Ophiostomatales, *Ophiostoma ulmi* s.l. for the sake of this review), and it is famous for being one of the most destructive diseases ever reported in the history of plant pathology. As a result of the disease, during the last century, adult elm trees were nearly wiped out from Europe, Asia, and North America. Two pandemics occurred, the first caused by *O. ulmi* started in Europe in the 1910s (Spierenburg, 1921) and rapidly spread in North America (Brasier, 2000; Guries, 2001). Around 1940, as most of the susceptible trees were killed, the effect of the disease diminished in Europe (Brasier, 1979). Just a few years later, in the 1950s, a second, and more destructive outbreak caused the death of elm trees in Europe, Western Asia, and North America (Brasier and Kirk, 2001), reducing many majestic trees to weedy shrubs (Mittempergher, 1989). This second, still active outbreak is due to a different species, the highly virulent *O. novo-ulmi* (Brasier, 1991), which has replaced *O. ulmi*. Moreover, two subspecies of *O. novo-ulmi* are known: *O. novo-ulmi* ssp. *novo-ulmi*, and *O. novo-ulmi* ssp. *americana* (Brasier and Kirk, 2001).

The spread of this disease was particularly quick and effective because *O. ulmi* s.l. is supposed to have replaced the native non-aggressive species *O. quercus* in its ancient association with the elm bark beetles of the genus *Scolytus* in Europe (Brasier, 1990). *Ophiostoma quercus* is a fungus that colonizes a wide array of hardwood and conifer hosts, including elms (Taerum et al., 2018). Adult beetles contaminated with fungal spores emerge from pupal chambers in spring from the bark of dying infected elms and fly to feed at the crotches of young twigs of healthy elms. Infected beetles contaminate healthy elms by carrying the pathogen spores into the host's vascular tissues. Spores germinate into a growing mycelium and reach the wide spring vessels, where the pathogen moves into a yeast multiplication phase (Webber and Brasier, 1984). Later, female beetles move to dying elms, mostly ought to the disease, to lay eggs under the bark of the stem and main branches, which is an ideal environment for both larval development (Rudinsky, 1962) and pathogen fructification (Webber and Brasier, 1984). Both asexual and sexual pathogen fruiting structures generate spores embedded in a sticky mucilage that facilitates their adhesion to the beetles. The new contaminated beetles emerge from the bark and move toward the crown of new healthy elms, completing the cycle (**Figure 1**).

Some other organisms are known for playing a less evident, but indeed important role in the dynamics of the beetle-fungi association. *Tarsonemus crassus* and *Proctolaelaps scolyti* are two mite species associated with *Scolytus* spp. that can carry *O. novo-ulmi* spores within their sporothecae or in the digestive system, respectively (**Figure 1**). They were described for significantly increasing the beetle's spore spread efficiency (Moser et al., 2010).

Elm bark beetles also carry other ascomycetes such as *Geosmithia* spp., generally considered as saprotrophs or endophytes (Kolařík et al., 2008). In elms they were consistently isolated from beetles' galleries, but never from dead wood or healthy trees (Pepori et al., 2015; **Figure 1**). A high frequency horizontal gene transfer of the cerato-ulmin gene between *O. novo-ulmi* and *Geosmithia* spp. has been recently reported (Bettini et al., 2014), suggesting that the two species do not just share the same habitat and vectors, but they show much closer relationships. A recent study (Pepori et al., 2018), providing direct and indirect evidence, supports the hypothesis that many *Geosmithia* isolates specific to elm recently turned to be mycoparasites of *O. novo-ulmi*. This may lead to the long term stabilization of population dynamics of various organisms involved in this complex disease.

CASE STUDY 2: CYPRESS CANKER DISEASE

Cypress canker is caused by the fungal pathogen *Seiridium cardinale*, found first in California on Monterey cypress [*Hesperocyparis* (*Cupressus*) *macrocarpa*], which over a period of only a few years was completely destroyed in the plantations located in inland districts (Wagener, 1939). Monterey cypress, which is extremely susceptible and widely traded for ornamental purposes, had a major role in spreading the disease to other host species worldwide. In the course of the following decades, the disease was introduced through the trade of *H. macrocarpa* to Oceania, Europe, South America, and Africa, where it spread over various cypress species (Barthelet and Vinot, 1944; Grasso, 1951; Graniti, 1998; Della Rocca et al., 2013), with a tremendous impact. *Seiridium cardinale* is a wound pathogen and it occurs in the presence of small wounds due to abiotic or biotic agents (cold, hail, forced growth by fertilizers, insects, rodents) in the periderm of stems and branches through which the conidia or mycelium enter the inner bark (Danti et al., 2013).

TABLE 1 | Organisms involved in three tree pandemics, i.e., Dutch elm disease, cypress canker, and pine wilt disease.

Host plant	Invasive pathogenic associated organism	Native non-pathogenic associated organism	Insect vector system	Facilitator/antagonist organism(s)
Ulmus spp.	*Ophiostoma novo-ulmi*	*Ophiostoma quercus*	*Scolytus* spp.	*Geosmithia* spp., *Proctolaelaps scolyti*, *Tarsonemus crassus*
Cupressus spp.	*Seiridium cardinale*	*Pestalotiopsis funerea*	*Phloeosinus* spp., *Orsillus maculatus*	*Megastigmus wachtli*
Pinus spp.	*Bursaphelenchus xylophilus*	*Bursaphelenchus mucronatus*	*Monochamus* spp.	Tree resistance and environmental conditions

Dispersal of the agent is little known in the area of origin, which has recently identified with California (Della Rocca et al., 2013). Wind is an unlikely vector because spores (conidia) are embedded in a sticky mucilage (Wagener, 1928, 1939; Panconesi and Ongaro, 1982). Insects are often assumed to be important carriers of the fungus, and some evidence for this has been obtained for bark beetles (Covassi et al., 1975) in the area of introduction in the Mediterranean region, especially when they moved from their breeding systems in an infected tree to a healthy one because of maturation feeding or new colonization attempts (**Figure 1**). As the fungus readily produces infectious spores in laboratory cultures when seeds are added to the substrate, and fruiting bodies are more abundant on cones than on the bark of infected trees (Intini and Panconesi, 1974; Battisti et al., 2000), cone and seed insects have been also considered. The seed bug *Orsillus maculatus* feeds on cypress seeds and inhabits the cone throughout its development. It shows a perfect overlap with the range of its major host, *Cupressus sempervirens*, in the Mediterranean region (Rouault et al., 2005). The cypress seed bug may feed on the seeds from outside the cone, penetrating through the cone scales with the mouthparts (adult), or from inside (nymph). However, the ovipositor cannot penetrate the cone scales, and therefore an incidental opening must be available for egg-laying to be possible (**Figure 1**).

Typically, such openings are provided when scales shrink and separate after colonization of the cone by the native, non-aggressive fungus (*Pestalotiopsis funerea*) that is introduced into the cone when the seed bug lays eggs into an emergence hole of the seed wasp *Megastigmus wachtli* (Roques and Raimbault, 1986). The seed wasp lays its eggs in the young cone and then emerges as an adult through a hole, thus creating a perfect way for the seed bug to access the inside of the cone for oviposition (Rouault et al., 2007). In an experiment performed in a cypress stand in northern Italy, it was shown that the fungus attack of the cones was related to insect feeding, and the seed bug appeared to be a major agent as traces of its feeding or oviposition were found in nearly all the cones killed by the fungi (Battisti et al., 1999). In addition, conidia are highly produced in fruiting bodies on the scales of infected cones and can be transported by rain or other occasional vectors to other parts of the tree, where they can eventually infect tissues (**Figure 1**).

The relationship between the seed bug *O. maculatus* and the fungi pathogenic to the cypress, depends ultimately upon the availability of holes suitable for egg laying in cones. Other cone and seed insects, especially the seed wasp *M. wachtlii*, produce such holes (**Figure 1**). In all likelihood, the relationship evolved over a long period of coexistence between insects and the non-aggressive fungus *P. funerea*. However, the introduction of another more aggressive species, such as *S. cardinale*, with similar niche requirements may lead to dramatic consequences for the survival of the tree and the perpetuation of the whole system (Zocca et al., 2008).

CASE STUDY 3: PINE WILT DISEASE

Pine wilt disease is caused by a species of nematode, *Bursaphelenchus xylophilus*, commonly known as pine wood nematode, and it is one of the most important forest diseases globally (Futai, 2013). It was first reported in the early 20th century and has in the last four decades devastated pine forests in eastern Asia and recently in Europe (Portugal and Spain), where the impacted area is expanding (Økland et al., 2010; Vicente et al., 2012; Naves et al., 2016). The most likely origin of the different introductions is North America (Li et al., 2018; Mallez et al., 2018).

The disease is characterized by systemic wilting symptoms derived from sudden interruption of water transport in stem tissues (Fukuda, 1997), induced by *B. xylophilus* (**Figure 1**). In its native range, the nematode is vectored by native North American longhorn beetle species, *Monochamus carolinensis*, *M. mutator*, *M. scutellatus*, *M. titillator* (Coleoptera: Cerambycidae), and in Asia and Europe by congeneric, native longhorn beetles, *M. alternatus* and *M. galloprovincialis*, respectively. The possibility for *B. xylophilus* to switch among vector species in very different geographic areas is the key to understand its success and spread, which are mainly related to the beetle activity (flight) and human-assisted passive (with timber) dispersal (de la Fuente et al., 2018).

Colonization of beetles by the nematodes happens in the insect pupation galleries created in the wood (**Figure 1**). Juvenile nematodes in the dispersal phase are attracted by chemical signals released by the pupae (Zhao et al., 2013) and enter the tracheal system of young adult beetles. After emergence, beetles mature by feeding on the bark of young twigs of healthy host trees. The nematodes then leave the insect and enter the host tree through the feeding wounds. This is referred to as the primary infection, after which the nematodes molt to adult stage, start propagation, and spread throughout the tree to cause wilting symptoms. A secondary infection is possible, and it is associated with the oviposition into the bark of weak or dying trees (Kobayashi et al., 1984). A precise mechanism of pathogenicity has not been

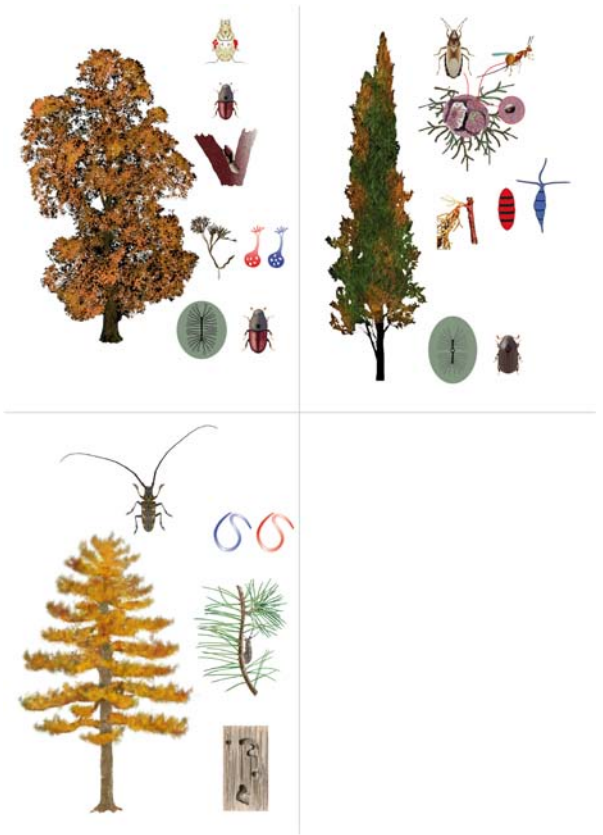

FIGURE 1 | Agents involved in the development of tree pandemics causing dieback of elms (Dutch elm disease), cypress (cypress canker), and pines (pine wood nematode). The non-native, aggressive microorganism is in red color and the native, non-aggressive microorganism in blue color. Elm: elm bark beetles do both bark breeding on main stem and branches, and maturation feeding on twigs, through which they carry the indigenous saprotrophic fungus *Ophiostoma quercus* (blue) among trees, with the help of phoretic mites that carry the fungus in special parts of the body called mycangia. The introduction of the congeneric *O. ulmi* s.l. (red), a fungus having niche requirements similar to *O. quercus* but far more aggressive, caused the almost complete replacement of the endemic fungus. At the same time elm bark beetles and associated mites transport several species of *Geosmithia* (gray), which seems to have developed a mycoparasitic activity toward *O. ulmi* s.l. Cypress: cypress bark beetles do both bark breeding and maturation feeding on twigs, through which they carry the indigenous non-aggressive fungus *Pestalotiopsis funerea* (blue) among trees. The introduction of *Seiridium cardinale* (red), a fungus having niche requirements similar to *P. funerea* but far more aggressive, caused the development of lethal bark cankers. Both fungi, however, have another spreading pathway that involves seed cones. A fungus-infected cone can be inhabited by the nymphs of a true seed bug (*Orsillus maculatus*), the adults of which may carry a heavy spore load at emergence. Cones are infected when eggs are laid within the cone, most frequently via the emergence holes of a seed wasp (*Megastigmus wachtli*). Pine: pine sawyer beetles (*Monochamus* spp.) do both wood boring in stems and maturation feeding on twigs, through which they carry the nematodes of the genus *Bursaphelenchus* among trees. The association has evolved independently among native species of beetles and nematodes (in blue) in various parts of the world, and it is generally associated with mild and occasional symptoms on the host pines. The introduction of the congeneric *Bursaphelenchus xylophilus* (red) from North America to Asia and Europe, caused the development of large outbreaks of pine wilt disease. The invasive nematode impact depends on the susceptibility of the local host plant species and on the local environmental conditions.

clarified yet, although it has been suggested that a hypersensitive reaction occurs in susceptible pine tissue, involving water transport and sudden appearance of disease symptoms (Fukuda, 1997). Such a reaction, however, is not always immediate and the nematode can survive asymptomatically in pine tissues until conducive conditions are established (Takeuchi, 2008).

The pine wilt disease caused by *B. xylophilus* and native *Monochamus* in North America is sporadically causing severe symptoms and damage. Similar results have been observed with combinations of congeneric native nematodes and vectors in Asia and Europe. *Bursaphelenchus mucronatus* is a phylogenetically sister species of *B. xylophilus* in Asia and Europe, where it occurs with two subspecies in each region (Kanzaki and Giblin-Davis, 2018). In all native nematode-native vector associations, the symptoms appear only when trees are challenged by strongly adverse conditions such as heavy environmental stresses such as abnormal water, light, and temperature conditions (Kanzaki and Giblin-Davis, 2018). In the introduction range of *B. xylophilus*, however, typical wilting symptoms on susceptible pine species may appear also when environmental conditions are not that stressful. To cause tissue and systemic symptoms, nematodes must in any case overcome host resistance, which is based on a complex biochemical interaction between the nematode and the host, where the insect vector does not seem to play an important role. The response of the tree to the nematode has been analyzed and a few resistance-related genes have been identified, especially in resistant species that show only weak reactions (Hirao et al., 2012). This suggests that nematodes do not propagate or disperse widely within the tree even if the nematode succeeds during the primary infection.

DISCUSSION AND CONCLUSION

The three pandemics analyzed here show that non-native pathogens have efficiently replaced native non-aggressive organisms and caused a significant impact. The mechanisms through which this had happened, however, differ substantially among the three case studies.

In the pine wilt disease, both nematodes and vectors are taxonomically close. The non-aggressive and aggressive nematodes belong to the same genus as well as the native and non-native pine sawyers (Cesari et al., 2005; Kanzaki and Giblin-Davis, 2018). A different situation is observed for Dutch elm disease and cypress canker, as in both cases there is limited information about the nature of the vectors in the native range of the aggressive fungus. Non-aggressive and aggressive fungi, however, are taxonomically close in both diseases. Even if the origin of *O. ulmi* s.l. is still unknown, it is strictly related to *O. quercus* (Brasier, 1990; Taerum et al., 2018) and this fact has greatly facilitated replacement of the latter. It has been hypothesized that repeated hybridization of the two species may have occurred, with introgression in *O. ulmi* of useful characters such as vegetative compatibility genes from *O. quercus*, eventually resulting in genetic swamping (Brasier, 2001). In cypress canker, the fungi are members of the same family, i.e., Pestalotiopsidaceae (Senanayake et al., 2015).

Affinity of the ecological niche occupied by the fungi and nematodes in native and non-native areas is a trait shared in the three case studies and it seems to be more important than taxonomic relatedness. For the pine wood nematode, the ecological niche is virtually the same, with possible differences due to the host plant species and related morphology, which could be more or less permissive to the nematode invasion in the tissues (Futai, 2013). The niche of non-aggressive fungi associated with elms and cypresses matches perfectly with that of the invasive pathogens. In addition, all the vectors considered here have a limited specialization and high adaptation potential, so that a newcomer can easily find a way to be transported and the fitness of the new association is maximized. In addition, the non-native pathogens display a higher Darwinian fitness that increases after episodic selection episodes such as hybridization with native species and gene introgression (Brasier, 1995), facilitating the complete replacement of the native species (Brasier, 2001).

The key for success of the invasion and development of the pandemic relies on the increase in fitness of arthropod vectors. In all three systems, the arrival of the aggressive pathogen resulted in larger amounts of breeding material for the vectors and in the consequent spread and population growth. This is, however, a transient condition at least in a local scale, as long as the host plants die and cannot support more growth. On a larger scale, however, it could be favorable to vectors capable of long-distance dispersal, as it seems to be in the three systems (Rouault et al., 2005; Javal et al., 2018; Kanzaki and Giblin-Davis, 2018). In that case, the disease may wax and wane in space and time as long as the host plant regenerates and become suitable to colonization. This is the typical case of the Dutch elm disease dynamics after the introduction of the aggressive fungus (Brasier et al., 2004). Reconciling the dynamics of diseases over sub-epidemic level is possible through (i) changes in the genetics of the players, such as in the pine wood nematode (Li et al., 2018), (ii) the antagonistic role of some organisms, such as the *Geosmithia* competitor of *O. novo-ulmi* (Pepori et al., 2018) and the egg parasitoids of the seed bug (Rouault et al., 2007), and iii. a decreasing demographic plasticity of the pathogen (Garbelotto et al., 2015).

Humans may become leading forces in shaping new associations (Rosenzweig, 2001; Olden et al., 2004), especially when action is taken to modify the responses of the local native communities to the invader. In all three case studies, tree plantations are clearly more exposed than natural forests to pandemics, as shown for a number of other pests and pathogens (Wingfield et al., 2015). Unraveling the relationships that result from the accidental introduction of a non-native pathogen with the local communities of host trees and associated organisms is a fundamental challenge for future research on the ecology of forest ecosystems worldwide. New models and tools are required to address these challenges, such as species distribution models that are commonly used by governmental institutions for planning surveillance programs and decide where to concentrate efforts and resources (Lantschner et al., 2018; Poland and Rassati, 2019). The new associations in the invaded environment can completely alter the predictions for establishment and spread of certain non-native pathogens and may results in pandemics with tremendous consequences on human economy and ecosystems.

AUTHOR CONTRIBUTIONS

AS and AB conceived and wrote the manuscript.

FUNDING

This project has received funding from the European Union's Horizon 2020 Program for Research and Innovation under grant agreement no. 771271 "HOMED."

ACKNOWLEDGMENTS

We thank Christer Magnusson for useful comments to the manuscript, Paolo Paolucci for drawing **Figure 1** and Mizuki Uemura for language editing.

REFERENCES

Barthelet, J., and Vinot, M. (1944). Notes sur les maladies des cultures méridionales. *Ann. Epiphyt.* 10, 11–23.

Battisti, A., Cantini, R., Feci, E., Frigimelica, G., Guido, M., and Roques, A. (2000). Detection and evaluation of seed damage of cypress, *Cupressus sempervirens* L., in Italy. *Seed Sci. Technol.* 28, 729–738.

Battisti, A., Roques, A., Colombari, F., Frigimelica, G., and Guido, M. (1999). Efficient transmission of an introduced pathogen via an ancient insect-fungus association. *Naturwissenschaften* 86, 479–483. doi: 10.1007/s001140050658

Bettini, P. P., Frascella, A., Kolařík, M., Comparini, C., Pepori, A. L., Santini, A., et al. (2014). Widespread horizontal transfer of the cerato-ulmin gene between *Ophiostoma novo-ulmi* and *Geosmithia* species. *Fungal Biol.* 118, 663–674. doi: 10.1016/j.funbio.2014.04.007

Biere, A., and Tack, A. J. M. (2013). Evolutionary adaptation in three-way interactions between plants, microbes and arthropods. *Fun. Ecol.* 27, 646–660. doi: 10.1111/1365-2435.12096

Brasier, C. M. (1979). Dual origin of recent dutch elm disease outbreaks in Europe. *Nature* 281, 78–79.

Brasier, C. M. (1990). China and the origins of Dutch elm disease: an appraisal. *Plant Pathol.* 39, 5–16. doi: 10.1111/j.1365-3059.1990.tb02470.x

Brasier, C. M. (1991). Ophiostoma novo-ulmi sp. nov., causative agent of current Dutch elm disease pandemics. *Mycopathologia* 115, 151–161. doi: 10.1007/bf00462219

Brasier, C. M. (1995). Episodic selection as a force in fungal microevolution, with special reference to clonal speciation and hybrid introgression. *Can. J. Bot.* 73(Suppl. 1), S1213–S1221.

Brasier, C. M. (2000). "Intercontinental spread and continuing evolution of the Dutch elm disease pathogens," in *The Elms: Breeding, Conservation and Disease Management*, ed. C. P. Dunn (Dordrecht: Kluwer Academic Publishers), 61–72. doi: 10.1007/978-1-4615-4507-1_4

Brasier, C. M. (2001). Rapid evolution of introduced plant pathogens via interspecific hybridization. *Bioscience* 51, 123–133.

Brasier, C. M., Buck, K., Paoletti, M., Crawford, L., and Kirk, S. (2004). Molecular analysis of evolutionary changes in populations of *Ophiostoma novo-ulmi*. *For. Syst.* 13, 93–103.

Brasier, C. M., and Kirk, S. A. (2001). Designation of the EAN and NAN races of *Ophiostoma novo-ulmi* as subspecies: their perithecial size differences

and geographical distributions. *Mycol. Res.* 105, 547–554. doi: 10.1017/s0953756201004087

Cesari, M., Marescalchi, O., Francardi, V., and Mantovani, B. (2005). Taxonomy and phylogeny of European *Monochamus* species: first molecular and karyological data. *J. Zool. Syst. Evol. Res.* 43, 1–7. doi: 10.1111/j.1439-0469.2004.00279.x

Covassi, M., Intini, M., and Panconesi, A. (1975). Preliminary notes on the relationship between *Coryneum cardinale* Wag. and *Phloeosinus* aubei Perr. in Tuscany. *Redia* 56, 159–166.

Crutzen, P. J. (2002). Geology of mankind. *Nature* 415:23. doi: 10.1038/415023a

Crutzen, P. J., and Stoermer, E. F. (2000). The Anthropocene. *IGBP Glob. Ch. Newsl.* 41, 17–18.

Danti, R., Della Rocca, G., and Panconesi, A. (2013). "Cypress canker," in *Infectious Forest Diseases*, eds P. Gonthier and G. Nicolotti (Wallingford: CABI), 359–375. doi: 10.1079/9781780640402.0359

de la Fuente, B., Saura, S., and Beck, P. S. A. (2018). Predicting the spread of an invasive tree pest: the pine wood nematode in Southern Europe. *J. Appl. Ecol.* 55, 2374–2382.

Della Rocca, G., Osmundson, T., Danti, R., Doulis, A., Pecchioli, A., Donnarumma, F., et al. (2013). AFLP analyses of california and mediterranean populations of *Seiridium cardinale* provide insights on its origin, biology and spread pathways. *For. Path.* 43, 211–221. doi: 10.1111/efp.12019

Fukuda, K. (1997). Physiological process of the symptom development and resistance mechanism in pine wilt disease. *J. For. Res.* 2, 171–181. doi: 10.1007/bf02348216

Futai, K. (2013). Pine wood nematode, *Bursaphelenchus xylophilus*. *Ann. Rev. Phytopathol.* 51, 61–83. doi: 10.1146/annurev-phyto-081211-172910

Garbelotto, M., Della Rocca, G., Osmundson, T., di Lonardo, V., and Danti, R. (2015). An increase in transmission-related traits and in phenotypic plasticity is documented during a fungal invasion. *Ecosphere* 6, 1–16.

Graniti, A. (1998). Cypress canker: a pandemic in progress. *Ann. Rev. Phytopathol.* 36, 91–114. doi: 10.1146/annurev.phyto.36.1.91

Grasso, V. (1951). A new pathogen of *Cupressus macrocarpa* Hartw. in italy. *It. For. Mont.* 6, 62–65.

Guries, R. P. (2001). "Elms: past, present, and future," in *Proceeding of the National Conference on Wilt Diseases of Shade Trees*, ed. C. L. Ash (St. Paul, MN): APS Press), 29–36.

Hirao, T., Fukatsu, E., and Watanabe, A. (2012). Characterization of resistance to pine wood nematode infection in *Pinus thunbergii* using suppression subtractive hybridization. *BMC Plant Biol.* 12:13. doi: 10.1186/1471-2229-12-13

Intini, M., and Panconesi, A. (1974). Studies on the in vitro fructification of *Coryneum cardinale* Wag. *Riv. Patol. Veg.* 10, 337–342.

Javal, M., Roux, G., Sauvard, D., and Roques, A. (2018). Asian long-horned beetle dispersal potential estimated in computer- linked flight mills. *J. Appl. Ent.* 142, 282–286. doi: 10.1111/jen.12408

Kanzaki, N., and Giblin-Davis, R. M. (2018). Diversity and plant pathogenicity of *Bursaphelenchus* and related nematodes in relation to their vector bionomics. *Curr. For. Rep.* 4, 85–100. doi: 10.1007/s40725-018-0074-7

Kobayashi, F., Yamane, A., and Ikeda, T. (1984). The Japanese pine sawyer beetle as the vector of pine wilt disease. *Annu. Rev. Entomol.* 29, 115–135. doi: 10.1146/annurev.ento.29.1.115

Kolařík, M., Kubátová, A., Hulcr, J., and Pažoutová, S. (2008). *Geosmithia* fungi are highly diverse and consistent bark beetle associates: evidence from their community structure in temperate Europe. *Microb. Ecol.* 55, 65–80. doi: 10.1007/s00248-007-9251-0

Lantschner, M. V., de la Vega, G., and Corley, J. C. (2018). Predicting the distribution of harmful species and their natural enemies in agricultural, livestock and forestry systems: an overview. *Int. J. Pest Man.* 1–17. doi: 10.1080/09670874.2018.1533664

Lewis, S. I., and Maslin, M. A. (2015). Defining anthropocene. *Nature* 519, 171–180. doi: 10.1038/nature14258

Li, J., Cheng, X., Lin, R., Xiao, S., Yi, X., Mao, Z., et al. (2018). Comparative whole-genome analysis reveals genetic adaptation of the invasive pinewood nematode. preprint repository. *bioRxiv* [Preprint]. doi: 10.1038/nature14258

Lu, M., Wingfield, M. J., Gillette, N. E., Mori, S. R., and Sun, J. H. (2010). Complex inter-actions among host pines and fungi vectored by an invasive bark beetle. *New Phytol.* 187, 859–866. doi: 10.1111/j.1469-8137.2010.03316.x

Luchi, N., Mancini, V., Feducci, M., Santini, A., and Capretti, P. (2012). *Leptoglossus occidentalis* and *Diplodia pinea*: a new insect-fungus association in Mediterranean forests. *For. Pathol.* 42, 246–251. doi: 10.1111/j.1439-0329.2011.00750.x

Mallez, S., Castagnone, C., Lombaert, E., Castagnone-Sereno, P., and Guillemaud, T. (2018). Inference of the worldwide invasion routes of the pinewood nematode, *Bursaphelenchus xylophilus*, using ABC analysis on microsatellite data. preprint repository. *bioRxiv* [Preprint]. doi: 10.1101/452326

Mittempergher, L. (1989). Il declino dell'olmo: da latifoglia nobile a cespuglio. *Ann. Acc. It. Sc. For.* 38, 585–609.

Moser, J. C., Konrad, H., Blomquist, S. R., and Kirisits, T. (2010). Do mites phoretic on elm bark beetles contribute to the transmission of dutch elm disease? *Naturwissenschaften* 97, 219–227. doi: 10.1007/s00114-009-0630-x

Naves, P., Bonifácio, L., and de Sousa, E. (2016). "The pine wood nematode and its local vectors in the Mediterranean Basin," in *Insects and Diseases in Mediterranean Forests*, eds T. D. Paine and F. Lieutier (Basel: Springer International Publishing), 329–378. doi: 10.1007/978-3-319-24744-1_12

Økland, B., Skarpaas, O., Schroeder, M., Magnusson, C., Lindelow, A., and Thunes, K. (2010). Is eradication of the pinewood nematode (*Bursaphelenchus xylophilus*) likely? an evaluation of current contingency plans. *Risk Anal.* 30, 1424–1439. doi: 10.1111/j.1539-6924.2010.01431.x

Olden, J. D., Poff, N. L., Douglas, M. R., Douglas, M. E., and Fausch, K. D. (2004). Ecological and evolutionary consequences of biotic homogenization. *Trends Ecol. Evol.* 19, 18–24. doi: 10.1016/j.tree.2003.09.010

Panconesi, A., and Ongaro, L. (1982). Seiridium (Coryneum) cardinale (Wag.) sutton & gibson in cypress stands of monte morello (Firenze). *Riv. Patol. Veg.* 18, 109–121.

Pepori, A. L., Bettini, P. P., Comparini, C., Sarrocco, S., Bonini, A., Frascella, A., et al. (2018). *Geosmithia-Ophiostoma*: a new fungus-fungus association. *Microb. Ecol.* 75, 632–646. doi: 10.1007/s00248-017-1062-3

Pepori, A. L., Kolařík, M., Bettini, P. P., Vettraino, A. M., and Santini, A. (2015). Morphological and molecular characterisation of *Geosmithia* species on European elms. *Fungal Biol.* 119, 1063–1074. doi: 10.1016/j.funbio.2015.08.003

Poland, T. M., and Rassati, D. (2019). Improved biosecurity surveillance of non-native forest insects: a review of current methods. *J. Pest Sci.* 92, 37–49. doi: 10.1007/s10340-018-1004-y

Roques, A., and Raimbault, J. P. (1986). Distribution and biological cycle of the Cypress seed chalcid, *Megastigmus wachtli* (Seitn.) *(Hymenoptera, Torymidae)*, in the mediterranean. *J. Appl. Entomol.* 101, 370–381. doi: 10.1111/j.1439-0418.1986.tb00871.x

Rosenzweig, M. L. (2001). The four questions: what does the introduction of exotic species do to diversity. *Evol. Ecol. Res.* 3, 361–367.

Rouault, G., Battisti, A., and Roques, A. (2007). Oviposition sites of the cypress seed bug *Orsillus maculatus* and response of the egg parasitoid *Telenomus* gr. *floridanus*. *BioControl* 52, 9–24. doi: 10.1007/s10526-006-9002-z

Rouault, G., Cantini, R., Battisti, A., and Roques, A. (2005). Geographic distribution and ecology of two species of *Orsillus* (*Hemiptera: Lygaeidae*) associated with cones of native and introduced cupressaceae in Europe and the mediterranean basin. *Can. Entomol.* 137, 450–470. doi: 10.4039/n04-044

Rudinsky, J. A. (1962). Ecology of scolytidae. *Annu. Rev. Entomol.* 7, 327–348. doi: 10.1146/annurev.en.07.010162.001551

Santini, A., Liebhold, A., Migliorini, D., and Woodward, S. (2018). Tracing the role of human civilization in the globalization of plant pathogens. *ISME J.* 12, 647–652. doi: 10.1038/s41396-017-0013-9

Schluter, D. (2009). Evidence for ecological speciation and its alternative. *Science* 323, 737–741. doi: 10.1126/science.1160006

Senanayake, I. C., Maharachchikumbura, S. S. N., Hyde, K. D., Bhat, D. J., Jones, E. B. G., McKenzie, E. H. C., et al. (2015). Towards unraveling relationships in xylariomycetidae (*Sordariomycetes*). *Fungal Divers.* 73, 73–144. doi: 10.1007/s13225-015-0340-y

Sousa, E., Bravo, M. A., Pires, J., Naves, P., Penas, A. C., Bonifâcio, L., et al. (2001). *Bursaphelenchus xylophilus* (*Nematoda*; *Aphelenchoididae*) associated with *Monochamus galloprovincialis* (*Coleoptera*; *Cerambycidae*) in portugal. *Nematology* 3, 89–91.

Spierenburg, T. (1921). Een onbekende ziekte in de iepen. *Tijd. Plant.* 27, 53–61.

Taerum, S. J., de Beer, Z. W., Marincowitz, S., Jankowiak, R., and Wingfield, M. J. (2018). *Ophiostoma quercus*: an unusually diverse and globally widespread

tree-infecting fungus. *Fungal Biol.* 122, 900–910. doi: 10.1016/j.funbio.2018.05.005

Takeuchi, Y. (2008). "Host fate following infection by the pine wood nematode," in *Pine Wilt Disease*, eds B. G. Zhao, K. Futai, J. R. Sutherland, and T. Takeuchi (Tokyo: Springer), 235–249. doi: 10.1007/978-4-431-75655-2_23

Vicente, C., Espada, M., Vieira, P., and Mota, M. (2012). Pine wilt disease: a threat to european forestry. *Eur. J. Plant. Pathol.* 133, 89–99. doi: 10.1007/s10658-011-9924-x

Wagener, W. W. (1928). *Coryneum* canker of Cypress. *Science* 67:584. doi: 10.1126/science.67.1745.584

Wagener, W. W. (1939). The canker of *Cupressus* induced by *Coryneum cardinale* n. sp. *J. Agric. Res.* 58, 1–46.

Webber, J. F., and Brasier, C. M. (1984). "The transmission of Dutch elm disease: a study of the process involved," in *Invertebrate-Microbial Interactions*, eds J. M. Anderson, A. D. M. Rayner, and D. Walton (Cambridge: Cambridge University Press), 271–306.

Wingfield, M. J., Brockerhoff, E. G., Wingfield, B. D., and Slippers, B. (2015). Planted forest health: the need for a global strategy. *Science* 349, 832–836. doi: 10.1126/science.aac6674

Zhao, L., Zhang, S., Wei, W., Hao, H., Zhang, B., and Butcher, R. A. (2013). Chemical signals synchronize the life cycles of a plant-parasitic nematode and its vector beetle. *Curr. Biol.* 23, 2038–2043. doi: 10.1016/j.cub.2013.08.041

Zocca, A., Zanini, C., Aimi, A., Frigimelica, G., La Porta, N., and Battisti, A. (2008). Spread of plant pathogens and insect vectors at the northern range margin of cypress in Italy. *Acta Oecol.* 33, 307–313. doi: 10.1016/j.actao.2008.01.004

Conflict of Interest Statement: The authors declare that the research was conducted in the absence of any commercial or financial relationships that could be construed as a potential conflict of interest.

frontiers in Physiology

MINI REVIEW
published: 15 May 2019
doi: 10.3389/fphys.2019.00603

Drosophila Cellular Immunity Against Parasitoid Wasps: A Complex and Time-Dependent Process

*Chami Kim-Jo, Jean-Luc Gatti and Marylène Poirié**

INRA, CNRS, Institut Sophia Agrobiotech, Université Côte d'Azur, Sophia Antipolis, France

Host-parasitoid interactions are among the most studied interactions between invertebrates because of their fundamental interest – the evolution of original traits in parasitoids – and applied, parasitoids being widely used in biological control. Immunity, and in particular cellular immunity, is central in these interactions, the host encapsulation response being specific for large foreign bodies such as parasitoid eggs. Although already well studied in this species, recent data on *Drosophila melanogaster* have unquestionably improved knowledge of invertebrate cellular immunity. At the same time, the venomics of parasitoids has expanded, notably those of *Drosophila*. Here, we summarize and discuss these advances, with a focus on an emerging "time-dependent" view of interactions outcome at the intra- and interspecific level. We also present issues still in debate and prospects for study. Data on the *Drosophila*-parasitoid model paves the way to new concepts in insect immunity as well as parasitoid wasp strategies to overcome it.

Keywords: immunity, encapsulation, hematopoiesis, *Drosophila*, parasitoid wasp, venom, *Leptopilina*

OPEN ACCESS

Edited by:
Patrizia Falabella,
University of Basilicata, Italy

Reviewed by:
Jalal Jalali Sendi,
University of Guilan, Iran
István Andó,
Hungarian Academy of Sciences, Hungary
Alexandre B. Leitão,
University of Cambridge, United Kingdom

***Correspondence:**
Marylène Poirié
marylene.poirie@univ-cotedazur.fr

Specialty section:
This article was submitted to Invertebrate Physiology, a section of the journal Frontiers in Physiology

Received: *02 April 2019*
Accepted: *29 April 2019*
Published: *15 May 2019*

Citation:
Kim-Jo C, Gatti J-L and Poirié M (2019) Drosophila Cellular Immunity Against Parasitoid Wasps: A Complex and Time-Dependent Process. Front. Physiol. 10:603. doi: 10.3389/fphys.2019.00603

INTRODUCTION

Eighty percent of known animal species are insects (Larsen et al., 2017), of which at least 20% have a parasitoid lifestyle (Forbes et al., 2018). The reproductive strategy of parasitoid species is unique among insects: they lay in or on other insects, their larvae developing by consuming host tissues, usually resulting in death. Most endoparasitoids are koinobionts, that is, their host can pursue its development with which their own offspring development will synchronize. They have thus evolved different strategies to circumvent the host immune response that, when successful, leads to the encapsulation of the parasitoid egg, i.e., its embedding by specialized hemocytes, together with melanization and production of Reactive Species (Carton et al., 2008; Nappi, 2010; Lu et al., 2014; Nakhleh et al., 2017). Encapsulation has notably been described in *Drosophila* species whose larvae are often attacked by endoparasitoid wasps (e.g. from the *Leptopilina*, *Ganaspis*, and *Asobara* genera) (Carton et al., 1986; Novković et al., 2011). Here, we will mainly rely on the *Drosophila melanogaster* interaction with *Leptopilina* wasps (Hymenoptera, Figitidae), one of the most advanced models for characterizing interaction mechanisms and the genetic bases of resistance and virulence (Dubuffet et al., 2009). It has helped to improve knowledge of hematopoiesis and cellular immunity in *Drosophila* and indirectly in other invertebrates. For thorough reviews of recent advances in *Drosophila* hematopoiesis, see Letourneau et al. (2016) and Banerjee et al. (2019). For a detailed follow-up of the cellular encapsulation of the wasp egg, see also Anderl et al. (2016).

THE *DROSOPHILA* ENCAPSULATION RESPONSE TO PARASITISM

In *D. melanogaster*, the first noticeable events after wasp oviposition are the increased number of circulating plasmatocytes followed by the appearance of circulating lamellocytes – a hemocyte type produced in response to parasitism (**Figure 1**) – and activation of the phenoloxidase (PO) cascade (Carton et al., 2008, 2009; Nappi, 2010). Plasmatocytes form a first layer of cells surrounding the parasitoid egg to which the lamellocytes adhere, forming tight junctions, giving rise to a multilayer melanized capsule that is completed 48 h post parasitism (**Figure 2**; Russo et al., 1996; Bajgar et al., 2015). The production of cytotoxic radicals *via* the PO cascade is supposed to kill the parasitoid egg (Nappi and Vass, 1993; Nappi et al., 1995). For this response to be effective, timing may be essential. The encapsulation should be completed in less than 48 h because at that time the parasitoid egg has hatched (see **Figure 2**), and a moving larva is more likely to escape from the forming capsule.

THE CONTROVERSIAL ORIGIN OF THE MAIN CIRCULATING IMMUNE CELLS THAT FORM THE CAPSULE

The number of circulating hemocytes increases during the *D. melanogaster* larval stages from a few hundred to around 7,000 (Lanot et al., 2001; Petraki et al., 2015). They come from embryonic progenitor cells, the prohemocytes, which circulate in the hemolymph or are found in the larval lymph gland or in subcuticular hematopoietic hubs called sessile compartment (**Figure 1**; Honti et al., 2010; Makki et al., 2010; Fauvarque and Williams, 2011; Gold and Brückner, 2015; Leitão and Sucena, 2015; Ghosh et al., 2018).

The three main types of differentiated hemocytes in *Drosophila* larvae are now considered as distinct lineages that are formed from the prohemocyte progenitor (**Figure 1**). 95% of the circulating cells are phagocytic plasmatocytes that clear pathogens and dead cells, participate in wound healing, and synthesize extracellular matrix proteins (Martinek et al., 2008) and antimicrobial peptides (Charroux and Royet, 2009). Larval plasmatocyte populations express different subsets of markers (Jung et al., 2005; Honti et al., 2014) and two different adults populations have distinct immune functions (Clark et al., 2011). Crystal cells – about 5% of circulating cells – are characterized by the expression of the specific marker Lozenge and harbor large paracrystalline inclusions which contain prophenol-oxidases (PPO1 and PPO2). Upon injury, activation of the JNK pathway and TNF homolog Eiger lead to their disruption and the release of PPO zymogens in the hemolymph (Bidla et al., 2007; Dudzic et al., 2015). The third cell type, the lamellocytes, are large flat cells with adherent properties that are rare in healthy larvae but can represent up to 50% of circulating hemocytes after wasp parasitism. They form the successive outer layers of the capsule and produce a specific pro-phenoloxidase (PPO3), required with PPO2 for a complete melanisation of the capsule (Irving et al., 2001; Dudzic et al., 2015).

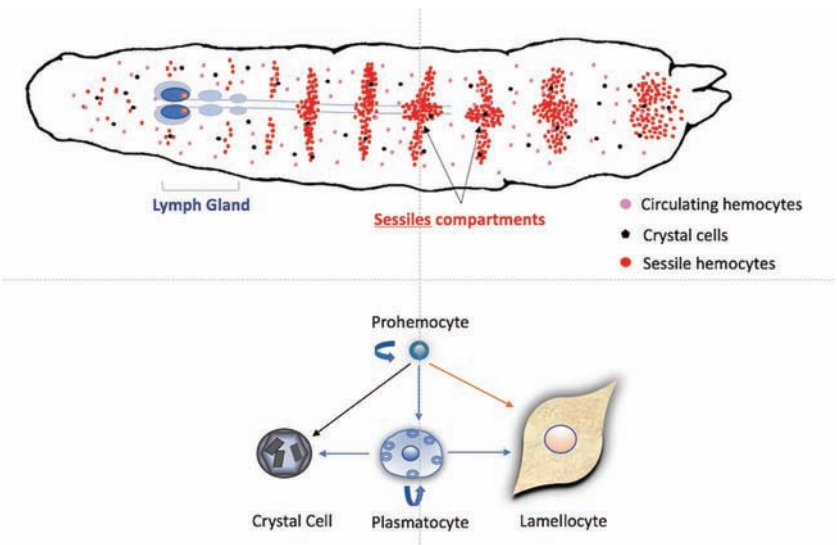

FIGURE 1 | Schematic hematopoiesis in a *Drosophila melanogaster* larva. Hemocytes, mainly plasmatocytes and crystal cells, are circulating in the larval hemolymph. These circulating hemocytes can derive from embryonic prohemocytes or are also formed within the sessile compartment during most of the larval stages. This compartment is composed of sub-cuticular groups of cells, mainly prohemocytes and plasmatocytes, present in the different larval segments. At the end of the L3 stage, the first lobes of the lymph gland increase in size due to the proliferation of hemocytes that will be released just after pupation in healthy larvae. In normal conditions, self-renewing prohemocytes are considered as progenitors for the three main hemocytes types. After parasitoid oviposition, circulating or sessile plasmatocytes can also proliferate and transdifferentiate into crystal cells and lamellocytes. In parasitized hosts, lamellocytes can also differentiate from prohemocytes within the lymph gland and be released earlier than pupation to participate in the encapsulation.

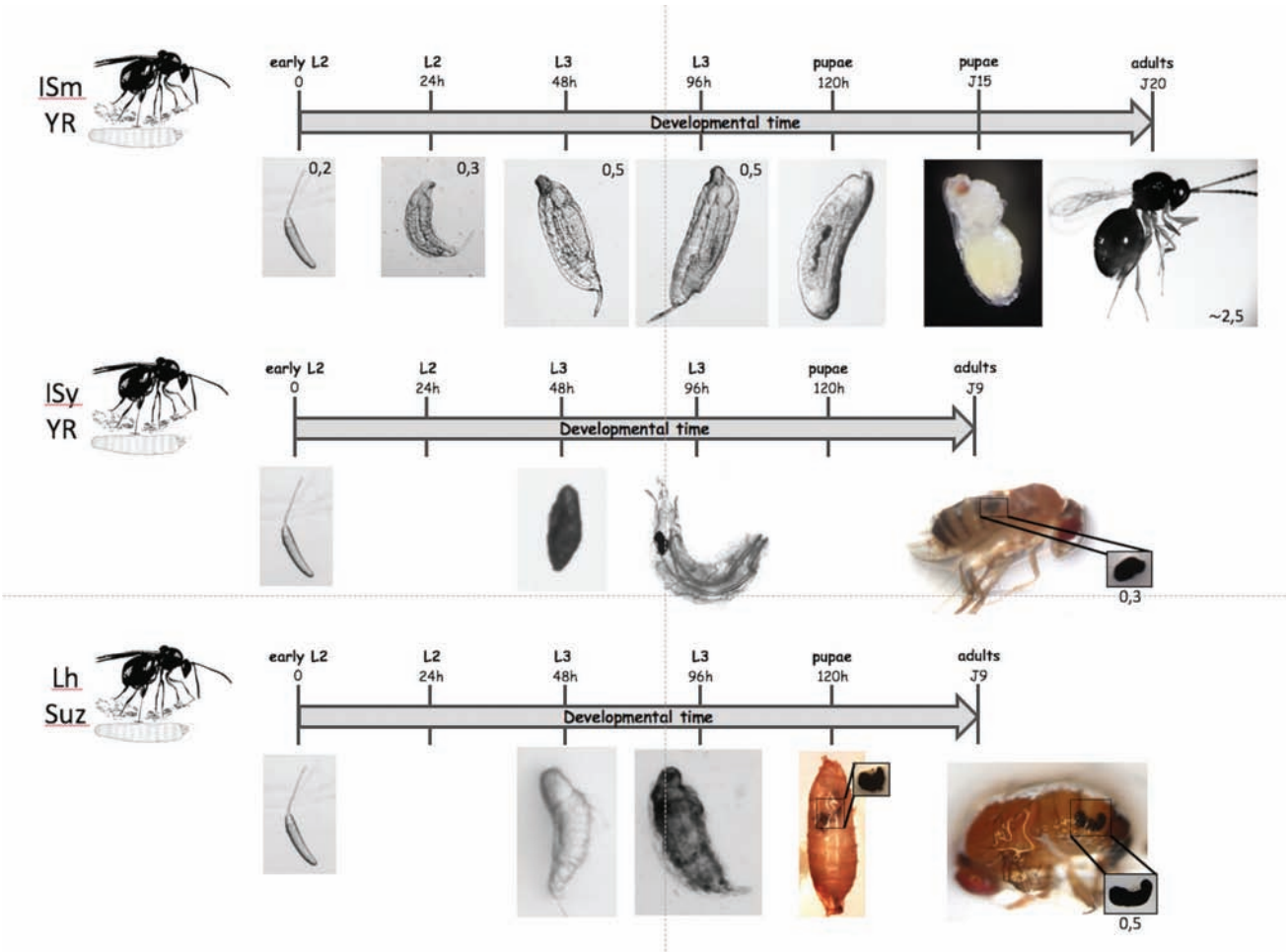

FIGURE 2 | Different possible outcomes for parasitoids. On the top: when a *D. melanogaster* L2 larva is parasitized by the virulent *L. boulardi* ISm line, the parasitoid egg develops normally and the parasitoid larva hatches from its chorion 24 to 48 h later after parasitism. The parasitoid larva continues its moderate growth until the fly larva pupates and after a few days the puparium is mainly occupied by the parasitoid that has eaten almost all the fly larva tissues. Twenty days after oviposition, an adult parasitoid egress from the pupal case instead of a fly. On the center: when a *D. melanogaster* resistant L2 larva is parasitized by the avirulent *L. boulardi* G486 line, the parasitoid egg is rapidly encapsulated and a melanized capsule is formed after 48 h that remains visible in the larva. The capsule is retrieved in the emerging adult fly. On the bottom: when a *D. suzukii* larva is parasitized by the generalist *L. heterotoma* wasp, the egg hatches and the parasitoid larva remains alive after 48 h, with no observed capsule or melanisation. After 96 h, the parasitoid larva is dead or dying and is slowly embedded in a cell-formed melanized capsule. The capsule continues to enlarge until pupation and it is well visible through the pupal case and then retrieved in the abdomen of the emerging fly. The upper scale indicates the development time from oviposition and the observed stages. The scales provided on the pictures are given in millimeters (mm).

Interestingly, the PPO3 gene seems specific to the melanogaster subgroup, suggesting that PPO production by lamellocytes is a recently evolved defense mechanism against parasitic wasps (Salazar-Jaramillo et al., 2014; Dudzic et al., 2015). The precise tissue origin of lamellocytes involved in encapsulation is still debated: they can be derived from sessile or circulating plasmatocytes (Anderl et al., 2016) or released as mature lamellocytes following accelerated proliferation and bursting of the lymph gland (Letourneau et al., 2016). All these recent advances about hematopoiesis have benefited from the genetic tools in *Drosophila* and also from the identification of hemocytes surface markers such as P1 for plasmatocytes or L1/Atilla for lamellocytes (Kurucz et al., 2007). The use of markers has improved discrimination and the tracking of different cell types but also, coupled with cell cytometry, demonstrated the presence of transient precursor populations (Anderl et al., 2016).

Lamellocyte Production From the Sessile Compartment

Until recently, *Drosophila* hemocytes were thought to be produced in two waves, one during embryogenesis and the other in the lymph gland at the end of the larval stage (Gold and Brückner, 2015). However, new studies suggest a much higher plasticity, with functional hematopoietic sites distributed along the larva and also present in the adult fly (Gold and Brückner, 2015; Ghosh et al., 2018). The larva thus contains two hematopoietic compartments, the sessile compartment and the lymph gland.

Hemocytes in the sessile compartments proliferate (self-renewal) and differentiate into plasmatocytes that can transdifferentiate into crystal cells by a Notch signaling-dependent process (Márkus et al., 2009; Leitão and Sucena, 2015). These new hemocytes can reach the hemolymph to contribute gradually to the pool of circulating larval hemocytes. In healthy larvae, they are mainly released at the onset of metamorphosis but simple stimuli such as light brush strokes can induce this release, indicating that these hemocytes fate also depends upon systemic and/or local signals including neuronal ones (Makhijani and Brückner, 2012; Tokusumi et al., 2017). An immune challenge such as oviposition of wasp can also cause their premature mobilization and induce their trans-differentiation into lamellocytes (Márkus et al., 2009; Honti et al., 2010; Anderl et al., 2016). Indeed, few hours after parasitism, a novel population of cells derived from plasmatocytes, the lamelloblasts, appears in the circulation, proliferate actively and develop into lamellocytes (Anderl et al., 2016). Plasmatocytes transdifferentiation into lamellocyte-like cells can also occur directly on the wasp egg. Different signaling pathways are important for the regulation of lamellocytes proliferation upon parasitism (Letourneau et al., 2016), including the Toll and Jak-Stat pathways (Morin-Poulard et al., 2013; Louradour et al., 2017). Activation of Jak-Stat induces the Charlatan (*Chl*) protein (a transcription factor that interacts with CoREST, a transcription repressor complex exhibiting histone deacetylase and demethylase activities) that is involved in lamellocytes transdifferentiation from plasmatocytes (Stofanko et al., 2010).

Lamellocyte Production From the Lymph Gland

At the end of the third stage, the lymph gland is composed of a large pair of primary anterior lobes organized into three domains: the cortical zone (CZ), the medullary zone (MZ), and the posterior signaling center (PSC), followed by pairs of small posterior lobes, each separated by a pair of pericardial cells (**Figure 1**). The differentiation of lymph gland hemocytes starts during the third instar: First, the cortical zone (CZ) of the primary lobes expands due to prohemocytes proliferation and differentiation into plasmatocytes, a small number of crystal cells and occasionally a few lamellocytes. Then, the progenitors of the medullary zone (MZ) become quiescent. As development progresses, almost all lymph gland hemocytes differentiate, and 8 h after pupation, all cells have been released into the circulation (Grigorian et al., 2011). The proliferation and differentiation of hemocytes is controlled by a wide range of signals from the posterior signaling center (PSC), CZ, and MZ, and from systemic sources such as neurotransmitters and growth factors from the brain, and levels of nutritional compounds. In the PSC, high levels of reactive oxygen species (ROS) (Owusu-Ansah and Banerjee, 2009; Letourneau et al., 2016; Louradour et al., 2017), activation of the Wingless signaling pathway (Sinenko et al., 2009) and expression of the EBF transcription factor Collier (Benmimoun et al., 2012; Oyallon et al., 2016) are required for the maintenance of a pool of pluripotent progenitors. The PSC secretes also diffusible signals such as hedgehog (Hh) and the platelet-derived growth factor/vascular endothelial growth factor-like factor (PVF1) to activate different pathways in the lymph gland compartments (Mondal et al., 2011, 2014). Hh acts directly on the MZ progenitors to maintain them in their pluripotent state. PVF1 acts on differentiating hemocytes, stimulating the secretion of adenosine deaminase-related growth factor-A (ADGF-A), which leads to the inactivation of the adenosine/AdoR (adenosine receptor) pathway in MZ cells by modulating the extracellular adenosine level. This double control allows the maintenance of the balance between progenitors and differentiated cells. Other signaling pathways are involved such as JAK/STAT and Toll, or the insulin/IGF (IlS) and target of rapamycin (TOR) pathways and components of the nutrient detection system (Morin-Poulard et al., 2013; Shim et al., 2013). The prohemocyte fate is also controlled by local signals from the neighboring heart tube and through the regulation of the PSC morphology (Morin-Poulard et al., 2016).

Six hours after parasitic wasp infestation, hemocyte proliferation starts in the lymph gland leading to a massive differentiation of lamellocytes (Lanot et al., 2001). The burst of the lymph gland, releasing all hemocytes into the hemolymph, occurs after 24–48 h, depending on the experimental conditions and possibly the *D. melanogaster* strain used. The mechanism(s) responsible for the anticipated differentiation in the gland have not yet been fully identified, but they could be triggered by the production of ROS and the local immune response at the oviposition site (Sinenko et al., 2011). In response, the PSC secretes the epidermal growth factor receptor (EGFR) ligand Spitz that binds to receptor and activates the Ras/Erk pathway resulting in the appearance of dpERK-positive lamellocytes in circulation (Lusk et al., 2017). Expression of a dominant-negative form of EGFR in the lymph gland and circulating hemocytes suppresses the lamellocyte induction by wasp oviposition (Sinenko et al., 2011), suggesting a role of this pathway in lamellocyte differentiation also for the other compartments. Spitz is the major EGFR ligand, but other activators and inhibitors may participate whose roles have to be established in case of parasitism (Lusk et al., 2017). More and more evidence suggests that signals secreted by different tissues upon wasp oviposition play a role in encapsulation. For example, the release of the cytokine Edin from the fat body (Vanha-aho et al., 2015) or the activation of JAK/STAT signaling in somatic muscles induced by Upd2 and Upd3 secretion from hemocytes (Yang et al., 2015), both required for the larvae to mount a normal encapsulation response.

The origin of the lamellocytes forming the capsule is still debated. Indeed, although both sessile and lymph gland lamellocytes may participate, which participate the most and the most precociously in the formation of the capsule remains unanswered. Interesting elements have been brought on both sides without the issue really being decided today. Further development of specific labeling of the lamellocytes from the respective compartments (lineage sorting) should help to solve this issue.

IN SEARCH FOR NEW GENES AND SIGNALING PATHWAYS INVOLVED IN ENCAPSULATION

Most studies have used wide genomic analyses or mutant flies to decipher the pathways involved in hematopoiesis and

encapsulation. The identification of new pathways could, however, also benefit from the analysis of resistance genes identified in natural populations. We work on *D. melanogaster* strains, one resistant (YR) the other susceptible (YS) to *Leptopilina boulardi* (strain G486; Carton et al., 1992) that differ mainly by their allele at a major "resistance" gene, *Rlb*, the resistant allele being dominant. *Rlb* was localized in a small region of chromosome 2R (Hita et al., 1999, 2006) that contains two genes: CG33136 and *edl*/*mae* (ETS-domain lacking)/(modulator of the activity of ETS). Interestingly, Edl interacts *via* its SAM (sterile alpha motif) domain with several ETS transcription factors (Baker et al., 2001) such as the transcriptional activator Pointed (mainly Pointed P2) and the repressor Yan/Aop (Vivekanand, 2018), both involved in the EGF pathway. When activated, the EGF signal triggers the mitogen-activated protein kinase/extracellular signal-regulated kinase (ERK) kinase (MEK) known as Rolled. Among many targets, rolled phosphorylates Pointed and Yan, thus modulating their function by changing their SAM domain binding affinity (Vivekanand, 2018). The universal output of the EGF pathway is induction of gene expression, mostly through the Pointed transcriptional activator. It regulates the proliferation and differentiation of many cell types in *Drosophila,* and Yan and Pointed have been involved in plasmatocyte and lamellocyte differentiation (Zettervall et al., 2004; Dragojlovic-Munther and Martinez-Agosto, 2013). It is thus possible, although still to be proven, that the balance between Edl, Yan and Pointed finely regulate hemocyte differentiation in case of parasitism, thus participating in *Drosophila* immune resistance.

VARIATION IN *DROSOPHILA* IMMUNE RESPONSE AND PARASITISM OUTCOME, A QUESTION OF TIMING?

Intraspecific Variation

The timing of increase of the hemocyte population in circulation is likely important for encapsulation success. When the total number of circulating hemocytes of the *D. melanogaster* YR and YS strains (see above) was compared post-parasitism by *L. boulardi* G486, an increase in hemocyte load occurred after 6 h for YR compared to 15 h for YS (Russo et al., 2001). Therefore, the earlier increase in hemocytes load in the YR strain might explain its resistance phenotype. Whether it is due to a differential regulation of the hematopoietic tissues response between resistant and susceptible strains will deserve further studies.

Interspecific Variation

The response to parasitism of different *Drosophila* species may differ from that of *D. melanogaster*. Indeed, species of the *melanogaster* subgroup all produce lamellocytes that actively participate in the encapsulation, but very different cells are involved in other species such as the multinucleated giant hemocytes found in the *ananassae* subgroup (Márkus et al., 2015) or the nematocyte cell types in species from the *Drosophila* subgroup (Kacsoh et al., 2014; Bozler et al., 2017). The inducible production by parasitism of cells of different nature and origin in *Drosophila* species is intriguing from both a physiological and evolutionary point of view. We can indeed wonder about the mechanisms that led to this specific cellular evolution. Other *Drosophila* species from the *melanica* subgroup, while having lamellocytes, succeed in killing *L. heterotoma* eggs or larvae without forming a capsule, possibly through the production of cytotoxic radicals (Nappi and Streams, 1969; Carton et al., 2009). Another example of parasitoid elimination after the egg stage without encapsulation was provided by Paredes et al. (2016): it involves a lipid competition-based protection against some parasitoid wasp species conferred to the fly by the endosymbiont *Spiroplasma poulsonii*.

The immune response may also differ depending on the species of *Drosophila* even with the same cells involved. Indeed, the *D. suzukii* encapsulation response to *Leptopilina* wasp eggs shows a timing very far from that known in *D. melanogaster* (Iacovone et al., 2018). The immune response was not noticeable on *L. heterotoma* parasitoid eggs during the first 48 h (**Figure 2**) and only a thin coat of lightly colored cells wrapped the hatched larvae 72 h post-oviposition. Most parasitoid larvae died 96 h post-oviposition and were melanized, but large complete capsules were only observed at pupation and retrieved in emerged adult flies. Thus, although many hemocytes circulate in *D. suzukii* (Kacsoh and Schlenke, 2012) the immune response of this species seems largely delayed compared to that of *D. melanogaster*.

HOW PARASITIC WASPS TARGET THE *DROSOPHILA* IMMUNE SYSTEM

The advanced knowledge on *Drosophila* immunity is a great asset to decipher mechanisms ensuring parasitic success which, for *Drosophila* endoparasitoids, mainly relies on injection of venom containing immunosuppressive proteins (Poirié et al., 2014; Moreau and Asgari, 2015). The venom effect on the hemocytes, the lymph gland or the melanisation has been described for *Leptopilina* species (Dubuffet et al., 2009; Heavner et al., 2014). The *Leptopilina* and *Ganaspis* venom contains not only soluble proteins but also peculiar vesicles with an unclear biogenesis (Rizki and Rizki, 1990; Dubuffet et al., 2009; Ferrarese et al., 2009; Gatti et al., 2012), which are likely involved in parasitic success. These purified vesicles seemingly target the host lamellocytes, changing their shape from discoidal to bipolar, which supposedly prevent them to adhere and form a capsule, or inducing their lysis (Rizki and Rizki, 1984, 1990, 1994). Venomics analyzes allowed identifying the main venom proteins in *L. heterotoma* and *L. boulardi*, among which P40 associated with the vesicles of *L. heterotoma* (Heavner et al., 2017) and LbGAP (Colinet et al., 2013; Goecks et al., 2013), a Rho GTPase activating protein secreted in high amounts in *L. boulardi* and associated with the vesicles in the venom reservoir (Labrosse, 2003; Labrosse et al., 2005). LbGAP interacts *in vitro* with Rac1 and Rac2 (Colinet et al., 2007), both required for successful encapsulation (Williams et al., 2005, 2006), and it also immunolocalizes in lamellocytes of parasitized hosts

(Colinet et al., 2007) like the *L. heterotoma* P40 protein (Chiu et al., 2006). The venom vesicles may therefore act as shuttles transporting virulence proteins and targeting them into *Drosophila* immune cells. Their mode of entry may represent a mechanism that shapes the host range of parasitoids, making it essential to decipher [e.g., identification of a specific receptor(s) on the lamellocytes] for understanding the host-parasitoid interaction in these species.

CONCLUSION AND PERSPECTIVES

Despite the recent rapid knowledge increases in insect cell immunity and encapsulation, particularly in the *Drosophila* model, some main gaps remain to be filled. The mechanisms of early recognition of a parasitoid egg as well as triggering and synchronization of the main actors of capsule formation are among the most important, as is the more precise identification of the role of ROS and NOS, factors from non-immune tissues. One can also mention the detailed formation of the capsule that will benefit from the development of markers to identify both the cell origin and type. On the parasitoids side, the ways of targeting the host immune compartments are diverse and the identification of molecular mechanisms remains a major challenge. Recent data have revealed a greater complexity of insect immunity against parasitoids than expected, with the presence of hematopoietic niches and the identification of pathways being reminiscent of vertebrate models (Sheehan et al., 2018). Finally, the natural variability of the host immune response and the mechanisms of virulence of parasitoids may open the way to new concepts. Understanding the short-term evolution of the immune interactions could well be announced as a major theme in the near future.

AUTHOR CONTRIBUTIONS

CK-J, J-LG and MP discussed the contents of the manuscript and contributed to the writing and editing.

FUNDING

CK-J PhD was funded, and work was performed in the context of the LABEX SIGNALIFE "Investments for the future" ANR-11-LABX-0028 (http://signalife.unice.fr). The team received funding from the Department of Plant Health (SPE) (http://www.spe.inra.fr) from the National Institute for Agronomic Research (INRA) and the European Union's Seventh Framework Program for research, technological development and demonstration, under grant agreement no. 613678 (DROPSA) (http://dropsaproject.eu).

ACKNOWLEDGMENTS

We acknowledge Dr. M. Crozatier, Dr. L. Boyer, and Pr. Istvan Ando for fruitful discussions. We also thank S. Lemauf and A. Iacovone for the pictures of *Leptopilina* wasp development and parasitism.

REFERENCES

Anderl, I., Vesala, L., Ihalainen, T. O., Vanha-aho, L.-M., Andó, I., Rämet, M., et al. (2016). Transdifferentiation and proliferation in two distinct hemocyte lineages in *Drosophila melanogaster* larvae after wasp infection. *PLoS Pathog.* 12, e1005746–e1005734. doi: 10.1371/journal.ppat.1005746

Bajgar, A., Kucerova, K., Jonatova, L., Tomcala, A., Schneedorferova, I., Okrouhlik, J., et al. (2015). Extracellular adenosine mediates a systemic metabolic switch during immune response. *PLoS Biol.* 13, 1–23. doi: 10.1371/journal.pbio.1002135

Baker, D. A., Mille-Baker, B., Wainwright, S. M., Ish-Horowicz, D., and Dibb, N. J. (2001). Mae mediates MAP kinase phosphorylation of Ets transcription factors in *Drosophila*. *Nature* 411, 330–334. doi: 10.1038/35077122

Banerjee, U., Girard, J. R., Goins, L. M., and Spratford, C. M. (2019). *Drosophila* as a genetic model for hematopoiesis. *Genetics* 211, 367–417. doi: 10.1534/genetics.118.300223

Benmimoun, B., Polesello, C., Waltzer, L., and Haenlin, M. (2012). Dual role for insulin/TOR signaling in the control of hematopoietic progenitor maintenance in *Drosophila*. *Development* 139, 1713–1717. doi: 10.1242/dev.080259

Bidla, G., Dushay, M. S., and Theopold, U. (2007). Crystal cell rupture after injury in *Drosophila* requires the JNK pathway, small GTPases and the TNF homolog Eiger. *J. Cell Sci.* 120, 1209–1215. doi: 10.1242/jcs.03420

Bozler, J., Kacsoh, B. Z., and Bosco, G. (2017). Nematocytes: discovery and characterization of a novel aculeate hemocyte in *Drosophila falleni* and *Drosophila phalerata*. *PLoS One* 12, e0188133–e0188117. doi: 10.1371/journal.pone.01881331

Carton, Y., Boulétreau, M., Van Lenteren, J. C., and van Alphen, J. J. M. (1986). "The Drosophila parasitic wasps" in *The genetic and biology of Drosophila*. Vol. 3 (London: Academic Press), 347–389.

Carton, Y., Frey, F., and Nappi, A. (1992). Genetic determinism of the cellular immune reaction in *Drosophila melanogaster*. *Heredity* 69, 393–399. doi: 10.1038/hdy.1992.141

Carton, Y., Frey, F., and Nappi, A. J. (2009). Parasite-induced changes in nitric oxide levels in *Drosophila paramelanica*. *J. Parasitol.* 95, 1134–1141. doi: 10.1645/GE-2091.1

Carton, Y., Poirié, M., and Nappi, A. J. (2008). Insect immune resistance to parasitoids. *J. Insect Sci.* 15, 67–87. doi: 10.1111/j.1744-7917.2008.00188.x

Charroux, B., and Royet, J. (2009). Elimination of plasmatocytes by targeted apoptosis reveals their role in multiple aspects of the *Drosophila* immune response. *Proc. Natl. Acad. Sci. USA* 106, 9797–9802. doi: 10.1073/pnas.0903971106

Chiu, H., Morales, J., and Govind, S. (2006). Identification and immuno-electron microscopy localization of p40, a protein component of immunosuppressive virus-like particles from *Leptopilina heterotoma*, a virulent parasitoid wasp of *Drosophila*. *J. Gen. Virol.* 87, 461–470. doi: 10.1099/vir.0.81474-0

Clark, R. I., Woodcock, K. J., Geissmann, F., Trouillet, C., and Dionne, M. S. (2011). Multiple TGF-β superfamily signals modulate the adult *Drosophila* immune response. *Curr. Biol.* 21, 1672–1677. doi: 10.1016/j.cub.2011.08.048

Colinet, D., Deleury, E., Anselme, C., Cazes, D., Poulain, J., Azema-Dossat, C., et al. (2013). Extensive inter- and intraspecific venom variation in closely related parasites targeting the same host: the case of *Leptopilina* parasitoids of *Drosophila*. *Insect Biochem. Mol. Biol.* 43, 601–611. doi: 10.1016/j.ibmb.2013.03.010

Colinet, D., Schmitz, A., Depoix, D., Crochard, D., and Poirié, M. (2007). Convergent use of RhoGAP toxins by eukaryotic parasites and bacterial pathogens. *PLoS Pathog.* 3:e203. doi: 10.1371/journal.ppat.0030203

Dragojlovic-Munther, M., and Martinez-Agosto, J. A. (2013). Extracellular matrix-modulated heartless signaling in *Drosophila* blood progenitors regulates their differentiation via a Ras/ETS/FOG pathway and target of rapamycin function. *Dev. Biol.* 384, 313–330. doi: 10.1016/j.ydbio.2013.04.004

Dubuffet, A., Colinet, D., Anselme, C., Dupas, S., Carton, Y., and Poirié, M. (2009). Variation of *Leptopilina boulardi* success in *Drosophila* hosts: what is inside the black box? *Adv. Parasitol.* 70, 147–188. doi: 10.1016/S0065-308X(09)70006-5

Dudzic, J. P., Kondo, S., Ueda, R., Bergman, C. M., and Lemaitre, B. (2015). *Drosophila* innate immunity: regional and functional specialization of prophenoloxidases. *BMC Biol.* 13, 1–16. doi: 10.1186/s12915-015-0193-6

Fauvarque, M. O., and Williams, M. J. (2011). *Drosophila* cellular immunity: a story of migration and adhesion. *J. Cell Sci.* 124, 1373–1382. doi: 10.1242/jcs.064592

Ferrarese, R., Morales, J., Fimiarz, D., Webb, B. A., and Govind, S. (2009). A supracellular system of actin-lined canals controls biogenesis and release of virulence factors in parasitoid venom glands. *J. Exp. Biol.* 212, 2261–2268. doi: 10.1242/jeb.025718

Forbes, A. A., Bagley, R. K., Beer, M. A., Hippee, A. C., and Widmayer, H. A. (2018). Quantifying the unquantifiable: why hymenoptera, not Coleoptera, is the most speciose animal order. *BMC Ecol.* 18:21. doi: 10.1186/s12898-018-0176-x

Gatti, J.-L., Schmitz, A., Colinet, D., and Poirié, M. (2012). "Diversity of virus-like particles in Parasitoids' venom: viral or cellular origin?" in *Parasitoid Viruses.* eds. N. E. Beckage, and J.-M. Drezen (San Diego: Academic Press), 181–192.

Ghosh, S., Mandal, S., and Mandal, L. (2018). Detecting proliferation of adult hemocytes in *Drosophila* by BrdU incorporation. *Wellcome Open Res.* 3, 47–12. doi: 10.12688/wellcomeopenres.14560.2

Goecks, J., Mortimer, N. T., Mobley, J. A., Bowersock, G. J., Taylor, J., and Schlenke, T. A. (2013). Integrative approach reveals composition of Endoparasitoid wasp venoms. *PLoS One* 8:e64125. doi: 10.1371/journal.pone.0064125

Gold, K. S., and Brückner, K. (2015). Macrophages and cellular immunity in *Drosophila* melanogaster. *Semin. Immunol.* 27, 357–368. doi: 10.1016/j.smim.2016.03.010

Grigorian, M., Mandal, L., and Hartenstein, V. (2011). Hematopoiesis at the onset of metamorphosis: terminal differentiation and dissociation of the *Drosophila* lymph gland. *Dev. Genes Evol.* 221, 121–131. doi: 10.1007/s00427-011-0364-6

Heavner, M. E., Hudgins, A. D., Rajwani, R., Morales, J., and Govind, S. (2014). Harnessing the natural *Drosophila*-parasitoid model for integrating insect immunity with functional venomics. *Curr. Opin. Insect Sci.* 6, 61–67. doi: 10.1016/j.cois.2014.09.016

Heavner, M. E., Ramroop, J., Gueguen, G., Ramrattan, G., Dolios, G., Scarpati, M., et al. (2017). Novel organelles with elements of bacterial and eukaryotic secretion systems Weaponize parasites of *Drosophila*. *Curr. Biol.* 27, 2869–2877.e6. doi: 10.1016/j.cub.2017.08.019

Hita, M., Espagne, E., Lemeunier, F., Pascual, L., Carton, Y., Periquet, G., et al. (2006). Mapping candidate genes for *Drosophila melanogaster* resistance to the parasitoid wasp *Leptopilina boulardi*. *Genet. Res.* 88, 81–91. doi: 10.1017/S001667230600841X

Hita, M. T., Poirié, M., Leblanc, N., Lemeunier, F., Lutcher, F., Frey, F., et al. (1999). Genetic localization of a *Drosophila melanogaster* resistance gene to a parasitoid wasp and physical mapping of the region. *Genome Res.* 9, 471–481.

Honti, V., Csordás, G., Kurucz, E., Márkus, R., and Andó, I. (2014). The cell-mediated immunity of *Drosophila melanogaster*: hemocyte lineages, immune compartments, microanatomy and regulation. *Dev. Comp. Immunol.* 42, 47–56. doi: 10.1016/j.dci.2013.06.005

Honti, V., Csordás, G., Márkus, R., Kurucz, E., Jankovics, F., and Andó, I. (2010). Cell lineage tracing reveals the plasticity of the hemocyte lineages and of the hematopoietic compartments in *Drosophila melanogaster*. *Mol. Immunol.* 47, 1997–2004. doi: 10.1016/j.molimm.2010.04.017

Iacovone, A., Ris, N., Poirié, M., and Gatti, J.-L. (2018). Time-course analysis of *Drosophila suzukii* interaction with endoparasitoid wasps evidences a delayed encapsulation response compared to *D. melanogaster*. *PLoS One* 13:e0201573. doi: 10.1371/journal.pone.0201573

Irving, P., Troxler, L., Heuer, T. S., Belvin, M., Kopczynski, C., Reichhart, J.-M., et al. (2001). A genome-wide analysis of immune responses in *Drosophila*. *Proc. Natl. Acad. Sci. USA* 98, 15119–15124. doi: 10.1073/pnas.261573998

Jung, S.-H., Evans, C. J., Uemura, C., and Banerjee, U. (2005). The *Drosophila* lymph gland as a developmental model of hematopoiesis. *Development* 132, 2521–2533. doi: 10.1242/dev.01837

Kacsoh, B. Z., Bozler, J., and Schlenke, T. A. (2014). A role for nematocytes in the cellular immune response of the Drosophilid *Zaprionus indianus*. *Parasitology* 141, 697–715. doi: 10.1017/S0031182013001431

Kacsoh, B. Z., and Schlenke, T. A. (2012). High Hemocyte load is associated with increased resistance against Parasitoids in *Drosophila suzukii*, a relative of *D. melanogaster*. *PLoS One* 7:e34721. doi: 10.1371/journal.pone.0034721

Kurucz, E., Váczi, B., Márkus, R., Laurinyecz, B., Vilmos, P., Zsámboki, J., et al. (2007). Definition of *Drosophila* hemocyte subsets by cell-type specific antigens. *Acta Biol. Hung.* 58, 95–111. doi: 10.1556/ABiol.58.2007.Suppl.8

Labrosse, C. (2003). Les facteurs immunosuppresseurs dans le système hôte-parasitoïde *Leptopilina boulardi-Drosophila melanogaster*. Thèse de doctorat. Université de Tours.

Labrosse, C., Stasiak, K., Lesobre, J., Grangeia, A., Huguet, E., Drezen, J. M., et al. (2005). A RhoGAP protein as a main immune suppressive factor in the *Leptopilina boulardi* (hymenoptera, Figitidae)-*Drosophila melanogaster* interaction. *Insect Biochem. Mol. Biol.* 35, 93–103. doi: 10.1016/j.ibmb.2004.10.004

Lanot, R., Zachary, D., Holder, F., and Meister, M. (2001). Postembryonic hematopoiesis in *Drosophila*. *Dev. Biol.* 230, 243–257. doi: 10.1006/dbio.2000.0123

Larsen, B. B., Miller, E. C., Rhodes, M. K., and Wiens, J. J. (2017). Inordinate fondness multiplied and redistributed: the number of species on earth and the new pie of life. *Q. Rev. Biol.* 92, 229–265. doi: 10.1086/693564

Leitão, A. B., and Sucena, É. (2015). *Drosophila* sessile hemocyte clusters are true hematopoietic tissues that regulate larval blood cell differentiation. *elife* 4:239. doi: 10.7554/eLife.06166

Letourneau, M., Lapraz, F., Sharma, A., Vanzo, N., Waltzer, L., and Crozatier, M. (2016). *Drosophila* hematopoiesis under normal conditions and in response to immune stress. *FEBS Lett.* 590, 4034–4051. doi: 10.1002/1873-3468.12327

Louradour, I., Sharma, A., Morin-Poulard, I., Letourneau, M., Vincent, A., Crozatier, M., et al. (2017). Reactive oxygen species-dependent toll/NF-κB activation in the *Drosophila* hematopoietic niche confers resistance to wasp parasitism. *elife* 6:e25496. doi: 10.7554/eLife.25496

Lu, A., Zhang, Q., Zhang, J., Yang, B., Wu, K., Xie, W., et al. (2014). Insect prophenoloxidase: the view beyond immunity. *Front. Physiol.* 5:252. doi: 10.3389/fphys.2014.00252

Lusk, J., Lam, V., and Tolwinski, N. (2017). Epidermal growth factor pathway signaling in *Drosophila* embryogenesis: tools for understanding cancer. *Cancer* 9, 16–12. doi: 10.3390/cancers9020016

Makhijani, K., and Brückner, K. (2012). Of blood cells and the nervous system: hematopoiesis in the *Drosophila* larva. *Fly* 6, 254–260. doi: 10.4161/fly.22267

Makki, R., Meister, M., Pennetier, D., Ubeda, J.-M., Braun, A., Daburon, V., et al. (2010). A short receptor downregulates Jak/STAT signalling to control the *Drosophila* cellular immune response. *PLoS Biol.* 8:e1000441. doi: 10.1371/journal.pbio.1000441

Márkus, R., Laurinyecz, B., Kurucz, E., Honti, V., Bajusz, I., Sipos, B., et al. (2009). Sessile hemocytes as a hematopoietic compartment in *Drosophila melanogaster*. *Proc. Natl. Acad. Sci. USA* 106, 4805–4809. doi: 10.1073/pnas.0801766106

Márkus, R., Lerner, Z., Honti, V., Csordás, G., Zsámboki, J., Cinege, G., et al. (2015). Multinucleated giant hemocytes are effector cells in cell-mediated immune responses of *Drosophila*. *J. Innate Immun.* 7, 340–353. doi: 10.1159/000369618

Martinek, N., Shahab, J., Saathoff, M., and Ringuette, M. (2008). Haemocyte-derived SPARC is required for collagen-IV-dependent stability of basal laminae in *Drosophila* embryos. *J. Cell Sci.* 121, 1671–1680. doi: 10.1242/jcs.021931

Mondal, B. C., Mukherjee, T., Mandal, L., Evans, C. J., Sinenko, S. A., Martinez-Agosto, J. A., et al. (2011). Interaction between differentiating cell- and niche-derived signals in hematopoietic progenitor maintenance. *Cell* 147, 1589–1600. doi: 10.1016/j.cell.2011.11.041

Mondal, B. C., Shim, J., Evans, C. J., and Banerjee, U. (2014). Pvr expression regulators in equilibrium signal control and maintenance of *Drosophila* blood progenitors. *elife* 3:e03626. doi: 10.7554/eLife.03626

Moreau, S., and Asgari, S. (2015). Venom proteins from parasitoid wasps and their biological functions. *Toxins* 7, 2385–2412. doi: 10.3390/toxins7072385

Morin-Poulard, I., Sharma, A., Louradour, I., Vanzo, N., Vincent, A., and Crozatier, M. E. (2016). Vascular control of the *Drosophila* haematopoietic microenvironment by slit/Robo signalling. *Nat. Commun.* 7, 1–12. doi: 10.1038/ncomms11634

Morin-Poulard, I., Vincent, A., and Crozatier, M. (2013). The *Drosophila* JAK-STAT pathway in blood cell formation and immunity. *Jak-Stat* 2:e25700. doi: 10.4161/jkst.25700

Nakhleh, J., Moussawi El, L., and Osta, M. A. (2017). The melanization response in insect immunity. *Adv In Insect Physiol.* 52, 83–109. doi: 10.1016/bs.aiip.2016.11.002

Nappi, A. J. (2010). Cellular immunity and pathogen strategies in combative interactions involving *Drosophila* hosts and their endoparasitic wasps. *Invertebr. Surviv. J.* 7, 198–210. Available at: http://www.isj.unimo.it/index.php/ISJ/article/view/222

Nappi, A. J., and Streams, F. A. (1969). Abortive development of the cynipid parasite *Pseudeucoila bochei* (hymenoptera) in species of the *Drosophila melanica* group. *Ann. Entomol. Soc. Am.* 63, 321–327.

Nappi, A. J., and Vass, E. (1993). Melanogenesis and the generation of cytotoxic molecules during insect cellular immune reactions. *Pigment Cell Res.* 6, 117–126. doi: 10.1111/j.1600-0749.1993.tb00590.x

Nappi, A. J., Vass, E., Frey, F., and Carton, Y. (1995). Superoxide anion generation in *Drosophila* during melanotic encapsulation of parasites. *Eur. J. Cell Biol.* 68, 450–456.

Novković, B., Mitsui, H., Suwito, A., and Kimura, M. T. (2011). Taxonomy and phylogeny of *Leptopilina* species (hymenoptera: Cynipoidea: Figitidae) attacking frugivorous drosophilid flies in Japan, with description of three new species. *Entomol. Sci.* 14, 333–346. doi: 10.1111/j.1479-8298.2011.00459.x

Owusu-Ansah, E., and Banerjee, U. (2009). Reactive oxygen species prime *Drosophila* haematopoietic progenitors for differentiation. *Nature* 461, 537–541. doi: 10.1038/nature08313

Oyallon, J., Vanzo, N., Krzemień, J., Morin-Poulard, I., Vincent, A., and Crozatier, M. (2016). Two independent functions of collier/early B cell factor in the control of *Drosophila* blood cell homeostasis. *PLoS One* 11, e0148978–e0148916. doi: 10.1371/journal.pone.0148978

Paredes, J. C., Herren, J. K., Schüpfer, F., and Lemaitre, B. (2016). The role of lipid competition for endosymbiont-mediated protection against parasitoid wasps in Drosophila. *mBio* 7, 1–8. doi: 10.1128/mBio.01006-16

Petraki, S., Alexander, B., and Brückner, K. (2015). Assaying blood cell populations of the *Drosophila melanogaster* larva. *JoVE* 105, 1–11. doi: 10.3791/52733

Poirié, M., Colinet, D., and Gatti, J.-L. (2014). Insights into function and evolution of parasitoid wasp venoms. *Curr Opin insect science* 6, 52–60.

Rizki, R. M., and Rizki, T. M. (1984). Selective destruction of a host blood cell type by a parasitoid wasp. *Proc. Natl. Acad. Sci. USA* 81, 6154–6158.

Rizki, R. M., and Rizki, T. M. (1990). Parasitoid virus-like particles destroy *Drosophila* cellular immunity. *Proc. Natl. Acad. Sci. USA* 87, 8388–8392. doi: 10.1073/pnas.87.21.8388

Rizki, T. M., and Rizki, R. M. (1994). Parasitoid-induced cellular immune deficiency in *Drosophila*. *Ann. N. Y. Acad. Sci.* 712, 178–194. doi: 10.1111/j.1749-6632.1994.tb33572.x

Russo, J., Brehélin, M., and Carton, Y. (2001). Haemocyte changes in resistant and susceptible strains of *D. melanogaster* caused by virulent and avirulent strains of the parasitic wasp *Leptopilina boulardi*. *J. Insect Physiol.* 47, 167–172. doi: 10.1016/S0022-1910(00)00102-5

Russo, J., Dupas, S., Frey, F., Carton, Y., and Brehelin, M. (1996). Insect immunity: early events in the encapsulation process of parasitoid (*Leptopilina boulardi*) eggs in resistant and susceptible strains of *Drosophila*. *Parasitology* 112, 135–142. doi: 10.1017/S0031182000065173

Salazar-Jaramillo, L., Paspati, A., van de Zande, L., Vermeulen, C. J., Schwander, T., and Wertheim, B. (2014). Evolution of a cellular immune response in drosophila: a phenotypic and genomic comparative analysis. *Genome Biol. Evol.* 6, 273–289. doi: 10.1093/gbe/evu012

Sheehan, G., Garvey, A., Croke, M., and Kavanagh, K. (2018). Innate humoral immune defences in mammals and insects: The same, with differences? *Virulence* 9, 1625–1639.

Shim, J., Gururaja-Rao, S., and Banerjee, U. (2013). Nutritional regulation of stem and progenitor cells in *Drosophila*. *Development* 140, 4647–4656. doi: 10.1242/dev.079087

Sinenko, S. A., Mandal, L., Martinez-Agosto, J. A., and Banerjee, U. (2009). Dual role of wingless signaling in stem-like hematopoietic precursor maintenance in *Drosophila*. *Dev. Cell* 16, 756–763. doi: 10.1016/j.devcel.2009.03.003

Sinenko, S. A., Shim, J., and Banerjee, U. (2011). Oxidative stress in the haematopoietic niche regulates the cellular immune response in *Drosophila*. *EMBO Rep.* 13, 83–89. doi: 10.1038/embor.2011.223

Stofanko, M., Kwon, S. Y., and Badenhorst, P. (2010). Lineage tracing of lamellocytes demonstrates *Drosophila* macrophage plasticity. *PLoS One* 5:e14051. doi: 10.1371/journal.pone.0014051

Tokusumi, Y., Tokusumi, T., and Schulz, R. A. (2017). The nociception genes painless and Piezo are required for the cellular immune response of *Drosophila* larvae to wasp parasitization. *Biochem. Biophys. Res. Commun.* 486, 893–897. doi: 10.1016/j.bbrc.2017.03.116

Vanha-aho, L.-M., Anderl, I., Vesala, L., Hultmark, D., Valanne, S., and Rämet, M. (2015). Edin expression in the fat 492 body is required in the Defense against parasitic wasps in *Drosophila* melanogaster. *PLoS Pathog.* 11:e1004895. doi: 10.1371/journal.ppat.1004895.s004

Vivekanand, P. (2018). Lessons from *Drosophila* pointed, an ETS family transcription factor and key nuclear effector of the RTK signaling pathway. *Genesis* 56:e23257. doi: 10.1002/dvg.23257

Williams, M. J., Andó, I., and Hultmark, D. (2005). *Drosophila melanogaster* Rac2 is necessary for a proper cellular immune response. *Genes Cells* 10, 813–823. doi: 10.1111/j.1365-2443.2005.00883.x

Williams, M. J., Wiklund, M.-L., Wikman, S., and Hultmark, D. (2006). Rac1 signalling in the *Drosophila* larval cellular immune response. *J. Cell Sci.* 119, 2015–2024. doi: 10.1242/jcs.02920

Yang, H., Kronhamn, J., Ekstrom, J. O., Korkut, G. G., and Hultmark, D. (2015). JAK/STAT signaling in *Drosophila* muscles controls the cellular immune response against parasitoid infection. *EMBO Rep.* 16, 1664–1672. doi: 10.15252/embr.201540277

Zettervall, C.-J., Anderl, I., Williams, M. J., Palmer, R., Kurucz, E., Andó, I., et al. (2004). A directed screen for genes involved in *Drosophila* blood cell activation. *Proc. Natl. Acad. Sci. USA* 101, 14192–14197. doi: 10.1073/pnas.0403789101

Conflict of Interest Statement: The authors declare that the research was conducted in the absence of any commercial or financial relationships that could be construed as a potential conflict of interest.

frontiers in Physiology

ORIGINAL RESEARCH
published: 27 May 2019
doi: 10.3389/fphys.2019.00604

Chemical Ecology of *Capnodis tenebrionis* (L.) (Coleoptera: Buprestidae): Behavioral and Biochemical Strategies for Intraspecific and Host Interactions

Giuseppe Bari[1†], Andrea Scala[2†], Vita Garzone[1], Rosanna Salvia[2], Cem Yalcin[1,3], Pasqua Vernile[1], Antonella Maria Aresta[4], Osvaldo Facini[5], Rita Baraldi[5], Sabino A. Bufo[2], Heiko Vogel[6], Enrico de Lillo[1‡], Francesca Rapparini[5*‡] and Patrizia Falabella[2*‡]*

[1] Department of Soil, Plant and Food Sciences, University of Bari Aldo Moro, Bari, Italy, [2] Department of Science, University of Basilicata, Potenza, Italy, [3] Syngenta, Izmir, Turkey, [4] Department of Chemistry, University of Bari Aldo Moro, Bari, Italy, [5] Department of Biology, Agriculture and Food Sciences, Biometeorology Institute, National Research Council, Bologna, Italy, [6] Department of Entomology, Max Planck Institute for Chemical Ecology, Jena, Germany

This study focuses on several aspects of communication strategies adopted by adults of the Mediterranean flat-headed root-borer *Capnodis tenebrionis* (Coleoptera: Buprestidae). Morphological studies on the structures involved in mate recognition and acceptance revealed the presence of porous areas in the pronota in both sexes. These areas were variable in shape and size, but proportionally larger in males. The presence of chaetic, basiconic, and coeloconic sensilla in the antennae of both males and females was verified. Bioassays revealed stereotyped rituals in males and the involvement of female pronotal secretions in mate recognition and acceptance. During the mating assays, the female's pronotum was covered by a biologically inert polymeric resin (DenFil^{TM}), which prevented males from detecting the secretions and from completing the copulation ritual. The use of the resin allowed for the collection of chemical compounds. GC-MS analysis of the resin suggested it may be used to retain compounds from insect body surfaces and revealed sex-specific chemical profiles in the cuticles. Since adult *C. tenebrionis* may use volatile organic compounds (VOCs) emitted from leaves or shoots, the VOC emission profiles of apricot trees were characterized. Several volatiles related to plant-insect interactions involving fruit tree species of the Rosaceae family and buprestid beetles were identified. To improve understanding of how VOCs are perceived, candidate soluble olfactory proteins involved in chemoreception (odorant-binding proteins and chemosensory proteins) were identified using tissue and sex-specific RNA-seq data. The implications for chemical identification, physiological and ecological functions in intraspecific communication and insect–host interactions are discussed and potential applications for monitoring presented.

Keywords: chemoreception, mating, Mediterranean flat-headed root-borer, scanning electron microscopy, soluble olfactory proteins, volatile organic compounds

OPEN ACCESS

Edited by:
Graziano Fiorito, Stazione Zoologica Anton Dohrn, Italy

Reviewed by:
Lindy Holden-Dye, University of Southampton, United Kingdom
Carmelo Peter Bonsignore, Mediterranea University of Reggio Calabria, Italy

****Correspondence:***
Enrico de Lillo
enrico.delillo@uniba.it
Francesca Rapparini
f.rapparini@ibimet.cnr.it
Patrizia Falabella
patrizia.falabella@unibas.it

[†] These authors have contributed equally to this work as first authors

[‡] These authors have contributed equally to this work as last authors

Specialty section:
This article was submitted to Invertebrate Physiology, a section of the journal Frontiers in Physiology

Received: *21 January 2019*
Accepted: *29 April 2019*
Published: *27 May 2019*

Citation:
Bari G, Scala A, Garzone V, Salvia R, Yalcin C, Vernile P, Aresta AM, Facini O, Baraldi R, Bufo SA, Vogel H, de Lillo E, Rapparini F and Falabella P (2019) Chemical Ecology of Capnodis tenebrionis (L.) (Coleoptera: Buprestidae): Behavioral and Biochemical Strategies for Intraspecific and Host Interactions. Front. Physiol. 10:604. doi: 10.3389/fphys.2019.00604

INTRODUCTION

Capnodis tenebrionis (L.) (Coleoptera: Buprestidae), commonly known as the Mediterranean flat-headed root-borer, affects many species of Rosaceae, particularly apricot, peach, plum, nectarine, cherry, and almond (Malagon et al., 1990; Ben-Yehuda et al., 2000; Marannino and de Lillo, 2007; Morton and García del Pino, 2008). The beetle is common in Central and Southern Europe, Northern Africa and the Middle East (Garrido et al., 1987; Tezcan, 1995; Martin et al., 1998; Cınar et al., 2004; Marannino and de Lillo, 2007; Sharon et al., 2010). *Capnodis tenebrionis* can be a key pest in some areas and cultivation conditions, particularly in organic orchards and/or in arid and semiarid environments, where plants are susceptible to the destructive action of larvae on roots and control strategies have to be applied (Bonsignore and Bellamy, 2007; del Mar Martinez de Altube et al., 2008). Recent outbreaks in areas like Emilia Romagna and Southern France, previously less affected by this pest, may be a consequence of global warming, especially for trees growing on clayey and poorly irrigated soils, and may be related to the beetle preference for the high temperature (Bonsignore and Vacante, 2009).

Adult beetles feed on the bark of shoots, buds, and leaf petioles, and usually prefer weakened and diseased trees rather than vigorous ones (Rivnay, 1946; Garrido, 1984; Bonsignore and Bellamy, 2007). These adults can seriously damage young trees in nurseries, orchards and greenhouses, but rarely affect established, well-cultivated and irrigated fruit-bearing orchards (García del Pino and Morton, 2005). Females lay eggs in the cracks of dry soil or under stones, close to trees and rarely on the bark (Ben-Yehuda et al., 2000). Neonate larvae crawl within the soil, penetrate the roots and feed on the root cortical and subcortical tissues (Mendel et al., 2003). Damage caused by larvae becomes obvious as the tree dries out or begins to secrete resin (Marannino et al., 2004; del Mar Martinez de Altube et al., 2008). One-year-old trees can be killed by a single larva; a few larvae can lead to the death of a mature tree within 1 or 2 years (Ben-Yehuda et al., 2000; García del Pino and Morton, 2005).

Whether *C. tenebrionis* secretes volatiles – long-distance airborne sex or aggregation pheromones – is not yet known (Bari et al., 2004; Rodriguez-Saona et al., 2006; Sharon et al., 2010), and how beetles find, select and accept partners has yet to be described. However, male-biased aggregation on host trees may be linked to mating (Bonsignore et al., 2008; Bonsignore and Jones, 2013). Additionally, cuticular hydrocarbons, which have been discovered in another buprestid, *Agrilus planipennis* (F.), may function as contact pheromones and be involved in the beetle's mating behavior (Lelito et al., 2009; Silk et al., 2009). Plant-produced chemicals could be involved in host location by *C. tenebrionis* (Sharon et al., 2010). It is well known that volatile organic compounds (VOCs) released by plants provide olfactory cues to help herbivorous insects locate nutritional resources and suitable oviposition sites, within both natural and agricultural ecosystems (Bruce et al., 2005, and references therein). VOC emissions from healthy plants result in a species-specific pattern that can be altered by abiotic and biotic factors (Niinemets et al., 2013). Emissions of VOCs from both healthy and stressed plants have been suggested to explain the host preference behavior of adult *C. tenebrionis* when testing the effect of air headspace of apricot twigs in an olfactometer assay (Sharon et al., 2010). Although species-by-species surveys of VOCs emissions have been carried out for forested ecosystems, VOC emissions from agricultural species, especially fruit trees, remain poorly characterized (Staudt et al., 2010; Najar-Rodriguez et al., 2013).

Since adult mating behavior likely involves the emission and recognition of pheromone cues, studying these behaviors may suggest the putative role of the structures involved in their release and perception. Similarly, knowledge of which volatiles are released by trees may clarify how adult beetles choose trees for feeding or mating. Both sets of data could improve monitoring strategies of *C. tenebrionis* in the field. Antennae in insects are the typical organs involved in chemical perception; a chemical message (host plant volatiles, pheromones or allomones) is transduced into a neuronal impulse starting from the olfactory sensory neuron (Jacquin-Joly and Merlin, 2004; Leal, 2013). Olfactory, gustatory, and ionotropic receptors, soluble olfactory proteins such as odorant-binding proteins (OBPs) and chemosensory proteins (CSPs) mediate chemical perception in insects (Fan et al., 2010; Mamidala et al., 2013). There is still no consensus about the role of each olfactory gene family in Coleoptera and few studies investigated this issue in coleopteran insects (Engsontia et al., 2008; Mitchell et al., 2012; Andersson et al., 2013). Concerning buprestids, Mamidala et al. (2013) focused on gene families associated with odor processing and xenobiotic degradation in the invasive *A. planipennis*. A detailed study of the distribution and structure of *A. planipennis* antennal sensilla showed that males had significantly more uniporous gustatory sensilla than females (Crook et al., 2008), supporting the hypothesis that mate recognition by males involves female-released contact cues. The antennal morphology and the sensillar arrangement of *C. tenebrionis* adults are still poorly known, as are the antennal pathways that allow for volatile or non-volatile compound binding, transport and olfactory neuron responses.

To understand the chemical ecology of *C. tenebrionis*, an investigation was carried out with the following goals: (1) to characterize the behavior and the structures involved in mate recognition and acceptance, (2) to identify the types of cues involved in mate recognition, (3) to describe the antennal sensillar morphology in males and females, (4) to characterize the qualitative pattern of constitutive VOC emissions by the host plant under non-stressed conditions and determine how these emissions act as infochemicals in host recognition and preference, (5) to recognize and evaluate the expression level of OBPs and CSPs, proteins involved in chemoreception, on the basis of the functional annotation and the analysis of conserved amino acid patterns. The identification and the evaluation of OBPs and CSPs expression level was performed starting from the transcriptomic analysis of antennae, the main organs involved in chemoreception in which soluble olfactory proteins are commonly highly expressed, in comparison to the

level of the expression of the same proteins in the rest of the insect body.

MATERIALS AND METHODS

Source of Adult Beetles

Due to the prolonged life cycle of *C. tenebrionis* and the difficulties in the rearing of the insect in laboratory and artificial conditions, the present study was carried out from 2011 to 2017, and on adults collected from infested orchards of apricot, cherry, peach, and plum in the District of Bari and Matera (Southern Italy). Adult beetles were collected from March to October from the host plants by hand or with a net. Active, healthy adults were held in ventilated polystyrene (17 cm × 25 cm × 7 cm) (de Lillo, 1998) or metal net cages (30 cm × 30 cm × 30 cm) (5–15 beetles per cage). Beetles were maintained under controlled conditions (28 ± 1°C, 45 ± 5%RH, 16:8 L:D photoperiod) or at room temperature, depending on the assay and observations to be performed. Insects were fed with fresh apricot and plum twigs. Cages were inspected every 2–7 days in order to renew twigs, and to remove feces and dead adults.

Females laid eggs on cellulose discs; eggs were incubated at 27 ± 1°C in darkness for 8–15 days until neonates hatched. Twenty-four-hour-old neonates were transferred with a fine brush onto Petri dishes (Ø 5 cm) containing artificial diet (Gindin et al., 2009). Diet included root cortex flour of 2- to 3-year-old Myrobalan (*Prunus cerasifera* L.) trees. Diet was replaced every 2 weeks up to pupation. Larvae were reared in a dark chamber with controlled temperature at 27 ± 1°C. Cuticular extractions were performed on newly emerged (virgin) adults.

Light Microscopy Examination of the Pronotum

Ten males and 10 females were randomly selected from a large collection of dead specimens and their pronota were removed under a dissecting stereomicroscope (Weatler, Ernst Leitz, Wetzlar, Germany). The pronotum of each specimen was mapped and pencil-drawn at 20X through a camera lucida mounted on a dissecting stereomicroscope (SZH, Olympus, Tokyo, Japan). Particular care was given to the details of the pronotum surface covered with a whitish dust (fields of secretion). The drawings were digitized (Perfection 3200 Photo, Epson, Nagano, Japan), and the smooth and rough surface fields of each specimen were measured (in pixels) using a graphic editing software (Adobe® Photoshop® CS5 Extended). The coverage percentage of smooth and rough fields was compared to the whole surface of the pronotum for both genders. Non-normally distributed continuous data were analyzed using the non-parametric Mann–Whitney *U* test.

SEM Examination of the Adult Pronotum and Antennae

Pronota were dissected from six males and six females, randomly selected from a large collection of dead specimens. The outer and inner surfaces were cleaned by washing the pronota in a solution composed of (1) ethylene 95% and xylene (1:1) (Sands, 1984) for 10 min (for three males and three females) or (2) sodium lauryl sulfate (25 g), sodium hydroxide (25 g), liquid soap (25 g) and distilled water (500 mL) (for three males and three females) (Porcelli and Di Palma, 2001) for a few days, followed by a treatment with Essig's fluid for a further day (Wilkey, 1962).

After three females and three males were frozen, their pairs of antennae were cut at the base of the scape and shaken for 24 h (15 shakes per min) in a solution containing a denture-cleaning tablet (Polident®, Brentford, Middlesex, United Kingdom) (1.2 g/100 mL of distilled water). Finally, antennae were washed in distilled water.

Cleaned pronota were air-dried at room temperature and antennae were dried in a dehydrator. Both structures were platinum-coated using a sputter coater (S150A, Edwards High Vacuum International, Crawley, United Kingdom) and examined under a scanning electron microscope (SEM) (Tabletop Microscope 3000, Hitachi, Tokyo, Japan) at 5 kV of accelerating voltage. At the same time, antennae of other three frozen females and three frozen males were not treated with Polident but directly platinum-coated and examined under SEM. The results (not shown) were compared with the antennae treated with Polident. Surfaces and sensilla were largely covered by adhering dusts and particles in antennae not treated with Polident, whereas they were clean and well exposed when antennae were treated with Polident. No damages of these structures were observed.

SEM Examination of the Pronotal Resin Copy

Males and females were collected in early spring after their overwintering. They were reared as previously described (see section "Source of Adult Beetles") and were assayed at the appearance of a white waxy secretion on the pronotum. These adults were assayed in a Y-shaped olfactometer (Bari et al., 2004) and females able to attract males and males moved toward the arm baited by females were used for subsequent observations. The pronota of these live beetles were coated with a polymeric resin-based dental restorative material (DenFil™, Vericom Ltd., Co., Gyeonggi-do, South Korea). This creamy composite is silicon-like at room temperature, hardens under ultraviolet light (UV) within about 20 s (or under light source for longer time) and contains barium aluminosilicate (average particle size ≥ 1 μm), fumed silica (average particle size 0.04 μm), bisphenol A glycidyl-dimethacrylate, triethylene-glycol dimethacrylate and other trace compounds. The resin was applied using forceps with flattened tips to cover the whole pronotum area including its lateral margins. After the resin hardened under a white fluorescent light, it was lifted gently and removed. Resin was applied on both male and female pronota. After the resin was removed from the beetle's surface, a resin copy of the pronotum with its secretions and the most external layers was made (**Figure 1**). Pure resin material was hardened and used as a blank (negative) control. Resin copy was studied under an SEM (Tabletop microscope 3000, Hitachi, Tokyo, Japan), at 5 kV of accelerating voltage. The chemical spectrum of the beetle-covering compounds of the pronotum

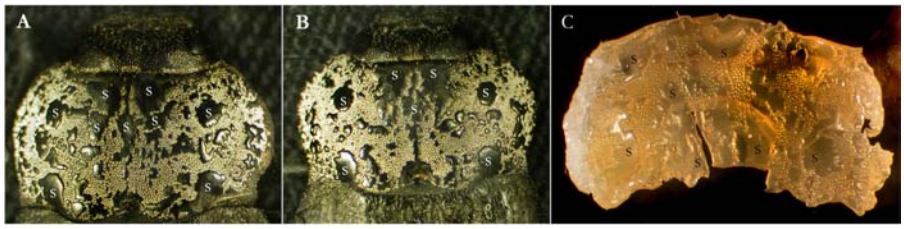

FIGURE 1 | Pronota of *C. tenebrionis*: smooth fields and rough fields on the pronotum of the adult female **(A)** and male **(B)**. Resin copy **(C)** removed from the pronotum. S, smooth fields; R, rough fields.

adhering to the resin was analyzed using an energy dispersive spectrometer (EDS) on surface spots.

Pre-mating and Mating Behavior

Although the age and mating status of field-caught beetles were unknown, adults caught in early spring (March-April 2011) were presumed to be sexually immature. Some females (about a dozen) were dissected after collection and sperms were not found in their spermatechae. The beetles were reared as previously described (see section "Source of Adult Beetles"), until the appearance of the white waxy secretion on the pronotum. Males and females were assayed in a Y-shaped olfactometer (Bari et al., 2004), and only females able to attract males and males moved toward the arm baited by females were used for the mating bioassay. Males (n = 22) and females (n = 25) were coupled in mating arenas (15 cm × 34 cm × 6 cm) at 28 ± 1°C under fluorescent light. The assay was repeated over several consecutive days. Each observation (n = 200) lasted 30 min at most and the behavior of each individual was studied before, during and shortly after copulation. Coupling duration was also recorded. Males were kept separate from females for at least 12 h before the assay. Coupling behavior was repeatedly observed for the same individuals, in order to determine whether females and males mated once or more than once under the experimental conditions. The outline of the beetle's body was approximated to an ellipse. Therefore, the body length (from the head tip to the tip of the elytra end) and width of the pronotum of mated couples were measured with a caliper; the surface of this ellipse was calculated. Pearson's bivariate analysis and Student's t-test (n = 19, $p < 0.05$, two-tailed) were performed in order to verify the relationship between mating duration and body size of mated couples.

Assuming that sexually mature males could ascertain female maturity via a contact pheromone released on the pronotum's secretory area, soon after the selection of adults by the olfactometer assays, the following procedure was carried out: (1) Ten males and 10 females (the most active following the olfactometer assay) were placed in mating arenas (glass container, 15 cm × 34 cm × 6 cm in size, with bottom and lateral sides covered by white paper). Once individual's readiness to mate was verified, they were separated until just before copulation. (2) Afterward, the lateral half (right or left) of the pronota of five out of ten selected females was coated with Denfil in order to evaluate the repellency of the resin on males (this assay was considered a sort of control). After the resin hardened, couples were again placed together and the males' behavior was observed for up to 30 min. This assay was repeated five times with different male-female combinations. (3) Next, the uncoated half of the female's pronotum was also treated by resin to hide the whole pronotum from the male's antennae; couples were formed again and the male's behavior was observed for up to 30 min. In addition, five additional couples were formed and observed, in which each female began with a whole uncoated pronotum that was then covered entirely. (4) Finally, the resin was removed from the pronota of all females, couples (n = 10) were again paired and individuals were left to mate.

Chemical Analysis of Pronotum Secretions and the Whole Beetle Body

The pronota of adults showing white wax secretion were used. The hardened resin acted like a negative, revealing the pronotum secretions and outer cuticular layers. After the resin copies were removed, they were dipped in a solution of 0.3 mL of n-hexane and sonicated for 20 min in an ultrasonic bath. A pure polymerized resin was used as a blank. In 2014, resin copies of the pronota were obtained from males and females caught in the field in early spring (after their overwintering) and selected from among those which positively responded to the Y-olfactometer and mating assays. In 2015, resin copies were produced by three groups: virgin males and females obtained by rearing larvae (without overwintering); mated males and females caught in the field (after their overwintering); adults caught in the field (after their overwintering) which were demonstrated to be attracted (males) and attractive (females) by the olfactometer bioassay. In 2015, cuticular chemicals were also directly extracted from the whole bodies of virgin males and females (without overwintering) whose larvae had been reared on artificial diets in order to highlight further chemicals potentially emitted from other body territories. Beetles used in the preparation of the whole body extracts were the most vigorous and active in cages. They were starved for 24 h in order to avoid contamination with food or feces during the extraction. Specimens were freeze-killed and left to dry at room temperature for 20 min. They were individually dipped in 3 mL aliquots of n-hexane for 15 min each. After removing the whole bodies, extracts were sonicated for 20 min in an ultrasonic bath. Three specimens were used as replicas for each year, gender, and treatment (resin copy of the pronotum, whole body, field-caught adults, virgin adults).

In all cases, the *n*-hexane was concentrated in a gentle stream of nitrogen to 0.3 mL and stored at −20°C till the analysis (Spikes et al., 2010). Of the extracted solution, 1–3 μL was injected in the GC-MS^n system (GCMSD 5975C, Thermo Electron Corporation, Austin, TX, United States) composed by a TRACE ultragas chromatograph (GC) interfaced to a Finnigan PolarisQ ion trap mass spectrometer (MS). The GC was provided by a capillary column made by HP-5MS (30 m length, 0.25 mm I.D. with 0.25 mm film thickness, 5 inch cage, Agilent, Palo Alto, CA, United States). The applied GC conditions were as follows: injector temperature (splitless mode), 200°C; carrier gas (helium) flow rate, 0.8 mL/min; the oven temperature program was raised from an initial 50°C (1 min) to 240°C at 10°C/min and 20°C/min up to 300°C (5 min) (Ginzel et al., 2006); transfer line temperature was 280°C. The applied MS conditions were as follows: EI^+ operating mode; source temperature, 250°C; electron energy, 70 eV; current, 200 μA at the filament; spectra acquisition (total ion current, TIC), from 50 to 650 m/z. To better identify the cuticular compounds of the whole beetle body, 3 μL of a C7–C40 saturated alkane standard (STD) Supelco 49452U was injected under the same conditions.

Compounds were identified based on their MS spectra (NIST05, WILEY Masslib) and the obtained peak values for STD. The differences between male, female and control (pure resin) chromatograms were evaluated.

Plant VOCs: Collection and Analysis

Volatile compounds were collected from the apricot (*Prunus armeniaca* L.) cultivar FARBALY®, which was selected because it represents a widely used cultivar, often attacked by *C. tenebrionis*. Three-year-old potted plants were grown in well-watered universal potting soil in the nursery of IBIMET-CNR in Bologna, Italy, under natural conditions of light, temperature, and humidity. VOC emissions were taken from three healthy leaves of non-fruit-bearing branches of four plants during fruit ripening (July–August 2015). The physiological status of the leaves was monitored through measurements of carbon assimilation, stomatal conductance and transpiration rates using the LI-COR 6400 Photosynthesis System (LI-COR Biosciences Inc., Lincoln, NE, United States) by placing each fully developed leaf in a 6 cm^2 cuvette. Measurements were performed at reference CO_2 (400 μmol mol^{-1}), flow rate (500 μmol min^{-1}), photosynthetic active radiation (PAR) (1000 μmol m^{-2} s^{-1}) and at 30°C with 30–50% of relative humidity. Carbon assimilation was measured for approximately 2–4 min, until photosynthetic intensity stabilized. VOC emissions were analyzed simultaneously with gas exchange measurements. Air samples were taken from the cuvette using steel tubes packed with 200 mg of Tenax GC®and Carbograph (Markes International, Ltd., Llantrisant, United Kingdom) connected to an external pump (Pocket Pump SKC Inc., Eighty Four, PA, United States), adsorbing at a flow rate of 200 mL min^{-1} for 30 min. All the adsorbent tubes were kept at −20°C until analysis to avoid any chemical alteration and/or artifacts. Traps were analyzed using a thermal-desorber (Markes International, Series 2 Unity) connected to a 7890A gas chromatograph coupled with a 5975C mass detector (GC-MS, Agilent Technologies, Wilmington, DE, United States) (Baraldi et al., 2018). Identification of the sampled compounds was carried out by comparing their retention times and mass spectra with those of authentic standards (Rapparini et al., 2004).

Olfactometer Assays With Plant VOCs

Adult beetles were assayed during 2013 using a transparent glass Y-olfactometer (55.6 mm internal diameter) composed of a common stem (about 15 cm long) bearing two lateral arms (about 10 cm long) separated at a 75° angle on the horizontal plane. The inner bottom of the tube housed a strip of fine metal netting to provide traction for the beetle. The olfactometer was placed horizontally and was illuminated by a white fluorescent light tube (700 lux), mounted at about 1 m above the olfactometer. The assay was carried out using cis-3-hexen-1-ol 98.0% (Aldrich), benzaldehyde 99.0% (Fluka), 2-hexanone reagent grade 98.0% (Sigma-Aldrich), 1-pentanol ≥ 99.0% Sigma-Aldrich), 3-methyl-1-butanol reagent grade (Sigma-Aldrich), S-(−)-limonene analytical standard (Fluka), β-myrcene analytical standard (Fluka) as volatile compounds, at a concentration of 1M in HPLC grade *n*-hexane. These compounds were selected based on the results of a previous electro-antennographic study of the response of *C. tenebrionis* adults to some chemicals (Bari et al., 2004), and VOC emissions of *Prunus* species (Baraldi et al., 1999). Each volatile compound was tested on 15 males and 15 females selected among the most active adults caught in the field during spring and reared under controlled conditions for at least 1 month. A 0.5 cm^2 square piece of filter paper (Whatman™, Maidstone, Kent, United Kingdom) was added with 5 μL of the volatile compound solution and introduced in the terminal glass bulb of one arm (the baited arm). Pure solvent was introduced on the glass bulb of the other arm (the control arm). Air passed through an activated charcoal filter and distilled water in a 1 L flask, and continued through flowmeters into the arms at an airstream of 0.9 L min^{-1} arm^{-1}. A single adult was introduced into the stem and allowed to move freely toward the arms and against the air flow. Each test lasted 15 min and arm choice was recorded. Responses were classified as "no-choice" when adults did not select an olfactometer arm within 15 min. After five adults had been assayed, the olfactometer arms were flipped 180° to minimize directional bias. The assay was carried out in a dark room, lighted only by the fluorescent tube above the olfactometer, and at 28 ± 1°C. At the end of the observations with the same volatile compound, the olfactometer was rinsed with soapy water and analytical grade acetone, and air-dried. After each assay, the adults were returned to the cages as above and used for the next assays. Each assayed adult was considered a replica. Results were expressed as response index calculated as:

$$= \frac{\text{number of adults moved to the baited arm} - \text{number of adults moved to non-baited arm}}{\text{total number of assayed adults per each tested VOC}} \times 100 \quad (1)$$

RNA Extraction and cDNA Synthesis

Antennae from 30 females and 30 males, caught in the field in early spring (after their overwintering), were cut from the base of the scape of live insects; a single male

body and a single female body, both without antennae, were collected. Samples were frozen in liquid nitrogen, homogenized in centrifuge tubes containing TRI Reagent (Sigma, St. Louis, MO, United States) and stored at −80°C until RNA extraction. Total RNA was extracted using TRI Reagent following the manufacturer's instructions (Sigma, St. Louis, MO, United States). A DNase (Turbo DNase, Ambion Inc., Austin, TX, United States) treatment was carried out to eliminate any contaminating DNA. After DNase enzyme removal, RNA was further purified using the RNeasy MinElute Cleanup Kit (Qiagen, Venlo, Netherlands) following the manufacturer's protocol and eluted in 20 μL of RNA storage solution (Ambion Inc., Austin, TX, United States). RNA integrity was verified on an Agilent 2100 Bioanalyzer using RNA nano chips (Agilent Technologies, Palo Alto, CA), while RNA quantity was determined by a NanoDrop ND1000 spectrophotometer (Thermo Scientific, Waltham, MA, United States).

Sequencing and *de novo* Transcriptome Assembly

Transcriptome sequencing of all RNA samples was performed with poly(A)+ enriched mRNA fragmented to an average of 150 nucleotides. Sequencing was carried out by the Max Planck Genome Center[1] using standard TruSeq procedures on an Illumina HiSeq2500 sequencer. Quality control measures, including the filtering of high-quality reads based on the score given in FASTQ files, the removal of reads containing primer/adaptor sequences and the trimming of read lengths, were carried out using CLC Genomics Workbench v9.1. The *de novo* transcriptome assembly was carried out using the same software, which is designed to assemble large transcriptomes using sequences from short-read sequencing platforms. All obtained sequences (contigs) were used for BLASTX searches (Altschul et al., 1997) against the National Center for Biotechnology Information (NCBI) non-redundant (nr) database, considering all hits with an e-value < 1E-5. The transcriptome was annotated using BLAST, gene ontology and InterProScan searches using BLAST2GO PRO v4.1[2](Götz et al., 2008). To optimize annotation of the obtained data, we used GO slim, a subset of GO terms that provides a high level of annotations and allows a global view of the result.

[1]http://mpgc.mpipz.mpg.de/home/
[2]www.blast2go.de

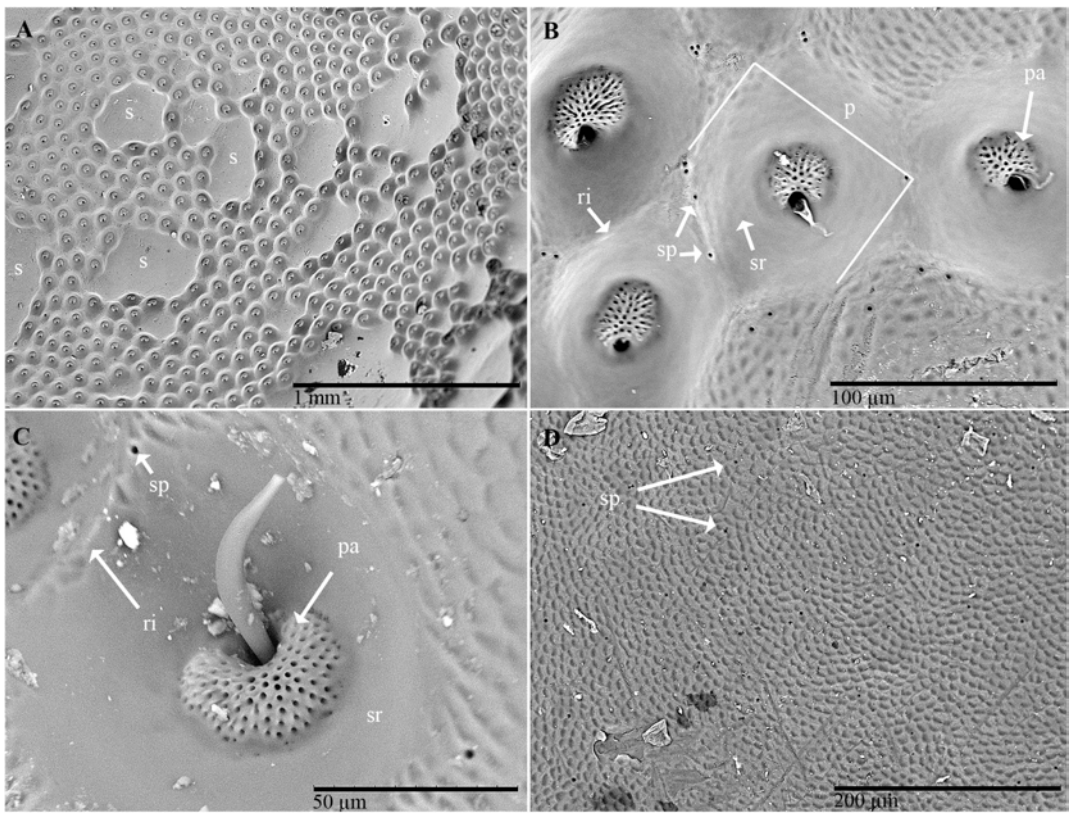

FIGURE 2 | Scanning electron micrographs of *C. tenebrionis*: general view **(A)** and details of a few glandular openings **(B)** on rough fields of the male's pronotum; **(C)** glandular openings on the male's pronotum; **(D)** outer surface of the female's pronotum. Specimens in panels **(A,B,D)** were washed according to Porcelli and Di Palma (2001); the specimen in panel **(C)** was washed according to Sands (1984). s, smooth fields; p, pore pit complex; pa, pore pit area; r, rim; sp, single pore; sr, smooth ring.

Digital Gene Expression Analysis

The tblastn program was used, with available sequences of OBP and CSP proteins from different insect species, as a "query" to identify candidate unigenes encoding putative OBPs and CSPs in *C. tenebrionis* adult males and females. All candidate proteins were manually checked by the blastx program at the NCBI.

The abundance in the expression level of each "unique" nucleotide sequences (contigs) was calculated on the basis of the reads per kilobase per million mapped reads method (RPKM) (Mortazavi et al., 2008), following the formula:

$$RPKM(A) = (10,00,000 \times C \times 1000)/(N \times L)$$

where RPKM (A) is the abundance of gene A, C is the number of reads that uniquely align to gene A, N is the total number of reads that uniquely align to all genes, and L is the number of bases in gene A.

RESULTS

Light Microscopy Examination of the Pronotum

Smooth and rough fields were observed on both antimers of the adult pronota (**Figure 1**). The pronotum is provided with one pre-scutellar dimple, shaped like a horseshoe, on the posterior margin. Two pairs of almost rounded and prominent smooth fields are found on the lateral sides. Size and distribution of smooth and rough fields, in both males and females, are not perfectly symmetrical and were not perfectly the same (for size and position) in all studied specimens. In addition, the borders of these areas appear quite irregular.

The average percentage of the surface size of the rough fields in comparison to the whole pronotum surface was not statistically different between the two genders.

SEM Examination of the Adult Pronotum and Antennae

Examination of the outer surface of the pronotum by SEM revealed the presence of groups of slight depressions ("pore pits") on the rough fields (**Figures 2A–C**). Most of the pore pits were hexagonal or round (**Figures 2A,B**), but some were irregularly outlined. The center of each complex was depressed and exhibited a cribrous (perforated) circular- or ovoid-shaped area, 50–60 μm in diameter, composed of 60–80 small circular or ovoid pores (each 5–10 μm in diameter) and one large pore (20–30 μm in diameter) (**Figures 2B,C**). In many cases, waxy filaments were observed to protrude from the pores (**Figures 2B,C**). The cribrous area was surrounded by a smooth ring delimited by a slight rim (**Figures 2B,C**). The diameter of the whole pore pit complex was between 80 and 120 μm at the rim level.

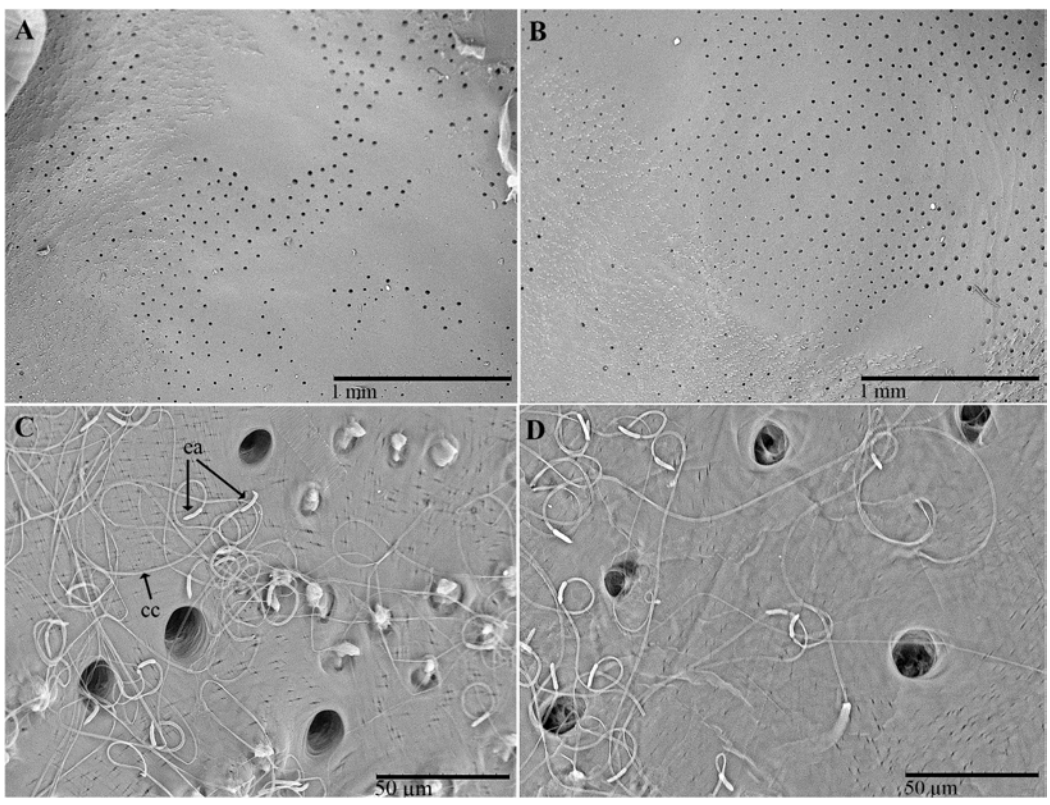

FIGURE 3 | Scanning electron micrographs of *C. tenebrionis*: glandular openings on the inner surface of the female **(A,C)** and male pronota **(B,D)**, washed according to Porcelli and Di Palma (2001). ea, end apparatus; cc, conducting canal.

Differences were observed among the specimens due to the cleaning procedure used. Short filaments (**Figure 2C**) of different thicknesses were detected protruding from the treated pores, according to Sands (1984). No filaments or filament residues were observed on the treated pronota, according to Porcelli and Di Palma (2001) (**Figure 2B**). Many smallish pores randomly scattered in varying densities on smooth and rough fields, often on the rims of pits, were also detected (**Figure 2D**). These pores consisted of a circular hole, ranging from 1 to 5 μm in diameter, with a slight border (**Figure 2B**).

Several groups of pores (from 10 to 20 μm in diameter) were observed on the inner surface of the pronotum (**Figures 3A–D**). The overall distribution of these grouped pores appeared to correspond roughly to the distribution of the pore pits of the rough fields on the outer surface. An abundance of filamentous cuticular gland structures was connected to each of these pores and covered the inner surface of the cuticle (**Figures 3C,D**). The structures were 150–200 μm long and uniform in diameter. The far end of the structure (measured from the pore pit, or the receiving canal) was thicker and spindle-shaped than the filament (also known as the conducting canal) that entered the pore.

No particular differences were detected between the outer and inner surfaces of the pronota belonging to males and those belonging to females.

The size and shape of the antennae in males and females are very similar. No relevant morphometric differences between genders were detected. The antennae are serrate-truncate, composed of 11 articles, long 4.7 ± 0.7 (SD) mm in males ($n = 3$), and 4.6 ± 0.8 mm ($n = 3$) in females (**Figure 4**). The cross-section is almost rounded for articles I–IV, whereas it appears triangular for articles V–IX. The scape is subglobose and larger than the other articles (591.7 ± 35.1 μm in females and 566.7 ± 52.5 μm in males). The pedicel is subcylindrical, short and stocky, and seems to be longer in females (259.3 ± 20.6 μm) than in males (218.7 ± 26.1 μm). Both articles III and IV have the shape of a barrel, whereas articles V–XI are wedge-shaped.

Male and female antennae are provided with three types of sensilla: chaetic, basiconic, and coeloconic (Altner and Prillinger, 1980; Zacharuk, 1980). The chaetic sensilla are present along the whole antenna and vary in length (38–109 μm). They are similarly distributed between males and females, are more or less evenly distributed on articles I–IV and are concentrated on the dorsal and subdorsal sides of the more distal articles (**Figure 5A**). The number of chaetic sensilla decreased from articles VI to XI. These sensilla have an apparently rigid shaft that sinks into a socket; there is no rim. This shaft usually shows longitudinal grooves with no evidence of pores, a type of external morphology that is inferred to have a mechanoreceptive function.

Three subtypes of chaetic sensilla can be distinguished on the base of the shaft (**Figures 5B,C,E**); each is inserted into an individual socket that is without a rim. Chaetic sensillum subtype I has a shaft flattened in cross-section, lightly marked with longitudinal grooves and ends with a sharp tip. These sensilla seem to be more numerous than the other subtypes (**Figure 5B**) and are clearly discernible on the scape and pedicel. Chaetic sensillum subtype II has an apparently smooth shaft surface, a relatively sharp tip and a geniculate shaft, bent just above its insertion on the antennal cuticle (**Figure 5C**). These sensilla are found on the subdorsal side of the antenna. Chaetic sensillum

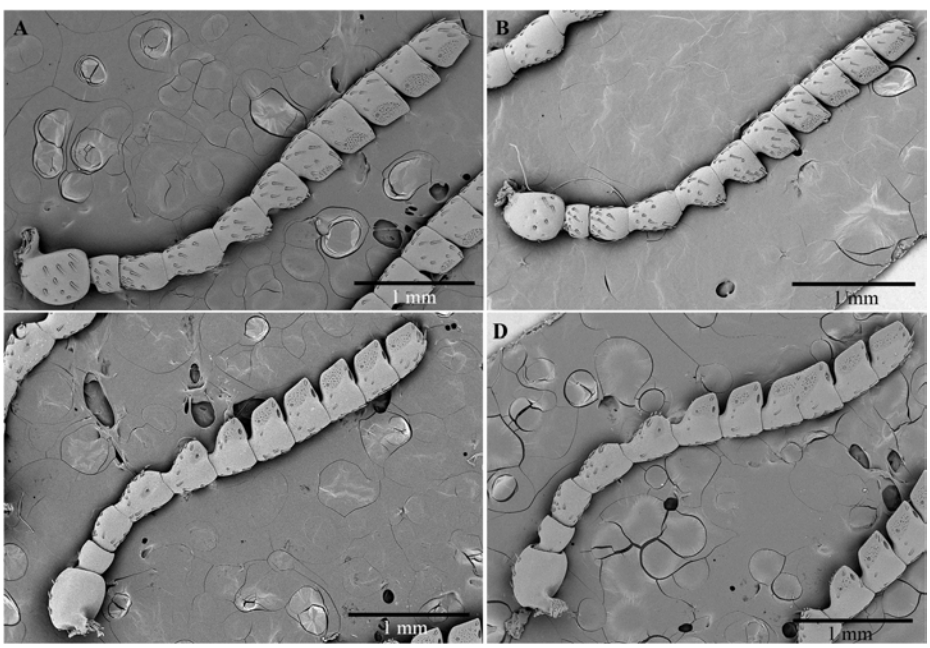

FIGURE 4 | Scanning electron micrographs of antennae of *C. tenebrionis*: general view of the antiaxial side of a female **(A)** and a male **(B)**; paraxial side of a female **(C)** and a male **(D)**.

subtype III has a shaft thicker than subtype I, with a furrowed surface and a rounded tip (**Figure 5D**).

The basiconic sensilla are peg-shaped with a short shaft (<10 μm long), tapering to a blunt tip (**Figures 5D,F**). Each has longitudinal grooves and is recessed into its own rimless socket. Basiconic sensilla of subtype III, which were observed on the scape, are short and have a smooth surface (**Figure 5C**). Basiconic sensilla of subtype II, which arise from an "eyelid"-shaped socket, have a grooved surface and a blunt tip with distal and subdistal depressions resembling pores (**Figures 5D**, **6A,C**). The number of these sensilla increases from article V to X on the ventral and subdistal sides. Males seem to have more basiconic sensilla than do females. The abundant presence of matrices near and at the base of these sensilla suggests that they are involved in the rubbing action of the antennae on the beetle's surfaces (like that made by the males on the pronotum of the females during mating) and on other surfaces. The abundance of these sensilla on male antennae implies that short-range contact cues can be significantly perceived for mate recognition. Their role in host location and recognition has to be considered, given the fact that females possess basiconic sensilla in the same position even though they have fewer of them.

The coeloconic sensilla – short, smooth-sided pegs with no distinct sockets at their base – are found in recessed cuticular pits located on the distal surface of articles (**Figures 6A,B**). The distribution of coeloconic sensilla is similar in both sexes. The number of pits on an antenna and for the same gender varies. Each sensorial pit can contain from 1 to 98 short sensilla. The number of these pits increases from articles VI to X and decreases on XI. On the paraxial side, the pits are more numerous in females than in males. A few pits (1–3) are also visible on the distal side (i.e., the side of an article opposing the side of the more distal subsequent article) of each articles IV–XI and increase their size until they reach article X. The porous walls of coeloconic sensilla (**Figures 6D,E**) suggest an olfactory chemoreceptive role.

SEM Examination of the Pronotal Resin Copy

The resin applied on the pronotum of each beetle produced a "negative" copy of the pronotum surface (**Figures 1**, **7A**)

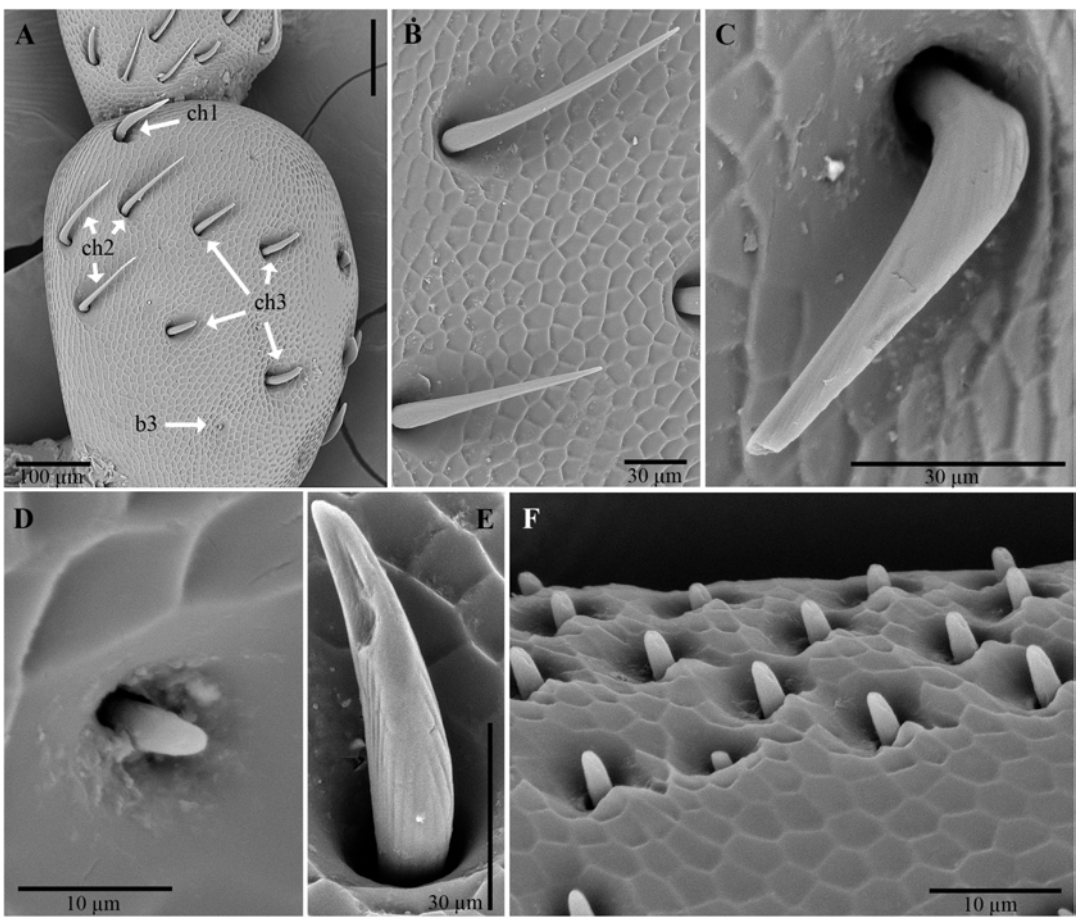

FIGURE 5 | Scanning electron micrographs of antennae of *C. tenebrionis*: antiaxial view of the scape of a male **(A)**; chaetic sensilla subtype I **(B)**, subtype II **(C)** and III **(E)**, and a basiconic sensillum subtype III **(D)** on the antiaxial side of a scape of a female; basiconic sensillum subtype II **(F)** on the antiaxial side of the article IX of a female. b3, basiconic sensillum subtype III; ch1, chaetic sensillum subtype I; ch2, chaetic sensillum subtype II; ch3, chaetic sensillum subtype III.

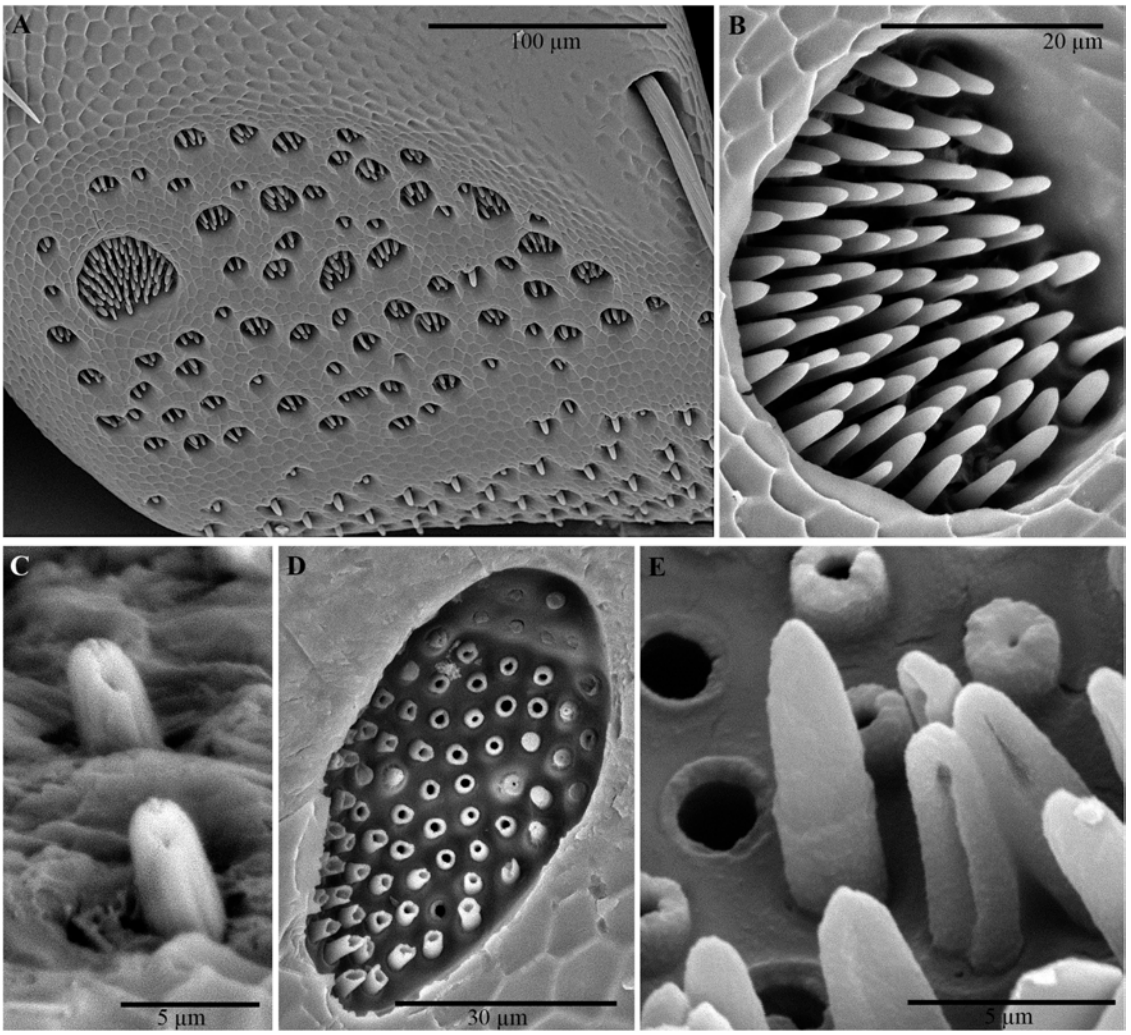

FIGURE 6 | Scanning electron micrographs of antennae of *C. tenebrionis*: antiaxial view of article IX of a female showing several sensorial pits with coeloconic sensilla on the upper side and basiconic sensilla subtype II on the lower side **(A)**; detail of the coeloconic sensilla into a large pit **(B)**; basiconic sensilla subtype II on the antiaxial side of the article VII of a male **(C)**; cross dissected coeloconic sensilla in a sensorial pit on the paraxial side of the article IX of a female **(D)**; detail of dissected coeloconic sensilla on the antiaxial side of the article XI of a male **(E)**.

and removed part of the white powder secreted on that surface (**Figures 7B,D**). On this copy, the rough fields assumed the shape of circular craters with electron-dense borders (**Figures 7B,C**). They delimited groups of electron-dense filaments (**Figures 7B,C**) containing a high percentage of carbon (**Figure 7D**). A sparse, random distribution of small electron-lucent spots was also observed all around the copy on both rough and smooth fields (**Figure 7B**). These spots may correspond to the simple pores sparsely distributed on the outer surface of the pronotum. According to the energy-dispersive spectra, the highest percentage of carbon (C) was detected on the electron-dense areas of the copy corresponding to the rough fields (82.3% vs. 39.5%), while the percentage of all other elements [barium (Ba), aluminum (Al), silicon (Si), carbon and oxygen (O), constitutive compounds of the resin] was the highest on the areas corresponding to the smooth fields of the pronotum (figure not shown).

Pre-mating and Mating Behavior

Males adopted the following behavioral sequence (**Figures 8A–D**) when successfully mated with females whose pronota were not coated with resin:

(1) The male oriented himself toward (turned toward) the female, usually moving via the shortest path toward her, but never proceeding on the line she had previously followed;
(2) The male stopped walking (its movement was arrested). At this time, the male became motionless unless the female began to move, in which case, the male suddenly sped up and quickly reached the female;
(3) The male aligned his body with the female's;

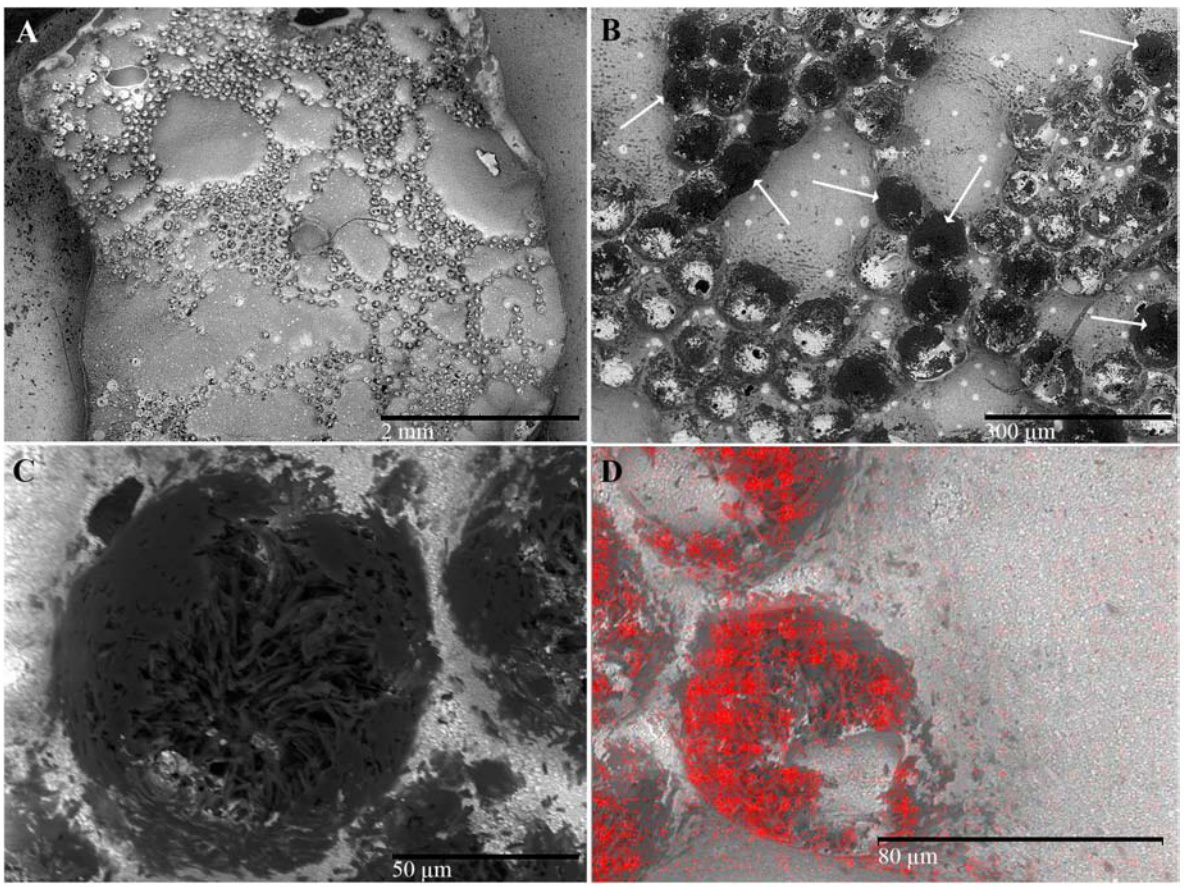

FIGURE 7 | Scanning electron micrographs of *C. tenebrionis*: general view of the resin copy **(A)**, detail of a group of glandular openings **(B)**, and a single opening **(C)** in which bundles of filaments are clearly visible; **(D)** evidence from an energy-dispersive spectrometer showing that the resin surface of a circular area corresponds to the gland opening (carbon detection is red in color). Circular areas (shown by arrows), more or less electron dense, refer to the porous surface of the pronotum.

(4) The male mounted the female from her posterior end, touching the cuticle of her dorsal side with his antennae as he moved up her body;
(5) Once the male had reached the pronotum, with his antennae, he extruded the aedeagus and moved his antennae rapidly from side to side across the female's pronotum;
(6) He inserted the aedeagus into the female's genital opening. The male rested his antennae on the pronotum of the female and on the first and second pair of legs on the elytrae, while the third pair of legs was usually placed on the substrate. For most of the time, both individuals remained motionless during copulation. If the female attempted to move, the male started shaking his body and moving his antennae quickly;
(7) If the female began to wiggle, the male quickly beat her pronotum with his antennae. When mating ended, the female started to move away while the male dismounted from her dorsum.

Among all the assayed coupling combinations, 76.0% of the assayed females (19 out of 25) and 86.4% of the assayed males (19 out of 22) were able to mate successfully at least once, and four males mated twice during the brief experimental period. All mated males displayed the above-described sequence. Unmated males performed steps 1 to 5, stopping their pre-mating activity when they touched the females' pronota. Additionally, mating was assayed from 10 a.m. till 5 p.m. on subsequent days within 2 weeks; no difference was observed in the behavior and success of the individuals during that period of time.

Copulation lasted from 0:52 to 13:26 min, averaging about 5:28 ± 3:05 (SD) min. This duration seemed to be unaffected by the size of the individuals. There was no correlation among mating duration, male and female body size (rduration/male = −0.03; rduration/female = 0.36; rmale/female = 0.22, $n = 19$, $p < 0.05$).

Females with half of their pronota coated by resin were still attractive and all assayed males performed steps 1 to 6 (the experiment was stopped at step 6). This assay confirmed that the resin did not interfere with mate receptivity and validated the procedure. Males performed steps 1 to 4 when paired with a female whose pronotum was entirely coated by resin. In this case, instead of proceeding to step 5, males left the females. When they returned, they performed again only steps 1 to 4. In this

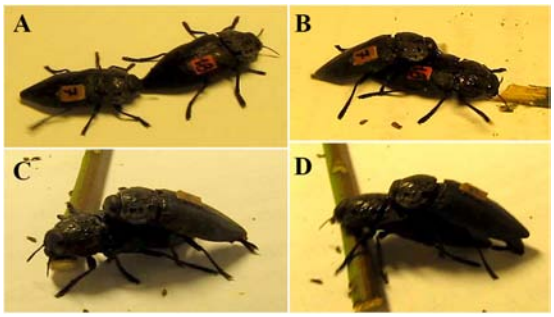

FIGURE 8 | Mating behavioral sequence of *C. tenebrionis*: male oriented toward the female, stopped walking and aligned his body with the female's – steps 1, 2, and 3 **(A)**, male mounted female – step 4 **(B)**, male touched female pronotum and extruded the aedeagus and started the coupling – steps 5 and 6 **(C,D)**.

condition, males were not able to copulate with females. Finally, after the resin was removed, females paired with the same males as they had previously and seemed to be still sexually attractive as determined by the performance of all steps (1–7).

Chemical Analysis of Pronotum Secretions and Whole Beetle Bodies

Hexane extracts from resin copies of the female and male pronota contained saturated, unsaturated and branched hydrocarbons in chain lengths ranging from C_8 to C_{36}. In the 2014 assay of the pronotum resin in copies of sexually mature specimens, the chromatograms showed very few qualitative differences between the genders: C_{13} and C_{25} (**Table 1**) were extracted only from females. With regard to the 2015 assay, GC/MS analysis of the cuticular pronotum extracts identified more peaks in attractive females and attracted males than in virgin and mated adults. In particular, methyl-nonacosane (MeC_{29}) and tetratriacontane (C_{34}) (**Table 1**) were not discovered in virgin and mated males. Interestingly, these hydrocarbons were found only in the female cuticular profile. More consistent differences were found in the hydrocarbon profiles of extracts from the whole bodies of male and female virgin adults. The highest peaks for females corresponded to C_{23} (peak 3), C_{27} (peak 22), MeC_{29} (peak 34), and C_{34} (peak 44) (**Figure 9** and **Table 2**).

Constitutive Volatile Profile of *Prunus armeniaca* Leaves

The applied dynamic headspace sampling, combined with TD-GC-MS analysis, allowed to directly collect and identify a total of 33 volatiles from the emission of intact leaves of *P. armeniaca* (**Table 3**). The detected profile includes a wide range of acids, alcohols, aldehydes, esters, ketones, and terpenes. Although many fruit trees of the Rosaceae family are considered low terpene emitters (Rapparini et al., 2001; Staudt et al., 2010), in the leaf emission profile of *P. armeniaca*, we identified several compounds which belong to this chemical class: C_{10}-monoterpene (E)-β-ocimene, C_{16}-homoterpene (*E*)-4,8-dimethyl-1,3,7-nonatriene (DMNT) and C_{15}-sesquiterpene (*E,E*)-α-farnesene. Traces of other monoterpenes, i.e., β-myrcene and linalool, were also detected. Another class of volatiles emitted by apricot leaves comprises benzenoids (e.g., benzoic acid, benzyl alcohol, benzaldehyde, benzothiazole), which are derived from the aromatic amino acid phenyl alanine. The identified alkanes and organic acids are typical constituents of leaf epicuticular waxes. The profile of emitted volatiles from apricot leaves shows the emission of the phenylpropene methyl eugenol and of the terpenoid cleavage product geranyl acetone.

Olfactometer Assays With Plant VOCs

Responses were usually distinct between adults according to gender. The females were attracted most by (Z)-3-hexen-1-ol and 3-methyl-butanol, whereas the males were attracted most by 3-methyl-butanol and 1-pentanol (**Table 4**). Benzaldehyde and 2-hexanone for the females, and s-limonene, (Z)-3-hexen-1-ol and 2-hexanone for the males appeared to act as repellents (**Table 4**).

Identification of Candidate Chemosensory Genes

Sequencing and *de novo* assembly of the transcriptomes derived from the antennae and whole bodies of *C. tenebrionis* adult males and females led to the identification of 51,394 nucleotide sequences (contigs). These contigs, each of which encodes for a putative protein characterized by a specific function, were functionally annotated using the Blast2GO software[3]. Our

[3]www.blast2go.com

TABLE 1 | Peaks produced by the hexane extracts of resin copies obtained by the pronota of sexually mature male and female pronota in 2014, and by the pronota of attracted males and attractive females in 2015.

	♀ Sexually mature	♂ Sexually mature	♀ Attractive	♂ Attracted
C_8	+	+	−	−
C_{10}	+	+	−	−
C_{13}	+	−	−	−
C_{14}	−	−	+	−
C_{15}	−	−	+	−
Cyclohexene	−	−	+	+
C_{22}	−	−	+	−
C_{24}	+	+	+	−
C_{25}	+	−	−	−
C_{26}	+	+	−	+
C_{28}	+	+	−	−
MeC_{24}	−	−	−	+
MeC_{25}	−	−	−	+
C_{30}	+	+	−	−
C_{31}	+	+	−	−
MeC_{29}	−	−	+	−
C_{32}	−	−	−	+
C_{34}	−	−	+	−
C_{35}	−	−	−	+
C_{36}	−	−	+	+

+ and − indicate, respectively, presence or absence of compounds.

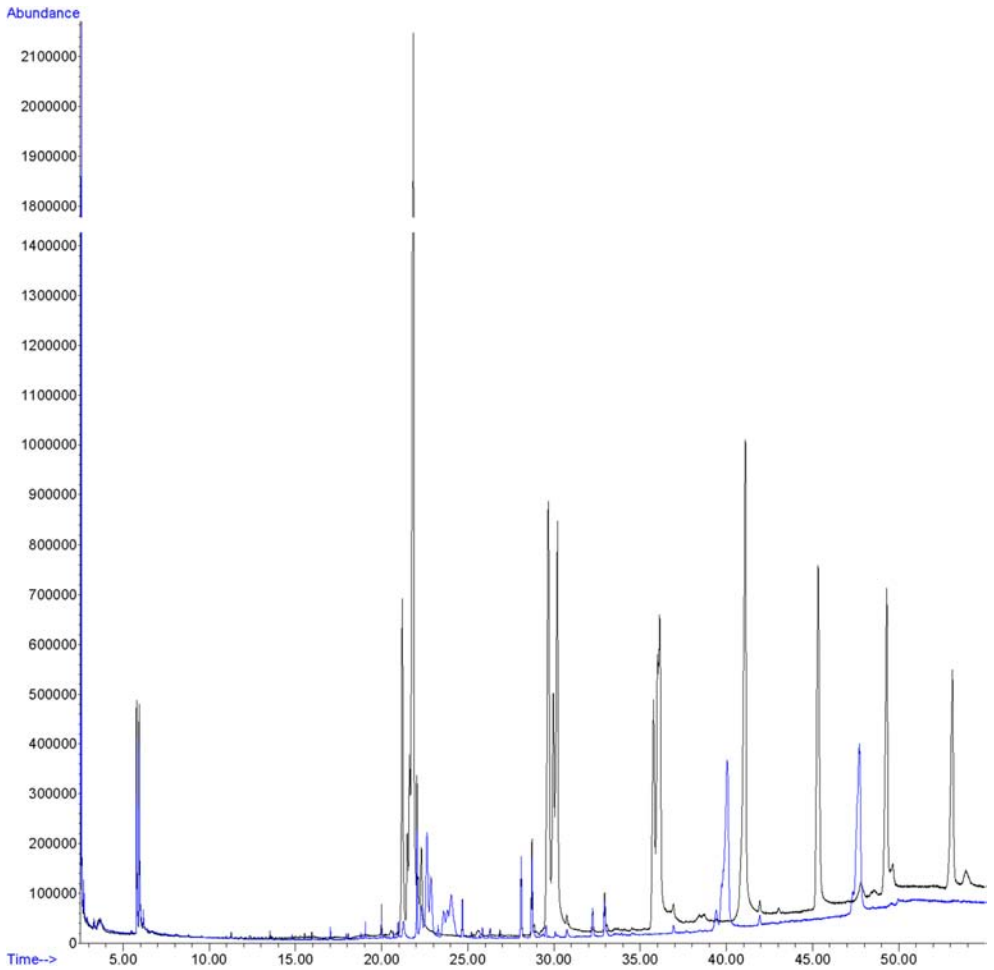

FIGURE 9 | GC profile of cuticular extracts from the whole bodies of virgin females (black line) and virgin males (blue line) of *C. tenebrionis*.

analysis allowed the identification of 14 putative OBPs and 11 putative CSPs (**Table 5**). The alignment of the 14 identified *C. tenebrionis* OBPs and the 11 identified *C. tenebrionis* CSPs is shown in **Supplementary Material S1**. Furthermore, analysis of the identified putative OBP and CSP genes using the RPKM method, allowed for the evaluation of expression level differences between adult males and females (measured in antennae and whole bodies) (**Figure 10**).

Our results showed that 13 out of the 14 identified putative OBPs and all the 11 identified putative CSPs displayed highest expression levels in the antennae of *C. tenebrionis* males and females.

DISCUSSION

The examination of *C. tenebrionis* using light and SEMicroscopy revealed pores on the inner and outer surfaces of the pronotum of both genders. The pore arrangement was not perfectly symmetrical and porous fields were larger in males than in females when the surfaces of whole pronotum were compared. No further differences were found between the genders. Whether other jewel beetles share the unexpectedly large porous fields found on the pronota of male *C. tenebrionis* is unknown. Gland pores were previously detected on pronota of other male Coleoptera, including many long-horned beetles, and in some species were related to sex or aggregation pheromone secretions (Noldt et al., 1995; Ray et al., 2006; Hanks et al., 2007; Lacey et al., 2007; Hanks and Millar, 2016). Behavioral assays on *C. tenebrionis* did not point to the secretion of aggregation cues by males or females (Bari et al., 2004; Sharon et al., 2010), which is confirmed by field observations (Bonsignore and Jones, 2013). On the contrary, pre-mating and mating behavior assigns a relevant role to females' pronota of this species. Males were unable to recognize the sexual suitability of females with pronota that had been entirely coated even though they did find and mount the females. These data suggest that males need confirmation of the readiness of a female to mate. Cuticular hydrocarbons or other cues have to be secreted on the pronota of sexually mature females of *C. tenebrionis*. These cues can be perceived by the contact chemosensilla of the male antennae during the mate recognition process as was

shown for *A. planipennis,* although the location of secretory gland openings are currently unknown (Silk et al., 2009; Silk and Ryall, 2015). Perhaps the volatile cues involved in male attraction and orientation are perceived even when the female's pronotum is coated. Moreover, males may exploit other means (e.g., in our experimental model, visual) to find females and plant-emitted compounds may also be involved (Sharon et al., 2010; Bonsignore and Jones, 2013) as has been observed for *A. planipennis* (Silk and Ryall, 2015).

The SEM study identified chaetic, basiconic and coeloconic sensilla on the antennae. The morphology of *C. tenebrionis* antennae is in agreement with Volkovitsh (2001). Sensorial pits containing coeloconic sensilla increase in number according to the article's distance from the antennal base. Basiconic

TABLE 2 | Peaks produced by the hexane extracts from the whole bodies of virgin males and females of *C. tenebrionis*.

Peak number	Retention time	Compound	Wholebody ♀	Wholebody ♂
1	20.07	C_{21}	+	–
2	21.00	C_{22}	+	–
3	22.04	C_{23}	+	–
4	22.93	3 MeC_{23}	+	–
5	23.15	5,9-dimethyl C_{23}	+	–
6	23.29	C_{24}	–	–
7	23.39	3,7+3,9 dimethyl C_{23}	–	–
8	23.80	$6MeC_{24}$	–	–
9	24.05	$4MeC_{24}$	+	–
10	24.43	$2MeC_{34}$	–	–
11	24.68	C_{25}	+	+
12	25.19	$7MeC_{25}$	–	–
13	25.53	$5MeC_{25}$	+	–
14	25.84	$3MeC_{25}$	+	+
15	26.00	5,9 dimethyl C_{25}	+	–
16	26.29	C_{26}	+	+
17	26.42	3,7+3,9 MeC_{26}	+	–
18	26.85	10+12 MeC_{26}	+	–
19	27.10	6 MeC_{26}	+	–
20	27.31	4 MeC_{26}	+	–
21	27.58	2 MeC_{26}	+	–
22	28.11	C_{27}	+	+
23	28.71	11+13 MeC_{27}	+	–
24	28.93	7 MeC_{27}	+	–
25	29.11	5 MeC_{27}	+	–
26	29.40	11,13 MeC_{27}	+	–
27	29.53	3 MeC_{27}	+	+
28	30.07	C_{28}	+	+
29	30.19	3,7 dimethyl C_{27}	+	–
30	30.68	12+14 7 MeC_{28}	+	–
31	31.06	6 MeC_{28}	+	–
32	31.27	4 MeC_{28}	+	–
33	31.70	2 MeC_{28}	+	–
34	32.29	C_{29}	+	+
35	32.93	7 MeC_{29}	+	+
36	33.57	11,15 6 MeC_{29}	+	–
37	33.92	3 MeC_{29}	+	+
38	34.59	C_{30}	+	–
39	34.71	3,11 dimethyl C_{30}	+	–
40	35.74	C_{31-ene}	+	–
41	36.96	C_{31}	+	+
42	37.66	13 MeC_{31}	+	+
43	41.94	C_{33}	+	+
44	45.08	C_{34}	+	–
45	47.70	11,15 dimethyl C_{35}	+	+
46	48.50	MeC_{35}	+	+
47	49.65	12+14+16 MeC_{36}	+	–
48	53.10	12,22 dimethyl C_{36}	+	+

+/– indicates the presence or absence of the relative compound in extracts of male and female bodies.

TABLE 3 | Volatile compounds identified from leaves of *P. armeniaca* based on TD-GC-MS measurements.

Compounds	RT	Formula
Acids		
Acetic acid	9.09	$C_2H_4O_2$
Hexanoic acid	29.45	$C_6H_{14}O_2$
Octanoic acid	41.46	$C_8H_{16}O_2$
Nonanoic acid	46.54	$C_9H_{18}O_2$
Decanoic acid	50.11	$C_{10}H_{20}O_2$
Alcohols		
1-Butanol	10.16	$C_4H_{10}O$
2-Butoxy ethanol	23.41	$C_6H_{14}O_2$
2-Ethyl 1-hexanol	31.81	$C_8H_{18}O$
Alkanes		
Decane	30.36	$C_{10}H_{22}$
Undecane	37.08	$C_{11}H_{24}$
Aliphatic aldehydes		
Octanal	29.32	$C_8H_{16}O$
Nonanal	36.22	$C_9H_{18}O$
Decanal	42.24	$C_{10}H_{20}O$
Ketones		
Cyclohexanone	21.38	$C_6H_{10}O$
2-Heptanone	21.77	$C_7H_{14}O$
6-Methyl-5-hepten-2-one	23.20	$C_8H_{14}O$
Esters		
3-Ethoxy ethyl propanoate	28.45	$C_7H_{14}O_3$
(*Z*)-3-Hexenyl acetate	29.93	$C_8H_{14}O_2$
2-Butoxy ethyl acetate	35.33	$C_8H_{16}O_3$
Benzenoids		
Benzaldehyde	25.75	C_7H_6O
Benzyl alcohol	31.26	C_7H_8O
Methyl salicylate	41.47	$C_8H_8O_3$
Benzothiazole	42.71	C_7H_5NS
Terpenes		
β-Myrcene	26.40	$C_{10}H_{16}$
(*E*)-β-Ocimene	33.05	$C_{10}H_{16}$
Linalool	36.33	$C_{10}H_{18}O$
(*E*)-4,8-Dimethyl-1,3,7-nonatriene (DMNT)	37.90	$C_{11}H_{18}$
(*E,E*)-α-farnesene	54.70	$C_{15}H_{24}$
Others		
Cyclohexane isothiocyanate	42.38	$C_7H_{11}NS$
Methyl eugenol	50.68	$C_{11}H_{14}O_2$
Geranyl acetone	52.60	$C_{11}H_{18}O_2$

sensilla placed on the ventral margin of the antennae possess the morphological characteristics of contact chemosensilla that could be involved in testing substances on touched surfaces. Sensorial pits (also referred to as "fossae" by Volkovitsh, 2001) containing fields of coeloconic sensilla are common among buprestid species and have been used to develop the systematics of the taxon (Volkovitsh, 2001). In the numerous examples shown by Volkovitsh (2001), uniporous sensilla and several types of basiconic sensilla dominate.

The pre-copulatory behavior observed in the current study and adopted by males for finding females in a small mating arena, and the potential presence of a pheromone (Bari et al., 2004) may imply the involvement of a short-distance cue. This hypothesis is supported by studies that suggest males of *A. planipennis* were able to find females at short distance (≤5 cm) through a short-range volatile pheromone (Pureswaran and Poland, 2009; Silk and Ryall, 2015). It is worth noting that *C. tenebrionis* adults tend to aggregate especially when exposed directly to sunlight (Bonsignore et al., 2008; Bonsignore and Jones, 2013). This exposure and the black color of the body can increase body temperature (Garzone et al., unpublished observations) and stimulate the evaporation of less volatile chemicals secreted by the beetle. Both factors might contribute to the aggregation tendency, and the way mates are found and sexual maturity perceived at a short distance.

The biologically inert resin was used for the current bioassays and did not cause any repellence or interference with the beetle behavior. The fluid resin was applied to a body part (pronotum, in our case) and, after hardening, easily removed. It detached compounds from the surfaces of the insects without harming or killing them. Compounds detached by the resin were organic compounds, according to the EDS analysis, and likely came from glandular secretions and the outermost cuticular layers. Previous analytical studies have been performed on solid-phase microextraction fibers (SPMEs) and solvent extraction of parts or whole body of beetles belonging to Buprestidae and few other taxa (Fukaya, 2003; Ginzel et al., 2006; Lelito et al., 2009; Silk et al., 2009; González-Núñez et al., 2012; Yew and Chung, 2015; Yang et al., 2017; etc.). Hydrocarbons are the major components of the cuticular coating of adult insects (Lockey, 1991), even though a wide range of more polar lipids have also been found and shown to have attractive properties (Yew and Chung, 2015; Hanks and Millar, 2016). The cuticular organic compounds sampled from the pronotum resin copies of attracted males and attractive females, and among the extracts of the whole bodies of virgin males and females of *C. tenebrionis*, appeared to differ qualitatively. These differences could support the assumption that the pronota of attractive females can emit cues that play specific roles in pre-mating and require further investigations in comparing sexually immature and mature females. These differences partially support the results of Cui et al. (2018); they found many more expressed OBPs in male antennae of *Agrilus mali* Matsumura than in female ones and these OBPs showed strong binding affinity to C_{2-15} compounds. In the current study, C_{13} and C_{14-15} were found only in the solvent extracts of the pronotum resin copies of sexually mature females and of attractive females, respectively. Current data are not in accordance with González-Núñez et al. (2012), who did not discover qualitative differences between males and females of *C. tenebrionis* in the levels of more than 40 cuticular hydrocarbons extracted by solvent from the whole body of both genders. The cuticular extracts did not elicit any male behavior at the time of mating, leading to the assumption that there is no contact pheromone in *C. tenebrionis*. Our finding – that methyl-nonacosane and tetratriacontane peaks only in the pronotum resin copies of females attracting males of *C. tenebrionis* – is in agreement with that of Lelito et al. (2009). They found 3-methyl-tricosane in limited quantities on the cuticle of young females of *A. planipennis,* and the levels of this chemical increased with the beetle's age and achievement of sexual maturity. Mfarrej and Sharaf (2011) recognized three aliphatic hydrocarbons produced by adults of *Capnodis carbonaria* (Klug.): hexacosane was found in the male cuticle, *n*-heptacosane in the female body and nonacosane in the male hindgut. The female body extract *n*-heptacosane was the most active hydrocarbon used to trap *C. carbonaria* adults. In the current research, hexacosane, heptacosane, and nonacosane were extracted from the bodies of both genders (peaks 16, 22, 34, **Table 2**) and their biological activity needs to be investigated. Finally, 9-methyl-pentacosane was found to be the main component of the contact pheromone in *A. planipennis* (Silk and Ryall, 2015).

Unlike males, females of *C. tenebrionis* respond highly positively in a preliminary olfactometer assay to (Z)-3-hexen-1-ol, suggesting the compound is involved in host finding. A high electron-antennographic response was previously shown for this green leaf volatile in *C. tenebrionis* (Bari et al., 2004). The current data on behavioral differences between males and females appear to contradict earlier data showing more virgin males than virgin females in oaks infested by *A. biguttatus* (F.) (Silk and Ryall, 2015; Vuts et al., 2016), but the numbers are in accordance with the data on *Coroebus florentinus* Herbst. (Furstenau et al., 2012) and *A. planipennis* infesting cork oak (Silk and Ryall, 2015).

Analysis of the volatile emission profile of healthy apricot plants increases the pool of chemicals to be assayed under olfactometer and electron-antennography in order to evaluate their influence on the behavior of adult *C. tenebrionis*. Although most of *Prunus* species are considered low VOC emitters (Baraldi et al., 1999; Rapparini et al., 2001; Karlik et al., 2002; Staudt

TABLE 4 | Response index of females (F, *n* = 15) and males (M, *n* = 15) of *C. tenebrionis* to some VOCs.

VOCs	*C. tenebrionis*	
	Male	**Female**
(Z)-3-Hexen-1-ol	−13.33	46.67
1-Pentanol	6.67	−13.33
Benzaldehyde	0	−33.33
3-Methyl-butanol	26.67	26.67
β-Myrcene	−6.67	−6.67
2-Hexanone	−13.33	−26.67
s-Limonene	−40.00	−13.33

et al., 2010), some of the constitutive volatiles released at leaf level may play a key functional role for long-lived adults of *C. tenebrionis* in host locations. If the host foliage of fruit trees may be an important point of this plant-insect interaction, leaf volatiles are used as olfactory cues by several buprestid species belonging to the *Agrilus* genus to locate feeding and mating sites in natural forests (Koch et al., 2015; Vuts et al., 2016, and references therein). The current data represent a basic profile of healthy plants and requires to be compared with that of plants stressed by biotic and abiotic factors which can favor the emission of more attractive VOCs for the beetle.

Recent findings on the relationship between buprestid beetles and trees showed that the apple buprestid *A. mali* use multiple OBPs to discriminate among compounds belonging to different chemical families, showing high affinity for alcohols, esters and terpenes (Cui et al., 2018). Among terpenes, the observed leaf emissions of (*E*)-β-ocimene, (*E*)-4,8-dimethyl-1,3,7-nonatriene (DMNT) and (E,E)-α-farnesene from apricot leaves may serve as relevant signals for the buprestid *Capnodis*. These compounds have been found to be the principal volatiles in the constitutive emissions from leaf-bearing shoots of different *Prunus* genotypes (Staudt et al., 2010) and other Rosaceae (Reidel et al., 2017; Yang et al., 2018), including fruit species frequently attacked by *C. tenebrionis*. These volatiles are commonly induced by herbivory in different trees, including rosaceous fruit species (Staudt et al., 2010; Giacomuzzi et al., 2016, 2017; Copolovici et al., 2017). The volatiles (*E*)-β-ocimene and DMNT, identified in leaf emissions of *Quercus robur*, showed positive electroantennography (EAG) responses in adult buprestid *A. biguttatus* (Vuts et al., 2016). In another fruit tree-insect relationship, DMNT and the monoterpene linalool have been found to elicit a high EAD response from adult females of a common apple moth (Lepidoptera: Totricidae). These two terpenes are often considered key volatiles in herbivore deterrence (Borrero-Echeverry et al., 2015).

Volatile benzenoids, which are qualitatively abundant in the emission profile of the analyzed, healthy apricot plants, play important roles in plant communication with the environment (Dudareva et al., 2013). Among them, benzaldehyde is considered a breakdown product of prunasin, a cyanogenic glycoside commonly found in *Prunus* species and other Rosaceae (Santamour, 1998). This aromatic aldehyde represents a key compound in plant–insect interactions of several fruit tree species of Rosaceae (Staudt et al., 2010; Najar-Rodriguez et al., 2013; Lu et al., 2015), but its attraction was not confirmed in the current olfactometer assay.

Interestingly, the release of methyl eugenol and geranyl acetone from intact apricot foliage was never previously detected in the leaf emission of other *Prunus* species. Geranyl acetone is a carotenoid-derived compound that in stone-fruit species has been previously detected only in the volatile emissions of fruits and flowers of *P. cerasifera* (Reidel et al., 2017). Unique

TABLE 5 | List of the identified odorant-binding proteins (OBPs) in *C. tenebrionis* adult males and females and list of the identified chemosensory proteins (CSPs) in *C. tenebrionis* adult males and females.

Unigene reference	Gene name	ORF (bp)	BLASTx annotation	*E*-value	AA identity (%)
Capnodis_C409	*CtenOBP1*	411	Odorant-binding protein 10 (*Agrilus mali*)	3e-47	59
Capnodis_C789	*CtenOBP2*	681	PREDICTED: general odorant-binding protein 67-like (*Aedes albopictus*)	5e-07	28
Capnodis_C4812	*CtenOBP3*	450	General odorant-binding protein 19d (*Agrilus planipennis*)	1e-41	54
Capnodis_C7413	*CtenOBP4*	405	Uncharacterized protein LOC108739404 (*Agrilus planipennis*)	2e-49	68
Capnodis_C8196	*CtenOBP5*	393	General odorant-binding protein 83a isoform X2 (*Agrilus planipennis*)	4e-55	65
Capnodis_C8312	*CtenOBP6*	531	PREDICTED: general odorant-binding protein 70 isoform X1 (*Tribolium castaneum*)	8e-38	53
Capnodis_C12606	*CtenOBP7*	423	Odorant-binding protein 3 (*Agrilus mali*)	2e-45	60
Capnodis_C16094	*CtenOBP8*	453	General odorant-binding protein 19d (*Agrilus planipennis*)	2e-31	45
Capnodis_C17506	*CtenOBP9*	408	Odorant-binding protein (*Dendrolimus kikuchii*)	8e-11	35
Capnodis_C17816	*CtenOBP10*	642	OBP16 (*Holotrichia parallela*)	7e-11	26
Capnodis_C18027	*CtenOBP11*	411	PREDICTED: general odorant-binding protein 56d-like (*Habropoda laboriosa*)	7e-18	34
Capnodis_C21011	*CtenOBP12*	831	General odorant-binding protein 71 (*Agrilus planipennis*)	1e-29	45
Capnodis_C34461	*CtenOBP13*	189	Odorant-binding protein 3 (*Agrilus mali*)	6e-33	54
Capnodis_C43694	*CtenOBP14*	399	Odorant-binding protein 7 (*Agrilus mali*)	4e-12	32
Capnodis_C4	*CtenCSP1*	240	Ejaculatory bulb-specific protein 3 (*Agrilus planipennis*)	1e-39	73
Capnodis_C120	*CtenCSP2*	369	Chemosensory protein 2 (*Agrilus mali*)	4e-37	53
Capnodis_C856	*CtenCSP3*	393	Ejaculatory bulb-specific protein 3 (*Agrilus planipennis*)	5e-49	74
Capnodis_C857	*CtenCSP4*	393	Ejaculatory bulb-specific protein 3 (*Agrilus planipennis*)	9e-50	74
Capnodis_C2805	*CtenCSP5*	399	Chemosensory protein 1 (*Agrilus mali*)	8e-63	83
Capnodis_C6098	*CtenCSP6*	366	Ejaculatory bulb-specific protein 3-like isoform X1 (*Agrilus planipennis*)	8e-56	84
Capnodis_C6962	*CtenCSP7*	429	Ejaculatory bulb-specific protein 3-like (*Agrilus planipennis*)	3e-56	72
Capnodis_C7044	*CtenCSP8*	396	Chemosensory protein 4 (*Agrilus mali*)	2e-66	76
Capnodis_C7625	*CtenCSP9*	1005	Chemosensory protein 7, partial (*Agrilus mali*)	4e-68	81
Capnodis_C12217	*CtenCSP10*	330	Chemosensory protein 8 (*Agrilus mali*)	1e-53	92
Capnodis_C30511	*CtenCSP11*	303	Uncharacterized protein LOC108734435 (*Agrilus planipennis*)	5e-43	69

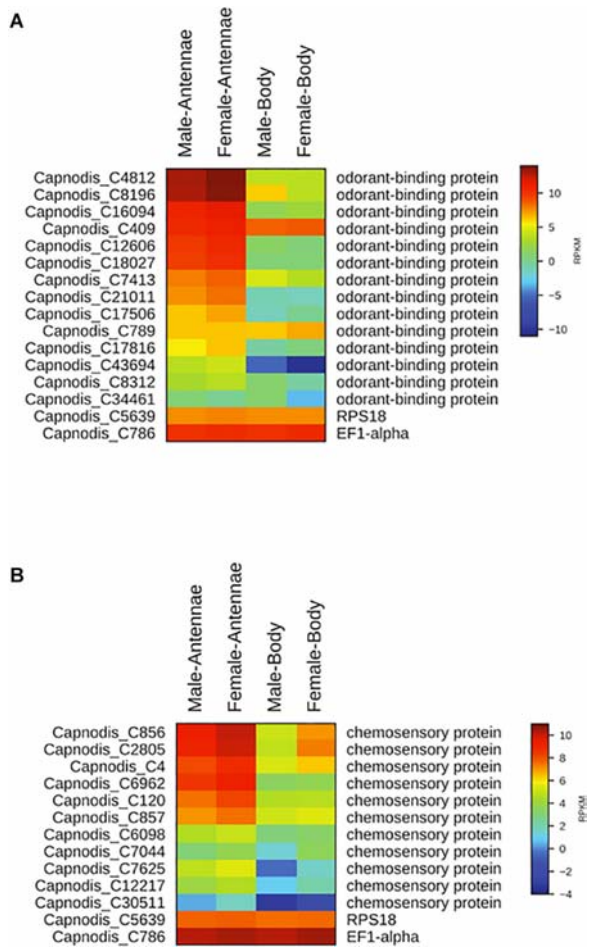

FIGURE 10 | Heat map showing differences in the expression of OBPs between *C. tenebrionis* adult males and females (measured in antennae and whole bodies) **(A)** and heat map showing differences in the expression of CSPs between *C. tenebrionis* adult males and females (measured in antennae and whole bodies) **(B)**. The housekeeping genes RPS18 and EF1-alpha are used for normalization and have been shown to confirm the uniform expression of these control genes across samples. The map is based on log_2-transformed RPKM values shown in the gradient heat map (blue represents weakly expressed genes, and red represents strongly expressed genes).

compounds may contribute to the chemical fingerprint of plant hosts and may play a key role in insect recognition of plant odors.

The identification of the C_6-ester (*Z*)-hexenyl acetate and nonanal from intact, healthy leaves of apricot plants confirms previous findings on leaf emissions from apricot (Yang et al., 2018) and other fruit tree species of Rosaceae (Najar-Rodriguez et al., 2013; Giacomuzzi et al., 2017; Reidel et al., 2017). Although this C_6-ester is frequently present when the corresponding alcohol (*Z*)-3-hexenol is emitted by plants, as both are products of the same lipoxygenase pathway (Dudareva et al., 2013), we did not detect this C_6-alcohol in the emissions of intact and healthy plants. Typically, C_5- and C_6-alcohols, together with related aldehydes, are produced and emitted after tissue damage (Dudareva et al., 2013). Recent findings on field-grown apricot plants showed induced emissions of (*Z*)-3-hexenol at leaf level in response to Coleoptera beetles (Scolytidae), which typically attack fruit trees of Rosaceae (Yang et al., 2018).

If the majority of the constitutive leaf volatiles identified in apricot is widespread in both pome- and stone-fruit trees of Rosaceae, leaf volatiles that are induced by both abiotic and biotic factors may be also relevant for the ability of *C. tenebrionis* to locate host trees. In a previous study, volatiles emitted from stressed nitrogen-rich peach plants enhanced the attractiveness of *C. tenebrionis* females (Sharon et al., 2010). Intraspecific variability in aphid-induced emissions rates of several VOCs, including (*E*)-β-ocimene, DMNT and (*E,E*)-β-farnesene, were associated with the resistance traits of different *Prunus* genotypes to aphid attack (Staudt et al., 2010). However, in another tree-insect system involving the buprestid *A. planipennis*, the lack of an association between insect resistance and intraspecific differences in leaf VOCs emission was shown (Koch et al., 2015). Whether the VOCs identified in our investigation confer direct or indirect protection to apricot trees against *C. tenebrionis* remains to be established.

The exact function of each olfactory gene family in Coleoptera is still not completely known, as few studies have yet been performed on the genes involved in olfaction in coleopterans (Engsontia et al., 2008; Mitchell et al., 2012; Andersson et al., 2013; Antony et al., 2016). Because many OBPs, CSPs and ORs isolated and characterized in moths, dipterans and hemipterans have been shown to have affinities to host plant volatile compounds or pheromones (He et al., 2011; Harada et al., 2012; Yin et al., 2012), the exact function of these proteins in coleopteran communication is starting to be studied. Mamidala et al. (2013) performed a complete studies on candidate genes involved in the perception, processing and degradation of volatiles in the invasive buprestid *A. planipennis*, identifying 9 OBPs, 2 ORs, 1 SNMP, 6 IRs, 6 ionotropic glutamate receptors (IGluRs), 2 GRs and 4 CSPs in the antennal transcriptome. The identified number of odorant genes provided insight into the olfactory processes of *A. planipennis* in detecting host- and mate-locating cues. Cui et al. (2018) cloned and characterized by binding assays two OBPs, both of which were identified in the antennal transcriptome of the apple buprestid beetle *A. mali*. In our study, 14 OBPs and 11 CSPs were identified in the antennae, the main organs involved in chemoreception in which soluble olfactory proteins are commonly highly expressed, and body transcriptome of adult males and females of the invasive buprestid *C. tenebrionis*. All the identified CtenOBPs were shown to share over 26% residues with OBPs from other coleopterans, although insect OBPs commonly share only 10–15% of their residues between species (Pelosi et al., 2017). The BLASTx results indicated that 4 CtenOBPs showed amino acid identities (32–60%) with *A. mali* OBPs. In particular, CtenOBP7 and CtenOBP13 shared 60% and 54% amino acid identity. respectively, with OBP3 of *A. mali* (AmalOBP3). AmalOBP3 was functionally characterized in competitive fluorescence-binding assays (Cui et al., 2018) and showed binding affinity toward both (Z)-3-hexenol and 3-methyl-1-butanol. In our work, (Z)-3-hexenol and 3-methyl-1-butanol attracted females and both adult genders of *C. tenebrionis*, respectively, in olfactometer

assays. In addition, both CtenOBP7 (Capnodis_C12606) and CtenOBP13 (Capnodis_C34461) were most highly expressed in antennae (**Figure 10**). The high amino acid sequence similarity between CtenOBP7, CtenOBP13 and AmalOBP3, as well as the binding affinity of AmalOBP3 with two molecules that we showed to be attractive for the insect and the high expression level of CtenOBP7 and CtenOBP13 provide the basis for our hypothesis that in *C. tenebrionis* these OBPs may be involved in the recognition of (Z)-3-hexenol and 3-methyl-1-butanol. Furthermore, the higher expression of CtenOBP7 and CtenOBP13 in antennae than in the whole body suggests that these OBPs may play important roles in the detection of general odorants such as the host plant volatiles as reported in other insect species (Landolt, 1997; Smyth and Hoffmann, 2003). Moreover, 5 of the 14 identified CtenOBPs shared high amino acid identities (45–68%) with *A. planipennis* OBPs at NCBI. Gas chromatography-electroantennogram detection bioassays demonstrated that *A. planipennis* antennae were highly responsive to (Z)-3-hexenol (de Groot et al., 2008). The high amino acid sequence similarity between the 5 CtenOBPs and *A. planipennis* OBPs suggests that these CtenOBPs may be involved in the detection of host plant volatiles. In order to determine the exact binding mechanisms between soluble olfactory proteins in *C. tenebrionis* and putative ligands, extensive studies with chemical ligands are needed since multiple OBPs and CSPs are often used in the mechanisms of insects' chemical perception (Hekmat-Scafe et al., 2002; Zhou, 2010). The biochemical characterization of CtenOBPs and CSPs will contribute to increasing our knowledge of the molecular mechanisms underlying the complex chemical communication system in this insect.

This study on the intraspecific and interspecific interactions in *C. tenebrionis* has summarized some aspects of the morphology of the insect's pronotum and antennae, on its pre-copulatory behavior and on beetle–plant communication; understanding the chemical ecology of this pest will be useful in the development of environmentally friendly management strategies for its control. The information collected to date seems to pair the chemical ecology of *C. tenebrionis* with that of *A. planipennis* (Silk and Ryall, 2015).

ETHICS STATEMENT

Insects used in this work were treated as well as possible given the constraints of the experimental design.

AUTHOR CONTRIBUTIONS

PF and AS contributed to the design and implementation of the research and analysis of the results on the identification of candidate chemosensory genes with support from SB and RS. EdL contributed to the design and implementation of the research, and to the analysis of the results on the morphology of antennae and pronotum, pre-mating and mating behavior, and olfactometer assays with support from GB, VG, PV, and CY. FR designed and performed the experiments on the VOC emission from plants with support from OF and RB. FR performed the TD-GC-MS analyses of VOCs. AA contributed at the GC-MS analysis of beetle extractions and at the interpretation of the results. HV performed the *de novo* transcriptome assembly and analysis. EdL, PF, FR, and AS supervised the research, interpreted the data, and wrote the manuscript with contributions from all other authors.

FUNDING

This research was supported in part by Fondazione Cassa di Risparmio di Puglia [Grant 2012 – "Bio-ecologia del *Capnodis tenebrionis* (L.) (Insecta: Coleoptera: Buprestidae): interazioni intraspecifiche della riproduzione e interspecifiche del riconoscimento della pianta ospite"] and by University of Basilicata (RIL funds).

ACKNOWLEDGMENTS

We thank Matteo Mari and Mafalda Govoni of IBIMET for the technical assistance in VOCs experiments on plants, Carmela Stigliano and Pasquale Trotti of DiSSPA for the technical assistance in SEM observations, Antonio Franco of DiS for the assistance in the identification of candidate chemosensory genes. We also thank Emily Wheeler for editorial assistance.

SUPPLEMENTARY MATERIAL

The Supplementary Material for this article can be found online at: https://www.frontiersin.org/articles/10.3389/fphys.2019.00604/full#supplementary-material

MATERIAL S1 | Alignment of amino acid sequences of candidate OBPs from *Capnodis tenebrionis* **(A)**. Alignment of amino acid sequences of candidate CSPs from *Capnodis tenebrionis* **(B)**.

REFERENCES

Altner, H., and Prillinger, L. (1980). Ultrastructure of invertebrate chemo-, thermo-, and hygroreceptors and its functional significance. *Int. Rev. Cytol.* 67, 69–139. doi: 10.1016/S0074-7696(08)62427-4

Altschul, S. F., Madden, T. L., Schaffer, A. A., Zhang, J., Zhang, Z., Miller, W., et al. (1997). Gapped BLAST and PSI-BLAST: a new generation of protein database search programs. *Nucleic Acids Res.* 25, 3389–3402. doi: 10.1093/nar/25.17.3389

Andersson, M. N., Grosse-Wilde, E., Keeling, C. I., Bengtsson, J. M., Yuen, M. M., and Li, M. (2013). Antennal transcriptome analysis of the chemosensory gene families in the tree killing bark beetles, *Ips typographus* and *Dendroctonus ponderosae* (Coleoptera: Curculionidae: Scolytinae). *BMC Genomics* 14:198. doi: 10.1186/1471-2164-14-198

Antony, B., Soffan, A., Jakše, J., Abdelazim, M. M., Aldosari, S. A., Aldawood, A. S., et al. (2016). Identification of the genes involved in odorant reception and detection in the palm weevil *Rhynchophorus ferrugineus*, an important

quarantine pest, by antennal transcriptome analysis. *BMC Genomics* 17:69. doi: 10.1186/s12864-016-2362-6

Baraldi, R., Neri, L., Costa, F., Facini, O., Rapparini, F., and Carriero, G. (2018). Ecophysiological and micromorphological characterization of green roof vegetation for urban mitigation. *Urban For. Urban Green.* 37, 24–32. doi: 10.1016/j.ufug.2018.03.002

Baraldi, R., Rapparini, F., Rossi, F., Latella, A., and Ciccioli, P. (1999). Volatile organic compound emissions from flowers of the most occurring and economically important fruit tree species. *Phys. Chem. Earth* 6, 729–732. doi: 10.5194/bg-9-3777-2012

Bari, G., de Cristofaro, A., de Lillo, E., and Germinara, G. S. (2004). "Studio preliminare sulle interazioni intraspecifiche ed interspecifiche in *Capnodis tenebrionis* (L.) (Coleoptera: Buprestidae)," in *Proceedings of the Atti Congresso Nazionale Italiano di Entomologia, 10-15 Giugno 2002*, Catania, 725–731.

Ben-Yehuda, S., Assael, F., and Mendel, Z. (2000). Improved chemical control of *Capnodis tenebrionis* and *C. carbonaria* in stone-fruit plantations in Israel. *Phytoparasitica* 28, 1–16. doi: 10.1007/BF02994021

Bonsignore, C. P., and Bellamy, C. (2007). Daily activity and flight behaviour of adults of *Capnodis tenebrionis* (Coleoptera: Buprestidae). *Eur. J. Entomol.* 104, 425–431. doi: 10.14411/eje.2007.062

Bonsignore, C. P., and Jones, T. M. (2013). Aggregation and mating success of *Capnodis tenebrionis* (Coleoptera: Buprestidae). *Insect Sci.* 21, 203–212. doi: 10.1111/1744-7917.12035

Bonsignore, C. P., Manti, F., and Vacante, V. (2008). Field and tree distribution of *Capnodis tenebrionis* (Linnaeus, 1767) (Col., Buprestidae) adults in an apricot orchard in Italy. *J. Appl. Entomol.* 132, 216–224. doi: 10.1111/j.1439-0418.2007.01235.x

Bonsignore, C. P., and Vacante, V. (2009). Il problema di *Capnodis tenebrionis* (Linnaeus) nei fruttiferi. *Prot. Colture* 5, 18–25.

Borrero-Echeverry, F., Becher, P. G., Birgersson, G., Bengtsson, M., Witzgall, P., and Saveer, A. M. (2015). Flight attraction of *Spodoptera littoralis* (Lepidoptera, Noctuidae) to cotton headspace and synthetic volatile blends. *Front. Ecol. Evol.* 3:56. doi: 10.3389/fevo.2015.00056

Bruce, T. J. A., Wadhams, L. J., and Woodcock, C. M. (2005). Insect host location: a volatile situation. *Trends Plant Sci.* 10, 269–274. doi: 10.1016/j.tplants.2005.04.003

Cınar, M., Cimen, I., and Bolu, H. (2004). The cherry pests, their natural enemies and observations on some important species in Elazığ and Mardin provinces of Turkey. *Türk. Entomol. Derg.* 28, 213–220. doi: 10.23902/trkjnat.357444

Copolovici, L., Pag, A., Kännaste, A., Bodescu, A., Tomescu, D., Copolovici, D., et al. (2017). Disproportionate photosynthetic decline and inverse relationship between constitutive and induced emissions upon feeding of *Quercus robur* leaves by large larvae of gypsy moth (*Lymantria dispar*). *Environ. Exp. Bot.* 138, 184–192. doi: 10.1016/j.envexpbot.2017.03.014

Crook, D. J., Khrimian, A., Francese, J. A., Fraser, I., Poland, T. M., Sawyer, A. J., et al. (2008). Development of a host-based semiochemical lure for trapping emerald ash borer *Agrilus planipennis* (Coleoptera: Buprestidae). *Environ. Entomol.* 37, 356–365. doi: 10.1603/0046-225X(2008)37[356:DOAHSL]2.0.CO;2

Cui, X., Liu, D., Sun, K., He, K., He, Y., and Shi, X.-Q. (2018). Expression profiles and functional characterization of two odorant-binding proteins from the Apple Buprestid Beetle *Agrilus mali* (Coleoptera: Buprestidae). *J. Econ. Entomol.* 111, 1420–1432. doi: 10.1093/jee/toy066

de Groot, P., Grant, G. G., Poland, T. M., Scharbach, R., Buchan, L., Nott, R. W., et al. (2008). Electrophysiological response and attraction of emerald ash borer to green leaf volatiles (GLVs) emitted by host foliage. *J. Chem. Ecol.* 34, 1170–1179. doi: 10.1007/s10886-008-9514-3

de Lillo, E. (1998). Andamento dell'ovideposizione di *Capnodis tenebrionis* (L.) (Coleoptera: Buprestidae). *Entomologica* 32, 141–153. doi: 10.15162/0425-1016/709

del Mar Martinez de Altube, M., Strauch, O., Fernandez, de Castro, G., and Martinez Pena, A. (2008). Control of the flat-headed root borer *Capnodis tenebrionis* (Linné) (Coleoptera: Buprestidae) with the entomopathogenic nematode *Steinernema carpocapsae* (Weiser) (Nematoda: Steinernematidae) in a chitosan formulation in apricot orchards. *BioControl* 53, 531–539. doi: 10.1007/s10526-007-9094-0

Dudareva, N., Klempien, A., Muhlemann, J. K., and Kaplan, I. (2013). Biosynthesis, function and metabolic engineering of plant volatile organic compounds. *New Phytol.* 198, 16–32. doi: 10.1111/nph.12145

Engsontia, P., Sanderson, A. P., Cobb, M., Walden, K. K., Robertson, H. M., and Brown, S. (2008). The red flour beetle's large nose: an expanded odorant receptor gene family in *Tribolium castaneum*. *Insect Biochem. Mol. Biol.* 38, 387–397. doi: 10.1016/j.ibmb.2007.10.005

Fan, J., Francis, F., Liu, Y., Chen, J. L., and Cheng, D. F. (2010). An overview of odorant-binding protein functions in insect peripheral olfactory reception. *Genet. Mol. Res.* 10, 3056–3069. doi: 10.4238/2011.December.8.2

Fukaya, M. (2003). Recent advances in sex pheromone studies on the white-spotted longicorn beetle, *Anoplophora malasiaca*. *Jap. Agric. Res. Q.* 37, 83–88. doi: 10.6090/jarq.37.83

Furstenau, B., Rosell, G., Guerrero, A., and Quero, C. (2012). Electrophysiological and behavioral responses of the Black-Banded Oak Borer, *Coroebus florentinus*, to conspecific and host-plant volatiles. *J. Chem. Ecol.* 38, 378–388. doi: 10.1007/s10886-012-0110-1

García del Pino, F., and Morton, A. (2005). Efficacy of entomopathogenic nematodes against neonate larvae of *Capnodis tenebrionis* (L.) (Coleoptera: Buprestidae) in laboratory trials. *BioControl* 50, 307–316. doi: 10.1007/s10526-004-0894-1

Garrido, A. (1984). Bioecologia de *Capnodis tenebrionis* L. (Col. Buprestidae) y orientaciones parasu control. *Bol. Sanid. Veg. Plagas* 10, 205–221.

Garrido, A., del Busto, T., and Malagon, J. (1987). Metodo de recogida de huevos de *Capnodis tenebrionis* L., (Coleop.: Buprestidae) y algunos factores abioticos que pueden condicionar la puesta. *Bol. Sanid. Veg. Plagas* 13, 303–309.

Giacomuzzi, V., Capellin, L., Khomenko, I., Biasioli, F., Schütz, S., Tasin, M., et al. (2016). Emission of volatile compounds from apple plants infested with *Pandemis heparana* larvae, antennal response of conspecific adults, and preliminary field trial. *J. Chem. Ecol.* 42, 1265–1280. doi: 10.1007/s10886-016-0794-8

Giacomuzzi, V., Capellin, L., Nones, S., Khomenko, I., Biasioli, F., Knight, A., et al. (2017). Diel rhythms in the volatile emission of apple and grape foliage. *Phytochemistry* 138, 104–115. doi: 10.1016/j.phytochem.2017.03.001

Gindin, G., Kuznetsova, T., Protasov, A., Ben Yehuda, S., and Mendel, Z. (2009). Artificial diet for two flat-headed borers, *Capnodis* spp. (Coleoptera: Buprestidae). *Eur. J. Entomol.* 106, 573–581. doi: 10.14411/eje.2009.072

Ginzel, M. D., Moreira, J. A., Ray, A. M., Millar, J. G., and Hanks, L. M. (2006). (*Z*)-9-nonacosane - Major component of the contact sex pheromone of the beetle. *Megacyllene caryae*. *J. Chem. Ecol.* 32, 435–451. doi: 10.1007/s10886-005-9010-y

González-Núñez, M., Durán, J. R. E., Del Moral De la Vega, J., Ortiz Hernández, A., Vargas Osuna, E., de Aguilar Cormenzana, J. M., et al. (2012). *Investigación de Métodos Compatibles con la Agricultura Ecológica Para el Control del "Gusano cabezudo" (Capnodis tenebrionis (Linnaeus, 1758). Trabajos y Estudios Sobre Agricultura Ecológica*. Madrid: Ministerio de Agricultura, Alimentación y Medio Ambiente.

Götz, S., García-Gómez, J. M., Terol, J., Williams, T. D., Nagaraj, S. H., Nueda, M. J., et al. (2008). High-throughput functional annotation and data mining with the Blast2GO suite. *Nucleic Acids Res.* 36, 3420–3435. doi: 10.1093/nar/gkn176

Hanks, L. M., and Millar, J. G. (2016). Sex and aggregation-sex pheromones of cerambycid beetles: basic science and practical applications. *J. Chem. Ecol.* 42, 631–654. doi: 10.1007/s10886-016-0733-8

Hanks, L. M., Millar, J. G., Moreira, J. A., Barbour, J. D., Lacey, E. S., McElfresh, J. S., et al. (2007). Using generic pheromone lures to expedite identification of aggregation pheromones for the cerambycid beetles *Xylotrechus nauticus*, *Phymatodes lecontei*, and *Neoclytus modestus modestus*. *J. Chem. Ecol.* 33, 889–907. doi: 10.1007/s10886-007-9275-4

Harada, E., Nakagawa, J., Asano, T., Taoka, M., Sorimachi, H., Ito, Y., et al. (2012). Functional evolution of duplicated odorant-binding protein genes, Obp57d and Obp57e, in *Drosophila*. *PLoS One* 7:e29710. doi: 10.1371/journal.pone.0029710

He, P., Zhang, J., Liu, N. Y., Zhang, Y. N., Yang, K., and Dong, S. L. (2011). Distinct expression profiles and different functions of odorant binding proteins in *Nilaparvata lugens*. *PLoS One* 6:e28921. doi: 10.1371/journal.pone.0028921

Hekmat-Scafe, D. S., Scafe, C. R., McKinney, A. J., and Tanouye, M. A. (2002). Genome-wide analysis of the odorant-binding protein gene family in *Drosophila melanogaster*. *Genome Res.* 12, 1357–1369. doi: 10.1101/gr.239402

Jacquin-Joly, E., and Merlin, C. (2004). Insect olfactory receptors: contributions of molecular biology to chemical ecology. *J. Chem. Ecol.* 30, 2359–2397. doi: 10.1007/s10886-004-7941-3

Karlik, J. F., McKay, H. A., Welch, J. M., and Winer, A. M. (2002). A survey of California plant species with a portable VOC analyzer for biogenic emission inventory development. *Atmos. Environ.* 36, 5221–5233. doi: 10.1016/S1352-2310(02)00569-1

Koch, J. L., Carey, D. W., Mason, M. E., Poland, T. M., and Knight, K. S. (2015). Intraspecific variation in *Fraxinus pennsylvanica* responses to emerald ash borer (*Agrilus planipennis*). *New For.* 46, 995–1011. doi: 10.1007/s11056-015-9494-4

Lacey, E. S., Moreira, J. A., Millar, J. G., Ray, A. M., and Hanks, L. M. (2007). Male produced aggregation pheromone of the cerambycid beetle *Neoclytus mucronatus mucronatus*. *Entomol. Exp. Appl.* 122, 171–179. doi: 10.1007/s10886-009-9633-5

Landolt, J. P. (1997). Sex attractant and aggregation pheromones of male phytophagous insects. *Am. Entomol.* 43, 12–22. doi: 10.1093/ae/43.1.12

Leal, W. S. (2013). Odorant reception in insects: roles of receptors, binding proteins, and degrading enzymes. *Annu. Rev. Entomol.* 58, 373–391. doi: 10.1146/annurev-ento-120811-153635

Lelito, J. P., Böröczky, K., Jones, T. H., Fraser, I., Mastro, V. C., Tumlinson, J. H., et al. (2009). Behavioral evidence for a contact sex pheromone component of the emerald ash borer, *Agrilus planipennis* Fairmare. *J. Chem. Ecol.* 35, 104–110. doi: 10.1007/s10886-008-9583-3

Lockey, K. H. (1991). Insect hydrocarbon classes - Implications for chemotaxonomy. *Insect Biochem.* 21, 91–97. doi: 10.1016/0020-1790(91)90068-P

Lu, P. F., Wang, R., Wang, C. Z., Luo, Y. Q., and Qiao, H. L. (2015). Sexual differences in electrophysiological and behavioral responses of *Cydia molesta* to peach and pear volatiles. *Entomol. Exp. Appl.* 157, 279–290. doi: 10.1111/eea.12362

Malagon, J., Garrido, A., del Busto, T., and Castaner, M. (1990). Influencia de algunos factores abioticos en la oviposicion de *Capnodis tenebrionis* (L.) Coleoptera, Buprestidae. *Invest. Agrar. Prod. Prot. Veg.* 5, 441–446.

Mamidala, P., Wijeratne, A. J., Wijeratne, S., Poland, T., Qazi, S. S., Doucet, D., et al. (2013). Identification of odor-processing genes in the Emerald Ash Borer, *Agrilus planipennis*. *PLoS One* 8:e56555. doi: 10.1371/journal.pone.0056555

Marannino, P., and de Lillo, E. (2007). *Capnodis tenebrionis* (L. 1758) (Coleoptera: Buprestidae): morphology and behaviour of the neonate larvae, and soil humidity effects on the egg eclosion. *Ann. Soc. Entomol. France* 43, 145–154. doi: 10.1080/00379271.2007.10697504

Marannino, P., Tarasco, E., and de Lillo, E. (2004). Biological notes on larval hatching in *Capnodis tenebrionis* (L.) (Coleoptera Buprestidae) and evaluation of entomopathogenic nematodes in controlling neonate larvae. *Redia* 86, 101–105.

Martin, P., Soria, F. J., Villagran, M., and Ocete, M. E. (1998). Preferencia alimentaria en laboratorio del adulto de *Capnodis tenebrionis* L. (Coleoptera: Buprestidae) sobre seis especies vegetales. *Bol. Sanid. Veg. Plagas* 24, 107–112.

Mendel, Z., Fabienne, A., and Ben-Yehuda, S. (2003). Host selection and root colonization of cyanogenic stonefruit species by *Capnodis* spp. (Coleoptera: Buprestidae). *Ann. Entomol. Soc. Am.* 96, 127–134. doi: 10.1603/0013-8746(2003)096%5B0127:hsarco%5D2.0.co;2

Mfarrej, M. F., and Sharaf, N. S. (2011). Host selection of peach rootborer *Capnodis tenebrionis* L. (Coleoptera: Buprestidae) to stone-fruit trees in Jordan. *Jordan J. Agric. Sci.* 7, 682–689.

Mitchell, R. F., Hughes, D. T., Luetje, C. W., Millar, J. G., Soriano-Agatón, F., and Hanks, L. M. (2012). Sequencing and characterizing odorant receptors of the cerambycid beetle *Megacyllene caryae*. *Insect Biochem. Mol. Biol.* 42, 499–505. doi: 10.1016/j.ibmb.2012.03.007

Mortazavi, A., Williams, B. A., McCue, K., Schaeffer, L., and Wold, B. (2008). Mapping and quantifying mammalian transcriptomes by RNA-Seq. *Nat. Methods* 5, 621–628. doi: 10.1038/nmeth.1226

Morton, A., and García del Pino, F. (2008). Effectiveness of different species of entomopathogenic nematodes for biocontrol of the Mediterranean flatheaded rootborer, *Capnodis tenebrionis* (Linné) (Coleoptera: Buprestidae) in potted peach tree. *J. Invertebr. Pathol.* 97, 128–133. doi: 10.1016/j.jip.2007.09.003

Najar-Rodriguez, A., Orschel, B., and Dorn, S. (2013). Season-long volatile emissions from peach and pear trees *in situ*, overlapping profiles, and olfactory attraction of an oligophagous fruit moth in the laboratory. *J. Chem. Ecol.* 39, 418–429. doi: 10.1007/s10886-013-0262-7

Niinemets, Ü., Kännaste, A., and Copolovici, L. (2013). Quantitative patterns between plant volatile emissions induced by biotic stresses and the degree of damage. *Front. Plant Sci.* 4:262. doi: 10.3389/fpls.2013.00262

Noldt, U., Fettköther, R., and Dettner, K. (1995). Structure of the sex pheromone producing prothoracic glands of the male old house borer, *Hylotrupes bajulus* (L.) (Coleoptera: Cerambycidae). *Int. J. Insect Morphol. Embryol.* 24, 223–234. doi: 10.1016/0020-7322(95)93345-d

Pelosi, P., Iovinella, I., Zhu, J., Wang, G., and Dani, F. R. (2017). Beyond chemoreception: diverse tasks of soluble olfactory proteins in insects. *Biol. Rev.* 93, 184–200. doi: 10.1111/brv.12339

Porcelli, F., and Di Palma, A. (2001). Formation of the monomerous female antenna in *Diaspis echinocacti* (Bouché) 1833 (Rhynchota Diaspididae). I. The second instar antenna. *Boll. Zool. Agrar. Bachicoltura* 33, 85–109.

Pureswaran, D. S., and Poland, T. M. (2009). The role of olfactory cues in short-range mate finding by the Emerald Ash Borer, *Agrilus planipennis* Fairmare (Coleoptera: Buprestidae). *J. Insect Behav.* 22, 205–216. doi: 10.1007/s10905-008-9166-8

Rapparini, F., Baraldi, R., and Facini, O. (2001). Seasonal variation of monoterpene emission from *Malus domestica* and *Prunus avium*. *Phytochemistry* 57, 681–687. doi: 10.1016/S0031-9422(01)00124-8

Rapparini, F., Baraldi, R., Miglietta, F., and Loreto, F. (2004). Isoprenoid emission in trees of *Quercus pubescens* and *Quercus ilex* with lifetime exposure to naturally high CO2 environment. *Plant Cell Environ.* 27, 381–391. doi: 10.1111/j.1365-3040.2003.01151.x

Ray, A. M., Lacey, E. S., and Hanks, L. M. (2006). Predicted taxonomic patterns in pheromone production by longhorned beetles. *Naturwissenschaften* 93, 543–550. doi: 10.1007/s00114-006-0142-x

Reidel, R. V. B., Cioni, P. L., and Pistelli, L. (2017). Volatile emission of different plant parts and fruit development from Italian cherry plums (*Prunus cerasifera* and *P. cerasifera 'Pissardii'*). *Biochem. Syst. Ecol.* 75, 10–17. doi: 10.1016/j.bse.2017.10.001

Rivnay, E. (1946). Physiological and ecological studies on the species of *Capnodis* in Palestine (Col., Buprestidae). III. Studies on the adult. *Bull. Entomol. Res.* 37, 273–280. doi: 10.1017/S0007485300023944

Rodriguez-Saona, C., Poland, T. M., Miller, J. R., Stelinski, L. L., Grant, G. G., de Groot, P., et al. (2006). Behavioral and electrophysiological responses of the emerald ash borer, *Agrilus planipennis*, to induced volatiles of Manchurian ash, *Fraxinus mandshurica*. *Chemoecology* 16, 75–86. doi: 10.1007/s00049-005-0329-1

Sands, D. P. A. (1984). Dissolving wax from scale insects: a method for assessing parasitism and determining instars of *Ceroplastes* spp. and *Gascardia destructor* (Newstead) (Homoptera: Coccidae). *J. Aust. Entomol. Soc.* 23, 295–296. doi: 10.1111/j.1440-6055.1984.tb01965.x

Santamour, F. S. (1998). Amygdalin in *Prunus* leaves. *Phytochemistry* 47, 1537–1538. doi: 10.1016/S0031-9422(97)00787-5

Sharon, R., Peles, S., Gordon, D., and Harari, A. R. (2010). Intraspecific attraction and host tree selection by adult *Capnodis tenebrionis*. *Isr. J. Plant Sci.* 58, 53–60. doi: 10.1560/IJPS.58.1.53

Silk, P., and Ryall, K. (2015). Semiochemistry and chemical ecology of the emerald ash borer *Agrilus planipennis* (Coleoptera: Buprestidae). *Can. Entomol.* 147, 277–289. doi: 10.4039/tce.2014.58

Silk, P. J., Ryall, K., Lyons, D. B., Sweeney, J., and Wu, J. (2009). A contact pheromone component of the emerald ash borer *Agrilus planipennis* Fairmare (Coleoptera: Buprestidae). *Naturwissenschaften* 96, 601–608. doi: 10.1007/s00114-009-0513-1

Smyth, R. R., and Hoffmann, M. P. (2003). A male-produced aggregation pheromone facilitating *Acalymma vittatum* [F.] (Coleoptera: Chrysomelidae) early season host plant colonization. *J. Insect Behav.* 16, 347–359. doi: 10.1023/A:1024824025210

Spikes, A. E., Paschen, M. A., Millar, J. G., Moreira, J. A., Hamel, P. B., Schiff, N. M., et al. (2010). First contact pheromone indentified for a longhorned beetle (Coleoptera: Cerambycidae) in the subfamily Prioninae. *J. Chem. Ecol.* 36, 943–954. doi: 10.1007/s10886-010-9837-8

Staudt, M., Jackson, B., El-Aouni, H., Buatois, B., Lacroze, J. P., Poëssel, J. L., et al. (2010). Volatile organic compound emissions induced by the

aphid *Myzus persicae* differ among resistant and susceptible peach cultivars and a wild relative. *Tree Physiol.* 30, 1320–1334. doi: 10.1093/treephys/tpq072

Tezcan, S. (1995). Investigations on the harmful species of Buprestidae (Coleoptera) of cherry or-chards in the Kemalpasa (Izmir) district (Turkey). *Turk. Entomol. Derg.* 19, 221–230.

Volkovitsh, M. G. (2001). The comparative morphology of antennal structures in Buprestidae (Coleoptera): evolutionary trends, taxonomic and phylogenetic implications. Part 1. *Acta Mus. Morav. Sci. Biol.* 86, 43–169.

Vuts, J., Woodcock, C. M., Sumner, M. E., Caulfield, J. C., Reed, K., Inward, D. J. G., et al. (2016). Responses of the two-spotted oak buprestid, *Agrilus biguttatus* (Coleoptera: Buprestidae), to host tree volatiles. *Pest Manag. Sci.* 72, 845–851. doi: 10.1002/ps.4208

Wilkey, R. F. (1962). A simplified technique for clearing, staining and permanently mounting small arthropods. *Ann. Entomol. Soc. Am.* 55:606. doi: 10.1093/aesa/55.5.606

Yang, L., Cheng, P., Zhu, X.-F., Zhang, Z. G., and Li, H. (2018). Composition and dynamic variations of the natural volatiles of *Prunus armeniaca*. *Int. J. Agric. Biol.* 20, 169–182. doi: 10.17957/IJAB/15.0507

Yang, S., Zhang, X. F., Gao, Y. L., Chen, D., She, D. M., Zhang, T., et al. (2017). Male-produced aggregation pheromone of coffee bean weevil, *Araecerus fasciculatus*. *J. Chem. Ecol.* 43, 978–985. doi: 10.1007/s10886-017-0894-0

Yew, J. Y., and Chung, H. (2015). Insect pheromones: an overview of function, form, and discovery. *Progr. Lipid Res.* 59, 88–105. doi: 10.1016/j.plipres.2015.06.001

Yin, J., Feng, H., Sun, H., Xi, J., Cao, Y., and Li, K. (2012). Functional analysis of general odorant binding protein 2 from the meadow moth, *Loxostege sticticalis* L. (Lepidoptera: Pyralidae). *PLoS One* 7:e33589. doi: 10.1371/journal.pone.0033589

Zacharuk, R. Y. (1980). Ultrastructure and function of insect chemosensilla. *Ann. Rev. Entomol.* 25, 27–47. doi: 10.1146/annurev.en.25.010180.000331

Zhou, J. J. (2010). Odorant-binding proteins in insects. *Vitam. Horm.* 83, 241–272. doi: 10.1016/S0083-6729(10)83010-9

Conflict of Interest Statement: CY is currently employed by company Syngenta in Turkey. CY was a masters student at CiHEAM IAM-B while undertaking part of this study which was performed at the University of Bari Aldo Moro.

The remaining authors declare that the research was conducted in the absence of any commercial or financial relationships that could be construed as a potential conflict of interest. Syngenta had no role in study design, data collection and analysis, decision to publish, or preparation of the manuscript.

frontiers in Physiology

CORRECTION
published: 26 June 2020
doi: 10.3389/fphys.2020.00668

Corrigendum: Chemical Ecology of *Capnodis tenebrionis* (L.) (Coleoptera: Buprestidae): Behavioral and Biochemical Strategies for Intraspecific and Host Interactions

Giuseppe Bari[1†], *Andrea Scala*[2†], *Vita Garzone*[1], *Rosanna Salvia*[2], *Cem Yalcin*[1,3], *Pasqua Vernile*[1], *Antonella Maria Aresta*[4], *Osvaldo Facini*[5], *Rita Baraldi*[5], *Sabino A. Bufo*[2], *Heiko Vogel*[6], *Enrico de Lillo*[1*‡], *Francesca Rapparini*[5*‡] and *Patrizia Falabella*[2*‡]

[1] Department of Soil, Plant and Food Sciences, University of Bari Aldo Moro, Bari, Italy, [2] Department of Science, University of Basilicata, Potenza, Italy, [3] Syngenta, Izmir, Turkey, [4] Department of Chemistry, University of Bari Aldo Moro, Bari, Italy, [5] Department of Biology, Agriculture and Food Sciences, Biometeorology Institute, National Research Council, Bologna, Italy, [6] Department of Entomology, Max Planck Institute for Chemical Ecology, Jena, Germany

Keywords: chemoreception, mating, mediterranean flat-headed root-borer, scanning electron microscopy, soluble olfactory proteins, volatile organic compounds

OPEN ACCESS

Edited and reviewed by:
Graziano Fiorito,
University of Naples Federico II, Italy

***Correspondence:**
Enrico de Lillo
enrico.delillo@uniba.it
Francesca Rapparini
f.rapparini@ibimet.cnr.it
Patrizia Falabella
patrizia.falabella@unibas.it

†These authors have contributed equally to this work and share first authorship

‡These authors have contributed equally to this work and share last authorship

Specialty section:
This article was submitted to Invertebrate Physiology, a section of the journal Frontiers in Physiology

Received: *25 April 2020*
Accepted: *25 May 2020*
Published: *26 June 2020*

Citation:
Bari G, Scala A, Garzone V, Salvia R, Yalcin C, Vernile P, Aresta AM, Facini O, Baraldi R, Bufo SA, Vogel H, de Lillo E, Rapparini F and Falabella P (2020) Corrigendum: Chemical Ecology of Capnodis tenebrionis (L.) (Coleoptera: Buprestidae): Behavioral and Biochemical Strategies for Intraspecific and Host Interactions. Front. Physiol. 11:668. doi: 10.3389/fphys.2020.00668

A Corrigendum on

Chemical Ecology of *Capnodis tenebrionis* (L.) (Coleoptera: Buprestidae): Behavioral and Biochemical Strategies for Intraspecific and Host Interactions
by Bari, G., Scala, A., Garzone, V., Salvia, R., Yalcin, C., Vernile, P., et al. (2019). Front. Physiol. 10:604. doi: 10.3389/fphys.2019.00604

In the original article, there was a mistake in **Table 1** and **Table 2** as published. The **Table 1** and **Table 2** had incorrect column headers due to an inversion of the symbols ♀ and ♂ with the consequent incorrect interpretation of the symbols + and – within the same Tables. The corrected **Table 1** and **Table 2** appear below.

The authors apologize for this error and state that this does not change the scientific conclusions of the article in any way. The original article has been updated.

TABLE 1 | Peaks produced by the hexane extracts of resin copies obtained by the pronota of sexually mature male and female pronota in 2014, and by the pronota of attracted males and attractive females in 2015.

	♀ **Sexually mature**	♂ **Sexually mature**	♀ **Attractive**	♂ **Attracted**
C_8	+	+	−	−
C_{10}	+	+	−	−
C_{13}	+	−	−	−
C_{14}	−	−	+	−
C_{15}	−	−	+	−
Cyclohexene	−	−	+	+
C_{22}	−	−	+	−
C_{24}	+	+	+	−
C_{25}	+	−	−	−
C_{26}	+	+	−	+
C_{28}	+	+	−	−
MeC_{24}	−	−	−	+
MeC_{25}	−	−	−	+
C_{30}	+	+	−	−
C_{31}	+	+	−	−
MeC_{29}	−	−	+	−
C_{32}	−	−	−	+
C_{34}	−	−	+	−
C_{35}	−	−	−	+
C_{36}	−	−	+	+

+ and – indicate, respectively, presence or absence of compounds.

TABLE 2 | Peaks produced by the hexane extracts from the whole bodies of virgin males and females of *C. tenebrionis*.

Peak number	**Retention time**	**Compound**	**Wholebody ♀**	**Wholebody ♂**
1	20.07	C_{21}	+	−
2	21.00	C_{22}	+	−
3	22.04	C_{23}	+	−
4	22.93	3 MeC_{23}	+	−
5	23.15	5,9-dimethyl C_{23}	+	−
6	23.29	C_{24}	−	−
7	23.39	3,7+3,9 dimethyl C_{23}	−	−
8	23.80	$6MeC_{24}$	−	−
9	24.05	$4MeC_{24}$	+	−
10	24.43	$2MeC_{34}$	−	−
11	24.68	C_{25}	+	+
12	25.19	$7MeC_{25}$	−	−
13	25.53	$5MeC_{25}$	+	−
14	25.84	$3MeC_{25}$	+	+
15	26.00	5,9 dimethyl C_{25}	+	−
16	26.29	C_{26}	+	+
17	26.42	3,7+3,9 MeC_{26}	+	−
18	26.85	10+12 MeC_{26}	+	−
19	27.10	6 MeC_{26}	+	−
20	27.31	4 MeC_{26}	+	−
21	27.58	2 MeC_{26}	+	−
22	28.11	C_{27}	+	+
23	28.71	11+13 MeC_{27}	+	−
24	28.93	7 MeC_{27}	+	−
25	29.11	5 MeC_{27}	+	−
26	29.40	11,13 MeC_{27}	+	−
27	29.53	3 MeC_{27}	+	+
28	30.07	C_{28}	+	+
29	30.19	3,7 dimethyl C_{27}	+	−
30	30.68	12+14 7 MeC_{28}	+	−
31	31.06	6 MeC_{28}	+	−
32	31.27	4 MeC_{28}	+	−
33	31.70	2 MeC_{28}	+	−
34	32.29	C_{29}	+	+
35	32.93	7 MeC_{29}	+	+
36	33.57	11,15 6 MeC_{29}	+	−
37	33.92	3 MeC_{29}	+	+
38	34.59	C_{30}	+	−
39	34.71	3,11 dimethyl C_{30}	+	−
40	35.74	C_{31-ene}	+	−
41	36.96	C_{31}	+	+
42	37.66	13 MeC_{31}	+	+
43	41.94	C_{33}	+	+
44	45.08	C_{34}	+	−
45	47.70	11, 15 dimethyl C_{35}	+	+
46	48.50	MeC_{35}	+	+
47	49.65	12+14+16 MeC_{36}	+	−
48	53.10	12,22 dimethyl C_{36}	+	+

+/– indicates the presence or absence of the relative compound in extracts of male and female bodies.

frontiers in Physiology

ORIGINAL RESEARCH
published: 19 June 2019
doi: 10.3389/fphys.2019.00716

TGF-β Signaling Interferes With the *Drosophila* Innate Immune and Metabolic Response to Parasitic Nematode Infection

*Yaprak Ozakman and Ioannis Eleftherianos**

Infection and Innate Immunity Laboratory, Department of Biological Sciences, The George Washington University, Washington, DC, United States

OPEN ACCESS

Edited by:
Michel Cusson, Natural Resources Canada, Canada

Reviewed by:
Jae Park, The University of Tennessee, Knoxville, United States
Wolfgang Blenau, Leipzig University, Germany

***Correspondence:**
Ioannis Eleftherianos
ioannise@gwu.edu

Specialty section:
This article was submitted to Invertebrate Physiology, a section of the journal Frontiers in Physiology

Received: *10 February 2019*
Accepted: *23 May 2019*
Published: *19 June 2019*

Citation:
Ozakman Y and Eleftherianos I (2019) TGF-β Signaling Interferes With the Drosophila Innate Immune and Metabolic Response to Parasitic Nematode Infection. Front. Physiol. 10:716. doi: 10.3389/fphys.2019.00716

The common fruit fly, *Drosophila melanogaster*, is an outstanding model to study the molecular basis of anti-pathogen immunity. The parasitic nematode *Heterorhabditis gerrardi,* together with its mutualistic bacteria *Photorhabdus asymbiotica,* infects a wide range of insects, including *D. melanogaster*. Recently, we have shown that transforming growth factor-β (TGF-ß) signaling in *D. melanogaster* is regulated in response to parasitic nematode infection. In the current study, we investigated the contribution of two TGF-ß signaling branches, the activin and the bone morphogenetic protein (BMP), to *D. melanogaster* immune function against *H. gerrardi*. We used *D. melanogaster* larvae carrying mutations in the genes coding for the TGF-ß extracellular ligands *daw* and *dpp*. We have demonstrated that the number of circulating hemocytes in uninfected *daw* and *dpp* mutants decreases twofold compared to background controls, yet no significant changes in hemocyte numbers and survival of the TGF-ß mutants are observed upon nematode infection. However, we have shown that nematode-infected *daw* mutants express *Dual oxidase* at higher levels and phenoloxidase activity at lower levels compared to their background controls. To elucidate the contribution of TGF-ß signaling in the metabolic response of *D. melanogaster* to parasitic nematodes, we estimated lipid and carbohydrate levels in *daw* and *dpp* mutant larvae infected with *H. gerrardi*. We have found that both nematode-infected mutants contain lipid droplets of larger size, with *daw* mutant larvae also containing elevated glycogen levels. Overall, our findings indicate that the regulation of activin and BMP branches of TGF-ß signaling can alter the immune and metabolic processes in *D. melanogaster* during response to parasitic nematode infection. Results from this study shed light on the molecular signaling pathways insects activate to regulate mechanisms for fighting potent nematode parasites, which could lead to the identification of novel management strategies for the control of damaging pests.

Keywords: *D. melanogaster*, *Heterorhabditis*, immunity, parasitism, TGF-ß signaling

INTRODUCTION

The fruit fly, *Drosophila melanogaster*, is an established insect model to study innate immune responses against pathogenic infection due to the availability of a wide range of genetic tools (Rämet, 2012). The nematode parasite *Heterorhabditis* forms an excellent experimental tool to dissect the molecular basis of nematode parasitism and mutualism in relation to the insect immune system (Hallem et al., 2007). The nematodes live in mutualistic relationship with the Gram-negative bacteria *Photorhabdus* and together they can infect a variety of insect species (Gerrard et al., 2006; Plichta et al., 2009). *Heterorhabditis* nematodes infect their insect hosts at the infective juvenile stage. Upon entering the insect body cavity, the nematode regurgitates its mutualistic bacteria into the hemolymph to overcome the insect immune response (Stock and Blair, 2008; Castillo et al., 2011).

Investigation of the dynamic interaction between *Heterorhabditis* and *Photorhabdus* species in relation to key aspects of the insect immune system has been facilitated in recent years by the establishment of the tripartite system that involves the fruit fly *D. melanogaster* as the model insect host (ffrench-Constant et al., 2007; Hallem et al., 2007). *D. melanogaster* has evolved certain immune mechanisms to fight against parasitic nematode infection (Castillo et al., 2011). The anti-nematode immunity of *D. melanogaster* includes both humoral and cellular responses in addition to the phenoloxidase cascade that results in melanin formation (Eleftherianos et al., 2016a). Nematode infection also induces stress signaling cascades that result in the synthesis of nitric oxide (NO) and differential regulation of genes involved in the production of reactive oxygen species (ROS) (Castillo et al., 2015; Yadav et al., 2017).

Transforming growth factor-β (TGF-β) signaling pathway is pivotal in cell-cell communication and is involved in several cellular processes, including cell proliferation and differentiation as well as tissue homeostasis and regeneration in mammals (Harradine and Akhurst, 2009). In *D. melanogaster*, it regulates developmental mechanisms including axis formation, body patterning, and morphogenesis (Masucci et al., 1990; Lecuit et al., 1996; Dobens and Raftery, 1998). Similar to vertebrates, the TGF-ß pathway in *D. melanogaster* is composed of two signaling branches: the bone morphogenetic protein (BMP) and the activin branches. The TGF-ß signaling pathway is initiated by the binding of an extracellular ligand to a transmembrane receptor complex of serine/threonine kinases (Raftery and Sutherland, 1999; Shi and Massagué, 2003). BMP signaling includes three ligands: decapentaplegic (dpp), glass-bottom boat (gbb), and screw (scw); and the activin subfamily ligands include *activin-ß* (*actß*), *dawdle* (*daw*), and *myoglianin* (*myo*; Peterson and O'Connor, 2014). Following the activation of the receptor through ligand binding, receptor complex phosphorylates downstream transcription factors that regulate the activation of target genes (Zi et al., 2012).

Recently, a link between TGF-ß signaling pathway activity and interaction with parasitic nematode infection has been found in *D. melanogaster* (Eleftherianos et al., 2016b; Patrnogic et al., 2018a,b). More precisely, both activin and BMP branches of TGF-ß signaling pathway are involved in the immune response to sterile injury and *Micrococcus luteus* bacterial infection in flies (Clark et al., 2011). Also, gene transcript levels of both *dpp* and *daw* are upregulated by *Heterorhabditis gerrardi* and *H. bacteriophora* nematode infection in flies (Eleftherianos et al., 2016b). In addition, inactivation of *dpp* increases fly survival and activates humoral immunity in response to *H. bacteriophora* assault (Patrnogic et al., 2018a).

In the current study, we investigated the potential contribution of activin and BMP branches of TGF-β signaling in *D. melanogaster* immunity against *H. gerrardi* infection. For this, we infected larvae carrying loss-of-function mutations in *daw* or *dpp* with *H. gerrardi* infective juveniles to estimate their survival ability, cellular immune activity including changes in hemocyte numbers, ROS and NO activation, and melanization response. In addition, in order to understand whether TGF-ß signaling regulates the *D. melanogaster* metabolic response to nematode parasites, we measured metabolic processes, including lipid and carbohydrate metabolism in *H. gerrardi*-infected larvae with inactivated *daw* or *dpp* genes. Similar studies in insect model hosts are expected to facilitate our understanding of the link between activation of conserved signaling pathways and their components and host immune capacity in response to potent nematode parasites.

MATERIALS AND METHODS

Fly and Nematode Stocks

All flies were reared on instant *D. melanogaster* diet (Formula 4–24 *D. melanogaster* medium) supplemented with yeast (Carolina Biological Supply), maintained at 25°C, and a 12:12-h light:dark photoperiodic cycle. A fly line with spontaneous dpp^{s1} mutation and a line carrying P-bac insertion Pbac{XP}daw^{05680} were used. Line w^{1118} was used as the background control in all experiments. All lines were obtained from Bloomington Drosophila Stock Center. Validation of mutant lines was performed using quantitative RT-PCR (**Supplementary Figure S1**). *H. gerrardi* nematodes were amplified in the larvae of the wax moth *Galleria mellonella* using the water trap technique (White, 1927). Nematodes were used 1–4 weeks after collection.

Larval Infection

Infections of *D. melanogaster* late 2nd instar larvae with nematodes were performed in microtiter 96-well plates containing 100 µl of 1.25% agarose in each well. Infective juveniles were washed and adjusted to the final density of 100 nematodes in 10 µl of sterile distilled water. Nematodes were pipetted into the wells of the microtiter plate and a single larva was transferred to each well. The plate was covered with a Masterclear real-time PCR film (Eppendorf) and holes were pierced for ventilation. Sterile distilled water was used as negative control. Control larvae maintained with water were able to survive, grow normally, and eventually pupate during the course of the experiment. Infected and uninfected larvae were kept at room temperature in the 96-well plate. At 3- and 24-h time point, infected and uninfected larvae were collected and frozen

at −80°C or immediately used in experiments. Each infection was performed three times with biological duplicates. For survival experiments, the survival of larvae kept in nematode-free solution or in nematode solution was counted every 12 h for 60 h. Four independent survival experiments were conducted.

RNA Analysis

Total RNA was extracted from 5 to 10 *D. melanogaster* larvae, using TRIzol™ reagent according to manufacturer's protocol. Reverse transcription was performed using the High Capacity cDNA Reverse Transcription Kit (Applied Biosystems) and 350 ng RNA. Quantitative RT-PCR (qRT-PCR) experiments were carried out with gene-specific primers (**Table 1**) and 3.5 ng cDNA, using iQ SYBR Green Supermix (Bio-Rad Laboratories) and a CFX96 Real-Time PCR detection system (Bio-Rad Laboratories), following the manufacturer's instructions. Each experiment was run in biological duplicates and repeated three times.

Hemolymph Collection and Total Hemocyte Counts

To extract hemolymph from nematode-infected and uninfected *D. melanogaster* mutant and background control larvae, 10 individuals were bled into 30 µl of 2.5× protease inhibitor cocktail (Sigma P2714). Hemolymph samples were loaded on a hemocytometer and total numbers of cells were counted using 40× magnification of a compound microscope (Olympus CX21). Each experiment was repeated three times.

Phenoloxidase Activity Assay

D. melanogaster larvae were infected with *H. gerrardi* nematodes as previously described, and 10 larvae were collected at 24 h post infection. Phenoloxidase activity was measured according to a previously published protocol with slight modifications (Duvic et al., 2002). Hemolymph of each sample was collected, added to a Pierce® Spin Column, and spun at 4°C and 13,000 rpm for 10 min. Protein concentrations were estimated using Pierce™ BCA Protein Assay Kit (Thermo Fisher Scientific). A mix containing 15 µg of protein, 5 mM $CaCl_2$, and 2.5× protease inhibitor were added to 160 µl of L-DOPA solution (in phosphate buffer, pH 6.6) in a clear microplate well. Absorbance was measured at 29°C at 492 nm for 60 min. Absorbance of the blank was subtracted from the absorbance of the samples. Each experiment was run in biological duplicates and repeated three times.

Metabolic Assays

D. melanogaster larvae were infected with *H. gerrardi* nematodes as previously described, and five larvae were collected at 24 h post infection. Larvae were washed several times in cold 1 ml 1× PBS and homogenized in either 100 µl of 1× PBS to determine glucose and glycogen levels or 100 µl of cold PBST (1× PBS + 0.05% Tween 20) to measure triglyceride levels, as previously described (Tennessen et al., 2014). Proteins were quantified by Pierce™ BCA Protein Assay Kit (Thermo Fisher Scientific). To determine the amount of triglycerides in infected and uninfected larvae, samples were diluted 1:1 in PBS-Tween and added to 200 µl of the Infinity™ Triglycerides Liquid Stable Reagent (Thermo Fisher Scientific) in a clear microplate well. Covered samples were incubated at 37°C for 30 min, and absorbance was measured at 540 nm. The amount of triglycerides was determined by the glycerol standard curve. To determine the amount of glucose and glycogen, samples were initially diluted 1:3 in PBS and then separated into two sets for further dilutions. The first set of samples was diluted 1:1 in amyloglucosidase stock solution (1.5 µl of amyloglucosidase in 1 ml of PBS, Sigma) and the second set was diluted 1:1 in PBS. Samples (30 µl) were incubated at 37°C for 60 min in a clear microplate well. Hexokinase (Glucose Assay Reagent, Sigma) reagent (100 µl) was added to each well and samples were incubated at room temperature for 15 min. Absorbance was measured at 340 nm, and the amount of glucose was determined by the second set of samples, which were diluted in PBS. The amount of glycogen was calculated by subtracting the absorbance of glucose from the absorbance of first set of samples (samples diluted with amyloglucosidase stock). The amounts of triglycerides, glucose, and glycogen were calculated relative

TABLE 1 | Primers and their sequences used in quantitative RT-PCR experiments.

Gene	Accession no.	Primer (5′-3′)	Sequence	T_m (°C)
Daw	CG16987	Forward	GGTGGATCAGCAGAAGGACT	57
		Reverse	GCCACTGATCCAGTGTTTGA	
Dpp	CG9885	Forward	CCTTGGAGCCTCTGTCGAT	57
		Reverse	TGCACTCTGATCTGGGATTTT	
PPO1	CG5779	Forward	CAACTGGCTTCGTTGAGTGA	60
		Reverse	CGGGCAGTTCCAATACAGTT	
PPO2	CG8193	Forward	CCCGCCTATACCGAGA	59
		Reverse	CGCACGTAGCCGAAAC	
PPO3	CG2952	Forward	GGCGAGCTGTTCTACT	58
		Reverse	GAGGATACGCCCTACTG	
Nos	CG6713	Forward	AACGTTCGACAAATGCGCAA	60
		Reverse	GTTGCTGTGTCTGTGCCTTC	
Duox	CG3131	Forward	ACGTGTCCACCCAATCGCACGAG	60
		Reverse	AAGCGTGGTGGTCCAGTCAGTCG	
RpL32	CG7939	Forward	GATGACCATCCGCCCAGCA	60
		Reverse	CGGACCGACAGCTGCTTGGC	

to the amount of proteins in each sample. Each experiment was run in biological duplicates and repeated three times.

Lipid Droplet Staining

D. melanogaster larvae were infected with *H. gerrardi* nematodes as previously described, and 15 larvae were collected at 24 h post infection. Fat body tissues of larvae were dissected and fixed in 4% paraformaldehyde in PBS at room temperature for 30 min. Tissues were washed two times in PBS and then incubated in the dark for 30 min in 0.05% Nile red diluted 1:1,000 in 1 mg/ml of methanol. Tissues were mounted in ProLong™ Diamond AntiFade Mountant with DAPI (Life Technologies). Images were taken by Zeiss LSM 510 confocal microscope. Quantification of lipid droplet size was performed by selecting the area of the five largest lipid droplets per cell from 20 fat body cells. ImageJ software (National Institutes of Health) was used for quantifications. The experiment was repeated three times.

Statistical Analysis

GraphPad Prism7 was used for data plotting and statistical analyses. Log-rank (Mantel-Cox) test was used for statistical analysis of the survival results. Statistical analyses of all other experiments were performed using unpaired *t*-test.

RESULTS

Nematode Infection Does Not Alter the Survival of TGF-ß Mutants

We assessed the ability of *daw* and *dpp* mutant larvae to survive the infection by *H. gerrardi* symbiotic nematodes. For this, we monitored larval survival every 12 h and up to 60 h post nematode infection. We found no significant differences in survival between uninfected TGF-ß mutants and their background control (**Figure 1**). Also, we did not observe any significant changes in survival between nematode-infected TGF-ß mutants and control individuals. These results indicate that activin and BMP branches of TGF-ß signaling do not contribute to the survival ability of *D. melanogaster* larvae to infection by *H. gerrardi* nematodes.

Uninfected *daw* and *dpp* Mutants Contain Fewer Circulating Hemocytes

In *D. melanogaster*, circulating hemocytes play a major role in immune surveillance, and their number can change drastically during pathogenic or non-pathogenic bacterial infection (Eleftherianos et al., 2014; Vlisidou and Wood, 2015; Shokal et al., 2017). To investigate whether inactivating the activin or BMP branches of TGF-ß signaling alters the total number of circulating hemocytes in uninfected *D. melanogaster* or those infected with nematode parasites, we counted hemocytes in larvae carrying loss-of-function mutations in *daw* or *dpp* following treatment with water (control) or infection with *H. gerrardi*. We used two time points to examine changes in hemocyte numbers over time: 3 h post infection as an early time point and 24 h post infection as a later point when nematode infection is established. Both uninfected *daw* and *dpp* mutants contained significantly reduced numbers of hemocytes relative to their w^{1118} background control at the 3-h time point (*daw*, $p = 0.0014$ and *dpp*, $p = 0.0078$; **Figure 2**). Similarly, at 24 h, we observed that uninfected *daw* mutants contained significantly fewer hemocytes compared to w^{1118} larvae ($p = 0.0119$). We then estimated the total

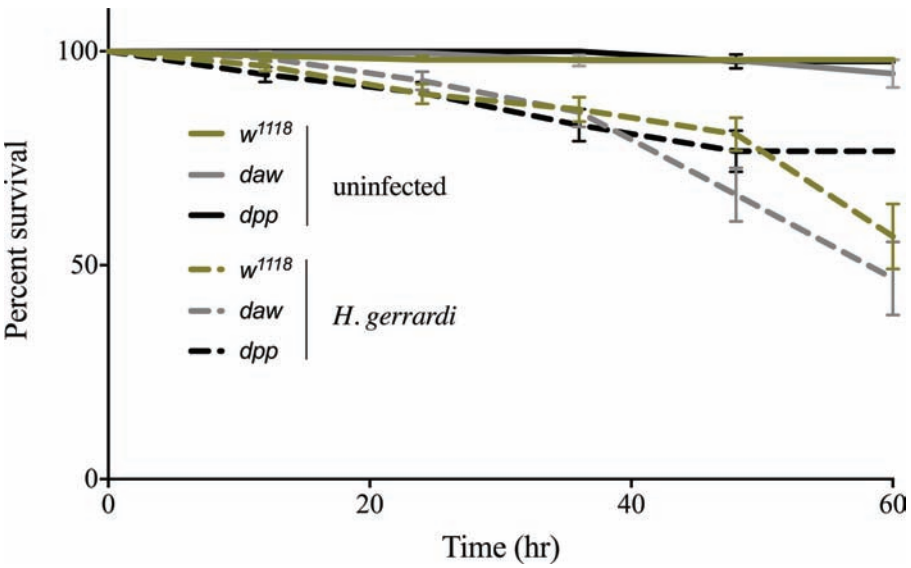

FIGURE 1 | Survival analysis of TGF-ß mutant larvae upon infection with the parasitic nematode *H. gerrardi*. *Daw* and *dpp* mutants together with their background control (*w1118*) larvae were infected with *H. gerrardi* symbiotic nematodes. Treatment with water served as negative control. Larval survival was counted every 12 h following infection. There is no significant difference in the survival of uninfected *daw* and *dpp* mutants relative to their background control (*w1118*). In addition, no significant difference is found between nematode-infected *daw* or *dpp* mutants and *w1118* individuals (non-significant differences are not indicated).

number of hemocytes in response to *H. gerrardi* and found that at 3 h post nematode infection, hemocyte numbers in *daw* mutants and w^{1118} control larvae were significantly lower relative to uninfected controls (*daw*, $p = 0.0008$; control, $p = 0.0023$). However, at the same time point, *dpp* mutants did not show any significant changes in hemocytes numbers in response to *H. gerrardi* infection. We also did not observe any differences in hemocyte numbers between infected or uninfected mutants and w^{1118} larvae at the 24-h time point. These results indicate that both activin and BMP branches of TGF-ß signaling in *D. melanogaster* are potentially involved in regulating the number of circulating hemocytes in the absence of infection.

Nematode-Infected *daw* Mutants Express *Duox* at Higher Levels

The production of reactive oxygen species (ROS) and nitric oxide (NO), mediated by dual oxidase (Duox) and nitric oxide synthase (Nos) enzymes, respectively, constitutes an essential regulator of diverse biological processes that include the immune response against bacterial infection (Marletta, 1994; Kuraishi et al., 2013; Eleftherianos et al., 2014). In addition, in mammals in the absence of infection, TGF-ß signaling is potentially regulated by ROS and NO responses (Saura et al., 2005; Jain et al., 2013). However, ROS and NO responses in *D. melanogaster* in the context of parasitic nematode infection and whether TGF-ß signaling participates in the regulation of these processes have not been examined yet. To investigate a potential link between these responses and TGF-ß signaling, we used qRT-PCR and gene-specific primers to determine the transcript levels of (*Nos*) and (*Duox*) in *daw* and *dpp* mutant larvae 24 h after infection with *H. gerrardi* nematodes. We found no statistically significant differences in *Nos* transcript levels between nematode-infected *daw* or *dpp* mutants and their w^{1118} background controls (**Figure 3A**). However, the expression of *Duox* in infected *daw* mutants was upregulated compared to w^{1118} larvae ($p = 0.00419$, **Figure 3B**) and *dpp* mutants ($p = 0.0022$, **Figure 3B**). These results suggest a link between the ROS response and the activin branch of TGF-ß signaling in *D. melanogaster* upon response to parasitic nematode infection.

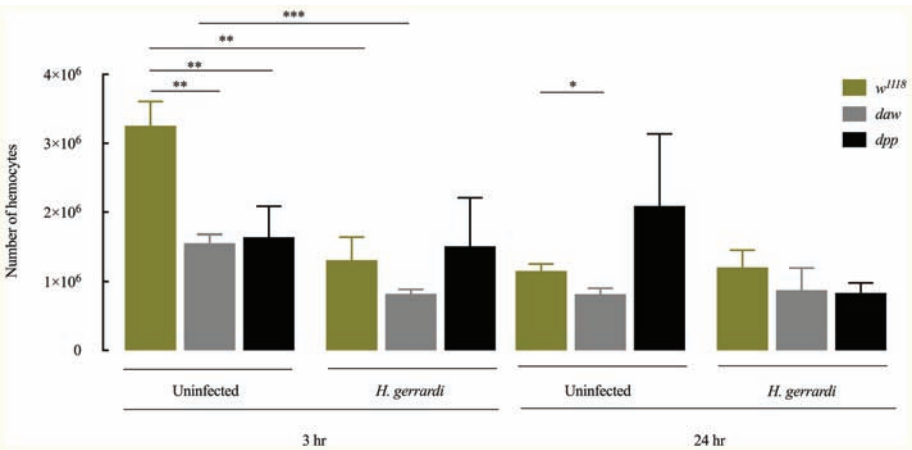

FIGURE 2 | Total number of circulating hemocytes in *Drosophila melanogaster* TGF-ß mutant larvae upon infection with the parasitic nematodes *Heterorhabditis gerrardi*. Hemolymph samples were collected at 3 and 24 h after infection. Numbers of hemocytes in uninfected *daw* and *dpp* mutants are significantly reduced at 3 h relative to their background control (*w1118*). *Daw* mutants contain significantly reduced numbers of hemocytes upon nematode infection. Asterisks indicate significant differences between experimental treatments (*$p < 0.05$, **$p < 0.01$, ***$p < 0.001$; non-significant differences are not indicated).

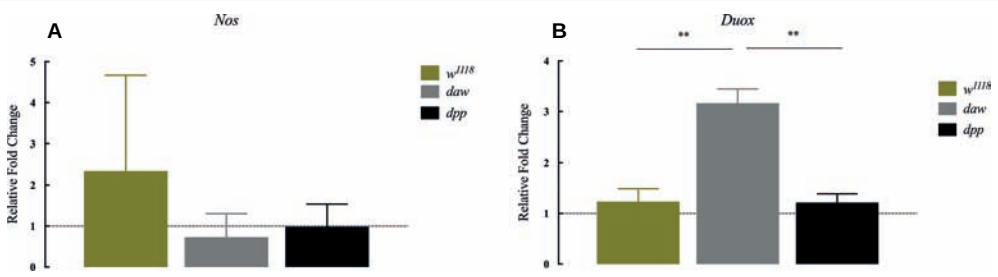

FIGURE 3 | Expression of *Nos* and *Duox* in *Drosophila melanogaster* TGF-ß mutant larvae at 24 h after infection with the parasitic nematodes *Heterorhabditis gerrardi*. *Nos* and *Duox* gene transcript levels in infected larvae are shown as relative fold change normalized to uninfected controls. **(A)** There is no significant change in the expression of *Nos* between the TGF-ß mutants relative to their background control (*w1118*). **(B)** Expression of *Duox* in *daw* mutants is upregulated compared to the background controls (**$p = 0.00419$ and **$p = 0.0022$, respectively; non-significant differences are not indicated).

The Activin Signaling Suppresses the Phenoloxidase Response in Response to *H. gerrardi*

Previous results indicate that ubiquitous knockdown of *daw* in *D. melanogaster* adult flies results in the formation of melanotic tumors suggesting an association between the TGF-ß activin branch and regulation of the melanization response (Clark et al., 2011). To investigate whether inactivation of TGF-ß signaling in *D. melanogaster* modifies the phenoloxidase response in the context of nematode infection, we challenged BMP and activin loss-of-function mutant larvae with *H. gerrardi* parasites, and 24 h later, we estimated the expression of prophenoloxidase genes *PPO1*, *PPO2*, and *PPO3* using qRT-PCR and gene-specific primers (Tang, 2009). We found no statistically significant differences in the transcript levels of *PPO1* and *PPO2* in *daw* or *dpp* mutants relative to w^{1118} control larvae upon *H. gerrardi* infection (**Figures 4A,B**). However, *PPO3* transcript levels were significantly reduced in nematode-infected *daw* ($p = 0.0140$) and *dpp* mutants ($p = 0.0169$) compared to w^{1118} controls (**Figure 4C**). We then determined the phenoloxidase enzyme activity in the hemolymph of *daw* and *dpp* mutant larvae infected with *H. gerrardi*. We found that phenoloxidase activity in *daw* mutant larvae was significantly reduced upon nematode infection relative to uninfected counterparts ($p = 0.0008$, **Figure 4D**). These results imply that the activin branch of TGF-ß signaling in *D. melanogaster* might be involved in suppressing phenoloxidase response in response to *H. gerrardi* nematode infection.

Size of Lipid Droplets Increases in Nematode-Infected *daw* and *dpp* Mutants

Lipid droplets are vital energy storage organelles found in many organisms. Recent findings suggest that lipid droplets increase in size in *D. melanogaster* infected with *Steinernema carpocapsae* nematodes, which implies a participation in the interaction with certain nematode parasites (Yadav et al., 2018). To determine lipid droplet status in the fat body of TGF-ß-deficient larvae, we stained lipid droplets with Nile red (red) and DAPI (blue) and measured lipid droplet sizes in *daw* and *dpp* loss-of-function mutant larvae (**Figures 5A–C**). We found that lipid droplets in uninfected *dpp* mutants significantly increased in size compared to w^{1118} controls (**Figure 5B**; $p = 0.0458$). However, uninfected *daw* mutants had significantly smaller lipid droplets relative to w^{1118} larvae (**Figure 4B**; $p < 0.0001$). Then, we determined lipid droplet sizes 24 h post *H. gerrardi* infection in *daw* and *dpp* mutants. Size of lipid droplets significantly increased in nematode-infected *daw* and *dpp* mutants compared to uninfected larvae (**Figure 5C**; $p < 0.0001$). Also, nematode infected w^{1118} controls contained significantly smaller lipid droplets relative to uninfected individuals (**Figure 5C**; $p = 0.0221$). To further assess changes

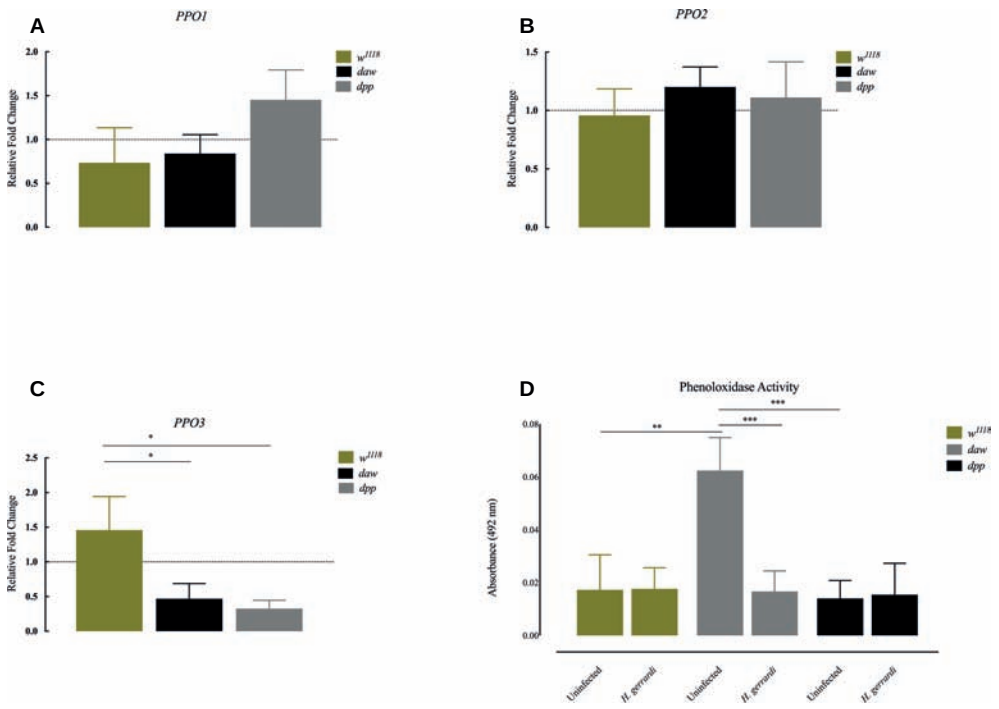

FIGURE 4 | Expression of *PPO* genes and activity of phenoloxidase in *Drosophila melanogaster* TGF-ß mutant larvae at 24 h after infection with the parasitic nematodes *Heterorhabditis gerrardi*. Transcript levels of *PPO1*, *PPO2*, and *PPO3* in nematode-infected larvae are shown as relative fold change normalized to uninfected controls. **(A,B)** There is no significant change in the expression of *PPO1* and *PPO2* between nematode-infected *daw* and *dpp* mutants relative to their background control (*w1118*). **(C)** Expression of *PPO3* is reduced in nematode-infected *daw* (*$p = 0.0140$) and *dpp* mutants (*$p = 0.0169$) compared to their background control (*w1118*). **(D)** Phenoloxidase activity in the hemolymph of *daw* mutants is significantly reduced upon *H. gerrardi* nematode infection compared to uninfected individuals (**$p = 0.0022$, ***$p = 0.0008$; non-significant differences are not indicated).

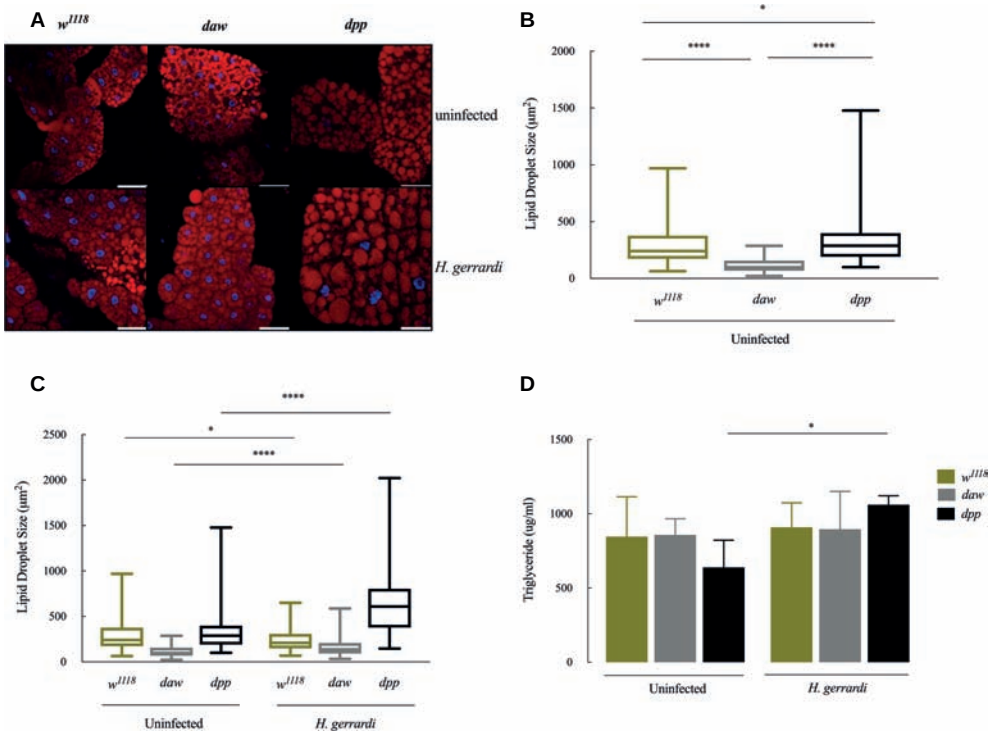

FIGURE 5 | Lipid metabolism in *Drosophila melanogaster* TGF-ß mutant larvae at 24 h upon infection with the parasitic nematodes *Heterorhabditis gerrardi.* **(A)** Confocal microscopy images of lipid droplets in the fat body of *H. gerrardi*-infected and uninfected *D. melanogaster daw* and *dpp* mutants and their background controls (*w1118*). **(B)** Size of lipid droplets in the fat body of uninfected *daw* and *dpp* mutants compared to their background controls (*w1118*). Size of lipid droplets in uninfected *dpp* mutants significantly increases compared to background controls (*w1118*) and *daw* mutants. Size of lipid droplets in uninfected *daw* mutants significantly decreases relative to background controls (*w1118*). **(C)** Fat body lipid droplet sizes in *daw* and *dpp* mutants responding to *H. gerrardi* infection relative to uninfected larvae. Size of lipid droplets significantly increases in *daw* and *dpp* mutants infected with *H. gerrardi* nematodes compared to uninfected larvae. Infected background control (*w1118*) larvae contain significantly lipid droplets of smaller size relative to uninfected individuals. **(D)** Triglyceride levels in TGF-ß mutant larvae 24 h after infection with *H. gerrardi.* Triglyceride content in nematode-infected *dpp* mutant larvae significantly increases compared to uninfected larvae. Scale bar is 100 µm. Asterisks indicate significant differences between experimental treatments (*$p < 0.05$, ****$p < 0.0001$; non-significant differences are not indicated).

in lipid metabolism in TGF-ß-deficient *D. melanogaster* larvae in the context of nematode infection, we estimated triglyceride concentrations in *daw* and *dpp* mutant larvae challenged with *H. gerrardi* (**Figure 5D**). Triglyceride levels in *dpp* mutants infected with the parasitic nematodes were significantly elevated compared to uninfected larvae ($p = 0.0193$), but there were no statistically significant changes in *daw* mutants relative to uninfected individuals. These findings suggest that both BMP and activin branches of TGF-ß signaling in *D. melanogaster* regulate fat body lipid droplet size during response to nematode infection.

Nematode-Infected *dpp* Mutants Have Elevated Glycogen Levels

In *D. melanogaster*, glucose is an essential resource for energy production. Glycogen is synthesized and stored several tissues and is required for energy metabolism (Mattila and Hietakangas, 2017). In mammals, there is a direct link between regulation of carbohydrate homeostasis and TGF-ß signaling in the absence of an infection (Yadav et al., 2011). To investigate whether TGF-ß signaling affects carbohydrate metabolism in *D. melanogaster* anti-nematode response, we estimated glucose and glycogen levels 24 h post infection with *H. gerrardi*. We found that upon nematode infection, infected w^{1118} control larvae had significantly increased glucose levels compared to uninfected individuals (**Figure 6A**; $p = 0.0381$). However, we did not observe any statistically significant changes in infected *daw* and *dpp* mutant larvae relative to uninfected controls. We found that only nematode-infected *daw* mutants had significantly elevated levels of glycogen relative to uninfected larvae (**Figure 6B**; $p = 0.0482$). These results indicate that the activin branch of TGF-ß signaling in *D. melanogaster* might participate in modulating glycogen metabolism in the context of nematode infection.

DISCUSSION

In this study, we explored the contribution of activin and BMP branches of TGF-β signaling in regulating immune activity in *D. melanogaster*. For this, we analyzed changes in larval survival capacity, hemocyte numbers, activation of ROS and NO, and melanization response in uninfected *daw* or *dpp* loss-of-function mutant larvae as well as in larvae infected with *H. gerrardi* parasitic nematodes. We have found a significant

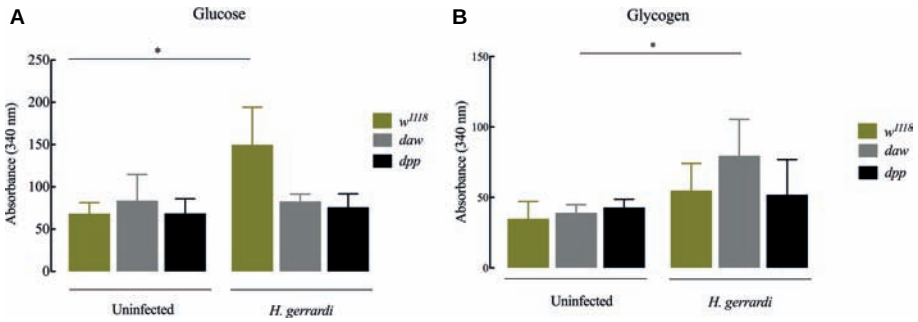

FIGURE 6 | Carbohydrate metabolism in *Drosophila melanogaster* TGF-ß mutant larvae at 24 h upon infection with the parasitic nematodes *H. gerrardi.* **(A)** Level of glucose in infected *daw* and *dpp* mutant larvae. Nematode-infected background controls (*w1118*) have significantly higher levels of glucose relative to uninfected larvae (*p = 0.0381). **(B)** Level of glycogen in infected *daw* and *dpp* mutant larvae. Nematode-infected *daw* mutants have significantly higher levels of glycogen relative to uninfected larvae (*p = 0.0482; non-significant differences are not indicated).

decrease in the number of circulating hemocytes in uninfected *daw* and *dpp* mutants compared to their background controls, but no significant change in hemocyte numbers following nematode infection. However, *daw* mutants have higher expression of *Duox* and decreased phenoloxidase activity in response to nematode infection compared to their background controls. We further examined the metabolic activity of *daw* and *dpp* mutant larvae in the presence or absence of *H. gerrardi* infection and found an increase in the size of lipid droplets in both mutants as well as elevated glycogen levels in *daw* mutants upon nematode challenge.

Hemocytes are the central regulators of the cellular immune response against microbial infection in insects, and previous information supports the notion that total number of circulating hemocytes constitutes a robust indication for the level of activation of the cellular arm of the insect innate immune system to act against foreign invaders (Parsons and Foley, 2016). To investigate the contribution of activin and BMP signaling on cellular immune activity in the context of parasitic nematode infection, we estimated changes in hemocyte numbers in uninfected *D. melanogaster daw* and *dpp* mutant larvae and larvae infected with *H. gerrardi* nematodes. Our results indicate that both *daw* and *dpp* uninfected mutants contain significantly fewer hemocytes relative to their background controls. Interestingly, a recent study has shown that the activin branch extracellular ligand Actβ is expressed in sensory neurons, and silencing of Actβ results in fewer hemocyte numbers in *D. melanogaster* larvae in the absence of infection (Makhijani et al., 2017). In agreement with this recent study, our results support the concept that the activin branch of TGF-ß signaling participates in the regulation of hemocyte population at the larval stage of *D. melanogaster*. In contrast, we did not detect any significant changes in hemocyte numbers between nematode-infected *daw* or *dpp* mutants and their background controls, which probably explains the lack of alteration in the survival of the TGF-β mutants in response to *H. gerrardi*. This result further implies that *H. gerrardi* infection has no effect on the total number of circulating hemocytes in *D. melanogaster* larvae. Therefore, current findings suggest that *H. gerrardi* infection does not alter the dynamics of hemocyte numbers in *D. melanogaster* and that the activin and BMP branches of TGF-ß signaling modulate the amount of hemocytes in the uninfected state of the larval stage.

The phenoloxidase enzyme in the melanization cascade regulates the formation of melanin at wound sites and around invading pathogens in the insect hemolymph (Eleftherianos and Revenis, 2011). Previous findings signify that ubiquitous silencing of *daw* in the adult fly causes melanotic tumors mostly in the abdomen, indicating that activin signaling controls the inhibition of the melanization response (Clark et al., 2011). Similarly, here we have found that uninfected *daw* mutants contain significantly higher levels of hemolymph phenoloxidase compared to *dpp* mutants and their background controls. This might suggest a direct or indirect interaction between phenoloxidase activity and activin signaling in response to nematode infection, which will form a subject of our future studies. It is also important to consider that *Photorhabdus* bacteria released from *Heterorhabditis* nematodes into the insect hemolymph secrete molecules, such as rhabduscin and hydroxystilbene, that interfere with the melanization cascade and suppress phenoloxidase activity in the infected insects (Eleftherianos et al., 2007; Crawford et al., 2012). Here, we have found that symbiotic *H. gerrardi* nematodes (containing mutualistic *P. asymbiotica* bacteria) fail to alter phenoloxidase activity in background control and *dpp* mutant larvae, but they are able to suppress the activity of the enzyme in *daw* mutants. This implies that phenoloxidase activity in the hemolymph of *D. melanogaster* larvae during infection with *H. gerrardi* symbiotic nematodes is regulated by the activin signaling of the TGF-β pathway.

Immune cells are required to maintain their cellular metabolism to function efficiently in combating pathogens (Loftus and Finlay, 2016). During infection, *Staphylococcus aureus* induces changes in the host extracellular environment by reducing oxygen and nutrient availability, which generates significant metabolic stress in the mammalian host (Vitko et al., 2015). In the current study, we aimed at understanding the contribution of activin and BMP branches of TGF-ß signaling to metabolic changes in uninfected *D. melanogaster* larvae as well as during nematode infection. It has been previously shown

that the BMP ligand *gbb* is essential in the fat body of uninfected *D. melanogaster* larvae to maintain lipid homeostasis and metabolism. *Gbb* loss-of function mutants also display abnormalities in fat body morphology (Ballard et al., 2010). Here, we have also found a significant increase in the size of lipid droplets in uninfected *dpp* mutants compared to background controls indicating the contribution of BMP signaling in maintaining lipid metabolism. However, uninfected *daw* mutants contain significantly smaller lipid droplets suggesting the disruption of lipid metabolism in these larvae. A previous study reported that in *D. melanogaster* embryos histones bound to cytosolic lipid droplets can eliminate both Gram-positive and Gram-negative bacteria *in vitro*. (Anand et al., 2012). In addition, infection with the intracellular bacteria *Mycobacterium tuberculosis*, *M. bovis*, and *M. leprae* leads to the accumulation of lipid droplets in macrophages and Schwann cells in mammalian hosts (D'Avila et al., 2006; Russell et al., 2009; Mattos et al., 2011). Also, infection with the intracellular parasite *Trypanosoma cruzi* in rats induces an increase in the size of lipid droplets in macrophages (Melo et al., 2003). In the fat body of *D. melanogaster,* size of lipid droplets increases in response to infection with the parasitic nematode *S. carpocapsae* carrying the mutualistic bacteria *Xenorhabdus nematophila* (Yadav et al., 2018). In contrast, here we have demonstrated that upon infection with *H. gerrardi* nematodes, which contain the mutualistic bacteria *P. asymbiotica*, size of lipid droplets in the fat body of background control larvae significantly decreases compared to uninfected individuals, suggesting reduced lipid accumulation in this tissue. Such alterations in host lipid metabolism might be an indication of pathogen-specific immune or metabolic responses (Govind, 2008). In our experiments, infection with *H. gerrardi* causes a significant increase in the size of lipid droplets in both *daw* and *dpp* mutant larvae, suggesting that both activin and BMP branches might be involved in the regulation of lipid metabolism in *D. melanogaster* during response to nematode insult.

The current findings highlight the overlapping interactions between the two TGF-ß signaling pathway branches activin and BMP with immune activity and maintenance of lipid and carbohydrate metabolism in uninfected *D. melanogaster* larvae as well as during infection with potent parasitic nematodes. Future research to examine the molecular and functional details of these interactions will contribute toward clarifying the exact role of activin and BMP branches in the host anti-nematode immune response. Due to conservation of innate immune signaling and function in humans, the identification of key immune signaling components will create the basis for identifying novel antihelminth treatment strategies. Alternatively, a better understanding of how parasitic nematodes interact with the immune and metabolic processes of model insects host could potentially lead to the development of innovative tactics for the effective management of agricultural insect pests and vectors of human diseases.

AUTHOR CONTRIBUTIONS

YO designed and conducted the experiments, analyzed the data, constructed the figures, interpreted the results, and wrote drafts of the manuscript. IE designed the experiments, interpreted the results, and revised the manuscript.

FUNDING

This research is funded by the National Institute of Allergy and Infectious Diseases (grants 1R01AI110675 and 1R56AI110675).

ACKNOWLEDGMENTS

We thank Kyle Devine for maintaining and amplifying the laboratory fly lines and members of the Department of Biological Sciences at George Washington University for providing feedback to manuscript drafts.

SUPPLEMENTARY MATERIAL

The Supplementary Material for this article can be found online at: https://www.frontiersin.org/articles/10.3389/fphys.2019.00716/full#supplementary-material

REFERENCES

Anand, P., Cermelli, S., Li, Z., Kassan, A., Bosch, M., and Sigua, R. (2012). A novel role for lipid droplets in the organismal antibacterial response. *elife* 1:e00003. doi: 10.7554/eLife.00003

Ballard, S. L., Jarolimova, J., and Wharton, K. A. (2010). Gbb/BMP signaling is required to maintain energy homeostasis in *Drosophila*. *Dev. Biol.* 337, 375–385. doi: 10.1016/j.ydbio.2009.11.011

Castillo, J. C., Creasy, T., Kumari, P., Shetty, A., Shokal, U., Tallon, L. J., et al. (2015). *Drosophila* anti-nematode and antibacterial immune regulators revealed by RNA-Seq. *BMC Genomics* 16:519. doi: 10.1186/s12864-015-1690-2

Castillo, J. C., Reynolds, S. E., and Eleftherianos, I. (2011). Insect immune responses to nematode parasites. *Trends Parasitol.* 27, 537–547. doi: 10.1016/j.pt.2011.09.001

Clark, R. I., Woodcock, K. J., Geissmann, F., Trouillet, C., and Dionne, M. S. (2011). Multiple TGF-β superfamily signals modulate the adult *Drosophila* immune response. *Curr. Biol.* 21, 1672–1677. doi: 10.1016/j.cub.2011.08.048

Crawford, J. M., Portmann, C., Zhang, X., Roeffaers, M. B., and Clardy, J. (2012). Small molecule perimeter defense in entomopathogenic bacteria. *Proc. Natl. Acad. Sci. USA* 109, 10821–10826. doi: 10.1073/pnas.1201160109

D'Avila, H., Melo, R. C., Parreira, G. G., Werneck-Barroso, E., Castro-Faria-Neto, H. C., and Bozza, P. T. (2006). *Mycobacterium bovis* bacillus Calmette-Guérin induces TLR2-mediated formation of lipid bodies: intracellular domains for eicosanoid synthesis in vivo. *J. Immunol.* 176, 3087–3097. doi: 10.4049/jimmunol.176.5.3087

Dobens, L. L., and Raftery, L. A. (1998). *Drosophila* oogenesis: a model system to understand TGF-ß/Dpp directed cell morphogenesis. *Ann. N. Y. Acad. Sci.* 857, 245–247. doi: 10.1111/j.1749-6632.1998.tb10123.x

Duvic, B., Hoffmann, J. A., Meister, M., and Royet, J. (2002). Notch signaling controls lineage specification during *Drosophila* larval hematopoiesis. *Curr. Biol.* 12, 1923–1927. doi: 10.1016/S0960-9822(02)01297-6

Eleftherianos, I., Boundy, S., Joyce, S. A., Aslam, S., Marshall, J. W., Cox, R. J., et al. (2007). An antibiotic produced by an insect-pathogenic bacterium

suppresses host defenses through phenoloxidase inhibition. *Proc. Natl. Acad. Sci. USA* 104, 2419–2424. doi: 10.1073/pnas.0610525104

Eleftherianos, I., Castillo, J. C., and Patrnogic, J. (2016b). TGF-ß signaling regulates resistance to parasitic nematode infection in *Drosophila melanogaster*. *Immunobiology* 221, 1362–1368. doi: 10.1016/j.imbio.2016.07.011

Eleftherianos, I., More, K., Spivack, S., Paulin, E., Khojandi, A., and Shukla, S. (2014). Nitric oxide levels regulate the immune response of *Drosophila melanogaster* reference laboratory strains to bacterial infections. *Infect. Immun.* 82, 4169–4181. doi: 10.1128/IAI.02318-14

Eleftherianos, I., and Revenis, C. (2011). Role and importance of phenoloxidase in insect hemostasis. *J. Innate Immun.* 3, 28–33. doi: 10.1159/000321931

Eleftherianos, I., Shokal, U., Yadav, S., Kenney, E., and Maldonado, T. (2016a). "Insect immunity to entomopathogenic nematodes and their mutualistic bacteria" in *The molecular biology of Photorhabdus bacteria*. ed. R. H. ffrench-Constant (Cham, Switzerland: Springer), 124–148.

ffrench-Constant, R. H., Eleftherianos, I., and Reynolds, S. E. (2007). Nematode symbionts shed light on invertebrate immunity. *Trends Parasitol.* 23, 514–517. doi: 10.1016/j.pt.2007.08.021

Gerrard, J. G., Joyce, S. A., Clarke, D. J., ffrench-Constant, R. H., Nimmo, G. R., Looke, D. F., et al. (2006). Nematode symbiont for *Photorhabdus asymbiotica*. *Emerg. Infect. Dis.* 12, 1562–1564. doi: 10.3201/eid1210.060464

Govind, S. (2008). Innate immunity in *Drosophila*: pathogens and pathways. *Insect Sci.* 15, 29–43. doi: 10.1111/j.1744-7917.2008.00185.x

Hallem, E. A., Rengarajan, M., Ciche, T. A., and Sternberg, P. W. (2007). Nematodes, bacteria, and flies: a tripartite model for nematode parasitism. *Curr. Biol.* 17, 898–904. doi: 10.1016/j.cub.2007.04.027

Harradine, K. A., and Akhurst, R. J. (2009). Mutations of TGF-ß signaling molecules in human disease. *Ann. Med.* 6, 403–414. doi: 10.1080/07853890600919911

Jain, M., Rivera, S., Monclus, E. A., Synenki, L., Zirk, A., and Eisenbart, J. (2013). Mitochondrial reactive oxygen species regulate transforming growth factor-*β* signaling. *J. Biol. Chem.* 288, 770–777. doi: 10.1074/jbc.M112.431973

Kuraishi, T., Hori, A., and Kurata, S. (2013). Host-microbe interactions in the gut of *Drosophila melanogaster*. *Front. Physiol.* 4:375. doi: 10.3389/fphys.2013.00375

Lecuit, T., Brook, W. J., Ng, M., Calleja, M., Sun, H., and Cohen, S. M. (1996). Two distinct mechanisms for long-range patterning by decapentaplegic in the *Drosophila* wing. *Nature* 381, 387–393. doi: 10.1038/381387a0

Loftus, R. M., and Finlay, D. K. (2016). Immunometabolism: cellular metabolism turns immune regulator. *J. Biol. Chem.* 291, 1–10. doi: 10.1074/jbc.R115.693903

Makhijani, K., Alexander, B., Rao, D., Petraki, S., Herboso, L., Kukar, K., et al. (2017). Regulation of *Drosophila* hematopoietic sites by activin-beta from active sensory neurons. *Nat. Commun.* 8:15990. doi: 10.1038/ncomms15990

Marletta, M. A. (1994). Nitric oxide synthase: aspects concerning structure and catalysis. *Cell* 78, 927–930. doi: 10.1016/0092-8674(94)90268-2

Masucci, J. D., Miltenberger, R. J., and Hoffmann, F. M. (1990). Pattern-specific expression of the *Drosophila* decapentaplegic gene in imaginal disks is regulated by 3′ cis-regulatory elements. *Genes Dev.* 4, 2011–2023. doi: 10.1101/gad.4.11.2011

Mattila, J., and Hietakangas, C. (2017). Regulation of carbohydrate energy metabolism in *Drosophila melanogaster*. *Genetics* 207, 1231–1253. doi: 10.1534/genetics.117.199885

Mattos, K. A., Lara, F. A., Oliveira, V. G., Rodrigues, L. S., D'Avila, H., Melo, R. C. N., et al. (2011). Modulation of lipid droplets by *Mycobacterium leprae* in Schwann cells: a putative mechanism for host lipid acquisition and bacterial survival in phagosomes. *Cell. Microbiol.* 13, 259–273. doi: 10.1111/j.1462-5822.2010.01533.x

Melo, R. C. N., D'Avila, H., Fabrino, D. L., Almeida, P. E., and Bozza, P. T. (2003). Macrophage lipid body induction by Chagas disease in vivo: putative intracellular domains for eicosanoid formation during infection. *Tissue Cell* 35, 59–67. doi: 10.1016/S0040-8166(02)00105-2

Parsons, B., and Foley, E. (2016). Cellular immune defenses of *Drosophila melanogaster*. *Dev. Comp. Immunol.* 58, 95–101. doi: 10.1016/j.dci.2015.12.019

Patrnogic, J., Heryanto, C., and Eleftherianos, I. (2018a). Wounding-induced upregulation of the bone morphogenic protein signalling pathway in *Drosophila* promotes survival against parasitic nematode infection. *Gene* 673, 112–118. doi: 10.1016/j.gene.2018.06.052

Patrnogic, J., Heryanto, C., and Eleftherianos, I. (2018b). Transcriptional up-regulation of the TGF- β intracellular signaling transducer mad of *Drosophila* larvae in response to parasitic nematode infection. *Innate Immun.* 24, 349–356. doi: 10.1177/1753425918790663

Peterson, A. J., and O'Connor, M. B. (2014). Strategies for exploring TGF-ß signaling in *Drosophila*. *Methods* 68, 183–193. doi: 10.1016/j.ymeth.2014.03.016

Plichta, K. L., Joyce, S. A., Clarke, D., Waterfield, N., and Stock, S. P. (2009). *Heterorhabditis gerrardi* n. sp. (Nematoda: Heterorhabditidae): the hidden host of *Photorhabdus asymbiotica* (Enterobacteriaceae: gamma-Proteobacteria). *J. Helminthol.* 83, 309–230. doi: 10.1017/S0022149X09222942

Raftery, L. A., and Sutherland, D. J. (1999). TGF-beta family signal transduction in *Drosophila* development: from mad to Smads. *Dev. Biol.* 210, 251–268. doi: 10.1006/dbio.1999.9282

Rämet, M. (2012). The fruit fly *Drosophila melanogaster* unfolds the secrets of innate immunity. *Acta Paediatr.* 101, 900–905. doi: 10.1111/j.1651-2227.2012.02740.x

Russell, D. G., Cardona, P. J., Kim, M. J., Allain, S., and Altare, F. (2009). Foamy macrophages and the progression of the human tuberculosis granuloma. *Nat. Immunol.* 10, 943–948. doi: 10.1038/ni.1781

Saura, M., Zaragoza, C., Herranz, B., Griera, M., Diez-Marques, L., Rodriguez-Puyol, D., et al. (2005). Nitric oxide regulates transforming growth factor-beta signaling in endothelial cells. *Circ. Res.* 97, 1115–1123. doi: 10.1161/01.RES.0000191538.76771.66

Shi, Y., and Massagué, J. (2003). Mechanisms of TGF-ß signaling from cell membrane to the nucleus. *Cell* 113, 685–700. doi: 10.1016/S0092-8674(03)00432-X

Shokal, U., Kopydlowski, H., and Eleftherianos, I. (2017). The distinct function of *Tep2* and *Tep6* in the immune defense of *Drosophila melanogaster* against the pathogen *Photorhabdus*. *Virulence* 88, 1668–1682. doi: 10.1080/21505594.2017.1330240

Stock, S. P., and Blair, H. G. (2008). Entomopathogenic nematodes and their bacterial symbionts: the inside out of a mutualistic association. *Symbiosis* 46, 65–75.

Tang, H. (2009). Regulation and function of the melanization reaction in *Drosophila*. *Fly* 3, 105–111. doi: 10.4161/fly.3.1.7747

Tennessen, J. M., Barry, W. E., Cox, J., and Thummel, C. S. (2014). Methods for studying metabolism in *Drosophila*. *Methods* 68, 105–115. doi: 10.1016/j.ymeth.2014.02.034

Vitko, N. P., Spahich, N. A., and Richardson, A. R. (2015). Glycolytic dependency of high-level nitric oxide resistance and virulence in *Staphylococcus aureus*. *MBio* 6:e00045-15. doi: 10.1128/mBio.00045-15

Vlisidou, I., and Wood, W. (2015). *Drosophila* blood cells and their role in immune responses. *FEBS J.* 282, 1368–1382. doi: 10.1111/febs.13235

White, G. F. R. (1927). A method for obtaining infective nematode larvae from cultures. *Science* 66, 302–303. doi: 10.1126/science.66.1709.302-a

Yadav, S., Daugherty, S., Shetty, A. C., and Eleftherianos, I. (2017). RNAseq analysis of the *Drosophila* response to the entomopathogenic nematode *Steinernema*. *G3* 7, 1955–1967. doi: 10.1534/g3.117.041004

Yadav, S., Frazer, J., Banga, A., Pruitt, K., Harsh, S., Jaenike, J., et al. (2018). Endosymbiont-based immunity in *Drosophila* melanogaster against parasitic nematode infection. *PLoS One* 13:e0192183. doi: 10.1371/journal.pone.0192183

Yadav, H., Quijano, C., Kamaraju, A. K., Gavrilova, O., Malek, R., Chen, W., et al. (2011). Protection from obesity and diabetes by blockade of tgf-beta/smad3 signaling. *Cell Metab.* 14, 67–79. doi: 10.1016/j.cmet.2011.04.013

Zi, Z., Chapnick, D. A., and Liu, X. (2012). Dynamics of TGF-ß/Smad signaling. *FEBS Lett.* 586, 1921–1928. doi: 10.1016/j.febslet.2012.03.063

Conflict of Interest Statement: The authors declare that the research was conducted in the absence of any commercial or financial relationships that could be construed as a potential conflict of interest.

frontiers in Physiology

ORIGINAL RESEARCH
published: 19 June 2019
doi: 10.3389/fphys.2019.00715

Aphidius ervi Teratocytes Release Enolase and Fatty Acid Binding Protein Through Exosomal Vesicles

Rosanna Salvia[1], Annalisa Grimaldi[2], Rossana Girardello[2], Carmen Scieuzo[1], Andrea Scala[1], Sabino A. Bufo[1,3], Heiko Vogel[4] and Patrizia Falabella[1]**

[1]*Department of Sciences, University of Basilicata, Potenza, Italy,* [2]*Department of Biotechnology and Life Sciences, University of Insubria, Varese, Italy,* [3]*Department of Geography, Environmental Management & Energy Studies, University of Johannesburg, Johannesburg, South Africa,* [4]*Department of Entomology, Max Planck Institute for Chemical Ecology, Jena, Germany*

The molecular bases of the host-parasitoid interactions in the biological system *Acyrthosiphon pisum* (Harris) (Homoptera, Aphididae) and *Aphidius ervi* (Haliday) (Hymenoptera, Braconidae) have been elucidated allowing the identification of a gamma-glutamyl transpeptidase, the active component of maternal venom secretion, and teratocytes, the embryonic parasitic factors responsible for host physiology regulation after parasitization. Teratocytes, cells deriving from the dissociation of the serosa, the parasitoid embryonic membrane, are responsible for extra-oral digestion of host tissues in order to provide a suitable nutritional environment for the development of parasitoid larvae. Teratocytes rapidly grow in size without undergoing any cell division, synthesize, and release in the host hemolymph two proteins: a fatty acid binding protein (*Ae*-FABP) and an enolase (*Ae*-ENO). *Ae*-FABP is involved in transport of fatty acids deriving from host tissues to the parasitoid larva. *Ae*-ENO is an extracellular glycolytic enzyme that functions as a plasminogen like receptor inducing its activation to plasmin. Both *Ae*-FABP and *Ae*-ENO lack their signal peptides, and they are released in the extracellular environment through an unknown secretion pathway. Here, we investigated the unconventional mechanism by which teratocytes release *Ae*-FABP and Ae-ENO in the extracellular space. Our results, obtained using immunogold staining coupled with TEM and western blot analyses, show that these two proteins are localized in vesicles released by teratocytes. The specific dimension of these vesicles and the immunodetection of ALIX and HSP70, two exosome markers, strongly support the hypothesis that these vesicles are exosomes.

Keywords: teratocytes, *Aphidius ervi*, enolase, *Aphidius ervi*, fatty acid binding protein, vesicles, exosomes, unconventional protein secretion

OPEN ACCESS

Edited by:
Senthil-Nathan Sengottayan, Manonmaniam Sundaranar University, India

Reviewed by:
Sergio Angeli, Free University of Bozen-Bolzano, Italy
Aram Megighian, University of Padova, Italy

***Correspondence:**
Annalisa Grimaldi
annalisa.grimaldi@uninsubria.it
Patrizia Falabella
patrizia.falabella@unibas.it

Specialty section:
This article was submitted to Invertebrate Physiology, a section of the journal Frontiers in Physiology

Received: *19 February 2019*
Accepted: *23 May 2019*
Published: *19 June 2019*

Citation:
Salvia R, Grimaldi A, Girardello R, Scieuzo C, Scala A, Bufo SA, Vogel H and Falabella P (2019) Aphidius ervi Teratocytes Release Enolase and Fatty Acid Binding Protein Through Exosomal Vesicles. Front. Physiol. 10:715. doi: 10.3389/fphys.2019.00715

INTRODUCTION

Teratocytes are specialized cells derived from the embryonic serosal membrane dissociation during parasitoid egg hatching in some hymenopteran endoparasitoid species (Dahlman and Vinson, 1993; Hotta et al., 2001; Strand, 2014). Teratocytes, together with other parasitic factors of maternal origin, such as polydnaviruses, venom, and ovarian proteins, are the

"arsenal" of the parasitism success (Burke and Strand, 2014). Teratocytes rapidly grow in size without cell division, become highly polyploid, and release molecules impacting physiology, development, and nutritional suitability of colonized hosts (Dahlman and Vinson, 1993; Dahlman et al., 2003; Beckage and Gelman, 2004; Pennacchio and Strand, 2006). These large cells are characterized by a microvillar cell membrane, abundant endoplasmic reticulum, and numerous mitochondria, indicating that they are metabolically active (Pennacchio et al., 1994; Zhang et al., 1994). Teratocytes have been shown to synthesize and secrete a variety of proteins at all stages of parasitoid development (De Buron and Beckage, 1997). The nutritional role of teratocytes is generally mediated by digestion of selected host tissues, which release nutrients in a suitable form for the developing larvae (Falabella et al., 2000, 2009; Nakamatsu et al., 2002; Strand, 2014).

In the host-parasitoid system *Acyrthosiphon pisum* (Harris) (Homoptera, Aphididae) and *Aphidius ervi* (Haliday) (Hymenoptera, Braconidae), the cells of the serosal membrane dissociate into free teratocytes as soon as the parasitoid larva emerges in the host hemocoel. Five days after oviposition, 30 ± 5 free teratocytes can be observed in the host. After release, their number remains almost the same up to 7 days after parasitization and then decreases drastically to 18 ± 5 and 2 ± 1 teratocytes on days 8 and 9, respectively (Sabri et al., 2011). When released, the teratocytes are 40 ± 10 μm in diameter and increase in size during the two following days up to approximately 200 μm. At the same time, the cytoplasm fraction becomes progressively crowded with vesicles (Sabri et al., 2011).

Several proteins are synthesized and secreted by *A. ervi* teratocytes into the host hemocoel, and among them, two proteins with an apparent molecular mass of about 15 and 45 kDa are found in high abundance in the hemolymph of parasitized hosts (Falabella et al., 2000). These proteins lack the signal peptide, and they have been characterized as a fatty acid binding protein (*Ae*-FABP) (Falabella et al., 2005) and an enolase (*Ae*-ENO), respectively (Falabella et al., 2009; Grossi et al., 2016).

Ae-FABP shows a high affinity for C14-C18 saturated fatty acids (FAs) and for oleic and arachidonic acids (Falabella et al., 2005). The immunolocalization profile of *Ae*-FABP showed that it is distributed around lipid particles, abundantly present in the hemocoel of parasitized host aphids and in the midgut lumen of parasitoid larvae, suggesting that the protein acts essentially as a vector in host hemolymph, transferring FAs from the sites of host lipid digestion to the growing parasitoid larvae (Caccia et al., 2012). Enolase plays an important role in the glycolytic pathway (Walsh et al., 1989). When present in the extracellular environment on the surface of prokaryotic and eukaryotic cells, enolase evidences a main role in the activation of enzymes that allow the invasion of tissues by pathogens and tumor cells (Liu and Shih 2007; Marcilla et al., 2012; Silva et al., 2014). *Ae*-ENO is an extracellular enolase that contributes to the success of parasitism, acting as a receptor able to bind a host plasminogen-like molecule, which, once activated, induces the digestion of the host tissues. *In vivo* immunodetection experiments have shown that *Ae*-ENO is localized in round spots in the teratocyte cytoplasm and released into the host hemocoel, resulting in strong immunoreactivity in host embryos (Falabella et al., 2009). Accumulation of *Ae*-ENO in cytoplasmic vesicles oriented toward the cell membrane is observed followed by protein release outside of the cell. These vesicles seem to be localized on the cellular plasma membrane especially in microvilli, probably allowing the release of *Ae*-ENO into the extracellular space (Grossi et al., 2016).

Here, we demonstrate a possible secretory mechanism for *Ae*-ENO, extensible also to *Ae*-FABP, mediated by vesicles acting as mean of exocytosis, which was already speculated by Grossi et al. (2016). This mechanism seems to be shared by some micro-organisms that use an extracellular enolase to invade host tissues (Chavez-Munguia et al., 2011) and by several parasitic helminths releasing proteins, including enolase, through extracellular vesicles (Marcilla et al., 2012). Furthermore, we demonstrate that these vesicles are exosomes, mediating the extracellular transport of proteins lacking a signal peptide. We propose a non-canonical protein transport mechanism that represents the model of a possible strategy shared by different cell types and organisms involved in such processes.

MATERIALS AND METHODS

Insect Rearing

Aphidius ervi was reared on the host *Acyrthosiphon pisum* maintained on plants of *Vicia faba* L. Both insect cultures were started with material originally collected on alfalfa plants, in Southern Italy. Aphids and parasitoids were kept in separate environmental chambers both at 20 ± 1°C, relative humidity of 75 ± 5%, and an 18:6 light/dark photoperiod. Experimental third instar aphids were singly exposed in a glass vial to a few *A. ervi* females and returned to plants until dissection.

Teratocyte Collection and Stimulation

Teratocytes were collected as described by Falabella et al. (2000) from pea aphids, 5 days after parasitization by *A. ervi* and cultured in 1× phosphate-buffered saline (PBS) (pH 7.2). Briefly, aphids were dissected, and the released teratocytes were transferred into a 1.5 ml tube (Eppendorf, Hamburg, Germany) containing ice-cold PBS and allowed to settle for approximately 5 min on ice. The medium was then removed and replaced with an equal volume of PBS and teratocytes re-suspended by gentle swirling of the tube. This washing procedure was repeated at least three times.

Since ATP, through activation of the P2P7 ATP receptor, massively increases the release of vesicles (Bianco et al., 2005, Drago et al., 2017), teratocytes were exposed to 5 mM of ATP in PBS for 30 min to induce the production and release of vesicles in the extracellular environment.

Light Microscopy

Samples were collected 5 and 6 days after *A. ervi* female oviposition (as described above, paragraph 2.1). Briefly, each parasitized aphid was dissected in a Petri dish in 100 µl 1× PBS. A stereo microscope (Nikon, Tokyo, Japan) was used for dissections, and *A. ervi* larvae (5 days after parasitization) and teratocytes (5 and 6 days after parasitization) were carefully transferred in a drop of 1× PBS and then observed by a Nikon Eclipse 80i at 10× magnification. Images were recorded by a Nikon Digital Sight DS-U1 camera (Nikon, Tokyo, Japan).

Vesicle Isolation and Collection

After ATP exposure, teratocytes were gently removed using a micropipette and fixed for subsequent analyses, as described below. The incubation medium was subjected to differential centrifugation at 4°C as follows: 300 *g* for 5 min in order to remove debris, the obtained supernatant was then centrifuged at 1,200 g for 20 min, in order to separate any microvesicles (in the pellet) from exosomes (in supernatant). The exosome-rich supernatant was further centrifuged at 120,000 *g* for 1 h at 4°C in an ultracentrifuge (Beckman Coulter, Brea, CA, USA). The pellet, supposedly containing exosomes, was either resuspended in Laemmli buffer (Laemmli, 1970) for western blotting, or in 200 µl of ice-cold 1× PBS for further immunogold staining.

Scanning Electron Microscopy

To obtain 3D imaging by scanning electron microscopy (SEM), teratocytes were collected from the parasitized hosts as already described (Falabella et al., 2009) and were attached to a small glass slide (9 mm × 9 mm) coated with 0.1% poly-L-lysine (Hotta et al., 2001). Subsequently, cells were fixed with Karnovsky fixative (2% paraformaldehyde and 2.5% glutaraldehyde) in 0.1 M cacodylate buffer (pH 7.2) for 1 h at room temperature. To obtain fine three-dimensional SEM imaging, an improved osmium maceration technique was employed (Franzetti et al., 2012). Teratocytes were fixed with 1% glutaraldehyde in 0.1 M Na-cacodylate buffer (pH 7.4) for 1 h at room temperature. After washes in Na-cacodylate buffer, specimens were post-fixed in a solution of 1% osmium tetroxide, 1.25% potassium ferrocyanide for 2 h. After several washings, cells were dehydrated in an increasing series of ethanol (70, 90, and 100%), and the small glass mounted on stubs gold and coated with a Sputter K250 coater (Emitech, Corato, Italy).

To obtain fine resolution of intracellular structures, teratocytes were fixed and post-fixed as described above, dehydrated in an increasing series of ethanol, embedded in an Epon-Araldite 812 mixture (Sigma-Aldrich, St. Louis, MO, USA), and sectioned with a Reichert Ultracut S ultramicrotome (Leica, Wetzlar, Germany). Semithin sections (700 nm in thickness) were collected on glass, and dried slices were treated with sodium methoxide to remove resin in excess. After mounting glasses on stubs, slices were subjected to critical point drying with CO_2, gold coated with a Sputter K250 coater, and then observed with a SEM-FEG XL-30 microscope. All the samples were observed with a SEM-FEG XL-30 microscope (Philips, Eindhoven, The Netherlands).

Transmission Electron Microscopy

For ultrastructural studies at TEM, teratocytes were recovered from hosts and dissected directly into fixative (0.1 M Na-cacodylate buffer at pH 7.4 containing 2% glutaraldehyde). After 2 h, cells were washed in the same buffer and post-fixed for 1 h with 1% osmium tetroxide in cacodylate buffer, pH 7.4. After standard serial ethanol dehydration, specimens were embedded in an Epon-Araldite 812 mixture (Sigma-Aldrich, St. Louis, MO, USA). Ultrathin sections (70–80) were obtained with a Reichert Ultracut S ultramicrotome (Leica, Wetzlar, Germany), collected on 200 mesh copper grids, counterstained with uranyl acetate and lead citrate, and observed by using a Jeol JEM-1010 electron microscope (Jeol, Tokyo, Japan) equipped with an Olympus Morada digital camera (Olympus, Tokyo, Japan).

Glycogen Staining at Transmission Electron Microscopy

Teratocytes were stained by following the Thiéry method (1967). Cells were prepared by fixation in 2% glutaraldehyde, dehydrate in ethanol, and embedded in Epon araldite. Ultrathin sections (80–90 nm in thickness), obtained as above described, were collected on 200 mesh gold grids, incubated in 1% periodic acid in water for 30 min. After several washing in water, sections were treated with 1% thiosemicarbozide in 10% acetic acid, at RT for 30 min, washed in graded acetic acid series to water, stained for 30 min in 1% silver proteinate (Sigma-Aldrich, St. Louis, MO, USA) in double distilled water, washed in double distilled water. In control experiment, thiosemicarbozide treatment was omitted, and sections were incubated only with silver proteinate. All sections were counterstained only with aqueous uranyl acetate and observed by Jeol JEM-1010 electron microscope (Jeol, Tokyo, Japan). Images were recorded with the Olympus Morada digital camera (Olympus, Tokyo, Japan).

Immunogold Labeling

For immunogold cytochemistry, teratocytes were fixed for 2 h with 4% paraformaldehyde and 0.5% glutaraldehyde in PBS, and then washed in the same buffer. After a standard step of serial ethanol dehydration, cells were embedded in an Epon-Araldite 812 mixture (Sigma-Aldrich, St. Louis, MO, USA) and sectioned with a Reichert Ultracut S ultramicrotome (Leica, Wetzlar, Germany). Ultrathin sections (80–90 nm in thickness) were collected on 200 mesh gold grids. After etching with 3% NaOH in absolute ethanol (Causton, 1984), sections were incubated for 30 min with PBS containing 2% bovine serum albumin (BSA) and then for 1 h at room temperature (RT), with the following primary antibodies (working dilution 1:40): rabbit polyclonal antibodies anti-Ae-ENO (Grossi et al., 2016) and anti-Ae-FABP (Falabella et al., 2005) and mouse monoclonal antibodies anti-Alix (Salvia et al., 2017) and

anti-HSP70 (Sigma-Aldrich, St Louis, MO, USA). After several washing in PBS, samples were incubated for 1 h at RT with secondary goat anti-rabbit IgG (H + L)-gold conjugate (working dilution 1:100, particle size 6 nm, GE Healthcare Amersham, Buckinghamshire, UK) to detect Ae-ENO and anti-Ae-FABP, and with goat anti-mouse IgG (H + L)-gold conjugate (working dilution 1:100, particle size 6 nm, GE Healthcare Amersham, Buckinghamshire, UK) to detect Alix and HSP70, or with a protein G gold-conjugated 1:100, particle size 6 nm, GE Healthcare Amersham, Buckinghamshire, UK, to detect the mouse primary antibodies. The PBS used for antibody dilutions contained 2% BSA. In control sections, primary antibodies were omitted, and sections were treated with BSA containing PBS and incubated only with the secondary antibody goat anti-rabbit or with Protein G gold conjugated.

Isolated exosomes (obtained as above described) were prepared for immunogold staining (Thery et al., 2006). Briefly, 5 µl of exosome suspension was fixed in 50 µl of 2% paraformaldehyde. Five microliters of the mix were transferred onto 300 Mesh Formvar–carbon-coated electron microscopy grids (Pacific Grid Tech[1]). After 20 min, grids were transferred on drops of 100 µl of PBS with the sample membrane side facing down. After three washing in PBS, grids were pre-incubated for 30 min in blocking solution, and then immunostaining was performed as described above for teratocytes. All samples were counterstained with uranyl acetate in water and observed with a Jeol 1010 EX electron microscope (Jeol, Tokyo, Japan), and data were recorded with a MORADA digital camera system (Olympus, Tokyo, Japan).

[1]www.grid-tech.com

Western Blot

The exosome pellet obtained as described above was resuspended in Laemmli buffer (Laemmli, 1970) and loaded on SDS PAGE (12.5%). The two *A. ervi* proteins (Ae-ENO and Ae-FABP) were detected using antibodies anti-*Ae-ENO* (Grossi et al., 2016) and anti-*Ae*-FABP (Falabella et al., 2005) as primary antibody (both diluted 1:5,000 in 5% milk), and anti-rabbit conjugated to horseradish peroxidase (Life Technologies, Carlsbad, CA, USA) (diluted 1:5,000 in tris-buffered saline and 0.1% Tween 20 (TBS-T)), as secondary antibody. The two exosomes markers, Alix and HSP70 (Meckes and Raab-Traub, 2011), were detected by using Anti-Alix antibody, kindly provided by Dr. Toshiro Aigaki, and anti-HASP70 antibody (Sigma-Aldrich, St Louis, MO, USA) (diluted 1:5,000 in 5% milk). The anti-mouse conjugated to horseradish peroxidase as secondary antibody (Life Technologies, Carlsbad, CA, USA) was used diluted 1:15,000 in TBS-T. Finally, the Western blot Chemiluminescent HRP Substrate (ECL) (Luminata™ Crescendo, Western HRP Substrate, Millipore, Temecula, CA, USA) was used to detect target proteins, and signals were measured with Chemidoc™ MP System (Bio-Rad, Milan, Italy).

RESULTS

Light Microscopy

Teratocytes and *Aphidius ervi* larva were collected and observed after dissection of the host aphid, 5 and 6 days after parasitization (**Figures 1A,B**). After dissection, teratocytes were easily visualized, since they appeared as giant and buoyant spherical cells. As reported by Sabri et al. (2011),

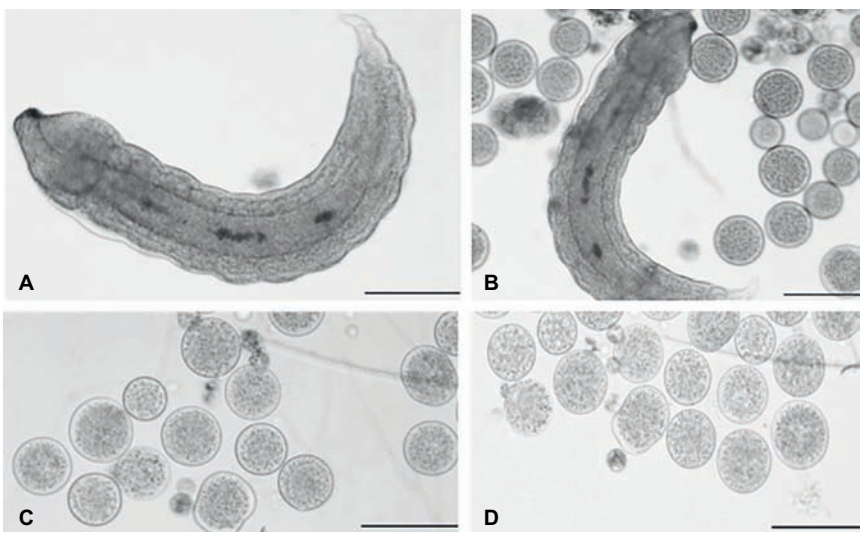

FIGURE 1 | Light microscopy of teratocytes. *Aphidius ervi* larva **(A)**. Teratocytes and *Aphidius ervi* larva observed in the host hemocoel 5 days after parasitization **(B)**. Teratocytes observed at 5 days after parasitization **(C)**. Teratocytes observed at 6 days after parasitization **(D)**. A stereo microscope Nikon SMZ800 was used for dissections, and images were observed at a light microscopy using Nikon Eclipse 80i at 10× magnification. The images were recorded by Nikon Digital Sight DS-U1 camera and ImageJ software. Bars in **(A)**–**(D)**, 100 µm.

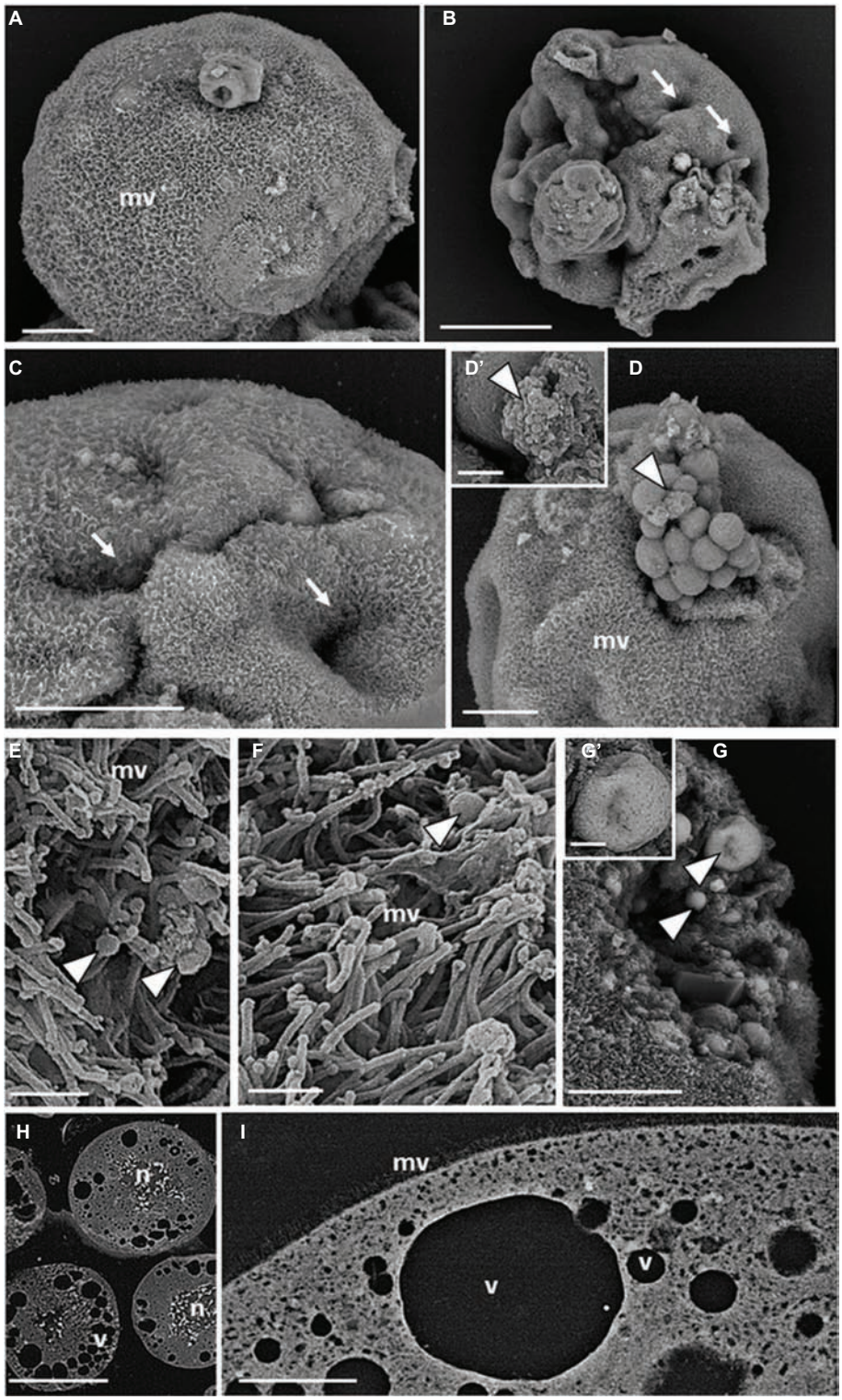

FIGURE 2 | SEM micrographs of teratocytes. Teratocytes isolated from pea aphids 5 days after parasitization by *A. ervi* have a surface covered with numerous microvilli **(A)** and are characterized by the presence of indentations or dimple-like structures **(B,C)**. Spherical vesicles and structures similar to exosomes protrude from the plasma membrane [arrowheads in **(D,D′)**]. Numerous exosome-like structures [arrowheads in **(E,F)**] are interspersed among the microvilli. Spherical vesicles filled with smaller vesicles with circular profiles are visible in the cytoplasm [arrowheads in **(G,G′)**]. Large stellate nuclei **(H)** and vacuoles **(H,I)** are visible in the sectioned teratocytes. (mv) microvilli, (n) nucleus, (v) vacuoles. Bars in **(A,C,D,G)**: 20 μm; bar in **(B)**: 50 μm; bars in **(D′,G′)**: 2.5 μm; bars in **(E,F)**: 1 μm; bar in **(H)**: 100 μm; bar in **(I)**: 10 μm.

approximately 30 teratocytes in the hemocoel of each parasitized aphid dissected after 5 days following parasitization were counted. The same number was observed also 6 days after parasitization. Microscope observations showed that the size of teratocytes after their release was about 50 μm diameter (**Figure 1C**) and increased the following day to approximately 100 μm (**Figure 1D**).

Morphological Analysis With Scanning Electron Microscopy

SEM revealed that the surface of teratocytes, collected 5 days after parasitization, was covered by a dense mat of microvilli (**Figure 2A**) and was characterized by the presence of indentations or dimple-like structures (**Figures 2B,C**). In addition, a blebbing phenomenon often became the dominant surface feature of some cells and spherical vesicles appeared on the external side of the microvilli-covered plasma membrane (**Figure 2D**). Smaller vesicular-shaped bodies, with a size ranging from 30 to 100 nm corresponding with the range of exosome-like structures, were grouped next to the large spherical vesicles (**Figure 2D′**) or interspersed among the microvilli (**Figures 2E,F**). Spherical vesicular formations of different sizes, limited by a membrane and filled with smaller vesicles with circular profiles (ranging size 50–100 nm), were also visible in the cytoplasm and underneath the plasma membrane (**Figures 2G,G′**). Analysis of sectioned teratocytes highlighted the presence of stellate nuclei (**Figure 2H**), localized in the center of the cytoplasm, and extended their ramifications toward the plasma membrane. Vacuoles of different sizes, occupying a substantial volume of the cytoplasm and in close proximity to the plasma membrane, were clearly evident (**Figures 2H,I**).

Transmission Electron Microscopy: Morphological Analysis, Histochemical, and Immunogold Staining

Further analyses of teratocyte intracellular structures were performed by ultrastructural analyses of thin sections with TEM. The plasma membrane formed a dense lawn of microvilli and underneath it, and numerous mitochondria with a regular shape were present (**Figure 3A**). Substantial amounts of rough endoplasmic reticulum (ER) and lipid droplets (LP) could be observed in the finely granular cytoplasm (**Figure 3A**). Such densely packed granules were shown to be glycogen by histochemical analysis (**Figure 3B**; Thiéry, 1967). No positively stained structures were found in non-oxidized thiocarbohydrazide-silver proteinate treated sections (**Figure 3C**), thus confirming that the cytoplasm of teratocytes contained a huge amount of glycogen. Taken together, these results suggest a possible specific role of teratocytes as a nutritional resource for the growth of parasitoid larvae. Indeed, several studies showed that braconid-wasp larvae consume teratocytes while feeding in the host hemocoel (Vinson and Iwantsch, 1980). Moreover, the accumulation of a great amount of glycogen and lipid in their cytoplasm confirmed that these cells had a high metabolic activity. These observations correlate well with the consistent secretory activity of these cells (Falabella et al., 2000). In fact, besides the presence of numerous vesicles (30–100 nm in size) mainly localized underneath the plasma membrane (**Figure 3D**), microvilli with enlarged tips (**Figure 3D**) as well as secretory exosome-like vesicles were observed along the external cell surface (**Figure 3E**), in close proximity to the microvilli and emanating from them (**Figure 3F**). Spherical organelles with a diameter of 250–1,000 nm, characterized by a single outer membrane enclosing a variable number of small spherical or ellipsoidal vesicles within a matrix and with heterogeneous sizes between 30 and 100 nm, were scattered in the cytoplasm and located in close vicinity of the plasma membrane (**Figure 3G**). Some of these organelles were exosome-like vesicles in the extracellular environment (**Figure 3H**). These structures, based on morphological criteria at the ultrastructural level, resembled the multivesicular body (MVB) organelles already described by several authors (Haigler et al., 1979; Cooney et al., 2002; Russell et al., 2006; Piper and Katzmann, 2007) and observed in almost all cell types of multicellular organisms.

TEM immunogold labeling, performed on ultrathin sections of teratocytes, clearly showed that anti-*Ae*-ENO (**Figures 4A–C** and inserts), anti-Ae-FABP (**Figures 4D,E**), anti-HSP70 (**Figures 4F,G** and inserts), and anti-Alix (**Figures 4H–J** and inserts) antibodies marked exosome-like vesicles released from microvilli, located underneath the plasma membrane, in MVB or freely dispersed in the cytoplasm.

The same result was obtained by immunostaining assays performed on exosome-like structures released by teratocytes stimulated for 30′ with 5 mM ATP (**Figures 4K–N**). No signal was detected in control experiments (**Figures 4O–R**), the primary antibodies were omitted, and samples were incubated only with the anti-rabbit secondary antibody (**Figures 4O,Q**) or with the gold-conjugated protein G (**Figures 4P,R**).

Western Blot

Western blot analyses were performed on exosome-like vesicles released by teratocytes stimulated with ATP, as described in the Materials and Methods section, paragraph 2.4. The signals detected with anti-*Ae*-FABP and anti-*Ae*-ENO antibodies (**Figure 5**, lanes 1, 2) unequivocally demonstrated that both proteins are localized in vesicles. Moreover, to confirm that collected vesicles are exosomes, anti-ALIX and anti-HSP70 antibodies, specific exosome markers, were used. Results strongly support the hypothesis that vesicles released by teratocytes are exosomes (**Figure 5**, lanes 3, 4).

DISCUSSION

Proteins destined to be secreted from cells or expressed at the cell surface usually enter the endomembrane pathway, mediated by the presence of a signal peptide that labels them for entering endoplasmic reticulum (ER) (Arnoys and Wang, 2007).

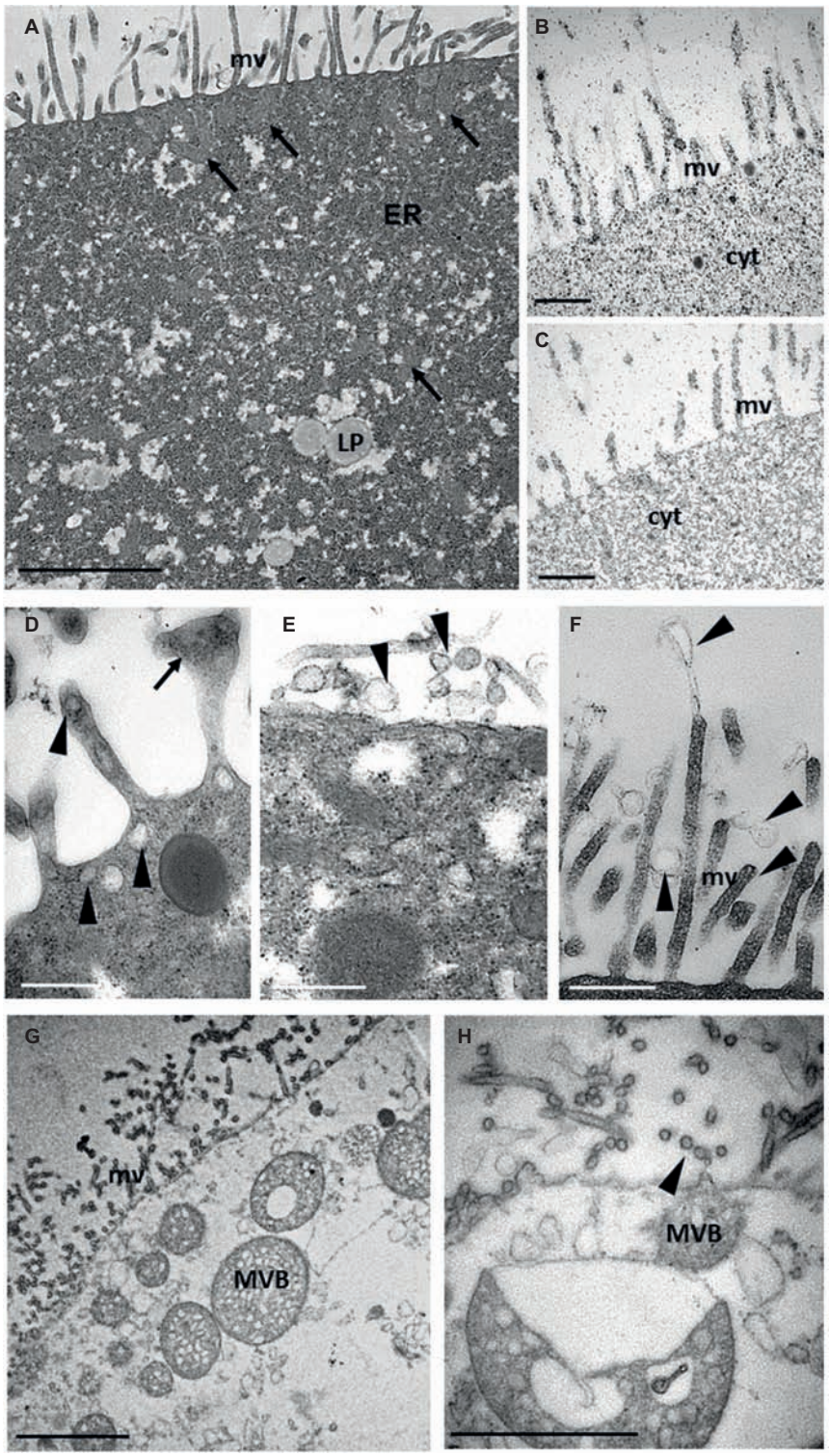

FIGURE 3 | TEM ultrastructural analysis of teratocytes intracellular structures. A thick layer of microvilli (mv) covers the plasma membrane. Numerous mitochondria (arrows) are present under the coat of microvilli (arrows). Lipid droplets (LP) and abundant rough endoplasmic reticulum (ER) are visible in the cytoplasm **(A)**. Glycogen granules black stained by Thiery reaction are visible in the cytoplasm **(B)**. No black staining is detected in control sections **(C)**. Secretory vesicles (arrowheads) are visible in close proximity of the plasma membrane and of microvilli, some of which showing an enlarged tips (arrow) **(D)**. Secretory exosome-like structures (arrowheads) emanating from the plasma membrane **(E)** and from microvilli **(F)** can be observed. Multivesicular bodies (MVB) like structures having a single limiting outer membrane and containing internal vesicles of homogeneous size are visible in close proximity of plasma membrane **(G)**. Detail of a MVB exocyting exosome-like structures (arrowhead) **(H)**. Bars in **(A,G)**: 2 μm; bars in **(B–F)**: 500 nm; bar in **(H)**: 1 μm.

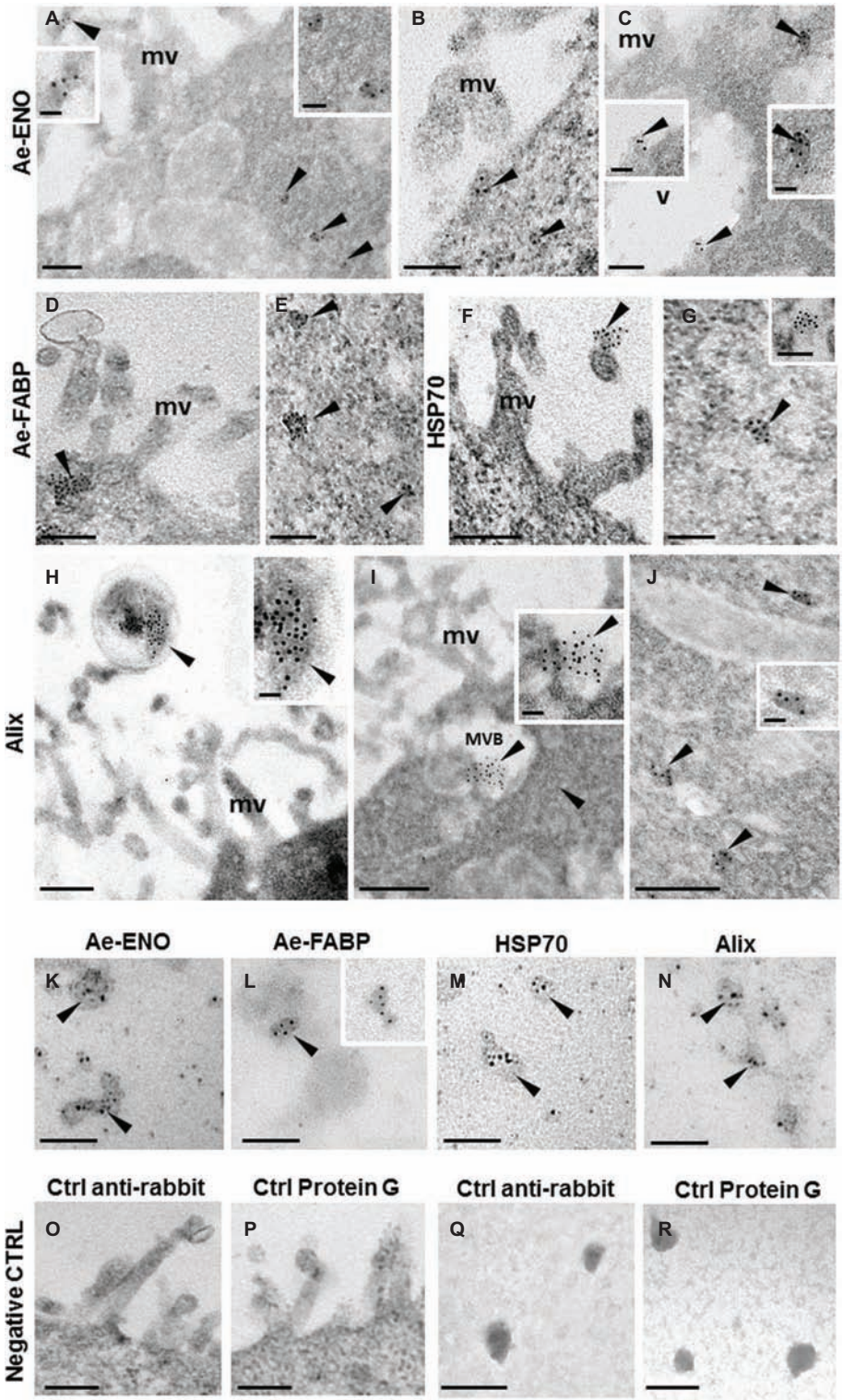

FIGURE 4 | Immunogold staining at TEM of *Ae*-ENO, *Ae*-FABP HSP70, and Alix. Gold nanoparticles (arrowheads) are visible in exosome-like vesicles released from teratocyte microvilli **(A,F,H)** underneath the plasma membrane **(B–D)**, in the multivesicular body located next to the plasma membrane **(I)** and in those dispersed in the cytoplasm **(A,C,E,G,J)**. Immunostaining assays performed on exosome-like structures released by teratocytes stimulated for 30′ with ATP 5 mM **(K–N)**. No signal was detected in control experiments, where the primary antibodies were omitted, and samples were incubated only with the anti-rabbit secondary antibody **(O,Q)** or with the protein G gold-conjugated **(P,R)**. (mv) microvilli; (MVB) multivesicular body; (v) vacuole. Bars in **(A–G)** and in **(K–R)**: 100 nm; bars in **(H–J)**: 200 nm; bars in inserts 40 nm.

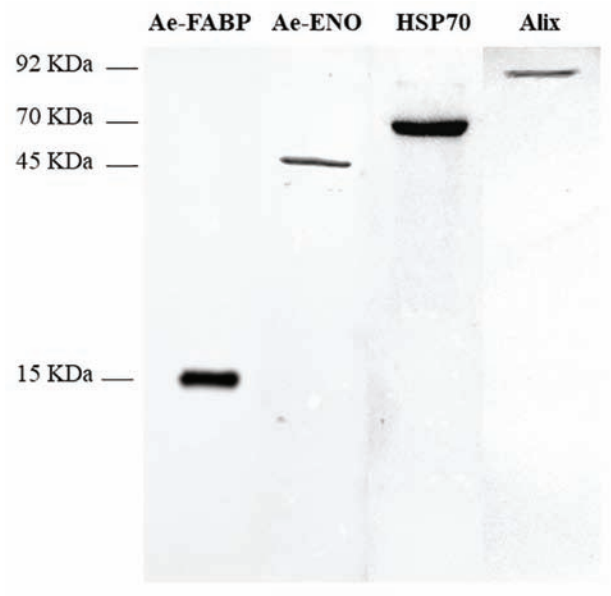

FIGURE 5 | Western blot analyses performed on exosome-like vesicles released from teratocytes stimulated with ATP. The incubation with anti-*Ae*-FABP (15 kDa) and anti-*Ae*-ENO antibodies (45 kDa) confirmed that both proteins are released by vesicles. The incubation with anti-HSP70 (70 kDa) and anti-ALIX (92 kDa) antibodies, specific exosomal markers, strongly supports the hypothesis that vesicles are exosomes.

A number of secreted proteins without known secretion signals have been found (Kinseth et al., 2007), and several unconventional secretory pathways have been discovered or suggested (Nickel and Rabouille, 2009; Duran et al., 2010; Manjithaya et al., 2010). These proteins without typical secretion signals were shown to be involved in wound healing, cancer angiogenesis, cancer metastasis, inflammation, cytoprotection, and neurodegeneration (Lee et al., 2012; Pegtel et al., 2014; Bebelman et al., 2018; Groot Kormelink et al., 2018; Jabalee et al., 2018; Kawahara and Hanayama, 2018; Pinheiro et al., 2018; Rackov et al., 2018). In addition, these proteins are often released during stress conditions, and some of them have distinct intracellular and extracellular functions (Iraci et al., 2016). Therefore, it has been speculated that unconventional secretion might have developed early in the evolution before conventional secretion to rapidly connect diverse processes without going through extraordinary regulations (Radisky et al., 2009).

In this work, we investigated the unconventional mechanism of release of *Ae*-ENO and *Ae*-FABP proteins in the extracellular environment the hemocoel of parasitoid host. These two cytoplasmic proteins are synthetized and then released by *A. ervi* teratocytes, and their abundance suggests their critical role in the success of parasitism (Falabella et al., 2005, 2009). Fatty acid binding proteins (FABPs) belong to a family of small proteins (14–15 kDa), usually located in the cytosol and characterized by their ability to bind hydrophobic ligands non-covalently and with high affinity. FABPs are commonly involved in lipid metabolism by uptake and transport of long-chain fatty acids (FAs), and they interact with other transport systems and enzymes and are involved in signal transduction, gene expression, growth, and differentiation (Zimmerman and Veerkamp, 2002; Corsico et al., 2004). *Ae*-FABP is involved in transport of fatty acids from digestion sites of host lipids, through the host hemolymph, to the parasitoid larvae, and shows a particularly high affinity for C14–C18 saturated fatty acids (FAs) and for oleic and arachidonic acids (Falabella et al., 2005; Caccia et al., 2012).

Enolase is the eighth enzyme of the glycolytic pathway (Walsh et al., 1989) but is also defined as "moonlight protein" (Jeffery, 1999) since along with the classical role in glycolysis it also has several other functions, depending on its cellular location and/or cellular types (Aaronson et al., 1995; Subramanian and Miller, 2000; Gao et al., 2015; Ji et al., 2016). Among these different roles, enolase is an important extracellular protein related to different physiological and pathological processes. As extracellular protein enolase works as plasminogen receptor inducing its activation in plasmin, it is thus involved in tissue invasion processes. This strategy is shared by several different cellular types, both of eukaryotic and prokaryotic origin, such as parasites, yeasts, pathogenic bacterial cells, tumor cells, and cells belonging to the immune system, involved in physiological and pathological tissue invasion processes (Pancholi, 2001; Liu and Shih, 2007; Vanegas et al., 2007; Wygrecka et al., 2009; De la Torre-Escudero et al., 2010; Nogueira et al., 2010; Floden et al., 2011; Sanderson-Smith et al., 2012; Toledo et al., 2012; Ceruti et al., 2013; Godier and Hunt, 2013; Hsiao et al., 2013). In all these cases, enolase lacks its canonical signal peptide (required for entry into the secretory pathway), and thus, it is transported to the external cell surface through a mechanism not fully understood to date (López-Villar et al., 2006; Avilán et al., 2011; Ghosh and Jacobs-Lorena, 2011).

The extracellular localization of *Ae*-FABP and *Ae*-ENO is unusual, and the mechanism of release to the extracellular environment by teratocytes for both proteins has not been elucidated yet.

To date, four types of unconventional protein secretion mechanisms have been described: (1) direct transfer across the plasma membrane; (2) ABC transporter-based secretion for acylated peptides and yeast mating peptides; (3) underneath certain regions of the plasma membrane followed by release into the extracellular medium as a result of membrane blebbing and incorporation into exosomes; and (4) Golgi bypass pathway for proteins that enter the ER but bypass the Golgi apparatus to reach the plasma membrane (Nickel, 2003; Nickel and Rabouille, 2009; Rabouille, 2017).

Here, we demonstrate that *Ae*-ENO and *Ae*-FABP are released into the extracellular space by exosomal exocytosis.

According to the minimal experimental requirements for extracellular vesicle analysis recommended by the international Society for Extracellular Vesicles (ISEV) (Lötvall et al., 2014), we performed SEM, TEM, and western blot analyses on teratocytes and vesicles released *in vitro*.

Light microscopy observations showed that 5 days after *A. ervi* parasitization, serosa cells dissociate into around

30 free teratocytes with a size ranging from approximately 50 μm (5 days after parasitization) to about 100 μm (6 days after parasitization), according to the observations reported by Sabri et al. (2011). Ultrastructural analysis results showed that teratocytes exhibited numerous long and diffuse microvilli on their cell surface, and from them evaginated vesicular-shaped bodies with a size ranging from 30 to 100 nm, similar to exosome-like structures (Mathivanan et al., 2010), confirming the secretory activity of these cells (Falabella et al., 2000). We observed that both proteins, *Ae*-ENO and *Ae*-FABP, localized below the plasma membrane, in multivesicular bodies (MVBs) or freely dispersed in the cytoplasm, and in exosome-like structures released by teratocytes to the extracellular environment. Moreover, we collected exosomes released by teratocytes *in vitro,* and we detected the presence of both proteins by western blot analyses. In addition to the size range, specific exosome molecular markers are used to identify the exosomes and differentiate those from other vesicular structures. Exosomes contain a distinct set of proteins such as Alix, TSG101, HSP70, and the tetraspanins CD63, CD81, and CD9. In particular, Alix (identified in 68% of exosome studies) and HSP70 (89%) are highly associated with exosomes (Mathivanan et al., 2010). For this reason, we chose these two latter proteins as exosomes markers and verified their presence through immunogold staining, TEM observations, and western blot by using specific antibodies. HSP70 and Alix proteins are found in the cytoplasm of teratocytes, in their membrane blebs, and in the vesicles released from them. The results here presented confirmed that *Ae*-ENO and *Ae*-FABP are contained in exosomal like vesicles and led us to conclude that the unconventional secretion pathway of *Ae*-ENO and *Ae*-FABP could be effectively mediated by exosomes. Also, enolases, such as other enzymes associated with glycolysis (aldolase, GAPDH, etc.), are reported in ExoCarta[2] as exosome markers. Also in helminths, among proteins secreted by exosome-like vesicles during infections, it has been identified an extracellular enolase (Bernal et al., 2006). Why exosomes contain so many glycolytic enzymes is unclear. It is possible that exosomes increase glycolytic activity in the target cells (Samoil et al., 2018). The unconventional secretion mechanisms of *Ae*-ENO and *Ae*-FABP are the same observed in two trematodes, *Echinostoma caproni* and *Fasciola hepatica*, which utilize exosome-like vesicles in the establishment of the infection of their hosts (Marcilla et al., 2012). Extracellular vesicles represent an important means of cellular communication transferring proteins, lipids, and genetic information (Mathivanan et al., 2010; Meckes and Raab-Traub, 2011; Willms et al., 2016). In eukaryotic cells, there are several extracellular organelles that are released, or shed, into the microenvironment (Mathivanan et al., 2010; Meckes and Raab-Traub, 2011). Across all eukaryotic kingdoms of life, extracellular vesicles have been pointed out as a ubiquitous mechanism for transferring information between cells and organisms. Their roles in normal physiology are not the only their remarkable point of interest. Extracellular vesicles mediate targeted intercellular communication under physiological and pathophysiological conditions. Parasite-derived extracellular vesicles can communicate information and transfer genetic material to host cells or other parasites (Mathivanan et al., 2010). Host-derived extracellular vesicles can play a key role in host defense and are candidates for generating a vaccine against pathogenic infection (Coakley et al., 2015).

Teratocytes of other parasitoid wasps, such as Braconidae, Aphididae, and Miramidae, are reported to secrete several proteins responsible for immunosuppression and inhibition of metamorphosis of hosts (Ali et al., 2013; Strand, 2014). Some of secreted proteins were identified and characterized: the teratocytes of *Microplitis mediator* have been shown to secrete collagens (Quin et al., 2000); *Microplitis croceipes* teratocytes secrete at least 15 different proteins, including TSP14, a protein with a signal peptide, that is involved in the developmental arrest of the host (Hoy and Dahlman 2002); *Cotesia plutellae* teratocytes release serpins and GTPase-activating proteins, both with signal peptides, involved in the inhibition of host cellular immunity (Ali et al., 2013); a chitinase, with signal peptide, released by teratocytes of *Toxoneuron nigriceps* was reported to promote the host cuticle digestion, allowing the parasitoid larva to emerge from the host body (Consoli et al., 2007). To date, the characterized proteins released by teratocytes of other parasitoid wasps seem to be secreted through a conventional mechanism involving the presence of signal peptide. To the best of our knowledge, this is the first study showing the mechanism of unconventional secretion of regulatory proteins released by teratocytes and lacking the signal peptide.

Enolase, in particular, is a protein of great interest, since it has been reported to be correlated to the progression of cancer and could represent a new therapeutic target (Dowling et al., 2007; Cappello et al., 2009, 2011); it was shown that enolase localizes to the surface of tumor metastasis cells and is responsible for the degradation of the extracellular matrix (Chang et al., 2006; Hsiao et al., 2013) similar to *A. ervi* enolase (Grossi et al., 2016). There is little evidence regarding the secretory pathway of enolase: *Saccharomyces cerevisiae* is reported to have autophagosome-mediated membrane compartments for the unconventional secretion of proteins (Bruns et al., 2011), or by SNARE-driven unconventional secretion (Miura et al., 2012). However, the mechanism by which enolase is transported to the surface of tumor cells remains unclear.

This work contributes to increase our knowledge regarding the unconventional mechanism of extracellular transport of proteins lacking canonical signal peptides. More generally, our study could contribute to clarifying the complex role of exosomal vesicles, more often considered as good diagnostic and drug-delivery tools, taking a central role in research of these fields, to understand the role that these vesicles play in the intercellular

[2]http://www.exocarta.org/

communication and to open new interesting scenarios for the regulation of physiological and pathological events.

DATA AVAILABILITY

All datasets generated for this study are included in the manuscript.

AUTHOR CONTRIBUTIONS

PF designed the experiments, wrote, and critically revised the manuscript. SB and HV contributed to the data interpretation and critically revised the manuscript. RS performed light microscopy observations, collected vesicles, and prepared samples for subsequent SEM and TEM analyses. RS, AS, and CS performed the western blot experiments. AG and RG performed microscopy observations at SEM and TEM and immunogold labeling. All authors read and approved the manuscript.

FUNDING

This work was supported by the University of Basilicata (RIL funds) and University of Insubria (FAR funds).

ACKNOWLEDGMENTS

We thank Dr. Marco Mosti of Bioplanet srl for kindly providing an *Aphidius ervi* colony. We also thank Dr. Toshiro Aigaky, for providing the anti-Alix antibody, and Prof. Terenzio Congiu, for his excellent technical assistance in scanning electron microscopy.

REFERENCES

Aaronson, R. M., Graven, K. K., Tucci, M., McDonald, R. J., and Farber, H. W. (1995). Non-neuronal enolase is an endothelial hypoxic stress protein. *J. Biol. Chem.* 270, 27752–27757. doi: 10.1074/jbc.270.46.27752

Ali, M. R., Seo, J., Lee, D., and Kim, Y. (2013). Teratocyte-secreting proteins of an endoparasitoid wasp, *Cotesia plutellae*, prevent host metamorphosis by altering endocrine signals. *Comp. Biochem. Physiol. A Mol. Integr. Physiol.* 166, 251–262. doi: 10.1016/j.cbpa.2013.06.028

Arnoys, E. J., and Wang, J. L. (2007). Dual localization: proteins in extracellular and intracellular compartments. *Acta Histochem.* 109, 89–110. doi: 10.1016/j.acthis.2006.10.002

Avilán, L., Gualdrón-López, M., Quiñones, W., González-González, L., Hannaert, V., Michels, P. A., et al. (2011). Enolase: a key player in the metabolism and a probable virulence factor of trypanosomatid parasites-perspectives for its use as a therapeutic target. *Enzyme Res.* 2011:932549. doi: 10.4061/2011/932549

Bebelman, M. P., Smit, M. J., Pegtel, D. M., and Baglio, S. R. (2018). Biogenesis and function of extracellular vesicles in cancer. *Pharmacol. Ther.* 188, 1–11. doi: 10.1016/j.pharmthera.2018.02.013

Beckage, N. E., and Gelman, D. B. (2004). Wasp parasitoid disruption of host development: implications for new biologically based strategies for insect control. *Annu. Rev. Entomol.* 49, 299–330. doi: 10.1146/annurev.ento.49.061802.123324

Bernal, D., Carpena, I., Espert, A. M., De la Rubia, J. E., Esteban, J. G., Toledo, R., et al. (2006). Identification of proteins in excretory/secretory extracts of *Echinostoma friedi* (Trematoda) from chronic and acute infections. *Proteomics* 6, 2835–2843. doi: 10.1002/pmic.200500571

Bianco, F., Pravettoni, E., Colombo, A., Schenk, U., Moller, T., Matteoli, M., et al. (2005). Astrocyte-derived ATP induces vesicle shedding and IL-1 beta release from microglia. *J. Immunol.* 174, 7268–7277. doi: 10.4049/jimmunol.174.11.7268

Bruns, C., McCaffery, J. M., Curwin, A. J., Duran, J. M., and Malhotra, V. (2011). Biogenesis of a novel compartment for autophagosome-mediated unconventional protein secretion. *J. Cell Biol.* 195, 979–992. doi: 10.1083/jcb.201106098

Burke, G. R., and Strand, M. R. (2014). Systematic analysis of a wasp parasitism arsenal. *Mol. Ecol.* 23, 890–901. doi: 10.1111/mec.12648

Caccia, S., Grimaldi, A., Casartelli, M., Falabella, P., de Eguileor, M., Pennacchio, F., et al. (2012). Functional analysis of a fatty acid binding protein produced by *Aphidius ervi* teratocytes. *J. Insect Physiol.* 58, 621–627. doi: 10.1016/j.jinsphys.2011.12.019

Cappello, M., Ferri-Borgogno, S., Cappello, P., and Novelli, F. (2011). Alpha-enolase: a promising therapeutic and diagnostic tumor target. *FEBS J.* 278, 1064–1074. doi: 10.1111/j.1742-4658.2011.08025.x

Cappello, P., Tomaino, B., Chiarle, R., Ceruti, P., Novarino, A., Castagnoli, C., et al. (2009). An integrated humoral and cellular response is elicited in pancreatic cancer by alpha-enolase, a novel pancreatic ductal adenocarcinoma-associated antigen. *Int. J. Cancer* 125, 639–648. doi: 10.1002/ijc.24355

Causton, B. E. (1984). "The choice of resins for electron immunocytochemistry" in *Immunolabelling for electron microscopy*. eds. J. M. Polack, and I. M. Varndell (Amsterdam: Elsevier), 17–28.

Ceruti, P., Principe, M., Capello, M., Cappello, P., and Novelli, F. (2013). Three are better than one: plasminogen receptors as cancer theranostic targets. *Exp. Hematol. Oncol.* 2, 1–12. doi: 10.1186/2162-3619-2-12

Chang, G. C., Liu, K. J., Hsieh, C. L., Hu, T. S., Charoenfuprasert, S., Liu, H. K., et al. (2006). Identification of alpha-enolase as an autoantigen in lung cancer: its overexpression is associated with clinical outcomes. *Clin. Cancer Res.* 12, 5746–5754. doi: 10.1158/1078-0432.CCR-06-0324

Chavez-Munguia, B., Segovia-Gamboa, N., Salazar-Villatoro, L., Omana-Molina, M., Espinosa-Cantellano, M., and Martinez-Palomo, A. (2011). *Naegleria fowleri*: enolase is expressed during cyst differentiation. *J. Eukaryot. Microbiol.* 58, 463–468. doi: 10.1111/j.1550-7408.2011.00574.x

Coakley, G., Maizels, R. M., and Buck, A. H. (2015). Exosomes and other extracellular vesicles: the new communicators in parasite infections. *Trends Parasitol.* 31, 477–489. doi: 10.1016/j.pt.2015.06.009

Consoli, F. L., Lewis, D., Keeley, L., and Vinson, S. B. (2007). Characterization of a cDNA encoding a putative chitinase from teratocytes of the endoparasitoid *Toxoneuron nigriceps*. *Entomol. Exp. Appl.* 122, 271–278. doi: 10.1111/j.1570-7458.2006.00514.x

Cooney, J. R., Hurlburt, J. L., Selig, D. K., Harris, K. M., and Fiala, J. C. (2002). Endosomal compartments serve multiple hippocampal dendritic spines from a widespread rather than a local store of recycling membrane. *J. Neurosci.* 22, 2215–2224. doi: 10.1523/JNEUROSCI.22-06-02215.2002

Corsico, B., Liou, H. L., and Storch, J. (2004). The a-helical domain of liver fatty acid binding protein is responsible for the diffusion-mediated transfer of fatty acids to phospholipid membranes. *Biochemistry* 43, 3600–3607. doi: 10.1021/bi0357356

Dahlman, D. L., Rana, R. L., Schepers, E. J., Schepers, T., Di Luna, F. A., and Webb, B. A. (2003). A teratocyte gene from a parasitic wasp that is associated with inhibition of insect growth and development inhibits host protein synthesis. *Insect Mol. Biol.* 12, 527–534. doi: 10.1046/j.1365-2583.2003.00439.x

Dahlman, D. L., and Vinson, S. B. (1993). "Teratocytes: developmental and biochemical characteristics" in *Parasites and pathogens of insects*. eds. N. E. Beckage, S. N. Thompson, and B. A. Federici (New York: Academic Press), 145–165.

De Buron, J. D., and Beckage, N. E. (1997). Developmental changes in teratocytes of the braconid wasp *Cotesia congregate* in larvae of the tobacco hornworm *Manduca sexta*. *J. Insect Physiol.* 43, 915–930. doi: 10.1016/S0022-1910(97)00056-5

De la Torre-Escudero, E., Manzano-Roman, R., Perez-Sanchez, R., Siles-Lucas, M., and Oleaga, A. (2010). Cloning and characterization of plasminogen-binding surface-associated enolase from *Schistosoma bovis*. *Vet. Parasitol.* 173, 76–84. doi: 10.1016/j.vetpar.2010.06.011

Dowling, P., Meleady, P., Dowd, A., Henry, M., Glynn, S., and Clynes, M. (2007). Proteomic analysis of isolated membrane fractions from superinvasive cancer cells. *Biochim. Biophys. Acta* 1774, 93–101. doi: 10.1016/j.bbapap.2006.09.014

Drago, F., Lombardi, M., Prada, I., Gabrielli, M., Joshi, P., Cojoc, D., et al. (2017). ATP modifies the proteome of extracellular vesicles released by microglia and influences their action on astrocytes. *Front. Pharmacol.* 8:910. doi: 10.3389/fphar.2017.00910

Duran, J. M., Anjard, C., Stefan, C., Loomis, W. F., and Malhotra, V. (2010). Unconventional secretion of Acb1 is mediated by autophagosomes. *J. Cell Biol.* 188, 527–536. doi: 10.1083/jcb.200911154

Falabella, P., Perugino, G., Caccialupi, P., Riviello, L., Varricchio, P., Tranfaglia, A., et al. (2005). A novel fatty acid binding protein produced by teratocytes of the aphid parasitoid *Aphidius ervi*. *Insect Mol. Biol.* 14, 195–205. doi: 10.1111/j.1365-2583.2004.00548.x

Falabella, P., Riviello, L., De Stradis, M. L., Stigliano, C., Varricchio, P., Grimaldi, A., et al. (2009). *Aphidius ervi* teratocytes release an extracellular enolase. *Insect Biochem. Mol. Biol.* 39, 801–813. doi: 10.1016/j.ibmb.2009.09.005

Falabella, P., Tremblay, E., and Pennacchio, F. (2000). Host regulation by the aphid parasitoid *Aphidius ervi*: the role of teratocytes. *Entomol. Exp. Appl.* 97, 1–9. doi: 10.1046/j.1570-7458.2000.00710.x

Floden, A. M., Watt, J. A., and Brissette, A. (2011). *Borrelia burgdorferi* enolase is a surface-exposed plasminogen binding protein. *PLoS One* 6:e27502. doi: 10.1371/journal.pone.0027502

Franzetti, E., Huang, Z. J., Shi, Y. X., Xie, K., Deng, X. J., Li, J. P., et al. (2012). Autophagy precedes apoptosis during the remodeling of silkworm larval midgut. *Apoptosis* 17, 305–324. doi: 10.1007/s10495-011-0675-0

Gao, S., Li, H., Feng, X. J., Li, M., Liu, Z. P., Cai, Y., et al. (2015). α-Enolase plays a catalytically independent role in doxorubicin-induced cardiomyocyte apoptosis and mitochondrial dysfunction. *J. Mol. Cell. Cardiol.* 79, 92–103. doi: 10.1016/j.yjmcc.2014.11.007

Ghosh, A. K., and Jacobs-Lorena, M. (2011). Surface-expressed enolases of plasmodium and other pathogens. *Mem. Inst. Oswaldo Cruz* 106, 85–90. doi: 10.1590/S0074-02762011000900011

Godier, A., and Hunt, B. J. (2013). Plasminogen receptors and their role in the pathogenesis of inflammatory, autoimmune and malignant disease. *J. Thromb. Haemost.* 11, 26–34. doi: 10.1111/jth.12064

Groot Kormelink, T., Mol, S., de Jong, E. C., and Wauben, M. H. M. (2018). The role of extracellular vesicles when innate meets adaptive. *Semin. Immunopathol.* 40, 439–452. doi: 10.1007/s00281-018-0681-1

Grossi, G., Grimaldi, A., Cardone, R. A., Monné, M., Reshkin, S. J., Girardello, R., et al. (2016). Extracellular matrix degradation via enolase/plasminogen interaction: evidence for a mechanism conserved in Metazoa. *Biol. Cell.* 108, 161–178. doi: 10.1111/boc.201500095

Haigler, H. T., McKanna, J. A., and Cohen, S. (1979). Direct visualization of the binding and internalization of a ferritin conjugate of epidermal growth factor in human carcinoma cells A-431. *J. Cell Biol.* 81, 382–395. doi: 10.1083/jcb.81.2.382

Hotta, M., Okuda, T., and Tanaka, T. (2001). *Cotesia kariyai* teratocytes: growth and development. *J. Insect Physiol.* 47, 31–41. doi: 10.1016/S0022-1910(00)00089-5

Hoy, H. L., and Dahlman, D. L. (2002). Extended *in vitro* culture of *Microplitis croceipes* teratocytes and secretion of TSP14 protein. *J. Insect Physiol.* 48, 401–409. doi: 10.1016/S0022-1910(02)00054-9

Hsiao, K. C., Shih, N. Y., Fang, H. L., Huang, T. S., Kuo, C. C., Chu, P. Y., et al. (2013). Surface α-enolase promotes extracellular matrix degradation and tumor metastasis and represents a new therapeutic target. *PLoS One* 8:e69354. doi: 10.1371/journal.pone.0069354

Iraci, N., Leonardi, T., Gessler, F., Vega, B., and Pluchino, S. (2016). Focus on extracellular vesicles: physiological role and signalling properties of extracellular membrane vesicles. *Int. J. Mol. Sci.* 617:171. doi: 10.3390/ijms17020171

Jabalee, J., Towle, R., and Garnis, C. (2018). The role of extracellular vesicles in cancer: cargo, function, and therapeutic implications. *Cell* 7:E93. doi: 10.3390/cells7080093

Jeffery, C. (1999). Moonlighting proteins. *Trends Biochem. Sci.* 24, 8–11. doi: 10.1016/S0968-0004(98)01335-8

Ji, H., Wang, J., Guo, J., Li, Y., Lian, S., Guo, W., et al. (2016). Progress in the biological function of alpha-enolase. *Anim. Nutr.* 2, 12–17. doi: 10.1016/j.aninu.2016.02.005

Kawahara, H., and Hanayama, R. (2018). The role of exosomes/extracellular vesicles in neural signal transduction. *Biol. Pharm. Bull.* 41, 1119–1125. doi: 10.1248/bpb.b18-00167

Kinseth, M. A., Anjard, C., Fuller, D., Guizzunti, G., Loomis, W. F., and Malhotra, V. (2007). The Golgi-associated protein GRASP is required for unconventional protein secretion during development. *Cell* 130, 524–534. doi: 10.1016/j.cell.2007.06.029

Laemmli, U. K. (1970). Cleavage of structural proteins during the assembly of the head of bacteriophage T4. *Nature* 227, 680–685. doi: 10.1038/227680a0

Lee, C., Mitsialis, S. A., Aslam, M., Vitali, S. H., Vergadi, E., Konstantinou, G., et al. (2012). Exosomes mediate the cytoprotective action of mesenchymal stromal cells on hypoxia-induced pulmonary hypertension. *Circulation* 126, 2601–2611. doi: 10.1161/CIRCULATIONAHA.112.114173

Liu, K., and Shih, N. Y. (2007). The role of enolase in tissue invasion and metastasis of pathogens and tumor cells. *J. Cancer Mol.* 3, 45–48.

López-Villar, E., Monteoliva, L., Larsen, M. R., Sachon, E., Shabaz, M., Pardo, M., et al. (2006). Genetic and proteomic evidences support the localization of yeast enolase in the cell surface. *Proteomics* 6, 107–118. doi: 10.1002/pmic.200500479

Lötvall, J., Hill, A. F., Hochberg, F., Buzás, E. I., Di Vizio, D., Gardiner, C., et al. (2014). Minimal experimental requirements for definition of extracellular vesicles and their functions: a position statement from the International Society for Extracellular Vesicles. *J. Extracell. Vesicles* 3:26913. doi: 10.3402/jev.v3.26913

Manjithaya, R., Anjard, C., Loomis, W. F., and Subramani, S. (2010). Unconventional secretion of *Pichia pastoris* Acb1 is dependent on GRASP protein, peroxisomal functions, and autophagosome formation. *J. Cell Biol.* 188, 537–546. doi: 10.1083/jcb.200911149

Marcilla, A., Trelis, M., Cortes, A., Sotillo, J., Cantalapiedra, F., Minguez, M. T., et al. (2012). Extracellular vesicles from parasitic helminths contain specific excretory/secretory proteins and are internalized in intestinal host cells. *PLoS One* 7:e45974. doi: 10.1371/journal.pone.0045974

Mathivanan, S., Ji, H., and Simpson, R. J. (2010). Exosomes: extracellular organelles important in intercellular communication. *J. Proteome* 73, 1907–1920. doi: 10.1016/j.jprot.2010.06.006

Meckes, D. G., and Raab-Traub, N. (2011). Microvesicles and viral infection. *J. Virol.* 85, 12844–12854. doi: 10.1128/JVI.05853-11

Miura, N., Kirino, A., Endo, S., Morisaka, H., Kuroda, K., Takagi, M., et al. (2012). Tracing putative trafficking of the glycolytic enzyme enolase via SNARE-driven unconventional secretion. *Eukaryot. Cell* 11, 1075–1082. doi: 10.1128/EC.00075-12

Nakamatsu, Y., Fujii, S., and Tanaka, T. (2002). Larvae of an endoparasitoid *Cotesia kariyai* (hymenoptera: Braconidae), feed on the host fat body directly in the second stadium with the help of teratocytes. *J. Insect Physiol.* 48, 1041–1052. doi: 10.1016/S0022-1910(02)00192-0

Nickel, W. (2003). The mystery of nonclassical protein secretion. A current view on cargo proteins and potential export routes. *Eur. J. Biochem.* 270, 2109–2119. doi: 10.1046/j.1432-1033.2003.03577.x

Nickel, W., and Rabouille, C. (2009). Mechanisms of regulated unconventional protein secretion. *Nat. Rev. Mol. Cell Biol.* 10, 148–155. doi: 10.1038/nrm2617

Nogueira, S. V., Fonseca, F. L., Rodrigues, M. L., Mundodi, V., Abi-Chacra, E. A., Winters, M. S., et al. (2010). Paracoccidioides brasiliensis enolase is a surface protein that binds plasminogen and mediates interaction of yeast forms with host cells. *Infect. Immun.* 78, 4040–4050. doi: 10.1128/IAI.00221-10

Pancholi, V. (2001). Multifunctional a-enolase: its role in diseases. *Cell. Mol. Life Sci.* 58, 902–920. doi: 10.1007/PL00000910

Pegtel, D. M., Peferoen, L., and Amor, S. (2014). Extracellular vesicles as modulators of cell-to-cell communication in the healthy and diseased brain. *Philos. Trans. R. Soc. Lond. Ser. B Biol. Sci.* 369, 20130516. doi: 10.1098/rstb.2013.0516

Pennacchio, F., and Strand, M. R. (2006). Evolution of developmental strategies in parasitic Hymenoptera. *Annu. Rev. Entomol.* 51, 233–258. doi: 10.1146/annurev.ento.51.110104.151029

Pennacchio, F., Vinson, S. B., and Tremblay, E. (1994). Morphology and ultrastructure of the serosal cells (teratocytes) in *Cardiochiles nigriceps* Viereck (Hymenoptera: Braconidae) embryos. *Int. J. Insect Morphol.* 23, 93–104. doi: 10.1016/0020-7322(94)90003-5

Pinheiro, A., Silva, A. M., Teixeira, J. H., Gonçalves, R. M., Almeida, M. I., Barbosa, M. A., et al. (2018). Extracellular vesicles: intelligent delivery strategies for therapeutic applications. *J. Control. Release* 289, 56–69. doi: 10.1016/j.jconrel.2018.09.019

Piper, R. C., and Katzmann, D. J. (2007). Biogenesis and function of multivesicular bodies. *Annu. Rev. Cell Dev. Biol.* 23, 519–547. doi: 10.1146/annurev.cellbio.23.090506.123319

Quin, Q., Gong, H., and Ding, T. (2000). Two collagenases are secreted by teratocytes from Microplitis mediator (Hymenoptera: Braconidae) cultured in vitro. *J. Invert. Pathol.* 76, 79–80. doi: 10.1006/jipa.2000.4950

Rabouille, C. (2017). Pathways of unconventional protein secretion. *Trends Cell Biol.* 27, 230–240. doi: 10.1016/j.tcb.2016.11.007

Rackov, G., Garcia-Romero, N., Esteban-Rubio, S., Carrión-Navarro, J., Belda-Iniesta, C., and Ayuso-Sacido, A. (2018). Vesicle-mediated control of cell function: the role of extracellular matrix and microenvironment. *Front. Physiol.* 9:651. doi: 10.3389/fphys.2018.00651

Radisky, D. C., Stallings-Mann, M., Hirai, Y., and Bissell, M. J. (2009). Single proteins might have dual but related functions in intracellular and extracellular microenvironments. *Nat. Rev. Mol. Cell Biol.* 10, 228–234. doi: 10.1038/nrm2633

Russell, M. R. G., Nickerson, D. P., and Odorizzi, G. (2006). Molecular mechanisms of late endosome morphology, identity and sorting. *Curr. Opin. Cell Biol.* 18, 422–428. doi: 10.1016/j.ceb.2006.06.002

Sabri, A., Hance, T., Leroy, P. D., Frere, I., Haubruge, E., Destain, J., et al. (2011). Placenta-like structure of the aphid endoparasitic wasp *Aphidius ervi*: a strategy of optimal resources acquisition. *PLoS One* 6:e18847. doi: 10.1371/journal.pone.0018847

Salvia, R., Grossi, G., Amoresano, A., Scieuzo, C., Nardiello, M., Giangrande, C., et al. (2017). The multifunctional polydnavirus TnBVANK1 protein: impact on host apoptotic pathway. *Sci. Rep.* 7:11775. doi: 10.1038/s41598-017-11939-x

Samoil, V., Dagenais, M., Ganapathy, V., Aldridge, J., Glebov, A., Jardim, A., et al. (2018). Vesicle-based secretion in schistosomes: analysis of protein and microRNA (miRNA) content of exosome-like vesicles derived from *Schistosoma mansoni*. *Sci. Rep.* 8:3286. doi: 10.1038/s41598-018-21587-4

Sanderson-Smith, M. L., De Oliveira, D. M., Ranson, M., and McArthur, J. D. (2012). Bacterial plasminogen receptors: mediators of a multifacted relationship. *J Biomed Biotechnol* 2012, 1–14. doi: 10.1155/2012/272148

Silva, R. C., Padovan, A. C., Pimenta, D. C., Ferreira, R. C., da Silva, C. V., and Briones, M. R. (2014). Extracellular enolase of *Candida albicans* is involved in colonization of mammalian intestinal epithelium. *Front. Cell. Infect. Microbiol.* 4:66. doi: 10.3389/fcimb.2014.00066

Strand, M. R. (2014). Teratocytes and their function in parasitoid. *Curr. Opin. Insect Sci.* 6, 68–73. doi: 10.1016/j.cois.2014.09.005

Subramanian, A., and Miller, D. M. (2000). Structural analysis of alpha-enolase. Mapping the functional domains involved in down-regulation of the c-myc protooncogene. *J. Biol. Chem.* 275, 5958–5965. doi: 10.1074/jbc.275.8.5958

Thery, C., Amigorena, S., Raposo, G., and Clayton, A. (2006). Isolation and characterization of exosomes from cell culture supernatants and biological fluids. *Curr. Protoc. Cell Biol.* Chapter 3, Supplement 30, Unit 3.22, 1–29. doi: 10.1002/0471143030.cb0322s30

Thiéry, J. P. (1967). Mise en évidence des polysaccharides sur coupes fines en microscopie électronique. *J. Microsc.* 6, 987–1018.

Toledo, A., Coleman, J. L., Kuhlow, C. J., Crowley, J. T., and Benacha, J. L. (2012). The enolase of *Borrelia burgdorferi* is a plasminogen receptor released in outer membrane vesicles. *Infect. Immun.* 80, 359–368. doi: 10.1128/IAI.05836-11

Vanegas, G., Quinones, W., Carrasco-Lopez, C., Concepcion, J. L., Albericio, F., and Avilan, L. (2007). Enolase as a plasminogen binding protein in *Leishmania mexicana*. *Parasitol. Res.* 101, 1511–1516. doi: 10.1007/s00436-007-0668-7

Vinson, S. B., and Iwantsch, G. F. (1980). Host regulation by insect parasitoids. *Q. Rev. Biol.* 55, 143–165. doi: 10.1086/411731

Walsh, J. L., Keith, T. J., and Knull, H. R. (1989). Glycolytic enzyme interactions with tubulin and microtubules. *Biochim. Biophys. Acta* 999, 64–70.

Willms, E., Johansson, H. J., Mäger, I., Lee, Y., Blomberg, K. E., Sadik, M., et al. (2016). Cells release subpopulations of exosomes with distinct molecular and biological properties. *Sci. Rep.* 6:22519. doi: 10.1038/srep22519

Wygrecka, M., Marsh, L. M., Rory, E. M., Henneke, I., Guenther, A., Lohmeyer, J., et al. (2009). Enolase-1 promotes plasminogen-mediated recruitment of monocytes to the acutely inflamed lung. *Blood* 113, 5588–55984. doi: 10.1182/blood-2008-08-170837

Zhang, D., Dahlman, D. L., Jarlfors, U. E., Southgate, H. H., and Wiley, S. P. (1994). Ultrastructure of *Microplitis croceipes* (Cresson) (Braconidae: Hymenoptera) teratocytes. *Int. J. Insect Morphol.* 23, 173–187. doi: 10.1016/0020-7322(94)90016-7

Zimmerman, A. W., and Veerkamp, J. H. (2002). New insights into the structure and function of fatty acid-binding proteins. *Cell. Mol. Life Sci.* 59, 1096–1116. doi: 10.1007/s00018-002-8490-y

Conflict of Interest Statement: The authors declare that the research was conducted in the absence of any commercial or financial relationships that could be construed as a potential conflict of interest.

frontiers in Physiology

ORIGINAL RESEARCH
published: 21 June 2019
doi: 10.3389/fphys.2019.00747

Jinggangmycin-Induced UDP-Glycosyltransferase 1-2-Like Is a Positive Modulator of Fecundity and Population Growth in *Nilaparvata lugens* (Stål) (Hemiptera: Delphacidae)

Lin Quan Ge[1]†, Sui Zheng[1†], Hao Tian Gu[1], Yong Kai Zhou[1], Ze Zhou[1], Qi Sheng Song[2] and David Stanley[3]*

[1] School of Horticulture and Plant Protection, Yangzhou University, Yangzhou, China, [2] Division of Plant Sciences, University of Missouri, Columbia, MO, United States, [3] Biological Control of Insects Research Laboratory, United States Department of Agriculture – Agricultural Research Service, Columbia, MO, United States

The antibiotic jinggangmycin (JGM) is broadly applied in Chinese rice producing regions to control rice blight, a fungal disease. Aside from protecting rice plants from the disease, JGM leads to the unexpected action of stimulating brown planthopper (BPH; *Nilaparvata lugens*; Hemiptera: Delphacidae) reproduction to the extent it can influence population sizes. The JGM-induced BPH population growth has potential for severe agricultural problems and we are working to understand and mitigate the mechanisms of the enhanced reproduction. UDP-glucuronosyltransferases (UGTs) are multifunctional detoxification enzymes responsible for biotransformation of diverse lipophilic compounds. The biological significance of this enzyme family in insect fecundity is not fully understood, however, upregulated *UGT12* in JGM-treated BPH, may influence fecundity through metabolism of developmental hormones. This idea prompted our hypothesis that *Nl*UGT12 is a positive modulator of BPH reproductive biology. JGM treatment led to significant increases in accumulations of mRNA encoding *Nl*UGT12, numbers of eggs laid, oviposition period, juvenile hormone III titers, and fat body, and ovarian protein contents. dsUGT12 treatment suppressed *NlUGT12* expression and reversed JGM-enhanced effects, resulting in under-developed ovaries and reduced expression of juvenile hormone acid methyltransferase and the JH receptor, methoprene tolerant. Application of the JH analog, methoprene, on dsUGT12 treated-females partially reversed the dsUTG12 influence on vitellogenin synthesis and on *NlUGT12* expression. These results represent an important support for our hypothesis.

Keywords: *Nilaparvata lugens*, UDP-glycosyltrasferase 1-2-like, jinggangmycin, fecundity, population growth

OPEN ACCESS

Edited by:
Anne-Nathalie Volkoff, Institut National de la Recherche Agronomique, France

Reviewed by:
Kai Lu, Fujian Agriculture and Forestry University, China
Xiao-Yue Hong, Nanjing Agricultural University, China

****Correspondence:***
Lin Quan Ge
lqge@yzu.edu.cn

† These authors have contributed equally to this work as co-first authors

Specialty section:
This article was submitted to Invertebrate Physiology, a section of the journal Frontiers in Physiology

Received: *22 November 2018*
Accepted: *31 May 2019*
Published: *21 June 2019*

Citation:
Ge LQ, Zheng S, Gu HT, Zhou YK, Zhou Z, Song QS and Stanley D (2019) Jinggangmycin-Induced UDP-Glycosyltransferase 1-2-Like Is a Positive Modulator of Fecundity and Population Growth in Nilaparvata lugens (Stål) (Hemiptera: Delphacidae). Front. Physiol. 10:747. doi: 10.3389/fphys.2019.00747

INTRODUCTION

The brown planthopper (BPH), *Nilaparvata lugens* (Stål) (Hemiptera: Delphacidae), is a classic pesticide-induced resurgence insect pest. The fungicide jinggangmycin (JGM), a product of *Streptomyces var. jinggangen*, is applied for rice sheath blight (*Rhizoctonia solani*) control in China (Peng et al., 2014). JGM foliar sprays alter BPH male and female physiological parameters and enhance fecundity, by up to 99%. A few examples of these physiological changes include enhanced flight capacity, thermotolerance, body weights, protein and lipid contents, and JH titers (Jiang et al., 2012). It is an attractive product due to its low cost, efficacy in the field, low toxicity and environmental residue. The current concern is that it also has real potential to spark agroecological catastrophes that may follow JGM-stimulated BPH fecundity.

JGM increased BPH fecundity via increased fatty acid metabolism (Jiang et al., 2016; Li et al., 2016), however, the broad impact of JGM led us to consider additional pathways that might also influence BPH reproduction. From digital gene (DEG) expression profiles, we identified a UDP-glycosyltransferase 1-2 like (*UGT12*) gene that was up-regulated in adult females following foliar JGM treatments (200 ppm) at 2 days after emergence (2 DAE). The UGTs form a superfamily of enzymes that catalyze the transfer of a glycosyl group from a nucleotide sugar, such as UDP-glucuronic acid or UDP-glucose, to a variety of small hydrophobic molecules (aglycones), thereby making them hydrophilic for efficient excretion (Mackenzie et al., 1997; Meech and Machenzie, 1997; Meech et al., 2019). Members of this superfamily are ubiquitous and act in many biological processes, including olfaction (Lazard et al., 1991), steroid metabolism, and detoxification of exogenous substrates (Meech and Machenzie, 1997).

In insects, these enzymes typically utilize UDP-glucose as the sugar donor (Ahmad and Hopkins, 1993a). As in vertebrates, endogenous and exogenous substrates undergo glycosylation in insects. Insect UGTs act in detoxification of plant allelochemicals, cuticle formation, pigmentation, olfaction, and ecdysteroid (20E) metabolism (Tompson et al., 1987; Hopkins and Kramer, 1992; Ahmad and Hopkins, 1993a,b; Wang et al., 1999). The UGT enzyme activity has been reported in tissues, such as fat body, of many insect orders, including fruit flies, *Drosophila melanogaster* (Diptera: Drosophilidae) (Real et al., 1991). The presence of UGT enzymes in the antenna of *D. melanogaster* indicate a role in olfaction (Wang et al., 1999). UGT activity was also recorded in silkworms, *Bombyx mori* (Lepidoptera: Bombycidae) (Luque et al., 2002). Many endogenous compounds, like 20E (Svoboda and Weirich, 1995) and cuticle tanning precursors (Hopkins and Kramer, 1992; Ahmad et al., 1996) are glycosylated by UGTs. UGTs in *Helicoverpa armigera* Hübner (Lepidoptera: Noctuidae) are factors for host plant adaptation and insecticide resistance (Heckel, 2010). Li et al. (2016) found that *UGT2B17* operates in chlorantraniliprole resistance in *Plutella xylostella* (L.) (Lepidoptera: Plutellidae).

It remains unknown whether UGT-encoding genes act in insect reproduction, although they may act indirectly. Collier et al. (2012), for example, reported that UGT1a genes are expressed in murine placentas and fetal livers in a model of intracytoplasmic sperm injection and *in vitro* fertilization. These genes promote enhanced steroid hormone clearance, which may mediate negative outcomes. In their review of the UGT superfamily, Meech et al. (2019) note that UGT-encoding genes are expressed in a range of reproduction-functioning tissues, including ovary, uterus, cervix, placenta, breast, testes, and prostate. We infer UGTs influence reproductive events by catalyzing various metabolic steps that influence levels of steroid hormones and other biomolecules. From this, we posed the hypothesis that NlUGT12 acts as a positive modulator of BPH reproductive biology. In this paper we report on the outcomes of experiments designed to test our hypothesis.

MATERIALS AND METHODS

Rice Variety, Insect, and Pesticide

Rice seeds (*Oryza sativa* L.) of the variety Ningjing 2 (Japonica rice) were sown in rectangular field cement tanks (200 cm × 100 cm × 60 cm, L, W, H). Rice plants at the tillering stage were used for all experiments.

The *Nilaparvata lugens* strain was obtained from the China National Rice Research Institute (CNRRI: Hangzhou, China). BPH were reared on rice plants in cement tanks covered with fine mesh under natural conditions from April to October and thereafter overwintered in an insectary at 26 ± 2°C and 14L:10D at Yangzhou University. Technical grade JGM ($C_{20}H_{35}O_{13}N$) (61.7% a.i) (Qianjing Biochemistry Co. Ltd., Haining, Zhejiang Province, China) was used in all trials. Third instar BPH was used in all experiments (Ge et al., 2009; Wang et al., 2010).

Experimental Design

Rice plants were sprayed with 200 ppm JGM and control plants were treated with tap water. Each treatment was repeated three times (3 pots) and distributed randomly. The 72 h-post-spray nymphs were selected for RNAi experiments and maintained in a climate chamber (Model: RXZ 328A) (Jiangnan Instrument Factory, Ningbo, Zhejiang, China) at 26 ± 2°C and L16:D8 in glass jars (6-cm diameter, 12-cm height) with a rice stem until emergence.

dsRNA Synthesis

Based on our digital gene (DEG) expression profiles, we selected UGT12 (accession no. XM022331295) as a RNAi target in the JGM-treated BPH. To synthesize double-stranded RNA (dsRNA), a 575 bp (the fragment from 861 to 1435 bp) was amplified with T_7 RNA polymerase promoter linked primers (**Table 1**). The thermocycler (T-100, Bio-Rad Co., California, United States) was programmed at pre-denaturing at 94°C for 4 min, followed by 35 cycles of denaturing at 94°C for 30 s, annealing at 55.2°C for 30 s and extension at 72°C for 1 min, with a final extension at 72°C for 10 min. The products were sequenced and then used as queries in BLAST searches to control identity in NCBI (98–99% identity) prior to dsRNA synthesis. The GFP gene (accession no. ACY56286) was used as a negative control (Chen et al., 2010). All dsRNAs were synthesized

TABLE 1 | PCR primers used in this study.

Purpose	Primer ID	Sequence (5′-3′)	Size (bp)
qPCR analysis	Q-UGT12-F	ACACTGCCTACGAACTGGAA	157
	Q-UGT12-R	CTCCATCCTCTGACTCGTCC	
	Q-Vg-F	GCTTGTCAGAATGCCACC	184
	Q-Vg-R	TCTTGCCAGAAGGATTGC	
	Q-VgR-F	AGGCAGCCACACAGATAACCGC	136
	Q-VgR-R	AGCCGCTCGCTCCAGAACATT	
	Q-JHAMT-F	AAATACGGCAATAAGAAC	112
	Q-JHAMT-R	GAAGACAATAAAACGAGA	
	Q-Met-F	CCGCACCCAACAACAATACA	288
	Q-Met-R	CCAATCCGTTTACCACCACA	
	actin-F	TGCGTGACATCAAGGAGAAGC	186
	actin-R	CCATACCCAAGAAGGAAGGCT	
dsRNA	UGT12-F	GGACGAGTCAGAGGATGGAG	575
synthesis	UGT12-R	AGGTGAGATCAAAGCAGGCT	
	UGT12-T7F	Taatacgactcactataggg (T_7 promoter) GGACGAGTCAGAGGATGGAG	
	UGT12-T7R	Taatacgactcactataggg (T_7 promoter) AGGTGAGATCAAAGCAGGCT	
	GFP-F	AAGGGCGAGGAGCTGTTCACCG	688
	GFP-R	CAGCAGGACCATGTGATCGCGC	
	GFP-T7F	Taatacgactcactataggg (T_7 promoter) AAGGGCGAGGAGCTGTTCACCG	
	GFP-T7R	Taatacgactcactataggg (T_7 protometer) CAGCAGGACCATGTGATCGCGC	

F, forward; R, reverse. Lowercase letters labeled sequences represent for T_7 promoter.

using a T_7 RiboMAX^{TM} Express RNAi System (Promega, Madison, WI, United States) according to the manufacturer's protocols. The dsRNA products were diluted with 50 μL diethylpyrocarbonate-treated water and stored at −80°C. The purified dsRNAs were quantified using spectroscopy at 260 nm and separated by agarose gels to validate their integrity.

Silencing UGT12

BPH were released into potted rice and treated with JGM as just described. The dsRNA treatments induced high mortality of second instar nymphs (over 95%) (Ge et al., 2017). Third-instar nymphs (20/treatment) were collected 3 days after the JGM treatments, and subjected to RNAi via an artificial diet as described by Dong et al. (2011), with slight modifications. Earlier studies found a high efficiency of dsRNA ingestion-mediated gene silencing in BPH (Fu et al., 2001). Glass cylinders (15.0-cm L × 2.5-cm D) have been used as feeding chambers, with four dsRNA concentrations, 0.12, 0.075, 0.05, and 0.025 μg/μL. In this study, the optimal dsRNA concentration, 0.075 μg/μL, was determined from preliminary experiments with the noted concentrations. The artificial diet (40 μL) was held between two layers of stretched Parafilm M membrane enclosing the two open ends of the chamber (the diet capsule), which was replaced every second day. Six days later, fifth (final) instar nymphs were transferred into a glass jar (12-cm H × 6-cm D), and maintained on rice plants under 26 ± 2°C, RH 90%, and 16L:8D photoperiod. The newly emerged females were collected separately and soluble protein content (fat body and ovary, 15 BPH/replicate or $n = 15$, $N = 3$ replicates), JH (whole body, $n = 5$, $N = 3$) and ecdysone titers (whole body, $n = 5$, $N = 3$), body weight ($n = 10$, $N = 3$), and longevity ($N = 19$) were recorded. We used whole bodies to determine the expression levels of *NlVg*, *NlVgR* (vitellogenin receptor, VgR), *NlJHAMT*, *NlMet*, and *NlUGT12* ($n = 5$, $N = 3$ for each gene) at 2 or 3 DAE and similarly whole bodies were used to determine Vg, JHAMT, Met, and UGT12. All the replicates were biologically independent. We separately selected 3 groups, 10 virgin females/group, to determine *NlUGT12* RNAi efficiency at 1, 3, 5, and 7 DAE. Others were used to isolate reproductive tracts at 2, 4, and 6 DAE. We recorded the pre-oviposition period, oviposition period, adult female longevity, and fecundity of 20 mated pairs (untreated ♀ × ♂). The eggs laid were counted under a microscope and rice stalks were replaced every second day.

Extraction and cDNA Synthesis

Total RNA was extracted using the Trizol reagent (Invitrogen, Carlsbad, CA, United States) according to the manufacturer's instructions. The concentration and purity of RNA sample were measured using a Nanodrop 2000C spectrophotometer (Thermo Fisher Scientific, West Palm Beach, FL, United States) and the integrity was checked by 1.5% agarose gel electrophoresis. Genomic DNA was cleared bussing DNase treatment. The first-strand cDNA was synthesized from 1 μg of the total RNA using a PrimeScript RT Reagent Kit with gDNA Eraser (TaKaRa, Tokyo, Japan) in a final volume of 20 μL.

Quantitative Real-Time PCR (qPCR)

Primers for qPCR were designed at http://primer3.ut.ee/ (Rozen and Skaletsky, 2000) (**Table 1**). Primer sets were validated

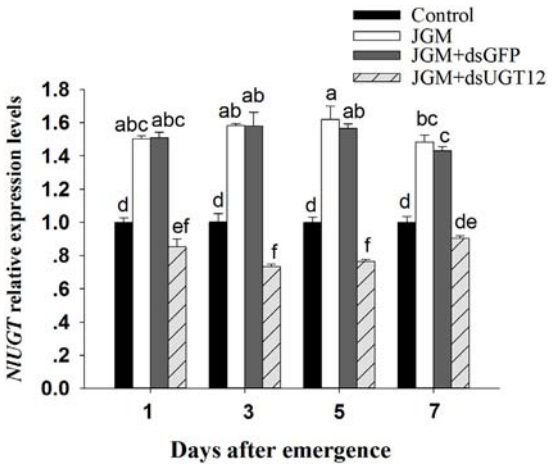

FIGURE 1 | Effects of JGM+dsUGT12 treatments on expression levels at different days post emergence (DAE). *NlUGT12* expression value of untreated females was converted to 1. The histogram bars show mean relative gene expression ($n = 3$ independent biological replicates) and the error bars represent one standard deviation (Tukey, $P < 0.05$). Gene expression was normalized to the β-actin reference gene.

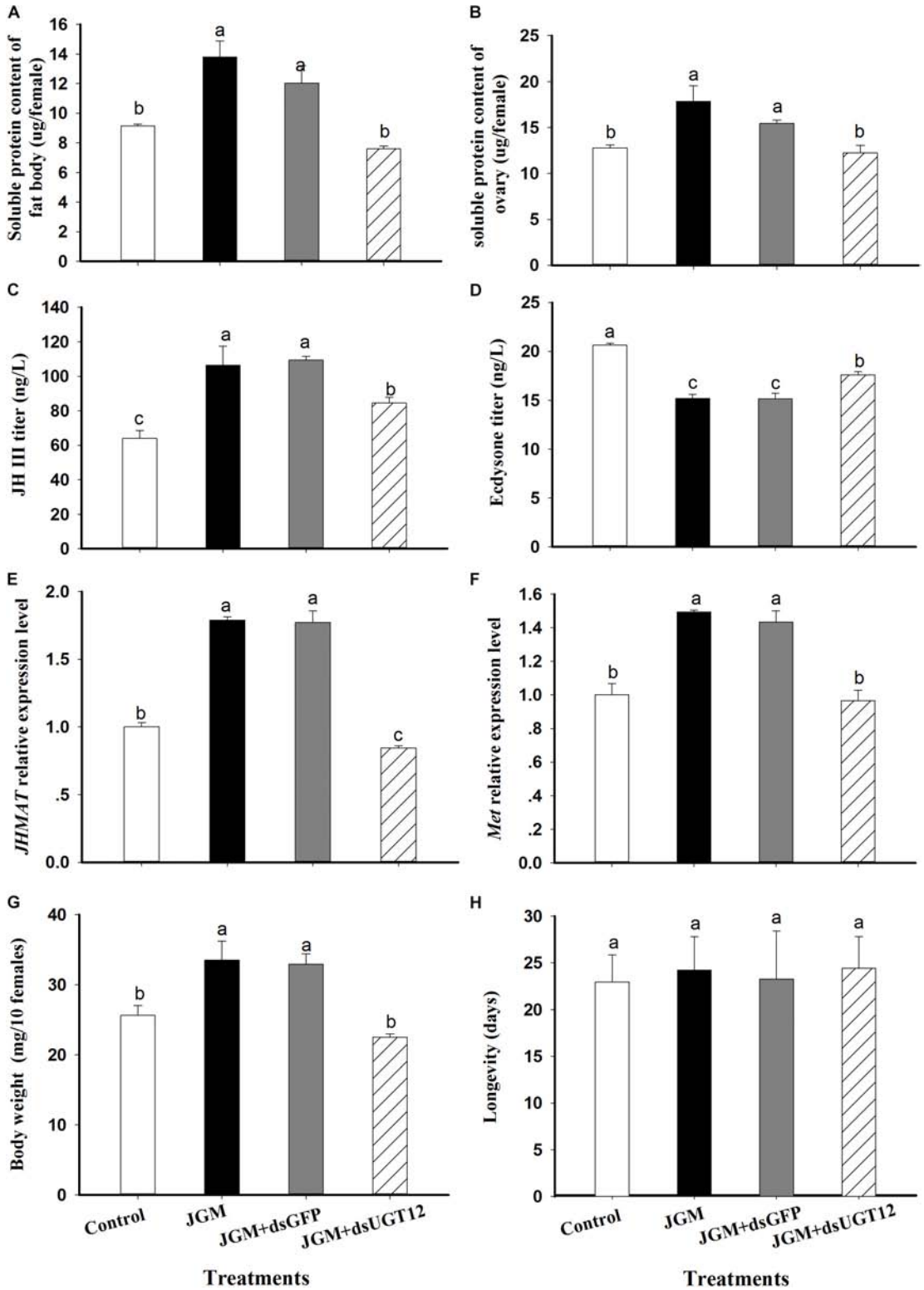

FIGURE 2 | Effects of JGM+dsUGT12 treatments on female physiology at 2 DAE. For all panels, unless noted differently, $n = 3$ independent biological replicates. **(A)** The histogram bars show mean fat body soluble protein content (μg/female,±SE) at 2 DAE. **(B)** The histogram bars show mean ovarian soluble protein content (μg/female). **(C)** the histogram bars show mean JH III titer (ng/L) in adult females ($n = 3$). **(D)** The histogram bars show mean ecdysone titer (ng/L) in adult female. **(E)** The histogram bars show mean *JHAMT* mRNA relative expression level. **(F)** The histogram bars show mean *Met* mRNA relative expression level. **(G)** The histogram bars show mean body weight (mg/10 females). **(H)** The histogram bars show mean longevity of adult females ($n = 19$ independent biological replicates).

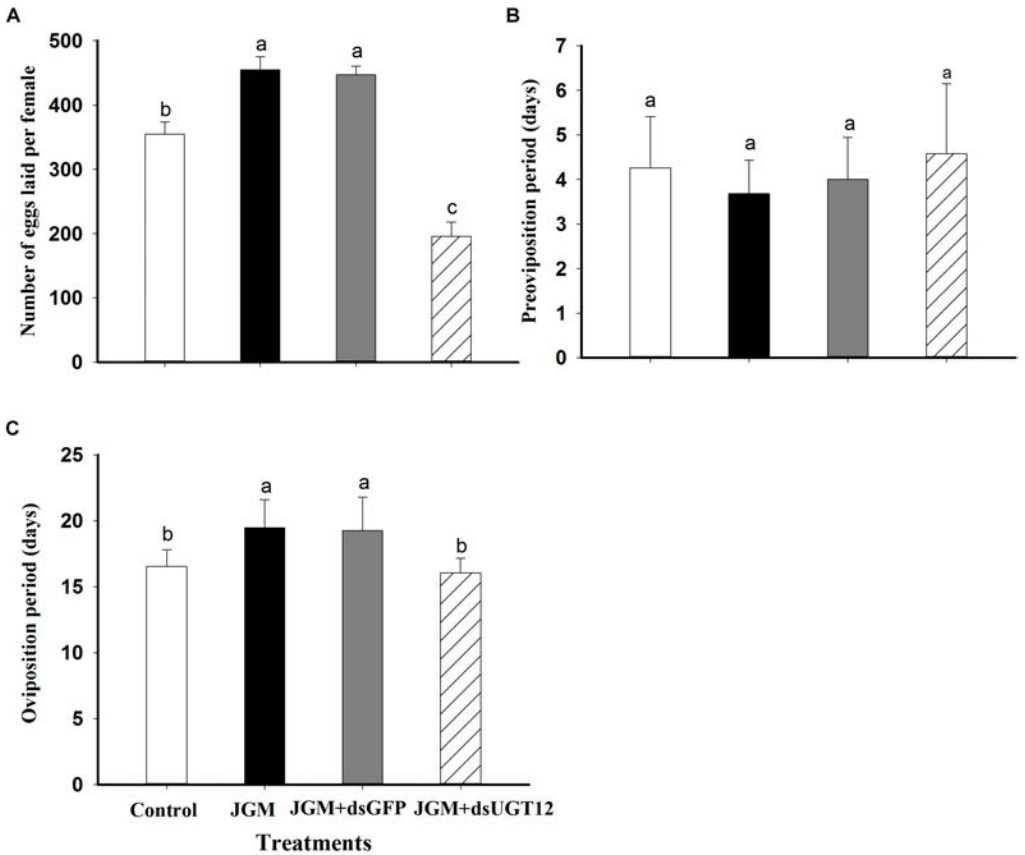

FIGURE 3 | Effects of JGM+dsUGT12 treatment on adult females reproduction parameters. **(A)** The histogram bars show mean numbers of eggs laid (n = 19 independent biological replicates). **(B)** The histogram bars show pre-oviposition period (days) (n = 19 independent biological replicates). **(C)** The histogram bars show oviposition period (days) (n = 19 independent biological replicates).

by relative standard curves for each gene transcript and amplification efficiency (E) along with correlation coefficient (R^2) were calculated for each primer pair. All qPCR reactions were performed in biologically independent triplicates in a CFX96 real-time PCR system (Bio-Rad Co., Ltd., California, United States). Each 10 μL reaction contained 5 μL 2 × SYBR Premix^{EX} TaqII Master Mix (TaKaRa, Tokyo, Japan), 0.4 μL reverse primer (10 μM), 1 μL cDNA template and 3.2 μL of deionized water. The thermocycler was programmed at 95°C for 30 s, followed by 35 cycles at 95°C for 5 s, 55.2°C for 15 s, and 72°C for 1 min. A β-actin (EU179846) cDNA fragment was amplified with actin-F and actin-R primers (**Table 1**) as a reference gene (Chen et al., 2010). The relative mRNA levels of target genes were quantified using the $2^{-\Delta\Delta Ct}$ method (Livak and Schmittgen, 2001). Three biologically independent replicates based on independent RNA sample preparations were performed for each gene.

Effects of Dietary dsRNA on Biological Performance Parameters

Protein contents in the fat bodies and ovaries were determined using the Bradford protocol (Bradford, 1976; Gong et al., 1980) with Coomassie Brilliant Blue G 250 (Shanghai Chemical Agent Co., Ltd., Shanghai, China). The fat bodies and ovaries were isolated under a zoom-stereomicroscope (model XTL20, Beijing Tech Instrument Co., Ltd., Beijing, China) in a cooled petri dish. The isolated ovaries and fat bodies were placed in pre-weighed separate ice-cold centrifuge tubes. The tubes were re-weighted on a Mettler-Toledo electronic balance (EC 100 model; 1/10000 g sensitivity), homogenized on ice in 5 mL phosphate buffered saline (PBS; 137 nM NaCl; 2.68 nM KCl; 1.47 mM KH_2PO_4; and 8.10 mM Na_2HPO_4, pH 7.0), and centrifuged at 10,000 × g at 4°C for 20 min. The supernatants were collected as sample preparations. A standard curve was established based on a standard protein (bovine serum albumin (Shanghai Biochemistry Research Institute, Shanghai, China). The absorbance at 595 nm was determined in a UV755B spectrometer (Shanghai Precision Instrument Co., Ltd., Shanghai, China). The protein content in the sample solution was calculated from the standard curve.

For body weight measurement, 10 females at 2 DAE were used as a replicate for each treatment, and control group. Females were placed in pre-weighed centrifuge tubes and weighed on the balance just described. The treatment and control groups had three biologically independent replicates.

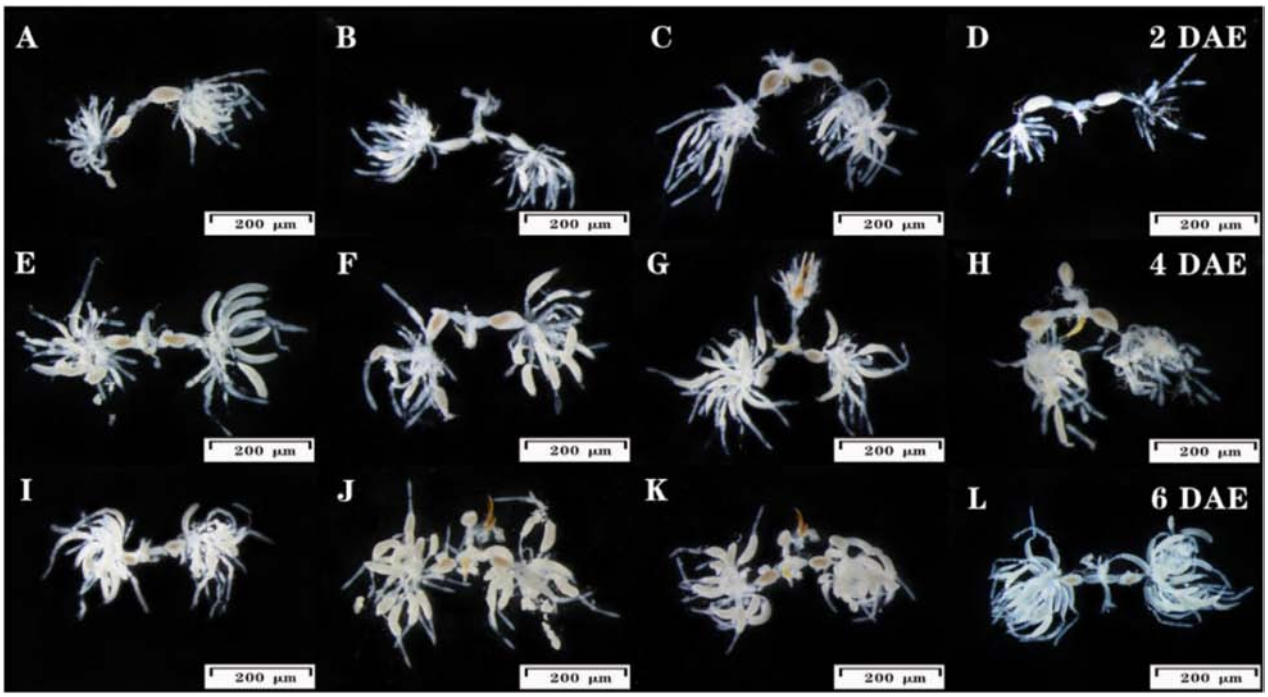

FIGURE 4 | Effects of JGM+dsUGT12 on female reproductive tract at 2, 4, and 6 DAE. The third instar nymphs amenable to JGM spraying were treated with dsUGT12 diet. **(A–L)** reproductive tracts were dissected from mated females and photographed. Ovaries from at least ten females of each group were dissected and observed under a microscope. Scale bar, 200 μm.

We followed the manufacturer's instructions to determine JH III (n = 5, N = 3) and ecdysone titers (n = 5, N = 3) of whole body using an insect double sandwich ELISA kit (Qiaodu biological technology Co., Ltd., Shanghai, China). Each treatment was performed in biologically independent triplicates.

Hormone Treatment

Methoprene (Sigma Chemical Co., Ltd.,cn, United States, weight, 100 mg, Purity, 99.5%) was dissolved in 1 mL acetone to produce a 100 μg/μL stock solution, and stored at −20°C (Ayoade et al., 1999). The stock solutions were diluted to concentrations indicated in Results with acetone and topically applied to the backs of newly emerged, RNAi-treated (100 ng/μL) females using a syringe (Terumo), and a micro applicator (Burkard). The BPH were transferred into glass jars described above and maintained on rice plants at 26 ± 2°C, RH 90%, and 16L:8D photoperiod. The insects were collected at 24 and 48 h, and *NlVg* and *NlUGT12* expression levels, and Vg protein synthesis post methoprene administration were determined. Each treatment was performed in biologically independent triplicates.

Ovary Isolation

The ovaries were isolated from the 2, 4, and 6 DAE females. There were four treatment groups: untreated controls, JGM-treated, JGM+dsGFP-treated, and JGM+dsUGT12-treated in 1 × PBS, n = at least 10 ovaries/group. After extensive washing, ovaries were photographed with a Leica DMR connected to a Fuji FinePix S_2 Pro digital camera (Germany).

Western Blot Analysis

Isolated fat bodies were homogenized in precooled lysis buffer (8 M urea, 4% CHAPS, 40 nM Tris pH 8.0, 5 nM EDTA, 1 mM PMSF, and 10 mM DTT) (Amersco, Solon, OH, United States) and 0.2 mM protease inhibitor (Roche Diagnostics, Basel, Switzerland), held at 4°C for 1 h and centrifuged at 12,000 × g at 4°C for 20 min. Protein concentration was detected using a bicinchoninic acid (BCA) method (CWOO14S, CWBIO Biological Co., Taizhou, Jiangsu Province, China). Aliquots of 30 μg protein were separated by 8% SDS-PAGE, electroblotted (Model: 1658001, Bio-Rad, Co., Ltd., California, United States) onto polyvinglidene fluoride membrane (PVDF) (Millipore, Billerica, MA, United States). After blocking with 5% non-fat milk (Amersco, Solon, OH, United States) in Tris–buffered saline (TBS) for 2 h at room temperature, the membranes were incubated with *N. lugens* primary antibodies for β-*actin* (1:2000) and *NlVg* (1:5000) at 4°C overnight. After washing three times for 15 min each with 0.5% Tween-20 in TBS (TBST), the membranes were incubated with goat anti-rabbit immunoglobulin G horseradish peroxidase-conjugated secondary antibody (Sigma, St. Louis, MO, United States) for 1 h at room temperature (Lu et al., 2016). The immunoreactivity was detected using the SuperSignal West Pico Chemiluminescent Substrate ECL (Pierce, Rockford, IL, United States) and the membrane was imaged with a GBOX-Chemi XT4 Imager (Syngene, Cambridge, United Kingdom). Vg protein abundance was compared with the internal control, β-actin. The Vg antibody was a gift from Professor Qiang Zhou (Sun Yat-sen University). The mean gray

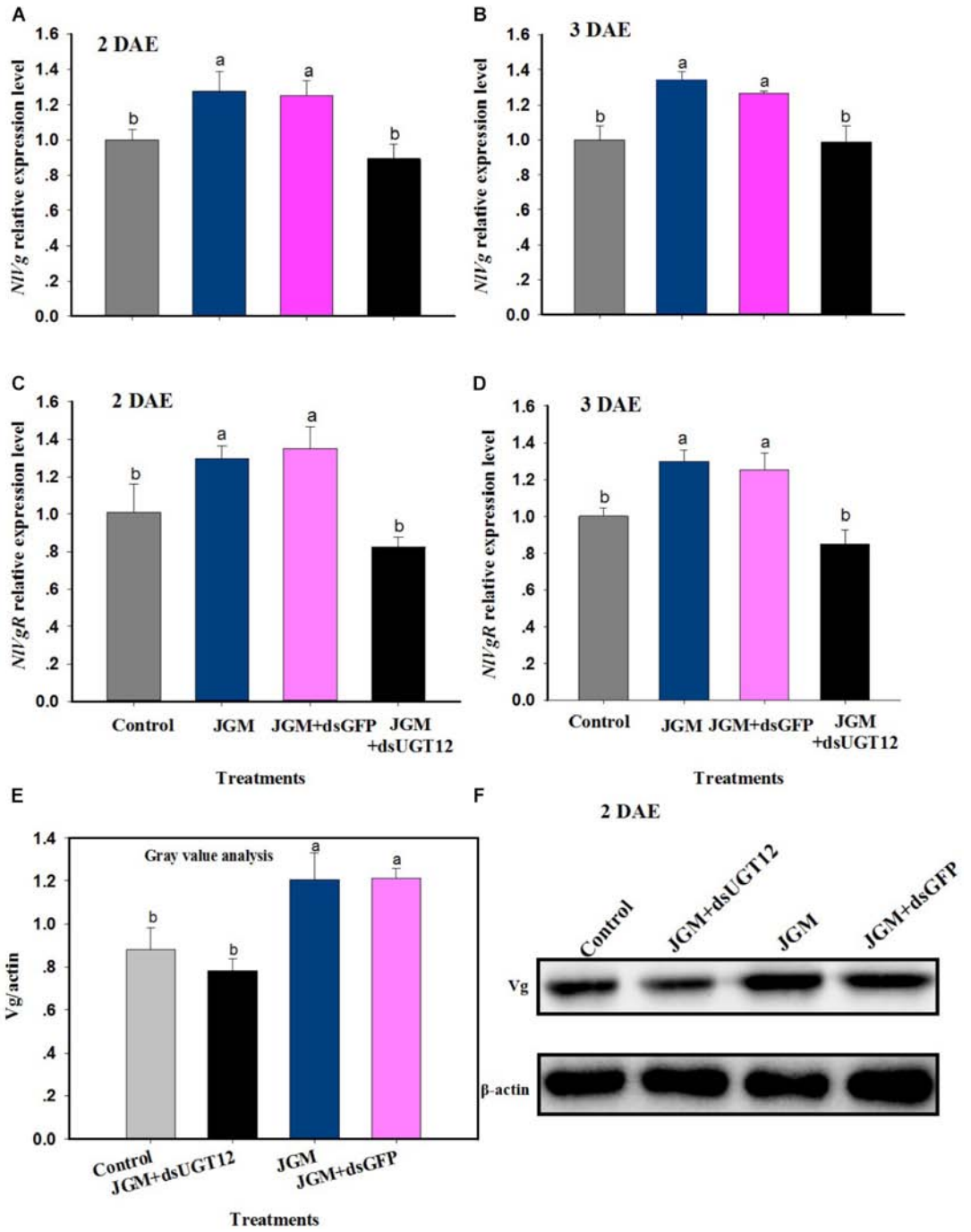

FIGURE 5 | Effects of JGM+dsUGT12 treatment on *NlVg, NlVgR* expression and Vg protein synthesis. **(A,B)** The histogram bars show mean *NlVg* expression level at 2 DAE and 3 DAE, respectively. **(C,D)** The histogram bars show mean *NlVgR* expression level at 2 DAE and 3 DAE. **(E)** The histogram bars show mean gray values of each band at 2 DAE. **(F)** Effects of JGM+dsUGT12-treated on protein levels of Vg in the fat body of adult females at 2 DAE. Western blot analysis was performed using Vg antibody specific for *N. lugnes*.

values of each band were normalized to β-actin using NIH image J software[1], $n = 3$ biologically independent replicates (**Supplementary Material**).

[1]https://imagej.nih.gov/ij/

Population Growth

We set up four mating groups: 1/ controls, untreated males × untreated females; 2/ control-♂ × JGM-treated females (JGM-♀); 3/ control-♂ × JGM+dsGFP-treated females (JGM+dsGFP-♀); and 4/ control-♂ × JGM+dsUGT12-treated

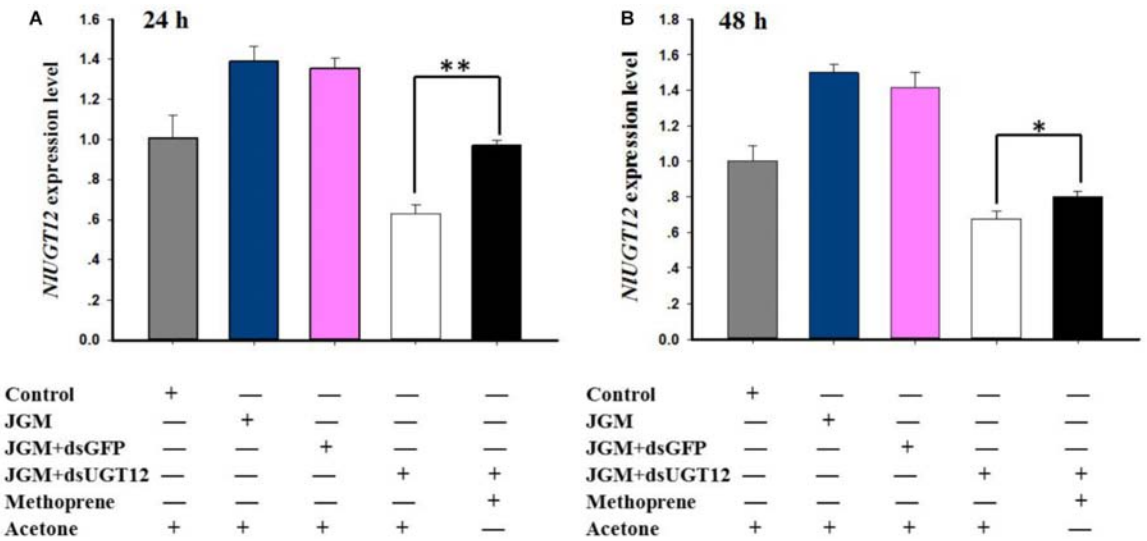

FIGURE 6 | Effects of methoprene topical application on *NlUGT12* expression level. **(A)** The histogram bars show *NlUGT12* expression level at 24 h post administered (** denotes significant difference at $P < 0.01$). **(B)** The histogram bars showed *NlUGT12* expression level at 48 h post administered (The asterisk represents significant difference at $P < 0.05$).

females (JGM+dsUGT12-♀). The experiment was arranged with a randomized complete block design with five biologically independent replicates. Two pairs of newly emerged BPH were released onto rice plants and covered with an 80-mesh nylon cylindrical cage (20 cm D × 80 cm H) in each pot. Ten days later, we started counting the next generation neonates each day, which were transferred into new plastic plots with rice plants covered as described until the parent females died. Numbers of neonates in the new plastic plot were recorded every second day until adult emergence. Numbers of unhatched eggs on the rice stems were recorded. Hatching rate was also recoded (total neonates/total neonates plus unhatched eggs). The population growth index (PGI) was expressed as N1/N0, with N1 representing the total neonates of next generation and unhatched eggs, and N0 representing the insects released (N0 = 4).

Statistical Analysis

The normal distributions and homogeneity of variances (determined using the Bartlett test) were verified before performing analysis of variance (ANOVA) tests. A one-way ANOVA was performed for the number of eggs laid (N = 19), the pre-oviposition period (N = 19), the oviposition period (N = 19), the longevity of the females (N = 19), the contents of soluble protein (fat body and ovary, n = 15, N = 3), JH III and ecdysone titer (n = 5, N = 3), body weight (n = 10, N = 3), longevity (N = 19), the number of offspring (N = 5), hatching rate (N = 5), gender ratio (N = 5), western blot (n = 20, N = 3), and *NlVg, NlVgR, NlJHAMT, NlMet* and *NlUGT12* expression levels (n = 5, N = 3). All data were expressed as means ± standard error of the mean (SEM) from three independent biological replicates, unless otherwise noted in figure legends. Two-way (days after emergence and dsRNA treatment) ANOVAs were performed to analyze the data in **Figure 1**. Multiple comparisons of the means were conducted using Fisher's Protected Significant Difference (PLSD) test. All analyses were conducted using the data processing system (DPS) of Tang and Feng (2002). Biological parameter data were analyzed using an analysis of variance (ANOVA) with one factor and statistical data are presented in **Table 2**.

RESULTS

dsUGT12 Treatments Reduce JGM-Enhanced NlUGT12 Expression

Compared to untreated controls, the JGM treatments led to substantially increased accumulations of mRNA encoding NlUGT12 over the 7-day experiment. The dsUGT12 treatments reversed the enhancing influence of JGM, with accumulations of NlUG12-encoding mRNA below control levels except for day 7 (down from the JGM influence by 39–53%) (**Figure 1**). The pattern did not differ across days (all statistics are listed in **Table 3**). We recorded an interactive effect between DAE and JGM+dsRNA treatments.

dsUGT12 Treatments Alter Protein Contents and Related Parameters in JGM-Treated BPH

Compared to controls, the JGM treatments led to substantially increased fat body and ovarian proteins, JH III titer, accumulations of mRNA encoding JHAMT and Met, and body weights. The treatments led to reduced 20E titers. None of the treatments influenced adult female lifespans (**Figure 2**). dsUGT12 treatment in nymphs effectively reversed the positive

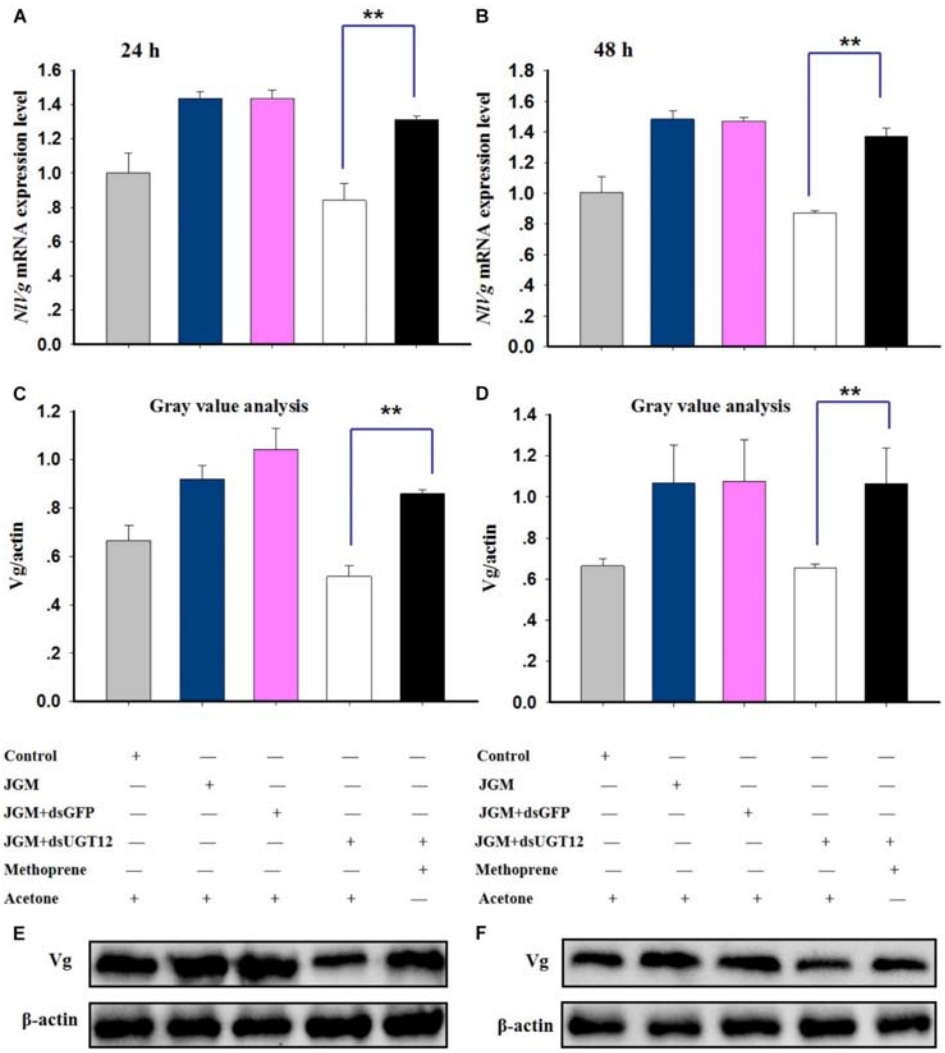

FIGURE 7 | Effects of methoprene topical application on *NlVg* expression and Vg protein expression levels. The histogram bars show *NlVg* expression level at 24 h **(A)** and 48 h **(B)** (** denotes significant difference at $P < 0.01$). The histogram bars show mean gray values of Vg protein levels at 24 h **(C)** and 48 h **(D)** (** denotes significant difference at $P < 0.01$). The Vg protein levels of JGM+dsUGT12-treated female fat bodies was quantified 24 h **(E)** and 48 h **(F)** post methoprene topical application relative to the other groups which received the equivalent amount of acetone.

influences of JGM. In general, the dsUGT12 treatment yielded values not different from untreated controls, with the exception of *JHAMT* expression (**Figure 2E**) with results slightly but significantly lower than control results.

dsUGT12 Treatments Reduce Egg Deposition in JGM-Treated BPH

Untreated control BPH deposited about 370 eggs/female, which was substantially increased in the JGM-treated group. The dsUGT12 treatment led to reduced egg laying in JGM-treated BPHs, significantly below results with untreated controls (**Figure 3A**). JGM treatments had no influence on the pre-oviposition period (**Figure 3B**) although the treatments led to significant increase in oviposition period, which was reversed by the dsUGT12 treatment (**Figure 3C**).

dsUGT12 Treatments Led to Dysfunctional Ovaries in JGM-Treated BPH

dsUGT12 treatment (**Figures 4D,H,L**) impeded ovarian development compared to JGM-treatments (**Figures 4B,C,F,G,J,K**) at 2, 4, and 6 DAE. The ovarioles of JGM-treated groups contained two or more banana–shaped oocytes (**Figure 4B**) at 2 DAE while there were no such oocytes in untreated controls, nor in the JGM+dsUGT12-treated group during the same time period (**Figures 4A,D**). Ovaries of the untreated control group (**Figures 4A,E,I**), the JGM-treated group (**Figures 4B,F,J**), and JGM+dsGFP group (**Figures 4C,G,K**) contained mature eggs (light brown colored) at 4 and 6 DAE, but the JGM+dsUGT12-treated group contained no mature eggs (**Figures 4H,L**).

TABLE 2 | Statistical analyses of biological parameter data.

Experiment	Statistic
dsUGT12 reduced *NlUGT12* expression at different days after emergence	$F = 1030.8$, df = 3, 47, $P = 0.0001$
Effects of dsUGT12 silencing on *NlUGT12* expression at DAEs	$F = 1.4$, df = 3, 47, $P = 0.2552$
Effects of dsUGT12 silencing on interactive effect between DAEs and JGM+dsRNA treatments	$F = 8.8$, df = 3, 47, $P = 0.0001$
dsUGT12 reduced JH titer, 2 DAE	$F = 34.2$, df = 3, 11, $P = 0.0001$
dsUGT12 increased 20E titer, 2 DAE	$F = 130.6$, df = 3, 11, $P = 0.0001$
dsUGT12 reduced protein content of fat body and ovary, 2 DAE	$F = 36.9$, df = 3, 11, $P = 0.0001$ for fat body $F = 21.4$, df = 3, 11, $P = 0.0004$ for ovary
dsUGT12 reduced *JHAMT* and *Met* expression, 2 DAE	$F = 325.3$, df = 3.11, $P = 0.0001$ for *JHAMT* $F = 75.4$, df = 3, 11, $P = 0.0001$ for *Met*
dsUGT12 reduced body weight, 2 DAE	$F = 30.1$, df = 3, 11, $P = 0.0001$
dsUGT12 reduced number of laid eggs	$F = 39.3$, df = 3, 75, $P = 0.0001$
dsUGT12 reduced oviposition period	$F = 23.5$, df = 3, 75, $P = 0.0001$
dsUGT12 was not significant difference for preoviposition period	$F = 2.1$, df = 3, 75, $P = 0.1077$
dsUGT12 was not significant difference for longevity of females	$F = 0.659$, df = 3, 75, $P = 0.5802$
dsUGT12 reduced *NlVg* expression, 2DAE	$F = 74.6$, df = 3, 11, $P = 0.0001$
dsUGT12 reduced *NlVg* expression, 3 DAE	$F = 23.5$, df = 3, 11, $P = 0.0003$
dsUGT12 reduced *NlVgR* expression, 2 DAE	$F = 16.3$, df = 3, 11, $P = 0.0009$
dsUGT12 reduced *NlVgR* expression, 3 DAE	$F = 27.9$, df = 3, 11, $P = 0.0001$
dsUGT12+methoprene rescued *NlUGT12* expression, 24 h	$F = 59.2$, df = 4, 14, $P = 0.0001$
dsUGT12+methoprene rescued *NlUGT12* expression, 48 h	$F = 99.8$, df = 4, 14, $P = 0.0001$
dsUGT12+methoprene rescued *NlVg* expression, 24 h	$F = 39.6$, df = 4,14, $P = 0.0001$
dsUGT12+methoprene rescued *NlVg* expression, 48 h	F = 66.5, df = 4, 14, $P = 0.0001$
dsUGT12 reduced number of offspring	$F = 16.9$, df = 3, 19, $P = 0.0001$
dsUGT12 reduced eggs hatching rate	$F = 18.6$, df = 3, 19, $P = 0.0001$
dsUGT12 let to no significant difference for gender ratio	$F = 1.62$, df = 3, 19, $P = 0.1847$

TABLE 3 | Influence of JGM+dsUGT12 treatment on the number of offspring, hatching rate, and gender ratio.

Treatments	Number of eggs laid	Hatching rate	Gender ratio	PGI (N1/N0)
Control	386.0 ± 25.7b	0.91 ± 0.03a	1.44 ± 0.42ab	96.5
JGM	516.6 ± 56.2a	0.95 ± 0.02a	1.92 ± 0.41a	129.2
JGM+dsGFP	534.8 ± 97.3a	0.94 ± 0.02a	2.02 ± 0.46a	113.7
JGM+dsUGT12	286.4 ± 54.2c	0.83 ± 0.05b	1.65 ± 0.55ab	71.6

**Means ± SE of five replicates. Means with columns followed by different letters are significantly different at the 5% level ($p < 0.05$, Tukey test). Control Group, control-♀ × control-♂; JGM Group, JGM-♀ × control-♂; JGM+dsGFP Group, JGM+dsGFP-♀ × control-♂; JGM+dsUGT12 Group, JGM+dsUGT12-♀ × control-♂.*

dsUGT12 Treatments Reversed the Enhancing Influence of JGM on *NlVg* Expression and Vg Synthesis

Jinggangmycin treatments led to increased accumulations of mRNAs encoding NlVg and NlVgR relative to the controls. The dsUGT12 treatments reversed the enhancing influence of JGM at 2 DAE and 3 DAE (**Figures 5A,B**). We recorded similar results with *NlVgR* at 2 and 3 DAE (**Figures 5C,D**). With respect to Vg protein contents, dsUGT12 treatment overcame the JGM-induced results (**Figure 5E**). Western blot analysis yielded similar results (**Figure 5F** and **Supplementary Figure S1**).

Methoprene Application Rescues *NlUGT12* Expression and Vg Synthesis

Jinggangmycin led to increased accumulations of mRNA encoding NlUGT12 which, again, were reversed by the dsUGT12 treatments. Topical methoprene application onto newly emerged adult females partially rescued *NlUGT12* expression in the dsUGT12-treated group at 24 h (**Figure 6A**) and 48 h post treatment (**Figure 6B**). Methoprene applications similarly rescued *NlVg* expression (**Figures 7A,B**) and Vg contents (**Figures 7C,D**). Western blot analysis yielded similar results (**Figures 7E,F** and **Supplementary Figure S2**).

dsUGT12 Treatment Led to Reduced Egg Laying and Hatch Rates

Compared to untreated controls, JGM treatments significantly increased the number of eggs laid (by 34%), gender ratio (by 33%), and PGI (by 34%). dsUGT12 treatments led to reduced numbers of deposited eggs (by 45%) and egg hatching rates (by 13%), gender ratio (by 14%), and PGI (by 45%) in the JGM+dsUGT12 treated group compare to JGM treated group (**Table 2**). dsGFP treatments had no effect on JGM-enhanced

egg deposition (**Table 2**). None of the treatments influenced the BPH gender ratios.

DISCUSSION

The results presented in this paper strongly support our hypothesis that *NlUGT12* is a positive modulator of BPH reproductive biology. Several points are germane to the point. First, JGM treatments led to increased fat body and ovarian protein contents, increased JHIII titers, decreased 20E titers, increased JHAMT and Met expression, increased body weights, increased egg deposition and duration of the oviposition period, elevated expression of *Nlvg* and *NlvgR* and production of Vg protein, and elevated *UGT12* expression. Second, a dsRNA construct specific to NlUGT12 effectively reversed the JGM enhanced influence. Third, JH analog methoprene treatment partially rescued dsUGT12 effect. We infer that *NlUGT12* acts via its cognate protein NlUGT12, as a positive modulator of BPH reproduction.

Overall, our results tend to show that NlUGT12 modulates fecundity and population growth in *N. lugens,* probably by regulating JH and Vg synthesis. Indeed, JGM is a very broadly-applied treatment for rice sheath blight (*R. solani*) control in China (Peng et al., 2014). These treatments lead to increased egg deposition. Because egg development is mediated by JH, we considered the possibility that the JGM effect on reproduction acts through JH. JGM exposure leads to increased JH, but not 20E, titers and to increases in mRNA encoding two JH-related proteins, JHAMT and the JH receptor, Met. JHAMT acts at the final step in converting inactive precursors into active JH and increases in JHAMT expression is consistent with increased JH titers. Similarly, increases in Met expression are consistent with enhancing the physiological functioning of JH. 20E titers were decreased under JGM exposure, from which we infer the JGM effects are focused on reproductive, rather than developmental events. Most results indicate that suppressing *NlUGT12* expression reverses the enhancing influences of JGM. We considered the possibility of a direct connection between *NlUGT12* and JH actions, from which we determined the reversing influence of a JH analog, methoprene, on dsRNA-mediated *NlUGT12* suppression.

Insect eggs reflect heavy resource investments, particularly proteins. Increased amounts of fat body protein are consistent with increased Vg synthesis, transport, and receptor-mediated ovarian uptake, a necessary foundation of increased egg laying. The increased protein supports increased egg production and deposition, which is seen, also, in higher numbers of deposited eggs. These JGM-mediated increases may be seen in increased body weights, particularly in females. We determined the influence of JGM on oviposition periods because insect egg-laying processes take time. Although it varies according to the rice developmental stage, BPHs typically lay eggs in groups, in rows usually in rice sheaths but also on leaves. We recorded increased oviposition periods, which is consistent with increased egg deposition. We considered egg hatch rates as an indicator of egg quality, which was not influenced by JGM.

UDP-glucuronosyltransferases act in multiple processes, including detoxification of ingested plant allelochemicals and inactivation of steroid hormones (Ahmad and Hopkins, 1993a; Kojima et al., 2010; Ahn et al., 2011). Phylogenetic analysis (Hughes, 2013) indicates the closest relatives of baculovirus EGT are the UGT33 and UGT34 families of lepidopteran UGTs. Baculoviral EGT disrupts the hormonal balance of insect hosts by catalyzing the inactivating conjugation of 20Es with a sugar moiety from UDP-glucose or UDP-galactose (Evans and O'Reilly, 1999), which leads to abnormal larval growth (Shikata et al., 1998; Hughes, 2013). Because UPDs act in 20E metabolism, we infer that *NlUGT12* positively modulates reproduction and the JGM-driven increases in reproduction via influencing developmental hormone titers.

The idea that NlUGT12 acts via influencing hormone titers is strongly supported by our findings. Silencing *NlUGT12* led to diminished JH III titers and increased 20E titers, relative to the outcomes of JGM and JGM+dsGFP treatments, from which we infer that NlUGT12 directly influences developmental hormone titers. mRNAs encoding JHAMT, which acts in JH biosynthesis and Met, the receptor responsible for JH actions, were diminished in BPHs following dsNlUGT12 treatments, again, supporting our view of *NlUGT12* as a central player in BPH hormonal homeostasis. The *Vg* and *VgR* directly act in insect fecundity. Their synthesis, transport and uptake are regulated mainly by JHs and, again, dsUGT12 treatments in JGM treated group led to reduced JH titers, which reduces *Vg* and *VgR* expression and subsequent ovarian Vg uptake. We infer that NlUGT12 exerts its actions via developmental hormones.

Topically applied methoprene, a JH analog, reversed the influences of the JGM+dsUGT12 treatments on *NlUGT12* and *NlVg* expression, and on Vg synthesis. Our interpretation is that *NlUGT12* influences JH synthesis, which regulates *NlVg* expression and Vg protein synthesis. The reduced protein contents of fat bodies and ovaries in JGM+dsUGT12-treated females may preclude synthesis of yolk protein from vitellogenin, accompanied by restricted ovarian development and reproduction.

AUTHOR CONTRIBUTIONS

LG designed the research. SZ, YZ, ZZ, and HG conducted the experiments. LG wrote the first draft of the manuscript. QS and DS revised the final draft of the manuscript.

FUNDING

This research was financially supported by the National Key R&D Program of China (2017YFD0200400), the National Natural Science Foundation of China (31872283), the Natural Science Foundation of Jiangsu Province, China (BK20171283), and the Jiangsu Agricultural Scientific SEL Innovation Fund [CX(125)1057].

ACKNOWLEDGMENTS

We thank Prof. Qiang Zhou of Sun Yat-sen University for providing *Nilaparvata lugens* Vg antibody. Mention of trade names or commercial products in this article is solely for the purpose of providing specific information and does not imply recommendation or endorsement by the United States Department of Agriculture. All programs and services of the United States Department of Agriculture are offered on a non-discriminatory basis without regard to race, color, national origin, religion, sex, age, marital status, or handicap.

SUPPLEMENTARY MATERIAL

The Supplementary Material for this article can be found online at: https://www.frontiersin.org/articles/10.3389/fphys.2019.00747/full#supplementary-material

REFERENCES

Ahmad, S. A., and Hopkins, T. L. (1993a). β-glucosylation of plant phenolics by phenol β-glucosyltransferase in larval tissues of the tobacco hornworm, *Manduca sexta* (L.). *Insect Biochem. Mol. Biol.* 23, 581–589. doi: 10.1016/0965-1748(93)90031-m

Ahmad, S. A., and Hopkins, T. L. (1993b). Phenol β-glucosyltransferases in six species of insects: properties and tissure localization. *Comp. Biochem. Physiol. B* 104, 515–519. doi: 10.1016/0305-0491(93)90276-B

Ahmad, S. A., Hopkins, T. L., and Kramer, K. J. (1996). Tyrosine β-glucosyltransferase in the tabacco hornworm, *Manduca sexta* (L): properties, tissue localization, and developmental profile. *Insect Biochem. Mol. Biol.* 26, 49–57. doi: 10.1016/0965-1748(95)00060-7

Ahn, S. J., Badenes-Pérez, F. R., Reichelt, M., Svatoš, A., Schneider, B., Gershenzon, J., et al. (2011). Metabolic detoxification of capsaicin by UDP-glycosyltransferase in three *Helicoverpa* species. *Arch. Insect Biochem. Physiol.* 78, 104–118. doi: 10.1002/arch.20444

Ayoade, O., Morooka, S., and Tojo, S. (1999). Enhancement of short wing formation and ovarian growth in the genetically defined macropterous strain of the brown planthopper, *Nilaparvata lugens*. *J. Insect Physiol.* 45, 93–100. doi: 10.1016/s0022-1910(98)00103-6

Bradford, M. (1976). A rapid and sensitive method for the quantitation of microgram quantities of protein utilizing the principle of protein dye binding. *Anal. Biochem.* 72, 248–254. doi: 10.1016/0003-2679(76)90527-3

Chen, J., Zhang, D., Yao, Q., Zhang, J., Dong, X., Tian, H., et al. (2010). Feeding-based RNA interference of a trehalose phosphate synthase gene in the brown planthooper, *Nilaparvata lugens*. *Insect Mol. Biol.* 19, 777–786. doi: 10.1111/j.1365-2583.2010.01038.x

Collier, A. C., Milam, K. A., Rougee, L. R. A., Sugawara, A., Yamauchi, Y., and Ward, M. A. (2012). Upregulation of Ugt1a genes in placentas and fetal livers in a murine mndel of assisted reproduction. *Placenta* 33, 77–80. doi: 10.1016/j.placenta.2011.11.002

Dong, X. L., Zhai, Y. F., Zhang, J. Q., Sun, Z. X., Chen, J., and Zhang, W. Q. (2011). Fork head transcription factor is required for ovarian mature in brown planthooper, *Nilaparvata lugens* (Stål). *BMC Mol. Biol.* 12:53. doi: 10.1186/1471-2199-12-53

Evans, O. P., and O'Reilly, D. R. (1999). Expression and structural characterization of a baculovirus ecdysteroid UDP-glucosyltransferase. *J. Gen. Virol.* 80, 485–492. doi: 10.1099/0022-1317-80-2-485

Fu, Q., Zhang, Z. T., Lai, F. X., and Sun, Z. X. (2001). A chemically defined diet enables the continuous rearing of the brown planthopper, *Nilaparvata lugens* (Stål). *Appl. Entomol. Zool.* 36, 111–116. doi: 10.1303/aez.2001.111

Ge, L. Q., Gu, H. T., Huang, B., Song, Q. S., Stanley, D., Liu, F., et al. (2017). An adenylyl cyclase like-9 gene (NlAC9) influences growth and fecundity in the brown planthopper, *Nilaparvata lugens* (Stål) (Hemiptera: Delphacidae). *PLoS One* 12:e0189214. doi: 10.1371/journal.pone.0189214

Ge, L. Q., Hu, J. H., Wu, J. C., Yang, G. Q., and Gu, H. N. (2009). Insecticide-induced changes in protein, RNA, and DNA contents in ovary and fat body of female *Nilaparvata lugens* (Hemiptera: Delphacidae). *J. Econ. Entomol.* 102, 1506–1514. doi: 10.1603/029.102.0415

Gong, H., Zhai, C. H., Wei, D. Y., and Zhang, J. Z. (1980). On the vitellogenesis of *Coccinella septempuntata* L: the occurrence of vitellogenin as influenced by artificial diet. *Acta Entomol. Sin.* 23, 252–257. doi: 10.1016/0020-1790(84)90064-7

Heckel, D. G. (2010). "Molecular genetics of insecticide resistance in Lepidoptera," in *Molecular Biology and Genetics of the Lepidoptera*. eds M. R. Goldsmith and F. Marec (Milton Park: Taylor &Francis). 239–269. doi: 10.1201/9781420060201-c13

Hopkins, T. L., and Kramer, K. J. (1992). Insect cuticle sclerotization. *Annu. Rev. Entomol.* 37, 273–302. doi: 10.1146/annurev.en.37.010192.001421

Hughes, A. L. (2013). Origin of ecdysteroid UDP-glycosyltransferases of baculoviruses through horizontal gene transfer from Lepidoptera. *Coevolution* 1, 1–7. doi: 10.1080/23256214.2013.858497

Jiang, L. B., Zhao, K. F., Wang, D. J., and Wu, J. C. (2012). Effects of different treatment methods of the fungicide jinggangmycin on reproduction and vitellogenine gene (*NlVg*) expression in the brown planthopper *Nilaparvata lugens* Stål (Hemiptera: Delphacidae). *Pestic. Biochem. Physiol.* 102, 51–55. doi: 10.1016/j.pestbp.2011.10.0009

Jiang, Y. P., Li, L., Liu, Z. Y., You, L. L., Wu, Y., Ge, L. Q., et al. (2016). Adipose triglyceride lipase (Atgl) mediates the antibiotic jinggangmycin-stimulated reproduction in the brown planthopper, *Nilaparvata lugens* Stål. *Sci. Rep.* 6:18984. doi: 10.1038/srep18984

Kojima, W., Fujii, T., Suwa, M., Miyazawa, M., and Iashikawa, Y. (2010). Physiological adaptation of the Asian corn borer *Ostrinina furnacalis* to chemical defenses of its host plant, maize. *J. Insect Physiol.* 56, 1349–1355. doi: 10.1016/j.jinsphys.2010.04.021

Lazard, D., Zupko, K., Poria, Y., Nef, P., Lazarovits, J., and Horn, S. (1991). Odorant signal termination by olfactory UDP glucuronosyltransferase. *Nature* 349, 790–793. doi: 10.1038/349790a0

Li, L., Jiang, Y. P., Liu, Z. Y., You, L. L., Wu, Y., Xu, B., et al. (2016). Jinggangmycin increases fecundity of the brown planthopper, *Nilaparvata lugens* (Stål) via fatty acid synthase gene expression. *J. Proteom.* 130, 140–149. doi: 10.1016/j.prot.2015.09.022

Livak, K. J., and Schmittgen, T. D. (2001). Analysis of relative gene expression data using real-time quantitative PCR and the 2-ΔΔCt Method. *Methods* 25, 402–408. doi: 10.1006/meth.2001.1262

Lu, K., Chen, X., Liu, W. T., Zhang, X. Y., Chen, M. X., and Zhou, Q. (2016). Nutritional signaling regulates vitellogenin synthesis and egg development through juvenile hormone in *Nilaparvata lugens* (Stål). *Int. J. Mol. Sci.* 17:269. doi: 10.3390/ijms17030269

Luque, T., Okano, K., and O'Reilly, D. R. (2002). Characterization of a novel silkworm (Bombyx mori) phenol UDP-glucosyltransferase. *FEBS J.* 269, 819–825. doi: 10.1046/j.0014-2956.2001.02723

Mackenzie, P. I., Owens, I. S., Burchell, B., Bock, K. W., Bairoch, A., Belanger, A., et al. (1997). The UDP glycosyltransferase gene superfamily: recommended nomenclature updata based on evolutionary divergence. *Pharmacogenetics* 7, 255–269. doi: 10.1097/00008571-199708000-00001

Meech, R., Hu, D. G., McKinnon, R. A., Mubarokah, S. N., Haines, A. Z., Nair, P. C., et al. (2019). The UDG-Glycosyltransferase (UGT) superfamily: new members, new functions, and novel paradigms. *Physiol. Rev.* 99, 1153–1222. doi: 10.1152/physrev.00058.2017

Meech, R., and Machenzie, P. I. (1997). Structure and function of uridine diphosphate glucuronosyltransferases. *Clin. Exp. Pharmacol. Physiol.* 24, 907–915. doi: 10.1111/j.1440-1681.1997.tb02718.x

Peng, D., Li, S. D., Wang, J. X., Chen, C., and Zhou, M. (2014). Integrated biological and chemical control of rice sheath blight by *Bacillus subtlis* NMJ-18 and jinggangmycin. *Pest Manag. Sci.* 70, 258–263. doi: 10.1002/ps.3551

Real, M. D., Ferré, J., and Chapa, F. J. (1991). UDP-glucosyltrasferase activity toward exogenous substrates in *Drosophila melanogaster*. *Anal. Biochem.* 194, 349–352. doi: 10.1016/0003-2697(91)90239-p

Rozen, S., and Skaletsky, H. (2000). Primer 3 on the WWW for general users and for biologist programmers. *Methods Mol. Biol.* 132, 365–386. doi: 10.1385/1-59259-192-2:365

Shikata, M., Shibata, H., Sakurai, M., Sano, Y., Hashimoto, Y., and Matsumoto, T. (1998). The ecdysteroid UDP-glucosyltransferase gene of *Autographa californica* nucleopolyhedrovirus alters the moulting and metamorphosis of a non-target insect, the silkworm, *Bombyx mori* (Lepidoptera, Bombycidae). *J. Gen. Virol.* 79, 1547–1551. doi: 10.1515/znc-2004-9-1021

Svoboda, J., and Weirich, G. (1995). Sterol metabolism in the tobacco hornworm, *Manduca sexta*-A review. *Lipids* 30, 263–267. doi: 10.1007/bf02537831

Tang, Q. Y., and Feng, M. G. (2002). *DPS Data Processing System for Practical Statistics-4*. Beijing: Scientific Press, 47–71.

Tompson, M., Feldlaufer, M., Lozano, R., Rees, H., Lusby, W., Svoboda, J., et al. (1987). Metabolism of 26-[14C] hydroxyecdyson 26-phosphate in the tobacco hornworm, *Manduca sexta* L., to a new wcdysteroid conjugate: 26-[14C] hydroxyecdysone 22-glucoside. *Arch. Insect Biochem. Physiol.* 4, 1–15. doi: 10.1002/arch.940040102

Wang, L. P., Shen, J., Ge, L. Q., Wu, J. C., Yang, G. Q., and Jahn, G. C. (2010). Insecticide-induced increase in the protein content of male accessory glands and its effect on the fecundity of females in the brown planthopper *Nilaparvata lugens* Stål (Hemiptera: Delphacidae). *Crop Prot.* 29, 1280–1285. doi: 10.1016/j.cropro.2010.07.009

Wang, X., Hasan, G., and Pikielny, C. W. (1999). Preferential expression of biotransformation enzymes in the olfactory organs of *Drosophila melanogaster*, the antennae. *J. Biol. Chem.* 274, 10309–10315. doi: 10.1074/jbc.274.15.10309

Conflict of Interest Statement: The authors declare that the research was conducted in the absence of any commercial or financial relationships that could be construed as a potential conflict of interest.

frontiers in Physiology

ORIGINAL RESEARCH
published: 21 June 2019
doi: 10.3389/fphys.2019.00795

Activation of Immune Genes in Leafhoppers by Phytoplasmas and Symbiotic Bacteria

*Elena Gonella[1], Mauro Mandrioli[2], Rosemarie Tedeschi[1], Elena Crotti[3], Marianna Pontini[1] and Alberto Alma[1]**

[1] Dipartimento di Scienze Agrarie, Forestali e Alimentari (DISAFA), Università degli Studi di Torino, Grugliasco, Italy, [2] Dipartimento di Scienze della Vita (DSV), Università degli Studi di Modena e Reggio Emilia, Modena, Italy, [3] Dipartimento di Scienze per gli Alimenti, la Nutrizione e l'Ambiente (DeFENS), Università degli Studi di Milano, Milan, Italy

Insect immunity is a crucial process in interactions between host and microorganisms and the presence of pathogenic, commensal, or beneficial bacteria may result in different immune responses. In Hemiptera vectors of phytoplasmas, infected insects are amenable to carrying high loads of phytopathogens, besides hosting other bacterial affiliates, which have evolved different strategies to be retained; adaptation to host response and immunomodulation are key aspects of insect-symbiont interactions. Most of the analyses published to date has investigated insect immune response to pathogens, whereas few studies have focused on the role of host immunity in microbiota homeostasis and vectorial capacity. Here the expression of immune genes in the leafhopper vector of phytoplasmas *Euscelidius variegatus* was investigated following exposure to *Asaia* symbiotic bacteria, previously demonstrated to affect phytoplasma acquisition by leafhoppers. The expression of four genes related to major components of immunity was measured, i.e., defensin, phenoloxidase, kazal type 1 serine protease inhibitor and Raf, a component of the Ras/Raf pathway. The response was separately tested in whole insects, midguts and cultured hemocytes. Healthy individuals were assessed along with specimens undergoing early- and late-stage phytoplasma infection. In addition, the adhesion grade of *Asaia* strains was examined to assess whether symbionts could establish a physical barrier against phytoplasma colonization. Our results revealed a specific activation of Raf in midguts after double infection by *Asaia* and flavescence dorée phytoplasma. Increased expression was observed already in early stages of phytoplasma colonization. Gut-specific localization and timing of Raf activation are consistent with the role played by *Asaia* in limiting phytoplasma acquisition by *E. variegatus*, supporting the involvement of this gene in the anti-pathogen activity. However, limited attachment capability was found for *Asaia* under *in vitro* experimental conditions, suggesting a minor contribution of physical phytoplasma exclusion from the vector gut wall. By providing evidence of immune modulation played by *Asaia*, these results contribute to elucidating the molecular mechanisms regulating interference

OPEN ACCESS

Edited by:
Michel Cusson,
Natural Resources Canada, Canada

Reviewed by:
Arash Zibaee,
University of Guilan, Iran
Jalal Jalali Sendi,
University of Guilan, Iran
Olga Makarova,
Freie Universität Berlin, Germany

***Correspondence:**
Alberto Alma
alberto.alma@unito.it

Specialty section:
This article was submitted to Invertebrate Physiology, a section of the journal Frontiers in Physiology

Received: *12 December 2018*
Accepted: *06 June 2019*
Published: *21 June 2019*

Citation:
Gonella E, Mandrioli M, Tedeschi R, Crotti E, Pontini M and Alma A (2019) Activation of Immune Genes in Leafhoppers by Phytoplasmas and Symbiotic Bacteria. Front. Physiol. 10:795. doi: 10.3389/fphys.2019.00795

with phytoplasma infection in *E. variegatus*. The involvement of Raf suggests that in the presence of reduced immunity (reported in Hemipterans), immune genes can be differently regulated and recruited to play additional functions, generally played by genes lost by hemipterans.

Keywords: insect immunity, plant pathogen, symbiotic bacterium, *Asaia*, Raf

INTRODUCTION

The interactions of organisms with the surrounding environment are related to their ability in responding to damage and non-self particles. In insects, responses are carried out via innate immunity exclusively, by means of both humoral and cellular defense. A major component of humoral and cellular immune response is the production of antimicrobial peptides (AMPs), which takes place in different organs and tissues, including the digestive tract, salivary glands, and fat body (Tsakas and Marmaras, 2010; Li et al., 2016; Shao et al., 2017). Many AMPs such as defensins are highly conserved in different orders of insects, while others are not evenly distributed (Tedeschi et al., 2017). Moreover, other important components of insect immunity are commonly found, such as phenoloxidase-related machinery and other genes. Insect immune responses are differentially stimulated by either pathogenic or beneficial microorganisms (Tedeschi et al., 2017). Indeed, besides activating responses to neutralize infections by entomopathogens, insects may modulate their immunity in the presence of bacterial symbionts to regulate their density and to maintain the microbiota balance (Login et al., 2011; Eleftherianos et al., 2013; Skidmore and Hansen, 2017). Differently from what is reported for entomopathogens that induce very similar responses, the interaction with non-pathogenic microbes depends on specific traits of insect–microorganism interactions: divergent reactions have indeed been recorded even for closely related microorganisms in the same host. For example, some pathogens of animals or plants, vectored by insects, may establish different interplay with their vectors, which in turn react with different responses. Although pathogenic agents for humans are often perceived as harmful agents by infected insects (Weiss and Aksoy, 2011), in the case of plant pathogens, exclusively transmitted by Hemiptera, divergent kinds of interactions have been observed. Infection by the α-proteobacterial '*Candidatus* Liberibacter asiaticus' resulted in downregulation of immune genes in nymphs of the psyllid *Diaphorina citri* Kuwayama, suggesting that the pathogen is able to modulate the vector immune response to promote its colonization of the hosts (Vyas et al., 2015). Considering plant pathogenic Mollicutes, *Spiroplasma citri* was shown to induce a specific response in the vector *Circulifer haematoceps* (Mulsant and Rey), consisting of increased phagocytosis and upregulation of a gene related to hexamerin, a protein playing a crucial role in phenoloxidase activation (Eliautout et al., 2016). However, the response is balanced by the capability of *S. citri* to inhibit phenoloxidase activity and escape phagocytosis (Eliautout et al., 2016). In phytoplasmas, diverse insect responses have been reported following infection by different strains in the same host species, i.e., immune response or immune priming from infections (Galetto et al., 2018). Moreover, some phytoplasmas counteract the insect response by expressing genes involved in limiting the products of immunity (Makarova et al., 2015).

The leafhopper *Euscelidius variegatus* Kirschbaum (Hemiptera: Cicadellidae) is a polyphagous polyvoltine species capable of transmitting phytoplasmas belonging to different taxonomic groups, including chrysanthemum yellows phytoplasma (CYp, 16SrI group) and flavescence dorée phytoplasma (FDp, 16SrV group), under laboratory conditions. These pathogens have been shown to have opposite effects on *E. variegatus*, with CYp slightly enhancing the fitness of the leafhopper (Bosco and Marzachì, 2016) and FDp reducing its survival and fecundity (Bressan et al., 2005). Transcriptomic analysis of leafhoppers infected with either CYp or FDp has demonstrated that only infection by FDp resulted in activation of insect immune response (Galetto et al., 2018). Besides carrying phytoplasmas, *E. variegatus* harbors bacterial symbionts, like many other Auchenorrhyncha (Baumann, 2005); among these, the acetic acid bacterium *Asaia* has been experimentally documented to limit the acquisition of FDp, after oral administration (Gonella et al., 2018). Symbiont-mediated control mechanisms against phytopathogens include competitive nutrient uptake by symbiotic bacteria, erection of a physical barrier preventing gut establishment and crossing by pathogens, symbiont-mediated immune response of the insect, and the release of antagonistic compounds (Gonella et al., 2019). In *E. variegatus*, the involvement of either *Asaia*-mediated mechanisms stimulating the host immune response or physical exclusion were suggested (Gonella et al., 2018); however, little experimental evidence has been provided on the effects of symbiotic bacteria on *E. variegatus* immunity (Tedeschi et al., 2017) and no data are available on the influence of phytoplasma-symbiont multiple infection on the insect response. Additionally, interest in the molecular machinery involved in the immune response of hemipteran species is hampered by the limited immune repertoire possessed by these insects, as reported for many species (Arp et al., 2016; Skidmore and Hansen, 2017). Such a reduced response is thought to result from the need of Hemiptera to maintain stable relationships with bacterial symbionts. On the other hand, symbiotic bacteria may compensate for the reduction of immunity of their hosts by stimulating insects' responses to protect them from enemies or directly protecting their hosts from pathogens (Eleftherianos et al., 2013). Moreover, insect immune activation is a candidate strategy used by endosymbionts to modulate the density of other bacteria (Skidmore and Hansen, 2017), including vector-transmitted disease agents, actually altering the insect transmission competence (Weiss and Aksoy, 2011; Kliot et al., 2014). The immune response may be especially crucial for those

phytopathogens that cause decreased vector fitness (Cassone et al., 2014; Nachappa et al., 2014; Alma et al., 2015; Olson and Blair, 2015), as in the case of FDp and *E. variegatus*.

In this study, we examined the question as to whether reduced phytoplasma acquisition observed after *Asaia* infection is related to stimulation of the insect immune system, and whether this mechanism is tissue-specific and related to phytoplasma infection timing. To this end, we investigated the expression pattern of four immune genes in *E. variegatus* whole adult leafhoppers, dissected midguts and cultured hemocytes, after exposure to *Asaia* strains and/or FDp. We selected genes involved in different immune pathways to explore possible peculiar regulation of immune genes in insects with reduced immunity such as Hemiptera. In particular, we analyzed phenoloxidase and kazal type 1 serine protease inhibitor, since both genes have been reported to respond to FDp infection (Galetto et al., 2018), together with the *defensin* gene that is one of the most commonly activated genes after bacterial challenges. Moreover, special attention was given to the *Raf* gene, a component of the Ras/Raf pathway, which is known in *Drosophila* as involved in the response to septic injury and in hemocyte proliferation and survival (Asha et al., 2003). The latter was selected since during the latent period (before the insect becomes infective) phytoplasmas multiply in different organs/tissues, including hemocytes, affecting their proliferation/survival (Bosco et al., 2007). Finally, an alternative hypothetical mechanism of interference with FDp acquisition was tested, involving the production of air-liquid interface (ALI) biofilm (**Supplementary Table S1**), i.e., masking of gut epithelial receptors through adhesion to insect gut wall.

MATERIALS AND METHODS

Insect Material and Bacterial Strains

A laboratory mass rearing of *E. variegatus* present at the DISAFA laboratories was used as a source of healthy adult leafhoppers for this work. Leafhoppers were kept on oat plants (*Avena sativa* L.) in growth chambers at 25°C with a photoperiod of 16:8 (L:D). Three groups of *E. variegatus* individuals were used for our experiments: healthy adults, specimens at the early stage of phytoplasma colonization, and individuals chronically infected by FDp. The first group was directly collected from the lab colony, while the second and the third groups were obtained by exposing insects to broad beans (*Vicia faba* L.) infected by FDp (strain FD-C). Adults at the early FD phytoplasma infection stage (EFDi) were chosen immediately after being submitted to a 5-day acquisition access period. Late FDp-infected (LFDi) *E. variegatus* were obtained by rearing nymphs on infected broad beans until adult emergence and for at least 21 days (**Figure 1**).

Bacterial colonization experiments in *E. variegatus* were performed using the spontaneous rifampicin-resistant mutant strains SF2.1Rif^R and SF15.14Rif^R of *Asaia*, the first being a non-ALI forming strain, and the latter an ALI-producer isolate that was reported to reduce FDp acquisition in *E. variegatus* (Gonella et al., 2018). *Escherichia coli* strain DH5α pKan(DsRed) (Crotti et al., 2009) was also used as a non-symbiotic control. Before use, the strains of *Asaia* were cultivated overnight at 30°C in GLY medium (Favia et al., 2007) under the selection of rifampicin (100 μg/ml), whereas *E. coli* DH5α pKan(DsRed) was cultured overnight at 37°C in Luria-Bertani (LB) medium under the selection of kanamycin (50 μg/ml).

Bacterial Colonization of *E. variegatus* Individuals

Asaia strains SF2.1 Rif^R and SF15.14 Rif^R, as well as *E. coli* DH5α pKan(DsRed), were individually administered to *E. variegatus* adults from the healthy, EFDi, and LFDi groups, following the protocol described by Crotti et al. (2009). Briefly, cultivated bacterial cells were harvested by centrifugation (10 min, 800 *g*), washed three times with 0.9% NaCl, and adjusted to 10^8 cells/ml in 5% (w/v) sucrose solution in TE (10 mM Tris HCl, 1 mM EDTA, pH 8) (Crotti et al., 2009; Gonella et al., 2012). Insects were allowed to feed for 48 h on artificial feeding systems (Gonella et al., 2015) containing the cell suspensions. Specimens directly collected from the mass rearings without any further treatment were used as reference samples for the gene expression analysis, while adults maintained in the artificial feeding systems with added sterile sugar solution were taken as a control. Five insects for each group and treatment (total number of specimens: 75), corresponding to 5 biological replicates, were directly collected and stored at −80°C in RNA later® (Sigma-Aldrich, St. Louis, MO, United States) until RNA extraction, while further individuals were submitted to midgut dissection.

Midgut Dissection and Establishment of Hemocyte Cell Cultures

To obtain midgut samples, *E. variegatus* individuals were dissected in Phosphate Buffered Solution (PBS, 137 mM NaCl, 2.7 mM KCl, 10 mM Na_2HPO_4, 2 mM KH_2PO_4; pH 7.4) made with Diethyl pyrocarbonate-treated water, by using sterile forceps under a stereomicroscope. Five replicates for each insect group and treatment, each one consisting of midguts from three adults, were collected and stored at −80°C in RNA later® (Sigma-Aldrich, St. Louis, MO, United States) until RNA extraction. Dissected midguts from *E. variegatus* adults directly collected from our lab colony without any further treatment were used as reference samples, and the midguts of insects fed with a sterile sugar diet were employed as a control.

Primary hemocyte cell cultures were established following the method described by Tedeschi et al. (2017). Specifically, groups of two adults were washed in 0.115% sodium hypochlorite, 75% ethanol and MilliQ sterile water for 10, 30, and 20 s, respectively, and then dried on a filter paper for a couple of seconds. Washed insects were placed in a single well of a sterile 24-well cell culture plate (Costar®, Corning®, NY, United States) containing 1 ml of Hert-Hunter 70 medium (Marutani-Hert et al., 2009), supplemented with 10 ml/L L-glutamine (Invitrogen, Carlsbad, CA, United States). Gentamicin (Sigma-Aldrich, St. Louis, MO, United States) at a final concentration of 50 μg/ml, penicillin/streptomycin (Sigma-Aldrich, St. Louis, MO, United States) at a final concentration of 50 U/ml and 50 μg/ml, respectively, and the antimycotic agent nystatin (Sigma-Aldrich, St. Louis, MO, United States) at a final

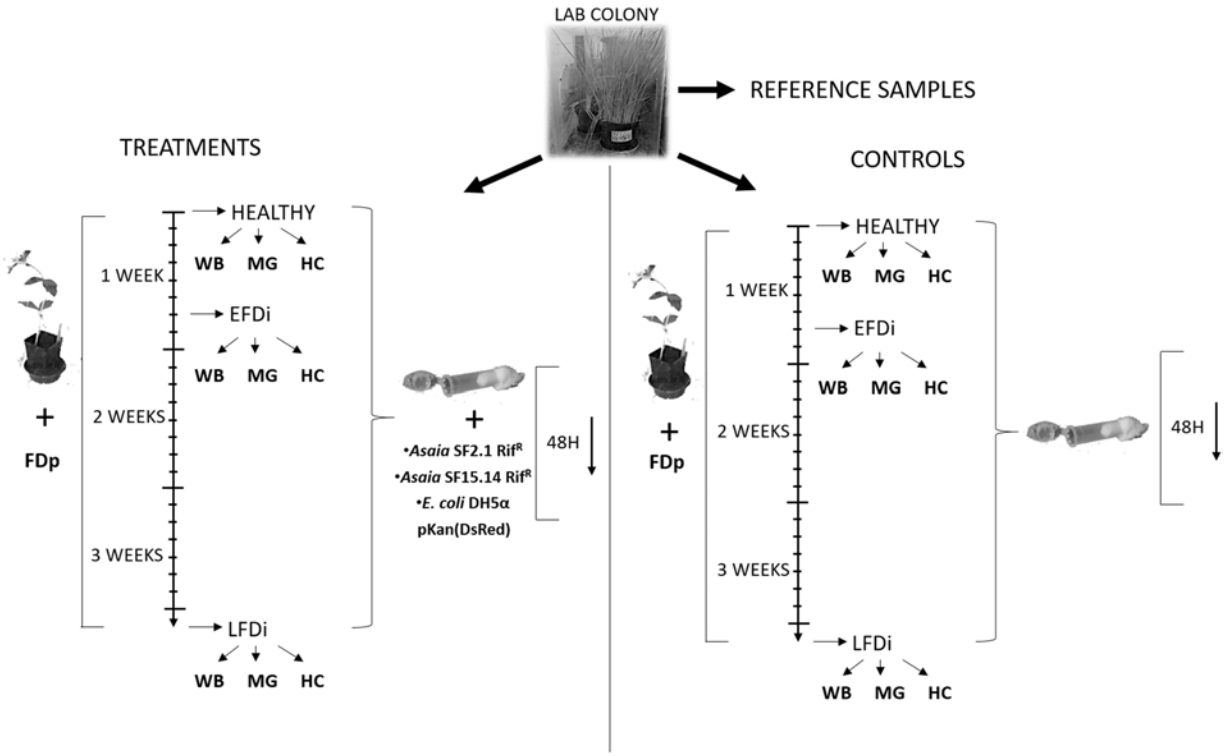

FIGURE 1 | Experimental set up of the trials for expression analysis of immune-related genes. Nymphs of *E. variegatus* were collected from our lab colony as reference samples for gene expression studies, or dedicated to treatments or controls. Insects of the healthy group were directly collected from the lab colony, while those of the EFDi group were exposed to FDp for 5 days and those of the LFDi group were exposed to FDp for 21 days. Afterward, leafhoppers used for treatments were fed either with *Asaia* SF15.14Rif^R, *Asaia* SF2.1Rif^R, or *E. coli* DH5α pKan(DsRed) through artificial feeding systems, whereas specimens for the controls were maintained on a sterile sugar diet. Within each group whole insect bodies (WB), midguts (MG), and hemocytes (HC) were taken separately.

concentration of 100 U/ml, were also added. Plates were incubated at 24 – 26°C for 24 h, to allow cell establishment in the medium, and subsequently incubated for further 24 h with 10^8 cells/ml bacterial suspension [*Asaia* SF2.1 Rif^R and SF15.14 Rif^R, and *E. coli* DH5α pKan(DsRed)] in the same medium deprived of antibiotics, after removal of the hemocytes culture supernatant. For each of healthy, EFDi and IFDi sample groups, five replicates were treated with bacteria, five replicates were incubated with a sterile antibiotic-free medium in the absence of bacteria as a control, and five replicates were left untreated to be used as the reference samples for gene expression analyses. At the end of treatments, cells were centrifuged at 800 *g* for 5 min at room temperature and immediately subjected to RNA extraction after discarding the supernatant.

RNA Extraction, cDNA Synthesis, and Quantitative Real Time PCR (qPCR)

RNA extraction was performed with the "SV Total RNA Isolation System" (Promega, Fitchburg, WI, United States), according to the supplier's suggestions. Briefly, insect tissues were lysed and homogenized with a sterile pestle in 175 μl RNA Lysis Buffer; then samples were heated at 70°C for 3 min after adding 350 μl of RNA Dilution Buffer. Cleared lysate solutions were obtained by centrifugation, and subsequently provided with 200 μl 95% ethanol and transferred in the supplied Spin Column Assembly. Once samples were washed with RNA Wash Solution, they were incubated for 15 min at room temperature with DNase incubation mix, then 200 μl of DNase Stop Solution were added to stop the reaction. Finally, samples were washed twice with RNA Wash Solution and resuspended in 50 μl nuclease-free water. After extraction, RNA quality and concentration were assessed with a ND-1000 spectrophotometer (NanoDrop, Wilmington, DE, United States) and by electrophoresis on a denaturing agarose gel (**Supplementary Figure S1**). First strand cDNA was synthesized by using the "Reverse Transcription System" (Promega) and Random Primers with 9 μl of RNA, following the manufacturer's instructions. cDNA was used as a template for qPCR analysis with primer pairs specifically targeting the following genes: *defensin, Raf, phenoloxidase*, and *kazal type 1 serine protease inhibitor*. A list of primers is presented in **Table 1**. Raf-specific primers were specifically designed on conserved sequences identified by the alignment of Raf sequences of *D. citri* (XM_008488867.2), *Nilaparvata lugens* (Stål) (XM_022347672.1) and *Acyrthosiphon pisum* (Harris) (XM_001952258.4) using the on-line software Primer 3[1]. A preliminary survey was conducted by amplification of cytoplasmic actin with the following parameters: initial

[1]http://bioinfo.ut.ee/primer3/

TABLE 1 | Primers used in this study.

Primer pair	Target gene	Sequence (5′→3′)	Size (bp)	Source
EvDef F	Defensin	ATGCATTCTTCCATTACTGCTG	200	Tedeschi et al., 2017
EvDef R		CAGCTGCCTCCCTTCTTGC		
Raf F	Raf	CAAGTGGAGAGGATTCAGCAG	200	This study
Raf R		GTGTGTTGGAGCCAGGTCTAT		
PO2_F1020	Phenoloxidase	CAATGTGGTTCCCTCAGGAT	115	Galetto et al., 2018
PO2_R1085		CTGCGAGGTCTCATTTCTGT		
kaz1_F70	Kazal type 1 serine protease inhibitor	CTGGTTCGCAGGCAAATACC	103	Galetto et al., 2018
kaz1_R172		GGCATGACACTCGGTACACT		
actF	Actin	AGCAGGAGATGGCCACC	300	Tedeschi et al., 2017
actR		TCCACATCTGCTGGAAGG		
fAY	16S rRNA	GCACGTAATGGTGGGCACTT	300	Marcone et al., 1996
rEY		CGAAGTTAAGCCACTGCTTTC		

denaturation at 95°C for 3 min, then 50 cycles consisting of denaturation at 95°C for 30 s, annealing at 58°C for 40 s and elongation at 72°C for 45 s. Even if a possible influence of immune challenge on actin expression was reported (de-Morais et al., 2005), stable actin expression was observed among sample groups and treatments (**Supplementary Table S2**), as previously observed by Capone et al. (2013) and Tedeschi et al. (2017). Consequently, *actin* was selected to be amplified as a reference gene. Moreover, samples belonging to the EFDi and LFDi groups were quantitatively checked for FDp infection by 16SrV group phytoplasma-specific PCR reactions, conducted with the fAY/rEY primer pair as described by Galetto et al. (2005); only positive samples were considered in this study. qPCRs were performed on a CFX Connect™ Real-Time PCR Detection System (Bio-Rad, Hercules, CA, United States). Reactions were conducted in clear HardShell® Low-Profile 96-Well PCR Plates (Bio-Rad) with a 25 μl mixture containing 12.5 μl of 2 × SsoFast™ EvaGreen® Supermix (Bio-Rad), 0.1 μl of each primer (100 mM), 100 ng of sample cDNA and 11.3 μl of double distilled H_2O, sealed with adhesive Microseal® PCR Plate Sealing Film (Bio-Rad); samples were analyzed in triplicate. An initial denaturation at 95°C for 3 min was followed by 50 cycles consisting of denaturation at 95°C for 30 s and annealing at 54°C (for qPCR targeting defensin and Raf) or 58°C (for qPCR targeting phenoloxidase and kazal type 1 serine protease inhibitor) for 20 s. A final step for melting curve analysis from 70 to 95°C, measuring fluorescence every 0.5°C, was added. Results were analyzed using the CFX Manager™ Software (Bio-Rad) for Ct determination. Normalization of primer efficiency was obtained by the one-point calibration (OPC) method, according to Brankatschk et al. (2012); normalized efficiencies of the target genes, with respect to the standard, ranged between 96 and 101%. Relative quantification of target genes was calculated using the $2^{-\Delta\Delta Ct}$ method (Livak and Schmittgen, 2001). Statistical analyses were performed with SPSS Statistics 25 (IBM Corp. Released 2017, Armonk, NY, United States). One-way analysis of variance (ANOVA) was applied and means separated by a Tukey's test ($P < 0.05$) when variance homogeneity was satisfied (Levene test, $P < 0.05$).

Evaluation of Strain Adhesion Capacity

Adhesion capacity of strains *Asaia* SF2.1Rif^R, *Asaia* SF15.14Rif^R, *E. coli* DH5α pKan(DsRed), and the positive control *E. coli* ATCC 25404 was evaluated by crystal violet staining assay (Barbato et al., 2016). *Asaia* strains were grown overnight in GE medium (2% glucose, 0.8% yeast extract, pH 7), while *E. coli* strains were cultured overnight in LB medium [added with 50 μg/ml kanamycin in case of *E. coli* DH5α pKan(DsRed)]. Following overnight growths, 200 μl of the bacterial suspensions containing 10^6 cell/ml of the different strains were transferred to a flat bottom, polystyrene microtiter plate. Eight replicates were inoculated for each strain and eight uninoculated controls were prepared, as well. Strains were grown at 24 or 30°C for 48 or 72 h. Following the incubation time, the optical density at 610 nm (OD 610 nm) was measured. Bacterial cultures were then removed and microtiter-adhering cells were gently washed with PBS three times. The microtiter plate was dried for 15 min and then stained with a solution of crystal violet (0.5 g/L crystal violet in 20% ethanol) for 15 min at room temperature. Finally, crystal violet solution was removed, the microtiter plate was washed twice with distilled water and let dry for 15 min. Crystal violet contained in adhering cells was then solubilized in 96% ethanol by pipetting. Absorbance (OD 610 nm) of solubilized crystal violet was measured by using a microtiter reader (Tecan Infinite F200Pro).

RESULTS

Expression of Immune Genes

Prior to measuring the expression of our target immune genes, cDNA from samples belonging to the EFDi and LFDi groups was subjected to phytoplasma quantification to confirm their infection status. We measured the average number of 16SrV phytoplasma cells per sample, which ranged between 1.04×10^2, detected in hemocytes, and 5.54×10^4 found in midguts. No significant differences were observed between treatments within the same sample origin, according to ANOVA performed on log-transformed values (whole insects: df = 7, 32, $F = 1.466$,

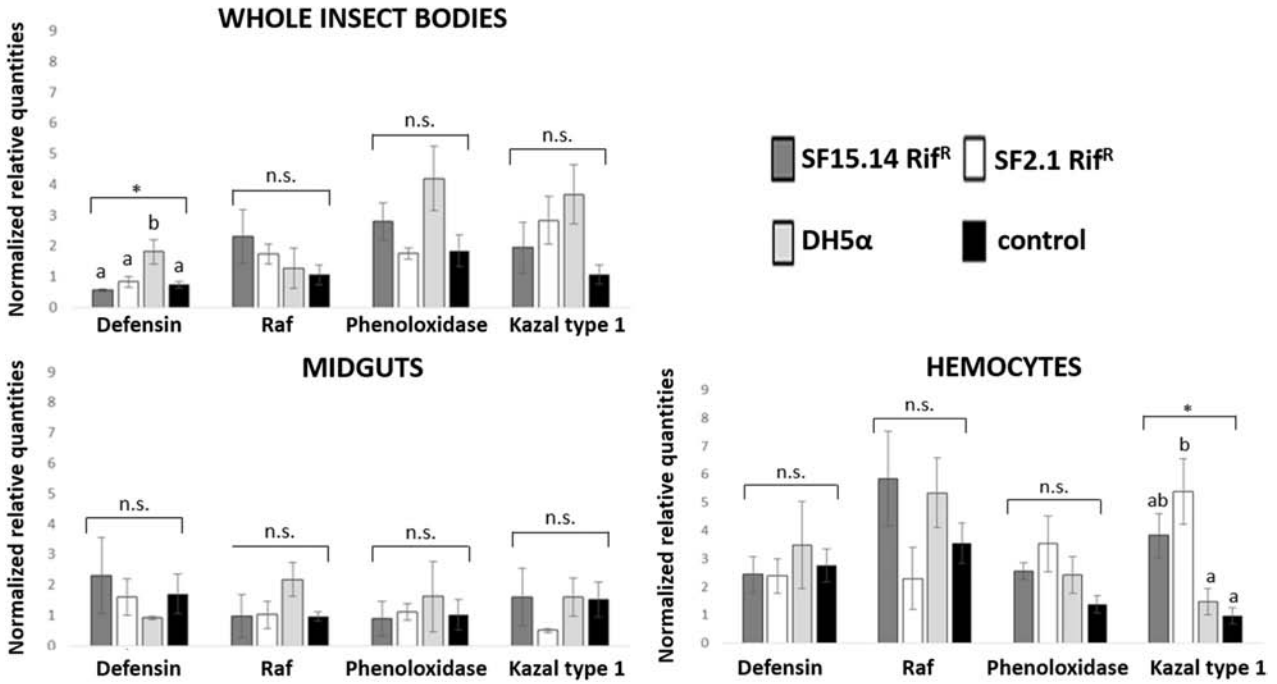

FIGURE 2 | Expression profiles of immune-related genes in *E. variegatus* samples of the healthy group. Gene expression was measured in the whole bodies, midguts, and cultured hemocytes of adults treated with *Asaia* SF15.14Rif^R, *Asaia* SF2.1Rif^R, and *E. coli* DH5α pKan(DsRed), along with the control. Normalized relative quantities, calculated by $2^{-\Delta\Delta Ct}$ method, are indicated for *defensin*, *Raf*, *phenoloxidase*, and *kazal type 1 serine protease inhibitor* genes. Bars indicate standard errors. Asterisks show significant differences according to ANOVA ($P < 0.05$); different letters indicate significantly different values according to Tukey's test (a < b). DH5α: *E. coli* DH5α pKan(DsRed); n.s., not significant.

$P = 0.215$; midguts: df = 7, 32, $F = 1.042$, $P = 0.422$; hemocytes: df = 7, 32, $F = 1.220$, $P = 0.321$). In the EFDi and LFDi sample groups, only the phytoplasma-positive samples were used for the immune gene expression analysis. Normalized relative quantities of immune genes considered in this study are reported in **Supplementary Table S3** and **Figures 2–4**. In the whole bodies of *E. variegatus* adults, the levels of transcripts showed little variability for all genes after supply of either bacteria, in each of the healthy, EFDi, and LFDi groups. Only in a few cases were significant differences observed in the expression values (**Supplementary Table S4**): defensin was overexpressed in healthy specimens fed with *E. coli* DH5α pKan(DsRed) (**Figure 2**), while phenoloxidase was activated after administering *Asaia* SF2.1Rif^R to individuals of the EFDi group (**Figure 3**). No differences were detected in LFDi insects (**Figure 4**). On the other hand, when considering midgut samples, significantly different transcript levels of *Raf* gene were found in the samples exposed to phytoplasmas (EFDi and LFDi groups) (**Figures 3**, **4**). In both cases, Raf was overexpressed in the midguts belonging to specimens fed with *Asaia* SF15.14Rif^R relative to the control, consisting of leafhoppers reared in the presence of phytoplasmas without bacteria. *Kazal type 1* gene was found to be upregulated as well, although only in EFDi midguts. In this case, the transcripts related to insects fed with *E. coli* DH5α pKan(DsRed) were significantly more abundant than those detected in the presence of *Asaia* SF15.14Rif^R. In the case of hemocyte samples, most significant differences were observed for the expression levels of *kazal type 1* gene. Strikingly, upregulation was observed in healthy (**Figure 2**) and LFDi samples (**Figure 4**), whereas kazal type 1 transcripts from the EFDi group were not significantly different, particularly when considering hemocytes treated with either bacteria (**Figure 3**). Moreover, in samples from the healthy group, kazal type 1 was overexpressed after exposure to *Asaia* SF2.1Rif^R relative to *E. coli* DH5α pKan(DsRed) and the control, while in samples from the LFDi group the most abundant transcripts were detected in the presence of *Asaia* SF15.14Rif^R. Other significant differences were recorded in hemocyte samples: defensin was downregulated in samples treated with *Asaia* SF2.1Rif^R relative to the control in EFDi samples, and Raf was upregulated in samples exposed to *Asaia* SF15.14Rif^R relative to those provided with *Asaia* SF2.1Rif^R in samples from the LFDi group (**Figures 2–4**).

Besides comparing gene expression profiles obtained for different treatments and sample groups, data were further analyzed to evaluate the temporal expression trend of each gene with respect to phytoplasma infection. Hence, normalized values obtained for single genes were examined, considering the healthy group as time 0 with respect to FDp infection, the EFDi group as time 0 + 5 days from the beginning of FDp infection, and finally the LFDi group as time 0 + 21 days from the beginning of phytoplasma infection. Statistical analysis performed to compare data from similarly treated samples from the healthy, EFDi and LFDi groups revealed a growing expression trend only for *Raf* and *kazal type 1* genes (**Figures 5**, **6**). Specifically, Raf was

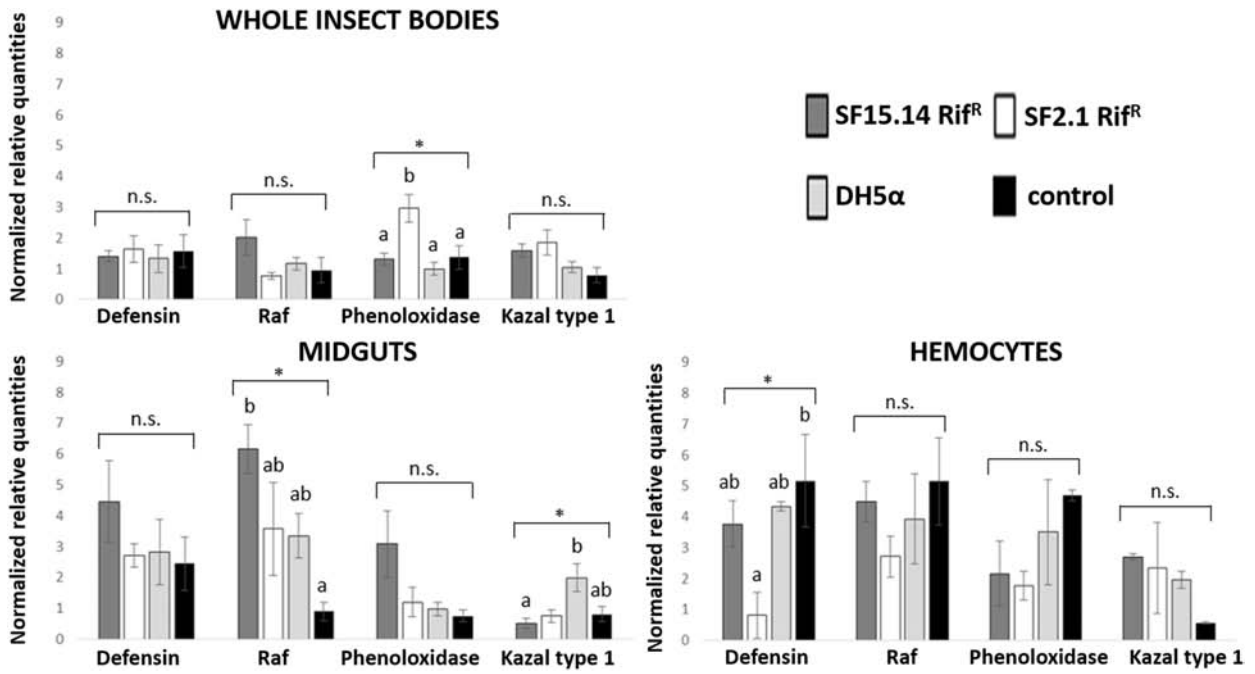

FIGURE 3 | Expression profiles of immune-related genes in *E. variegatus* samples of the EFDi group. Gene expression was measured in the whole bodies, midguts, and cultured hemocytes of adults treated with *Asaia* SF15.14Rif^R, *Asaia* SF2.1Rif^R, and *E. coli* DH5α pKan(DsRed), along with the control. Normalized relative quantities, calculated by $2^{-\Delta\Delta Ct}$ method, are indicated for *defensin*, *Raf*, *phenoloxidase*, and *kazal type 1 serine protease inhibitor* genes. Bars indicate standard errors. Asterisks show significant differences according to ANOVA ($P < 0.05$); different letters indicate significantly different values according to Tukey's test (a < b). DH5α: *E. coli* DH5α pKan(DsRed); n.s., not significant.

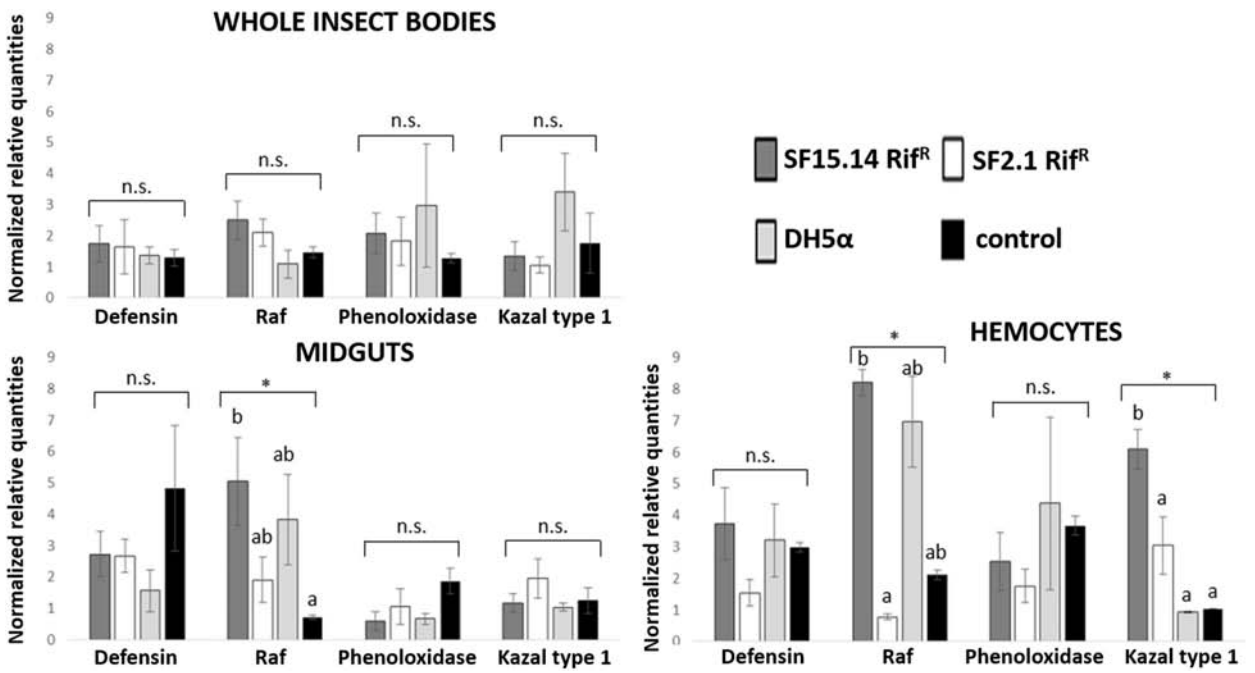

FIGURE 4 | Expression profiles of immune-related genes in *E. variegatus* samples of the LFDi group. Gene expression was measured in the whole bodies, midguts, and cultured hemocytes of adults treated with *Asaia* SF15.14Rif^R, *Asaia* SF2.1Rif^R, and *E. coli* DH5α pKan(DsRed), along with the control. Normalized relative quantities, calculated by $2^{-\Delta\Delta Ct}$ method, are indicated for *defensin*, *Raf*, *phenoloxidase*, and *kazal type 1 serine protease inhibitor* genes. Bars indicate standard errors. Asterisks show significant differences according to ANOVA ($P < 0.05$); different letters indicate significantly different values according to Tukey's test (a < b). DH5α: *E. coli* DH5α pKan(DsRed); n.s., not significant.

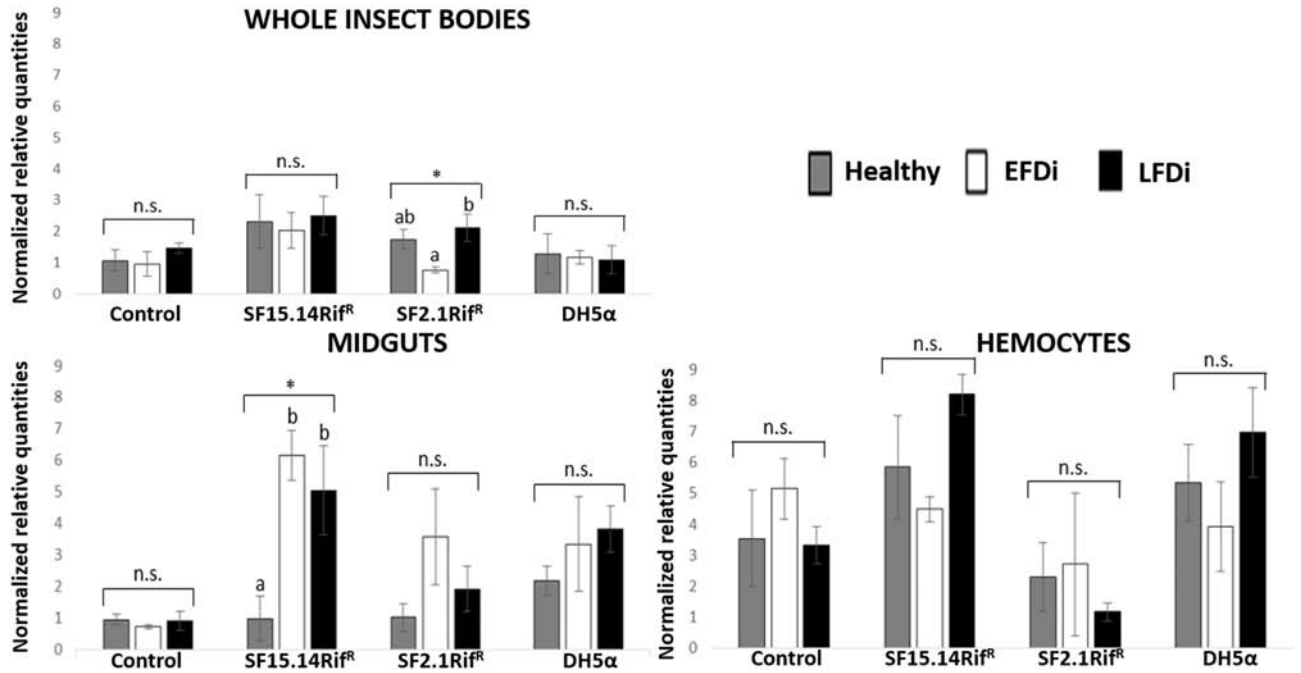

FIGURE 5 | Temporal trend of gene expression for *Raf* gene. Normalized relative quantities are displayed for whole insect bodies, midgut sections, and cultured hemocytes of insects treated with *Asaia* SF15.14Rif^R, *Asaia* SF2.1Rif^R, and *E. coli* DH5α pKan(DsRed), along with the control. Healthy: time 0 of FDp infection; EFDi time 0 + 5 days of FDp infection; LFDi: time 0 + 21 days of FDp infection. Asterisks show significant differences according to ANOVA ($P < 0.05$); different letters indicate significantly different values according to Tukey's test (a < b). DH5α: *E. coli* DH5α pKan(DsRed); n.s., not significant.

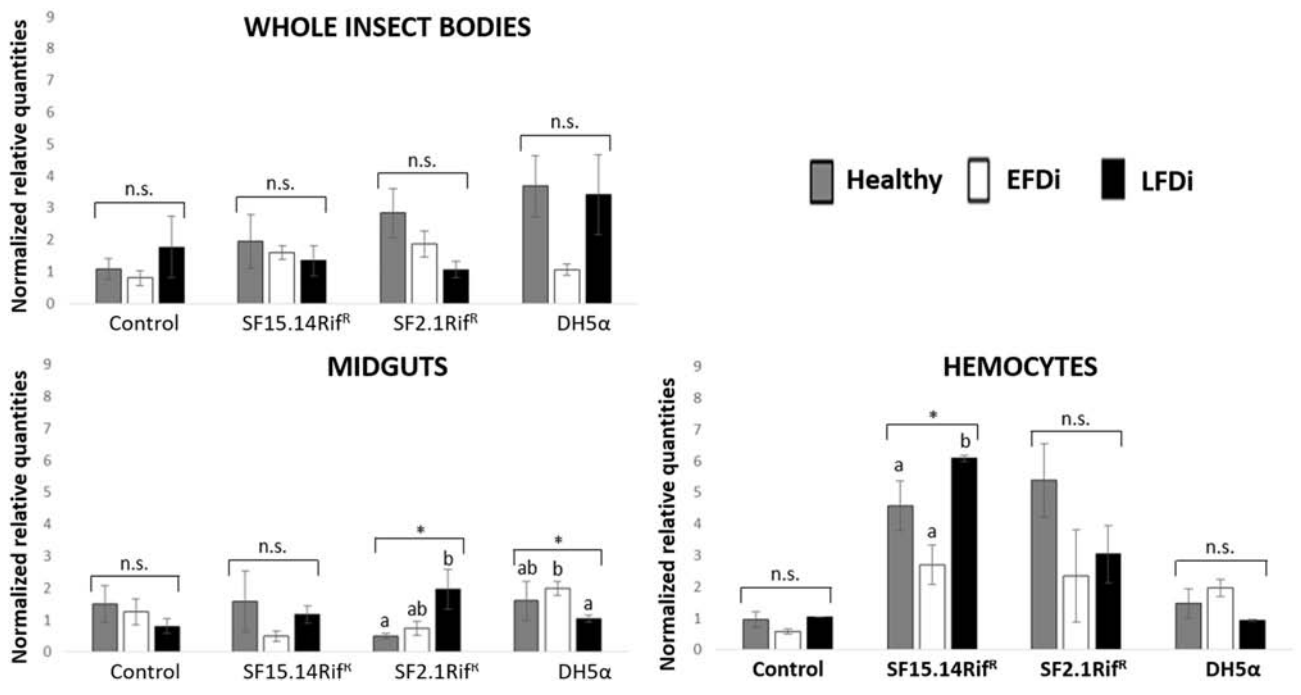

FIGURE 6 | Temporal trend of gene expression for *kazal type 1 serine protease inhibitor* gene. Normalized relative quantities are displayed for whole insect bodies, midgut sections, and cultured hemocytes of insects treated with *Asaia* SF15.14Rif^R, *Asaia* SF2.1Rif^R, and *E. coli* DH5α pKan(DsRed), along with the control. Healthy: time 0 of FDp infection; EFDi time 0 + 5 days of FDp infection; LFDi: time 0 + 21 days of FDp infection. Asterisks show significant differences according to ANOVA ($P < 0.05$); different letters indicate significantly different values according to Tukey's test (a < b). DH5α: *E. coli* DH5α pKan(DsRed); n.s., not significant.

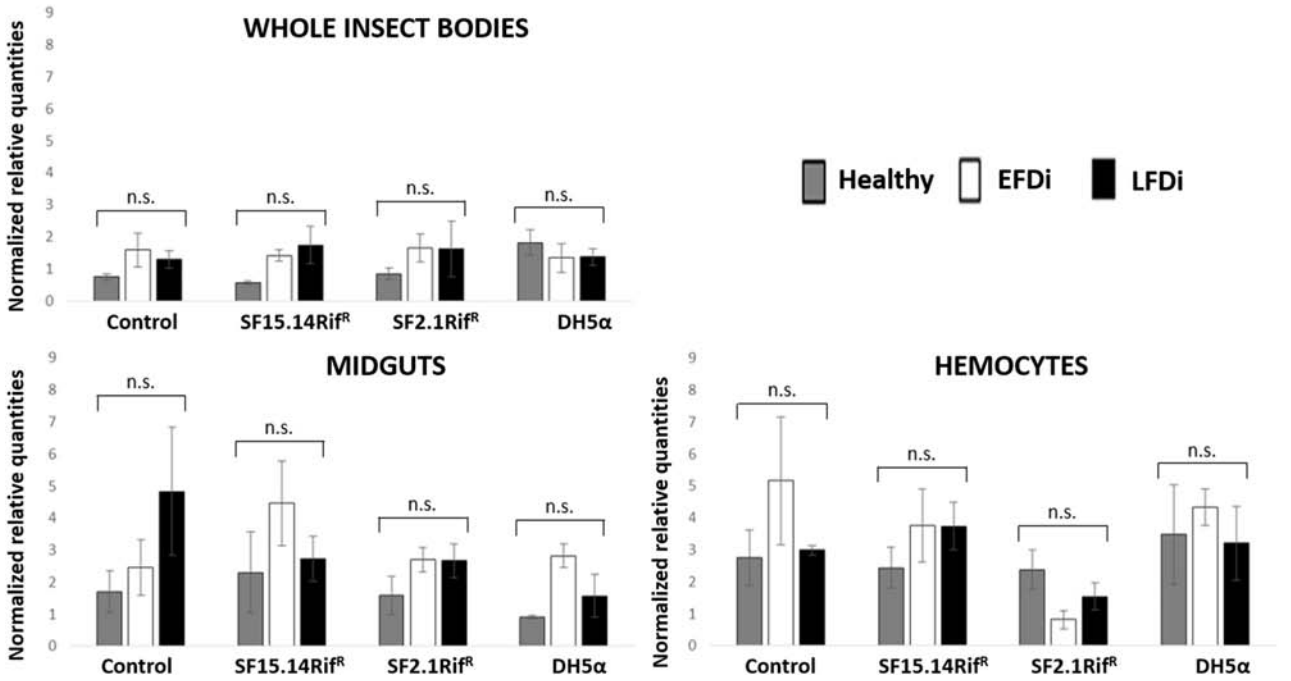

FIGURE 7 | Temporal trend of gene expression for *defensin* gene. Normalized relative quantities are displayed for whole insect bodies, midgut sections, and cultured hemocytes of insects treated with *Asaia* SF15.14Rif^R, *Asaia* SF2.1Rif^R, and *E. coli* DH5α pKan(DsRed), along with the control. Healthy: time 0 of FDp infection; EFDi time 0 + 5 days of FDp infection; LFDi: time 0 + 21 days of FDp infection. DH5α: *E. coli* DH5α pKan(DsRed); n.s., not significant.

overexpressed in the whole body of *E. variegatus* fed with *Asaia* SF2.1Rif^R as a consequence of chronical FDp infection (LFDi vs. healthy + EFDi), and in the midguts of insects provided with *Asaia* SF15.14Rif^R subsequent to FDp exposure (EFDi + LFDi vs. healthy) (**Figure 5** and **Supplementary Table S5**). Likewise, *kazal type 1* gene was upregulated in samples from the LFDi group (LFDi vs. healthy + EFDi), and precisely in midguts of insects fed with *Asaia* SF2.1Rif^R and *E. coli* DH5α pKan(DsRed), and in hemocytes following treatment with *Asaia* SF15.14Rif^R (**Figure 6** and **Supplementary Table S5**). Conversely, we did not find any significant trend in defensin or phenoloxidase in consequence of bacterial challenge (**Figures 7**, **8** and **Supplementary Table S5**). Instead, phenoloxidase was significantly overexpressed over time in hemocytes from the control group (**Figure 8**).

Adhesion Test

Adhesion capacity of *Asaia* strains was evaluated in comparison to the one shown by a well-known biofilm-producer strain, i.e., *E. coli* ATCC 25404, which was considered as positive control (Wood et al., 2006). *Asaia* SF2.1Rif^R and *E. coli* DH5α pKan(DsRed) weakly adhered to the polystyrene microtiter plate (**Supplementary Figure S2A** and **Supplementary Table S6**) in comparison with the positive control strain. Moreover, following a longer incubation (72 h) *E. coli* DH5α pKan(DsRed) displayed a decreasing adhesion capacity. *Asaia* SF15.14Rif^R was not able to adhere to the microtiter wells in our experimental conditions either considering incubation at 24 and 30°C, or 48 and 72 h. In wells inoculated with *Asaia* SF15.14Rif^R bacterial biomasses were observed on the medium surface that resembled the ALI films already described to be produced by this strain (**Supplementary Figure S2B**): it is likely that the shorter incubation times used in our experiments, in comparison to those described in Gonella et al. (2018) did not allow the complete film formation observed before. Conversely, strain *E. coli* ATCC 25404 showed itself to be a strong adherent strain.

DISCUSSION

Our investigation focused on the differential regulation of immune genes chosen to represent a range of elements shaping the leafhopper immune response, revealing localized regulation in *E. variegatus* adults, for all of the four genes taken into consideration. Indeed, even if gene expression variability generally appeared mitigated in whole-body samples for most of the genes, in midgut and hemocyte samples, significantly diverging gene expression levels were observed, in particular for the genes *Raf* and *kazal type 1*.

Raf is the only gene that exhibited consistent upregulation in response to exposure to a single bacterial strain, being overexpressed in the presence of *Asaia* SF15.14Rif^R. Since this strain was reported by Gonella et al. (2018) to induce a reduced FDp acquisition in *E. variegatus*, this gene might be involved in enhancing the insect response to phytoplasma infection. Specifically, *Raf* gene was more specifically activated in midgut samples when the presence of *Asaia* SF15.14Rif^R was combined with FDp infection (EFDi and LFDi groups),

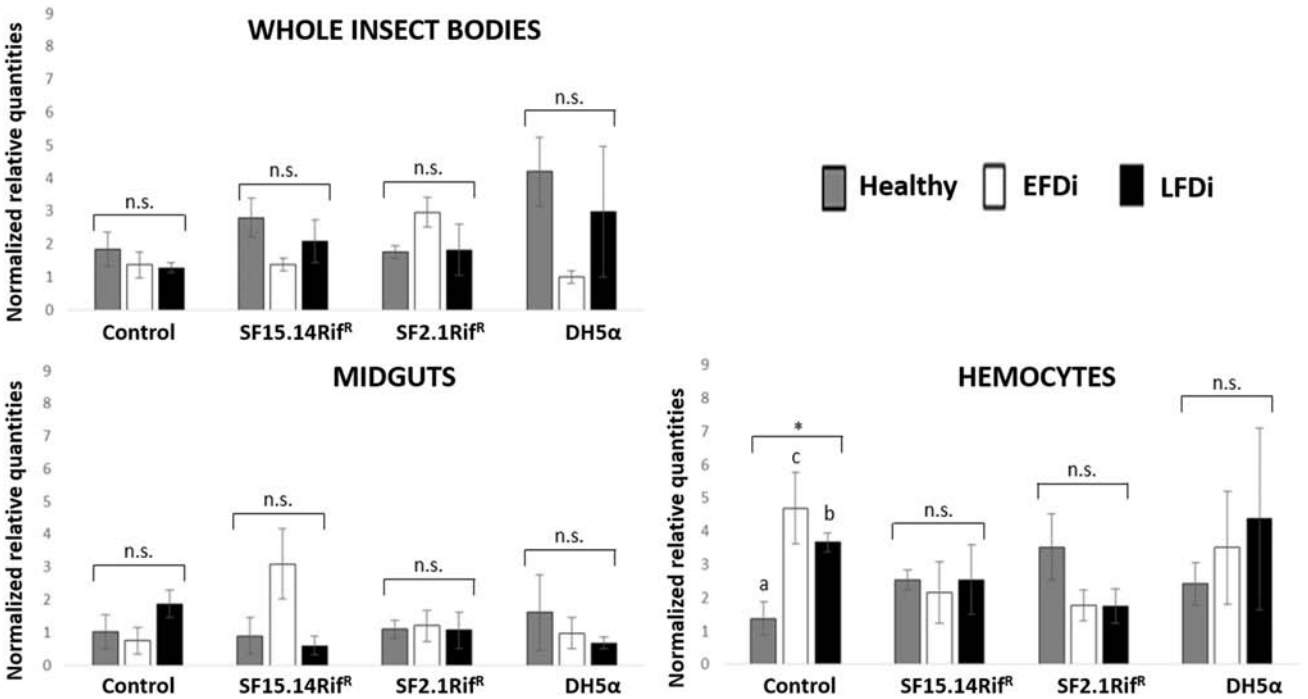

FIGURE 8 | Temporal trend of gene expression for *phenoxidase* gene. Normalized relative quantities are displayed for whole insect bodies, midgut sections, and cultured hemocytes of insects treated with *Asaia* SF15.14Rif^R, *Asaia* SF2.1Rif^R, and *E. coli* DH5α pKan(DsRed), along with the control. Healthy: time 0 of FDp infection; EFDi time 0 + 5 days of FDp infection; LFDi: time 0 + 21 days of FDp infection. Asterisk shows significant difference according to ANOVA ($P < 0.05$); different letters indicate significantly different values according to Tukey's test (a < b). DH5α: *E. coli* DH5α pKan(DsRed); n.s., not significant.

while the same gene was overexpressed in the hemocytes only at the late phase of phytoplasma infection. Our experimental evidence confirms that Raf expression is relevant in the immune response and in persistent infection and/or sepsis since Raf induction causes activation of the hematopoiesis (as reported in *Drosophila*) (Asha et al., 2003; Zettervall et al., 2004). Our observations also suggest that the midgut could be a crucial site for Raf activation, supporting a role for Raf in limiting the capability of FDp to colonize the gut, and crossing this barrier to reach the hemolymph. This indication is in accordance with previous results suggesting that gut homeostasis is maintained through a balance between cell damage, due to the collateral effects of bacteria killing, and epithelial repair by stem cell division (Buchon et al., 2009) and that Raf is involved in the control of *Drosophila* gut stem cell proliferation (Jin et al., 2015). Accordingly, in the midgut of insects fed with *Asaia* SF15.14Rif^R, a significant rise of Raf expression was recorded corresponding to the early stage of FDp infection, which is a crucial stage for phytoplasma passage from the midgut to the insect hemolymph.

In the case of kazal type 1 serine protease inhibitor, a hemocyte-specific response was observed following challenge with *Asaia*, while no significant activation relative to controls was observed in whole insects or dissected midguts following exposure to these strains. Nonetheless, different strains induced kazal type 1 overexpression in the hemocytes of healthy and LFDi individuals, namely strains SF2.1Rif^R and SF15.14Rif^R in the first and in the latter groups, respectively, whereas no significant upregulation was found in the EFDi hemocytes. Accordingly, significantly increased expression of kazal type 1 was found in late phytoplasma infection (LFDi), in hemocytes exposed to *Asaia* SF15.14Rif^R (while an increasing trend over FDp infection time was observed for strain SF2.1Rif^R in midgut samples). Hence, a response in the hemocytes could be speculated to be related to genus-specific traits rather than to the production of ALI biofilm. Previous work experimentally combing *Asaia* strains with FDp infection did not show inhibition of phytoplasma transmission by strain SF2.1Rif^R (Gonella et al., 2018), suggesting the absence of genus-specific interference with the pathogen. Moreover, although FDp itself was demonstrated to induce *kazal type 1* gene overexpression (Galetto et al., 2018), this pathogen can bloom to high concentrations in *E. variegatus* (Rashidi et al., 2014), indicating that phytoplasmas may be only partially susceptible to such a response. Furthermore, no clear temporal trend was observed for *kazal type 1* gene over FDp infection stages in the control group, in none of sample types, even though a slight increment was visible for whole-insect samples, in agreement with the upregulation reported by Galetto et al. (2018). This is indicative of limited activation of this gene in our experimental conditions. Taken together, this evidence does not support a role for kazal type 1 activation in limiting FDp acquisition by *E. variegatus*.

The expression of *defensin* and *phenoloxidase* genes was not as affected as that of *Raf* and *kazal type 1* genes in

response to bacterial infection. Defensin was overexpressed in the whole body of insects fed with *E. coli* DH5α pKan(DsRed) only considering healthy individuals. Conversely, considering the EFDi and LFDi insect groups and single-body parts, samples exposed to this strain did not exhibit higher defensin expression than those treated with *Asaia* strains or the control, confirming the limited activation of this AMP in *E. variegatus* in response to Gram-negative bacteria (Tedeschi et al., 2017). Relative defensin transcript levels were significantly reduced in the hemocytes of insects from the EFDi group, after challenge with *Asaia* SF2.1Rif^R. However, no further data sustained the downregulation of this gene operated by the non-ALI producer strain. In previous experiments performed with hemocyte cultures of *Anopheles stephensi* Liston and *Drosophila melanogaster* Meigen, the administration of a DsRed-tagged strain of *Asaia* SF2.1 and *E. coli* DH5α pKan(DsRed) did not induce the expression of *defensin* gene (Capone et al., 2013). However, it is worth considering that a higher load of bacterial cells (10^9 cell/ml) and shorter incubation times (0, 4, 8, 12 h) than the ones used in our experimental set up were used by Capone et al. (2013). Taking into account the tendency of defensin expression over FDp infection-time, statistical analysis did not demonstrate any significant variation. However, an increase in the expression levels was recorded in the midgut of control insects, never exposed to bacteria other than the phytoplasma. This is in agreement with evidence reported by Yang et al. (2017), showing that defensin is activated by insect infection with *Spiroplasma melliferum*, a close relative of phytoplasmas recognized as a model for phytoplasma infection (Naor et al., 2011). On the other hand, when analyzing the FDp infection temporal trend in the control hemocytes, enhanced expression was detected in correspondence to the early stage of pathogen infection, suggesting hemocyte-specific defensin stimulation, consistently with the key role of the hemolymph for phytoplasma multiplication, resulting in a higher load of phytopathogen cells, which in turn stimulated an insect response. However, our data suggest an overall limited role of defensin in altering the capacity of *E. variegatus* to acquire FDp.

Phenoloxidase exhibited mostly irregular expression profiles, without significant diversity of transcript levels corresponding to distinct bacterial treatments according to ANOVA analysis, with the only exception being EFDi whole insects. Such an erratic response suggests the absence of a specific induction mechanism related to a challenge with any of administered bacterial strains. Limited phenoloxidase activation in response to *Asaia* infection could be expected considering its symbiotic interplay with leafhoppers (Crotti et al., 2009). On the other hand, in *Anopheles* mosquitoes, the adaptation of *Asaia* to host body environment was suggested to be related to resistance to immune response, rather than to a low immunogenicity (Capone et al., 2013); however, these authors did not investigate phenoloxidase activation. Similarly, although being a non-symbiotic strain, *E. coli* DH5α pHM2(GFP) did not induce phenoloxidase-related responses in leafhoppers, as previously reported for *E. coli*-infected hemocytes of *C. haematoceps* (Eliautout et al., 2016). However, phenoloxidase was shown to be significantly activated in the hemocytes during the early stage of phytoplasma infection, as a transcript peak was detected for EFDi samples in the control group. This result supports the hypothesis put forward by Galetto et al. (2018) that an increment in the expression of phenoloxidase might be evident in the early stages of FDp infection, whereas a lack of activation is typical of *E. variegatus* individuals chronically infected by phytoplasma.

Besides demonstrating that *Asaia* SF15.14Rif^R elicited in *E. variegatus* a midgut-specific immune response, this work explored an alternative process that may modulate the interference exerted by this strain on FDp, i.e., physical exclusion by means of complete adhesion to the gut wall. However, the adhesion test did not show successful adhesion to microtiter plates for *Asaia* SF15.14Rif^R. This result might be affected by the experimental conditions that were applied in terms of incubation times or medium used. The artificial substrate may indeed imperfectly mimic the insect gut epithelia. As a matter of fact, in Hemiptera the gut content is in contact with the microvilli of midgut cells, in the absence of a peritrophic membrane (Nation, 2016). Therefore, the increased contact surface provided by microvilli may offer a more suitable substrate for bacterial adhesion. Acetic acid bacteria closely related to *Asaia* were reported to be specifically located near the host gut wall (Kounatidis et al., 2009; Vacchini et al., 2017); however, our results do not support massive attachment of *Asaia* SF15.14Rif^R to the gut epithelial layer. A possible explanation of limited attachment could be the production of flocculant flake-like bacterial masses (**Supplementary Figure S2B**). These masses have previously been proposed to play a role in entrapping phytoplasma cells or erecting a barrier against them, contributing to hampering pathogen establishment in the insect body (Gonella et al., 2018). Moreover, we cannot rule out the involvement of specific host factors under *in vivo* conditions necessary to mediate the bacterial adhesion. Future work is thus required to investigate the role of bacterial entrapment or physical containment in limiting FDp acquisition by *E. variegatus*.

CONCLUSION

This work sheds light on the molecular interplay occurring among insect hosts and bacteria, focusing on symbiotic and non-symbiotic strains, as well as on leafhopper-vectored plant pathogens. Among different immune-related genes indicative of distinct response mechanisms, *Raf* gene showed midgut-specific activation in response to *Asaia* strain SF15.14Rif^R after insect infection by FDp, while the pathogen alone did not stimulate the same reaction. It can therefore be suggested that *Asaia* strain SF15.14Rif^R may elicit a basal host immune activity that appears to act against other microorganisms, including phytoplasma. The elicitation of Raf-mediated response is thus predicted to be a major component of the interfering effect displayed by *Asaia* SF15.14Rif^R toward FDp acquisition by *E. variegatus*. Considering the limited number of immune genes reported for *E. variegatus* and other Hemiptera (Arp et al., 2016; Skidmore and Hansen, 2017; Tedeschi et al., 2017), our results suggest a compensation of lost defensive functions by genes that have minor functions in insects exhibiting a more complete immunity.

Investigating the role of other immune genes will help to further elucidate this phenomenon, as well as exploring possible differential response profiles in different conditions, such as for example when insects are exposed to different temperatures. On the other hand, a minor contribution to phytoplasma exclusion seems to be provided by *Asaia* attachment to the vector gut wall. Further possible mechanisms of phytoplasma segregation, involving a physical barrier created by *Asaia* SF15.14Rif^{R} though the production of ALI biofilm, need to be investigated.

AUTHOR CONTRIBUTIONS

EG, MM, RT, EC, and AA contributed to conception and design of the study. EG, EC, and MP carried out the experiments. EG performed the statistical analysis. AA, RT, and EC provided reagents and analytical tools. EG, MM, EC, and RT wrote sections of the manuscript. All authors contributed to manuscript revision, read and approved the submitted version.

FUNDING

This work was partially supported by the "INTEFLAVI" (Un approccio integrato alla lotta contro la flavescenza dorata della vite) project. Funding was provided by Fondazione Cassa di Risparmio di Cuneo.

ACKNOWLEDGMENTS

The authors are grateful to Luca Picciau and Giuseppe Galante for insect rearing and phytoplasma maintenance.

SUPPLEMENTARY MATERIAL

The Supplementary Material for this article can be found online at: https://www.frontiersin.org/articles/10.3389/fphys.2019.00795/full#supplementary-material

REFERENCES

Alma, A., Tedeschi, R., Lessio, F., Picciau, L., Gonella, E., and Ferracini, C. (2015). Insect vectors of plant pathogenic mollicutes in the euro-mediterranean region. *Phytopathogen Mollicutes* 5, 53–73. doi: 10.5958/2249-4677.2015.00063.8

Arp, A. P., Hunter, W. B., and Pelz-Stelinski, K. S. (2016). Annotation of the Asian citrus psyllid genome reveals a reduced innate immune system. *Front. Physiol.* 7:570. doi: 10.3389/fphys.2016.00570

Asha, H., Nagy, I., Kovacs, G., Stetson, D., Ando, I., and Dearolf, C. R. (2003). Analysis of Ras-induced overproliferation in *Drosophila* hemocytes. *Genetics* 163, 203–215.

Barbato, M., Mapelli, F., Magagnini, M., Chouaia, B., Armeni, M., Marasco, R., et al. (2016). Hydrocarbon pollutants shape bacterial community assembly of harbor sediments. *Mar. Pollut. Bull.* 104, 211–220. doi: 10.1016/j.marpolbul.2016.01.029

Baumann, P. (2005). Biology of bacteriocyte-associated endosymbionts of plant sap-sucking insects. *Ann. Rev. Microbiol.* 59, 155–189. doi: 10.1146/annurev.micro.59.030804.121041

Bosco, D., Galetto, L., Leoncini, P., Saracco, P., Raccah, B., and Marzachì, C. (2007). Interrelationships between "*Candidatus* Phytoplasma asteris" and its leafhopper vectors (Homoptera: Cicadellidae). *J. Econom. Entomol.* 100, 1504–1511. doi: 10.1603/0022-0493-100.5.1504

Bosco, D., and Marzachì, C. (2016). "Insect transmission of phytoplasmas," in *Vector-Mediated Transmission of Plant Pathogens*, ed. J. K. Brown (St. Paul, MN: APS Press), 319–327.

Brankatschk, R., Bodenhausen, N., Zeyer, J., and Bürgmann, H. (2012). Simple absolute quantification method correcting for quantitative PCR efficiency variations for microbial community samples. *Appl. Environ. Microbiol.* 78, 4481–4489. doi: 10.1128/AEM.07878-11

Bressan, A., Clair, D., Sémétey, O., and Boudon-Padieu, E. (2005). Effect of two strains of flavescence dorèe phytoplasma on the survival and fecundity of the experimental leafhopper vector *Euscelidius variegatus* Kirschbaum. *J. Invertebr. Pathol.* 89, 144–149. doi: 10.1016/j.jip.2005.03.001

Buchon, N., Broderick, N. A., Poidevin, M., Pradervand, S., and Lemaitre, B. (2009). *Drosophila* intestinal response to bacterial infection: activation of host defense and stem cell proliferation. *Cell Host Microbe* 5, 200–211. doi: 10.1016/j.chom.2009.01.003

Capone, A., Ricci, I., Damiani, C., Mosca, M., Rossi, P., Scuppa, P., et al. (2013). Interactions between *Asaia*, *Plasmodium* and *Anopheles*: new insights into mosquito symbiosis and implications in malaria symbiotic control. *Parasit. Vectors* 6:182. doi: 10.1186/1756-3305-6-182

Cassone, B. J., Michel, A. P., Stewart, L. R., Bansal, R., Mian, M. A. R., and Redinbaugh, M. G. (2014). Reduction in fecundity and shifts in cellular processes by a native virus on an invasive insect. *Genome Biol. Evol.* 6, 873–885. doi: 10.1093/gbe/evu057

Crotti, E., Damiani, C., Pajoro, M., Gonella, E., Rizzi, A., Ricci, I., et al. (2009). Asaia, a versatile acetic acid bacterial symbiont, capable of cross-colonizing insects of phylogenetically distant genera and orders. *Environ. Microbiol.* 11, 3252–3264. doi: 10.1111/j.1462-2920.2009.02048.x

de-Morais, G. S., Vitorino, R., Domingues, R., Tomer, K., Correia, A. J., Amado, F., et al. (2005). Proteomics of immune-challenged *Drosophila melanogaster* larvae haemolymph. *Biochem. Biophys. Res. Commun.* 328, 106–115. doi: 10.1016/j.bbrc.2004.12.135

Eleftherianos, I., Atri, J., Accetta, J., and Castillo, J. C. (2013). Endosymbiotic bacteria in insects: guardians of the immune system? *Front. Physiol.* 4:46. doi: 10.3389/fphys.2013.00046

Eliautout, R., Dubrana, M. P., Vincent-Monégat, C., Vallier, A., Braquart-Varnier, C., Poirié, M., et al. (2016). Immune response and survival of *Circulifer haematoceps* to *Spiroplasma citri* infection requires expression of the gene hexamerin. *Dev. Comp. Immunol.* 54, 7–19. doi: 10.1016/j.dci.2015.08.007

Favia, G., Ricci, I., Damiani, C., Raddadi, N., Crotti, E., Marzorati, M., et al. (2007). Bacteria of the genus *Asaia* stably associate with *Anopheles stephensi*, an Asian malarial mosquito vector. *Proc. Natl. Acad. Sci. U.S.A.* 104, 9047–9051. doi: 10.1073/pnas.0610451104

Galetto, L., Abbà, S., Rossi, M., Vallino, M., Pesando, M., Arricaus-Bouvery, N., et al. (2018). Two phytoplasmas elicit different responses in the insect vector *Euscelidius variegatus* Kirschbaum. *Infect. Immun.* 86:e042-18. doi: 10.1128/IAI.00042-18

Galetto, L., Bosco, D., and Marzachì, C. (2005). Universal and group-specific real-time PCR diagnosis of flavescence doree (16Sr-V), bois noir (16Sr-XII) and apple proliferation (16Sr-X) phytoplasmas from field-collected plant hosts and insect vectors. *Ann. Appl. Biol.* 147, 191–201. doi: 10.1111/j.1744-7348.2005.00030.x

Gonella, E., Crotti, E., Mandrioli, M., Daffonchio, D., and Alma, A. (2018). Asaia symbionts interfere with infection by "flavescence dorée" phytoplasma in leafhoppers. *J. Pest Sci.* 91, 1033–1046. doi: 10.1007/s10340-018-0973-1

Gonella, E., Crotti, E., Rizzi, A., Mandrioli, M., Favia, G., Daffonchio, D., et al. (2012). Horizontal transmission of the symbiotic bacterium Asaia sp. in the leafhopper *Scaphoideus titanus* Ball (Hemiptera: Cicadellidae). *BMC Microbiol.* 12(Suppl. 1):S4. doi: 10.1186/1471-2180-12-S1-S4

Gonella, E., Pajoro, M., Marzorati, M., Crotti, E., Mandrioli, M., Pontini, M., et al. (2015). Plant-mediated interspecific horizontal transmission of an intracellular symbiont in insects. *Sci. Rep.* 5:15811. doi: 10.1038/srep15811

Gonella, E., Tedeschi, R., Crotti, E., and Alma, A. (2019). Multiple guests in a single host: interactions across symbiotic and phytopathogenic bacteria in phloem-feeding vectors – a review. *Entomol. Exp. Appl.* 167, 171–185. doi: 10.1111/eea.12766

Jin, Y., Ha, N., Forés, M., Xiang, J., Gläßer, C., Maldera, J., et al. (2015). EGFR/Ras signaling controls *Drosophila* intestinal stem cell proliferation via capicua-regulated genes. *PLoS Genet.* 11:e1005634. doi: 10.1371/journal.pgen.1005634

Kliot, A., Cilia, M., Csosnek, H., and Ghanim, M. (2014). Implication of the bacterial endosymbiont *Rickettsia* spp. in interactions of the whitefly *Bemisia tabaci* with tomato yellow leaf curl virus. *J. Virol.* 88, 5652–5660. doi: 10.1128/JVI.00071-14

Kounatidis, I., Crotti, E., Sapountzis, P., Sacchi, L., Rizzi, A., Chouaia, B., et al. (2009). *Acetobacter tropicalis* is a major symbiont of the olive fruit fly (*Bactrocera oleae*). *Appl. Environ. Microbiol.* 75, 3281–3328. doi: 10.1128/AEM.02933-08

Li, Z., An, X. K., Liu, Y. D., and Hou, M. L. (2016). Transcriptomic and expression analysis of the salivary glands in white-backed planthoppers, *Sogatella furcifera*. *PLoS One* 11:e0159393. doi: 10.1371/journal.pone.0159393

Livak, K. J., and Schmittgen, T. D. (2001). Analysis of relative gene expression data using real-time quantitative PCR and the 2-ΔΔCt method. *Methods* 25, 402–408. doi: 10.1006/meth.2001.1262

Login, F. H., Balmand, S., Vallier, A., Vincent-Monegat, C., Vigneron, A., Weiss-Gayet, M., et al. (2011). Antimicrobial peptides keep insect endosymbionts under control. *Science* 334, 362–365. doi: 10.1126/science.1209728

Makarova, O., MacLean, A., and Nicolaisen, M. (2015). Phytoplasma adapt to the diverse environments of their plant and insect hosts by altering gene expression. *Physiol. Mol. Plant Pathol.* 91, 81–87. doi: 10.1016/j.pmpp.2015.06.003

Marcone, C., Ragozzino, A., Schneider, B., Lauer, U., Smart, C. D., and Seemüller, E. (1996). Genetic characterization and classification of two phytoplasmas associated with spartium witches'-broom disease. *Plant Dis.* 80, 365–371. doi: 10.1094/PD-80-0365

Marutani-Hert, M., Hunter, W. B., and Hall, D. G. (2009). Establishment of Asian citrus psyllid (*Diaphorina citri*) primary cultures. *In Vitro Cell. Dev. Biol. – Animal* 45, 317–320. doi: 10.1007/s11626-009-9188-3

Nachappa, P., Levy, J., Pierson, E., and Tamborindeguy, C. (2014). Correlation between "*Candidatus* Liberibacter solanacearum" infection levels and fecundity in its psyllid vector. *J. Invertebr. Pathol.* 115, 55–61. doi: 10.1016/j.jip.2013.10.008

Naor, V., Ezra, D., and Zahavi, T. (2011). The use of *Spiroplasma melliferum* as a model organism to study the antagonistic activity of grapevine endophytes against phytoplasma. *Bull. Insectol.* 64, S265–S266.

Nation, J. L. (2016). *Insect Physiology and Biochemistry*. Boca Raton, FL: CRC Press.

Olson, K. E., and Blair, C. D. (2015). Arbovirus-mosquito interactions: RNAi pathway. *Curr. Opin. Virol.* 15, 119–126. doi: 10.1016/j.coviro.2015.10.001

Rashidi, M., D'Amelio, R., Galetto, L., Marzachì, C., and Bosco, D. (2014). Interactive transmission of two phytoplasmas by the vector insect. *Ann. Appl. Biol.* 165, 404–413. doi: 10.1111/aab.12146

Shao, E., Lin, G., Liu, S., Ma, X., Chen, M., Lin, L., et al. (2017). Identification of transcripts involved in digestion, detoxification and immune response from transcriptome of *Empoasca vitis* (Hemiptera: Cicadellidae) nymphs. *Genomics* 109, 58–66. doi: 10.1016/j.ygeno.2016.11.006

Skidmore, I. H., and Hansen, A. K. (2017). The evolutionary development of plant-feeding insects and their nutritional endosymbionts. *Insect Sci.* 24, 910–928. doi: 10.1111/1744-7917.12463

Tedeschi, R., Monti, M., Gonella, E., Melchiori, G., Alma, A., and Mandrioli, M. (2017). Molecular and cellular analysis of immunity in the phytoplasma vector *Euscelidius variegatus*: exploiting immunity to improve biological control strategies. *Inv. Surv. J.* 14, 63–72.

Tsakas, S., and Marmaras, V. J. (2010). Insect immunity and its signalling: an overview. *Inv. Surv. J.* 7, 228–238. doi: 10.1111/j.1462-2920.2009.02048.x

Vacchini, V., Gonella, E., Crotti, E., Prosdocimi, E. M., Mazzetto, F., Chouaia, B., et al. (2017). Bacterial diversity shift determined by different diets in the gut of the spotted wing fly *Drosophila suzukii* is primarily reflected on acetic acid bacteria. *Environ. Microbiol. Rep.* 9, 91–103. doi: 10.1111/1758-2229.12505

Vyas, M., Fisher, T. W., He, R., Nelson, W., Yin, G., Cicero, J. M., et al. (2015). Asian citrus psyllid expression profiles suggest *Candidatus liberibacter asiaticus*-mediated alteration of adult nutrition and metabolism, and of nymphal development and immunity. *PLoS One* 10:e0130328. doi: 10.1371/journal.pone.0130328

Weiss, B., and Aksoy, S. (2011). Microbiome influences on insect host vector competence. *Trends Parasitol.* 27, 514–522. doi: 10.1016/j.pt.2011.05.001

Wood, T. K., González Barrios, A. F., Herzberg, M., and Lee, J. (2006). Motility influences biofilm architecture in *Escherichia coli*. *Appl. Microbiol. Biotechnol.* 72, 361–367. doi: 10.1007/s00253-005-0263-8

Yang, D., Zha, G., Li, X., Gao, H., and Yu, H. (2017). Immune responses in the haemolymph and antimicrobial peptide expression in the abdomen of *Apis mellifera* challenged with spiroplasma melliferum CH-1. *Microb. Pathog.* 112, 279–287. doi: 10.1016/j.micpath.2017.10.006

Zettervall, C. J., Anderl, I., Williams, M. J., Palmer, R., Kurucz, E., Ando, I., et al. (2004). A directed screen for genes involved in *Drosophila* blood cell activation. *Proc. Natl. Acad. Sci. U.S.A.* 101, 14192–14197. doi: 10.1073/pnas.0403789101

Conflict of Interest Statement: The authors declare that the research was conducted in the absence of any commercial or financial relationships that could be construed as a potential conflict of interest.

frontiers in Physiology

ORIGINAL RESEARCH
published: 21 June 2019
doi: 10.3389/fphys.2019.00745

Transcriptome and Metabolome Reprogramming in Tomato Plants by *Trichoderma harzianum strain* T22 Primes and Enhances Defense Responses Against Aphids

Mariangela Coppola[1], *Gianfranco Diretto*[2]*, *Maria Cristina Digilio*[1,3], *Sheridan Lois Woo*[3,4,5], *Giovanni Giuliano*[2], *Donata Molisso*[1], *Francesco Pennacchio*[3,4], *Matteo Lorito*[1,3,5] *and Rosa Rao*[1,3]*

[1] Department of Agricultural Sciences, Portici, Italy, [2] ENEA, Rome, Italy, [3] Task Force on Microbiome Studies, University of Naples Federico II, Naples, Italy, [4] Department of Pharmacy, University of Naples Federico II, Naples, Italy, [5] National Research Council, Institute for Sustainable Plant Protection, Portici, Italy

OPEN ACCESS

Edited by:
Patrizia Falabella,
University of Basilicata, Italy

Reviewed by:
Santiago Gutierrez,
Universidad de León, Spain
Federico Martinelli,
University of Florence, Italy

***Correspondence:**
Gianfranco Diretto
gianfranco.diretto@enea.it
Rosa Rao
rao@unina.it

Specialty section:
This article was submitted to Invertebrate Physiology, a section of the journal Frontiers in Physiology

Received: 15 February 2019
Accepted: 31 May 2019
Published: 21 June 2019

Citation:
Coppola M, Diretto G, Digilio MC, Woo SL, Giuliano G, Molisso D, Pennacchio F, Lorito M and Rao R (2019) Transcriptome and Metabolome Reprogramming in Tomato Plants by Trichoderma harzianum strain T22 Primes and Enhances Defense Responses Against Aphids. Front. Physiol. 10:745. doi: 10.3389/fphys.2019.00745

Beneficial fungi in the genus *Trichoderma* are among the most widespread biocontrol agents of plant pathogens. Their role in triggering plant defenses against pathogens has been intensely investigated, while, in contrast, very limited information is available on induced barriers active against insects. The growing experimental evidence on this latter topic looks promising, and paves the way toward the development of *Trichoderma* strains and/or consortia active against multiple targets. However, the predictability and reproducibility of the effects that these beneficial fungi is still somewhat limited by the lack of an in-depth understanding of the molecular mechanisms underlying the specificity of their interaction with different crop varieties, and on how the environmental factors modulate this interaction. To fill this research gap, here we studied the transcriptome changes in tomato plants (cultivar "Dwarf San Marzano") induced by *Trichoderma harzianum* (strain T22) colonization and subsequent infestation by the aphid *Macrosiphum euphorbiae*. A wide transcriptome reprogramming, related to metabolic processes, regulation of gene expression and defense responses, was induced both by separate experimental treatments, which showed a synergistic interaction when concurrently applied. The most evident expression changes of defense genes were associated with the multitrophic interaction *Trichoderma*-tomato-aphid. Early and late genes involved in direct defense against insects were induced (i.e., *peroxidase, GST, kinases and polyphenol oxidase, miraculin, chitinase*), along with indirect defense genes, such as *sesquiterpene synthase* and *geranylgeranyl phosphate synthase*. Targeted and untargeted semi-polar metabolome analysis revealed a wide metabolome alteration showing an increased accumulation of isoprenoids in *Trichoderma* treated plants. The wide array of transcriptomic and metabolomics changes nicely fit with the higher mortality of aphids when feeding on *Trichoderma* treated plants, herein reported, and with the previously observed attractiveness of these latter toward the aphid parasitoid *Aphidius ervi*.

Moreover, *Trichoderma* treated plants showed the over-expression of transcripts coding for several families of defense-related transcription factors (bZIP, MYB, NAC, AP2-ERF, WRKY), suggesting that the fungus contributes to the priming of plant responses against pest insects. Collectively, our data indicate that *Trichoderma* treatment of tomato plants induces transcriptomic and metabolomic changes, which underpin both direct and indirect defense responses.

Keywords: San Marzano, aphid, RNA-Seq, semi-polarmetabolome, defense

INTRODUCTION

Solanum lycopersicum represents one of the most widespread horticultural crops in the world, with a production of 177 million of tons in 2016 (FAOSTAT). Pests and pathogens cause remarkable crop losses only in part limited by control strategies, which are still largely based on chemical pesticides. The use of biocontrol agents and/or the implementation of bioinspired strategies of sustainable pest management (Pennacchio et al., 2012) is still limited, in spite of the health and environmental issues associated with pesticide release (Alewu and Nosiri, 2011) and the recent changes of the EU policy aiming to reduce their use (European directive 2009/128; Woo and Pepe, 2018). Among the different biocontrol options, the useof soil microorganisms to reduce crop losses and promote plant growth appears to be very promising. Indeed, many biological products (i.e., biopesticides, biostimulants, biofertilizers) already available on the market often contain beneficial fungi belonging to the genus *Trichoderma* (Woo et al., 2014; Woo and Pepe, 2018). Numerous strains of *Trichoderma* may have direct effects on plants, such as promotion of growth, nutrient uptake, efficiency of nitrogen use, seed germination rate and plant defenses against biotic and abiotic stress agents (Shoresh et al., 2010; Studholme et al., 2013; Lorito and Woo, 2015). In particular, as many other beneficial microbes (Pineda et al., 2015), some *Trichoderma* strains can activate Systemic Acquired Resistance (SAR) and/or Induced Systemic Resistance (ISR) (Segarra et al., 2007; Shoresh et al., 2010; Rubio et al., 2014; Martínez-Medina et al., 2017; Manganiello et al., 2018), whichconfer resistance against a wealth of phytopathogens (Van Wees et al., 2008). Indeed, *Trichoderma spp.* are widely used as biocontrol agents of plant pathogens (Lorito et al., 2010; Lorito and Woo, 2015; Manganiello et al., 2018), and are recognized as valuable Plant Growth Promoting Fungi (PGPFs) (Harman et al., 2004; Hermosa et al., 2012; Studholme et al., 2013; Mendoza-Mendoza et al., 2018). However, very few reports have addressed the role of these fungi in the modulation of plant defense responses against pest insects. Only in the last decade, the enhancement of indirect plant defense barriers against aphids was observed in plants colonized by *Trichoderma* (Guerrieri et al., 2004; Battaglia et al., 2013; Coppola et al., 2017a).

Plants have evolved both direct and indirect protection barriers to limit pest insects, such as the production of compounds able to directly interfere with physiology and reproduction of herbivores (i.e., direct defense), or to attract their natural enemies and exploit the ecological service they provide (i.e., indirect defense) (Walling, 2000; Kessler and Baldwin, 2002). The signals and the defense molecules locally produced at the damage site are often systemically circulated throughout the plant, while the released volatile blend modulates the interactions not only with higher trophic levels (i.e., herbivores and their natural enemies), but also with neighboring healthy plants, which can perceive the "alarm messages" emitted by injured conspecifics (Conrath, 2011; Coppola et al., 2017b).

The titer of different plant hormones, such as salicylic acid (SA), ethylene (ET), and jasmonic acid (JA), is modulated by damage and the induced changes activate hormone-dependent key-regulators of downstream plant defense pathways (Pieterse and van Loon, 1999, 2004; Thaler et al., 2002). Biotrophic pathogens generally trigger the SA pathway, while necrotrophic colonization activates both of ET and JA pathways (Pieterse and van Loon, 1999; Walling, 2000; Harman et al., 2004). Insect chewing on plant tissues mostly induce the JA pathway (Schilmiller et al., 2007; Pieterse et al., 2012), while sap feeders predominantly activate SA-dependent responses (Walling, 2000, 2008). However, these signaling pathways are tightly interconnected to allow a fine control of optimal resource allocation between plant growth and response to environmental stress agents; the underlying network of cross-modulating pathways is often manipulated by plant enemies to evade or actively suppress the defense barriers (Pieterse et al., 2012). The antagonism between SA, ET, and JA pathways, dictated by the need to prioritize the response against a specific type of biotic stressor, has been demonstrated in many plant species (Reymond and Farmer, 1998; Spoel and Dong, 2008; Pieterse et al., 2012). However, numerous attackers can exploit this antagonism to their own benefit by activating responses to which they are not sensitive, thus preventing/limiting energy investments in defense pathways detrimental for them (Erb et al., 2012).

This intricate network of molecular interactions among different stress agents has a further layer of complexity, which is added by the soil and plant-associated microbiota, deeply influencing the overall plant response (Berendsen et al., 2012; Bulgarelli et al., 2013; Pineda et al., 2017). Plants, along with the associated microbiota in the surrounding environment, are therefore the living milieu in which a complex network of multitrophic interactions among pests/and beneficial organisms takes place. Then, the molecular mechanisms driving plant defense responses against pests and in presence of a beneficial micro-organism can only be understood if analyzed at metaorganism level. These studies will shed light on the co-evolutionary forces shaping insect communities on plants and

will offer valuable insights for developing novel strategies of pest control that can mimic and/or modulate plant defense responses.

Here we pursue this objective by investigating transcriptomic and metabolomic changes induced in *Solanum lycopersicum* (cv "Dwarf San Marzano") by the beneficial fungus *Trichoderma harzianum* strain T22, and a pest insect, the aphid *Macrosiphum euphorbiae* (Thomas), when applied to the experimental plants alone or in combination.

MATERIALS AND METHODS

Fungal Cultures and Insects

T. harzianum strain T22 (T22) was maintained on potato dextrose agar (PDA; Hi Media) slants at room temperature and regularly sub-cultured. Conidia were collected from the surface of sporulating fungal cultures (5–7 d) in sterile distilled water, and adjusted to a concentration of 10^7 spores mL^{-1}.

The aphid *M. euphorbiae* was reared on tomato "Dwarf San Marzano" (hereafter indicated as SM), in a climatic chamber at 20 ± 1°C, 65 ± 10% RH, photoperiod of 16:8 hr light/dark.

Plant Material and Treatments

Seeds of *Solanum lycopersicum* cv "Dwarf San Marzano" (SM) were surface-sterilized in 2% (v/v) sodium hypochlorite for 20 min, then thoroughly rinsed in sterile distilled water. Seeds were treated with the fresh spore suspension of *T. harzianum* T22, as a seed coating (conc. 10^7 spores mL^{-1}), or with water as a control treatment (CTRL); stirred frequently to cover the seed surface uniformly, left to air dry for 24 h, then stored at 4°C until use. Treated seeds were germinated on wet sterile paper disks in the dark, in an environmental chamber at 24Â°C, then transplanted to sterile potting soil upon root emergence and grown in controlled conditions at 20 ± 2°C, with a photoperiod of 16:8 h light/dark. After 3 weeks, tomato seedlings were transplanted to 14-cm diameter plastic pots containing sterilized soil and grown for 2 weeks under the same environmental conditions. Plants from the T22 coated seeds also received a supplementary watering with the T22 spore suspension (20 mL; 10^7 sporemL^{-1}) after the transplant and, after that, on a weekly basis. Leaf samples were collected from all tomato plants (T22 and CTRL) 2 weeks after the last T22 watering treatment.

Aphid Infestation and Bioassay

A clonal population of *M. euphorbiae* was reared on SM in an environmental chamber at 20 ± 2°C, 65 ± 5% RH and a 16:8 h light/dark photoperiod. For the transcriptomic analysis, the control and *T. harzianum*-treated plants (T22) subjected to aphid infestation after 4 weeks of growth under the same environmental conditions indicated above. Three biological replicates, both for CTRL and T22 plants, were caged and infested with synchronized 1-day-old nymphs of *M. euphorbiae*. Five aphids per plant were settled and allowed to feed for 48 h, then removed from the plant in order to collect aphid-free leaf samples for the subsequent RNA extraction (samples named as "Aph" or "T22Aph").

For the aphid longevity assay, 10 plants for each CTRL or T22 treatment were infested with 5 newly born first instar nymphs of *M. euphorbiae*. The presence of aphids and of shed exuviae, as an indicator of molting occurrence, was daily monitored. Survival curves were compared by LogRank analysis.

RNA-Seq

Fully expanded leaves (5 leaves) of 3 tomato plants for each treatment were used for total RNA extraction: leaf samples treated with T22 (T22), infested by aphids (Aph), treated with T22 and infested by aphids (T22Aph), and untreated (CTRL). Total RNA was extracted using the Plant RNeasy mini kit (Qiagen) according to manufacturer's protocol. Samples were analyzed with the 2,100 Bioanalyzer system (Agilent Technologies) for size, quantification, and quality control of RNA. Only samples with a 260/280 nm absorbance >1.8 and a 260/230 nm absorbance >2 were sequenced. Three biological replicates were used for each experimental condition and controls. Total RNA (8 μg) of each sample was used for the library preparation and sequencing by an external sequencing service. A paired-end sequencing (2 × 30 Million of reads) on Illumina HiSeq 2,500 platform was chosen. RNA-Seq raw sequences were cleaned using Trim Galore package [http://www.bioinformatics.babraham.ac.uk/projects/trim_galore/]. Low-quality bases were trimmed from the sequences and the adapter sequences were removed by Cutadapt (Martin, 2011); default parameters for the pair-end sequences were used. Finally, if one of the pairs was filtered out due to the cleaning procedure, the other pair was also discarded from the downstream analyses.

The cleaned sequences were then mapped on the tomato genome (version 2.50) using Bowtie version 2.1.0 (Langmead and Salzberg, 2012) and Tophat version 2.0.8 (Kim et al., 2013). Quantification of the reads abundance per each gene (exon level) available from iTAG gene annotation (version 2.5) was done using AIR (https://transcriptomics.sequentiabiotech.com/).

To identify the set of Differentially Expressed Genes (DEGs) between the diverse experimental conditions, two different statistical approaches were used: the Negative Binomial test implemented in DESeq package (Anders and Huber, 2010) and the Negative Binomial test and Generalized Linear Model (GLM), as implemented in EdgeR package (Robinson et al., 2010), were used considering false discovery rate (FDR) <= 0.05. The data from the two methods were compared and where the values intersected, these results were considered and selected to compile the datasets used for the analysis of the differentially expressed genes.

RNA-Seq validation was carried out by Real Time RT-PCR, measuring the transcript levels of selected DEGs. Gene expression analysis was carried out using 2 technical replicates for each of the 3 biological replicates per sample. Relative quantification of gene expression was carried out using the $2^{-\Delta\Delta Ct}$ method (Livak and Schmittgen, 2001). The housekeeping gene EF-1α was used as endogenous reference gene for the normalization of the expression level of the target genes (Marum et al., 2012; Müller et al., 2015). Ten couples of primers were used to analyze each treatment condition. Primers and their main features are reported in the **Supplementary Table 1**.

Functional Annotation

GO and GOslim annotations were downloaded from the Biomart section of Ensembl Plant version SL2.50 (2014-10-EnsemblPlants) (Kinsella et al., 2011). Moreover, GO was used for GO enrichment of all DEGs together and DEGs UP or DOWN regulated, independently. The analysis was carried out by the Goseq Bioconductor package (Young et al., 2010) (method "BH," FDR ≤ 0.05).

Mapping of some enzymatic activities into specific molecular pathways was acquired from the KEGG database.

Semi-polar Metabolome Analysis

LC-ESI(+)-MS analysis of the leaf primary and secondary semi-polar metabolome was performed as previously described (Alboresi et al., 2016; Fasano et al., 2016) with slight modifications: 5 mg of freeze-dried, homogenized leaf powder were extracted with 0.75 mL cold 75% (v/v) methanol, 0.1% (v/v) formic acid, spiked with 10 µg/ml formononetin. After shaking for 40'at 20 Hz using a Mixer Mill 300 (Qiagen), samples were centrifuged for 15' at 20,000 g at 4°C; 0.6 mL of supernatant were removed and transferred to HPLC tubes. For each genotype, 4 independent biological replicates, consisting of 4 plants each, were analyzed; for each biological replicate, at least one technical replicate was carried out. LC-MS analyses were carried out using an LTQ-Orbitrap Discovery mass spectrometry system (Thermo Fisher Scientific) operating in positive electrospray ionization (ESI), coupled to an Accela U-HPLC system (Thermo Fisher Scientific, Waltham, MA). Liquid chromatography was carried out using a Phenomenex C18 Luna column (150 × 2.0 mm, 3 µm) and the mobile phase was composed by water −0.1% formic acid (A) and acetonitrile −0.1% formic acid (B). The gradient was: 95%A:5%B (1 min), a linear gradient to 25%A:75%B over 40 min, 2 min isocratic, before going back to the initial LC conditions in 18 min. Five microliter of each sample were injected and a flow of 0.2 mL was used throughout the LC runs. Detection was carried out continuously from 230 to 800 nm with an online Accela Surveyor photodiode array detector (PDA, Thermo Fisher Scientific, Waltham, MA). All solvents used were LC-MS grade quality (CHROMASOLV® from Sigma-Aldrich). Metabolites were quantified in a relative way by normalization on the internal standard (formononetin) amounts. ESI-MS ionization was performed using the following parameters: capillary voltage and temperature were set at 20V and 280°C; sheath and aux gas flow rate at, respectively, 30 and 20. Spray voltage was set to 3.5 kV and tube lens at 80 V. Targeted metabolite identification was performed by comparing chromatographic and spectral properties with authentic standards and reference spectra, in house database, literature data, and on the basis of the m/z accurate masses, as reported in the Pubchem database (http://pubchem.ncbi.nlm.nih.gov/) for monoisotopic mass identification, or on the Metabolomics Fiehn Lab Mass Spectrometry Adduct Calculator (http://fiehnlab.ucdavis.edu/staff/kind/Metabolomics/MS-Adduct-Calculator/) in the case of adduction detection.

Untargeted metabolomics was performed using the SIEVE software (Thermofisher scientific). After chromatogram alignment and retrieve of the all the detected frames (e.g., ions), an ANOVA + *t*-test statistical analysis was carried out to identify differentially accumulated molecules. Finally, a series of public metabolomic databases (KEGG, HMD, Golm Metabolome Database, PlantCyc) were interrogated and a list of tentative IDs was obtained. Further validation steps included isotopic pattern ratio (IPR), mass fragmentation when available and literature search.

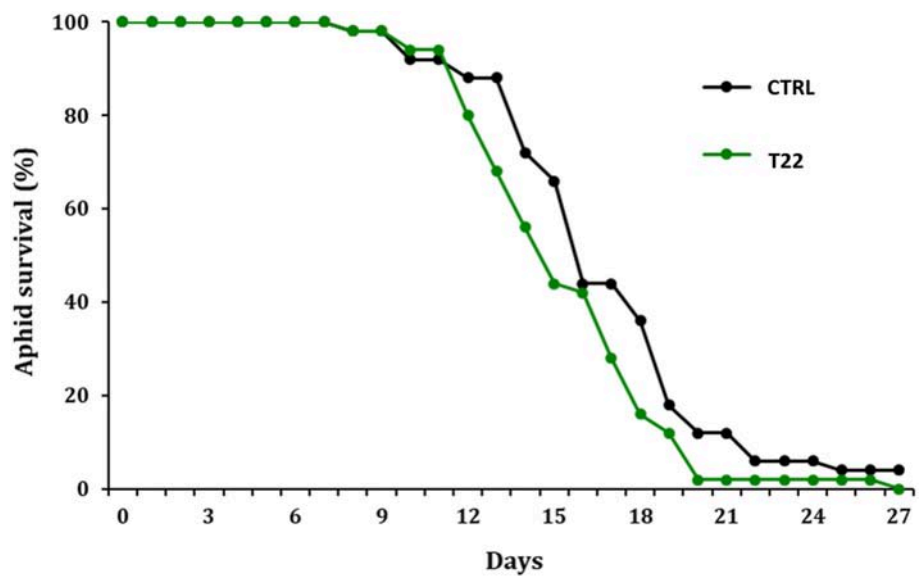

FIGURE 1 | Effect of *T. harzianum* T22 on aphid survival over time. Survival curves (percentage) of *M. euphorbiae* reared on the untreated water control and the *T. harzianum* T22 treated tomato plants are significantly different, $p < 0.05$ (LogRank test).

Principal component analysis (PCA) of untargeted semipolar metabolome was performed by using the SIEVE software (Thermofisher Scientific). Venn diagram representation of differentially accumulated metabolites (DAMs) was performed using the Venny 2.1 software [Oliveros, J. C. (2007–2015)]. Metabolite heat maps and hierarchical clustering were build and colored by using the GENE-E software (http://www.broadinstitute.org/cancer/software/GENE-E/) and as previously described (Diretto et al., 2010).

RESULTS

Trichoderma harzianum T22 Promotes Tomato Defense Against *M. euphorbiae*

The treatment of tomato plants with *T. harzianum* T22 negatively influenced the survival rate of *M. euphorbiae*. T22 plants showed an increased level of resistance to aphid infestation, as indicated by the significant difference registered between the T22 survival curve and that of CTRL (LogRank analysis, $\chi^2 = 4.72$, $p = 0.030$, $df = 1$) (**Figure 1**).

TABLE 1 | General overview of the transcriptomic rearrangement of Dwarf San Marzano tomato plants imposed by experimental treatments compared to untreated SM plants.

	T22	Aph	T22Aph
Total DEGs	978	1804	1527
Up-regulated	515	625	602
Down-regulated	463	1179	925

T22: treatment with T. harzianum T22, Aph: aphid infestation, T22 Aph: treatment with T. harzianum T22 followed by aphid infestation.

Plant Transcriptome Reprogramming Induced by *Trichoderma harzianum* T22 Root Colonization

In order to unravel the molecular mechanisms underlying the plant response to the combined action of *Trichoderma* infection and aphid infestation, transcriptomic and metabolomic analyses ofthe tomato cultivar "Dwarf San Marzano" were conducted by comparing *Trichoderma* treated and untreated plants, with and without aphid infestation.

Table 1 provides a general summary of differentially expressed genes for each treatment.

T22 plants showed a total of 978 differentially expressed genes (DEGs) of which 515 were up-regulated and 463 were down-regulated (**Supplementary Tables 2A,B**). The principal defense-related categories that may be linked to the induction in T22 treated plants of a precursor state of defense against insect attack are represented by "response to stress," "transport" and "response to stimulus" (**Figure 2**). The most abundant enriched Gene Ontology (GO) terms in the ontological category "Biological Process" were associated with metabolic processes, photosynthesis-related mechanisms, oxidation-reduction processes and response to stress (**Supplementary Figure 1**).

Several genes included in these categories were up-regulated. A short list of these genes is reported in **Table 2**. Among them, the induction of genes associated with photosynthesis, chlorophyll biosynthesis and sequestration and biosynthetic processes, may be linked with T22 beneficial effects on tomato

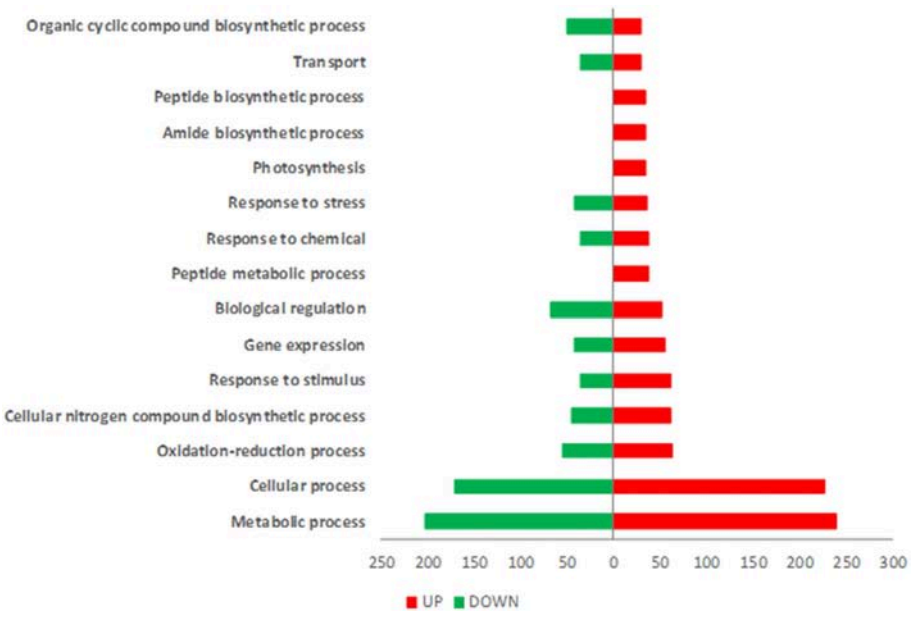

FIGURE 2 | GOs distribution of differentially expressed genes in SM plants treated with *T.harzianum*T22. Gene Ontology (GO) terms associated with up-regulated (red bars) and down-regulated (green bars) genes based on the "Biological Process" ontological domain (sequence cut-off: 5%).

TABLE 2 | Examples of tomato genes affected by Trichoderma T22 treatment.

Gene ID	logFC	Gene description
PHOTOSYNTHESIS		
Solyc03g114930.3	1,525559	Photosystem II reaction center PsbP family protein
Solyc09g064500.3	1,498658	Photosystem II reaction center Psb28 protei
Solyc06g060340.3	1,400894	Photosystem II subunit S
Solyc07g066150.1	1,153408	Photosystem I reaction center subunit V family protein
Solyc06g084045.1	1,119141	Photosystem II reaction center W
Solyc06g065490.3	1,117796	Photosystem II reaction center PsbP family protein
Solyc02g069450.3	1,097231	Photosystem I reaction center subunit III
Solyc08g006930.3	1,087737	Photosystem I reaction center subunit psaK
Solyc12g044280.2	1,064617	Photosystem I reaction center subunit VI
BIOSYNTHETIC PROCESSES		
Solyc01g056780.3	1,463119	50S ribosomal protein L34
Solyc11g066410.2	1,425305	50S ribosomal protein L9
Solyc02g068090.3	1,401681	30S ribosomal protein S21
Solyc06g082750.3	1,359268	50S ribosomal protein L17
Solyc11g068820.2	1,283545	50S ribosomal protein L27
Solyc04g079790.3	1,180683	30S ribosomal protein S9
Solyc04g074900.3	1,164445	40S ribosomal protein S21
Solyc07g062870.3	1,135344	30S ribosomal protein S20
Solyc09g097910.3	1,111600	30S ribosomal protein S1
CHLOROPHYLL BIOSYNTHESIS AND SEQUESTRATION		
Solyc08g062290.3	1,676942	Light-independent protochlorophyllide reductase subunit B
Solyc10g007320.3	1,376821	Uroporphyrinogen decarboxylase
Solyc10g077040.2	1,102132	Magnesium-protoporphyrin monomethyl ester
PHENYLPROPANOID OR FLAVONOID SYNTHESIS		
Solyc06g074710.1	−2,23399	Hydroxycinnamoyl-CoA shikimate/quinate hydroxycinnamoyl transferase
Solyc08g061480.3	−1,07068	Chalcone–flavonone isomerase
Solyc08g005120.3	−1,63331	Cinnamoyl-CoA reductase-like protein

Values of Log2 Fold Change and gene description are indicated.

plant physiology The up-regulation of plant genes involved in early signals of defense responses against environmental cues as, for example, Serine/threonine-protein kinase, Leucine-rich repeat protein kinase, LRKs, Glutathione S-transferase, and others (listed in **Supplementary Table 2A**) was also observed. Similarly, the up-regulation of genes coding for transcription factors (TF), such as Ethylene responsive transcription factors (ERF), WRKY, MYB, and bZIP TF (**Supplementary Table 2A**), was registered. These genes are likely involved in plant defense priming (Conrath et al., 2015).

As expected, the up-regulation of markers of SA (i.e., chitinase and1,3-B glucanase) and JA pathways (i e., metallocarboxypeptidase inhibitor and, Type I serine protease inhibitor; **Supplementary Table 2A**) were also observed. Overall, these data show that *Trichoderma* colonization of tomato plants positively affects several metabolic pathways, consistently with previous observations in tomato and other plant species (Alexandru et al., 2013; Mohapatra and Mittra, 2016; Ban et al., 2018). Since phenylpropanoids contribute to plant defenses (both direct and indirect) to insect herbivores, genes encoding for key-enzymes associated with phenylpropanoids biosynthesis were searched by using DEGs in a query to a KEGG database; in addition, a manual curation to enrich the aforementioned list was performed. Transcripts coding for 10 enzymes were retrieved among the DEGs that were up-regulated and the correspondence found between the enzymes and the gene identifiers is listed in **Table 3**. As shown in **Figure 3**, the enzymes act in different stages of phenylpropanoid biosynthesis, catalyzing key-steps as phenylalanine conversion in cinnamic acid (*Phenylalanine ammonia-lyase (PAL)* and *Caffeoyl-CoA O-methyltransferase*), or catalyzing final branches for lignin production (i.e., *Peroxiredoxin*) and anthocyanin synthesis and modification (*Anthocyanin 5-aromatic acyl transferase* and *Anthocyanidin reductase*). Interestingly, a transcript coding for *PAL* is greatly up-regulated in T22 samples. In addition, a series of genes coding for enzymes involved in early phenylpropanoid or flavonoid synthesis resulted down-regulated (**Table 2**). Overall, these data show that T22 colonization strongly affects and remodels phenylpropanoid pathway.

Plant Transcriptome Reprogramming Induced by Aphids

Studies on tomato-*M. euphorbiae* interaction and on the relative transcriptomic changes have been already reported, although using other tomato cultivars, different time points and diverse transcriptomic approaches (Avila et al., 2012; Coppola et al., 2013). Here we carried out a transcriptomic study of the SM cultivar challenged with *M. euphorbiae* for 48 h, through RNA-Seq approach.

Tomato plants infested by *M. euphorbiae* showed 625 up-regulated and 1179 down-regulated transcripts (**Supplementary Table 3**). Major GO categories associated with plant defense were "response to stress," "response to stimulus" and "oxidation-reduction process" (**Figure 4**). The distribution and the enrichment analysis of GO terms associated with DEGs induced by aphid infestation underlined the predominance of categories related to the regulation of gene expression as "RNA methylation," "ncRNA processing," "Ribosome assembly," "rRNA metabolic process," "translation," "mRNA cleavage," "defense response to bacterium" (**Supplementary Figure 2**). The increase of several transcripts coding for kinase/phosphatase/receptor-like kinase as well as of transcripts coding for proteins involved in oxidative burst and scavenging was observed (**Supplementary Table 3A**). Genes coding for several classes of pathogenesis-related proteins (PR) (PR5, PR10, Chitinase, Subtilisin), genes associated with salicylic acid and genes involved in ethylene signaling were also up-regulated upon aphid attack (**Supplementary Table 3A**). A large number of DEGs were down-regulated (**Supplementary Table 3B** and **Table 4**), including key genes of plant immunity, such as MAP Kinases and WRKY. Interestingly, a strong down-regulation was observed for transcripts associated with JA pathway, as those coding for lipoxygenases and protease inhibitors. Other down-regulated

TABLE 3 | Differentially expressed genes involved in phenylpropanoid biosynthesis.

Enzyme ID	Gene ID	logFC	Gene description
4.3.1.24	Solyc03g036470.2	4,802883	Phenylalanine ammonia-lyase
4.3.1.25			
2.1.1.104	Solyc02g093250.3	1,099098	Caffeoyl-CoA O-methyltransferase
1.11.1.7	Solyc06g082420.3	1,179331	Peroxidase
		1,476077	Peroxiredoxin
3.2.1.21	Solyc01g060020	1,892951	β-1,3-glucanase
	Solyc02g086700	1,878683	
Manual curation	Solyc10g008680.2	2,199016	Anthocyanin 5-aromatic acyltransferase (5AT)
Manual curation	Solyc10g009507.1	1,533819	Anthocyanidin reductase (ANR)
Manual curation	Solyc01g067290.2	1,270974	Isoflavone reductase-related family protein (IFR)
Manual curation	Solyc08g074620.3	1,113982	polyphenoloxidase precursor (PPO)
Manual curation_2.3.1.99	Solyc06g074710.1	−2,234000	hydroxycinnamoyl-CoAshikimate/quinate hydroxycinnamoyl transferase
Manual curation_2.1.1.104	Solyc03g032220.3	−1,286107	Caffeoyl-CoA O-methyltransferase
Manual curation	Solyc08g074682.1	−1,236095	polyphenoloxidase precursor (PPO)
Manual curation_ 1.2.1.44	Solyc08g005120.3	−1,633312	Cinnamoyl-CoA reductase-like protein
Manual curation	Solyc08g061480.3	−1,070684	Chalcone—flavonone isomerase (CHI)
Manual curation	Solyc08g074683.1	−1,310960	polyphenoloxidase precursor (PPO)

Enzyme and gene identifiers, fold change and gene description are listed. Colors associated to enzymes refers to ***Figure 3****.*

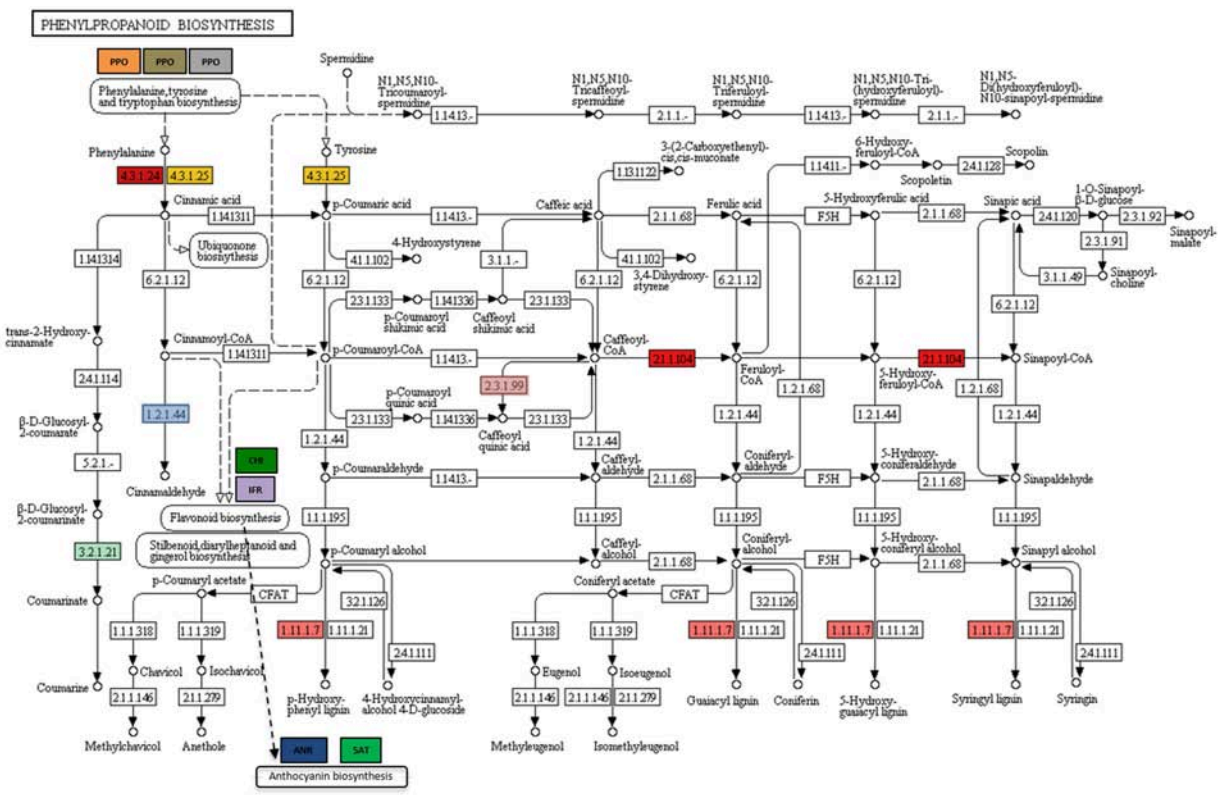

FIGURE 3 | Schematic diagram of the phenylpropanoid biosynthesis pathway as determined by DEGs in plants treated with T22 and queried to a KEGG database. The enzymes evidenced in color are encoded by genes found in the up-regulated DEGs of the tomato. A correspondence between enzymes and DEGs is shown in **Table 2**.

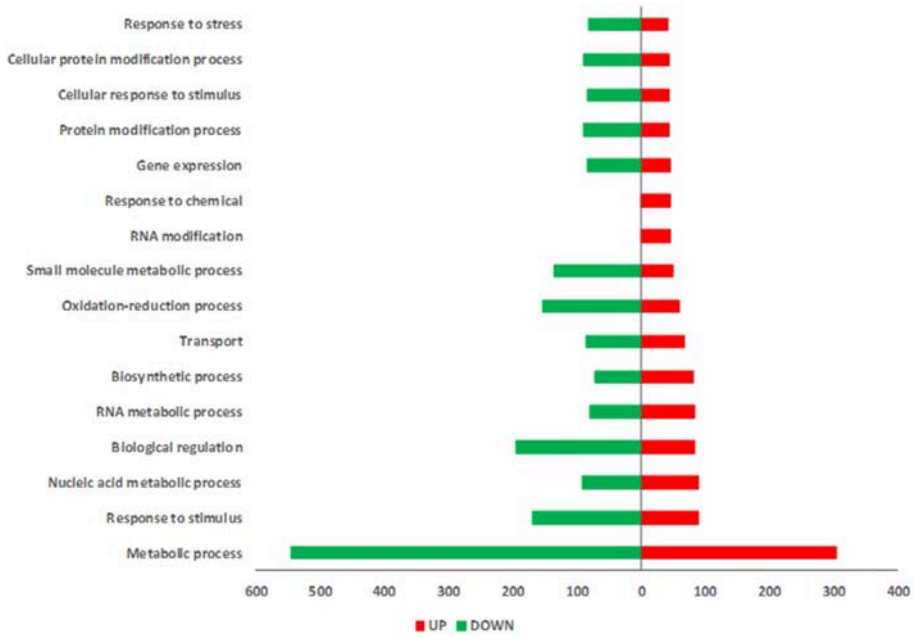

FIGURE 4 | GOs distribution of differentially expressed genes in SM plants infested by*M. euphorbiae*. Gene Ontology (GO) terms associated with up-regulated (red bars) and down-regulated (green bars) genes based on the "Biological Process" ontological domain (sequence cut-off: 5%).

transcripts code for glycosyltransferases and genes associated with terpene production, such as sesquiterpene synthase 1 and geranylgeranyl reductase.

Overall, at primary metabolism level, aphid infestation strongly repressed transcripts of enzymes associated with sugar (i.e., *Fructose-bisphosphatealdolase* and *Sucrose synthase*) and amino acid (i.e., *Threonine deaminase* and *Tryptophan synthase*) pathways, which are involved in the plant defense responses against biotic and abiotic stresses (Conklin and Last, 1995; Brader et al., 2001; Wilkinson et al., 2001; Chen et al., 2005; Tauzin and Giardina, 2014; Lv et al., 2017). Several other down-regulated genes were involved in photosynthetic activities, chlorophyll biosynthesis, polyamine and phenylpropanoids-related metabolism (**Table 4**).

Plant Transcriptome Reprogramming Induced by *Trichoderma harzianum* T22 Root Colonization and Aphid Infestation

In order to assess the impact of *T. harzianum* T22 on tomato defense response against aphids, the transcriptome of tomato plants treated with *Trichoderma* and subsequently infested by aphids (T22Aph) was analyzed. T22Aph transcriptome reprogramming involved 1527 transcripts: 602 up- and 925 down-regulated (**Supplementary Table 4**). *Trichoderma* colonization strongly affected GO categories involved in plant metabolism and stress response during aphid infestation (**Figure 5**). The enrichment analysis was performed in order to underline significant over-represented GO categories relative to Biological Process ontological domain. Interestingly, some enriched GO term categories were associated with direct and indirect defenses, as they include genes involved in isoprenoid biosynthesis, induced systemic resistance and JA-mediated signaling pathway (**Supplementary Figure 3**; **Supplementary Tables 4A,B**). An example of defense-related DEGs is shown in **Table 5**. Among early signals, calmodulin-binding proteins and Ca^{2+} transporters were also over-represented as several classes of kinases and receptor-kinases (serine/threonine kinases, receptor-like kinases, LRR-RLKs, MAPKKK). Furthermore, transcripts related to ROS production and scavenging such as GST, peroxidases, oxidoreductases, catalase, superoxide dismutase, and detoxification protein were up-regulated. Other up-regulated genes coded for Lipoxygenases, involved in early stages of JA biosynthesis, Polyphenol oxidase (PPO), Leucine aminopeptidase (LapA), and proteinase inhibitor (MCPI) involved in later stages of defense besides several classes of defense genes-related TF (GRAS, WRKY, MYB, bZIP). Moreover, a transcript encoding for a cysteine protease inhibitor (Multicystatine), associated with aphid growth inhibition (Rahbé et al., 2003; Emani, 2018), was up-regulated while the number of down-regulated transcripts encoding proteinase inhibitors was reduced in comparison with what observed following aphid infestation.

A strong impact on hormone-controlled defense pathways was observed: ethylene biosynthesis and signaling as well as salicylic acid biosynthesis and signaling were up-regulated in T22Aph plants (**Supplementary Table 4**; **Table 5**). Notably, compared to T22, T22Aph were characterized by a strong down-regulation of key-steps in the phenylpropanoid pathway (**Table 5**).

TABLE 4 | Example of defense-related down-regulated genes by aphid infestation.

Gene ID	logFC	Gene description
ETHYLENEBIOSYNTHESIS AND SIGNALING		
Solyc08g078180.1	−2,71739	Ethylene Response Factor A.1
Solyc04g071770.3	−1,81979	Ethylene-responsive transcription factor
JA SIGNALING PATHWAY		
Solyc03g020040.3	−2,64679	Pin-II type proteinase inhibitor 69
Solyc01g099160.3	−2,52785	Lipoxygenase
Solyc08g014000.3	−2,09537	Lipoxygenase A
Solyc11g022590.1	−1,94405	Trypsin inhibitor-like protein precursor
Solyc00g187050.3	−1,89562	Leucine aminopeptidase 2
Solyc08g074682.1	−1,87224	Polyphenoloxidase precursor
Solyc07g007250.3	−1,8422	Metallocarboxypeptidase inhibitor
Solyc09g084450.3	−1,79009	Proteinasi inhibitor I
Solyc12g010030.2	−1,77364	Leucine aminopeptidase
Solyc01g006540.3	−1,42694	Lipoxygenase C
Solyc09g008670.3	−1,38363	Threonine deaminase
Solyc04g077650.3	−1,27008	Serine carboxypeptidase
Solyc03g118540.3	−1,25772	Jasmonate ZIM-domain protein 7b
ISOPRENOID AND TERPENOID PATHWAY		
Solyc06g059930.3	−2,17858	Sesquiterpene synthase 1
Solyc10g005410.3	−2,1206	Terpene synthase
Solyc08g005710.3	−1,57829	Terpene synthase 41
PHENYLPROPANOID PATHWAY		
Solyc06g074710.1	−3,68386	Hydroxycinnamoyl-CoAshikimate/quinate hydroxycinnamoyltransferase
Solyc06g084050.3	−2,39253	Isochorismatesynthase 2
POLYAMINE BIOSYNTHESIS		
Solyc10g009380.3	−1,03958	Arginine N-methyltransferase
Solyc03g098300.1	−2,12424	Ornithine decarboxylase 2
Solyc01g010050.3	−1,77437	S-adenosylmethionine decarboxylase proenzyme
Solyc07g039310.1	−1,42553	Polyamineoxidase 5
SUGAR METABOLISM		
Solyc07g065900.3	−1,71894	Fructose-bisphosphate aldolase
Solyc09g092130.3	−1,0955	Sucrose-phosphate synthase
Solyc02g071590.2	−1,26851	Trehalose-6-phosphate synthase
Solyc03g112500.3	−7,11877	Raffinose synthase
AMINO ACID PATHWAY		
Solyc07g054280.1	−3,48542	Tyrosine decarboxylase
Solyc09g008670.3	−1,38363	Threonine deaminase
Solyc10g005320.3	−1,36504	Tryptophan synthase
Solyc06g019170.3	−2,25121	Delta-1-pyrroline-5-carboxylate synthetase
CHLOROPHYLL METABOLISM AND PHOTOSYNTHESIS-RELATED GENES		
Solyc01g060085.1	−3,38289	Ribulose bisphosphate carboxylase large chain
Solyc07g062530.3	−2,86058	Phosphoenolpyruvate carboxylase 2
Solyc12g013710.2	−2,81926	Light dependent NADH:protochlorophyllide oxidoreductase 1
Solyc03g005790.2	−2,65938	Chlorophyll a-b binding protein
Solyc04g006970.3	−2,1064	Phosphoenolpyruvate carboxylase
Solyc06g053620.3	−1,91070	Phosphoenolpyruvate carboxylasekinase 2
Solyc09g011080.3	−1,53137	Ribulose bisphosphate carboxylase/oxygenase activase
Solyc02g086650.3	−1,30017	Phosphoenolpyruvate/phosphate translocator
Solyc10g077040.2	−1,07567	Magnesium-protoporphyrin monomethyl ester cyclase

Values of Log2 Fold Change and gene description are indicated.

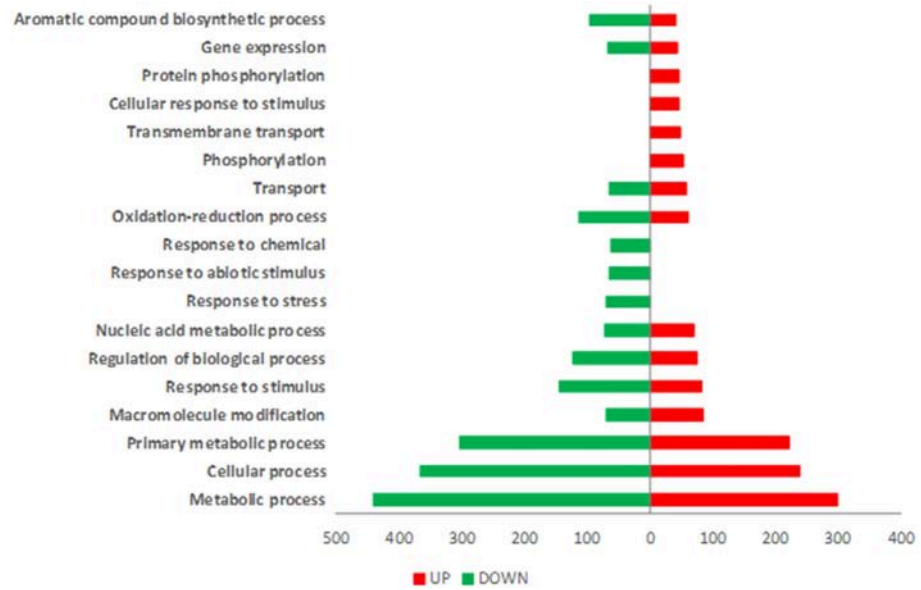

FIGURE 5 | GOs distribution of DEGs in T22-Aph plants, first treated with *T. harzianum* T22 and subsequently infested with aphids (SMT22 Aph). Gene Ontology (GO) terms associated with up-regulated (red bars) and down-regulated (green bars) genes based on the "Biological Process" ontological domain (sequence cut-off: 5%).

For a selected number of genes, transcript quantification was confirmed by Real Time RT-PCR (**Supplementary Figure 4**).

Key Genes Regulated by the Interaction T22-Tomato-Aphid

In order to assess the contribution of *T. harzianum* T22 in the priming of defenses against aphids, genes specifically regulated in the tripartite interaction were analyzed. **Supplementary Tables 5A,B** list unique genes modulated in their expression during the T22-Tomato-Aphid interaction (T22Aph samples, **Figure 6A**). These genes are specifically induced by aphid challenge in presence of *Trichoderma* priming. Among the up-regulated ones, genes involved in ethylene biosynthesis and signaling emerge (**Table 6**), as well as those associated with amino acid metabolism (*asparagine synthase 1*, *glutamate receptor 1.2*, *proline dehydrogenase*). Unique down-regulated genes (**Supplementary Table 5B**; **Table 6**) included several members of WRKY family of transcription factors, known for their promotion of JA signaling in the negative interplay with SA pathway (Li et al., 2004; Takatsuji, 2014).

Figure 6A shows that aphid repression of tomato genes (1179 down-regulated genes in Aph) was reduced by *T. harzianum* T22 colonization in T22Aph (925 down-regulated genes in T22Aph).

The intersection between down-regulated genes of Aph and T22Aph samples is shown through a Venn diagram representation (**Figure 6B**). Common genes repressed in both conditions are listed in **Supplementary Table 5C**. A large group of genes of phenylpropanoid pathways (i.e., *phenylalanine ammonia-lyase*, *caffeoyl-CoA O-methyltransferase,* and others) resulted down-regulated in both conditions. Interestingly, a large number of glycosyltransferases resulted strongly repressed in both conditions, indicating that they could represent a peculiar aspect of tomato-aphid interaction, independently from *T. harzianum* T22 influence (**Supplementary Table 5C**). Genes specifically repressed in the bipartite interaction (Aph) are 683 (**Figure 6B**; **Supplementary Table 5D**) and include JA-related genes as those coding for Phospholipase, Lipoxygenases A, C and D, Leucine aminopeptidase A1 and several classes of proteinase inhibitors (**Table 5**). In order to assess if *T. harzianum* T22 is able to overturn the expression of aphid-repressed genes in tomato, the 683 specifically down-regulated transcripts in Aph samples were compared with genes induced by T22 (T22; **Supplementary Table 2A**), underlining an overturning of the expression of three genes listed in **Table 7**. The transcription factor bHLH may be associated with JA signaling (Zhou and Memelink, 2016) while the steroid dehydrogenase, involved in steroid and squalene biosynthesis, is a precursor of triterpenes. Finally, the GDSL esterase/lipase belong to a very large subfamily of lipolytic enzymes.

Metabolomic Analysis

In order to analyse the downstream effects of the transcriptomic reprogramming induced by *M. euphorbiae* attack, in the absence or presence of the antagonist fungus *T. harzianum* T22, we performed a global metabolic profiling of the leaf semi-polar fraction by LC-ESI(+)-MS (for more details, see "Materials and methods). First of all, to gain a general overview of the metabolic changes occurring under the different experimental conditions, we carried an untargeted metabolomics analysis, using the SIEVE software (Thermo Fisher Scientific). Through alignment of all mass chromatograms with the subsequent retrieval of all detected ions, we built a 3D Principal Component Analysis (PCA) diagram (**Supplementary Figure 5**), which showed a clear separation of the leaves treated with

TABLE 5 | Group of defense-related DEGs identified in San Marzano plants treated with Trichoderma T22 and infested by aphid.

Gene ID	logFC	Gene description
ISOPRENOID PATHWAY		
Solyc07g052135.1	5,569388	Sesquiterpenesynthase
Solyc11g011240.1	1,544086	geranylgeranylpyrophosphatesynthase 1
ETHYLENEBIOSYNTHESIS AND SIGNALING		
Solyc05g051180.2	7,829771	Ethylene-responsive transcription factor
Solyc11g045520.2	2,490749	1-aminocyclopropane-1-carboxylate oxidase-like protein
Solyc05g051200.1	2,049015	Ethylene-responsive factor 1
Solyc08g008305.1	1,688514	Ethylene-responsive transcription factor ERF061
SALICYLIC ACID BIOSYNTHESIS AND SIGNALING		
Solyc08g080670.1	2,301690	Pathogenesis-related 5-like protein
Solyc08g080660.1	2,286811	Osmotin-like protein
Solyc07g009500.2	2,224245	Chitinase
Solyc09g090990.2	2,162828	PR10 protein
Solyc01g087840.3	2,161848	Subtilisin-like protease
Solyc08g079900.3	1,597817	subtilisin-like protease
Solyc01g005230.3	1,590776	S-adenosyl-L-methionine-dependent methyltransferase superfamily protein
JA SIGNALING PATHWAY		
Solyc08g029000.3	3,645744	Lipoxygenase
Solyc00g071180.3	2,670684	Multicystatin
Solyc06g061230.3	1,805861	Metallocarboxypeptidaseinhibitor
Solyc01g091170.3	1,389207	arginase 2 ARG2
Solyc12g010030.2	1,295502	Leucine aminopeptidase
Solyc08g074620.3	1,144778	polyphenoloxidase precursor
Solyc06g048820.1	1,020496	Wound-inducedprotein 1
PHENYLPROPANOID PATHWAY		
Solyc03g036470.2	−6,60171	Phenylalanine ammonia-lyase
Solyc09g091510.3	−2,13284	chalconesynthase 1
Solyc05g053550.3	−1,92049	chalconesynthase 2
Solyc11g013110.2	−1,49002	Flavonolsynthase
Solyc02g085020.3	−1,21211	dihydroflavonol 4-reductase

Values of Log2 Fold Change and gene description are indicated.

T. harzianum and, to a lower extent, infested by aphids in the presence of the fungus. To investigate the changes of known tomato leaf metabolites, we then performed a targeted metabolomic analysis in which we quantified, in a relative way, 135 metabolites involved in primary (amino acids, amines, sugars, organic acids, lipids, vitamins, etc) and secondary (alkaloids, amides, phenylpropanoids, isoprenoids) pathways. The complete metabolite dataset is reported in **Supplementary Table 7** and **Supplementary Figure 6**, while the lists of the differentially accumulated metabolites (DAM) in each comparison (T22/CTRL, Aph/CTRL, and T22Aph/T22) are reported in **Supplementary Table 6**.

Heatmap visualization was used as first attempt to understand the real impact of the aphid and fungus treatments on the leaf metabolome (**Supplementary Figure 6**). Globally, most of the alterations in leaves grown in the presence of *M. euphorbiae* or *T. harzianum* were of negative sign (e.g., lower levels in the treated over the control) and particularly affected secondary metabolism (alkaloids and phenylpropanoids). We used Venn diagram visualization (**Figure 7**; **Supplementary Table 8**) to highlight the number of common and specific DAMs in relation to the three interactions under study: interestingly, 29 metabolites resulted present in all the comparisons and 17 out of them displayed variations of the same sign. A group of metabolites was specifically highlighted in T22 plants, and included ADP, AMP, citric acid, dihydro-caffeic acid,2-hydroxyglutarate, phosphoenolpyruvate (PEP), coumarin, syringaldehyde and tetrahydrofolate being down-accumulated in T22 vs. CTRL and T22Aph vs. T22, and up-represented in Aph vs. CTRL; and Uroporphyrinogen III and Galactonate/Gluconate, showing an opposite trend. Interestingly, over-represented metabolites retrieved in T22 samples are precursors of salicylic acid: Salicylate β-D-glucose ester and Salicyloyl-L-aspartic acid, have a concentration three times higher than the control. Furthermore, Phenylalanine, Coumaric and chorismic acids, member of phenilpropanoids and known for their possible flow into primary steps of salicylic acid biosynthesis, in T22 samples are about 5 times higher than in control (**Supplementary Table 6**). Fourteen metabolites were found to be specifically associated with the presence of *T. harzianum* (T22 vs. CTRL and T22Aph vs. Aph comparisons), mostly with alterations of negative sign (indicated in **Supplementary Table 6** with a cross). Finally, 7 DAMs each were exclusive for T22Aph vs. T22; among them, δ-tomatine (an alkaloid), N-isovalerylglycine and threonine/homoserine (amino acids) and protoporphyrinogen IX, an isoprenoid associated with tissue necrosis, were detected at lower levels over the control. At the opposite, the amino acid glutamic acid, the sugar phosphate glycerate-2-P/glycerate-3-Pand the lipid CDP-choline displayed a higher accumulation in T22Aph leaves over the CTRL. T22 and T22Aph were found to share 32 metabolites: interestingly, most of them varied differently between the two comparisons, with the exception of shikimic acid and dihydrokaempferol-7-O-glucoside, and raffinose/melezitose, respectively, down- and over-accumulated in both T22 and T22Aph. In the group of compounds showing higher accumulation in T22Aph, two relevant alkaloids were found (α-/β-tomatine), together with other compounds (indicated in **Supplementary Table 6** with a hash mark). On the contrary, a group comprising the amide feruloylputrescine and other compounds (indicated in **Supplementary Table 6** with an asterisk), resulted more abundant in T22 vs. CTRL than T22Aph vs. T22. Notably, no common compounds were found between T22Aph and Aph.

Targeted semi-polar metabolomes were used to generate a Hierarchical Clustering (HCL), applied both on columns and rows, in order to study the global relationships within leaves treated with *M. euphorbiae* and/or *T. harzianum*T22 (**Figure 8**). Interestingly, two distinct groups were produced, with one-to-one interactions (aphid or fungus, Aph vs. CTRL and T22 vs. CTRL) on the left side, and the three-way interactions (T22Aph vs. T22) clustering alone. As expected, metabolites displaying similar trends of related accumulation over the controls grouped together like, for instance, a set of alkaloids in the initial part and one of phenylpropanoids in the central parts of the HCL.

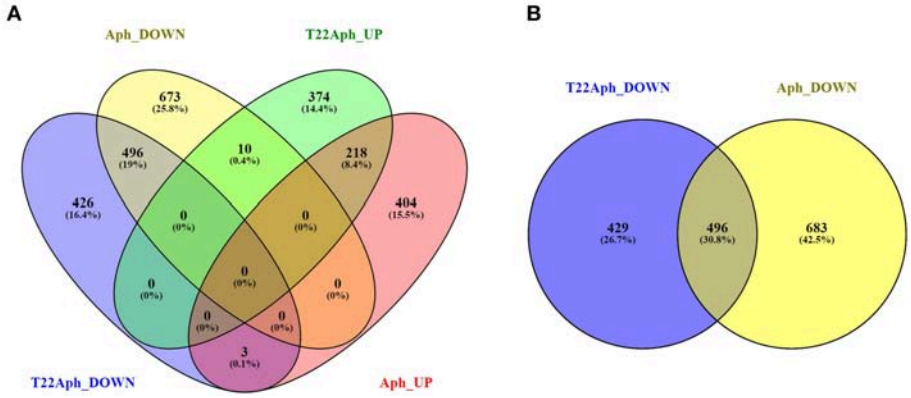

FIGURE 6 | Venn diagram visualization of DEGs. **(A)** DEGs of tomato plants infested by the aphid *M. euphorbiae* (Aph) are crossed to DEGs of tomato plants inoculated with *T. harzianum* T22 and subsequently infested by aphids (T22Aph). **(B)** Focus on the intersection of down-regulated genes of Aph and T22Aph plants.

TABLE 6 | Example of DEGs modulated by aphid challenge in presence of Trichoderma priming.

Gene ID	logFC	Gene description
ETHYLENE BIOSYNTHESIS AND SIGNALING		
Solyc12g056590.2	3,27892	Ethylene Response Factor D.2
Solyc06g065820.3	2,651662	Ethylene Response Factor H.1
Solyc11g045520.2	2,490749	1-aminocyclopropane-1-carboxylate oxidase-like protein
Solyc03g111620.1	2,051024	S-adenosyl-L-methionine-dependent methyltransferase superfamily protein
Solyc05g052030.1	1,803781	Ethylene responsive factor 4
Solyc08g008305.1	1,688514	Ethylene-responsive transcription factor ERF061
Solyc08g014120.3	1,60402	Ethylene responsive protein 33
WRKYS FAMILY OF TF		
Solyc09g010960.3	−3,58083	WRKY transcription factor 49
Solyc08g067360.3	−2,65237	WRKY transcription factor 45
Solyc03g007380.2	−2,44306	WRKY transcription factor 52
Solyc04g051690.3	−2,19968	WRKY transcription factor 51
Solyc08g067340.3	−1,89527	WRKY transcription factor 46
Solyc08g062490.3	−1,22158	WRKY transcription factor 50
Solyc08g082110.3	−1,16835	WRKY transcription factor 54
Solyc09g015770.3	−1,07513	WRKY transcription factor 81
Solyc09g014990.3	−1,07294	WRKY transcription factor 33

Values of Log2 Fold Change and gene description are indicated.

TABLE 7 | Overturned expression of genes in dipartite interactions (tomato-aphid and tomato-T22).

Gene ID	T22 (Log2FC)	Aph (Log2FC)	Gene description
Solyc03g118310.3	1,02474507	−1,95569	bHLH transcription factor 083
Solyc11g006300.2	1,42671042	−1,12261	3-oxo-5-alpha-steroid 4-dehydrogenase family protein
Solyc01g099030.3	1,06934649	−1,11098	GDSL esterase/lipase

Gene ID, Log2 Fold change in T22 and Aph samples, respectively, and gene description are listed.

Finally, we exploited the untargeted metabolomes to retrieve new ions not included in our targeted database and specific for the four conditions under investigation (**Supplementary Table 9**). Twenty-two ions were found, which were subjected to metabolomics database interrogation, and isotopic pattern ratio, literature search and standard (where available) validations. For nine of them, an identification already reported in tomato was found: this group of metabolites included three acids (5-amino-levulinic acid, hydroxypipecolic acid and glutaric acid) and one phenylpropanoid (caffeic acid hexose II), over-accumulated in T22Aph vs. T22. In addition, one ester-like (2-Amino-2-methylbutanoate), two lipids (CDP-DG(16:0/20:4(5Z,8Z,11Z,14Z)), LysoPE [22:6(4Z,7Z,10Z,13Z,16Z,19Z)/0:0)], and one alkaloid (C33H57NO8 (Jurubine-like), showing an opposite trend. Thirteen additional molecular ions were detected, which could not be identified as any of the known tomato metabolites, and were tentatively assigned according other metabolite identifications: four of them (2 acids: 3-hydroxybutyric acid-like, citric acid-like; an amine: N-methyl ethanolamine phosphate-like; a flavonoid: 6-hydroxy-4′-methoxyflavone-like; and an alkaloid: O-acetylnitraraine-like) and 3 ions (a flavonoid: 3′,4′-dihydroxychalcone-like; an alkaloid: beta-obscurine-like; and an unknown) were found at, respectively, higher and lower levels in T22Aph vs. T22. Interestingly, most of the cited molecules displayed an inverse statistically significant accumulation in the other two comparisons (Aph vs. CTRL and T22Aph vs. T22).

DISCUSSION

Plants colonized by *Trichoderma* have often shown multiple beneficial effects (Hermosa et al., 2012; Vitti et al., 2015). We

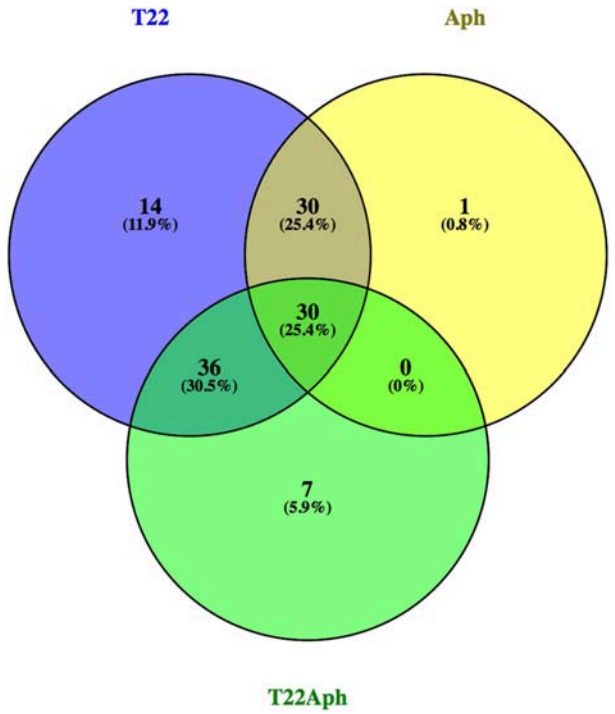

FIGURE 7 | Venn diagram visualization of differentially accumulated metabolites in three comparisons between tomato plants: infested with aphids vs. water control (Aph vs. CTRL); treated with T22 vs. water control (T22 vs. CTRL); treated with T22 plus infested with aphid vs. treated with T22 (T22 Aph vs. T22).

previously demonstrated an enhancement of the indirect defense barriers in tomato plants treated with *T. harzianum* T22, which were more attractive toward aphid parasitoids (Coppola et al., 2017a). This plant phenotype was associated with an increased level of methyl-salicylate and β-caryophyllene, known to be among the most active compounds in promoting *A. ervi* flight (Sasso et al., 2009; Coppola et al., 2017a).

Here we studied the impact of *T. harzianum* T22 colonization of tomato plant on direct defense responses to the aphid *M. euphorbiae*, and used transcriptomic and metabolomic approaches to shed light on the molecular mechanisms underlying the observed phenotypic changes.

Aphid Infestation Suppresses Plant Defense Responses

Aphid feeding on the tomato cv "Dwarf San Marzano" induced dramatic changes in thetranscriptome and metabolome of the plant, despite the very limited mechanical damage caused by the insect. Transcriptomic reprogramming was characterized by the deregulation of a large number of transcripts, the majority of which are down-regulated. The total number of DEGs was much higher than previously observed (Avila et al., 2012; Coppola et al., 2013), possibly due to the higher sensitivity of the digital method (RNA-Seq with respect to the analog one (microarray and/or the different tomato cultivars used in the two studies. However, the related GO categories distribution was in general agreement

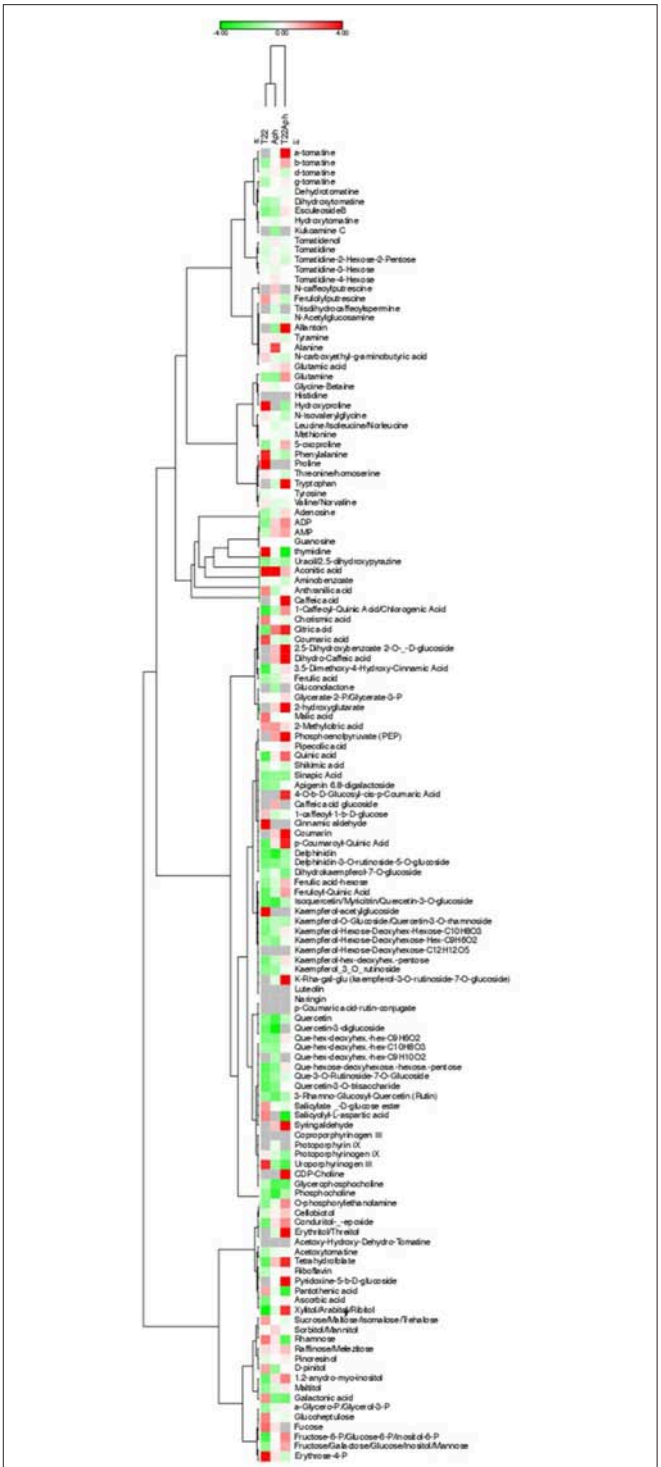

FIGURE 8 | Hierarchical Clustering (HCL) of semi-polar metabolome of tomato leaves grown in the absence and in the presence of the aphid *M. euphorbiae* and the fungus *T. harzianum*, alone or in combination. Colored squares represent the values of log2-transformed fold changes of a metabolite with respect to the corresponding control (water control CTRL for Aph and T22 samples; T22 for T22Aph), according to the color scale shown (green: down-accumulated; red: up-accumulated). Gray squares indicate no detectable accumulation of the corresponding metabolite. Hierarchical clustering was calculated both on columns and rows, applying the One Minus Pearson correlation with the average linkage algorithm.

with previous reports Avila et al., 2012; Coppola et al., 2013. All levels of defense responses were influenced in Aph samples: oxidative stress, signal transduction, TFs and late defenses. The down-regulation of key-genes of plant immunity such as MAP Kinases, WRKY and genes associated with direct (i.e., protease inhibitors, PIs) and indirect (i.e., sesquiterpene synthase 1) responses, is consistent with the aphid capacity to circumvent host defenses by secreting evolutionarily conserved effectors able to suppress plant immune responses (Will et al., 2007; Elzinga et al., 2014). Aphid ability to interfere with plant defense mechanisms is clearly evidenced by the down regulation of genes associated with sugar metabolism and amino acid biosynthesis. Fructose-1, 6-bisphosphate aldolase is a key-enzyme involved in glycolysis, gluconeogenesis, and the Calvin cycle. It plays significant roles in biotic and abiotic stress responses, as well as in regulating growth and development processes (Lv et al., 2017). Sucrose synthase is a glycosyltransferase enzyme that plays a key-role in sugar metabolism. Sucrose is engaged in plant defense by activating plant immune responses against pathogens (Tauzin and Giardina, 2014). Threonine deaminase is part of the phytochemical arsenal that plants use to deter herbivores. Together with PIs and other defense-related compounds, is tightly regulated by the JA signaling pathway (Chen et al., 2005). The enzyme acts in the insect gut to degrade the essential amino acids arginine and threonine, respectively. In aphids it was observed that a shortfall in threonine contribute to the poor performance of the *Aphis fabae* on *Lamium purpureum* (Wilkinson et al., 2001). Tryptophan biosynthesis and the enzymes involved are induced by a wealth of stress agents, such as for instance, ozone (Conklin and Last, 1995) and biotic stress (Brader et al., 2001). In addition, a strong down-regulation of transcripts encoding Proteinase inhibitors (PIs) and several other glycosyltransferases further demonstrated the aphid ability to repress plant defense responses. PIs are proteins involved in defense responses and are often induced upon attack by insect herbivores, as they are able to inhibit insect growth and survival by disrupting their digestive physiology (Ryan, 1990; Lawrence and Koundal, 2002; Zhu-Salzman and Zeng, 2015). In aphids, similarly to what observed in thrips, PIs may inhibit aphid salivary proteases during probing and feeding establishment (Pyati et al., 2011; van Bel and Will, 2016) reducing the insect ability to degrade sieve-tube sap that includes proteins involved in defense (Furch et al., 2015). It was proposed that plant protect sap-proteins degradation by glycosylation that appears to prevent proteolysis (Taoka et al., 2007; Russel et al., 2009). Considering that glycosyltransferases are enzymes that catalyse the transfer of a sugar residue from an activated donor to an acceptor molecule the concerted down-regulation of transcripts encoding PIs and glycosyltransferases in Aph plants could be part of the aphid strategies to reduce the effectiveness of plant defense. Interestingly, three down-regulated glycosyltransferases (Solyc10g084890.2, Solyc03g078780.2, Solyc10g085280.1) showed high homology to UGT76B, C and/or E enzymes, which in Arabidopsis are involved in flavonoid biosynthesis and/or defense responses (Yonekura-Sakakibara and Hanada, 2011). The former function is consistent with the reduction in flavonoids, particularly kaempferol and quercetin glucosides, as well in phenolic acid derivatives, observed in aphid-infested plants (**Supplementary Table 6**).

Other down-regulated transcripts associated with plant defense are those encoding sesquiterpene synthase 1, Z,Z-farnesyl pyrophosphate synthase and geranylgeranyl reductase (Dudareva et al., 2004; Schmidt et al., 2011). Terpenoids, including sesquiterpenes and diterpenes, constitute some of the commonly encountered chemical classes of phytoalexins, biochemicals that locally protect plant tissues (Li et al., 2015). They are pathogen- and insect-inducible, known for their role in the attraction of predators, parasitoids, and other natural antagonists (Aljbory and Chen, 2018).

Among down-regulated genes, transcripts involved in phenylalanine metabolism (PAL) were retrieved, indicating a strong perturbation in phenylpropanoid pathway. In fact, as shown by the KEGG analysis, down-regulated genes involved in phenylalanine metabolism are in the early steps of the pathway, allowing the hypothesis of a possible accumulation of phenylalanine, that has been underlined as a crucial channel of SA biosynthesis (Chen et al., 2009). This finding is consistent with the reduced accumulation of several metabolites belonging to phenylpropanoid family in Aph plants that are located downstream PAL in the pathway. The over-presence of caffeic acid glucoside and coumarin could be similarly interpreted: the effect of the partial suppression of a branch of the phenylpropanoid biosynthesis causes the accumulation of central metabolites that are not toxic *per se* for aphids, but are precursor of molecules toxic for other herbivores (Sun et al., 2016).

Trichoderma harzianum T22 Boosts the Plant Immune Response

The advantages conferred to the plant by *Trichoderma* were largely associated with biological control of phytopathogens (Woo et al., 2006; Lorito et al., 2010). However, in the past 30 years, particularly with the advancement of modern techniques to analyse plant-microbe interactions, it became increasingly evident that root colonization by *Trichoderma* is associated with a wealth of beneficial effects, by activating defense responses against multiple stressors (De Meyer et al., 1998; Yedidia et al., 1999; Harman et al., 2004; Lorito et al., 2010; Shoresh et al., 2010; Hermosa et al., 2012; Lorito and Woo, 2015; Manganiello et al., 2018). Regarding plant responses to phytopathogens, the production of microbe-associated molecular patterns (MAMPs) by *Trichoderma* enhances the sensitivity of first defense, by maintaining a level of "alert" near to the threshold of effective resistance (Lorito et al., 2010). In particular, *Trichoderma* is also known to be involved in priming, the activation of plant defense prior to invasion, whereby upon pathogen attack *Trichoderma* stimulates a faster response to the pathogen effectors or it produces compounds specifically recognized by plant receptors able to elicit defense mechanisms (Lorito et al., 2010; Mauch-Mani et al., 2017; Manganiello et al., 2018). Only very recently, this priming response was also proposed to have a role in tomato indirect defense against aphid (Balmer et al., 2015; Coppola et al., 2017a; Tan et al., 2017). Here, we observed the activation of

early signals of defense responses against insects in T22 plants that indicates the ability of these plants to mount more rapid and effective direct and indirect defense responses. Similarly, the up-regulation of transcripts coding for several types of TF is a peculiar feature of adaptive plant strategies that improve their defensive potential (Khong et al., 2008; Walling, 2008). On the other hand, the concurrent down-regulation of some defense-related functions observed in T22 plants is possibly due, at least in part, to fungal effectors that allow *T. harzianum* T22 to colonize plant roots as an avirulent symbiont (Shoresh et al., 2005).

Trichoderma, as many beneficial plant growth promoting rhizobacteria (PGPR), tends to activate induced systemic resistance (ISR) that involve signal transduction pathways responding to JA/ET, but includes also cross-talk with SA, as well as with phytohormones associated with plant development (Harman et al., 2004; Shoresh et al., 2005; Hermosa et al., 2012). A trade-off is established between plant biosynthetic pathways involving defense or cellular/growth functions that can be regulated by *Trichoderma* stimuli, such as 1-aminocyclopropane-1-carboxylic acid deaminase (ACCD) activity, that modulates ET biosynthesis, or indole-3-acetic acid (IAA), that stimulates plant growth (Pieterse et al., 2009; Hermosa et al., 2012).

Our findings indicates that fungal colonization of tomato has an impact on phosphorylation dynamics of several Serine/threonine- and Leucine-rich repeat protein kinases, that were up-regulated. These kinases are involved in recruiting signals from receptors sensing environmental conditions and phytohormones and recalibrating them into appropriate outputs such as changes in metabolism, and gene expression, to activate defense/resistance against invaders (Xu and Huang, 2017). This evidence supports the hypothesis that *Trichoderma* T22 strain triggers a "defense mood" in the tomato cultivar "Dwarf San Marzano," generating a pre-alerted state of "priming" to face more efficiently likely incoming attacks (Conrath, 2011; Conrath et al., 2015). However, it is of interest to note that this reinforcement of defense barriers is not univocally associated with *Trichoderma* infection of tomato plants. Indeed, what observed here in terms of direct defense for SM was quite different in the case of *Trichoderma longibrachiatum* strain MK1, which similarly increased plant attractiveness toward the aphid parasitoid *A. ervi*, but also promoted the development and reproduction of *M. euphorbiae* (Battaglia et al., 2013). This demonstrates that the plant response can be different to different fungal species, and can be specific for each tomato variety, as already suggested by Tucci et al. (2011).

The up-regulation of a Multicystatine and several other Proteinase inhibitors with the T22 treatments (observed in both T22 and T22Aph) correlated with the reduced aphid survivorship overtime. This plant defense barrier induced by T22 was reinforced by the concurrent reduction in the number of down-regulated transcripts by aphid feeding related to other protease inhibitors (4 in Aph and 2 in T22Aph), which further contributes to the disruption of the aphid-induced suppression of plant defense. Previous studies have demonstrated that *Trichoderma* interferes with nematode performance by inducing Protease inhibitors in tomato (Martínez-Medina et al., 2017). In addition, in wheat the fungus counteracts nematode growth, inducing chitinase, β-1, 3-glucanase and defense compounds such as total flavonoids and lignin (Zhang et al., 2017). The metabolomics analysis remarkably expands the understanding of effect induced by *T. harzianum* T22 on tomato defenses when coupled with insect feeding. Defense-related secondary metabolites were over-represented in T22Aph samples compared to T22 or with only aphid infestation (Aph). The defense barrier array involved alkaloids (α-/β-tomatine) that could be responsible for the reduction in aphid survival together with late defense gene products (PPO, LapA, Miraculin, and many others), phenolic acids and flavonoids.

The up-regulation of the enzymes participating at different stages in the phenylpropanoid biosynthesis, for example, involved in catalyzing key-steps such as the conversion of phenylalanine in cinnamic acid (Phenylalanine ammonia-lyase and Caffeoyl-CoA O-methyl transferase), or catalyzing final branches for lignin production (i.e., Peroxiredoxin), may be associated with the observed increased level of compounds implicated in the defense responses. In fact, phenylpropanoids or their precursors/derivates may exert direct toxicity against insect herbivores (Naoumkina et al., 2010) and, at the same time, are precursors to VOCs that contribute to plant indirect defense (Dudareva et al., 2013). Notably, *PAL* is the up-regulated gene with the highest fold change in T22 plants while it is down-regulated in aphid-infested plants (Aph). The observed transcriptomic reprogramming of phenylpropanoid pathway is consistent with the augmented accumulation of Phenylalanine, Coumaric and Chorismic acids, Salicylic acid precursors, as well as SA-related metabolites (Salicylate β-D-glucose ester and salicyolyl-L-aspartic acid) in T22 plants. These observations are summarized in **Figure 9**. Similarly, metabolites involved in PAL pathway were over-accumulated in T22 plants. This is consistent with the previously observed increased attractiveness toward *A. ervi* mediated by methyl-salicylate (Coppola et al., 2017a).

Furthermore, T22 plants showed higher accumulation of sugars quantities than CTRL plants, indicating a higher root uptake and photosynthesis efficiency, as confirmed by the over-representation of a series of transcripts of the Calvin cycle; this is in line with the reported beneficial effect of the fungus on the plant physiology (Lorito et al., 2010; Lorito and Woo, 2015) and consistent with previous observation on *Trichoderma* –tomato interaction (De Palma et al., 2019).

The higher content of sugar could be the result of the over-expression of a large group of genes associated with cellular and metabolic processes and many others identified by GO annotation (**Figure 3**; **Supplementary Table 2**). These processes produce substances such as nutrients, hormones, metabolites that contribute to the positive effects observed in plant growth promotion frequently induced by *Trichoderma* spp. (Tucci et al., 2011; Vinale et al., 2014; Lorito and Woo, 2015). It has been proposed that plant-derived sugars represent not only a carbon source for the fungus, but also a tool to modulate the extension of root colonization and the systemic induction of photosynthesis in leaves (Vargas et al., 2009). In addition, the increased expression of glycolytic enzymes can redirect the higher sugar flux to increase the carbon supply to biosynthetic pathways involved in the production

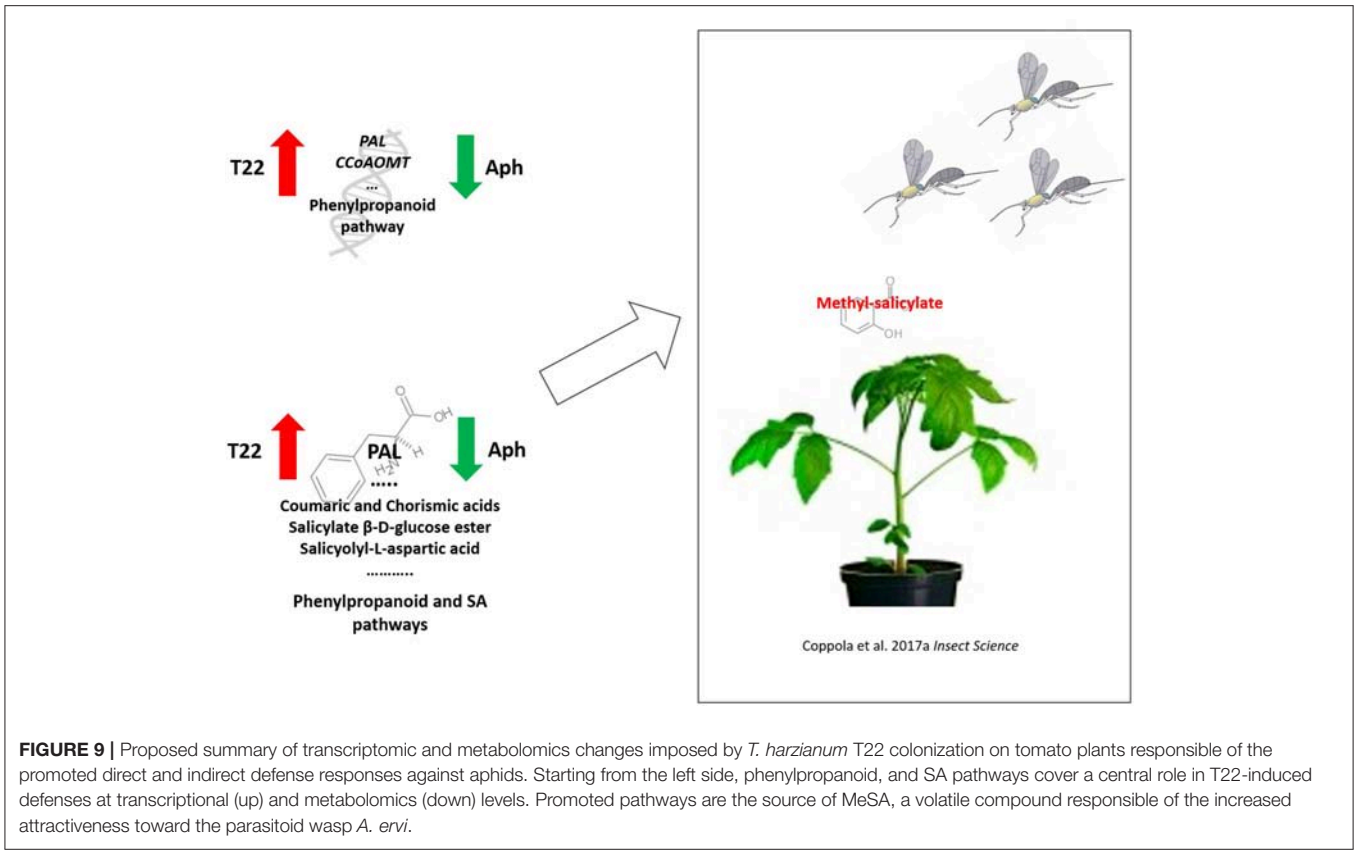

FIGURE 9 | Proposed summary of transcriptomic and metabolomics changes imposed by *T. harzianum* T22 colonization on tomato plants responsible of the promoted direct and indirect defense responses against aphids. Starting from the left side, phenylpropanoid, and SA pathways cover a central role in T22-induced defenses at transcriptional (up) and metabolomics (down) levels. Promoted pathways are the source of MeSA, a volatile compound responsible of the increased attractiveness toward the parasitoid wasp *A. ervi*.

of plant resistance-secondary metabolites (Fürstenberg-Hägg et al., 2013). In agreement with this hypothesis, a large group of terpenes and carotenoids/apocarotenoids genes were up-regulated in T22 leaves. In the same context, amino acid metabolism was strongly affected by *Trichoderma* and aphids: among the different transcript/metabolite data, a group of elements involved in glutamate metabolism was highlighted. For instance, a*sparagine synthetase 1* and *aspartate aminotransferase*, involved in glutamate production, were up-regulated in T22Aph; interestingly, a plant resistance mechanism due to increased levels of glutamate has been proved (Dixit et al., 2013). A possible explanation for this finding, besides its role in chlorophyll pathway (see below), could rely on the involvement of glutamate in tricarboxylic acidreplenishment and nitrogen remobilization upon insect attack (Ameye et al., 2018). In agreement with transcriptomic data, glutamate accumulation was observed in T22Aph vs. T22 leaves. In the same context, additional genes of glutamate synthesis/sensing/catabolism varied according the same trend: *proline dehydrogenase*, converting proline in Δ1-pyrroline-5-carboxylate, and which is known to contribute to the hypersensitive response and disease resistance (Cecchini et al., 2011), were up-regulated; similarly, *glutamate receptor 1.2*, for which a potential function as primary sensors in plant defense responses has been postulated (Forde and Roberts, 2014), displayed positive changes.On the contrary, *glutamate decarboxylase,* opposing glutamate accumulation by its conversion in γ-aminobutyrate, was down-expressed in T22Aph over CTRL leaves.

Key Events of the Tripartite Interaction

The hormonal balance during tomato-aphid interaction in presence of *T. harzianum* T22 is very delicate, variable and complex. *Trichoderma* spp. induction of ethylene and jasmonate (ET/JA) and salicylic acid (SA)-mediated signaling pathways has been reported in tomato cv. MicroTom (Manganiello et al., 2018). In our dataset, specific genes of the tripartite interaction are involved in ethylene biosynthesis and signaling, confirming the impact of *Trichoderma* on this pathway. ET production is part of the array of defense responses triggered in different plants by aphid feeding (Mantelin et al., 2009; Coppola et al., 2013). Indeed, the tomato *ERF Pti5* gene confers protection against aphids, both in susceptible and resistant genotypes (War et al., 2015).

The host plant regulation by hormonal management exerted by *T. harzianum* T22 in the tripartite interaction is also based on the down-regulation of several members of WRKY family of transcription factors, known for their promotion of JA signaling through the negative interplay with SA pathway (Li et al., 2004; Takatsuji, 2014). WRKYs represent keystones of communication between JA and SA and are involved in multiple defense responses (Phukan et al., 2016). These TFs appear to be aphid targets in the manipulation of plant host resistance (Kloth et al., 2016). Their down-regulation in T22Aph plants promotes JA-mediated defenses, at the expenses of SA signaling

which would interfere with *Trichoderma* colonization of plant roots. In other words, the aphid strategy based on the activation of the salycilate pathway to exert a negative regulation of JA signaling, to which they are sensitive, is outcompeted by the capacity of the Trichoderma strainT22 to counteract it, as it is is detrimental for the fungal entry and development in the plant tissues. Many TFs implicated in JA signaling have been identified and functionally characterized, including many basic helix–loop–helix (bHLH) type TFs (Zhou and Memelink, 2016). To date, four subclades of the bHLH TF family have been implicated in JA signaling in *Arabidopsis*, each with a different contribution to the JA response (Goossens et al., 2017). The redirection of the expression of a bHLH TF, up-regulated in T22 while down-regulated in Aph plants, represents a further contribute of *Trichoderma* colonization to defense priming against aphids and, possibly, other herbivores. Notably, allantoin, a purine metabolite that activates JA signaling in *Arabidopsis thaliana* (Takagi et al., 2016), was found to accumulate at higher levels in T22Aph vs. T22 (**Supplementary Tables 6**, **7**). In addition, a gene encoding a steroid dehydrogenase, (upregulated in T22Aph and down regulated in Aph) is involved in plant responses to stress through lipid signaling (Fürstenberg-Hägg et al., 2013). Membrane lipids serve as substrates for the generation of numerous signaling lipids such as phosphatidic acid, phosphoinositides, sphingolipids, lysophospholipids, oxylipins, N-acylethanolamines, free fatty acids and others. These molecules are tightly regulated and can be rapidly activated upon abiotic stress signals (Hou et al., 2016) or pathogen attack (Okazaki and Saito, 2014). Interestingly, O-phosphorylethanolamine, an intermediate of ethanolamine/choline synthesis, which can take part in the stress response-signaling machinery, was over-accumulated in T22Aph leaves (**Supplementary Tables 6**, **7**). Phloem lipids have been associated not only with intracellular signaling but also with a long-distance lipid signaling: lipid molecules could be released upon a stress perception and moving through the phloem they could bind receptors with the consequent modification of the sink tissue mediating a response (Benning et al., 2012). In this scenario, the possible alteration of lipid signaling following *T. harzianum* T22 colonization of tomato roots could contribute to tomato responses in the initial phase of perception and recognition of the injury.

Interestingly, among the metabolites identified by targeted/untargeted metabolomics, and previously reported in tomato, 5-amino-levulinic acid, while reduced in Aph, is highly overproduced in T22 and in T22Aph plants. This metabolite is known to be effective in counteracting the damages of different plant stressors (Yang et al., 2014). Similar accumulation pattern was registered for hydroxypipecolicacid, very recently identified as a mobile signal responsible of the induction of systemic disease resistance in Arabidopsis (Chen et al., 2018); chlorogenic and sinapic acids, which can improve host plants resistance (Nićiforović and Abramovič, 2013; Kundu and Vadassery, 2019); anthranilic acid, precursor of methyl anthranilate, which has been associated with the production of the volatile blend attracting herbivore parasitoids (Köllner et al., 2010).

Concerted regulation of genes and metabolites involved in chlorophyll metabolism is observed in the plant-fungus-insect interaction. Aphids repress, and *Trichoderma* induces, two early intermediates in chlorophyll biosynthesis; 5-amino-levulinic acid (ALA) and uroporphyrinogen III (UROIII); later intermediates (coproporphyrinogenIII (COPIII), protoporphyrin IX (PPIX)) show the opposite trend (**Supplementary Table 10**). This dual regulation is observed also for transcripts involved in chlorophyll biosynthesis: for instance, coproporphyrinogen III oxidase (CPOX) is induced by aphids, while transcripts encoding later steps (magnesium chelatase H subunit (MgCH), magnesium-protoporphyrin monomethyl ester cyclase (MPEC)) and a light harvesting chlorophyll a/b binding protein (LHC) are repressed. *Trichoderma* induces uroporphyrinogen decarboxylase (UROD) and protochlorophyllide reductase (POR) as well as MgCH, MPEC and two LHCs. Finally, in the triple interaction, aphid infestation seems to be epistatic over *Trichoderma* treatment, since it represses ALA and UROIII, strongly induces a fifth intermediate (protoporphyrinogen IX) and represses a series of transcripts involved in chlorophyll biosynthesis and sequestration (MgCH, PEC and 23 LHCs). Such a coordinated regulation of transcripts and metabolites belonging to a single pathway must have a biological meaning. Several genes in the chlorophyll pathway are known to be involved in plant defense responses: for instance, a null *UROD* mutation generates a disease lesion mimic phenotype in maize (Hu et al., 1998), and the *accelerated cell death 2* gene of *Arabidopsis*, showing constitutive activation of defenses in the absence of pathogen infection, encodes a red chlorophyll catabolite reductase (Mach et al., 2001). Two hypotheses have been proposed explaining the remodeling of chorophyll metabolism in defense responses: in the first hypothesis, a reduction in chlorophyll biosynthesis and accumulation in aphid-resistant cultivars would cause a decrease in photosynthetic efficiency, thus limiting the nutrient supply to aphids (Carrillo et al., 2014). This hypothesis is consistent with the data from the tripartite (plant-fungus-aphid) interaction. A second hypothesis is based on the well-known role of some tetrapyrrole chlorophyll precursors in generating Reactive Oxygen Species in the presence of light, which in turn activate defense responses. This hypothesis is consistent with some, but not other, data presented in this paper: for instance, both UROD and CPOX silencing causes the accumulation of photosensitizing tetrapyrroles and necrotic lesions in tobacco (Mock et al., 1998). In the tomato-Trichoderma-aphid system, UROD is induced by Trichoderma (presumably a way to alleviate the production of ROS by reducing the levels of photosensitizing COPIII and PPIX) while CPOX is induced by aphid infestation (presumably a way to reduce the levels of COPIII). It is not entirely clear from our data whether the interplay of these two responses enhances or diminishes resistance to aphids in the triple interaction.

In conclusion, our study suggests a wide, articulated and sophisticated contribute of *T. harzianum* T22 in the promotion of tomato endogenous defenses against phloem-feeders, by the instauration of a preparation to defense. This preparation ranges from transcriptomic to metabolomics changes, from early signals to late effector of defense responses. In the specific

tripartite system under investigation, the major contribute of the beneficial fungus appears to be the manipulation of phloem sap sentinel molecules, the regulation of hormonal balance and enhanced communication with natural enemies via terpenes and salycilate.

DATA AVAILABILITY

Publicly available datasets were analyzed in this study. This data can be found here: https://www.ncbi.nlm.nih.gov/Traces/study/?acc=PRJNA532377.

ETHICS STATEMENT

This article does not contain any studies with human participants or animals performed by any of the authors.

AUTHOR CONTRIBUTIONS

MC performed and analyzed transcriptomic data and draft the ms. GD and GG performed metabolomics, analyzed the results and contributed to manuscript writing. MD performed insect bioassays and analyzed the data. SW participated to the experimental design and contributed to manuscript writing. DM contributed to RNA isolation. ML contributed to the work plan and helped in results interpretation. FP contributed to the work plan and to data analyses and revised the manuscript. RR conceived and designed the study, supervised the experimental work and wrote the paper.

FUNDING

This work was supported by the European Union Horizon 2020 research and innovation programme, under grant agreement no. 773554 (EcoStack) (to FP) and by European FP7—ERANET ARIMNET2 Sustainable Tomato Production: plant defense enhancement, development of new biopesticides and optimization of environmental, water and chemical inputs—STomP (to MD). This project has received funding from the European Union's Horizon 2020 research and innovation programme under grant agreements no. 818431 (SIMBA) and no. 677379 (G2P-SOL). JGI Community Scientific Program 2016, Proposal 1966-CSP 2016; Project ProBio - IZSM (Portici), n. D01 6309, 14/12/2016; Project LINFA - MIUR-PON, n. 03PE_00026_1, 09/04/2014; KENYA-AID, n. 10306/CEFA/KEN, 18/05/2017. This output reflects only the author's view and the Research Executive Agency (REA) cannot be held responsible for any use that may be made of the information contained therein.

SUPPLEMENTARY MATERIAL

The Supplementary Material for this article can be found online at: https://www.frontiersin.org/articles/10.3389/fphys.2019.00745/full#supplementary-material

Supplementary Figure 1 | GO categories distribution for plants treated with *T. harzianum* T22 in the "Biological Process" domain. Colors indicate the enrichment score of each GO category for **(A)** up-regulated and **(B)** down-regulated genes.

Supplementary Figure 2 | GO categories distribution for SM plants infested by *M. euphorbiae* for 48 h in the "Biological Process" domain. Colors indicate the enrichment score of each GO category for **(A)** up-regulated and **(B)** down-regulated genes.

Supplementary Figure 3 | GO categories distribution for SM plants treated with *T. harzianum* T22 and subsequently infested by aphids in the "Biological Process" domain. Colors indicate the enrichment score of each GO category for **(A)** up-regulated and **(B)** down-regulated genes.

Supplementary Figure 4 | Expression analysis of selected defense genes from the tomato DEGs by Real Time RT-PCR in plants: treated with *T. harzianum* T22 (T22); infested by aphid *M. euphorbiae* (Aph) or treated with T22 and subsequently infested by aphid (T22Aph). Relative quantities (RQ) are calibrated to untreated plants (Ctrl), as indicated by the linear scale on the Y-axis. Asterisks indicate statistically significant differences compared to control condition (*$p < 0.05$; **$p < 0.01$; ***$p < 0.001$ *t*-test).

Supplementary Figure 5 | Principal Component Analysis (PCA) of the untargeted metabolomic analysis, of the semi-polar fraction, obtained from tomato leaves grown in the absence and in the presence of the aphid *M. euphorbiae,* and treated with the *T. harzianum* T22, alone or in combination with the aphids. Dots with same colors indicate biological experimental replicates. For more details, see Materials and Methods.

Supplementary Figure 6 | Heatmap (HM) of semi-polar metabolome of tomato leaves grown in the absence and in the presence of the aphid M. euphorbiae and the fungus *T. harzianum* T22, alone or in combination. Colored squares represent the values of log2-transformed fold changes of a metabolite in respect to the corresponding control (water control CTRL for Aph and T22 samples; T22 for T22Aph), according to the color scale shown (green: down-accumulated; red: up-accumulated). Gray squares indicate no detectable accumulation of the corresponding metabolite.

REFERENCES

Alboresi, A., Perin, G., Vitulo, N., Diretto, G., Block, M., Jouhet, J., et al. (2016). Light remodels lipid biosynthesis in nannochloropsis gaditana by modulating carbon partitioning between organelles. *Plant Physiol.* 171, 2468–2482. doi: 10.1104/pp.16.00599

Alewu, B., and Nosiri, C. (2011). "Pesticides and human health," in Pesticides in the Modern World – Effects of Pesticides Exposure, ed M. Stoytcheva (Mexicali: Autonomous University of Baja California), 231–50.

Alexandru, M., Lazăr, D., Ene, M., Sesan, T. E. (2013). Influence of some *Trichoderma* species on photosynthesis intensity and pigments in tomatoes. *Rom Biotech Lett*. 18, 8499–8510.

Aljbory, Z., and Chen, M. S. (2018). Indirect plant defense against insect herbivores: a review. *Insect Sci.* 25, 2–23. doi: 10.1111/1744-7917.12436

Ameye, M., Allmann, S., Verwaeren, J., Smagghe, G., Haesaert, G., Schuurink, R. C., et al. (2018). Green leaf volatile production by plants: a meta-analysis. *N. Phytol.* 220, 666–683. doi: 10.1111/nph.14671

Anders, S., and Huber, W. (2010). Differential expression analysis for sequence count data. *Genome Biol.* 11, 106-110. doi: 10.1186/gb-2010-11-10-r106

Avila, C. A., Arevalo-Soliz, L. M., Jia, L. L., Navarre, D. A., Chen, Z., Howe, G. A., et al. (2012). Loss of Function of FATTY ACID DESATURASE7 in Tomato enhances basal aphid resistance in a salicylate-dependent manner. *Plant Physiol.* 158, 2028–2041. doi: 10.1104/pp.111.191262

Balmer, A., Pastor, V., Gamir, J., Flors, V., and Mauch-Mani, B. (2015). The 'prime-ome': towards a holistic approach to priming. *Trends Plant Sci.* 20, 443–452. doi: 10.1016/j.tplants.2015.04.002

Ban, Q., Han, Y., He, Y., Jin, M., Han, S., Suo, J., et al. (2018). Functional characterization of persimmon β-galactosidase gene DkGAL1 in tomato reveals

cell wall modification related to fruit ripening and radicle elongation. *Plant Sci.* 274, 109–120. doi: 10.1016/j.plantsci.2018.05.014

Battaglia, D., Bossi, S., Cascone, P., Digilio, M. C., Prieto, J. D., Fanti, P., et al. (2013). Tomato below ground-above ground interactions: *Trichoderma longibrachiatum* affects the performance of *Macrosiphum euphorbiae* and its natural antagonists. *Mol. Plant Microbe Interact* 26, 1249–1256. doi: 10.1094/MPMI-02-13-0059-R

Benning, U. F., Tamot, B., Guelette, B. S., and Hoffmann-Benning, S. (2012). New aspects of phloem-mediated long-distance lipid signalling in plants. *Front. Plant Sci.* 3:53. doi: 10.3389/fpls.2012.00053

Berendsen, R. L., Pieterse, C. M., and Bakker, P. A. (2012). The rhizosphere microbiome and plant health. *Trends Plant Sci.* 17, 478–486. doi: 10.1016/j.tplants.2012.04.001

Brader, G., Tas, E., and Palva, E. T. (2001). Jasmonate-dependent Induction of indole glucosinolates in *Arabidopsis* by culture filtrates of the nonspecific pathogen *Erwinia carotovora*. *Plant Physiol.* 126, 849–860.

Bulgarelli, D., Schlaeppi, K., Spaepen, S., Ver Loren van Themaat, E., and Schulze-Lefert, P. (2013).Structure and functions of the bacterial microbiota of plants. *Annu. Rev. Plant Biol.* 64, 807–838. doi: 10.1146/annurev-arplant-050312-120106

Carrillo, E., Rubiales, D., and Castillejo, M. A. (2014). Proteomic analysis of pea (*Pisum sativum L.)* response during compatible and incompatible interactions with the pea aphid (*Acyrthosiphon pisum H.*). *Plant Mol. Biol. Report*. 32, 697–718. doi: 10.1007/s11105-013-0677-x

Cecchini, N. M., Monteoliva, M. I., and Alvarez, M. E. (2011). Proline dehydrogenase is a positive regulator of cell death in different kingdoms. *Plant Signal Behav*. 6, 1195–1197. doi: 10.4161/psb.6.8.15791

Chen, H., Wilkerson, C. G., Kuchar, J. A., Phinney, B. S., and Howe, G. A. (2005). Jasmonate-inducible plant enzymes degrade essential amino acids in the herbivore midgut. *Proc. Natl. Acad. Sci. U.S.A.* 102, 19237–19242. doi: 10.1073/pnas.0509026102

Chen, Y. C., Holmes, E. C., Rajniak, J., Kim, J. G., Tang, S., Fischer, C. R., et al. (2018). N-hydroxy-pipecolic acid is a mobile signal that induces systemic disease resistance in Arabidopsis. *Proc. Natl. Acad. Sci. U.S.A.* 22:115. doi: 10.1101/288449

Chen, Z., Zheng, Z., Huang, J., Lai, Z., and Fan, B. (2009). Biosynthesis of salicylic acid in plants. *Plant Signal Behav*. 4, 493–496. doi: 10.4161/psb.4.6.8392

Conklin, P. L., and Last, R. L. (1995). Differential accumulation of antioxidant mRNAs in *Arabidopsis thaliana* exposed to ozone. *Plant Physiol.* 109, 203–212. doi: 10.1104/pp.109.1.203

Conrath, U. (2011). Molecular aspects of defence priming. *Trends Plant Sci*. 16, 524–531. doi: 10.1016/j.tplants.2011.06.004

Conrath, U., Beckers, G. J., Langenbach, C. J., and Jaskiewicz, M. R. (2015). Priming for enhanced defense. *Annu. Rev. Phytopathol.* 53, 97–119. doi: 10.1146/annurev-phyto-080614-120132

Coppola, M., Cascone, P., Chiusano, M. L., Colantuono, C., Lorito, M., Pennacchio, F., et al. (2017a). *Trichoderma harzianum* enhances tomato indirect defense against aphids. *Insect Sci.* 24, 1025–1033. doi: 10.1111/1744-7917.12475

Coppola, M., Cascone, P., Madonna, V., Di Lelio, I., Esposito, F., Avitabile, C., et al. (2017b). Plant-to-plant communication triggered by systemin primes anti-herbivore resistance in tomato. *Sci. Rep*. 7:15522. doi: 10.1038/s41598-017-15481-8

Coppola, V., Coppola, M., Rocco, M., Digilio, M. C., D'Ambrosio, C., Renzone, G., et al. (2013). Transcriptomic and proteomic analysis of a compatible tomato-aphid interaction reveals a predominant salicylic acid-dependent plant response. *BMC Genomics* 14:515. doi: 10.1186/1471-2164-14-515

De Meyer, G., Bigirimana, J., Elad, Y., and Höfte, M. (1998). Induced systemic resistance in Trichoderma harzianum T39 biocontrol of *Botrytis cinerea*. *Eur. J. Plant Pathol.* 104, 279–286. doi: 10.1023/A:1008628806616

De Palma, M., Salzano, M., Villano, C., Aversano, R., Lorito, M., Ruocco, M., et al. (2019). Transcriptome reprogramming, epigenetic modifications and alternative splicing orchestrate the tomato root response to the beneficial fungus *Trichoderma harzianum*. *Horticul. Res*. 6:5. doi: 10.1038/s41438-018-0079-1

Diretto, G., Al-Babili, S., Tavazza, R., Scossa, F., Papacchioli, V., Migliore, M., et al. (2010). Transcriptional-metabolic networks in β-carotene-enriched potato tubers: the long and winding road to the Golden phenotype. *Plant Physiol.* 154, 899–912. doi: 10.1104/pp.110.159368

Dixit, S., Upadhyay, S. K., Singh, H., Sidhu, O. P., Verma, P. C., and Chandrashekar, K. (2013). Enhanced methanol production in plants provides broad spectrum insect resistance. *PLoS ONE* 8:e79664. doi: 10.1371/journal.pone.0079664

Dudareva, N., Klempien, A., Muhlemann, J. K., and Kaplan, I. (2013). Biosynthesis, function and metabolic engineering of plant volatile organic compounds. *N. Phytol.* 198, 16–32. doi: 10.1111/nph.12145

Dudareva, N., Pichersky, E., and Gershenzon, J. (2004). Biochemistry of plant volatiles. *Plant Physiol.* 135, 1893–1902. doi: 10.1104/pp.104.049981

Elzinga, D. A., De Vos, M., and Jander, G. (2014). Suppression of plant defenses by a Myzus persicae (green peach aphid) salivary effector protein. *Mol. Plant Microbe. Interact.* 27, 747–756. doi: 10.1094/MPMI-01-14-0018-R

Emani, C. (2018). *The Biology of Plant-Insect Interactions: A Compendium for the Plant Biotechnologist*, ed C. Emani (Boca Raton, FL: CRC Press). doi: 10.1201/9781315119571

Erb, M., Meldau, S., and Howe, G. A. (2012). Role of phytohormones in insect-specific plant reactions.*Trends Plant Sci.* 17, 250–259. doi: 10.1016/j.tplants.2012.01.003

Fasano, C., Diretto, G., Aversano, R., D'Agostino, N., Di Matteo, A., Frusciante, L., et al. (2016). Transcriptome and metabolome of synthetic Solanum autotetraploids reveal key genomic stress events following polyploidization. *N. Phytol*. 210, 1382–1394. doi: 10.1111/nph.13878

Forde, B. G., and Roberts, M. R. (2014). Glutamate receptor-like channels in plants: a role as amino acid sensors in plant defence? *F1000 Prime Rep*. 6:37.doi: 10.12703/P6-37

Furch, A. C., van Bel, A. J., and Will, T. (2015). Aphid salivary proteases are capable of degrading sieve-tube proteins. *J. Exp. Bot*. 66, 533–539. doi: 10.1093/jxb/eru487

Fürstenberg-Hägg, J., Zagrobelny, M., and Bak, S. (2013).Plant defense against insect herbivores. *Int. J. Mol. Sci.* 14, 10242–10297. doi: 10.3390/ijms140510242

Goossens, J., Mertens, J., and Goossens, A. (2017). Role and functioning of bHLH transcription factors in jasmonate signalling. *J. Exp. Bot*. 68, 1333–1347. doi: 10.1093/jxb/erw440

Guerrieri, E., Lingua, G., Digilio, M. C., Massa, N., and Berta, G. (2004). Do interactions between plant roots and the rhizosphere affect parasitoid behaviour? *Ecol. Entomol.* 29, 753–756. doi: 10.1111/j.0307-6946.2004.00644.x

Harman, G. E., Howell, C. R., Viterbo, A., Chet, I., and Lorito, M. (2004).Trichoderma species—opportunistic, avirulent plant symbionts. *Nat. Rev. Microbiol*. 2, 43–56. doi: 10.1038/nrmicro797

Hermosa, R., Viterbo, A., Chet, I., and Monte, E. (2012). Plant-beneficial effects of Trichoderma and of its genes. *Microbiology* 158, 17–25. doi: 10.1099/mic.0.052274-0

Hou, Q., Ufer, G., and Bartels, D. (2016). Lipid signalling in plant responses to abiotic stress. *Plant Cell Environ.* 39, 1029–1048. doi: 10.1111/pce.12666

Hu, G., Yalpani, N., Briggs, S. P., and Johal, G. S. (1998). A porphyrin pathway impairment is responsible for the phenotype of a dominant disease lesion mimic mutant of maize. *Plant Cell*. 10, 1095–1105. doi: 10.1105/tpc.10.7.1095

Kessler, A., and Baldwin, I. T. (2002). Plant responses to insect herbivory: the emerging molecular analysis. *Annu. Rev. Plant Biol.* 53, 299–328. doi: 10.1146/annurev.arplant.53.100301.135207

Khong, G. N., Richaud, F., Coudert, Y., Pati, P. K., Santi, C., Périn, C., et al. (2008). Modulating rice stress tolerance by transcription factors. *Biotech. Genet. Eng. Rev*. 25, 381–404. doi: 10.5661/bger-25-381

Kim, D., Pertea, G., Trapnell, C., Pimentel, H., Kelley, R., and Salzberg, S. (2013). TopHat2: accurate alignment of transcriptomes in the presence of insertions, deletions and gene fusions. *Genome Biol.* 14:36. doi: 10.1186/gb-2013-14-4-r36

Kinsella, R. J., Kähäri, A., Haider, S., et al. (2011). Ensembl BioMarts: a hub for data retrieval across taxonomic space. *Database*. 2011:bar030. doi: 10.1093/database/bar030

Kloth, K. J., Wiegers, G. L., Busscher-Lange, J., van Haarst, J. C., Kruijer, W., Bouwmeester, H. J., et al. (2016). AtWRKY22 promotes susceptibility to aphids and modulates salicylic acid and jasmonic acid signalling. *J. Exp. Bot*. 67, 3383–3396. doi: 10.1093/jxb/erw159

Köllner, T. G., Lenk, C., Zhao, N., Seidl-Adams, I., Gershenzon, J., Chen, F., et al. (2010). Herbivore-induced SABATH methyltransferases of maize that

methylate anthranilic acid using s-adenosyl-L-methionine. *Plant Physiol.* 153, 1795–1807. doi: 10.1104/pp.110.158360

Kundu, A., and Vadassery, J. (2019). Chlorogenic acid-mediated chemical defence of plants against insect herbivores. *Plant Biol.* 21, 185–189. doi: 10.1111/plb.12947

Langmead, B., and Salzberg, S. L. (2012). Fast gapped-read alignment with Bowtie 2. *Nat. Methods* 9, 357–359. doi: 10.1038/nmeth.1923

Lawrence, P. K., and Koundal, K. R. (2002). Plant protease inhibitors in control of phytophagous insects. *Electron. J. Biotechnol.* 5, 1–17. doi: 10.2225/vol5-issue1-fulltext-3

Li, J., Brader, G., and Palva, E. T. (2004). The WRKY70 transcription factor: a node of convergence for jasmonate-mediated and salicylate-mediated signals in plant defense. *Plant Cell.* 16, 319–331. doi: 10.1105/tpc.016980

Li, R., Tee, C. S., Jiang, Y. L., Jiang, X. Y., Venkatesh, P. N., Sarojam, R., et al. (2015). A terpenoid phytoalexin plays a role in basal defense of Nicotiana benthamiana against Potato virus X. *Sci. Rep.* 5:9682. doi: 10.1038/srep09682

Livak, K. J., and Schmittgen, T. D. (2001). Analysis of relative gene expression data using real-time quantitative PCR and the 2-Delta Delta CT method. *Methods* 25, 402–408. doi: 10.1006/meth.2001.1262

Lorito, M., and Woo, S. L. (2015). "Trichoderma: a multi-purpose tool for integrated pest management," in *Principles of Plant-Microbe Interactions*, ed B. Lugtenberg (Cham: Springer International Publishing), 345–353. doi: 10.1007/978-3-319-08575-3_36

Lorito, M., Woo, S. L., Harman, G. E., and Monte, E. (2010). Translational research on Trichoderma: from'omics to the field. *Annu. Rev. Phytopathol.* 48, 395–417. doi: 10.1146/annurev-phyto-073009-114314

Lv, G. Y., Guo, X. G., Xie, L. P., Xie, C. G., Zhang, X. H., Yang, Y., et al. (2017). Molecular characterization, gene evolution, and expression analysis of the fructose-1, 6-bisphosphate aldolase (FBA) gene family in wheat (*Triticum aestivum L.*). *Front. Plant Sci.* 8:1030. doi: 10.3389/fpls.2017.01030

Mach, J. M., Castillo, A. R., Hoogstraten, R., and Greenberg, J. T. (2001). The Arabidopsis-accelerated cell death gene ACD2 encodes red chlorophyll catabolite reductase and suppresses the spread of disease symptoms. *Proc. Natl. Acad. Sci. U.S.A.* 98, 771–776. doi: 10.1073/pnas.98.2.771

Manganiello, G., Sacco, A., Ercolano, M. R., Vinale, F., Lanzuise, S., Pascale, A., et al. (2018). Modulation of tomato response to Rhizoctonia solani by Trichoderma harzianum and its secondary metabolite harzianic acid. *Front. Microbiol.* 9:1966. doi: 10.3389/fmicb.2018.01966

Mantelin, S., Bhattarai, K. K., and Kaloshian, I. (2009). Ethylene contributes to potato aphid susceptibility in a compatible tomato host. *N. Phytol.* 183, 444–456. doi: 10.1111/j.1469-8137.2009.02870.x

Martin, M. (2011). Cutadapt removes adapter sequences from high-throughput sequencing reads. *EMBN J.* 17, 10–12. doi: 10.14806/ej.17.1.200

Martínez-Medina, A., Van Wees, S. C. M., and Pieterse, C. M. J. (2017). Airborne signals by Trichoderma fungi stimulate iron uptake responses in roots resulting in priming of jasmonic acid-dependent defences in shoots of Arabidopsis thaliana and Solanum lycopersicum. *Plant Cell Environ.* 40, 2691–2705. doi: 10.1111/pce.13016

Marum, L., Miguel, A., Ricardo, C. P., and Miguel, C. (2012). Reference gene selection for quantitative real-time PCR normalization in quercus suber. *PLoS ONE* 7:e35113. doi: 10.1371/journal.pone.0035113

Mauch-Mani, B., Baccelli, I., Luna, E., and Flors, V. (2017). Defence priming: an adaptive part of induced resistance. *Annu. Rev. Plant Biol.* 68, 485–512. doi: 10.1146/annurev-arplant-042916-041132

Mendoza-Mendoza, A., Zaid, R., Lawry, R., Hermosa, R., Monte, E., Horwitz, B. A., et al. (2018). Molecular dialogues between Trichoderma and roots: role of the fungal secretome. *Fungal Biol. Rev.* 32, 62–85. doi: 10.1016/j.fbr.2017.12.001

Mock, H. P., Heller, W., Molina, A., Neubohn, B., Sandermann, H. Jr., and Grimm, B. (1998). Expression of uroporphyrinogen decarboxylase or coproporphyrinogen oxidase antisense RNA in tobacco induces pathogen defense responses conferring increased resistance to tobacco mosaic virus. *J. Biol. Chem.* 274, 4231–4238. doi: 10.1074/jbc.274.7.4231

Mohapatra, S., and Mittra, B. (2016). Protein glutathionylation protects wheat (Triticum aestivum Var. Sonalika) against Fusarium induced oxidative stress. *Plant Physiol. Biochem.* 109, 319–325. doi: 10.1016/j.plaphy.2016.10.014

Müller, O. A., Grau, J., Thieme, S., Prochaska, S., Adlung, N., Sorgatz, A., et al. (2015). Genome-wide identification and validation of reference genes in infected tomato leaves for quantitative RT-PCR analyses. *PLoS ONE.* 10:e0136499. doi: 10.1371/journal.pone.0136499

Naoumkina, M. A., Zhao, Q., Gallego-Giraldo, L., Dai, X., Zhao, P. X., and Dixon, R. A. (2010). Genome-wide analysis of phenylpropanoid defence pathways. *Mol. Plant Pathol.* 11, 829–846. doi: 10.1111/j.1364-3703.2010.00648.x

Nićiforović, N., and Abramovič, H. (2013). Sinapic acid and its derivatives: natural sources and bioactivity. *Comprehen. Rev. Food Sci. Food Safety.* 13, 34–35 doi: 10.1111/1541-4337.12041

Okazaki, Y., and Saito, K. (2014). Roles of lipids as signaling molecules and mitigators during stress response in plants. *Plant J.* 79, 584–596. doi: 10.1111/tpj.12556

Pennacchio, F., Giordana, B., and Rao, R. (2012). "Applications of parasitoid virus and venom research in agriculture," in *Parasitoid Viruses, Symbionts and Pathogens,* ed J. Drezen (Gainesville, FL: University of Florida), 269–283. doi: 10.1016/B978-0-12-384858-1.00022-9

Phukan, U. J., Jeena, G. S., and Shukla, R. K. (2016). WRKY transcription factors: molecular regulation and stress responses in plants. *Front. Plant Sci.* 7:760. doi: 10.3389/fpls.2016.00760

Pieterse, C. M., Van der Does, D., Zamioudis, C., Leon-Reyes, A., and Van Wees, S. C. (2012). Hormonal modulation of plant immunity. *Annu. Rev. Cell Dev. Biol.* 28, 489–521. doi: 10.1146/annurev-cellbio-092910-154055

Pieterse, C. M., and van Loon, L. C. (1999). Salicylic acid-independent plant defence pathways. *Trends Plant Sci.* 4, 52–58. doi: 10.1016/S1360-1385(98)01364-8

Pieterse, C. M., and van Loon, L. C. (2004). NPR1: the spider in the web of induced resistance signalling pathways. *Curr. Opin. Plant Biol.* 7, 456–464. doi: 10.1016/j.pbi.2004.05.006

Pieterse, C. M. J., Leon-Reyes, A., Ent, S., and Wees, S. C. M. (2009). Networking by small-molecules hormones in plant immunity. *Nat. Chem. Biol.* 5, 308–316.doi: 10.1038/nchembio.164

Pineda, A., Kaplan, I., and Bezemer, T. M. (2017). Steering soil microbiomes to suppress aboveground insect pests. *Trends Plant Sci.* 22, 770–778. doi: 10.1016/j.tplants.2017.07.002

Pineda, A., Soler, R., Pozo, M. J., Rasmann, S., and Turlings, T. C. (2015). Editorial: Above-belowground interactions involving plants, microbes and insects. *Front. Plant Sci.* 6:318. doi: 10.3389/fpls.2015.00318

Pyati, P., Bandani, A. R., Fitches, E., and Gatehouse, J. A. (2011). Protein digestion in cereal aphids (Sitobion avenae) as a target for plant defence by endogenous proteinase inhibitors. *J. Insect Physiol.* 57, 881–891. doi: 10.1016/j.jinsphys.2011.03.024

Rahbé, Y., Deraison, C., Bonade-Bottino, M., Girard, C., Nardon, C., and Jouanin, L. (2003). Effects of the cysteine protease inhibitor oryzacystatin (OC-I) on different aphids and reduced performance of *Myzus persicae* on OC-I expressing transgenic oilseed rape. *Plant Sci.* 164, 441–450. doi: 10.1016/S0168-9452(02)00402-8

Reymond, P., and Farmer, E. E. (1998). Jasmonate and salicylate as global signals for defense gene expression. *Curr. Opin. Plant Biol.* 1, 404–411. doi: 10.1016/S1369-5266(98)80264-1

Robinson, M. D., McCarthy, D., and Smyth, G. K. (2010). edgeR: a Bioconductor package for differential expression analysis of digital gene expression data. *Bioinformatics.* 1, 139-40. doi: 10.1093/bioinformatics/btp616

Rubio, M. B., Quijada, N. M., Pérez, E., Domínguez, S., Monte, E., and Hermosa, R. (2014). Identifying beneficial qualities of Trichoderma parareesei for plants. *Appl. Environ. Microbiol.* 80, 1864–1873. doi: 10.1128/AEM.03375-13

Ryan, C. A. (1990). Protease inhibitors in plants: genes for improving defenses against insects and pathogens. *Annu. Rev. Phytopathol.* 28, 425–449. doi: 10.1146/annurev.py.28.090190.002233

Sasso, R., Iodice, L., Woodcock, C. M., Pickett, J. A., and Guerrieri, E. (2009). Electrophysiological and behavioural responses of *Aphidius ervi* (Hymenoptera: Braconidae) to tomato plant volatiles. *Chemoecology* 19, 195–201. doi: 10.1007/s00049-009-0023-9

Schilmiller, A. L., Koo, A. J., and Howe, G. A. (2007). Functional diversification of acyl-coenzyme A oxidases in jasmonic acid biosynthesis and action. *Plant Physiol.* 143, 812–824. doi: 10.1104/pp.106.092916

Schmidt, A., Nagel, R., Krekling, T., Christiansen, E., Gershenzon, J., and Krokene, P. (2011). Induction of isoprenyl diphosphate synthases, plant hormones and defense signalling genes correlates with traumatic resin duct

formation in Norway spruce (*Picea abies*). *Plant Mol. Biol.* 77, 577–590. doi: 10.1007/s11103-011-9832-7

Segarra, G., Casanova, E., Bellido, D., Odena, M. A., Oliveira, E., and Trillas, I. (2007). Proteome, salicylic acid, and jasmonic acid changes in cucumber plants inoculated with Trichoderma asperellum strain T34. *Proteomics* 7, 3943–3952. doi: 10.1002/pmic.200700173

Shoresh, M., Harman, G. E., and Mastouri, F. (2010). Induced systemic resistance and plant responses to fungal biocontrol agents. *Annu. Rev. Phytopathol.* 48, 21–43. doi: 10.1146/annurev-phyto-073009-114450

Shoresh, M., Yedidia, I., and Chet, I. (2005). Involvement of jasmonic acid/ethylene signaling pathway in the systemic resistance induced in cucumber by Trichoderma asperellum T203. *Phytopathology* 95, 76–84. doi: 10.1094/PHYTO-95-0076

Spoel, S. H., and Dong, X. (2008). Making sense of hormone crosstalk during plant immune responses. *Cell Host Microbe.* 3, 348–351. doi: 10.1016/j.chom.2008.05.009

Studholme, D. J., Harris, B., Le Cocq, K., Winsbury, R., Perera, V., Ryder, L., et al. (2013). Investigating the beneficial traits of Trichoderma hamatum GD12 for sustainable agriculture— insights from genomics. *Front. Plant Sci.* 4:258. doi: 10.3389/fpls.2013.00258

Sun, Z., Liu, Z., Zhou, W., Jin, H., Liu, H., Zhou, A., et al. (2016). Temporal interactions of plant - insect - predator after infection of bacterial pathogen on rice plants. *Sci. Rep.* 6:26043. doi: 10.1038/srep26043

Takagi, H., Ishiga, Y., Watanabe, S., Konishi, T., Egusa, M., Akiyoshi, N., et al. (2016). Allantoin, a stress-related purine metabolite, can activate jasmonate signaling in a MYC2-regulated and abscisic acid-dependent manner. *J. Experi. Botany* 67, 2519–2532. doi: 10.1093/jxb/erw071

Takatsuji, H. (2014). Development of disease-resistant rice using regulatory components of induced disease resistance. *Front. Plant Sci.* 5:630. doi: 10.3389/fpls.2014.00630

Tan, X. L., Chen, J. L., Benelli, G., Desneux, N., Yang, X. Q., Liu, T. X., et al. (2017). Pre-infestation of tomato plants by aphids modulates transmission-acquisition relationship among whiteflies, tomato yellow leaf curl virus (TYLCV) and plants. *Front. Plant Sci.* 8:1597. doi: 10.3389/fpls.2017.01597

Taoka, K., Ham, B. K., Xoconostle-Cázares, B., Rojas, M. R., and Lucas, W. J. (2007). Reciprocal phosphorylation and glycosylation recognition motifs control NCAPP1 interaction with pumpkin phloem proteins and their cell-to-cell movement. *Plant Cell.* 19, 1866–1884. doi: 10.1105/tpc.107.052522

Tauzin, A. S., and Giardina, T. (2014). Sucrose and invertases, a part of the plant defense response to the biotic stresses. *Front. Plant Sci.* 5:293. doi: 10.3389/fpls.2014.00293

Thaler, J. S., Fidantsef, A. L., and Bostock, R. M. (2002). Antagonism between jasmonate- and salicylate-mediated induced plant resistance: effects of concentration and timing of elicitation on defense-related proteins, herbivore, and pathogen performance in tomato. *J. Chem. Ecol.* 28, 1131–1159. doi: 10.1023/A:1016225515936

Tucci, M., Ruocco, M., De Masi, L., De Palma, M., and Lorito, M. (2011). The beneficial effect of *Trichoderma spp.* on tomato is modulated by the plant genotype. *Mol. Plant Pathol.* 12, 341–354. doi: 10.1111/j.1364-3703.2010.00674.x

van Bel, A. J. E., and Will, T. (2016). Functional evaluation of proteins in watery and gel saliva of aphids. *Front. Plant Sci.* 7:1840. doi: 10.3389/fpls.2016.01840

Van Wees, S. C., Van der Ent, S., and Pieterse, C. M. (2008). Plant immune responses triggered by beneficial microbes. *Curr. Opin. Plant Biol.* 11, 443–448. doi: 10.1016/j.pbi.2008.05.005

Vargas, W. A., Mandawe, J. C., and Kenerley, C. M. (2009). Plant-derived sucrose is a key element in the symbiotic association between Trichoderma virens and maize plants. *Plant Physiol.* 151, 792–808. doi: 10.1104/pp.109.141291

Vinale, F., Manganiello, G., Nigro, M., et al. (2014). A novel fungal metabolite with beneficial properties for agricultural applications. *Molecules* 19, 9760–9772. doi: 10.3390/molecules19079760

Vitti, A., La Monaca, E., Sofo, A., Scopa, A., Cuypers, A., and Nuzzati, M. (2015). Beneficial effects ofTrichoderma harzianum T-22 in tomato seedlings infected by Cucumber mosaic virus (CMV). *BioControl.* 60, 135–147. doi: 10.1007/s10526-014-9626-3

Walling, L. L. (2000). The myriad plant response to herbivores. *J. Plant Growth Regul.* 19, 195–216. doi: 10.1007/s003440000026

Walling, L. L. (2008). Avoiding effective defenses: strategies employed by phloem-feeding insects. *Plant Physiol.* 146, 859–866. doi: 10.1104/pp.107.113142

War, A. R., Paulraj, M. G., Ignacimuthu, S., and Sharma, H. C. (2015).Induced resistance to Helicoverpa armigera through exogenous application of jasmonic acid and salicylic acid in groundnut, *Arachis hypogaea*. *Pest Manag. Sci.* 71, 72–82. doi: 10.1002/ps.3764

Wilkinson, T. L., Adams, D., Minto, L. B., and Douglas, A. E. (2001). The impact of host plant on the abundance and function of symbiotic bacteria in an aphid. *J. Experi. Biol.* 204, 3027–3038.

Will, T., Tjallingii, W. F., Thonnessen, A., and van Bel, A. J. (2007). Molecular sabotage of plant defense by aphid saliva. *Proc. Natl. Acad. Scsi. U.S.A.* 104, 10536–10541. doi: 10.1073/pnas.0703535104

Woo, S. L., and Pepe, O. (2018). Microbial consortia: promising probiotics as plant biostimulants for sustainable agriculture. *Front. Plant Sci.* 9:1801. doi: 10.3389/fpls.2018.01801

Woo, S. L., Ruocco, M., Vinale, F., Nigro, M., Marra, R., Lombardi, N., et al. (2014). Trichoderma-based products and their widespread use in agriculture. *Open Mycol. J.* 8, 71–126. doi: 10.2174/1874437001408010071

Woo, S. L., Scala, F., Ruocco, M., and Lorito, M. (2006). The molecular biology of the interactions between *Trichoderma spp.*, phytopathogenic fungi, and plants. *Phytopathology* 96, 181–185. doi: 10.1094/PHYTO-96-0181

Xu, W., and Huang, W. (2017). Calcium-dependent protein kinases in phytohormone signaling pathways. *Int. J. Mol. Sci.* 20:E2436. doi: 10.3390/ijms18112436

Yang, Y., Sun, C., Ren, Y., Hao, S., and Jiang, D. (2014). New route toward building active ruthenium nanoparticles on ordered mesoporous carbons with extremely high stability. *Sci. Rep.* 4:4540. doi: 10.1038/srep04540

Yedidia, I., Benhamou, N., and Chet, I. (1999). Induction of defence responses in cucumber plants (*Cucumissativus L.*) by the biocontrol agent Trichoderma harzianum. *Appl. Environ. Microbiol.* 65:1061–1070.

Yonekura-Sakakibara, K., and Hanada, K. (2011). An evolutionary view of functional diversity in family 1 glycosyltransferases. *Plant J.* 66:182–193. doi: 10.1111/j.1365-313X.2011.04493.x

Young, M. D., Wakefield, M. J., Smyth, G. K., and Oshlack, A. (2010). Gene ontology analysis for RNA-seq: accounting for selection bias. *Genome Biol.* 11:R14. doi: 10.1186/gb-2010-11-2-r14

Zhang, Y., Bai, Y., Wu, G., Zou, S., Chen, Y., Gao, C., et al. (2017). Simultaneous modification of three homoeologs of Ta EDR 1 by genome editing enhances powdery mildew resistance in wheat. *Plant J.* 91, 714–724. doi: 10.1111/tpj.13599

Zhou, M., and Memelink, J. (2016). Jasmonate-responsive transcription factors regulating plant secondary metabolism. *Biotechnol. Adv.* 34, 441–449. doi: 10.1016/j.biotechadv.2016.02.004

Zhu-Salzman, K., and Zeng, R. (2015). Insect response to plant defensive protease inhibitors. *Annu. Rev. Entomol.* 60, 233–252. doi: 10.1146/annurev-ento-010814-020816

Conflict of Interest Statement: The authors declare that the research was conducted in the absence of any commercial or financial relationships that could be construed as a potential conflict of interest.

frontiers in Physiology

ORIGINAL RESEARCH
published: 04 July 2019
doi: 10.3389/fphys.2019.00746

An Egg Parasitoid Efficiently Exploits Cues From a Coevolved Host But Not Those From a Novel Host

*Valeria Bertoldi[1,2], Gabriele Rondoni[1,2], Jacques Brodeur[2] and Eric Conti[1,2]**

[1]Dipartimento di Scienze Agrarie, Alimentari ed Ambientali, Università degli Studi di Perugia, Perugia, Italy, [2]Département de Sciences Biologiques, Institut de Recherche en Biologie Végétale, Université de Montréal, Montréal, QC, Canada

Egg parasitoids have evolved adaptations to exploit host-associated cues, especially oviposition-induced plant volatiles and odors of gravid females, when foraging for hosts. The entire host selection process is critical for successful parasitism and relevant in defining host specificity of parasitoids. We hypothesized that naïve egg parasitoid females reared on their coevolved host are able to exploit cues related to the coevolved host but not those from a novel host. We used the egg parasitoid *Trissolcus japonicus*, its coevolved host *Halyomorpha halys*, and the non-coevolved host *Podisus maculiventris* to evaluate this hypothesis. *H. halys*, a polyphagous pest native from Eastern Asia, has invaded North America and Europe, resulting in serious damage to crops. *T. japonicus* is the most effective egg parasitoid of *H. halys* in its native area and thus considered a major candidate for biological control. This parasitoid was detected in North America and Europe as a result of accidental introductions. Laboratory host range of *T. japonicus* includes *P. maculiventris,* an American predatory stink bug used as a biological control agent of several pests. Using *T. japonicus* reared on its natural host *H. halys*, we tested in a Y-tube olfactometer the responses of naïve parasitoid females to volatiles from tomato plants with a deposited egg mass and feeding punctures of either *H. halys* or *P. maculiventris*. Additionally, using two different olfactometer set-ups, we tested *T. japonicus* responses to volatiles emitted by eggs and mature males and females of *H. halys* or *P. maculiventris*. Tomato plants subjected to oviposition and feeding by *H. halys* were preferred by the wasp compared to clean plants, suggesting a possible activation of an indirect defense mechanism. Furthermore, *T. japonicus* females were attracted by cues from gravid females and mature males of *H. halys* but not from eggs. By contrast, naïve parasitoid females never responded to cues associated with *P. maculiventris*, although this non-target host is suitable for complete parasitoid development. Such lack of responses might reduce the probability of *T. japonicus* locating and parasitizing *P. maculiventris* under field conditions. Our experimental approach properly simulates the parasitoid host-location process and could be combined with the required host specificity tests for risk assessment in biological control programs.

Keywords: *Trissolcus japonicus*, invasive species, *Halyomorpha halys*, herbivore-induced plant volatiles, predator, *Podisus maculiventris*, biological control

OPEN ACCESS

Edited by:
Patrizia Falabella, University of Basilicata, Italy

Reviewed by:
Raúl Alberto Laumann, Embrapa Genetic Resources and Biotechnology, Brazil
Tania Zaviezo, Pontifical Catholic University of Chile, Chile

***Correspondence:**
Eric Conti
eric.conti@unipg.it

Specialty section:
This article was submitted to Invertebrate Physiology, a section of the journal Frontiers in Physiology

Received: *14 December 2018*
Accepted: *31 May 2019*
Published: *04 July 2019*

Citation:
Bertoldi V, Rondoni G, Brodeur J and Conti E (2019) An Egg Parasitoid Efficiently Exploits Cues From a Coevolved Host But Not Those From a Novel Host. Front. Physiol. 10:746. doi: 10.3389/fphys.2019.00746

INTRODUCTION

Efficient exploitation of host-associated cues is a key feature for successful reproduction in insect parasitoids that need to invest their limited time on the location and parasitization of suitable hosts (Godfray, 1994; Vinson, 1998). This foraging process is especially challenging for egg parasitoids because their inactive and often inconspicuous hosts are hardly perceived from a distance (Vinson, 1998; Fatouros et al., 2008; Colazza et al., 2010). Egg parasitoid females have thus evolved adaptations to exploit host-related cues that are highly detectable and reliable indicators of the presence of suitable hosts, such as oviposition-induced plant volatiles and volatiles from gravid host females but also less reliable cues from males and nymphs (Hilker and Meiners, 2006; Conti and Colazza, 2012; Hilker and Fatouros, 2015).

In spite of such highly specialized adaptations, egg parasitoids often show a relatively wide host range, attacking species belonging to a given or related families, or even to different orders, on different plant species (Chantarasa-ard et al., 1984; Mansfield and Mills, 2002; Conti et al., 2004; Salerno et al., 2006; Zhang et al., 2011). Thus, foraging egg parasitoids can exploit different combinations of host-associated cues (Lewis et al., 1982; Vet and Groenewold, 1990; Turlings et al., 1993; Meiners and Hilker, 2000; Peñaflor et al., 2011). Alternatively, the nature of induced plant volatiles might be similar among different plant species, especially when plants belong to the same family (Colazza et al., 2004a,b; Mumm and Dicke, 2010).

Parasitoid host range may appear even wider under laboratory conditions, as some species show the capability to parasitize and develop within species that are not their natural hosts (Barratt et al., 1997; Babendreier et al., 2003). This aspect is interesting from an applied perspective since it allows rearing biocontrol agents on factitious hosts (Hoffmann et al., 2001; Cônsoli and Grenier, 2010) and consents the establishment of novel associations (Wyckhuys et al., 2009; Henry et al., 2010). On the other hand, this can be a limitation to classical biological control due to the apparently wide host range shown by these parasitoids in host-specificity tests, thus suggesting a risk that the candidate biocontrol agent may attack non-target species (Barron et al., 2003; Louda et al., 2003; Girod et al., 2018).

However, how high is the probability that, under field conditions, parasitoids would find and, subsequently, successfully parasitize non-target hosts? Considering that parasitoid host range is shaped not only by host recognition, acceptance, and suitability, but by the entire selection process, the role played by host-related cues in defining host specificity is relevant (Conti et al., 2004; Salerno et al., 2006). Exotic host species provide suitable models to examine the role of host selection cues in parasitoid host specificity. When an exotic herbivorous insect enters a new environment, multiple novel interactions may be established with native species, involving different trophic levels and resulting in unpredictable ecological consequences. From one side, native parasitoids (and other natural enemies) may adapt to the novel host, whereas from the other side, the invading species might disrupt the native trophic systems with possible negative consequences on natural control of native pest populations (Fand et al., 2013; Harvey, 2015; Martorana et al., 2017).

A relevant example is that of the brown marmorated stink bug (BMSB), *Halyomorpha halys* Stål (Hemiptera: Pentatomidae). Native to Eastern Asia, *H. halys* was first recorded in North America in 2003 (Hoebeke and Carter, 2003) and in Europe in 2004 (Wermelinger et al., 2008; Arnold, 2009; Haye et al., 2014). Since then *H. halys* has spread over the two continents and, because of its high polyphagy and capacity to build up large populations, it is causing serious damage to many agricultural systems (Hoebeke and Carter, 2003; Lee et al., 2013). In both invaded continents, several indigenous parasitoids and predators exploit the invasive herbivore, although their efficacy is generally low (Rice et al., 2014; Abram et al., 2015; Haye et al., 2015; Cornelius et al., 2016; Herlihy et al., 2016; Roversi et al., 2017; Costi et al., 2018; Morrison et al., 2018; Stahl, 2018). Interestingly, two native European parasitoids were found to be attracted to plant volatiles induced by oviposition of *H. halys* and to volatiles from males, which might be related to the low host specificity of these parasitoids (Rondoni et al., 2017). However, it has been documented both in America and Europe that *H. halys* may also act as an "evolutionary trap" for some native parasitoid species, which readily accept stink bug eggs as host but cannot successfully develop (Abram et al., 2014; Haye et al., 2015; Konopka et al., 2018). Additionally, *H. halys* may disrupt semiochemical networks, thus affecting the efficacy of local parasitoids (Martorana et al., 2017).

Therefore, in addition to relying on new associations with native parasitoids for control of *H. halys*, the introduction of coevolved parasitoids from the native area of the pest, in Asia, might be also considered. *Trissolcus japonicus* (Ashmead) (Hymenoptera: Scelionidae) is the dominant egg parasitoid of *H. halys* in its native area, with high parasitism rates (60–90%), and a candidate for biological control (Qiu et al., 2007; Yang et al., 2009; Dieckhoff et al., 2017). Nevertheless, its relatively large host range in Asia, together with results from host specificity tests indicating its ability to attack several *Pentatomoidea* species, are of concern to biocontrol practitioners (Haye et al., 2014; Lara et al., 2016; Matsuo et al., 2016; Hedstrom et al., 2017; Botch and Delfosse, 2018). Noticeably, the host range of *T. japonicus* in North America also includes *Podisus maculiventris* (Say) (Hemiptera: Pentatomidae) (Hedstrom et al., 2017; Botch and Delfosse, 2018), a predator of several insect pests including *H. halys* (Pote and Nielsen, 2017). When reared on *H. halys* eggs, *T. japonicus* showed a strong preference for its associated host (Botch and Delfosse, 2018). However, when reared on non-target hosts, this parasitoid showed reduced host-specificity, although a trade-off was observed in terms of reduced brood size and fertility, suggesting specialization to the coevolved host (Botch and Delfosse, 2018).

Because of such risks of non-target effects, *T. japonicus* has not yet been released in the field for biological control. In spite of that, this parasitoid is now present both in North America (Talamas et al., 2015; Milnes et al., 2016; Hedstrom et al., 2017; Morrison et al., 2018; Abram et al., 2019) and Europe (Stahl et al., 2018), likely as a consequence of accidental introductions (Milnes et al., 2016).

Therefore, it would be important to, first, confirm that *T. japonicus* exploits reliable volatile cues associated with its natural host *H. halys* and, second, determine if the parasitoid can also exploit cues associated with non-target *P. maculiventris*. It cannot be ruled out that the parasitoid could respond to cues from non-coevolved hosts as a consequence of learning (Giunti et al., 2015) or conditioning by rearing host (Godfray, 2007; Botch and Delfosse, 2018). However, our investigation is focused on naïve parasitoids reared on their naturally associated host *H. halys*. This species reliably represents the most available host for *T. japonicus* under field conditions in the invaded areas, where the population density of *H. halys* might be higher compared to that of the predatory stink bug *P. maculiventris*.

Here, we carried out olfactometer bioassays to test the following hypotheses: (1) naïve *T. japonicus* females have the innate capacity to efficiently exploit *H. halys* kairomones and oviposition-induced plant synomones and (2) although *T. japonicus* was shown to accept and develop in *P. maculiventris* eggs in the laboratory, naïve females reared on *H. halys* do not respond to cues associated with this new host because of lack of coevolution and learning experience. Using two types of Y-tube olfactometer set-ups (long- and close-distance assays), we tested the parasitoid response to plant and host volatiles, associated with *H. halys* and *P. maculiventris*.

MATERIALS AND METHODS

Insect Rearing

Adults of *H. halys* were originally collected from a population in Hamilton (Ontario, Canada) in 2012 and reared continuously thereafter in nylon ventilated cages (30 cm^3) with raw pumpkin seeds, carrots, green beans, grapes, and potted soybean plants, at 24 ± 1°C, 50 ± 5% relative humidity and a 16:8 h light:dark photoperiod. Eggs of *H. halys* were collected every 2 days and transferred to new cages to maintain the colony or used for parasitoid rearing. Eggs laid on the sides of the cages were collected daily for experiments.

Adults of *P. maculiventris* were originally collected from several locations in London and Ottawa (Ontario, Canada) regions in 2011 and 2012 and partly pooled with individuals provided from a greenhouse supply company (Anatis Bioprotection, Canada). Adults were fed with live mealworm larvae, *Tenebrio molitor* L. (Coleoptera: Tenebrionidae), fresh green beans, and bean plants, and reared in nylon cages at 24 ± 1°C, 50 ± 5% relative humidity and a 16:8 h light:dark photoperiod. Previous studies showed that *P. maculiventris* commonly feeds on plant tissues, especially when prey are scarce, probably to acquire water and nutrients (Ruberson et al., 1986; Valicente and O'Neil, 1995; De Clercq, 2008). First instar larvae, which do not feed, were provided with green beans for moisture. From the second instar onward, nymphs were kept in plastic cylinders and fed with mealworm and green beans. Eggs were collected every 2 days to maintain the colony and daily, from the sides of the cages, for experiments.

T. japonicus was obtained from the Beneficial Insects Introduction Research Unit, USDA Agricultural Research Service, Newark, DE, USA in 2017. Parasitoids were kept in nylon cages (30 cm^3) and provided with a 1:1 (vol/vol) honey water solution on a small piece of ParaFilm®. *T. japonicus* was reared on 24 h-old *H. halys* eggs. Each week, egg masses were glued (Pritt® stick glue) on filter paper, offered to parasitoids, and then transferred to Petri dishes for parasitoid development. After emergence, male and female parasitoids were kept together for mating. For the experiments, insects were isolated in glass tubes before being tested.

Plants

Seeds of tomato (*Lycopersicum esculentum* Mill. cv Rio Grande) were individually sown in plastic pots (Ø: 5.5–8 cm; h: 6.5 cm) filled with a mix of coarse sphagnum peat moss and perlite (Berger BM 6 soil). Plants were maintained in a climatic chamber (24 ± 2°C, 70 ± 5% RH, 12 h:12 h L/D) and irrigated every 3 days. A soluble mixture fertilizer (PlantProd 15N-30P-15K) was added 1 week after germination. Plants 3–4 weeks old were used for the olfactometer assays.

Plant Volatiles

Tomato plants used as a source of volatiles in bioassays were exposed to a reproductive stink bug female of either *H. halys* or *P. maculiventris*. The pentatomid female was placed in a clip cage for 24–72 h and allowed to feed and oviposit on the plant. Plants were regularly checked for finding egg masses, and the female was removed after egg detection on the abaxial leaf surface, whereas eggs were not removed to prevent mechanical damage to plant (Colazza et al., 2004a,b; Fatouros et al., 2005; Conti et al., 2010). When eggs were not found after 72 h, the plant was considered as having being exposed to only feeding activity. To reduce feeding damage by *H. halys* on the plants and to promote oviposition, five sunflower kernels were placed in the clip cage. No prey was provided to *P. maculiventris* to ensure plant feeding by this predaceous stink bug. The plants were tested 24 h after oviposition or after the end of the exposition period (72 h) when there was only feeding. The four treatments were: P + HhFeed: plants with *H. halys* feeding damage but no oviposition; P + HhEggs: plants with *H. halys* feeding damage and oviposition of an egg mass; P + PmFeed: plants where a *P. maculiventris* female had fed but did not oviposit; P + PmEggs: plants where a *P. maculiventris* female had fed and laid an egg mass. Clean tomato plants (CP) were used as control.

Stink Bug Volatiles

Volatile cues from males or females in their reproductive phase or freshly laid eggs of *H. halys* or *P. maculiventris* were tested in the olfactometer vs. clean air. Stink bug males were 1–2 weeks old, sexual maturity occurring about 1 week following emergence (Polajnar et al., 2016). Females were at least 1-week old and in their ovipositional phase, as evident by their physogastric abdomen (De Clercq, 2008; Polajnar et al., 2016). Four adult pentatomids (females or males) were used per bioassay, and

adults were not fed during the assays. Tested egg masses of either *H. halys* or *P. maculiventris* were <24 h old and composed of about 28 and 19 eggs, respectively, as naturally laid on the nylon sides of the rearing cages. The six treatments were volatiles from: *Hh*Fem: four *H. halys* females; *Hh*Mal: four *H. halys* males; *Pm*Fem: four *P. maculiventris* females; *Pm*Mal: four *P. maculiventris* males; *HhEggs*: a single egg mass of *H. halys*; and *PmEggs*: a single egg mass of *P. maculiventris*. Clean air was used in the control arm of the olfactometer against insect volatiles.

Olfactometer Bioassays

A Y-tube olfactometer, made from a glass body (stem: 80 mm; arms: 200 mm at 30° angle between arms; internal diameter 12 mm; outside diameter 15 mm), was used to determine the behavioral responses of female *T. japonicus* to host-associated cues. A stream of air from the laboratory compressed-air supply was purified by a charcoal filter made from a 500 ml flask (Pyrex) with four layers each of alternated charcoal and fiberglass. The stream was then bubbled through water in a second 500 ml flask (Pyrex) to humidify the air before it passed into the olfactometer. The air also passed through flow meters set in each arm at 0.5/0.6 L min^{-1}. The Y-tube was held in a cardboard box, black on the sides and white on bottom, with two holes for connection with the air flow tubes, and illuminated from above by two 18-W cool white fluorescent lamps. A thin pencil line drawn on the base of the olfactometer box at 100 mm from the beginning of stem divided the olfactometer into three parts: the left arm, the right arm, and the common area with the junction of the two arms.

Two different types of olfactometer setups were used: "long-distance" and "close-distance" olfactometer. In the "long-distance" setup, each air stream passed through a 4 L glass jar (Ø: 10–15 cm; h: 30 cm) containing the odor source and connected to the olfactometer arm through a plastic tube (inner diameter 8 mm and outer diameter 12 mm) of about 40 cm of length. For the "close-distance" setup, the source of volatiles were placed close to the olfactometer in two little chambers, each made from a modified 15 ml falcon tube with two holes, one on the cover and one on the bottom, both closed by a brass mesh. These chambers were connected with the tubes carrying the air and placed directly at the ends of the arms of the olfactometer, held with Parafilm wrapped on it. To avoid visual stimuli the chambers were kept outside from the illuminated box containing the olfactometer and in the dark. This type of set-up, similar to others used by Colazza et al. (1999), Conti et al. (2003) and Zhong et al. (2017), aimed at studying the searching behavior of the parasitoid once arrived close to the host colony. The volatiles from stink bug treated plants were tested in the "long-distance" olfactometer, whereas those from adults and eggs of *H. halys* and *P. maculiventris* were tested in both olfactometers. The rationale being that oviposition-induced plant volatiles are probably exploited from a longer range than volatiles from adult stink bugs and from eggs (Conti et al., 2003; Colazza et al., 2010; Hilker and Fatouros, 2015).

The assays were conducted from the 9:00 to 16:00, and the temperature in the bioassay room was maintained at 25°C. A *T. japonicus* female was introduced in the Y-tube at the entrance of the central stem and let move freely for 10 min. After up to five wasps (block) had been tested, the glass olfactometer was cleaned with a laboratory detergent and rinsed with hot tap water. Moreover, the tubes connecting the plants to each of the Y-tube arms were switched to avoid bias. All tested wasps were naïve, 3–8 days old, likely mated, and used only once. Each plant, group of adults or egg masses were used for a set of up to 10 bioassays, each carried out with different parasitoid females. For each treatment, 29–77 replicates were conducted. Overall, only five insects did not respond, i.e., they stayed in the common stem, and were removed from the analysis. The parasitoid's residence time, i.e., the durations and frequency of their presence in each olfactometer arm and in the common stem, was recorded using JWatcher 1.0 (Blumstein et al., 2006).

Data Analyses

For each treatment, percent residence time was calculated as the proportion of time spent in the treatment arm on the total time spent in both arms (i.e., excluding the time spent in the common stem). Percent data were normalized using arcsine square root transformation. Generalized linear models (GLMs, Gaussian error distribution) were fitted to test the attraction of *T. japonicus* females to the different sources of volatiles against clean air or clean plant (Zuur et al., 2009). The effect of blocks was initially included as a random effect in generalized mixed models, but its relevance, evaluated by means of likelihood ratio test, was never justified (Zuur et al., 2009). All analyses were run under R statistical environment (R Core Team, 2014).

RESULTS

"Long-Distance" Assays

Females *T. japonicus* responded to volatiles from tomato plants with feeding damage and an egg mass of *H. halys* (P + HhEggs vs. CP: $p = 0.0013$) but not to volatiles from plants with only feeding punctures by *H. halys* (P + HhFeed vs. CP: $p = 0.382$) (**Figure 1**). In contrast, parasitoid females did not respond to volatiles from plants with feeding damage and an egg mass of *P. maculiventris* (P + PmEggs vs. CP: $p = 0.522$). However, they seemed to be repelled by plants subjected only to feeding by *P. maculiventris* although the results were barely non-significant (P + PmFeed vs. CP: $p = 0.0567$). Finally, the parasitoids did not show a preference for clean control plants or clean air (CP vs. Air: $p = 0.659$) (**Figure 1**).

Parasitoid females did not respond in the "long-distance" olfactometer setup to volatiles emitted by *H. halys* eggs (HhEggs vs. Air: $p = 0.258$), gravid females (HhFem vs. Air: $p = 0.119$) or reproductive males (HhMal vs. Air: $p = 0.848$). Similarly, the parasitoid was not attracted to volatiles from *P. maculiventris* (PmEggs vs. Air: $p = 0.407$; PmFem vs. Air: $p = 0.297$; PmMal vs. Air: $p = 0.090$) (**Figure 2**).

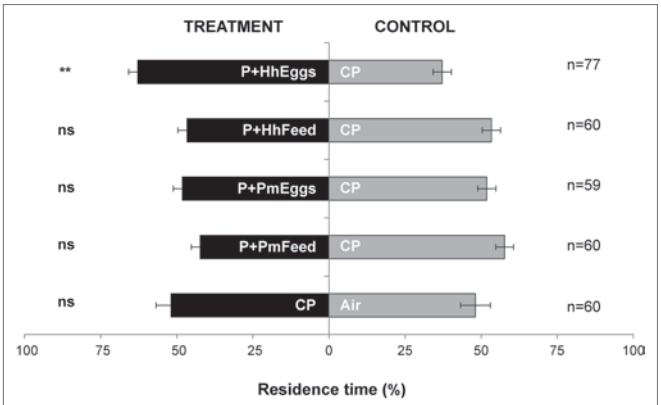

FIGURE 1 | Residence time (mean percentage ± SE) of *Trissolcus japonicus* females in the treatment vs. control arm of a Y-tube olfactometer designed for "long-distance" assays. Treatments were volatiles from tomato plants, where: a *Halyomorpha halys* female had fed and oviposited (P+HhEggs); a *H. halys* female had fed but did not oviposit (P+HhFeed); a *Podisus maculiventris* female had fed and oviposited (P+PmEggs); a *P. maculiventris* female had fed but did not oviposit (P+PmFeed). Volatiles from clean tomato plants were used as controls (CP). Data were analyzed by means of GLMs (**$P < 0.01$; ns: not significant).

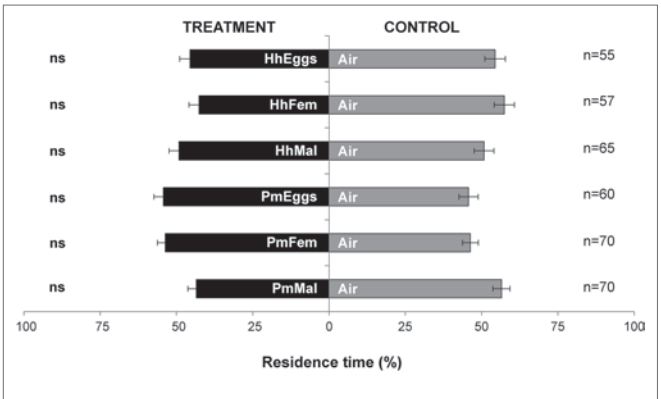

FIGURE 2 | Residence time (mean percentage ± SE) of *Trissolcus japonicus* females in the treatment vs. control arm of a Y-tube olfactometer designed for "long-distance" assays. Treatments were volatiles of: a single egg mass of *Halyomorpha halys* (HhEggs); *H. halys* gravid females (HhFem); *H. halys* mature males (HhMal); a single egg mass of *Podisus maculiventris* (PmEggs); *P. maculiventris* gravid females (PmFem); *P. maculiventris* mated males (PmMal). Air was used as control (Air). Data were analyzed by means GLMs (ns: not significant).

"Close-Distance" Assays

Females of *T. japonicus* were not attracted in the "close-distance" olfactometer setup to volatiles from *H. halys* eggs (HhEggs vs. Air: $p = 0.356$). In contrast, they significantly responded to cues from *H. halys* gravid females (HhFem vs. Air: $p = 0.0052$) and mature males (HhMal vs. Air: $p = 0.0487$). However, *T. japonicus* females never responded to *P. maculiventris* in the "close-distance" olfactometer setup (PmEggs vs. Air: $p = 0.439$; PmFem vs. Air: $p = 0.129$; PmMal vs. Air: $p = 0.620$) (**Figure 3**).

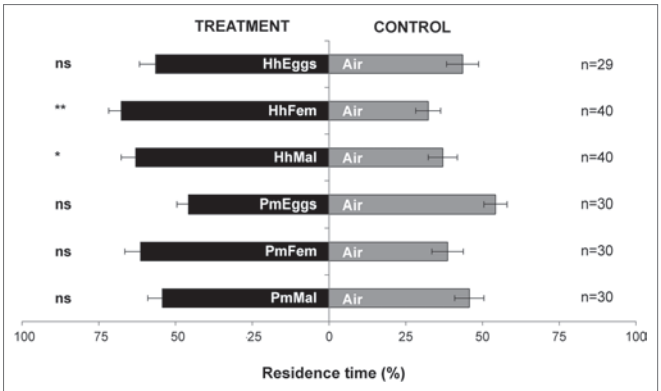

FIGURE 3 | Residence time (mean percentage ± SE) of *Trissolcus japonicus* females in the treatment vs. control arm of a Y-tube olfactometer designed for "close-distance" assays. Treatments were volatiles of: a single egg mass of *Halyomorpha halys* (HhEggs); *H. halys* gravid females (HhFem); *H. halys* males (HhMal); a single egg mass of *Podisus maculiventris* (PmEggs); *P. maculiventris* gravid females (PmFem); *P. maculiventris* males (PmMal). Air was used as control (Air). Data were analyzed by means of GLMs (**$p < 0.01$; *$p < 0.05$; ns: not significant).

DISCUSSION

Here, we demonstrated using "long-distance" olfactometer assays that naïve females of the egg parasitoid *T. japonicus*, reared from its coevolved host *H. halys*, positively respond to volatiles emitted by tomato plants being fed upon and bearing an egg mass of *H. halys*. Using "close-distance" olfactometer assays, we showed that the parasitoids have the capacity to detect and positively respond to cues associated with gravid females and mature males of *H. halys*. In contrast, naïve *T. japonicus* females reared on *H. halys* did not respond to any of the eight treatments involving odors associated with *P. maculiventris*. These results confirm our hypothesis about the capacity of the naïve egg parasitoid, reared on *H. halys*, to exploit cues related to its coevolved host but not those related to the novel association. However, we cannot exclude that experienced parasitoid females or those reared on *P. maculiventris* may also respond to cues from this novel host (Tognon et al., 2014, 2018; Botch and Delfosse, 2018). Additionally, in the "close-distance" setup, the parasitoid showed an apparently similar response to *P. maculiventris* females and *H. halys* males; thus we cannot exclude that a higher number of replications in the former would have resulted in significant values.

The ability of *T. japonicus* to exploit plant volatiles associated with *H. halys* eggs may be consistent with previous findings on host selection strategies developed by egg parasitoids in general and, more specifically, those attacking pentatomids (reviewed by Conti and Colazza, 2012), although we cannot exclude parasitoid response to a combination of plant and egg volatiles rather than just plant volatiles. An "early herbivore alert" (*sensu* Hilker and Meiners, 2006) by the plant denotes a particular type of indirect induced defense that has been observed in several other systems (Colazza et al., 2004a; Conti et al., 2010; Peñaflor et al., 2011). In our experiments, tomato plants subjected to *H. halys* oviposition and feeding were preferred over clean plants by females of *T. japonicus* in olfactometer assays, whereas those subjected only

to feeding were not. Similarly, in a different system, *Trissolcus basalis* (Wollaston) responded to leguminous plants on which *N. viridula* had fed and oviposited compared to control plants, but not to plants on which the host only had fed (Colazza et al., 2004a). The emission of volatiles from leguminous plants was systemic, thus maximizing the release surface and synomone volatilization; additionally, the synomone activity was tuned to parasitoid behavior since preference was higher toward fresh eggs and faded for older eggs that were not suitable for parasitoid development (Colazza et al., 2004a). Chemical analyses of the emitted volatiles showed an increase of (E)-β-caryophyllene (Colazza et al., 2004b). However, of significance, tomato plants that have been used in our system are not native from Asia, although their cultivation has spread worldwide from America in the 16th century, including Eastern China. Thus, tomato defensive responses to *H. halys* may be quite general, against several species, or might result from plant adaptation, although further investigations may provide different explanations.

Interestingly, previous papers showed responses of different parasitoids to volatiles emitted by the plant-herbivore complex and the activation of plant defenses against *H. halys* (Rondoni et al., 2017, 2018). Specifically, the egg parasitoids *Anastatus bifasciatus* (Geoffroy) (Hymenoptera: Eupelmidae) and *Ooencyrtus telenomicida* (Vassiliev) (Hymenoptera: Encyrtidae) positively responded in an olfactometer to volatiles emitted by faba bean plants with oviposition and feeding punctures of *H. halys* and to volatiles from males (Rondoni et al., 2017). Considering that *T. basalis* did not react to *H. halys* induced plant volatiles, exploitation of plant volatiles in this system most likely depends on parasitoid host range, which is much wider for *A. bifasciatus* and *O. telenomicida* compared to *T. basalis* (Rondoni et al., 2017). Thus, complex combinations of indirect (Rondoni et al., 2017) and direct (Rondoni et al., 2018) defense strategies can be activated by plants against invasive herbivore species, suggesting possible existence of general (non-specific), conserved plant defensive mechanisms. One of our olfactometer set-ups for the plant volatile assays tentatively simulated a long-range diffusion of the chemical blend from plants. *T. japonicus* response seems thus consistent with general hypothesis that induced-plant volatiles act as long-distance attractants (Vet and Dicke, 1992; Hilker and Fatouros, 2015), although this is not always the case since in different systems female egg parasitoids only respond to oviposition-induced plant volatiles from a very short distance in static olfactometer (Fatouros et al., 2005, 2009; Conti et al., 2010). Therefore, additive effects from different cues, originated from host and plant, are worth being investigated for *T. japonicus* on plants attacked by *H. halys*.

In our experiments, *T. japonicus* also responded to cues from gravid females and sexually mature males of *H. halys*, but only when using the "close-distance" olfactometer set up, with the volatile sources at the end of the olfactometer arm, whereas it did not respond to host odors in the "long-distance" setup. The reason for these different responses is not clear and possibly depends on the different distance of source from the olfactometer, different concentrations of chemical volatiles or emissions of volatile blends based on the different container sizes and insect crowding conditions, or on a combination of these and other factors. The chemical ecology of *H. halys* has been intensely studied and several compounds have been identified (Khrimian et al., 2014; Harris et al., 2015; Weber et al., 2017; Nixon et al., 2018). Zhong et al. (2017) found that females of *T. japonicus* were attracted in Y-tube assays by n-tridecane, a component of the *H. halys* defensive secretion, and that treatment with this compound significantly improved host-searching efficiency of female *T. japonicus*. By contrast, (E)-2-decenal, also a defensive secretion, was strongly repellent to the parasitoid (Zhong et al., 2017). Therefore, additional investigation will be necessary to understand the role of host-derived cues acting on a short range in host location by *T. japonicus*, including possible vibrational cues from *H. halys* adults, as was shown for other egg parasitoids associated with stink bugs (Laumann et al., 2007, 2011).

Detection of host eggs by parasitoids is more difficult than for larval or adult hosts, as eggs emit small amounts of volatiles, mostly useful as short-range cues (Vet et al., 1995; Vinson, 1998). Accordingly, we did not observe any preference for volatiles from a single egg mass of *H. halys* in the bioassays. This also suggests that *T. japonicus* response to plants with *H. halys* eggs was due to the volatiles emitted from plants as a consequence of oviposition, although it cannot be excluded that the parasitoid is attracted by a combination of both plant and egg volatiles. However, while visual cues may have a role when the parasitoid is close to the egg mass (Sugimoto et al., 1988), they do not appear crucial for egg location, whereas very short-range volatile kairomones from eggs are considered more important, as shown for the egg parasitoid *T. brochymenae* on *M. histrionica* (Conti et al., 2003).

The lack of response by *T. japonicus* to volatiles from any treatments involving *P. maculiventris*, although it was expected from a coevolutionary and behavioral/learning perspective, still needs to be explained from a semiochemical perspective. *P. maculiventris* is a predatory stink bug that also feeds on plant tissues (Ruberson et al., 1986; Valicente and O'Neil, 1995), but no evidence of feeding damage is reported (De Clercq, 2008). In laboratory conditions, *P. maculiventris* often landed on tomato plants to lay eggs and feed (Bertoldi, personal observations). Intriguingly, in our olfactometer observations, tomato plants subjected to feeding by *P. maculiventris* but without oviposition seemed to be almost repellent toward *T. japonicus*. One may consider that plants have the ability to discriminate between herbivorous and predaceous stink bugs and thus emit synomones only when attacked by herbivores, but no data support this speculation. In any case, it seems that oviposition and feeding activity of *P. maculiventris* did not activate the plant indirect defenses or that the parasitoid is not attracted to the combination of volatiles from plant and *P. maculiventris* eggs.

Concerning treatments with only volatiles associated with reproductive females or males of *P. maculiventris*, naïve *T. japonicus* females reared from *H. halys* eggs did not respond in either types of olfactometer. This absence of innate response is not surprising, because of the lack of coevolution of the novel host-parasitoid association, and may be explained by the *P. maculiventris* volatiles, which are mostly different from those of *H. halys* (Aldrich et al., 1984; Kitamura et al., 1984; Harris et al., 2015; Zhong et al., 2017).

From an applied perspective, our results are interesting in the context of *T. japonicus* being the most effective parasitoid of *H. halys* in its native area (Yang et al., 2009; Dieckhoff et al., 2017), as well as a candidate for classical biological control against *H. halys* in newly invaded areas. This parasitoid shows a number of positive attributes, such as high parasitism rate in the field (Qiu et al., 2007; Talamas et al., 2013), short developmental time (Yang et al., 2009), cold tolerance (Santacruz et al., 2017), and climate suitability (Avila and Charles, 2018).

In spite of the concerns raised by the large host range of *T. japonicus*, which involves several stink bug species including *P. maculiventris* (Haye et al., 2014; Matsuo et al., 2016; Hedstrom et al., 2017; Botch and Delfosse, 2018), our results suggest that the probability for *P. maculiventris* to be located by the exotic parasitoid in the field would be low; *T. japonicus* will mainly respond to volatile cues from *H. halys*. This should limit parasitism risk to *P. maculiventris* and potentially to other native Pentatomid species, although it might be possible for *T. japonicus* to detect and parasitize *P. maculiventris* especially where *H. halys* co-exist with other *Pentatomidae*. Additionally, *T. japonicus* was shown to adapt to new hosts or learn to respond to its odor and after that become more prone to choose the new host, reducing its specificity, although there is a cost for such adaptation (Botch and Delfosse, 2018). The effect of the rearing host on parasitoid behavior was also described for other species (Godfray, 2007; Tognon et al., 2014, 2018). Further studies are therefore required to evaluate the physiological and the ecological host range of *T. japonicus* in the areas of introduction and to evaluate the possible effects of adaptation to the new host on the parasitoid ability to exploit host associated volatiles. Testing parasitoid responses to host cues, whether they are newly introduced or candidate for released in biological control programs, would help to predict possible non-target effects. We think that this approach could be complementary to standard host-specificity tests because it examines different host selection steps resulting in a given host-parasitoid association.

AUTHOR CONTRIBUTIONS

VB, GR, JB, and EC conceived and designed the experiments. VB and GR performed the experiments and analyzed the data. VB, GR, JB, and EC interpreted results, drafted, and revised the article.

FUNDING

This research was supported by the Marie Skłodowska-Curie Research and Innovation Staff Exchange (RISE) H2020-MSCA-RISE-2015 of the European Union with the project Impact of invasive alien true bug species in native trophic webs INVASION (GA 690952).

ACKNOWLEDGMENTS

We thank Josée Doyon for insect rearing and technical assistance.

REFERENCES

Abram, P. K., Doyon, J., Brodeur, J., Gariepy, T. D., and Boivin, G. (2015). Susceptibility of *Halyomorpha halys* (Hemiptera: Pentatomidae) eggs to different life stages of three generalist predators. *Can. Entomol.* 147, 222–226. doi: 10.4039/tce.2014.41

Abram, P. K., Gariepy, T. D., Boivin, G., and Brodeur, J. (2014). An invasive stink bug as an evolutionary trap for an indigenous egg parasitoid. *Biol. Invasions* 16, 1387–1395. doi: 10.1007/s10530-013-0576-y

Abram, P. K., Talamas, E. J., Acheampong, S., Mason, P. G., and Gariepy, T. D. (2019). First detection of the samurai wasp, *Trissolcus japonicus* (Ashmead) (Hymenoptera, Scelionidae), in Canada. *J. Hymenopt. Res.* 68, 29–36. doi: 10.3897/jhr.68.32203

Aldrich, J. R., Kochansky, J. P., Lusby, W. R., and Sexton, J. D. (1984). Semiochemicals from a predaceous stink bug, *Podisus maculiventris* (Hemiptera: Pentatomidae). *J. Wash. Acad. Sci.* 74, 39–46.

Arnold, K. (2009). *Halyomorpha halys* (Stål, 1855), eine für die europäische fauna neu nachgewiesene wanzenart (Insecta: Heteroptera: Pentatomidae: Cappaeini). *Mitt Thüringer Entomol.* 16:19.

Avila, G. A., and Charles, J. G. (2018). Modelling the potential geographic distribution of *Trissolcus japoni*cus: a biological control agent of the brown marmorated stink bug, *Halyomorpha halys*. *BioControl* 63, 505–518. doi: 10.1007/s10526-018-9866-8

Babendreier, D., Kuske, S., and Bigler, F. (2003). Non-target host acceptance and parasitism by *Trichogramma brassicae* Bezdenko (Hymenoptera: Trichogrammatidae) in the laboratory. *Biol. Control* 26, 128–138. doi: 10.1016/S1049-9644(02)00121-4

Barratt, B. I. P., Evans, A. A., Ferguson, C. M., Barker, G. M., McNeill, M. R., and Phillips, C. B. (1997). Laboratory nontarget host range of the introduced parasitoids *Microctonus aethiopoides* and *M. hyperodae* (Hymenoptera: Braconidae) compared with field parasitism in New Zealand. *Environ. Entomol.* 26, 694–702. doi: 10.1093/ee/26.3.694

Barron, M. C., Barlow, N. D., and Wratten, S. D. (2003). Non-target parasitism of the endemic New Zealand red admiral butterfly (*Bassaris gonerilla*) by the introduced biological control agent *Pteromalus puparum*. *Biol. Control* 27, 329–335. doi: 10.1016/S1049-9644(03)00028-8

Blumstein, D. T., Evans, C. S., and Daniels, J. C. (2006). JWatcher (Version 1.0). Available at: http://www.jwatcher.ucla.edu (Accessed September 3, 2018).

Botch, P. S., and Delfosse, E. S. (2018). Host-acceptance behavior of *Trissolcus japonicus* (Hymenoptera: Scelionidae) reared on the invasive *Halyomorpha halys* (Heteroptera: Pentatomidae) and nontarget species. *Environ. Entomol.* 47, 403–411. doi: 10.1093/ee/nvy014

Chantarasa-ard, S., Hirashima, Y., and Hirao, J. (1984). Host range and host suitability of *Anagrus incarnatus* Haliday (Hymenoptera: Mymaridae): an egg parasitoid of *Delphacid Planthoppers*. *Appl. Entomol. Zool.* 19, 491–497. doi: 10.1303/aez.19.491

Colazza, S., Fucarino, A., Peri, E., Salerno, G., Conti, E., and Bin, F. (2004a). Insect oviposition induces volatile emission in herbaceous plants that attracts egg parasitoids. *J. Exp. Biol.* 207, 47–53. doi: 10.1242/jeb.00732

Colazza, S., McElfresh, J. S., and Millar, J. G. (2004b). Identification of volatile synomones, induced by *Nezara viridula* feeding and oviposition on bean spp., that attract the egg parasitoid *Trissolcus basalis*. *J. Chem. Ecol.* 30, 945–964. doi: 10.1023/B:JOEC.0000028460.70584.d1

Colazza, S., Peri, E., Salerno, G., and Conti, E. (2010). "Host searching by egg parasitoids: exploitation of host chemical cues" in *Egg parasitoids in agroecosystems with emphasis on Trichogramma*. eds. F. L. Cônsoli, J. R. P. Parra, and R. A. Zucchi (Dordrecht, NL: Springer), 97–147.

Colazza, S., Salerno, G., and Wajnberg, E. (1999). Volatile and contact chemicals released by *Nezara viridula* (Heteroptera: Pentatomidae) have a kairomonal

effect on the egg parasitoid *Trissolcus basalis* (Hymenoptera: Scelionidae). *Biol. Control* 16, 310–317. doi: 10.1006/bcon.1999.0763

Cônsoli, F. L., and Grenier, S. (2010). "*In vitro* rearing of egg parasitoids" in *Egg parasitoids in agroecosystems with emphasis on Trichogramma*. eds. F. L. Cônsoli, J. R. P. Parra, and R. A. Zucchi (Netherlands, NL: Springer), 293–313.

Conti, E., and Colazza, S. (2012). Chemical ecology of egg parasitoids associated with true bugs. *Psyche* 2012:651015. doi: 10.1155/2012/651015

Conti, E., Salerno, G., Bin, F., and Vinson, S. B. (2004). The role of host semiochemicals in parasitoid specificity: a case study with *Trissolcus brochymenae* and *Trissolcus simoni* on pentatomid bugs. *Biol. Control* 29, 435–444. doi: 10.1016/j.biocontrol.2003.08.009

Conti, E., Salerno, G., Bin, F., Williams, H. J., and Vinson, S. B. (2003). Chemical cues from *Murgantia histrionica* eliciting host location and recognition in the egg parasitoid *Trissolcus brochymenae*. *J. Chem. Ecol.* 29, 115–130. doi: 10.1023/A:1021980614512

Conti, E., Salerno, G., Leombruni, B., Frati, F., and Bin, F. (2010). Short-range allelochemicals from a plant–herbivore association: a singular case of oviposition-induced synomone for an egg parasitoid. *J. Exp. Biol.* 213, 3911–3919. doi: 10.1242/jeb.045922

Cornelius, M. L., Dieckhoff, C., Hoelmer, K. A., Olsen, R. T., Weber, D. C., Herlihy, M. V., et al. (2016). Biological control of sentinel egg masses of the exotic invasive stink bug *Halyomorpha halys* (Stål) in Mid-Atlantic USA ornamental landscapes. *Biol. Control* 103, 11–20. doi: 10.1016/j.biocontrol.2016.07.011

Costi, E., Haye, T., and Maistrello, L. (2018). Surveying native egg parasitoids and predators of the invasive *Halyomorpha hal*ys in Northern Italy. *J. Appl. Entomol.* 143, 299–307. doi: 10.1111/jen.12590

De Clercq, P. (2008). "Spined soldier bug, *Podisus maculiventris* Say (Hemiptera: Pentatomidae: Asopinae)" in *Encyclopedia of Entomology*. Vol. 4, ed. J. L. Capinera (Heidelberg: Springer), 3508–3510.

Dieckhoff, C., Tatman, K. M., and Hoelmer, K. A. (2017). Natural biological control of *Halyomorpha halys* by native egg parasitoids: a multi-year survey in northern Delaware. *J. Pest. Sci.* 90, 1143–1158. doi: 10.1007/s10340-017-0868-6

Fand, B. B., Suroshe, S. S., and Gautam, R. D. (2013). Fortuitous biological control of insect pests and weeds: a critical review. *The Bioscan.* 8, 1–10.

Fatouros, N. E., Bukovinszkine'Kiss, G., Kalkers, L. A., Gamborena, R. S., Dicke, M., and Hilker, M. (2005). Oviposition induced plant cues: do they arrest *Trichogramma* wasps during host location? *Entomol. Exp. Appl.* 115, 207–215. doi: 10.1111/j.1570-7458.2005.00245.x

Fatouros, N. E., Dicke, M., Mumm, R., Meiners, T., and Hilker, M. (2008). Foraging behavior of egg parasitoids exploiting chemical information. *Behav. Ecol.* 19, 677–689. doi: 10.1093/beheco/arn011

Fatouros, N. E., Pashalidou, F. G., Cordero, W. V. A., van Loon, J. J., Mumm, R., Dicke, M., et al. (2009). Anti-aphrodisiac compounds of male butterflies increase the risk of egg parasitoid attack by inducing plant synomone production. *J. Chem. Ecol.* 35, 1373–1381. doi: 10.1007/s10886-009-9714-5

Girod, P., Lierhmann, O., Urvois, T., Turlings, T. C., Kenis, M., and Haye, T. (2018). Host specificity of Asian parasitoids for potential classical biological control of *Drosophila suzukii*. *J. Pest. Sci.* 91, 1241–1250. doi: 10.1007/s10340-018-1003-z

Giunti, G., Canale, A., Messing, R. H., Donati, E., Stefanini, C., Michaud, J. P., et al. (2015). Parasitoid learning: current knowledge and implications for biological control. *Biol. Control* 90, 208–219. doi: 10.1016/j.biocontrol.2015.06.007

Godfray, H. C. J. (1994). *Parasitoids: Behavioral and evolutionary ecology*. (Princeton, NJ: Princeton University Press).

Godfray, H. C. J. (2007). "Parasitoids" in *Encyclopedia of Biodiversity*. ed. S. A. Levin (Oxford: Elsevier).

Harris, C., Abubeker, S., Yu, M., Leskey, T., and Zhang, A. (2015). Semiochemical production and laboratory behavior response of the brown marmorated stink bug, *Halyomorpha hal*ys. *PLoS One* 10:11. doi: 10.1371/journal.pone.0140876

Harvey, J. A. (2015). Conserving host–parasitoid interactions in a warming world. *Curr. Opin. Insect Sci.* 12, 79–85. doi: 10.1016/j.cois.2015.09.001

Haye, T., Abdallah, S., Gariepy, T., and Wyniger, D. (2014). Phenology, life table analysis and temperature requirements of the invasive brown marmorated stink bug, *Halyomorpha halys*, in Europe. *J. Pest. Sci.* 87, 407–418. doi: 10.1007/s10340-014-0560-z

Haye, T., Fischer, S., Zhang, J., and Gariepy, T. (2015). Can native egg parasitoids adopt the invasive brown marmorated stink bug, *Halyomorpha halys* (Heteroptera: Pentatomidae), in Europe? *J. Pest Sci* 88, 693–705. doi: 10.1007/s10340-015-0671-1

Hedstrom, C., Lowenstein, D., Andrews, H., Bai, B., and Wiman, N. (2017). Pentatomid host suitability and the discovery of introduced populations of *Trissolcus japonicus* in Oregon. *J. Pest. Sci.* 90, 1169–1179. doi: 10.1007/s10340-017-0892-6

Henry, L. M., May, N., Acheampong, S., Gillespie, D. R., and Roitberg, B. D. (2010). Host-adapted parasitoids in biological control: does source matter? *Ecol. Appl.* 20, 242–250. doi: 10.1890/08-1869.1

Herlihy, M. V., Talamas, E. J., and Weber, D. C. (2016). Attack and success of native and exotic parasitoids on eggs of *Halyomorpha halys* in three Maryland habitats. *PLoS One* 11:3. doi: 10.1371/journal.pone.0150275

Hilker, M., and Fatouros, N. E. (2015). Plant responses to insect egg deposition. *Annu. Rev. Entomol.* 60, 493–515. doi: 10.1146/annurev-ento-010814-020620

Hilker, M., and Meiners, T. (2006). Early herbivore alert: insect eggs induce plant defence. *J. Chem. Ecol.* 32, 1379–1397. doi: 10.1007/s10886-006-9057-4

Hoebeke, E. R., and Carter, M. E. (2003). *Halyomorpha halys* (Stål)(Heteroptera: Pentatomidae): a polyphagous plant pest from Asia newly detected in North America. *Proc. Entomol. Soc. Wash.* 105, 225–237.

Hoffmann, M. P., Ode, P. R., Walker, D. L., Gardner, J., van Nouhuys, S., and Shelton, A. M. (2001). Performance of *Trichogramma ostriniae* (Hymenoptera: Trichogrammatidae) reared on factitious hosts, including the target host, *Ostrinia nubilalis* (Lepidoptera: Crambidae). *Biol. Control* 21, 1–10. doi: 10.1006/bcon.2000.0912

Khrimian, A., Zhang, A., Weber, D. C., Ho, H. Y., Aldrich, J. R., Vermillion, K. E., et al. (2014). Discovery of the aggregation pheromone of the brown marmorated stink bug (*Halyomorpha halys*) through the creation of stereoisomeric libraries of 1-bisabolen-3-ols. *J. Nat. Prod.* 77, 1708–1717. doi: 10.1021/np5003753

Kitamura, C., Wakamura, S., and Takahashi, S. (1984). Identification and functions of ventral glands secretion of some Heteroptera. *Appl. Entomol. Zool.* 19, 33–41. doi: 10.1303/aez.19.33

Konopka, J. K., Poinapen, D., Gariepy, T., and McNeil, J. N. (2018). Understanding the mismatch between behaviour and development in a novel host-parasitoid association. *Sci. Rep.* 8:15677. doi: 10.1038/s41598-018-33756-6

Lara, J., Pickett, C., Ingels, C., Haviland, D. R., Grafton-Cardwell, E., Doll, D., et al. (2016). Biological control program is being developed for brown marmorated stink bug. *Calif. Agric.* 70, 15–23. doi: 10.3733/ca.v070n01p15

Laumann, R. A., Čokl, A., Lopes, A. P., Fereira, J. B., Moraes, M. C. B., and Borges, M. (2011). Silent singers are not safe: selective response of a parasitoid to substrate-borne vibratory signals of stink bugs. *Anim. Behav.* 82, 1175–1183. doi: 10.1016/j.anbehav.2011.08.017

Laumann, R. A., Moraes, M. C. B., Čokl, A., and Borges, M. (2007). Eavesdropping on sexual vibratory signals of stink bugs (Hemiptera: Pentatomidae) by the egg parasitoid *Telenomus podisi*. *Anim. Behav.* 73, 637–649. doi: 10.1016/j.anbehav.2006.09.011

Lee, D.-H., Short, B. D., Joseph, S. V., Bergh, J. C., and Leskey, T. C. (2013). Review of the biology, ecology, and management of *Halyomorpha halys* (Hemiptera: Pentatomidae) in China, Japan, and the Republic of Korea. *Environ. Entomol.* 42, 627–641. doi: 10.1603/EN13006

Lewis, W. J., Nordlund, D. A., Gueldner, R. C., Teal, P. E. A., and Tumlinson, J. H. (1982). Kairomones and their use for management of entomophagous insects. Kairomonal activity for *Trichogramma* spp. of abdominal tips, excretion, and a synthetic sex pheromone blend of *Heliothis zea* (Boddie) moths. *J. Chem. Ecol.* 8, 1323–1331. doi: 10.1007/BF00987765

Louda, S. M., Pemberton, R. W., Johnson, M. T., and Follett, P. (2003). Nontarget effects—the Achilles' heel of biological control? Retrospective analyses to reduce risk associated with biocontrol introductions. *Annu. Rev. Entomol.* 48, 365–396. doi: 10.1146/annurev.ento.48.060402.102800

Mansfield, S., and Mills, N. J. (2002). Host egg characteristics, physiological host range, and parasitism following inundative releases of *Trichogramma platneri* (Hymenoptera: Trichogrammatidae) in walnut orchards. *Environ. Entomol.* 31, 723–731. doi: 10.1603/0046-225X-31.4.723

Martorana, L., Foti, M. C., Rondoni, G., Conti, E., Colazza, S., and Peri, E. (2017). An invasive insect herbivore disrupts plant volatile-mediated tritrophic signalling. *J. Pest. Sci.* 90, 1079–1085. doi: 10.1007/s10340-017-0877-5

Matsuo, K., Honda, T., Itoyama, K., Toyama, M., and Hirose, Y. (2016). Discovery of three egg parasitoid species attacking the shield bug *Glaucias subpunctatus* (Hemiptera: Pentatomidae). *Japan. J. Appl. Entomol. Zool.* 60, 43–45. doi: 10.1303/jjaez.2016.43

Meiners, T., and Hilker, M. (2000). Induction of plant synomones by oviposition of a phytophagous insect. *J. Chem. Ecol.* 26, 221–232. doi: 10.1023/A:1005453830961

Milnes, J. M., Wiman, N. G., Talamas, E. J., Brunner, J. F., Hoelmer, K. A., Buffington, M. L., et al. (2016). Discovery of an exotic egg parasitoid of the brown marmorated stink bug, *Halyomorpha halys* (Stål) in the Pacific Northwest. *Proc. Entomol. Soc. Wash.* 118, 466–470. doi: 10.4289/0013-8797.118.3.466

Morrison, W. R. III, Blaauw, B. R., Nielsen, A. L., Talamas, E., and Leskey, T. C. (2018). Predation and parasitism by native and exotic natural enemies of *Halyomorpha halys* (Stål)(Hemiptera: Pentatomidae) eggs augmented with semiochemicals and differing host stimuli. *Biol. Control* 121, 140–150. doi: 10.1016/j.biocontrol.2018.02.016

Mumm, R., and Dicke, M. (2010). Variation in natural plant products and the attraction of bodyguards involved in indirect plant defense. *Can. J. Zool.* 88, 628–667. doi: 10.1139/Z10-032

Nixon, L. J., Morrison, W. R., Rice, K. B., Brockerhoff, E. G., Leskey, T. C., Guzman, F., et al. (2018). Identification of volatiles released by diapausing brown marmorated stink bug, *Halyomorpha halys* (Hemiptera: Pentatomidae). *PLoS One* 13:1. doi: 10.1371/journal.pone.0191223

Peñaflor, M. F. G. V., Erb, M., Miranda, L. A., Werneburg, A. G., and Bento, J. M. S. (2011). Herbivore-induced plant volatiles can serve as host location cues for a generalist and a specialist egg parasitoid. *J. Chem. Ecol.* 37, 1304–1313. doi: 10.1007/s10886-011-0047-9

Polajnar, J., Maistrello, L., Bertarella, A., and Mazzoni, V. (2016). Vibrational communication of the brown marmorated stink bug (*Halyomorpha halys*). *Physiol. Entomol.* 41, 249–259. doi: 10.1111/phen.12150

Pote, J. M., and Nielsen, A. L. (2017). Life stage specific predation of *Halyomorpha halys* (Stål) by generalist predators. *Biol. Control* 114, 1–7. doi: 10.1016/j.biocontrol.2017.07.007

Qiu, L. F., Yang, Z. Q., and Tao, W. Q. (2007). Biology and population dynamics of *Trissolcus halyomorphae*. *Sci. Silvae Sin.* 43, 62–65. doi: 10.11707/j.1001-7488.20071111

R Core Team (2014). R: a language and environment for statistical computing. R Foundation for Statistical Computing, Vienna.

Rice, K. B., Bergh, C. J., Bergmann, E. J., Biddinger, D. J., Dieckhoff, C., Dively, G., et al. (2014). Biology, ecology, and management of brown marmorated stink bug (Hemiptera: Pentatomidae). *J. Integr. Pest Manag.* 5, 1–13. doi: 10.1603/IPM14002

Rondoni, G., Bertoldi, V., Malek, R., Djelouah, K., Moretti, C., Buonaurio, R., et al. (2018). *Vicia faba* plants respond to oviposition by invasive *Halyomorpha halys* activating direct defences against offspring. *J. Pest. Sci.* 91, 671–679. doi: 10.1007/s10340-018-0955-3

Rondoni, G., Bertoldi, V., Malek, R., Foti, M. C., Peri, E., Maistrello, L., et al. (2017). Native egg parasitoids recorded from the invasive *Halyomorpha halys* successfully exploit volatiles emitted by the plant–herbivore complex. *J. Pest. Sci.* 90, 1087–1095. doi: 10.1007/s10340-017-0861-0

Roversi, P. F., Binazzi, F., Marianelli, L., Costi, E., Maistrello, L., and Sabbatini Peverieri, G. (2017). Searching for native egg-parasitoids of the invasive alien species *Halyomorpha halys* stål (Heteroptera Pentatomidae) in southern europe. *Redia* 99, 63–70. doi: 10.19263/REDIA-99.16.01

Ruberson, J. R., Tauber, M. J., and Tauber, C. A. (1986). Plant feeding by *Podisus maculiventris* (Heteroptera: Pentatomidae): effect on survival, development, and preoviposition period. *Environ. Entomol.* 15, 894–897. doi: 10.1093/ee/15.4.894

Salerno, G., Conti, E., Peri, E., Colazza, S., and Bin, F. (2006). Kairomone involvement in the host specificity of the egg parasitoid *Trissolcus basalis* (Hymenoptera: Scelionidae). *Eur. J. Entomol.* 103, 311–318. doi: 10.14411/eje.2006.040

Santacruz, E. N., Venette, R., Dieckhoff, C., Hoelmer, K., and Koch, R. L. (2017). Cold tolerance of *Trissolcus japonicus* and *T. cultratus*, potential biological control agents of *Halyomorpha halys*, the brown marmorated stink bug. *Biol. Control* 107, 11–20. doi: 10.1016/j.biocontrol.2017.01.004

Stahl, J. (2018). Benefits and risks of using native parasitoids for augumentative biological control of the invasive pest *Halyomorpha halys* in Europe. PhD thesis. Bremen (DE): University of Bremen.

Stahl, J., Tortorici, F., Pontini, M., Bon, M. C., Hoelmer, K., Marazzi, C., et al. (2018). First discovery of adventive populations of *Trissolcus japonicus* in Europe. *J. Pest Sci.* 1–9. doi: 10.1007/s10340-018-0969-x

Sugimoto, T., Shimono, Y., Hata, Y., Nakai, A., and Yahara, M. (1988). Foraging for patchily-distributed leaf-miners by the parasitoid, *Dapsilarthra rufiventris* (Hymenoptera: Braconidae): III. Visual and acoustic cues to a close range patch-location. *Appl. Entomol. Zool.* 23, 113–121. doi: 10.1303/aez.23.113

Talamas, E., Buffington, M., and Hoelmer, K. (2013). New synonymy of *Trissolcus halyomorphae* Yang. *J. Hymenopt. Res.* 33, 113–117. doi: 10.3897/jhr.33.5627

Talamas, E. J., Herlihy, M. V., Dieckhoff, C., Hoelmer, K. A., Buffington, M., Bon, M. C., et al. (2015). *Trissolcus japonicus* (Ashmead)(Hymenoptera, Scelionidae) emerges in North America. *J. Hymenopt. Res.* 43, 119–128. doi: 10.3897/JHR.43.4661

Tognon, R., Sant'Ana, J., Redaelli, L. R., and Meyer, A. L. (2018). Is it possible to manipulate scelionidae wasps' preference to a target host? *Neotrop. Entomol.* 47, 689–697. doi: 10.1007/s13744-018-0607-6

Tognon, R., Sant'Ana, J., and Jahnke, S. M. (2014). Influence of original host on chemotaxic behaviour and parasitism in *Telenomus podisi* Ashmead (Hymenoptera: Platygastridae). *Bull. Entomol. Res.* 104, 781–787. doi: 10.1017/S0007485314000649

Turlings, T. C., Wäckers, F. L., Vet, L. E., Lewis, W. J., and Tumlinson, J. H. (1993). "Learning of host-finding cues by hymenopterous parasitoids" in *Insect learning*. eds. D. R. Papaj and A. C. Lewis (Boston, MA: Springer), 51–78.

Valicente, F. H., and O'Neil, R. J. (1995). Effects of host plants and feeding regimes on selected life history characteristics of *Podisus maculiventris* (Say) (Heteroptera: Pentatomidae). *Biol. Control* 5, 449–461. doi: 10.1006/bcon.1995.1054

Vet, L. E., and Dicke, M. (1992). Ecology of infochemical use by natural enemies in a tritrophic context. *Annu. Rev. Entomol.* 37, 141–172. doi: 10.1146/annurev.en.37.010192.001041

Vet, L. E., and Groenewold, A. W. (1990). Semiochemicals and learning in parasitoids. *J. Chem. Ecol.* 16, 3119–3135. doi: 10.1007/BF00979615

Vet, L. E., Lewis, W. J., and Carde, R. T. (1995). "Parasitoid foraging and learning" in *Chemical ecology of insects 2*. eds. R. T. Cardé and W. J. Bell (Boston, MA: Springer), 65–101.

Vinson, S. B. (1998). The general host selection behavior of parasitoid Hymenoptera and a comparison of initial strategies utilized by larvaphagous and oophagous species. *Biol. Control* 11, 79–96. doi: 10.1006/bcon.1997.0601

Weber, D. C., Morrison, W. R., Khrimian, A., Rice, K. B., Leskey, T. C., Rodriguez-Saona, C., et al. (2017). Chemical ecology of *Halyomorpha halys*: discoveries and applications. *J. Pest. Sci.* 90, 989–1008. doi: 10.1007/s10340-017-0876-6

Wermelinger, B., Wyniger, D., and Forster, B. (2008). First records of an invasive bug in Europe: *Halyomorpha halys* Stal (Heteroptera: Pentatomidae), a new pest on woody ornamentals and fruit trees? *Mitt. Schweiz. Entomol. Ges.* 81, 1–8. doi: 10.5169/seals-402954

Wyckhuys, K. A., Koch, R. L., Kula, R. R., and Heimpel, G. E. (2009). Potential exposure of a classical biological control agent of the soybean aphid, *Aphis glycines*, on non-target aphids in North America. *Biol. Invasions* 11, 857–871. doi: 10.1007/s10530-008-9299-x

Yang, Z. Q., Yao, Y. X., Qiu, L. F., and Li, Z. X. (2009). A new species of *Trissolcus* (Hymenoptera: Scelionidae) parasitizing eggs of *Halyomorpha halys* (Heteroptera: Pentatomidae) in China with comments on its biology. *Ann. Entomol. Soc. Am.* 102, 39–47. doi: 10.1603/008.102.0104

Zhang, Y. Z., Si, S. L., Zheng, J. T., Li, H. L., Fang, Y., Zhu, C. D., et al. (2011). DNA barcoding of endoparasitoid wasps in the genus *Anicetus* reveals high levels of host specificity (Hymenoptera: Encyrtidae). *Biol. Contr.* 58, 182–191. doi: 10.1016/j.biocontrol.2011.05.006

Zhong, Y. Z., Zhang, J. P., Ren, L. L., Tang, R., Zhan, H. X., Chen, G. H., et al. (2017). Behavioral responses of the egg parasitoid *Trissolcus japonicus* to volatiles from adults of its stink bug host, *Halyomorpha halys*. *J. Pest. Sci.* 90, 1097–1105. doi: 10.1007/s10340-017-0884-6

Zuur, A. F., Ieno, E. N., Walker, N. J., Saveliev, A. A., and Smith, G. M. (2009). *Mixed effects models and extensions in ecology with R*. (New York: Springer).

Conflict of Interest Statement: The authors declare that the research was conducted in the absence of any commercial or financial relationships that could be construed as a potential conflict of interest.

frontiers in Physiology

ORIGINAL RESEARCH
published: 05 July 2019
doi: 10.3389/fphys.2019.00813

Trichoderma atroviride P1 Colonization of Tomato Plants Enhances Both Direct and Indirect Defense Barriers Against Insects

*Mariangela Coppola[1], Pasquale Cascone[2], Ilaria Di Lelio[1], Sheridan Lois Woo[2,3,4], Matteo Lorito[1,2,4], Rosa Rao[1,4], Francesco Pennacchio[1,4], Emilio Guerrieri[2] and Maria Cristina Digilio[1,4]**

[1] Department of Agricultural Sciences, University of Naples Federico II, Naples, Italy, [2] CNR–IPSP, Portici, Italy, [3] Department of Pharmacy, University of Naples Federico II, Naples, Italy, [4] Task Force on Microbiome Studies, University of Naples Federico II, Naples, Italy

OPEN ACCESS

Edited by:
Patrizia Falabella, University of Basilicata, Italy

Reviewed by:
Nadia Massa, University of Eastern Piedmont, Italy
Liang Sun, Chinese Academy of Agricultural Sciences, China

***Correspondence:**
Maria Cristina Digilio
digilio@unina.it

Specialty section:
This article was submitted to Invertebrate Physiology, a section of the journal Frontiers in Physiology

Received: *05 April 2019*
Accepted: *11 June 2019*
Published: *05 July 2019*

Citation:
Coppola M, Cascone P, Di Lelio I, Woo SL, Lorito M, Rao R, Pennacchio F, Guerrieri E and Digilio MC (2019) Trichoderma atroviride P1 Colonization of Tomato Plants Enhances Both Direct and Indirect Defense Barriers Against Insects. Front. Physiol. 10:813. doi: 10.3389/fphys.2019.00813

Numerous microbial root symbionts are known to induce different levels of enhanced plant protection against a variety of pathogens. However, more recent studies have demonstrated that beneficial microbes are able to induce plant systemic resistance that confers some degree of protection against insects. Here, we report how treatments with the fungal biocontrol agent *Trichoderma atroviride* strain P1 in tomato plants induce responses that affect pest insects with different feeding habits: the noctuid moth *Spodoptera littoralis* (Boisduval) and the aphid *Macrosiphum euphorbiae* (Thomas). We observed that the tomato plant–*Trichoderma* P1 interaction had a negative impact on the development of moth larvae and on aphid longevity. These effects were attributed to a plant response induced by *Trichoderma* that was associated with transcriptional changes of a wide array of defense-related genes. While the impact on aphids could be related to the up-regulation of genes involved in the oxidative burst reaction, which occur early in the defense reaction, the negative performance of moth larvae was associated with the enhanced expression of genes encoding for protective enzymes (i.e., Proteinase inhibitor I (PI), Threonine deaminase, Leucine aminopeptidase A1, Arginase 2, and Polyphenol oxidase) that are activated downstream in the defense cascade. In addition, *Trichoderma* P1 produced alterations in plant metabolic pathways leading to the production and release of volatile organic compounds (VOCs) that are involved in the attraction of the aphid parasitoid *Aphidius ervi*, thus reinforcing the indirect plant defense barriers. Our findings, along with the evidence available in the literature, indicate that the outcome of the tripartite interaction among plant, *Trichoderma*, and pests is highly specific and only a comprehensive approach, integrating both insect phenotypic changes and plant transcriptomic alterations, can allow a reliable prediction of its potential for plant protection.

Keywords: root symbionts, *Macrosiphum euphorbiae*, *Aphidius ervi*, VOCs, *Spodoptera littoralis*, plant induced defence

INTRODUCTION

Numerous strains of *Trichoderma* species are widely used in agriculture and commercialized as biocontrol agents (BCA) of plant pathogens (Harman et al., 2004), biostimulants, and biofertilizers (Woo et al., 2014).

Their ability to control plant pathogens is mediated by different mechanisms, including competition for nutrients (Chet et al., 1997), the ability to modify the rhizosphere (Benítez et al., 2004), the production of useful secondary metabolites (Vey et al., 2001; Vinale et al., 2014), and direct antagonism of disease agents (mycoparasitism) (Harman et al., 2004). It is also well known that root colonization by these and other non-pathogenic microorganisms may modulate plant defense reactions to challenge the pathogen attack, based on a localized or systemic response, namely, Localized Acquired Resistance (LAR) (Anees et al., 2010), associated with the induction of hormone pathways that involve the activation of Salicylic Acid in Systemic Acquired Resistance (SAR) and of Jasmonic Acid (JA) in Ethylene Induced Systemic Resistance (ISR) (Pieterse et al., 2009). In fact, *Trichoderma* colonization may stimulate plant defense, resulting in the establishment of ISR, which represents an effective response to pathogens, particularly active at the root level, as it has been shown with nematodes (Degenkolb and Vilcinskas, 2016). Moreover, it has been indicated that *Trichoderma* colonization induces a state of priming in the plant that leads to a faster defense response to pathogens (Conrath et al., 2015; Martìnez-Medina et al., 2017), achieved by increasing the intensity of the plant immune response to microbial elicitors by means of microbe-associated molecular patterns (MAMPs); this is mediated by *Trichoderma*, which reduces the effector-triggered susceptibility and concurrently enhances the effector-triggered immunity, thus resulting in a higher level of plant resistance due to a faster and more effective defense response to a future pathogen attack (Lorito et al., 2010).

These findings indicate that these beneficial fungi have a well-documented capacity to manipulate plant defense barriers against pathogens. Their use is completely in line with the mandate of EU Directive 2009/128/EC to achieve a sustainable (reduced) use of chemical plant protection products (PPPs) in agriculture, by promoting the implementation of integrated pest management (IPM) practices and the application of alternative non-synthetic approaches/tools to reduce the negative impact on human health and on the environment. However, it would be highly desirable if the plant metabolic changes induced by these beneficial microorganisms could be active also against insect pests.

To date, only limited studies have determined the insect control activity by plants exposed to *Trichoderma* colonization. Namely, the available information is limited to aphids (Coppola et al., 2019), thrips (Muvea et al., 2014), and caterpillars (Contreras-Cornejo et al., 2018). Battaglia et al. (2013) registered a growth-stimulation effect of *Trichoderma longibrachiatum* MK1 treatments, both on tomato plants and on aphids feeding on them. Maag et al. (2013) observed a positive impact on oilseed rape development following *T. atroviride* LU132 treatment, which was not associated with any change in the defense reaction against *Plutella xylostella*, and in the titer of defense-related hormones, such as JA and SA. Therefore, it is evident that there is a remarkable variability of plant metabolic changes induced by a specific *Trichoderma* strain that may influence feeding and development of different pests.

To unravel the functional basis of these interactions and to identify the crucial plant metabolic changes associated with defense responses relevant from a crop protection perspective, we used an experimental approach based on the integration of accurate bioassays and concurrent transcriptional analyses of plants, to determine and analyze the effect of root colonization by the symbiont, in order to identify the key regulatory genes underlying *Trichoderma*-induced plant defense response.

Three interacting organisms were considered in this study: (1) the tomato plant, *Solanum lycopersicum* L., a staple crop in many areas of the world[1]; (2) two major pests of tomato that adopt different strategies of plant attack: the noctuid moth *Spodoptera littoralis* (Boisduval), a chewing herbivore, and the aphid *Macrosiphum euphorbiae* (Thomas), a piercing–sucking feeder. For this latter, we also considered an effective biological control agent, the parasitic wasp *Aphidius ervi* (Haliday), which is effectively recruited by attractive volatile organic compounds (VOCs) emitted by the plant in response to pest attack, as reported for many other insect natural enemies (Rasmann et al., 2017 and references therein); and (3) the rhizosphere fungus *T. atroviride* strain P1, a laboratory strain known for its antagonistic activity against numerous phytopathogens, including the soil-borne plant pathogenic fungus *Rhizoctonia solani* (Tronsmo, 1989).

MATERIALS AND METHODS

Insect Rearing and Fungal Isolate

S. littoralis larvae were reared on artificial diet, as described in Di Lelio et al. (2014).

The aphid *M. euphorbiae* was reared on the tomato cultivar "San Marzano nano," in a greenhouse, under the following conditions: temperature, 20 ± 2°C; 65% ± 10% RH; 16L:8D photoperiod.

A. ervi, a parasitoid of several macrosiphine aphids, was reared on *Acyrthosiphon pisum* (Harris) as previously described (Guerrieri et al., 2002), under the same climatic conditions as the aphids, in a separate cabinet of the greenhouse.

T. atroviride strain P1 (ATCC 74058) was used in this study. The fungus was originally isolated from wood chips, selected for resistance to low temperature and some fungicides; it is a producer of VOCs (6-*n*-pentyl-6H-pyran-2-one; 6PP), and a good biological control agent (Tronsmo, 1991). The fungus was maintained on potato dextrose agar (PDA; HiMedia) at room temperature and sub-cultured regularly. Conidia were collected from the surface of sporulating fungal cultures (5–7 days) in sterile distilled water and adjusted to a concentration of 10^7 sp ml^{-1}.

[1]http://faostat.fao.org

Seed Treatment and Plant Rearing

S. lycopersicum var. "San Marzano nano" (dwarf; hereinafter indicated as "San Marzano Dwarf") is a tomato variety with determinate growth and a reduced size in comparison to the commercial variety of "San Marzano 2," thus facilitating its use for experiments under controlled growth conditions and/or space constraints (pot, cage, or jar for VOC collection).

The seeds were surface-sterilized in 2% (v/v) sodium hypochlorite for 20 min and then thoroughly rinsed in sterile distilled water. Coating was performed by immersion of seeds in a fresh suspension of *T. atroviride* P1 spores (concentration 10^7 sp ml^{-1}), followed by frequent stirring of the seeds in the slurry to uniformly cover the seed surface, followed by air drying for 24 h; control seeds were similarly treated with water. The seeds were germinated on wet sterile paper disks in the dark, in an environmental chamber at 24°C, and then transplanted to sterile potting soil upon root emergence and grown under controlled conditions at 20 ± 2°C, with a photoperiod of 16:8 h light/dark. After 3 weeks, tomato seedlings were transplanted to 14-cm-diameter plastic pots containing sterilized soil and grown for 2 weeks under the same environmental conditions.

Insect Bioassays

S. littoralis Bioassay

The *Spodoptera* bioassay started 7 weeks after sowing, in order to attain a sufficient plant size, requested for feeding the caterpillars. The bioassay started with 400 newly hatched larvae reared for the first two instars on tomato leaves, freshly cut from P1-tomato plants. After molting to third instar, 32 larvae were singly transferred into the wells of a polystyrene rearing tray (RT32W, Frontier Agricultural Sciences, United States), bottom-lined with 3 ml of 1.5% agar (w/v), to keep the leaf disks turgid, which were daily replaced. The rearing wells, each containing a leaf disk and a single larva, were closed by perforated plastic lids (RTCV4, Frontier Agricultural Sciences, United States). Environmental conditions for *S. littoralis* rearing and assays were 25 ± 1°C, 70 ± 5% RH, and 16L:8D photoperiod. The same procedure was repeated for the *Trichoderma*-free controls.

The survival rate was assessed daily until pupation. The larval weight was assessed daily starting at day 6 from hatching (third instar), in order to avoid mortality due to handling.

M. euphorbiae Bioassay

To assess the effect of *Trichoderma*–tomato plant interactions on *M. euphorbiae* survival, five apterous young adult aphids were gently transferred onto a single plant with the help of a paintbrush. After 24 h, the adult aphids were removed and only five nymphs of their newly laid progeny were left on the plant. Eleven plants were used for each treatment (P1-treated and untreated controls). Aphid survival, development (molting), and the number attaining the adult stage were recorded daily, until survival of the last aphid. The environmental conditions were as follows: 20 ± 1°C, 70 ± 10% UR, and 16L:8D photoperiod.

A. ervi Bioassay

Tomato plants inoculated with *T. atroviride* P1 and untreated controls were tested in a no-choice wind-tunnel bioassay for their attractiveness toward the parasitic wasp *A. ervi*, which attacks several macrosiphine aphids. For each experimental condition, a total of 10 plants were used over several days, and on each occasion, the different treatments were analyzed in a random sequence to reduce any time-related bias. One hundred parasitoid females were singly tested for each target and observed for a maximum of 5 min. The percentage of response (oriented flights, landings on the target) to each target plant was scored. The parameters of the bioassay were set as follows: temperature, 20 ± 1°C; 65 ± 5% RH; wind speed, 25 ± 5 cm s^{-1}; distance between releasing vial and target, 50 cm; photosynthetic photon flux density (PPFD) at releasing point, 700 μmol m^2 s^{-1}.

VOC Collection and Analysis

Volatiles from tomato plants inoculated with *T. atroviride* P1 and control plants were collected immediately after the wind-tunnel bioassay. The airtight entrainment system consisted of a glass jar (20 dm^3) connected to a circulating pump (closed loop), whose flow was adjusted to 200 cm^3 min^{-1}. Before re-entering the pump, the air passed through a glass narrow tube filled with a biphasic phase of 30 mg of Tenax and 20 mg of Carboxen (GERSTEL GmbH & Co., KG, Mulheim an der Ruhr, Germany). Glass jars and pipeline were cleaned with diethyl ether on each measurement, in order to avoid memory effects. Plants were singly placed inside glass jars and VOCs were collected from the system for 3 h (totalling 3.6 dm^3 of air sampled), under a PPFD of 700 μmol m^2 s^{-1}, a temperature of 25 ± 2°C, and an RH of 50 ± 10% in order to avoid anomalous plant responses caused by simultaneous uncontrolled decrease in [CO_2] and increase in RH inside the glass jar. All VOCs were eluted from a tube with redistilled diethyl ether. An Agilent 7890 GC-chromatograph coupled with an Agilent 5975C MSD spectrometer was used to analyze the VOCs (Cascone et al., 2015). The following chromatographic conditions were used: column HP-INNOWax polyethylene glycol (50 m, 200 μm, ID, and 0.4 μm film); splitless mode, oven program: 40°C for 1 min, then a 5°C min^{-1} ramp to 200°C, a 10°C min^{-1} ramp to 220°C, and a 30°C min^{-1} ramp to 260°C; final temperature was held for 3.6 min. Mass spectra were acquired within the 29–350 *m*/*z* interval operating the spectrometer at 70 eV and at scan speed mode. Three scans per second were obtained. The identification of VOCs was done based on both matches of the peak spectra with library spectral database, and comparison with pure standards (**Appendix 1**). All standards were purchased by Sigma-Aldrich (Milan, Italy). After identification, each VOC from the samples was quantified through regression lines built using a set of serial dilutions of pure standards covering similar spans of VOCs as in sampled leaves. Data were analyzed using Agilent MassHunter Workstation software (Agilent 7890A; Agilent Technologies, Santa Clara, CA, United States).

Statistical Analysis

Survival curves of *S. littoralis* and *M. euphorbiae* fed on P1 and control tomato plants were compared by Kaplan–Meier and Log-Rank analysis (GraphPad Prism 6.01). Normality of data was checked with Shapiro–Wilk test and Kolmogorov–Smirnov test,

while homoscedasticity was tested with Levene's test and Barlett's test. Student's *t* test was used to compare larval weights during development from day 6 to pupation.

The number of parasitoids responding, as oriented and un-oriented flight, to each target was compared by a *G* test for independence, as described in Sokal and Rohlf (1995), using the pairwise *G* test procedure (package RVAideMemoire) in R (Hervé, 2017).

The volatile emission patterns, measured as peak areas divided by fresh plant weight, were analyzed by PCA (principal component analysis), ANOVA test ($P < 0.05$), and multivariate analysis of variance (MANOVA). PCA was performed on data mean-centered and scaled to unit variance using the "ropls" R package (Thévenot et al., 2015).

RNA-Seq

Total RNA was extracted using the Plant RNeasy Mini Kit (Qiagen) according to the manufacturer's protocol from three leaves of three plants, 2 months after sowing. Samples were analyzed with the 2100 Bioanalyzer system (Agilent Technologies) for sizing, quantitation, and quality control of RNA. Only samples with a 260/280 nm absorbance >1.8 and a 260/230 nm absorbance >2 were sequenced. Three biological replicates were used for P1 and for control plants. Eight micrograms of total RNA for each sample was shipped for the library preparation and sequencing to an external sequencing service. A paired-end 2 × 30 M reads on Illumina HiSeq 2500 platform was chosen. RNA-seq raw sequences were cleaned using Trim Galore package[2]. Low-quality bases were trimmed from the sequences and then we removed the adapter sequences by Cutadapt (Martin, 2011); default parameters for the paired-end sequences were used. Finally, if one of the pairs was filtered out due to the cleaning procedure, the other pair was also discarded from the downstream analyses.

The cleaned sequences were then used as input for the mapping to the tomato genome (version 2.50) using Bowtie version 2.1.0 (Langmead and Salzberg, 2012) and Tophat version 2.0.8 (Kim et al., 2013). Quantification of the read abundance per gene (exon level) available from iTAG gene annotation (version 2.5) was done using AIR[3].

To identify the set of differentially expressed genes (DEGs) between the conditions/stages, two different statistical approaches—negative binomial test implemented in DESeq package (Anders and Huber, 2010) and negative binomial test and generalized linear model (GLM) implemented in EdgeR package (Robinson et al., 2010)—were used considering false discovery rate (FDR) ≤0.05. The results from the two methods were considered as an intersection to select the sets of DEGs.

Functional Annotation

GO and GOslim annotations for tomato were downloaded from the Biomart section of Ensembl Plant [version SL2.50 (2014-10-EnsemblPlants)] (Kinsella et al., 2011). Moreover, GO was used for GO enrichment of all DEGs together and of up- and down-regulated DEGs, independently. The analysis was carried out by the Goseq Bioconductor package (Young et al., 2010) (method "BH," FDR ≤0.05).

Mapping of enzymatic activities into molecular pathways was acquired from the KEGG database.

RESULTS

S. littoralis Bioassay

Tomato plants inoculated with *Trichoderma* P1 strain had a negative impact on survival and development of *S. littoralis* larvae. The survival rate, from third instar larva to pupation, was significantly lower for larvae fed on P1-treated leaves, compared to control plants (**Figure 1**) (Log-Rank test, $\chi^2 = 9.009$, df = 1, $P = 0.0027$). No difference between treated or untreated plants was noted in the quantity of leaves consumed by experimental larvae. P1 treatment had a negative impact on weight gain of *S. littoralis* larvae. While no statistically significant difference was registered on days 6–9, starting from day 10, the larvae feeding on P1-treated leaves were always significantly lighter than controls (**Figure 2**), and this difference was constant until pupation (Student's *t* test, $P \leq 0.0001$).

M. euphorbiae Bioassay

Aphid survival was measured starting from 1st instar nymphs. Survival was significantly impaired on P1-treated plants compared to controls (**Figure 3**) (Log-Rank test, $\chi^2 = 10.5$, df = 1, $P = 0.0012$). A decline in the survival rate started to be evident on day 8 and was consistent throughout the bioassay, while no difference in the times of molting (to young instars and surviving adults) was observed.

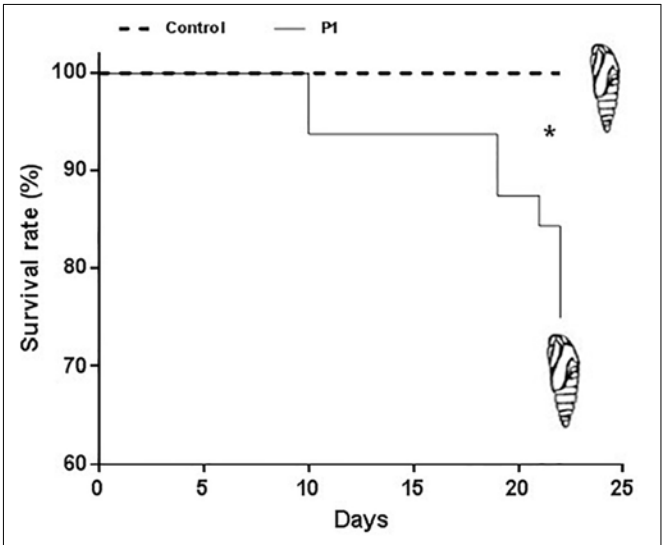

FIGURE 1 | Survival rate of *S. littoralis* larvae, from 3rd instar (time 0) to pupation, reared on tomato leaves obtained from plants treated with *Trichoderma atroviride* P1 or untreated control plants. Asterisk indicates that the two survival curves are significantly different (LogRank test, $P = 0.0027$).

[2]http://www.bioinformatics.babraham.ac.uk/projects/trim_galore/

[3]https://transcriptomics.sequentiabiotech.com/

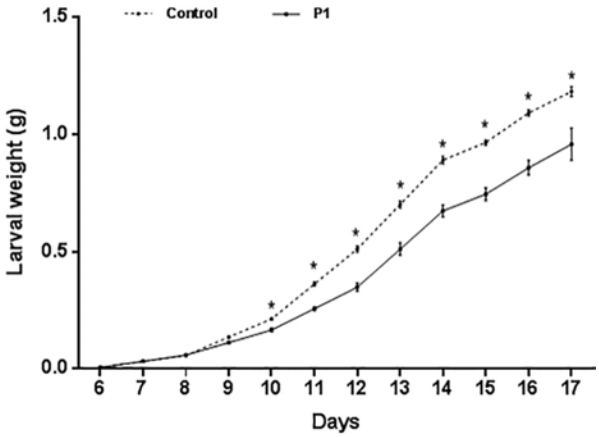

FIGURE 2 | Weight (grams, mean ± SE) of *S. littoralis* larvae, from third instar (day 6) to pupation, reared on tomato leaves obtained from plants treated with *T. atroviride* P1 or untreated control plants. Asterisks indicate a significant difference ($P < 0.0001$) according to Student's *t* test.

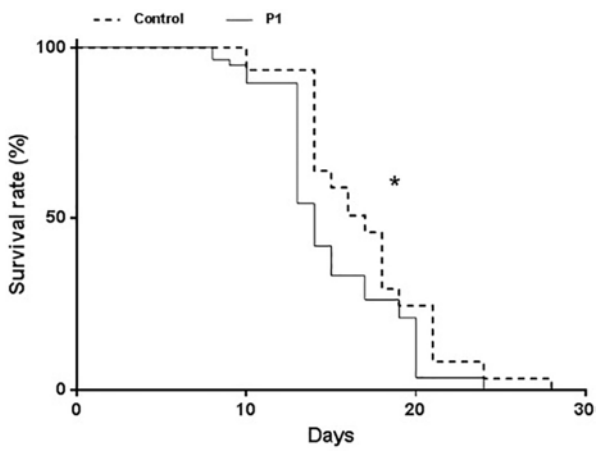

FIGURE 3 | Survival of *Macrosiphum euphorbiae* reared on tomato plants treated with *T. atroviride* P1 or untreated control plants. Asterisk indicates that the two survival curves are significantly different (LogRank test, $P = 0.0012$).

A. ervi Bioassay

The parasitoid behavior was influenced by P1 inoculation in comparison to control plants. Colonization by *T. atroviride* P1 resulted in a significant increase of attraction, with 75% oriented flights (*G* test, $\chi^2 = 50.01$, df = 1, $P < 0.001$) and 50% landings (*G* test, $\chi^2 = 13.21$, df = 1, $P < 0.001$) compared to untreated controls, where oriented flights and landings were 24 and 23%, respectively (**Figure 4**).

VOC Analysis

Gas chromatography (GC) and coupled GC-mass spectrometry (GC–MS) analyses of VOCs collected from treated and untreated tomato plants detected a total of 24 compounds (**Table 1**), with a greater number of VOCs released by the P1 plants.

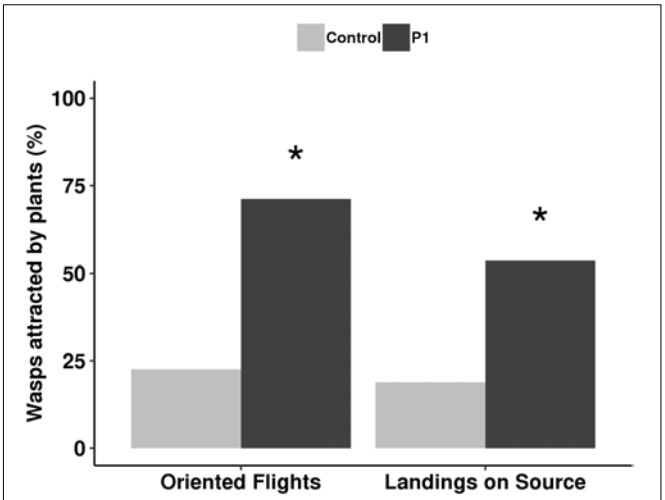

FIGURE 4 | Flight behavior of *Aphidius ervi* females (%) toward tomato plants inoculated with *T. atroviride* P1 and untreated controls. Asterisk indicates a significant difference, assigned by *G* test for independence ($P < 0.001$).

TABLE 1 | GC-MS detection of VOCs released by tomato plants obtained from seeds untreated (Control) and treated with *Trichoderma atroviride* strain P1.

		Mean values ± SE (mg g^{-1} fresh weight)		
	Compounds	**Control**		**P1**
1	2,4 dimethyl-1-heptene	2.3 ± 0.814		1.198 ± 0.61
2	z-3-hexenol	–	*	0.114 ± 0.051
3	ethylbenzene	0.217 ± 0.059		0.087 ± 0.087
4	α-pinene	0.159 ± 0.022	*	3.251 ± 0.625
5	isocumene	–		0.031 ± 0.031
6	benzaldehyde	0.229 ± 0.109		0.568 ± 0.107
7	β-pinene	–		0.384 ± 0.085
8	δ-2-carene	–	*	1.504 ± 0.518
9	1,4-dichlorobenzene	0.906 ± 0.035		0.849 ± 0.554
10	β-cymene	0.051 ± 0.023	*	0.943 ± 0.296
11	2-ethyl-1-hexanol	0.841 ± 0.062		–
12	limonene	–	*	1.01 ± 0.298
13	β-phellandrene	–		0.816 ± 0.725
14	acetophenone	0.235 ± 0.018		0.266 ± 0.081
15	*p*-tolualdehyde	0.282 ± 0.072		0.166 ± 0.096
16	camphor	0.063 ± 0.005		0.127 ± 0.038
17	naphthalene	4.333 ± 0.234		2.039 ± 0.805
18	1-dodecene	0.334 ± 0.02		0.108 ± 0.079
19	methyl salicylate	–	*	0.205 ± 0.093
20	2,4 dimethyl benzaldehyde	0.115 ± 0.025		0.652 ± 0.256
21	2,5 dimethyl benzaldehyde	–		0.779 ± 0.72
22	benzothiazole	0.147 ± 0.012		0.109 ± 0.055
23	carvone	–		0.071 ± 0.06
24	β-caryophyllene	–		0.03 ± 0.018

Asterisks indicate statistically significant differences (ANOVA test; $P < 0.05$, $n = 6$).

In particular, the *Trichoderma* treatment induced the *ex novo* production of z-3-hexenol, δ-2-carene, limonene, and methyl salicylate, not present in the control, and significantly

increased the quantity of emission in α-pinene and β-cymene (**Table 1**). The overall difference in volatile emissions can be fully appreciated on the basis of the PCA analysis, which clearly separated control plants from those inoculated with *T. atroviride* P1 (**Supplementary Figure S1**). The two principal components accounted for 46 and 22% of the total variation in VOC profiles (**Supplementary Figure S1A**).

Trichoderma P1 Massively Manipulates Tomato Plant Transcriptome

Trichoderma P1 inoculation to "Dwarf San Marzano" induced a wide transcriptome reprogramming involving 2513 gene transcripts; among them, 1247 were up-regulated, while 1266 were down-regulated. **Figure 5** shows the Gene Ontology (GO) distribution of DEGs in tomato plants treated with *Trichoderma* P1, based on the "Biological Process" ontological domain. Numerous defense-related genes are included in categories such as "Gene expression," "Transport," and "Response to stimulus." The enrichment analysis underlined the up-regulation of genes included in categories specifically associated with plant defense responses, such as "spermine and spermidine biosynthetic process," "isopentenyl diphosphate biosynthetic process," and "arginine catabolic process" (**Supplementary Figure S2**).

The activation of tomato defense mechanisms associated with *Trichoderma* colonization (Tucci et al., 2011; Hermosa et al., 2012) was clearly indicated in our experiments by the up-regulation of genes involved in early signals as Serine/threonine-protein kinase, Leucine-rich repeat protein kinase family protein, LRKs, glutathione S-transferase, calcium-binding protein, calmodulin-binding transcription activator, peroxidase, and superoxide dismutase 3 (**Supplementary Table S1**). In addition, a large number of up-regulated transcripts code for several classes of genes active late in the plant defense reaction, and therefore directly active against herbivores, such as proteinase inhibitors (PIs) (i.e., wound-induced PI I, Kunitz-type proteinase inhibitor, and metallocarboxypeptidase inhibitor). The transcription of these late genes is induced by JA, the end product of the octadecanoid pathway, which was promoted in P1-treated plants. In fact, transcripts coding for lipoxygenase and allene oxide synthase, two upstream genes of the path, were up-regulated. Other up-regulated late defense genes code for enzymes that reduce the nutritional value of the food ingested or interfere with insect digestion such as threonine deaminase, leucine aminopeptidase A1, arginase 2, and polyphenol oxidase. Interestingly, almost 20 transcripts encoding glycosyltransferases were up-regulated.

Several transcription factors (TFs) were up-regulated [ethylene responsive transcription factors (ERFs), WRKY, MYB, and bZIP TFs] (**Supplementary Table S1**) as well as genes involved in VOC production (i.e., Squalene monooxygenase and terpene) that are part of the gene expression cascade triggered in the plant defense response. The up-regulation of phenylalanine ammonia-lyase (PAL) and hydroxycinnamoyl-CoA shikimate/quinatehydroxycinnamoyl transferase suggests the activation of the phenylpropanoid pathway (**Supplementary Tables S1, S2** and **Supplementary Figure S2**), which is involved in plant direct and indirect defense (Dixon et al., 2002; Mumm et al., 2008). These findings are consistent with those observed in the KEGG analysis: using DEGs in a query to a KEGG database, key enzymes associated with phenylpropanoids and terpenoid biosynthesis were found (**Supplementary Figures S3, S4**), indicating that P1 plant treatment affected phenylalanine metabolism and mevalonate pathway that control the biosynthesis of terpenoids. In particular, the correspondence between enzymes and encoding transcripts was found for three enzymes involved in phenylpropanoid biosynthesis, and seven enzymes implicated in terpenoid biosynthesis (**Table 2**).

As expected, the plants treated with P1 showed the up-regulation of genes involved in the salicylic acid biosynthetic pathway (i.e., S-adenosyl-L-methionine-dependent methyltransferases superfamily protein, SAM), although a number of genes under SA control (i.e., PR1, PR10, Thaumatin, and Osmotin) were noted as down-regulated.

DISCUSSION

The colonization of tomato plants by *T. atroviride* strain P1 triggered plant metabolic changes that limited the survival and development of two pests, the moth *S. littoralis* and the aphid *M. euphorbiae*, which are characterized by different feeding habits, i.e., chewing and piercing-sucking, respectively, eliciting different defense response pathways (Erb and Reymond, 2019).

The *Spodoptera* caterpillars feeding on P1 plants, compared to controls, consumed the same amount of foliar tissue, but showed (1) a reduced larval survival rate, with a lower number of individuals attaining the pupal stage, and (2) a reduced weight gain over time, which resulted in a lower final weight. These developmental alterations are typically associated with the activity of digestive enzyme inhibitors, often aggravated

TABLE 2 | Correspondence between differentially expressed transcripts and enzymes involved in defense-related pathways affected by P1 treatment.

EC ID	Description	Gene ID	Log2 FC
Phenylpropanoid biosynthesis			
ec:4.3.1.25	Phenylalanine ammonia-lyase	Solyc09g007910.3	1, 61
ec:4.3.1.24	Phenylalanine ammonia-lyase 2	Solyc05g056170.3	1, 13
ec:1.11.1.7	Lactoperoxidase	Solyc02g083630.3	1, 3
Terpenoid biosynthesis			
ec:2.3.1.9	C-acetyltransferase	Solyc05g017760.2	1, 71
ec:2.3.3.10	Hydroxymethylglutaryl-CoA synthase	Solyc08g080170.2	2
ec:1.1.1.34	3-hydroxy-3-methylglutaryl CoA reductase	Solyc02g082260.2	3, 35
ec:4.1.1.33	Mevalonate disphosphate decarboxylase	Solyc11g007020.1	1, 86
ec:5.3.3.2	Isopentenyl diphosphate isomerase	Solyc04g056390.2	1, 46
ec:2.5.1.1	Geranyl-diphosphate synthase	Solyc11g011240.1	1, 13
ec:2.5.1.29	Geranylgeranyl pyrophosphate synthase 1	Solyc11g011240.1	1, 13

Enzyme identifiers (KEGG database), gene description and identifiers, and fold changes are listed.

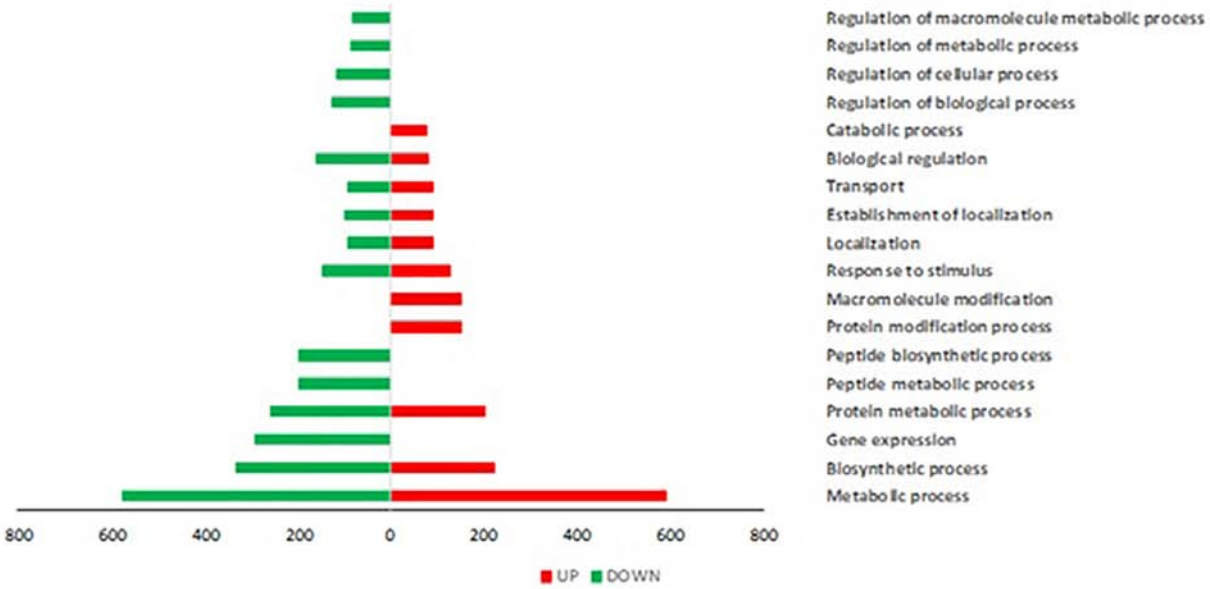

FIGURE 5 | Gene Ontology (GO) distribution of DEGs in tomato plants treated with *Trichoderma* P1, based on the "Biological Process" ontological domain (sequence cutoff: 5%). GO terms are associated to genes up-regulated (red bars, on the right) and down-regulated (green bars, on the left).

by the compensative hyper-production of unaffected enzymes, which further enhances the overall nutritional impairment (Broadway, 1996; Brito et al., 2001; Chen et al., 2005; Brioschi et al., 2007). Plant inoculation with *Trichoderma* P1 is able to enhance the production of PIs in the plant tissues, likely as a consequence of the jasmonate pathway activation. This is further corroborated by the induction of transcripts coding for different classes of PIs and other insect "anti-nutritional" proteins, such as Threonine deaminase, Polyphenol oxidase, and Leucine aminopeptidases, that hinder development. Similarly, maize plants colonized by the same *Trichoderma* species showed reduced leaf herbivory by *S. frugiperda* (Contreras-Cornejo et al., 2018), as a consequence of the octadecanoid pathway induction, leading to JA accumulation in the shoots. These plant changes were associated with an altered feeding behavior and symptoms of midgut damage (presented as a ventral dark area extending over 1/5 of the larva), induced by the exposure to *Trichoderma*-produced VOCs, 6-pentyl-2H-pyran-2-one, and 1-octen-3-ol (Contreras-Cornejo et al., 2018). Moreover, the fine-tuning of defense reactions is associated with arginine catabolic process (VanEtten et al., 1963; Winter et al., 2015), and the up-regulation of genes involved in such process confirms that P1-treated plants are in a "defense state" that is tightly regulated.

The aphid *M. euphorbiae* showed a significantly reduced survival rate when reared on P1-treated plants compared to controls. This effect cannot be related to the release of volatile compounds that affect aphid fixation and behavior (Digilio et al., 2012), as in the first days of the assay, the number of aphids fixed and feeding on plant was similar between P1-treated and control plants. The difference in aphid development can be attributed to the impact of *Trichoderma* on plant direct defenses, which include the production of anti-feedant or inhibitory compounds, such as oryzacystatin, which has inhibitory effect when administered to *Myzus persicae* (Rahbé et al., 2003) and *A. pisum* (Carrillo et al., 2011). The activation of tomato defense response, indicated by the up-regulation of genes active early and late in the plant defense reaction, may be responsible for the impaired aphid performance on P1-treated plants. Starting from early events, P1 effects on tomato transcriptome indicate the activation of the oxidative defense compartment, known for its effect on aphid survival (Coppola et al., 2013; Enders et al., 2014). In addition, the overexpression of PI genes in the attacked plant may reduce the activity of aphid salivary proteases that appear to degrade defense proteins present in the sieve-tube sap (Furch et al., 2015). Intriguingly, it was proposed that the plant protects sap protein degradation by glycosylation that prevents proteolysis (Taoka et al., 2007; Russel et al., 2009). The concerted up-regulation of PIs and glycosyltransferases in *Trichoderma*-treated tomato plants may therefore reduce the aphid ability to degrade sap proteins involved in the defense response. Among the 1247 up-regulated genes, 112 could be grouped as "kinases," indicating a strong impact of the beneficial fungus on the activation of defense signaling pathways. Much evidence shows the essential role of protein phosphorylation in the regulation of plant immunity (Park et al., 2012 and references therein). For instance, in *Arabidopsis*, SNF1/AMPK/SnRK1 protein kinases play a role in detecting the damages caused by insect feeding (Crozet et al., 2014), while in tobacco plants, kinases were found to be involved in the induction of responses to herbivores and wounds (Seo et al., 2007; Wu et al., 2007). Interestingly, it has been demonstrated that protein kinases play a key role in *Arabidopsis* responses against aphids (Shoala et al., 2018).

One of the peculiar aspects of *Trichoderma*–tomato interaction is the positive effect exerted by the fungus on TFs regulating defense gene expression (Segarra et al., 2009; Pieterse et al., 2014; Conrath et al., 2015; Rubio et al., 2017). In our data, genes coding for several families of defense-related TFs (i.e., ERF, WRKY, MYB, and bZIP) are all up-regulated, similarly to what was observed following the interaction of tomato plants with *T. harzianum* T22 (Coppola et al., 2019, this issue). These TFs are involved in innate immunity. For example, in *Arabidopsis*, AP2/ERF proteins are involved in JA inducible gene expression and known as octadecanoid-responsive elements that positively regulate the expression of JA- and ET-mediated defense-related genes (Pré et al., 2008). Specifically, in rice, OsERF3 plays positive roles in resistance against the chewing herbivores, influencing the expression of genes involved in the MAPK cascades and hormone biosynthesis (Lu et al., 2011). Similarly, MYB factors are implicated in JA signaling pathways, playing a role in the defense response against aphids and lepidoptera (AtMYB44 regulates resistance to the green peach aphid and diamondback moth by activating EIN2-affected defenses in *Arabidopsis*). Taken together, these data demonstrate that P1 treatment of tomato plants promoted the expression of a gene network underlying plant defense responses.

The fungus colonization promotes a plant transcriptome reprogramming in which both SA and JA pathways are potentiated, independently from the reported antagonism between these plant hormones (Walling, 2000, 2009; Coppola et al., 2013; Zhang et al., 2015; Li et al., 2016). Recently, higher constitutive levels of ABA and JA, and basal expression of ABA- and JA-related transcripts were found in soybean tolerant genotype (Chapman et al., 2018). In our dataset, the induction of ABA-related (i.e., Abscisic acid inducible protein) and the above-cited JA-related transcripts can be retrieved. In addition, our data are consistent with the recent finding of JA predominance over SA signaling occurring in cotton plants infested by aphids (Eisenring et al., 2018). The potentiation of physical barriers is also a reasonable hypothesis, since the induction of genes involved in cellulose biosynthesis and associated molecules is observed, as well as the up-regulation of several genes involved in phenylpropanoid pathway, which underlies the biosynthesis of lignin precursors and anti-microbial compounds (Naoumkina et al., 2010).

Tomato plants treated with *Trichoderma* P1 showed enhanced attractiveness toward the aphid parasitoid *A. ervi* compared to controls. Such behavioral observations are supported by differential VOC profiles, explaining the parasitoid altered behavior. The terpenoid biosynthesis, evidenced by the KEGG analysis, showed the enhanced expression of several transcripts coding for seven enzymes involved in this VOC-generating pathway. Parasitoid attraction to odor source may result from the release of a "blend" of compounds, rather than by single compounds (Bruce and Pickett, 2011). Among the six compounds whose release was significantly enhanced by the treatment with P1, two can have an important role in parasitoid response: z-3-hexenol and methyl salicylate. These two compounds are both released at a higher rate by tomato plants following aphid attack (Sasso et al., 2007) and have been shown to be detected by *A. ervi* antennae at a concentration as low as 0.1 and 0.01 mg/mL, respectively (Sasso et al., 2009). The same compounds are associated with a significantly higher attraction toward tomato, when the plant was challenged at the same time by *T. harzianum* T22 and *M. euphorbiae* in respect to plants challenged by either of the two (Coppola et al., 2017).

The significant differences in VOC release between treated and untreated plants are further corroborated by the up-regulation of genes involved in both the octadecanoid and salicylic acid pathways. In addition, several enzymes involved in early and late steps of phenylpropanoid biosynthesis, as well as in phenylalanine (PAL) metabolism, are coded by DEGs induced by P1 treatment in tomato. This result is consistent with many of the described effects on the enhancement of tomato defenses against insects described in this work. Phenylpropanoid metabolism generates a wealth of secondary metabolites, based on the few intermediates of the shikimate pathway as the core unit, which are molecules with antimicrobial activity (Didry et al., 1999; Naoumkina et al., 2010) and showing direct repellent activity (Vogt, 2010). PAL and the shikimate are channels for SA biosynthesis in plant (Chen et al., 2009). Thus, our transcriptomic results not only suggest a likely enhancement of physical barriers but also support an antixenotic/antibiotic effect on insects and are consistent with the registered increased emissions of MeSA.

CONCLUSION

In conclusion, P1-treated tomato plants exert a negative impact on the development of *S. littoralis* caterpillars and on *M. euphorbiae*. This direct defense barrier against aphids is nicely complemented by more intense attraction of *A. ervi*, an aphid parasitoid widely used in biocontrol plans and IPM strategies. This makes our results appealing from an applied perspective.

DATA AVAILABILITY

The datasets generated for this study can be found in dd, PRJNA533559.

ETHICS STATEMENT

Animal subjects involved in the study are insect pests (aphids and caterpillars) that we manage on agricultural crops by the use of biocontrol agents (BCA).

AUTHOR CONTRIBUTIONS

MCD, FP, RR, SW, and ML contributed to the study design. MC, PC, and IDL performed the experiments and analyzed the results. MC and MCD wrote the first draft of the manuscript. MC, SW, RR, FP, EG, and MCD wrote sections of the manuscript.

All authors contributed to revise the manuscript, read, and approved the submitted version.

FUNDING

This work was supported by the European Union Horizon 2020 Research and Innovation Program, under grant agreement no. 773554 (EcoStack), and by the FP7—ERANET ARIMNET2 "Sustainable Tomato Production: Plant Defense Enhancement, development of new biopesticides and optimization of environmental, water, and chemical inputs—STomP". This work was partially funded by the Italian Ministry of Foreign Affairs and International Cooperation project PGR00963; Community Scientific Program 2016, Proposal 1966-CSP 2016; Project ProBio – IZSM (Portici), n. D01 6309, 14/12/2016; Project LINFA – MIUR-PON, n. 03PE_00026_1, 09/04/2014; KENYA-AID, n. 10306/CEFA/KEN, 18/05/2017.

SUPPLEMENTARY MATERIAL

The Supplementary Material for this article can be found online at: https://www.frontiersin.org/articles/10.3389/fphys.2019.00813/full#supplementary-material

REFERENCES

Anders, S., and Huber, W. (2010). Differential expression analysis for sequence count data. *Genome Biol.* 11:R106. doi: 10.1186/gb-2010-11-10-r106

Anees, M., Tronsmo, A., Edel-Hermann, V., Hjeljord, L. G., Heraud, C., and Steinberg, C. (2010). Characterization of field isolates of *Trichoderma* antagonistic against *Rhizoctonia solani*. *Fungal Biol.* 114, 691–701. doi: 10.1016/j.funbio.2010.05.007

Battaglia, D., Bossi, S., Cascone, P., Digilio, M. C., Duran Prieto, J., Fanti, P., et al. (2013). Tomato belowground–aboveground interactions: *Trichoderma longibrachiatum* affects the performance of *Macrosiphum euphorbiae* and its natural antagonists. *MPMI* 26, 1249–1256. doi: 10.1094/MPMI-02-13-0059-R

Benítez, T., Rincón, A. M., Limón, M. C., and Codón, A. C. (2004). Biocontrol mechanisms of *Trichoderma* strains. *Int. Microbiol.* 7, 249–260.

Brioschi, D., Nadalini, L. D., Bengtson, M. H., Sogayar, M., Moura, D. S., and Silva-Filho, M. C. (2007). Up regulation of *Spodoptera frugiperda* trypsins and chymotrypsins allows its adaptation to soybean proteinase inhibitor. *Insect Biochem. Mol. Biol.* 37, 1283–1290. doi: 10.1016/j.ibmb.2007.07.016

Brito, L., Lopes, A. R., Parra, J. R. P., Terra, W. R., and Silva-Filho, M. C. (2001). Adaptation of tobacco budworm *Heliothis virescens* to proteinase inhibitors may be mediated by synthesis of new proteinases. *Comp. Biochem. Physiol.* 128B, 365–375. doi: 10.1016/s1096-4959(00)00325-0

Broadway, R. M. (1996). Dietary proteinase inhibitors alter complement of midgut proteases. *Arch. Insect Biochem. Physiol.* 32, 39–53. doi: 10.1002/(sici)1520-6327(1996)32:1<39::aid-arch3>3.3.co;2-h

Bruce, T. J., and Pickett, J. A. (2011). Perception of plant volatile blends by herbivorous insects—finding the right mix. *Phytochemistry* 72, 1605–1611. doi: 10.1016/j.phytochem.2011.04.011

Carrillo, L., Martinez, M., Alvarez-Alfageme, F., Castanera, P., Smagghe, G., Diaz, I., et al. (2011). A barley cysteine–proteinase inhibitor reduces the performance of two aphid species in artificial diets and transgenic *Arabidopsis* plants. *Transgen. Res.* 20, 305–319. doi: 10.1007/s11248-010-9417-2

Cascone, P., Iodice, L., Maffei, M. E., Bossi, S., Arimura, G.-I., and Guerrieri, E. (2015). Tobacco overexpressing β-ocimene induces direct and indirect responses against aphids in receiver tomato plants. *J. Plant Physiol.* 173, 28–32. doi: 10.1016/j.jplph.2014.08.011

Chapman, K. M., Marchi-Werle, L., Hunt, T. E., Heng-Moss, T. M., and Louis, J. (2018). Abscisic and jasmonic acids contribute to soybean tolerance to the soybean aphid (Aphis glycines Matsumura). *Sci. Rep.* 8:15148. doi: 10.1038/s41598-018-33477-w

Chen, H., Curtis, G., Wilkerson, C. G., Kuchar, J. A., Phinney, B. S., and Howe, G. A. (2005). Jasmonate-inducible plant enzymes degrade essential amino acids in the herbivore midgut. *PNAS* 102, 19237–19242. doi: 10.1073/pnas.0509026102

Chen, Z., Zheng, Z., Huang, J., Lai, Z., and Fan, B. (2009). Biosynthesis of salicylic acid in plants. *Plant Signal. Behav.* 4, 493–496. doi: 10.4161/psb.4.6.8392

Chet, I., Inbar, J., and Hadar, I. (1997). "Fungal antagonists and mycoparasites," in *The Mycota IV: Environmental and Microbial Relationships*, eds D. T. Wicklow and B. Söderström (Berlin: Springer-Verlag), 165–184.

Conrath, U., Beckers, G. J., Langenbach, C. J., and Jaskiewicz, M. R. (2015). Priming for enhanced defense. *Annu. Rev. Phytopathol.* 53, 97–119. doi: 10.1146/annurev-phyto-080614-120132

Contreras-Cornejo, H. A., Macías-Rodríguez, L., del-Val, Ek, and Larsen, J. (2018). The root endophytic fungus Trichoderma atroviride induces foliar herbivory resistance in maize plants. *Appl. Soil Ecol.* 124, 45–53. doi: 10.1016/j.apsoil.2017.10.004

Coppola, V., Coppola, M., Rocco, M., Digilio, M. C., D'Ambrosio, C., Renzone, G., et al. (2013). Transcriptomic and proteomic analysis of a compatible tomato–aphid interaction reveals a predominant salicylic acid-dependent plant response. *BMC Genomics* 14:515. doi: 10.1186/1471-2164-14-515

Coppola, M., Cascone, P., Chiusano, M. L., Colantuono, C., Lorito, M., Pennacchio, F., et al. (2017). Trichoderma harzianum enhances tomato indirect defense against aphids. *Insect Sci.* 24, 1025–1033. doi: 10.1111/1744-7917.12475

Coppola, M., Diretto, G., Digilio, M. C., Woo, S. L., Giuliano, G., Molisso, D., et al. (2019). Transcriptome and metabolome reprogramming in tomato plants by *Trichoderma harzianum* strain T22 primes and enhances defence responses against aphids. *Front. Physiol.* 10:745. doi: 10.3389/fphys.2019.00745

Crozet, P., Margalha, L., Confraria, A., Rodrigues, A., Martinho, C., Adamo, M., et al. (2014). Mechanisms of regulation of SNF1/AMPK/SnRK1 protein kinases. *Front. Plant Sci.* 5:190. doi: 10.3389/fpls.2014.00190

Degenkolb, T., and Vilcinskas, A. (2016). Metabolites from nematophagous fungi and nematicidal natural products from fungi as an alternative for biological control. part I: metabolites from nematophagous ascomycetes. *Appl. Microbiol. Biotechnol.* 100, 3799–3812. doi: 10.1007/s00253-015-7233-6

Didry, N., Seidel, V., Dubreuil, L., Tillequin, F., and Bailleul, F. (1999). Isolation and antibacterial activity of phenylpropanoid derivatives from *Ballota nigra*. *J. Ethnopharmacol.* 67, 197–202. doi: 10.1016/S0378-8741(99)00019-7

Digilio, M. C., Cascone, P., Iodice, L., and Guerrieri, E. (2012). Interactions between tomato volatile organic compounds and aphid behaviour. *J. Plant Interact.* 7, 322–325. doi: 10.1080/17429145.2012.727104

Di Lelio, I., Varricchio, P., Di Prisco, G., Marinelli, A., Lasco, V., Caccia, S., et al. (2014). Functional analysis of an immune gene of *S. littoralis* by RNAi. *J. Insect Physiol.* 64, 90–97. doi: 10.1016/j.jinsphys.2014.03.008

Dixon, R., Achnine, L., Kota, P., Liu, C. J., Reddy, M. S. S., and Wang, L. (2002). The phenylpropanoid pathway and plant defence—A genomics perspective. *Mol. Plant Pathol.* 3, 371–390. doi: 10.1046/j.1364-3703.2002.00131.x

Eisenring, M., Glauser, G., Meissle, M., and Romeis, J. (2018). Differential impact of herbivores from three feeding guilds on systemic secondary metabolite induction, phytohormone levels and plant-mediated herbivore interactions. *J. Chem. Ecol.* 44, 1178–1189. doi: 10.1007/s10886-018-1015-4

Enders, L. S., Bickel, R. D., Brisson, J. A., Heng-Moss, T. M., Siegfried, B. D., Zera, A. J., et al. (2014). Abiotic and biotic stressors causing equivalent mortality induce highly variable transcriptional responses in the soybean aphid. *G3* 5, 261–270. doi: 10.1534/g3.114.015149

Erb, M., and Reymond, P. (2019). Molecular interactions between plants and insect herbivores. *Annu. Rev. Plant Biol.* 70, 527–557. doi: 10.1146/annurev-arplant-050718-095910

Furch, A. C., van Bel, A. J., and Will, T. (2015). Aphid salivary proteases are capable of degrading sieve-tube proteins. *J. Exp. Bot.* 66, 533–539. doi: 10.1093/jxb/eru487

Guerrieri, E., Poppy, G. M., Powell, W., Rao, R., and Pennacchio, F. (2002). Plant-to-plant communication mediating in-flight orientation of *Aphidius ervi*. *J. Chem. Ecol.* 28, 1703–1715. doi: 10.1023/A:1020553531658

Harman, G. E., Howell, C. R., Viterbo, A., Chet, I., and Lorito, M. (2004). Trichoderma species-opportunistic, avirulent plant symbionts. *Nat. Rev. Microbiol.* 2, 43–56. doi: 10.1038/nrmicro797

Hermosa, R., Viterbo, A., Chet, I., and Monte, E. (2012). Plant-beneficial effects of *Trichoderma* and of its genes. *Microbiology* 158, 17–25. doi: 10.1099/mic.0.052274-0

Hervé, M. (2017). *RVAideMemoire: Testing and Plotting Procedures for Biostatistics. R Package Version 0.9-73*.

Kim, D., Pertea, G., Trapnell, C., Pimentel, H., Kelley, R., and Salzberg, S. L. (2013). TopHat2: accurate alignment of transcriptomes in the presence of insertions, deletions and gene fusions. *Genome Biol.* 14:R36. doi: 10.1186/gb-2013-14-4-r36

Kinsella, R. J., Kähäri, A., Haider, S., Zamora, J., Proctor, G., Spudich, G., et al. (2011). Ensembl biomarts: a hub for data retrieval across taxonomic space. *Database* 2011:bar030. doi: 10.1093/database/bar030

Langmead, B., and Salzberg, S. L. (2012). Fast gapped-read alignment with Bowtie 2. *Nat. Methods* 9, 357–359. doi: 10.1038/nmeth.1923

Li, Y., Dicke, M., Kroes, A., Liu, W., and Gols, R. (2016). Interactive effects of cabbage aphid and caterpillar herbivory on transcription of plant genes associated with phytohormonal signalling in wild cabbage. *J. Chem. Ecol.* 42, 793–805. doi: 10.1007/s10886-016-0738-3

Lorito, M., Woo, S. L., Harman, G. E., and Monte, E. (2010). Translational research on *Trichoderma*: from 'omics to the field. *Annu. Rev. Phytopathol.* 48, 395–417. doi: 10.1146/annurev-phyto-073009-114314

Lu, J., Ju, H., Zhou, G., Zhu, C., Erb, M., Wang, X., et al. (2011). An EAR-motif-containing ERF transcription factor affects herbivore-induced signaling, defense and resistance in rice. *Plant J.* 68, 583–596. doi: 10.1111/j.1365-313X.2011.04709.x

Maag, D., Kandula, D. R. W., Müller, C., Mendoza-Mendoza, A., Wratten, S. D., Stewart, A., et al. (2013). Trichoderma atroviride LU132 promotes plant growth but not induced systemic resistance to *Plutella xylostella* in oilseed rape. *BioControl* 59, 241–252. doi: 10.1007/s10526-013-9554-7

Martin, M. (2011). Cutadapt removes adapter sequences from high-throughput sequencing reads. 866 EMBNet. *Journal* 17, 10–12. doi: 10.14806/ej.17.1.200

Martìnez-Medina, A., Fernandez, I., Lok, G. B., Pozo, M. J., Pieterse, C. M. J., and Van Wees, S. C. M. (2017). Shifting from priming of salicylic acid- to jasmonic acid-regulated defences by *Trichoderma* protects tomato against the root knot nematode *Meloidogyne* incognita. *New Phytol.* 213, 1363–1377. doi: 10.1111/nph.14251

Mumm, R., Posthumusm, A., and Dicke, M. (2008). Significance of terpenoids in induced indirect plant defence against herbivorous arthropods. *Plant Cell Environ.* 31, 575–585. doi: 10.1111/j.1365-3040.2008.01783.x

Muvea, A. M., Meyhöfer, R., Subramanian, S., Poehling, H. M., Ekesi, S., and Maniania, N. K. (2014). Colonization of onion roots by endophytic fungi and their impacts on the biology of Thrips tabaci. *PLoS One* 9:e108242. doi: 10.1371/journal.pone.0108242

Naoumkina, M. A., Zhao, Q., Gallego-Giraldo, L., Dai, X., Zhao, P. X., and Dixon, R. A. (2010). Genome-wide analysis of phenylpropanoid defence pathways. *Mol. Plant Pathol.* 11, 829–846. doi: 10.1111/j.1364-3703.2010.00648.x

Park, C. J., Caddell, D. F., and Ronald, P. C. (2012). Protein phosphorylation in plant immunity: insights into the regulation of pattern recognition receptor-mediated signalling. *Front. Plant Sci.* 3:177. doi: 10.3389/fpls.2012.00177

Pieterse, C. M. J., Leon-Reyes, A., Van der Ent, S., and van Wees, S. C. M. (2009). Networking by small-molecule hormones in plant immunity. *Nat. Chem. Biol.* 5, 308–316. doi: 10.1038/nchembio.164

Pieterse, C. M., Zamioudis, C., Berendsen, R. L., Weller, D. M., Van Wees, S. C., and Bakker, P. A. (2014). Induced systemic resistance by beneficial microbes. *Annu. Rev. Phytopathol.* 52, 347–375. doi: 10.1146/annurev-phyto-082712-102340

Pré, M., Atallah, M., Champion, A., De Vos, M., Pieterse, C. M., and Memelink, J. (2008). The AP2/ERF domain transcription factor ORA59 integrates jasmonic acid and ethylene signals in plant defence. *Plant Physiol.* 147, 1347–1357. doi: 10.1104/pp.108.117523

Rahbé, Y., Deraison, C., Bonade ì-Bottino, M., Girard, C., Nardon, C., and Jouanin, L. (2003). Effects of the cysteine protease inhibitor oryzacystatin (OC-I) on different aphids and reduced performance of Myzus persicae on OC-I expressing transgenic oilseed rape. *Plant Sci.* 164, 441–450. doi: 10.1016/s0168-9452(02)00402-8

Rasmann, S., Bennett, A., Biere, A., Karley, A., and Guerrieri, E. (2017). Root symbionts: powerful drivers of plant above- and belowground indirect defences. *Insect Sci.* 24, 947–960. doi: 10.1111/1744-7917.12464

Robinson, M. D., McCarthy, D. J., and Smyth, G. K. (2010). edgeR: a bioconductor package for differential expression analysis of digital gene expression data. *Bioinformatics* 26, 139–140. doi: 10.1093/bioinformatics/btp616

Rubio, M. B., Pardal, A. J., Cardoza, R. E., Gutiérrez, S., Monte, E., and Hermosa, R. (2017). Involvement of the transcriptional coactivator ThMBF1 in the biocontrol activity of *Trichoderma harzianum*. *Front. Microbiol.* 8:2273. doi: 10.3389/fmicb.2017.02273

Russel, D., Oldham, N. J., and Davis, B. G. (2009). Site-selective chemical protein glycosylation protects from autolysis and proteolytic degradation. *Carbohydr. Res.* 344, 1508–1514. doi: 10.1016/j.carres.2009.06.033

Sasso, R., Iodice, L., Digilio, M. C., Carretta, A., Ariati, L., and Guerrieri, E. (2007). Host-locating response by the aphid parasitoid *Aphidius ervi* to tomato plant volatiles. *J. Plant Interact.* 2, 175–183.

Sasso, R., Iodice, L., Woodcock, C. M., Pickett, J. A., and Guerrieri, E. (2009). Electrophysiological and behavioural responses of *Aphidius ervi* (Hymenoptera: Braconidae) to tomato plant volatiles. *Chemoecology* 19:195. doi: 10.1007/s00049-009-0023-9

Segarra, G., Van der Ent, S., Trillas, I., and Pieterse, C. M. (2009). MYB72, a node of convergence in induced systemic resistance triggered by a fungal and a bacterial beneficial microbe. *Plant Biol.* 11, 90–96. doi: 10.1111/j.1438-8677.2008.00162.x

Seo, S., Katou, S., Seto, H., Gomi, K., and Ohashi, Y. (2007). The mitogen-activated protein kinases WIPK and SIPK regulate the levels of jasmonic and salicylic acids in wounded tobacco plants. *Plant J.* 49, 899–909. doi: 10.1111/j.1365-313x.2006.03003.x

Shoala, T., Edwards, M. G., Knight, M. R., and Gatehouse, A. M. R. (2018). OXI1 kinase plays a key role in resistance of *Arabidopsis* towards aphids (*Myzus persicae*). *Transgenic Res.* 27, 355–366. doi: 10.1007/s11248-018-0078-x

Sokal, R. R., and Rohlf, F. J. (1995). *Biometry: The Principles and Practice of Statistics in Biological Research*. San Francisco: W.H. Freeman And Company, 887.

Taoka, K., Ham, B. K., Xoconostle-Cázares, B., Rojas, M. R., and Lucas, W. J. (2007). Reciprocal phosphorylation and glycosylation recognition motifs control NCAPP1 interaction with pumpkin phloem proteins and their cell-to-cell movement. *Plant Cell* 19, 1866–1884. doi: 10.1105/tpc.107.052522

Thévenot, E. A., Roux, A., Xu, Y., Ezan, E., and Junot, C. (2015). Analysis of the human adult urinary metabolome variations with age, body mass index, and gender by implementing a comprehensive workflow for univariate and OPLS statistical analyses. *J. Proteome Res.* 14, 3322–3335. doi: 10.1021/acs.jproteome.5b00354

Tronsmo, A. (1989). Effect of fungicides and insecticides on growth of *Botrytis cinerea*, *Trichoderma viride* and *T. harzianum*. *Norw. J. Agric. Sci.* 3, 151–156. doi: 10.1016/S1043-4526(10)59002-8

Tronsmo, A. (1991). Biological and integrated controls of *Botrytis cinerea* on apple with *Trichoderma harzianum*. *Biol. Control* 1, 59–62. doi: 10.1016/1049-9644(91)90102-6

Tucci, M., Ruocco, M., De Masi, L., De Palma, M., and Lorito, M. (2011). The beneficial effect of *Trichoderma* spp. on tomato is modulated by the plant genotype. *Mol. Plant Pathol.* 12, 341–354. doi: 10.1111/j.1364-3703.2010.00674.x

VanEtten, C. H., Miller, R. W., Wolff, I. A., and Jones, Q. (1963). Amino acid composition of twenty-seven selected seed meals. *J. Agric. Food Chem.* 11, 399–410. doi: 10.1021/jf60129a016

Vey, A., Hoagland, R. E., and Butt, T. M. (2001). "Toxic metabolites of fungal biocontrol agents," in *Fungi as Biocontrol Agents: Progress, Problems and Potential*, eds T. M. Butt, C. Jackson, and N. Magan (Bristol: CAB International), 311–346. doi: 10.1079/9780851993560.0311

Vinale, F., Sivasithamparam, K., Ghisalberti, E. L., Woo, S. L., Nigro, M., Marra, R., et al. (2014). Trichoderma secondary metabolites active on plants and fungal pathogens. *Open Mycol. J.* 8, 127–139. doi: 10.2174/1874437001408010127

Vogt, T. (2010). Phenylpropanoid biosynthesis. *Mol. Plant* 3, 2–20. doi: 10.1093/mp/ssp106

Walling, L. L. (2000). The myriad plant responses to herbivores. *J. Plant Growth Regul.* 19, 195–216.

Walling, L. L. (2009). Avoiding effective defenses: strategies employed by phloem-feeding insects. *Plant Physiol.* 146, 859–866. doi: 10.1104/pp.107.113142

Winter, G., Todd, C. D., Trovato, M., Forlani, G., and Funck, D. (2015). Physiological implications of arginine metabolism in plants. *Front. Plant Sci.* 6:534. doi: 10.3389/fpls.2015.00534

Woo, S. L., Ruocco, M., Vinale, F., Nigro, M., Marra, R., Lombardi, N., et al. (2014). Trichoderma-based products and their widespread use in agriculture. *Open Mycol. J.* 8, 71–126. doi: 10.2174/1874437001408010071

Wu, J., Hettenhausen, C., Meldau, S., and Baldwin, I. T. (2007). Herbivory rapidly activates MAPK signaling in attacked and unattacked leaf regions, but not between leaves of *Nicotiana attenuata*. *Plant Cell* 19, 1096–1122. doi: 10.1105/tpc.106.049353

Young, M. D., Wakefield, M. J., Smyth, G. K., and Oshlack, A. (2010). Gene ontology analysis for RNA-seq: accounting for selection bias. *Genome Biol.* 11:R14. doi: 10.1186/gb-2010-11-2-r14

Zhang, S., Li, X., Sun, Z., Shao, S., Hu, L., Ye, M., et al. (2015). Antagonism between phytohormone signalling underlies the variation in disease susceptibility of tomato plants under elevated CO2. *J. Exp. Bot.* 66, 1951–1963. doi: 10.1093/jxb/eru538

Conflict of Interest Statement: The authors declare that the research was conducted in the absence of any commercial or financial relationships that could be construed as a potential conflict of interest.

APPENDIX 1

Standards Used for the Identification of Volatiles Collected by air-Entrainment of Head Space from Tomato Plants. (+)Longifolene, (Z)-3-hexen-1-ol, 3-carene, 6-methyl- 5-hepten-2-one, anisole-p-allyl, camphor, chlorobenzene, *cis*-nerolidol, decane, dodecene, eucalyptol, eugenol, hexanal, humulene (= α-caryophyllene), linalool, methyl salicylate, menthol, ocimene, p-cymene, p-dichlorobenzene (Is), phellandrene, R(+)limonene, S(−)limonene, skatol, terpinolene, (E)-β-caryophyllene, trans-nerolidol, trans-β-farnesene, α-copaene, α/cubebene, α-gurjunene, α-pinene, α-terpinene, α-terpineol, β-myrcene, and γ-terpinene.

frontiers in Physiology

ORIGINAL RESEARCH
published: 24 July 2019
doi: 10.3389/fphys.2019.00926

Gall Wasp Transcriptomes Unravel Potential Effectors Involved in Molecular Dialogues With Oak and Rose

*Sébastien Cambier[1†], Olivia Ginis[1], Sébastien J. M. Moreau[1], Philippe Gayral[1], Jack Hearn[2†], Graham N. Stone[2], David Giron[1], Elisabeth Huguet[1] and Jean-Michel Drezen[1]**

[1] UMR 7261 CNRS, Institut de Recherche sur la Biologie de l'Insecte, Faculté des Sciences et Techniques, Université de Tours, Tours, France, [2] Institute of Evolutionary Biology, The University of Edinburgh, Edinburgh, United Kingdom

OPEN ACCESS

Edited by:
Patrizia Falabella,
University of Basilicata, Italy

Reviewed by:
Sassan Asgari,
The University of Queensland, Australia
Edward F. Connor,
San Francisco State University, United States

***Correspondence:**
Jean-Michel Drezen
drezen@univ-tours.fr

†Present address:
Sébastien Cambier,
Environmental Research and Innovation Department, Luxembourg Institute of Science and Technology, Esch-sur-Alzette, Luxembourg
Jack Hearn,
Department of Vector Biology, Liverpool School of Tropical Medicine, Liverpool, United Kingdom

Specialty section:
This article was submitted to Invertebrate Physiology, a section of the journal Frontiers in Physiology

Received: 03 April 2019
Accepted: 09 July 2019
Published: 24 July 2019

Citation:
Cambier S, Ginis O, Moreau SJM, Gayral P, Hearn J, Stone GN, Giron D, Huguet E and Drezen J-M (2019) Gall Wasp Transcriptomes Unravel Potential Effectors Involved in Molecular Dialogues With Oak and Rose. Front. Physiol. 10:926. doi: 10.3389/fphys.2019.00926

To gain insight into wasp factors that might be involved in the initial induction of galls on woody plants, we performed high throughput (454) transcriptome analysis of ovaries and venom glands of two cynipid gall wasps, *Biorhiza pallida* and *Diplolepis rosae*, inducing galls on oak and rose, respectively. *De novo* assembled and annotated contigs were compared to sequences from phylogenetically related parasitoid wasps. The relative expression levels of contigs were estimated to identify the most expressed gene sequences in each tissue. We identify for the first time a set of maternally expressed gall wasp proteins potentially involved in the interaction with the plant. Some genes highly expressed in venom glands and ovaries may act to suppress early plant defense signaling. We also identify gall wasp cellulases that could be involved in observed local lysis of plant tissue following oviposition, and which may have been acquired from bacteria by horizontal gene transfer. We find no evidence of virus-related gene expression, in contrast to many non-cynipid parasitoid wasps. By exploring gall wasp effectors, this study is a first step toward understanding the molecular mechanisms underlying cynipid gall induction in woody plants, and the recent sequencing of oak and rose genomes will enable study of plant responses to these factors.

Keywords: oak gall wasp, rose gall wasp, gall induction, venom, ovary secretions

INTRODUCTION

Cynipoid wasps (Hymenoptera: Apocrita) constitute a diverse lineage of plant and insect parasites. Although most cynipoid lineages are parasitoids of insect larvae, the well-described family Cynipidae consists entirely of plant-galling wasps (Ronquist, 1999; Ronquist et al., 2015). Around 1400 species of gall wasps parasitizing different plants have been described (Ronquist et al., 2015). While some species gall non-woody herbs (Ronquist and Liljeblad, 2001; Abe et al., 2007), the most familiar species belong to two gall wasp tribes, the Cynipini and Diplolepidini, which induce galls on oak trees and rose bushes, respectively (Ronquist and Liljeblad, 2001; Ronquist et al., 2015).

These gall wasps have the capacity to modify plant host physiology, resulting in the development of complex gall structures that resemble novel plant organs but which are never produced by

healthy plants (Harper et al., 2004). Gall tissues provide food and physical protection for the larvae developing within them (Cornell, 1983; Price et al., 1987; Bailey et al., 2009). Structurally, cynipid galls can be divided into two parts: the larval chamber and the outer gall. The larval chamber, which is structurally similar in almost all cynipid galls (Stone et al., 2002), is lined with nutritive plant tissues on which the larva feeds, and is surrounded by a thin wall of sclerenchyma. The cynipid larva completes its entire development within this chamber. The diversity observed in cynipid gall morphology is the result of variation in the targeted plant organ (Shorthouse et al., 2005) and in gall tissues that develop outside the larval chamber, such as surrounding layers of woody or spongy tissue, complex air spaces within the gall, surface coats of sticky resins, hairs or spines (Stone and Schönrogge, 2003), and extrafloral nectaries (Nicholls et al., 2016; Pierce, 2019). Mature galls formed by members of the same genus may differ enormously in size, color and shape (Stone and Schönrogge, 2003; Bailey et al., 2009), and are diagnostic of the inducing gall wasp species. In consequence, galls are considered to be the extended phenotypes of galler genes (Dawkins, 1982; Stone and Schönrogge, 2003). Overall, this suggests gall wasps have evolved a genuine molecular dialogues with the plant that allows establishment of a precise developmental program resulting in the formation of specific galls as well as preventing or diverting plant defenses. However, while many studies have analyzed the developmental and morphological aspects of gall induction, the molecular mechanisms used by the gall wasps to modify plant host physiology during cecidogenesis (i.e., gall formation) are unknown (Giron et al., 2016; Nabity, 2016).

Cynipid gall development by wasps can be divided into three major steps: (i) initiation, (ii) growth, and (iii) maturation (Rohfritsch, 1992; Stone et al., 2002). Several lines of evidence suggest that gall initiation and development are governed by specific factors produced by gall wasp larvae (Leblanc and Lacroix, 2001). For example, pioneering work (Molliard, 1917) showed that injection of total and crude extracts of larvae of a herb gall wasp, *Aylax papaveris,* into the pistils of *Papaver rhoeas* flowers resulted in developmental responses mimicking the hypertrophy of the parietal placenta observed during cecidogenesis. Continued production of some stimuli by gall wasp larvae is suggested by the fact that in galls of *Diplolepis rosae* on *Rosa canina*, chambers hosting living gall wasp larvae are significantly larger than chambers hosting dead gall wasps or hymenopteran parasitoids. This shows that gall wasp larvae induce specific plant modifications that cannot be triggered or maintained by other Hymenoptera opportunistically developing in galls (Brooks and Shorthouse, 1997). In contrast, the role of maternal secretions (ovarian fluids or venom deposited on host plant cells or injected into them by adult female wasps during oviposition) in cecidogenesis is still a matter of debate. The initiation phase of gall induction is often considered to result from the action of secretions derived from the egg and larva and not from maternal secretions (Stone et al., 2002). However, some observations are compatible with initiation stimuli being present in maternal secretions. Magnus (1914) observed early modifications of plant cells (hypertrophy and hyperplasia) before hatching of *D. rosae* eggs that could not be explained simply by the mechanical wounding of plant tissue. Stimuli driving this response could derive from injected venom or ovary secretions lining the eggs. Bronner (1973) detected proteolytic, cellulolytic and pectinolytic activities at the surface and along the egg stalk of *Biorhiza pallida* naturally laid on oak buds. Bronner (1985) later observed a substance "deposited at oviposition" at the other end of *D. rosae* eggs and in contact with plant epidermal cells that died shortly after oviposition. More recently, cytoplasmic condensation, enlargement of the nucleus and nucleoli and fragmented vacuolation were observed in plant cells adjacent to *D. rosaefolii* maternal fluids deposited during oviposition on the abaxial surface of leaflets of *R. virginiana* (Leblanc and Lacroix, 2001). Limited autolysis of plant tissue led to the creation of a chamber into which the newly hatched larvae subsequently migrated. In this system, as in several other plant-cynipid associations (Shorthouse et al., 2005), tissue changes occur rapidly in zones adjacent to or below the egg's attachment to the host plant epidermis, where the female wasp deposits maternal fluids during oviposition, suggesting that the very first initiation steps of gall induction could depend on adult female gall wasp secretions. Furthermore, a morphological comparison of the venom apparatus in 25 species of Cynipoidea revealed that most gall inducing wasps have better-developed and more prominent structures than closely related parasitoid (i.e., non gall-inducing) wasps (Vårdal, 2006). This is compatible with the hypothesis that the venom of gall wasps could indeed be of functional importance in the interaction with the host plant, an issue recently addressed for other hymenopteran species interacting with plants such as fig wasps (Martinson et al., 2015; Elias et al., 2018) and a seed-parasitic wasp (Paulson et al., 2016).

In this study, we present anatomical data on the venom glands of two gall wasp species, *B. pallida* and *D. rosae*, the large sizes of which further suggest an important investment of the wasps in venomous secretions, and the first venom gland and ovary transcriptomes for any gall inducing cynipid. Our overall aim is to identify candidate genes involved in interactions between the gall wasp and either its host plant or its natural enemies, such as bacteria and fungi that may attack young galls (Taper et al., 1986; Taper and Case, 1987; Wilson, 1995). To achieve this, we first identify transcripts coding for potentially secreted proteins that are substantially differentially expressed between these two tissues. We then use annotation information to identify candidates with possible roles in gall wasp-plant or gall wasp-natural enemy interactions. We use these data to test the hypothesis advanced by Cornell (1983) that gall induction involves symbiotic viral partners by asking whether venom gland or ovary transcriptomes show any evidence of export of gall wasp genes or proteins within viral particles, a mechanism known to be involved in delivery of effectors used by hymenopteran parasitoids to manipulate the physiology of their insect hosts (Drezen et al., 2017). Finally, we assess the novelty of transcripts in gall-inducing cynipids through comparison with published venom gland transcriptomes for a panel of parasitoid Hymenoptera, including figitid cynipoids that represent the sister group and putative ancestral lifestyle of gall inducing cynipids.

MATERIALS AND METHODS

Gall Collection and Tissue Dissection

Oak (*Quercus robur*) bud galls of *B. pallida* were collected in May 2010 in Tours (France, 47° 21′ 22″N, 0° 42′ 10″E). Wild rose (*R. canina*) bud galls of *D. rosae* were harvested in November 2009 in Thilouze (France, 47°14′35″N, 0°34′43″E). Galls were incubated at room temperature until wasp emergence. At this time mature eggs are already present in the ovaries suggesting the wasps are ready for oviposition and that virulence factors are already produced as in most parasitoid wasps. A total of 135 female *B. pallida* and 146 female *D. rosae* were dissected immediately after emergence to isolate ovaries and venom glands (along with their contiguous reservoir for *B. pallida*). Dissections were performed on ice in a sterile phosphate-buffered saline (PBS) droplet. Five venom glands from each species were immediately used for microscopy observations (see below). The remaining venom glands and ovaries were preserved at −80°C in RA1 RNA extraction buffer containing β-mercaptoethanol according to the NucleoSpin RNA II Kit instructions (Macherey-Nagel, France) until enough material could be collected to perform total RNA extractions.

Fluorescence Microscopy and Confocal Microscopy Imaging of Venom Glands

For observation under fluorescence or confocal microscopy, each venom gland was transferred to a microscope slide with reaction wells containing 35 μl of 4% (w/v) paraformaldehyde for 15 min of incubation at room temperature in a dark moisture chamber. Venom glands were washed three times in PBS and cells were permeabilized in 0.1% (v/v) Triton X-100 for 5 min and washed three times in PBS. Actin was stained with fluorescein isothiocyanate (FITC) conjugated phalloidin (0.5 mg/ml final concentration in PBS) for 60 min at room temperature in a dark moisture chamber and washed three times in PBS. Nucleic acids were stained using 40 μl of Hoechst 33258 (10 μg/ml final concentration in PBS) for 10 min and washed three times in PBS. Microscope slides were then covered with a square glass coverslip and observed immediately under a fluorescence microscope (Olympus BX51 with CCD camera DP50) for *B. pallida,* or analyzed under an Olympus Fluoview 500 confocal laser-scanning microscope for *D. rosae*. Filter 330–380 nm and filter 465–495 nm were used for observations of nuclei and actin staining, respectively.

RNA Extraction and Quality Control

RNA extractions were performed using the NucleoSpin RNA II Kit guidelines (Macherey-Nagel, France). Total RNA yields were 120 μg and 19 μg for 130 *B. pallida* ovaries and venom glands, and 16 and 34 μg for 141 *D. rosae* ovaries and venom glands, respectively. Absence of RNase in samples was confirmed by comparing agarose gel electrophoresis profiles of RNA subsamples incubated for 2 h at 37°C to untreated RNA subsamples. RNA quality was evaluated by analyzing samples on a Bioanalyzer (Agilent, France).

cDNA Library Construction and Sequencing

cDNA libraries were constructed from RNA extracted from ovaries and venom glands of *B. pallida* and *D. rosae* using the SMARTer^{TM} PCR cDNA Synthesis Kit (Clontech, France) according to the supplier's instructions. In brief, 1 μg of total RNA was used to perform the first strand cDNA synthesis using a primer hybridizing to the polyA tail. From the single strand cDNA libraries, a cDNA amplification was performed by LD PCR to obtain the optimal amount of double stranded cDNA, which was used for 454 pyrosequencing using a GS FLX Titanium platform (GEH Biogenouest®, Rennes, France). It is noteworthy that the selection of molecules having a polyA tail for cDNA first strand synthesis is supposed to prevent sequencing of transcripts of bacterial origin. Indeed, only a very low level of bacterial RNA contamination could be detected in the sequenced libraries as illustrated by the very low level 23S ribosomal RNA contigs (Bp_contig 01854, Dr_contig 01575) of *Wolbachia* bacteria, a symbiont known to infect both *B. pallida* (Rokas et al., 2002) and *D. rosae* (Plantard et al., 1999).

Bioinformatic Treatment, Functional Annotation, and Sequence Analysis

Raw data generated by 454 pyrosequencing (Genbank/EMBL/DBJ accession number: PRJNA517634) were preprocessed using SnoWhite software (Dlugosch et al., 2013) to remove nonsense sequences including (i) adapters used for reverse transcription and 454 sequencing, (ii) primers, (iii) very short (<15 bp) sequences, and (iv) low quality sequences. In a first step, the preprocessed sequences were assembled with optimal parameters (-minlen 15 -it 0 -ig 0 - icc 0 -icl 5000 -mi 95 -ml 10 -ss 1 -sl 16 -a 15 -rip) using runAssembly (Newbler software, Roche version 2.6) supplied by Geneouest (France). In a second step, the same preprocessed sequences were mapped to the transcriptome resulting from the first assembly using runMapping (Newbler software, Roche version 2.6) with optimal parameters (-minlen 15 - notrim -ss 1 -sl 16 -sc 1 -ml 80% -mi 95% -a 15 -d 15) to obtain the final transcriptome used for the analysis. To annotate the obtained contigs we compared them with the available non-redundant (nr) NCBI protein database using blastx software with an *E*-value cut-off of 10^{-4}.

To assess the potential function of proteins encoded by contigs, we used the Gene Ontology (GO) controlled vocabulary and more particularly GOSlim, a subset of GO terms, which provides a higher level of annotation (Vincent et al., 2010). To this end, an automated GO-annotation of contigs was performed using the Blast2go software and a stringency cut-off of 10^{-6}.

To identify peptide signals and transmembrane domains the assembled sequences were translated into the correct open reading frames (ORFs) using Prodigal (Hyatt et al., 2010) and amino acid sequences were analyzed using signalP 4.0[1] (Nielsen, 2017). SignalP identifies potential signal peptides in amino acid sequences and locates their cleavage sites. In a previous study, we found that most proteins corresponding to highly expressed

[1]http://www.cbs.dtu.dk/services/SignalP/

genes and predicted to contain a peptide signal by SignalP were indeed confirmed by proteomic analysis to be present in the venom of the parasitoid wasp *Chelonus inanitus* (Vincent et al., 2010). In addition, we also used the DeepLoc-1.0 program that predicts the localization (subcellular or extracellular) of eukaryotic proteins[2].

Gall wasp contigs were specifically compared using blastx and tblastx programs to available parasitoid wasp transcriptomes from NCBI public databases and from a homemade database collecting sequences of venom components reported from a selection of parasitoid species. This set comprised two species (*Leptopilina boulardi* and *L. heterotoma*) (Colinet et al., 2013a,b; Poirié et al., 2014) in the family Figitidae, the sister group of Cynipidae within the superfamily Cynipoidea, two species in the family Pteromalidae of the superfamily Chalcidoidea [*Pteromalus puparum* (Zhu et al., 2010) and *Nasonia vitripennis]* (Danneels et al., 2010; de Graaf et al., 2010), and four more distantly related species in the Hymenoptera (*C. inanitus* (Vincent et al., 2010) and *Microplitis demolitor* (Burke and Strand, 2014), in the family Braconidae and *Pimpla hypochondriaca* (Dani et al., 2005) and *Hyposoter didymator* (Dorémus et al., 2013) in the family Ichneumonidae).

For gene expression analysis, the number of expressed reads was counted and normalized using RPKM (reads per kb million reads: number of reads $\times$ 10^9/contig length $\times$ total reads of the library) (Mortazavi et al., 2008). Contigs were considered as differentially expressed when RPKM values were at least 20 times higher in one tissue than in the other. Comparison of expression levels by qRT-PCR and 454 RPKM in our previous work using the same experimental approach revealed that the number of reads obtained using 454 sequencing reflected the level of expression and that this value was a good cut-off to define over- or under-expressed genes (Chevignon et al., 2014, 2015).

RESULTS

Fluorescence Microscopy and Confocal Microscopy Imaging of Venom Apparatuses

For informed selection of tissues to use for transcriptomic analyses we performed a detailed examination of the venom apparatus of the two gall-wasps species studied, which revealed two different organizations (**Figures 1A,B**). The venom apparatus of *B. pallida* includes a very large reservoir (approximately 2.5 to 3 mm long) relative to other similarly sized Hymenoptera, and a single tubular gland composed of a simple glandular epithelium (**Figure 2A**). Each glandular cell is connected to a central canal via a small duct (ductule) rich in actin that was stained positively by FITC-conjugated phalloidin (**Figure 2B**). Nuclei of these cells are large and round (**Figure 2C**). The dorsal side of the reservoir incorporates a loose secondary secretory zone characterized by cells with small isolated nuclei, round to triangular in shape and organized in a simple epithelium (**Figures 2B–D**). The remaining surface of the reservoir wall consists of a very loose simple epithelium, the cells of which have an elongated nucleus (**Figures 2C,D**). On its external side, the reservoir wall is lined with a loose network of long and striated skeletal muscles with fusiform nuclei (**Figures 2B–D**). Rupture of the reservoir in saline buffer resulted in leakage of a very dense and viscous venom (**Figure 2A**). Observation at high magnification revealed that the venom of *B. pallida* is full of spherical particles approximately 1 to 2 μm in diameter (**Figure 3**) that remained unstained by DAPI (for detection of nucleic acids) or FITC-conjugated phalloidin (data not shown).

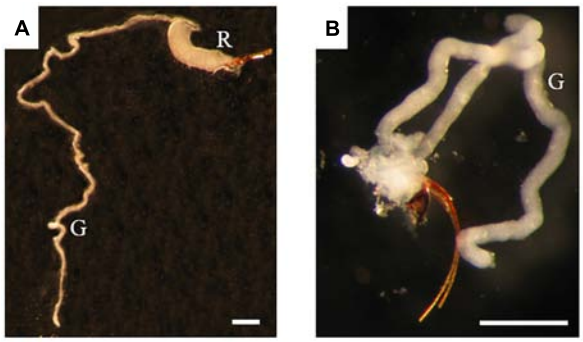

FIGURE 1 | Venom apparatus of *B. pallida* **(A)** and *D. rosae* **(B)** females. G, venom gland; R, venom reservoir. Scale bars = 0,6 mm.

The venom apparatus of *D. rosae* consists of a long and branched gland (approximately 400 μm long) whose central canal is supported by an internal helix containing actin (**Figure 4**). No ductules or reservoir are visible. Each glandular cell contains a large and round nucleus. The gland epithelium is surrounded by a loose network of skeletal muscular cells. Surrounding the muscular fibers is a mesenchymal tissue, the cells of which have fusiform nuclei. The venom could not be distinguished from saline buffer after rupture of the venom gland, indicating a lower density than venom of *B. pallida*, and neither did it contain spherical particles (data not shown).

Gall Wasp Ovary and Venom Gland 454 Sequencing Statistics and *de novo* Assembly

The 454 run provided a total of 292784 and 304506 reads respectively for *D. rosae* and *B. pallida* samples. Quality control using SnoWhite software resulted in a total of 287438 cleaned reads for *D. rosae* and 298180 reads for *B. pallida*, with average sequence lengths of 336 bp and 369 bp, respectively (**Table 1**).

To obtain an optimal assembly, sequences from ovary and venom gland cDNA libraries from the same species were merged together, using parameter settings that allowed us to obtain large contigs and to avoid chimeras (see Materials and Methods). The cleaned reads were assembled into 2061 contigs for *D. rosae* and 2304 contigs for *B. pallida* (**Table 1**). Similar high quality of sequencing and assembly was obtained for both species with contig sizes of an average length of 330 and 339 bp (N50 447

[2]http://www.cbs.dtu.dk/services/DeepLoc-1.0/index.php

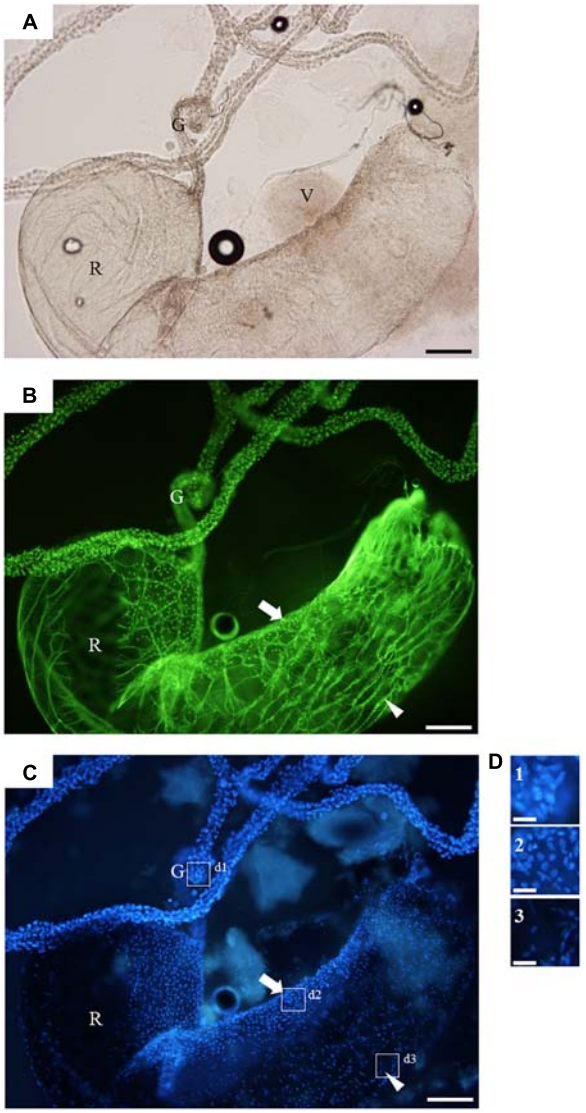

FIGURE 2 | The venom apparatus of *B. pallida* observed in fluorescence microscopy. **(A)** light microscopy, **(B)** FITC-conjugated phalloidin staining for actin detection, **(C)** DAPI staining for detection of nucleic acids, and **(D)** detailed view of **(C)**. G, venom gland; R, venom reservoir; V, venom; arrow, secondary secretory zone; arrowhead, muscular fiber; boxes d1, d2, and d3 refer to detailed views shown in panel **(D)**. Note the high density of the venom leaking from the ruptured reservoir in panel **(A)**, and the different shapes of nuclei that allow to discriminate between the different tissues composing the organ. Scale bars = 0,3 mm for **(A)**, **(B)**, and **(C)** or 50 μm for **(D)**.

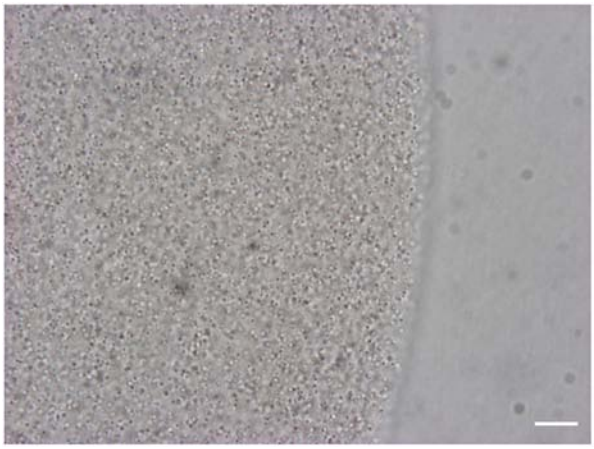

FIGURE 3 | View of the venom of *B. pallida* in light microscopy. At high magnification, numerous spherical particles of approximately 1 to 2 μm in diameter are visible in the venom of *B. pallida*. Scale bar = 50 μm.

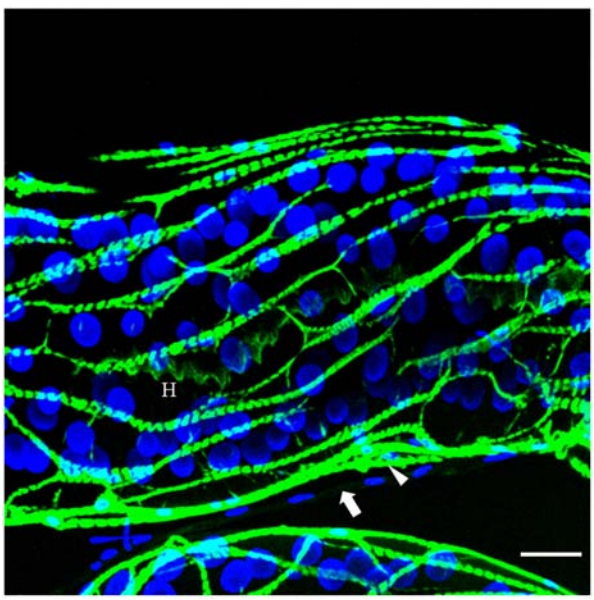

FIGURE 4 | The venom gland of *D. rosae* observed in confocal microscopy. Merge image of FITC-conjugated phalloidin staining for actin detection (green) and DAPI staining for detection of nucleic acids (blue). H, internal helix containing actin; arrow, surrounding mesenchymal tissue; arrowhead, muscular fiber. Note the round shape of the nuclei of glandular cells. Scale bars = 30 μm.

and 462 bp) for *D. rosae* and *B. pallida*, respectively (**Table 1** and **Supplementary Notes S1, S2**).

Initial Annotation and Origins of Expressed Genes

Contig annotation was performed by blastx comparison with sequences in non-redundant public databases using an *E*-value cut-off of $< 10^{-4}$ and a match was identified for 54 % of contigs from each wasp species (1117 contigs from *D. rosae* and 1253 contigs from *B. pallida*) (**Table 1**). The *E*-value of most contigs from both species ranged from 10^{-15} to 10^{-50} and 35% of contigs from *D. rosae* and 32% of contigs from *B. pallida* shared very high similarities with sequences in databases (*E*-value $< 10^{-50}$) (**Supplementary Figures S1a,c**).

For both *D. rosae* and *B. pallida*, 97% of matched contigs were identified as insect sequences, primarily hymenopteran (**Supplementary Figures S1b,d**) as expected. Interestingly,

TABLE 1 | General features of the *D. rosae* and *B. pallida* transcriptomes.

Species	*D. rosae*		*B. pallida*	
Tissue	**Ovary**	**Venom gland**	**Ovary**	**Venom gland**
Number of reads	163275	129509	182605	121901
	292784		304506	
Number of cleaned reads[a]	160430	127008	178899	119281
	287438		298180	
Average cleaned read length (bp)	343	326	368	370
	336		369	
Number of unique sequences assembled	64627		61682	
Number of contigs	2061		2304	
Number of reads assembled into contigs	224872		238802	
Range of coverage of contigs (reads)	2–17971		2–11614	
Contigs size range (bp; mean)	15–1350 (330)		15–1390 (339)	
N50 of contigs (bp)[b]	447		462	
Number of contigs with a hit (with no hit)[c]	1117 (944)		1253 (1051)	

[a]*Adapters, primers, very short reads (<15 bp), and low-quality reads were removed using SnoWhite software.* [b]*N50 size is the longest contig such that at least half of the total size of the contigs is contained in contigs larger than this value.* [c]*Contigs which present a hit in the NCBI nr database with the blastx approach with an E-value* $< 10^{-4}$.

among the non-matching contigs, two translated sequences coding for cellulases were similar to gene products from bacteria (58% similarity).

Relative Expression Levels of Contigs in Different Tissues Within Species

For each species, contigs could be divided into three categories based on their expression levels normalized using RPKM: (i) contigs expressed at least 20 times higher in venom glands than in ovaries (dark gray in **Figure 5**) – reported below as "differentially expressed in venom glands"; (ii) contigs expressed at least 20 times higher in ovaries than in venom glands (light gray, **Figure 5**) – reported below as "differentially expressed in ovaries"; and (iii) contigs expressed in both ovaries and venom glands with relative expression levels differing by less than 20-fold (intermediate gray in **Figure 5**). This latter category, which contains mostly housekeeping genes, is reported below as "equivalently expressed" in venom glands and ovaries. In contrast, the two differentially expressed categories represent transcripts of candidate genes coding for potential virulence factors, which in parasitoids are generally abundantly produced (either in venom gland or in the ovaries depending on the factor) and injected in large amounts into the host. The same proportion of genes (13 % of the total number of analyzed contigs) was found to be differentially expressed in venom glands of both species. The vast majority of contigs differentially expressed in venom glands of *B. pallida* and *D. rosae* were novel sequences with no significant sequence similarity with known gene products (respectively 80 and 89% of contigs) (**Figure 5**).

Gene Ontology Classification of Contigs

Gene ontology assignments were used to classify the functions of the gall wasp transcripts into biological processes, molecular functions, and cellular components for both species and for each relative expression level category (**Figure 6**). Contigs showing a blast hit (807 and 844 contigs, respectively for *D. rosae* and *B. pallida*) could be categorized into 19 different GO functional groups for each species. Globally, both species showed a similar profile of GO annotation, with high numbers of contigs mainly involved in "cellular" and "metabolic" processes and "global cell structure," as well as "binding" and "catalytic" activities.

Identification of Potential Virulence Factors

To identify potential virulence effectors more likely involved in gall induction we focused on genes coding for potentially secreted proteins, since virulence factors are likely to be found among secretion products of venom glands or ovarian epithelia, based on what we know about parasitoids. We therefore considered here proteins that are expected to be secreted by the classical ER-Golgi secretory pathway and do not contain a transmembrane domain that would suggest they are anchored to the cell surface (see Materials and Methods). Since numerous transcripts lacked the 5′ end and hence the region potentially encoding a signal peptide, we also retained proteins showing homology to known secreted proteins present in the databases. A total of 167 *B. pallida* contigs and 134 *D. rosae* contigs encode proteins containing a signal peptide or which are homologous to proteins known to contain a signal peptide. In both species, a higher proportion of genes potentially encoding proteins with predicted signal peptides was expressed in venom glands compared to ovaries (**Figure 5**), reflecting the important secretory function of the glandular epithelium of venom glands. In *B. pallida*, among contigs differentially expressed in the venom glands at least 29.5% of the contigs and 12% of contigs with no match in databases encode proteins with predicted signal peptides, which therefore likely correspond to venom proteins. By comparison, only 1 or 2 % of contigs belonging to the other categories coded for proteins with a signal peptide (**Figure 5A**), suggesting that ovaries are less actively secretory than venom glands (which could be expected since egg production is their major function). Similarly, in *D. rosae*, 21.4 % of the identified contigs and 13% of non-assigned contigs differentially expressed in the venom glands encode proteins with predicted signal peptides, compared to only 1 or 2 % for the other categories (**Figure 5B**). Interestingly, the DeepLoc1.0 analysis of the deduced sequences from contigs differentially expressed in venom glands from *B. pallida* and *D. rosae* confirmed a probable extracellular addressing for 38 of the 46 contigs predicted to encode a peptide signal for *B. pallida* and for 12 out of 17 contigs for *D. rosae* (**Tables 2**, **3**). It is noteworthy that *B. pallida* unassigned contigs differentially expressed in venom gland share no similarity with *D. rosae* contigs, except for one sequence (coding for a protein with a putative DNA binding domain -Pfam 05485-) belonging to the "equivalently expressed" category in *D. rosae*, indicating that most of the corresponding proteins are species-specific. In

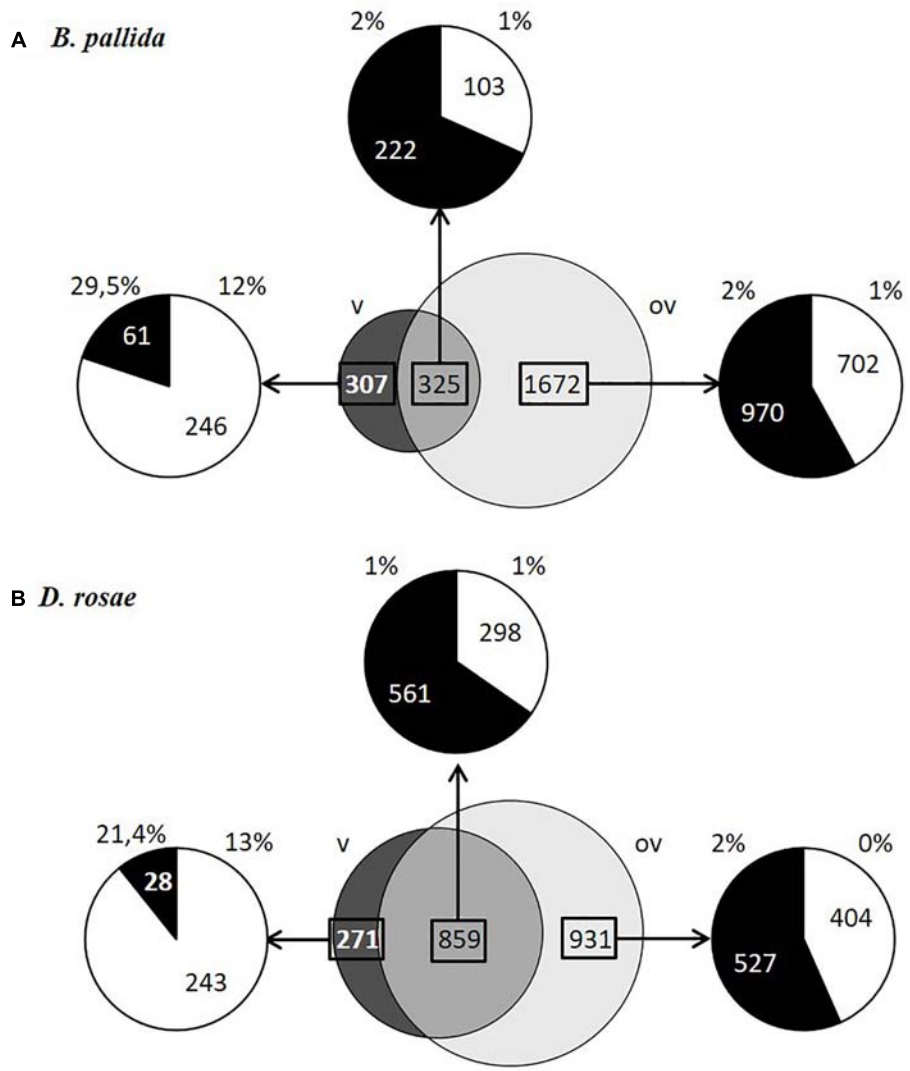

FIGURE 5 | Contig expression levels in ovaries and venom glands and percentage of contigs encoding proteins with signal peptides in *B. pallida* **(A)** and *D. rosae* **(B)**. In dark gray, contigs expressed at least 20 times higher in venom glands than in ovaries (v); in light gray, contigs expressed at least 20 times higher in ovaries than in venom glands (ov); in gray, contigs expressed in both ovaries and venom glands with relative expression levels differing by less than 20-fold. The distribution of contigs that had a blastx hit (black) or that are not assigned (NA; white) and the percentage of these contigs coding proteins with a signal peptide (SignalP4.0 prediction) are specified for each category of contigs.

the following sections, we consider possible candidate proteins putatively secreted by venom glands and ovaries in turn.

Identification of Potential Virulence Factors Differentially Expressed in the Venom Transcriptome of *B. pallida*

For *B. pallida*, 307 contigs (61 annotated) were differentially expressed in venom glands relative to ovaries. Of these, 46 potentially encoded amino acid sequences with a predicted signal peptide or with significant sequence similarity to known secreted proteins (**Figure 7A** and **Table 2**). These contigs are grouped according to functional annotation in **Table 2**. They encoded proteins mainly involved in transport, hydrolytic processes and protection against oxidative stress (**Table 2**). Genes encoding Apolipoprotein D (ApoD), a fatty acid transport protein, had the highest levels of expression with 20 different contigs displaying up to 75889 RPKM in venom glands. Genes encoding acid phosphatases were also highly expressed (up to 65960 RPKM for Bp_contig00098, whose expression was 6785 times higher in venom glands than in ovaries). The third most expressed category of genes encodes secreted peroxidases (up to 6168 RPKM). Other highly expressed contigs in venom gland matched genes whose products are potentially involved in nucleotide hydrolysis (two nucleoside hydrolases and one apyrase), plant tissue and glucoside degradation (two cellulases, two β-glucosidases, four myrosinase-like proteins), fatty acid degradation (at least seven esterases

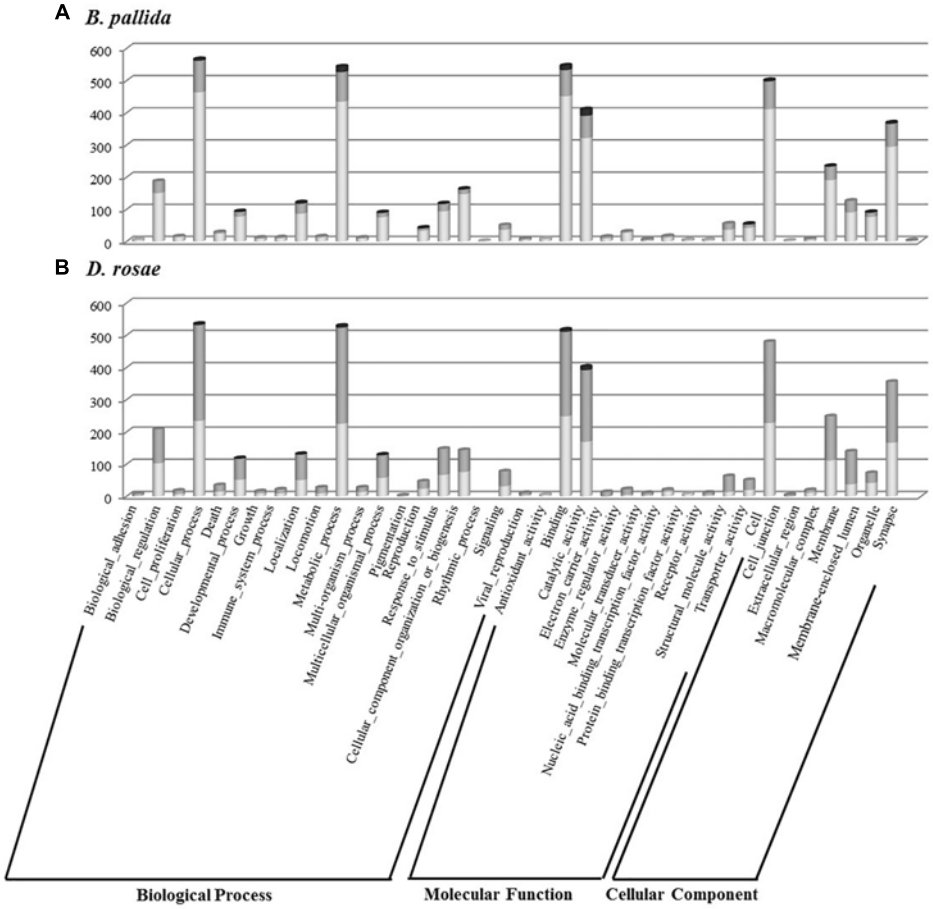

FIGURE 6 | Histogram presentation of Gene Ontology (GO) classification of *B. pallida* **(A)** and *D. rosae* **(B)** contigs. Results are given in the three GO categories at the level two of GO analysis for contigs highly expressed in venom gland (dark gray), those highly expressed in ovaries (light gray), and those equivalently expressed in the two tissues (gray).

or lipases and a phospholipase A2-like enzyme) and peptide hydrolysis (two leukotriene A-4 hydrolases). Genes involved in potential protection mechanisms against bacteria and fungi were also identified, including a lysozyme 3-like enzyme and a chitotriosidase 1-like enzyme of the GH18 chitinase superfamily. Several genes were identified that code for proteins with potential involvement in regulation of plant signaling, including an OV-16 antigen/phosphatidylethanolamine binding protein (PEBP) and a gene encoding a regucalcin-like protein potentially regulating Ca^{++} signaling. In contrast, 'housekeeping' genes involved in general cell metabolism were mainly equivalently expressed between venom glands and ovaries.

Identification of Potential Virulence Factors Differentially Expressed in the Venom Gland Transcriptome of *D. rosae*

In *D. rosae*, 271 contigs were differentially expressed in venom glands, most of which potentially code for proteins with no similarity to known proteins in databases and only 28 of which could be annotated. Of these, 17 contigs code for proteins with a predicted signal peptide or with high similarity to proteins possessing a signal peptide (**Table 3**). The global pattern of gene expression in the venom gland of *D. rosae* differs from patterns observed *in B. pallida* (**Figure 7B** and **Table 4**) – in particular, the cellulase genes whose transcripts were detected in the *B. pallida* venom gland were not detected in *D. rosae*. However, some venom gland transcripts were differentially expressed in both *B. pallida* and *D. rosae*, including one encoding a chitotriosidase-1-like enzyme (25217 RPKM), one an esterase (587 RPKM) and one encoding an apyrase (4664 RPKM), all of which were important components of the *D. rosae* venom gland transcriptome.

We also observed a different type of nucleotide hydrolase (ectonucleoside triphosphate diphosphohydrolase) to that observed in *B. pallida*, expressed at a relatively low level in *D. rosae* venom glands (28 RPKM). In *D. rosae,* 28.5% of the highly expressed venom gland genes identified were similar to genes encoding lysosomal enzymes (α-mannosidase, α-mannosidase-like isoform 2, α-mannosidase-like, β-mannosidase-like, chitooligosaccharidolytic beta-N-acetylglucosaminidase-like and Pro-X carboxypeptidase-like),

TABLE 2 | Biorhiza pallida contigs differentially expressed in venom glands[a].

Contig	Length (bp)	Relative expression[b]	Putative localization[c]	Accession number of best hit	*E*-value	Signal peptide[d]	Description[e]	Putative localization[c]
Bp_contig00785*	684	334	E	XP_003699771.1[$]	5,00E-40	Y	*apolipoprotein D-like*	E
Bp_contig02018*	529	9440	E	XP_003699771.1[$]	1,00E-25	Y	*apolipoprotein D-like*	E
Bp_contig02594	385	17419	E	XP_003699771.1[$]	7,00E-21	Y	*apolipoprotein D-like*	E
Bp_contig00009*	475	5671	E	XP_003699771.1[$]	3,00E-20	Y	*apolipoprotein D-like*	E
Bp_contig00011*	424	2800	E	XP_003699771.1[$]	2,00E-19	Y	*apolipoprotein D-like*	E
Bp_contig00439*	377	3045	E	XP_014230135.1[$]	3,00E-19	Y	*apolipoprotein D-like*	E
Bp_contig00005*	193	876	E	XP_014230135.1[$]	2,00E-18	Y	*apolipoprotein D-like*	E
Bp_contig02210	498	769	E	XP_014230135.1[$]	3,00E-15	Y	*apolipoprotein D-like*	E
Bp_contig00352	495	360	E	XP_023024212.1[$]	3,00E-11	Y	*apolipoprotein D-like*	E
Bp_contig00008	139	111	M	XP_015111737.1[$]	4,00E-10	Y	apolipoprotein D	E
Bp_contig00735*	731	4817	E	EFN80483.1	2,00E-09	Y	apolipoprotein D	E
Bp_contig00674	730	106	E	EGI66470.1	2,00E-09	N	apolipoprotein D	E
Bp_contig00012	225	223	E	OWR42187.1[$]	2,00E-08	Y	apolipoprotein D	E
Bp_contig02145*	458	250	M	OWR42187.1[$]	2,00E-08	Y	apolipoprotein D	E
Bp_contig00018	124	643	M	XP_014230135.1[$]	3,00E-07	Y	*apolipoprotein D-like*	E
Bp_contig00440	162	709	E	EFN69132.1	3,00E-06	N	apolipoprotein D	ER
Bp_contig00006	132	130	M	EFN80483.1	3,00E-06	N	apolipoprotein D	E
Bp_contig00007	130	70	E	EGI66470.1	4,00E-06	N	apolipoprotein D	E
Bp_contig00318	654	366	E	XP_003488538.1[$]	5,00E-06	Y	*apolipoprotein D-like*	E
Bp_contig00230	579	931	E	XP_003448594.1[$]	3,00E-05	Y	*apolipoprotein D-like*	E
Bp_contig00096	767	3555	E	EFN78070.1[$]	4,00E-27	Y	testicular acid phosphatase-like protein	CM
Bp_contig00098	222	6785	M	XP_001605452.1[$]	3,00E-12	Y	venom acid phosphatase Acph-1-like isoform 1 and 2	ER
Bp_contig00095	277	6628	M	AVZ66237.1[$]	1,00E-09	Y	venom acid phosphatase	L/V
Bp_contig00934	745	111	E	XP_003397066.1[$]	5,00E-60	Y	*peroxidase-like isoform 1 and 2*	E
Bp_contig00408*	563	1194	E	EFN60907.1	5,00E-30	Y	peroxidase	N
Bp_contig02115*	485	84	E	XP_017753112.1	3,00E-25	Y	*peroxidase-like*	E
Bp_contig00465	320	130	E	XP_001603589.1[$]	1,00E-20	Y	*peroxidase-like*	E
Bp_contig00208	898	706	ER	NP_001155173.1[$]	2,00E-52	Y	inosine-uridine preferring nucleoside hydrolase-like precursor	ER
Bp_contig00209	671	417	C	KZC11420.1	9,00E-26	N	putative uridine nucleosidase 2	C
Bp_contig00782	109	21	P	XP_003702963.1[$]	8,00E-09	Y	*apyrase-like*	E
Bp_contig00227*	792	654	E	WP_062062951.1[$]	8,00E-78	Y	cellulase	C
Bp_contig02577	196	48	E	BAM21527.1[$]	9,00E-18	Y	cellulase	E
Bp_contig01034*	689	87	E	EFN89852.1[$]	3,00E-49	Y	lipase 3	ER
Bp_contig00246	310	90	E	XP_015605711.1	9,00E-43	N	lipase 3 isoform X2	L/V
Bp_contig00247	310	39	E	XP_015605711.1	3,00E-42	N	lipase 3 isoform X2	L/V
Bp_contig00919	458	48	E	XP_969958.1[$]	3,00E-42	Y	inactive pancreatic lipase-related protein 1	E
Bp_contig00076	326	853	C	XP_029036643.1	1,00E-20	N	*ester hydrolase C11orf54 homolog*	C
Bp_contig01139*	670	157	E	EGI67126.1[$]	8,00E-14	Y	pancreatic triacylglycerol lipase	E
Bp_contig00248	165	120	M	EFN89852.1[$]	1,00E-11	Y	lipase 3	ER
Bp_contig01485	373	42	M	XP_001604598.1[$]	5,00E-11	Y	phospholipase A2-like	E
Bp_contig00075	378	1348	N	XP_029171997.1	7,00E-10	N	*ester hydrolase C11orf54 homolog*	C
Bp_contig01814	537	67	C	XP_011861823.1[$]	8,00E-53	Y	*chitotriosidase-1 isoform X2*	E
Bp_contig00478	583	438	E	XP_003696479.1[$]	4,00E-44	Y	*chitotriosidase-1-like*	E
Bp_contig01222	595	67	M	XP_012348776.1[$]	7,00E-88	Y	*myrosinase 1-like*	L/V
Bp_contig01009	417	39	M	XP_020295361.1[$]	5,00E-48	Y	alpha-glucosidase-like	E
Bp_contig00838	511	46	M	XP_014364862.1[$]	5,00E-47	Y	*myrosinase 1-like*	L/V

(Continued)

TABLE 2 | Continued

Contig	Length (bp)	Relative expression[b]	Putative localization[c]	Accession number of best hit	*E*-value	Signal peptide[d]	Description[e]	Putative localization[c]
Bp_contig01121	489	2167	C	XP_015608814.1[$]	3,00E-39	Y	*myrosinase 1-like*	L/V
Bp_contig02447	269	25	E	XP_015513216.1[$]	3,00E-26	Y	*myrosinase 1-like*	L/V
Bp_contig01316	506	166	E	XP_003394100.1[$]	9,00E-28	Y	*lysozyme 3-like*	E
Bp_contig01637*	263	46	E	KZC10586.1[$]	3,00E-15	Y	alpha-glucosidase	E
Bp_contig01673	515	51	C	EFN73602.1	6,00E-75	N	Lactase-phlorizin hydrolase	L/V
Bp_contig00267*	727	87	ER	XP_001607975.2	1,00E-57	Y	*leukotriene A-4 hydrolase-like*	C
Bp_contig00552	568	69	C	EFN66270.1	1,00E-38	N	leukotriene A-4 hydrolase	C
Bp_contig00420	207	75	E	RZC41298.1	8,00E-25	N	PBP domain containing protein	C
Bp_contig02290	172	42	E	XP_015178004.1	1,00E-21	N	peptidoglycan-recognition protein LC-like isoform X3	ER
Bp_contig00280*	708	1333	E	EFX65777.1	7,00E-19	Y	hypothetical protein DAPPUDRAFT_229540	CM
Bp_contig00419*	317	121	E	EFN69212.1[$]	4,00E-17	Y	OV-16 antigen/ PhosphatidylEthanolamine-Binding Protein	E
Bp_contig00275	438	1276	C	KYN12678.1	9,00E-16	N	*hypothetical protein ALC57_15147*	C
Bp_contig00415	246	28	M	XP_016839796.1[$]	1.00E-12	Y	*prolyl 4-hydroxylase subunit alpha-1 isoform X2*	ER
Bp_contig00572*	452	85	E	XP_003701165.1	5,00E-11	Y	*regucalcin-like*	L/V
Bp_contig00021	558	300	E	XP_001622620.1	1,00E-06	N	*predicted protein*	C

Contigs coding for a signal peptide according to SignalP 4.0.* [$] *Best hits coding for a signal peptide according to SignalP 4.0.* [a] *The annotation of B. pallida contigs was performed using a blastx approach (E-value < 10^{-4}).* [b] *Ratio between normalized (RPKM) contig expression in venom gland and ovaries.* [c] *Putative localization predicted using DeepLoc-1.0 : C, cytoplasm; CM, cell membrane; E, extracellular; ER, endoplasmic reticulum; L/V, lysosome or vacuole; M, mitochondrion; N, nucleus; P, plastid.* [d] *Contig or best hit coding for a signal peptide.* [e] *Gene names in italics are predicted description. Colors refer to functional groups defined in* ***Figure 7**.*

some of these genes reaching up to 1960 RPKM. A contig differentially expressed in the venom glands of *D. rosae* (829 RPKM) codes for a protein with a predicted peptide motif that shares similarity with Seele, a saposin-like protein of the Canopy1 family. A second contig (25 RPKM), for which no putative peptide signal could be detected, corresponds to an antichymotrypsin-2-like protein, a member of the serine protease inhibitor family. In addition, 28.6% of the highly expressed genes of the venom gland transcriptome correspond to eight contigs coding for potentially secreted proteins without any known function (the most expressed reaching 24964 RPKM).

Identification of Potential Virulence Factors Differentially Expressed in Ovaries of *B. pallida* or *D. rosae* or Classified in the Category "Equivalently Expressed"

Genes equivalently expressed in ovary and venom gland or those mainly expressed in ovary generally encode proteins involved in global cellular metabolism. However, in *B. pallida* transcriptomes, we found four contigs corresponding to genes coding for proteins previously identified as virulence factors in some parasitoid wasps (**Supplementary Table S1**). Three of them (carboxypeptidase B-like, venom acid phosphatase Acph-1-like isoform 1, putative alpha-N-acetylgalactosaminidase) were more expressed in venom gland than ovary, but by less than our chosen threshold for differential expression. The fourth contig codes for a protein similar to venom protein 5 from the ant *Brachymyrmex patagonicus* and was most expressed in the ovary. This suggests that the 20-fold difference in expression level is a very stringent threshold and that some virulence factors might remain in the "equivalently expressed" category.

Similarly in *D. rosae*, 73 contigs (4% of the contigs which are not differentially expressed in the venom gland) satisfy our criteria of potentially secreted virulence factors (**Supplementary Table S2**). Of these, two corresponded to gene products encoding members of the GH18 chitinase-like superfamily, classified in the category "equivalently expressed" in venom gland and ovary but more expressed in the venom gland. Five other contigs, more expressed in the ovaries (over or below the threshold) coded for proteins with sequence similarities to one venom serine carboxypeptidase-like, one venom carboxylesterase-6-like, one phospholipase A2-like, and two exonuclease 3′-5′ domain-like 2, that could correspond to virulence factors secreted by the ovaries.

Comparison Between Gall Wasp and Parasitoid Wasp Venom Gland Transcriptomes

The 307 and 271 contigs differentially expressed in venom glands of *B. pallida* and *D. rosae*, respectively, were compared to venom sequences for parasitoid wasps from four different families to identify similarities and differences between gallers and parasitoids. The comparison identified seven groups

TABLE 3 | Diplolepis rosae contigs differentially expressed in venom glands[a].

Contig	Length (bp)	Relative expression[b]	Putative localization[c]	Accession number of best hit	E-value	Signal peptide[d]	Description[e]	Putative localization[c]
Dr_contig00438	756	1156	GA	XP_012277362.1[$]	2,00E-47	Y	*chitooligosaccharidolytic beta-N-acetylglucosaminidase-like*	E
Dr_contig00333	508	25217	E	XP_001606170.2[$]	1,00E-35	Y	*chitotriosidase-1-like*	E
Dr_contig00372	973	59	C	XP_001600239.2[$]	4,00E-53	Y	5'-nucleotidase-like	E
Dr_contig00150	434	4664	E	XP_003694809.1[$]	2,00E-32	Y	*apyrase-like*	E
Dr_contig00076	358	28	M	XP_001948332.1	4,00E-13	N	ectonucleoside triphosphate diphosphohydrolase 5-like isoform 1 and 2	GA
Dr_contig01616	566	1502	ER	XP_003424313.1[$]	1,00E-50	Y	*xaa-Pro aminopeptidase 1-like*	ER
Dr_contig02302	184	984	N	EFN65087.1	1,00E-14	N	Xaa-Pro aminopeptidase 2	ER
Dr_contig02301	117	1144	E	XP_007537171.2[$]	5,00E-09	Y	*lysosomal Pro-X carboxypeptidase-like*	E
Dr_contig00694	743	1960	E	XP_015589369.1[$]	6,00E-90	Y	*lysosomal alpha-mannosidase-like isoform 2*	ER
Dr_contig00725	537	1569	E	XP_011498322.1[$]	3,00E-88	Y	*lysosomal alpha-mannosidase*	ER
Dr_contig01444	584	485	C	XP_012163913.1	3,00E-74	N	*beta-mannosidase-like*	C
Dr_contig00850	688	76	M	EGI69344.1	2,00E-61	N	Lysosomal alpha-mannosidase	C
Dr_contig01222	622	32	N	XP_014218055.1	4,00E-58	N	*lysosomal alpha-mannosidase-like*	C
Dr_contig02188	389	587	M	XP_011297371.1	3,00E-18	N	*esterase FE4*	ER
Dr_contig01475	462	682	C	XP_016921482.1	1,00E-76	N	*natterin-3-like*	C
Dr_contig00664	438	42	L/V	XP_014601538.1[$]	7,00E-75	Y	*sodium/potassium/calcium exchanger 3-like*	CM
Dr_contig00136	405	25	C	XP_015512769.1	9,00E-47	N	*antichymotrypsin-2-like*	C
Dr_contig00370*	779	829	ER	XP_003394069.1	4,00E-45	Y	*protein canopy-1-like*	ER
Dr_contig01769	374	35	C	KYN42454.1	3,00E-44	N	hypothetical protein ALC56_03113	M
Dr_contig00409*	896	5290	E	EGI63918.1	9,00E-44	Y	hypothetical protein G5I_07497	E
Dr_contig00606*	729	2408	E	XP_001607382.1[$]	3,00E-19	Y	*carbonic anhydrase 1-like*	E
Dr_contig01983*	378	86	E	XP_001601633.1[$]	6,00E-19	Y	*hypothetical protein LOC100113725*	E
Dr_contig00059*	387	8158	E	XP_001604826.2[$]	2,00E-18	Y	*hypothetical protein LOC100121232*	E
Dr_contig00056	208	1329	E	XP_003699351.1[$]	7,00E-18	Y	*uncharacterized protein LOC100875586*	E
Dr_contig00021	599	4540	M	TKR61321.1	6,00E-11	N	hypothetical protein L596_028442	M
Dr_contig00055*	293	24964	E	EFX75302.1[$]	8,00E-09	Y	hypothetical protein DAPPUDRAFT_306830	E
Dr_contig00288	450	19176	N	WP_124341075.1	2,00E-06	N	HAMP domain-containing protein	M
Dr_contig00057	176	1358	E	XP_003699351.1[$]	6,00E-06	Y	*uncharacterized protein LOC100875586*	E

Contigs coding for a signal peptide according to SignalP 4.0.* [$] *Best hits coding for a signal peptide according to SignalP 4.0.* [a] *The annotation of D. rosae contigs was performed using a blastx approach (E-value < 10^{-4}).* [b] *Ratio between normalized (RPKM) contig expression in venom gland and ovaries.* [c] *Putative localization predicted using DeepLoc-1.0 : C, cytoplasm; CM, cell membrane; E, extracellular; ER, endoplasmic reticulum; GA, Golgi apparatus; M, mitochondrion; N, nucleus.* [d] *Contig or best hit coding for a signal peptide.* [e] *Gene names in italics are predicted description. Colors refer to functional groups defined in* ***Figure 7**.*

of putative gall wasp venom proteins that are functionally related to gene products from parasitoid venom glands (**Table 4**). Esterases/lipases, nucleoside hydrolases, serine protease inhibitors, GH18 chitinase-like enzymes and acid phosphatases are shared venom components in both cynipid gall wasps and the selected parasitoids. The studied gall wasps also expressed apyrases or phospholipase A2 in their venom glands that are similar to sequences from the pteromalide *N. vitripennis* or the braconid wasp *M. demolitor*, respectively (**Table 4**).

This comparison also confirmed the novelty of most of the contigs differentially expressed in venom glands of both gall wasps (**Table 4**: eight groups of proteins for *B. pallida* and six groups for *D. rosae*), which lacked functional equivalents in previously described parasitoid venoms, including *L. boulardi*

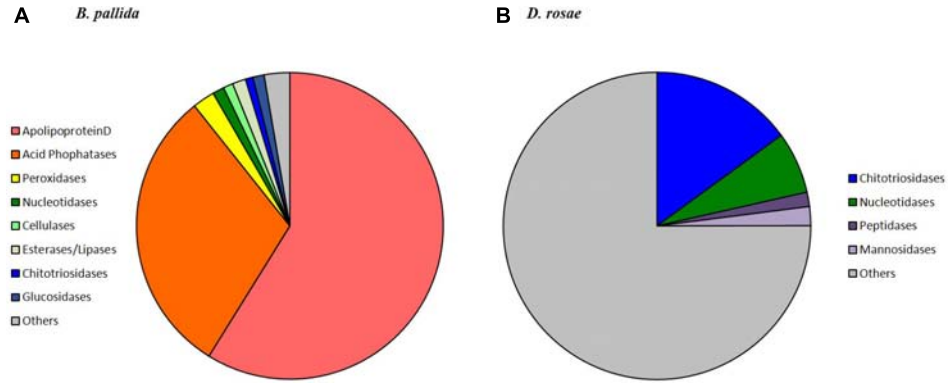

FIGURE 7 | Relative expression and annotation of *B. pallida* **(A)** and *D. rosae* **(B)** contigs differentially expressed in venom glands and potentially coding secreted proteins. Contigs considered here were only those returning a significant blastx hit (*E*-value $< 10^{-4}$) and having a predicted signal peptide or homologous to a protein possessing a signal peptide (contigs indicated by Y in **Tables 2**, **3** from SignalP4.0 prediction). For each category, the sum of the reads (RPKM) in venom gland was calculated. For detailed description of contigs see **Tables 2**, **3**.

TABLE 4 | Comparison between *B. pallida* and *D. rosae* sequences with known venom components from parasitoids[a].

Families	**Cynipidae**		**Figitidae**		**Pteromalidae**		**Ichneumonidae**		**Braconidae**	
Species	***Bp***	***Dr***	***Lb***	***Lh***	***Nv***	***Pp***	***Hd***	***Ph***	***Md***	***Ci***
Esterases/Lipases	■	■	▒	▒	▒	▒	▒	▒	▒	▒
Venom acid phosphatases	■		▒	▒	▒	▒				
Nucleoside hydrolases	■	■								
Serine protease inhibitors	■	■					▒		▒	
GH18 Chitinases-like	■	■	▒		▒					▒
Apyrases	■	■	▒							
Phospholipases A2	■	■							▒	
Apolipoproteins D	■	■								
Peroxidases	■	■								
Leukotriene A-4 hydrolases	■	■								
Cellulases	■	■								
Lysozyme 3-like	■	■								
Beta-Glucosidases	■	■								
PhosphatidylEthanolamine-Binding Proteins	■	■								
xaa-Pro aminopeptidases	■	■								
Lysosomal Pro-X carboxypeptidases	■	■								
Alpha-mannosidases	■	■								
Carbonic anhydrases	■	■								
Chitooligosaccharidolytic beta-N-acetylglucosaminidases	■	■								
Canopy 1-like proteins	■	■								

[a] *The most expressed sequences in venom glands from B. pallida and D. rosae (black cells) were compared to sequences expressed by venom glands of parasitoid species using a tblastx and a blastx approach. Only significant results concerning proteins with identified functions or domains are shown here, using a coding system to indicate presence (gray cells) or absence (white cells) of similar sequences in available transcriptomes and/or proteomes. Bp: B. pallida; Ci: Chelonus inanitus; Dr: D. rosae; Hd: Hyposoter didymator; Lb: Leptopilina boulardi; Lh: Leptopilina heterotoma; Md: Microplitis demolitor; Nv: Nasonia vitripennis; Ph: Pimpla hypochondriaca; Pp: Pteromalus puparum.*

and *L. heterotoma*, in the family Figitidae, sister group to the Cynipidae within the Cynipoidea (Ronquist et al., 2015).

DISCUSSION

This study presents the first global transcriptome data for the venom gland and ovary of two gall-inducing cynipid wasps, *B. pallida* and *D. rosae* and constitutes a first step toward identifying virulence factors associated with cynipid gall induction. We have compared these new data with data for closely related Figitid parasitoid wasps, given their phylogenetic proximity to gall wasps, in order to identify on the one hand factors that are potentially conserved between insect and plant parasites and on the other hand factors that are specific to plant-parasitic gall-wasps.

Parasitism is a complex trait and involves multiple mechanisms that act in combination to overcome host defenses and to manipulate host physiology. In parasitoid Hymenoptera, manipulation of host physiology generally starts at oviposition and is mainly controlled by secretions of the female venom glands and/or ovaries, injected with the eggs during oviposition, which can contain symbiotic viruses or virus-like particles produced by the female wasp (Strand and Pech, 1995; Moreau et al., 2009; Drezen et al., 2017). Our goal was to evaluate whether any of the proteins corresponding to genes differentially expressed by the venom glands or ovaries of the two gall inducing wasps studied here could potentially play a defensive role against natural enemies and/or be involved in interactions with molecules from their host plants. We suggest at least three main roles for the venom proteins of *B. pallida* and *D. rosae*, based on identification of putative components: i) controlled lysis of host plant tissues by venom hydrolases, providing space and food for the larvae after hatching from the egg, ii) moderation of the host plant response in reaction to tissue lysis and iii) defense of gall wasp eggs against antagonistic microbes that could benefit from a lowering of plant defenses to invade the newly colonized host tissues, and particularly the fungi that can cause high mortality in cynipid galls (Taper et al., 1986; Taper and Case, 1987; Wilson, 1995; Wilson and Carroll, 1997).

Venom Components That Potentially Contribute to Controlled Plant Cell Lysis

Our transcriptomic study revealed that the contigs highly expressed in the venom glands of *B. pallida* and *D. rosae* were almost all classified in the GO categories "metabolic" and "cellular" processes, "binding" and "catalytic" activities. Over-representation of the two latter categories has already been reported for genes expressed in the venom gland of a braconid parasitoid wasp *C. inanitus* (Vincent et al., 2010). It confirms that the venom arsenals of the two gall-inducing cynipids comprise enzymes, including hydrolases that are able to interact with a wide diversity of ligands. In *B. pallida*, the main hydrolases expressed in the venom glands were acid phosphatases, which have also been reported from a range of parasitoid wasps venoms (**Table 4**; Dani et al., 2005; Moreau and Guillot, 2005; Zhu et al., 2008; Manzoor et al., 2016). Since venom acid phosphatases are thought to play a role in cell histolysis and degeneration of targeted tissue (Zhu et al., 2008), we hypothesize that venom acid phosphatases in *B. pallida* may be involved in lysis of plant tissue. This could contribute to the observed collapse of plant tissues around cynipid eggs that precedes hatching, and which provides a space into which the emerging larva moves. The same function could apply to observed high expression of a cellulase (β-1,4-endoglucanase) gene in the venom glands of *B. pallida*, an enzyme involved in the degradation of cellulose plant cell walls. Genes coding ester hydrolases and lipases were also highly expressed in the venom gland of *B. pallida* and, to a lesser extent, also of *D. rosae*. These hydrolases are involved in fatty acid hydrolysis, and have been found in the venom of several parasitoid wasps (**Table 4**). Lipases and/or esterases in the venoms of the cynipid gall wasps could play a role in altering host plant tissues. In addition, we have observed high expression of a cellulase (β-1,4-endoglucanase) gene in the venom glands of *B. pallida*, an enzyme involved in the degradation of cellulose plant cell walls.

Cellulase has already been characterized in salivary secretions of root-knot cyst nematodes (Davis et al., 2004), but this is the first report of its presence in venom. In nematodes, the acquisition of this gene has been clearly shown to involve horizontal gene transfer (Danchin et al., 2010). In terms of mRNA abundance, myrosinase-like enzymes are among the most expressed venom gland products in *B. pallida*. Myrosinase enzymes are β-glucosidases with thioglucosidase activity, that are involved in protection of cruciferous plants against herbivores, glycosinolate hydrolysis producing compounds toxic for caterpillars (Rask et al., 2000; Burow and Halkier, 2017). Since oaks do not use the glycosynolate defense system one may reasonably consider that these enzymes more likely correspond to β-glucosidases and may provide readily available sugar to the larvae. Other hydrolases were found expressed by the venom gland of *D. rosae*, including several chitooligosaccharidolytic, proteolytic and peptidolytic enzymes. We also found expression of a natterin-3-like protein by the venom glands of *D. rosae*, suggesting a possible evolutionary convergence with the venom of a fish *Thalassophryne nattereri* (Magalhães et al., 2005). However, SignalP 4.0 did not identify a signal peptide in the amino acid sequence encoded either by the corresponding contig or the best hit sequence identified by Blastx comparison, so there is no indication yet that this protein is secreted.

Venom Components That Potentially Moderate Plant Responses to Damage

Biorhiza pallida and *D. rosae* venom glands express a second category of molecules, whose products appear to be involved in modulating the defense reactions of the host plant. Such a process is crucial for the initiation of long-term interactions, as observed for instance in nodulation induced by bacteria in the legume plant symbiosis (Nakagawa et al., 2011). A peroxidase was highly expressed by the venom gland of *B. pallida*, representing to our knowledge the first reported peroxidase in hymenopteran venom. This peroxidase may limit the oxidative stress induced in the oak root following oviposition by the sampled sexual generation of *B. pallida*.

Other putative regulators of plant "early danger signaling" (Dubreuil et al., 2010; Guiguet et al., 2016) identified among the transcripts from the venom glands or the ovaries of both species include an apyrase from *B. pallida*, a peroxiredoxin from *D. rosae* and several 5′ nucleotidases including ectoapyrase, differentially expressed in the venom of both gall wasps. The ectoapyrase could play a role in breaking down extracellular ATP (released by the action of venom hydrolases on plant cells), which is known to induce some plant defenses (Tanaka et al., 2010; Heil et al., 2012).

We also noted expression by the *B. pallida* venom gland of a regucalcin-like protein, similar to a regucalcin in the saliva of pea aphids (Carolan et al., 2009). In pea aphids, the regucalcin binds calcium ions to prevent calcium-mediated shut down of damaged phloem sieve tube elements, allowing prolonged aphid feeding (Carolan et al., 2009), *B. pallida* regucalcin could regulate

oak Ca^{++} level, although its precise role is difficult to predict (Stafford-Banks et al., 2014). The venom gland of *D. rosae* expresses the genes of two proteins able to interact with serine proteases, including a serpin, which belongs to a superfamily of irreversible inhibitors of serine proteases. Serpins have been described from several parasitoid venoms (**Table 4**), in which they prevent triggering of host immune responses (Moreau and Asgari, 2015). It is possible that the gall wasp serpin functions in an analogous way in the plant host. In plants, serpins are thought to have a role in the complex pathways involved in up-regulating the plant immune response (Habib and Fazili, 2007).

Venom Components That Potentially Contribute to Defense of Gall Wasp Eggs Against Antagonistic Microbes

The third important role that venoms of gall wasps seem to fulfill is protection against opportunistic pathogens. Antimicrobial properties of venoms are among the most conserved and widespread properties of hymenopteran venoms (Moreau, 2013), presumably because bacteria and fungi may compromise the quality of larval habitats (nest or host organisms), thus reducing the reproductive success of the species. Venom glands of both species differentially expressed genes coding for chitotriosidase 1-like enzymes of the GH18 chitinase superfamily, a group of chitinases already described in the venoms of several parasitoid wasps (4). In plants, chitotriosidase 1 degrades fungal chitin into monomers of *N*-acetyl-D-glucosamine, which seems to be the least effective compound for elicitation of an immune response (Kasprzewska, 2003; Cabrera et al., 2006; Hamel and Beaudoin, 2010). Degradation of fungal chitin by gall wasp venom chitinases could thus fulfill the dual functions of protecting the egg from direct fungal attack, and preventing a strong host plant defensive response.

Other venom-gland expressed genes may target gall wasp vulnerability to, and plant defenses against, bacteria. Transcripts of a *lysozyme 3-like* gene were identified in the *B. pallida* venom gland transcriptome. Lysozyme is an important component of the insect immune response against bacteria, characterized by its ability to break down bacterial cell walls. We also identified expression of an α-mannosidase gene in the venom gland of *D. rosae*. Mannose is a major sugar of bacterial cell walls and can elicit plant defense responses via the ROS pathway (Hwang and Hwang, 2011). Gall wasp α-mannosidase could limit the triggering of such defenses at the oviposition site, whilst degrading the outermost layers of challenging bacteria.

Contrasts in Venom Gland Structure and Gene Expression Patterns Between *B. pallida* and *D. rosae*

While there are some similarities in the venom gland molecular repertoire of the two gall wasp species studied here, they differ substantially from each other and also from parasitoid wasps (**Table 4**). The two gall wasps also differ substantially in the structure of their venom glands. We hypothesize that these differences at one level reflect deep phylogenetic divergence between *Diplolepis* and *Biorhiza* within the Cynipidae (Ronquist et al., 2015), and further reflect differences in host plants and plant organs galled. One of the most striking findings of this study is the apparently high production of apolipoprotein D (ApoD) in venom glands of *B. pallida* but not *D. rosae*. ApoD could be involved in the production of the abundant spherical particles we observed in *B. pallida* venom (**Figure 3**) that are responsible for its high viscosity, resembling plasmatic apolipoprotein particles observed in vertebrate models (Bergeron et al., 1998). In animals, ApoD is involved in the transport of fatty acids, steroids and other hormones (Rassart et al., 2000). ApoD has also been detected in some plants, where it plays an important function in defense against oxidative bursts (Charron et al., 2008). We speculate that the gall wasp venom ApoD could facilitate transport of fatty acids for the newly hatched larva, be part of a transport system for an as-yet unidentified vesicle-delivered gall wasp product, or play a role in regulation of oxidative stress in the newly colonized plant tissues.

Our microscopic observations have confirmed Vårdal's (2006) observation that, relative to the other Hymenoptera of similar size, *B. pallida* has an exceptionally large venom apparatus. Fluorescence microscopy revealed the existence of a secondary secretory zone located on the dorsal side of a large reservoir, both of which structures are absent from *D. rosae*. Future investigations will help to determine whether the secondary secretory zone is where the abundant spherical particles in *B. pallida* venom are produced. In *D. rosae*, instead of "a small sac-like structure" described by Vårdal (2006), we found in all the examined specimens a long and branched gland connected at the base of the ovipositor, the secretory epithelium of which was supported by a central helix of chitin and lined with muscles. *D. rosae* females (but not *B. pallida*) also possess two small accessory glands that were not included in the sample for transcriptomic analyses. In some gall-inducing sawflies (Symphyta), accessory glands produce gall-growth promoting substances (McCalla et al., 1962; Yamaguchi et al., 2012). Therefore, it would be of interest in future to sequence the transcriptome of the accessory glands of *D. rosae*. Another point of interest is the presence of muscular cells surrounding the reservoir of *B. pallida* and the venom gland of *D. rosae* indicating that venom ejection is probably under the control of a voluntary muscular contraction, in contrast to previous observations suggesting that cynipoids lack reservoir muscles (Vårdal, 2006). After venom ejection, the venom apparatuses could passively return to their initial state either thanks to an internal helix of chitin (in *D. rosae*), or to the high viscosity of the venom (in *B. pallida*).

Possible Acquisition of Gall Wasp Cellulases by Horizontal Gene Transfer From Bacteria

Another significant finding was the strong sequence similarities between cellulase genes expressed in venom glands and/or ovaries of *B. pallida* and genes of bacterial origin. Previous studies have identified horizontal gene transfer from bacteria as an important route for metabolic innovation in insect herbivores (Wybouw et al., 2016), and the similarity between cellulases in *B. pallida* and

bacteria could be explained in this way. Alternative explanations are the production of the cellulases by bacterial endosymbionts or entirely convergent similarity between bacterial and gall wasp cellulases sequences, the latter representing an ancient insect trait lost from some lineages. We consider it unlikely that high expression of cellulase genes in the *B. pallida* venom gland could be due to bacterial endosymbionts because the bacterial sequences in our libraries (all associated with *Wolbachia*) are present only at a low level and mostly in the ovaries. Wider phylogenetic analysis would probably rule out ancestral possession of these genes in insects and other Metazoan lineages. However, the case for a HGT origin would be strengthened by demonstrating that the observed transcripts originate from genes in the cynipid genome (e.g., by demonstrating the presence of flanking genes of definite insect origin and/or presence of introns) and by sequencing flanking regions of the cellulase genes or obtaining a high quality *B. pallida* genome assembly.

The acquisition and venom gland overexpression of a cellulase gene may have been important in the adaptation of gall wasps to parasitism of plants. Why ApoD and (putatively bacterial) cellulases are highly expressed in *B. pallida* but not in equivalent tissues of *D. rosae* remains an open question. However, study of parasitoid wasps has shown that major virulence factors may vary greatly even among congeneric species (Colinet et al., 2013a). Such diversity is probably the result of arms race coevolution between host and parasite, the latter having to shift regularly from one molecular strategy to another to circumvent host resistance (Colinet et al., 2013a).

No Evidence for a Role of Viral Genes or Viral Particles in the Gall Wasp Venom Gland

We observed that several genes, similar to those encoding lysosomal enzymes, were differentially expressed by venom glands of *B. pallida* and *D. rosae*. This supports the hypothesis that some genes encoding venom enzymes originated by duplication of genes coding for lysosomal or other cellular enzymes (Moreau and Guillot, 2005). Interestingly, in *D. rosae*, several typical venom components were found expressed by ovaries, suggesting that this organ has a secretory function complementary to the venom gland. However, we found no evidence for expression of genes of viral origin or for the production of symbiotic viruses or virus-like particles by the ovaries of the gall wasps studied. This contrasts with several parasitoid lineages in which complex viral machineries are used to deliver virulence factors and to manipulate the physiology of the insect hosts (Herniou et al., 2013; Pichon et al., 2015; Burke et al., 2018; Leobold et al., 2018). However, since the analysis of venom gland transcriptomes from *B. pallida* or *D. rosae* revealed a high proportion (80–89%) of novel sequences compared to venom glands from parasitoid wasps (17% in *H. didymator* and 50% in *C. inanitus*) (Vincent et al., 2010; Dorémus et al., 2013), such unannotated transcripts may comprise as yet unknown virus genes. Indeed, this was initially the case for genes later shown to be involved in symbiotic virus particle production of ichneumonid parasitoids (Volkoff et al., 2010). Ongoing sequencing and annotation of gall wasp and host plant genomes will contribute to future advances in this field. Moreover, successful knock down of a venom protein expression in a parasitoid cynipid wasp using RNA interference (Colinet et al., 2014) suggests that functional analysis could be used to study gall inducer factors after mass spectrometry confirmation of their secretion and of their injection at the oviposition site.

DATA AVAILABILITY

The datasets generated for this study can be found in the genbank/EMBL and PRJNA517634.

AUTHOR CONTRIBUTIONS

SC and OG were involved in the experimental approach, detailed analysis of the data set, and draft manuscript writing. SM was involved in the dissection of venom glands, cDNA library constructions, and sequence analysis. PG provided expertise on bioinformatics analyses. JH and GS provided expertise on oak and rose gallers and DG on plant–insect interactions. EH and J-MD were involved in the project conception and direction, and with GS and SM in final manuscript writing.

FUNDING

This work was funded by the ANR project Paratoxose (ANR-09-BLAN-0243-01). GS and JH were supported by the NERC grant NE/J010499 and JH by the NERC Ph.D. studentship.

ACKNOWLEDGMENTS

We thank Aurore Dubuffet, Mélanie Body, and Olivier Plantard for stimulating discussions.

SUPPLEMENTARY MATERIAL

The Supplementary Material for this article can be found online at: https://www.frontiersin.org/articles/10.3389/fphys.2019.00926/full#supplementary-material

REFERENCES

Abe, Y., Melika, G., and Stone, G. N. (2007). The diversity and phylogeography of cynipid gallwasps (Hymenoptera: Cynipidae) of the Oriental and eastern Palearctic regions, and their associated communities. *Oriental Insects* 41, 169–212. doi: 10.1080/00305316.2007.10417504

Bailey, R., Schönrogge, K., Cook, J. M., Melika, G., Csóka, G. Y., Thúroczy, C. S., et al. (2009). Host niches and defensive extended phenotypes structure

parasitoid wasp communities. *PLoS Biology* 7:e1000179. doi: 10.1371/journal.pbio.1000179

Bergeron, N., Kotite, L., Verges, M., Blanche, P., Hamilton, R. L., Krauss, R. M., et al. (1998). Lamellar lipoproteins uniquely contribute to hyperlipidemia in mice doubly deficient in apolipoprotein E and hepatic lipase. *Proc. Natl. Acad. Sci. U. S.A.* 95, 15647–15652. doi: 10.1073/pnas.95.26.15647

Bronner, R. (1973). Propriétés lytiques des śufs de Biorhiza pallida. *C. R. Hebd. Séances Acad. sci. D* 276, 189–192.

Bronner, R. (1985). Anatomy of the ovipositor and oviposition behavior of the gall wasp *Diplolepis rosae* (*Hymenoptera: Cynipidae*). *Can. Entomol.* 117, 849–858. doi: 10.4039/ent117849-7

Brooks, S. E., and Shorthouse, J. D. (1997). Developmental morphology of stem galls of *Diplolepis nodulosa* (*Hymenoptera: Cynipidae*) and those modified by the inquiline *Periclistus pirata* (*Hymenoptera: Cynipidae*) on *Rosa blanda* (*Rosaceae*). *Can. J. Bot.* 76, 365–381. doi: 10.1139/b98-001

Burke, G. R., Simmonds, T. J., Sharanowski, B. J., and Geib, S. M. (2018). Rapid viral symbiogenesis via changes in parasitoid wasp genome architecture. *Mol. Biol. Evol.* 35, 2463–2474. doi: 10.1093/molbev/msy148

Burke, G. R., and Strand, M. R. (2014). Systematic analysis of a wasp parasitism arsenal. *Mol. Ecol.* 23, 890–901. doi: 10.1111/mec.12648

Burow, M., and Halkier, B. A. (2017). How does a plant orchestrate defense in time and space? Using glucosinolates in *Arabidopsis* as case study. *Curr. Opin. Plant Biol.* 38, 142–147. doi: 10.1016/j.pbi.2017.04.009

Cabrera, J. C., Messiaen, J., Cambier, P., and van Cutsem, P. (2006). Size, acetylation and concentration of chitooligosaccharide elicitors determine the switch from defense involving PAL activation to cell death and water peroxide production in *Arabidopsis* cell suspensions. *Physiol. Plant.* 127, 44–56. doi: 10.1111/j.1399-3054.2006.00677.x

Carolan, J. C., Fitzroy, C. I., Ashton, P. D., Douglas, A. E., and Wilkinson, T. L. (2009). The secreted salivary proteome of the pea aphid *Acyrthosiphon pisum* characterized by mass spectrometry. *Proteomics* 9, 2457–2467. doi: 10.1021/pr100881q

Charron, J. B., Ouellet, F., Houde, M., and Sarhan, F. (2008). The plant apolipoprotein D ortholog protects *Arabidopsis* against oxidative stress. *BMC plant biol.* 8:86. doi: 10.1186/1471-2229-8-86

Chevignon, G., Cambier, S., Da Silva, C., Poulain, J., Drezen, J.-M., Huguet, E., et al. (2015). Transcriptomic response of *Manduca sexta* immune tissues to parasitization by the bracovirus associated wasp *Cotesia congregata*. *Insect Biochem. Mol. Biol.* 62, 86–99. doi: 10.1016/j.ibmb.2014.12.008

Chevignon, G., Thézé, J., Cambier, S., Poulain, J., Da Silva, C., Bézier, A., et al. (2014). Functional annotation of Cotesia congregata bracovirus: identification of the viral genes expressed in parasitized host immune tissues. *J. Virol.* 88, 8795–8812. doi: 10.1128/JVI.00209-14

Colinet, D., Deleury, E., Anselme, C., Cazes, D., Poulain, J., Azema-Dossat, C., et al. (2013a). Extensive inter- and intraspecific venom variation in closely related parasites targeting the same host: the case of *Leptopilina* parasitoids of *Drosophila*. *Insect Biochem. Mol. Biol.* 43, 601–611. doi: 10.1016/j.ibmb.2013.03.010

Colinet, D., Mathé-Hubert, H., Allemand, R., Gatti, J.-L., and Poirié, M. (2013b). Variability of venom components in immune suppressive parasitoid wasps: from a phylogenetic to a population approach. *J. Insect Physiol.* 59, 205–212. doi: 10.1016/j.jinsphys.2012.10.013

Colinet, D., Kremmer, L., Lemauf, S., Rebuf, C., Gatti, J. L., and Poirié, M. (2014). Development of RNAi in a *Drosophila* endoparasitoid wasp and demonstration of its efficiency in impairing venom protein production. *J. Insect Physiol.* 63, 56–61. doi: 10.1016/j.jinsphys.2014.02.011

Cornell, H. V. (1983). The Secondary chemistry and complex morphology of galls formed by the Cynipinae (*Hymenoptera*): why and how? *Am. Midl. Nat.* 110, 225–230.

Danchin, E. G., Rosso, M.-N., Vieira, P., Almeida-Engler, J., Coutinho, P. M., Henrissat, B., et al. (2010). Multiple lateral gene transfers and duplications have promoted plant parasitism ability in nematodes. *Proc. Natl. Acad. Sci. U. S. A.* 107, 7651–7656. doi: 10.1073/pnas.1008486107

Dani, M. P., Edwards, J. P., and Richards, E. H. (2005). Hydrolase activity in the venom of the pupal endoparasitic wasp, *Pimpla hypochondriaca*. *Comp. Biochem. Physiol. B* 141, 373–381. doi: 10.1016/j.cbpc.2005.04.010

Danneels, E. L., Rivers, D. B., and de Graaf, D. C. (2010). Venom proteins of the parasitoid wasp *Nasonia vitripennis*: recent discovery of an untapped pharmacopee. *Toxins* 2, 494–516. doi: 10.3390/toxins2040494

Davis, E. L., Hussey, R. S., and Baum, T. J. (2004). Getting to the roots of parasitism by nematodes. *Trends Parasitol.* 20, 134–141. doi: 10.1016/j.pt.2004.01.005

Dawkins, R. (1982). *The Extended Phenotype*. Oxford: Oxford University Press.

de Graaf, D. C., Aerts, M., Brunain, M., Desjardins, C. A., Jacobs, F. J., Werren, J. H., et al. (2010). Insights into the venom composition of the ectoparasitoid wasp *Nasonia vitripennis* from bioinformatic and proteomic studies. *Insect Mol. Biol.* 19, 11–26. doi: 10.1111/j.1365-2583.2009.00914.x

Dlugosch, K. M., Lai, Z., Bonin, A., Hierro, J., and Rieseberg, L. H. (2013). Allele identification for transcriptome-based population genomics in the invasive plant *Centaurea solstitialis*. *G3* 3, 359–367. doi: 10.1534/g3.112.003871

Dorémus, T., Urbach, S., Jouan, V., Cousserans, F., Ravallec, M., Demettre, E., et al. (2013). Venom gland extract is not required for successful parasitism in the polydnavirus-associated endoparasitoid *Hyposoter didymator* (Hym. *Ichneumonidae*) despite the presence of numerous novel and conserved venom proteins. *Insect Biochem. Mol. Biol.* 43, 292–307. doi: 10.1016/j.ibmb.2012.12.010

Drezen, J.-M., Leobold, M., Bézier, A., Huguet, E., Volkoff, A.-N., and Herniou, E. A. (2017). Endogenous viruses of parasitic wasps: variations on a common theme. *Curr. Opin. Virol.* 25, 41–48. doi: 10.1016/j.coviro.2017.07.002

Dubreuil, G., Deleury, E., Magliano, M., Jaouannet, M., Abad, P., and Rosso, M. N. (2010). Peroxiredoxins from the plant parasitic root-knot nematode. *Int. J. Parasitol.* 41, 385–396. doi: 10.1016/j.ijpara.2010.10.008

Elias, L. G., Silva, D. B., Silva, R., Peng, Y.-Q., Yang, D.-R., Lopes, N. P., et al. (2018). A comparative venomic fingerprinting approach reveals that galling and non-galling fig wasp species have different venom profiles. *PLoS One* 13:e0207051. doi: 10.1371/journal.pone.0207051

Giron, D., Huguet, E., Stone, G. N., and Body, M. (2016). Insect-induced effects on plants and possible effectors used by galling and leaf-mining insects to manipulate their host-plant. *J. Insect Physiol.* 84, 70–89. doi: 10.1016/j.jinsphys.2015.12.009

Guiguet, A., Dubreuil, G., Harris, M. O., Appel, H. M., Schultz, J. C., Pereira, M. H., et al. (2016). Shared weapons of blood and plant-feeding insects: surprising commonalities for manipulating hosts. *J. Insect Physiol.* 84, 4–21. doi: 10.1016/j.jinsphys.2015.12.006

Habib, H., and Fazili, K. M. (2007). Plant protease inhibitors: a defense strategy in plants. *Biotechnol. Mol. Biol. Rev.* 2, 68–85.

Hamel, L. P., and Beaudoin, N. (2010). Chitooligosaccharide sensing and downstream signaling: contrasted outcomes in pathogenic and beneficial plant-microbe interactions. *Planta* 232, 787–806. doi: 10.1007/s00425-010-1215-9

Harper, L. J., Schönrogge, K., Lim, K. Y., Francis, P., and Lichtenstein, C. P. (2004). Cynipid galls: insect-induced modifications of plant development create novel plant organs. *Plant Cell Environ.* 27, 327–335. doi: 10.1046/j.1365-3040.2004.01145.x

Heil, M., Ibarra-Laclette, E., Adame-Álvarez, R. M., Martínez, O., Ramirez-Chávez, E., Molina-Torres, J., et al. (2012). How plants sense wounds: damaged-self recognition is based on plant-derived elicitors and induces octadecanoid signaling. *PLoS One* 7:e30537. doi: 10.1371/journal.pone.0030537

Herniou, E. A., Huguet, E., Thézé, J., Bézier, A., Periquet, G., and Drezen, J. M. (2013). When parasitic wasps hijacked viruses: genomic and functional evolution of polydnaviruses. *Philos. Trans. R. Soc. of Lond. B Biol. sci.* 368:20130051. doi: 10.1098/rstb.2013.0051

Hwang, I. S., and Hwang, B. K. (2011). The pepper mannose-binding lectin gene CaMBL1 is required to regulate cell death and defense responses to microbial pathogens. *Plant Physiol.* 155, 447–463. doi: 10.1104/pp.110.164848

Hyatt, D., Chen, G. L., Locascio, P. F., Land, M. L., Larimer, F. W., and Hauser, L. J. (2010). Prodigal: prokaryotic gene recognition and translation initiation site identification. *BMC Bioinformatics.* 11:119. doi: 10.1186/1471-2105-11-119

Kasprzewska, A. (2003). Plant chitinases: regulation and function. *Cell. Mol. Biol. Lett.* 8, 809–824.

Leblanc, D. A., and Lacroix, C. R. (2001). Developmental potential of galls induced by Diplolepis rosaefolii (*Hymenoptera: Cynipidae*) on the leaves of rosa virginiana and the influence of Periclistus species on the diplolepis rosaefolii galls. *Int. J. Plant Sci.* 162, 29–46. doi: 10.1086/317900

Leobold, M., Bézier, A., Pichon, A., Herniou, E. A., Volkoff, A. N., and Drezen, J. M. (2018). The domestication of a large DNA virus by the wasp venturia canescens

involves targeted genome reduction through pseudogenization. *Genome Biol. Evol.* 10, 1745–1764. doi: 10.1093/gbe/evy127

Magalhães, G. S., Lopes-Ferreira, M., Junqueira-de-Azevedo, I. L., Spencer, P. J., Araújo, M. S., Portaro, F. C., et al. (2005). Natterins, a new class of proteins with kininogenase activity characterized from *Thalassophryne nattereri* fish venom. *Biochimie* 87, 687–699. doi: 10.1016/j.biochi.2005.03.016

Magnus, W. (1914). *Die Entstehung der Pflanzengallen Verursacht Durch Hymenopteren*. Germany: Fischer.

Manzoor, A., UlAbdin, Z., Webb, B. A., Arif, M. J., and Jamil, A. (2016). De novo sequencing and transcriptome analysis of female venom glands of ectoparasitoid *Bracon hebetor* (Say.) (*Hymenoptera: Braconidae*). *Comp. Biochem. Physiol. Part D Genom. Proteom.* 20, 101–110. doi: 10.1016/j.cbd.2016.08.002

Martinson, E. O., Hackett, J. D., Machado, C. A., and Arnold, A. E. (2015). Metatranscriptome analysis of fig flowers provides insights into potential mechanisms for mutualism stability and gall induction. *PLoS One* 10:e0130745. doi: 10.1371/journal.pone.0130745

McCalla, D. R., Genthe, M. K., and Hovanitz, W. (1962). Chemical nature of an insect gall growth-factor. *Plant Physiol.* 37, 98–103. doi: 10.1104/pp.37.1.98

Molliard, M. (1917). Production artificielle d'une galle. *C. R. SéancesAcad. Sci.* 165, 160–162.

Moreau, S. J. (2013). "It stings a bit but it cleans well": venoms of hymenoptera and their antimicrobial potential. *J. Insect Physiol.* 59, 186–204. doi: 10.1016/j.jinsphys.2012.10.005

Moreau, S. J., and Asgari, S. (2015). Venom proteins from parasitoid wasps and their biological functions. *Toxins* 7, 2385–2412. doi: 10.3390/toxins7072385

Moreau, S. J., and Guillot, S. (2005). Advances and prospects on biosynthesis, structures and functions of venom proteins from parasitic wasps. *Insect Biochem. Mol. Biol.* 35, 1209–1223. doi: 10.1016/j.ibmb.2005.07.003

Moreau, S. J., Huguet, E., and Drezen, J. M. (2009). "Polydnaviruses as tools to deliver wasp virulence factors to impair lepidopteran host immunity," in *Insect Infection and Immunity: Evolution, Ecology and Mechanisms*, ed. S. Reynolds (Oxford, UK: Oxford University Press), 137–158. doi: 10.1093/acprof:oso/9780199551354.003.0009

Mortazavi, A., Williams, B. A., McCue, K., Schaeffer, L., and Wold, B. (2008). Mapping and quantifying mammalian transcriptomes by RNA-Seq. *Nature Methods* 5, 621–628. doi: 10.1038/nmeth.1226

Nabity, P. D. (2016). Insect-induced plant phenotypes: revealing mechanisms through comparative genomics of galling insects and their hosts. *Am. J. Bot.* 103, 979–981. doi: 10.3732/ajb.1600111

Nakagawa, T., Kaku, H., Shimoda, Y., Sugiyama, A., Shimamura, M., Takanashi, K., et al. (2011). From defense to symbiosis: limited alterations in the kinase domain of LysM receptor-like kinases are crucial for evolution of legume-Rhizobium symbiosis. *Plant J.* 65, 169–180. doi: 10.1111/j.1365-313X.2010.04411.x

Nicholls, J. A., Melika, G., and Stone, G. N. (2016). Sweet tetra-trophic interactions: multiple evolutions of nectar secretion, a defensive extended phenotype in cynipid gallwasps. *Am. Nat.* 189, 67–77. doi: 10.1086/689399

Nielsen, H. (2017). "Predicting Secretory Proteins with SignalP," in *Protein function prediction* (Methods in Molecular Biology vol.1611), ed. D. Kihara (New York,NY: Humana Press), 59–73. doi: 10.1007/978-1-4939-7015-5_6

Paulson, A. R., Le, C. H., Dickson, J. C., Ehlting, J., von Aderkas, P., and Perlman, S. J. (2016). Transcriptome analysis provides insight into venom evolution in a seed-parasitic wasp. Megastigmus spermotrophus. *Insect Mol. Biol.* 25, 604–616. doi: 10.1111/imb.12247

Pichon, A., Bézier, A., Urbach, S., Aury, J.-M., Jouan, V., Ravallec, M., et al. (2015). Recurrent virus domestication leading to different parasite virulence strategies. *Sci. Adv.* 1:e1501150. doi: 10.1126/sciadv.1501150

Pierce, M. P. (2019). The ecological and evolutionary importance of nectar-secreting galls. *Ecosphere* 10:e02670. doi: 10.1002/ecs2.2670

Plantard, O., Rasplus, J.-Y., Mondor, G., Le Clainche, I., and Solignac, M. (1999). Distribution and phylogeny of *Wolbachia* inducing thelytoky in Rhoditini and 'Aylacini' (*Hymenoptera: Cynipidae*). *Insect Mol. Biol.* 8, 185–191. doi: 10.1046/j.1365-2583.1999.820185.x

Poirié, M., Colinet, D., and Gatti, J.-L. (2014). Insights into function and evolution of parasitoid wasp venoms. *Curr. Opin. Insect Sci.* 6, 52–60. doi: 10.1016/j.cois.2014.10.004

Price, P. W., Fernandes, G. W., and Waring, G. L. (1987). Adaptive nature of insect galls. *Environ. Entomol.* 16, 15–24. doi: 10.1093/ee/16.1.15

Rask, L., Andréasson, E., Ekbom, B., Eriksson, S., Pontoppidan, B., and Meijer, J. (2000). Myrosinase: gene family evolution and herbivore defense in brassicaceae. *Plant Mol. Biol.* 42, 93–113. doi: 10.1007/978-94-011-4221-2_5

Rassart, E., Bedirian, A., Do Carmo, S., Guinard, O., Sirois, J., Terrisse, L., et al. (2000). Apolipoprotein D. *Biochim. Biophys. Acta* 1482, 185–198.

Rohfritsch, O. (1992). "Patterns in gall development," in *Biology of Insect-Induced Galls*, eds J. D. Shorthouse and O. Rohfritsch (New York,NY: Oxford University Press), 69–86.

Rokas, A., Atkinson, R. J., Nieves-Aldrey, J.-L., West, S. A., and Stone, G. N. (2002). The incidence and diversity of *Wolbachia* in gallwasps (*Hymenoptera. Cynipidae*) on oak. *Mol. Ecol.* 11, 1815–1829. doi: 10.1046/j.1365-294x.2002.01556.x

Ronquist, F. (1999). Phylogeny, classification and evolution of the cynipoidea. *Zool. scr.* 28, 139–164. doi: 10.1046/j.1463-6409.1999.00022.x

Ronquist, F., and Liljeblad, J. (2001). Evolution of the gall wasp-host plant association. *Evolution* 51, 2503–2522. doi: 10.1111/j.0014-3820.2001.tb00765.x

Ronquist, F., Nieves-Aldrey, J.-L., Buffington, M. L., Liu, Z., Liljeblad, J., and Nylander, J. A. A. (2015). Phylogeny, evolution and classification of gall wasps: the plot thickens. *PLoS One* 10:e0123001. doi: 10.1371/journal.pone.0123301

Shorthouse, J. D., Leggo, J. J., Sliva, M. D., and Lalonde, R. G. (2005). Has egg location influenced the radiation of *Diplolepis* (*Hymenoptera: Cynipidae*) gall wasps on wild roses? *Basic Appl. Ecol.* 6, 423–434. doi: 10.1016/j.baae.2005.07.006

Stafford-Banks, C. A., Rotenberg, D., Johnson, B. R., Whitfield, A. E., and Ullman, D. E. (2014). Analysis of the salivary gland transcriptome of *Frankliniella occidentalis*. *PLoS One* 9:e94447. doi: 10.1371/journal.pone.0094447

Stone, G. N., and Schönrogge, K. (2003). The adaptive significance of insect gall morphology. *Trends Ecol. Evol.* 18, 512–522. doi: 10.1111/j.1558-5646.1998.tb02248.x

Stone, G. N., Schönrogge, K., Atkinson, R. J., Bellido, D., and Pujade-Villar, J. (2002). The population biology of oak gall wasps (*Hymenoptera: Cynipidae*). *Annu. Revi. Entomol.* 47, 633–678.

Strand, M. R., and Pech, L. L. (1995). Immunological basis for compatibility in parasitoid–host relationships. *Annu. Rev. Entomol.* 40, 31–56. doi: 10.1146/annurev.ento.40.1.31

Tanaka, K., Gilroy, S., Jones, A. M., and Stacey, G. (2010). Extracellular ATP signaling in plants. *Trends Cell Biol.* 20, 601–608. doi: 10.1016/j.tcb.2010.07.005

Taper, M. L., and Case, T. J. (1987). Interactions between oak tannins and parasite structure: unexpected benefits of tannins to gall wasps. *Oecologia* 71, 254–261. doi: 10.1007/BF00377292

Taper, M. L., Zimmerman, E. M., and Case, T. J. (1986). Sources of mortality for a cynipid gall wasp (*Dryocosmus dubiosus* (*Hymenoptera: Cynipidae*))—the importance of the tannin-fungus interaction. *Oecologia* 68, 437–445. doi: 10.1007/bf01036752

Vårdal, H. (2006). Venom gland and reservoir morphology in cynipoid wasps. *Arthropod Struct. dev.* 35, 127–136. doi: 10.1016/j.asd.2006.05.002

Vincent, B., Kaeslin, M., Roth, T., Heller, M., Poulain, J., Cousserans, F., et al. (2010). The venom composition of the parasitic wasp *Chelonus inanitus* resolved by combined expressed sequence tags analysis and proteomic approach. *BMC Genom.* 11:693. doi: 10.1186/1471-2164-11-693

Volkoff, A.-N., Jouan, V., Urbach, S., Samain, S., Bergoin, M., Wincker, P., et al. (2010). Analysis of virion structural components reveals vestiges of the ancestral ichnovirus genome. *Plos Pathogens* 6:e1000923. doi: 10.1371/journal.ppat.1000923

Wilson, D. (1995). Fungal endophytes which invade insect galls: insect pathogens, benign saprophytes, or fungal inquilines? *Oecologia* 103, 255–260. doi: 10.1007/BF00329088

Wilson, D., and Carroll, G. C. (1997). Avoidance of high-endophyte space by gall-forming insects. *Ecology* 78, 2153–2163. doi: 10.1890/0012-9658(1997)078\%5B2153:aohesb\%5D2.0.co;2

Wybouw, N., Pauchet, Y., Heckel, D. G., and Van Leeuwen, T. (2016). Horizontal gene transfer contributes to the evolution of arthropod herbivory. *Genome Biol. Evol.* 8, 1785–1801. doi: 10.1093/gbe/evw119

Yamaguchi, H., Tanaka, H., Hasegawa, M., Tokuda, M., Asami, T., and Suzuki, Y. (2012). Phytohormones and willow gall induction by a gall-inducing sawfly. *New Phytol.* 196, 586–595. doi: 10.1111/j.1469-8137.2012.04264.x

Zhu, J.-Y., Fang, Q., Wang, L., Hu, C., and Ye, G. Y. (2010). Proteomic analysis of the venom from the endoparasitoid wasp *Pteromalus puparum* (*Hymenoptera: Pteromalidae*). *Arch. Insect Biochem. Physiol.* 75, 28–44. doi: 10.1002/arch.20380

Zhu, J. Y., Ye, G. Y., and Hu, C. (2008). Molecular cloning and characterization of acid phosphatase in venom of the endoparasitoid wasp *Pteromalus puparum* (*Hymenoptera: Pteromalidae*). *Toxicon* 51, 1391–1399. doi: 10.1016/j.toxicon.2008.03.008

Conflict of Interest Statement: The authors declare that the research was conducted in the absence of any commercial or financial relationships that could be construed as a potential conflict of interest.

frontiers in Physiology

ORIGINAL RESEARCH
published: 06 September 2019
doi: 10.3389/fphys.2019.01106

Regulation of the Larval Transcriptome of *Diatraea saccharalis* (Lepidoptera: Crambidae) by Maternal and Other Factors of the Parasitoid *Cotesia flavipes* (Hymenoptera: Braconidae)

Bruna Laís Merlin and Fernando Luis Cônsoli†*

Insect Interactions Laboratory, Department of Entomology and Acarology, College of Agriculture "Luiz de Queiroz", University of São Paulo, Piracicaba, Brazil

OPEN ACCESS

Edited by:
Michel Cusson,
Natural Resources Canada, Canada

Reviewed by:
Don Stoltz,
Dalhousie University, Canada
M. Lukas Seehausen,
CABI, Switzerland

***Correspondence:**
Fernando Luis Cônsoli
fconsoli@usp.br

†ORCID:
Fernando Luis Cônsoli
orcid.org/0000-0002-2287-0782

Specialty section:
This article was submitted to Invertebrate Physiology, a section of the journal Frontiers in Physiology

Received: *04 January 2019*
Accepted: *12 August 2019*
Published: *06 September 2019*

Citation:
Merlin BL and Cônsoli FL (2019) Regulation of the Larval Transcriptome of Diatraea saccharalis (Lepidoptera: Crambidae) by Maternal and Other Factors of the Parasitoid Cotesia flavipes (Hymenoptera: Braconidae). Front. Physiol. 10:1106. doi: 10.3389/fphys.2019.01106

Koinobiont endoparasitoid wasps regulate the host's physiology to their own benefit during their growth and development, using maternal, immature and/or derived-tissue weaponry. The tools used to subdue the wasps' hosts interfere directly with host transcription activity. The broad range of host tissues and pathways affected impedes our overall understanding of the host-regulation process during parasitoid development. Next-generation sequencing and *de novo* transcriptomes are helpful approaches to broad questions, including in non-model organisms. In the present study, we used Illumina sequencing to assemble a *de novo* reference transcriptome of the sugarcane borer *Diatraea saccharalis*, to investigate the regulation of host gene expression by the larval endoparasitoid *Cotesia flavipes*. We obtained 174,809,358 reads and assembled 144,116 transcripts, of which 44,325 were putatively identified as lepidopteran genes and represented a substantial number of pathways that are well described in other lepidopteran species. Comparative transcriptome analyses of unparasitized versus parasitized larvae identified 1,432 transcripts of *D. saccharalis* that were up-regulated under parasitization by *C. flavipes*, while 1,027 transcripts were down-regulated. Comparison of the transcriptomes of unparasitized and pseudoparasitized *D. saccharalis* larvae led to the identification of 1,253 up-regulated transcripts and 972 down-regulated transcripts in the pseudoparasitized larvae. Analysis of the differentially expressed transcripts showed that *C. flavipes* regulated several pathways, including the Ca^{+2} transduction signaling pathway, glycolysis/gluconeogenesis, chitin metabolism, and hormone biosynthesis and degradation, as well as the immune system, allowing us to identify key target genes involved in the metabolism and development of *D. saccharalis*.

Keywords: calcium signaling regulation, gene expression, host regulation, host–parasitoid interactions, polydnavirus, sustainable pest management

INTRODUCTION

Parasitoids have developed a variety of adaptive processes to colonize and successfully develop in a range of host stages (Godfray, 1994). The processes that parasitoids employ vary with the parasitoids' developmental strategies, but all parasitoids manipulate the host's physiology and metabolism, in a process known as host regulation (Vinson and Iwantsch, 1980). Host regulation may rely on passive and/or active mechanisms (Schmidt et al., 2001). Parasitoids use passive mechanisms to elude host immune cells by hiding their eggs in tissues to which host hemocytes have limited access, or by covering their eggs with immunoevasive proteins produced in the wasp ovaries (Schmidt et al., 2001; Dorémus et al., 2013a). Mechanisms of active regulation are stimulated by maternal factors (ovarian proteins, venom, and viral particles) injected during oviposition, or by factors that parasitic larvae and/or teratocytes release during growth. Active mechanisms alter the host physiology in such a way that the host becomes a suitable environment to sustain parasitoid growth and development (Yu et al., 2007; Asgari and Rivers, 2011; Cônsoli and Vinson, 2012; Dorémus et al., 2013a; Strand and Burke, 2013; Strand, 2014). Strategies for host regulation by koinobionts can be quite variable. The venom may play no role in evading the host immune system in *Hyposoter didymator* (Thunberg) (Hymenoptera: Ichneumonidae), whereas it is pivotal in *Cotesia chilonis* (Munakata) (Hymenoptera: Braconidae) (Dorémus et al., 2013b; Teng et al., 2016).

Members of some subfamilies of Braconidae and Ichneumonidae have mutualistic associations with polydnaviruses (PDV). In the wasp, two forms of PDV DNAs are recognized: viral and insect. DNA sequences in the former category have a viral origin, but are not packaged. Instead, DNA sequences of non-viral origin are packaged for delivery to the parasitized host. The virus particles are released into the calyx lumen, to be injected with the wasp eggs at parasitization. DNA packaging occurs during viral morphogenesis, a process that is restricted to cells of the ovarian calyx of female wasps (Kroemer and Webb, 2004; Burke and Strand, 2012). PDV infects a range of cells of the host, affecting the host's cellular machinery to regulate several aspects of the host physiology (Strand, 2008). The expression of viral genes leads to regulation of ecdysteroidogenesis and of ecdysteroid secretion by prothoracic glands in the host during parasitization (Pruijssers et al., 2009; Kim et al., 2013; Ignesti et al., 2018). Proteins encoded by genes of the encapsidated form are also required to regulate the host immune response. The humoral immune response is affected by regulation of translation of proteins needed to activate the phenoloxidase cascade (Beck and Strand, 2007; Prasad et al., 2014), and the cellular immune response is affected through the disruption of the cellular cytoskeleton, and the hemocyte attachment and spreading behavior (Pruijssers and Strand, 2007; Kumar and Kim, 2016). PDV also regulates the host metabolism by affecting nutrient uptake and allocation (Thompson, 2001; Bottjen, 2011; Di Lelio et al., 2014; Kumar et al., 2016). Recent data showed that host regulation by PDV also influences the herbivore's interaction with the host plant, lowering the capacity of parasitized larvae to elicit the plant's immune response, by reducing the availability of salivary glucose oxidase (Tan et al., 2018).

Research to identify the bioactive molecules that parasitoids use to regulate their hosts and expand our understanding of the regulation of host gene expression has intensified, with next-generation sequencing techniques and bioinformatic tools supporting systemic analyses (Fang et al., 2010; Etebari et al., 2011; Provost et al., 2011; Laurino et al., 2016). Genomic analyses are elucidating the organization of the integrated and encapsidated forms of the PDV genome (Chevignon et al., 2014), and transcriptome analyses are depicting the profile of viral and host gene expression in parasitized hosts (Bitra et al., 2011; Provost et al., 2011; Dorémus et al., 2014; Ali et al., 2015). Integrative analyses have identified bioactive molecules present in maternal factors injected by the parasitoid (Laurino et al., 2016; Liu et al., 2017).

Diatraea saccharalis (F.) (Lepidoptera: Crambidae) is the major pest of sugarcane in Brazil causing direct and indirect damage. Losses in sugar and ethanol production due to insect damage to sugarcane can be as high as 10%, resulting in an economic loss of nearly US$ 4,6 billion/year (Oliveira et al., 2014). The larval boring behavior also limits the use of chemical strategies for the control of this pest, and the use of biological control through macrophages has been the best strategy to manage this pest (Botelho and Macedo, 2002). Among all natural enemies used to control the sugarcane borer, *Cotesia flavipes* (Cameron) (Hymenoptera: Braconidae) is the only parasitoid that is currently mass-produced to target the larval stage of this pest. *Cotesia flavipes* is exotic to Brazil. It is a common larval endoparasitoid of several species of Crambidae and other borers in Southeast Asia and Australia. *Cotesia flavipes* was introduced early in the 1970s from Trinidad, where it has been introduced earlier from Mauritius and India (Botelho and Macedo, 2002). Biological control with *C. flavipes* requires the constant release of adult wasps in the field, which keeps the infestation levels of *D. saccharalis* close to 2–3% (Botelho and Macedo, 2002). The successful exploitation of *D. saccharalis* by *C. flavipes* is partially due to the demonstrated capacity of this parasitoid to regulate its host physiology. *Cotesia flavipes* has been demonstrated to alter the host metabolism by affecting the availability of sugars and proteins circulating in the hemolymph and stored in the fat body tissues (Salvador and Cônsoli, 2008), and by influencing food consumption and utilization by parasitized larvae (Rossi et al., 2014). *Cotesia flavipes* also affects the host cellular and humoral immune response by affecting the total hemocyte population and phenoloxidase activity (Mahmoud et al., 2011, 2012). The suppression of the immune system of *D. saccharalis* by *C. flavipes* is highly effective, but the efficiency in escaping host immune response (egg encapsulation) is reduced in *Diatraea grandiosella* (Dyar) (Lepidoptera: Crambidae) (Alleyne and Wiedenmann, 2001) and completely ineffective in avoiding encapsulation by larvae of *Ostrinia nubilalis* (Walker) (Lepidoptera: Pyralidae) (Alleyne and Wiedenmann, 2001) and *Manduca sexta* (L.) (Lepidoptera: Sphingidae) (Rodríguez-Pérez et al., 2005). Like other species in the *flavipes* complex, *C. flavipes* is also associated with a polydnavirus (Cônsoli and Kitajima, 2006). PDV associated with

species in the *flavipes* complex as well as bracoviruses and ichnoviruses associated with other wasp species are known to have a key role in the immunosuppression of parasitized hosts (Ye et al., 2018). The failure of *C. flavipes* to immunosuppress *O. nubilalis* and *M. sexta* suggests a narrow physiological range for the *C. flavipes* PDV-produced imunnosuppressants (Alleyne and Wiedenmann, 2001; Rodríguez-Pérez et al., 2005).

The broad array of functional targets that parasitic wasps are able to regulate and the diversity of bioactive molecules that they produce to successfully control several attributes of the host biology and physiology have great potential for the development of sustainable biotechnologies for pest management (Beckage and Gelman, 2004). Successful exploitation of the host regulation process as a source of new targets and/or bioactive molecules relies on identification and understanding of the functional processes affected during this process. We investigated the process of regulation of the gene expression of the sugarcane borer *D. saccharalis* parasitized by the larval endoparasitoid *C. flavipes*. Our purpose was to identify target genes and the pathways of the host that are regulated by maternal factors injected by female wasps during parasitization, or by factors that are released by the developing immature parasitoids, using comparative transcriptome analyses of control, parasitized and pseudoparasitized larvae, based on a *de novo* transcriptome of *D. saccharalis* larvae.

We provide the first larval transcriptome of the sugarcane borer *D. saccharalis* and an in depth analysis of the gene expression regulation of sugarcane borer larvae by its endoparasitoid *C. flavipes*. Our data add to the existing literature of host regulation by parasitoids through the investigation of an undescribed system, and the investigation of the regulation of the host gene expression in natural and pseudoparasitized larvae. We expect our data will contribute to the discovery of target genes and/or pathways of the sugarcane borer amenable to manipulation that could be further exploited in the development of alternative strategies for pest control.

MATERIALS AND METHODS

Rearing of *D. saccharalis* and *C. flavipes*

A stock colony of *D. saccharalis* was reared on an artificial diet based on soy flour and wheat germ (King et al., 1985) under controlled laboratory conditions (25 ± 1°C; 60 ± 10% RH; photophase of 14 h). A stock colony of *C. flavipes* was maintained using fourth and fifth instars of *D. saccharalis* as hosts for parasitization. The stock colony of *D. saccharalis* was obtained from field collections in the region of Piracicaba, state of São Paulo, and has been maintained in culture for the last 10 years without introduction of field-collected insects. *Cotesia flavipes* was obtained from sugarcane mills insectaries, and it belongs to the original colony that was introduced from Trinidad into Brazil (Botelho and Macedo, 2002). The host larvae were offered individually to female wasps for a single sting. Once female wasps stung the larvae, larvae were individually transferred to rearing containers containing new artificial diet, until the parasitoid larvae exited from the host larvae. After cocoon formation, the masses of cocoons were collected and transferred to clean plastic dishes until the wasps emerged.

Irradiation of *C. flavipes* Cocoons

In order to obtain females that would lay inviable, sterile eggs for the pseudoparasitization experiments, cocoons containing late-stage pupae (7–8 days old) of the parasitoid *C. flavipes* were collected and subjected to ^{60}Co gamma irradiation at 75 Gy in a GammaCell 220 irradiator (MDS Nordion, Ottawa, ON, Canada) at the Laboratory of Radiology and Environment – Center of Nuclear Energy in Agriculture (CENA/USP), to sterilize the adults. Previous data from our laboratory showed the irradiation dosage applied led to the complete sterilization of the developing adults, with no harm to their successful emergence and host parasitization (Lopes, 2008). After irradiation, cocoons were maintained in controlled conditions until adults' emergence and parasitization.

Parasitization of *D. saccharalis* Larvae by *C. flavipes*

Newly molted fifth-instar of *D. saccharalis* were divided in three subgroups: (i) control, larvae that were not parasitized; (ii) parasitized, larvae that were individually parasitized by naïve, fed and mated *C. flavipes* females, exposing the hosts to virulence factors from the calyx fluids, PDV particles, venom, and larval and teratocyte secretions of the parasitoid; and (iii) pseudoparasitized, larvae that were individually parasitized by gamma-irradiated sterile *C. flavipes* females, exposing the hosts only to virulence factors from the calyx fluids, PDV particles, and venom of the wasp. Larvae that were subjected to parasitization or pseudoparasitization were stung only once by female wasps. Subsamples of parasitized and pseudoparasitized larvae were removed for later dissection to confirm the level of successful parasitization (parasitized) or female sterilization (pseudoparasitized) by inspection of the parasitoid larvae. All larvae were placed in individual tubes containing artificial diet and maintained in controlled laboratory conditions as described above, to allow them to develop.

Tissue Collection and RNA Extraction of *D. saccharalis*

Larvae of *D. saccharalis* parasitized and pseudoparasitized by *C. flavipes* and unparasitized control larvae were sampled 1, 3, 5, and 7 days after parasitization and immediately placed in RNA*later* stabilization solution (Thermo Fisher Scientific), and then stored at −80°C until RNA extraction. Each sampling period had three biological replicates, each replicate consisting of a pool of five larvae. Forced by a sudden limitation in funds, the total RNA later obtained from each sampling period had to be pooled, and each pooled sample represented one sample with a mixture of larvae sampled 1, 3, 5, and 7 days after parasitization.

Larval tissues were disrupted using a TissueLyser II LT^{TM} (Qiagen), following the manufacturer's recommendations. The processed tissues were transferred to 1.5 mL microtubes containing 1 mL TrizolTM reagent (Invitrogen). Samples were homogenized manually, centrifuged (12,000 g × 10 min × 4°C),

and the upper layer mixed with 200 μL chloroform. Samples were homogenized by inversion, incubated at room temperature for 3 min and centrifuged (12,000 g × 15 min × 4°C). The aqueous layer was collected, added to 500 μL isopropanol, incubated for 10 min and centrifuged (12,000 g × 10 min × 4°C). The pellet was washed with 75% ethanol and centrifuged (7,500 g × 5 min × 4°C) twice. The samples were allowed to dry at room temperature and the pelleted RNA was recovered in 30 μL RNAse-free water and incubated at 60°C for 15 min.

Total RNA was quantified using the EpochTM Microplate Spectrophotometer (Fisher Scientific). After quantification, samples collected at 1, 3, 5, and 7 days after parasitization were used in the preparation of an equimolar mixture for each biological replicate of the three treatments: (i) control, (ii) parasitized, and (iii) pseudoparasitized. Each biological replicate represented a pool of 20 larvae sampled at 1, 3, 5, and 7 days after parasitization. Each treatment was represented by three biological replicates, totaling 60 larvae for each treatment.

cDNA Sequencing

Differentially expressed genes of *D. saccharalis* larvae parasitized or pseudoparasitized by *C. flavipes* were identified by sequencing cDNA libraries using the Illumina© HiScanSQ platform, available at the Multiusers Center of Agricultural Biotechnology at the Department of Animal Sciences, ESALQ/USP.

RNA integrity was confirmed using the Agilent Bioanalyzer 1000 (Agilent Technologies). RNA samples were prepared for sequencing using the cDNA TruSeq RNA Library Prep Kit (Illumina©) following a paired-end (2 × 100 bp) strategy. Briefly, mRNA was purified from total RNA using oligo(dT) magnetic beads and fragmented into sequences of 200 nucleotides. Fragmented mRNA was ligated to random primers, followed by the reverse transcription reaction for cDNA library construction. The cDNA produced was end-repaired and purified using magnetic beads and ethanol washing. After the end repair, adenosine was added at the 3′ end of each cDNA fragment to guide the ligation of specific adapters. Adapters consisted of primers for transcription primers and a specific index to code each sample. Samples were enriched with limited-cycle PCR and analyzed to confirm the success of sample preparation.

De novo Transcriptome Assembly

Reads obtained from sequencing the cDNA libraries of the control, parasitized and pseudoparasitized larvae of *D. saccharalis* were visualized in FastQC software to verify the quality (Andrews, 2010). Reads were then analyzed using Trimmomatic-0.36 (Bolger et al., 2014) for clipping Illumina adapters and quality filtering by trimming the leading (LEADING:3) and trailing (TRAILING:3) nucleotides until the quality was higher than 3, and then using a sliding window of 4 nucleotides and trimming when scores were lower than 22 (SLIDINGWINDOW 4:22). Remaining reads shorter than 25 nucleotides were also excluded.

Reads obtained from all replicates of the three treatments (control, parasitized, and pseudoparasitized) were used to assemble a *de novo* transcriptome, using the pipeline available in the Trinity-v.2.4.0 software (Haas et al., 2013). Both paired and unpaired trimmed and quality filtered reads were used to assemble a *de novo* transcriptome that was used as the reference transcriptome for the RNASeq experiments. Assemblage was obtained using normalization of the reads coverage (<50), and the minimum contig size selected was 200 nucleotides.

The transcripts obtained were functionally annotated using the BlastX algorithm for putative identification of homologous sequences, with an *e*-value cut-off $< 10^{-3}$. Annotated sequences were cured and grouped into categories according to their function, using Blast2Go® (Conesa et al., 2005), with an *e*-value cut-off $< 10^{-6}$ and EggNOG-mapper 4.5.1 (Huerta-Cepas et al., 2017). Transcripts putatively identified as belonging to lepidopteran genes were checked against the KEGG database (Kyoto Encyclopedia of Genes and Genomes) (Kanehisa and Goto, 2000) to verify the metabolic pathways represented in the obtained *de novo* transcriptome.

Differential Gene Expression Analyses

The differential gene expression among the control and larvae of *D. saccharalis* parasitized and pseudoparasitized by *C. flavipes* was analyzed using the software RSEM (Li and Dewey, 2011). Reads from each library were counted against the *de novo* transcriptome and counts were normalized as transcripts per million reads (TPM). TPM values for each sample sequenced were used to calculate fold-change ratios for comparative analyses of the gene expression of control (NP) versus parasitized (P), and control versus pseudoparasitized (PP) larvae. Analyses were carried out using the statistical package EdgeR (Robinson et al., 2010), and the values of fold change obtained were corrected with the False Discovery Rate (FDR) method. Only transcripts that showed $p < 0.05$ and log fold change $> |2|$ between treatments were considered differentially expressed. Differentially expressed transcripts were grouped according to the physiological processes in which they are involved.

RESULTS

De novo Transcriptome Assembly

Reads obtained from the control and larvae of *D. saccharalis* parasitized and pseudoparasitized by *C. flavipes* had a mean quality score >32 for each nucleotide position, with less than 2% being filtered (**Supplementary Table S1**). Quality filtering and trimming yielded 174,809,358 reads, which resulted in the assembly of 144,116 transcripts (**Supplementary Table S2**). Annotation of the *de novo* assembly allowed a putative identification of 84,678 transcripts, of which 14,177 sequences were allocated to different gene ontology categories.

One-third of the annotated transcripts were similar to genes belonging to Lepidoptera and approximately 15% to Hymenoptera (**Figure 1A**). Of the 44,325 transcripts expressed by *D. saccharalis* that were similar to Lepidoptera sequences, 26% were similar to *Amyelois transitella* (Walker) (Lepidoptera: Crambidae), 22% to *Helicoverpa armigera* (Hübner) (Lepidoptera: Noctuidae), and 11.5% to *Bombyx mori* (L.) (Lepidoptera: Bombycidae) sequences (**Figure 1B**). Annotation of 7,928 transcripts resulted in

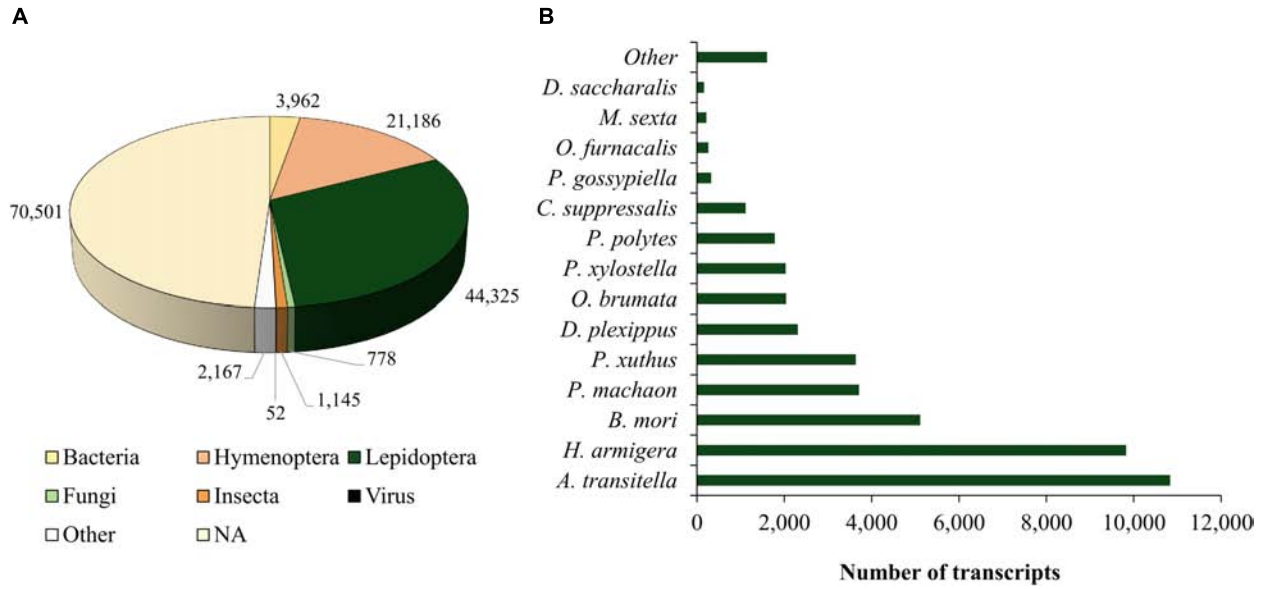

FIGURE 1 | Distribution of alignments and transcripts of *de novo* assembly of control larvae of *Diatraea saccharalis* parasitized and pseudoparasitized by *Cotesia flavipes* after search for similarity in NCBI databank; **(A)** Groups represented by *de novo* assembly; **(B)** Lepidoptera species obtained in the annotation of transcripts of *D. saccharalis: Manduca sexta; Ostrinia furnacalis; Pectinophora gossypiella; Chilo suppressalis; Papilio polistes; Ophemerata brunata; Danaus plexippus; Papilio xuthus; Papilio machaon; Bombyx mori; Helicoverpa armigera; Amyelois transitella*.

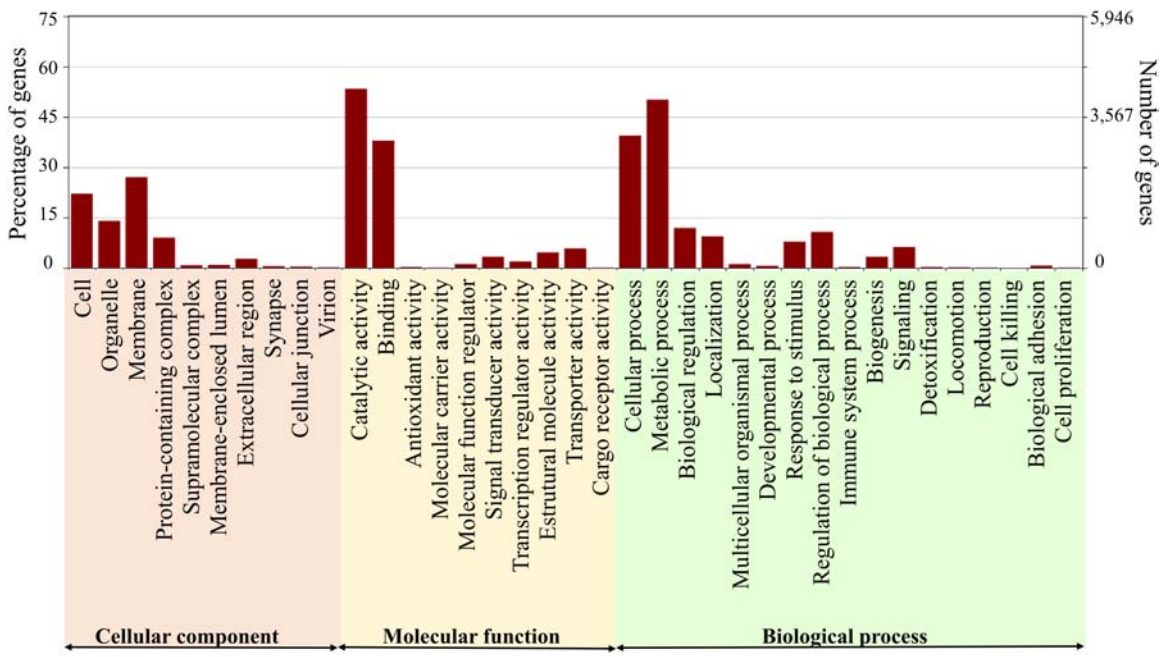

FIGURE 2 | Distribution of functionally annotated transcripts of *Diatraea saccharalis* in gene ontologies.

their grouping in categories of cellular component (10), molecular function (10), and biological process (17) (**Figure 2**). The enzyme codes generated from the annotation of the transcriptome of *D. saccharalis* led to the identification of 7,006 transcripts represented in the metabolic pathways using KEGG (Kanehisa and Goto, 2000), confirming the quality and representativeness of the *de novo* assembly obtained (**Supplementary Figure S1**).

Differential Gene Expression Analyses

Unparasitized, parasitized and pseudoparasitized larvae of *D. saccharalis* by *C. flavipes* shared more than 50% of the

transcripts from the *de novo* assembly (**Figure 3**). *D. saccharalis* larvae non-parasitized and pseudoparasitized by *C. flavipes* had about 1% exclusive transcripts, while parasitized larvae had more than 20% exclusive transcripts (**Figure 3**).

Differential expression gene analysis indicated that a total of 2,459 transcripts of *D. saccharalis* larvae were differentially expressed when parasitized by *C. flavipes*. The majority of the differentially expressed transcripts (1,764) were down- or up-regulated, 625 were expressed exclusively in parasitized hosts, and 70 were completely inhibited by parasitization. A smaller number of differentially expressed genes (2,225) were identified in larvae of *D. saccharalis* pseudoparasitized by *C. flavipes*. The number of transcripts unique to pseudoparasitized larvae (643) was close to the number of unique transcripts in parasitized larvae (625), but 97 transcripts were completely inhibited in pseudoparasitized larvae compared with the 70 transcripts in parasitized larvae. A total of 1,485 transcripts were up- or down-regulated in pseudoparasitized larvae. Although the number of differentially expressed genes differed between parasitized and pseudoparasitized larvae, we found that both sets of differentially expressed genes represented the same functional groups.

The 1,027 transcripts down-regulated in parasitized larvae differed by fold changes from −4 to more than −10,000-fold, with the majority differing in expression by fold-change values between −4 and −100-fold (**Figure 4**). Fold-change values of the 1,432 up-regulated transcripts in parasitized larvae ranged from 4 to 1,000 times. Fold-change values for differentially expressed genes in pseudoparasitized larvae were similar to the values observed for parasitized larvae. Values for fold change for the 972 sequences of *D. saccharalis* that were down-regulated in pseudoparasitized larvae ranged from −4 to −100, while the fold changes for the 1,253 up-regulated sequences were mainly between 4 and 1,000-fold (**Figure 4**).

A serine protease inhibitory protein (IIL_32799_c0_g1_i4: logFC = 7) and a defensin precursor (IIL_25072_c0_g1_i1: logFC = 12.74) were included in the group of transcritps with the highest fold-change differences after parasitization, while cuticular proteins (IIL_26787_c0_g1_i3: logFC = –10.12; IIL_31999_c0_g2_i4: logFC = –10.10) were the most strongly regulated in parasitized larvae. In pseudoparasitized larvae, genes of the immune humoral response, i.e., trypsin and Toll proteins (IIL_33635_c0_g1_i23: logFC = 6.84; IIL_34261_c0_g1_i7: logFC = 7.36), were among the most strongly regulated. Expression of genes coding for cuticular proteins was also strongly inhibited in pseudoparasitized larvae (IIL_31999_c0_g2_i4: logFC = –14.23; IIL_28404_c0_g3_i1: logFC = –11.54; IIL_21160_c0_g1_i1: logFC = –10.57; IIL_23374_c0_g1_i1: logFC = –9.95).

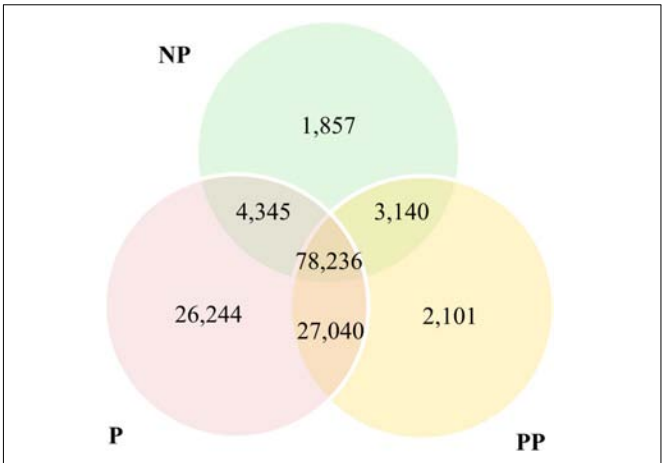

FIGURE 3 | Venn diagram of transcripts of the *de novo* assembly of *Diatraea saccharalis* larvae expressed in control (NP) and parasitized (P) and pseudoparasitized (PP) larvae by *Cotesia flavipes*.

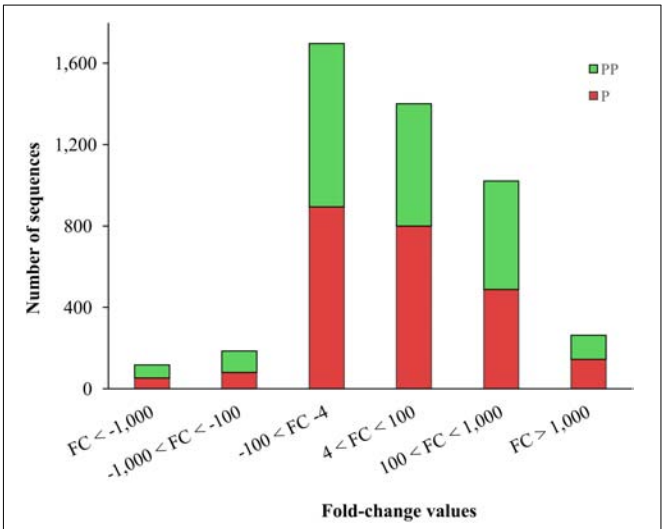

FIGURE 4 | Fold change of differentially expressed genes of *Diatraea saccharalis* larvae parasitized (P) or pseudoparasitized (PP) by *Cotesia flavipes*.

Regulation of Cell Cycle and Apoptosis

The expression of genes involved in cell cycle regulation was affected in parasitized and pseudoparasitized larvae, but a much higher number of differentially expressed transcripts was detected in parasitized than in pseudoparasitized larvae. DNA duplication and cell cycle progression were affected by the down-regulation of cyclin-dependent kinases in both conditions (IIL_22184_c0_g1_i1: cyclin-dependent kinase 20, logFC = –2.91 in P; logFC = −3.39 in PP; IIL_27801_c0_g1_i3: cyclin-dependent kinase 10, logFC = −2.87 in P; −2.29 in PP; IIL_29239_c4_g1_i2: cyclin-dependent kinase 2, logFC = –4.01 in P).

Larval parasitization by *C. flavipes* also led to the down-regulation of inducers of cell apoptosis in parasitized and pseudoparasitized *D. saccharalis*, such as the apoptosis-inducing factor 1 (IIL_32688_c2_g2_i1: logFC = −2.74 in P; IIL_32688_c2_g2_i3: logFC = –2.06 in P; IIL_32688_c2_g2_i6: logFC = –2.55 in P; IIL_32688_c2_g2_i7: logFC = −3.85 in P; −3.87 in PP) and programed cell death 4 (IIL_3726_c0_g2_i1: logFC = –9.85 in P). However, the apoptotic chromatin condensation inducer in the nucleus-like and the death-associated kinase related isoform X2 were up-regulated

(IIL_32093_c0_g1_i2: logFC = 8.84 in P, logFC = 8.78 in PP). Caspase 1 and 4 were also up-regulated (IIL_30089_c3_g1_i4: logFC = 7.65 in P; logFC = 8.68 in PP; IIL_31764_c1_g1_i11: logFC = 8.42 in P; IIL_31764_c1_g1_i12: logFC = 3.05 in P; logFC = 2.78 in PP). Enzymes involved in regulation of transduction signaling pathways that result in cellular apoptosis and degradation of reactive oxygen species, and detoxification (ABC transporters, glutathione S-transferase and cytochrome P450) were up-regulated in both parasitized and pseudoparasitized *D. saccharalis* larvae.

Regulation of Ribosomal Genes and Host Transcription/Translation Factors

Most of the ribosomal-protein genes were found to be regulated in parasitized and pseudoparasitized larvae. Thirty-seven ribosomal genes were down-regulated and 12 were up-regulated in parasitized larvae. A smaller number of ribosomal protein genes were affected in pseudoparasitized larvae, with 26 down-regulated and 10 up-regulated genes. Mitochondrial 28S ribosomal, 39S ribosomal L13, and 40S ribosomal L subunits were down-regulated in both larvae attacked by *C. flavipes* (**Figure 5A**).

Host transcription factors were targeted for regulation in both parasitized and pseudoparasitized larvae (**Figures 5B,C**). We identified a total of 61 transcription factors that were differentially expressed. Twenty-two were equally regulated in parasitized and pseudoparasitized larvae. Levels of expression of another 24 transcription factors were altered exclusively in parasitized larvae, e.g., the nuclear transcription factor E75B (IIL_29251_c0_g1_i5: logFC = −2.10) and POU class transcription factor (IIL_24864_c0_g1_i1: logFC = −2.54; IIL_24864_c0_g1_i2: logFC = −2.02). However, the histone deacelylase 6 isoform X2 (IIL_24484_c0_g1_i2: logFC = −3.22) and 15 other gene expression regulators were altered only in pseudoparasitized larvae (**Figure 5B**). *Cotesia flavipes* regulation of host gene expression also targeted the transcription repressor factor 'transcriptional repressor YY1-like isoform X1' (transcript IIL_30586_c0_g1_i2, logFC = 9 in P; logFC = 9.85 in PP). Post-transcriptional regulation of the host was also observed in larvae of *D. saccharalis* parasitized or pseudoparasitized by *C. flavipes*, with up-regulation of the translational repressor factor 'eukaryotic translation initiation factor 4E-binding 2′ (4E-BPs) (IIL_30132_c1_g1_i4: logFC = 2.40 in P, logFC = 2.61 in PP; IIL_31514_c0_g1_i13: logFC = 4.63 in P). 4E-BPs bind to eukaryotic translation initiation factors (eIFs), preventing translation. eIFs are proteins that direct ribosomes to the 5′-cap of mature mRNA. Besides the up-regulation of repressors of eIFs, larvae of *D. saccharalis* that were parasitized or pseudoparasitized by *C. flavipes* also had the expression levels of several eIFs (eukaryotic translation initiation factor 2, 3F and 5B) down-regulated (**Figure 5C**).

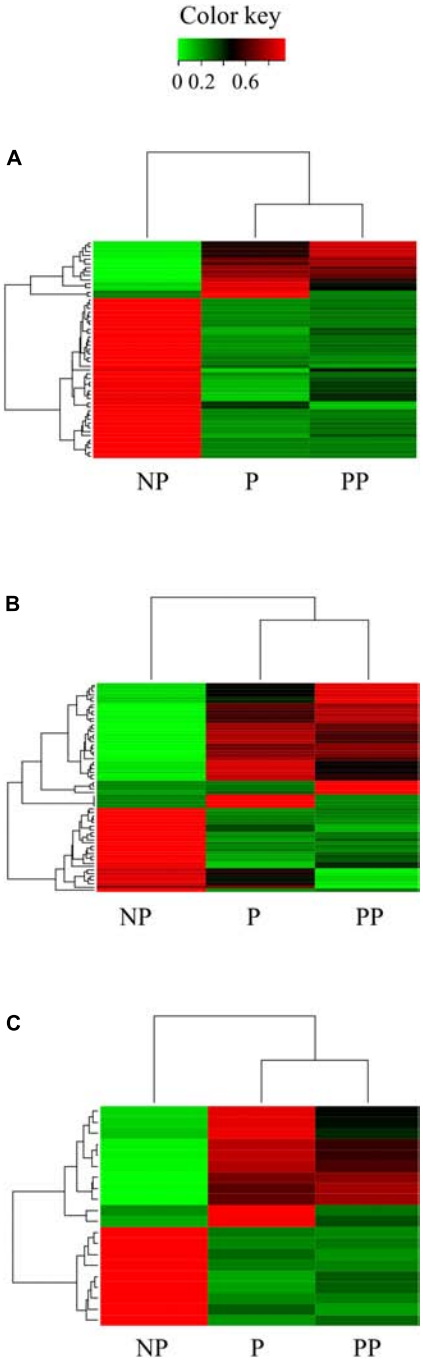

FIGURE 5 | Heatmap of sequences of **(A)** ribosomal proteins, **(B)** transcription factors, and **(C)** translation factors regulated in larvae *Diatraea saccharalis* parasitized and pseudoparasitized by *Cotesia flavipes*.

Hormonal Regulation

Regulation of target pathways by *C. flavipes* was observed not only through the regulation of transcription factors, but also of other genes belonging to the pathway. The host hormone metabolism was affected by regulation of the E75B transcription factor (IIL_29251_c0_g1_i5) and of another 28 transcripts in parasitized and 19 transcripts in pseudoparasitized larvae involved in hormone metabolism. Parasitized and pseudoparasitized larvae shared 15 differentially expressed genes that are involved in hormone metabolism (**Table 1**).

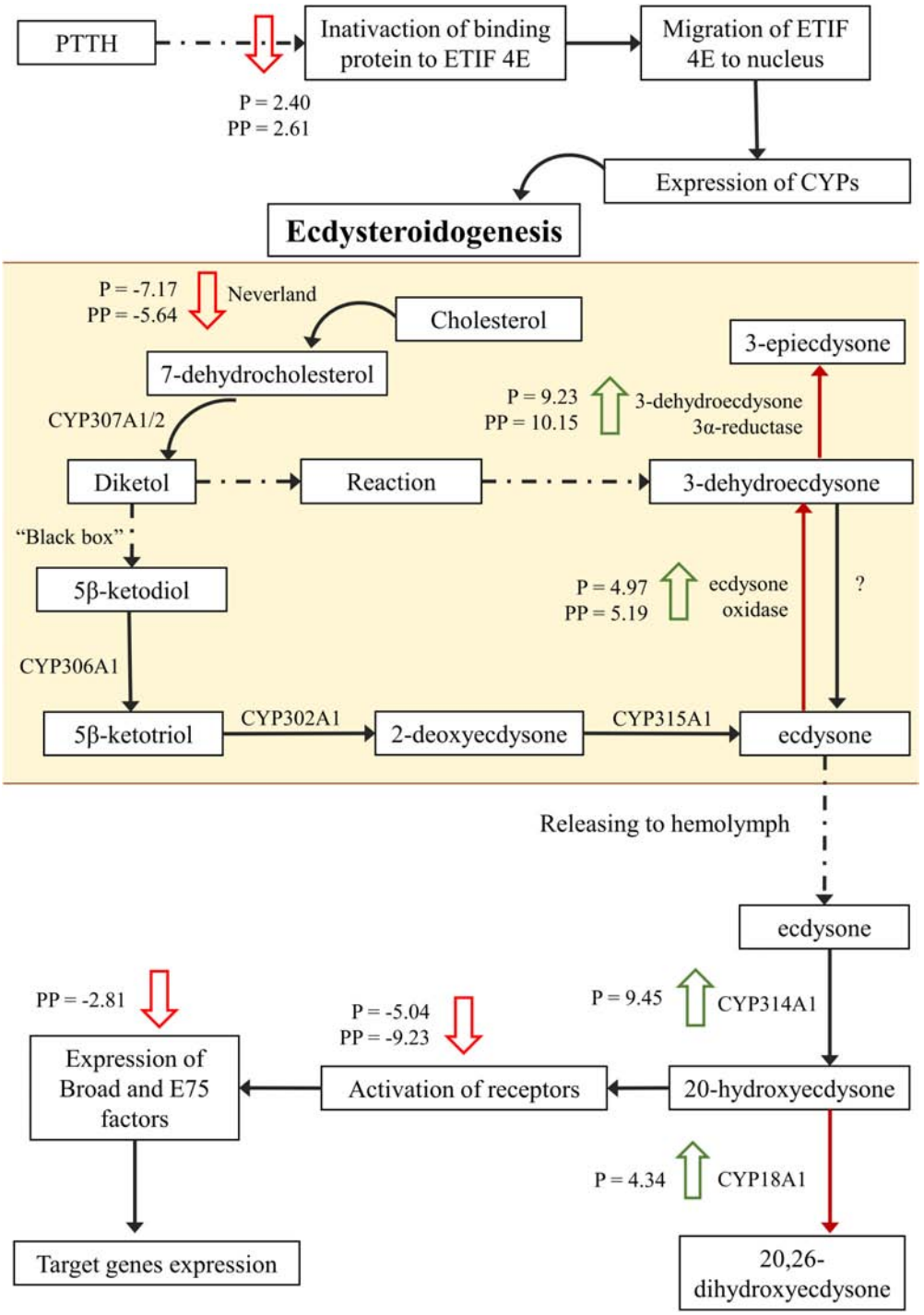

FIGURE 6 | Simplified pathways for ecdysteroid synthesis and release in prothoracic glands. Dashed arrows indicate different reactions and red arrows indicate ecdysteroid inactivation. Large green arrows indicate superexpression of enzymes in *Diatraea saccharalis* parasitized (P) and/or pseudoparasitized (PP) by *Cotesia flavipes*. Large red arrows indicate inhibition of expression in parasitized and/or pseudoparasitized larvae. CYP, cytochrome P450 enzymes; ETIF, eukaryotic translation initiation factor; PPTH, prothoracicotropic hormone.

Positive regulation of farnesyl diphosphate synthases 1 and 2 (IIL_32117_c1_g1_i1; IIL_34096_c0_g1_i1) and cytochrome P450 18A1 (IIL_31541_c0_g3_i2; IL_31541_c0_g3_i6), enzymes involved in isoprenoid biosynthesis and in the hydroxylation of ecdysone to 20-hydroxyecdysone respectively, was observed in parasitized larvae. Nevertheless, up-regulation of enzymes

involved in the degradation of JH and ecdysteroids was also detected in both the parasitized and pseudoparasitized conditions (**Table 1** and **Figure 6**). Additionally, down-regulation of hormone receptors occurred in parasitized and pseudoparasitized larvae (**Table 1**), but ecdysone-inducible translation factors, such as 74EF and E75, were inhibited only in pseudoparasitized larvae (**Table 1**).

Regulation of Cuticle Proteins and Peritrophic Membrane

Larval parasitization by *C. flavipes* also regulated larval cuticle formation and pigmentation. More than 100 cuticle proteins with RR-1 and RR-2 motifs, and larval and pupal cuticle proteins were inhibited in parasitized and pseudoparasitized larvae. Twenty-three cuticle proteins were down-regulated only in parasitized larvae and 51 only in pseudoparasitized larvae. Genes coding for enzymes involved in cuticle sclerotization and melanization, such as peroxidase isoform X1 (IIL_32355_c3_g1_i9: logFC = –8.75 in P; logFC = –8.78 in PP) and laccase 2 precursor (IIL_33503_c0_g1_i1: logFC = –2.93 in P; logFC = –3.75 in PP) were also down-regulated.

The peritrophic matrix lining the larval midgut of *D. saccharalis* was negatively affected by parasitization, through inhibition of peritrophin-1 (IIL_31190_c0_g1_i4: logFC = −2.72 in P; logFC = −3.11 in PP) and peritrophin precursor (IIL_32010_c0_g1_i1: logFC = −2.98 in P; logFC = −3.22 in PP), both of which are protein components of the peritrophic matrix.

Regulation of Cellular Organization and Motility

Forty-three (43) genes involved in cellular organization and motility were down-regulated, while 35 were up-regulated in parasitized larvae. The transcripts filamin A isoform X1 (IIL_34274_c0_g2_i5: logFC = –10.69), dynactin subunit 5 (IIL_28346_c0_g1_i1: logFC = –10.91) and myosin heavy chain isoform X34 (IIL_33425_c0_g2_i10: logFC = −12.54) had their expression reduced over 1,000-fold in parasitized larvae. Genes involved in the inhibition of actin reorganization (Saarikangas et al., 2010), G-coupled protein Mth-3 receptor isoform X4 (IIL_31157_c3_g1_i3: logFC = 8) and twinfilin factor (IIL_34395_c1_g2_i3: logFC = 8.26), were strongly up-regulated in parasitized larvae. Other important genes involved in the regulation of cell adhesion and spread, α-tubulins, rho GTPase activators, and integrins, were represented by several isoforms in the transcriptome; a clear pattern of regulation could not be detected, as some isoforms were up- while others were down-regulated.

Pseudoparasitization by *C. flavipes* altered the expression of 81 transcripts of *D. saccharalis* larvae related to cellular cytoskeleton organization for cell motility and adhesion (down-regulated = 53, up-regulated = 28). In addition to the observed regulation of actin and myosin transcripts in parasitized larvae, down-regulation of signal activators of the transduction pathways that result in cell motility (Blanchoin et al., 2014), i.e., formin (IIL_28739_c0_g2_i2: logFC = –3.55), cdc42 factor (IIL_33959_c2_g1_i2: logFC = −10.01), and rho GTPase 6 activator isoform X2 (IIL_25884_c0_g1_i2: logFC = –3.41), was also observed in pseudoparasitized larvae.

The reorganization of the cytoskeleton for cell motility depends on calcium (Ca^{+2}) signaling (Pinto et al., 2015; Tsai et al., 2015), and Ca^{+2} channels were regulated in parasitized larvae. The plasma membrane Ca^{+2}-transporting ATPase 2 and Ca^{+2}/Na^{+1} exchanger 1 isoform X1, which transport calcium to the extracellular space, were down-regulated (**Table 2**), but the influx Ca^{+2} channels ionotropic glutamate receptor, glutamate receptor kainate 2-like, and glutamate *N*-methyl-D-aspartate (NMDA) receptor associated 1 were up-regulated (**Table 2**). Phospholipase A2 and sphingosine 1-phosphate lyase were also down-regulated in parasitized larvae. These two proteins are channel regulators and they interfere with the levels of secondary messengers, through activation of G-protein (**Table 2**). The same pattern of regulation of influx and efflux Ca^{+2} channels was observed in pseudoparasitized larvae (**Table 2**). Genes encoding the Ca^{+2}-modulated protein calmodulin and the Ca^{+2}-activated proteins calcineurin A and B were up-regulated only in pseudoparasized larvae. No difference in their expression profile was detected in parasitized larvae (**Table 2**).

Regulation of the Immune System

Cotesia flavipes parasitizing larvae of *D. saccharalis* also regulated many transcripts involved with the immune system. We detected differential expression of 155 transcripts in parasitized larvae and 130 transcripts in pseudoparasitized larvae, most of them common to both conditions (**Figure 7**). In parasitized larvae, the wasps induced the synthesis of 19 antimicrobial peptides (AMPs), of which attacin, cecropin, scolexin and gloverin were highly expressed (**Figure 7A**). In pseudoparasitized larvae, only nine differentially expressed AMPs were detected. Expression of cecropin (IIL_23051_c0_g1_i2: logFC = 2.55 in P) and defensin (IIL_25072_c0_g1_i1: logFC = 12.74 in P) was not altered in pseudoparasitized larvae. AMP synthesis in insects is regulated by the *Imd* (*immune deficiency*) and *Toll* pathways of the immune system (De Gregorio et al., 2002), and Toll-like proteins (IIL_34261_c0_g1_i8: logFC = 2.59 in P; IIL_34261_c0_g1_i10: logFC = 2.05 in P; IIL_34261_c0_g1_i11: logFC = 2.59 in P; logFC = 2.55 in PP; IIL_34261_c0_g1_i4: logFC = 4.85 in P; logFC = 5.20 in PP; IIL_34261_c0_g1_i7: logFC = 6.79 in P; logFC = 7.36 in PP) and Toll receptors (IIL_28993_c0_g1_i1: logFC = 4.94 in PP) were up-regulated in both parasitized and pseudoparasitized larvae.

Cotesia flavipes also affected a group of pattern-recognition peptides involved in the humoral response of *D. saccharalis* larvae. Peptidoglycan-recognition peptide, lipopolysaccharide binding, and lipopolysaccharide-induced tumor necrosis factor-α were up-regulated in parasitized and pseudoparasitized larvae (**Figure 7E**).

Contrary to the activation of the humoral immune response through the stimulation of AMPs expression, genes involved in activation of the cellular immune response were down-regulated in larvae of *D. saccharalis* parasitized and pseudoparasitized by *C. flavipes* (**Figure 7B**). Sequences of macrophage mannose receptor 1-like, c-type lectin (IIL_33289_c2_g8_i1: logFC = –2.06 in P; logFC = –2.17 in PP; IIL_31980_c2_g1_i1: logFC = –5.26

TABLE 1 | Putative identification and fold-change values of transcripts related to the endocrine system of larvae of *Diatraea saccharalis* parasitized (P) and pseudoparasitized (PP) by *Cotesia flavipes*.

Putative identification	Transcripts	LogFC*[1] in P	FDR*[2]	LogFC in PP	FDR
3-dehydroecdysone 3α-reductase	IIL_29686_c0_g1_i1	9.23	3.14×10^{-5}	10.15	2.28×10^{-6}
Parathyroid hormone-responsive B1	IIL_33372_c0_g2_i2	−3.21	1.77×10^{-3}	−3.01	1.70×10^{-2}
Cytochrome P450 monooxygenase CYP18A1	IIL_31541_c0_g3_i2	2.92	2.58×10^{-4}	–	–
	IIL_31541_c0_g3_i6	4.34	4.16×10^{-3}	–	–
Nuclear receptor coactivator 5 isoform X1	IIL_33867_c3_g1_i3	8.00	1.86×10^{-4}	–	–
Rieske-domain Neverland	IIL_25348_c0_g1_i1	−7.17	2.95×10^{-5}	−5.64	4.27×10^{-3}
Ecdysone 20-monooxygenase isoform X2 (CYP314A1)	IIL_33026_c0_g13_i2	8.78	2.68×10^{-5}	–	–
	IIL_33026_c0_g13_i3	9.45	1.21×10^{-5}	–	–
Ecdysone oxidase	IIL_33220_c0_g1_i8	2.35	1.58×10^{-2}	–	–
	IIL_34436_c2_g2_i1	4.97	1.62×10^{-3}	5.19	9.92×10^{-3}
Juvenile hormone epoxide hydrolase	IIL_33751_c1_g1_i1	2.19	6.10×10^{-3}	2.20	1.50×10^{-2}
	IIL_33751_c1_g1_i5	2.21	8.98×10^{-3}	2.72	3.32×10^{-2}
	IIL_33290_c1_g1_i4	2.81	7.71×10^{-3}	2.88	2.18×10^{-2}
	IIL_33290_c1_g1_i7	2.88	5.23×10^{-3}	2.97	1.47×10^{-2}
	IIL_33290_c1_g1_i1	5.55	2.50×10^{-3}	5.08	1.22×10^{-2}
Juvenile hormone esterase-like	IIL_29119_c0_g1_i2	2.77	6.23×10^{-3}	2.71	3.32×10^{-2}
Farnesyl diphosphate synthase 1	IIL_32117_c1_g1_i1	8.50	3.80×10^{-5}	–	–
Farnesyl diphosphate synthase 2	IIL_34096_c0_g1_i1	7.76	4.41×10^{-4}	–	–
Ecdysone-induced 74EF isoform X1	IIL_33545_c3_g1_i3	–	–	−3.26	3.81×10^{-2}
Ecdysone-inducible E75 isoform X1	IIL_29251_c0_g1_i2	–	–	−2.81	3.85×10^{-2}
Phosphomevalonate kinase isoform X1	IIL_33071_c1_g4_i5	–	–	4.08	4.36×10^{-2}
Geranylgeranyltransferase type-1 subunit α	IIL_33557_c0_g1_i2	5.08	3.45×10^{-4}	5.08	2.46×10^{-3}
Krueppel homolog 2	IIL_30739_c1_g3_i2	4.42	4.28×10^{-3}	–	–
Prostamide/prostaglandin F synthase-like	IIL_27864_c0_g1_i2	−2.76	2.16×10^{-2}	−5.98	1.26×10^{-3}
Probable nuclear hormone receptor HR3 isoform X2	IIL_27960_c0_g1_i4	−5.04	9.87×10^{-4}	−9.23	3.47×10^{-5}
Steroid receptor partial	IIL_413_c0_g1_i1	−2.32	3.49×10^{-2}	−3.46	1.33×10^{-2}
Gonadotropin-releasing hormone receptor	IIL_42622_c0_g1_i1	4.75	7.69×10^{-3}	5.64	6.02×10^{-3}
Nuclear hormone receptor FTZ-F1 isoform X2	IIL_34249_c0_g1_i2	–	–	−8.54	8.85×10^{-4}
Neuropeptide receptor A13	IIL_28896_c0_g1_i1	4.88	4.22×10^{-2}	–	–
FMRFamide receptor-like	IIL_32921_c0_g1_i1	−2.79	1.47×10^{-3}	–	–
Gonadotropin-releasing hormone receptor II	IIL_32102_c1_g6_i1	2.95	1.99×10^{-3}	–	–
β-2-octopamine receptor	IIL_16542_c0_g1_i2	8.20	1.51×10^{-4}	8.41	6.39×10^{-4}

*[1] - fold change values; *[2]– FDR - statistic values.*

in P; logFC = −11.49 in PP), immunolectin (2a and 4) and hemolin (IIL_31301_c0_g1_i1: logFC = −7.49 in P; logFC = −7.70 in PP; IIL_31301_c0_g1_i2: logFC = −8.12 in P; logFC = −7.88 in PP) were all inhibited in parasitized and pseudoparasitized hosts (**Figure 7B**).

Phenoloxidases that participate in both the humoral and cellular immune response were severely regulated in parasitized and pseudoparasitized larvae, through inhibition of the expression of serine proteases (**Figure 7C**) that activate the prophenoloxidase cascade, and stimulation of the expression of 16 serine protease inhibitors (serpins) (**Figure 7D**). All of the serine proteases analyzed in this case carried the clip-domain typical of proteases that function as immune factors (Kanost and Jiang, 2015). Twelve additional serpin transcripts were up-regulated only in parasitized larvae, while four other serpin transcripts were up-regulated exclusively in pseudoparasitized larvae. Up-regulation of the NF-κ-β inhibitor cactus (IIL_31869_c2_g1_i4: logFC = 3.19; IIL_31869_c2_g1_i6: logFC = 2.43) was detected only in parasitized larvae, while down-regulation of the nuclear factor NF-κ-β p110 subunit (IIL_30756_c0_g3_i8: logFC = −2.26) was detected only in pseudoparasitized larvae. The expression of a particular set of isoforms of phenoloxidase subunits 1 and 2 was affected differently in parasitized and pseudoparasitized larvae of *D. saccharalis*. PO 1 and 2 were up-regulated in parasitized larvae, but the expression of these transcripts in pseudoparasitized larvae was similar to that observed in non-parasitized larvae (**Figure 7F**).

Regulation of Host Metabolism

Cotesia flavipes also targeted genes involved in nutrient metabolism and transport. Several transcripts involved in carbohydrate metabolism were up-regulated in parasitized larvae, particularly those from the glycolysis and gluconeogenesis pathways. Phosphoglucose isomerase (IIL_34193_c0_g2_i3: logFC = 3.48), phosphoglucomutase (IIL_34190_c0_g1_i5:

TABLE 2 | Putative identification and fold-change values of sequences related to Calcium signaling pathway in larvae of *Diatraea saccharalis* parasitized (P) and pseudoparasitized (PP) by *Cotesia flavipes*.

Putative identification	Transcripts	LogFC*1 in P	FDR*2	LogFC in PP	FDR
Channels					
Ca^{+2} uptake mitochondrial isoforma X1	IIL_34181_c0_g1_i8	8.89	4.26×10^{-5}	8.62	5.53×10^{-4}
Plasma membrane Ca^{+2} transporting ATPase 2	IIL_33345_c1_g1_i12	−2.25	2.49×10^{-2}	–	–
	IIL_33345_c1_g1_i4	−2.33	2.33×10^{-3}	–	–
	IIL_33345_c1_g1_i5	−2.59	2.42×10^{-2}	−3.13	1.84×10^{-3}
Ca^{+2} homeostasis endoplasmatic reticulum isoforma X1	IIL_33424_c0_g1_i9	–	–	9.15	1.39×10^{-4}
Canal de K + interno ATP-sensível 12	IIL_32994_c0_g1_i1	−2.88	2.23×10^{-2}	–	–
Voltage-dependent L-type Ca^{+2} channel subunit β-2	IIL_34061_c0_g1_i1	−2.59	1.03×10^{-3}	−2.27	1.41×10^{-2}
	IIL_29702_c0_g1_i16	−2.74	1.18×10^{-2}	−4.54	3.29×10^{-3}
Sphingosine 1-phosphate lyase	IIL_32913_c0_g1_i3	10.21	3.26×10^{-7}	11.18	5.81×10^{-9}
Glutamate receptor kainate 2-like	IIL_31765_c1_g1_i2	2.91	3.95×10^{-3}	–	–
	IIL_30235_c0_g1_i1	−3.23	2.07×10^{-4}	−2.17	1.94×10^{-2}
Glutamate *N*-methyl-D-aspartate receptor associated 1	IIL_31082_c0_g2_i5	8.49	4.74×10^{-5}	9.99	7.18×10^{-6}
	IIL_31765_c1_g1_i4	3.09	2.55×10^{-2}	3.44	3.40×10^{-2}
Inositol 1,4,5-trisphosphate receptor	IIL_33132_c1_g2_i2	−2.42	2.82×10^{-2}	–	–
Ryanodine receptor	IIL_34501_c1_g1_i4	–	–	−2.35	2.21×10^{-2}
Na^{+}/CA^{+2} exchanger 1 isoform X1	IIL_23004_c0_g1_i1	−2.44	1.61×10^{-2}	–	–
Carrier					
Ca^{+2} and integrin-binding 1-like	IIL_28526_c0_g1_i1	8.99	1.41×10^{-5}	9.44	3.68×10^{-5}
Ca^{+2} binding E63-1	IIL_31127_c4_g2_i21	–	–	8.48	1.08×10^{-2}
	IIL_31127_c4_g2_i5	10.21	1.19×10^{-4}	11.40	5.36×10^{-11}
	IIL_31127_c4_g2_i17	–	–	−3.19	1.95×10^{-3}
	IIL_31127_c4_g2_i20	4.02	1.19×10^{-2}	–	–
	IIL_31127_c4_g2_i22	8.88	9.49×10^{-9}	8.21	1.73×10^{-6}
	IIL_31127_c4_g2_i9	5.96	3.46×10^{-5}	5.25	6.72×10^{-3}
	IIL_31127_c4_g2_i1	4.79	1.53×10^{-3}	5.18	6.35×10^{-3}
	IIL_31127_c4_g2_i14	−4.49	4.72×10^{-5}	−3.93	1.65×10^{-4}
	IIL_31127_c4_g2_i7	10.57	1.34×10^{-7}	10.45	9.84×10^{-7}
Sarcoplasmatic Ca^{+2} binding 1 isoform X2	IIL_29360_c0_g1_i2	–	–	8.36	4.41×10^{-4}
FK506 binding	IIL_28237_c0_g1_i4	–	–	−4.61	6.74×10^{-3}
	IIL_30991_c0_g1_i2	9.22	2.92×10^{-6}	8.65	2.34×10^{-4}
	IIL_31707_c0_g1_i4	3.80	1.80×10^{-2}	3.82	4.41×10^{-2}
Direct response					
Calcineurin A	IIL_23753_c0_g1_i1	9.80	1.25×10^{-7}	9.38	2.38×10^{-3}
Calcineurin B	IIL_31789_c3_g1_i2	–	–	9.18	3.38×10^{-3}
	IIL_31789_c3_g1_i3	–	–	8.59	8.22×10^{-3}
Calcyphosin isoform X3	IIL_29400_c0_g1_i4	−11.35	5.95×10^{-11}	–	–
Calmodulin	IIL_31731_c1_g2_i5	–	–	7.25	2.72×10^{-2}
	IIL_31846_c1_g2_i6	–	–	−3.36	7.59×10^{-3}
Calpain-B-like isoform X3	IIL_29647_c2_g3_i9	10.16	1.65×10^{-8}	10.29	3.64×10^{-7}
Calphotin-like	IIL_27019_c0_g1_i1	−3.10	3.30×10^{-4}	−3.63	6.03×10^{-4}
EF-hand Ca^{+2} binding domain-containing 2	IIL_30305_c1_g1_i32	–	–	7.50	2.28×10^{-2}
Phospholipase A2	IIL_31392_c0_g1_i8	6.27	1.05×10^{-4}	–	–

**1 – fold change values in log format; *2– FDR – statistic values.*

logFC = 2.69), aldose 1-epimerase-like (IIL_31340_c4_g3_i2: logFC = 3.15 in P; logFC = 3.48 in PP), and fructose-1,6-bisphosphatase (IIL_30548_c2_g3_i1: logFC = 7.62) were up-regulated, while only two were down-regulated. Hexokinase-2-like isoform X2 (glycolysis) (IIL_33352_c0_g3_i1: logFC = –2.64 in P; logFC = −2.51 in PP) and enolase (gluconeogenesis) (IIL_28113_c0_g1_i1: logFC = –8.78 in P; logFC = –9.51 in PP) were both inhibited in parasitized and pseudoparasitized larvae. The trehalose pathway was also affected in larvae parasitized and pseudoparasitized by *C. flavipes*,

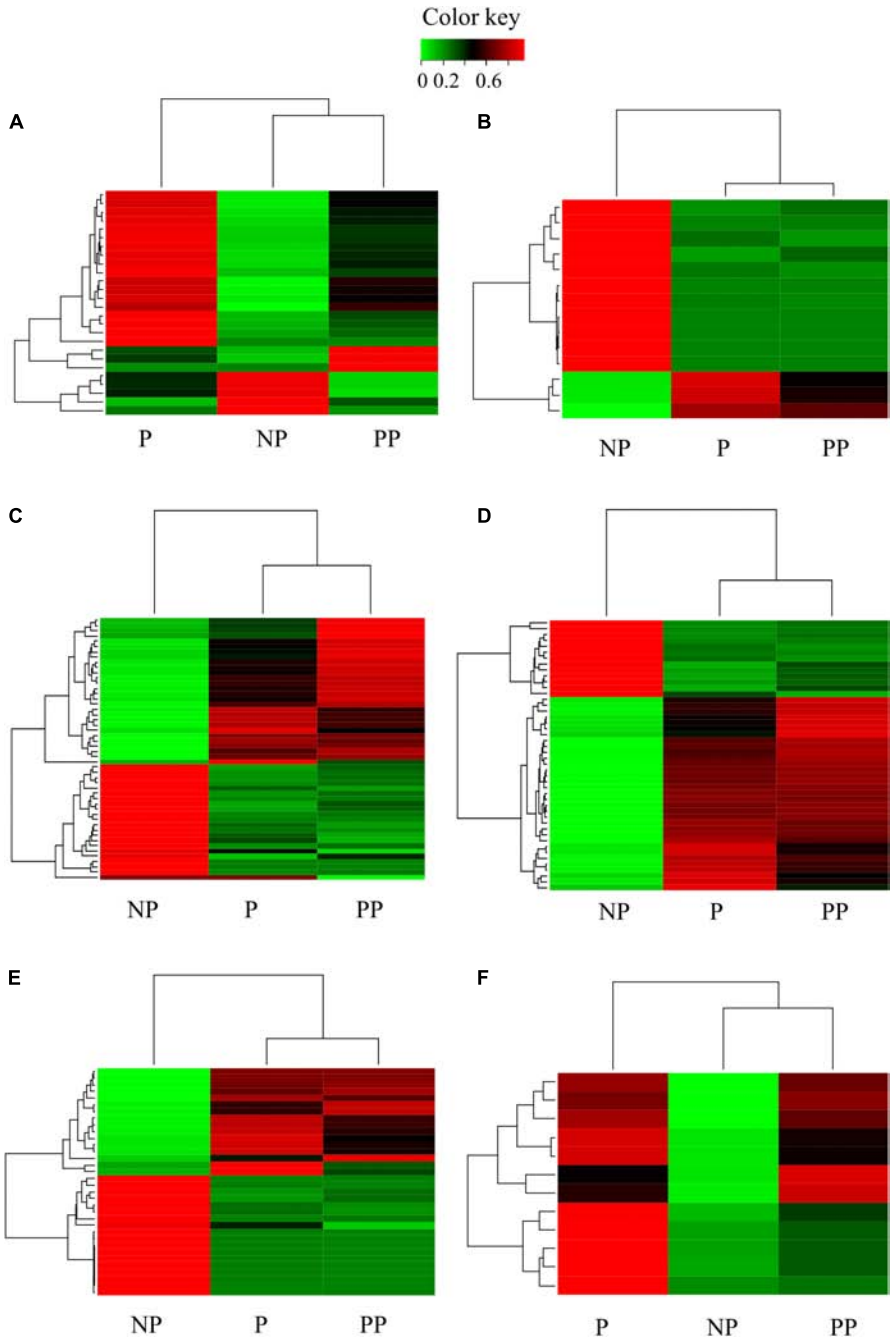

FIGURE 7 | Heatmap of immune response transcripts of larvae of *Diatraea saccharalis* parasitized (P) and pseudoparasitized (PP) by *Cotesia flavipes*: **(A)** AMPs synthesis; **(B)** cellular response; **(C)** immune system activation; **(D)** immune system inactivation; **(E)** peptidoglycan recognition; **(F)** phenoloxidase enzymes.

with the up-regulation of trehalose-6-phosphate synthase (IIL_32431_c0_g1_i3: logFC = 2.07 in P; IIL_32431_c0_g1_i6: logFC = 11.58 in P, logFC = 11.79 in PP).

The carrier protein apolipo-D (IIL_29978_c0_g3_i3: logFC = −2 in P; IIL_29978_c0_g3_i6: logFC = −4.78 in P; logFC = −9.66 in PP) and long-chain fatty acid transport 4-like (IIL_31821_c1_g1_i11: logFC = −6.06 in P; logFC = 4.69 in PP; IIL_31821_c1_g1_i14: logFC = −4.07 in P; logFC = −4.83 in PP) were down-regulated in parasitized and pseudoparasitized larvae. Sugar and trehalose transporters were represented by a number of isoforms with no clear pattern of regulation, as some were up- and others were down-regulated.

Regulation of nutrient metabolism and transport was followed by regulation of lipid and protein storage by *C. flavipes*. The lipid storage droplets surface-binding 1 isoform X1 (IIL_34294_c2_g1_i2: logFC = 2.89 in P; logFC = 2.17 in PP;

IIL_34294_c2_g1_i4: logFC = 10.39 in P; logFC = 10.18 in PP), arylphorin subunit α (IIL_28532_c2_g2_i4: logFC = 4.45 in P; logFC = 4.20 in PP) and acidic juvenile hormone-suppressible 1-like protein (IIL_DN34340_c0_g1_i6: logFC = 2.79 in P) were up-regulated.

DISCUSSION

Differential gene expression showed that *C. flavipes* interferes with the expression of 2,459 transcripts (5%) of *D. saccharalis*, revealing the large number of target genes involved in many physiological processes that are essential for the successful growth and development of the parasitoid. A similar number of transcripts (2,225) were regulated in larvae of *D. saccharalis* that were pseudoparasitized by *C. flavipes*. The similar numbers of differentially expressed genes in parasitized and pseudoparasitized larvae of *D. saccharalis* indicate that most of the virulence factors required for host regulation by *C. flavipes* are injected by the female wasp during parasitization, and would include venom, ovarian proteins and viral particles.

The role of venom and PDVs in the process of host regulation has been demonstrated by injecting them individually into the hosts of parasitoids, including a number of host-parasitoid associations involving braconids, such as *Chelonus inanitus* (L.) – *Spodoptera littoralis* (Boisduval) (Lepidoptera: Noctuidae) (Hochuli et al., 1999), *Protapanteles liparidis* (Bouché) – *Lymantria dispar* (L.) (Lepidoptera: Erebidae) (Hoch et al., 2009), *Cotesia plutellae* (Kurdjummov) – *Plutella xylostella* (L.) (Lepidoptera: Plutellidae) (Yu et al., 2007), and the system studied here, *C. flavipes* – *D. saccharalis* (Lopes, 2008). The synthesis and release of molecules by teratocytes (Nakamatsu et al., 2002) and the anal vesicle of the larval parasitoid and their participation in host regulation have been demonstrated in several host-parasitoid associations (Kaeslin et al., 2006). Our data showed that the release of molecules by the developing parasitoid larvae and/or teratocytes also contributes to host regulation. However, the contribution of virulence factors from teratocytes and/or larval secretions does not have a strong impact on gene expression, at least in the host genes we identified in this study.

Regulation of Cell Cycle and Apoptosis

Activation of secondary messengers is required to trigger signal transduction and allow cells to perceive changes in the surrounding environment (Clapham, 2007). Calcium (Ca^{+2}) ions are among the most important transduction-signal mediators, affecting cell excitability, exocytosis, motility, apoptosis and transcription (van Haasteren et al., 1999; Bernstein, 2015; Humeau et al., 2017). The increase in intracellular levels of Ca^{+2} is perhaps the most universal signaling cascade required for cell proliferation (Pinto et al., 2015). Ca^{+2} signaling was strongly regulated in larvae of *D. saccharalis* parasitized and pseudoparasitized by *C. flavipes*. *Cotesia flavipes* inhibited the expression of Ca^{+2} efflux channels and stimulated Ca^{+2} influx channels. Muscle contraction requires the release of calcium from the sarcoplasmic reticulum to the muscle sarcolema to promote the disassociation of the troponin–tropomyosin complex from the binding sites of the actin filament, allowing myosin to bind to actin for cell contraction. Alteration on muscle contraction can be related to change of host behavior induced by parasitoids, as *Glyptapanteles* sp. that induces their caterpillar host to behave as a bodyguard of the parasitoid pupae and knocks off predators with violent head-swings (Grosman et al., 2008). An increase in calcium availability reduces cell adhesion and activates caspases involved in cytolysis and DNA degradation during apoptosis. Calcium regulation can also lead to a disruption in the cell cycle (Mattson and Chan, 2003; Devreotes and Horwitz, 2015; Humeau et al., 2017).

Some caspases and Ca^{+2}-dependent molecules (caspase activators), such as calpain and calcineurin, were up-regulated in *D. saccharalis* larvae parasitized and pseudoparasitized by *C. flavipes* (Mattson and Chan, 2003; Humeau et al., 2017). Apoptosis of *High Five* cells was induced in the presence of viral protein associated with *Microplitis bicoloratus* Chen (Hymenptera: Braconidae) and *Toxoneuron nigriceps* (Viereck) (Hymenoptera: Braconidae), through their interaction with cell proteins that activate caspases (Yu et al., 2016; Salvia et al., 2017). *Cotesia flavipes* also regulated Ca^{+2} channels, Ca^{+2} modulators and Ca^{+2}-dependent molecules, altering several physiological processes ranging from cell proliferation to apoptosis activation.

Hormonal Regulation

Targeting of the host endocrine system for regulation is well described for several host-parasitoid systems. In the *D. saccharalis* – *C. flavipes* system, we observed intensive regulation of synthesis and degradation of juvenile hormone (JH) and ecdysteroids. *Cotesia flavipes* induced synthesis of juvenile hormone in both parasitized and pseudoparasitized larvae. Regulation of JH by *C. flavipes* is obtained by virulence factors injected with the eggs, and the same effect was observed in larvae in which virulence factors from teratocytes and parasitoid larvae were not available (pseudoparasitized larvae). JH regulation is important to maintain the parasitized host at the larval stage as long as is necessary for the parasitoid larva to fully develop (Lawrence, 1986; Grossniklaus-Bürgin et al., 1998; Noriega, 2014), but also to regulate the expression of juvenile hormone-dependent genes, such as methionine-rich protein (Salvador and Cônsoli, 2008), and the allocation of nutrients to host growth and development (Jones, 1995; Cônsoli and Vinson, 2012). Contrariwise, the juvenile hormone-degrading enzymes esterase and epoxide hydrolase were also up-regulated. However, up-regulation of genes involved in JH synthesis was much more pronounced than the up-regulation seen in JH-degrading enzymes. Additionally, we cannot rule out the possibility that the up-regulation of the translational regulatory factors observed in parasitized and pseudoparasitized larvae of *D. saccharalis* could be interfering with the synthesis of enzymes involved in the synthesis and degradation of JH. A multiomic approach would be required for a full understanding of the functional regulation of JH titers in parasitized larvae. However, JH regulation varies widely among host-parasitoid systems and often depends on the strategy of parasitoid development. Endoparasitoids such as *G. liparidis* and *Tranosema rostrale* (Brischke) (Hymenoptera: Ichneumonidae), maintain elevated JH titers by reducing the

host JH esterases (Béliveau et al., 2000; Schafellner et al., 2007). The larval parasitoid *T. nigriceps* does not interfere with the JH esterase levels in the host, but regulates other components of the hormone pathways (Li et al., 2003). On the other hand, in egg-pupal or larval-pupal parasitoids that complete their development in the host pupal stage, such as *C. inanitus*, JH esterase levels are elevated to induce reduction in JH titers in order to induce a precocious onset of the pupal stage in the host *S. littoralis* (Kaeslin et al., 2005).

Cotesia flavipes parasitization of *D. saccharalis* larvae led to the down-regulation of enzymes acting on ecdysteroid synthesis and of several eukaryotic translation initiation factors. Eukaryotic translation initiation factors also participate in regulating the activity of prothoracic glands as signaling factors (Gu et al., 2017). Down-regulation of ecdysteroid synthesis was followed by the negative regulation of many orphan nuclear receptors, such as the nuclear hormone receptors HR3, E75 and E74. Activation of orphan nuclear receptors is dependent on ecdysteroid induction. E75 responds faster to ecdysteroid activation than HR3, and both of these are also considered transcription factors by some authors (Hannas and LeBlanc, 2010). These orphan receptors heterodimerize to act as fundamental regulators of changes in development and redirection of metamorphosis induced by ecdysteroids. The HR3 receptor orchestrates the transition from larva to prepupa and the E75 receptor modulates this transition (Thummel, 2005; Li K. et al., 2015). Disruption of the expression of the E75 and HR3 receptors will affect the onset of metamorphosis, as they are in charge of activating and deactivating genes in preparation for pupation, in response to the first ecdysteroid peak (Horner et al., 1995; Lam et al., 1997; Guo et al., 2015). In addition to inhibiting the E75 and HR3 receptors to control cell response to ecdysteroid stimulation, *C. flavipes* induced the overexpression of ecdysone oxidase and CYP P450 18A1, which are ecdysteroid-inactivating enzymes (Guittard et al., 2011; Li Z. et al., 2015). Thus, ecdysteroid availability and cell recognition are negatively affected in parasitized and pseudoparasitized larvae, demonstrating that cells would be unresponsive to ecdysteroid stimulation even if hormone synthesis was not affected.

Down-regulation of ecdysteroid titers will block important pathways for host ecdysis such as chitin metabolism and cuticle degradation and synthesis (Charles, 2010). Thus, the strong down-regulation of cuticle proteins, chitinases and chitin-synthesis proteins in parasitized and pseudoparasitized larvae is a consequence of the regulation of genes involved in ecdysteroid synthesis, as observed in *D. saccharalis* larvae parasitized by *C. flavipes*.

Regulation of Cellular Organization and Motility

Bracoviruses are reported to interfere with host cell activities, mainly disrupting the cell cytoskeleton by expressing proteins that irreversibly bind to gene-expression factors (Suderman et al., 2008; Bitra et al., 2012). Several genes that are important to the cell cytoskeleton (actin and myosin) and to cell migration and attachment (integrin) were regulated in larvae of *D. saccharalis* parasitized and pseudoparasitized by *C. flavipes*. Regulation of these genes interferes with the ability of hemocytes to move, attach to and spread over the surface of the invader egg during egg encapsulation (Webb and Luckhart, 1994; Kwon and Kim, 2008; Devreotes and Horwitz, 2015). Disruption of the cell cytoskeleton also affects the cell activity in the host. PDV viral ankyrins interfere with the cytoskeleton organization of cells of the prothoracic gland, affecting the synthesis and transport of ecdysteroids (Valzania et al., 2014). Thus, regulation of genes that affect the cell cytoskeleton organization, cell motility, attachment and spread would be associated with virulence factors produced by the bracovirus associated with *C. flavipes*.

Regulation of the Immune System

Regulation of the host immune responses is an important function of the virulence factors that female parasitic wasps inject into their hosts during parasitization. Host humoral and cellular immune responses are targeted by parasitic wasps to prevent the encapsulation process (Vinson, 1990; Schmidt et al., 2001; Barat-Houari et al., 2006; Mahmoud et al., 2011; Meng et al., 2016). Initial reports on *D. saccharalis – C. flavipes* demonstrated larval parasitization induced an increase in the population of host hemocytes and in the phenoloxidase activity in permissive and non-permissive hosts. Interestingly, increase in host hemocytes did not correlate with parasitoid encapsulation by the host (Alleyne and Wiedenmann, 2001; Mahmoud et al., 2012). A large number of genes of *D. saccharalis* were differentially regulated in larvae parasitized or pseudoparasitized by *C. flavipes*. Expression of C-type lectins and hemolins was severely affected in these parasitized or pseudoparasitized larvae. Regulation of the expression of these genes would affect pattern recognition of pathogens and cell adhesion, and the similarities in the expression profiles in parasitized and pseudoparasitized larvae show that the maternally associated virulence factors are responsible for altering the expression of these genes. Down-regulation of C-type lectins and hemolins indicates that the host immune response is compromised upon parasitization (Fang et al., 2011; Wang et al., 2012). Hemolin plays several roles in the immune response of insects. Hemolin is highly important to mount the cell response to bacterial infections (Sun et al., 1990; Schmidt et al., 1993; Lanz-Mendoza et al., 1996), but hemolin has also been shown to affect the humoral immune response by interfering with phenoloxidase activation (Terenius et al., 2007). Additionally, hemolin has been suggested to be important in the immune response against viruses attacking lepidopterans (Terenius, 2008; Qian et al., 2017), and the down-regulation observed in larvae of *D. saccharalis* parasitized and pseudoparasitized by *C. flavipes* is likely required to prevent the host from defending against the polydnavirus particles injected by female wasps. Inhibition of hemolin expression in larvae of *Manduca sexta* (L.) (Lepidoptera: Sphingidae) parasitized by *Cotesia congregata* (Say) (Hymenoptera: Braconidae) was shown to occur soon after the polydnavirus gene *Cc*V1 was expressed (Labropoulou et al., 2008).

Besides the possible regulation of phenoloxidases by hemolin, two other genes (serine proteases and serpins) belonging to the prophenoloxidase cascade (PPO) were regulated in larvae

parasitized and pseudoparasitized by *C. flavipes*. Inhibition of the expression of serine proteases and overexpression of serine protease inhibitors (serpins) (Irving et al., 2000; Gorman and Paskewitz, 2001) show that inhibiting the activation of phenoloxidase is important for suppressing the immune response of the host against *C. flavipes*. PPO and phenoloxidases bind to foreign and hemocyte surfaces and participate in the process of hemocyte melanization and encapsulation of large pathogens and parasitoids (Ling and Yu, 2005).

Regulation of the immune system of *D. saccharalis* also involved controlling the expression of a key member of the immune response, the nuclear factor kappa-light-chain-enhancer of activated B cells (NF-κ-β). NF-κ-β is a complex of proteins that once activated, controls DNA transcription, cell survival and cytokine production and participates in several cell responses, including the response to infections (Perkins, 2007). *Cotesia flavipes* inhibited the activity of NF-κ-β in parasitized and pseudoparasitized larvae of *D. saccharalis* by inducing the overexpression of cactus, an NF-κ-β inhibitory factor (Shrestha et al., 2009). Regulation of NF-κ-β then leads to a change in cell function, impacting hematopoietic and immune signaling. Gueguen et al. (2013) proposed that regulation of NF-κ-β by PDV vankyrins leads to an immune deficiency that contributes to the successful colonization of the host and survival of the developing parasitoid larvae. The similar profile of gene expression in larvae of *D. saccharalis* parasitized and pseudoparasitized by *C. flavipes* demonstrates that the regulation of the host immune system seems to rely exclusively on maternal virulence factors.

Regulation of the host's immune response is certainly important for successful parasitization, but parasitoids also must maintain their host's immune responses active up to a certain level, in order to provide a healthy environment to support their own development. For this reason, antimicrobial peptides (AMPs) are not always inhibited in parasitized hosts. Up-regulation of AMPs was observed in larvae of *D. saccharalis* parasitized and pseudoparasitized by *C. flavipes*, although the levels of regulation were much higher in parasitized than in pseudoparasitized larvae, indicating that other virulence factors or late factors of regulation are required to maintain the high levels of expression observed in parasitized larvae. Activation of AMP expression requires activation of the *Toll* and *Imd* pathways (De Gregorio et al., 2002; Myllymaki et al., 2014), and several Toll-like proteins were up-regulated by *C. flavipes*.

Regulation of Host Metabolism

Modulation of the host's energy metabolism will vary according to the strategy of parasitoid development, and is usually accompanied by manipulation of the host's endocrine system. Although glycolysis and gluconeogenesis have opposing functions, they share several enzymes that play reversible roles in each pathway (Thompson, 2003). These pathways are regulated by the activation of insulin-like peptides in response to the host's nutritional environment (Mirth and Riddiford, 2007). The sugar content in the hemolymph of *D. saccharalis* larvae parasitized by *C. flavipes* is maintained almost unaltered throughout parasitoid development (Salvador and Cônsoli, 2008; Rossi et al., 2014). Maintenance of sugar levels in the hemolymph of larvae of *M. sexta* parasitized by *C. congregata* has been found to occur through increased gluconeogenesis and trehalose synthesis (Thompson and Dahlman, 1999; Thompson, 2001). The expression levels of trehalose-6-synthase were elevated in parasitized and pseudoparasitized larvae of *D. saccharalis*, but activation of gluconeogenesis in parasitized/pseudoparasitized larvae is not fully understood. *Cotesia flavipes* inhibited the initial steps of gluconeogenesis (enolase down-regulation) while activating the final steps (up-regulation of phosphoglucose isomerase, phosphoglucomutase, fructose-1,6-bisphosphatase, and aldose 1-epimerase-like). Although our data suggest that regulation of the sugar content in the host is a means to make this nutrient available to the developing parasitoid, we cannot discard the possibility that some of the intermediates also participate in other physiological processes. For example, enolases can act as DNA-binding proteins and affect gene transcription or participate in muscle growth and development, among other processes (Ji et al., 2016). Contrary to the inhibition of enolase observed in *D. saccharalis* parasitized by *C. flavipes*, the aphid parasitoid *Aphidius ervi* Haliday (Hymenoptera: Braconidae) increases the availability of enolase in the host, releasing enolases produced by teratocytes (Falabella et al., 2009).

Similarly, the positive regulation of the expression of host proteins and enzymes involved in lipid synthesis could be a strategy of the parasitoid to maintain a suitable nutritional environment for its development. Nevertheless, because *C. flavipes* regulates several translational regulatory factors, it is difficult to understand the outcome of regulating any of these components individually (Kim, 2007).

CONCLUSION

We identified several pathways and key genes of the host *D. saccharalis* that are regulated by the wasp *C. flavipes*, using a *de novo* assembly of a transcriptome of this non-model species. We conclude that most of the regulation of gene expression of *D. saccharalis* is controlled by virulence factors transmitted by the female wasp along with the egg, as the gene-expression profile in parasitized larvae was similar to that in pseudoparasitized larvae. Our undesired need to pool RNA samples at different sampling time after host parasitization in order to build one sequencing library frustrated our expectations to clearly identify and differentiated early and late target genes of the virulence factors of *C. flavipes*. Nevertheless, we depicted the efficiency of the virulence factors of *C. flavipes* in regulating gene expression of *D. saccharalis*, and propose that *C. flavipes* regulates a large number of physiological processes of *D. saccharalis* by targeting mechanisms that control the availability of calcium ions, due to the importance of this molecule in almost every aspect of the cell life cycle. Finally, our data provide an overview of the changes induced in the host by *C. flavipes*, generating a large body of information for future functional studies.

AUTHOR CONTRIBUTIONS

BM and FC designed and planned the research, and revised and edited the final manuscript. FC secured the funds, supervised the data analysis, and revised, edited, and amended the initial draft of the manuscript. BM collected and analyzed the data, and wrote the initial draft of the manuscript.

FUNDING

We thank Coordenação de Aperfeiçoamento de Pessoal de Nível Superior - Brazil (CAPES) - Finance Code 001 for the scholarship granted to BM. We also thank Conselho Nacional de Desenvolvimento Científico e Tecnológico (CNPq) (Grant No. 2013/312094) and Fundação de Amparo à Pesquisa do Estado de São Paulo (FAPESP) (Grant No. 2005/00355-7) for providing funds to FC. Research carried out using the computational resources of the Center for Mathematical Sciences Applied to Industry (CeMEAI) was funded by FAPESP (Grant 2013/07375-0).

SUPPLEMENTARY MATERIAL

The Supplementary Material for this article can be found online at: https://www.frontiersin.org/articles/10.3389/fphys.2019.01106/full#supplementary-material

REFERENCES

Ali, M. R., Lim, J., and Kim, Y. (2015). Transcriptome of a specialized extra-embryonic cell, teratocyte, and its host immunosuppressive role revealed by ex vivo RNA interference. *Insect Mol. Biol.* 24, 13–28. doi: 10.1111/imb.12132

Alleyne, M., and Wiedenmann, R. N. (2001). Encapsulation and hemocyte numbers in three lepidopteran stemborers parasitized by *Cotesia* flavipes-complex endoparasitoids. *Entomol. Exp. Appl.* 100, 279–293. doi: 10.1046/j.1570-7458.2001.00875.x

Andrews, S. (2010). *FastQC: a Quality Control Tool for High Throughput Sequence Data*. Available at:http://www.bioinformatics.babraham.ac.uk/projects/fastqc (accessed May 12, 2017).

Asgari, S., and Rivers, D. B. (2011). Venom proteins from endoparasitoid wasps and their role in host-parasite interactions. *Annu. Rev. Entomol.* 56, 313–335. doi: 10.1146/annurev-ento-120709-144849

Barat-Houari, M., Hilliou, F., Jousset, F. X., Sofer, L., Deleury, E., Rocher, J., et al. (2006). Gene expression profiling of *Spodoptera frugiperda* hemocytes and fat body using cDNA microarray reveals polydnavirus-associated variations in lepidopteran host genes transcript levels. *BMC Genomics* 7:160. doi: 10.1186/1471-2164-7-160

Beck, M. H., and Strand, M. R. (2007). A novel polydnavirus protein inhibits the insect prophenoloxidase activation pathway. *Proc. Natl. Acad. Sci. U.S.A.* 104, 19267–19272. doi: 10.1073/pnas.0708056104

Beckage, N. E., and Gelman, D. B. (2004). Wasp parasitoid disruption of host development: implications for new biologically based strategies for insect control. *Annu. Rev. Entomol.* 49, 299–330. doi: 10.1146/annurev.ento.49.061802.123324

Béliveau, C., Laforge, M., Cusson, M., and Bellemare, G. (2000). Expression of a *Tranosema rostrale* polydnavirus gene in the spruce budworm, *Choristoneura fumiferana*. *J. Gen. Virol.* 81, 1871–1880. doi: 10.1099/0022-1317-81-7-1871

Bernstein, L. H. (2015). Role of calcium, the actin skeleton, and lipid structures in signaling and cell motility. *Arch. Med.* S 1, 1–10.

Bitra, K., Suderman, R. J., and Strand, M. R. (2012). Polydnavirus Ank proteins bind NF-κB homodimers and inhibit processing of Relish. *PLoS Pathog* 8:e1002722. doi: 10.1371/journal.ppat.1002722

Bitra, K., Zhang, S., and Strand, M. R. (2011). Transcriptomic profiling of *Microplitis demolitor Bracovirus* reveals host, tissue and stage-specific patterns of activity. *J. Gen. Virol.* 92, 2060–2071. doi: 10.1099/vir.0.032680-32680

Blanchoin, L., Boujemaa-Paterski, R., Sykes, C., and Plastino, J. (2014). Actin dynamics, architecture, and mechanisms in cell motility. *Physiol. Rev.* 94, 235–263. doi: 10.1152/physrev.00018.2013

Bolger, A. M., Lohse, M., and Usadel, B. (2014). Trimmomatic: a flexible trimmer for Illumina sequence data. *Bioinformatics* 30, 2114–2120. doi: 10.1093/bioinformatics/btu170

Botelho, P. S. M., and Macedo, N. (2002). *Cotesia* flavipes para o controle de Diatraea saccharalis. In *Controle Biologico no Brasil: Parasitoides e Predadores*. eds J. R. P. Parra, P. S. M. Botelho, B.S. Correa-Ferreira, & J. M. S. Bento. (Manole: Sao Paulo:) pp. 409-426

Bottjen, R. C. (2011). *Characterization of the Viral Protein Tyrosine Phosphatase-H2 and The Metabolic consequences of Microplitis Demolitor Bracoviral Infection in Pseudoplusia includens*. Master's Thesis, University of Georgia, Athens.

Burke, G. R., and Strand, M. R. (2012). Polydnaviruses of parasitic wasps:domestication of viruses to act as gene delivery vectors. *Insects* 3, 91–119. doi: 10.3390/insects3010091

Charles, J. P. (2010). The regulation of expression of insect cuticle protein genes. *Insect Biochem. Mol. Biol.* 40, 205–213. doi: 10.1016/j.ibmb.2009.12.005

Chevignon, G., Theze, J., Cambier, S., Poulain, J., Da Silva, C., Bezier, A., et al. (2014). Functional annotation of *Cotesia* congregata *Bracovirus*: identification of viral genes expressed in parasitized host immune tissues. *J. Virol.* 88, 8795–8812. doi: 10.1128/JVI.00209-214

Clapham, D. E. (2007). Calcium Signaling. *Cell* 131, 1047–1058. doi: 10.1016/j.cell.2007.11.028

Conesa, A., Götz, S., García-Gómez, J. M., Terol, J., Talón, M., and Robles, M. (2005). Blast2GO: a universal tool for annotation, visualization and analysis in functional genomics research. *Bioinformatics* 21, 3674–3676. doi: 10.1093/bioinformatics/bti610

Cônsoli, F. L., and Kitajima, E. W. (2006). Symbiofauna associated with the reproductive system of *Cotesia flavipes* and *Doryctobracon areolatus* (*Hymenoptera*. *Braconidae*). *Braz. J. Morphol. Sci.* 23, 463–470.

Cônsoli, F. L., and Vinson, S. B. (2012). "Parasitoids (*Hymenoptera*)," in *Insect Bioecology and Nutrition for Integrated Pest Management*, eds J. R. P. Parra, and A. R. Panizzi (CRC press), 750.

De Gregorio, E., Spellman, P. T., Tzou, P., Rubin, G. M., and Lemaitre, B. (2002). The Toll and Imd pathways are the majors regulators of the immune response in *Drosophila*. *Embo J.* 21, 2568–2579. doi: 10.1093/emboj/21.11.2568

Devreotes, P., and Horwitz, A. R. (2015). Signaling networks that regulate cell migration. *Cold Spring Harb. Perspect. Biol.* 7:a005959. doi: 10.1101/cshperspect.a005959

Di Lelio, I., Caccia, S., Coppola, M., Buonanno, M., Di Prisco, G., Varricchio, P., et al. (2014). A virulence factor encoded by a polydnavirus confers tolerance to transgenic tobacco plants against lepidopteran larvae, by impairing nutrient absorption. *PLoS One* 9:e113988. doi: 10.1371/journal.pone.0113988

Dorémus, T., Cousserans, F., Gyapay, G., Jouan, V., Milano, P., Wajnberg, E., et al. (2014). Extensive transcription analysis of the *Hyposoter didymator* ichnovirus genome in permissive and non-permissive lepidopteran host species. *PLoS One* 9:e104072. doi: 10.1371/journal.pone.0104072

Dorémus, T., Jouan, V., Urbach, S., Cousserans, F., Wincker, P., Ravallec, M., et al. (2013a). *Hyposoter didymator* uses a combination of passive and active strategies to escape from the *Spodoptera frugiperda* cellular immune response. *J. Insect Physiol.* 59, 500–508. doi: 10.1016/j.ijrobp.2016.01.022.This

Dorémus, T., Urbach, S., Jouan, V., Cousserans, F., Ravallec, M., Demettre, E., et al. (2013b). Venom gland extract is not required for successful parasitism in the polydnavirus-associated endoparasitoid *Hyposoter didymator* (Hym. *Ichneumonidae)* despite the presence of numerous novel and conserved venom proteins. Insect Biochem. *Mol. Biol.* 43, 292–307. doi: 10.1016/j.ibmb.2012.12.010

Etebari, K., Palfreyman, R. W., Schlipalius, D., Nielsen, L. K., Glatz, R. V., and Asgari, S. (2011). Deep sequencing-based transcriptome analysis of *Plutella xylostella* larvae parasitized by *Diadegma semiclausum*. *BMC Genomics* 12:446. doi: 10.1186/1471-2164-12-446

Falabella, P., Riviello, L., Stradis, M. L., De Stigliano, C., Varricchio, P., Grimaldi, A., et al. (2009).). Aphidius ervi teratocytes release an extracellular enolase. *Insect Biochem. Mol. Biol.* 39, 801–813. doi: 10.1016/j.ibmb.2009.09.005

Fang, Q., Wang, F., Gatehouse, J. A., Gatehouse, A. M. R., Chen, X., Hu, C., et al. (2011). Venom of parasitoid, *Pteromalus puparum*, suppresses host, *Pieris rapae*, immune promotion by decreasing host C-type lectin gene expression. *PLoS One* 6:e26888. doi: 10.1371/journal.pone.0026888

Fang, Q., Wang, L., Zhu, J., Li, Y., Song, Q., Stanley, D. W., et al. (2010). Expression of immune-response genes in lepidopteran host is suppressed by venom from an endoparasitoid, *Pteromalus puparum*. *BMC Genomics* 11:484. doi: 10.1186/1471-2164-11-484

Godfray, H. C. J. (1994). *Parasitoids: Behavioral and Evolutionary Ecology*. New Jersey: Princeton University Press.

Gorman, M. J., and Paskewitz, S. M. (2001). Serine proteases as mediators of mosquito immune responses. *Insect Biochem. Mol. Biol.* 31, 257–262. doi: 10.1016/S0965-1748(00)00145-

Grosman, A. H., Janssen, A., de Brito, E. F., Cordeiro, E. G., Colares, F., Fonseca, J. O., et al. (2008). Parasitoid increases survival of its pupae by inducing hosts to fight predators. *PLoS One* 3:e2276. doi: 10.1371/journal.pone.0002276

Grossniklaus-Bürgin, C., Pfister-Wilhelm, R., Meyer, V., Treiblmayr, K., and Lanzrein, B. (1998). Physiological and endocrine changes associated with polydnavirus/venom in the parasitoid-host system *Chelonus inanitus-Spodoptera littoralis*. *J. Insect Physiol.* 44, 305–321. doi: 10.1016/S0022-1910(97)00144-143

Gu, S. H., Hsieh, Y. C., and Lin, P. L. (2017). Signaling involved in PTTH-stimulated 4E-BP phosphorylation in prothoracic gland cells of *Bombyx mori*. *J. Insect Physiol.* 96, 1–8. doi: 10.1016/j.jinsphys.2016.10.007

Gueguen, G., Kalamarz, M. E., Ramroop, J., Uribe, J., and Govind, S. (2013). Polydnaviral ankyrin proteins aid parasitic wasp survival by coordinate and selective inhibition of hematopoietic and immune NF-kappa B signaling in insect hosts. *PLoS Pathog* 9:e1003580. doi: 10.1371/journal.ppat.1003580

Guittard, E., Blais, C., Maria, A., Parvy, J. P., Pasricha, S., Lumb, C., et al. (2011). CYP18A1, a key enzyme of *Drosophila* steroid hormone inactivation, is essential for metamorphosis. *Dev. Biol.* 349, 35–45. doi: 10.1016/j.ydbio.2010.09.023

Guo, W.-C., Liu, X.-P., Fu, K.-Y., Shi, J.-F., Lü, F.-G., and Li, G.-Q. (2015). Functions of nuclear receptor HR3 during larval-pupal molting in *Leptinotarsa decemlineata* (Say) revealed by in vivo RNA interference. *Insect Biochem. Mol. Biol.* 63, 23–33. doi: 10.1016/j.ibmb.2015.05.010

Haas, B. J., Papanicolaou, A., Yassour, M., Grabherr, M., Blood, P. D., Bowden, J., et al. (2013). De novo transcript sequence reconstruction from RNA-seq using the Trinity platform for reference generation and analysis. *Nat. Protoc.* 8, 1494–1512. doi: 10.1038/nprot.2013.084

Hannas, B. R., and LeBlanc, G. A. (2010). Expression and ecdysteroid responsiveness of the nuclear receptors HR3 and E75 in the crustacean *Daphnia magna*. *Mol. Cell. Endocrinol.* 315, 208–218. doi: 10.1016/j.mce.2009.07.013

Hoch, G., Marktl, R. C., and Schopf, A. (2009). Gamma radiation-induced pseudoparasitization as a tool to study interactions between host insects and parasitoids in the system *Lymantria dispar* (Lep., *Lymantriidae*)-*Glyptapanteles liparidis (Hym., Braconidae*). *Biocontrol Sci. Technol.* 19, 23–34. doi: 10.1080/09583150802434059

Hochuli, A., Pfister-Wilhelm, R., and Lanzrein, B. (1999). Analysis of endoparasitoid-released proteins and their effects on host development in the system *Chelonus inanitus* (*Braconidae*)-*Spodoptera littoralis* (Noctuidae). *J. Insect Physiol.* 45, 823–833. doi: 10.1016/S0022-1910(99)00051-57

Horner, M. A., Chen, T., and Thummel, C. S. (1995). Ecdysteroid regulation and DNA binding properties of *Drosophila* nuclear hormone receptor superfamily members. *Dev. Biol.* 168, 490–502. doi: 10.1006/dbio.1995.1097

Huerta-Cepas, J., Forslund, K., Coelho, L. P., Szklarczyk, D., Jensen, L. J., von Mering, C., et al. (2017). Fast genome-wide functional annotation through orthology assignment by eggNOG-mapper. *Mol. Biol. Evol.* 34, 2115–2122. doi: 10.1093/molbev/msx148

Humeau, J., Bravo-San Pedro, J. M., Vitale, I., Nuñez, L., Villalobos, C., Kroemer, G., et al. (2017). Calcium signaling and cell cycle: progression or death. *Cell Calcium* 70, 3–15. doi: 10.1016/j.ceca.2017.07.006

Ignesti, M., Ferrara, R., Romani, P., Valzania, L., Serafini, G., Pennacchio, F., et al. (2018). A polydnavirus-encoded ANK protein has a negative impact on steroidogenesis and development. *Insect Biochem. Mol. Biol.* 95, 26–32. doi: 10.1016/j.ibmb.2018.03.003

Irving, J. A., Pike, R. N., Lesk, A. M., and Whisstock, J. C. (2000). Phylogeny of the serpin superfamily: implications of patterns of amino acid conservation for structure and function. *Genome Res.* 10, 1845–1864. doi: 10.1101/gr.GR-1478R

Ji, H., Wang, J., Guo, J., Li, Y., Lian, S., Guo, W., et al. (2016). Progress in the biological function of alpha-enolase. *Anim. Nutr.* 2, 12–17. doi: 10.1016/j.aninu.2016.02.005

Jones, G. (1995). Molecular mechanisms of action of juvenile hormone. *Annu. Rev. Entomol.* 40, 147–169. doi: 10.1146/annurev.en.40.010195.001051

Kaeslin, M., Pfister-Wilhelm, R., Molina, D., and Lanzrein, B. (2005). Changes in the haemolymph proteome of *Spodoptera littoralis* induced by the parasitoid *Chelonus inanitus* or its polydnavirus and physiological implications. *J. Insect Physiol.* 51, 975–988. doi: 10.1016/j.jinsphys.2005.04.012

Kaeslin, M., Wyler, T., Grossniklaus-Bürgin, C., and Lanzrein, B. (2006). Development of the anal vesicle, salivary glands and gut in the egg-larval parasitoid *Chelonus inanitus*: tools to take up nutrients and to manipulate the host? *J. Insect Physiol.* 52, 269–281. doi: 10.1016/j.jinsphys.2005.11.006

Kanehisa, M., and Goto, S. (2000). KEGG: kyoto encyclopedia of genes and genomes. *Nucleic Acids Res.* 28, 27–30. doi: 10.1093/nar/28.1.27

Kanost, M. R., and Jiang, H. (2015). Clip-domain serine proteases as immune factors in insect hemolymph. *Curr. Opin. Insect Sci.* 11, 47–55. doi: 10.1016/j.cois.2015.09.003

Kim, Y. (2007). An evidence for host translation inhibitory factor encoded in a Polydnavirus, *Cotesia glomerata Bracovirus*, genome and its expression in parasitized cabbage white butterfly, *Pieris rapae*. *J. Asia. Pac. Entomol.* 10, 351–356. doi: 10.1016/S1226-8615(08)60375-60371

Kim, Y., Hepat, R., and Kim, Y. (2013). A copy of cystatin from the diamondback moth *Plutella xylostella* is encoded in the polydnavirus *Cotesia plutellae Bracovirus*. *J. Asia. Pac. Entomol.* 16, 449–455. doi: 10.1016/j.aspen.2013.06.006

King, E. G., Hartley, G. G., Martin, D. F., and Laster, M. L. (1985). Large-scale rearing of a sterile backcross of the tobacco budworm (*Lepidoptera*: Noctuidae)1. *J. Econ. Entomol.* 78, 1166–1172. doi: 10.1093/jee/78.5.1166

Kroemer, J. A., and Webb, B. A. (2004). Polydnavirus genes and genomes: emerging gene families and new insights into Polydnavirus replication. *Annu. Rev. Entomol.* 49, 431–456. doi: 10.1146/annurev.ento.49.072103.120132

Kumar, S., Gu, X., and Kim, Y. (2016). A viral histone H4 suppresses insect insulin signal and delays host development. *Dev. Comp. Immunol.* 63, 66–77. doi: 10.1016/j.dci.2016.05.012

Kumar, S., and Kim, Y. (2016). Glyceraldehyde-3-phosphate dehydrogenase is a mediator of hemocyte-spreading behavior and molecular target of immunosuppressive factor CrV1. *Dev. Comp. Immunol.* 54, 97–108. doi: 10.1016/j.dci.2015.09.003

Kwon, B., and Kim, Y. (2008). Transient expression of an EP1-like gene encoded in *Cotesia plutellae Bracovirus* suppresses the hemocyte population in the diamondback moth, *Plutella xylostella*. *Dev. Comp. Immunol.* 32, 932–942. doi: 10.1016/j.dci.2008.01.005

Labropoulou, V., Douris, V., Stefanou, D., Magrioti, C., Swevers, L., and Iatrou, K. (2008). Endoparasitoid wasp *Bracovirus*-mediated inhibition of hemolin function and lepidopteran host immunosuppression. *Cell. Microbiol.* 10, 2118–2128. doi: 10.1111/j.1462-5822.2008.01195.x

Lam, G. T., Jiang, C., and Thummel, C. S. (1997). Coordination of larval and prepupal gene expression by the DHR3 orphan receptor during *Drosophila* metamorphosis. *Development* 124, 1757–1769.

Lanz-Mendoza, H., Bettencourt, R., Fabbri, M., and Faye, I. (1996). Regulation of the insect immune response: the effect of hemolin on cellular immune mechanisms. *Cell. Immunol.* 169, 47–54. doi: 10.1006/cimm.1996.0089

Laurino, S., Grossi, G., Pucci, P., Flagiello, A., Bufo, S. A., Bianco, G., et al. (2016). Identification of major *Toxoneuron nigriceps* venom proteins using an integrated transcriptomic/proteomic approach. *Insect Biochem. Mol. Biol.* 76, 49–61. doi: 10.1016/j.ibmb.2016.07.001

Lawrence, P. O. (1986). Host-parasite hormonal interactions: an overview. *J. Insect Physiol.* 32, 295–298. doi: 10.1016/0022-1910(86)90042-90049

Li, B., and Dewey, C. N. (2011). RSEM: accurate transcript quantification from RNA-Seq data with or without a reference genome. *BMC Bioinformatics* 12:323. doi: 10.1186/1471-2105-12-323

Li, K., Guo, E., Hossain, M. S., Li, Q., Cao, Y., Tian, L., et al. (2015). *Bombyx* E75 isoforms display stage- and tissue-specific responses to 20-hydroxyecdysone. *Sci. Rep.* 5:12114. doi: 10.1038/srep12114

Li, Z., You, L., Zeng, B., Ling, L., Xu, J., Chen, X., et al. (2015). Ectopic expression of ecdysone oxidase impairs tissue degeneration in *Bombyx mori*. *Proc. Biol. Sci.* 282:20150513. doi: 10.1098/rspb.2015.0513

Li, S., Falabella, P., Kuriachan, I., Vinson, S. B., Borst, D. W., Malva, C., et al. (2003). Juvenile hormone synthesis, metabolism, and resulting haemolymph titre in *Heliothis virescens* larvae parasitized by *Toxoneuron nigriceps*. *J. Insect Physiol.* 49, 1021–1030. doi: 10.1016/S0022-1910(03)00185-189

Ling, E., and Yu, X.-Q. (2005). Prophenoloxidase binds to the surface of hemocytes and is involved in hemocyte melanization in *Manduca sexta*. *Insect Biochem. Mol. Biol.* 35, 1356–1366. doi: 10.1016/j.ibmb.2005.08.007

Liu, N.-Y., Wang, J.-Q., Zhang, Z.-B., Huang, J.-M., and Zhu, J.-Y. (2017). Unraveling the venom components of an encyrtid endoparasitoid wasp *Diversinervus elegans*. *Toxicon* 136, 15–26. doi: 10.1016/j.toxicon.2017.06.011

Lopes, C. S. (2008). *Regulação do desenvolvimento e resposta imune de lagartas de Diatraea saccharalis (Fabricius) (lepidoptera: Crambidae) por Cotesia flavipes (Cameron) (Hymenoptera: Braconidae).* Piracicaba-SP: Universidade de São Paulo

Mahmoud, A. M. A., De Luna-Santillana, E. J., Guo, X., and Rodríguez-Perez, M. A. (2012). Parasitism by *Cotesia flavipes* alters the haemocyte population and phenoloxidase activity of the sugarcane borer, *Diatraea saccharalis*. *Can. Entomol.* 144, 599–608. doi: 10.4039/tce.2012.41

Mahmoud, A. M. A., De Luna-Santillana, E. J., and Rodríguez-Perez, M. A. (2011). Parasitism by the endoparasitoid, *Cotesia flavipes* induces cellular immunosuppression and enhances susceptibility of the sugar cane borer, *Diatraea saccharalis* to *Bacillus thuringiensis*. *J. Insect Sci.* 11, 1–15. doi: 10.1673/031.011.11901

Mattson, M. P., and Chan, S. L. (2003). Calcium orchestrates apoptosis. *Nat. Cell Biol.* 5, 1041–1043. doi: 10.1038/ncb1203-1041

Meng, E., Tang, B., Hou, Y., Chen, X., Chen, J., and Yu, X. Q. (2016). Altered immune function of *Octodonta nipae* (Maulik) to its pupal endoparasitoid, *Tetrastichus brontispae* Ferrière. *Comp. Biochem. Physiol. Part B Biochem. Mol. Biol.* 198, 100–109. doi: 10.1016/j.cbpb.2016.04.001

Mirth, C. K., and Riddiford, L. M. (2007). Size assessment and growth control: how adult size is determined in insects. *BioEssays* 29, 344–355. doi: 10.1002/bies.20552

Myllymaki, H., Valanne, S., and Ramet, M. (2014). The *Drosophila* Imd signaling pathway. *J. Immunol.* 192, 3455–3462. doi: 10.4049/jimmunol.1303309

Nakamatsu, Y., Fujii, S., and Tanaka, T. (2002). Larvae of an endoparasitoid, *Cotesia kariyai* (*Hymenoptera*: *Braconidae*), feed on the host fat body directly in the second stadium with the help of teratocytes. *J. Insect Physiol.* 48, 1041–1052. doi: 10.1016/S0022-1910(02)00192-190

Noriega, F. G. (2014). Juvenile hormone biosynthesis in insects: what is new, what do we know, and what questions remain? *Int. Sch. Res. Not.* 2014, 1–16. doi: 10.1155/2014/967361

Oliveira, C. M., Auad, A. M., Mendes, S. M., and Frizzas, M. R. (2014). Crop losses and the economic impact of insect pests on brazilian agriculture. *Crop Prot.* 56, 50–54. doi: 10.1016/j.cropro.2013.10.022

Perkins, N. D. (2007). Integrating cell-signalling pathways with NF-κB and IKK function. *Nat. Rev. Mol. Cell Biol.* 8, 49–62. doi: 10.1038/nrm2083

Pinto, M. C. X., Kihara, A. H., Goulart, V. A. M., Tonelli, F. M. P., Gomes, K. N., Ulrich, H., et al. (2015). Calcium signaling and cell proliferation. *Cell. Signal.* 27, 2139–2149. doi: 10.1016/j.cellsig.2015.08.006

Prasad, S. V., Hepat, R., and Kim, Y. (2014). Selectivity of a translation-inhibitory factor, CpBV15β, in host mRNAs and subsequent alterations in host development and immunity. *Dev. Comp. Immunol.* 44, 152–162. doi: 10.1016/j.dci.2013.12.001

Provost, B., Jouan, V., Hilliou, F., Delobel, P., Bernardo, P., Ravallec, M., et al. (2011). Lepidopteran transcriptome analysis following infection by phylogenetically unrelated polydnaviruses highlights differential and common responses. *Insect Biochem. Mol. Biol.* 41, 582–591. doi: 10.1016/j.ibmb.2011.03.010

Pruijssers, A. J., Falabella, P., Eum, J. H., Pennacchio, F., Brown, M. R., and Strand, M. R. (2009). Infection by a symbiotic polydnavirus induces wasting and inhibits metamorphosis of the moth *Pseudoplusia includens*. *J. Exp. Biol.* 212, 2998–3006. doi: 10.1242/jeb.030635

Pruijssers, A. J., and Strand, M. R. (2007). PTP-H2 and PTP-H3 from *Microplitis demolitor Bracovirus* localize to focal adhesions and are antiphagocytic in insect immune cells. *J. Virol.* 81, 1209–1219. doi: 10.1128/JVI.02189-2186

Qian, C., Wang, F., Zhu, B., Wang, L., Wei, G., Sun, Y., et al. (2017). Identification of a hemolin protein from *Actias selene* mediates immune response to pathogens. *Int. Immunopharmacol.* 42, 74–80. doi: 10.1016/j.intimp.2016.11.020

Robinson, M. D., McCarthy, D. J., and Smyth, G. K. (2010). edgeR: a Bioconductor package for differential expression analysis of digital gene expression data. *Bioinformatics* 26, 139–140. doi: 10.1093/bioinformatics/btp616

Rodríguez-Pérez, M. A., Dumpit, R. F., Lenz, J. M., Powell, E. N., Tam, S. Y., and Beckage, N. E. (2005). Host refractoriness of the tobacco hornworm, *Manduca sexta*, to the braconid endoparasitoid *Cotesia flavipes*. *Arch. Insect Biochem. Physiol.* 60, 159–171. doi: 10.1002/arch.20102

Rossi, G. D., Salvador, G., and Cônsoli, F. L. (2014). The parasitoid, *Cotesia flavipes* (Cameron) (*Hymenoptera*: *Braconidae*), influences food consumption and utilization by larval *Diatraea saccharalis* (F.) (*Lepidoptera*: *Crambidae*).*Arch. Insect Biochem. Physiol.* 87, 85–94. doi: 10.1002/arch.21182

Saarikangas, J., Zhao, H., and Lappalainen, P. (2010). Regulation of the actin cytoskeleton-plasma membrane interplay by phosphoinositides. *Physiol. Rev.* 90, 259–289. doi: 10.1152/physrev.00036.2009

Salvador, G., and Cônsoli, F. L. (2008). Changes in the hemolymph and fat body metabolites of *Diatraea saccharalis* (*Fabricius*) (*Lepidoptera*: *Crambidae*) parasitized by *Cotesia flavipes* (Cameron) (*Hymenoptera*: *Braconidae*). *Biol. Control* 45, 103–110. doi: 10.1016/j.biocontrol.2007.12.007

Salvia, R., Grossi, G., Amoresano, A., Scieuzo, C., Nardiello, M., Giangrande, C., et al. (2017). The multifunctional polydnavirus TnBVANK1 protein: impact on host apoptotic pathway. *Sci. Rep.* 7, 1–16. doi: 10.1038/s41598-017-11939-x

Schafellner, C., Marktl, R. C., and Schopf, A. (2007). Inhibition of juvenile hormone esterase activity in *Lymantria dispar* (*Lepidoptera*, Lymantriidae) larvae parasitized by *Glyptapanteles liparidis* (*Hymenoptera*, *Braconidae*). *J. Insect Physiol.* 53, 858–868. doi: 10.1016/j.jinsphys.2007.05.010

Schmidt, O., Faye, I., Lindström-Dinnetz, I., and Sun, S.-C. (1993). Specific immune recognition of insect hemolin. *Dev. Comp. Immunol.* 17, 195–200. doi: 10.1016/0145-305X(93)90038-R

Schmidt, O., Theopold, U., and Strand, M. (2001). Innate immunity and its evasion and supression by *hymenopteran endoparasitoids*. *BioEssays* 23, 344–351. doi: 10.1002/bies.1049

Shrestha, S., Kim, H. H., and Kim, Y. (2009). An inhibitor of NF-kB encoded in *Cotesia plutella Bracovirus* inhibits expression of antimicrobial peptides and enhances pathogenicity of *Bacillus thuringiensis*. *J. Asia. Pac. Entomol.* 12, 277–283. doi: 10.1016/j.aspen.2009.06.004

Strand, M. R. (2008). The insect cellular immune response. *Insect Sci.* 15, 1–14. doi: 10.1111/j.1744-7917.2008.00183.x

Strand, M. R. (2014). Teratocytes and their functions in parasitoids. *Curr. Opin. Insect Sci.* 6, 68–73. doi: 10.1016/j.cois.2014.09.005

Strand, M. R., and Burke, G. R. (2013). Polydnavirus-wasp associations: evolution, genome organization, and function. *Curr. Opin. Virol.* 3, 587–594. doi: 10.1016/j.coviro.2013.06.004

Suderman, R. J., Pruijssers, A. J., and Strand, M. R. (2008). Protein tyrosine phosphatase-H2 from a polydnavirus induces apoptosis of insect cells. *J. Gen. Virol.* 89, 1411–1420. doi: 10.1099/vir.0.2008/000307-300

Sun, S. C., Lindstrom, I., Boman, H. G., Faye, I., and Schmidt, O. (1990). Hemolin: an insect-immune protein belonging to the immunoglobulin superfamily. *Science.* 250, 1729–1732. doi: 10.1126/science.2270488

Tan, C., Peiffer, M., Hoover, K., Rosa, C., Acevedo, F. E., and Felton, G. W. (2018). Symbiotic polydnavirus of a parasite manipulates caterpillar and plant immunity. *Proc. Natl. Acad. Sci. U.S.A.* 115, 5199–5204. doi: 10.1073/pnas.1717934115

Teng, Z. W., Xu, G., Gan, S. Y., Chen, X., Fang, Q., and Ye, G. Y. (2016). Effects of the endoparasitoid *Cotesia chilonis* (*Hymenoptera*: *Braconidae*) parasitism, venom, and calyx fluid on cellular and humoral immunity of its host *Chilo suppressalis* (Lepidoptera: Crambidae) larvae. *J. Insect Physiol.* 85, 46–56. doi: 10.1016/j.jinsphys.2015.11.014

Terenius, O. (2008). Hemolin-A lepidopteran anti-viral defense factor? *Dev. Comp. Immunol.* 32, 311–316. doi: 10.1016/j.dci.2007.09.006

Terenius, O., Bettencourt, R., Lee, S. Y., Li, W., Söderhäll, K., and Faye, I. (2007). RNA interference of Hemolin causes depletion of phenoloxidase activity in *Hyalophora cecropia*. *Dev. Comp. Immunol.* 31, 571–575. doi: 10.1016/j.dci.2006.09.006

Thompson, S. N. (2001). Parasitism enhances the induction of glucogenesis by the insect, *Manduca sexta* L. *Int. J. Biochem. Cell Biol.* 33, 163–173. doi: 10.1016/S1357-2725(00)00079-70

Thompson, S. N. (2003). Trehalose - the insect "blood" sugar. *Adv. Insect Physiol.* 31, 205–228.

Thompson, S. N., and Dahlman, D. L. (1999). Blood sugar formation due to abnormally elevated gluconeogenesis: aberrant regulation in a parasitized insect. Manduca sexta Linnaeus. *Biochim. Biophys. Acta Mol. Basis Dis.* 1454, 133–142. doi: 10.1016/S0925-4439(99)00031-39

Thummel, C. S. (2005). Dueling orphans–interacting nuclear receptors coordinate *Drosophila* metamorphosis. *BioEssays* 19, 669–672. doi: 10.1002/bies.950190806

Tsai, F.-C., Kuo, G.-H., Chang, S.-W., and Tsai, P.-J. (2015). Ca2+ signaling in cytoskeletal reorganization, cell migration, and cancer metastasis. *Biomed Res. Int.* 2015:409245. doi: 10.1155/2015/409245

Valzania, L., Romani, P., Tian, L., Li, S., Cavaliere, V., Pennacchio, F., et al. (2014). A polydnavirus ank protein acts as virulence factor by disrupting the function of prothoracic gland steroidogenic cells. *PLoS One* 9:e95104. doi: 10.1371/journal.pone.0095104

van Haasteren, G., Li, S., Muda, M., Susini, S., and Schlegel, W. (1999). Calcium signalling and gene expression. *J. Recept Signal Transduct. Res.* 19, 481–492. doi: 10.3109/10799899909036666

Vinson, S. B. (1990). How parasitoids deal with the immune system of their host: an overview. *Arch. Insect Biochem. Physiol.* 13, 3–27. doi: 10.1002/arch.940130103

Vinson, S. B., and Iwantsch, G. F. (1980). Host regulation by insect parasitoids. *Quartely Rev. Biol.* 55, 143–165. doi: 10.1086/411731

Wang, J. L., Liu, X. S., Zhang, Q., Zhao, H. B., and Wang, Y. F. (2012). Expression profiles of six novel C-type lectins in response to bacterial and 20E injection in the cotton bollworm (*Helicoverpa armigera*). *Dev. Comp. Immunol.* 37, 221–232. doi: 10.1016/j.dci.2012.04.004

Webb, B., and Luckhart, S. (1994). Evidence for an early immunosuppressive role for related *Campoletis sonorensis* venom and ovarian proteins in *Heliothis virescens*. *Arch. Insect Biochem. Physiol.* 26, 147–163. doi: 10.1002/arch.940260208

Ye, X. Q., Shi, M., Huang, J. H., and Chen, X. X. (2018). Parasitoid polydnaviruses and immune interaction with secondary hosts. *Dev. Comp. Immunol.* 83, 124–129. doi: 10.1016/j.dci.2018.01.007

Yu, D. S., Chen, Y. B., Li, M., Yang, M. J., Yang, Y., Hu, J. S., et al. (2016). A polydnaviral genome of *Microplitis bicoloratus Bracovirus* and molecular interactions between the host and virus involved in NF-κB signaling. *Arch. Virol.* 161, 3095–3124. doi: 10.1007/s00705-016-2988-2983

Yu, R. X., Chen, Y. F., Chen, X. X., Huang, F., Lou, Y. G., and Liu, S. S. (2007). Effects of venom/calyx fluid from the endoparasitic wasp *Cotesia plutellae* on the hemocytes of its host Plutella xylostella in vitro. *J. Insect Physiol.* 53, 22–29. doi: 10.1016/j.jinsphys.2006.09.011

Conflict of Interest Statement: The authors declare that the research was conducted in the absence of any commercial or financial relationships that could be construed as a potential conflict of interest.

frontiers in Physiology

ORIGINAL RESEARCH
published: 18 September 2019
doi: 10.3389/fphys.2019.01069

Botanical Origin of Pesticide Residues in Pollen Loads Collected by Honeybees During and After Apple Bloom

*Riccardo Favaro[1], Lisbeth Marie Bauer[1], Michele Rossi[2], Luca D'Ambrosio[3], Edith Bucher[2] and Sergio Angeli[1]**

[1] Faculty of Science and Technology, Free University of Bozen-Bolzano, Bolzano, Italy, [2] Laboratorio Biologico, Agenzia Provinciale per l'Ambiente e la Tutela del Clima, Bolzano, Italy, [3] Laboratorio Analisi Alimenti, Agenzia Provinciale per l'Ambiente e la Tutela del Clima, Bolzano, Italy

Honeybees closely rely on insect-pollinated plants for their survival. Each forager bee displays a tendency of loyalty toward specific plant species during the many daily foraging flights. Due to the ease of collection, pollen loads have been extensively used as a proxy for detection of pesticide residues. Pollen is the main protein food source for colonies, and its contamination has also been addressed as a reason for the colony losses phenomenon. As honeybees fly over a variable but wide range territory, they might collect pollen from both agricultural, urban and wild environments, also displaying considerable preferences in botanical sources between colonies of the same apiary. It is thus difficult to address the source of the pesticide contamination, when pollen is analyzed as a whole. In the current study, a practical and reliable approach has been proposed to narrow down the source of contamination. Pollen loads have been collected from colonies placed in eight locations over large apple orchard extensions in Trentino-South Tyrol region (Italy), during and 2 weeks after apple blossom. The pollen loads have been separated by the color due to the predominant plant species. On each color group, palynology and multi-residual chemical analyses have been performed in parallel. The pollen hazard quotient (PHQ) was used to estimate the risk to honeybees of each color group and of the total collected pollen. Apple and dandelion pollen were the main portions of the first collection, while a greater variety emerged after the apple blossom. Dandelion was always present in the samples. The frequency and the amount of pesticide residues differed according to the collection periods, the locations and the pollen color groups. The amount of insecticide residues increased after the apple blossom, while no difference between the period was found on fungicide residues. The PHQ values were higher after the blossom due to the insecticide contribution, with highest values of 160,000 and 150,000. The variations within samples did not allow to identify a unique source of contamination, whereas it seems that the pollen from plants outside the agricultural areas has as much residues as the pollen from apple orchards.

Keywords: palynology, pesticide drift, pollen color, colony loss, agricultural landscape, PHQ, multi-residue analysis

OPEN ACCESS

Edited by:
Patrizia Falabella, University of Basilicata, Italy

Reviewed by:
Notburga Oeggl-Wahlmueller, University of Innsbruck, Austria
Ales Gregorc, University of Maribor, Slovenia

****Correspondence:***
Sergio Angeli
sergio.angeli@unibz.it

Specialty section:
This article was submitted to Invertebrate Physiology, a section of the journal Frontiers in Physiology

Received: *06 March 2019*
Accepted: *05 August 2019*
Published: *18 September 2019*

Citation:
Favaro R, Bauer LM, Rossi M, D'Ambrosio L, Bucher E and Angeli S (2019) Botanical Origin of Pesticide Residues in Pollen Loads Collected by Honeybees During and After Apple Bloom. Front. Physiol. 10:1069. doi: 10.3389/fphys.2019.01069

INTRODUCTION

Pollinating insects, such as honeybees (*Apis mellifera* L.), are a crucial part of ecosystems for their contribution to plant reproduction. While the role of honeybees has been reappraised in view of the contribution of other wild pollinators (Garibaldi et al., 2013), they are still prominent in commercial orchards, since production, fruit growth and fruit durability are affected by pollination and seed development (Garratt et al., 2014). Due to the recent decrease of wild pollinators, insect-pollinated fruit production started to rely on managed honeybee hives (Calderone, 2012). In order to enhance the yield, honeybee hives are brought to fruit tree orchards during the flowering period, and beekeepers play a key role tightly related to fruit growers.

The use of pesticides in integrated crop management practice allows the farmers to protect their yields, but the chemical treatments are well-recognized as one of the main causes affecting pollinators decline (Potts et al., 2016). To combine crop protection and pollinator protection is a big challenge of today's agriculture. While avoiding spraying of harmful chemicals during the flowering period ensure to prevent the pollinators from direct exposures, feeding on nectar and pollen represent the main source of contamination (Sanchez-Bayo and Goka, 2014).

Pesticides not only affect the target organisms, but also spread in the ecosystems, contaminating soil, water and plants. Residues on plants have been extensively investigated in recent years (Botías et al., 2016; Long and Krupke, 2016; Lentola et al., 2017). Persistent and systemic molecules, such as neonicotinoids, are absorbed and translocated in the entire plant matrix (Sur and Stork, 2003), lately being found also in nectar and pollen (Blacquiere et al., 2012; Böhme et al., 2018).

Pollen contamination has been the subject of many studies as honeybees rely on it for the majority of their protein supply. A study of the annual pollen intake by Keller et al. (2005), reports the amount of collected pollen per hive ranging from 5.6 to 222 kg, depending on the colony size, the food availability and the season length, while other data show an estimated average value of 20 kg (McLellan, 1977). In order to support this large supply, honeybees take continuous surveys of the surrounding territory, making them reliable bioindicators of environmental pollution (Porrini et al., 2002). One particular aspect of the bee ecology is posed by the tendency of each colony to choose the food source autonomously, for which hives of the very same apiary may collect pollens from different plant species at the same time. On the other hand, single honeybees display loyalty to food source during their daily foraging flights, tuning their search on a specific botanical species as long as it continues to provide flowers (Porrini et al., 2002). Thus, a single honeybee tends to gather pollen loads composed of mainly one plant species.

Several studies provided pollen residues data (Škerl et al., 2009; Genersch et al., 2010; Lambert et al., 2012; Kasiotis et al., 2014; Böhme et al., 2018). These studies provide indications of the amount of pesticide residues found in the collected pollens, but there also have been attempts to estimate the hazard of these pollens on honeybee health (Stoner and Eitzer, 2013; Böhme et al., 2018).

The distribution of pesticide in the environment seems to be not equal, as runoff water and airborne movements spread pesticides from agricultural areas to wild plants (Botías et al., 2016). For instance, crops report higher residue levels than the surrounding vegetation (Longley and Sotherton, 1997), but wildflowers too resulted to be an important source of pesticide contaminations (Botías et al., 2015). Residues analysis of the mixed pollen offer a whole picture of the present contaminants, but lack providing the information about their source. Böhme et al. (2018) provided a first attempt of source recognition performing chemical residues of the collected pollen and in parallel performing palynological analyses. However, also in this case pesticide residues could not be attributed to a specific plant species, as pollen samples were analyzed as mixed samples collected by the bees in a specific period.

In the current study, we aimed to fill the gap of the contamination source knowledge, thus analyzing the amount of pesticide residues in pollen loads. After a single collection from honeybees, the pollen loads were divided by color and each group was characterized botanically. Given the overwhelming abundance of apple orchards in the study area, we focused our attention on pesticide residues during and after apple blossom. As no other crops were blooming during the collections, this peculiar situation offered the chance to focus mainly on the pollens collected from apple orchards and the surrounding environments.

MATERIALS AND METHODS

Biological Material

Honeybees [*Apis mellifera* ssp. *carnica* (Pollmann)] were kept in standard 10-frames Dadant-Blatt beehives for nomadic beekeeping. In each beehive, the brood was spread at least over four frames. Bee colonies were managed according to good beekeeping practice and had undergone regular sanitary treatments against the parasitic mite *Varroa destructor* (Anderson & Trueman).

Field Experimental Setup

The experiments took place in the Italian region Trentino-South Tyrol between April and May 2017. In the lower valleys, this alpine region is characterized by a wide extension of apple orchards composed by many small lots belonging to different farmers (Tasser et al., 2009). Dandelion (*Taraxacum* spp.) is the predominant herbaceous flowering plant on the apple orchard floor during blossom. Its abundance leads to competition with apple trees for pollinators, as already noticed by Free (1968). The woods on the surrounding mountain slopes are characterized mainly by broadleaves species (*Castanea sativa* Mill., *Fraxinus ornus* L., *Quercus pubescens* Willd., *Ostrya carpinifolia* Scop.), and pines (*Pinus sylvestris* L.).

In this region apple trees flower usually in April with temporal shifts of some weeks depending on local conditions. The pollen samples were collected in two periods: during the middle of the main apple blooming (during king flower = F collection) and 2 weeks after the end of the blooming (after flowering = AF

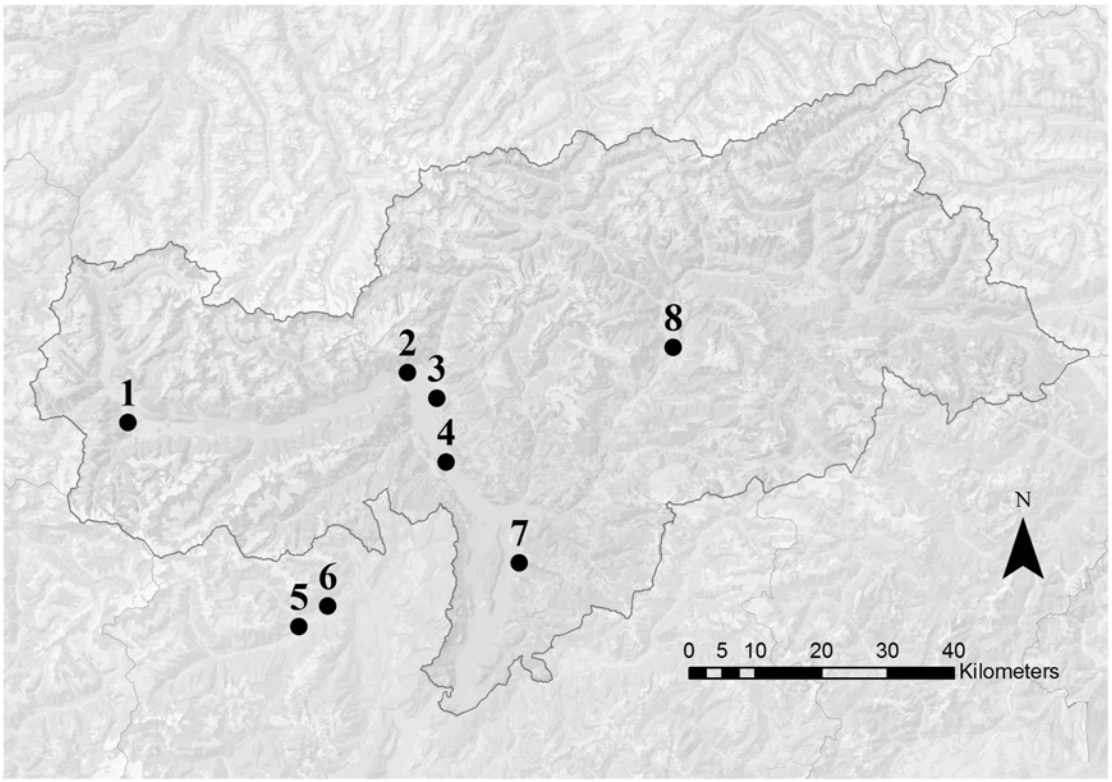

FIGURE 1 | Map of South Tyrol (Italy). Dots indicate the approximate position of the apiary locations. Numbers refer to the information reported in **Table 1**. Apiaries 5 and 6 were located in the nearby Trento province.

collection). Eight voluntary beekeepers participated to the study with their beehives: six apiaries were located along the two main valleys of the province of Bolzano and two apiaries in a valley of the province of Trento (**Figure 1**). In order to ensure the beekeepers privacy, only altitude and the nearest town are reported for each location (**Table 1**). Every beekeeper had a permanent apiary within the apple orchard extension in the low valley, in which two beehives were randomly chosen for pollen collection. In each location, the surrounding agricultural landscape was dominated by apple orchards. Even if the use of different cultivar influences slightly timing and number of pesticide treatments, only one common regulation for the apple orchards management exists (AGRIOS, 2017). For this reason, the allowed pesticides were known but not the timing of their application.

TABLE 1 | Sample collection specifications.

Location	Town	Altitude	F collection date	AF collection date
1	Sluderno (BZ)	1008	21.-24.4.2017	5.- 8.5.2017
2	Tirolo (BZ)	646	10.-13.4.2017	2.-5.5.2017
3	Merano (BZ)	620	19.-22.4.2017	4.-7-5.2017
4	Nalles (BZ)	345	11.-14.4.2017	3.-6.5.2017
5	Croviana (TN)	902	22.-25.4.2017	11.-14.5.2017
6	Malè (TN)	953	22.-25.4.2017	10.-13.5.2017
7	Laives (BZ)	335	6.-8.4.2017	9.-12.5.2017
8	Bressanone (BZ)	670	22.4-25.4.2017	26.-29.5.2017

The nearest town to the apiary is reported. The altitude (m a.s.l) refers to the apiary position. Differences in the time between the two collections depend by different duration of apple blossom, due to cultivar and climatic conditions.

Samples were collected by standard pollen traps (Pollen trap "Metalori," Il Pungiglione S.C.S., Italy). The two collection periods lasted four consecutive days (**Table 1**), during which the beekeepers daily gathered, labeled and froze the pollen loads at −20°C daily in sterilized glass jars. Afterward, pollen samples were transported in freezers to the Free University of Bolzano and stored there at −80°C until analysis.

Palynological Analyses

Pollen samples from every apiary location, collected over a 4 days period, were mixed together to avoid differences linked to the colony. For a first botanical separation, pollen loads were separated by color. The *green* and the *orange* pollen loads were taken out of a representative amount of 50 grams from the *total* fresh pollen loads collected by each beekeeper. The pollen loads were manually separated according to the color (Kirk, 2006) under a neutral light bulb (True-Light led, CRI 96) until reaching samples of at least 10 g each. Once separated, the pollen sample colors were measured in L*a*b color scale with a Chroma meter (Minolta CR-400, Konica Minolta,

United States). The abundance of each color in the pollen samples was expressed as a weight percentage over the *total*. The pollen composition of the *total*, *green*, *orange,* and *leftover* samples collected during the flowering, as well as of the *total, orange,* and *leftover* samples collected after the flowering were analyzed by light-microscopy.

The pollen loads of the AF collection were divided by color and every subsample was weighted. From each subsample two pollen loads were randomly chosen for the palynological analysis. The pollen loads were dissolved in 2 ml Milli-Q water and two drops of 60 μl were placed on a microscope slide. After drying, one drop of glycerine jelly with fuchsine (Lanzoni S.r.l, Bologna, Italy) was placed above and covered with a thin glass sheet. Under a microscope, 1000 grains of pollen were counted for each slide and identified based on their morphology at the family, genus or species level, when possible (Bucher, 2004). The taxa found in the slides were assigned to the weight of the corresponding subsamples allowing an estimation of the frequency classes.

The method for the palynological analysis was further implemented in a more accurate and time-saving approach. Performing parallel trials on the same samples with different methods, no difference was found in abundance classes and more biodiversity in rare occurring pollen types. Therefore, for each sample of the F collection, 1 g of pollen was taken and diluted with 30 ml of Milli-Q water and then agitated at 100 rps for 30 min. 1 ml of the solution was further diluted in 6 ml of Milli-Q water and again agitated at 100 rps for 30 min. Two drops of 60 μl were placed on a microscope slide. After drying, one drop of glycerine jelly with fuchsine (Lanzoni S.r.l) was placed above and covered with a thin glass sheet. Under a microscope, 1000 grains of pollen were counted for each slide and identified based on their morphology at the family, genus or species level, when possible (Bucher, 2004). The pollen composition thus referred to the proportion of the number of grains belonging to a level over the total.

We considered the following seven groups for color separation: *total*, *green*, *orange,* and *leftover* pollen loads collected during the apple flowering. *Total*, *orange,* and *leftover* were instead considered in the pollen samples from the second collection period. The *leftover* pollen group referred to a mixture of pollen colors obtained by removing the *green* and the *orange* portions. The pollen groups were kept separated by locations, so that for each location there were seven pollen groups.

Multi-Residual Pesticides Analyses

A total of 56 pollen samples were chemically analyzed considering the 7 pollen groups per location and the 8 locations above described. Samples of 5 grams each were prepared following the multi-residual QuEChERS (Anastassiades et al., 2003) method (Standard Operating Procedure EN15662:2008). The preparations were then analyzed by GC–MS and LC–MS were used to identify 270 active principles and some of their metabolites. The residues were quantified by standard calibration curves using the Agilent MassHunter Quantitative Analysis Software. The limit of quantification (LOQ) was 0.01 mg/kg for all the substances. When below this limit, the results were not considered in the study.

Toxicological Evaluation

In order to assess the effects of pesticide residues in pollen on honeybees, we decided to use the Pollen Hazard Quotient (PHQ) proposed by Stoner and Eitzer (2013) dividing the concentration (ppb) of each residue found in the analyses by the known LD_{50} value (μg/bee). As a nurse honeybee can consume up to 9.5 mg of pollen a day (Rortais et al., 2005). Böhme et al. (2018) considered relevant a PHQ of 50. Taking into account a PHQ value of 1,000 would imply the consumption of 1% of the LD_{50} in a day, or 10% after 10 days of average nursing period (Stoner and Eitzer, 2013). A further improvement of the PHQ concept considered the summing of all the PHQs in each pollen sample to reach a total PHQ value (tPHQ) (Böhme et al., 2018).

In this study, we considered tPHQ in order to compare the harm of the different pollen groups and collection periods to the honeybee colonies. The LD50 values were acquired by the US EPA ecotoxicology database (US EPA ECOTOX, 2018), the Agritox database (AGRITOX, 2018) and the Pesticide Properties Database of the University of Hertfordshire (Ppdb., 2018). Both contact and oral doses were considered. In the attempt to rely on a worst-case scenario, the lowest of the available values were chosen to calculate the PHQ values.

Statistical Analysis

The frequency of the residuals and the tPHQ of the pollen samples were analyzed using the software R (R Core Team, 2018). The effect of the collection period, the color group and the type of pesticide on the number of residues per sample were tested using a Linear Mixed-Effect Model (lme4 package, Bates et al., 2015).

The effect of the pollen type and the collection period on the tPHQ were tested with the same approach. Data were Tukey-transformed to fit a parametric distribution. In both the analysis, the locations were considered as a random effect. All the values reported in the paper are expressed as mean ± standard deviation, when not specified differently. The plots were created using the R package ggplot2 (Wickham, 2016).

RESULTS

Botanical Characterization of Pollen During and After Apple Flowering

The chromatic separation of pollen loads allowed to divide four groups: *green*, *orange*, *yellow*, *dark yellow*. Small fractions of other remaining colors were grouped together.

Although some variation between locations, the color composition of the pollen collected during the blossom (F collection) showed that *green* and *orange* were the main groups, being on average 49.1 ± 21 and 30.5 ± 20%, respectively. Together they accounted for the majority of the pollen composition (79.6 ± 10.3%). The other groups presented a more variable incidence: 8.5 ± 9.7% the *yellow*, 4 ± 7.8% the *dark yellow*, 8 ± 3.5% the minor colors. The palynology analyses of

the *green* and *orange* components of the F collection confirmed the predominance of apple (*Malus* spp. = 60.9 ± 16.6%) and dandelion (*Taraxacum* spp. = 99.6 ± 0.6%) on the two groups, respectively. The palynology analysis of the *total* pollen composition showed a high occurrence of willow (42.8 ± 25.9%), Asteraceae T-form (dominated by *Taraxacum* spp., 21.3 ± 15.4%) and apple (18.3 ± 16.9%) (**Table 2**). It was not possible to perform also the palynological analysis of the total pollen samples from the Meran site, as we did not reach a sufficient amount of pollen.

In the second pollen collection (AF), the pollen composition showed an increased variability, with standard deviation easily exceeding the average values. While the *green* group remained the most represented (53.8 ± 35.5%), *dark yellow* reached higher values (19.2 ± 28.4%) similar to *orange* (18.1 ± 21.1%). The *yellow* and the minor colors decreased to 3.3 ± 4.2 and 5.5 ± 5.6%, respectively. The *green* component was no longer represented by apple, but from a variety of other plant species (**Table 3**), since the palynology analysis revealed traces of *Malus* spp. pollen in only two locations. This was expected, as the apple blossom ended 2 weeks before. The *orange* fraction was still dominated by *Taraxacum* spp. but in a slightly lower amount (81.4 ± 17.2%).

The variation of pollen composition in the main color groups revealed also a change in the chromametric scale (L*a*b) although these differences were not detected at operator sight. The *green* group, identified as 57.6, 0.3, 32.7 in the F collection became 51.3, 0.8, 27.8 in the AF collection. The *orange* group shifted from 54.8, 18.6, 39.3 in the F collection to 51.3, 18.8, 35.1 in the AF collection.

TABLE 2 | Pollen composition of the total samples collected during apple blossom.

Location	Pollen abundance			
	>45%	**16–45%**	**3–16%**	**<3%**
Sluderno (BZ)	*Salix* sp.	–	Asteraceae T-Form	*Malus/Pyrus* sp. *Viburnum* sp.
Tirolo (BZ)	*Salix* sp.	*Malus/Pyrus* sp.	Asteraceae T-form *Platanus* sp.	*Acer palmatum* Thunb. *Ligustrum/ Syringa* sp.
Nalles (BZ)	*Malus/Pyrus* sp.	–	Asteraceae T-form *Fraxinus ornus* L.	*Acer* sp. *Aesculus* sp. Lamiaceae M-form *Ligustrum/ Syringa* sp. *Viburnum* sp. Juglandaceae Papaveraceae
Croviana (TN)	–	Asteraceae T-form *Malus/Pyrus* sp.	*Salix* sp. *Viburnum* sp.	*Aesculus* sp. *Ligustrum/ Syringa* sp. *Betula* sp.
Malè (TN)	*Salix* sp.	Asteraceae T-form	–	*Malus/Pyrus* sp. *Acer* sp. *Fraxinus ornus* L. *Ligustrum/ Syringa* sp. *Quercus* sp.
Laives (BZ)	–	*Salix* sp. *Malus/Pyrus* sp. Asteraceae T-form	–	*Acer* sp. *Ligustrum/ Syringa* sp. Brassicaceae *Prunus* sp.
Bressanone (BZ)	*Salix* sp.		Asteraceae T-form *Malus/Pyrus* sp. *Fraxinus ornus* L. Brassicaceae *Aesculus* sp.	Rosaceae *Prunus* sp. Papaveraceae *Viburnum* sp. *Fragaria/ Potentilla* form

Values report the frequency classes of the botanical source over 1000 grains of pollen counted for each slide. Pollens were identified based on their morphology at the family, genus or species level, when possible. Merano is not reported because of lack of sufficient pollen amount for the analyses. While the group Asteraceae T-form in palynological studies comprises more genera from the Asteraceae family, here refers mainly to the genus Taraxacum.

Pesticide Residues in Pollen Samples

The multi-residual analysis on pollen loads from eight locations, collected in two periods, was performed on a total of 56 samples. 36 pesticides were detected considering all samples, of which 13 insecticides, 21 fungicides, and 2 herbicides (**Table 4**). Overall, fungicides occurred the most, as in each sample we found from 2 up to 10 substances, while insecticides ranged from 0 to 6 residues per sample. No sample was free of pesticides. The statistical analysis of the number of residues showed a higher occurrence of fungicides in the samples (lmer, $t = -3.05$, $p < 0.005$), with an average difference of 2.7 substances per sample from the insecticides (**Table 5**). The collection period had a highly significant effect on the insecticide residues (lmer, $t = -2.871$, $p < 0.01$) (**Figure 2**), as their number increased of 1.375 residues per sample during the second collection (AF). On the contrary, there was no effect of the collection period on the number of fungicides per sample (lmer, $t = -1.39$, $p = 0.17$) (**Figure 3**). The number of fungicide residues in *orange* pollen was significantly lower than in the *total* and in the *green* pollens during the F collection (lmer, $t = -3.38$, $p < 0.005$), as well as the number of insecticides (lmer, $t = -2.13$, $p < 0.05$). After flowering, the number of residues in *orange* pollen raised significantly in insecticides (lmer, $t = 5.29$, $p < 0.01$) but not in fungicides (lmer, $t = 0.661$, $p = 0.52$). Also the *leftover* samples showed a reduced occurrence of insecticide residues during the apple blossom (lmer, $t = -2.43$, $p < 0.05$).

The presence and the amount of residues varied according to the collection period and the pollen group. Among the insecticides, Flonicamid, Phosmet, Imidacloprid, Methoxyfenozid and Chlorpyrifos-methyl were the most frequent, being found in 23, 21, 21, 17, and 17 samples, respectively. Penconazole, Cyprodinil, and Fluazinam were instead the most frequent fungicides (in 50, 38, and 31 samples, respectively). We detected only two

TABLE 3 | Pollen composition of the total samples collected 2 weeks after the end of apple blossom.

Location	Pollen abundance				
	>45%	**16–45%**	**3–16%**	**<3%**	
Sluderno (BZ)	Asteraceae T form	Poaceae *Lonicera* sp.	*Pinus* sp.	Rhamnaceae *Salix* sp. *Malus/Pyrus* sp. Rosaceae *Berberis* sp.	*Fragaria/Potentilla* sp. *Allium* sp. *Aesculus* sp. *Knautia* sp. Cyperaceae
Tirolo (BZ)	*Quercus* sp.	*Fraxinus ornus* L.	*Trachycarpus* sp.	*Pinus* sp. *Robinia* sp. Asteraceae A form *Viburnum* sp. *Trifolium repens* L.	*Kolkwitzia* sp. Polygonaceae *Weigelia* sp. *Veronica* sp. Apiaceae
Merano (BZ)	*Trachycarpus* sp.	–	Ranuncolaceae *Quercus ilex* Asteraceae T form *Robinia pseudoacacia* L.	*Ilex* sp. *Viburnum* sp. *Malus/Pyrus* sp. *Liriodendron* sp. *Aesculus* sp. *Lonicera* sp.	Rhamnaceae *Acer* sp. *Pinus* sp. *Weigelia* sp. Geraniaceae *Tulipa* sp.
Nalles (BZ)	*Gleditsia* sp.	–	*Robinia pseudoacacia* L. *Trachycarpus* sp. *Acer* sp. *Cornus* sp. *Liriodendron* sp. Brassicaceae	Ranuncolaceae Asteraceae T form *Aesculus* sp. *Thalictrum* sp.	*Pinus* sp. *Allium* sp. *Trollius* sp. *Aruncus* sp.
Croviana (TN)	–	*Fraxinus ornus* L. *Quercus* sp. *Asteraceae T form*	Brassicaceae	*Pinus* sp. *Salix* sp.	Apiaceae *Clemantis* sp.
Malè (TN)	*Fraxinus ornus* L.	–	Asteraceae T form *Malus/Pyrus* sp.	*Pinus* sp. *Picea* sp. *Acer* sp. *Prunus* sp.	Geraniaceae Caryophillaceae *Knautia* sp.
Laives (BZ)	Asteraceae T form	–	*Gleditisia* sp. *Trachycarpus* sp. *Liriodendron* sp. *Fraxinus ornus*	*Cornus* sp. *Aesculus* sp. *Rubus* sp. *Acer* sp.	*Anemone* sp. *Viburnum* sp. *Pinus* sp.
Bressanone (BZ)	*Parthenocissus* sp.	–	*Rubus* sp. *Tilia* sp. Rosaceae	*Plantago* sp. *Potentilla/Fragaria* sp. Asteraceae H form Asteraceae T form Poaceae *Vitis* sp.	Papaveraceae *Echium* sp. Lamiaceae *Knautia* sp. *Fraxinus ornus* *Aruncus* sp.

Values report the frequency classes of the botanical source expressed as weight proportion over the total. Pollens were identified based on their morphology at the family, genus or species level, when possible. While the group Asteraceae T-form in palynological studies comprises more genera from the Asteraceae family, here refers mainly to the genus Taraxacum.

herbicides, Metamitron in six samples, and MCPA in six samples (**Table 4**).

The analysis revealed the highest concentrations of insecticides in the AF collection, where Chlorpyrifos-methyl and Phosmet reached 2.27 and 2.1 ppm respectively (**Table 4**). Some substances were present only in the F collection (Etofenprox, Flonicamid), while others appeared after the flowering (Indoxacarb, Fenoxycarb, Spirotetramat) (**Table 4**). We also found residues of insecticides classified harmful to bees in the F collection: Chlorpyrifos-ethyl and Imidacloprid were

TABLE 4 | Summary of the 36 pesticides detected in honey bee pollen loads collected during and after apple blossom and separated by color.

Pesticide	Type	Period	Group	Mean ± SD	Maximum	Frequency	LD_{50} contact	LD_{50} oral	PHQ_{max}
Boscalid	Fg	F	Total	0.062	0.062	1	200 b	160 b	0.3875
			Green	0.1	0.1	1			0.625
			Orange	0.04	0.04	1			0.25
			Leftover	–	–	–			–
		AF	Total	0.016	0.016	1			0.1
			Orange	0.02	0.02	1			0.125
			Leftover	0.052	0.052	1			0.325
Bupirimate	Fg	F	Total	0.384 ± 0.41	0.088	2	50 b	200 b	1.76
			Green	0.198 ± 0.25	0.49	3			9.8
			Orange	0.078	0.078	1			1.56
			Leftover	–	–	–			–
		AF	Total	–	–	–			–
			Orange	–	–	–			–
			Leftover	–	–	–			–
Captan	Fg	F	Total	1.103 ± 1.7	3.1	3	200 b	100 b	31
			Green	0.17	0.17	1			1.7
			Orange	0.15	0.15	1			1.5
			Leftover	0.26 ± 0.5	1.3	6			13
		AF	Total	–	–	–			–
			Orange	0.47 ± 0.62	1.4	4			14
			Leftover	0.22 ± 0.29	0.69	5			6.9
Chlorpyrifos-ethyl	Is	F	Total	–	–	–	0.01 a	0.25 a	–
			Green	–	–	–			–
			Orange	0.02	0.02	1			2000
			Leftover	–	–	–			–
		AF	Total	0.76 ± 0.25	0.94	2			94000
			Orange	0.98 ± 0.73	1.5	2			150000
			Leftover	1.1 ± 0.7	1.6	2			160000
Chlorpyrifos-methyl	Is	F	Total	0.13 ± 0.13	0.23	2	0.38	0.11	2090
			Green	0.076	0.076	1			690
			Orange	0.034	0.034	1			309
			Leftover	0.028	0.028	1			254
		AF	Total	0.12 ± 0.05	0.15	4			1363
			Orange	0.66 ± 1.1	2.27	4			20636
			Leftover	0.16 ± 0.1	0.24	4			2181
Cyflufenamid	Fg	F	Total	–	–	–	100 c	100 c	–
			Green	0.03	0.03	1			0.3
			Orange	–	–	–			–
			Leftover	–	–	–			–
		AF	Total	0.011	0.011	1			0.11
			Orange	–	–	–			–
			Leftover	0.011	0.011	1			0.11
Cyprodinil	Fg	F	Total	0.241 ± 0.4	1.1	7	100 b	150 b	11
			Green	0.31 ± 0.51	1.5	8			15
			Orange	0.1 ± 0.13	0.38	7			3.8
			Leftover	0.15 ± 0.28	0.69	7			6.9
		AF	Total	–	–	–			–
			Orange	–	–	–			–
			Leftover	0.043	0.043	1			0.43

(Continued)

TABLE 4 | Continued

Pesticide	Type	Period	Group	Mean ± SD	Maximum	Frequency	LD_{50} contact	LD_{50} oral	PHQ_{max}
Difenoconazole	Fg	F	Total	0.067	0.067	1	100 b	177 b	0.67
			Green	0.16	0.16	1			1.6
			Orange	0.06	0.06	1			0.6
			Leftover	0.062	0.062	1			0.6
		AF	Total	0.1 ± 0.12	0.38	5			3.8
			Orange	0.1 ± 0.15	0.34	4			3.4
			Leftover	0.1 ± 0.12	0.28	4			2.8
Dithianon	Fg	F	Total	0.39 ± 0.45	0.71	2	100 b	25.4 b	28
			Green	–	–	–			–
			Orange	–	–	–			–
			Leftover	–	–	–			–
		AF	Total	–	–	–			–
			Orange	0.05	0.05	2			2
			Leftover	–	–	–			–
Dodina	Fg	F	Total	0.1	0.12	2	100 c	200 c	1.2
			Green	0.32 ± 0.26	0.51	2			5.1
			Orange	0.1	0.12	2			1.2
			Leftover	0.07 ± 0.1	0.16	3			1.6
		AF	Total	0.04	0.08	3			0.8
			Orange	0.026	0.026	1			0.2
			Leftover	0.02	0.02	4			0.2
Etofenprox	Is	F	Total	0.02	0.02	2	0.015 b	0.024 b	1333
			Green	0.11	0.11	2			7333
			Orange	0.016	0.016	1			1066
			Leftover	0.02 ± 0.02	0.046	3			3066
		AF	Total	–	–	–			–
			Orange	–	–	–			–
			Leftover	–	–	–			–
Fenoxycarb	Is	F	Total	–	–	–	100 b	204 b	–
			Green	–	–	–			–
			Orange	–	–	–			–
			Leftover	–	–	–			–
		AF	Total	–	–	–			–
			Orange	–	–	–			–
			Leftover	0.046	0.046	1			0.46
Flonicamid	Is	F	Total	0.02 ± 0.01	0.06	7	100 b	60.5 b	1
			Green	0.03 ± 0.02	0.1	7			1.6
			Orange	0.02	0.03	4			0.5
			Leftover	0.04 ± 0.03	0.08	5			1.3
		AF	Total	–	–	–			–
			Orange	–	–	–			–
			Leftover	–	–	–			–
Fluazinam	Fg	F	Total	0.13 ± 0.1	0.29	7	200 b	100 b	2.9
			Green	0.15 ± 0.11	0.32	6			3.2
			Orange	0.11 ± 0.1	0.23	5			2.3
			Leftover	0.05 ± 0.03	0.08	5			0.8
		AF	Total	0.36 ± 0.17	0.68	7			6.8
			Orange	0.47 ± 0.4	1.1	8			11
			Leftover	0.52 ± 0.3	0.87	7			8.7

(Continued)

TABLE 4 | Continued

Pesticide	Type	Period	Group	Mean ± SD	Maximum	Frequency	LD_{50} contact	LD_{50} oral	PHQ_{max}
Fludioxonil	Fg	F	Total	–	–	–	100 b	100 b	–
			Green	0.018	0.018	1			0.18
			Orange	–	–	–			–
			Leftover	0.021	0.021	1			0.21
		AF	Total	–	–	–			–
			Orange	–	–	–			–
			Leftover	–	–	–			–
Folpet	Fg	F	Total	0.2	0.2	1	200 b	236 b	1
			Green	0.15	0.15	1			0.7
			Orange	–	–	–			–
			Leftover	–	–	–			–
		AF	Total	0.2 ± 0.1	0.32	5			1.6
			Orange	0.43 ± 0.4	1.1	6			5.5
			Leftover	0.3 ± 0.2	0.65	5			3.25
Imidacloprid	Is	F	Total	0.041	0.041	1	0.0439 a	0.0039 a	10512
			Green	–	–	–			–
			Orange	–	–	–			–
			Leftover	–	–	–			–
		AF	Total	0.06 ± 0.05	0.18	7			46153
			Orange	0.068 ± 0.03	0.11	6			28205
			Leftover	0.094 ± 0.1	0.32	7			82051
Indoxacarb	Is	F	Total	–	–	–	0.07 b	0.194 b	–
			Green	–	–	–			–
			Orange	–	–	–			–
			Leftover	–	–	–			–
		AF	Total	–	–	–			–
			Orange	–	–	–			–
			Leftover	0.085	0.085	1			1214
MCPA	He	F	Total	0.029	0.029	1	200 c	200 c	0.1
			Green	–	–	–			–
			Orange	0.04 ± 0.05	0.1	3			0.5
			Leftover	–	–	–			–
		AF	Total	–	–	–			–
			Orange	0.01	0.01	2			0.05
			Leftover	–	–	–			–
Metamitron	He	F	Total	–	–	–	100 c	97.2 c	–
			Green	–	–	–			–
			Orange	–	–	–			–
			Leftover	–	–	–			–
		AF	Total	0.06	0.07	2			0.72
			Orange	0.09 ± 0.1	0.22	3			2.2
			Leftover	0.02 ± 0.01	0.03	2			0.3
Methoxyfenozid	Is	F	Total	0.3 ± 0.05	0.34	2	100 a	100 b	3.4
			Green	0.5 ± 0.3	0.79	2			7.9
			Orange	0.2 ± 0.26	0.45	2			4.5
			Leftover	–	–	–			–
		AF	Total	0.03 ± 0.01	0.042	4			0.4
			Orange	0.03 ± 0.01	0.04	4			0.4
			Leftover	0.047	0.052	3			0.4

(Continued)

TABLE 4 | Continued

Pesticide	Type	Period	Group	Mean ± SD	Maximum	Frequency	LD_{50} contact	LD_{50} oral	PHQ_{max}
Metrafenon	Fg	F	Total	–	–	–	100 b	114 b	–
			Green	–	–	–			–
			Orange	–	–	–			–
			Leftover	–	–	–			–
		AF	Total	–	–	–			–
			Orange	0.021	0.021	1			0.2
			Leftover	–	–	–			–
Myclobutanil	Fg	F	Total	–	–	–	33.9 c	33.9 c	–
			Green	0.03 ± 0.01	0.046	3			1.3
			Orange	–	–	–			–
			Leftover	–	–	–			–
		AF	Total	0.09	0.09	1			2.6
			Orange	–	–	–			–
			Leftover	0.034	0.034	1			1
Paclobutrazol	Fg	F	Total	–	–	–	40 b	2 b	–
			Green	–	–	–			–
			Orange	–	–	–			–
			Leftover	–	–	–			–
		AF	Total	0.014	0.014	1			7
			Orange	–	–	–			–
			Leftover	–	–	–			–
Penconazole	Fg	F	Total	0.12 ± 0.04	0.35	8	30 b	112 b	11.6
			Green	0.2 ± 0.16	0.57	8			19
			Orange	0.2 ± 0.3	0.8	7			26
			Leftover	0.06 ± 0.04	0.15	8			5
		AF	Total	0.05 ± 0.04	0.1	5			3.3
			Orange	0.05 ± 0.02	0.075	5			2.5
			Leftover	0.06 ± 0.04	0.14	5			4.6
Penthiopyrad	Fg	F	Total	0.25 ± 0.47	1.1	5	500 b	500 b	2.2
			Green	0.38 ± 0.6	1.3	4			2.6
			Orange	0.7	0.7	1			1.4
			Leftover	0.26 ± 0.3	0.5	2			1
		AF	Total	0.12 ± 0.17	0.5	7			1
			Orange	0.14 ± 0.14	0.4	6			0.8
			Leftover	0.18 ± 0.26	0.74	7			1.5
Phosmet	Is	F	Total	0.175 ± 0.25	0.47	3	1.06 a	0.15 a	3133
			Green	0.17 ± 0.1	0.24	2			1600
			Orange	0.072	0.072	1			500
			Leftover	0.033	0.033	1			220
		AF	Total	0.48 ± 0.13	0.62	4			4133
			Orange	0.52 ± 0.4	1.14	5			7600
			Leftover	0.09 ± 0.7	2.1	5			14000
Pirimicarb	Is	F	Total	0.036	0.036	1	12.56 a	4 b	9
			Green	0.05	0.05	1			12.5
			Orange	0.036	0.036	1			9
			Leftover	–	–	–			–
		AF	Total	–	–	–			–
			Orange	–	–	–			–
			Leftover	–	–	–			–

(Continued)

TABLE 4 | Continued

Pesticide	Type	Period	Group	Mean ± SD	Maximum	Frequency	LD_{50} contact	LD_{50} oral	PHQ_{max}
Pyraclostrobin	Fg	F	Total	0.053	0.053	1	100 b	73.1 b	0.7
			Green	0.074	0.074	1			1
			Orange	0.015	0.015	1			0.2
			Leftover	0.06 ± 0.03	0.082	2			1.1
		AF	Total	0.011	0.011	1			0.2
			Orange	–	–	–			–
			Leftover	–	–	–			–
Pyrimethanil	Fg	F	Total	0.2 ± 0.2	0.5	4	100 b	100 b	5
			Green	0.37 ± 0.42	0.97	4			9.7
			Orange	0.2 ± 0.2	0.52	4			5.2
			Leftover	0.18 ± 0.12	0.3	3			3
		AF	Total	0.11 ± 0.11	0.23	3			2.3
			Orange	0.07 ± 0.05	0.13	3			1.3
			Leftover	0.16 ± 0.07	0.22	2			2.2
Quinoxyfen	Fg	F	Total	0.05 ± 0.04	0.12	4	100 b	100 b	1.2
			Green	0.1 ± 0.1	0.25	4			2.5
			Orange	0.041	0.041	1			0.4
			Leftover	0.05 ± 0.05	0.11	3			1.1
		AF	Total	0.02	0.02	2			0.2
			Orange	0.13 ± 0.14	0.29	3			2.9
			Leftover	0.02 ± 0.01	0.042	3			0.4
Spirotetramat	Is	F	Total	–	–	–	100 a	107 a	–
			Green	–	–	–			–
			Orange	–	–	–			–
			Leftover	–	–	–			–
		AF	Total	–	–	–			–
			Orange	–	–	–			–
			Leftover	0.01	0.01	1			0.1
Tau-fluvalinate	Is	F	Total	0.13 ± 0.1	0.21	2	12 b	12.6 b	17.5
			Green	0.4 ± 0.72	1.5	4			125
			Orange	0.4	0.4	1			33
			Leftover	0.08	0.08	1			6
		AF	Total	0.01	0.01	1			0.8
			Orange	0.03 ± 0.02	0.05	2			4
			Leftover	0.015	0.015	1			1
Tetraconazole	Fg	F	Total	0.11 ± 0.1	0.18	2	63 b	130 b	2.8
			Green	0.4 ± 0.6	1.1	3			17.5
			Orange	0.017 ± 0.2	0.02	3			0.3
			Leftover	0.02 ± 0.01	0.03	5			0.5
		AF	Total	0.011	0.011	1			0.2
			Orange	–	–	–			–
			Leftover	–	–	–			–
Thiacloprid	Is	F	Total	–	–	–	37.83 a	17.32 b	–
			Green	0.024	0.024	1			1.4
			Orange	0.11	0.11	1			6.3
			Leftover	–	–	–			–
		AF	Total	–	–	–			–
			Orange	–	–	–			–
			Leftover	–	–	–			–

(Continued)

TABLE 4 | Continued

Pesticide	Type	Period	Group	Mean ± SD	Maximum	Frequency	LD_{50} contact	LD_{50} oral	PHQ_{max}
Trifloxystrobin	Fg	F	Total	0.1	0.1	1	200 b	200 b	0.5
			Green	–	–	–			–
			Orange	–	–	–			–
			Leftover	–	–	–			–
		AF	Total	–	–	–			–
			Orange	–	–	–			–
			Leftover	–	–	–			–

Type reports the pesticide type according to Pesticide Properties DataBase (Fg = fungicide; Is = insecticide; He = herbicide). Concentration values are expressed in ppm (mg/Kg). PHQ has been calculated as pesticide residue concentration in ppb/LD50. Letters indicate the sources for LD50 values: (a) US EPA ECOTOX database. (b) EU AGRITOX database. (c) Pesticide Properties DataBase.

TABLE 5 | Number of pesticides detected in pollen samples from different color group, during and after apple blossom, for each location.

Location	Collection	n° insecticides					n° fungicides				
		Total	Green	Orange	Leftover	Mean	Total	Green	Orange	Leftover	Mean
1	F	1	3	1	1		5	6	3	6	
2	F	1	3	2	0		5	4	2	2	
3	F	4	5	3	2		8	9	4	6	
4	F	5	6	6	4		8	9	9	8	
5	F	1	2	1	1		5	9	3	7	
6	F	1	2	1	2		8	6	6	7	
7	F	1	2	1	0		5	5	3	6	
8	F	6	5	6	2		7	4	4	4	
	Average	2,5	3,5	2,6	1,5	2,53	6,4	6,5	4,3	5,75	5,72
	Sum	20	28	21	12		51	52	34	46	
1	AF	2		2	3		3		2	4	
2	AF	4		6	3		5		6	6	
3	AF	5		6	5		8		8	8	
4	AF	3		5	5		8		7	8	
5	AF	2		3	2		5		4	5	
6	AF	2		3	2		5		3	6	
7	AF	0		1	0		0		6	0	
8	AF	4		6	5		9		8	8	
	Average	2,75	–	4	3,125	3,29	5,375		5,5	5,625	5,50
	Sum	22	–	32	25		43		44	45	
	Mean					2,91					5,61

Values indicate the number of insecticide or fungicide residues found in pollen samples. The average of each color group is reported on the "average" row. The sum of the number of residues of each color group is reported on the "sum" row. The mean of the number of all the insecticide and fungicide residues is reported on the "mean" label.

found at the maximum concentration of 0.2 ppm (*orange* pollen) and 0.041 ppm (*total* pollen), respectively.

Pollen Hazard Quotient

In the attempt to evaluate the toxicological effect of the residues found on pollen to adult honeybees, we calculated the PHQ for each substance found in a sample and then we summed them together in tPHQ (Stoner and Eitzer, 2013; Böhme et al., 2018). The PHQ value depends on the residues concentration and the substance LD_{50}. We found the highest values of PHQ in insecticide residues, where Chlorpyrifos-ethyl reached a PHQ of 160,000 in an AF *leftover* sample (**Table 4**). As 1,000 PHQ accounts for 1% of the LD50 consumed by a nurse bee in a day, this value of Chlorpyrifos-ethyl means a consumption of 160% of the LD50 in a day. Other high PHQ resulted from Imidacloprid (28,205), Chlorpyrifos-methyl (20,636), Phosmet (7,600) and Chlorpyrifos-ethyl again (150,000) all in *orange* AF samples (**Table 4**). The highest Imidacloprid PHQ was 82,051 from a *leftover* pollen sample as well as the highest Phosmet PHQ (14,000). Fungicides usually have higher LD_{50}, thus lower PHQs. We found Captan having the higher PHQ of 31 (*total* pollen, F collection), followed by Dithianon (27.95 in *total* pollen, F

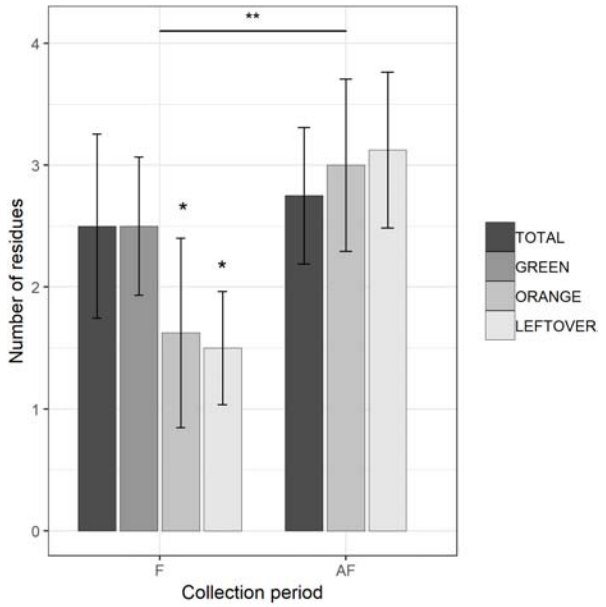

FIGURE 2 | Number of insecticide residues detected in each sample, during (F) and 2 weeks after the end of apple blossom (AF). Asterisks show statistical significance (*$p < 0.05$, **$p < 0.01$). Error bars report standard error of the mean. Pollen color groups are reported in scale of grays.

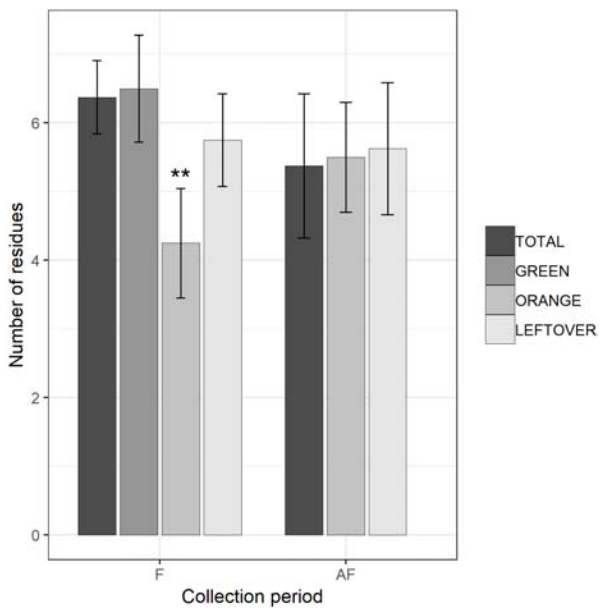

FIGURE 3 | Number of fungicide residues detected in each sample, during (F) and 2 weeks after the end of apple blossom (AF). Asterisks show statistical significance (**$p < 0.01$). Error bars report standard error of the mean. Pollen color groups are reported in scale of grays.

collection) and Penconazole (26.67 in *orange* pollen, F collection). Overall, the mean PHQ of fungicides (2,55 ± 7.02) was much lower than the PHQ of insecticides (6,080 ± 19,030). The PHQ of the herbicides was negligible, having a mean of 0.4 ± 0.57, with Metamitron reaching a maximum value of 2.26. The insecticide residues accounted for the 74 ± 40% of the tPHQ in the samples. In 69% of the samples, the insecticide contribution was higher than 90%.

The tPHQs varied according to the collection period and pollen group (**Figure 4**). In the pollen collected during the apple blossom, the mean tPHQs resulted in 2,354 ± 5,455 for *total*, 498 ± 1,013 for *orange*, 509 ± 703 for *green* and 651 ± 1,089 for *leftover* pollen samples. The values significantly increased in the AF collection (lmer, $t = -6.446$, $p < 0.001$), where the *total* pollen scored 39,525 ± 38,244, the *orange* pollen 42,787 ± 52,824 and the *leftover* pollen 61,082 ± 67,241 (**Figure 4**). Due to the high data variability, it was not possible to detect statistical differences between pollen groups, although consistent variations were found. However, pollen color groups collected from the same apiary showed remarkable differences in terms of tPHQ (**Figure 5**).

Since the purpose of the experiment was to detect the pesticides contribution of different pollen groups, we did not test the pollen toxicological effects, nor did we monitor the colonies health. However, none of the beehives involved in the experiment collapsed by the end of the trial.

DISCUSSION

This study provides for the first time insight into the contribution of plant specific residues in bee-collected pollen. The study was performed in a context of large apple orchard extensions in Trentino-South Tyrol (Italy). Our results clearly showed the source of pesticide contaminations according to the separation of pollen loads by their color, then assessing the number of residues and their potential toxicity. Here we combined two well-known practices, palynology and multi-residual analysis, with the purpose to obtain a more detailed picture of the agricultural landscape effect on pesticide contamination. The color of the pollen loads successfully allowed to separate the main plant species pollen during and after apple blossom, apple and dandelion, from the pollen of the surrounding plants. Although the pollen analysis revealed that not all the pollen of a giving color group belonged to a single species, this single species represented the main fraction, in particular in the *orange* group, which was almost totally composed by dandelion (99% during F collection, **Table 2**). *Green* pollen had a lower amount of apple pollen, but still representing 61%. The remaining received contributions by other green pollen species, such as *Salix* spp., which color ranges from yellowish green to full green (Kirk, 2006).

It was surprising that *Salix* spp. (42.8%) was the most abundant pollen during the F collection, even if the hives were placed in the midst of full blooming apple orchards. Indeed, dandelion and apple were only 21.3 and 18.3% of the collected pollen loads. This finding not only confirmed the studies of Free (1996, 1968), addressing dandelion as a competitor of apple flowers, but also showed that other plants from the surroundings (e.g., willows) might exhibit an even stronger appeal. Mitchell et al. (2009) suggested an effect of the nectar and pollen availability on flowers due to temperature, and the constancy of

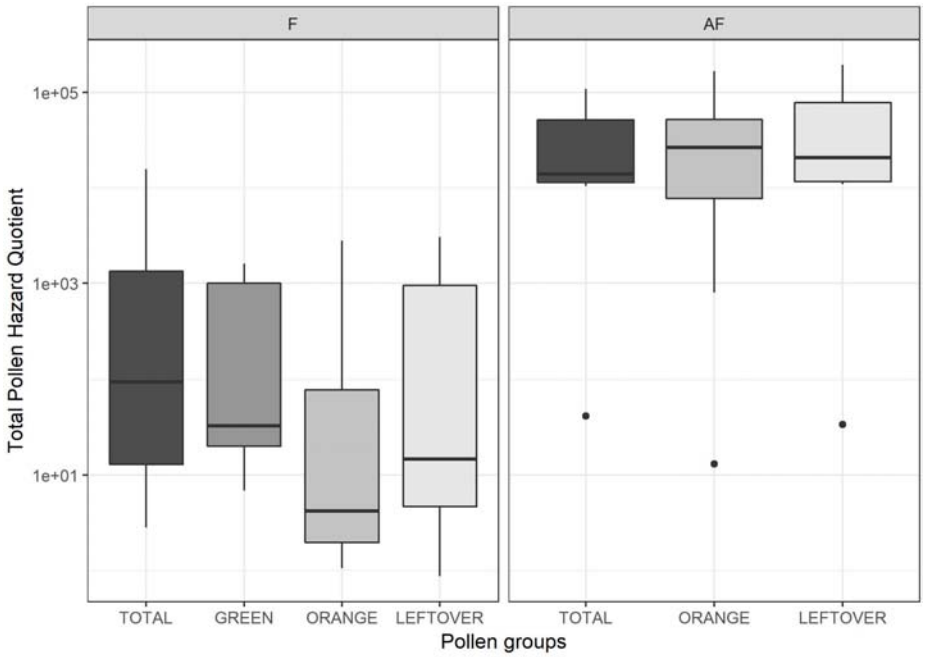

FIGURE 4 | Total Pollen Hazard Quotient (PHQ) of the pesticide residues detected in each sample, during (on the left frame, F) and 2 weeks after apple blossom (on the right frame, AF). Values are reported on a logarithmic scale. Dots indicate outliers.

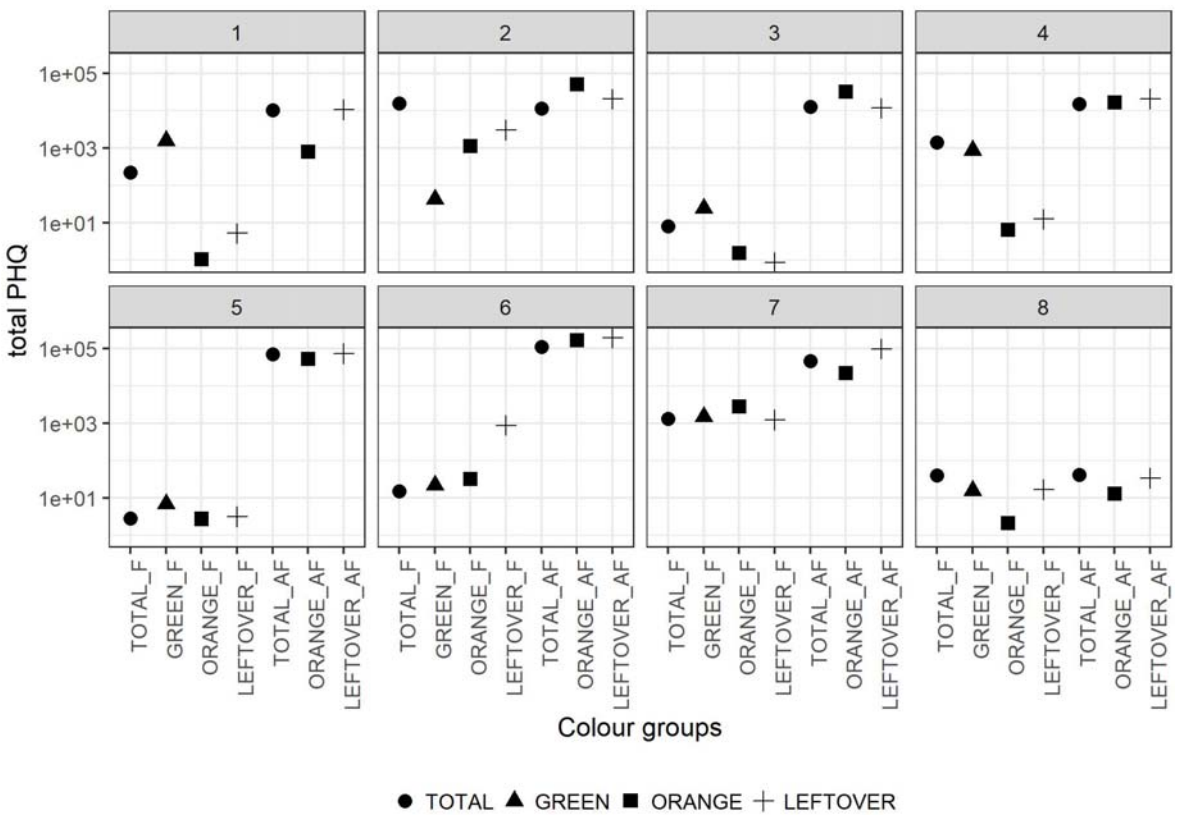

FIGURE 5 | Total PHQ of the pollen color groups in the eight locations. Dots shapes refer to the pollen color group. The values in y-axis are reported in logarithmic scale. In the x-axis the labels combine the pollen group and the collection period (F = apple flowering, AF = after apple flowering).

bees on one flower species. Similar results were found when hives were placed in the center of a large apple commercial production providing only 25% of apple pollen while willow reached almost 60% (Olsen et al., 1979).

While the main two components during the F collection were the *green* and the *orange* (79.6%), the lack of apple flowers in the AF collection led to increased variability of the other pollens. The *orange* component dropped from 30.5 to 18%, and other plant species from the surrounding environment became the most abundant. These plants, such as *Fraxinus ornus*, *Gleditisia* sp., *Parthenocissus* sp., *Quercus* sp., *Trachycarpus* sp., are not associated with apple orchards and showed that bees went for other food sources out of the orchards once the blossom was over. In two locations (1 and 7), the *orange* pollen was dominant, this likely due to still a large amount of dandelion in the apple orchards at the time of collection. According to scientific literature in melissopalinology (Persano and Oddo Ricciardelli D'Albore, 1989) the Asteraceae T form includes echinolophate pollen grains belonging to *Taraxacum* and other genera from the Asteraceae family, which cannot be distinguished easily by light microscopy. However, from our field observations we deduced that the Asteraceae T form corresponded mainly to the genus *Taraxacum* as it was in full flowering in immediate vicinity of the bee hives during the sampling period. Furthermore, *Taraxacum* is considered a typical element of the undergrowth of apple orchards.

We detected a total of 36 substances, a lower amount than found in other studies (i.e., Mullin et al., 2010; Böhme et al., 2018). This is probably due to the lower agricultural diversity of our experimental area, where only apple trees are cultivated. Yet, we found a number of molecules higher than Stoner and Eitzer (2013) (18 molecules), Chauzat et al. (2006) (19 molecules) and close to Colwell et al. (2017) (39 molecules), whom collected pollen from more complex agricultural landscapes. The pollen from apple monoculture reached a range of pesticides comparable to that of a study comprising three different crops (Colwell et al., 2017). In our study, we did not find any pollen sample free of pesticide. As the apiaries were inside apple orchards, the contamination was expected. This finding agrees with the study of Böhme et al. (2018), which found residues in all the pollen samples from the "fruit" area (30% surface occupied by permanent vine, pome, stone, and soft fruits).

The number of fungicide residues per sample did not vary between the collections, as these substances were allowed in apple orchards also during flowering. Because of the use of most insecticides was forbidden during apple blossom, the higher number and concentration of insecticide residues found in the second collection resulted likely from the treatments applied after the end of the apple blossom. During the F collection, the *green* pollen showed a number of residues very close to that of *total* pollen, while the *orange* had a lower occurrence of both fungicides and insecticides. Nevertheless, residual concentrations at the F collection were lower than the AF collection. It is likely that these amounts were remains from the pre-floral treatments and degraded from their initial amount. In a study on residues on pollen loads (Škerl et al., 2009) reported that residues of the insecticide Diazinon reduced from 1.98 ppm 1 day after application to 0.03 ppm 10 days after (application of 15 L/ha of "Oleodiazinon"). In addition, Thiacloprid shrank from 0.09 ppm to undetectable in 6 days after treatment (application of 0.2 L/ha of "Calypso SC480"). Imidacloprid half-life was 8.2 days after foliar application (Juraske et al., 2009), and 32 days according to Vogeler et al. (1992) (but not allowed before apple blossom). Moreover, the pesticide molecules might have broken in their metabolites during the process of degradation, and then being undetected by the analyses.

The presence of pesticides also varied between pollen groups. Some of the molecules found in pollen loads from the first collection were not allowed to be sprayed during apple blossom (Imidacloprid, Chlorpyrifos-methyl, Phosmet, Etofenprox, and Flonicamid), as stated by the local guidelines (AGRIOS, 2017). The guidelines provide rules for the allowed chemicals, the number of use and the prohibition periods. However, the farmers are free to choose the treatments within this range. It was not possible then, to know exactly what pesticides were applied in the surroundings of the study sites.

Chlorpyrifos-methyl and Phosmet were found only in few locations, Etofenprox was detected at the same concentrations in two locations both in *green* and *total* pollen but Flonicamid resulted in seven locations both in *green* and *total* samples and four times in *orange* samples. We detected Imidacloprid in a *total* pollen sample during flowering, but not in the *green* pollen from the same location. As Imidacloprid was allowed only after apple blossom, this residue might come from other sources than apple flowers.

Whether these residuals belonged to treatments prior to the prohibition period, we cannot know. On the other hand, we detected only few samples with bee-friendly insecticides (Pirimicarb, Tau-fluvalinate, and Thiacloprid), allowed by the guidelines. Surprisingly, we also found residues of Chlorpyrifos-ethyl in one location during apple blossom and in two locations at the AF collection, even if the use of this pesticide was forbidden starting from spring 2017 (AGRIOS, 2017).

Application of PHQs allowed to summarize the detailed information provided by the frequency and the concentration of the residues detected in the view of honeybee toxicity.

Hazard Quotient (HQ) is a concept adopted by EU guidelines (Campbell et al., 2000) for the evaluation of side effects of chemicals on honeybees and used for the estimation of risk by pesticide exposure to honeybees (Rortais et al., 2005; Halm et al., 2006), then applied on pollen by Stoner and Eitzer (2013). The sum of the contribution of each residue provides the total PHQ. We found differences in tPHQ values between the two collection period. The pollen collected after the apple blossom had a much higher toxicological risk to honeybees, and this was indeed expected as the main treatments against aphids occurred on those weeks. However, due to the variability of the data, it was not possible to state any effect of the pollen color group on the tPHQ. While the values varied among color group in the same location, no common trends arose. Although not linked with pollen groups, this study presents, however, particularly high tPHQ values, with the majority of samples that easily exceed 40,000 after the apple blossom. Compared to previous studies, only Stoner and Eitzer (2013) had some values higher than 40,000, while

in McArt et al. (2017) only Indoxacarb and Thiamethoxam had mean PHQ above 4,000. A maximum PHQ value exceeding 500 was reported only four times in Böhme et al. (2018).

Even ignoring more complex mechanisms, such as pesticide synergisms and antagonisms, the current PHQs might be of a great risk to honeybee colonies. A PHQ of 40,000 means, indeed, an assumption of 40% the LD50 in a day. At the end of this study, however, we have not been reported of any colony loss by the beekeepers. One possible answer to this survival is the social behavior of the honeybee, which, acting as a superorganism, allows them a resilience attitude to tolerate environmental stressors (Straub et al., 2015). Moreover, though the tPHQ concept comes in handy to risk estimation, it can be strongly affected by minimal variations of very toxic residuals. For instance, imidacloprid oral LD50 is 0,0039 μg/bee (US EPA ECOTOX, 2018). The highest residue we found was 180 ppb, which lead to a PHQ of 46153, 99.3% of the tPHQ of that pollen sample. Few molecules (chlorpyrifos-ethyl, chlorpyrifos-methyl, imidacloprid) influence most of the value, and minimal variation drastically change the output.

Dandelion pollen remained abundant during apple blossom, partially reducing after it but still representing a major fraction of the collection. *Taraxacum* spp. bloom usually starts few weeks before apple bloom and last through the summer (Cockfield et al., 2007). It reaches the peak bloom right before the apple full blossom, becoming an important competitor for pollinators (Free, 1968) thus decreasing but maintaining a moderate flowering until autumn. In the year of the experiment, a master thesis work (Ungerer, 2017) reported dandelion to bloom until the end of May in three locations of this study region. Dandelion is closely associated with apple orchards and very abundant on beneath (Olsen et al., 1979; Cockfield and Beers, 2008), also in the experimental locations (Ungerer, 2017, authors observation). In the experimental locations, where the absence of other crops than apple enclosed the most of the dandelion in apple orchards, this species was a reliable proxy of the pesticide treatments in orchards after the end of apple bloom. We cannot exclude a dandelion contribution from spots outside apple plantations (road edges, garden patches or ditch sides), but the overwhelming orchards surface was likely to contribute the most. It should be noticed that the local guidelines suggested mowing the orchard floor if flowers were present at the time of pesticide treatment. Regulation compliance may explain the very low amount of *orange* pollen found in few locations during the AF collection (0.5, 1.16, and 3.7%), but Ungerer (2017) also reported an average orchard floor height of 28.8 cm during the same days of the AF collection, and dandelion flowers in all the three sample sites.

While ground floor mowing may prevent bees from direct contamination during spraying, soil and leaves can absorb systemic insecticides and translocate them to nectar and pollen (Blacquiere et al., 2012) of the ground cover plants. As a result, plant with a constant flowering such as dandelion may continuously bring contaminated flowers throughout the season. The consistent amount of insecticide residues detected on the AF *orange* samples might be explained either by the lack of mowing before treatments, or the contamination of dandelion plants after flower cut, and the subsequent appearance of new flowers with pesticide residues. The latest hypothesis is supported by the high tPHQ of the *orange* portions, in spite of their low abundance in the collection. High residuals of imidacloprid were found in *orange* samples, strongly affecting their tPHQ.

After the removal of the *green* and *orange* pollen, the *leftover* represented mostly plants not associated with the apple orchard. The study of Ungerer (2017) also reported the herbaceous plants occurring in the orchard floors during the season. Combining these data with the palynological analysis of the collected pollen loads allowed understanding how much they contribute to the pollen loads. During the apple blossom, dandelion was a major fraction of the honeybee-collected pollen loads, but all the other species contribute for only 0.41%. These species (*Aegopodium podagraria* L., *Cardamine hirsuta* L., *Lamium album* L., *Ranunculus* spp., *Stellaria media* L., *Veronica persica* Poir.) are indeed reported as poorly or not attractive to honeybees (Contessi, 2016). After the apple blossom, their contribution remained very low (1.1%), dandelion was still an important portion, while most of the pollen came from ornamental or wild trees in the surrounding urban and forest area. The number of residues and the tPHQ of the *leftover* pollen groups did not differ from the *green* and the *orange* pollen groups, suggesting a pesticide contamination of the surrounding environment as high as in the apple orchards. The reasons beyond these findings may lay on pollen trans-contamination or pesticide drift. The first implies a theoretical transfer of residues between pollen loads while stored before color separation, leading to an averaging of the residues concentrations. This mechanism seemed however unlikely, as the pollen was deep-frozen after the collection and separated while still cold, remaining at room temperature only in the pollen trap drawer during the day of collection. Moreover, pollen groups from the same locations displayed consistent differences in concentrations and tPHQ values. Pesticides can reach the area outside crops by drift during and after spraying and by volatilization from soil and plant surface (Himel et al., 1990), generating pesticide-enriched rainfalls (Jensen et al., 2007), and atmospheric dust deposition (Wheatley, 1973). Spray drift is a mechanism of pesticide droplets moving through air or water (Felsot et al., 2010), and a constant concern of pesticide use (Damalas, 2015). The droplets spread according to droplet size and weather conditions, and the drift can reach a long distance when adjuvants reduce evaporation of small droplets (Bretthauer, 2011). As a result, airborne pesticide residues transport over distances of several miles may be responsible for adverse effects on non-target species (Plimmer, 1990), and the residues we found on plant pollen outside the apple orchards confirm it. Whether we do not know the relative distance of these plants from the orchards, some of them are strictly forest species (*Fraxinus ornus* L., *Quercus* spp., *Pinus* spp., *Robinia pseudoacacia* L.), most likely occurring on the fringes of the side valley woods. Their contribution to the pollen composition exceed 45% in some of the locations (2, 5, and 6) during the second collection and the tPHQ of their pollen had values equal to the *orange* or *total* ones, suggesting those areas being rich in pesticide residues as much as apple orchards.

At the best of our knowledge, it was not possible to state if the pollen from any color group posed a higher risk to the honeybees than another, nor we found any group less toxic. Each location had its own intrinsic differences between pollen groups, and the pollen collected after the flowering, when treatments were allowed again, was richer in residues and potentially more harmful than the pollen collected during the flowering. However, the variations between pollen groups in the same location clearly showed that it is actually possible to recognize the residue contamination by different pollen sources. This study also provides evidences of pesticide contamination in the surrounding environment, urban or forest, as high as in agricultural fields. Future studies that consider this approach should increase the number of locations. Moreover, the method itself can be improved, enhancing the specificity of pollen groups.

DATA AVAILABILITY

The raw data supporting the conclusions of this manuscript will be made available by the authors, without undue reservation, to any qualified researcher.

AUTHOR CONTRIBUTIONS

SA and RF conceived and designed the study. LB managed the sample collections and part of the palynology analyses. EB and MR performed the palynology analyses on the total pollen samples. LD performed the chemical multi-residual analyses. RF performed the data collection and statistical analyses, and prepared the draft of the manuscript. SA approved the final version of the manuscript.

FUNDING

This study was partially funded by the project TN2214 STEFANIE financed by the Autonomous Province of Bolzano (Italy).

ACKNOWLEDGMENTS

We are grateful to the beekeepers who contributed to this research, and Dr. Salvatore Barone, Mr. Andreas Platzer, and the Südtiroler Imkerbund for the support in the study completion and the data reading.

REFERENCES

AGRIOS (2017). *Agrios Guidelines*. Availabele at: http://www.provincia.bz.it/agricoltura-foreste/agricoltura/downloads/Direttive_AGRIOS_2017.pdf (accessed March 01, 2019).

AGRITOX, (2018). *Agence Nationale de Sécurité Sanitaire Agritox Database 2018*. Available at: http://www.agritox.anses.fr/guides/guide-agritox-anglais.html (accessed March 01, 2019).

Anastassiades, M., Lehotay, S. J., Štajnbaher, D., and Schenck, F. J. (2003). Fast and easy multiresidue method employing acetonitrile extraction/partitioning and "dispersive solid-phase extraction" for the determination of pesticide residues in produce. *J. AOAC Int.* 86, 412–431.

Bates, D., Mächler, M., Bolker, B., and Walker, S. (2015). Fitting linear mixed-effects models using lme4. *J. Stat. Softw.* 67, 1–48.

Blacquiere, T., Smagghe, G., Van Gestel, C. A., and Mommaerts, V. (2012). Neonicotinoids in bees: a review on concentrations, side-effects and risk assessment. *Ecotoxicology* 21, 973–992. doi: 10.1007/s10646-012-0863-x

Böhme, F., Bischoff, G., Zebitz, C. P., Rosenkranz, P., and Wallner, K. (2018). Pesticide residue survey of pollen loads collected by honeybees (*Apis mellifera*) in daily intervals at three agricultural sites in South Germany. *PLoS One* 13:e0199995. doi: 10.1371/journal.pone.0199995

Botías, C., David, A., Horwood, J., Abdul-Sada, A., Nicholls, E., Hill, E., et al. (2015). Neonicotinoid residues in wildflowers, a potential route of chronic exposure for bees. *Environ. Sci. Technol.* 49, 12731–12740. doi: 10.1021/acs.est.5b03459

Botías, C., David, A., Hill, E. M., and Goulson, D. (2016). Contamination of wild plants near neonicotinoid seed-treated crops, and implications for non-target insects. *Sci. Total Environ.* 566, 269–278. doi: 10.1016/j.scitotenv.2016.05.065

Bretthauer, S. (2011). Spray drift management. *Outlooks Pest Manag.* 22, 262–267. doi: 10.1564/22dec05

Bucher, E. (2004). *Das Pollenbild der Südtiroler Honige*. Bolzano: Landesagentur für Umwelt und Arbeitsschutz, Biologisches Labor.

Calderone, N. W. (2012). Insect pollinated crops, insect pollinators and US agriculture: trend analysis of aggregate data for the period 1992–2009. *PLoS One* 7:e37235. doi: 10.1371/journal.pone.0037235

Campbell, P. J., Brown, K. C., Harrison, E. G., Bakker, F., Barrett, K. L., Candolfi, M. P., et al. (2000). A hazard quotient approach for assessing the risk to non-target arthropods from. *J. Pest Sci.* 73:117.

Chauzat, M. P., Faucon, J. P., Martel, A. C., Lachaize, J., Cougoule, N., and Aubert, M. (2006). A survey of pesticide residues in pollen loads collected by honey bees in France. *J. Econ. Entomol.* 99, 253–262. doi: 10.1603/0022-0493-99.2.253

Cockfield, S. D., and Beers, E. H. (2008). Management of dandelion to supplement control of western flower thrips (Thysanoptera: Thripidae) in apple orchards. *J. Entomol. Soc. Br. Columbia* 105, 89–96.

Cockfield, S. D., Beers, E. H., and Zack, R. S. (2007). Phenology of western flower thrips Frankliniella occidentalis (Pergande) (Thysanoptera: Thripidae) on plant species in and near apple orchards in Washington State. *J. Entomol. Soc. Br. Columbia* 104, 35–44.

Colwell, M. J., Williams, G. R., Evans, R. C., and Shutler, D. (2017). Honey bee-collected pollen in agro-ecosystems reveals diet diversity, diet quality, and pesticide exposure. *Ecol. Evol.* 7, 7243–7253. doi: 10.1002/ece3.3178

Contessi, A. (2016). *Le Api: Biologia, Allevamento, Prodotti*, 4th Edn. Milano, IT: Edagricole.

Damalas, C. A. (2015). Pesticide drift: seeking reliable environmental indicators of exposure assessment. In *Environmental Indicators*, eds *R. Armon., O. Hänninen*. Dordrecht, NL: Springer.

Felsot, A. S., Unsworth, J. B., Linders, J. B., Roberts, G., Rautman, D., Harris, C., et al. (2010). Agrochemical spray drift; assessment and mitigation—a review. *J. Environ. Sci. Health B* 46, 1–23. doi: 10.1080/03601234.2010.515161

Free, J. B. (1966). "The foraging behaviour of bees and its effect on the isolation and speciation of plants," in *Reproductive Biology and Taxonomy of Vascular Plants*, ed. J. G. Hawkes (Oxford: Pergamon Press), 76–92.

Free, J. B. (1968). Dandelion as a competitor to fruit trees for bee visits. *J. Appl. Ecol.* 5, 169–178.

Garibaldi, L. A., Steffan-Dewenter, I., Winfree, R., Aizen, M. A., Bommarco, R., Cunningham, S. A., et al. (2013). Wild pollinators enhance fruit set of crops regardless of honey bee abundance. *Science* 339, 1608–1611. doi: 10.1126/science.1230200

Garratt, M. P., Breeze, T. D., Jenner, N., Polce, C., Biesmeijer, J. C., and Potts, S. G. (2014). Avoiding a bad apple: insect pollination enhances fruit quality and economic value. *Agric. Ecosyst. Environ.* 184, 34–40. doi: 10.1016/j.agee.2013.10.032

Genersch, E., Von Der Ohe, W., Kaatz, H., Schroeder, A., Otten, C., Büchler, R., et al. (2010). The German bee monitoring project: a long term study to understand periodically high winter losses of honey bee colonies. *Apidologie* 41, 332–352. doi: 10.1051/apido/2010014

Halm, M. P., Rortais, A., Arnold, G., Taséi, J. N., and Rault, S. (2006). New risk assessment approach for systemic insecticides: the case of honey bees and imidacloprid (Gaucho). *Environ. Sci. Tech.* 40, 2448–2454. doi: 10.1021/es051392i

Himel, C. M., Loats, H., and Bailey, G. W. (1990). "Pesticide sources to the soil and principles of spray physics," in *Pesticides in the Soil Environment: Processes, Impact, and Modeling*, ed. H. H. Cheng, (Madison, WI: Soil Science Society of America).

Jensen, A. R., Spliid, N. H., and Svensmark, B. (2007). Determination of volatilization (dissipation) and secondary deposition of pesticides in a field study using passive dosimeters. *Int. J. Environ. Anal. Chem.* 87, 913–926. doi: 10.1080/03067310701455955

Juraske, R., Castells, F., Vijay, A., Muñoz, P., and Antón, A. (2009). Uptake and persistence of pesticides in plants: measurements and model estimates for imidacloprid after foliar and soil application. *J. Hazard. Mater.* 165, 683–689. doi: 10.1016/j.jhazmat.2008.10.043

Kasiotis, K. M., Anagnostopoulos, C., Anastasiadou, P., and Machera, K. (2014). Pesticide residues in honeybees, honey and bee pollen by LC–MS/MS screening: reported death incidents in honeybees. *Science of the Total Environment* 485, 633–642. doi: 10.1016/j.scitotenv.2014.03.042

Keller, I., Fluri, P., and Imdorf, A. (2005). Pollen nutrition and colony development in honey bees: part 1. *Bee World* 86, 3–10. doi: 10.1080/0005772x.2005.11099641

Kirk, W. (2006). *A Colour Guide to Pollen Loads of the Honey Bee*, 2nd Edn. Congresbur: International Bee Research Association.

Lambert, O., Piroux, M., Puyo, S., Thorin, C., Larhantec, M., Delbac, F., et al. (2012). Bees, honey and pollen as sentinels for lead environmental contamination. *Environ. Pollut.* 170, 254–259. doi: 10.1016/j.envpol.2012.07.012

Lentola, A., David, A., Abdul-Sada, A., Tapparo, A., Goulson, D., and Hill, E. M. (2017). Ornamental plants on sale to the public are a significant source of pesticide residues with implications for the health of pollinating insects. *Environ. Pollut.* 228, 297–304. doi: 10.1016/j.envpol.2017.03.084

Long, E. Y., and Krupke, C. H. (2016). Non-cultivated plants present a season-long route of pesticide exposure for honey bees. *Nat. Commun.* 7:11629. doi: 10.1038/ncomms11629

Longley, M., and Sotherton, N. W. (1997). Measurements of pesticide spray drift deposition into field boundaries and hedgerows: 2. autumn applications. *Environ. Toxicol. Chem.* 16, 173–178. doi: 10.1002/etc.5620160211

McArt, S. H., Fersch, A. A., Milano, N. J., Truitt, L. L., and Böröczky, K. (2017). High pesticide risk to honey bees despite low focal crop pollen collection during pollination of a mass blooming crop. *Sci. Rep.* 7:46554. doi: 10.1038/srep46554

McLellan, A. R. (1977). Honeybee colony weight as an index of honey production and nectar flow: a critical evaluation. *J. Appl. Ecol.* 14, 401–408.

Mitchell, R. J., Irwin, R. E., Flanagan, R. J., and Karron, J. D. (2009). Ecology and evolution of plant–pollinator interactions. *Ann. Bot.* 103, 1355–1363. doi: 10.1093/aob/mcp122

Mullin, C. A., Frazier, M., Frazier, J. L., Ashcraft, S., Simonds, R., and Pettis, J. S. (2010). High levels of miticides and agrochemicals in North American apiaries: implications for honey bee health. *PLoS One* 5:e9754. doi: 10.1371/journal.pone.0009754

Olsen, L. G., Hoopingarner, R., and Martin, E. C. (1979). Pollen preferences of honeybees sited on four cultivated crops. *J. Apicult. Res.* 18, 196–200. doi: 10.1080/00218839.1979.11099967

Persano Oddo, L., and Ricciardelli D'Albore, G. (1989). Nomenclatura melissopalinologica. *Apicoltura* 5, 63–72.

Plimmer, J. R. (1990). Pesticide loss to the atmosphere. *Am. J. Ind. Med.* 18, 461–466. doi: 10.1002/ajim.4700180418

Porrini, C., Ghini, S., Girotti, S., Sabatini, A. G., Gattavecchia, E., and Celli, G. (2002). "Use of honey bees as bioindicators of environmental pollution in Italy," in *Honey Bees: Estimating the Environmental Impact of Chemicals*, eds J. Devillers, and M. H. Pham-Delegue, (London: CRC Press).

Potts, S. G., Imperatriz-Fonseca, V., Ngo, H. T., Aizen, M. A., Biesmeijer, J. C., Breeze, T. D., et al. (2016). Safeguarding pollinators and their values to human well-being. *Nature* 540:220. doi: 10.1038/nature20588

Ppdb. (2018). *Pesticide Properties DataBase, Univesity of Hertfordshire, 2018*. Available at: http://sitem.herts.ac.uk/aeru/ppdb/en/atoz.htm#A (accessed March 01, 2019).

R Core Team, (2018). *R: A Language and Environment for Statistical Computing*. Vienna: R Foundation for Statistical Computing.

Rortais, A., Arnold, G., Halm, M. P., and Touffet-Briens, F. (2005). Modes of honeybees exposure to systemic insecticides: estimated amounts of contaminated pollen and nectar consumed by different categories of bees. *Apidologie* 36, 71–83. doi: 10.1051/apido:2004071

Sanchez-Bayo, F., and Goka, K. (2014). Pesticide residues and bees–a risk assessment. *PLoS One* 9:e94482. doi: 10.1371/journal.pone.0094482

Škerl, M. I. S., Bolta, ŠV., Èesnik, H. B., and Gregorc, A. (2009). Residues of pesticides in honeybee (*Apis mellifera carnica*) bee bread and in pollen loads from treated apple orchards. *Bull. Environ. Contam. Toxicol.* 83, 374–377. doi: 10.1007/s00128-009-9762-0

Stoner, K. A., and Eitzer, B. D. (2013). Using a hazard quotient to evaluate pesticide residues detected in pollen trapped from honey bees (*Apis mellifera*) in Connecticut. *PLoS One* 8:e77550. doi: 10.1371/journal.pone.0077550

Straub, L., Williams, G. R., Pettis, J., Fries, I., and Neumann, P. (2015). Superorganism resilience: eusociality and susceptibility of ecosystem service providing insects to stressors. *Curr. Opin. Insect Sci.* 12, 109–112. doi: 10.1016/j.cois.2015.10.010

Sur, R., and Stork, A. (2003). Uptake, translocation and metabolism of imidacloprid in plants. *Bull. Insectol.* 56, 35–40.

Tasser, E., Ruffini, F. V., and Tappeiner, U. (2009). An integrative approach for analysing landscape dynamics in diverse cultivated and natural mountain areas. *Landsc. Ecol.* 24, 611–628. doi: 10.1007/s10980-009-9337-9

Ungerer, V. (2017). *Vegetationskundliche Erhebungen des Blühenden Unterwuchses in Südtirols Apfelanlagen und dessen Bedeutung für die Honigbiene*. Dissertation/master's thesis Freising: Hochschule Weihenstephan-Triesdorf - University of Applied Sciences.

US EPA ECOTOX (2018). *United States Environmental Protection Agency Ecotoxicology Database 2018*. Available at: https://cfpub.epa.gov/ecotox/ (accessed March 01, 2019).

Vogeler, K., Clark, T., and Brauner, A. (1992). *Metabolism of [methylene-14C]-imidacloprid (NTN 33893) in Apples*. Report No. PF3676 (internal report). Leverkusen: Bayer AG.

Wheatley, G. A. (1973). "Pesticides in the atmosphere," in *Environmental Pollution by Pesticides*, ed. C. A. Edwards, (Boston, MA: Springer).

Wickham, H. (2016). *ggplot2: Elegant Graphics for Data Analysis*. New York, NY: Springer-Verlag.

Conflict of Interest Statement: The authors declare that the research was conducted in the absence of any commercial or financial relationships that could be construed as a potential conflict of interest.

frontiers in Physiology

ORIGINAL RESEARCH
published: 19 November 2019
doi: 10.3389/fphys.2019.01425

Relationship Between Performance of Carob Moth, *Ectomyelois ceratoniae* Zeller (Lepidoptera: Pyralidae) and Phytochemical Metabolites in Various Pomegranate Cultivars

Zahra Abedi[1], Ali Golizadeh[1], Mahmoud Soufbaf[2], Mahdi Hassanpour[1], Ali Jafari-Nodoushan[3] and Hamid-Reza Akhavan[4]*

[1] Department of Plant Protection, Faculty of Agriculture and Natural Resources, University of Mohaghegh Ardabili, Ardabil, Iran, [2] Department of Plant Protection, Nuclear Agriculture Research School, Nuclear Science and Technology Research Institute, Karaj, Iran, [3] Agriculture and Natural Resources Research Center of Yazd, Yazd, Iran, [4] Department of Food Science and Technology, Faculty of Agriculture, Shahid Bahonar University of Kerman, Kerman, Iran

OPEN ACCESS

Edited by:
Michel Cusson, Natural Resources Canada, Canada

Reviewed by:
Jose Eduardo Serrão, Universidade Federal de Viçosa, Brazil
Habib Abbasipour, Shahed University, Iran

***Correspondence:**
Ali Golizadeh
golizadeh@uma.ac.ir

Specialty section:
This article was submitted to Invertebrate Physiology, a section of the journal Frontiers in Physiology

Received: *20 January 2019*
Accepted: *04 November 2019*
Published: *19 November 2019*

Citation:
Abedi Z, Golizadeh A, Soufbaf M, Hassanpour M, Jafari-Nodoushan A and Akhavan H-R (2019) Relationship Between Performance of Carob Moth, Ectomyelois ceratoniae Zeller (Lepidoptera: Pyralidae) and Phytochemical Metabolites in Various Pomegranate Cultivars. Front. Physiol. 10:1425. doi: 10.3389/fphys.2019.01425

The carob moth, *Ectomyelois ceratoniae* Zeller (Lepidoptera: Pyralidae), is the main pest of pomegranate, *Punica granatum* L., in Iran and many parts of the world. In this study, the effects of 11 commercial cultivars of pomegranate (Aban-Mahi, Esfahani-Daneghermez, Gabri, Gorche-Tafti, Malase-Danesyah, Malase-Yazdi, Shahvare-Daneghermez, Shahvare-Danesefid, Tabolarze-Mehrmahi, Tafti, and Toghe-Gardan) were evaluated on life history variables, nutritional performance, and energy reserves of *E. ceratoniae* under the following laboratory conditions: 30 ± 1°C, 60 ± 5% RH, and a photoperiod of 14:10 (L:D) hours. In addition, biochemical characteristics of the tested cultivars were assessed in order to understand any possible correlation between important demographic parameters and nutritional properties with biochemical features of pomegranate juice. Our research showed that various pomegranate cultivars have significant effects on life history, demographical parameters, nutritional indices, and energy reserves of *E. ceratoniae*. The shortest development time was observed on Shahvare-Danesefid cultivar and the longest was on Esfahani-Daneghermez and Malase-Danesyah cultivars. The highest intrinsic rate of increase (r_m) was observed on Shahvare-Danesefid and the lowest was on Esfahani-Daneghermez. Six major anthocyanin compounds were detected in juice of various pomegranate cultivars. Significant positive or negative correlations were observed between life history variables and nutritional characteristics with biochemical traits of pomegranate cultivars. The results indicated that Shahvare-Danesefid was a relatively susceptible pomegranate cultivar and Esfahani-Daneghermez was the least appropriate (most resistant) cultivar for feeding of *E. ceratoniae*, which could be useful in the development of integrated pest management strategies for this pest.

Keywords: *Ectomyelois ceratoniae*, pomegranate, feeding response, physiological characteristics, demographic parameters, phytochemical metabolites

INTRODUCTION

The carob moth, *Ectomyelois ceratoniae* Zeller (Lepidoptera: Pyralidae), has been recognized as one of the most destructive insect pests of pomegranate and other fruits such as date, almond, carob, nuts, walnut, fig, and pistachio, with a broad distribution in Iran and many tropical and subtropical regions (Warner et al., 1990; Ranjbar et al., 2011; Kishani-Farahani et al., 2012; Soufbaf et al., 2017). Pomegranate, *Punica granatum* L. (Ponicaceae), is the main host of the carob moth *E. ceratoniae* in Iran. The larvae feed inside the fruit, resulting in contamination with saprophytic fungi and causing great damage during the cropping season and after harvest, conditions that make the fruit unfit for human consumption (Shakeri, 2004).

The use of resistant cultivars could be an effective approach in integrated pest management (IPM) strategies targeting the carob moth (*E. ceratoniae*) in pomegranate orchards (Ramzi et al., 2014; Sobhani et al., 2015). Host plant resistance is an alternative for pest management as it is both economically and environmentally acceptable (Golizadeh et al., 2009; Soufbaf et al., 2010; Golizadeh and Abedi, 2016). Evaluating the resistance of various cultivars and crop species to pests may offer useful information about their suitability or unsuitability for the target pest species (Tsai and Wang, 2001). Host plant resistance to insects can also be manipulated using chemical elicitation of secondary metabolites, which can confer resistance to insects (War et al., 2012). Proper use of resistant cultivars in pest management strategies requires knowledge of life table parameters and biological variables of pests (Nawrot et al., 2010; Golizadeh and Abedi, 2017; Gvozdenac et al., 2018; Karimi-Pormehr et al., 2018).

Previously, Norouzi et al. (2008) studied population growth traits of the carob moth fed with different fruits like pomegranate, pistachio, fig, and date; their results showed that the reproductive output of *E. ceratoniae* on pomegranate and pistachio was higher than that on fig and date. Zare et al. (2013) investigated the biological characteristics of this pest on three pomegranate cultivars and indicated that Malase-danesyah cultivar was the least susceptible host for *A. ceratoniae*. Mortazavi et al. (2016) evaluated the effects of four diets including pistachio, pomegranate, semi-artificial and artificial diets on this pest, measured some of the biological variables and reported that pomegranate was the most suitable host for *E. ceratoniae*.

Various defense characteristics of host plants affect the fitness of herbivorous insects (Harvey et al., 2007; Nouri-Ganbalani et al., 2018). Secondary plant chemicals act as feeding inhibitors, deterrents, repellents, and antidigestive compounds that interfere with herbivore physiology and reduce its developmental and survival rates as well as its potential fecundity (War et al., 2011; Nikooei et al., 2015). Pomegranate juice is a potential source of secondary metabolites such as anthocyanins, ellagic acid, phytoestrogenic flavonoids, organic acids, tannins, and antioxidants (Tezcan et al., 2009; Fischer et al., 2011). Anthocyanins are polyphenolic compounds (flavonoids) responsible for the blue, red, and purple colors of most fruits and flowers, which are major compounds of pomegranate juices (Du et al., 1975; Alighourchi et al., 2008; Turfan et al., 2011; Mirsaeedghazi et al., 2014; Akhavan et al., 2015). Important anthocyanins in pomegranate juice are cyanidin 3-glucoside, cyanidin 3,5-diglucoside, delphinidin 3-glucoside, delphinidin 3,5 diglucoside, pelargonidin 3-glucoside, and pelargonidin 3,5-diglucoside (Alighourchi et al., 2008; Turfan et al., 2011; Mirsaeedghazi et al., 2014).

Pomegranate is native to Iran and northern India, however nowadays it is widely cultivated in subtropical regions of the world (Sarkhosh et al., 2009). Iran is the first producer of pomegranate with 6400 ha of pomegranate orchard and total production of 700,000 ton annually. The high quality of pomegranates in Iran has made it an important export commodity and some commercial cultivars have been exported from Iran to other parts of the world (Zare et al., 2013; Ashtari et al., 2019). Therefore, the findings of this study could be used wherever these cultivars are cultivated.

The aim of the present study was to determine whether the life history and nutritional traits of *E. ceratoniae* vary as a function of the commercial pomegranate cultivar used to rear larvae, using a two-sex life table method. In parallel, we wanted to examine how the biochemical properties and/or nutritional quality of the cultivars we tested can affect life history variables and the nutritional performance of *E. ceratoniae*. To this end, we quantified some pomegranate compounds, especially major anthocyanins in the juice of various pomegranate varieties, and examined the relationship between their levels and selected biological variables in the pest; prior to this study, no published information was available on the correlation between such variables in *E. ceratoniae* and plants contents in major anthocyanins and other biochemical compounds of pomegranate juice. Our findings will inform the development of novel carob moth management approaches, including the use of resistant cultivars to reduce pest damage in orchard systems.

MATERIALS AND METHODS

Pomegranate Cultivars Tested

Fruits of 11 pomegranate (*P. granatum*) cultivars, including Aban-Mahi, Esfahani-Daneghermez, Gabri, Gorche-Tafti, Malase-Danesyah, Malase-Yazdi, Shahvare-Daneghermez, Shahvare-Danesefid, Tabolarze-Mehrmahi, Tafti, and Toghe-Gardan, which are commercially important in Iran, were selected from mature trees grown in Agricultural and Natural Resources Research Center (ANRRC) of Yazd, Iran (31° 54′ 54′ ′ N, 54° 16′ 37′ ′ E). Commercially ripe fresh fruits were randomly selected and harvested from different mature trees to represent the population of the plantation during September 2016. All cultivars were grown within the same geographical zone, using similar agronomic practices. The fruits were transported by a ventilated car to the laboratory, where pomegranates with defects (sunburns, cracks, cuts, and bruises in peel) were discarded. Approximately 10 kg (n = 60) of pomegranate fruit was sampled for each cultivar. Five pomegranates of each cultivar were used for juice extraction, which was kept frozen at −80°C until analysis. The remainder of the fruits was placed in paper bags, stored in refrigerators at 2°C and then used for feeding of larvae.

Insect Rearing

Larvae used to establish the colony of *E. ceratoniae* were collected in orchards at the Agricultural and Natural Resources Research Center, Yazd (Iran), between August and October 2016. The pomegranate fruits infested with carob moth larvae were maintained in a growth chamber at 30 ± 1°C, relative humidity of 60 ± 5%, and under a photoperiod of 14 h:10 h (L:D). New adults that emerged from infested fruits were caught with an electric aspirator and transferred to the mating cages (50 cm × 50 cm × 100 cm) for 24 h (Navarro et al., 1986). Adults were fed with a 10% honey-water solution. After mating and flying in mating cages, 20 pairs of adult moths were placed in a transparent cylindrical plexiglass container (30 cm × 18 cm) with two holes in the cap covered by organza mesh, and the egg-loaded organza was replaced daily with a new one until nearly all the moths died. The newly laid eggs were separately transferred on 11 pomegranate cultivars. Larvae were reared on each pomegranate cultivar in plastic containers (diameter: 20 cm, depth: 6 cm) with a hole covered by a mesh net for ventilation and maintained under the abovementioned standard rearing conditions. Before initiating the experimental work, insects on each pomegranate cultivar were reared for two generations on the same cultivar, and then eggs from the third generation were used to conduct the experiments.

Life History Variables and Body Weight in Immature Stages

The experiments on each pomegranate cultivar started using same-aged eggs (within 24 h after oviposition) laid by females reared as larvae on the same cultivar. Sixty eggs of *E. ceratoniae* were individually transferred into Petri dishes (diameter 9 cm, depth 2 cm). In order to ventilation, the middle part of the lid of Petri dish was cut in a circle (diameter 3 cm) and then covered with a cloth mesh. The Petri dishes contained a part of pomegranate fruit for feeding of larvae. The fruit pieces were replaced with fresh ones every 2 days during the larval development. The fifth instar larvae of *E. ceratoniae* reared on each cultivar were weighed separately 24 h after their emergence. The Petri dishes were checked daily, and the duration of immature stages (egg, larval, pre-pupal, and pupal stages), and immature survival rate were recorded. Pupal weight of *E. ceratoniae* was measured within 24 h of pupation on each pomegranate cultivar (Sartorius AG Germany GCA803S, d = 0.001 ct). All experiments on pomegranate cultivars were carried out under the following laboratory conditions: 30 ± 1°C, relative humidity of 60 ± 5%, and a photoperiod of 14:10 (L:D).

Life History Variables in Adults

After emergence of adult moths, a pair of female and male moths was transferred to the same mating cages as described above and maintained for 24 h. Then, each pair was placed in a transparent plastic tube fitted with mesh lids (6 cm diameter and 15 cm depth). Experimental tubes were checked daily and the number of *E. ceratoniae* eggs deposited in each tube was recorded. In this way, each pair was daily transferred to a new tube, the number of eggs laid by adults was counted, and the experiments were continued up to the death of the last adult female and male moth. To supply a source of carbohydrate for adult feeding, a small cotton wick soaked in 10% honey solution was inserted into the egg- laying container. In this experiment, adult preoviposition period (APOP: the time between the emergence of an adult female and the start of its oviposition), total preoviposition period (TPOP: the duration from egg to first oviposition), oviposition period, fecundity (eggs laid during the reproductive period), and adult longevity were recorded. Resulting data were analyzed based on the age-stage, two-sex life table model developed by Chi and Liu (1985) and Chi (1988).

Nutritional Indices and Quantitative Analysis of Stored Macromolecules in Larvae

The gravimetric method described by Waldbauer (1968) was used to determine the nutritional responses (larval weight, food consumed, feces produced, and weight gain) of *E. ceratoniae* fourth-instar larvae on 11 pomegranate cultivars (40 replicates for each cultivar). Nutritional indices were evaluated on the basis of dry weight. Fourth-instar larvae were placed on fruit of each pomegranate cultivar after weighing and transfer into Petri dishes (9 cm in diameter, depth 2 cm). Larval weight was recorded daily, before and after feeding, for a 1-week experimental period. The fresh food provided, the remaining food, and feces at the end of each experiment were weighed daily. The quantity of ingested food was calculated by subtracting the weight of remaining food at the end of each experiment from the weight of fresh food at the beginning. To obtain the dry weight percentage of the food and larvae, 20 specimens of food and larvae for each cultivar were weighed, oven-dried at 60°C for 48 h, and then weighed again. Nutritional indices of larval *E. ceratoniae* were calculated using the Waldbauer (1968) as follows: efficiency of conversion of ingested food (ECI) = P/E; efficiency of conversion of digested food (ECD) = P/E-F; relative consumption rate (RCR) = E/A*T; relative growth rate (RGR) = P/A*T; where A = mean dry weight of larvae over the feeding period (g), E = dry weight of food consumed (g), F = dry weight of feces produced (g), P = dry weight gain of larvae (g), and T = duration of feeding period (day).

To measure the energy content of *E. ceratoniae* larvae (protein and glycogen contents), we used the whole body of fourth-instar larvae feeding on each pomegranate cultivar. All assays were replicated three times.

Total protein concentration of individual larvae was assessed using the Bradford (1976), bovine serum albumin (BSA) as a standard.

Glycogen content was assayed using the anthrone reagent as described (Yuval et al., 1998) and whole body lipid of *E. ceratoniae* larva was extracted according to the Van Handel (1985) method.

Biochemical Traits of Pomegranate Cultivars

Biochemical traits of pomegranate were assessed to examine the correlation between the main life-table parameters, nutritional

indices, and energy reserves of *E. ceratoniae*, on the one hand, and biochemical compounds founds in various pomegranate cultivars. All assays (each pomegranate cultivar) were done in three replicates. All biochemical metabolites of pomegranate were measured using pomegranate juice. Before juice extraction, fruits of 11 pomegranate cultivars (five from each cultivar) were washed in cold tap water and dried, and the damaged pomegranates were discarded. The juicy sacs from fruit pericarp were separated by hand and the juices were obtained using a manual juicer via pressing the arils. The juice samples (200 mL) were immediately centrifuged (10,000 rpm for 2 min at 4°C), divided into small vials and frozen at −80°C until analysis (Alighourchi et al., 2013).

Anthocyanin Analysis

Delphinidin 3,5-diglucoside, delphinidin 3-diglucoside, cyanidin 3,5-diglucoside, cyanidin 3-glucoside, pelargonidin 3,5-diglucoside, and pelargonidin 3-glucoside standards were purchased from Apin Chemicals, Co., Ltd. (Oxon, United Kingdom). Anthocyanins in juices were determined by high-performance liquid chromatography (HPLC) using an HPLC system equipped with an Empower software, a pump (Waters 600), a Rheodyne 7125i six-way injector with 20 μL sample loop, and a UV–Vis detector (Waters model 2487). Twenty microliters of purified juice was injected onto the HPLC column. Calculation of concentrations was based on the external standard method and anthocyanins were identified by comparison of their retention times with those of pure standards.

Total Protein Concentration Measurements

Protein content of pomegranate cultivars we tested was determined according to the Bradford (1976) using BSA as a standard.

Carbohydrate Content Determination

The carbohydrate content was assayed using the Anthrone reagent (0.05% in sulfuric acid) (Bemani et al., 2012).

Condensed Tannin (CT) Content Determination

Condensed tannin content reactive to Sulphosphovanillin reagent (orthophosphoric acid 0.6% aqueous vanillin solution 4:1 v/v) was analyzed according to Tanner and Brunner (1979). Quantification of condensed tannin content was carried out using calibration curves of catechin as an external standard.

Total Monomeric Anthocyanin Pigment Content (TMAC)

Total anthocyanin contents were measured by pH differential method using two buffer systems: potassium chloride, pH 1.0 (0.025M) and sodium acetate, pH 4.5 (0.4M) (Wrolstad et al., 2005). Results were expressed as mg of cyaniding-3-glucoside per 100 mL of pomegranate juice.

Total Phenolic Content (TPC)

Total phenolic content was determined using Folin–Ciocalteu method described by Tezcan et al. (2009). The result was expressed as milligram of gallic acid equivalent per 100 mL of pomegranate juice.

Flavonoid Content Determination

Total flavonoid content was measured by aluminum chloride colorimetric assay (Jia et al., 1999). Total flavonoid content was expressed as milligram catechin equivalents per one milliliter of extract.

Antioxidant Activity Determination

Evaluation of antioxidant activity was done based on radical scavenging properties of the juice using 2,2-diphenyl-1-picrylhydrazyl (DPPH) method (Tezcan et al., 2009).

Titrable Acidity (TA), pH, and Soluble Solids Content

Total titrable acidity was determined by titration to pH = 8.1 with 0.1M NaOH solution and expressed as grams citric acid per liter of juice. The pH measurements were performed using a digital pH meter at 20°C. Total soluble solid content (SSC) was determined with a digital refractometer. Results were reported as°Brix at 20°C (Alighourchi et al., 2008).

Statistical Analysis

Before analysis, all data were examined for normality using Kolmogorov–Smirnov test by SPSS v. 16.0 statistical program (SPSS Inc, 2007). The life table parameters including the intrinsic rate of increase (r_m), gross reproductive rate (*GRR*), net reproductive rate (R_0), mean generation time (T), and finite rate of increase (λ) were analyzed according to the age-stage, two-sex life table using TWOSEX-MSChart (Chi, 2016). The variability of life table parameters was estimated in bootstrap procedure and the bootstrap values on 11 pomegranate cultivars were compared using paired bootstrap test ($P < 0.05$) (Chi, 2016). The developmental time, immature survival rate, and fecundity were used for calculation of age-specific survivorship (l_x) and age-specific fecundity (m_x) for both male and female (Chi and Su, 2006). Additionally, weights of fifth instar larvae and pupae, nutritional indices, energy reserves of *E. ceratoniae* and biochemical traits of various pomegranate cultivars were analyzed by one-way ANOVA with mean separation at 5% level of significance by Tukey test (SAS Institute, 2002). Correlation between some important demographic parameters, nutritional indices, and storage macromolecule amounts of *E. ceratoniae* with biochemical compounds of various pomegranate cultivars was evaluated through Pearson's correlation test. A dendrogram of pomegranate cultivars based on life table parameters, nutritional indices, and storage macromolecules of *E. ceratoniae* on tested pomegranate cultivars was constructed by Ward's method using SPSS.

RESULTS

Immature Life History Variables and Body Weight

Developmental time of *E. ceratoniae* on various pomegranate cultivars is given in **Table 1**. There were significant differences in mean incubation periods among the pomegranate cultivars. The longest egg incubation period was on the Esfahani-Daneghermez and Malase-Danesyah cultivars, while the shortest was observed on the Toghe-Gardan cultivar. The longest larval period was seen on the Esfahani-Daneghermez cultivar and the shortest on the Shahvare-Danesefid cultivar. The pre-pupal period of *E. ceratoniae* on the Shahvare-Danesefid cultivar was significantly shorter than on the other cultivars except for Malase-Yazdi. The longest pupal period was observed on the Esfahani-Daneghermez and Malase-Danesyah cultivars, whereas a shorter period was observed on the Toghe-Gardan cultivar. The shortest developmental time from egg to adult emergence was on the Shahvare-Danesefid cultivar (36.41 ± 0.31 days) and the longest was on the Esfahani-Daneghermez (41.80 ± 0.26 days) and Malase-Danesyah (41.46 ± 0.28 days) cultivars. The immature survival rate ranged from 0.68 ± 0.06 to 0.87 ± 0.05 with the lowest and highest survival rates observed on Esfahani-Daneghermez and Shahvare-Danesefid cultivars, respectively (**Table 1**). Finally, *E. ceratoniae* displayed the highest sex ratio on the Shahvare-Danesefid cultivar, while the lowest one was seen on the Esfahani-Daneghermez and Malase Danesyah cultivars (**Table 1**).

The age-specific survival rate (l_x) of *E. ceratoniae* on different cultivars is shown in **Figure 1**. Overall, age-specific survival rate curves were similar among insects fed different cultivars. However, female adults were longer-lived on the Aban-Mahi cultivar and the l_x curve was more extended on this cultivar.

Table 2 shows the weight of fifth instars and pupae of *E. ceratoniae* when reared on various pomegranate cultivars. The mean weight of fifth-instar larvae varied from 0.0425 ± 0.001 g on the Malase-Danesyah cultivar to 0.0615 ± 0.001 g on Shahvare-Danesefid (F = 31.66; df = 10, 546; $P < 0.0001$). Moreover, pupal weight showed significant variation as a function of the pomegranate cultivar tested (F = 25.35; df = 10, 514; $P < 0.0001$). The highest values were observed on the Shahvare-Danesefid and Toghe-Gardan cultivars and the lowest ones were recorded on the Malase-Danesyah and Esfahani-Daneghermez cultivars (**Table 2**).

Longevity and Reproductive Variables

The data on pre-oviposition and oviposition periods, fecundity and lifespan of *E. ceratoniae* adults on the tested pomegranate cultivars are presented in **Table 3**. Significant effects were observed for adult pre-oviposition period (APOP) of *E. ceratoniae*. Total pre-oviposition period (TPOP) varied significantly as a function of the pomegranate cultivars used as food source. The TPOP was longest on the Esfahani-Daneghermez cultivar and shortest on Toghe-Gardan. Moreover, the oviposition period was the longest when *E. ceratoniae* females were reared on the Shahvare-Danesefid cultivar and the shortest

TABLE 1 | The mean (± SE) duration (days) and survival rate (%) of immature stages and sex ratio of *Ectomyelois ceratoniae* fed on various pomegranate cultivars.

Pomegranate cultivar	Egg incubation (days)	Larval period (days)	Pre-pupal period (days)	Pupal period (days)	Development time (days)	Pre-adult survival	Sex ratio
Aban-Mahi	3.77 ± 0.06 cd (52)	26.49 ± 0.32 ad (46)	1.98 ± 0.020 a (45)	6.31 ± 0.08 b (45)	38.58 ± 0.33 c (45)	0.76 ± 0.05 ab (60)	0.37 ± 0.06 ab (60)
Esfahani-Daneghermez	4.21 ± 0.06 a (51)	28.59 ± 0.24 a (45)	1.99 ± 0.002 a (43)	6.93 ± 0.04 a (41)	41.80 ± 0.26 a (41)	0.68 ± 0.06 b (60)	0.30 ± 0.06 b (60)
Gabri	3.96 ± 0.04 b (55)	27.92 ± 0.23 b (51)	1.96 ± 0.030 a (48)	6.19 ± 0.08 b (47)	39.88 ± 0.24 b (47)	0.78 ± 0.05 ab (60)	0.37 ± 0.06 ab (60)
Gorche-Tafti	3.84 ± 0.05 cd (55)	25.72 ± 0.21 de (52)	1.96 ± 0.030 a (51)	5.86 ± 0.07 cd (50)	37.43 ± 0.23 d (50)	0.83 ± 05 ab (60)	0.40 ± 0.07 ab (60)
Malase-Danesyah	4.20 ± 0.06 a (49)	28.31 ± 0.24 ab (46)	1.99 ± 0.005 a (44)	6.88 ± 0.05 a (42)	41.46 ± 0.28 a (42)	0.70 ± 0.06 b (60)	0.32 ± 0.06 b (60)
Malase-Yazdi	3.89 ± 0.06 bcd (53)	26.71 ± 0.25 c (48)	1.94 ± 0.030 ab (46)	6.29 ± 0.09 b (45)	38.62 ± 0.28 c (45)	0.75 ± 0.05 ab (60)	0.35 ± 0.06 ab (60)
Shahvare-Daneghermez	3.91 ± 0.04 bc (53)	26.77 ± 0.30 c (50)	1.99 ± 0.003 a (47)	6.25 ± 0.09 b (47)	39.03 ± 0.30 c (47)	0.79 ± 0.05 ab (60)	0.36 ± 0.06 ab (60)
Shahvare-Danesefid	3.80 ± 0.05 cd (57)	24.86 ± 0.24 f (54)	1.77 ± 0.060 b (53)	5.92 ± 0.09 c (52)	36.41 ± 0.31 f (52)	0.87 ± 0.05 a (60)	0.44 ± 0.07 a (60)
Tabolarze-Mehrmahi	3.83 ± 0.05 cd (54)	26.46 ± 0.25 cd (52)	1.99 ± 0.003 a (50)	6.17 ± 0.07 b (48)	38.48 ± 0.29 c (48)	0.80 ± 0.05 ab (60)	0.37 ± 0.06 ab (60)
Tafti	3.87 ± 0.04 bcd (56)	25.85 ± 0.23 d (51)	1.99 ± 0.002 a (50)	5.83 ± 0.07 cd (48)	37.67 ± 0.24 d (48)	0.81 ± 0.05 ab (60)	0.40 ± 0.06 ab (60)
Toghe-Gardan	3.73 ± 0.06 d (57)	25.09 ± 0.27 ef (52)	1.96 ± 0.030 a (51)	5.66 ± 0.07 d (50)	36.43 ± 0.28 e (50)	0.84 ± 0.05 ab (60)	0.42 ± 0.06 ab (60)

Mean values in a column followed by different lowercase letters are significantly different ($P < 0.05$, paired bootstrap test). The numbers in parentheses indicate sample size.

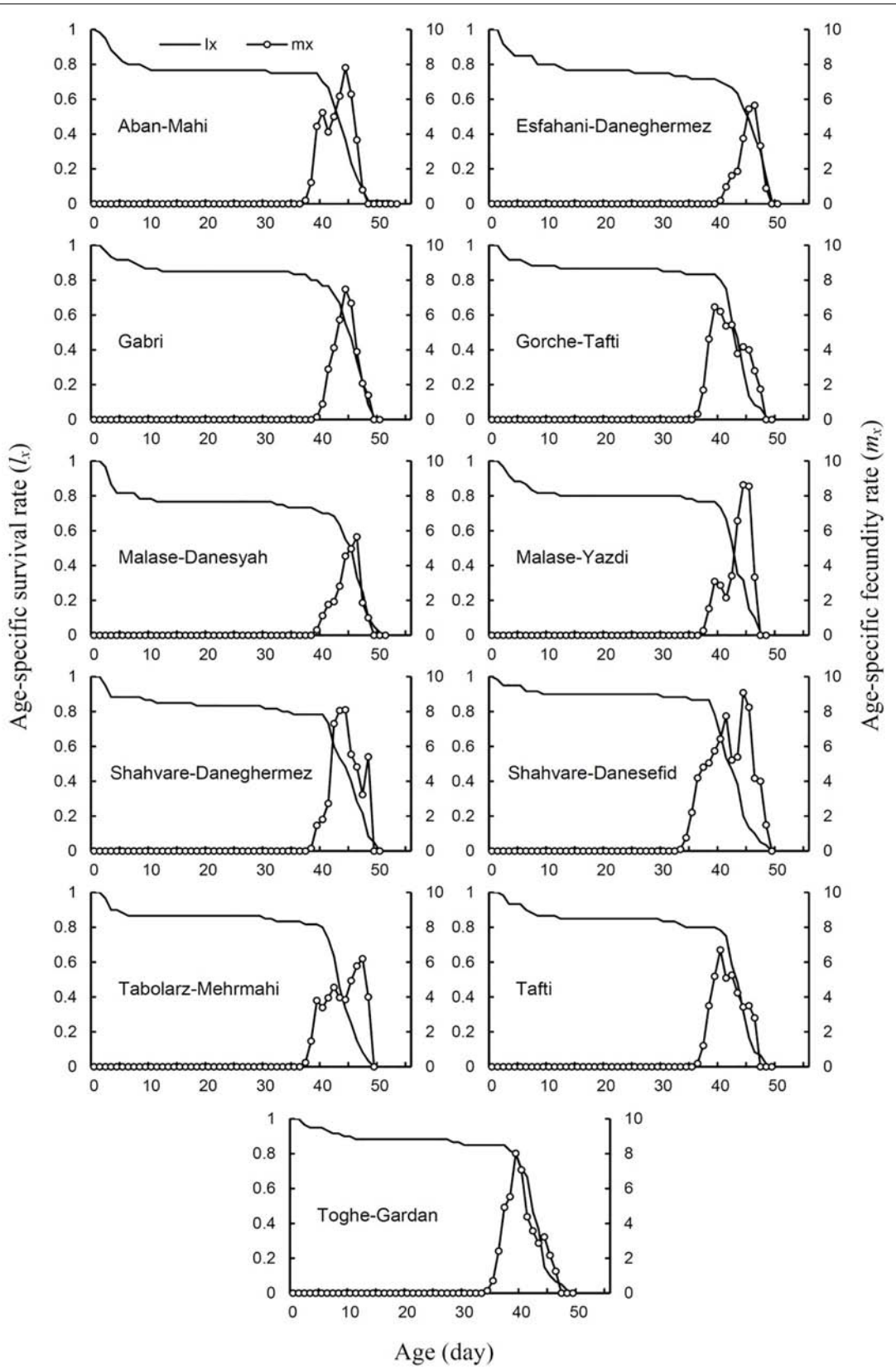

FIGURE 1 | Age-specific survival rate (l_x) and age-specific fecundity (m_x) of *Ectomyelois ceratoniae* on various pomegranate cultivars.

TABLE 2 | The mean (± SE) (g) weight of fifth instar larvae and pupa stage of *Ectomyelois ceratoniae* reared on various pomegranate cultivars.

Pomegranate cultivar	Fifth instar larvae	Pupa
Aban-Mahi	0.0504 ± 0.001 cd (46)	0.0410 ± 0.001 bc (45)
Esfahani-Danehghermez	0.0435 ± 0.001 ef (45)	0.0347 ± 0.001 e (41)
Gabri	0.0468 ± 0.001 def (51)	0.0387 ± 0.001 cd (47)
Gorche-Tafti	0.0542 ± 0.001 bc (52)	0.0418 ± 0.001 abc (50)
Malase-Danehsyah	0.0425 ± 0.001 f (46)	0.0342 ± 0.001 e (42)
Malase-Yazdi	0.0466 ± 0.001 def (48)	0.0362 ± 0.001 de (45)
Shahvare-Danehghermez	0.0455 ± 0. 001 def (50)	0.0391 ± 0.001 bcd (47)
Shahvare-Danehsefid	0.0615 ± 0.001 a (54)	0.0442 ± 0.001 a (52)
Tabolarze-Mehrmahi	0.0484 ± 0.001 de (52)	0.0393 ± 0.001 bcd (48)
Tafti	0.0566 ± 0.001 b (51)	0.0420 ± 0.001 ab (48)
Toghe-Gardan	0.0581 ± 0.002 ab (52)	0.0448 ± 0.001 a (50)

Mean values in a column followed by different lowercase letters are significantly different on the basis of ANOVA with Tukey test ($P < 0.05$). The numbers in parentheses indicate sample size.

when reared on the Esfahani-Daneghermez, Malase-Danesyah, and Malase-Yazdi cultivars. Total fecundity (mean number of eggs laid during the reproductive period) of *E. ceratoniae* varied significantly as a function of the 11 pomegranate cultivars tested; the highest values were observed on the Shahvare-Danesefid (82.74 ± 2.01 eggs) and Toghe-Gardan (70.46 ± 2.30 eggs) cultivars and the lowest was on Esfahani-Daneghermez (36.91 ± 1.35 eggs) (**Table 3**).

Age-specific fecundity rates (m_x) for *E. ceratoniae* reared on the pomegranate cultivars tested are shown in **Figure 1**. The width of the m_x curve (i.e., the fecundity period) was the greater on the Shahvare-Danesefid cultivar than the others.

Longevity of both male and female adults of *E. ceratoniae* was lowest when larvae were reared on the Esfahani-Daneghermez, Malase-Danesyah, and Malase-Yazdi cultivars (**Table 3**).

Adult Life Table Parameters

Life tables were constructed from developmental time, survival, and fecundity data (**Table 4**). All computed parameters were significantly affected by the pomegranate cultivar. Insects reared on Shahvare-Danesefid had the highest gross reproductive rate (*GRR*) while those reared on Esfahani-Daneghermez showed the lowest *GRR* value. The net reproductive rate (R_0) was the lowest on the Esfahani-Daneghermez cultivar and the highest on the Shahvare-Danesefid cultivar. The intrinsic rate of increase (r_m) values ranged from 0.053 ± 0.004 to 0.090 ± 0.004 female progeny per female per day on the pomegranate cultivars under study (**Table 4**). The r_m value was highest when *E. ceratoniae* were reared on the Shahvare-Danesefid cultivar and lowest on the Esfahani-Daneghermez cultivar. Variation in the finite rate of increase (λ) was similar to that observed for the intrinsic rate of increase while the mean generation time (T) of *E. ceratoniae* was shortest on the Toghe-Gardan cultivar (**Table 4**).

Nutritional Indices and Storage Macromolecules of Larvae

Measurements of the nutritional performance of *E. ceratoniae* fourth-instar larvae are shown in **Table 5**. Nutritional indices were significantly different among larvae feeding on various pomegranate cultivars. The larvae fed on Shahvare-Danesefid showed a higher level of food consumption as compared with those reared on other cultivars (F = 23.15; df = 10, 439; $P < 0.0001$). Also, the highest weight gain of larvae (F = 47.91; df = 10, 439; $P < 0.0001$) was observed when larvae were fed on Shahvare-Danesefid (**Table 5**). Larvae reared on the Shahvare-Danesefid and Gorche-Tafti cultivars showed the highest efficiency of conversion of ingested food (ECI) (F = 22.89; df = 10, 439; $P < 0.0001$) as well as efficiency of conversion of digested food (ECD) (F = 22.77; df = 10, 439; $P < 0.0001$) compared with larvae fed on the other cultivars (**Table 5**). The highest RCR (F = 2.48; df = 10, 439; P = 0.0068) was observed on the Esfahani-Daneghermez and Tabolarze-MehrMahi cultivars, while larvae reared on Gorche-Tafti had a lowest RCR. In addition, the highest value of relative growth rate (RGR) (F = 7.93; df = 10, 439; $P < 0.0001$) was obtained for larvae reared on the Shahvare-Danesefid cultivar (**Table 5**).

TABLE 3 | Biological parameters of *Ectomyelois ceratoniae* adults reared on various pomegranate cultivars.

Pomegranate cultivar	APOP (days)	TPOP (days)	Oviposition period (days)	Fecundity (no. eggs laid)	Female adult longevity (days)	Male adult longevity (days)
Aban-Mahi	1.04 ± 0.05 b (22)	39.92 ± 0.41 ef (22)	4.55 ± 0.23 cd (22)	58.61 ± 2.05 c (22)	6.27 ± 0.25 bc (22)	5.47 ± 0.20 c (23)
Esfahani-Daneghermez	1.22 ± 0.10 ab (18)	43.11 ± 0.40 a (18)	3.39 ± 0.18 e (18)	36.91 ± 1.35 f (18)	5.33 ± 0.19 d (18)	4.47 ± 0.23 d (23)
Gabri	1.18 ± 0.08 ab (22)	41.64 ± 0.28 bc (22)	4.22 ± 0.18 d (22)	51.51 ± 1.94 d (22)	6.14 ± 0.23 c (22)	5.76 ± 0.23 abc (25)
Gorche-Tafti	1.17 ± 0.07 ab (24)	38.52 ± 0.32 gh (24)	5.03 ± 0.25 abc (24)	67.03 ± 2.28 b (24)	6.82 ± 0.27 abc (24)	5.96 ± 0.14 ab (26)
Malase-Danesyah	1.16 ± 0.09 ab (19)	42.23 ± 0.45 ab (19)	3.68 ± 0.19 e (19)	40.37 ± 1.63 ef (19)	5.53 ± 0.16 d (19)	4.57 ± 0.22 d (23)
Malase-Yazdi	1.28 ± 0.10 a (21)	40.30 ± 0.49 de (21)	3.67 ± 0.20 e (21)	44.97 ± 2.02 e (21)	5.48 ± 0.23 d (21)	4.91 ± 0.21 d (24)
Shahvare-Daneghermez	1.18 ± 0.08 ab (22)	41.09 ± 0.33 cd (22)	5.01 ± 0.17 abc (22)	60.02 ± 1.99 c (22)	6.90 ± 0.23 ab (22)	5.72 ± 0.15 abc (25)
Shahvare-Danesefid	1.11 ± 0.06 ab (26)	37.45 ± 0.52 hi (26)	5.50 ± 0.20 a (26)	82.74 ± 2.01 a (26)	7.04 ± 0.21 a (26)	5.84 ± 0.18 abc (26)
Tabolarze-Mehrmahi	1.09 ± 0.06 ab (22)	39.72 ± 0.43 ef (22)	4.64 ± 0.23 bcd (22)	51.33 ± 2.08 d (22)	6.28 ± 0.23 bc (22)	5.51 ± 0.20 bc (26)
Tafti	1.21 ± 0.09 ab (24)	38.92 ± 0.37 fg (24)	4.66 ± 0.23 bcd (24)	60.34 ± 2.29 c (24)	6.82 ± 0.27 abc (24)	5.96 ± 0.15 ab (24)
Toghe-Gardan	1.08 ± 0.05 ab (25)	37.23 ± 0.35 i (25)	5.16 ± 0.20 ab (25)	70.46 ± 2.30 a (25)	7.19 ± 0.27 a (25)	6.04 ± 0.16 a (25)

Mean values in a column followed by different lowercase letters are significantly different ($P < 0.05$, paired bootstrap test). The numbers in parentheses indicate sample size. APOP, adult pre-oviposition period; TPOP, total pre-oviposition period.

Values measured for the energy reserves of *E. ceratoniae* fourth-instar larvae on various pomegranate cultivars are given in **Table 6**. There was significant variation in energy contents of *E. ceratoniae* larvae reared on different cultivars. The highest whole-body protein content of larvae (F = 16.05; df = 10, 32; P = 0.0068) was observed in those fed on the Shahvare-Danesefid cultivar (F = 3.16; df = 10, 32; P = 0.0118). Similarly, the larvae fed on this cultivar showed the highest whole-body glycogen

TABLE 4 | Mean (± SE) of two-sex life-table parameters for *Ectomyelois ceratoniae* reared on various pomegranate cultivars.

Pomegranate cultivar	Sample size (n)	*GRR* (female/female)	R_0 (female/female)	r_m (female/female/day)	λ (female/day)	*T* (days)
Aban-Mahi	60	44.98 ± 6.71 b	21.59 ± 3.65 bc	0.072 ± 0.004 cde	1.075 ± 0.004 cde	42.50 ± 0.48 c
Esfahani-Daneghermez	60	23.90 ± 4.30 c	5.27 ± 4.46 e	0.053 ± 0.004 g	1.054 ± 0.005 g	45.33 ± 0.38 a
Gabri	60	35.44 ± 5.51 bc	19.05 ± 3.30 bcd	0.066 ± 0.004 def	1.068 ± 0.004 def	44.26 ± 0.30 b
Gorche-Tafti	60	46.48 ± ±7.40 b	26.83 ± 4.49 ab	0.080 ± 0.004 abc	1.083 ± 0.005 abc	41.10 ± 0.33 fg
Malase-Danesyah	60	25.85 ± 4.64 c	12.71 ± 2.47 d	0.057 ± 0.005 fg	1.058 ± 0.005 fg	44.56 ± 0.40 ab
Malase-Yazdi	60	40.50 ± 5.53 b	15.67 ± 2.84 cd	0.064 ± 0.004 efg	1.066 ± 0.005 efg	42.44 ± 0.41 cd
Shahvare-Daneghermez	60	48.47 ± 7.12 b	21.84 ± 3.87 bc	0.070 ± 0.004 cde	1.073 ± 0.004 cde	43.84 ± 0.36 b
Shahvare-Danesefid	60	74.64 ± 10.55 a	36.05 ± 5.60 a	0.090 ± 0.004 a	1.093 ± 0.004 a	40.02 ± 0.50 gh
Tabolarze-Mehrmahi	60	45.40 ± 8.44 b	18.88 ± 3.31 bcd	0.069 ± 0.004 cde	1.071 ± 0.005 cde	42.34 ± 0.44 cde
Tafti	60	41.03 ± 5.85 b	24.01 ± 3.84 abc	0.077 ± ±0.004 bcd	1.080 ± 0.004 bcd	41.34 ± 0.34 ef
Toghe-Gardan	60	46.29 ± 7.84 b	29.29 ± 4.58 ab	0.084 ± 0.004 ab	1.088 ± 0.004 ab	39.90 ± 0.32 h

Mean values in a column followed by different lowercase letters are significantly different ($P < 0.05$, paired bootstrap test). GRR, gross reproductive rate; R_0, net reproductive rate; r_m, intrinsic rate of increase; λ, finite rate of increase; T, mean generation time.

TABLE 5 | The mean (± SE) nutritional indices of *Ectomyelois ceratoniae* reared on various pomegranate cultivars.

Pomegranate cultivar	Sample size (n)	Food consumed (g/larvae)	Larval weight gain (g)	ECI (%)	ECD (%)	RCR (g/g/day)	RGR (g/g/day)
Aban-Mahi	40	2.70 ± 0.06 cd	0.020 ± 0.002 de	1.93 ± ±0.12 bc	1.99 ± ±0.13 bc	4.11 ± ±0.14 ab	0.076 ± ±0.004 bc
Esfahani-Danehghermez	40	2.59 ± ±0.04 d	0.014 ± 0.001 e	1.44 ± ±0.08 d	1.49 ± ±0.08 d	4.53 ± ±0.14 a	0.064 ± ±0.004 c
Gabri	40	2.65 ± ±0.05 cd	0.016 ± 0.001 e	1.57 ± ±0.09 cd	1.62 ± ±0.09 cd	4.24 ± ±0.14 ab	0.065 ± ±0.004 c
Gorche-Tafti	40	3.10 ± 0.07 b	0.031 ± ±0.008 b	2.69 ± ±0.10 a	2.78 ± ±0.10 a	3.41 ± ±0.16 b	0.090 ± ±0.005 ab
Malase-Danehsyah	40	2.63 ± ±0.05 cd	0.015 ± ±0.009 e	1.47 ± ±0.08 d	1.52 ± ±0.08 d	4.36 ± ±0.14 ab	0.063 ± ±0.004 c
Malase-Yazdi	40	2.62 ± 0.05 cd	0.016 ± 0.004 e	1.59 ± ±0.10 cd	1.64 ± ±0.10 cd	4.25 ± ±0.14 ab	0.065 ± ±0.004 c
Shahvare-Danehghermez	40	2.66 ± ±0.04 cd	0.017 ± 0.003 e	1.69 ± ±0.11 bcd	1.74 ± ±0.11 bcd	4.20 ± ±0.16 ab	0.067 ± ±0.004 c
Shahvare-Danehsefid	40	3.62 ± 0.07 a	0.039 ± ±0.006 a	2.84 ± ±0.08 a	2.92 ± ±0.08 a	3.74 ± ±0.12 ab	0.105 ± ±0.003 a
Tabolarze-Mehrmahi	40	2.76 ± 0.07 cd	0.019 ± 0.001 de	1.78 ± ±0.12 bcd	1.84 ± ±0.13 bcd	4.63 ± ±0.64 a	0.074 ± ±0.007 bc
Tafti	40	2.80 ± ±0.09 cd	0.023 ± 0.001 cd	2.09 ± ±0.10 b	2.18 ± ±0.11 b	3.91 ± ±0.17 ab	0.080 ± ±0.005 bc
Toghe-Gardan	40	2.89 ± 0.08 bc	0.025 ± ±0.003 c	2.14 ± ±0.09 b	2.20 ± ±0.10 b	3.66 ± ±0.18 ab	0.076 ± ±0.004 bc

The means followed by different letters in the same column are significantly different (Tukey test, $P < 0.05$). ECI, efficiency of conversion of ingested food; ECD, efficiency of conversion of digested food; RCR, relative consumption rate; RGR, relative growth rate.

TABLE 6 | The mean (± SE) energy reserves of fourth-instar larvae of *Ectomyelois ceratoniae* reared on various pomegranate cultivars.

Pomegranate cultivar	Sample size (n)	Protein content (μg/larva)	Glycogen content (μg/larva)	Lipid content (μg/larva)
Aban-Mahi	3	491.67 ± 8.90 cde	58.45 ± 6.27 ab	59.87 ± 7.59 abc
Esfahani-Danehghermez	3	468.67 ± 1.20 e	39.63 ± 12.16 ab	45.89 ± 4.59 cd
Gabri	3	492.02 ± 5.57 cde	40.33 ± 11.19 ab	52.85 ± 3.56 cd
Gorche-Tafti	3	505.50 ± 8.13 bcd	63.29 ± 6.87 ab	67.12 ± 7.83 abc
Malase-Danehsyah	3	482.33 ± 6.86 de	29.90 ± 8.41 b	34.15 ± 6.15 d
Malase-Yazdi	3	494.67 ± 7.66 bcde	38.45 ± 3.73 ab	47.05 ± 3.49 cd
Shahvare-Danehghermez	3	503.33 ± 9.70 bcde	50.60 ± 4.45 ab	60.17 ± 3.75 abc
Shahvare-Danehsefid	3	574.33 ± 7.22 a	73.34 ± 10.71 a	81.83 ± 1.66 a
Tabolarze-Mehrmahi	3	502.50 ± 4.77 bcde	46.95 ± 2.82 ab	56.40 ± 2.39 bcd
Tafti	3	520.01 ± 5.69 bc	65.60 ± 2.84 ab	80.02 ± 1.90 a
Toghe-Gardan	3	529.83 ± 3.01 b	70.60 ± 12.31 ab	77.20 ± 1.26 ab

Mean values in a column followed by different lowercase letters are significantly different on the basis of ANOVA with Tukey test ($P < 0.05$).

content (F = 3.16; df = 10, 32; P = 0.0118). Larvae fed on the Shahvare-Danesefid and Tafti cultivars showed the highest lipid content (F = 11.07; df = 10, 32; $P < 0.0001$) while the lowest value was observed for larvae reared on the Malase-Danesyah cultivar (**Table 6**).

A dendrogram based on population growth parameters, nutritional indices, and energy reserves of *E. ceratoniae* on various pomegranate cultivars is shown in **Figure 2**. The dendrogram revealed two clusters labeled A (including sub-clusters A1 and A2) and B. Different pomegranate cultivars tested were grouped within each cluster according to the *E. ceratoniae* criteria. Cluster B included Shahvare-Danesefid; sub-cluster A2 consisted of Esfahani-Daneghermez and Malase-Danesyah and other cultivars were in sub-cluster A1.

Biochemical Traits of Pomegranate Cultivars

Concentrations of the major anthocyanins measured in the pomegranate cultivars that we examined are listed in **Table 7**. Six compounds, namely cyanidin 3-glucoside (0.48–11.91 mg/L), cyanidin 3,5-diglucoside (1.90–54.47 mg/L), delphinidin 3-glucoside (0.78–4.28 mg/L), delphinidin 3,5-diglucoside (0.072–40.59 mg/L), pelargonidin 3-glucoside (0.118–0.55 mg/L), and pelargonidin 3,5-diglucoside (0.37–3.52 mg/L), were detected as major anthocyanin constituents from various pomegranate juice cultivars. There were significant differences among various pomegranate cultivars for all the detected anthocyanin compounds (**Table 7**). Esfahani-Daneghermez cultivar showed the highest value of cyanidin 3-glucoside (F = 710.64; df = 10, 32; $P < 0.0001$) compound compared with other cultivars. The cyanidin 3,5-diglucoside (F = 979.90; df = 10, 32; $P < 0.0001$) was significantly higher in Esfahani-Daneghermez. Also, the highest value of delphinidin 3-glucoside (F = 473.38; df = 10, 32; $P < 0.0001$), delphinidin 3,5-diglucoside (F = 24.31; df = 10, 32; $P < 0.0001$), pelargonidin 3-glucoside (F = 52.35; df = 10, 32; $P < 0.0001$) and pelargonidin 3,5-diglucoside (F = 12.74; df = 10, 32; $P < 0.0001$) compounds were measured in Esfahani-Daneghermez (**Table 7**).

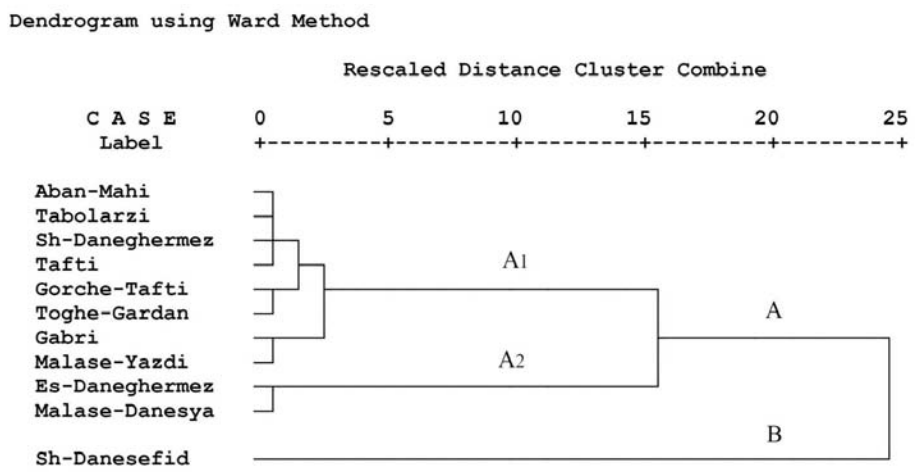

FIGURE 2 | Dendrogram of different pomegranate cultivars based on life table parameters, nutritional indices and energy reserves of *Ectomyelois ceratoniae* reared on various pomegranate cultivars.

TABLE 7 | The means (± SE) major anthocyanins constituents (mg/L) of various pomegranate cultivars.

Pomegranate cultivar	Sample size (n)	Cyanidin 3-glucoside	Cyanidin 3,5-diglucoside	Delphinidin 3-glucoside	Delphinidin 3,5 diglucoside	Pelargonidin 3- glucoside	Pelargonidin 3,5- diglucoside
Aban-Mahi	3	2.13 ± 0.05 d	7.73 ± 0.37 d	1.19 ± 0.02 e	1.38 ± 0.40 c	0.17 ± 0.010 bcd	0.56 ± 0.040 d
Esfahani-Danehghermez	3	11.91 ± 0.04 a	54.47 ± 1.47 a	4.28 ± 0.09 a	40.59 ± 7.94 a	0.51 ± 0.020 a	3.52 ± 0.080 a
Gabri	3	2.61 ± 0.03 d	13.36 ± 0.24 c	1.56 ± 0.02 d	2.61 ± 0.07 bc	0.24 ± 0.006 bc	1.17 ± 0.020 bcd
Gorche-Tafti	3	1.11 ± 0.02 e	4.17 ± 0.03 ef	0.95 ± 0.00 ef	1.28 ± 0.03 c	0.13 ± 0.001 *cd*	0.43 ± 0.020 d
Malase-Danehsyah	3	5.44 ± 0.12 c	39.83 ± 0.96 b	3.52 ± 0.15 b	2.01 ± 0.57 b	0.25 ± 0.004 b	2.36 ± 0.090 ab
Malase-Yazdi	3	9.94 ± 0.24 b	37.44 ± 0.64 b	3.16 ± 0.04 c	9.33 ± 0.70 b	0.55 ± 0.070 a	2.92 ± 0.280 a
Shahvare-Danehghermez	3	0.48 ± 0.06 e	6.02 ± 0.17 de	1.06 ± 0.03 ef	1.42 ± 0.01 c	0.15 ± 0.002 bcd	1.14 ± 0.010 bcd
Shahvare-Danehsefid	3	0.86 ± 0.01 e	3.39 ± 0.04 ef	0.90 ± 0.01 f	0.072 ± 0.01 c	0.118 ± 0.001 d	0.37 ± 0.002 d
Tabolarze-Mehrmahi	3	1.16 ± 0.38 e	15.81 ± 0.02 c	1.72 ± 0.00 d	0.197 ± 0.05 c	0.16 ± 0.006 bcd	2.23 ± 0.910 abc
Tafti	3	0.64 ± 0.13 e	1.90 ± 0.07 f	0.78 ± 0.02 f	0.81 ± 0.06 c	0.119 ± 0.001 d	0.74 ± 0.390 cd
Toghe-Gardan	3	0.83 ± 0.01 e	3.61 ± 0.13 ef	0.92 ± 0.01 ef	0.89 ± 0.04 c	0.122 ± 0.002 d	0.37 ± 0.010 d

Mean values in a column followed by different lowercase letters are significantly different on the basis of ANOVA with Tukey test ($P < 0.05$).

Biochemical characteristics of tested pomegranate cultivars used for feeding of *E. ceratoniae* are given in **Tables 8**, **9**. No significant differences were observed in total protein content (F = 1.10; df = 10, 32; P = 0.41) among the pomegranate cultivars. The carbohydrate content varied from 92.61 mg/mL in Esfahani-Daneghermez to 138.33 mg/mL in Shahvare-Danesefid cultivar (F = 16.22; df = 10, 32; $P < 0.0001$). Furthermore, a higher content of condensed tannins was measured in Esfahani-Daneghermez and Shahvare-Daneghermez, whereas a lower content was detected in Shahvare-Danesefid and Toghe-Gardan cultivars (F = 12.18; df = 10, 32; $P < 0.0001$) (**Table 8**). There was a significant difference for the total phenolic (TPC) (F = 45.22; df = 10, 32; $P < 0.0001$) and total monomeric anthocyanin pigment (TMAC) (F = 38.99; df = 10, 32; $P < 0.0001$) contents of different pomegranate cultivars. A higher value of TPC and TMAC was measured in Esfahani-Daneghermez cultivar and the lowest value of TMAC was detected in Shahvare-Danesefid and Tafti cultivars. The highest flavonoid content was measured in Esfahani-Daneghermez, whereas the lowest content was observed in the Shahvare-Danesefid and Toghe-Gardan cultivars (F = 44.70; df = 10, 32; $P < 0.0001$) (**Table 8**).

Antioxidant activity (AA%) varied from 49.17 in Tafti to 60.13 (AA%) in the Esfahani-Daneghermez cultivar (F = 8.30; df = 10, 32; $P < 0.0001$). Moreover, the highest pH value was observed in the Shahvare-Danesefid cultivar while the lowest value was in the Malase-Danesyah cultivar (F = 34.32; df = 10, 32; $P < 0.0001$). The highest total titrable acidity value was obtained for the Malase-Danesyah cultivar, whereas the lowest value was seen for the Shahvare-Danesefid cultivar (F = 24.37; df = 10, 32; $P < 0.0001$). The percentage of juice showed limited variation, ranging from 50.15 to 61.32 for the pomegranate cultivars under investigation (F = 2.66; df = 10, 32; P = 0.0265). The soluble solids content was lowest in the Tabolarze-Mehrmahi cultivar (F = 2.42; df = 10, 32; P = 0.040) (**Table 9**).

Correlation Analysis

Tables 10, **11** show coefficients obtained for analyses of correlation between life table parameters and physiological characteristics of *E. ceratoniae* fed on different cultivars, on

TABLE 8 | Some biochemical characteristics of tested various pomegranate juice cultivars.

Pomegranate cultivar	Sample size (n)	Total Protein (mg/mL)	Carbohydrate content (mg/mL)	CT (mg/mL)	TPC (mg/100 mL)	TMAC (mg/L)	Flavonoid (mg/mL)
Aban-Mahi	3	0.139 ± 0.004 a	102.78 ± 4.99 bc	20.01 ± 1.05 abcd	277.35 ± 9.33 abc	138.07 ± 8.09 cde	98.37 ± 6.15 b
Esfahani-Danehghermez	3	0.133 ± 0.003 a	92.61 ± 5.61 c	23.55 ± 0.58 a	308.61 ± 1.21 a	244.52 ± 5.81 a	132.44 ± 11.37 a
Gabri	3	0.132 ± 0.002 a	97.06 ± 3.19 bc	21.08 ± 1.14 abc	246.68 ± 11.13 bcd	152.24 ± 8.50 bcd	90.84 ± 0.83 b
Gorche-Tafti	3	0.136 ± 0.005 a	131.45 ± 0.89 a	16.21 ± 1.39 cde	165.35 ± 6.96 ef	99.69 ± 13.72 efg	40.44 ± 3.46 cd
Malase-Danehsyah	3	0.130 ± 0.002 a	94.39 ± 4.36 bc	21.55 ± 0.57 ab	294.68 ± 5.77 ab	172.93 ± 8.46 bc	108.04 ± 4.45 ab
Malase-Yazdi	3	0.136 ± 0.002 a	95.44 ± 6.65 bc	19.95 ± 0.74 abcd	259.68 ± 1.73 abc	181.20 ± 4.69 b	98.77 ± 3.48 b
Shahvare-Danehghermez	3	0.134 ± 0.001 a	117.67 ± 0.92 ab	23.15 ± 0.71 a	202.68 ± 25.16 de	169.73 ± 5.37 bcd	63.11 ± 6.36 c
Shahvare-Danehsefid	3	0.138 ± 0.002 a	138.33 ± 0.73 a	14.01 ± 0.64 e	131.35 ± 4.37 f	90.78 ± 7.92 *g*	27.11 ± 3.53 d
Tabolarze-Mehrmahi	3	0.131 ± 0.002 a	99.61 ± 5.24 bc	18.01 ± 1.80 bcde	236.68 ± 9.02 cd	132.31 ± 3.09 def	93.11 ± 3.71 b
Tafti	3	0.134 ± 0.001 a	134.61 ± 1.02 a	16.01 ± 0.70 de	144.68 ± 5.29 f	91.38 ± 8.23 *g*	37.77 ± 4.66 cd
Toghe-Gardan	3	0.133 ± 0.004 a	135.83 ± 1.11 a	14.28 ± 0.46 e	130.68 ± 3.46 f	95.83 ± 5.37 fg	32.44 ± 4.16 d

Mean values in a column followed by different lowercase letters are significantly different on the basis of ANOVA with Tukey test ($P < 0.05$). CT, condensed tannins; TPC, total phenolic content; TMAC, total monomeric anthocyanin pigment content.

TABLE 9 | Some biochemical characteristics of tested various pomegranate juice cultivars.

Pomegranate cultivar	Sample size (n)	DPPH (inhibition%)	pH	TA (g/L)	Juice (%)	SSC (°Brix)
Aban-Mahi	3	51.71 ± 0.58 cd	3.55 ± 0.08 de	2.33 ± 0.07 bc	51.13 ± 1.65 b	16.67 ± 0.67 ab
Esfahani-Danehghermez	3	60.13 ± 0.96 a	3.30 ± 0.08 ef	2.73 ± 0.07 abc	53.42 ± 3.55 b	17.01 ± 0.58 a
Gabri	3	57.80 ± 2.39 abc	3.38 ± 0.05 ef	2.79 ± 0.23 ab	57.04 ± 2.17 ab	17.17 ± 0.44 a
Gorche-Tafti	3	50.83 ± 0.57 d	4.07 ± 0.09 ab	1.33 ± 0.13 ef	61.18 ± 1.08 a	15.33 ± 0.34 bc
Malase-Danehsyah	3	58.48 ± 2.54 ab	3.21 ± 0.05 f	2.99 ± 0.11 a	51.68 ± 2.39 b	17.33 ± 0.67 a
Malase-Yazdi	3	54.47 ± 0.51 abcd	3.28 ± 0.04 ef	2.87 ± 0.18 ab	56.50 ± 3.29 ab	16.83 ± 0.44 ab
Shahvare-Danehghermez	3	52.23 ± 1.13 bcd	3.73 ± 0.08 cd	2.13 ± 0.13 cd	55.80 ± 1.38 ab	16.33 ± 0.33 abc
Shahvare-Danehsefid	3	50.94 ± 0.95 d	4.15 ± 0.04 a	0.93 ± 0.13 f	61.32 ± 1.02 a	16.01 ± 0.58 abc
Tabolarze-Mehrmahi	3	54.48 ± 0.51 abcd	3.83 ± 0.05 bcd	1.60 ± 0.11 de	50.15 ± 1.78 b	15.01 ± 0.58 c
Tafti	3	49.17 ± 1.20 d	4.01 ± 0.07 abc	1.27 ± 0.06 ef	54.82 ± 1.11 ab	17.33 ± 0.67 a
Toghe-Gardan	3	49.94 ± 0.67 d	3.96 ± 0.04 abc	1.40 ± 0.11 ef	52.38 ± 3.77 b	17.5 ± 0.51 a

Mean values in a column followed by different lowercase letters are significantly different on the basis of ANOVA with Tukey test ($P < 0.05$). DPPH, 2,2 diphenyl-1-picrylhydrazyl; TA, total titrable acidity; SSC, soluble solids content.

the one hand, and different biochemical traits of the various pomegranate cultivars tested, on the other hand; significant positive or negative correlations were observed (**Tables 10**, **11**).

These analyses revealed high positive correlation between developmental time and contents of all major anthocyanin compounds of pomegranate cultivars, while a significant negative correlation was observed between R_0 and r_m, and all major anthocyanin contents (**Table 10**).

Fecundity and pupal weight, as well as the nutritional indices ECI and RGR, were also negatively correlated with contents of all major anthocyanins, whereas RCR was positively correlated with these same variables (**Table 10**).

The life history variables and physiological characteristics of *E. ceratoniae* listed in **Table 11** were not significantly correlated with total protein contents of the various pomegranate cultivars. However, significant positive or negative correlations were observed for life history variables and physiological characteristics with carbohydrate and condensed tannins of pomegranate cultivars. Very high positive correlations were observed between the carbohydrate content of the cultivars and *E. ceratoniae* fecundity, pupal weight, protein content of larvae, R_0 and r_m; developmental time, on the other hand, was negatively correlated with this biochemical trait of pomegranate cultivars. Moreover, a significant negative correlation was observed between condensed tannins of various pomegranate cultivars and *E. ceratoniae* fecundity, pupal weight, protein content of larva, R_0, r_m, ECI and RGR (**Table 11**).

Significant correlations were observed for life history variables and physiological characteristics of *E. ceratoniae* with total phenolic content, total monomeric anthocyanin pigment content, and DPPH of pomegranate cultivars. Specifically, fecundity, pupal weight, protein content of larva, R_0, r_m, ECI and RGR all displayed a significant negative correlation with total phenolic content, total monomeric anthocyanin pigment content, DPPH of pomegranate cultivars; conversely, developmental time and RCR were positively correlated with these biochemical traits of pomegranate cultivars (**Table 11**).

DISCUSSION

Research on plant-herbivore interactions is one of the most important and multidisciplinary undertakings in plant biology, involving various disciplines to describe chemical and ecological processes influencing the outcome of plant-herbivore interactions (War et al., 2012). The results of the present study indicated that *E. ceratoniae* is able to complete its development, survive, and reproduce on all pomegranate cultivars examined; however, its growth rates significantly varied among the tested cultivars. The present research

TABLE 10 | Correlation coefficients (r) of some life history parameters and physiological characteristics of *Ectomyelois ceratoniae* fed on different pomegranate cultivars with major anthocyanins constituents of various pomegranate cultivars.

Parameter	Cyanidin 3-glucoside	Cyanidin 3,5-diglucoside	Delphinidin 3-glucoside	Delphinidin 3,5-diglucoside	Pelargonidin 3- glucoside	Pelargonidin 3,5-diglucoside
Development time	0.665 (0.026)	0.813 (0.002)	0.819 (0.002)	0.606 (0.048)	0.593 (0.05)	0.758 (0.007)
Fecundity	−0.750 (0.008)	−0.850 (0.001)	−0.850 (0.001)	−0.571 (0.067)	−0.732 (0.011)	−0.877 (0.000)
Weight of pupa	−0.774 (0.005)	−0.890 (0.000)	−0.894 (0.000)	−0.555 (0.077)	−0.751 (0.008)	−0.888 (0.000)
Protein content of larva	−0.590 (0.056)	−0.664 (0.026)	−0.662 (0.026)	−0.503 (0.115)	−0.572 (0.066)	−0.660 (0.027)
R_0	−0.790 (0.004)	−0.876 (0.000)	−0.872 (0.000)	−0.697 (0.017)	−0.752 (0.008)	−0.886 (0.000)
r_m	−0.752 (0.008)	−0.866 (0.001)	−0.867 (0.001)	−0.619 (0.042)	−0.718 (0.013)	−0.867 (0.001)
ECI	−0.580 (0.062)	−0.683 (0.021)	−0.683 (0.021)	−0.424 (0.194)	−0.605 (0.049)	−0.742 (0.009)
RCR	0.510 (0.109)	0.659 (0.027)	0.655 (0.029)	0.420 (0.198)	0.523 (0.099)	0.796 (0.003)
RGR	−0.534 (0.090)	−0.619 (0.042)	−0.620 (0.042)	−0.371 (0.261)	−0.569 (0.068)	−0.664 (0.026)

Correlations were evaluated based on Pearson's correlation test ($P < 0.05$). The number in parenthesis is P_{value}.

TABLE 11 | Correlation coefficients (r) of some life history parameters and physiological characteristics of *Ectomyelois ceratoniae* fed on different pomegranate cultivars with biochemical traits of various pomegranate cultivars.

Parameter	Total pProtein	Carbohydrate	CT	TPC	TMAC	DPPH
Development time	−0.517 (0.103)	−0.832 (0.001)	0.886 (0.000)	0.883 (0.000)	0.876 (0.000)	0.912 (0.000)
Fecundity	0.543 (0.084)	0.893 (0.000)	−0.794 (0.004)	−0.884 (0.000)	−0.841 (0.001)	−0.824 (0.002)
Weight of pupa	0.467 (0.147)	0.873 (0.000)	−0.846 (0.001)	−0.883 (0.000)	−0.888 (0.000)	−0.870 (0.001)
Protein content of larva	0.409 (0.212)	0.818 (0.002)	−0.821 (0.002)	−0.853 (0.001)	−0.770 (0.006)	−0.695 (0.018)
R_0	0.490 (0.126)	0.867 (0.001)	−0.832 (0.001)	−0.890 (0.000)	−0.903 (0.000)	−0.839 (0.001)
r_m	0.511 (0.108)	0.899 (0.000)	−0.881 (0.000)	−0.916 (0.000)	−0.908 (0.000)	−0.880 (0.000)
ECI	0.580 (0.061)	0.849 (0.001)	−0.834 (0.001)	−0.801 (0.003)	−0.803 (0.003)	−0.739 (0.009)
RCR	−0.504 (0.114)	−0.856 (0.001)	0.727 (0.011)	0.792 (0.004)	0.743 (0.009)	0.743 (0.009)
RGR	0.590 (0.056)	0.779 (0.005)	−0.802 (0.003)	−0.732 (0.010)	−0.751 (0.008)	−0.662 (0.026)

Correlations were evaluated based on Pearson's correlation test ($P < 0.05$). The number in parenthesis is P_{value}.

demonstrates the existence of interactions between biochemical characteristics of various pomegranate cultivars with growth rate, life table parameters, and nutritional indices of this pest. There are complex interactions of macronutrients with other dietary characteristics influencing lifespan and reproduction rate (Coskun et al., 2005; Chen et al., 2009). Primary plant metabolites, including nitrogen, protein, and carbohydrates have been shown to strongly affect the feeding and growth of insect herbivores (Soufbaf et al., 2012; Golizadeh and Abedi, 2017); however, less attention has been given to secondary plant metabolites and their effects on insect performance (Harvey, 2005; Ode, 2006; Mardani-Talaee et al., 2016).

In the present research, *E. ceratoniae* developed more slowly on Esfahani-Daneghermez and Malase-Danesyah cultivars, suggesting that the nutritional quality of these cultivars is less suitable for the feeding of larvae. It has been proposed that low nutritive quality of host diet is a possible measure offering resistance against insect herbivores (War et al., 2012; Akandeh et al., 2016). Variations in the duration of immature stages of *E. ceratoniae* might be attributed to differences in macronutrients and biochemical traits of the tested pomegranate cultivars. The shortest development time of *E. ceratoniae* on Shahvare-Danesefid cultivar may be explained by the higher carbohydrate value in this cultivar. Moreover, the secondary metabolites could be another factor affecting development time (Soufbaf et al., 2012; Nouri-Ganbalani et al., 2018). The content of major anthocyanin compounds and other secondary metabolites in Shahvare-Danesefid cultivar was lower than that of other tested pomegranate cultivars. There is a negative correlation between the development time of *E. ceratoniae* and macronutrients (especially carbohydrate) of pomegranate cultivars. Development time was positively correlated with major anthocyanin constituents, condensed tannins, total phenolic content, total monomeric anthocyanin pigment content, flavonoid, DPPH, and total titrable acidity of pomegranate cultivars, suggesting that pest development rate is negatively affected by respective metabolites and that these factors play a decisive role in the fitness of this insect. The longer development time of *E. ceratoniae* on Esfahani-Daneghermez cultivar may be due to higher levels of secondary metabolites n this cultivar. The range of larval and pupal periods of *E. ceratoniae* on tested cultivars is somewhat in agreement with the findings of Norouzi et al. (2008), Zare et al. (2013), and Mortazavi et al. (2016).

It has been reported that body weight is associated with the quality and quantity of food, which is one of the main biological indices of insect population dynamics (Li et al., 2004). The lower pupal weight of carob moths on Malase-Danesyah and Esfahani-Daneghermez cultivars indicated that the larvae fed on these cultivars did more poorly than on the other cultivars. The range of pupal weight for *E. ceratoniae* in the current study was greater than that reported by Mortazavi et al. (2016). The variations in nutritional quality or secondary compounds among the pomegranate cultivars can influence the larval and pupal development and can be reflected in the pupal weight of *E. ceratoniae*. The reduced body weight of this pest on cultivars Malase-Danesyah and Esfahani-Daneghermez might be attributed to the lower carbohydrate content and higher contents of secondary metabolites in these cultivars.

In this study, adults reared as larvae on the Shahvare-Danesefid and Toghe-Gardan cultivars presented higher fecundity and longevity, indicating suitability of these cultivars for reproduction of this pest. Regarding the larval and pupal weights, it is evident that the fecundity values can be correlated with the weights of larvae and pupae on the respective cultivars (Golizadeh and Abedi, 2016). This is illustrated by the present study, in which it was found that the development times of *E. ceratoniae* fed on pomegranate cultivars were positively correlated with levels of the major anthocyanin constituents and secondary compounds, suggesting that phytochemical metabolites play a negative role in the growth of this insect. In this study, the range of male and female longevities of *E. ceratoniae* was close to those reported earlier for *E. ceratoniae* reared on three pomegranate cultivars, including Malase-danesyah, Gabri, and Shahvar (Zare et al., 2013).

The results of the present investigation revealed that pomegranate cultivar is a major factor influencing life table parameters of *E. ceratoniae* so that its best and worst performances were observed on the Shahvare-Danesefid and Esfahani-Daneghermez cultivars, respectively. The reduced R_0, *GRR*, r_m and λ of this pest on Esfahani-Daneghermez cultivar might be attributed to the positive correlation of these factors with primary metabolites as well as negative correlation with secondary metabolites of tested cultivars. Normally, higher r_m is related to shorter developmental time, lower mortality, and greater fecundity, which is true for *E. ceratoniae* reared on Shahvare-Danesefid. The range of r_m values of *E. ceratoniae* on various pomegranate cultivars tested in the present study was smaller than that reported by Norouzi et al. (2008), Zare et al. (2013), and Mortazavi et al. (2015). Such discrepancy might be attributable to either genetic differences in pest populations or variations in the experimental conditions and cultivars used for feeding of this pest.

The lower food consumption by *E. ceratoniae* on Esfahani-Daneghermez is likely attributable to the poor nutritional quality of this cultivar. The higher ECI value for *E. ceratoniae* on the Shahvare-Danesefid and Gorche-Tafti cultivars indicated that the larvae were able to convert digested food to body mass and that the weights of larvae improved on these cultivars. Furthermore, a significant correlation between ECI with starch and carbohydrate content indicated that larvae efficiently utilized carbohydrate for better growth. In contrast, the larvae reared on Esfahani-Daneghermez and Malase-Danesyah cultivars showed a lower ability to convert the ingested food into biomass, which led to the reduction in food consumption and weight of larvae (Nathan et al., 2005). The highest RCR value of *E. ceratoniae* on Esfahani-Daneghermez and Tabolarze-Mehrmahi could be due to the higher level of secondary compounds in these cultivars. Moreover, the variation in RGR and whole-body protein contents of populations reared on different pomegranate cultivars may have resulted from differences in primary plant metabolites among the cultivars.

In the present study, cluster analysis with respect to life table parameters, nutritional indices, and energy reserves of

E. ceratoniae on tested pomegranate cultivars revealed two separate main clusters. Shahvare-Danesefid cultivar is the only member in cluster B as the most susceptible cultivar. The grouping within each class might be due to a high level of physiological similarity of pomegranate cultivars. Cluster A can be divided into two distinct sub-clusters (A1 and A2). Sub-cluster A2 consisted of Esfahani-Daneghermez and Malase-Danesyah (most relatively unsuitable cultivars), and other cultivars were grouped in sub-cluster A1 based on their similarity in primary and secondary metabolite contents (partially unsuitable cultivars).

CONCLUSION

Results of the present study point to the apparent adaptability of *E. ceratoniae* to feeding on various pomegranate cultivars, albeit with different degrees of success. Our results indicate that insects fed on the Shahvare-Danesefid cultivar displayed the fastest development and highest adult fecundity and longevity, immature survival rate and nutritional performance, apparently as a consequence of the higher primary metabolite and lower secondary metabolite contents of the host plant. Therefore, this cultivar was the most suitable (least resistant) cultivar for *E. ceratoniae*, among those tested here. Moreover, the Esfahani-Daneghermez cultivar was the least suitable (most resistant) pomegranate cultivar for *E. ceratoniae*, apparently as a consequence of the higher secondary metabolite contents of the host plant. Consequently, Esfahani-Daneghermez was designated as the most unsuitable cultivar among those tested in the present work; we recommend that it be grown in areas where damage by *E. ceratoniae* is typically high, with the view to protecting or at least delaying infestation of pomegranate by this pest.

AUTHOR CONTRIBUTIONS

All authors read and approved the manuscript. This research is a part of Ph.D. thesis of ZA. AG as supervisor and ZA proposed the research subject and wrote the manuscript. ZA conducted the experiments. MS, MH, AJ-N, and H-RA participated in the data analysis and acted as advisors.

FUNDING

This study was funded by the University of Mohaghegh Ardabili and Iran National Science Foundation (INSF).

ACKNOWLEDGMENTS

This work received financial support from the University of Mohaghegh Ardabili and Iran National Science Foundation (INSF) which is greatly appreciated.

REFERENCES

Akandeh, M., Soufbaf, M., Kocheili, F., and Rasekh, A. (2016). Gamma irradiation on canola seeds affects herbivore-plant and host-parasitoid interactions. *Neotrop. Entomol.* 46, 256–263. doi: 10.1007/s13744-016-0460-4

Akhavan, H., Barzegar, M., Weidlich, H., and Zimmermann, B. F. (2015). Phenolic compounds and antioxidant activity of juices from ten iranian pomegranate cultivars depend on extraction. *J. Chem. N.Y.* 2015, 1–7. doi: 10.1155/2015/907101

Alighourchi, H., Barzegar, M., and Abbasi, S. (2008). Anthocyanins characterization of 15 iranian pomegranate (*Punica granatum* L.) varieties and their variation after cold storage and pasteurization. *Eur. Food Res. Technol.* 227, 881–887. doi: 10.1007/s00217-007-0799-1

Alighourchi, H. R., Barzegar, M., Sahari, M. A., and Abbasi, S. (2013). Effect of sonication on anthocyanins, total phenolic content, and antioxidant capacity of pomegranate juices. *Int. Food Res. J.* 20, 1703–1709.

Ashtari, M., Khademia, O., Soufbaf, M., Afsharmanesh, H., and Askari-Sarcheshmeh, M. A. (2019). Effect of gamma irradiation on antioxidants, microbiological properties and shelf life of pomegranate arils cv. *'Malas Saveh'*. *Sci. Hortic.* 244, 365–371. doi: 10.1016/j.scienta.2018.09.067

Bemani, M., Izadi, H., Mahdian, K., Khani, A., and Samih, M. A. (2012). Study on the physiology of diapause, cold hardiness and supercooling point of overwintering pupae of the pistachio fruit hull borer. *Arimania comaroffi*. *J. Insect Physiol.* 58, 897–902. doi: 10.1016/j.jinsphys.2012.04.003

Bradford, M. M. (1976). A rapid and sensitive method for the quantitation of microgram quantities of protein utilizing the principle of protein-dye binding. *Anal. Biochem.* 72, 248–254. doi: 10.1016/0003-2697(76)90527-3

Chen, Y., Ni, X., and Buntin, G. D. (2009). Physiological, nutritional, and biochemical bases of corn resistance to foliage-feeding fall armyworm. *J. Chem. Ecol.* 35, 297–306. doi: 10.1007/s10886-009-9600-1

Chi, H. (1988). Life-table analysis incorporating both sexes and variable development rates among individuals. *Environ. Entomol.* 17, 26–34. doi: 10.1093/ee/17.1.26

Chi, H. (2016). *TWOSEX-MSChart: A Computer Program for the Age-Stage, Two-Sex Life Table Analysis*. Available at: http://140.120.197.173/Ecology/Download/TWOSEX-MSchart.zip (accessed November 20, 2017).

Chi, H., and Liu, H. (1985). Two new methods for the study of insect population ecology. *Bull. Inst. Zool. Academia Sinica* 24, 225–240.

Chi, H., and Su, H. Y. (2006). Age-stage, two-sex life tables of *Aphidius gifuensis* (Ashmead) (Hymenoptera: Braconidae) and its host *Myzus persicae* (Sulzer) (Homoptera: Aphididae) with mathematical proof of the relationship between female fecundity and the net reproductive rate. *Environ. Entomol.* 35, 10–21. doi: 10.1603/0046-225X-35.1.10

Coskun, M., Ozalp, P., Sulanc, M., and Emre, I. (2005). Effects of various diets on the oviposition and sex ratio of *Pimpla turionellae* L. *Int. J. Agric. Biol.* 7, 129–132.

Du, C. T., Wang, P. L., and Francis, F. J. (1975). Anthocyanins of pomegranate, *Punica granatum*. *J. Food Sci.* 40, 417–418. doi: 10.1111/j.1365-2621.1975.tb02217.x

Fischer, U. A., Carle, R., and Kammerer, D. R. (2011). Identification and quantification of phenolic compounds from pomegranate (*Punica granatum* L.) peel, mesocarp, aril and differently produced juices by *HPLC-DAD-ESI/MSn*. *Food Chem.* 127, 807–821. doi: 10.1016/j.foodchem

Golizadeh, A., and Abedi, Z. (2016). Comparative performance of the Khapra beetle, *Trogoderma granarium* Everts (Coleoptera: Dermestidae) on various wheat cultivars. *J. Stored Prod. Res.* 69, 159–165. doi: 10.1016/j.jspr.2016.08.003

Golizadeh, A., and Abedi, Z. (2017). Feeding performance and life table parameters of Khapra beetle, *Trogoderma granarium* Everts (Coleoptera: Dermestidae) on various barley cultivars. *Bull. Entomol. Res.* 14, 1–10. doi: 10.1017/S0007485317000207

Golizadeh, A., Kamali, K., Fathipour, Y., and Abbasipour, H. (2009). Life table of the diamondback moth, *Plutella xylostella* (L.) (Lepidoptera: Plutellidae) on five cultivated brassicaceous host plants. *J. Agr. Sci. Tech-Iran.* 11, 115–124.

Gvozdenac, S. M., Prvulovi, D. M., Radovanovi, M. N., Ovuka, S., Mikli, V. J., Canski, J. M. A., et al. (2018). Life history of *Plodia interpunctella* Hübner on sunflower seeds: effects of seed qualitative traits and the initial seed damage. *J. Stored Prod. Res.* 79, 89–97. doi: 10.1016/j.jspr.2018.08.003

Harvey, J. A. (2005). Factors affecting the evolution of development strategies in parasitoid wasps: the importance of functional constraints and incorporating complexity. *Entomol. Exp. Appl.* 117, 1–13. doi: 10.1111/j.1570-7458.2005.00348.x

Harvey, J. A., Gols, R., Wagenaar, R., and Bezemer, T. M. (2007). Development of an insect herbivore and its pupal parasitoid reflect differences in direct plant defense. *J. Chem. Ecol.* 33, 1556–1569. doi: 10.1007/s10886-007-9323-0

Jia, Z., Tang, M., and Wu, J. (1999). The determination of flavonoid contents in mulberry and their scavenging effects on superoxide radicals. *Food Chem.* 64, 555–559. doi: 10.1016/S0308-8146(98)00102-2

Karimi-Pormehr, M. S., Borzoui, E., Naseri, B., Rafiee Dastjerdi, H., and Mansouri, S. M. (2018). Two-sex life table analysis and digestive physiology of *Sitotroga cerealella* (Olivier) (Lepidoptera: Gelechiidae) on different barley cultivars. *J. Stored Prod. Res.* 75, 64–71. doi: 10.1016/j.jspr.2017.10.005

Kishani-Farahani, H., Goldansaz, S. H., and Sabahi, Q. (2012). A survey on the overwintering larval parasitoids of *Ectomyelois ceratoniae* in three regions in Iran. *Crop Prot.* 36, 52–57. doi: 10.1016/j.cropro.2012.01.018

Li, Y., Hill, C. B., and Hartman, G. L. (2004). Effect of three resistant soybean genotypes on the fecundity, mortality, and maturation of soybean aphid (Homoptera: Aphididae). *J. Econ. Entomol.* 97, 1106–1111. doi: 10.1603/0022-0493(2004)097%5B1106:eotrsg%5D2.0.co;2

Mardani-Talaee, M., Nouri-Ganblani, G., Razmjou, J., Hassanpour, M., Naseri, B., and Asgharzadeh, A. (2016). Effects of chemical, organic and bio-fertilizers on some secondary metabolites in the leaves of bell pepper (*Capsicum annuum*) and their impact on life table parameters of *Myzus persicae* (Hemiptera: Aphididae). *J. Econ. Entomol.* 109, 1231–1240. doi: 10.1007/s13744-017-0494-2

Mirsaeedghazi, H., Emam-Djomeh, Z., and Ahmadkhaniha, R. (2014). Effect of frozen storage on the anthocyanins and phenolic components of pomegranate juice. *J. Food Sci. Technol.* 51, 382–386. doi: 10.1007/s13197-011-0504-z

Mortazavi, S., Samih, M. A., Ghajarieh, H., and Jafari, A. (2015). Effect of some diets on demographic parameters of *Ectomyelois ceratoniae* (Zeller) (Lepidoptera: Pyralidae) in vitro. *J. Plant Protec. Res.* 55, 212–219. doi: 10.1515/jppr-2015-0028

Mortazavi, S., Samih, M. A., Ghajarieh, H., and Jafari, A. (2016). Effect of some diets on biological parameters of *Apomyelois ceratoniae* in laboratory and efficiency of natural pheromone traps in pomegranate orchards. *J. Crop Protec.* 5, 115–124. doi: 10.18869/modares.jcp.5.1.115

Nathan, S. S., Chung, P. G., and Murugan, K. (2005). Effect of biopesticides applied separately or together on nutritional indices of the rice leaffolder *Cnaphalocrocis medinalis*. *Phytoparasitica* 33, 187–195. doi: 10.1007/BF03029978

Navarro, S., Donahaye, E., and Calderon, M. (1986). Development of the carob moth, *Spectrobates ceratoniae*, on stored almonds. *Phytoparasitica* 14, 177–186. doi: 10.1007/BF02980485

Nawrot, J., Gawlak, M., Szafranek, J., Szafranek, B., Synak, E., Warchalewski, J. R., et al. (2010). The effect of wheat grain composition, cuticular lipids and kernel surface microstructure on feeding, egg-laying, and the development of the granary weevil, *Sitophilus granarius* (L.). *J. Stored Prod. Res.* 46, 133–141. doi: 10.1016/j.jspr.2010.02.001

Nikooei, M., Fathipour, Y., Jalali Javaran, M., and Soufbaf, M. (2015). How different genetically manipulated Brassica genotypes affect life table parameters of *Plutella xylostella* (Lepidoptera: Plutellidae). *J. Econ. Entomol.* 108, 515–524. doi: 10.1093/jee/tov018

Norouzi, A., Talebi, A., and Fathipour, A. Y. (2008). Development and demographic parameters of the Carob moth *Apomyelois ceratoniae* on four diet regimes. *B. Insectol.* 61, 291–297.

Nouri-Ganbalani, G., Borzoui, E., Shahnavazi, M., and Nouri, A. (2018). Induction of resistance against *Plutella xylostella* (L.) *(Lep.: Plutellidae*) by jasmonic acid and mealy cabbage aphid feeding in *Brassica napus L. Front. Physiol.* 9:859. doi: 10.3389/fphys.2018.00859

Ode, P. J. (2006). Plant chemistry and natural enemy fitness: effects on herbivore and natural enemy interactions. *Annu. Rev. Entomol.* 51, 163–185. doi: 10.1146/annurev.ento.51.110104.151110

Ramzi, S., Sahragard, A., and Zibaee, A. (2014). Effects of *Citrullus colocynthis* agglutinin on intermediary metabolism of *Ectomyelois ceratoniae* Zeller (Lepidoptera: Pyralidae). *J. Asia Pac. Entomol.* 17, 273–279. doi: 10.1016/j.aspen.2014.01.005

Ranjbar, M., Sendi, J. J., and Zibaee, A. (2011). Proteolytic activity in the midgut of *Ectomyelois ceratoniae* Zeller (Lepidoptera: Pyralidae), pomegranate carob moth. *ISJ Invert. Surviv. J.* 8, 132–142. doi: 10.2478/v10045-012-0061-0

Sarkhosh, A., Zamani, Z., Fatahi, R., and Ranjbar, H. (2009). Evaluation of genetic diversity among Iranian soft-seed pomegranate accessions by fruit characteristics and RAPD markers. *Sci. Hortic.* 121, 313–319. doi: 10.1016/j.scienta.2009.02.024

SAS Institute (2002). *The SAS system for Windows*. Cary, NC: SAS Institute.

Shakeri, M. (ed.) (2004). "A review on investigations on pomegranate neck worm in Iran," in *A Proceeding on Evaluation of Finding and Current Problems Associated With Spectrobates Ceratoniae* Management in Pomegranate, (Tehran: Ministry of Jihad-e- Agriculture).

Sobhani, M., Goldansaz, S. H., Hatami, B., and Hosseini, S. A. (2015). A field screening of pomegranate cultivars for resistance to the carob moth, *Ectomyelois ceratoniae*, and compatibility with its larval parasitoids. *Int. J. Pest Manage.* 61, 346–352. doi: 10.1080/09670874.2015.1069418

Soufbaf, M., Fathipour, Y., Karimzadeh, J., and Zalucki, M. P. (2010). Bottom-up effect of different host plants on *Plutella xylostella* (Lepidoptera: Plutellidae): a life-table study on canola. *J. Econ. Entomol.* 103, 2019–2027. doi: 10.1603/EC10010

Soufbaf, M., Fathipour, Y., Zalucki, M. P., and Hui, C. (2012). Importance of primary metabolites in canola in mediating interactions between a specialist leaf-feeding insect and its specialist solitary endoparasitoid. *Arthropod Plant Int.* 6, 241–250. doi: 10.1007/s11829-012-9182-7

Soufbaf, M., Salehi, B., Kalantarian, N., Zanganeh, A. H., Fathollahi, H., Babaei, M., et al. (2017). Is sterile insect technique's efficiency affected by pomegranate variety in mixed cultivars? New insights from a case study on the carob moth, *Apomyelois ceratoniae* Zeller (Lepidoptera: Pyralidae) in Iran. *Orient. Insects.* 52, 1–11. doi: 10.1080/00305316.2017.1397064

SPSS Inc (2007). *SPSS Base 16.0 User's Guide*. Chicago, IL: SPSS Incorporation.

Tanner, H., and Brunner, H. R. (1979). *Getraenke Analytik. Verlag Heller Chemie-Und Verwaltungsgeselschaft mbH. D*-7170. Germany: schwaebisch Hall.

Tezcan, F., Gültekin-Özgüven, M., Diken, T., Özçelik, B., and Erim, F. B. (2009). Antioxidant activity and total phenolic, organic acid and sugar content in commercial pomegranate juices. *Food Chem.* 115, 873–877. doi: 10.1016/j.foodchem.2008.12.103

Tsai, J. H., and Wang, J. J. (2001). Effects of host plant on biology and life table parameters of *Aphis spiraecola* (Hom: *Aphididae*). *Environ Entomol.* 30, 44–50. doi: 10.1603/0046-225X-30.1.44

Turfan, O., Turkyılmaz, M., Yemis, O., and Ozkan, M. (2011). Anthocyanin and colour changes during processing of pomegranate (*Punica granatum* L., *cv. Hicaznar*) juice from sacs and whole fruit. *Food Chem.* 129, 1644–1651. doi: 10.1016/j.foodchem.2011.06.024

Van Handel, E. (1985). Rapid determination of total lipids in mosquitoes. *J. Am. Mosquito Contr.* 1, 302–304.

Waldbauer, G. P. (1968). The consumption and utilization of food by insects. *Adv. Insect Physiol.* 5, 229–288. doi: 10.1016/S0065-2806(08)60230-1

War, A. R., Paulraj, M. G., Ahmad, T., Buhroo, A. A., Hussain, B., Ignacimuthu, S., et al. (2012). Mechanisms of plant defense against insect herbivores. *Plant Signal. Behav.* 7, 1306–1320. doi: 10.4161/psb.21663

War, A. R., Paulraj, M. G., War, M. Y., and Ignacimuthu, S. (2011). Differential defensive response of groundnut to *Helicoverpa armigera* (Hubner)

(Lepidoptera: Noctuidae). *J. Plant Interact.* 6, 1–11. doi: 10.1080/17429145.2011.587898

Warner, R. L., Barnes, M. M., Laird, E. F., and Lanham, M. D. (1990). Chemical control of carob moth, *Ectomyelois ceratoniae* (Lepidoptera.: *Pyralidae*), and various nitidulid beetles (Coleoptera) on 'Deglet Noor' dates in California. *J. Econ. Entomol.* 83, 2357–2361. doi: 10.1093/jee/83.6.2357

Wrolstad, R. E., Durst, R. W., and Lee, J. (2005). Tracking color and pigment changes in anthocyanin products. *Trends Food Sci. Tech.* 16, 423–428. doi: 10.1016/j.tifs.2005.03.019

Yuval, B., Kaspi, R., Shloush, S., and Warburg, M. S. (1998). Nutritional reserves regulate male participation in mediterranean fruit fly leks. *Ecol. Entomol.* 23, 211–215. doi: 10.1046/j.1365-2311.1998.00118.x

Zare, D., Sendi, J. J., Jafary Nodoushan, A., and Khosravi, A. (2013). Life table parameters and biological characteristics of *Apomyelois ceratoniae* Zeller (Lepidoptera: Pyralidae) on three cultivars of pomegranate. *Arch. Phytopathol. Plant Protect.* 46, 766–773. doi: 10.1080/03235408.2012.752141

Conflict of Interest: The authors declare that the research was conducted in the absence of any commercial or financial relationships that could be construed as a potential conflict of interest.

Advantages of publishing in Frontiers

OPEN ACCESS
Articles are free to read for greatest visibility and readership

FAST PUBLICATION
Around 90 days from submission to decision

HIGH QUALITY PEER-REVIEW
Rigorous, collaborative, and constructive peer-review

TRANSPARENT PEER-REVIEW
Editors and reviewers acknowledged by name on published articles

Frontiers
Avenue du Tribunal-Fédéral 34
1005 Lausanne | Switzerland

Visit us: www.frontiersin.org
Contact us: info@frontiersin.org | +41 21 510 17 00

REPRODUCIBILITY OF RESEARCH
Support open data and methods to enhance research reproducibility

DIGITAL PUBLISHING
Articles designed for optimal readership across devices

FOLLOW US
@frontiersin

IMPACT METRICS
Advanced article metrics track visibility across digital media

EXTENSIVE PROMOTION
Marketing and promotion of impactful research

LOOP RESEARCH NETWORK
Our network increases your article's readership